

UC Berkeley

UC Berkeley Electronic Theses and Dissertations

Title

Bioorthogonal Chemistries for Labeling Living Systems

Permalink

<https://escholarship.org/uc/item/616516jm>

Author

Sletten, Ellen

Publication Date

2011

Peer reviewed|Thesis/dissertation

Bioorthogonal Chemistries for Labeling Living Systems

by

Ellen May Sletten

A dissertation submitted in partial satisfaction of the

requirements for the degree

Doctor of Philosophy

in

Chemistry

in the

Graduate Division

of the

University of California, Berkeley

Committee in charge:

Professor Carolyn R. Bertozzi, Chair

Professor Matthew B. Francis

Professor Seung-Wuk Lee

Fall 2011

Bioorthogonal Chemistries for Labeling Living Systems

© 2011

By Ellen May Sletten

Abstract

Bioorthogonal Chemistries for Labeling Living Systems

by

Ellen May Sletten

Doctor of Philosophy in Chemistry

University of California, Berkeley

Professor Carolyn R. Bertozzi, Chair

Bioorthogonal is defined as not interfering or interacting with biology. Chemical reactions that are bioorthogonal have recently become valuable tools to visualize biomolecules in their native environments, particularly those that are not amenable to traditional genetic modification. The field of bioorthogonal chemistry is rather young, with the first published account of the term bioorthogonal in 2003, yet it is expanding at a rapid rate. The roots of this unique subset of chemistry are in classic protein modification and subsequent bioconjugation efforts to obtain uniformly and site-specifically functionalized proteins. These studies are highlighted in Chapter 1. Chapter 2 opens with a summary of the bioorthogonal chemical reporter strategy, a two-step approach where a bioorthogonal functional group is installed into a biomolecule of interest, most often using endogenous metabolic machinery, and detected through a secondary covalent reaction with an appropriately functionalized chemical partner. It is this chemical reporter strategy that empowers bioorthogonal chemistry and allows for a wide variety of biological species to be assayed.

Chapter 2 proceeds to outline the discovery of the Staudinger ligation, the first chemical reaction developed for use in the bioorthogonal chemical reporter strategy. The Staudinger ligation employed the azide as the chemical reporter group and, since its debut in 2000, many laboratories have capitalized on the exquisite qualities of the azide (small, abiotic, kinetically stable) that make it a versatile chemical reporter group. The success of the azide prompted the development of other bioorthogonal chemistries for this functional group. One of these chemistries, Cu-free click chemistry, is the 1,3-dipolar cycloaddition between cyclooctynes and azides. The cycloaddition is promoted at physiological conditions by the ~18 kcal/mol of ring strain contained within cyclooctyne, and further modifications to the cyclooctyne reagents have led to increased reactivity through augmentation of the ring strain or optimization of orbital overlap. When I began my graduate work, a difluorinated cyclooctyne (DIFO), which was 60-fold more reactive than other existing bioorthogonal chemistries, had just been synthesized and employed for labeling azides on live cells and within living mice. DIFO performed very well on

cultured cells, but it was outperformed by the slower Staudinger ligation in the more complex environment of the mouse. We hypothesized that DIFO was too hydrophobic to be effective in mice and designed a more hydrophilic cyclooctyne reagent, a dimethoxyazacyclooctyne (DIMAC). DIMAC was synthesized in nine steps in a 10% overall yield (Chapter 3). As predicted, DIMAC displayed reaction kinetics similar to early generation cyclooctynes, but exhibited improved water-solubility. Consequently, DIMAC labeled cell-surface azides with comparable efficiencies to the early generation cyclooctynes but greater signal-to-noise ratios were achieved due to minimal background staining. Encouraged by these results, we assayed the ability for DIMAC to label azides in living mice and found that DIMAC was able to modify azides *in vivo* with moderate signal over background. However, the Staudinger ligation was still the superior bioorthogonal reaction for labeling azides *in vivo*. Our results collectively indicated that both hydrophilicity and reactivity are important qualities when optimizing the cyclooctynes for *in vivo* reaction with azides (Chapter 4).

We were also interested in modifying DIMAC so that it would become fluorescent upon reaction with an azide. Previous work in the lab had established that fluorogenic reagents could be easily created if a functional group was cleaved from the molecule upon reaction with an azide. We envisioned a leaving group could be engineered into the azacyclooctyne scaffold by strategically positioning a labile functional group across the ring from a nitrogen atom. The cyclooctyne structure should be stable, as it is rigid and intramolecular reactions are not favorable. However, upon reaction with an azide, a significant amount of strain is liberated and the intramolecular reaction should readily occur. Efforts toward the synthesis of this modified DIMAC reagent are chronicled in Chapter 5.

Chapter 6 is a very short account of our early work to use DIFO-based reagents for proteomics. The results contained in this chapter are preliminary and further endeavors towards this goal are underway by others within the group.

Chapters 7, 8 and 9 are devoted to strategies to increase the second-order rate constant of Cu-free click chemistry. In Chapter 7, various routes toward a tetrafluorinated cyclooctyne are outlined, although none of them successfully yielded this putatively highly reactive cyclooctyne. Chapter 8 describes the synthesis of a difluorobenzocyclooctyne (DIFBO), which is more reactive than DIFO, but unstable due to its propensity to form trimer products. However, DIFBO can be kinetically stabilized by encapsulation in β -cyclodextrin. Only β -cyclodextrin and not the smaller (α) or larger (γ) cyclodextrins were able to protect DIFBO. We did observe an intriguing result when complexation with the larger γ -cyclodextrin was attempted. It appears as though two DIFBO molecules can fit inside the γ -cyclodextrin and dimeric products, which were not apparent in the absence of γ -cyclodextrin, were observed. We hypothesized that all oligomer products of DIFBO were derived from a common cyclobutadiene intermediate. While DIFBO was chemically interesting, it was not a useful reagent for labeling azides in biological settings. Thus, Chapter 9 is devoted to the modification of DIFBO, with the aim of identifying a reactive yet stable cyclooctyne. The data from Chapter 9 suggest we are rapidly approaching the reactivity/stability limit for cyclooctyne reagents.

The results contained within Chapters 7-9 indicated that it was time to explore other bioorthogonal chemistries. When embarking on the development of a new bioorthogonal chemical reaction, we aimed to explore unrepresented reactivity space, such that the new reaction would be orthogonal to existing bioorthogonal chemistries. We became attracted to the highly strained hydrocarbon quadricyclane and performed a screen to find a suitable reactive partner for this potential chemical reporter group (Chapter 10). Through this analysis, we discovered that quadricyclane cleanly reacts with Ni bis(dithiolene) reagents and this transformation appeared to be a good prototype for a new bioorthogonal chemical reaction. After a thorough mechanistic investigation and many rounds of modification to the Ni bis(dithiolene) species, a nickel complex with suitable reaction kinetics, water-solubility, and stability was obtained (Chapter 11). Gratifyingly, this Ni bis(dithiolene) reagent selectively modified quadricyclane-labeled bovine serum albumin, even in the presence of cell lysate (Chapter 12). Other results in Chapter 12 highlight that this new bioorthogonal ligation reaction is indeed orthogonal to Cu-free click chemistry as well as oxime ligation chemistry. Additionally, quadricyclane-dependent labeling is observed on live cells, although further optimization is necessary.

The final chapter of this dissertation outlines the current state of the field. There are now many methods to modify biomolecules including several new, although relatively untested, bioorthogonal chemistries. The rapid pace of this field makes it an exciting time to be pursuing bioorthogonal chemistry.

This dissertation is dedicated to everyone who has made this journey possible.

Bioorthogonal Chemistries for Labeling Living Systems

Table of Contents

List of Figures	vii
List of Schemes	xiii
List of Tables	xv
Acknowledgements	xvi
Chapter 1. Chemistry Meets Biology	
Introduction	1
Protein Modification	1
Canonical Residue Modification	1
N-Terminal Modification	5
Native Chemical Ligation	7
Selective Protein Modification through Protein and Peptide Fusions	9
Fluorogenic Bisarsenical Reagents	9
Peptide Tags Detected through the Chelation of Transition Metals	10
Enzymatic Modification of Peptide Tags	11
From Protein Modification to Bioorthogonal Chemistry	14
References	18
Chapter 2. Bioorthogonal Chemistry	
The Bioorthogonal Chemical Reporter Strategy	25
The Staudinger Ligation	26
Cu-Catalyzed Azide-Alkyne Cycloaddition (CuAAC)	34
Strain-Promoted Azide-Alkyne Cycloaddition	36
References	39
Chapter 3. A Hydrophilic Azacyclooctyne	
Cu-Free Click Chemistry	44
Initial Attempts at Cu-Free Click Chemistry in Mice	45
Design of a More Hydrophilic Cyclooctyne	48
Synthesis of a Hydrophilic Azacyclooctyne	49
Kinetic and Structural Analysis of DIMAC	54
Materials and Methods	56
General Experimental Procedure	56
Experimental Procedures	57
Kinetics	68
X-Ray Crystallography	68
References	69

Chapter 4. Labeling Azido-Glycans with DIMAC	
Labeling of Azides <i>in vitro</i> with DIMAC	71
Labeling of Azides <i>in vivo</i> with DIMAC	78
Materials and Methods	82
General Experimental Procedure	82
Experimental Procedures	83
Cell Culture	84
Western Blot Analysis of Azide-Labeled Cell Lysates	84
Cell-Surface Azide Labeling and Detection	85
Mice	86
Compound Administration	86
Splenocyte Analysis after Cu-Free Click Chemistry <i>in vivo</i>	86
Labeling of Splenocyte Cell-Surface Azides <i>ex vivo</i>	86
Lysis of Murine Organs and Western Blot Analysis	86
Western Blot Analysis of Serum Glycoproteins	87
References	87
Chapter 5. Towards a Fluorogenic Cyclooctyne	
Strategies for <i>in vivo</i> Imaging of Azides using the Staudinger Ligation	89
Design of a Fluorogenic Cyclooctyne	91
Synthesis of Fluorogenic Azacyclooctyne 5.12	93
Future Steps Towards the Synthesis of a Fluorogenic Azacyclooctyne	96
Materials and Methods	96
General Experimental Procedure	96
Experimental Procedures	96
X-Ray Crystallography	103
References	103
Chapter 6. Cu-Free Click Chemistry as a Tool for Proteomics	
Introduction to Proteomics	105
Reagent Design	106
Synthesis of Pull-Down Reagent	107
Evaluation of Pull-Down Reagent	108
Conclusions and Future Directions	110
Materials and Methods	111
General Experimental Procedure	111
Experimental Procedures	111
N ₃ -BSA Pull-Down Assay	114
H2 Ras Pull-Down Assay	114
References	114

Chapter 7. Towards a Tetrafluorinated Cyclooctyne	
The Benefits of a Highly Reactive Cyclooctyne	118
Design of a More Reactive Cyclooctyne	119
Initial Synthetic Attempts Toward TetraFO	120
New Synthetic Strategies Toward TetraFO	122
Synthesis of TetraFO using a Ring-Expansion Strategy	123
Materials and Methods	127
General Experimental Procedure	127
Experimental Procedures	127
References	134
Chapter 8. Synthesis and Stabilization of Difluorobenzocyclooctyne	
Fused Phenyl Rings Activate Cyclooctynes for Reaction with Azides	138
Design of a More Reactive Cyclooctyne	139
Stabilization of DIFBO	142
Precedent for Proposed Oligomerization Mechanism	149
Unexpected Lessons from DIFBO	150
Materials and Methods	151
General Experimental Procedure	151
Experimental Procedures	151
CPMAS ¹³ C NMR Procedure	155
Analysis of DIFBO-Cyclodextrin Complexes	155
X-Ray Crystallography	156
Cell Culture	157
Cell-Surface Labeling and Detection	157
References	158
Chapter 9. Reactivity of Monobenzocycloalkynes	
Difluoro and monobenzocyclooctyne	161
Reactivity of DIFBO in a Biological Setting	164
Efforts to Stabilize DIFBO	165
A More Subtle Strain-Release Strategy	166
Cu-Free Click Chemistry Conclusions	171
Materials and Methods	172
General Experimental Procedure	172
Experimental Procedures	172
Kinetics	181
Western Blot Analysis of β -Cyclodextrin-DIFBO Treated Lysates	182
References	183
Chapter 10. The Road to a New Bioorthogonal Reaction	
A Guide to Bioorthogonal Reaction Development	185
A New Chemical Reporter Group	187
Finding a Reaction Partner for Quadricyclane	191

A Prototype Reaction	196
Materials and Methods	197
General Experimental Procedure	197
Experimental Procedures	198
Kinetics	200
References	201
Chapter 11. Mechanistic Investigation and Modifications of Quadricyclane-Ni bis(dithiolene) Chemistry	
Mechanistic Investigation	205
Molecular Orbital Analysis	205
Kinetic Analysis	206
Stability Analysis of the Ligation Product	208
Mechanistic Modifications	213
Rate Enhancement	213
Stability Enhancement	218
Further Mechanistic Modifications	220
Kinetic Analysis of Ni bis(dithiolene) 11.44	221
Stability Analysis of Ni bis(dithiolene) 11.44	224
Summary of Mechanistic Modifications	230
Materials and Methods	231
General Experimental Procedure	231
Experimental Procedures	231
Kinetics	237
Stability Analysis of 11.44	237
References	238
Chapter 12. A Bioorthogonal Quadricyclane Ligation	
Selective Protein Modification with the Quadricyclane Ligation	241
The Quadricyclane Ligation is Orthogonal to Existing Bioorthogonal Chemistries	245
Live Cell Labeling with the Quadricyclane Ligation	247
Future Direction for the Quadricyclane Ligation	255
Materials and Methods	256
General Experimental Procedure	256
Experimental Procedures	256
Preparation of QC-BSA	259
Western Blot Procedures	260
Cell Culture	260
Cell-Surface Labeling and Detection	261
References	263

Chapter 13. The Growth of a Field	
Protein Modification	265
Canonical Residue Modification	265
N-Terminal Modification	269
C-Terminal Modification	270
Selective Protein Modification through Protein and Peptide Fusions	271
Bisboronic Acid Reagents	271
Peptide Tags Detected through Chelation of Transition Metals	272
Binding-Promoted Covalent Modification	274
Enzymatic Modification of Peptide Tags	274
Bioorthogonal Chemistry for the Carbonyl	277
The Staudinger Ligation	280
Cu-Catalyzed Azide-Alkyne Cycloaddition	282
Cu-Free Click Chemistry	286
The Tetrazine Ligation	292
Photoclick Chemistry	298
Emerging Bioorthogonal Chemistries	301
Azirine Ligation	301
Light-Induced Hetero-Diels-Alder Reaction	301
Oxanorbornadiene-Azide Cycloaddition	303
Boronic Acids	303
Pyrroline-Carboxy-Lysine Condensation	305
Conclusion	307
References	308
Appendix A	331
¹ H NMR Spectra	332
Appendix B	462
¹³ C NMR Spectra	463
Appendix C	570
¹⁹ F NMR Spectra	571
Appendix D	615
2D NMR Spectra	616
HPLC Traces	619
UV/Vis/NIR Spectra	624
Appendix E	632
X-Ray Crystallography Data	633

List of Figures

Figure 1.1	Classic bioconjugation reactions for the modification of Cys and Lys residues.	2
Figure 1.2	Modern methods to modify Lys, Tyr, and Trp.	4
Figure 1.3	Methods for N-terminal modification.	6
Figure 1.4	Native chemical ligation and intein-based technologies.	8
Figure 1.5	Fluorogenic bisarsenical reagents for site-specific labeling of recombinant proteins with tetracysteine motifs.	10
Figure 1.6.	Site-specific protein modification through the detection of artificial peptide tags by metal-mediated chelation with chemical reagents.	11
Figure 1.7	Protein modification through enzymatic elaboration of peptide tags.	13
Figure 1.8	Metabolic oligosaccharide engineering pioneered by Reutter and coworkers.	15
Figure 1.9	Selective chemistries for aldehydes/ketones.	15
Figure 1.10	The metabolic incorporation and detection of ketones in cell-surface glycans.	16
Figure 1.11	The site-specific incorporation and detection of a ketone in T4 lysozyme.	17
Figure 2.1	A bioorthogonal chemical reaction and the bioorthogonal chemical reporter strategy.	25
Figure 2.2	The mechanism of the Staudinger reduction and the Staudinger ligation.	27
Figure 2.3	The Staudinger ligation.	27
Figure 2.4	The Staudinger ligation enables selective biomolecule labeling in a variety of environments.	28
Figure 2.5	Azide-modified monosaccharides for incorporation into glycoproteins.	29
Figure 2.6	Global metabolic incorporation of unnatural amino acids into proteins.	30
Figure 2.7	Selected unnatural amino acid metabolites.	30
Figure 2.8	Azido-lipid and azido-SAM analogues.	31
Figure 2.9	Activity-based protein profiling using the bioorthogonal chemical reporter strategy.	32
Figure 2.10	A coumarin-based fluorogenic phosphine for the Staudinger ligation.	33
Figure 2.11	Peptide coupling via the traceless Staudinger ligation.	33
Figure 2.12	The 1,3-dipolar cycloaddition of azides and alkynes to yield triazole products.	34

Figure 2.13	Cu(I)-catalyzed formal cycloaddition between azides and terminal alkynes.	35
Figure 2.14	Metabolic incorporation of alkynes into proteins and detection by CuAAC.	35
Figure 2.15	The strain-promoted cycloaddition.	36
Figure 2.16	Cyclooctynes selectively react with azides in a variety of environments.	37
Figure 2.17	Initial optimization of cyclooctyne reagents for reaction with azides.	38
Figure 3.1	Difluorinated cyclooctyne allows for direct imaging of azides on live cells.	44
Figure 3.2	DIFO labels azides on live cells and in living mice.	46
Figure 3.3	Azide-dependent labeling with phosphine and DIFO probes is evident in many organs within live mice. DIFO displays significant background reactivity with serum albumin.	47
Figure 3.4	Early generation cyclooctynes do not display robust azide-dependent labeling <i>in vivo</i> .	48
Figure 3.5	Strategies for cyclooctyne synthesis from a ketone.	53
Figure 3.6	Kinetic plot for reaction of DIMAC with benzyl azide.	55
Figure 3.7	Crystal structure of DIMAC.	56
Figure 4.1	DIMAC labels azides in cell lysates.	72
Figure 4.2	Dose- and time-dependent cell-surface labeling of azides with DIMAC.	73
Figure 4.3	Cytotoxicity analysis of DIMAC.	74
Figure 4.4	Comparison of ALO's and DIMAC's ability to label cell-surface azido-glycans.	75
Figure 4.5	Cell-surface azido-glycan labeling with ALO-DIMAC-, DIFO-, and Phos-biotin reagents.	76
Figure 4.6	Cell-surface azido-glycan labeling with DIMAC-FLAG.	77
Figure 4.7	DIMAC-FLAG labels cell-surface azido-glycans on splenocytes in live mice.	78
Figure 4.8	The Staudinger ligation is the superior bioorthogonal reaction for labeling azides <i>in vivo</i> .	79
Figure 4.9	DIMAC-FLAG labels azides in many organisms within the mouse.	80
Figure 4.10	Comparison of the cyclooctyne reagents' ability to label azides in mice.	81

Figure 5.1	A FRET-based fluorogenic phosphine for the Staudinger ligation.	90
Figure 5.2	A bioluminogenic phosphine reagent for the Staudinger ligation.	91
Figure 5.3	Strategy for a fluorogenic azacyclooctyne.	92
Figure 5.4	Crystal structure of bicyclic ether 5.29 .	95
Figure 6.1	Target pull-down reagent for purification of azido-glycoproteins using DIFO.	106
Figure 6.2	Work-flow for the capture, purification, and elution of azide-labeled proteins.	108
Figure 6.3	Azide-specific capture and elution of BSA using pull-down reagent 6.1 .	109
Figure 6.4	Enrichment of azide-labeled BSA from cell lysate using pull-down reagent 6.1 .	109
Figure 6.5	Pull-down reagent 6.1 enriches proteins from cell lysate in an azide-dependent manner.	110
Figure 7.1	DIFO-Alexa Fluor conjugates label azides in higher organisms.	119
Figure 8.1	Dibenzocyclooctyne.	138
Figure 8.2	Difluorobenzocyclooctyne.	139
Figure 8.3	Crystal structure of trimer products 8.8 and 8.9 .	141
Figure 8.4	α , β , and γ Cyclodextrin.	142
Figure 8.5	^1H NMR and CPMAS ^{13}C NMR spectra of β -cyclodextrin compared to the DIFBO- β -cyclodextrin inclusion complex.	144
Figure 8.6	DIFBO- β -cyclodextrin is stable for over 2 months.	145
Figure 8.7	Only β -cyclodextrin prevents trimerization of DIFBO.	147
Figure 8.8	Oxidized dimers of DIFBO.	148
Figure 8.9	A hemicarcerand stabilizes cyclobutadiene.	150
Figure 9.1	Kinetic plot for the reaction of DIFBO with benzyl azide.	162
Figure 9.2	Kinetic plot for the reaction of MOBO with benzyl azide.	163
Figure 9.3	Comparison of NOFO, MOBO, DIFO and DIFBO.	163
Figure 9.4	Western blot assay to determine if DIFBO selectively reacts with azides in cell lysate.	165
Figure 9.5	Methods to stabilize DIFBO.	166
Figure 9.6	Kinetic plot for reaction of thiaDIFBO with benzyl azide.	170
Figure 9.7	Thiacycloheptynes.	170
Figure 10.1	A step-by-step guide to bioorthogonal reaction development.	185

Figure 10.2	Schematic for a double labeling experiment using bioorthogonal chemistries.	187
Figure 10.3	Crystal structure of 3-(<i>p</i> -cyanophenoxy) quadricyclane.	188
Figure 10.4	Selected [2+2+2] cycloaddition reactions with quadricyclane.	188
Figure 10.5	Stability of quadricyclane to PBS and cysteine.	190
Figure 10.6	Kinetic plot for the reaction of PTAD with quadricyclane.	195
Figure 11.1	Molecular orbital analysis of the reaction between Ni bis(dithiolene) and quadricyclane or norbornadiene.	205
Figure 11.2	UV/Vis/NIR analysis of Ni bis(dithiolene) and the ligation product.	206
Figure 11.3	Kinetic plots to determine the second-order rate constant for the reaction between 7-acetoxy quadricyclane and bis(dithiobenzil)nickel (II).	208
Figure 11.4	NMR analysis of the photodegradation of 10.49 .	209
Figure 11.5	UV/Vis/NIR analysis of the photodegradation of 10.49 .	210
Figure 11.6	Diethyldithiocarbamate prevents photodegradation of 10.49 .	212
Figure 11.7	Known Ni bis(dithiolene) complexes with electron withdrawing substituents.	215
Figure 11.8	UV/Vis/NIR analysis of the reaction between quadricyclane 10.4 and Ni bis(dithiolene) 11.25 .	216
Figure 11.9	Ni bis(dithiolene) 11.25 is reduced by polar solvents.	217
Figure 11.10	Electronic deactivation of Ni bis(dithiolene) 11.25 .	218
Figure 11.11	UV/Vis/NIR analysis of the reaction between quadricyclane 10.4 and Ni bis(dithiolene) 11.44 .	222
Figure 11.12	Kinetic plots to determine the second-order rate constant for the reaction between 10.4 and 11.44 .	223
Figure 11.13	Ni bis(dithiolene) 11.44 is stable to PBS.	224
Figure 11.14	Ni bis(dithiolene) 11.44 is moderately stable to excess amino acid.	225
Figure 11.15	Ni bis(dithiolene) 11.44 is not stable to reducing agent.	226
Figure 11.16	Ni bis(dithiolene) 11.44 can be rescued by the addition of K ₃ Fe(CN) ₆ .	227
Figure 11.17	Ni bis(dithiolene) 11.44 is stable to oxidized insulin over multiple hours.	228
Figure 11.18	Ni bis(dithiolene) 11.44 is reduced by BSA.	229
Figure 11.19	Ni bis(dithiolene) 11.44 is reduced by thioredoxin and glutathione S-transferase.	229

Figure 11.20	The reaction between 11.44 and 10.5 proceeds in the presence of live cells.	230
Figure 12.1	Schematic for the preparation and labeling of quadricyclane-modified BSA with 11.44 .	242
Figure 12.2	Ni bis(dithiolene) 12.2 selectively labels quadricyclane-modified BSA.	243
Figure 12.3	Reaction of 12.2 with QC-BSA can be prevented by pretreatment with 12.3 .	244
Figure 12.4	Oxidizing agent increases the efficiency of labeling of QC-BSA by 12.2 in a mixture of proteins.	245
Figure 12.5	The quadricyclane ligation is orthogonal to Cu-free click chemistry and the oxime ligation.	247
Figure 12.6	Cytotoxicity of 12.3 and the adduct of 10.4 and 12.3 as compared to NiCl ₂ and Cu(I).	248
Figure 12.7	Modification of cell-surfaces with quadricyclane and live-cell labeling with 12.2 .	260
Figure 12.8	Schematic for a double live-cell labeling experiment with DIMAC-QC and 12.2 .	252
Figure 12.9	Live-cell double labeling experiment with DIMAC-QC and 12.2 .	253
Figure 12.10	Cytotoxicity of diethyldithiocarbamate.	254
Figure 12.11	Diethyldithiocarbamate reduces background labeling on live cells.	255
Figure 12.12	Proposed quadricyclane-modified metabolites.	256
Figure 13.1	New methods for the modification of Cys.	266
Figure 13.2	New methods for the modification of Lys and Tyr.	268
Figure 13.3	The cyanobenzothiazole condensation for modification of N-terminal Cys residues.	269
Figure 13.4	Unnatural amino acids containing 1,2-aminothiols.	270
Figure 13.5	Methods for C-terminal protein modification.	271
Figure 13.6	A fluorogenic bisboronic acid reagent for labeling tetraserine motifs.	272
Figure 13.7	Metal-assisted detection of peptide tags.	273
Figure 13.8	Site-specific modification of proteins with small molecules through the enzymatic elaboration of peptide tags.	276
Figure 13.9	Aniline catalyzes the oxime ligation on live cells.	278
Figure 13.10	New chemistries for the aldehyde which form irreversible linkages.	279
Figure 13.11	Peptide cyclization by the traceless Staudinger ligation.	281
Figure 13.12	The Staudinger-phosphite ligation.	281
Figure 13.13	Recent alkynyl- and azidosugars employed for metabolic labeling of glycans.	282

Figure 13.14	Azido- and alkynyl-derivatized amino acids.	283
Figure 13.15	A selection of azido- and alkynyl- fatty acids, isoprenoids, and phospholipids.	284
Figure 13.16	Propargyl choline 13.25 is metabolically elaborated into choline phospholipids.	284
Figure 13.17	Azido- and alkynyl-nucleosides for DNA or RNA modification.	285
Figure 13.18	Ligands and additives for CuAAC.	286
Figure 13.19	Cyclooctynes for Cu-free click chemistry.	287
Figure 13.20	BARAC is the superior reagent for labeling azido-glycoproteins on live cells.	289
Figure 13.21	A fluorogenic coumarin-fused BARAC.	289
Figure 13.22	Dibenzocyclooctadiyne as a linker molecule for modifying azido-biomolecules with azide probes.	290
Figure 13.23	A photo-caged dibenzocyclooctyne.	290
Figure 13.24	Cyclooctyne-modified metabolites.	292
Figure 13.25	The mechanism of the tetrazine ligation.	292
Figure 13.26	The three original versions of the tetrazine ligation.	294
Figure 13.27	Applications of the tetrazine ligation to pretargeted antibody labeling.	295
Figure 13.28	A fluorogenic and cell-permeable tetrazine for intracellular labeling of <i>trans</i> -cyclooctene.	296
Figure 13.29	New <i>trans</i> -cyclooctene reagents.	297
Figure 13.30	The inaugural report of photoclick chemistry.	298
Figure 13.31	Optimized tetrazoles for photoclick chemistry.	299
Figure 13.32	Applications of photoclick chemistry to live-cell labeling.	300
Figure 13.33	The azirine ligation.	301
Figure 13.34	The photo-induced hetero-Diels-Alder reaction between <i>ortho</i> -quinone methides and vinyl ethers.	302
Figure 13.35	The oxanorbornadiene-azide cycloaddition.	303
Figure 13.36	Boronic acids as bioorthogonal reagents.	305
Figure 13.37	Condensation cascade of pyrroline-carboxyllysine and 2-aminobenzaldehyde reagents.	306
Figure 13.38	Incorporation of pyrroline-carboxyllysine into proteins.	307

List of Schemes

Scheme 3.1	Retrosynthesis of azacyclooctene 3.5 .	49
Scheme 3.2	Synthesis of 6-bromo-1,2,3-trimethoxy- α ,D-glucopyranoside.	49
Scheme 3.3	Conversion of 6-bromoglucopyranoside 3.9 to azacyclooctene 3.14 .	50
Scheme 3.4	Bromination of azacyclooctene 3.14 .	50
Scheme 3.5	Attempts at the synthesis of an azacyclooctene through vinyl triflate 3.21 .	51
Scheme 3.6	Synthesis of vinyl triflate 3.27 .	52
Scheme 3.7	Synthesis of dimethoxyazacyclooctyne 3.30 .	53
Scheme 3.8	Synthesis of dimethoxyazacyclooctyne 3.35 .	54
Scheme 3.9	Reaction of DIMAC with benzyl azide.	55
Scheme 4.1	Synthesis of DIMAC-biotin.	71
Scheme 4.2	Synthesis of DIMAC-FLAG.	77
Scheme 5.1	Retrosynthesis of tetrahydroxylated pyrrolizidine.	92
Scheme 5.2	Retrosynthesis of azacyclooctyne 5.12 .	93
Scheme 5.3	Synthesis of Boc-protected azacyclooctene and failed dibromination.	94
Scheme 5.4	Inversion of stereochemistry at C-2.	94
Scheme 5.5	Bromination of azacyclooctene 5.27 .	95
Scheme 6.1	Synthesis of target pull-down reagent.	107
Scheme 7.1	Two approaches to tetrafluorinated cyclooctyne.	120
Scheme 7.2	Efforts toward 3,3,8,8-tetrafluoro-1,2-dione.	121
Scheme 7.3	Synthesis of tetrafluorinated alkene 7.17 .	121
Scheme 7.4	Bromination of 7.17 to yield bromolactone 7.18 .	122
Scheme 7.5	A homologation strategy for the mild synthesis of a cyclooctyne.	122
Scheme 7.6	Retrosynthetic analysis of second-generation DIFO reagents.	123
Scheme 7.7	Retrosynthetic analysis of tetraFO 7.24 by a homologation strategy.	124
Scheme 7.8	Synthesis of tetrafluorinated ketone 7.26 .	124
Scheme 7.9	Attempted homologation of ketone 7.26 .	125
Scheme 7.10	Tiffeneau-Demjanov rearrangement of tetrafluorinated ketone 7.26 .	126
Scheme 7.11	Corey-Fuchs alkyne formation from 7.26 .	126
Scheme 8.1	Synthesis of difluorobenzocyclooctyne.	140
Scheme 8.2	Trimerization of DIFBO.	141
Scheme 8.3	Isolation of DIFBO-benzyl azide cycloadducts.	141

Scheme 8.4	Synthesis and purification of DIFBO- β -cyclodextrin complex.	143
Scheme 8.5	Proposed mechanism of DIFBO dimerization and trimerization.	149
Scheme 8.6	Dimerization of a thiacycloheptyne to yield a stable cyclobutadiene.	150
Scheme 9.1	DIFBO is extracted from β -cyclodextrin and reacts with benzyl azide.	161
Scheme 9.2	Synthesis and reactivity of MOBO.	162
Scheme 9.3	Synthesis and attempted homologation of 2,2-dimethylbenzosuberone.	166
Scheme 9.4	Synthesis and attempted homologation of 2-fluoro-2-methylbenzosuberone.	167
Scheme 9.5	Synthesis and attempted homologation of difluorinated benzosuberone 9.21 .	167
Scheme 9.6	Synthesis of difluorobenzocyclononyne.	168
Scheme 9.7	Synthesis of thiaDIFBO.	169
Scheme 9.8	Reactivity of thiaDIFBO with benzyl azide.	169
Scheme 9.9	Synthesis and trapping of monobenzothia- cycloheptyne 9.35 .	171
Scheme 10.1	A generic [2+2+2] reaction between quadricyclane and π -electrophiles.	187
Scheme 10.2	Synthesis of 7-acetoxy quadricyclane.	189
Scheme 10.3	Synthesis of triazole-functionalized quadricyclane.	191
Scheme 10.4	Synthesis of triazole linker.	191
Scheme 10.5	Reaction between PTAD and 7-acetoxy quadricyclane.	195
Scheme 10.6	Synthesis of bis(isopropyl) PTAD 10.48 .	196
Scheme 10.7	Reaction between bis(dithiobenzil)nickel(II) and 7-acetoxy quadricyclane.	197
Scheme 11.1	Reactivity of Ni bis(dithiolene) with quadricyclane and norbornadiene.	206
Scheme 11.2	Reaction between 7-acetoxy quadricyclane and bis(dithiobenzil)nickel(II).	207
Scheme 11.3	Photodegradation of 10.49 .	209
Scheme 11.4	Reduction of neutral Ni bis(dithiolene) to the anionic form.	210
Scheme 11.5	Preparation and kinetic analysis of substituted Ni bis(dithiolene) complexes.	213
Scheme 11.6	Retrosynthesis of Ni bis(dithiolene) complexes through a dithiol-2-one intermediate.	214
Scheme 11.7	Synthesis of Ni bis(dithiolene) 11.25 .	215

Scheme 11.8	Reaction between quadricyclane 10.4 and Ni bis(dithiolene) 11.25 .	216
Scheme 11.9	Reduction of Ni bis(dithiolene) to anionic species 11.24 .	217
Scheme 11.10	Synthesis of Ni bis(dithiolene) 11.27 .	219
Scheme 11.11	Synthesis of alkynes 11.36 and 11.37 .	219
Scheme 11.12	Synthesis of Ni bis(dithiolene) complexes 11.28 and 11.29 .	220
Scheme 11.13	Synthesis of sulfonated Ni bis(dithiolene) 11.44 .	221
Scheme 11.14	Reaction between quadricyclane 10.4 and Ni bis(dithiolene) 11.44 .	222
Scheme 11.15	Reduction of 11.44 to anionic species 11.46 .	226
Scheme 12.1	Synthesis of biotinylated Ni bis(dithiolene) 12.2 .	241
Scheme 12.2	Synthesis of tetrasulfonated Ni bis(dithiolene) 12.3 .	243
Scheme 12.3	Synthesis of DIMAC-quadricyclane.	251

List of Tables

Table 7.1	Selected homologation attempts.	125
Table 10.1	Compounds screened for reactivity with quadricyclane.	192
Table 11.1	Additives screened for inhibition of the photodegradation of 10.49 .	211

Acknowledgements

Graduate school has been an amazing experience. I have learned so much over the past five years thanks to the wisdom, support, encouragement, help, and friendship of so many people.

First, a huge thank you to my advisor Carolyn Bertozzi. Carolyn is a brilliant scientist and fantastic communicator, a powerful combination in the academic world. These qualities were immediately evident upon my first conversation with her and I instantly knew that I wanted to be apart of her research group. Just observing how Carolyn thinks about a problem, critiques slides, and edits a manuscript has been an invaluable experience. While our field is based on empirical data, Carolyn has taught me that the presentation of the results and the ability to look toward the “big picture” is an equally essential component for having a successful scientific career.

In addition to being a great scientist, Carolyn is one of the most caring people I have ever met. She has always been there when I have needed her, whether it be related to science or not. Carolyn has given me the freedom to pursue my interests throughout the course of graduate school. Even if she predicts an idea to have a 5% chance of working (as she labeled my quest for a new bioorthogonal reaction), she is supportive and helpful along the way. I doubt I will ever find an environment with so much freedom to conduct research coupled with ready access to a wealth of instrumentations, supplies, and expertise. The Bertozzi group really is a unique place and it has been a great atmosphere to learn all aspects necessary for becoming a principle investigator.

Carolyn has filled the laboratory with an awesome group of people, which has been priceless from both the scientific perspective as well as the enjoyment perspective because I have spent many, many hours with my labmates. Latimer 805 became my second (or first!) home for the past five years, and I was lucky to have two great guys work in the space next to me for my tenure in graduate school. During my first two years, Scott Laughlin, a senior graduate student, worked beside me. He put up with my first year naivety and taught me many basic biological techniques. I still wish I could run a Western blot as perfectly as he can! Scott has stayed in Berkeley for his postdoctoral work, and it has been great to have his expertise and friendship close by. Once Scott graduated, a postdoc John Jewett moved into the hood adjacent to mine. John and I immediately became great friends and I can't imagine what my PhD would have been like without John. We were working on similar projects and bounced ideas off each other all day. The synthetic work in this thesis greatly benefited from these daily conversations. When John entered 805, we also had a critical mass of Red Sox fans and we listened to baseball games every afternoon. Baseball and columns go great together! Aside from science and New England sports, John fueled my coffee addiction, kept me up-to-date on the latest documentaries, unclogged my sink, fixed my pump, made me (and everyone else) glass art and constantly informed me Vermont was better than New Hampshire.

The other member of the west side of 805 was Hitomi Nakamura, an outstanding undergraduate that I had the opportunity to work with. I couldn't have asked for a better undergraduate student to mentor. Hitomi is extremely intelligent and hard working. She

did a great job on a number of very difficult projects. She deserved to have more successful results than she obtained as an undergraduate. The science gods must be saving her success for graduate school! She has a great career ahead of her in whatever avenue of science she chooses.

When I joined the Bertozzi group as a first year, a number of older students in the laboratory were instrumental in helping me get started on my projects, adjust to the dynamics of a large research group, and prepare my first presentations. Jeremy Baskin was a third year when I joined the group. He was always willing to talk about projects and he warned me of all the challenges in cyclooctyne synthesis. Starting off in the laboratory would have been much more difficult if Jeremy hadn't been there to help me. Nick Agard, the founder of Team Octyne, was also very helpful in synthetic design before he graduated after my first year. I also need to thank the undergraduates that were part of Team Octyne, Anderson Lo and Jay Codelli, for helpful discussions. Zsafia Botyanszki, an undergraduate working in 805, was also a good friend and resource during my first few years of graduate school. Pamela Chang was the resident mouse expert when I joined the lab and I couldn't have tested DIMAC *in vivo* without her guidance. I am grateful that she didn't give up on me after the first day in the animal facility when I dropped the mouse and it ran all over the room! I also need to thank Sarah Hubbard for all her help on the proteomics project in my first year.

I was apart of one of the largest classes to join the Bertozzi group and all my classmates deserve acknowledgement: Karen Dehnert, Kim Sogi, Kanna Palaniappan, Allison Cohen, Andy Hsieh, and Sonny Hsiao. We all certainly bonded over practice quals every Sunday of our second year. Karen has been a great friend over the past five years and I have missed her since she left the lab in June. Karen was always willing to help and I took advantage of her masterful editing skill on many occasions! Karen and I were "conference buddies" throughout grad school and we had lots of fun in Hawaii, San Diego, and Vegas together. Aside from being a friend and colleague, Karen is a master of board games and I look forward to Bolkus and Dominion rematches in the future! Kim has also been a great friend, and together with Alison Narayan, we have spent many hours running and working out together. We have countered the exercise with lots of great meals and Kim (or maybe just Berkeley in general) has turned me into a food snob. Our Indian cooking marathon with Ali's mother-in-law, cherry pitting messes, and massive party spreads are great memories of my time in Berkeley. Ali deserves special thanks for all our walks home together where we shared stories and helped each other through the difficult moments of grad school. It is these moments that truly build a friendship that will last a lifetime. Kanna, coupled with Gary Tong, have also been fun to hang out with over the years. Additionally, Kanna has been a great resource within the laboratory. Allison was my labmate in 805 for three years and it was great to get to know her better. She was a wonderful addition to 805. Sloan Siegrist has also been an awesome addition to 805. She was the brave biologist that entered the chemistry room and Allison, John, and I have all benefited from her expertise. Sloan is eager to collaborate and learn chemistry as well as spread her love of bacteria. I wish her the best as the new senior member of 805!

I have had the opportunity to mentor some great people over the past few years. Chelsea Gordon, Brendan Beahm, and Lauren Wagner all joined the laboratory as

chemistry students when I was a fourth year. Chelsea and Brendan were both working on the metabolic engineering project and instantly became frequent visitors to 805, Chelsea for her insightful questions and Brendan for his bromance with John plus some science thrown in there. That same year, I had the pleasure of working with chemical biology students Gabriela de Almeida and Paresh Agarwal when they rotated with me. Gaby shared a hood with Hitomi and I and its amazing anything got done. There were a few casualties during that time including my manifold and, as I learned much later, a schlenk flask of phenylphosphine. Gaby countered these mishaps with drawings, stories, lots of laughs, and dubbing me “boss lady.” It was a fun (but stinky) time in 805. Paresh has quite the opposite personality of Gaby, but he is easy to work with and has done great things with a fairly rough idea that I gave him. Collectively, its been really fun to become friends with and to watch these four grow as scientists over their first years of graduate school. I will miss seeing them on a daily basis but always have the memories of mounds of pineapple, milk tasting, “mama bird”, betting Blue and flooded basements from our week at Princeton together.

Thanks to current and former Bertozzi group members Kimberly Beatty, Mike Boyce, Mark Breidenbach, Brian Carlson, Ramesh Jasti, Ben Swarts, Jason Hudak, Peng Wu, Phung Gip, Brian Belardi, David Rapuka, and Brian Smart for advice over the years. The Bertozzi group has an incredible support staff that keeps the lab running. Without them I’m not sure I would have a PhD! Thank you Asia Avelino, Olga Martinez, Karen Carkhuff, Sia Kruschke, and Cheryl McVaugh. Particular thanks to Olga for being willing to solve any instrument or order related problem— we couldn’t ask for a better lab manager. And a big thank you to Asia— the gateway to Carolyn. I will surely miss our gossiping, venting, and scheming over the years. I wish every principle investigator had an administrative assistant as awesome as her! I also acknowledge the staff within the entire chemistry department. Thanks to Rudi Nunlist and Chris Canlas in the NMR facility for always being willing to set up new ^{19}F or solid-state experiments and everyone in the mass spectrometry facility. Also thank you to Antonio DiPasquale, the most enthusiastic X-ray crystallographer ever, for solving the crystal structures in this thesis.

The faculty that comprise the Berkeley chemistry department are top-notch and I am fortunate to have gotten to know a number of them over my tenure in graduate school. Thank you to my qualifying exam committee: Matt Francis, Chris Chang, and Dean Toste. Particularly, thanks to Matt for his support over the years and many letters of recommendation. I had the opportunity to teach for K. Peter Volhardt, Richmond Sarpong, and Bob Bergman. Bob has become a great mentor and I am grateful that he entrusted me to GSI CHEM 200/260. I learned a great deal from teaching that course and I view it as a significant part of my graduate education. It will be a sad day when Bob retires from teaching.

My teaching partner for CHEM 200/260 was Jane Wang. I didn’t really know Jane at the start but after a few months of teaching for Bob we got to know each other very well and Jane has been a good friend ever since. I also want to thank all the girls in bookclub— Ali, Karen, Kim, Chelsea, Leah Witus, Allie Obermeyer, and Jess Wood— for lots of great dinners and a few great books. Thanks to my original roommate Ellie Browne as well as Ashley Russell for many years together in the Woolsey house. Meg Stratton, who I met

when we were undergraduates at Stonehill together, has been a fabulous addition to Berkeley over the past year. I'm so glad she decided to postdoc in the Kuriyan lab and I wish we had overlapped here longer. I want to thank everyone at Stonehill who prepared me for my graduate studies. Leon Tilley taught the first organic chemistry course I ever took, and through my three years working in Louis Liotta's lab, I learned first-hand how to perform organic synthesis. I thank them in addition to Magda James-Pederson, Marilena Hall, Maria Curtin, Paul House and Barbara Anzivino for making the Stonehill chemistry department a great place while I was there. Kara Bren at the University of Rochester has also been a supportive mentor ever since I worked in her laboratory as an undergraduate.

Last, but certainly not least, I thank my parents for always being there for me, giving me so many opportunities, and raising me to be confident, articulate and independent. I would not have a PhD if it weren't for their constant love and support. One of the first things my mom always asks about a completed paper or project is "are you happy with it?". My efforts to answer yes to that question have been instrumental in my success in graduate school. Chemistry graduate school is full of failed experiments but as long as I tried my best I was able to keep a positive outlook throughout these past five years. Thank you mom and dad for teaching me this (and so much more!). Thanks to my brother Phil and my grandparents, Doris and Dale Hesch and Ruth and Carl Sletten. My grandfather Carl did not get to witness my graduate work but I am forever connected to him through science as one of the last moments we had together was conversing about my undergraduate research. And thanks to my extended family, who don't really understand why I have been in school so long, but are supportive and inquisitive nonetheless. I love you all.

Chapter 1

Chemistry Meets Biology

Introduction

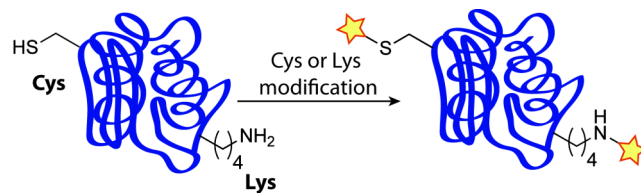
During the past century, the chemical modification of biomolecules has evolved from a means of defining protein composition to a highly selective method for monitoring cellular events. Proteins, with their myriad of side chain functionalities, complex tertiary structures, and diverse biological functions, were early favorites for chemical modification, initially with the goal of defining their amino acids components¹ and identifying side chain structures involved in enzyme catalysis.² However, organisms contain an array of different biomolecules, which are all essential components, and recent attention has been drawn toward developing general methods to study any biological species of interest.

Chemical biologists have focused on chemistry-based methods to study all biomolecules and metabolites. These techniques are particularly useful for studying post-translational modifications and metabolites not directly encoded by the genome. This field has dramatically expanded in the past decade, something that I aim to highlight in this dissertation. The first two chapters of this dissertation depict the state of bioorthogonal chemistry when I began my doctoral work, while the last chapter showcases the rapid progression of the field and describes the advances made within the last five years. My contributions to the field are described in the middle ten chapters.

Protein Modification

Canonical Residue Modification

The roots of bioorthogonal chemistry- chemistry that does not interfere or interact with biology- lie in classic protein bioconjugation methods. Classic protein bioconjugation primarily encompasses simple second-order reactions that selectively target the functionalities present in the side chains of the canonical, proteogenic amino acids.^{1,3,4} Of those, cysteine and lysine are the most commonly modified residues. The thiol group of cysteine can undergo disulfide exchange to form mixed disulfides (Figure 1.1, entry 1) as well as alkylation with alkyl halides or Michael addition with α , β -unsaturated electrophiles to yield thioethers (Figure 1.1, entries 2-3). Further, as cysteine is one of the rarest amino acids, cysteine modification can often be used as a method for single-site protein modification. Although considerably more prevalent than cysteine within proteins, lysine residues are often chosen as points of modification due to the surplus of methods available to selectively modify primary amines. Lysines can be treated with activated esters, sulfonyl chlorides, isocyanates or isothiocyanates to afford amides, sulfonamides, ureas or thioureas, respectively (Figure 1.1, entries 4-7). Lysine residues also undergo reductive amination reactions with aldehydes.^{6,7,8} It is of note that reagents which target lysine residues often additionally modify the N-terminus of proteins.



Entry	Residue	Reagent	Product
1	Cys		
2	Cys		
3	Cys		
4	Lys		
5	Lys		
6	Lys		
7	Lys		

Figure 1.1. Classic bioconjugation reactions for the modification of Cys and Lys residues. Cys residues are modified through disulfide exchange, alkylation with iodoacetamide reagents, and Michael addition with maleimides (entries 1-3, respectively). Lys residues are modified through amide, sulfonamide, urea, and thiourea formation with NHS-activated esters, sulfonyl chlorides, isocyanates and isothiocyanates (entries 4-7, respectively).

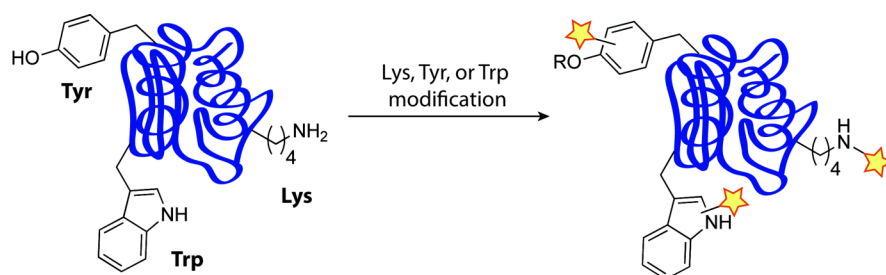
By comparison, the remaining 18 amino acids have been minimally exploited for residue-selective modification reactions. The phenol moiety of tyrosine has been modified through electrophilic aromatic substitution reactions with diazonium salts, iodine, or nitrous acid.^{9,10} Glutamate and aspartate residues have been targeted for bioconjugation through coupling with amines via carbodiimide reagents,^{11,12,12} although the potential to crosslink proteins limits the utility of this technique. Pyrocarbonates have also been employed to successfully modified histidine residues.^{13,12,14,15}

Using these classical methods, conjugation of small molecule probes such as biotin and fluorophores to proteins is quite routine. Similar methods are widely used to immobilize proteins on chromatography matrices, soluble polymers, plastic surfaces, and microarray chips. More recently, new methods have been developed for the modification of cysteine, lysine, tyrosine, and tryptophan (Figure 1.2). Many of these modern methods involve metal-mediated transformations.¹⁴ Additionally, the N-terminus has emerged as a popular target for protein modification (Figure 1.3).

While the classic bioconjugation techniques for cysteine and lysine have been widely used, new methods are continually being developed. Francis and coworkers have modified the lysine conjugation method of reductive amination by altering the reducing agent. In this variant of the reductive amination, an iridium catalyst is used instead of sodium cyanoborohydride (Figure 1.2, entry 1).¹⁶

Many recent efforts to discover bioconjugation reactions have focused on the modification of aromatic residues and often employ transition metal-mediated transformations that are compatible with aqueous conditions.¹⁷ These residues are relatively rare on protein surfaces, and thus offer opportunities for controlled single-site modification.¹⁸ Initial work toward metal-mediated tyrosine modification involved the oxidative coupling of two phenol groups. This method was first explored by Kodadek and coworkers using a Ni(II) catalyst and a co-oxidant to crosslink two proteins (Figure 1.2, entry 2).¹⁹ Finn and coworkers have since validated this method as a bioconjugation tool by coupling biotin and alkyne reagents to tyrosine residues on the capsid proteins of a virus particle.²⁰ Francis and coworkers have also explored the modification of tyrosine residues through a three-component Mannich reaction with aldehydes and anilines (Figure 1.2, entry 3)^{21,18,17} as well as through palladium π -allyl chemistry (Figure 1.2, entry 4).¹³

Additionally, Francis and coworkers have developed a bioconjugation reaction for tryptophan, the rarest amino acid. Tryptophan modification was accomplished using a rhodium carbenoid that was generated *in situ* from $\text{Rh}_2(\text{OAc})_4$ and a diazo compound (Figure 1.2, entry 5).²² A reliable method for selective tryptophan modification is advantageous due to the scarcity of this residue; unfortunately, this reaction requires acidic conditions (pH \sim 2), which hinders the study of many proteins in their native conformations.



Entry	Residue	Reagents/Catalyst	pH	Product
1	Lys	 $[Cp^*Ir-(bipy)(H_2O)]SO_4$ $NaHCO_2$	7.4	
2	Tyr	 $Ni(OAc)_2$ Gly-Gly-His MMPP	7	
3	Tyr	 R	6.5	
4	Tyr	 $Pd(OAc)_2$	8.5-9	
5	Trp	 $R = (CH_2CH_2O)_3CH_3$ $Rh(OAc)_4$ $HONH_3Cl$	1.5-2	

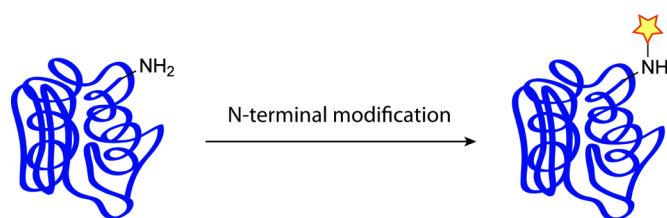
Figure 1.2. Modern methods to modify Lys, Tyr, and Trp. Lys is modified through a reductive amination using an Ir hydride as the reductant (entry 1). Tyr is modified by a Ni(II)-mediated radical coupling with magnesium monoperoxyphthalate (MMPP) as a stoichiometric oxidant (entry 2), a three-component Mannich reaction with aldehyde and aniline reagents (entry 3), or a Pd-catalyzed π -allylation (entry 4). Trp modification is performed using a Rh carbenoid (entry 5).

N-Terminal Modification

While the previous methods target a single type of residue, it is often desirable to singly modify a whole protein. This approach was first actualized by exploiting the N-terminus. The initial effort to selectively modify a protein's N-terminus capitalized on the decreased pKa of the N-terminal amine relative to the amino groups on lysine side chains,²³ but these efforts were impeded by the abundance of lysine residues relative to the N-terminus. Although these attempts were ineffective, they prompted the development of other chemistries for the N-terminal modification of peptides and proteins. The most general of these modifications is the transamination reaction. Transamination of the N-terminus dates back to 1956, when it was attempted by Bonetti and coworkers at 100 °C, a temperature that often denatures proteins (Figure 1.3, entry 1a).²⁴ Almost a decade later, Dixon and coworkers performed a transamination at room temperature using glyoxylate, catalytic base, and Cu(I), which facilitated imine formation between the N-terminus and the glyoxylate (Figure 1.3, entry 1b).²⁵

Even with the improvements made by Dixon and coworkers, the transamination reaction did not receive considerable attention until Francis and coworkers reported a biomimetic transamination that proceeded under physiological conditions without the need for metal or base additives (Figure 1.3, entry 1c).²⁶ This transamination reaction occurs via condensation of the N-terminal amine with pyridoxal-5-phosphate and subsequent hydrolysis to result in a pyruvamide. The protein can then be further modified through the ketone of the pyruvamide via reactions with hydrazide or aminoxy reagents (see Chapter 2). The Francis group has extensively characterized this transamination reaction and discovered that Ala, Gly, Asp, Glu, and Asn are the optimal N-terminal residues for the transamination. While transamination is possible with other N-terminal residues, the yields are variable.²⁷

Other chemical methods for N-terminal modification rely on a specific residue at the N-terminus. For example, N-terminal serine or threonine residues undergo periodate oxidation to form glyoxylamides (Figure 1.3, entry 2).²⁸ The glyoxylamide's aldehyde moiety can then be modified with hydrazide and aminoxy reagents. A Pictet-Spengler reaction can selectively modify N-terminal tryptophan residues with aldehyde probes (Figure 1.3, entry 3).¹³ There is also evidence that this reaction can be used to modify N-terminal histidine residues.²⁶ The advantage of the Pictet-Spengler reaction is that a carbon-carbon linkage of the probe and protein is obtained in a one-step procedure, whereas hydrazide/aminoxy based methods do not form an irreversible linkage between the probe and protein. Additionally, aldehyde probes can be selectively conjugated to proteins containing N-terminal cysteine residues (as well as Ser, Thr, Trp, His, and Asn) via a bicyclic lactam-forming reaction (Figure 1.3, entry 4).²⁹ N-terminal cysteine residues have also been exploited in the highly successful method of protein modification known as native chemical ligation (Figure 1.3, entry 5).



Entry	N-terminal residue	Reagents	Product
1	a) Any	Pyridoxal (100 °C)	
	b) Any	Glyoxylate NaOAc Cu(I)	
	c) Ala, Gly, Asp, Glu, Asn ^a	Pyridoxal-5-phosphate	
2	Ser, Thr	NaIO ₄	
3	Trp		
4	Cys, Ser, Thr, His, Trp, Asn		 Various heterocycles ^c
5	Cys		

^a These are the optimal residues.

^b The probe is inserted through a subsequent chemical labeling step.

^c Structure of the product is dependent on the N-terminal residue.

Figure 1.3. Methods for N-terminal modification. Modification of the N-terminus is achieved through transamination with aldehydes, oxidation with periodate, Pictet-Spengler reaction between an N-terminal tryptophan and an aldehyde, bicyclic lactam formation with acyl-aldehyde reagents, or native chemical ligation with thioester reagents (entries 1-5, respectively).

Native Chemical Ligation

In 1994, Kent and coworkers reported the ligation of thioesters with N-terminal cysteine residues to result in a “native” amide bond, a reaction now termed native chemical ligation (NCL, Figure 1.4A).³⁰ Mechanistically, this transformation involves a rapid equilibration of the thioester and cysteine thiol (*i.e.*, thioesterification), which is interrupted by an irreversible intramolecular attack of the amino-terminus of the protein on the thioester to ultimately result in a stable amide bond (*i.e.*, S-N acyl shift). The formation of a native amide bond via a S-N acyl shift was first discovered by Wieland and coworkers in 1953, but was not applied as a protein modification technique until much later.³¹ NCL can be used to selectively ligate two highly functionalized molecules under physiological conditions without the use of protecting groups. As such, NCL has become a powerful tool for protein modification, protein synthesis, and semisynthesis. Through NCL, proteins larger than the traditional limits of solid phase peptide synthesis have been chemically generated and studied.³² Further, NCL has allowed for portions of proteins to be isotopically labeled for structural biology studies^{33,34} or for the selective addition of post-translational modifications and chemical probes.³⁵

Many of the applications of native chemical ligation have been enhanced by expressed protein ligation (EPL, Figure 1.4B) and protein-*trans* splicing (PTS, Figure 1.4C) technologies. EPL and PTS both rely on NCL’s biological relative: self-splicing proteins.³⁶ Protein self-splicing is a natural phenomenon where a domain of a protein, referred to as an intein, is extruded in a post-translational process that mechanistically mimics NCL. EPL is the NCL of a chemically prepared species (often containing an N-terminal cysteine) with a recombinantly expressed thioester-containing protein. PTS is similar to EPL in that a synthetically generated compound can be joined to a recombinantly expressed protein through a native amide bond; however, in PTS the two components must have complementary peptide sequences instead of a thioester and an N-terminal cysteine.

EPL exploits inteins as a means to biologically create a C-terminal thioester, which can then be modified through native chemical ligation (Figure 1.4B). Using recombinant expression techniques, a desired polypeptide is fused with an intein that has been mutated so that it is unable to undergo an S-N acyl shift. Often a chitin-binding domain is added to the fusion protein on the C-terminal side of the intein to facilitate purification. The expressed fusion protein is isolated on a chitin affinity matrix and, following the removal of all other biomolecules, the desired protein is cleaved from the chitin matrix via NCL with a synthetic peptide or other molecule containing an N-terminal cysteine residue.^{37,38}

Further expansion of NCL and protein splicing occurred with the discovery that the intein domain can be separated into two polypeptides (Int_C and Int_N). The two polypeptides must have affinity for each other, and when they noncovalently interact, splicing occurs to result in the union of two originally separate species (Figure 1.4C).³⁹ These split-inteins are used in PTS and allow two species to be connected via the addition of simple peptide sequences. PTS has allowed for the extension of NCL into living systems, facilitating the study of protein-protein interactions,⁴⁰ the synthesis of cyclic peptides,^{41,42} and the semi-synthesis of proteins *in vivo*.⁴³ Yao and coworkers have also

performed traditional NCL in *E. coli* by the detection of overexpressed N-terminal cysteine-containing proteins with thioester fluorophore conjugates.⁴⁴ In this study only the proteins modified with the thioester fluorophore were detected, but there are many natural thioester containing species that could also modify the protein of interest, including coenzyme A (CoA) derivatives and polyketide and fatty acid synthases. These naturally occurring thioesters primarily limit NCL to *in vitro* techniques, such as the preparation of semisynthetic protein samples.

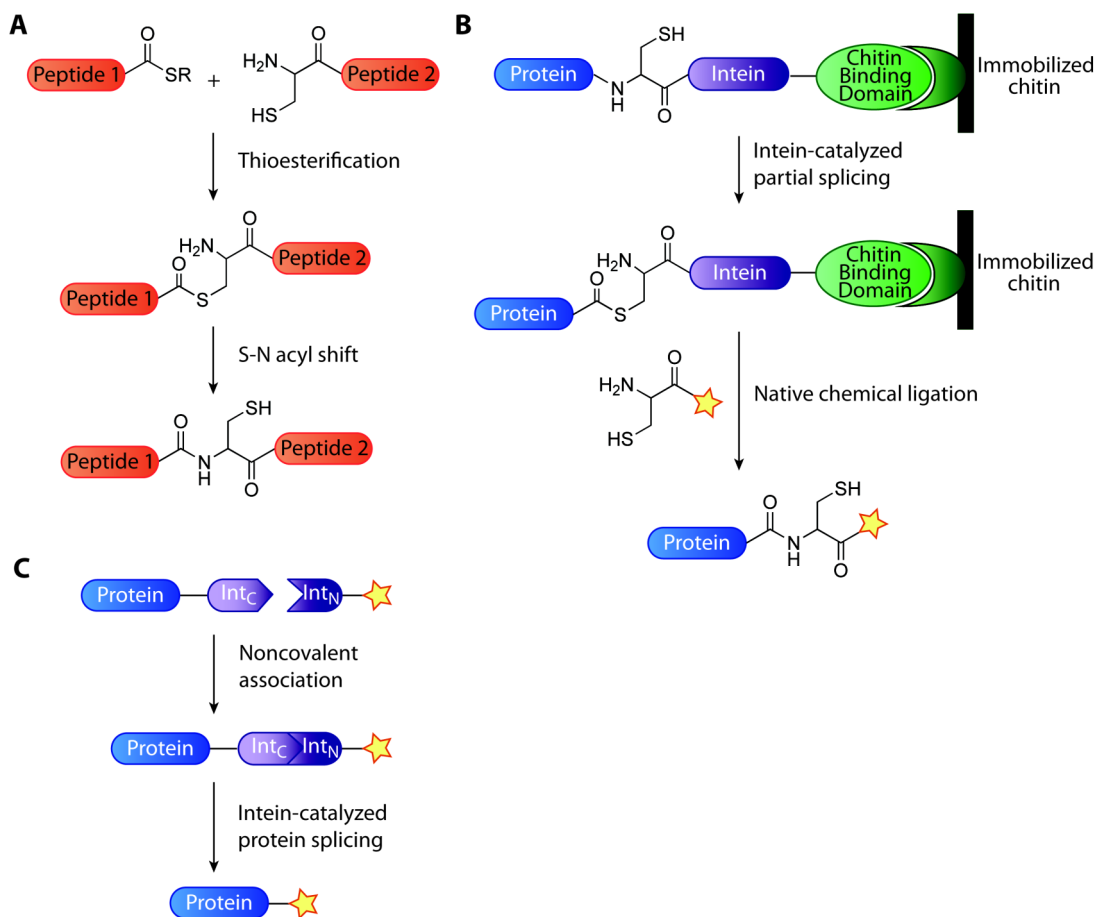


Figure 1.4. Native chemical ligation and intein-based technologies. A. Native chemical ligation of two peptides. Peptide 1 contains a C-terminal thioester that undergoes thioesterification with the N-terminal cysteine of peptide 2. A S-N acyl transfer results in a native peptide bond. B. Expressed protein ligation. A protein is recombinantly expressed fused to a mutated intein and a chitin binding domain to facilitate purification. The intein is mutated so that it undergoes thioester formation but not S-N acyl exchange, allowing for the recombinant protein to be selectively cleaved from the immobilized chitin by a species containing an N-terminal cysteine. C. Protein-trans splicing. A protein is recombinantly expressed fused to a portion of a split intein (Int_C). The complementary portion of the

intein (Int_N) is connected to an unnatural chemical species. When the two inteins associate noncovalently, splicing occurs to generate a modified protein.

Selective Protein Modification Through Protein and Peptide Fusions

Many research groups have sought to selectively modify a protein in its native environment through the fusion of unique peptide sequences or enzymes to a protein of interest. The process of tagging a protein of interest with a series of amino acids is facile, as it only involves standard cloning methods. This technique has been widely used in the preparation of fluorescent protein chimeras. Fluorescent proteins, most notably the green fluorescent protein (GFP), have become an essential tool for biologists. These proteins enable visualization of the localization, dynamics, and interactions of proteins within live cells and organisms.^{43,45,46,47} The genetic fusion of GFP to a protein results in 100% efficiency of labeling, minimizing the possibility that certain subsets of proteins are invisible to a study. Unfortunately, the large size of these fluorescent proteins (~200 residues) can disrupt the function of proteins fused to them.⁴⁸ In an effort to reduce the size of the unnatural amino acid sequence appended to a target protein, while still incorporating a unique label using the simple and highly efficient method of genetic engineering, peptide sequences with high affinity for secondary reagents have been developed.

Fluorogenic Bisarsenical Reagents

The landmark study employing peptide sequences to target proteins in live cells was the genetic implementation of a tetracysteine-containing peptide (CCXXCC) and its subsequent detection via bisarsenical dyes.^{49,47} This method was developed by Tsien and coworkers, and since its introduction, bisarsenical dyes that span the visible spectrum have been developed. The most frequently used are fluorescein arsenical hairpin binder (FIAsH, Figure 1.5A) and resorufin arsenical hairpin binder (ReAsH, Figure 1.5B).^{48,50} These dyes are initially nonfluorescent because the arsenic is chelated with ethane dithiol (EDT), and upon ligand exchange of EDT with the tetracysteine motif, the dyes become fluorescent. Dyes that become fluorescent upon a specific event are termed “fluorogenic”. Fluorogenic probes are highly desirable because they display low levels of background fluorescence, require minimal washing procedures, and allow for real-time imaging.

Although the bisarsenical dyes are fluorogenic, they do exhibit background fluorescence due to cross-reactivity with other biological thiols. The background fluorescence due to nonspecific ligand exchange makes it difficult to detect low abundance and dispersed proteins.^{51,52} In order to overcome this limitation, Tsien and coworkers have developed a labeling mixture that includes hydrophobic molecules to avert non-specific binding of the dyes and increased concentrations of EDT to avoid the reaction of the dyes with other thiol-containing biomolecules.⁵³ Additionally, the peptide sequence has been optimized for an enhanced association constant, allowing more stringent washing conditions.⁵⁴

Numerous studies have employed the tetracysteine methodology, demonstrating its importance in chemical biology. The tetracysteine tag and bisarsenical dyes have been used to study mRNA translation,⁵⁵ G-protein-coupled receptor activation,⁵⁶ amyloid formation,⁵⁷ ATP-gated P2X receptors,⁵⁸ and trafficking of HIV-1 complexes.⁵⁶ The tetracysteine methodology also allows electron microscopy,⁵⁹ pulse-chase,⁶⁰ Western blotting,⁶¹ and affinity purification⁶² experiments to be performed on suitably modified proteins.

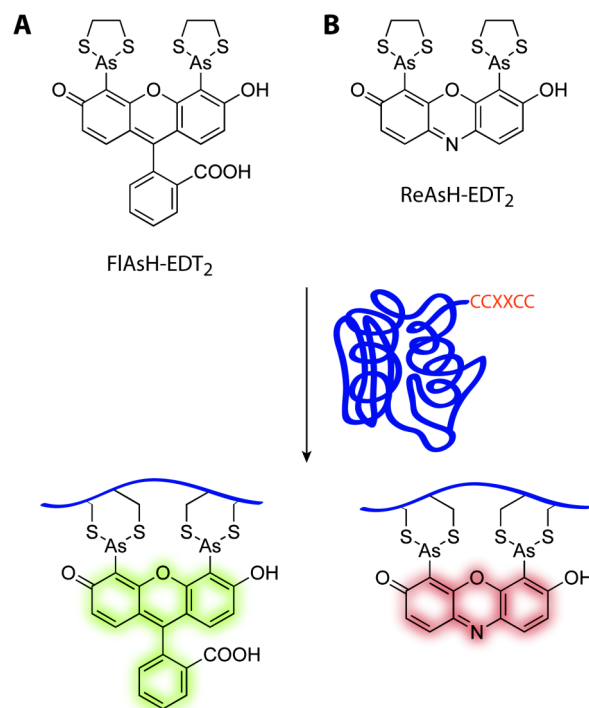


Figure 1.5. Fluorogenic bisarsenical reagents for site-specific labeling of recombinant proteins with tetracysteine motifs. A. Fluorescein arsenical hairpin binder (FIAsh) B. Resorufin arsenical hairpin binder (ReAsH).

Peptide Tags Detected Through the Chelation of Transition Metals

The hexahistidine peptide, extensively used for purification of recombinantly expressed proteins, has also been exploited for labeling proteins in cellular systems. The imidazole side chains within the polyhistidine motif bind to nickel-nitrilotriacetate (Ni-NTA) with good affinity.⁶³ Consequently, rhodamine derivatives,⁶⁴ cyanine dyes,⁶⁵ and fluorescein⁶⁶ have all been conjugated to Ni-NTA and used for imaging proteins containing His₆ or His₁₀ sequences (Figure 1.6, entry 1). These methods have not seen widespread use perhaps due to the fact that the paramagnetic nature of Ni(II) often quenches fluorescence.⁶⁷ Lippard and coworkers have sought to address this problem, reporting a chlorinated fluorescein probe that is not as readily quenched by Ni(II).⁶⁸

Longer peptide tags have been used to detect proteins in complex systems. Through library screens, Imperiali and coworkers have discovered peptides that become luminescent upon binding to terbium(III) (Figure 1.6, entry 2).^{69,69} Tb³⁺-binding sequences have been used to identify tagged ubiquitin in cell lysates⁷⁰ and to study, through luminescence resonance energy transfer, peptide-protein interactions between phosphopeptides and Src homology 2 domains.⁶² The applications of lanthanide-binding tags are primarily limited to *in vitro* studies due to the cell-impermeability of these metals and their potential toxicity if they are able to cross the cell membrane.⁷¹

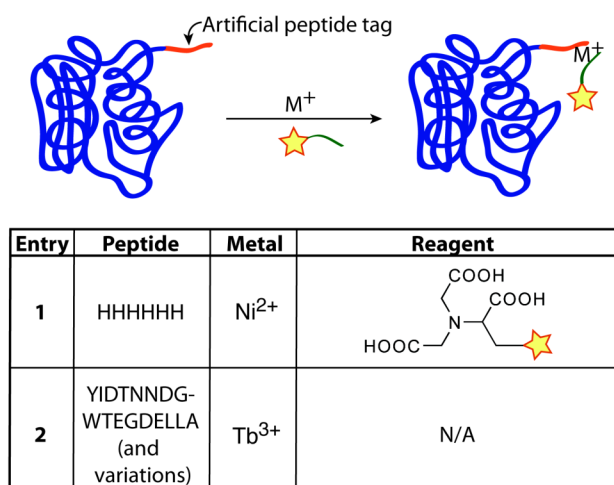


Figure 1.6. Site-specific protein modification through the detection of artificial peptide tags by metal-mediated chelation with chemical reagents. Polyhistidine peptides chelate Ni(II) and are detected with Ni-NTA reagents (entry 1). Peptides that have been engineered to bind terbium(III) can be visualized following chelation, due to the luminescent properties of Tb(III) (entry 2).

Enzymatic Modification of Peptide Tags

The unifying disadvantage of peptide tags is that a covalent linkage between the peptide and detection moiety is not obtained. One way to overcome this is to employ peptide sequences that can be uniquely modified by enzymes that exclusively recognize them.^{72,73} Often times these enzymes are coaxed to accept a small-molecule substrate that is modified with an unnatural group, facilitating further detection. The optimal enzyme-mediated strategies employ a small perturbation to the protein of interest (*i.e.*, a short tag) and only require a few steps in the overall labeling procedure.

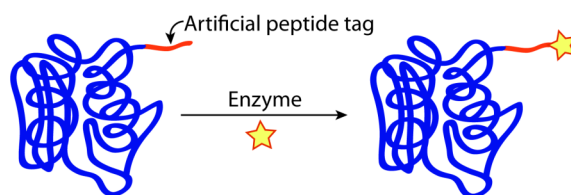
This technique has been popularized by Alice Ting, who initially demonstrated the utility of this strategy with the enzyme biotin ligase. This method utilizes the biotin ligase from *E. coli*, BirA, to biotinylate a lysine within a 15-residue acceptor peptide (Figure 1.7, entry 1).⁷⁴ The acceptor peptide for BirA is orthogonal to the peptide recognized by

mammalian biotin ligases and, consequently, is well suited for modifying proteins in mammalian systems. Proteins were adorned with quantum dots through a two-step labeling procedure that involved treatment of acceptor peptide-tagged cell-surface proteins with biotin ligase followed by introduction of streptavidin-conjugated quantum dots.⁷⁵ This method installs biotin, BirA's natural substrate, but Ting and coworkers also demonstrated that BirA can accept a ketone-containing analogue of biotin, termed keto-biotin, as a substrate.⁷⁶ The ketone can subsequently be modified with hydrazide or aminoxy compounds as demonstrated by the conjugation of fluorescein and benzophenone to cell-surface proteins tagged with the acceptor peptide. Unfortunately, the poor promiscuity of BirA prevented the ligation of molecules other than biotin and keto-biotin to proteins.

The success of the biotin ligase technology prompted Ting and coworkers to develop other enzyme-mediated protein tagging strategies. They focused their attention on transglutaminase (TGase, Figure 1.7, entry 2),⁷⁷ which had been employed previously for the *in vitro* modification of glutamine-tagged proteins with amine-conjugated probes.^{77,78} Ting and coworkers were the first to perform transglutaminase labeling on live cells.⁷⁷ Site-specific modification of proteins has also been accomplished through the exploitation of bacterial sortases (Figure 1.7, entry 3). Sortase A (SrtA), the most commonly used enzyme, naturally catalyzes the addition of proteins to the bacterial cell wall.

The enzyme recognizes a peptide sequence (LPXTG) near the C-terminus, cleaves the Thr-Gly bond, and forms an amide bond between the new C-terminal threonine and the N-terminal glycine of a polyglycine species.⁷² SrtA only recognizes the polyglycine sequence, and thus large, unnatural groups can be ligated to a protein using this method. Sortase has been used for many *in vitro* applications including peptide-, protein-, and carbohydrate-peptide ligations.^{73,74}

Cell-surface proteins have also been selectively modified using phosphopantetheinyl transferases (PPtases) from *E. coli* (AcpS) and *B. subtilis* (Sfp). PPtases catalyze the addition of a CoA activated-phosphopantetheine group to the serine of an acyl or peptidyl carrier protein (Figure 1.7, entry 4).⁷⁵ AcpS and Sfp do not load mammalian carrier proteins, and, therefore, these enzymes and their complementary bacterial carrier proteins can be used orthogonally within a mammalian system.⁷⁶ These enzymes are highly promiscuous and can introduce a variety of functionality into proteins, including biotin and cyanine dyes.^{77,78} PPtases have been used to study the trafficking of the transferrin receptor 1⁷⁹ and yeast cell-wall protein Sag1.⁸⁰ In the latter work, a two-color labeling strategy was employed that takes advantage of the pseudo-orthogonality of AcpS and Sfp. Sfp is not selective for the type of carrier protein it labels, while AcpS only modifies acyl carrier proteins. Thus, if a cell is exhaustively labeled with AcpS and then subjected to Sfp, two separate proteins may be selectively tagged and simultaneously studied.⁸⁰



Entry	Enzyme	Small Molecule	Product
1	BirA		
2	TGase	$\text{H}_2\text{N}-(\text{---})_5$	
3	SrtA	$-(\text{Gly})_n$	
4	AcpS or Sfp	CoA	
5	hAGT ^b		

^a Probe is inserted through a subsequent chemical labeling step.

^b Enzyme is fused to the protein of interest and no peptide tag is employed.

Figure 1.7. Protein modification through the enzymatic elaboration of peptide tags. Biotin ligase (BirA) catalyzes the attachment of biotin (not shown) or keto-biotin to proteins containing the appropriate peptide substrate (entry 1). Transglutaminase (TGase) catalyzes the attachment of primary amine-containing probes to proteins tagged with polyglutamine sequences (entry 2). Sortase A catalyzes the attachment of a polyglycine-containing probe to proteins that contain an LPXTG motif near the C-terminus (entry 3). Phosphopantetheinyl transferases (AcpS or Sfp) catalyze the attachment of a coenzyme A (CoA) probe to proteins containing the appropriate protein/peptide substrate (entry 4). A protein is recombinantly expressed as a fusion with the human repair protein O⁶-alkylguanine-DNA alkyltransferase (hAGT). The enzyme hAGT is alkylated at a cysteine residue with the benzyl group from O⁶-benzylguanosine derivatives (entry 5).

The carrier protein/phosphopantetheinyl transferase system of protein modification suffers the same liability as GFP in that carrier proteins (80-120 residues) are often substantial perturbations to the protein of interest. In order to overcome this limitation, Walsh and coworkers performed phage display selections to obtain an 11 amino acid peptide, called ybbR, that was selectively modified by Sfp.⁸¹ Further phage display screening resulted in two more effective peptide sequences: one for Sfp and one for AcpS. The two new peptides (A1 and S6) both contain twelve residues and are superior to ybbR. Additionally, these peptides display orthogonal reactivity to each other because A1 is selective for modification by AcpS and S6 is selective for Sfp.⁸² This makes the two-color labeling strategy originally demonstrated by Johnsson and coworkers⁸⁰ considerably more straightforward.

Johnsson and coworkers have also developed a protein-labeling method that utilizes the human DNA repair protein O⁶-alkylguanine-DNA alkyltransferase (hAGT), which repairs guanosine residues that are alkylated at the 6-oxo position by transferring the alkyl group to a resident cysteine.⁸³ Through this work, it was found that when O⁶-benzylguanosine derivatives are introduced to cells, the benzyl group is readily transferred to hAGT. Thus, if hAGT is fused to a protein of interest, guanosine derivatives can be utilized to specifically label the desired protein (Figure 1.7, entry 5).^{84,85} This technology is known as the SNAP-tag.

From Protein Modification to Bioorthogonal Chemistry

While peptide-tag/small-molecule probe combinations provide a means of detecting certain proteins within a living system, they cannot be extended to the study of biomolecules that are not directly genetically encoded (*e.g.* post-translational modifications and small-molecule metabolites). This deficiency prompted the development of new methods for analyzing biomolecules in their native environments.

In the late 1990s, the Bertozzi group was interested in exploring glycosylation using chemical tools. Toward this end, it was necessary to overcome two obstacles: 1) appending an unnatural moiety to a specific set of glycans and 2) the selective detection of the unnatural glycans. The first difficulty was overcome by building on the work of Reutter and coworkers, who demonstrated that unnatural *N*-acetylmannosamine (ManNAc) derivatives could be incorporated into cell-surface sialic acids in live cells and animals (Figure 1.8).^{86,87} Reutter and coworkers introduced varying lengths of alkyl chains into sialoglycans to study host-virus interactions⁸⁸ and neuronal cell differentiation.⁸⁹ These unnatural carbohydrates have also been used to study polysialic acid.⁹⁰ The introduction of unnatural functionality into glycans using unnatural monosaccharide precursors became known as metabolic oligosaccharide engineering.⁹¹ Reutter's work showed that a metabolic strategy could be used to modify glycans; however, only small perturbations were accepted. Thus, the existing methods to selectively modify proteins in native settings via unique peptide sequences were not applicable to a metabolism-based labeling strategy.

Luckily, other work from the early 1990s had established that ketone or aldehyde containing peptides, proteins, and polymers could be selectively modified with hydrazide or aminoxy reagents.^{19,92,93,94} These amine nucleophiles are enhanced by the alpha effect

and form stable oxime or hydrazone linkages under physiological conditions (Figure 1.9). While other biological nucleophiles such as amines and alcohols do condense with ketones and aldehydes, the equilibrium at pH 7 favors the carbonyl.⁹⁵ Due to the thermodynamic stability of the oxime and hydrazone linkages, this chemistry is selective in complex environments. Rideout and coworkers had even demonstrated that the selective condensation of hydrazine and aldehyde groups could be harnessed to assemble toxins from inactive prodrugs within live cells.^{96,97}

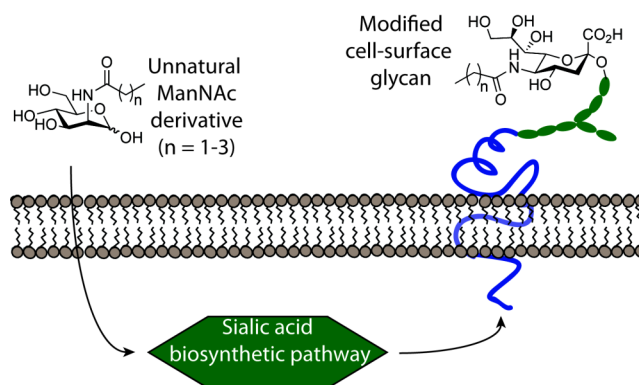


Figure 1.8. Metabolic oligosaccharide engineering pioneered by Reutter and coworkers. N-Acetyl mannosamine derivatives with elongated acetyl groups (propyl, butyl, pentyl) are substrates for the sialic acid biosynthetic pathway, and cells are able to incorporate the unnatural metabolites into cell-surface sialoglycans with good efficiencies.

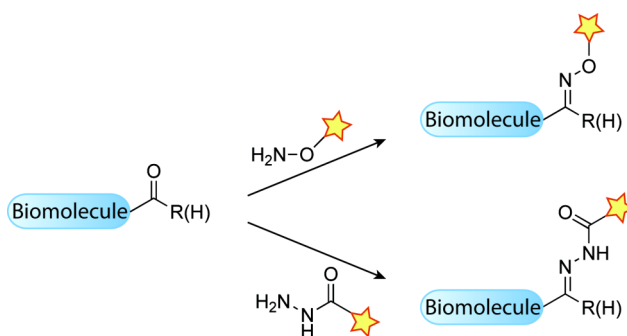


Figure 1.9. Selective chemistries for aldehydes/ketones. Aldehydes and ketones can condense with aminoxy (top) or hydrazide (bottom) reagents to form stable oxime or hydrazone linkages, respectively.

Combining Reutter's metabolic oligosaccharide engineering strategy with the condensation chemistry of carbonyl compounds and alpha effect amine nucleophiles, the Bertozzi group introduced a two-step procedure for the selective covalent labeling of glycans. A ketone-containing N-acetylmannosamine derivative, known as N-levulinoylmannosamine (ManLev), was synthesized and introduced into glycans in a variety of mammalian cell lines.⁹⁸ The enzymes of the sialic acid biosynthetic pathway proved to be promiscuous enough to accept ManLev, and ketones were displayed on cell-surface glycans.^{99,100} The keto-glycans were then modified with biotin-hydrazide and detected by flow cytometry (Figure 1.10). This method was also used to promote gene transfer and adenoviral uptake through the targeting of an anti-adenovirus antibody to ketone-containing glycans.¹⁰¹

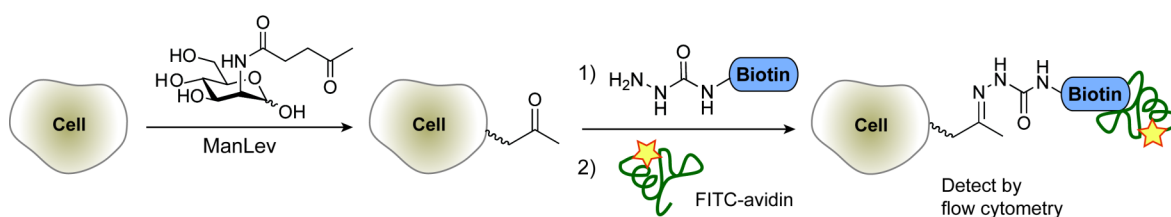


Figure 1.10. The metabolic incorporation of ketones into cell-surface glycans by treatment with N-levulinoylmannosamine (ManLev) and subsequent detection through condensation with hydrazide probes.

Around the same time, a similar strategy was reported by Schultz and coworkers for the selective modification of ketone-containing T4 lysozyme.¹⁰² In this case, the ketone was incorporated using the amber stop codon unnatural amino acid mutagenesis strategy, which was well-established, although not particularly user friendly at this time.^{103,104,105} This method utilizes the codon UAG (the amber nonsense stop codon), which normally directs termination of protein synthesis, to instead encode an unnatural amino acid loaded onto a complementary tRNA.¹⁰⁶ The tolerance of the ribosome for unnatural amino acids allows for their incorporation into proteins during normal translation. A tRNA recognizing the amber stop codon was synthetically loaded with a keto-amino acid and subjected to the mutated T4 lysozyme gene in an *in vitro* transcription/translation system. The keto-T4 lysozyme was then detected by treatment with a fluorescein-hydrazide probe (Figure 1.11).

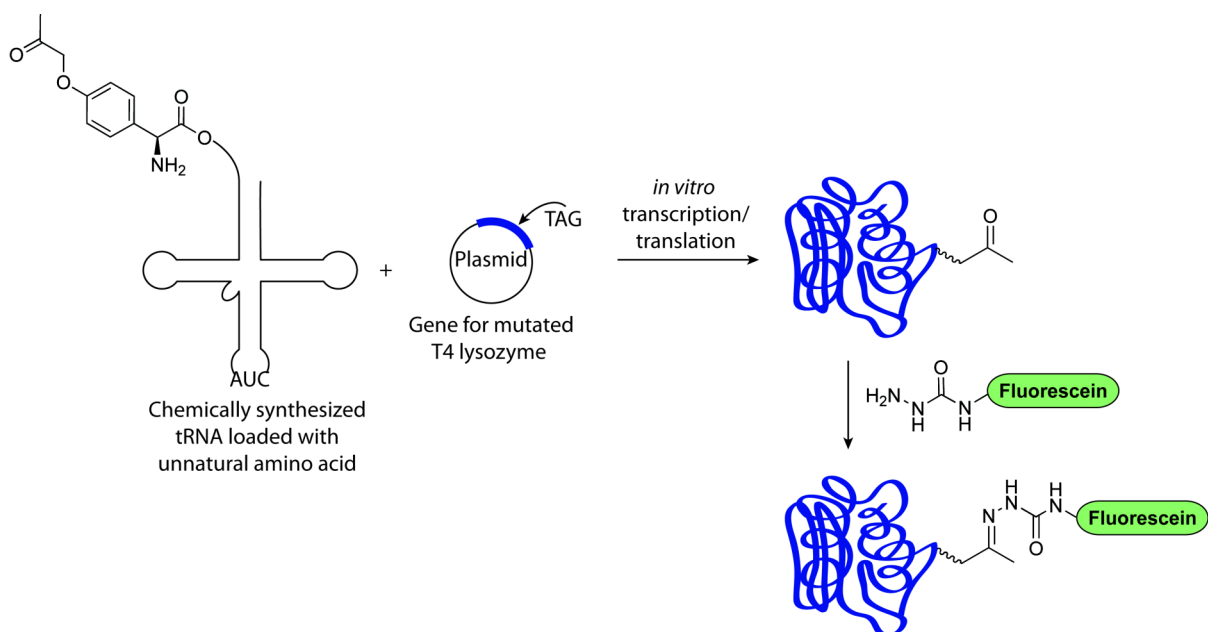


Figure 1.11. The site-specific incorporation of a ketone into T4 lysozyme and subsequent chemical modification with a fluorescent hydrazide.

These initial studies foreshadowed the power selective chemical reactions could have as an instrument for biological discovery and biotechnology. However, the reaction between carbonyl compounds and alpha effect nucleophiles was not ideal. Ketones and aldehydes are endogenously found in many intracellular metabolites and cofactors such as pyruvate, oxaloacetate, free sugars, and pyridoxal phosphate, which limit the utility of these groups to studying extracellular biological events. An additional disadvantage of ketone and aldehyde condensation reactions is that the optimal pH of the reaction is between 3 and 5, below physiological pH.⁹⁵ Furthermore, when monosaccharides other than ManNAc were modified with ketones, robust metabolic labeling was not observed,¹⁰⁷ suggesting a smaller unnatural group was necessary for widespread use of this chemical labeling strategy. Despite these limitations, the ketone was a crucial functional group in creating the field of bioorthogonal chemistry, which the following chapter is dedicated to.

References

- (1) Glazer, A. N. Specific chemical modification of proteins. *Annu. Rev. Biochem.* **1970**, *39*, 101-130.
- (2) Kaiser, E. T.; Lawrence, D. S.; Rokita, S. E. The chemical modification of enzymatic specificity. *Annu. Rev. Biochem.* **1985**, *54*, 565-595.
- (3) Francis, M. B. New Methods for Protein Bioconjugation. In *Chemical Biology: From small molecules to systems biology and drug design*; Wiley-VHC, 2008; Vol. 3, pp. 593-634.
- (4) Hermanson, G. T. *Bioconjugate techniques*; Academic Press, 1996.
- (5) Antos, J. M.; Francis, M. B. Transition metal catalyzed methods for site-selective protein modification. *Curr. Opin. Chem. Biol.* **2006**, *10*, 253-262.
- (6) McFarland, J. M.; Francis, M. B. Reductive alkylation of proteins using iridium catalyzed transfer hydrogenation. *J. Am. Chem. Soc.* **2005**, *127*, 13490-13491.
- (7) Joshi, N. S.; Whitaker, L. R.; Francis, M. B. A three-component Mannich-type reaction for selective tyrosine bioconjugation. *J. Am. Chem. Soc.* **2004**, *126*, 15942-15943.
- (8) Kodadek, T.; Duroux-Richard, I.; Bonnafous, J.-C. Techniques: Oxidative cross-linking as an emergent tool for the analysis of receptor-mediated signalling events. *Trends Pharmacol. Sci.* **2005**, *26*, 210-217.
- (9) Meunier, S.; Strable, E.; Finn, M. G. Crosslinking of and coupling to viral capsid proteins by tyrosine oxidation. *Chem. Biol.* **2004**, *11*, 319-326.
- (10) McFarland, J. M.; Joshi, N. S.; Francis, M. B. Characterization of a three-component coupling reaction on proteins by isotopic labeling and nuclear magnetic resonance spectroscopy. *J. Am. Chem. Soc.* **2008**, *130*, 7639-7644.
- (11) Romanini, D. W.; Francis, M. B. Attachment of peptide building blocks to proteins through tyrosine bioconjugation. *Bioconjugate Chem.* **2008**, *19*, 153-157.
- (12) Tilley, S. D.; Francis, M. B. Tyrosine-selective protein alkylation using π -allylpalladium complexes. *J. Am. Chem. Soc.* **2006**, *128*, 1080-1081.
- (13) Antos, J. M.; Francis, M. B. Selective tryptophan modification with rhodium carbenoids in aqueous solution. *J. Am. Chem. Soc.* **2004**, *126*, 10256-10257.
- (14) Dixon, H. B. F. N-Terminal modification of proteins-a review. *J. Protein Chem.* **1984**, *3*, 99-108.
- (15) Cennamo, C.; Carafoli, B.; Bonetti, E. P. Non-enzymatic transamination between peptides and pyridoxal. Isolation of the 2,4-dinitrophenylhydrazones of some keto-peptides. *J. Am. Chem. Soc.* **1956**, *78*, 3523-3527.
- (16) Dixon, H. B. Transamination of peptides. *Biochem. J.* **1964**, *92*, 661-666.
- (17) Gilmore, J. M.; Scheck, R. A.; Esser-Kahn, A. P.; Joshi, N. S.; Francis, M. B. N-Terminal protein modification through a biomimetic transamination reaction. *Angew. Chem. Int. Ed.* **2006**, *45*, 5307-5311.
- (18) Scheck, R. A.; Dedeo, M. T.; Iavarone, A. T.; Francis, M. B. Optimization of a biomimetic transamination reaction. *J. Am. Chem. Soc.* **2008**, *130*, 11762-11770.

- (19) Geoghegan, K. F.; Stroh, J. G. Site-directed conjugation of nonpeptide groups to peptides and proteins via periodate oxidation of a 2-amino alcohol. Application to modification at N-terminal serine. *Bioconjugate Chem.* **1992**, *3*, 138-146.
- (20) Li, X.; Zhang, L.; Hall, S. E.; Tam, J. P. A new ligation method for N-terminal tryptophan-containing peptides using the Pictet-Spengler reaction. *Tetrahedron Lett.* **2000**, *41*, 4069-4073.
- (21) de la Figuera, N.; Fiol, S. Fernández, J.-C.; Forns, P.; Fernández-Forner, D.; Albericio, F. Role of the acid group in the Pictet-Spengler reaction of α -amino acids. *Synlett* **2006**, 1903-1907.
- (22) Tam, J. P.; Yu, Q.; Miao, Z. Orthogonal ligation strategies for peptide and protein. *Pept. Sci.* **1999**, *51*, 311-332.
- (23) Dawson, P. E.; Muir, T. W.; Clark-Lewis, I.; Kent, S. B. Synthesis of proteins by native chemical ligation. *Science* **1994**, *266*, 776-779.
- (24) Wieland, T.; Bokelmann, E.; Bauer, L.; Lang, H. U.; Lau, H. Über peptidsynthesen. 8. Mitteilung bildung von S-haltigen peptiden durch intramolekulare wanderung von aminoacylresten. *Justus Liebigs Ann. Chem.* **1953**, *583*, 129-149.
- (25) Dawson, P. E.; Kent, S. B. H. Semisynthesis of native proteins by chemical ligation. *Annu. Rev. Biochem.* **2000**, *69*, 923-960.
- (26) Camarero, J. A.; Shekhtman, A.; Campbell, E. A.; Chlenov, M.; Gruber, T. M. Bryant, D. A.; Darst, S. A.; Cowburn, D.; Muir, T. W. Autoregulation of a bacterial sigma factor explored by using segmental isotopic labeling and NMR. *Proc. Natl. Acad. Sci. U.S.A.* **2002**, *99*, 8536-8541.
- (27) Yamazaki, T.; Otomo, T.; Oda, N.; Kyogoku, Y.; Uegaki, K.; Ito, N.; Ishino, Y.; Nakamura, H. Segmental isotope labeling for protein NMR using peptide splicing. *J. Am. Chem. Soc.* **1998**, *120*, 5591-5592.
- (28) Schwarzer, D.; Cole, P. A. Protein semisynthesis and expressed protein ligation: Chasing a protein's tail. *Curr. Opin. Chem. Biol.* **2005**, *9*, 561-569.
- (29) Muralidharan, V.; Muir, T. W. Protein ligation: An enabling technology for the biophysical analysis of proteins. *Nat. Methods* **2006**, *3*, 429-438.
- (30) Muir, T. W. Semisynthesis of proteins by expressed protein ligation. *Annu. Rev. Biochem.* **2003**, *72*, 249-289.
- (31) Muir, T. W.; Sondhi, D.; Cole, P. A. Expressed protein ligation: A general method for protein engineering. *Proc. Natl. Acad. Sci. U.S.A.* **1998**, *95*, 6705-6710.
- (32) Ozawa, T.; Nogami, S.; Sato, M.; Ohya, Y.; Umezawa, Y. A fluorescent indicator for detecting protein-protein interactions in vivo based on protein splicing. *Anal. Chem.* **2000**, *72*, 5151-5157.
- (33) Scott, C. P.; Abel-Santos, E.; Wall, M.; Wahnon, D. C.; Benkovic, S. J. Production of cyclic peptides and proteins in vivo. *Proc. Natl. Acad. Sci. U.S.A.* **1999**, *96*, 13638-13643.
- (34) Evans, T. C., Jr; Martin, D.; Kolly, R.; Panne, D.; Sun, L.; Ghosh, I.; Chen, L.; Benner, J.; Liu, X. Q.; Xu, M. Q. Protein trans-splicing and cyclization by a naturally split intein from the dnaE gene of *Synechocystis* species PCC6803. *J. Biol. Chem.* **2000**, *275*, 9091-9094.

- (35) Giritat, I.; Muir, T. W. Protein semi-synthesis in living cells. *J. Am. Chem. Soc.* **2003**, *125*, 7180-7181.
- (36) Yeo, D. S. Y.; Srinivasan, R.; Uttamchandani, M.; Chen, G. Y. J.; Zhu, Q.; Yao, S. Q. Cell-permeable small molecule probes for site-specific labeling of proteins. *Chem. Commun.* **2003**, *39*, 2870-2871.
- (37) Tsien, R. Y. The green fluorescent protein. *Annu. Rev. Biochem.* **1998**, *67*, 509-544.
- (38) Shaner, N. C.; Steinbach, P. A.; Tsien, R. Y. A guide to choosing fluorescent proteins. *Nat. Methods* **2005**, *2*, 905-909.
- (39) Lippincott-Schwartz, J.; Patterson, G. H. Development and use of fluorescent protein markers in living cells. *Science* **2003**, *300*, 87-91.
- (40) Shaner, N. C.; Patterson, G. H.; Davidson, M. W. Advances in fluorescent protein technology. *J. Cell Sci.* **2007**, *120*, 4247-4260.
- (41) Andresen, M.; Schmitz-Salue, R.; Jakobs, S. Short tetracysteine tags to β -tubulin demonstrate the significance of small labels for live cell imaging. *Mol. Biol. Cell* **2004**, *15*, 5616-5622.
- (42) Adams, S. R.; Campbell, R. E.; Gross, L. A.; Martin, B. R.; Walkup, G. K.; Yao, Y.; Llopis, J.; Tsien, R. Y. New biarsenical ligands and tetracysteine motifs for protein labeling in vitro and in vivo: Synthesis and biological applications. *J. Am. Chem. Soc.* **2002**, *124*, 6063-6076.
- (43) Griffin, B. A.; Adams, S. R.; Tsien, R. Y. Specific covalent labeling of recombinant protein molecules inside live cells. *Science* **1998**, *281*, 269-272.
- (44) Stroffekova, K.; Proenza, C.; Beam, K. The protein-labeling reagent FLASH-EDT₂ binds not only to CCXXCC motifs but also non-specifically to endogenous cysteine-rich proteins. *Pflug. Arch. Eur. J. Phys.* **2001**, *442*, 859-866.
- (45) Griffin, B. A.; Adams, S. R.; Jones, J.; Tsien, R. Y. Fluorescent labeling of recombinant proteins in living cells with FLaSH. In *Applications of Chimeric Genes and Hybrid Proteins - Part B: Cell Biology and Physiology*; Academic Press, 2000; Vol. Volume 327, pp. 565-578.
- (46) Martin, B. R.; Giepmans, B. N. G.; Adams, S. R.; Tsien, R. Y. Mammalian cell-based optimization of the biarsenical-binding tetracysteine motif for improved fluorescence and affinity. *Nat. Biotech.* **2005**, *23*, 1308-1314.
- (47) Rodriguez, A. J.; Shenoy, S. M.; Singer, R. H.; Condeelis, J. Visualization of mRNA translation in living cells. *J. Cell Biol.* **2006**, *175*, 67-76.
- (48) Hoffmann, C.; Gaietta, G.; Bunemann, M.; Adams, S. R.; Oberdorff-Maass, S.; Behr, B.; Vilardaga, J.-P.; Tsien, R. Y.; Ellisman, M. H.; Lohse, M. J. A FLaSH-based FRET approach to determine G protein-coupled receptor activation in living cells. *Nat. Methods* **2005**, *2*, 171-176.
- (49) Roberti, M. J.; Bertocini, C. W.; Klement, R.; Jares-Erijman, E. A.; Jovin, T. M. Fluorescence imaging of amyloid formation in living cells by a functional, tetracysteine-tagged α -synuclein. *Nat. Methods* **2007**, *4*, 345-351.
- (50) Chaumont, S.; Khakh, B. S. Patch-clamp coordinated spectroscopy shows P2X₂ receptor permeability dynamics require cytosolic domain rearrangements but not Panx-1 channels. *Proc. Natl. Acad. Sci. U.S.A.* **2008**, *105*, 12063-12068.

- (51) Arhel, N.; Genovesio, A.; Kim, K.-A.; Miko, S.; Perret, E.; Olivo-Marin, J.-C.; Shorte, S.; Charneau, P. Quantitative four-dimensional tracking of cytoplasmic and nuclear HIV-1 complexes. *Nat. Methods* **2006**, *3*, 817-824.
- (52) Gaietta, G.; Deerinck, T. J.; Adams, S. R.; Bouwer, J.; Tour, O.; Laird, D. W.; Sosinsky, G. E.; Tsien, R. Y.; Ellisman, M. H. Multicolor and electron microscopic imaging of connexin trafficking. *Science* **2002**, *296*, 503 -507.
- (53) Taguchi, Y.; Shi, Z.-D.; Ruddy, B.; Dorward, D. W.; Greene, L.; Baron, G. S. Specific biarsenical labeling of cell surface proteins allows fluorescent- and biotin-tagging of amyloid precursor protein and prion proteins. *Mol. Biol. Cell* **2009**, *20*, 233-244.
- (54) Terpe, K. Overview of tag protein fusions: From molecular and biochemical fundamentals to commercial systems. *Appl. Microbiol. Biotechnol.* **2003**, *60*, 523-533.
- (55) Guignet, E. G.; Hovius, R.; Vogel, H. Reversible site-selective labeling of membrane proteins in live cells. *Nat. Biotech.* **2004**, *22*, 440-444.
- (56) Kapanidis, A. N.; Ebright, Y. W.; Ebright, R. H. Site-specific incorporation of fluorescent probes into protein: Hexahistidine-tag-mediated fluorescent labeling with (Ni²⁺:nitrilotriacetic acid)-fluorochrome conjugates. *J. Am. Chem. Soc.* **2001**, *123*, 12123-12125.
- (57) Lata, S.; Reichel, A.; Brock, R.; Tampé, R.; Piehler, J. High-affinity adaptors for switchable recognition of histidine-tagged proteins. *J. Am. Chem. Soc.* **2005**, *127*, 10205-10215.
- (58) Goldsmith, C. R.; Jaworski, J.; Sheng, M.; Lippard, S. J. Selective labeling of extracellular proteins containing polyhistidine sequences by a fluorescein-nitrilotriacetic acid conjugate. *J. Am. Chem. Soc.* **2006**, *128*, 418-419.
- (59) Nitz, M.; Franz, K. J.; Maglathlin, R. L.; Imperiali, B. A powerful combinatorial screen to identify high-affinity terbium(III)-binding peptides. *ChemBioChem* **2003**, *4*, 272-276.
- (60) Martin, L. J.; Sculimbrene, B. R.; Nitz, M.; Imperiali, B. Rapid combinatorial screening of peptide libraries for the selection of lanthanide-binding tags (LBTs). *QSAR Comb. Sci.* **2005**, *24*, 1149-1157.
- (61) Franz, K. J.; Nitz, M.; Imperiali, B. Lanthanide-binding tags as versatile protein coexpression probes. *ChemBioChem* **2003**, *4*, 265-271.
- (62) Sculimbrene, B. R.; Imperiali, B. Lanthanide-binding tags as luminescent probes for studying protein interactions. *J. Am. Chem. Soc.* **2006**, *128*, 7346-7352.
- (63) Fricker, S. P. The therapeutic application of lanthanides. *Chem. Soc. Rev.* **2006**, *35*, 524-533.
- (64) Chen, I.; Ting, A. Y. Site-specific labeling of proteins with small molecules in live cells. *Curr. Opin. Chem. Biol.* **2005**, *16*, 35-40.
- (65) Foley, T. L.; Burkart, M. D. Site-specific protein modification: Advances and applications. *Curr. Opin. Chem. Biol.* **2007**, *11*, 12-19.
- (66) Chen, I.; Howarth, M.; Lin, W.; Ting, A. Y. Site-specific labeling of cell surface proteins with biophysical probes using biotin ligase. *Nat. Methods* **2005**, *2*, 99-104.

- (67) Howarth, M.; Takao, K.; Hayashi, Y.; Ting, A. Y. Targeting quantum dots to surface proteins in living cells with biotin ligase. *Proc. Natl. Acad. Sci. U.S.A.* **2005**, *102*, 7583 -7588.
- (68) Lin, C.-W.; Ting, A. Y. Transglutaminase-catalyzed site-specific conjugation of small-molecule probes to proteins in vitro and on the surface of living cells. *J. Am. Chem. Soc.* **2006**, *128*, 4542-4543.
- (69) Dutton, A.; Singer, S. J. Crosslinking and labeling of membrane proteins by transglutaminase-catalyzed reactions. *Proc. Natl. Acad. Sci. U.S.A.* **1975**, *72*, 2568 -2571.
- (70) Sato, H.; Ikeda, M.; Suzuki, K.; Hirayama, K. Site-specific modification of Interleukin-2 by the combined use of genetic engineering techniques and transglutaminase. *Biochemistry* **1996**, *35*, 13072-13080.
- (71) Mazmanian, S. K.; Liu, G.; Ton-That, H.; Schneewind, O. Staphylococcus aureus sortase, an enzyme that anchors surface proteins to the cell wall. *Science* **1999**, *285*, 760 -763.
- (72) Marraffini, L. A.; DeDent, A. C.; Schneewind, O. Sortases and the art of anchoring proteins to the envelopes of gram-positive bacteria. *Microbiol. Mol. Biol. Rev.* **2006**, *70*, 192-221.
- (73) Samantaray, S.; Marathe, U.; Dasgupta, S.; Nandicoori, V. K.; Roy, R. P. Peptide-sugar ligation catalyzed by transpeptidase sortase: A facile approach to neoglycoconjugate synthesis. *J. Am. Chem. Soc.* **2008**, *130*, 2132-2133.
- (74) Mao, H.; Hart, S. A.; Schink, A.; Pollok, B. A. Sortase-mediated protein ligation: A new method for protein engineering. *J. Am. Chem. Soc.* **2004**, *126*, 2670-2671.
- (75) Johnsson, N.; George, N.; Johnsson, K. Protein chemistry on the surface of living cells. *ChemBioChem* **2005**, *6*, 47-52.
- (76) Joshi, A. K.; Zhang, L.; Rangan, V. S.; Smith, S. Cloning, expression, and characterization of a human 4'-phosphopantetheinyl transferase with broad substrate specificity. *J. Biol. Chem.* **2003**, *278*, 33142 -33149.
- (77) Yin, J.; Liu, F.; Li, X.; Walsh, C. T. Labeling proteins with small molecules by site-specific posttranslational modification. *J. Am. Chem. Soc.* **2004**, *126*, 7754-7755.
- (78) George, N.; Pick, H.; Vogel, H.; Johnsson, N.; Johnsson, K. Specific labeling of cell surface proteins with chemically diverse compounds. *J. Am. Chem. Soc.* **2004**, *126*, 8896-8897.
- (79) Yin, J.; Lin, A. J.; Buckett, P. D.; Wessling-Resnick, M.; Golan, D. E.; Walsh, C. T. Single-cell FRET imaging of transferrin receptor trafficking dynamics by Sfp-catalyzed, site-specific protein labeling. *Chem. Biol.* **2005**, *12*, 999-1006.
- (80) Vivero-Pol, L.; George, N.; Krumm, H.; Johnsson, K.; Johnsson, N. Multicolor imaging of cell surface proteins. *J. Am. Chem. Soc.* **2005**, *127*, 12770-12771.
- (81) Yin, J.; Straight, P. D.; McLoughlin, S. M.; Zhou, Z.; Lin, A. J.; Golan, D. E.; Kelleher, N. L.; Kolter, R.; Walsh, C. T. Genetically encoded short peptide tag for versatile protein labeling by Sfp phosphopantetheinyl transferase. *Proc. Natl. Acad. Sci. U.S.A.* **2005**, *102*, 15815 -15820.

- (82) Zhou, Z.; Cironi, P.; Lin, A. J.; Xu, Y.; Hrvatin, S.; Golan, D. E.; Silver, P. A.; Walsh, C. T.; Yin, J. Genetically encoded short peptide tags for orthogonal protein labeling by Sfp and AcpS phosphopantetheinyl transferases. *ACS Chem. Biol.* **2007**, *2*, 337-346.
- (83) Pegg, A. E. Repair of O⁶-alkylguanine by alkyltransferases. *Mut. Res.* **2000**, *462*, 83-100.
- (84) Keppler, A.; Gendreizig, S.; Gronemeyer, T.; Pick, H.; Vogel, H.; Johnsson, K. A general method for the covalent labeling of fusion proteins with small molecules in vivo. *Nat. Biotech.* **2003**, *21*, 86-89.
- (85) Keppler, A.; Pick, H.; Arrivoli, C.; Vogel, H.; Johnsson, K. Labeling of fusion proteins with synthetic fluorophores in live cells. *Proc. Natl. Acad. Sci. U.S.A.* **2004**, *101*, 9955-9959.
- (86) Keppler, O. T.; Stehling, P.; Herrmann, M.; Kayser, H.; Grunow, D.; Reutter, W.; Pawlita, M. Biosynthetic modulation of sialic acid-dependent virus-receptor interactions of two primate polyoma viruses. *J. Biol. Chem.* **1995**, *270*, 1308-1314.
- (87) Kayser, H.; Zeitler, R.; Kannicht, C.; Grunow, D.; Nuck, R.; Reutter, W. Biosynthesis of a nonphysiological sialic acid in different rat organs, using N-propanoyl-D-hexosamines as precursors. *J. Biol. Chem.* **1992**, *267*, 16934-16938.
- (88) Herrmann, M.; von der Lieth, C. W.; Stehling, P.; Reutter, W.; Pawlita, M. Consequences of a subtle sialic acid modification on the murine polyomavirus receptor. *J. Virol.* **1997**, *71*, 5922-5931.
- (89) Schmidt, C.; Stehling, P.; Schnitzer, J.; Reutter, W.; Horstkorte, R. Biochemical engineering of neural cell surfaces by the synthetic N-propanoyl-substituted neuraminic acid precursor. *J. Biol. Chem.* **1998**, *273*, 19146-19152.
- (90) Mahal, L. K.; Charter, N. W.; Angata, K.; Fukuda, M.; Koshland, D. E.; Bertozzi, C. R. A small-molecule modulator of poly- α -2,8-sialic acid expression on cultured neurons and tumor cells. *Science* **2001**, *294*, 380-381.
- (91) Keppler, O. T.; Horstkorte, R.; Pawlita, M.; Schmidt, C.; Reutter, W. Biochemical engineering of the N-acyl side chain of sialic acid: Biological implications. *Glycobiology* **2001**, *11*, 11R-18R.
- (92) Shao, J.; Tam, J. P. Unprotected peptides as building blocks for the synthesis of peptide dendrimers with oxime, hydrazone, and thiazolidine linkages. *J. Am. Chem. Soc.* **1995**, *117*, 3893-3899.
- (93) Rose, K. Facile synthesis of homogeneous artificial proteins. *J. Am. Chem. Soc.* **1994**, *116*, 30-33.
- (94) Canne, L. E.; Ferre-D'Amare, A. R.; Burley, S. K.; Kent, S. B. H. Total chemical synthesis of a unique transcription factor-related protein: cMyc-Max. *J. Am. Chem. Soc.* **1995**, *117*, 2998-3007.
- (95) Jencks, W. P. Studies on the mechanism of oxime and semicarbazone formation. *J. Am. Chem. Soc.* **1959**, *81*, 475-481.
- (96) Rideout, D.; Calogeropoulou, T.; Jaworski, J.; McCarthy, M. Synergism through direct covalent bonding between agents: A strategy for rational design of chemotherapeutic combinations. *Biopolymers* **1990**, *29*, 247-262.

- (97) Rideout, D. Self-assembling drugs: A new approach to biochemical modulation in cancer chemotherapy. *Cancer Invest.* **1994**, *12*, 189-202.
- (98) Mahal, L. K.; Yarema, K. J.; Bertozzi, C. R. Engineering chemical reactivity on cell surfaces through oligosaccharide biosynthesis. *Science* **1997**, *276*, 1125 -1128.
- (99) Yarema, K. J.; Mahal, L. K.; Bruehl, R. E.; Rodriguez, E. C.; Bertozzi, C. R. Metabolic delivery of ketone groups to sialic acid residues. *J. Biol. Chem.* **1998**, *273*, 31168 -31179.
- (100) Jacobs, C. L.; Goon, S.; Yarema, K. J.; Hinderlich, S.; Hang, H. C.; Chai, D. H.; Bertozzi, C. R. Substrate specificity of the sialic acid biosynthetic pathway. *Biochemistry* **2001**, *40*, 12864-12874.
- (101) Lee, J. H.; Baker, T. J.; Mahal, L. K.; Zabner, J.; Bertozzi, C. R.; Wiemer, D. F.; Welsh, M. J. Engineering novel cell surface receptors for virus-mediated gene transfer. *J. Biol. Chem.* **1999**, *274*, 21878 -21884.
- (102) Cornish, V. W.; Hahn, K. M.; Schultz, P. G. Site-specific protein modification using a ketone handle. *J. Am. Chem. Soc.* **1996**, *118*, 8150-8151.
- (103) Noren, C.; Anthony-Cahill, S.; Griffith, M.; Schultz, P. A general method for site-specific incorporation of unnatural amino acids into proteins. *Science* **1989**, *244*, 182 -188.
- (104) Bain, J. D.; Diala, E. S.; Glabe, C. G.; Dix, T. A.; Chamberlin, A. R. Biosynthetic site-specific incorporation of a non-natural amino acid into a polypeptide. *J. Am. Chem. Soc.* **1989**, *111*, 8013-8014.
- (105) Ellman, J.; Mendel, D.; Anthony-Cahill, S.; Noren, C. J.; Schultz, P. G. Biosynthetic method for introducing unnatural amino acids site-specifically into proteins. *Meth. Enzymol.* **1991**, *202*, 301-336.
- (106) Wang, L.; Schultz, P. G. Expanding the genetic code. *Angew. Chem. Int. Ed.* **2005**, *44*, 34-66.
- (107) Hang, H. C.; Bertozzi, C. R. Ketone isosteres of 2-N-acetamidoglycans as substrates for metabolic cell surface engineering. *J. Am. Chem. Soc.* **2001**, *123*, 1242-1243.

Chapter 2

Bioorthogonal Chemistry

The Bioorthogonal Chemical Reporter Strategy

Bioorthogonal chemistry is chemistry that does not interfere or interact with biology (Figure 2.1A).¹ The use of bioorthogonal chemistry to probe biomolecules in living systems typically follows a two-step process, which has become known as the bioorthogonal chemical reporter strategy. First, a metabolic substrate, small molecule ligand, or enzyme inhibitor is adorned with a bioorthogonal functional group and introduced to the biological system. The structural perturbation imposed by the functional group, also referred to as a “chemical reporter,” must be minimal so as not to undermine the molecule’s natural bioactivity. Once the labeled molecule has been delivered to its target (e.g., a metabolically labeled glycan, lipid, or protein, or an inhibitor-bound receptor or enzyme), the second step involves a bioorthogonal chemical reaction with an appropriately functionalized probe (Figure 2.1B).²

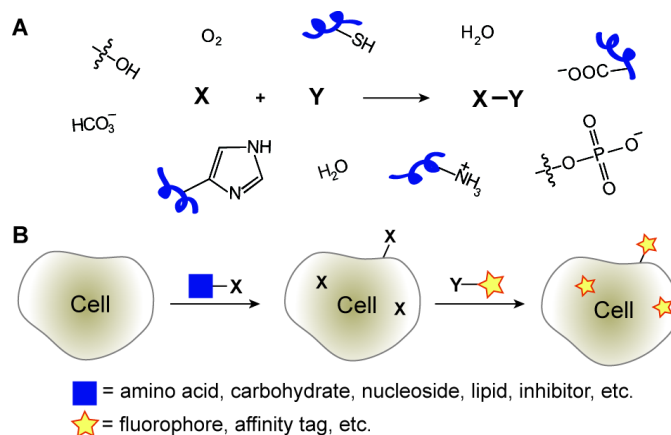


Figure 2.1. A. A generic bioorthogonal chemical reaction between X and Y that proceeds in biological systems. B. A common experimental platform for biomolecule probing using bioorthogonal chemistry. First, a non-native functional group, often called a “chemical reporter,” is installed in a biomolecule of interest. The modified biomolecule is subsequently labeled using a bioorthogonal chemical reaction.

From a chemist's perspective, bioorthogonal reaction development has unusually restrictive boundary conditions. The reaction must form a stable covalent linkage between two functional groups that are bio-inert and ideally nontoxic. The reaction must have fast kinetics so that product is formed at a reasonable rate even when reactant concentrations are very low, as is required in many biological labeling experiments. Also, such fast kinetics must be achieved in the physiological ranges of pH and temperature. For optimal utility as chemical reporters, at least one of the bioorthogonal reactive partners should be small and highly stable.

The Staudinger Ligation

Taking the above stipulations into consideration, Bertozzi and coworkers became interested in the reduction of azides with triphenylphosphine and water (Figure 2.2A), a famously mild transformation that was reported by Hermann Staudinger in 1919.³ Advantageous features of this reaction were the small size of the azide,^{4,5,6} its kinetic stability,⁷ and its absence from biological systems.⁸ Also, the azide's behavior as a "soft electrophile" that prefers "soft nucleophiles" (such as phosphines) situates this functional group in a reaction space that is distinct from most of biology,⁹ wherein nucleophiles are typically "hard". That organic azides would be well tolerated by cells and organisms was hinted at by the established use of aryl azides as photocrosslinkers¹⁰ and by the favorable toxicity profiles of commercially approved drugs such as azidothymidine¹¹. Additionally, phosphines, the other reactive group, are naturally absent from living systems. Mechanistically, the classic Staudinger reduction (Figure 2.2A) proceeds through nucleophilic attack of the phosphine (**2.1**) on the azide (**2.2**), followed by loss of nitrogen to yield an aza-ylide species (**2.3**). In aqueous environments, the aza-ylide is rapidly hydrolyzed to produce a phosphine oxide (**2.4**) and an amine (**2.5**). The Staudinger reduction appeared well-suited as a prototype for bioorthogonal reaction development because the two participants were abiotic, mutually and selectively reactive, essentially unreactive with biological functionalities, and tolerant of water. The main problem was that the initial covalent linkage formed (intermediate **2.3**) was later lost to hydrolysis. Thus, this reaction needed to be modified to redirect the aza-ylide intermediate to a stably ligated product. This was achieved by introducing an ester group *ortho* to the phosphorous atom on one of the aryl rings (**2.6**). Formation of the aza-ylide intermediate (**2.7**) proceeded analogously to the Staudinger reduction; however, the ester group offered a new path of reactivity in which the nucleophilic nitrogen atom reacted with the electrophilic trap to form intermediate **2.8**, which, upon hydrolysis, yielded a stable amide-linked product (**2.9**).¹²

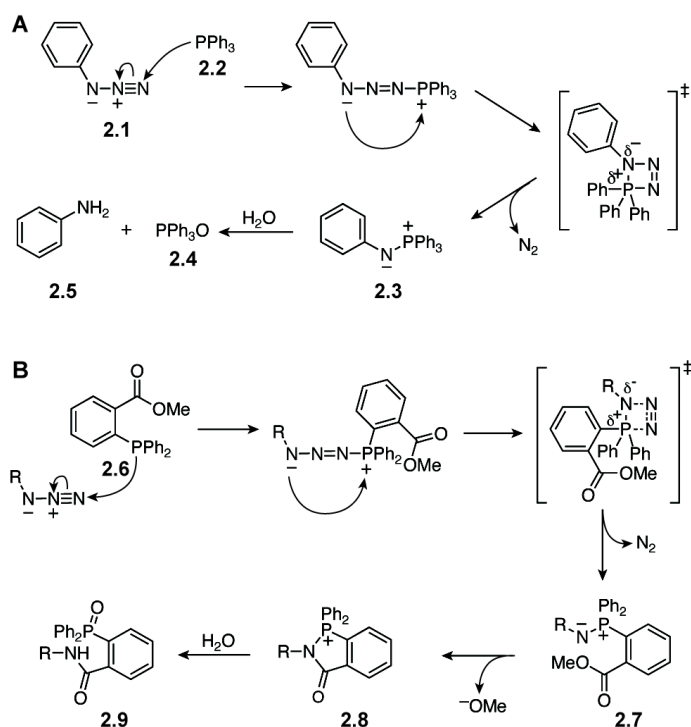


Figure 2.2. The mechanism of the Staudinger reduction (A) and Staudinger ligation (B).

This adjustment to the Staudinger reduction was sufficient to generate a bioorthogonal chemical reaction. The engineered phosphines were exquisitely selective for azides in a variety of environments. Equally exciting was the efficiency with which azides could be incorporated into sialoglycans by metabolic labeling with N-azidoacetyl mannosamine (ManNAz).¹²

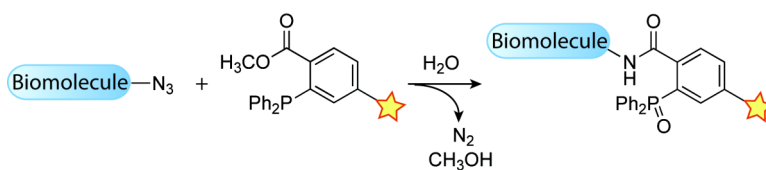


Figure 2.3. The bioorthogonal Staudinger ligation between an azide and triarylphosphine reagent to yield an amide bond ligation product.

Phosphine-biotin (**2.10**) and phosphine-FLAG probes (**2.11**) displayed selective labeling of azide-modified glycoproteins (Figure 2.3A) in cell lysates (Figure 2.3B).¹³ Additionally, the phosphine reagents proved to be non-toxic, and therefore the Staudinger ligation can be performed on live cells. Flow cytometry data from a typical experiment in which cell-surface glycans were labeled with Ac_4ManNAz and then reacted with a phosphine probe are shown in Figure 2.3C.^{12,14}

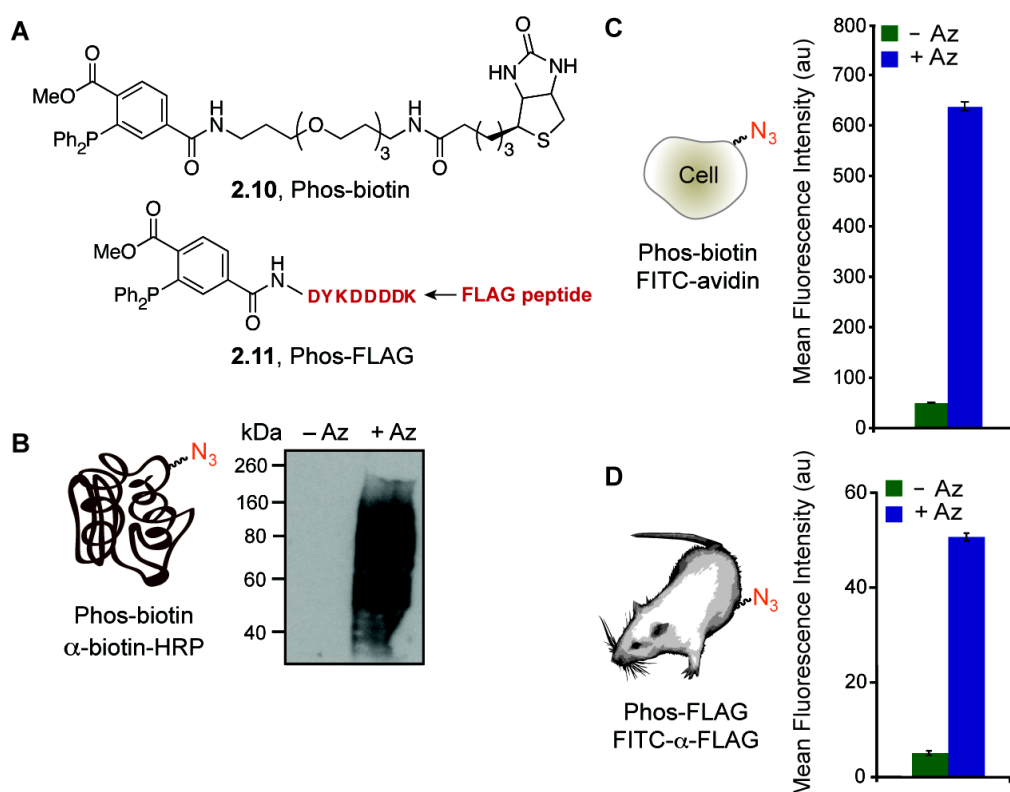


Figure 2.4. The Staudinger ligation enables selective biomolecule labeling in a variety of environments. A. Phosphine-biotin (Phos-biotin, **2.10**) and Phosphine-FLAG (Phos-FLAG, **2.11**) probes for the detection of azides through the Staudinger ligation. B/C. Selective labeling of azide-modified glycoproteins in lysates and on live cells. Jurkat cells were treated with (+ Az, blue bars) or without (- Az, green bars) peracetylated-N-azidoacetyl mannosamine ($Ac_4ManNAz$), which is metabolized to N-azidoacetyl neuraminic acid and incorporated into glycoproteins. B. Lysates were treated with Phos-biotin (**2.10**, 250 μ M) overnight, and analyzed by Western blot probing with an α -biotin-horse radish peroxidase (α -biotin-HRP) antibody. C. Live cells were treated with Phos-biotin (**2.10**, 250 μ M) for 1 h, followed by incubation with a fluorescent avidin protein (FITC-avidin) and analyzed by flow cytometry. D. Mice were injected with (blue bars) or without (green bars) $Ac_4ManNAz$ once daily for 7 d. On the eighth day, phosphine conjugated to the FLAG peptide (**2.11**, Phos-FLAG) was injected into the mice. After 3 h, the mice were sacrificed, their splenocytes were isolated, incubated with a fluorescent anti-FLAG antibody (FITC- α -FLAG), and analyzed by flow cytometry. Au = arbitrary units.

These results showcased the exquisite selectivity that the triarylphosphine reagent had for the azide, and the Staudinger ligation appeared equipped for use *in vivo*. Mice were injected once daily for 7 days with $Ac_4ManNAz$ and on the eighth day the mice were injected with a phosphine reagent connected to the FLAG peptide (Phos-FLAG, **2.11**). After 90 min, the mice were sacrificed, their splenocytes were harvested, incubated with a fluorescent α -FLAG antibody, and the degree of labeling was measured by flow cytometry

(Figure 2.3D). The results indicated that the Staudinger ligation enabled the selective *in vivo* covalent modification of cell-surface glycans with chemical probes.¹⁵ This unprecedented feat was a testament to the mutual selectivity of the Staudinger ligation reagents; no previously reported reaction could have reliably formed products in such a complex reaction vessel.

The entirety of the Staudinger ligation was an enormous advance for the field, but the real gem of this early work was the azide. The benefits of its small size were immediately apparent. Unlike the previously studied keto-sugars, several glycan biosynthetic pathways were quite accommodating of azidosugar substrates in cell culture and in living mice (Figure 2.4).^{14,16,17,18,19} In fact, the azide was so small that the efficiency of metabolic incorporation of ManNAz (**2.12**) through the sialic acid biosynthetic pathway was equivalent to the degree of incorporation of N-azidoacetyl neuraminic acid (**2.13**), a substrate for the sialic acid salvage pathway. In contrast, the larger modification of an aryl azide showed minimal incorporation through the sialic acid biosynthetic pathway (metabolic labeling with **2.14**) while significant labeling was achieved through the sialic acid salvage pathway (metabolic labeling with **2.15**).²⁰ The 9-position of sialic acid was also successfully modified with an aryl azide by introduction of sialic acid **2.16**.²¹ Furthermore, azides could be incorporated into mucin-type O-linked glycans¹⁸ and O-GlcNAcylated proteins¹⁷ using N-azidoacetyl galactosamine (**2.16**) and N-azidoacetyl glucosamine precursors (**2.17**).

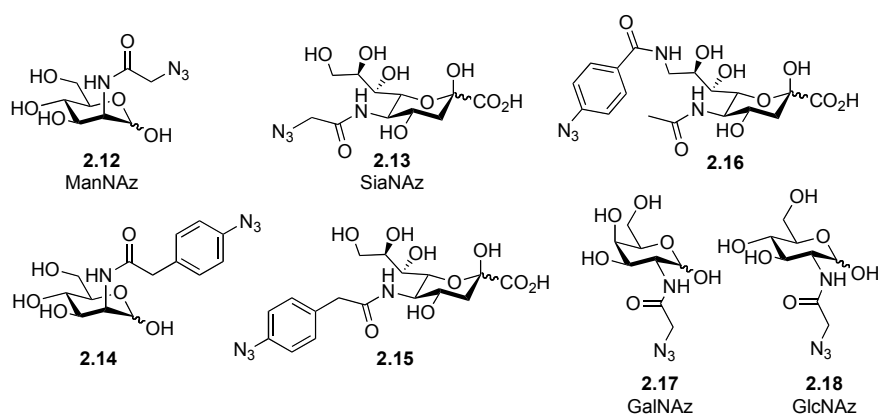


Figure 2.5. Azide-modified monosaccharides for incorporation into glycoproteins by metabolic oligosaccharide engineering.

A metabolic labeling strategy followed by detection with the Staudinger ligation was also applied to proteins by Tirrell and coworkers.¹³ The Tirrell group has pioneered the use of auxotrophic cell lines to globally replace a canonical amino acid with an unnatural group of similar size, which is still accepted by the aminoacyl-tRNA synthetases (aaRSs) (Figure 2.5).^{22,23,24} This concept dates back to the 1950s, when methionine residues were shown to be replaced by their selenium analogs by adding selenomethionine

to methionine-depleted growth media.²⁵ Surrogates for methionine, leucine, tryptophan, or phenylalanine are commonly incorporated into proteins expressed in *E. coli*, although reports can be found for replacement of almost any amino acid with an unnatural derivative. The yields are optimal when the *E. coli* strain is rendered auxotrophic for the amino acid being targeted for replacement, and overexpression of the required aaRS can be helpful as well.^{26,27,28} Fortunately, the small size of the azide readily allowed incorporation of azidohomoalanine (**2.19**, Figure 2.7) as a methionine surrogate. The resulting azido-proteins were labeled with Phos-FLAG (**2.11**) and analyzed by Western blot (Figure 2.6).¹³

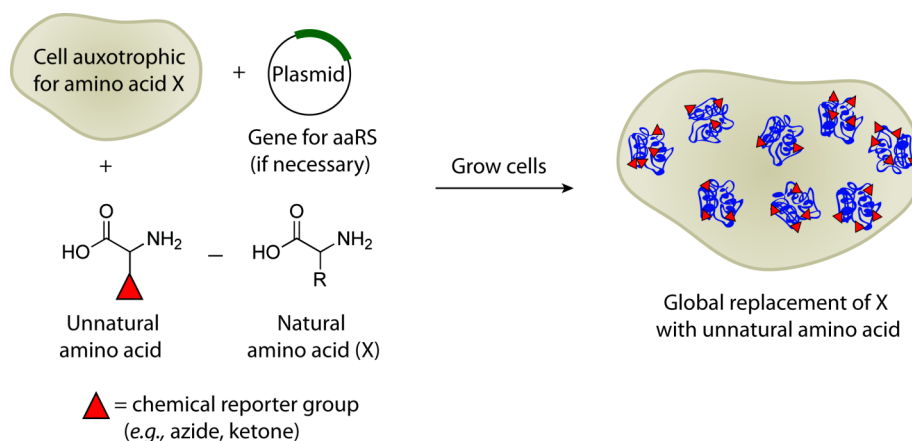


Figure 2.6. Global metabolic incorporation of unnatural amino acids into proteins using auxotrophic cell lines and promiscuous aminoacyl tRNA synthetases (aaRSs).

The ease of metabolic incorporation of the azide into proteins also showcased the benefits of the Staudinger ligation over oxime ligation chemistry, as a ketone-bearing amino acid *p*-acetylphenylalanine (**2.21**) could only be metabolically introduced into proteins if a mutant phenylalanine tRNA synthetase was employed.²⁶ This mutant tRNA synthetase also allowed for the incorporation of *p*-azido-, *p*-bromo-, and *p*-iodophenylalanines into proteins (**2.20**, **2.22-2.23**).^{29,30} The latter halogen derivatives can be modified using Pd-catalyzed cross-coupling methodologies.^{31,32}

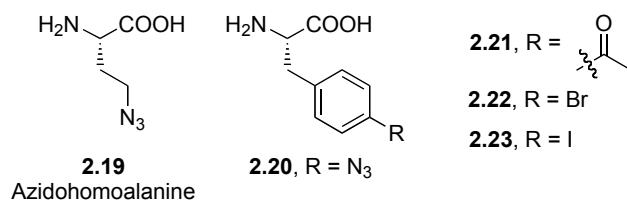


Figure 2.7. Selected unnatural amino acids metabolically incorporated into proteins.

Shortly after the report of the Staudinger ligation, azides were incorporated into farnesyl (**2.24**) and geranylgeranyl metabolites (**2.25**) as well as S-adenosyl methionine (SAM) analogues (**2.26**, **2.27**) (Figure 2.8). Upon introduction of an azido-farnesyl group to live cells and Staudinger ligation mediated enrichment, Zhou and coworkers discovered new farnesylated proteins.³³ Additionally, Rajski and coworkers probed DNA-methyltransferase activity using azido-SAM mimics and phosphine secondary reagents.^{34,35}

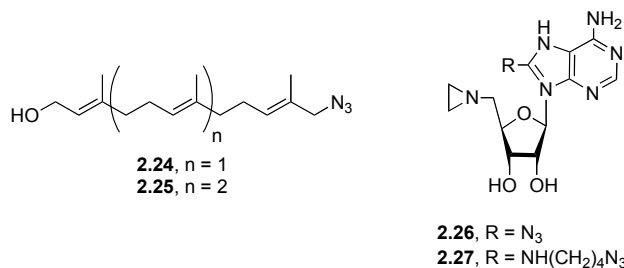


Figure 2.8. Azido-lipid and azido-SAM analogues.

The Staudinger ligation also proved to be a valuable tool for activity-based protein profiling. Activity-based protein profiling (ABPP) allows for the study of specific classes of enzymes based on their catalytic mechanism, often through the use of mechanism-based covalent inhibitors conjugated to a probe (*i.e.*, fluorophore or biotin). The bioorthogonal chemical reporter strategy eliminated the need for a large chemical probe during the covalent labeling process (Figure 2.9).^{36,37} In its initial form, ABPP employed an electrophilic group (known as a warhead) that covalently modifies the targeted class of enzymes and is conjugated to an affinity probe such as a biotin or a fluorophore. While useful for tagging active enzymes from cell lysates, such large probes often had poor pharmacokinetic properties that prevented their use *in vivo*.³⁸ Overkleeft and coworkers applied the Staudinger ligation to ABPP by targeting proteasomes in live cells with an azide-functionalized vinyl sulfone.³⁹ Once the enzymes were covalently modified, cell lysates were generated and subsequently reacted with a biotinylated triarylphosphine probe through the Staudinger ligation. Additionally, Ploegh and coworkers have used an azido-epoxide warhead, a triarylphosphine-biotin probe, and streptavidin-Alexa Fluor 647 for live-cell imaging of cathepsin proteases.⁴⁰

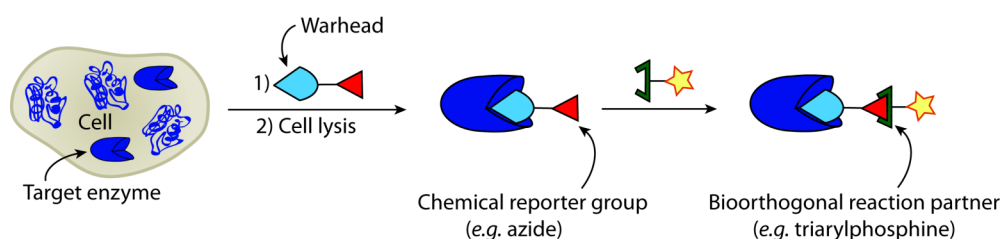


Figure 2.9. Activity-based protein profiling using the bioorthogonal chemical reporter strategy. A warhead group is functionalized with a chemical reporter and introduced to cells. Following cell lysis, a bioorthogonal chemical reaction facilitates identification or visualization of the modified enzymes.

Clearly, the Staudinger ligation had an immediate impact on the chemical biology community, but there were also limitations to this reaction. The phosphine reagents slowly underwent oxidation within biological systems, and appeared to be metabolized by cytochrome P450⁴¹ or flavin monooxygenase⁴² enzymes in mice. Additionally, the kinetics of the reaction were somewhat slow (typical second-order rate constant of $0.0020 \text{ M}^{-1}\text{s}^{-1}$),⁴³ which necessitated the use of high concentrations of phosphine reagent. This, in turn, was found to be problematic for fluorescence imaging applications because excess probe reagent was difficult to wash away, resulting in high background signal.⁴⁴

A detailed mechanistic study revealed that the rate-determining step of the Staudinger ligation is the initial nucleophilic attack of the phosphine on the azide.⁴³ Thus, increasing the electron density on the phosphorous atom could, in principle, increase the rate of the Staudinger ligation. While the addition of electron donating groups to the aryl substituents did indeed increase the rate of the desired reaction, these more reactive substrates were also rapidly oxidized in air.

Frustrated by our inability to improve the intrinsic kinetics of the Staudinger ligation, we turned to alternate means of reducing background fluorescence in cell imaging experiments. An appealing feature of the Staudinger ligation is that its mechanism lends itself to the invention of fluorogenic reagents for real-time biomolecule imaging. This was first exploited within the Bertozzi group by replacing one of the aryl rings of **2.6** with a coumarin dye (compound **2.28**, Figure 2.10).⁴⁵ Fluorescence of **2.28** was quenched by the lone pair of electrons on the phosphorus atom. Phosphine oxidation during the course of the Staudinger ligation relieved the quenching effect, producing a highly fluorescent biomolecule-bound product (**2.29**).

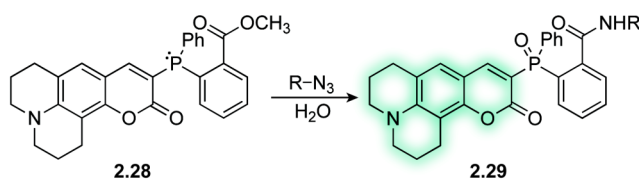


Figure 2.10. A coumarin-based fluorogenic phosphine for the Staudinger ligation. This molecule becomes fluorescent upon phosphine oxidation.

The Staudinger ligation has also been adapted for applications beyond biomolecule labeling, most significantly as a tool for protein synthesis. “Traceless” versions of the Staudinger ligation have been developed to produce amide bonds without inclusion of the phosphine oxide moiety.⁴⁶ Raines and coworkers merged this concept with thioester chemistry reminiscent of NCL in order to develop a traceless Staudinger ligation for peptide couplings (Figure 2.11).^{47,48,49} This traceless Staudinger-mediated peptide coupling involves the attack of a peptide containing a C-terminal phosphothioester (**2.30**) with an azide-labeled peptide. Attack of the phosphine in **2.30** on the azide results in aza-ylide **2.31**, which rearranges to **2.32**. Hydrolysis of **2.32** facilitates the ligation of the two original peptides via a native amide bond (**2.33**). Unlike the canonical NCL process, Raines’s method does not require the presence of a cysteine residue at the ligation site.^{47,48} Additional reagents have been synthesized for the traceless Staudinger ligation including an ester-linked version.⁵⁰ Optimization of the phosphine reagents for steric, electronic, and coulombic factors has also been performed.^{51,52}

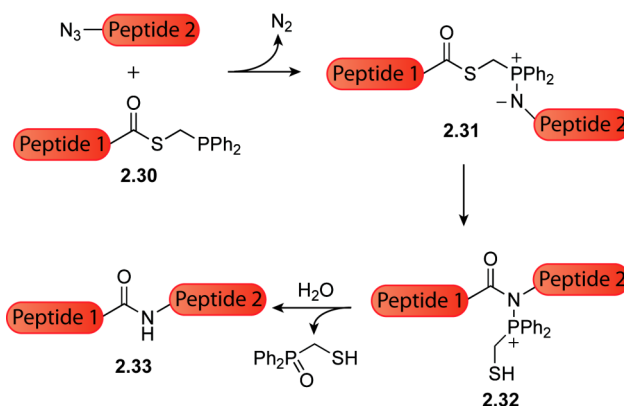


Figure 2.11. Peptide coupling via the traceless Staudinger ligation. The phosphine appended to peptide 1 through a C-terminal thioester (**2.30**) attacks the azide attached to peptide 2 in a manner analogous to the original Staudinger ligation to yield aza-ylide **2.31**, which rearranges to **2.32**. Hydrolysis of **2.32** results in coupling product **2.33** plus a phosphine oxide byproduct.

While still the reaction of choice for a wide range of bioconjugation applications, the slow kinetics of the Staudinger ligation remains an unsolved problem and an obstacle for *in vivo* chemistry. Consequently, during the mid-2000s, we and others turned our attention to new chemistries for the azide.

Cu-Catalyzed Azide-Alkyne Cycloaddition (CuAAC)

An alternate mode of reactivity for the azide is its participation as a 1,3-dipole in a [3+2] cycloaddition with alkenes and alkynes (Figure 2.12). This reaction, first reported in the late 1800s,⁵³ has been proposed to proceed via a concerted cycloaddition since the 1950s, when Rolf Huisgen introduced the concept of 1,3-dipolar cycloadditions.⁵⁴ However, the high temperatures or pressures required to promote cycloaddition of azides and most dipolarophiles are not compatible with living systems.⁵⁵ Nevertheless, the potential of this transformation, especially the cycloaddition of azides and alkynes to form aromatic triazole products ($\Delta G^\circ \sim -61$ kcal/mol),⁵⁶ was too great for it to be overlooked.

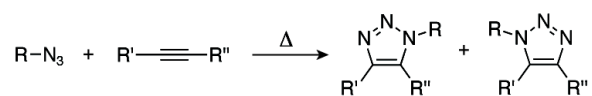


Figure 2.12. The 1,3-dipolar cycloaddition of azides and alkynes to yield regioisomeric triazole products.

In separate efforts, Sharpless and Meldal discovered that the formal 1,3-dipolar cycloaddition of azides with terminal alkynes to produce 1,4-disubstituted 1,2,3-triazoles could be effectively catalyzed by Cu(I) (Figure 2.13).^{57,58} This reaction, now termed the copper-catalyzed azide-alkyne 1,3-dipolar cycloaddition (CuAAC), takes advantage of Cu-acetylide formation to activate terminal alkynes toward reaction with azides. The result of Cu(I) catalysis is a reaction that proceeds roughly seven orders of magnitude faster than the uncatalyzed cycloaddition,⁵⁶ and the reaction can be further accelerated by the use of specific ligands for Cu(I).^{59,60} CuAAC has all the properties of a “click” reaction (including efficiency, simplicity, and selectivity), as defined by Sharpless and coworkers.⁶¹ In fact, it has become the quintessential click reaction and is often referred to simply as “click chemistry.” CuAAC has gained widespread use in organic synthesis, combinatorial chemistry, polymer chemistry, materials chemistry, and chemical biology.^{62,63,64} The formal cycloaddition between azides and terminal alkynes can also be catalyzed by Ru(II) to obtain 1,5-disubstituted 1,2,3-triazole products,⁶⁵ but this reaction is used far less frequently than CuAAC.

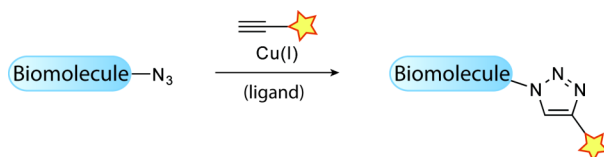


Figure 2.13. Cu(I) catalyzed formal cycloaddition between an azide and terminal alkyne to yield a 1,4-triazole product.

The first report of CuAAC as a bioconjugation strategy was demonstrated by Finn and coworkers through the attachment of dyes to cowpea mosaic virus.⁶⁶ Since that time, CuAAC has been applied in many azido-biomolecule labeling experiments. The Tirrell group has used click chemistry with a fluorogenic azidocoumarin dye (**2.34**) to study newly synthesized proteins that contain homopropargylglycine (**2.35**) as a methionine surrogate or ethynylphenylalanine (**2.36**) as a phenylalanine surrogate; however, the latter required a mutant tRNA synthetase (Figure 2.14).⁶⁷ Click chemistry has also been applied to proteomic analysis of newly synthesized proteins containing azidohomoalanine (**2.19**), a process termed bioorthogonal noncanonical amino acid tagging (BONCAT).⁶⁸

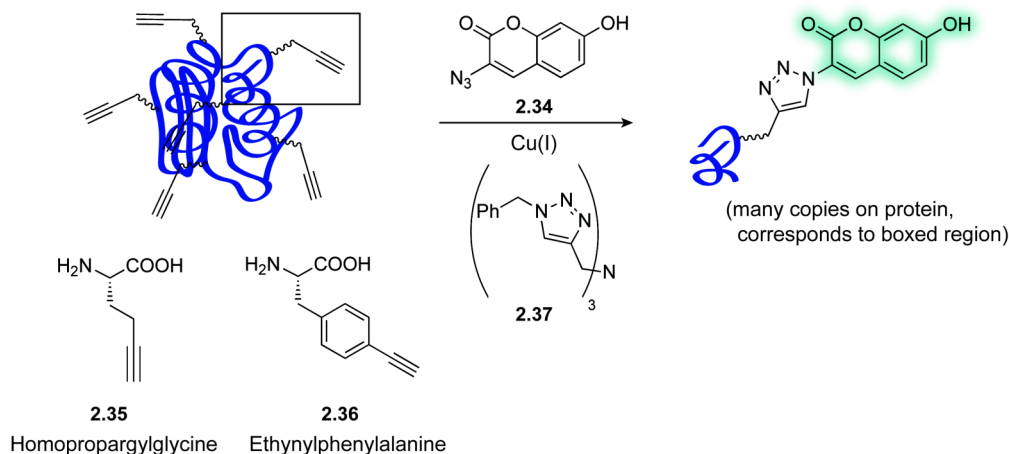


Figure 2.14. Metabolic incorporation of alkynyl functionality into proteins and subsequent detection by Cu(I)-catalyzed click chemistry with a fluorogenic azidocoumarin dye.

CuAAC has been employed for ABPP with great success by the Cravatt group. In a report that was published concurrent to Overkleeft's use of the Staudinger ligation, Cravatt and coworkers targeted serine hydrolases in live cells with an azide functionalized phenyl sulfonate warhead.⁶⁹ Cell lysates were treated with an alkyne-rhodamine probe in the presence of Cu(I). Cravatt and coworkers further showed that this two-step procedure allowed the extension of ABPP to live mice.⁶⁹ Shortly after their original report, Cravatt and coworkers used this strategy to profile breast cancer cells. They also determined that

the Cu(I)-catalyzed labeling procedure is more effective when the alkyne is attached to the electrophilic trap and detection is performed with an azido-probe.⁷⁰

The reagents necessary for click chemistry are small and simple. In addition, CuAAC gives one flexibility regarding the choice of chemical reporter group because both azides and terminal alkynes are compact, stable, and readily metabolically incorporated. CuAAC also benefits from fast reaction kinetics without compromising selectivity. These advantages have resulted in many fields of chemistry exploiting CuAAC. Unfortunately, CuAAC has a limited scope in terms of chemical biology applications due to the toxicity of Cu(I).⁷¹

Strain-Promoted Azide-Alkyne Cycloaddition

To overcome the liability of CuAAC, the Bertozzi group sought to avoid the use of transition metal catalysts altogether, hoping that a more biologically compatible method of activating alkynes toward reaction with azides could be found by mining the classic mechanistic literature. One intriguing strategy for enhancing the rate of the cycloaddition is the addition of ring strain. The first reports of rate-enhancement via ring strain precede the Huisgen era and date back to the 1930s when Alder and Stein discovered that dicyclopentadiene reacted considerably faster than cyclopentadiene in reactions with azides.^{72,73} Studies on strained alkenes and alkynes continued through the 1960s, and during this time, Wittig and Krebs reported that cyclooctyne, the smallest stable cycloalkyne, reacted “like an explosion” when combined with phenylazide to form triazole products.⁷⁴ The explosiveness of this transformation was noted years prior by Blomquist and Liu shortly after cyclooctyne was first synthesized, although they were unaware that the blast they observed was a result of a highly selective chemical reaction.⁷⁵ These early reports concerning the reactivity of cyclooctyne with azide were the foundation of the strain-promoted cycloaddition (Figure 2.15).

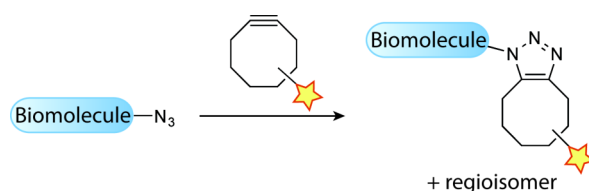


Figure 2.15. The strain-promoted cycloaddition between an azide and cyclooctyne to yield a triazole product.

Cyclooctyne **2.38** (Figure 2.16A, OCT) was the first cyclooctyne synthesized for the purpose of labeling azido-biomolecules.⁷⁶ OCT was further conjugated to biotin (OCT-biotin, **2.39**) and the FLAG peptide (OCT-FLAG, **2.40**) for detection of the cycloadducts in biological samples. While linear alkynes are essentially unreactive with azides at physiological temperature, OCT-biotin readily reacted with azide-labeled glycans

on proteins, within cell lysates, and on live cultured cells (Figure 2.16B/C). Most importantly, the compound exhibited no apparent toxicity, in stark contrast to the reagents for the Cu-catalyzed reaction. However, with a second-order rate constant of $0.0024 \text{ M}^{-1}\text{s}^{-1}$ in model reactions, OCT was no faster than the Staudinger ligation, and the compound also displayed unfavorable water-solubility properties.

Two modifications of OCT were made in an effort to accelerate the reaction and to improve its physical properties. The “aryl-less octyne” **2.41** (ALO, Figure 2.17A) had better water solubility but its kinetic properties were similar to those of OCT ($k = 0.0013 \text{ M}^{-1}\text{s}^{-1}$).⁷⁷ The first significant rate enhancement was achieved by addition of an electron-withdrawing fluorine atom at the propargylic position to yield a monofluorinated cyclooctyne (MOFO, **2.42**).⁷⁷ MOFO proved more reactive than OCT and ALO ($k = 0.0043 \text{ M}^{-1}\text{s}^{-1}$), and accordingly labeled azides in cell lysates and on cell-surfaces more rapidly when OCT-biotin (**2.39**), ALO-biotin (**2.43**), and MOFO-biotin (**2.44**) were compared (Figure 2.17B). A nonfluorinated version of MOFO (NOFO, **2.47**) was also synthesized to explore the effects of propargylic fluorination. NOFO proved to have similar reaction kinetics to ALO ($k = 0.0012 \text{ M}^{-1}\text{s}^{-1}$).

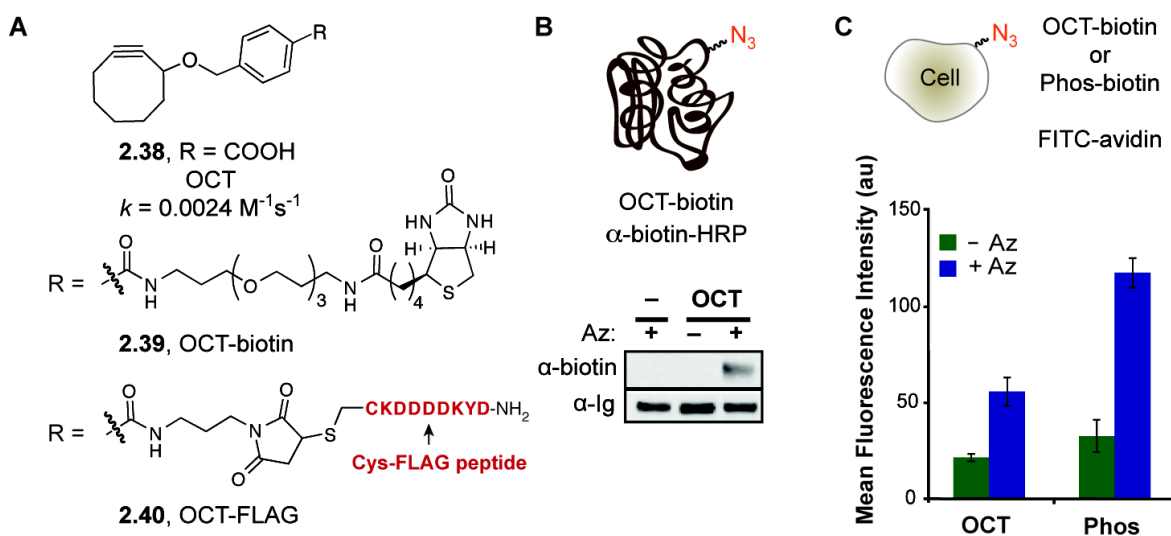


Figure 2.16. Cyclooctyne selectively reacts with azides through a strain-promoted cycloaddition. **A**. The original cyclooctyne OCT (**2.38**) as well as biotin and FLAG conjugates of OCT (**2.39** and **2.40**, respectively). **B**. OCT-biotin selectively labels an azide-modified form of the recombinant glycoprotein GlyCAM-IgG. Purified GlyCAM-IgG or azido-GlyCAM-IgG were incubated with 0 or 250 μM OCT-biotin (**2.39**) overnight at rt. The samples were analyzed by Western blot probing with an α -biotin-HRP antibody. An α -IgG antibody confirmed equal protein loading. **C**. OCT-biotin labels live cells in an azide-dependent manner. Jurkat cells were grown in the presence (+ Az, blue bars) or absence (- Az, green bars) of Ac₄ManNAz (25 μM). The cells were incubated with 100 μM OCT-biotin (**2.39**) or Phos-biotin (**2.10**) for 1 h at rt, followed by treatment with FITC-avidin and analyzed by flow cytometry.

The Tirrell group was quick to label proteins with cyclooctyne reagents. OCT-biotin (**2.39**) was used in a flow cytometry assay to screen for incorporation of azidonorleucine into recombinant proteins. This study successfully identified a key mutation in the methionyl-tRNA synthetase, which allowed for incorporation of this long-chain azido-amino acid.⁷⁸

While labeling of cell-surface glycans with cyclooctyne reagents was apparent, the efficiency of labeling was subpar. The Staudinger ligation still outperformed the cyclooctyne reagents in both Western blot and live cell-labeling experiments.⁷⁷ Thus, the major focus surrounding the strain-promoted cycloaddition was further enhancing the water-solubility and reactivity of these reagents so that dynamic biological processes could be monitored in real-time.

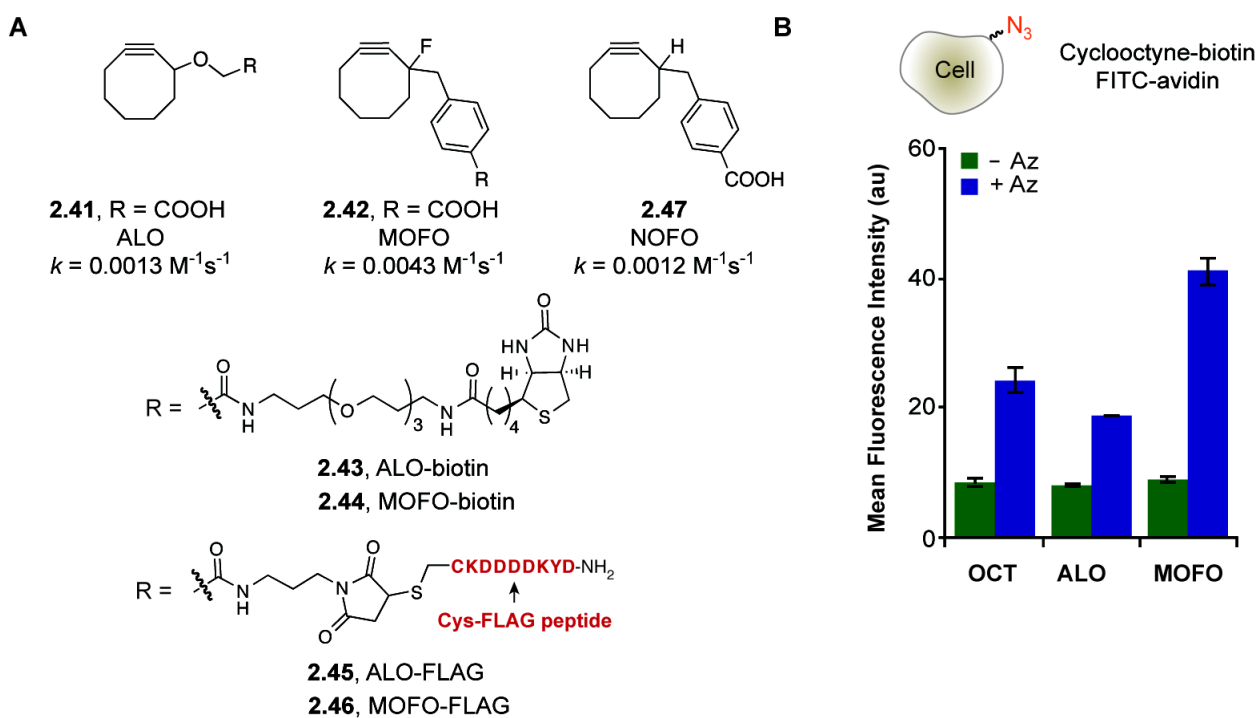


Figure 2.17. Initial improvements to cyclooctyne reagents for reaction with azides in biological systems. A. A more water-soluble aryl-less octyne (ALO, **2.41**), a more reactive monofluorinated cyclooctyne (MOFO, **2.42**) and a nonfluorinated cyclooctyne (NOFO, **2.47**) for determining the effect of propargylic fluorination on rate of reaction with azide. Also shown are biotin and FLAG conjugates of ALO and MOFO for further biological labeling experiments. B. Comparison of cyclooctyne reagents' ability to label cell-surface glycans. Jurkat cells were grown in the presence (+ Az, blue bars) or absence (- Az, green bars) of Ac_4ManNAz ($25 \mu\text{M}$ for 3 d). The cells were incubated with OCT-biotin, ALO-biotin, or MOFO-biotin ($250 \mu\text{M}$) for 1 h at rt, followed by treatment with FITC-avidin and analyzed by flow cytometry.

References

- (1) Sletten, E. M.; Bertozzi, C. R. Bioorthogonal chemistry: Fishing for selectivity in a sea of functionality. *Angew. Chem. Int. Ed.* **2009**, *48*, 6974-6998.
- (2) Prescher, J. A.; Bertozzi, C. R. Chemistry in living systems. *Nat. Chem. Biol.* **2005**, *1*, 13-21.
- (3) Staudinger, H.; Meyer, J. Über neue organische phosphorverbindungen III. Phosphinmethylenderivate und phosphinimine. *Helv. Chim. Acta* **1919**, *2*, 635-646.
- (4) Hendricks, S. B.; Pauling, L. The crystal structures of sodium and potassium trinitrides and potassium cyanate and the nature of the trinitride group. *J. Am. Chem. Soc.* **1925**, *47*, 2904-2920.
- (5) Sidgwick, N. V.; Sutton, L. E.; Thomas, W. 107. Dipole moments and structures of the organic azides and aliphatic diazo-compounds. *J. Chem. Soc.* **1933**, 406-412.
- (6) Knaggs, I. E. Crystal structure of cyanuric triazide. *Nature* **1935**, *135*, 268-268.
- (7) Bock, V. D. Hiemstra, H.; van Maarseveen, J. H. Cu(I)-catalyzed alkyne-azide "click" cycloadditions from a mechanistic and synthetic perspective. *Eur. J. Org. Chem.* **2006**, *2006*, 51-68.
- (8) Griffin, R. J. The medicinal chemistry of the azido group. *Prog. Med. Chem.* **1994**, *31*, 121-232.
- (9) Bräse, S.; Gil, C.; Knepper, K.; Zimmermann, V. Organic azides: An exploding diversity of a unique class of compounds. *Angew. Chem. Int. Ed.* **2005**, *44*, 5188-5240.
- (10) Kotzyba-Hibert, F.; Kapfer, I.; Goeldner, M. Recent trends in photoaffinity labeling. *Angew. Chem. Int. Ed.* **1995**, *34*, 1296-1312.
- (11) Schinazi, R. F.; Chu, C. K.; Eriksson, B. F.; Sommadossi, J.-P.; Doshi, K. J.; Boudinot, F. D.; Oswald, B.; McClure, H. M. Antiretroviral activity, biochemistry, and pharmacokinetics of 3'-azido-2',3'-dideoxy-5-methylcytidine. *Ann. N.Y. Acad. Sci.* **1990**, *616*, 385-397.
- (12) Saxon, E.; Bertozzi, C. R. Cell surface engineering by a modified Staudinger reaction. *Science* **2000**, *287*, 2007-2010.
- (13) Kiick, K. L.; Saxon, E.; Tirrell, D. A.; Bertozzi, C. R. Incorporation of azides into recombinant proteins for chemoselective modification by the Staudinger ligation. *Proc. Natl. Acad. Sci. U.S.A.* **2002**, *99*, 19-24.
- (14) Saxon, E.; Luchansky, S. J.; Hang, H. C.; Yu, C.; Lee, S. C.; Bertozzi, C. R. Investigating cellular metabolism of synthetic azidosugars with the Staudinger ligation. *J. Am. Chem. Soc.* **2002**, *124*, 14893-14902.
- (15) Prescher, J. A.; Dube, D. H.; Bertozzi, C. R. Chemical remodelling of cell surfaces in living animals. *Nature* **2004**, *430*, 873-877.
- (16) Vocadlo, D. J.; Hang, H. C.; Kim, E.-J.; Hanover, J. A.; Bertozzi, C. R. A chemical approach for identifying O-GlcNAc-modified proteins in cells. *Proc. Natl. Acad. Sci. U.S.A.* **2003**, *100*, 9116-9121.
- (17) Hang, H. C.; Yu, C.; Kato, D. L.; Bertozzi, C. R. A metabolic labeling approach toward proteomic analysis of mucin-type O-linked glycosylation. *Proc. Natl. Acad. Sci. U.S.A.* **2003**, *100*, 14846-14851.

- (18) Laughlin, S. T.; Agard, N. J.; Baskin, J. M.; Carrico, I. S.; Chang, P. V.; Ganguli, A. S.; Hangauer, M. J.; Lo, A.; Prescher, J. A.; Bertozzi, C. R. Metabolic labeling of glycans with azido sugars for visualization and glycoproteomics. *Meth. Enzymol.* **2006**, *415*, 230-250.
- (19) Dube, D. H.; Prescher, J. A.; Quang, C. N.; Bertozzi, C. R. Probing mucin-type O-linked glycosylation in living animals. *Proc. Natl. Acad. Sci. U.S.A.* **2006**, *103*, 4819-4824.
- (20) Luchansky, S. J.; Goon, S.; Bertozzi, C. R. Expanding the diversity of unnatural cell-surface sialic acids. *ChemBioChem* **2004**, *5*, 371-374.
- (21) Han, S.; Collins, B. E.; Bengtson, P.; Paulson, J. C. Homomultimeric complexes of CD22 in B cells revealed by protein-glycan cross-linking. *Nat. Chem. Biol.* **2005**, *1*, 93-97.
- (22) Link, A. J.; Mock, M. L.; Tirrell, D. A. Non-canonical amino acids in protein engineering. *Curr. Opin. Biotechnol.* **2003**, *14*, 603-609.
- (23) Hendrickson, T. L.; Crécy-Lagard, V. de; Schimmel, P. Incorporation of nonnatural amino acids into proteins. *Annu. Rev. Biochem.* **2004**, *73*, 147-176.
- (24) Budisa, N. Prolegomena to future experimental efforts on genetic code engineering by expanding its amino acid repertoire. *Angew. Chem. Int. Ed.* **2004**, *43*, 6426-6463.
- (25) Cowie, D. B.; Cohen, G. N. Biosynthesis by *Escherichia coli* of active altered proteins containing selenium instead of sulfur. *Biochem. Biophys. Acta* **1957**, *26*, 252-261.
- (26) Kast, P.; Hennecke, H. Amino acid substrate specificity of *Escherichia coli* phenylalanyl-tRNA synthetase altered by distinct mutations. *J. Mol. Biol.* **1991**, *222*, 99-124.
- (27) Ibba, M.; Kast, P.; Hennecke, H. Substrate specificity is determined by amino acid binding pocket size in *Escherichia coli* phenylalanyl-tRNA synthetase. *Biochemistry* **1994**, *33*, 7107-7112.
- (28) Kothakota, S.; Mason, T. L.; Tirrell, D. A.; Fournier, M. J. Biosynthesis of a periodic protein containing 3-thienylalanine: A step toward genetically engineered conducting polymers. *J. Am. Chem. Soc.* **1995**, *117*, 536-537.
- (29) Sharma, N.; Furter, R.; Kast, P.; Tirrell, D. A. Efficient introduction of aryl bromide functionality into proteins in vivo. *FEBS Lett.* **2000**, *467*, 37-40.
- (30) Kirshenbaum, K.; Carrico, I. S.; Tirrell, D. A. Biosynthesis of proteins incorporating a versatile set of phenylalanine analogues. *ChemBioChem* **2002**, *3*, 235-237.
- (31) Kodama, K.; Fukuzawa, S.; Nakayama, H.; Kigawa, T.; Sakamoto, K.; Yabuki, T.; Matsuda, N.; Shirouzu, M.; Takio, K.; Tachibana, K.; Yokoyama, S. Regioselective carbon-carbon bond formation in proteins with palladium catalysis; New protein chemistry by organometallic chemistry. *ChemBioChem* **2006**, *7*, 134-139.
- (32) Kodama, K.; Fukuzawa, S.; Nakayama, H.; Sakamoto, K.; Kigawa, T.; Yabuki, T.; Matsuda, N.; Shirouzu, M.; Takio, K.; Yokoyama, S.; Tachibana, K. Site-specific functionalization of proteins by organopalladium reactions. *ChemBioChem* **2007**, *8*, 232-238.
- (33) Kho, Y.; Kim, S. C.; Jiang, C.; Barma, D.; Kwon, S. W.; Cheng, J.; Jaunbergs, J.; Weinbaum, C.; Tamanoi, F.; Falck, J.; Zhao, Y. A tagging-via-substrate technology

- for detection and proteomics of farnesylated proteins. *Proc. Natl. Acad. Sci. U.S.A.* **2004**, *101*, 12479 -12484.
- (34) Comstock, L. R.; Rajski, S. R. Conversion of DNA methyltransferases into azidonucleosidyl transferases via synthetic cofactors. *Nucleic Acids Res.* **2005**, *33*, 1644 -1652.
- (35) Comstock, L. R.; Rajski, S. R. Efficient synthesis of azide-bearing cofactor mimics. *J. Org. Chem.* **2004**, *69*, 1425-1428.
- (36) Speers, A. E.; Cravatt, B. F. Chemical strategies for activity-based proteomics. *ChemBioChem* **2004**, *5*, 41-47.
- (37) Uttamchandani, M.; Li, J.; Sun, H.; Yao, S. Q. Activity-based protein profiling: New developments and directions in functional proteomics. *ChemBioChem* **2008**, *9*, 667-675.
- (38) Evans, M. J.; Cravatt, B. F. Mechanism-based profiling of enzyme families. *Chem. Rev.* **2006**, *106*, 3279-3301.
- (39) Ovaa, H.; van Swieten, P. F.; Kessler, B. M.; Leeuwenburgh, M. A.; Fiebigler, E.; van den Nieuwendijk, A. M. C. H.; Galardy, P. J.; van der Marel, G. A.; Ploegh, H. L.; Overkleeft, H. S. Chemistry in living cells: Detection of active proteasomes by a two-step labeling strategy. *Angew. Chem. Int. Ed.* **2003**, *42*, 3626-3629.
- (40) Hang, H. C.; Loureiro, J.; Spooner, E.; van der Velden, A. W. M.; Kim, Y.-M.; Pollington, A. M.; Maehr, R.; Starnbach, M. N.; Ploegh, H. L. Mechanism-based probe for the analysis of cathepsin cysteine proteases in living cells. *ACS Chem. Biol.* **2006**, *1*, 713-723.
- (41) Isin, E. M.; Guengerich, F. P. Complex reactions catalyzed by cytochrome P450 enzymes. *BBA-Gen. Subjects* **2007**, *1770*, 314-329.
- (42) Phillips, I. R.; Shephard, E. A. Flavin-containing monooxygenases: Mutations, disease and drug response. *Trends Pharmacol. Sci.* **2008**, *29*, 294-301.
- (43) Lin, F. L.; Hoyt, H. M.; van Halbeek, H.; Bergman, R. G.; Bertozzi, C. R. Mechanistic investigation of the Staudinger ligation. *J. Am. Chem. Soc.* **2005**, *127*, 2686-2695.
- (44) Chang, P. V.; Prescher, J. A.; Hangauer, M. J.; Bertozzi, C. R. Imaging cell surface glycans with bioorthogonal chemical reporters. *J. Am. Chem. Soc.* **2007**, *129*, 8400-8401.
- (45) Lemieux, G. A.; de Graffenried, C. L.; Bertozzi, C. R. A fluorogenic dye activated by the Staudinger ligation. *J. Am. Chem. Soc.* **2003**, *125*, 4708-4709.
- (46) Soellner, M. B.; Nilsson, B. L.; Raines, R. T. Reaction mechanism and kinetics of the traceless Staudinger ligation. *J. Am. Chem. Soc.* **2006**, *128*, 8820-8828.
- (47) Nilsson, B. L.; Kiessling, L. L.; Raines, R. T. Staudinger ligation: A peptide from a thioester and azide. *Org. Lett.* **2000**, *2*, 1939-1941.
- (48) Nilsson, B. L.; Kiessling, L. L.; Raines, R. T. High-yielding Staudinger ligation of a phosphinothioester and azide to form a peptide. *Org. Lett.* **2001**, *3*, 9-12.
- (49) Soellner, M. B.; Tam, A.; Raines, R. T. Staudinger ligation of peptides at non-glycyl residues. *J. Org. Chem.* **2006**, *71*, 9824-9830.
- (50) Saxon, E.; Armstrong, J. I.; Bertozzi, C. R. A "traceless" Staudinger ligation for the chemoselective synthesis of amide bonds. *Org. Lett.* **2000**, *2*, 2141-2143.

- (51) Tam, A.; Soellner, M. B.; Raines, R. T. Electronic and steric effects on the rate of the traceless Staudinger ligation. *Org. Biomol. Chem.* **2008**, *6*, 1173-1175.
- (52) Tam, A.; Raines, R. T. Coulombic effects on the traceless Staudinger ligation in water. *Bioorg. Med. Chem. Lett.* **2009**, *17*, 1055-1063.
- (53) Michael, A. Ueber die einwirkung von diazobenzolimid auf acetylendicarbons uremethylester. *J. Prakt. Chem.* **1893**, *48*, 94-95.
- (54) Huisgen, R. 1,3-Dipolar cycloadditions. Past and future. *Angew. Chem. Int. Ed.* **1963**, *2*, 565-598.
- (55) Hartzel, L. W.; Benson, F. R. Synthesis of 4-alkyl-1,2,3-triazoles from acetylenic compounds and hydrogen azide. *J. Am. Chem. Soc.* **1954**, *76*, 667-670.
- (56) Himo, F.; Lovell, T.; Hilgraf, R.; Rostovtsev, V. V.; Noodleman, L.; Sharpless, K. B.; Fokin, V. V. Copper(I)-catalyzed synthesis of azoles. DFT study predicts unprecedented reactivity and intermediates. *J. Am. Chem. Soc.* **2005**, *127*, 210-216.
- (57) Rostovtsev, V. V.; Green, L. G.; Fokin, V. V.; Sharpless, K. B. A stepwise Huisgen cycloaddition process: Copper(I)-catalyzed regioselective "ligation" of azides and terminal alkynes. *Angew. Chem. Int. Ed.* **2002**, *41*, 2596-2599.
- (58) Tornøe, C. W.; Christensen, C.; Meldal, M. Peptidotriazoles on solid phase: [1,2,3]-Triazoles by regiospecific copper(I)-catalyzed 1,3-dipolar cycloadditions of terminal alkynes to azides. *J. Org. Chem.* **2002**, *67*, 3057-3064.
- (59) Rodionov, V. O.; Presolski, S. I.; Díaz Díaz, D.; Fokin, V. V.; Finn, M. G. Ligand-accelerated Cu-catalyzed azide-alkyne cycloaddition: A mechanistic report. *J. Am. Chem. Soc.* **2007**, *129*, 12705-12712.
- (60) Chan, T. R.; Hilgraf, R.; Sharpless, K. B.; Fokin, V. V. Polytriazoles as copper(I)-stabilizing ligands in catalysis. *Org. Lett.* **2004**, *6*, 2853-2855.
- (61) Kolb, H. C.; Finn, M. G.; Sharpless, K. B. Click chemistry: Diverse chemical function from a few good reactions. *Angew. Chem. Int. Ed.* **2001**, *40*, 2004-2021.
- (62) Kolb, H. C.; Sharpless, K. B. The growing impact of click chemistry on drug discovery. *Drug Discov. Today* **2003**, *8*, 1128-1137.
- (63) Breinbauer, R.; Köhn, M. Azide-alkyne coupling: A powerful reaction for bioconjugate chemistry. *ChemBioChem* **2003**, *4*, 1147-1149.
- (64) Dondoni, A. Triazole: The keystone in glycosylated molecular architectures constructed by a click reaction. *Chem. Asian J.* **2007**, *2*, 700-708.
- (65) Zhang, L.; Chen, X.; Xue, P.; Sun, H. H. Y.; Williams, I. D.; Sharpless, K. B.; Fokin, V. V.; Jia, G. Ruthenium-catalyzed cycloaddition of alkynes and organic azides. *J. Org. Chem.* **2005**, *127*, 15998-15999.
- (66) Wang, Q.; Chan, T. R.; Hilgraf, R.; Fokin, V. V.; Sharpless, K. B.; Finn, M. G. Bioconjugation by copper(I)-catalyzed azide-alkyne [3 + 2] cycloaddition. *J. Am. Chem. Soc.* **2003**, *125*, 3192-3193.
- (67) Beatty, K. E.; Xie, F.; Wang, Q.; Tirrell, D. A. Selective dye-labeling of newly synthesized proteins in bacterial cells. *J. Am. Chem. Soc.* **2005**, *127*, 14150-14151.
- (68) Dieterich, D. C.; Link, A. J.; Graumann, J.; Tirrell, D. A.; Schuman, E. M. Selective identification of newly synthesized proteins in mammalian cells using bioorthogonal noncanonical amino acid tagging (BONCAT). *Proc. Natl. Acad. Sci. U.S.A.* **2006**, *103*, 9482-9487.

- (69) Speers, A. E.; Adam, G. C.; Cravatt, B. F. Activity-based protein profiling in vivo using a copper(I)-catalyzed azide-alkyne [3 + 2] cycloaddition. *J. Am. Chem. Soc.* **2003**, *125*, 4686-4687.
- (70) Speers, A. E.; Cravatt, B. F. Profiling enzyme activities in vivo using click chemistry methods. *Chem. Biol.* **2004**, *11*, 535-546.
- (71) Wolbers, F.; ter Braak, P.; Le Gac, S.; Luttge, R.; Andersson, H.; Vermes, I.; van den Berg, A. Viability study of HL60 cells in contact with commonly used microchip materials. *Electrophoresis* **2006**, *27*, 5073-5080.
- (72) Alder, K.; Stein, G. Über das abgestufte additionsvermögen von ungesättigten ringsystemen. *Justus Liebigs Ann. Chem.* **1933**, *501*, 1-48.
- (73) Alder, K.; Stein, G.; Finzenhagen, H. Über das abgestufte additionsvermögen von ungesättigten ringsystemen. *Justus Liebigs Ann. Chem.* **1931**, *485*, 211-222.
- (74) Wittig, G.; Krebs, A. Zur Existenz niedergliedriger Cycloalkine, I. *Chem. Ber.* **1961**, *94*, 3260-3275.
- (75) Blomquist, A. T.; Liu, L. H. Many-membered carbon rings. VII. Cycloöctyne. *J. Am. Chem. Soc.* **1953**, *75*, 2153-2154.
- (76) Agard, N. J.; Prescher, J. A.; Bertozzi, C. R. A strain-promoted [3 + 2] azide-alkyne cycloaddition for covalent modification of biomolecules in living systems. *J. Am. Chem. Soc.* **2004**, *126*, 15046-15047.
- (77) Agard, N. J.; Baskin, J. M.; Prescher, J. A.; Lo, A.; Bertozzi, C. R. A comparative study of bioorthogonal reactions with azides. *ACS Chem. Biol.* **2006**, *1*, 644-648.
- (78) Link, A. J.; Vink, M. K. S.; Agard, N. J.; Prescher, J. A.; Bertozzi, C. R.; Tirrell, D. A. Discovery of aminoacyl-tRNA synthetase activity through cell-surface display of noncanonical amino acids. *Proc. Natl. Acad. Sci. U.S.A.* **2006**, *103*, 10180-10185.

Chapter 3

A Hydrophilic Azacyclooctyne

Cu-Free Click Chemistry

At the beginning of my doctoral work, the potential of cyclooctynes as bioorthogonal reactive partners for azides was just becoming a reality in the Bertozzi group. A difluorinated cyclooctyne (DIFO, **3.1**, Figure 3.1A) with enhanced reaction kinetics had just been synthesized.¹ This cyclooctyne was 60-times more reactive than previous bioorthogonal chemistries for the azide (the Staudinger ligation and early generation cyclooctynes for the strain-promoted cycloaddition, **2.38**, **2.41-2.42**) and DIFO transformed the strain-promoted cycloaddition into Cu-free click chemistry. The large second-order rate constant for the reaction of DIFO with benzyl azide ($k = 0.076 \text{ M}^{-1}\text{s}^{-1}$) was attributed to the two propargylic fluorine atoms lowering the LUMO level of the cyclooctyne. Since the report of DIFO, this rate-enhancement has been confirmed by DFT studies,^{2,3} although theoretical work has shown that other factors such as distortion energy and bond polarization also contribute to the reactivity of DIFO.⁴

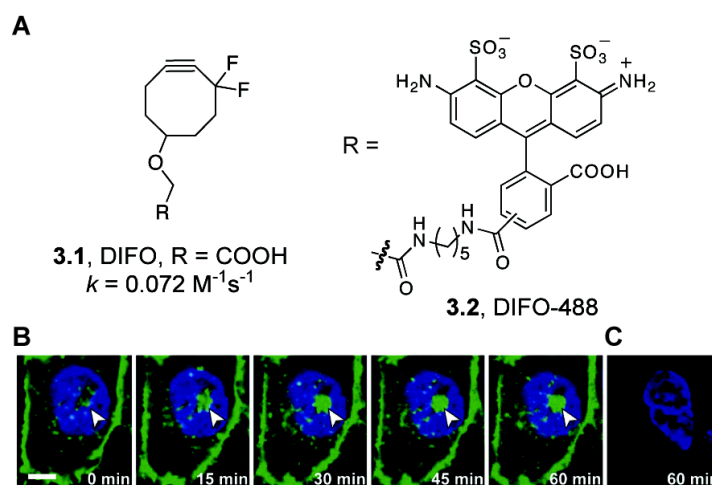


Figure 3.1. A. Difluorinated cyclooctyne (DIFO) **3.1** and an Alexa Fluor-488 conjugate (DIFO-488, **3.2**) for direct imaging of azides. B/C. DIFO-488 enables dynamic live cell labeling of azides. B. Chinese Hamster Ovary (CHO) cells were grown in the presence of peracetylated N-azidoacetyl mannosamine (Ac₄ManNAz, 100 μM) for 3 d. The cells were washed and incubated with DIFO-488 (100 μM) for 1 min. Images were then collected at varying time points and glycan endocytosis over this time was observed. Green = DIFO-488. Blue = Hoechst 3342 nuclear stain. C. CHO cells treated with DIFO as described in part B but not grown in the presence of azidosugar.

The highly reactive nature of DIFO allowed dynamic imaging experiments to be performed using bioorthogonal chemistry for the first time. Sialic acid containing glycans on live Chinese Hamster Ovary (CHO) cells were labeled with azides through the metabolic incorporation of N-azidoacetyl mannosamine (ManNAz) and subsequently treated with DIFO-488 (**3.2**). The azido-glycoproteins could be visualized after only 1 min of labeling, facilitating the study of glycan endocytosis (Figure 3.1B/C).¹

Initial Attempts at Cu-Free Click Chemistry in Mice

The success of DIFO reagents at imaging azido-glycan dynamics prompted the use of DIFO in higher organisms. The laboratory mouse is widely regarded as the model organism of choice for human disease,⁵ and thus, a major goal for Cu-free click chemistry was for it to proceed efficiently in this organism. To analyze the ability for DIFO to label azides in mice, DIFO was conjugated to the FLAG peptide (DIFO-FLAG, **3.3**, Figure 3.2A).¹⁶ DIFO-FLAG was injected into mice that were treated with or without Ac₄ManNAz once daily for 7 days prior. Three hours after injection of DIFO-FLAG, the mice were sacrificed and the organs were harvested. Mice treated with and without azide were also injected with Phos-FLAG (**2.10**) as a control. A live-cell analysis of the splenocytes treated with DIFO-FLAG vs. Phos-FLAG revealed that, while Cu-free click chemistry had more favorable reaction kinetics *in vitro* and displayed enhanced azide-dependent labeling on live cells than the Staudinger ligation (Figure 3.2B), the Staudinger ligation was the superior reaction for labeling cell-surface azido-glycans in mice (Figure 3.2C).⁶

Some insight regarding the sub par performance of DIFO *in vivo* was gained upon Western blot analysis of organ lysates (heart, liver, and intestines). While both DIFO and Phos displayed azide-dependent labeling in these organs (Figure 3.3A/B), DIFO exhibited a striking amount of background labeling centered around 65 kDa.⁶ A series of immunoprecipitation experiments indicated that the band at 65 kDa in the vehicle treated mice corresponded to mouse serum albumin (MSA, Figure 3.3C-F), a highly abundant protein known to strongly bind hydrophobic molecules.⁷ Thus, we hypothesized that the hydrophobicity of DIFO was severely limiting its bioavailable concentration inside the mouse, precluding efficient labeling of azido-glycans.

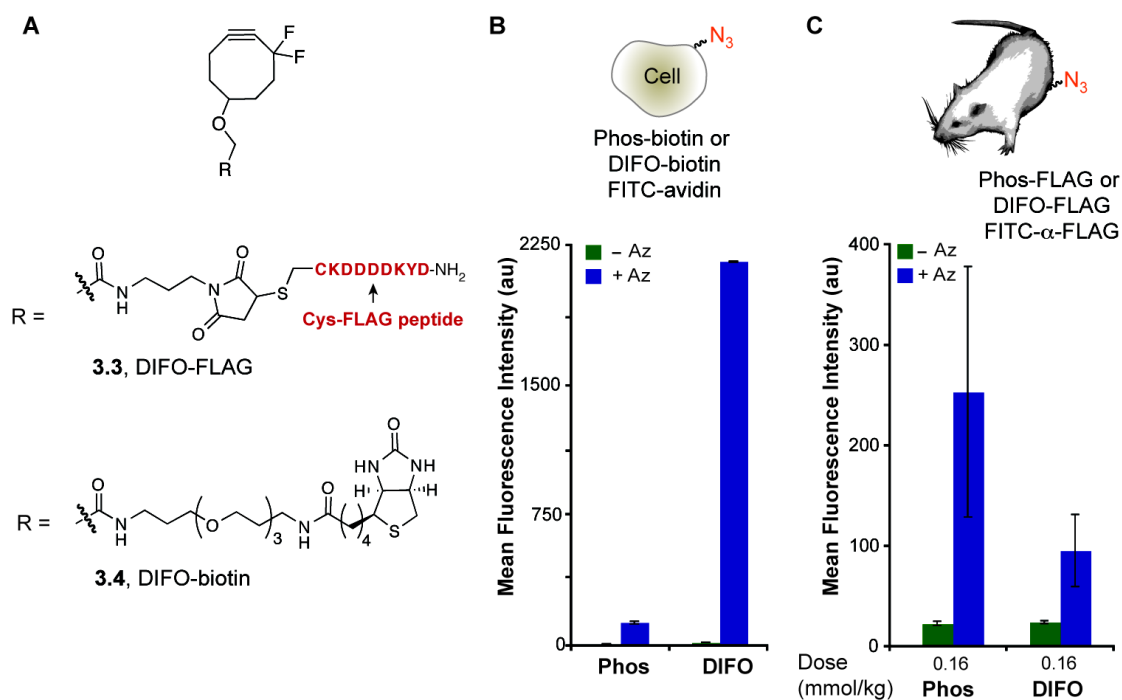


Figure 3.2. A. DIFO conjugated to the FLAG peptide (**3.3**) or biotin (**3.4**) for labeling azides on live cells and in living mice. B. Cu-free click chemistry with DIFO is superior to the Staudinger ligation at labeling cell-surface azides. Jurkat cells were grown in the presence (blue bars) or absence (green bars) of Ac₄ManNAz (25 μM) for 3 d. The cells were incubated with Phos-biotin (**2.10**) or DIFO-biotin (**3.4**) (100 μM) for 1 h at rt, followed by treatment with FITC-avidin and analyzed by flow cytometry. C. The Staudinger ligation is the superior reaction for labeling cell-surface associated azido-glycans in mice. Mice were injected once daily with (blue bars) or without (green bars) Ac₄ManNAz for 7 d. On the eighth day, Phos-FLAG (**2.11**) or DIFO-FLAG (**3.3**) was injected (0.16 mmol/kg, IP). After 3 h, the mice were sacrificed, their splenocytes were isolated, incubated with FITC-α-FLAG and analyzed by flow cytometry. Au = arbitrary units.

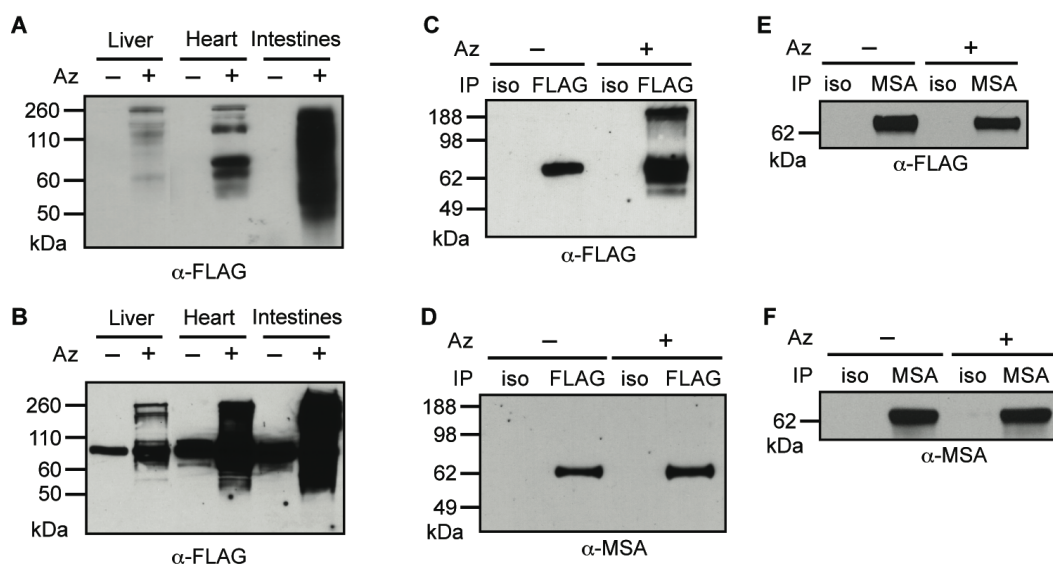


Figure 3.3. A/B. Cu-free click chemistry and Staudinger ligation products are observed in a variety of tissues *in vivo*. Mice were injected with Ac₄ManNAz (300 mg/kg, + Az) or vehicle (70% DMSO, – Az) once daily for 7 d. On day 8, the mice were injected with either or (A) Phos-FLAG (0.8 mmol/kg) or (B) DIFO-FLAG (0.16 mmol/kg). Three hours post-injection of the FLAG conjugate, the mice were euthanized, and organs (liver, heart, intestines) were harvested and homogenized. The organ lysates were analyzed by Western blot probing with α -FLAG-HRP. Each lane represents organ lysate from a single representative mouse. C-F. DIFO-FLAG binds mouse serum albumin (MSA). Liver lysates generated as described in (B) were immunoprecipitated with (C-D) an α -FLAG antibody (FLAG) or an isotype control (iso), or (E-F) an α -MSA antibody (MSA) or an isotype control (iso). The samples were analyzed by Western blot probing for (C, E) FLAG or (D, F) MSA.

Other results obtained when earlier generation cyclooctynes (OCT, ALO, MOFO) were analyzed for their ability to label azides within mice supported the hypothesis that the hydrophobic nature of the cyclooctynes was hindering Cu-free click chemistry *in vivo*. Of the three earlier generation cyclooctynes, ALO-FLAG (**2.45**) was the only cyclooctyne reagent, which displayed azide-dependent labeling *in vivo*, even though OCT-FLAG (**2.40**) and MOFO-FLAG (**2.46**) both exhibited improved reaction kinetics with azides (Figure 3.4).⁶ We attributed this result to the fact that ALO-FLAG did not contain an aryl ring and was more hydrophilic than OCT-FLAG and MOFO-FLAG. Taking all these data into consideration, we felt Cu-free click chemistry *in vivo* would be improved by a considerably more hydrophilic cyclooctyne.

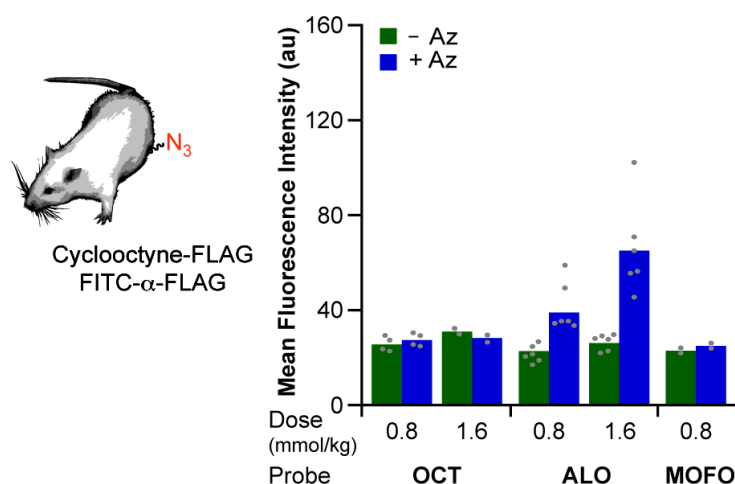


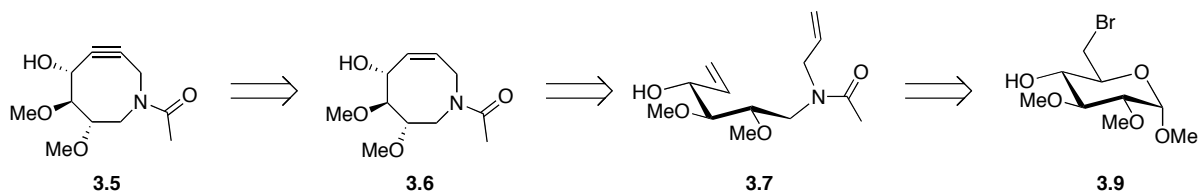
Figure 3.4. Early generation cyclooctynes do not display robust azide-dependent labeling *in vivo*. Mice were injected with either $Ac_4ManNAz$ (300 mg/kg, IP, blue bars) or vehicle (70% DMSO, green bars) once daily for 7 d. On day 8, the mice were injected IP with various doses (as indicated) of OCT-FLAG (**2.40**), ALO-FLAG (**2.45**), or MOFO-FLAG (**2.46**). After 3 h, the mice were euthanized, and splenocytes were isolated, labeled with FITC- α -FLAG and analyzed by flow cytometry. Each point represents the average mean fluorescence intensity value of three replicate samples from an individual mouse. Each bar represents the average mean fluorescence intensity value of splenocytes isolated from separate mice ($n = 3-6$). Au = arbitrary units. For all *in vivo* experiments, *ex vivo* reactions of isolated splenocytes with FLAG conjugates verified the presence of cell-surface azides for all of these probes.

Design of a More Hydrophilic Cyclooctyne

To design a more hydrophilic cyclooctyne, we looked toward nature's most abundant cyclic molecules: carbohydrates. Carbohydrates not only contain polar functionality appended to their core ring structure, but also have an oxygen to break up the hydrocarbon chain. We envisioned applying these two components to a cyclooctyne with our heteroatom of choice being the nitrogen of an exocyclic amide. Additionally, for synthetic ease and long-term stability of the cyclooctyne,⁸ we chose to append ether groups off the core scaffold.

Our initial target cyclooctyne was azacyclooctyne **3.5** (Scheme 3.1), which could be obtained from a carbohydrate starting material. Strained-alkyne formation could be achieved from cyclooctene **3.6** through a bromination-double elimination sequence commonly employed for cyclooctyne synthesis.⁹ The azacyclooctene core could be formed through ring-closing metathesis of **3.7**. Amide **3.7** could be prepared from an appropriately functionalized glucopyranoside (**3.9**) by a one-pot zinc reduction/reductive amination with allylamine.

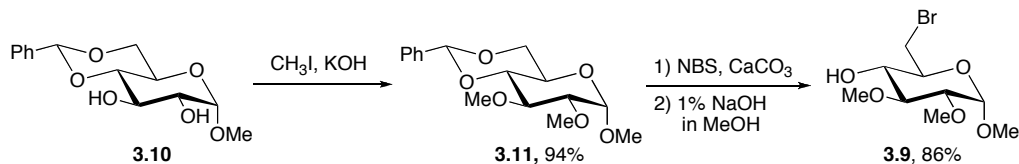
Scheme 3.1. Retrosynthesis of hydrophilic azacyclooctyne **3.5**.



Synthesis of a Hydrophilic Azacyclooctyne

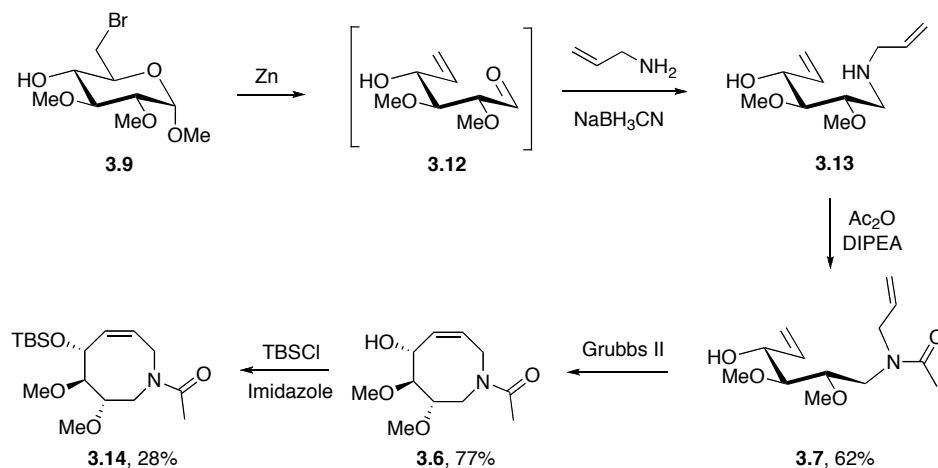
Standard carbohydrate chemistry commencing from commercially available methyl 4,6-O-benzylidene- α ,D-glucopyranoside (**3.10**) facilitated the formation of **3.9** (Scheme 3.2).¹⁰ The C-2 and C-3 hydroxyl groups were converted to methyl ethers by alkylation with methyl iodide to yield **3.11** in 92% yield. Subjecting **3.11** to N-bromosuccinimide under radical conditions converted the benzylidene protecting group into a C-4 benzoate group and concomitantly installed a bromine atom at the C-6 position.¹¹ Saponification of the benzoate group resulted in the desired glucopyranoside **3.9** in 88% yield over 2 steps.

Scheme 3.2. Synthesis of 6-bromo-1,2,3-trimethoxy- α ,D-glucopyranoside (**3.9**).



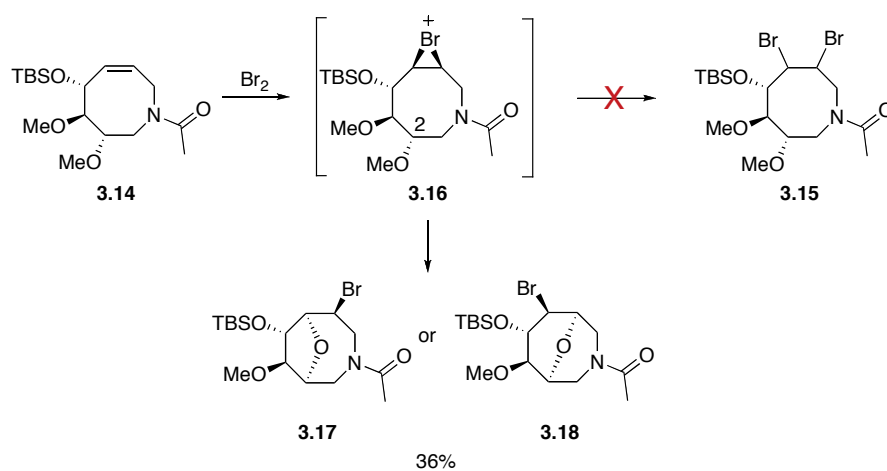
Methyl 6-deoxy-6-bromo-2,3-di-O-methyl- α ,D-glucopyranoside **3.9** was treated with zinc, which reduced the bromine atom causing a chain elimination reaction that displaced the anomeric methoxy group and yielded *in situ* generated aldehyde **3.12**, which immediately underwent reductive amination with allylamine to afford **3.13**.¹² The amine was acetylated with acetic anhydride before purification. This sequence resulted in 62% yield of amide **3.7**, that upon treatment with Grubbs second-generation catalyst gave desired azacyclooctene **3.6**.¹³ The allylic alcohol was protected as a *tert*-butyl dimethyl silyl ether using standard conditions to give **3.14** (Scheme 3.3).

Scheme 3.3. Conversion of 6-bromoglucopyranoside **3.9** to azacyclooctene **3.14**.



All attempts to isolate **3.15** through subjecting **3.14** to bromine were unsuccessful. Instead, a bicyclic compound containing only one bromine atom (either isomer **3.17** or **3.18**) was isolated (Scheme 3.4). This monobrominated product presumably arose from the intramolecular reaction of the C-2 methoxy group with the bromonium ion in intermediate **3.16**. Reactivity of this type is well-precedented when cyclooctene-ols are subjected to bromine;¹⁴ however, it was unexpected that the much less nucleophilic methoxy group rapidly underwent this transformation.

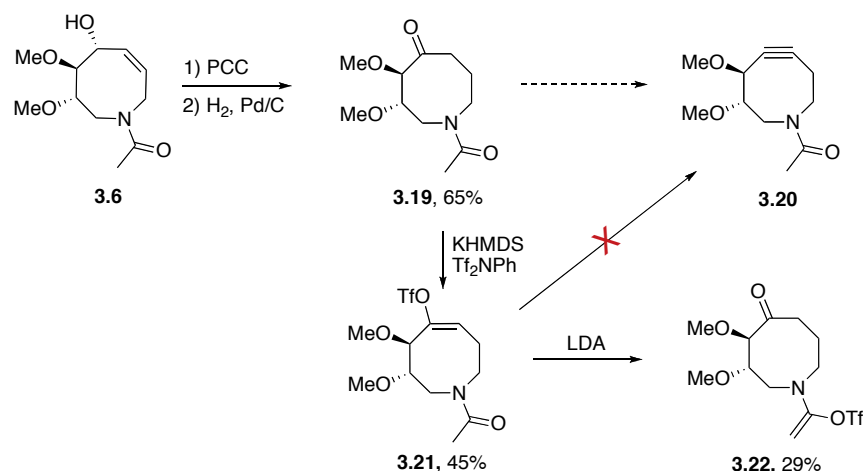
Scheme 3.4. Bromination of azacyclooctene **3.14**.



It appeared that alkyne formation from an alkene precursor was not going to be a productive synthetic pathway for the azacyclooctyne, as it was complicated by reactivity of the appended polar functionality. Instead, we looked to another common strained alkyne synthon– the ketone.¹⁵ The allylic alcohol of **3.6** was easily converted to ketone **3.19** through oxidation with PCC followed by reduction with H₂ and Pd/C. Conversion of ketone **3.19** to the strained alkyne would result in a different azacyclooctene than the original target molecule (**3.20**). Luckily, bioorthogonal reaction development gives one the flexibility to change a target molecule as long as it still contains the initial requirements. In this case, the nitrogen atom within the ring as well as the polar functional groups appended to the ring were still present. The main modification was the propargylic hydroxyl group in **3.5** was eliminated. This was the intended point of attachment of a chemical probe; however, a probe group could also be envisioned off the exocyclic acetyl group.

The synthesis of MOFO (**2.42**) and DIFO (**3.1**) both proceeded through ketone synthons by formation of a vinyl triflate and subsequent *syn*-elimination of triflic acid with LDA.^{1,16} Performing this same sequence on ketone **3.19** (Scheme 3.5) did yield vinyl triflate **3.21**; however, when **3.21** was subjected to LDA, transfer of the triflate to the acetyl group (compound **3.22**) was observed. A screen of other bases did not yield the desired cyclooctyne.

Scheme 3.5. Attempts at the synthesis of an azacyclooctyne through vinyl triflate **3.21**.

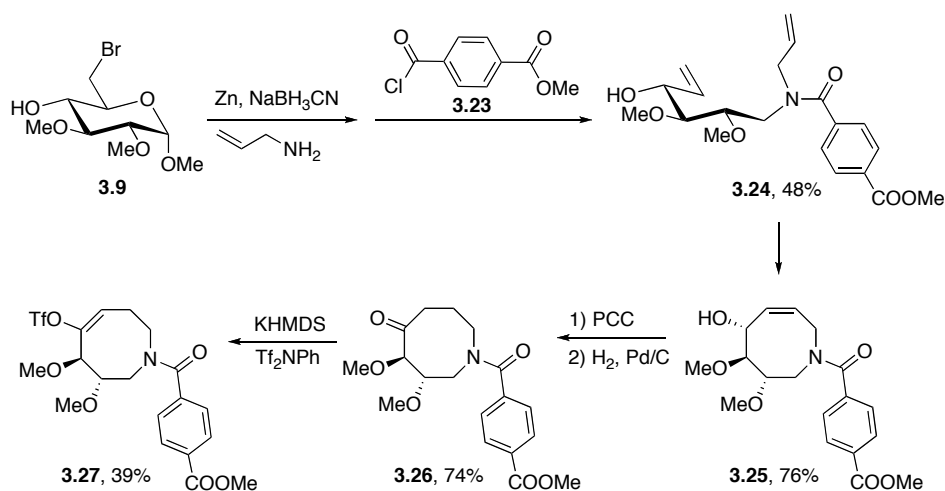


The results from compound **3.21** suggested that enolizable protons on the acetyl group were problematic for the harsh basic conditions necessary to convert **3.21** to **3.20**. To solve this problem, we exchanged the acetyl group for a linker group that did not contain any enolizable protons. Altering the acetyl group necessitated exchanging the activated carbonyl compound employed after the one-pot zinc reduction/reductive amination reaction. We chose methyl 4-(chlorocarbonyl)benzoate (**3.23**) as the activated

carbonyl compound as it would not only remove enolizable protons but it contained a methyl ester, which would allow for easy conjugation of probes to the azacyclooctyne. Although it should be noted that the addition of the aryl group was not ideal for reaching the end goal of a hydrophilic cyclooctyne.

The synthesis with the aryl linker group (Scheme 3.6) proceeded analogously to the synthesis of **3.19** without problems to yield ketone **3.26**. The ketone was again converted to a vinyl triflate (**3.27**) and subjected to LDA. Without enolizable protons, compound **3.27** was surprisingly stable toward LDA and numerous other strong bases. When forcing conditions were employed, only decomposition and hydrolysis of the methyl ester were observed. These results indicated vinyl triflate formation, like bromination, was not a productive alkyne formation strategy for a hydrophilic azacyclooctyne.

Scheme 3.6. Synthesis of vinyl triflate **3.27** containing an aryl ring linker group.



While vinyl triflate precursors have been the most advantageous precursor for cyclooctynes in our hands, there are a number of synthetic pathways for formation of a strained alkyne from a ketone. Another option involves formation of a selenadiazole by condensation with semicarbazide and oxidation with selenium dioxide. The selenadiazole can undergo thermal or nucleophile-promoted extrusion of N₂ and Se to yield an alkyne.^{17,18,19,20} Alternatively, oxidation to a diketone followed by condensation with hydrazine yields a bis(hydrazone) which upon treatment with a metal oxide (generally lead tetraacetate) results in an alkyne.^{21,22}

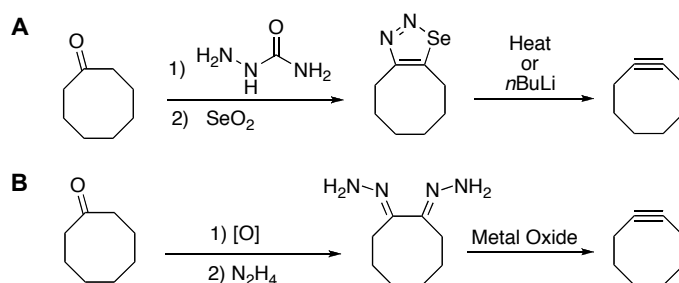
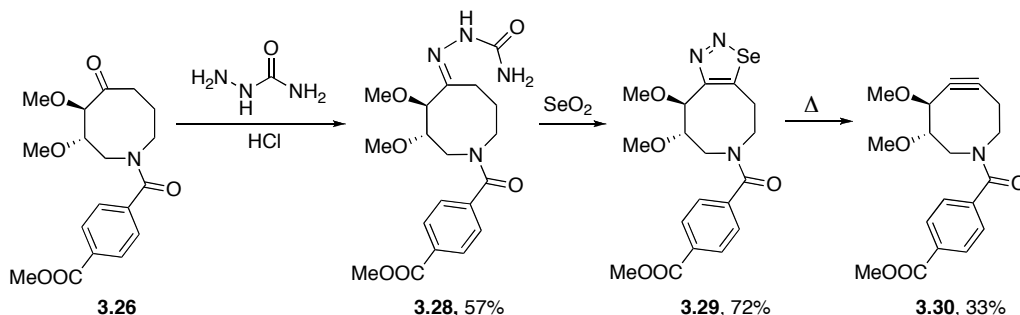


Figure 3.5. Strategies for cyclooctyne synthesis from a ketone. A. Selenadiazole formation followed by fragmentation to the cyclooctyne. B. Oxidation to the diketone, condensation with hydrazine, and treatment of the bishydrazone with a metal oxide to form the desired cyclooctyne.

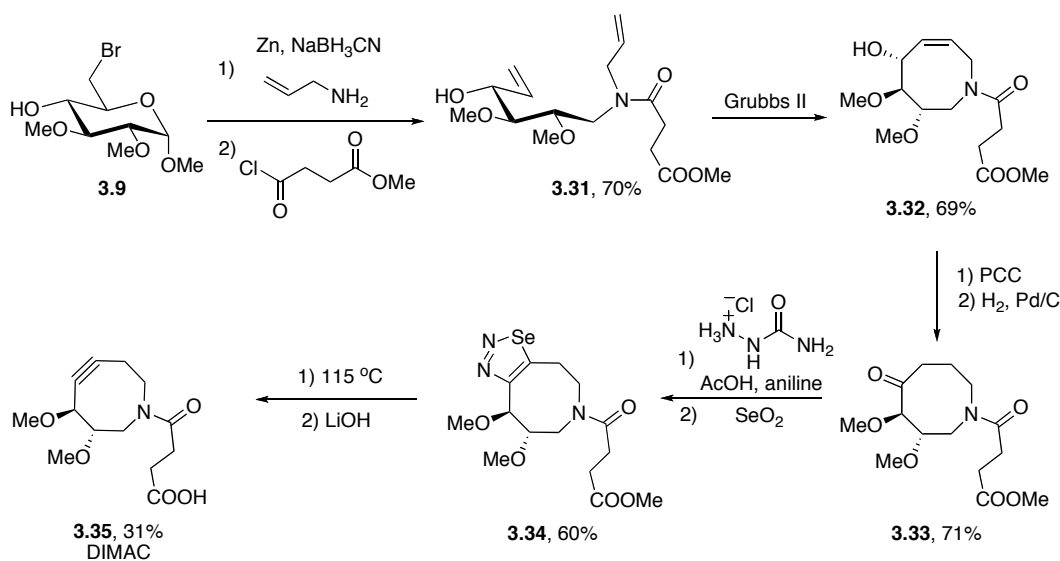
The selenadiazole strategy appeared attractive, as the thermal elimination of Se and N₂ had the potential to be compatible with a variety of hydrophilic functional groups and did not employ a heavy metal, which could be a concern for toxicity during *in vivo* experiments. Additionally, this method had previously been employed in the synthesis of oxa- and thiacyclooctynes.^{23,24} Ketone **3.26** was condensed with semicarbazide under acidic conditions to yield semicarbazone **3.28**. Compound **3.28** was oxidized with SeO₂ to the desired selenadiazole (**3.29**), and gratifyingly, when heated in refluxing toluene, azacyclooctyne **3.30** was isolated in 33% yield. With compound **3.30**, we had successfully synthesized the first azacyclooctyne; however, the aryl ring in the linker group hindered its water-solubility, which was the motivation for the synthesis of **3.30**. Thus, before moving to biological experiments, we removed the aryl linker group. Luckily the selenadiazole strategy did not necessitate harsh basic conditions and allowed a linker group with enolizable protons to be employed.

Scheme 3.7. Synthesis of azacyclooctyne **3.30**.



The synthetic pathway, which successfully yielded **3.30** was repeated with replacement of the aryl linker group with two methylene units (Scheme 3.8). To this end, methyl succinyl chloride was employed as the activated carbonyl group utilized for amide bond formation to yield **3.31**. As was the case for the transformation of **3.24** to **3.26**, the change in linker region did not affect the chemistry necessary to obtain ketone **3.33**. Ketone **3.33** was converted to selenadiazole **3.34** by aniline-catalyzed condensation²⁵ with semicarbazide and oxidation with selenium dioxide. Upon heating selenadiazole **3.34** in *m*-xylene for 3 days, the desired azacyclooctyne was produced in 47% yield. Simple saponification of the methyl ester with LiOH yielded the desired compound **3.35**, DIMethoxy AzaCyclooctyne (DIMAC), ready for kinetic analysis and conjugation to an epitope tag of choice.²⁶

Scheme 3.8. Synthesis of dimethoxyazacyclooctyne (DIMAC).



Kinetic and Structural Analysis of DIMAC

The ability for DIMAC to react with azides was analyzed using the model compound benzyl azide (Scheme 3.9). The cycloaddition reaction proceeded cleanly with a second-order rate constant of $3.0 \times 10^{-3} \text{ M}^{-1}\text{s}^{-1}$ to yield triazole products **3.36** and **3.37** in a 1:1.4 ratio. This rate constant is slightly higher than OCT and ALO ($1\text{-}2 \times 10^{-3} \text{ M}^{-1}\text{s}^{-1}$), perhaps due to added ring strain from the shorter C-N bond length or the sp^2 character of the amide nitrogen.²⁷

Scheme 3.9. Reaction of DIMAC with benzyl azide to yield two triazole products.

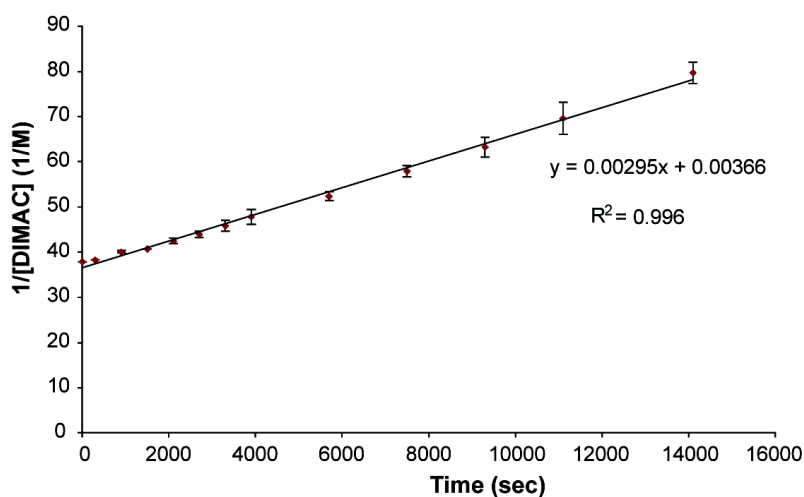
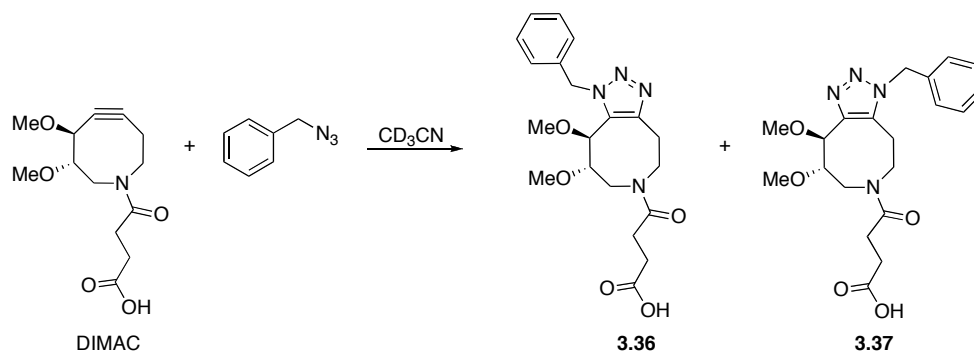


Figure 3.6. Plot of 1/[DIMAC] vs. time for the reaction of DIMAC with benzyl azide in CD₃CN at rt. The slope of the line represents the second-order rate constant for the reaction.

We further explored the structure of DIMAC through X-ray crystallography. An X-ray crystal structure of DIMAC shows that the two strained bond angles in DIMAC are similar in the solid state at 157.5 and 157.0 degrees. The alkyne bond length is 1.2 Å, which is relatively consistent with linear alkynes. The amide does indeed introduce a true sp^2 center to the cyclooctyne core as 120° angles are observed between the three substituents on the nitrogen. Additionally, as expected, the C-N bond lengths are shortened relative to the $C(sp^3)$ - $C(sp^3)$ bonds in the azacyclooctyne ring (1.48 Å vs. 1.54 Å). These two factors likely contribute to the rate-enhancement of DIMAC relative to the all carbon analogues OCT and ALO.

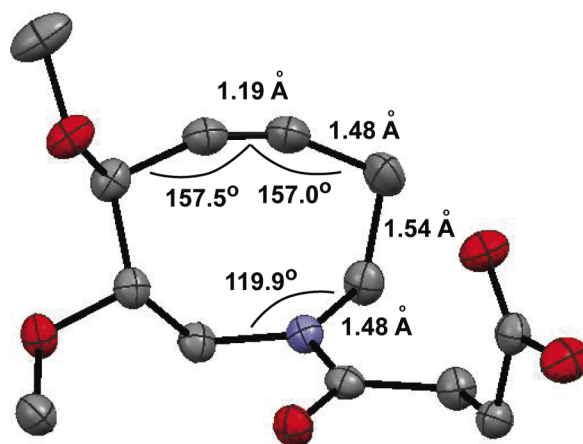


Figure 3.7. Crystal structure of DIMAC. Thermal ellipsoid plot for DIMAC **3.35** at 50% probability. Gray atoms correspond to carbon, red atoms correspond to oxygen, and the blue atom is nitrogen. The hydrogen atoms have been removed for clarity.

With the synthesis and kinetic analysis of DIMAC complete, it was time to test if the increased water-solubility of DIMAC improved Cu-free click chemistry *in vitro* and *in vivo*.

Materials and Methods

General Experimental Procedure

All chemical reagents were purchased from Sigma-Aldrich, Acros, and TCI chemicals and used without purification unless noted otherwise. Anhydrous DMF and MeOH were purchased from Aldrich or Acros in sealed bottles; all other solvents were purified as described by Pangborn *et al.*²⁸ In all cases, magnesium sulfate was used as a drying agent and solvent was removed by reduced pressure with a Buchi Rotovapor R-114 equipped with a Welch self-cleaning dry vacuum. Products were further dried by reduced pressure with an Edwards RV5 high vacuum. Thin layer chromatography was performed with Silicycle[®] 60 Å silica gel plates. Unless otherwise specified, R_f values are reported in the solvent system the reaction was monitored in. Flash chromatography was performed using Merck 60 Å 230-400 mesh silica or a Biotage Flash+[®] system with Biotage[®] 10S, 10M, 40S or 40M prepacked silica gel columns. All ¹H and ¹³C NMR spectra are reported in ppm and referenced to solvent peaks. When mixtures of rotomers are present the minor rotomer is designated as “rot”. Spectra were obtained on Bruker AV-300, AVQ-400, AVB-400, DRX-500, AV-500 or AV-600 instruments. IR spectra were obtained using a Varian 3100 FT-IR using thin films on NaCl plates. Optical rotations were measured using a Perkin Elmer 241 polarimeter. High resolution fast atom bombardment (FAB) and electrospray ionization (ESI) mass spectra were obtained from the UC Berkeley Mass Spectrometry Facility. Elemental analysis was performed at the UC Berkeley

Microanalytical Facility. X-ray crystallography was performed at the UC Berkeley X-ray Crystallography Facility.

Experimental Procedures

Methyl 4,6-O-benzylidene-2,3-di-O-methyl- α ,D-glucopyranoside (3.11). Methyl 4,6-O-benzylidene- α ,D-glucopyranoside (1.416 g, 5.176 mmol, 1 equiv, Acros) was dissolved in toluene (55 mL, anhydrous). To this solution, KOH was added (1.73 g, 30.8 mmol, 6 equiv) followed by methyl iodide (2.20 mL, 35.3 mmol, 7 equiv.). The mixture was heated to reflux while stirring under N₂ and monitored by TLC (1:1 hexane/ethyl acetate) for the disappearance of **3.10** (R_f = 0.2). Upon reaction completion (approx 4 h), the mixture was cooled to rt and toluene (50 mL) was added and the organic layer was washed with H₂O (3 x 30 mL). The organic extracts were evaporated to dryness and twice azeotroped (50 mL) with toluene to result in **3.11** as a white powder (1.516 g, 4.885 mmol, 94%, R_f = 0.7). Mp 123.2-124.0 °C (lit.²⁹ 121-123 °C). ¹H NMR (400 MHz, CDCl₃): δ 7.48-7.46 (m, 2H), 7.34-7.28 (m, 3H), 5.51 (s, 1H), 4.82 (d, J = 3.4 Hz, 1H), 4.25 (dd, J = 9.9, 4.5 Hz, 1H), 3.79 (td, J = 5.1, 4.4 Hz, 1H), 3.70 (t, J = 10.1 Hz, 1H), 3.66 (t, J = 9.2 Hz, 1H), 3.60 (s, 3H), 3.52 (s, 3H), 3.50 (t, J = 9.3 Hz, 1H), 3.41 (s, 3H), 3.26 (dd, J = 9.2, 3.7 Hz, 1H). ¹³C NMR (100 MHz, CDCl₃): δ 137.4, 129.0, 128.3, 126.1, 101.4, 98.4, 82.2, 81.5, 79.9, 69.1, 62.3, 61.1, 59.4, 55.3. HRMS (FAB): calcd. for C₁₆H₂₃O₆ [M + H]⁺, 311.14946; found, 311.14930.

Methyl 6-bromo-6-deoxy-2,3-di-O-methyl- α ,D-glucopyranoside (3.9). Methyl 4,6-O-benzylidene- α ,D-glucopyranoside (37.97 g, 122.4 mmol, 1 equiv.) was dissolved in CCl₄ (1.5 L, anhydrous) and CaCO₃ (13.54 g, 135.3 mmol, 1.11 equiv.) was added. This mixture was heated to reflux under N₂. N-bromosuccinimide (24.228 g, 136.13 mmol, 1.11 equiv, recrystallized) was then added, and the reaction was monitored by TLC (1:1 hexane/ethyl acetate) for the disappearance of **3.11** (R_f = 0.7). Upon completion (approx 1 h), the reaction was cooled to rt and evaporated to dryness. The residue was dissolved in CH₂Cl₂ (1 L) and washed with 10% Na₂SO₃ (1 x 1 L) and sat. NaHCO₃ (1 x 1 L). Each aqueous wash was extracted with CH₂Cl₂ (2 x 500 mL). All organic layers were combined, dried, decanted, and evaporated to dryness. The residue was dissolved in a solution of 1% NaOH in methanol (1.5 L). After 1 h, the solution was neutralized with 3M HCl and evaporated to dryness. The residue was dissolved in H₂O (1.5 L) and extracted with CH₂Cl₂ (8 x 500 mL). The organic layers were combined, dried, decanted, and evaporated to dryness. The crude product was purified by flash chromatography on 5 Biotage 40M columns with a gradient solvent system of 4:1 hexane/ethyl acetate to 1:1 hexane/ethyl acetate to result in pure **3.9** as a clear oil (30.10 g, 105.6 mmol, 86%, R_f = 0.3). ¹H NMR (400 MHz, CDCl₃): δ 4.73 (d, J = 3.5 Hz, 1H), 3.60-3.53 (m, 3H), 3.49 (s, 3H), 3.49-3.43 (m, 1H), 3.35-3.24 (m, 8H), 3.11 (dd, J = 9.1, 3.5 Hz, 1H). ¹³C NMR (100 MHz, CDCl₃): δ 97.3, 82.7, 81.7, 71.6, 69.9, 61.2, 58.5, 55.3, 33.5. HRMS (FAB): calcd. for C₉H₁₇BrO₅Li [M + Li]⁺, 291.041939; found, 291.041570.

N-allyl-N-((2*R*,3*S*,4*R*)-4-hydroxy-2,3-dimethoxyhex-5-enyl)acetamide (3.7). Methyl 6-bromo-6-deoxy-2,3-di-O-methyl- α ,D-glucopyranoside (2.80 g, 9.83 mmol, 1 equiv.) was dissolved in 19:1 1-propanol/water (330 mL). To this solution NaBH₃CN (2.62 g, 42.9 mmol, 4.2 equiv.), allylamine (22 mL, 293 mmol, 29.9 equiv.), and zinc (31.9 g, 486 mmol, 49.4 equiv., acid treated) were added. The solution was heated to reflux for 1.5 h, at which point not starting material remained. The mixture was cooled to rt, filtered through Celite, and the filtrate was evaporated to dryness. The resulting residue was dissolved in 200 mL of 6:4:1 CH₂Cl₂/MeOH/1.5 M HCl and stirred for 3 h checking to make sure the pH was acidic the entire time and adding 3M HCl as necessary. The mixture was then basified and with 10% NaOH and extracted with CH₂Cl₂ (3 x 200 mL). The organics were combined, dried, decanted, and evaporated to dryness. The crude product was dissolved in MeOH (150 mL, anhydrous) and diisopropylethylamine (1.65 mL, 9.47 mmol, 0.964 equiv.) and acetic anhydride (0.90 mL, 9.5 mmol, 0.96 equiv.) were added. The reaction stirred for 4 h at rt, at which point the methanol was removed by evaporation. The residue was dissolved in water (50 mL) and extracted with CH₂Cl₂ (3 x 75 mL). The organic layers were combined, dried, decanted, and evaporated to dryness to yield crude **3.7**, which was purified by silica gel chromatography on a Biotage 40M column with a toluene/acetone solvent system (8:1 to 1:1; product elutes at 4:1). This procedure resulted in 1.57 g pure **3.7** (6.11 mmol, 62%). R_f = 0.6 in 9:1 CH₂Cl₂/MeOH. ¹H NMR (400 MHz, CDCl₃): δ 5.87-5.80 (m, 1H), 5.68-5.64 (m, 1H), 5.23 (dd, *J* = 17.2, 4.7 Hz, 1H), 5.10-4.98 (m, 3H), 4.22-4.17 (m, 1H), 4.04-3.79 (m, 2H), 3.67-3.56 (m, 1H), 3.44-3.37 (m, 4H), 3.32-3.27 (m, 4H), 3.13-3.04 (m, 1H), 2.04 (s, 1.2H), 1.96 (s, 1.8H). ¹³C NMR (100 MHz, CDCl₃): δ 171.8, 171.6, 138.4, 138.4, 133.64, 132.9, 117.2, 116.6, 116.2, 116.1, 83.6, 83.0, 80.4, 80.2, 72.4, 71.4, 60.6, 60.5, 59.8, 59.7, 53.0, 49.3, 48.6, 47.9, 21.9, 21.7. IR: 3405, 3081, 2932, 2829, 1628, 1417, 1097 cm⁻¹. HRMS (FAB): calcd. for C₁₃H₂₄NO₄⁺ [M+H]⁺, 258.1705; found, 258.1709.

N-acetyl-(3*S*,4*S*,5*R*,6*Z*)-3,4-bis(methoxy)-5-hydroxy-3,4,5,8-tetrahydroazocine (3.6). Compound **3.7** (42.3 mg, 0.164 mmol) and Grubbs 2nd generation catalyst (11.9 mg, 14.0 μ mol, 8.5 mol%) were combined in CH₂Cl₂ (10 mL) and heated to reflux. The reaction was monitored by TLC (20:3:1:3 CH₂Cl₂/CH₃CN/CH₃OH/hexane) for the disappearance of **3.7** (R_f = 0.37, approx. 30 min). The completed reaction was cooled to rt, filtered through Celite, and the filtrate was evaporated to dryness. The crude product was chromatographed through silica gel using 80:12:3:40 CH₂Cl₂/CH₃CN/MeOH/hexane to yield pure **3.6** as a 1:0.2 mixture of rotamers (28.9 mg, 0.126 mmol, 77%, R_f = 0.31). ¹H NMR (400 MHz, CDCl₃): δ 5.71 (ddd, *J* = 11.8, 6.6, 2.4 Hz, 1H), 5.64 (d, *J* = 32 Hz, 0.4H), 5.53 (dm, *J* = 9.8 Hz, 1H), 4.60-4.48 (m, 0.4H), 4.42 (t, *J* = 8.4 Hz, 1H), 4.29 (apparent d, *J* = 17.5 Hz, 1H), 4.14 (dd, *J* = 13.8, 32 Hz, 1H), 3.80 (dd, *J* = 17.5, 5.1 Hz, 1H), 3.76-3.67 (m, 1.4H), 3.64 (s, H), 3.58 (s, 3H), 3.54 (s, 0.6H), 3.52-3.38 (m, 0.4H), 3.34 (s, 0.6H), 3.25-3.20 (m, 0.2H), 3.00 (dd, *J* = 9.4, 7.5 Hz, 1H), 2.87 (dd, *J* = 13.8, 9.6 Hz), 2.23 (s, 0.6H), 2.14 (s, 3H). ¹³C NMR (125 MHz, CDCl₃): δ 171.0, 170.9, 134.6, 32.7, 125.5, 124.0, 85.6, 85.4, 82.3, 80.8, 68.0, 67.0, 61.1, 60.6, 58.2, 58.1, 49.1, 47.1, 45.2,

45.0, 22.2, 22.1. IR: 3439, 2931, 2872, 1651, 1417, 1361, 1251, 1190, 1098 cm^{-1} . HRMS (FAB): calcd. for $\text{C}_{11}\text{H}_{20}\text{NO}_4^+$ $[\text{M}+\text{H}]^+$, 230.1392; found, 230.1391.

1-((5*R*,6*R*,7*S*,*Z*)-5-(*tert*-butyldimethylsilyloxy)-6,7-dimethoxy-5,6,7,8-tetrahydroazocin-1(2*H*)-yl)ethanone (3.14). Azacyclooctene **3.6** (82 mg, 0.27 mmol, 1 equiv.) was dissolved in DMF (4.0 mL, anhydrous). To this solution was added imidazole (94 mg, 1.4 mmol, 5.0 equiv.) and *tert*-butyldimethylsilyl chloride (325 mg, 2.1 mmol, 7.7 equiv.). The mixture was heated to 85 °C for 5 h, at which point the reaction was quenched with water (10 mL) and extracted with ether (3 x 10 mL). The organics were combined and washed with sat. NaHCO_3 (15 mL) and brine (15 mL). The ether was dried, decanted, and evaporated to dryness to yield crude **3.14**. The crude product was purified by silica gel chromatography on a Biotage 40M column using a hexane/ethyl acetate solvent system (8:1 to 1:2). This procedure resulted in 26 mg of pure **3.14** (0.076 mmol, 28%) as a 1:0.8 mixture of rotamers. $R_f = 0.2$ in 1:1 hexane/ethyl acetate. $^1\text{H NMR}$ (300 MHz, CDCl_3): δ 5.58 (ddt, $J = 11.5, 5.9, 1.4$ Hz, 1rotH), 5.51- 5.38 (m, 2H, 1rotH), 4.58-4.52 (m, 1H, 1rotH), 4.42- 4.33 (m, 1H, 1rotH), 4.14-4.04 (m, 1H), 3.92-3.76 (m, 1H, 1rotH), 3.62 (dd, $J = 16.9, 3.6$ Hz, 1rotH), 3.52-3.35 (m, 7H, 8rotH), 3.22 (dd, $J = 8.4, 4.1$ Hz, 1H), 3.09-3.02 (m, 1H, 1rotH), 2.15 (s, 3rotH), 2.08 (s, 3H), 0.88 (s, 9H, 9rotH) 0.06-0.03 (m, 6H, 6rotH).

1-((1*S*,5*S*,6*S*,7*S*,8*R*)-5-bromo-7-(*tert*-butyldimethylsilyloxy)-8-methoxy-9-oxa-3-azabicyclo[4.2.1]nonan-3-yl)ethanone (3.17) or 1-((1*S*,5*R*,6*S*,7*S*,8*R*)-6-bromo-7-(*tert*-butyldimethylsilyloxy)-8-methoxy-9-oxa-3-azabicyclo[3.3.1]nonan-3-yl)ethanone (3.18). TBS-protected azacyclooctene **3.14** (26 mg, 0.076 mmol, 1.0 equiv.) was dissolved in CH_2Cl_2 (2.0 mL, anhydrous). Bromine (13 μL , 0.51 mmol, 6.6 equiv., diluted in 2 mL CH_2Cl_2) was added to the solution of **3.14** over 15 min. After 3 h, the reaction was quenched with H_2O (10 mL). The organic layer was then washed with sat. NaHCO_3 (10 mL) followed by H_2O (10 mL). The organics were dried, decanted, evaporated to dryness, and purified on a Biotage 10S column with a hexane/ethyl acetate solvent system. This procedure resulted in pure **3.17** or **3.18** (11 mg, 0.027 mmol, 36%) as a ~1:1 mixture of rotamers. $R_f = 0.53$ in 1:1 toluene/acetone. $^1\text{H NMR}$ (400 MHz, CDCl_3): δ 5.10 (d, $J = 14.2$ Hz, 1H), 4.63 (d, $J = 13.8$ Hz, 1H), 4.37 (d, $J = 13.7$ Hz, 1H), 4.20- 4.15 (m, 2H), 4.08-3.98 (m, 6H), 3.90 (d, $J = 13.4$ Hz, 1H), 3.38- 3.37 (m, 4H), 3.35- 3.33 (m, 4H), 3.30-3.27 (m, 2H), 2.88 (dd, $J = 14.1, 3.9$ Hz, 1H), 2.81 (dd, $J = 13.7, 4.2$ Hz, 1H), 2.17 (s, 3H), 2.10 (s, 3H), 0.91 (s, 18H), 0.14 -0.10 (m, 6H), 0.07 (s, 6H). $^{13}\text{C NMR}$ (150 MHz, CDCl_3): δ 169.5, 169.4, 83.82, 83.76, 74.01, 73.96, 72.6, 72.1, 69.0, 68.7, 58.5, 58.2, 54.9, 53.8, 45.0, 43.7, 39.9, 38.6, 29.9, 26.32, 26.30, 26.0, 21.5, 21.3, 18.60, 18.59, -3.9, -4.0, -4.2, -4.5. HRMS (ESI): calcd. for $\text{C}_{16}\text{H}_{31}\text{O}_4\text{NBrSi}^+$ $[\text{M} + \text{H}]^+$, 408.1200; found, 408.1207.

N-acetyl (3*S*,4*S*,6*Z*)-3,4-bis(methoxy)-5-one-3,4,8-trihydroazocaine. Compound **3.6** (13.6 mg, 0.0593 mmol, 1.00 equiv.) was dissolved in CH_2Cl_2 (2 mL) and PCC (18.6 mg, 0.0863 mmol, 1.46 equiv.) was added. The reaction was stirred at rt and monitored by TLC (20:3:1:3 $\text{CH}_2\text{Cl}_2/\text{CH}_3\text{CN}/\text{CH}_3\text{OH}/\text{hexane}$) for the disappearance of **3.6** ($R_f = 0.30$). When there was no more **3.6** present (approx. 9 h), water was added and the mixture was

extracted with three portions of 4 mL of CH₂Cl₂. The organic layers were combined, dried, decanted and evaporated to dryness. The residue was purified via silica gel chromatography using 40:1 CH₂Cl₂/MeOH to yield *N*-acetyl (3*S*,4*S*,6*Z*)-3,4-bis(methoxy)-5-one-3,4,8-trihydroazocaine as a 1:1 mixture of rotamers (9.6 mg, 0.042 mmol, 71%, R_f = 0.4). ¹H NMR (500 MHz, CDCl₃): δ 6.23-6.19 (ddd, *J* = 11.9, 4.2, 3.1 Hz, 0.5H), 5.97 (s, 1H), 5.78 (d, 11.8 Hz, 0.5H), 4.35 (dd, *J* = 17.5, 4.3 Hz, 0.5H), 4.09 (d, *J* = 19.7 Hz, 0.5 Hz), 3.95 (d, *J* = 19.6 Hz, 0.5H), 3.91-3.86 (m, 0.5H), 3.82-3.79 (m, 1.5H), 3.75 (q, *J* = 5.5 Hz, 0.5H), 3.70-3.61 (m, 1.75H), 3.54 (s, 3H), 3.46-3.38 (m, 3.25H), 2.05 (s, 1.5H), 1.95 (s, 1.5H). ¹³C NMR (125 MHz, CDCl₃): δ 202.5, 201.7, 171.5, 170.9, 136.9, 132.3, 129.1, 126.3, 88.8, 87.5, 80.8, 79.2, 59.4, 59.1, 58.8, 58.1, 51.0, 50.5, 47.9, 46.2, 21.3, 21.2. IR: 2917, 2849, 2360, 2342, 1689, 1661, 1463, 1091 cm⁻¹. HRMS (FAB): calcd. for C₁₁H₁₈NO₄⁺ [M+H]⁺, 228.1236; found, 228.1234.

(3*S*,4*R*)-1-acetyl-3,4-dimethoxyazocan-5-one (3.19). *N*-acetyl (3*S*,4*S*,6*Z*)-3,4-bis(methoxy)-5-one-3,4,8-trihydroazocaine (39 mg, 0.17 mmol, 1.0 equiv.) was dissolved in EtOH (10 mL). The solution was flushed with nitrogen and Pd/C was added until the solution was light gray. The reaction mixture was flushed with hydrogen and remained stirring under a H₂ atmosphere overnight. The following morning, the Pd/C was removed by filtration through Celite. The filtrate was evaporated to dryness and pushed through a plug of silica with 40:1 CH₂Cl₂/MeOH. This procedure resulted in 36 mg of pure **3.19** (0.16 mmol, 91%) as a 1:0.7 mixture of rotamers. R_f = 0.4 in 1:1 toluene/acetone. ¹H NMR (500 MHz, CDCl₃): δ 4.05 (dd, *J* = 13.8, 4.2 Hz, 1H), 3.92 (d, *J* = 8.1 Hz, 1rotH), 3.82-3.78 (m, 1H), 3.76-3.76 (m, 1rotH), 3.69-3.46 (m, 4H, 6rotH), 3.40 (s, 3rotH), 3.30 (s, 3H), 3.32-3.23 (m, 1H, 1rotH), 3.13 (dt, *J* = 14.6, 5.5 Hz, 1H), 2.71 (dd, *J* = 13.5, 10.7 Hz, 1H), 2.51-2.35 (m, 2H, 2rotH), 2.21-2.11 (m, 2H, 2rotH), 1.99 (s, 3rotH), 1.96 (s, 3H). ¹³C NMR (100 MHz, CDCl₃): δ 209.5 (rot), 209.0, 172.2 (rot), 171.8, 88.5, 86.4 (rot), 82.4 (rot), 80.5, 59.9, 59.3 (rot), 58.8 (rot), 58.0, 50.5, 49.5 (rot), 47.6, 47.2 (rot), 41.2, 37.9 (rot), 26.1 (rot), 25.6, 22.0, 22.0 (rot). HRMS (ESI): calcd. for C₁₁H₂₀O₄N⁺ [M + H]⁺, 230.1387; found, 230.1390.

(3*S*,4*R*,*E*)-1-acetyl-3,4-dimethoxy-1,2,3,4,7,8-hexahydroazocin-5-yl trifluoromethanesulfonate (3.21). Potassium bis(trimethylsilyl)amide (0.28 mL, 0.14 mmol, 1.5 equiv., 0.5M in toluene) was further diluted in THF (1.5 mL, anhydrous) and cooled to -78 °C. Ketone **3.19** (22 mg, 0.95 mmol, 1.0 equiv.) was dissolved in THF (1.5 mL, anhydrous) and added to the bis(trimethylsilyl)amide solution over 30 min. After addition of **3.19**, the mixture was stirred for an additional hour at which point *N*-phenyltrifluoromethanesulfonimide (59 mg, 0.14 mmol, 1.5 equiv.) was added and the reaction mixture was warmed to 0 °C over 2.5 h. The mixture was evaporated to dryness and purified by silica gel chromatography with a dichloromethane/methanol solvent system (100:1, 80:1, 60:1, 40:1). This procedure resulted in 16 mg of **3.21** (0.044 mmol, 45%) as a 1:0.9 mixture for rotamers. R_f = 0.4 in 9:1 CH₂Cl₂/MeOH. ¹H NMR (400 MHz, CDCl₃): δ 6.03 (t, *J* = 7.8 Hz, 1H), 5.98 (dd, *J* = 9.8, 8.1 Hz, 1rotH), 4.12 (d, *J* = 7.9 Hz, 1H), 4.03-3.93 (m, 2H, 2rotH), 3.75-3.68 (m, 1H), 3.62-3.55 (m, 1H, 1rotH), 3.50-3.47 (m, 4H, 3rotH), 3.44-3.41 (m, 3H, 4rotH), 3.36- 3.28 (m, 1H), 3.02-2.98 (m, 1rotH), 2.62

(apparent dt, $J = 7.8, 4.7$ Hz, 1H), 2.49-2.43 (m, 1rotH), 2.35-2.22 (m, 3H, 1rotH), 2.02 (s, 3rotH). ^{19}F NMR (376 MHz, CDCl_3): δ -73.60 (s, 3F), -73.67 (s, 3rotF). HRMS (ESI): calcd. for $\text{C}_{12}\text{H}_{19}\text{O}_6\text{NF}_3\text{S}^+ [\text{M} + \text{H}]^+$, 362.0880; found, 362.0885.

1-((3S,4R)-3,4-dimethoxy-5-oxoazocan-1-yl)vinyl trifluoromethanesulfonate (3.22).

Vinyl triflate **3.21** (7 mg, 0.019 mmol, 1.0 equiv.) was dissolved in THF 1.5 mL, anhydrous) and cooled to 0 °C. Lithium diisopropylamide (0.8 mL of 0.2 M solution in THF prepared from *n*BuLi and diisopropylamine, 0.16 mmol, 8.3 equiv.) was added dropwise over 1 h at which point the reaction was quenched with methanolic ammonium chloride and evaporated to dryness. The crude product was purified by silica gel chromatography with a toluene/acetone solvent system. This produced resulted in 2 mg of **3.22** (0.0055 mmol, 29%). $R_f = 0.7$ in 1:1 toluene/acetone. ^1H NMR (500 MHz, CDCl_3) δ 4.56 (q, $J = 14.8$ Hz, 2H), 3.82 (d, $J = 4.5$ Hz, 1H), 3.75-3.72 (m, 3H), 3.66-3.62 (m, 1H), 3.57 (s, 3H), 3.55 (s, 3H), 3.55-3.48 (m, 1H), 2.67 (td, $J = 11.2, 3.9$ Hz, 1H), 2.50-2.38 (m, 2H), 1.97-1.92 (m, 1H).

Methyl 4-(allyl((2R,3S,4R)-4-hydroxy-2,3-dimethoxyhex-5-enyl)carbamoyl)benzoate (3.24).

Methyl 6-bromo-6-deoxy-2,3-di-O-methyl- α ,D-glucopyranoside (9.73 g, 34.1 mmol, 1 equiv.) was dissolved in 19:1 1-propanol/water (800 mL). To this solution NaBH_3CN (9.54 g, 152 mmol, 4.5 equiv.), allylamine (76 ml, 1.01 mol, 29.7 equiv.), and zinc (113 g, 1.79 mol, 52.6 equiv., acid treated) were added. The solution was heated to to ~ 85 °C for 2 h stirring with a mechanical stirred. The mixture was cooled to rt, filtered through Celite, and the filtrate was evaporated to dryness. The resulting residue was dissolved in 660 mL of 6:4:1 $\text{CH}_2\text{Cl}_2/\text{MeOH}/1.5$ M HCl and stirred for 3 h checking to make sure the pH was acidic the entire time and adding 3M HCl as necessary. The mixture was then basified and with 10% NaOH and extracted with CH_2Cl_2 (3 x 500 mL). The organics were combined, dried, decanted, and evaporated to dryness. The crude product was dissolved in MeOH (500 mL, anhydrous) and diisopropylethylamine (6.50 mL, 37.4 mmol, 1.10 equiv.) and methyl 4-(chlorocarbonyl)benzoate (6.89 g, 34.8 mmol, 1.02 equiv.) were added. The reaction stirred for 2.5 h at rt, at which point reaction was quenched with water and the MeOH was removed by evaporation. The resulting aqueous solution was extracted with CH_2Cl_2 (3 x 500 mL). The organic layers were combined, dried, decanted, and evaporated to dryness to yield crude **3.24**, which was purified by silica gel chromatography on a Biotage 40M column with a toluene/acetone solvent system (25:1, 20:1, 15:1). This procedure resulted in 6.13 g pure **3.24** (16.3 mmol, 48%) as a 1:0.5 mixture of rotamers. $R_f = 1:1$ toluene/acetone. ^1H NMR (500 MHz, CDCl_3): δ 7.88 (d, $J = 8.1$ Hz, 2H, 2rotH), 7.35 (d, $J = 7.6$ Hz, 2rotH), 7.29 (d, $J = 7.9$ Hz, 2H), 5.86-5.79 (m, 1H), 5.77-5.72 (m, 1rotH), 5.65-5.58 (m, 1rotH), 5.55- 5.50 (m, 1H), 5.19 (d, $J = 17.2$ Hz, 1H), 5.11-4.89 (m, 4H, 4rotH), 4.19-4.15 (m, 1H, 1rotH), 3.96 (dd, $J = 14.7, 4.6$ Hz, 1rotH), 3.84-3.73 (m, 5H, 6rotH), 3.44-3.39 (m, 3H, 1rotH), 3.31- 3.21 (m, 5H, 7rotH), 3.11-3.03 (m, 2H, 1rotH), 2.92-2.84 (m, 1H). ^{13}C NMR (125 MHz, CDCl_3 , no rotamer tabulated): δ 171.0, 166.0, 140.4, 138.0, 132.7, 126.1, 117.25, 115.5, 83.3, 79.1, 75.2, 71.6, 60.0, 59.2, 52.0, 46.3. HRMS (ESI): calcd. for $\text{C}_{20}\text{H}_{28}\text{O}_6\text{N}^+ [\text{M} + \text{H}]^+$, 378.1911; found, 378.1914.

Methyl 4-((3*S*,4*S*,5*R*,*Z*)-5-hydroxy-3,4-dimethoxy-1,2,3,4,5,8-hexahydroazocine-1-carbonyl)benzoate (3.25). Compound **3.24** (590 mg, 1.56 mmol) and Grubbs 2nd generation catalyst (113 mg, 0.133 mmol, 8.5 mol%) were combined in CH₂Cl₂ (100 mL) and heated to reflux. The reaction was monitored by TLC (1:1 toluene/acetone) for the disappearance of **3.24** (*R*_f = 0.5, approx. 25 min). The completed reaction was cooled to rt, filtered through Celite, and the filtrate was evaporated to dryness. The crude product was chromatographed on a Biotage 40S column using a toluene/acetone solvent system (10:1, 7:1, 4:1; product elutes at 7:1). This procedure yielded pure **3.25** as a 1:0.2 mixture of rotamers (414 mg, 1.18 mmol, 76%). *R*_f = 0.4 in 1:1 toluene/acetone. ¹H NMR (400 MHz, CDCl₃, no rotamer tabulated): δ 7.95 (d, *J* = 8.1 Hz, 2H), 7.38 (d, *J* = 8.2 Hz, 2H), 5.61 (d, *J* = 10.4 Hz, 1H), 5.25 (d, *J* = 12.0 Hz, 1H), 4.57 (t, *J* = 7.5 Hz, 1H), 4.19 (dd, *J* = 13.6, 2.9 Hz, 1H), 4.08 (d, *J* = 18.4 Hz, 1H), 3.81 (s, 3H), 3.66-3.64 (m, 1H), 3.60-3.50 (m, 4H), 3.47 (s, 3H), 3.37-3.30 (m, 1H), 2.95 (apparent t, *J* = 8.3 Hz, 1H), 2.90-2.84 (m, 1H). ¹³C NMR (100 MHz, CDCl₃, no rotamer tabulated): δ 170.4, 166.0, 139.7, 134.0, 131.3, 129.6, 126.7, 124.2, 85.9, 79.7, 67.1, 61.1, 58.2, 52.2, 51.6, 46.3. HRMS (ESI): calcd. for C₁₈H₂₄O₆N⁺ [M+H]⁺, 350.1598; found, 350.1602.

Methyl 4-((3*S*,4*R*)-3,4-dimethoxy-5-oxoazocane-1-carbonyl)benzoate (3.26).

Azacyclooctene **3.25** (414 mg, 1.18 mmol, 1.0 equiv.) was dissolved in CH₂Cl₂ (75 mL, anhydrous) and pyridinium chlorochromate (PCC, 390 mg, 1.8 mmol, 1.5 equiv.) was added. The mixture was stirred overnight at rt. The following morning the reaction was not complete and more PCC (110 mg) was added and the solution was heated to reflux. After 3 h, the reaction was complete and cooled to rt. It was quenched with water (75 mL) and extracted with CH₂Cl₂ (3 x 100 mL). The organics were combined, dried, decanted, and evaporated to dryness. The crude product was purified by silica gel chromatography on a Biotage 40S column using a toluene/acetone solvent system. The product elutes with 7:1 toluene/acetone. *R*_f = 0.8 in 1:1 toluene/acetone. The resulting enone (306 mg, 0.88 mmol, 74%; HRMS (ESI): calcd. for C₁₈H₂₂O₆N⁺ [M+H]⁺, 348.1442; found, 348.1446.) was immediately hydrogenated to ketone **3.26**. The enone was dissolved in ethanol (80 mL) and this solution was flushed with nitrogen. Palladium on carbon (34 mg) was added and the reaction mixture was flushed with hydrogen. It was stirred overnight under a hydrogen atmosphere. The following morning the mixture was filtered through Celite, washed with ethanol, and the filtrate was evaporated to dryness to yield 304 mg of pure **3.26** (0.87 mmol, 74% from **3.25**) as a 1:0.5 mixture of rotamers. *R*_f = 0.7 in 1:1 toluene/acetone. ¹H NMR (600 MHz, CDCl₃): δ 7.96 (d, *J* = 7.5 Hz, 2H, 2rotH), 7.37-7.29 (m, 2H, 2rotH), 4.13 (dd, *J* = 13.5, 3.3 Hz, 1H), 3.99 (d, *J* = 8.0 Hz, 1H), 3.81 (bs, 3H, 5rotH), 3.70 (bs, 1rotH), 3.63 (bs, 1rotH), 3.52-3.46 (m, 3H, 1rotH), 3.40 (bs, 1rotH), 3.33-3.23 (m, 5H, 5rotH), 3.11 (dd, *J* = 9.5, 3.7 Hz, 1rotH), 3.02-3.00 (m, 1H), 2.87 (t, *J* = 12.1 Hz, 1H), 2.54-2.44 (m, 1H, 1rotH), 2.37- 2.19 (m, 1H, 2rotH), 2.06-1.90 (m, 2H, 1rotH). ¹³C NMR (150 MHz, CDCl₃): δ 209.7 (rot), 209.5, 171.7, 171.3 (rot), 166.3, 166.3 (rot), 140.6 (rot), 140.6, 130.9, 130.5 (rot), 129.8, 129.5 (rot), 126.5 (rot), 126.0, 87.9, 86.3 (rot), 81.5 (rot), 80.2, 59.8, 59.0 (rot), 58.4 (rot), 57.7, 53.5 (rot), 52.2, 50.7, 49.3 (rot), 47.1 (rot), 47.8, 41.7, 37.7 (rot), 26.1 (rot), 25.6. HRMS (ESI): calcd. for C₁₈H₂₄O₆N⁺ [M + H]⁺, 350.1598; found, 350.1603.

Methyl 4-((3*S*,4*R*,*E*)-3,4-dimethoxy-5-(trifluoromethylsulfonyloxy)-1,2,3,4,7,8-hexahydroazocine-1-carbonyl)benzoate (3.27). Potassium bis(trimethylsilyl)amide (1.4 mL, 0.70 mmol, 1.3 equiv., 0.5 M in toluene) was further diluted in THF (6 mL, anhydrous) and cooled to -78 °C. Ketone **3.26** (195 mg, 0.558 mmol, 1.0 equiv.) was dissolved in THF (2 mL, anhydrous) and this solution was added dropwise to the solution of base over 45 min. Upon addition of all **3.26**, the mixture was stirred for 1.5 h at -78 °C, at which point, N-phenyltrifluoromethanesulfonamide (360 mg, 1.0 mmol, 1.5 equiv.) in THF (2 mL, anhydrous) was added. The reaction was stirred for 30 min at -78 °C and then warmed to -20 °C when it was quenched with methanolic ammonium chloride (2 mL). The mixture was evaporated to dryness and purified by silica gel chromatograph on a Biotage 12M column with a toluene/acetone solvent system. The product elutes with 15:1 toluene/acetone. This procedure resulted in **3.27** (105 mg, 0.218 mmol, 39%) as a 1:0.5 mixture of rotamers. $R_f = 0.6$ in 1:1 toluene/acetone. $^1\text{H NMR}$ (400 MHz, CDCl_3): δ 8.07 (d, $J = 8.1$ Hz, 2H, 2rotH), 7.49 (d, $J = 8.3$ Hz, 2rotH), 7.39 (d, $J = 8.1$ Hz, 2H), 6.11 (t, $J = 8.7$ Hz, 1rotH), 5.98 (t, $J = 8.8$ Hz, 1H), 4.15 (d, $J = 9.2$ Hz, 1H), 4.09-3.97 (m, 1H, 2rotH), 3.93 (s, 3H, 3rotH), 3.78-3.68 (m, 1H), 3.65-3.27 (m, 9H, 6rotH), 3.14-3.12 (m, 1rotH), 2.76 (s, 3rotH), 2.70-2.56 (m, 1H, 1rotH), 2.47-2.40 (m, 1rotH), 2.17-2.13 (m, 1H). $^{19}\text{F NMR}$ (376 MHz, CDCl_3): δ -73.61 (s, 3F), -73.63 (s, 3rotF). HRMS (ESI): calcd. for $\text{C}_{19}\text{H}_{23}\text{O}_8\text{NF}_3\text{S}^+ [\text{M} + \text{H}]^+$, 482.1091; found, 482.1100.

Methyl 4-((3*S*,4*S*,*E*)-5-(2-carbamoylhydrazono)-3,4-dimethoxyazocane-1-carbonyl)benzoate (3.28). Ketone **3.26** (477 mg, 1.36 mmol, 1.0 equiv.) was dissolved in ethanol (10 mL) in the presence of molecular sieves. To this solution, semicarbazide hydrochloride (1.42 g, 12.7 mmol, 9.4 equiv.) and acetic acid (~ 100 μL) was added. The mixture was monitored by TLC in 1:1 toluene/acetone for the disappearance of **3.26** ($R_f = 0.7$). Acetic acid (~ 100 μL) was added every 4 h until the reaction was complete. After 9.5 h the reaction was evaporated to dryness. The residue was dissolved in water (100 mL) and extracted with ethyl acetate (3 x 100 mL). The organics were combined, dried, decanted, and evaporated to dryness. The crude product was purified by silica gel chromatography eluting with 10:3:1 ethyl acetate/methanol/water. This procedure resulted in **3.28** (316 mg, 0.778 mmol, 57%) as a mixture of hydrazone regioisomers and rotamers which was taken directly onto next step. See appendix for NMR spectra. HRMS (ESI): calcd. for $\text{C}_{19}\text{H}_{27}\text{O}_6\text{N}_4^+ [\text{M} + \text{H}]^+$, 407.1925; found, 407.1930.

Methyl 4-((8*S*,9*S*)-8,9-dimethoxy-4,5,6,7,8,9-hexahydro-[1,2,3]selenadiazolo[5,4-*d*]azocine-6-carbonyl)benzoate (3.29). Semicarbazone **3.28** (181 mg, 0.447 mmol, 1.0 equiv.) was dissolved in dioxane (0.6 mL). Selenium dioxide (111 mg, 1.47 mmol, 3.3 equiv.) was dissolved in dioxane (0.6 mL) and water (0.4 mL). The SeO_2 solution was added dropwise to the solution of semicarbazone **3.28**. The mixture was stirred at rt overnight. The following day an additional 50 mg of SeO_2 was added and the reaction was allowed to stir at rt for another 24 h, at which point the dioxane was evaporated and water was added (20 mL). The aqueous solution was extracted with CH_2Cl_2 (3 x 30 mL). The organics were combined, dried, decanted and evaporated to dryness. The crude product was purified on a Biotage 40S column using a $\text{CH}_2\text{Cl}_2/\text{MeOH}$ solvent system. The product

elutes between 80:1 and 50:1 CH₂Cl₂/MeOH. This procedure resulted in pure **3.29** (141 mg, 0.321 mmol, 72%) as a 1:0.5 mixture of rotamers. ¹H NMR (400 MHz, CDCl₃): δ 8.08 (d, *J* = 7.9 Hz, 2H, 2rotH), 7.49 (d, *J* = 6.9 Hz, 2rotH), 7.35 (d, *J* = 7.6 Hz, 2H), 5.54 (s, 1H), 5.38 (s, 1rotH), 4.42-4.39 (m, 1H, 1rotH), 4.13 (d, *J* = 10.3 Hz, 1H), 3.94 (s, 3H, 3rotH), 3.74-3.22 (m, 10H, 8rotH), 3.06 (s, 3rotH), 3.01-2.95 (m, 1rotH), 2.80 (apparent t, *J* = 11.1 Hz, 1H). ¹³C NMR (125 MHz, CDCl₃): δ 171.7 (rot), 171.4, 166.44 (rot), 166.37, 161.1 (rot), 158.9, 157.1, 155.8 (rot), 141.2, 141.0 (rot), 131.03, 130.92 (rot), 130.1, 129.6 (rot), 127.3 (rot), 126.1, 81.8 (rot), 80.0, 79.1, 78.6 (rot), 58.5, 57.9, 57.9 (rot), 57.7 (rot), 53.6 (rot), 52.5, 52.5 (rot), 50.9, 50.5 (rot), 48.1, 26.4, 25.1 (rot). HRMS (ESI): calcd. for C₁₈H₂₂O₅N₃Se⁺ [M + H]⁺, 440.0719; found, 440.0726.

Dimethoxyazacyclooctyne with aryl linker (3.30). Selenadiazole **3.29** (41 mg, 0.093 mmol, 1.0 equiv.) was dissolved in toluene (3 mL, anhydrous). This mixture was heated to reflux for 3 d, at which point water (10 mL) was added and extracted with CH₂Cl₂ (3 x 10 mL). The organics were combined, dried, decanted and evaporated to dryness. The crude product was purified by silica gel chromatography with a toluene/acetone solvent system. The desired cyclooctyne elutes with 15:1 toluene/acetone to yield 10 mg of **3.30** (0.030 mmol, 33%) as a 1:0.3 mixture of rotamers. ¹H NMR (500 MHz, CDCl₃): δ 8.10 (d, *J* = 10.1 Hz, 2rotH), 8.07 (d, *J* = 10.2 Hz, 2H), 7.56 (d, *J* = 10.0 Hz, 2rotH), 7.44 (d, *J* = 10.2 Hz, 2H), 4.67- 4.64 (m, 1rotH), 4.45 (d, *J* = 16.6 Hz, 2H), 4.26 (dt, *J* = 9.9, 3.4 Hz, 1H), 4.14-4.11 (m, 1rotH), 4.05-4.01 (m, 4H, 4rotH), 3.84 (s, 3H), 3.77 (dd, *J* = 17.5, 7.2 Hz, 1H), 3.55 (s, 3H), 3.45 (s, 3rotH), 3.33-3.25 (m, 1H, 2rotH), 3.21-3.19 (m, 1rotH), 3.16-3.15 (m, 1rotH), 3.12 (dd, *J* = 16.9, 10.9 Hz, 1H), 2.70 (s, 3rotH), 2.67-2.58 (m, 1H), 2.40 (dm, *J* = 20.2 Hz, 1rotH), 2.25 (ddd, *J* = 20.3, 5.4, 3.4 Hz, 1H). ¹³C NMR (125 MHz, CDCl₃, no rotamer peaks tabulated): δ 171.9, 166.5, 141.5, 131.3, 130.2, 126.1, 95.2, 93.0, 86.4, 77.8, 59.5, 57.8, 55.2, 52.7, 52.6, 22.3. HRMS (ESI): calcd. for C₁₈H₂₂O₅N⁺ [M + H]⁺, 332.1492; found, 332.1497.

(2*S*, 3*S*, 4*R*) N-allyl, N-(methyl succinyl)-4-hydroxy-2,3-dimethoxyhex-5-ene amine (3.31). Pyranoside **3.9** (18.2 g, 63.8 mmol, 1.0 equiv.) was dissolved in 19:1 1-propanol/H₂O (1.5 L) in an Erlenmeyer flask equipped with an overhead stirring unit. To this solution, allylamine (150 mL, 2.0 mol, 31 equiv.), zinc (223.9 g, 3.423 mol, 54 equiv., acid treated), and NaBH₃CN (18.97 g, 301.9 mmol, 5 equiv.) were added. The reaction was heated to 90 °C and monitored by TLC (ethyl acetate) for the disappearance of **3.9** (*R*_f = 0.7). Upon reaction completion (approx 1 h), the mixture was cooled to rt and filtered through Celite. The filtrate was evaporated to dryness and dissolved in 6:4:1 MeOH/CH₂Cl₂/1.5M HCl (1.32 L) and stirred for 1 h (adding 3M HCl as necessary to keep the solution acidic) at which point, H₂O (300 mL) was added and the mixture was extracted with CH₂Cl₂ (3 x 600 mL). The organics were dried, decanted, and evaporated to a residue. The resulting crude amine was dissolved in methanol (600 mL, anhydrous). To this solution, N,N-diisopropylethylamine (12.2 mL, 70.0 mmol, 1.1 equiv) followed by methyl succinyl chloride (8.6 mL, 70 mmol, 1.1 equiv.) were added and the mixture was stirred at rt under N₂ for 1 h, at which point the reaction was quenched with H₂O (100 mL) and the methanol was removed via rotary evaporation. To the resulting aqueous solution,

H₂O (500 mL) was added and extracted with CH₂Cl₂ (3 x 650 mL). The organic extracts were combined, dried, decanted, and evaporated to dryness. The crude product was purified via flash chromatography using 3 Biotage 40M columns with a gradient solvent system starting with 25:1 toluene/acetone and ending with 3:1 toluene/acetone (product begins to elute at 10:1 toluene/acetone) to result in pure **3.31** as a colorless oil (14.8 g, 44.9 mmol, 70%). R_f = 0.6 in 1:1 toluene/acetone. $[\alpha]_D^{28}$ -38.8° (c 0.943, CH₂Cl₂). 1:0.5 mixture of rotamers (designated rot) ¹H NMR (500 MHz, CDCl₃): δ 5.98-5.88 (m, 1H, 1rotH), 5.79-5.71 (m, 1H, 1rotH), 5.36 (d, *J* = 17.2 Hz, 1rotH), 5.35 (d, *J* = 17.2 Hz, 1H), 5.24-5.11 (m, 3H, 3rotH), 4.32-4.27 (m, 1H, 1rotH), 4.16-4.13 (m, 1H, 1rotH), 4.07-4.03 (m, 1H), 3.98-3.94 (m, 1rotH), 3.78 (dd, *J* = 13.9, 3.6 Hz, 1H), 3.72-3.67 (m, 4H, 3rotH), 3.63-3.59 (m, 2rotH), 3.52 (s, 3H, 3 rotH), 3.45-3.38 (m, 3H, 4rotH), 3.25-3.21 (m, 1H, 1rotH), 3.15 (t, *J* = 4.2 Hz, 1H), 2.85-2.80 (m, 1rotH), 2.73-2.60 (m, 5H, 3rotH), 2.33 (d, *J* = 6.5 Hz, 1rotH). ¹³C NMR (125 MHz, CDCl₃): δ 173.9, 173.7, 172.2, 172.1, 138.4, 133.6, 132.8, 117.2, 116.7, 116.31, 116.25, 83.4, 82.7, 80.5, 80.4, 72.4, 71.5, 60.7, 60.6, 59.8, 59.7, 52.02, 51.95, 51.9, 48.9, 48.3, 48.2, 29.5, 29.2, 28.2, 28.1. IR: 3441 (b), 3082, 2981, 2933, 2832, 1737, 1641 cm⁻¹. HRMS (FAB): calcd for C₁₆H₂₈NO₆ [M + H]⁺, 330.191663; found, 330.192190. Anal. calcd for C₁₆H₂₇NO₆: C, 58.34; H, 8.26, N, 4.25; found: C, 58.41; H, 8.22, N, 4.38.

(5R, 6S, 7S, Z) N-(methyl succinyl)-5-hydroxy-6,7-dimethoxyazacyclooct-3-ene (3.32).

Compound **3.31** (790 mg, 2.40 mmol, 1 equiv.) was dissolved in dichloromethane (200 mL, anhydrous) and heated to reflux while stirring under N₂. Once at reflux, Grubbs second generation catalyst (163.3 mg, 0.1927 mmol, 0.08 equiv.) was added and the reaction was carefully monitored by TLC in 1:1 toluene/acetone for the disappearance of **3.31** (R_f = 0.6) adding more catalyst if necessary (at 2.25 h 61 mg catalyst added). Upon completion (approx 5 h), the mixture was cooled to rt, evaporated to dryness, and *immediately* purified via flash chromatography using a Biotage 40M column with a gradient of 8:1 toluene/acetone, 6:1 toluene/acetone, 4:1 toluene/acetone. This procedure resulted in pure **3.32** as a brown oil (500 mg, 1.66 mmol, 69%, R_f = 0.4). $[\alpha]_D^{28}$ -82.6° (c 1.12, CH₂Cl₂). 1:0.2 mixture of rotamers. ¹H NMR (500 MHz, CDCl₃): δ 5.63 (ddd, *J* = 11.9, 6.4, 2.0 Hz, 1H), 5.56-5.54 (m, 2rotH), 5.48-5.45 (m, 1H), 4.41-4.30 (m, 2rotH), 4.35 (t, *J* = 8.0 Hz, 1H), 4.30 (apparent d, *J* = 17.5 Hz, 1H), 4.07 (dd, *J* = 13.8, 3.1 Hz, 1H), 3.73 (dd, *J* = 17.2, 5.0 Hz, 1H, 2rotH), 3.66 (s, 3H, 3rotH), 3.62-3.56 (m, 4H, 3rotH), 3.50 (s, 3H), 3.45 (s, 3rotH), 3.42-3.39 (m, 2rotH), 3.27 (s, 1H), 3.08 (apparent dd, *J* = 9.0 Hz, 5.6 Hz, 1rotH), 2.93 (dd, *J* = 9.4, 7.7 Hz, 1H, 1rotH), 2.81 (dd, *J* = 13.8, 9.6 Hz, 1H), 2.68-2.52 (m, 4H, 4rotH). ¹³C NMR (100 MHz, CDCl₃): δ 173.3, 173.1, 171.5, 134.5, 132.4, 125.3, 123.7, 85.5, 85.2, 81.4, 80.5, 68.1, 66.8, 60.8, 60.1, 58.0, 57.8, 51.6, 47.8, 46.0, 45.3, 45.2, 29.0, 28.7, 28.3. IR: 3472 (b), 2933, 2828, 1735, 1636 cm⁻¹. HRMS (FAB): calcd. for C₁₄H₂₄NO₆ [M + H]⁺, 302.160363; found, 302.159780.

(6R, 7S, Z) N-(methyl succinyl)-6,7-dimethoxy-5-oxoazacyclooct-3-ene. To a solution of **3.32** (436 mg, 1.51 mmol, 1 equiv) in dichloromethane (100 mL, anhydrous), pyridinium chlorochromate (494 mg, 2.29 mmol, 1.5 equiv.) was added. The mixture was heated to 40 °C and stirred under N₂ overnight. The following day, the reaction was cooled

to rt, water (75 mL) was added, and extracted with CH₂Cl₂ (3 x 100 mL). The organic extracts were combined, dried, decanted, and evaporated to dryness to result in crude product, which was purified via flash chromatography using a Biotage 40S column with a gradient solvent system of 8:1 toluene/acetone, 6:1 toluene/acetone, 4.5:1 toluene/acetone to yield pure (6*R*, 7*S*, *Z*) N-(methyl succinyl)-6,7-dimethoxy-5-oxoazacyclooct-3-ene as a clear oil (360 mg, 1.21 mmol, 80%). R_f = 0.6 in 1:1 toluene/acetone. [α]_D²⁸ +35.5° (c 4.46, CH₂Cl₂). 1:1 mixture of rotamers. ¹H NMR (500 MHz, CDCl₃): δ 6.17 (apparent d, *J* = 11.8 Hz, 1H), 5.95-5.88 (m, 2H), 5.69 (d, *J* = 11.9 Hz, 1H), 4.26 (dd, *J* = 17.4, 4.3 Hz, 1H), 4.11 (d, *J* = 19.7 Hz, 1H), 3.96 (d, *J* = 19.7 Hz, 1H), 3.81-3.71 (m, 6H), 3.61-3.59 (m, 8H), 3.48-3.30 (m, 13H), 2.62-2.40 (m, 7H), 2.36-2.31 (m, 1H). ¹³C NMR (125 MHz, CDCl₃): δ 203.2, 202.2, 173.8, 173.7, 172.5, 171.9, 137.5, 132.5, 129.1, 126.3, 89.1, 87.3, 81.1, 79.3, 59.6, 59.09, 59.07, 58.3, 51.9, 51.8, 50.4, 49.7, 48.5, 46.8, 29.1, 29.0, 28.02, 27.95. IR: 3590, 3516, 2944, 2830, 1743, 1691, 1655 cm⁻¹. HRMS (FAB): calcd. for C₁₄H₂₂NO₆ [M + H]⁺, 300.144713; found, 300.144130. Anal. calcd for C₁₄H₂₁NO₆: C, 56.18; H, 7.07, N, 4.68; found: C, 56.17; H, 7.09, N, 4.57.

(3*S*, 4*R*) N-(methyl succinyl)-3,4-dimethoxy-5-oxoazacyclooctane (3.33). (6*R*, 7*S*, *Z*) N-(methyl succinyl)-6,7-dimethoxy-5-oxoazacyclooct-3-ene (331 mg, 1.11 mmol, 1 equiv.) was dissolved in ethanol (60 mL) and 10 % Pd/C (27.8 mg) was added. The mixture was stirred overnight at rt under H₂ (1 atm). The following day, the mixture was filtered through Celite and the filtrate was evaporated to dryness to yield **3.33** (295 mg, 0.980 mmol, 89%). R_f = 0.5 in 1:1 toluene/acetone. [α]_D²⁸ +29.7° (c 6.24, CH₂Cl₂). 1:0.7 mixture of rotamers. ¹H NMR (500 MHz, CDCl₃): δ 4.00 (dd, *J* = 14.0, 4.5 Hz, 1H), 3.87 (d, *J* = 8.0 Hz, 1H), 3.75-3.69 (m, 3rotH), 3.65-3.39 (m, 8H, 6rotH), 3.34 (s, 3rotH), 3.29-3.20 (m, 3H, 2rotH), 3.08 (dt, *J* = 14.5, 5.0 Hz, 1H), 2.69-2.25 (m, 6H, 8rotH), 2.12-2.07 (m, 3H), 1.96 (s, 1rotH). ¹³C NMR (125 MHz, CDCl₃): δ 209.7, 209.0, 173.8, 173.5, 172.8, 172.4, 88.4, 86.1, 82.3, 80.4, 59.8, 59.1, 58.8, 57.9, 51.9, 51.8, 49.4, 48.3, 47.8, 47.5, 41.3, 37.7, 29.2, 28.9, 28.5, 28.3, 26.0, 25.3. IR: 3587, 3518, 2940, 2831, 1743, 1711, 1655 cm⁻¹. HRMS (ESI): calcd. for C₁₄H₂₃NO₆Na [M + Na]⁺, 324.1418; found, 324.1420. Anal. calcd for C₁₄H₂₃NO₆: C, 55.80; H, 7.69, N, 4.65; found: C, 55.91; H, 7.77, N, 4.63.

Compound 3.34. Ketone **3.33** (1.528 g, 5.075 mmol, 1 equiv.) was dissolved in 1:1 water/ethanol containing 100 mM aniline²⁵ (40 mL). To this solution, semicarbazide hydrochloride (5.898 g, 52.66 mmol, 10 equiv.) and AcOH (4 mL) was added. The reaction was stirred at rt and monitored by TLC (1:1 toluene/acetone) for the disappearance of **3.33** (R_f = 0.5). After the reaction was complete (approx 8 h), the reaction was neutralized with 10% NaOH and the ethanol was removed via evaporation under reduced pressure. The aqueous layer was extracted with ethyl acetate (4 x 75 mL). The ethyl acetate was combined, dried, decanted, and evaporated to dryness to result in crude semicarbazone that was directly converted to selenadiazole **3.34**. The crude semicarbazone was dissolved in dioxane (10 mL). A solution of SeO₂ (2.587 g, 23.31 mmol, 4.6 equiv.) in 1:1 dioxane/water (8 mL) was added dropwise over 4 h to the semicarbazone solution. The mixture was stirred at rt and analyzed by ESI-MS for the presence of **3.34** ([M+H]⁺ = 392) and absence of semicarbazone ([M+H]⁺ = 359, [M+Na]⁺

= 381). Upon reaction completion (approx 3 h after addition of all SeO₂), the dioxane was removed under reduced pressure and water (10 mL) was added. The aqueous solution was extracted with ethyl acetate (3 x 40 mL) and the organic extracts were combined, dried, decanted, and evaporated to dryness. The crude product was purified by flash chromatographed using a Biotage 40M column with CH₂Cl₂, 80:1 CH₂Cl₂/MeOH, 60:1 CH₂Cl₂/MeOH to result in pure **3.34** as a yellow oil (1.18 g, 3.03 mmol, 60%). R_f = 0.3 in 60:1 CH₂Cl₂/MeOH. [α]_D²⁸ +17.6° (c 1.27, CH₂Cl₂). 1:0.8 mixture of rotamers. ¹H NMR (500 MHz, CDCl₃): δ 5.39 (s, 1rotH), 5.37 (d, *J* = 5.4 Hz, 1H), 4.36 (m, 1rotH), 4.07-4.02 (m, 2rotH), 3.91 (q, *J* = 5.3 Hz, 1H), 3.73 (bs, 2H), 3.67 (s, 3rotH), 3.65 (s, 3H), 3.59-3.53 (m, 4H, 3rotH), 3.45-3.39 (m, 2H, 2rotH), 3.33-3.19 (m, 3H, 5rotH), 2.91-2.83 (m, 1rotH), 2.74-2.53 (m, 5H, 1rotH), 2.48-2.36 (m, 2rotH). ¹³C NMR (125 MHz, CDCl₃): δ 173.9, 173.7, 173.4, 171.7, 161.2, 159.3, 157.0, 156.3, 82.6, 80.1, 78.8, 77.9, 58.7, 58.5, 57.94, 57.88, 52.0, 51.9, 51.3, 50.5, 50.1, 49.8, 29.6, 29.1, 28.4, 28.3, 26.3, 25.4. IR: 3580, 3057, 2983, 2931, 2828, 1741, 1649 cm⁻¹. HRMS (FAB): calcd. for C₁₄H₂₂N₃O₅Se [M + H]⁺, 392.072467; found, 392.071460.

(6*S*, 7*S*) N-(methyl succinyl)-6,7-dimethoxyazacyclooct-4-yne. Selenadiazole **3.34** (350 mg, 0.90 mmol, 1.0 equiv.) was dissolved in *m*-xylene (320 mL) and heated to 115 °C. The reaction was monitored by TLC (1:1 toluene/acetone) for the disappearance of **3.34** (R_f = 0.60, UV active, red spot when visualized with vanillin) and appearance of azacyclooctyne methyl ester (R_f = 0.65, green spot when visualized with vanillin). Upon completion (approx 2 d), the reaction was cooled to rt and filtered, and then the filtrate was evaporated to dryness. The crude product was purified via flash chromatography using silica gel and a toluene/acetone solvent system starting at 20:1 and ending with 8:1. This procedure resulted in pure (6*S*, 7*S*) N-(methyl succinyl)-6,7-dimethoxyazacyclooct-4-yne as a slightly yellow oil (120 mg, 0.423 mmol, 47%, 55% brsm, R_f = 0.6). [α]_D²⁸ +7.5° (c 0.64, CH₂Cl₂). 1:0.15 mixture of rotamers. ¹H NMR (400 MHz, D₂O): δ 4.38 (apparent d, *J* = 7.9 Hz, 1rotH), 4.24 (dt, *J* = 8.6, 2.6 Hz, 1H, 1rotH), 4.17 (dd, 14.9, 5.4 Hz, 1H), 4.06 (d, *J* = 14.3 Hz, 1H), 4.00 (s, 1rotH), 3.88 (t, *J* = 9.2 Hz, 1rotH), 3.72-3.68 (m, 4H, 3rotH), 3.55-3.44 (m, 3H, 4rotH), 3.38-3.29 (m, 4H, 3rotH), 3.05 (dd, *J* = 14.3, 9.1 Hz, 1H, 1rotH), 2.90-2.64 (m, 5H, 5rotH), 2.33 (dt, *J* = 16.9, 3.2 Hz, 1H), 2.25 (apparent d, *J* = 16.8 Hz, 1rotH). ¹³C NMR (100 MHz, CDCl₃): δ 173.6 (broad), 172.5, 171.6, 99.0, 96.0, 93.0, 91.0, 87.0, 85.2, 77.8, 77.4, 59.8, 59.3, 57.5, 57.4, 56.4, 55.7, 53.2, 52.3, 52.02, 51.98, 29.5, 29.3, 28.7, 28.3, 22.1, 21.1. IR: 3489, 2931, 2827, 2203, 1736, 1648 cm⁻¹. HRMS (FAB): calcd. for C₁₄H₂₂NO₅ [M + H]⁺, 284.149798; found, 284.150650.

(6*S*, 7*S*) N-(succinate)-6,7-dimethoxyazacyclooct-4-yne (3.35). (6*S*, 7*S*) N-(methyl succinyl)-6,7-dimethoxyazacyclooct-4-yne (27.3 mg, 0.0964 mmol, 1.0 equiv.) was dissolved in 2:1 water/dioxane (1.5 mL) and LiOH (45.7 mg, 1.91 mmol, 20 equiv., crushed) was added. The reaction was stirred overnight at rt. The following day the mixture was neutralized with 3M HCl and the dioxane was removed via reduced pressure. Additional water (3 mL) was added to the resulting aqueous solution, this solution was acidified with 3M HCl and extracted with ethyl acetate (5 x 10 mL). The organic extracts were combined, dried, decanted, and evaporated to dryness. The crude product was

purified via flash chromatography using silica gel and a gradient solvent system starting with 8:1 toluene/acetone and ending with 1:1 toluene/acetone. This procedure resulted in pure **3.35** as an off-white solid (17.1 mg, 0.0636 mmol, 66%). $R_f = 0.3 - 0.4$ in 1:1 toluene/acetone. $[\alpha]_D^{28} -14.6^\circ$ (c 0.357, H₂O). 1:0.1 mixture of rotamers. ¹H NMR (400 MHz, D₂O): δ 4.37 (dt, $J = 7.8, 2.3$ Hz, 1rotH), 4.13 (dt, $J = 8.7, 2.8$ Hz, 1H, 1rotH), 4.18 (dd, $J = 14.9, 5.4$ Hz, 1H), 4.06 (d, $J = 14.3$ Hz, 1H), 3.91 (s, 1rotH), 3.89 (t, $J = 8.4$ Hz, 1rotH), 3.71 (t, $J = 8.5$ Hz, 1H), 3.56 (s, 3H, 3rotH), 3.56-3.46 (m, 2rotH), 3.37-3.28 (m, 4H, 2rotH), 3.04 (dd, $J = 14.3, 9.0$ Hz, 1H, 1rotH), 2.88-2.64 (m, 5H, 5rotH), 2.32 (dt, $J = 16.6, 3.4$ Hz, 1H), 2.24 (apparent d, 16.8 Hz, 1rotH). ¹³C NMR (125 MHz, D₂O, no rotamer peaks tabulated): δ 177.0, 174.9, 99.0, 89.7, 84.1, 76.1, 58.0, 56.4, 54.1, 51.9, 29.0, 27.7, 20.6. IR: 3434, 2935, 2830, 2358, 2207, 1729, 1642 cm⁻¹. HRMS (ESI): calcd. for C₁₃H₁₉NO₅Na [M + Na]⁺, 292.1155; found, 292.1157.

Kinetics

The reaction in Scheme 3.6 was monitored by ¹H NMR for 4 h at rt. DIMAC and benzyl azide were separately dissolved in CD₃CN and mixed together in a 1:1 ratio at concentrations between 20 and 30 mM. *Tert*-butyl acetate (approx 0.3 equiv) was used as an internal standard. The percent conversion was calculated by the disappearance of DIMAC relative to the *tert*-butyl acetate as determined by integration. No products other than **3.36** and **3.37** were apparent by ¹H NMR. The triazole isomers were produced in a ~ 1:1.4 ratio. The second-order rate constant was determined by plotting 1/[**3.35**] versus time. The plot was fit to a linear regression and the slope corresponds to the second-order rate constant. Shown are data from two replicate experiments.

X-Ray Crystallography

A colorless prism 0.12 x 0.08 x 0.04 mm in size was mounted on a Cryoloop with Paratone oil. Data were collected in a nitrogen gas stream at 150(2) K using phi and omega scans. Crystal-to-detector distance was 60 mm and exposure time was 5 seconds per frame using a scan width of 2.0°. Data collection was 99.8% complete to 67.00° in ϕ . A total of 16229 reflections were collected covering the indices, $-6 \leq h \leq 6$, $-9 \leq k \leq 9$, $-17 \leq l \leq 17$. 2383 reflections were found to be symmetry independent, with an R_{int} of 0.0357. Indexing and unit cell refinement indicated a primitive, monoclinic lattice. The space group was found to be P2(1) (No. 4). The data were integrated using the Bruker SAINT software program and scaled using the SADABS software program. Solution by direct methods (SIR-2008) produced a complete heavy-atom phasing model consistent with the proposed structure. All non-hydrogen atoms were refined anisotropically by full-matrix least-squares (SHELXL-97). All hydrogen atoms were placed using a riding model. Their positions were constrained relative to their parent atom using the appropriate HFIX command in SHELXL-97. Absolute stereochemistry was unambiguously determined to be *S* at both C2 and C3, respectively.

References

- (1) Baskin, J. M.; Prescher, J. A.; Laughlin, S. T.; Agard, N. J.; Chang, P. V.; Miller, I. A.; Lo, A.; Codelli, J. A.; Bertozzi, C. R. Copper-free click chemistry for dynamic in vivo imaging. *Proc. Natl. Acad. Sci. U.S.A.* **2007**, *104*, 16793-16797.
- (2) Chenoweth, K.; Chenoweth, D.; Goddard III, W. A. Cyclooctyne-based reagents for uncatalyzed click chemistry: A computational survey. *Org. Biomol. Chem.* **2009**, *7*, 5255-5258.
- (3) Schoenebeck, F.; Ess, D. H.; Jones, G. O.; Houk, K. N. Reactivity and regioselectivity in 1,3-dipolar cycloadditions of azides to strained alkynes and alkenes: A computational study. *J. Am. Chem. Soc.* **2009**, *131*, 8121-8133.
- (4) Ess, D. H.; Jones, G. O.; Houk, K. N. Transition states of strain-promoted metal-free click chemistry: 1,3-Dipolar cycloadditions of phenyl azide and cyclooctynes. *Org. Lett.* **2008**, *10*, 1633-1636.
- (5) Peters, L. L.; Robledo, R. F.; Bult, C. J.; Churchill, G. A.; Paigen, B. J.; Svenson, K. L. The mouse as a model for human biology: A resource guide for complex trait analysis. *Nat. Rev. Genet.* **2007**, *8*, 58-69.
- (6) Chang, P. V.; Prescher, J. A.; Sletten, E. M.; Baskin, J. M.; Miller, I. A.; Agard, N. J.; Lo, A.; Bertozzi, C. R. Copper-free click chemistry in living animals. *Proc. Natl. Acad. Sci. U.S.A.* **2010**, *107*, 1821-1826.
- (7) Mano, N.; Sato, K.; Goto, J. Specific affinity extraction method for small molecule-binding proteins. *Anal. Chem.* **2006**, *78*, 4668-4675.
- (8) Detert, H.; Anthony-Mayer, C.; Meier, H. Anti-Bredt enol ethers by transannular cyclization of cycloalkynols. *Angew. Chem. Int. Ed.* **1992**, *31*, 791-792.
- (9) Brandsma, L.; Verkruijsse, H. D. An improved synthesis of cyclooctyne. *Synthesis* **1978**, 290-290.
- (10) Jones, K.; Wood, W. W. The preparation and attempted alkylation of some 6-cyano-carbohydrates. *Carbohydr. Res.* **1986**, *155*, 217-222.
- (11) Chretien, F.; Khaldi, M.; Chapleur, Y. An improved procedure for the ring opening of benzylidene acetals with N-bromosuccinimide. *Synthetic Comm.* **1990**, *20*, 1589-1596.
- (12) Sletten, E. M.; Liotta, L. J. A flexible stereospecific synthesis of polyhydroxylated pyrrolizidines from commercially available pyranosides. *J. Org. Chem.* **2006**, *71*, 1335-1343.
- (13) Miller, S. J.; Kim, S.-H.; Chen, Z.-R.; Grubbs, R. H. Catalytic ring-closing metathesis of dienes: Application to the synthesis of eight-membered rings. *J. Am. Chem. Soc.* **1995**, *117*, 2108-2109.
- (14) Bonney, K. J.; Braddock, D. C.; White, A. J. P.; Yaqoob, M. Intramolecular bromonium ion assisted epoxide ring-opening: Capture of the oxonium ion with an added external nucleophile. *J. Org. Chem.* **2011**, *76*, 97-104.
- (15) Krebs, A.; Wilke, J. Angle strained cycloalkynes. In *Wittig Chemistry*; Springer-Verlag: Berlin/Heidelberg, **1983**; Vol. 109, pp. 189-233.
- (16) Agard, N. J.; Baskin, J. M.; Prescher, J. A.; Lo, A.; Bertozzi, C. R. A comparative study of bioorthogonal reactions with azides. *ACS Chem. Biol.* **2006**, *1*, 644-648.

- (17) Meier, H.; Voigt, E. Bildung und fragmentierung von cycloalkeno-1,2,3-selenadiazolen. *Tetrahedron* **1972**, *28*, 187-198.
- (18) Meier, H.; Petersen, H. Synthese von 5-substituierten cyclooctynen. *Synthesis* **1978**, 596-598.
- (19) Petersen, H.; Meier, H. Synthese von cycloocteninen. *Chem. Ber.* **1980**, *113*, 2383-2397.
- (20) Meier, H.; Gugel, H. Synthese des 5,6-didehydro-11,12-dihydro-dibenzo-[a,e]cyclooctens - eines hochgespannten cycloalkyns. *Synthesis* **1976**, 338-339.
- (21) Krebs, A.; Kimling, H. 3.3.6.6-Tetramethyl-1-thiacycloheptin ein isolierbares siebenring-acetylen. *Tetrahedron Lett.* **1970**, *11*, 761-764.
- (22) Leupin, W.; Wirz, J. Cyclooct-1-en-5-yne. Preparation, spectroscopic characteristics and chemical reactivity. *Helv. Chim. Acta* **1978**, *61*, 1663-1674.
- (23) Meier, H.; Stavridou, E.; Roth, S.; Mayer, W. 1-Oxa-3-cyclooctin. *Chem. Ber.* **1990**, *123*, 1411-1414.
- (24) Meier, H.; Stavridou, E.; Storek, C. 1-Thia-2-cyclooctyne—A strained cycloalkyne with polarized triple bond. *Angew. Chem. Int. Ed.* **1986**, *25*, 809-810.
- (25) Dirksen, A.; Hackeng, T. M.; Dawson, P. E. Nucleophilic catalysis of oxime ligation. *Angew. Chem.* **2006**, *118*, 7743-7746.
- (26) Sletten, E. M.; Bertozzi, C. R. A hydrophilic azacyclooctyne for Cu-free click chemistry. *Org. Lett.* **2008**, *10*, 3097-3099.
- (27) Meier, H.; Hanold, N.; Molz, T.; Bissinger, H. J.; Kolshorn, H.; Zountsas, J. Strained cycloalkenynes. *Tetrahedron* **1986**, *42*, 1711-1719.
- (28) Pangborn, A. B.; Giardello, M. A.; Grubbs, R. H.; Rosen, R. K.; Timmers, F. J. Safe and convenient procedure for solvent purification. *Organometallics* **1996**, *15*, 1518-1520.
- (29) Capon, B.; Overend, W. G.; Sobell, M. The kinetics of the acid-catalysed hydrolysis of some methyl 4,6-O-benzylidene-hexosides. *Tetrahedron* **1961**, *16*, 106-112.

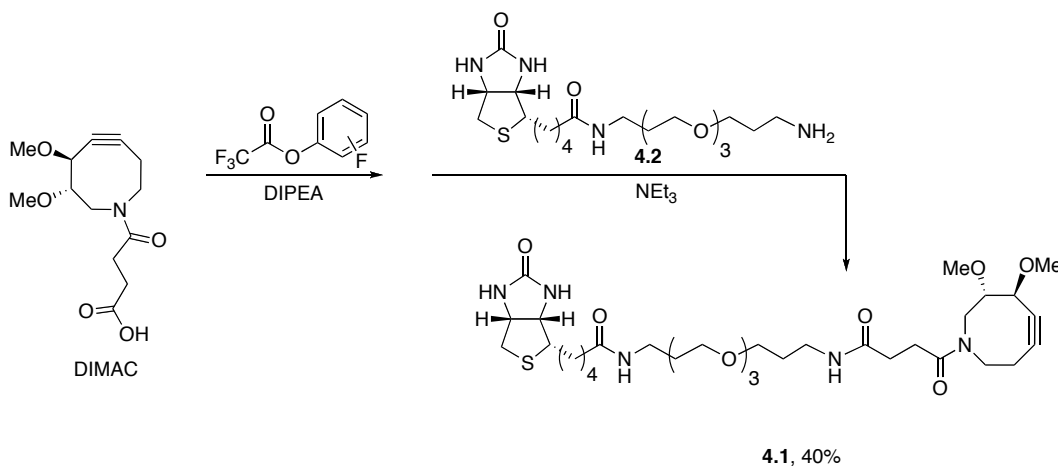
Chapter 4

Labeling Azido-Glycans with DIMAC

Labeling of Azides *in vitro* with DIMAC

With the hydrophilic azacyclooctyne DIMAC synthesized, we were eager to discover the advantages of a more water-soluble cyclooctyne. In order to detect the cycloadducts in biological experiments, a biotin conjugate of DIMAC (DIMAC-biotin, **4.1**, Scheme 4.1) was prepared by activation of the acid with a pentafluorophenol group followed by amide bond formation with amine containing biotin **4.2**.¹ The hydrophilicity of **4.1** was immediately evident during the preparation of 2.5 mM stock solutions. DIMAC-biotin **4.1** was readily soluble in aqueous buffer, whereas the analogous OCT-MOFO- or DIFO- biotin conjugates (**2.39**, **2.44**, **3.4**, respectively) required an organic cosolvent (30% DMF). Thus, DIMAC seemed poised to have minimal hydrophobic interactions when labeling azides in living systems.

Scheme 4.1. Synthesis of DIMAC-biotin **4.1**.



We first tested the ability of DIMAC to label glycan-associated azides within cell lysates and on the surfaces of live cells. Jurkat cells were grown in the presence (+Az) or absence (-Az) of 25 μ M N-azidoacetylmannosamine (Ac₄ManNAz) for three days resulting in the metabolic labeling of cell-surface glycans with N-azidoacetyl sialic acid (SiaNAz) residues. Cell lysates were incubated overnight with 250 μ M DIMAC-biotin, ALO-biotin or Phos-biotin (the latter two for comparison purposes) and then analyzed by Western blot probing with a horseradish peroxidase conjugated α -biotin antibody (α -biotin-HRP). All the reagents labeled glycoproteins from the lysate in an azide-dependent manner. However, the more hydrophobic cyclooctyne ALO produced a greater extent of non-specific protein labeling (Figure 4.1).

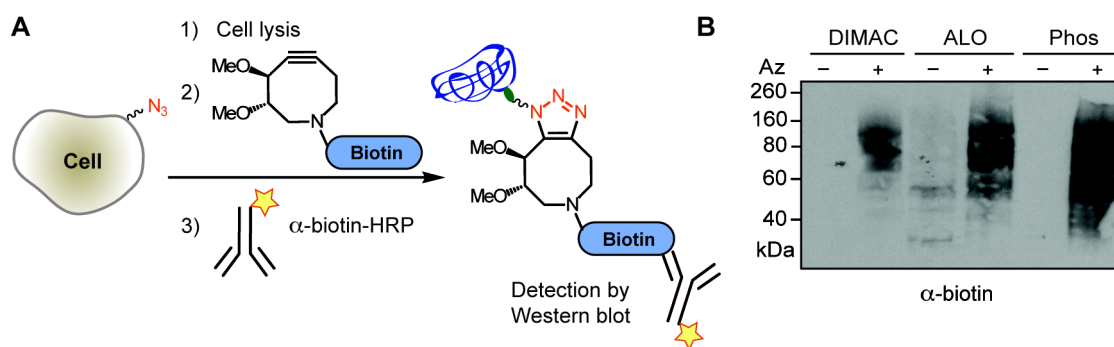


Figure 4.1. DIMAC labels azido-glycoproteins in cell lysate. A. Schematic of experiment. B. Cells were treated with (+) or without (-) Ac_4ManNAz ($25\ \mu\text{M}$) for 3 d and lysates were generated. The cell lysate ($35\ \mu\text{g}$) was reacted with $250\ \mu\text{M}$ DIMAC-biotin (**4.1**), ALO-biotin (**2.43**) or Phos-biotin (**2.10**) overnight at rt. The resulting protein mixtures were analyzed by Western blot probing with α -biotin conjugated to horse-radish peroxidase (α -biotin-HRP).

To test DIMAC's reactivity with azides on live cells, Jurkat cells were again incubated with $25\ \mu\text{M}$ Ac_4ManNAz for three days and then treated with various concentration of DIMAC-biotin for 1 h or $250\ \mu\text{M}$ DIMAC-biotin for various amounts of time (Figure 4.2). The cells were incubated with fluorescein isothiocyanate modified avidin (FITC-avidin) and analyzed by flow cytometry. DIMAC exhibited time- and dose-dependent labeling consistent with other early generation cyclooctynes. Notably, at the longer time points and higher concentrations there was still minimal signal for cells treated with no azidosugar, a testament to the hydrophilic nature of the cyclooctyne. Importantly, DIMAC did not show any cytotoxicity during cell labeling as assayed by propidium iodide and AnnexinV staining (Figure 4.3).

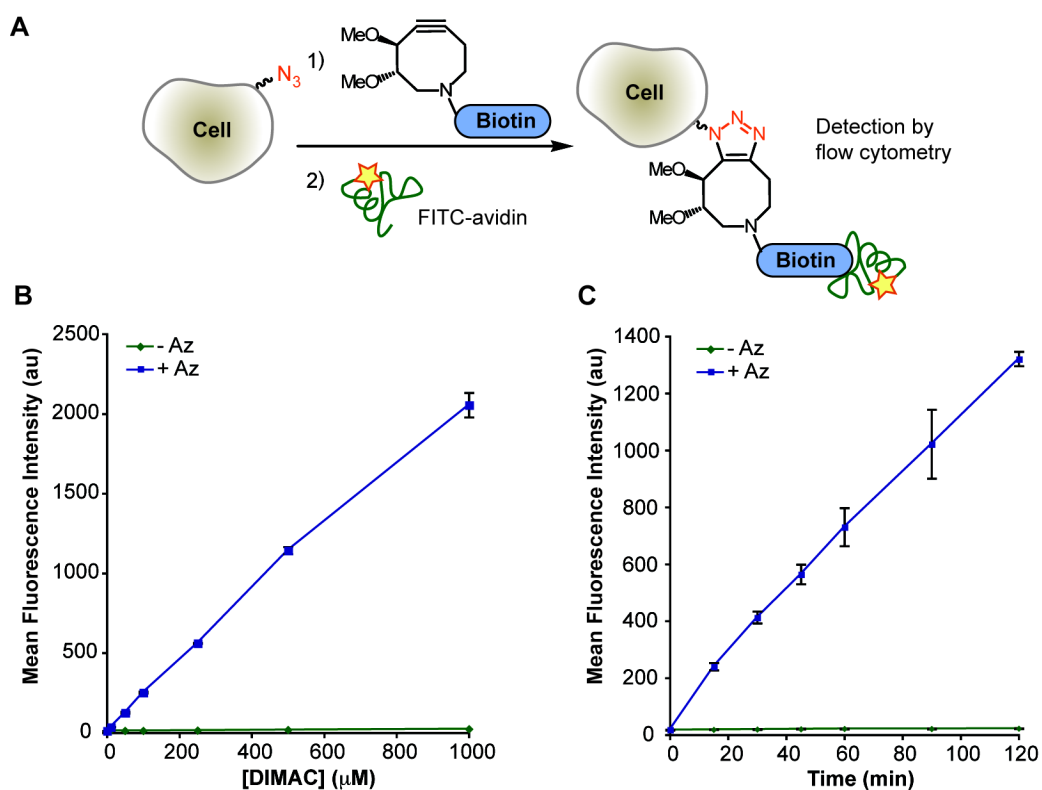


Figure 4.2. Dose- and time-dependent cell-surface glycan labeling with DIMAC-biotin **4.1**. **A.** Schematic for live cell labeling of Jurkat cells with DIMAC-biotin. **B/C.** Jurkat cells were grown in the presence (+ Az, blue square) or absence (– Az, green diamond) of 25 μM Ac_4ManNAz for 3 d. The cells were treated with DIMAC-biotin **4.1** in **(B)** varying concentrations for 1 h or **(C)** varying times at a concentration of 250 μM . The cells were then treated with FITC-avidin and analyzed by flow cytometry. The error bars represent standard deviations from three replicate samples.

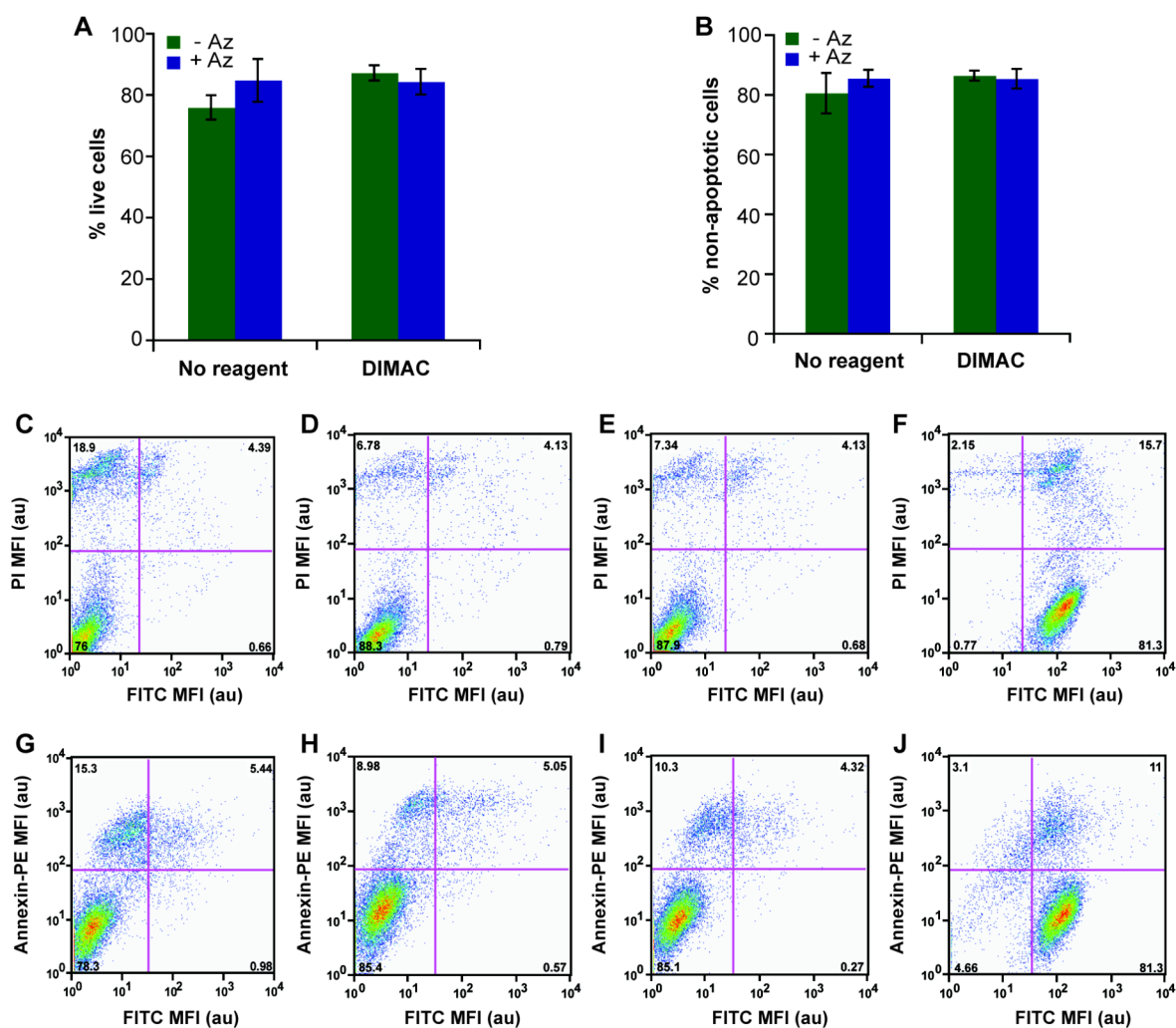


Figure 4.3. Cytotoxicity analysis of DIMAC-biotin. A/B. Jurkat cells were incubated in the presence (+ Az) or absence (– Az) of Ac₄ManNAz for 3 d. Cells were treated with no reagent (FACS buffer) or DIMAC-biotin conjugate **4.1** (250 μM **4.1** in FACS buffer) for 1 h at rt, incubated with FITC-avidin, and washed. Prior to flow cytometry analysis, half the cells were treated with (A) propidium iodide and the other half were treated with (B) Annexin-V-PE using the BD Pharmingen Annexin-V Apoptosis Detection Kit following the provided procedure. The samples were diluted and analyzed by flow cytometry. The error bars represent standard deviations from three replicate samples. C-J. Representative FL2 vs. FL1 scatter plots. In all plots, the x-axis indicates the degree of cell-surface azido-glycan labeling as measured by FITC fluorescence (FITC MFI). For plots C-F, the y-axis represents the degree of propidium iodide staining (PI MFI, cell death marker), while the y-axis in plots G-J represents the degree of Annexin-V staining (Annexin-PE MFI, early apoptosis marker). Plots C,D,G,H represent cells treated without azide and plots E,F,I,J represent cells treated with azide. Plots C,G,E,I represent cells treated with no reagent while plots D,H,F,J represent cells treated with DIMAC-biotin.

A comparison experiment on Jurkat cells was performed between DIMAC-biotin **4.1** and ALO-biotin **2.43** (250 μ M, 1 h). DIMAC-biotin and ALO-biotin selectively label cell surfaces in an azide-dependent manner with comparable efficiencies (Figure 4.4A). ALO-biotin, however, showed significantly higher non-specific background labeling. The DIMAC reagent labeled cells with a signal:background ratio of 26:1 whereas the ratio for ALO-biotin was 14:1. The fluorescence of cells lacking azides but treated with DIMAC-biotin followed by FITC-avidin was indistinguishable from those treated with FITC-avidin alone (Figure 4.4B).

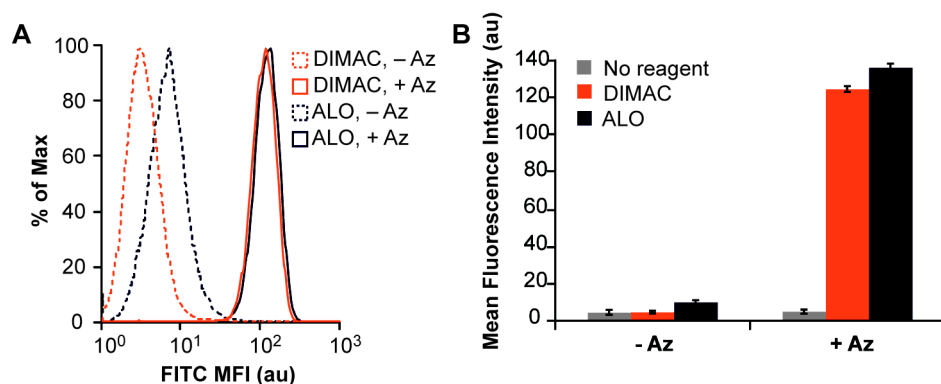


Figure 4.4. Cell-surface glycan labeling with DIMAC-biotin and ALO-biotin. Jurkat cells were grown in the presence (+ Az) or absence (– Az) of Ac_4ManNAz for 3 d. Cells were incubated with no reagent (FACS buffer containing 3% DMF, gray), DIMAC-biotin (250 μ M **4.1** in FACS buffer containing 3% DMF, orange) or ALO-biotin (250 μ M **2.43** in FACS buffer containing 3% DMF, navy) for 1 h at rt, incubated with FITC-avidin, and analyzed by flow cytometry. A. Histograms of representative samples. MFI = mean fluorescence intensity (arbitrary units). B. Bar graph of the average of three replicates. The error bars represent standard deviations of three replicate experiments.

DIMAC was also compared to Phos-biotin of the Staudinger ligation and to DIFO-biotin (Figure 4.5). As expected, DIMAC did not label cell-surface azides with similar efficiencies to these reagents. In fact, DIMAC-biotin yielded a similar degree of labeling to 100-fold less DIFO-biotin. Nevertheless, the hydrophilicity of DIMAC appeared very promising in terms of minimizing non-specific background labeling, which was the main goal for this water-soluble cyclooctyne. All the *in vitro* experiments indicated that DIMAC should be tested *in vivo* for its ability to label murine azido-glycans.

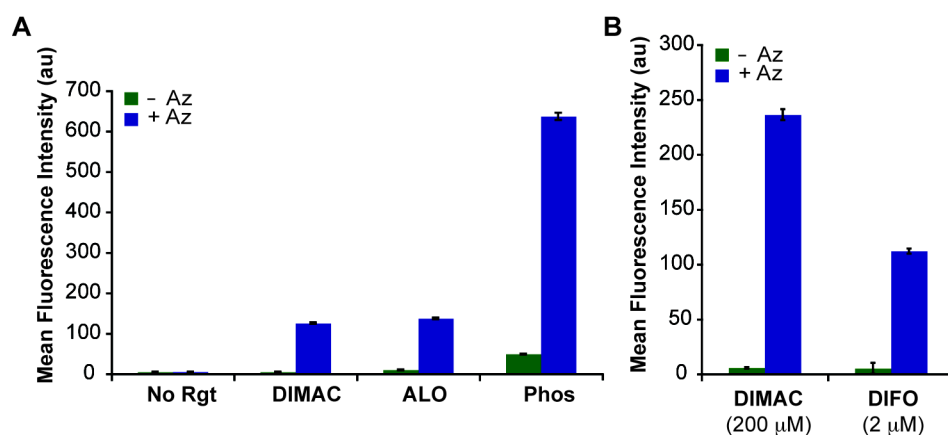


Figure 4.5. Cell-surface glycan labeling with DIMAC-biotin, DIFO-biotin, ALO-biotin, and Phos-biotin. Jurkat cells were incubated in the presence (+ Az, blue bars) or absence (– Az, green bars) of 25 μM Ac₄ManNAz for 3 d. Cells were treated with no reagent (FACS buffer), DIMAC-biotin (200 μM **4.1** in FACS buffer), ALO-biotin (200 μM **2.43** in FACS buffer with 3% DMF), Phos-biotin (200 μM **2.10** in FACS buffer with 3% DMF), or DIFO-biotin (2 μM **3.4** in FACS buffer with 0.03% DMF) for 1 h at rt, incubated with FITC-avidin, and analyzed by flow cytometry. The error bars represent standard deviations from three replicate samples. Au = arbitrary units.

Previous work had shown that the biotin conjugates were ineffective *in vivo* and FLAG conjugates proved to have superior solubility properties for use in mice.² DIMAC-FLAG (**4.3**) was synthesized through a two-step process involving the coupling of DIMAC (**3.35**) and maleimide-amine **4.4**³ to yield **4.5** followed by Michael addition of the sulfhydryl residue of the Cys-FLAG peptide onto the maleimide. HPLC purification afforded pure DIMAC-FLAG in 40% yield (Scheme 4.2).⁴ Phos-FLAG was also prepared as a control for the *in vivo* experiments. DIMAC-FLAG exhibited the expected azide-dependent labeling on Jurkat cells treated with or without Ac₄ManNAz (Figure 4.6), indicating this reagent was ready for use in mice.

Scheme 4.2. Synthesis of DIMAC-FLAG 4.3.

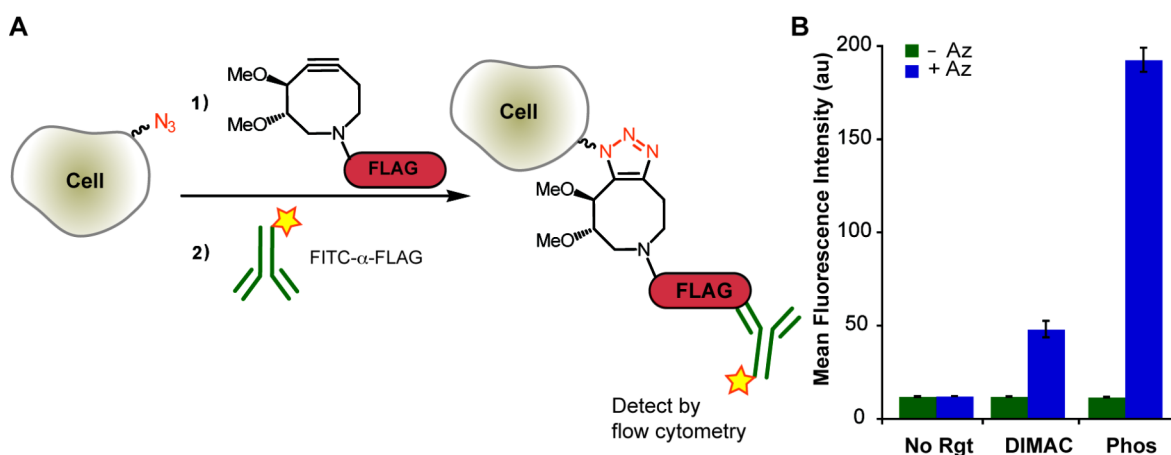
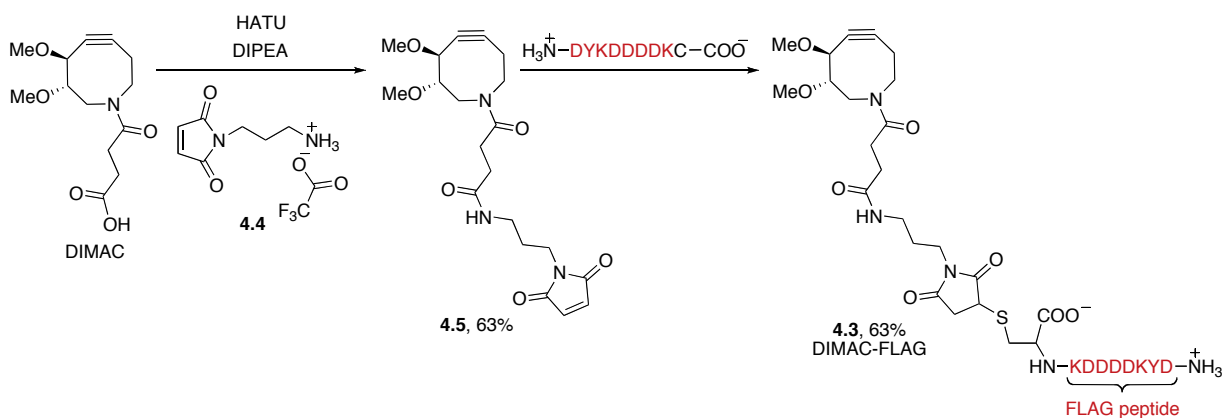


Figure 4.6. Cell-surface glycan labeling with DIMAC-FLAG (4.3). A. Schematic for live cell labeling of Jurkat cells with DIMAC-FLAG. Jurkat cells were grown in the presence (+Az, blue bars) or absence (-Az, green bars) of 25 μM Ac₄ManNAz for 3 d. The cells were treated with DIMAC-FLAG (4.3) or Phos-FLAG (2.11) (250 μM for 1 h). The cells were then treated with FITC- α -FLAG and analyzed by flow cytometry. The error bars represent standard deviations from three replicate samples.

Labeling of Azides *in vivo* with DIMAC^a

Azides were incorporated into sialoglycans in mice by injection of Ac₄ManNAz (300 mg/kg, IP) once a day for 7 days. On the eighth day, DIMAC-FLAG (**4.3**) or Phos-FLAG (**2.11**) were injected IP. Two different doses of DIMAC-FLAG (0.8 mmol/kg and 1.6 mmol/kg) were tested. Three hours later, the mice were sacrificed, their splenocytes were isolated, incubated with fluorescein isothiocyanate (FITC)-conjugated α -FLAG (FITC- α -FLAG) and the degree of labeling was analyzed by flow cytometry. The heart, liver, kidney, intestines, and thymus were also collected and organ lysates were generated. Western blot analyses were performed on these organs as well as on serum proteins that were collected during a cardiac bleed.

The live splenocyte labeling experiments allowed for quantitative comparison of the two doses of DIMAC-FLAG and for comparison to Phos-FLAG. Gratifyingly, we found that DIMAC-FLAG displayed azide-dependent labeling at both doses with a reasonable dose-dependence also being observed (Figure 4.7).

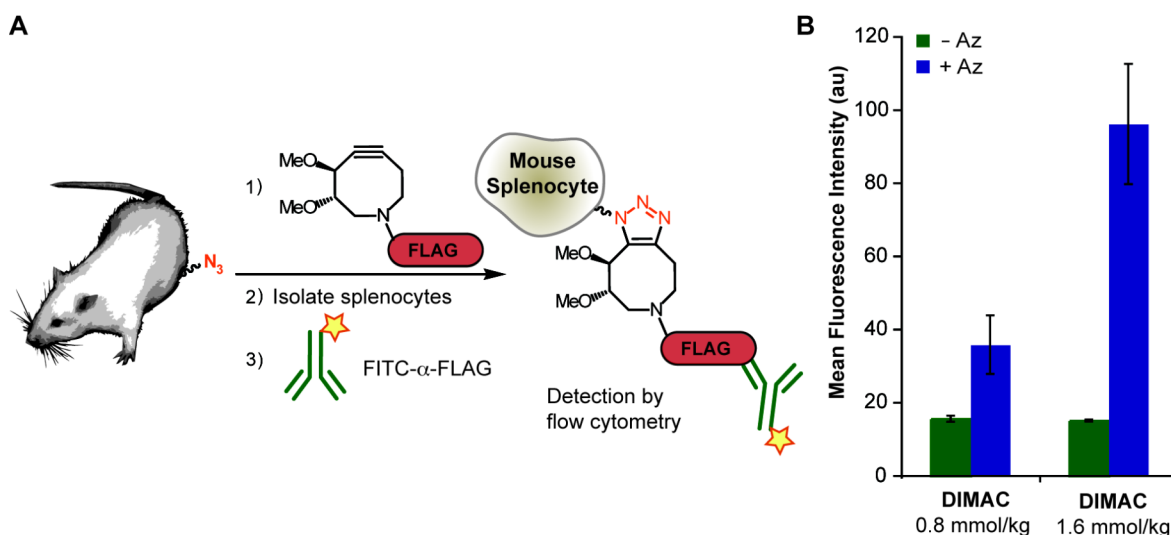


Figure 4.7. DIMAC-FLAG labels cell-surface azidoglycans on splenocytes of live mice. A. Schematic of experiment. B. Mice were injected with either Ac₄ManNAz (300 mg/kg, IP, blue bars) or vehicle (70% DMSO, IP, green bars) once daily for 7 d. On day 8, the mice were injected IP with DIMAC-FLAG (0.8 mmol/kg or 1.6 mmol/kg). After 3 h, the mice were euthanized, and splenocytes were isolated, labeled with FITC- α -FLAG and analyzed by flow cytometry. Error bars represent the standard deviation of the average MFI value of splenocytes isolated from separate mice (n = 3-5). Au = arbitrary units.

^a Pamela Chang and Jeremy Baskin contributed to results in this section.

When the efficiency of azide-labeling with DIMAC-FLAG was compared to Phos-FLAG, it was apparent that the Staudinger ligation was still dramatically outperforming Cu-free click chemistry *in vivo* (Figure 4.8). In fact, when the splenocytes were treated with additional Phos-FLAG *ex vivo*, we found no additional increase in labeling for the splenocytes that came from mice treated with azide and Phos-FLAG; however, there was an increase in signal for the splenocytes treated with azide and with DIMAC-FLAG (Figure 4.8A). This result indicates that all accessible azides are labeled by the *in vivo* Staudinger ligation but not by *in vivo* Cu-free click chemistry. An α -FLAG Western blot of serum proteins from mice treated with and without azide followed by Phos-FLAG or DIMAC-FLAG also indicated that the Staudinger ligation outperformed DIMAC-FLAG *in vivo* (Figure 4.8B).

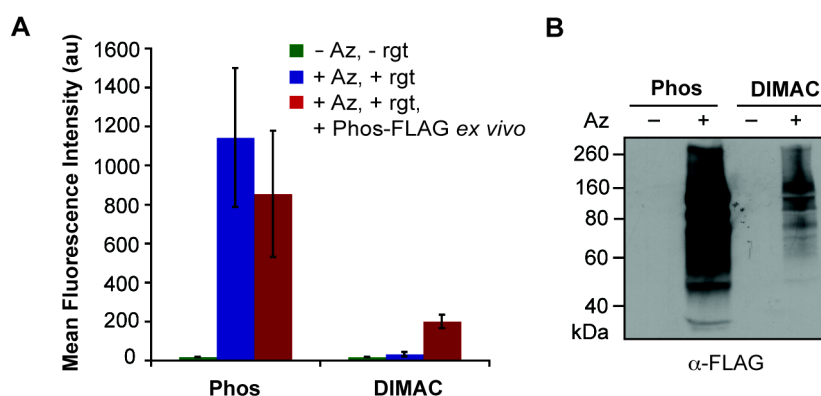


Figure 4.8. The Staudinger ligation is the superior bioorthogonal reaction for labeling azides in live mice. Mice were injected with either Ac₄ManNAz (300 mg/kg, IP, blue bars, red bars) or vehicle (70% DMSO, green bars) once daily for 7 d. On day 8, the mice were injected IP with Phos-FLAG or DIMAC-FLAG (0.8 mmol/kg). A. After 3 h, the mice were euthanized and the splenocytes were isolated. Half the cells were labeled with FITC- α -FLAG and analyzed by flow cytometry immediately (green and blue bars). The other half was incubated with Phos-FLAG (250 μ M) for 1 h. These cells were then incubated with Phos-FLAG and analyzed by flow cytometry (red bars, data for vehicle treated mice not shown). Error bars represent the standard deviation of the average MFI value of splenocytes isolated from separate mice (n = 3). Au = arbitrary units. B. After 3 h, the mice were anesthetized and whole blood was collected by cardiac puncture from the closed thorax. After removal of red blood cells and leukocytes, serum samples were analyzed by Western blot probing with an α -FLAG-HRP.

We wondered if the decreased efficiency of labeling of DIMAC-FLAG *in vivo* as compared to cultured live cell labeling experiments was due to background reactivity, as at the onset of the synthesis of DIMAC we hypothesized this was the main problem with DIFO-FLAG (Figure 3.2). To assess the background labeling of DIMAC-FLAG, we performed Western blot analyses of organ lysates (Figure 4.9). DIMAC gives robust azide-dependent signal in the liver, heart, kidneys, and intestine. The most intense signal appears in the intestines, most likely due to its proximity to the injection site (all injections were intraperitoneal). In the heart and kidney blots, faint signal is observed in the vehicle treated mice around 65 kDa. This band could correlate to mouse serum albumin (as was the case for DIFO). Due to the intrinsic reactivity differences between DIFO and DIMAC, it is difficult to conclude whether the decrease in background labeling is due to the hydrophilicity or reactivity of the reagents. We suspect that both are contributing factors. A better comparison would be that of DIMAC and ALO; however, ALO did not display efficient enough labeling *in vivo* for azide-dependent labeling in the heart and kidney to be observed.

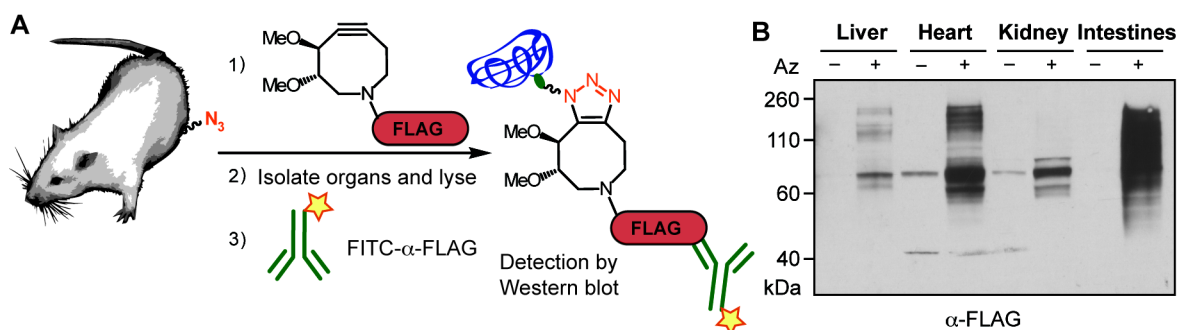


Figure 4.9. DIMAC-FLAG labels azides in many organisms within the mouse. A. Schematic for the experiment. B. Mice were injected with Ac₄ManNAz (300 mg/kg, IP, + Az) or vehicle (70% DMSO, – Az) once daily for 7 d. On day 8, the mice were injected with DIMAC-FLAG (0.8 mmol/kg, IP). Three hours post-injection of the FLAG conjugate, the mice were euthanized, and organs (liver, heart, kidney, intestines) were harvested and homogenized. The organ lysates were analyzed by Western blot probing with α -FLAG-HRP. Each lane represents an organ lysate from a single representative mouse.

Interestingly, DIMAC-FLAG did not display significant background labeling when serum samples were analyzed by Western blot, even though the protein we suspected was responsible for background reactivity, MSA, was a serum protein (Figure 4.10A). This is in stark contrast to DIFO, which displayed robust labeling of MSA in the serum (Figure 4.10B). This result could indicate that the hydrophilicity of DIMAC caused it to be readily cleared from the serum. Additional pharmacokinetic studies, ideally with radiolabeled cyclooctynes, will be necessary to answer this question.

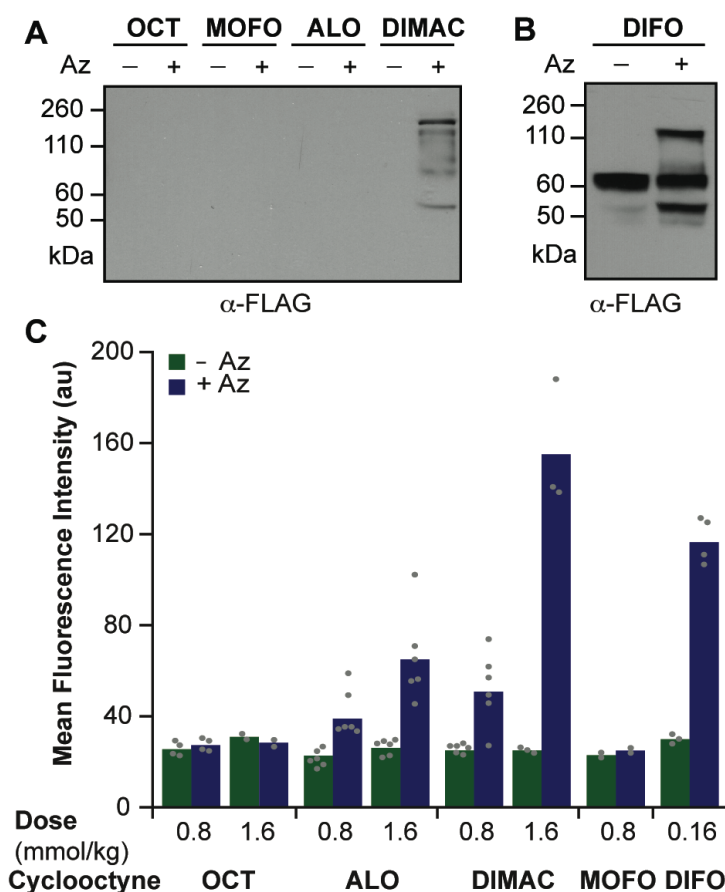


Figure 4.10. Comparison of cyclooctyne reagents' ability to label azides *in vivo*. Mice were injected with either Ac₄ManNAz (300 mg/kg, IP, +, blue bars) or vehicle (70% DMSO, -, green bars) once daily for 7 d. On day 8, the mice were injected IP with various doses (as indicated) of OCT-FLAG (**2.39**), ALO-FLAG (**2.45**), DIMAC-FLAG (**4.3**), MOFO-FLAG (**2.46**), or DIFO-FLAG (**3.3**). **A**. After 3 h, the mice were anesthetized and whole blood was collected by cardiac puncture from the closed thorax. After removal of red blood cells and leukocytes, serum samples were analyzed by Western blot probing with an α -FLAG-HRP. **B**. After 3 h, the mice were euthanized, and splenocytes were isolated, labeled with FITC- α -FLAG and analyzed by flow cytometry. Each point represents the average MFI value of three replicate samples from an individual mouse. Each bar represents the average MFI value of splenocytes isolated from separate mice (n = 3-11). MFI = Mean fluorescence intensity in arbitrary units (au). For all *in vivo* experiments, *ex vivo* reactions of isolated splenocytes with FLAG conjugates verified the presence of cell-surface azides for all of these probes

While a direct quantitative comparison of DIMAC-FLAG to the earlier generation cyclooctynes was precluded due to the large amount of compound and mice necessary to perform these experiments simultaneously, serum samples frozen from mice treated with

earlier generation cyclooctynes could be compared to the DIMAC serum samples by Western blot (Figure 4.10A). These Western blot data highlighted that the hydrophilicity of DIMAC was critical to improving Cu-free click chemistry *in vivo*, as all these cyclooctynes react with azides with similar efficiencies but only DIMAC displays robust signal (if the blot is further exposed ALO also displays azide-dependent labeling).⁴ Additionally, splenocyte labeling experiments from the earlier generation cyclooctyne *in vivo* experiments could be normalized for comparison with the DIMAC (and DIFO) experiments (Figure 4.10C). These normalized data also indicate that DIMAC-FLAG was more efficient than cyclooctynes with similar reaction kinetics at labeling cell-surface azido-glycoproteins *in vivo*. However, from these data it is evident that the reaction kinetics of DIFO outweigh the hydrophilicity of DIMAC when comparing the effects of these two factors at labeling azides *in vivo*, as DIFO and DIMAC show comparable labeling efficiencies only when 10 times as much DIMAC-FLAG is employed relative to the concentration of DIFO-FLAG.

Overall, the hydrophilicity of DIMAC did improve azide-dependent labeling *in vivo*. However, our results from the *in vivo* experiments clearly indicate that improved reaction kinetics are critical for efficient labeling of azides in mice. There also appears to be a quality that the Staudinger ligation possesses which enables it to outperform Cu-free click chemistry *in vivo*, despite its sluggish reaction kinetics and propensity to undergo nonspecific phosphine oxidation. Steps toward further understanding the success of the Staudinger ligation *in vivo* should be pursued, as this insight will be valuable in optimizing other reactions for use in mice. Additionally, a more thorough study of the pharmacokinetics of the cyclooctyne reagents should be performed including analysis of binding to serum proteins, clearance times, and oxidation by cytochromes P450.⁵ Preliminary *in vitro*^{6,7} and *in vivo*⁸ studies regarding the oxidation of cytochromes P450 have not indicated that the cyclooctynes are metabolized by these enzymes. However, further studies need to be performed as the literature suggests internal alkynes can act as covalent inhibitors of some classes of cytochromes P450.⁹

Materials and Methods

General Experimental Procedure

All chemical reagents were purchased from Sigma-Aldrich, Acros, and TCI chemicals and used without purification unless noted otherwise. Anhydrous DMF and MeOH were purchased from Aldrich or Acros in sealed bottles; all other solvents were purified as described by Pangborn *et al.*¹⁰ In all cases, magnesium sulfate was used as a drying agent and solvent was removed by reduced pressure with a Buchi Rotovapor R-114 equipped with a Welch self-cleaning dry vacuum. Products were further dried by reduced pressure with an Edwards RV5 high vacuum. Lyophilization was performed on a LABCONCO FreeZone[®] instrument equipped with an Edwards RV2 pump. Thin layer chromatography was performed with Silicycle[®] 60 Å silica gel plates. Unless otherwise specified, R_f values are reported in the solvent system the reaction was monitored in.

Chromatography was performed using Merck 60 Å 230-400 mesh silica. All ^1H and ^{13}C NMR spectra are reported in ppm and referenced to solvent peaks. When mixtures of rotamers are present the minor rotamer is designated as “rot”. Spectra were obtained on Bruker AV-300, AVQ-400, AVB-400, DRX-500, AV-500 or AV-600 instruments. Electrospray ionization (ESI) mass spectra were obtained from the UC Berkeley Mass Spectrometry Facility. HPLC was performed on a Varian Pro Star instrument with a C18 column.

Experimental Procedures

DIMAC-biotin conjugate (4.1). DIMAC (**3.35**) (4.8 mg, 0.018 mmol, 1.0 equiv.) was dissolved in CH_3CN (1 mL, anhydrous) and cooled to $0\text{ }^\circ\text{C}$. *N,N*-Diisopropylethylamine (10 μL , 0.06, 3 equiv.) was added and this solution was stirred under N_2 for 10. Pentafluorophenyl trifluoroacetate (10 μL , 0.06 mmol, 3 equiv.) was then added dropwise and the reaction was allowed to warm to rt. The reaction was monitored by TLC (1:1 toluene/acetone) for the disappearance of **3.35** ($R_f = 0.3\text{-}0.4$). Upon reaction completion (approx 1 h), the mixture was filtered, and the filtrate was evaporated to dryness. Pentafluorophenyl activated DIMAC was purified via flash chromatography using silica gel and anhydrous toluene and anhydrous ether in a gradient solvent system of 10:1 toluene/ether to 4:1 toluene/ether. This product was dried under reduced pressure and immediately used for the coupling to biotin. *N*-(13-amino-4,7,10-trioxatridecanyl)biotinamide¹ (7.8 mg, 0.018 mmol, 1 equiv.) was dissolved in DMF (0.5 mL, anhydrous) and cooled to $0\text{ }^\circ\text{C}$. *N,N*-Diisopropylethylamine (2 drops) was added. The pentafluorophenyl activated DIMAC was dissolved in DMF (0.5 mL, anhydrous) and this solution was added dropwise to the biotin solution at $0\text{ }^\circ\text{C}$. Upon addition of all activated DIMAC, the reaction was warmed to rt and monitored by ESI-MS for the formation of **4.1** ($[\text{M}+\text{H}]^+ = 698$, $[\text{M}+\text{Na}]^+ = 720$). Upon reaction completion (approx 6 h), the mixture was evaporated to dryness and purified by flash chromatography on silica gel. A gradient solvent system was used beginning at 50:3:1 EtOAc/MeOH/ H_2O and ending with 8:3:1 EtOAc/MeOH/ H_2O . This procedure resulted in pure **4.1** (5.0 mg, 0.0072 mmol, 40%). $R_f = 0.4$ in 5:3:1 EtOAc/MeOH/ H_2O . ^1H NMR (500 MHz, D_2O): 4.58 (dd, $J = 7.9$, 4.9 Hz, 1H), 4.40 (dd, $J = 7.9$, 4.5 Hz, 1H), 4.36 (dt, $J = 7.8$, 2.0 Hz, 0.1H), 4.22 (dt, $J = 8.6$, 2.5 Hz, 1H), 4.12 (dd, 14.9, 5.4 Hz, 0.9H), 4.05 (d, $J = 14.2$ Hz, 0.9H), 4.00 (d, $J = 16.2$ Hz, 0.1H), 3.82 (t, $J = 8.4$ Hz, 0.1H), 3.71-3.65 (m, 8.9H), 3.57-3.45 (m, 7.1H), 3.37-3.19 (m, 8.9H), 3.03 (dd, $J = 14.3$, 9.0 Hz, 1H), 2.97 (dd, $J = 13.1$, 5.0 Hz, 1H), 2.92-2.88 (m, 0.1H), 2.79-2.75 (m, 2.9H), 2.65-2.62 (m, 1H), 2.58-2.49 (m, 2H), 2.32 (dt, $J = 16.8$, 3.0 Hz, 0.9H), 2.24 (t, $J = 7.2$ Hz, 2.1H), 1.79-1.53 (m, 8H), 1.44-1.33 (m, 2H). ^{13}C NMR (125 MHz, D_2O): 176.7, 174.7, 174.5, 165.2, 98.9, 89.9, 84.3, 76.1, 69.5, 69.3, 68.4, 68.3, 62.0, 60.2, 58.0, 56.5, 55.3, 54.2, 52.0, 39.6, 36.3, 36.2, 35.4, 30.7, 28.24, 28.18, 27.8, 27.6, 25.1, 20.8. HRMS (ESI): calcd for $\text{C}_{33}\text{H}_{55}\text{N}_5\text{O}_9\text{SNa}$ $[\text{M} + \text{Na}]^+$, 720.3618; found, 720.3593.

DIMAC-maleimide conjugate (4.5). DIMAC (100 mg, 0.37 mmol, 1.0 equiv.) was dissolved in CH₃CN (8 mL, anhydrous) and cooled to 0 °C. N,N-diisopropylethylamine (0.33 mL, 1.9 mmol, 5.1 equiv.) was added followed by maleimide-amine-TFA salt **4.4**³ (158 mg, 0.589 mmol, 1.6 equiv.) and HATU (162 mg, 0.427 mmol, 1.2 equiv.). The mixture was warmed to rt and allowed to react for 4 h at which point, the reaction was evaporated to dryness. The crude product was purified by silica gel chromatography using a toluene/acetone solvent system (5:1, 3:1, 1:1). This procedure produced pure DIMAC-maleimide **4.5** (141 mg, 0.348 mmol, 94%). $R_f = 0.2$ in 1:1 toluene/acetone. 1:0.1 mixture of rotamers (designated rotH). ¹H NMR (600 MHz, D₂O): δ 1.78 (quin, $J = 6.8$ Hz, 2H, 2rotH), 2.21-2.25 (m, 1 rotH), 2.32 (dt, $J = 16.8, 3.2$ Hz, 1H), 2.50-2.60 (m, 2H, 2rotH), 2.62-2.69 (1H, 1rotH), 2.73-2.82 (2H, 1rotH), 2.84-2.92 (m, 1rotH), 3.02 (dd, $J = 14.3, 9.0$ Hz, 1H), 3.05-3.08 (m, 1rotH), 3.12-3.21 (m, 2H, 3rotH), 3.28-3.34 (m, 4H), 3.36 (s, 3rotH), 3.51-3.56 (m, 5H, 3rotH), 3.69 (t, $J = 8.8$ Hz, 1H), 3.67-3.73 (m, 2rotH), 3.82 (t, $J = 8.4$ Hz, 1rotH), 4.00 (d, $J = 15.9$ Hz, 1rotH), 4.05 (d, $J = 14.2$ Hz, 1H), 4.16 (dd, $J = 14.9, 5.5$ Hz, 1H), 4.20 (dt, $J = 8.6, 2.5$ Hz, 1H), 4.22-4.24 (m, 1rotH), 4.35 (dt, $J = 7.9, 2.3$ Hz, 1rotH), 6.83 (s, 2H, 2rotH). ¹³C NMR (150 MHz, D₂O, no rotamer peaks tabulated): δ 20.8, 27.1, 28.4, 30.9, 35.1, 36.7, 52.1, 54.3, 56.7, 58.1, 76.2, 84.4, 90.8, 99.0, 134.4, 173.2, 174.75, 174.77. HRMS (ESI): calcd. for C₂₀H₂₇O₆N₃Na⁺ [M+Na]⁺, 428.1792; found, 428.1785.

DIMAC-FLAG conjugate (4.3). DIMAC-maleimide **4.5** (43 mg, 0.11 mmol, 1.0 equiv.) was dissolved in N,N-dimethylformamide (0.5 mL) and cooled to 0 °C. The DYKDDDDKC peptide³ (122 mg, 0.109 mmol, 1.0 equiv.) was dissolved in water (1 mL) and added to the DIMAC-maleimide solution. The reaction was warmed to rt overnight. After 16 h, the reaction was evaporated to dryness and purified by HPLC using a CH₃CN/H₂O solvent system with 0.1% TFA increasing the amount of CH₃CN from 0% to 35% over 30 minutes. DIMAC-FLAG elutes after 20 minutes (91 mg, 0.060 mmol, 56%). HRMS (ESI): calcd. for C₆₄H₉₀N₁₄O₂₇S [M-2H]²⁻, 759.2916; found, 759.2941.

Cell Culture

Jurkat (human T cell lymphoma) cells and isolated splenocytes were maintained in a 5% CO₂, water-saturated atmosphere and grown in RPMI 1640 media supplemented with 10% FBS, penicillin (100 units/ml), and streptomycin (0.1 mg/ml). Cell densities were maintained between 1 x 10⁵ and 2 x 10⁶ cells per mL.

Western Blot Analysis of Azide-Labeled Cell Lysates

Jurkat cells were grown in media supplemented with or without 25 μM Ac₄ManNAz (+Az or -Az respectively) for 3 d. The cells were concentrated (500 × g, 3 min) and washed three times by sequential resuspension with 10 mL chilled PBS and concentration. The cell pellet was resuspended in lysis buffer (150 mM NaCl, 20 mM Tris, 1% NP-40 substitute (Sigma-Aldrich), pH 7.4; 500 μL buffer per 2.8 × 10⁷ cells)

containing protease inhibitors (Roche) and disrupted by sonication with one 30 s 6 W pulse. Following sonication, insoluble debris were removed by centrifugation (20000 × g, 10 min) and the supernatant was kept. The protein concentration of each lysate was determined using the Bio-RAD[®] D_c protein assay.

Thirty-five micrograms of total protein from each lysate was reacted with 250 μM DIMAC-biotin, ALO-biotin, Phos-biotin or no reagent overnight at rt. SDS-PAGE loading buffer (4X, BioRAD) was added to each sample and the proteins were separated via electrophoresis and transferred to a nitrocellulose membrane. Equal protein loading and successful transfer were confirmed by visualizing the proteins with Ponceau S. The membrane was blocked with 5-10% BSA in PBST (PBS pH 7.4 containing 0.1% Tween 20) for 2 h at rt. The membrane was incubated with horseradish peroxidase-conjugated α-biotin (1:100,000 dilution, Jackson Laboratories) in PBST for 1 h. The membrane was washed with PBST (3 x 15 min). Detection was performed by chemiluminescence using Pierce SuperSignal West Pico Chemiluminescent Substrate.

Cell-Surface Azide Labeling and Detection

Jurkat cells were incubated in untreated media or media containing 25 μM Ac₄ManNAz. After 3 d, the cells were twice concentrated (500 x g, 3 min, 4 °C) and resuspended in 10 mL FACS buffer (PBS containing 1% FCS, 2 x 10 mL) and cells (approx 500,000 per a well) were placed in a 96 well V-bottom plate. The cells were concentrated by centrifugation (2500 x g, 3 min, 4 °C), resuspended in 200 μL cold FACS buffer, and again concentrated by centrifugation (2500 x g, 3 min, 4 °C). The cells were then treated for 1 h (unless otherwise noted) at rt with the specified reagent (no reagent, cyclooctyne-biotin, Phos-biotin, Phos-FLAG, DIMAC-FLAG, etc.). After 1 h, the cells were thrice concentrated by centrifugation (2500 x g, 3 min, 4 °C) and resuspended in 200 μL cold FACS buffer. Following and additional concentration by centrifugation (2500 x g, 3 min, 4 °C), cells were resuspended in FACS buffer (100 μL) containing FITC-avidin (1:200 dilution of 1 mg/mL stock, Sigma-Aldrich) or FITC-M2-α-FLAG (1:900 of Sigma-Aldrich stock) and incubated in the dark at 4 °C for 15 min (avidin) or 30 min (α-FLAG). Following the incubation, cells were concentrated by centrifugation, resuspended in 200 μL cold FACS buffer. For FITC-α-FLAG experiments the cells were diluted to 400 μL for flow cytometry analysis. For FITC-avidin experiments, the cells were concentrated by centrifugation, and another FITC-avidin incubation was performed. After the second FITC-avidin labeling, the cells were thrice concentrated by centrifugation (2500 x g, 3 min, 4 °C) and resuspended in 200 μL cold FACS buffer. The cells were then diluted to 400 μL for flow cytometry analysis. Flow cytometry was performed on a BD Biosciences FACSCalibur flow cytometer equipped with a 488-nm argon laser. All flow cytometry experiments were performed with three replicate samples.

Mice

Wild type B6D2F1 mice (aged 5-8 weeks) were purchased from The Jackson Laboratory or Charles River Laboratories. Animals were handled in accordance with Animal Use Protocol R234-0609B (approved by the Animal Care and Use Committee at the University of California, Berkeley).

Compound Administration

B6D2F1 mice were administered Ac₄ManNAz (300 mg/kg in 70% DMSO from a 116 mM stock solution) or vehicle (70% DMSO) intraperitoneally once daily for 7 days. Twenty-four hours after the final Ac₄ManNAz bolus, mice were injected intraperitoneally with either Phos-FLAG (0.8 mmol/kg water from a 133 mM stock solution) or DIMAC-FLAG (0.8 mmol/kg and 1.6 mmol/kg in water from a 133 mM or 267 mM stock solution, respectively). All doses of azidosugar, vehicle, and FLAG-conjugates were administered in approximately 150 µl of 70% DMSO or water. Three hours post-injection of the FLAG conjugates, the mice were euthanized, and a panel of organs was harvested.

Splenocyte Analysis after Cu-Free Click Chemistry in vivo

Splenocytes from mice treated first with Ac₄ManNAz or vehicle followed by the appropriate FLAG conjugate were isolated and probed for the presence of cell-surface FLAG epitopes using the procedure outlined above. Briefly, isolated splenocytes were incubated directly with FITC-α-FLAG in FACS buffer (PBS + 1% FBS, 1:900 dilution from Sigma stock) for 30 min on ice. The cells were then washed once with labeling buffer and analyzed by flow cytometry.

Labeling of Splenocyte Cell-Surface Azides ex vivo

Splenocytes isolated as described above were further reacted *ex vivo* with Phos-FLAG to probe for the presence of unreacted azides. Briefly, splenocytes were incubated with Phos-FLAG (250 µM) for 1 h at room temperature in FACS buffer. The cells were then rinsed three times with labeling buffer, treated with FITC-α-FLAG for 30 min on ice, rinsed with labeling buffer once, and analyzed by flow cytometry (see above for more details).

Lysis of Murine Organs and Western Blot Analysis

Organs (liver, heart, kidney and intestines) harvested from mice injected first with either Ac₄ManNAz or vehicle and then Phos-FLAG or DIMAC-FLAG were rinsed with cold PBS and minced. The organs were then transferred into 1.5 mL of lysis buffer (150 mM NaCl, 1.0% NP-40, 20 mM Tris-HCl, 1 mM EDTA, pH 7.4) containing protease inhibitors (Complete, Roche) and homogenized using a Dounce homogenizer. The lysates were centrifuged (13,500 x g for 10 min) to remove cell debris, and the supernatant was

collected. Protein concentrations were determined using the *DC* protein assay kit (Bio-Rad). The samples (100 µg of protein per lane) were analyzed by Western blot, probing with HRP-α-FLAG in a similar manner as describe above.

Western Blot Analysis of Serum Glycoproteins

Whole blood was collected from anesthetized mice injected first with either Ac₄ManNAz or vehicle and then Phos-FLAG or DIMAC-FLAG by cardiac puncture from the closed thorax. The samples were allowed to clot, and the serum was then isolated by removal of the agglutinated red blood cells and leukocytes. The samples were then centrifuged (13,500 x g for 10 min) to remove residual cell debris, and the supernatant was collected and diluted with lysis buffer (150 mM NaCl, 1.0% NP-40, 20 mM Tris-HCl, 1 mM EDTA, pH 7.4) containing protease inhibitors (Complete, Roche). Protein concentrations were determined using the *DC* protein assay kit (Bio-Rad). The samples (50 µg of protein per lane) were analyzed by Western blot, probing with a horseradish peroxidase-α-FLAG antibody conjugate (HRP-α-FLAG) in a similar manner as described above.

References

- (1) Wilbur, D. S.; Hamlin, D. K.; Vessella, R. L.; Stray, J. E.; Buhler, K. R.; Stayton, P. S.; Klumb, L. A.; Pathare, P. M.; Weerawarna, S. A. Antibody fragments in tumor pretargeting. Evaluation of biotinylated Fab colocalization with recombinant streptavidin and avidin. *Bioconjugate Chem.* **1996**, *7*, 689-702.
- (2) Prescher, J. A.; Dube, D. H.; Bertozzi, C. R. Chemical remodelling of cell surfaces in living animals. *Nature* **2004**, *430*, 873-877.
- (3) Baskin, J. M.; Prescher, J. A.; Laughlin, S. T.; Agard, N. J.; Chang, P. V.; Miller, I. A.; Lo, A.; Codelli, J. A.; Bertozzi, C. R. Copper-free click chemistry for dynamic in vivo imaging. *Proc. Natl. Acad. Sci. U.S.A.* **2007**, *104*, 16793 -16797.
- (4) Chang, P. V.; Prescher, J. A.; Sletten, E. M.; Baskin, J. M.; Miller, I. A.; Agard, N. J.; Lo, A.; Bertozzi, C. R. Copper-free click chemistry in living animals. *Proc. Natl. Acad. Sci. U.S.A.* **2010**, *107*, 1821-1826.
- (5) Ruiz-Garcia, A.; Bermejo, M.; Moss, A.; Casabo, V. G. Pharmacokinetics in Drug Discovery. *J. Pharm. Sci.* **2008**, *97*, 654-690.
- (6) Beebe, L. E.; Roberts, E. S.; Fornwald, L. W.; Hollenberg, P. F.; Alworth, W. L. Mechanism-based inhibition of mouse P450_{2b-10} by selected arylalkynes. *Biochem. Pharmacol.* **1996**, *52*, 1507-1513.
- (7) Foroozesh, M.; Primrose, G.; Guo, Z.; Bell, L. C.; Alworth, W. L.; Guengerich, F. P. Aryl acetylenes as mechanism-based inhibitors of cytochrome P450-dependent monooxygenase enzymes. *Chem. Res. Toxicol.* **1997**, *10*, 91-102.
- (8) Mico, B. A.; Federowicz, D. A.; Ripple, M. G.; Kerns, W. In vivo inhibition of oxidative drug metabolism by, and acute toxicity of, 1-aminobenzotriazole (ABT): A tool for biochemical toxicology. *Biochem. Pharmacol.* **1988**, *37*, 2515-2519.

- (9) Ortiz de Montellano, P. R.; Kunze, K. L. Self-catalyzed inactivation of hepatic cytochrome P-450 by ethynyl substrates. *J. Biol. Chem.* **1980**, *255*, 5578 -5585.
- (10) Pangborn, A. B.; Giardello, M. A.; Grubbs, R. H.; Rosen, R. K.; Timmers, F. J. Safe and convenient procedure for solvent purification. *Organometallics* **1996**, *15*, 1518-1520.

Chapter 5

Towards a Fluorogenic Azacyclooctyne

Strategies for *in vivo* Imaging of Azides using the Staudinger Ligation

One of the main conclusions from the previous chapter is that the phosphine-FLAG (**2.11**) reagent is a privileged structure for labeling cell-surface azides in mice. However, the ultimate goal for bioorthogonal chemistry *in vivo* is to be able to visualize azide dynamics in real-time, as can be achieved on cell-surfaces with DIFO reagents. This goal necessitates azide-reactive compounds that are directly conjugated to an imaging moiety, rather than the FLAG peptide. Many imaging modalities for *in vivo* imaging exist, including optical imaging, positron emission tomography (PET), single photon emission computed tomography (SPECT), magnetic resonance imaging (MRI), and bioluminescence imaging (BLI).¹ Since the initial success of the Staudinger ligation *in vivo*,² a number of these modalities have been explored with phosphine probes with only minimal success. SPECT and MRI modalities have been pursued through collaborative projects, while a number of students within the group have attempted to image azido-glycans *in vivo* with phosphine-fluorophore conjugates through optical imaging.

Optical imaging *in vivo* necessitates fluorophores that are red-shifted due to complications from tissue autofluorescence and endogenous chromophores that readily absorb higher energy light.^{3,4} Red-shifted and near-infrared (NIR) fluorophores were conjugated to phosphine reagents and injected into mice with or without azides on their cell-surfaces, but no azide-dependent labeling was observed. Most likely, the slow kinetics of the Staudinger ligation necessitated too much excess reagent, which prevented specific labeling from being observed.

A possible solution to this problem is to engineer a phosphine reagent that does not become fluorescent until reaction with an azide, such as the fluorogenic phosphine-coumarin **2.28**. Unfortunately, phosphine reagent **2.28** is fluorogenic upon phosphine oxidation, a problematic background reaction for the Staudinger ligation.⁵ Luckily, there were other strategies for the preparation of a fluorogenic phosphine reagent. A key step in the mechanism of the Staudinger ligation is intramolecular amide bond formation with concomitant ester cleavage, and mechanistic studies indicated that the alcohol leaving group could be varied widely in structure without detriment to rate or yield.⁶ This feature was exploited in a FRET-based fluorogenic phosphine reagent QPhos (**5.1**, Figure 5.1A).⁷ Fluorescein was conjugated to one of the phosphine's aryl substituents through an amide linkage and, disperse red-1, a FRET quencher, was appended through the ester linkage. Upon reaction of **5.1** with an azide, the quencher is released and the resulting phosphine oxide (**5.2**) is fluorescent.

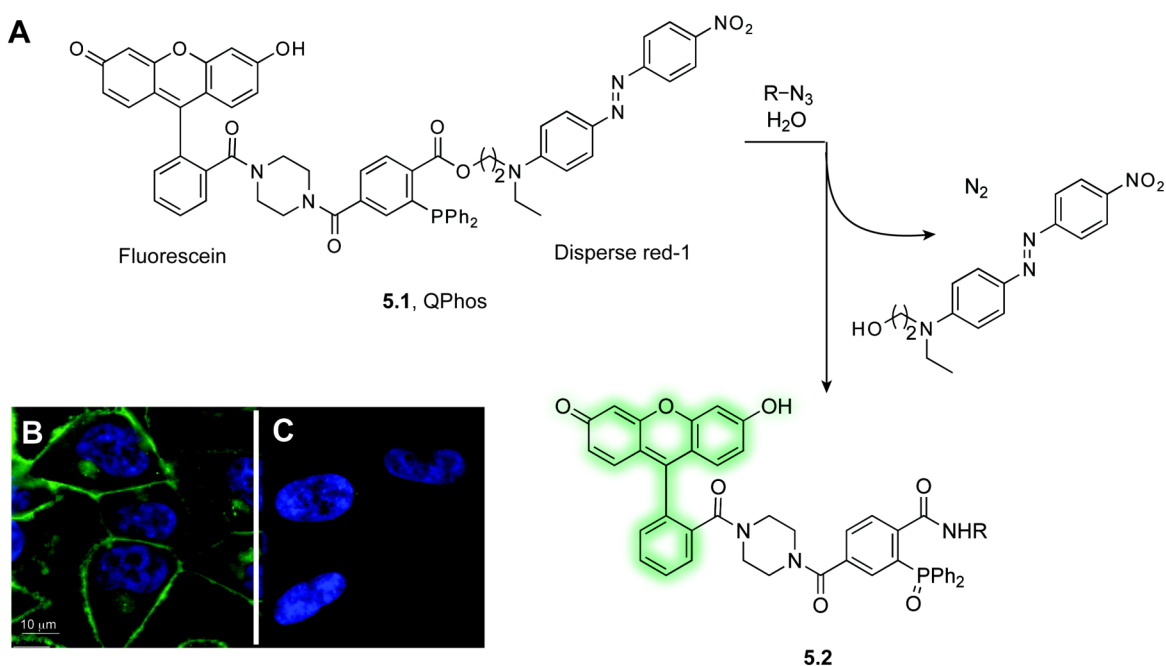


Figure 5.1. A. A FRET-based fluorogenic phosphine for the Staudinger ligation. B/C. HeLa cells were grown in the presence (B) or absence (C) of Ac₄ManNAz. The cells were washed, incubated with 50 μM **5.1** for 8 h at 37 °C and imaged. Green = fluorescein. Blue = Hoechst 33342 nuclear stain.

QPhos allowed for direct imaging of azides on live cultured cells, the first direct imaging of azides on live cells (Figure 5.1B/C). Unfortunately, the imperfect spectral properties of fluorescein for *in vivo* imaging⁸ undermined the use of fluorogenic phosphine **5.1** in live animals. Red-shifted variants of the fluorogenic phosphine were synthesized, but these compounds underwent nonspecific phosphine oxidation more readily than the Staudinger ligation.⁹

Recent work in the group has focused on the more sensitive imaging modality of bioluminescence,¹⁰ and bioluminogenic phosphine reagent **5.3** was synthesized.¹¹ In a manner similar to fluorogenic reagent **5.1**, compound **5.3** releases luciferin (**5.4**) during its Staudinger ligation with phosphines (Figure 5.2). Once liberated, luciferin readily enters cells wherein heterologously expressed luciferase catalyzes its oxidation to **5.5** and the concomitant emission of light.¹² Compound **5.3** enabled very sensitive detection of azides on cell-surface glycoproteins and initial results in luciferase transgenic mice appear promising.

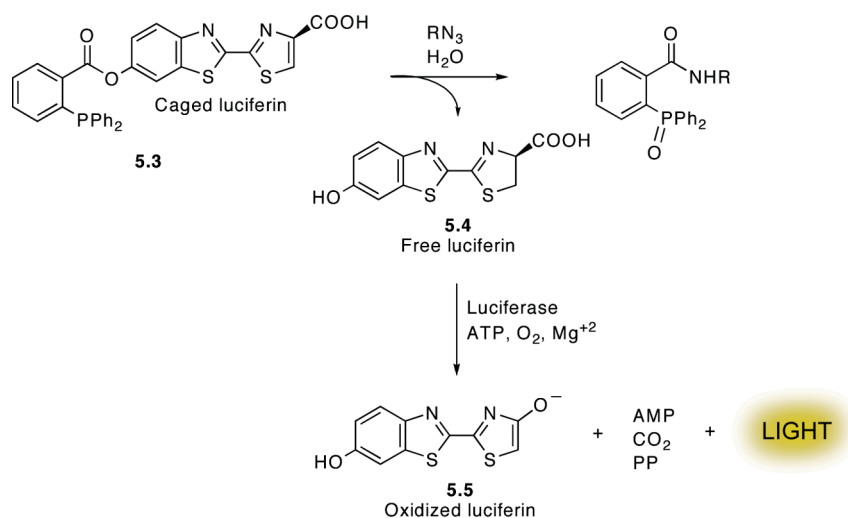


Figure 5.2. A bioluminescent phosphine reagent for sensitive detection of azides by the Staudinger ligation. Upon reaction of **5.3** with an azide, luciferin is released and oxidized by luciferase to an excited state, which readily emits a photon of light.

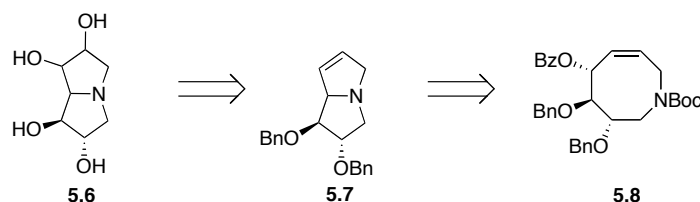
Design of a Fluorogenic Cyclooctyne

Fluorogenic and bioluminescent versions of the Staudinger ligation were relatively easy to develop, as the mechanism of the Staudinger ligation has many elementary steps that could be exploited. In contrast, Cu-free click chemistry is a single-step process where all atoms in the starting material remain in the product, leaving no obvious mechanism for developing a fluorogenic cyclooctyne. Nevertheless, the potential of a fluorogenic cyclooctyne is great. If the fast reaction kinetics of Cu-free click chemistry could be combined with azide-dependent fluorescence, imaging of azido-biomolecules in environments where excess reagent could not be washed away, most notably inside a living animal, would be possible. A number of strategies for the development of a fluorogenic cyclooctyne exist including exploiting additional conjugation due to triazole formation,¹³ utilizing the triazole as a ligand for a luminogenic lanthanide metal (such as europium),¹⁴ or engineering a leaving group into the cyclooctyne. While exploiting the additional conjugation present upon triazole formation appeared to be the easiest method for obtaining a fluorogenic cyclooctyne, the spectral properties of these reagents could not be easily tuned. Phosphine **5.1** and **5.3** highlighted the advantages an engineered leaving group can have for applications in different imaging modalities, and, unlike the phosphine reagents, cyclooctynes should be compatible with red-shifted fluorophores.

We directed our attention to engineering a cyclooctyne, which expelled a leaving group upon reaction with azides. In work performed before beginning my doctoral research, I synthesized polyhydroxylated pyrrolizidine (**5.6**) and noted a facile intramolecular S_N2 reaction of azacyclooctene **5.8** to form bicycle **5.7** in the presence of 25% trifluoroacetic acid (Scheme 5.1).¹⁵ This was a highly unexpected result as the amine

should be protonated under these conditions and benzoate is not a highly activated leaving group. Simple molecular modeling of **5.8** suggested that the amine and benzoate group were perfectly aligned for an intramolecular S_N2 reaction.

Scheme 5.1. Retrosynthesis of tetrahydroxylated pyrrolizidine mediated by an intramolecular cyclization.



Building on this result, we designed a strategy for a fluorogenic cyclooctyne that relied on strain-release to promote an intramolecular S_N2 reaction (Figure 5.3). An azacyclooctyne containing a fluorophore and an appropriately positioned quencher group across the ring from the nitrogen (compound **5.9**) was proposed. There should be ample ring strain in **5.9** to prevent an intramolecular reaction between the nucleophilic amine and the quencher group. However, upon reaction with an azide, a considerable amount of ring strain is released and triazole **5.10** (which should adopt a structure similar to compound **5.8**) can undergo an intramolecular S_N2 reaction to yield **5.11**. With the quencher group expelled, **5.11** should be fluorescent.

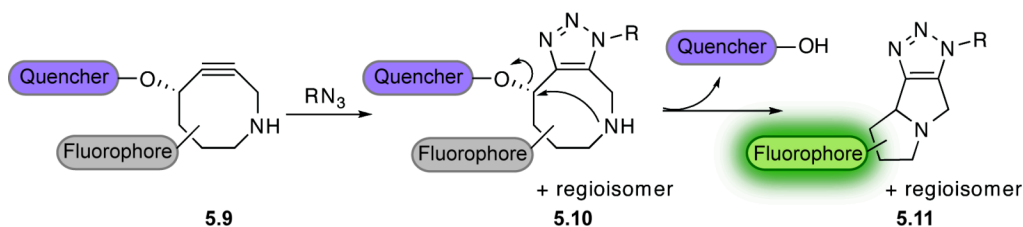
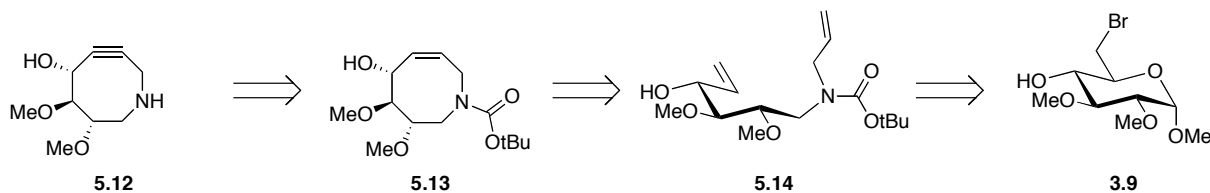


Figure 5.3. Strategy for a fluorogenic azacyclooctyne.

Model azacyclooctyne **5.12** was our initial target (Scheme 5.2). While a fluorophore could not easily be attached to **5.12**, the strain-release strategy could be tested. Retrosynthetically, the synthesis of **5.12** was nearly identical to that of azacyclooctyne **3.35**. However, we were relying on alkyne formation through a bromination and double elimination of **5.13**, which proved difficult for azacyclooctyne **3.5** (see Chapter 3). We were optimistic that a more thorough screen of bromination conditions would make this sequence possible. Azacyclooctene **5.13** could be prepared from 6-bromoglucopyranoside **3.9** though the same synthetic pathway employed for the synthesis of DIMAC, the exception being that the amine produced from the one-pot zinc reduction/reductive

amination reaction was protected with a Boc group (**5.14**). We envisioned the Boc group would prevent undesired intramolecular reactions throughout the synthesis. Once the strained alkyne was installed, removal of the Boc group would yield the desired compound. Other results with DIMAC (**3.35**) suggested that the alkyne would be stable to Boc deprotection conditions (see Chapter 12).

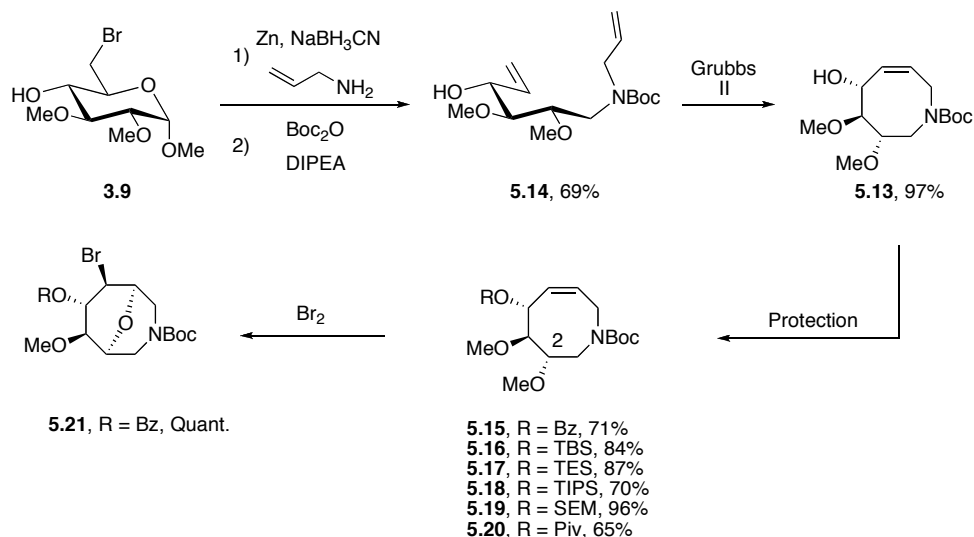
Scheme 5.2. Retrosynthesis of target azacyclooctyne **5.12**.



Synthesis of Fluorogenic Azacyclooctyne 5.12

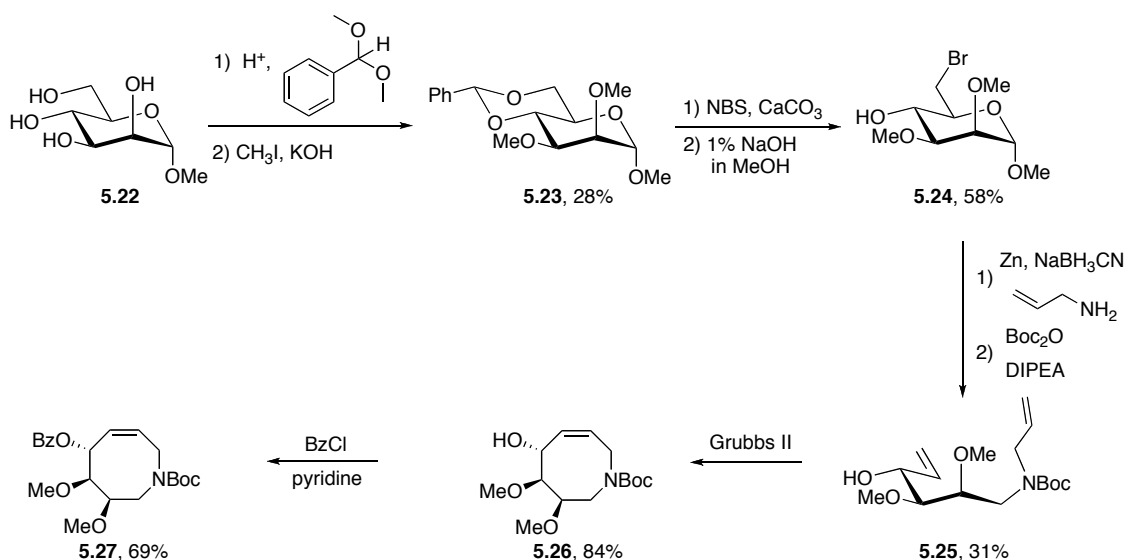
The synthesis of azacyclooctene **5.13** proceeded without incident. Briefly, methyl-6-bromo-6-deoxy-2,3-di-O-methyl- α ,D-glucopyranoside (**3.9**) was subjected to Zn, NaBH_3CN and allylamine followed by Boc anhydride to yield **5.14**. Cyclization was achieved through a ring-closing metathesis reaction. The resulting allylic alcohol in **5.13** was protected as a benzoate to yield **5.15**, the precursor necessary for alkyne formation through a bromination/double elimination pathway. When azacyclooctene **5.15** was subjected to bromination conditions only bicyclic ether **5.21** was formed. Swapping the benzoate for a variety of protecting groups (**5.16-5.20**) also did not yield the desired dibrominated compound. In fact, aside from the TES group, which was not stable to bromine, the protecting group seemed to have little effect on the outcome of the reaction and the bicyclic product was observed. Optimization of reaction temperature, time, and solvent were also unsuccessful. Thus, a more drastic modification was necessary to allow for a bromination strategy to be utilized.

Scheme 5.3. Synthesis of Boc-protected azacyclooctene and failed dibromination.



Unfortunately, the target structure of compound **5.9** was much less flexible than initial target azacyclooctyne **3.5**. Since the C-2 methoxy group proved to be remarkably reactive, we hypothesized that it must be situated directly under the olefin, facilitating reaction with the intermediate bromonium ion. We sought to alter the conformation of the ring by reversing the stereochemistry at this position. Towards this end, we employed methyl α -D-mannopyranoside (**5.22**) as a starting material. Inverting the stereochemistry at the C-2 position did not impede any of the synthetic transformations in the early steps of the synthesis and compound **5.27** was obtained without difficulty as shown in Scheme 5.4.

Scheme 5.4. Inversion of the stereochemistry at the C-2 position.



When azacyclooctene **5.27** was exposed to bromine, the brown color did not disperse as rapidly as it did with the C-2 epimer (**5.15**) under analogous conditions. However, the result was similar. The C-2 methoxy group still appeared to react with the bromonium ion (**5.28**) and yield **5.29**. The identity of **5.29** was confirmed by X-ray crystallography (Figure 5.4). These results indicate that bromine addition to **5.27** and **5.15** proceed from different faces of the azacyclooctene. This suggests that either the C-2 methoxy group is directing the bromination rather than the larger benzoate group or epimerization of the C-2 methoxy group considerably alters the conformation of the azacyclooctene (**5.15** or **5.27**). It should be noted that it is possible that the desired dibrominated compound was formed and is sufficiently unstable that the C-2 methoxy group can displace one of the bromine atoms. However, the low nucleophilicity of methyl ethers makes this mechanism unlikely.

Scheme 5.5. Bromination of azacyclooctene **5.27**.

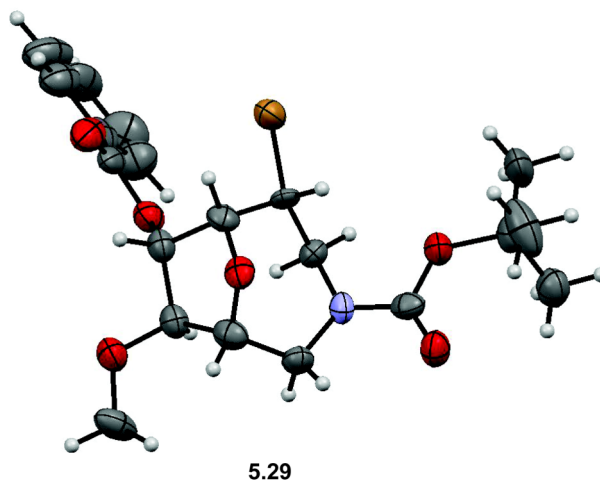
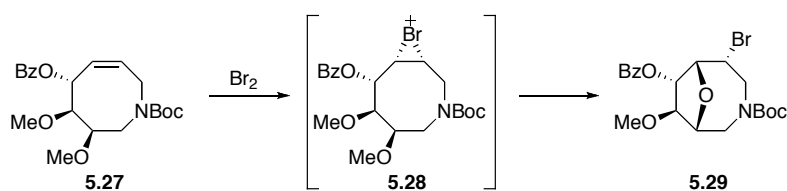


Figure 5.4. Crystal structure of bicyclic ether **5.29**. Thermal ellipsoid plot for **5.29** at 50% probability. Gray atoms correspond to carbon, red atoms correspond to oxygen, the blue atom is nitrogen, and the brown atom is bromine. Hydrogen atoms (white) were placed using a riding model.

Future Steps Toward the Synthesis of a Fluorogenic Azacyclooctyne

The C-2 methoxy group appears very prone to transannular reaction. Some potential strategies to prevent this reactivity are removal of the C-2 methoxy group or implementation of a protecting which tethers the C-2 and C-3 hydroxyl groups together. Additionally, strategies for alkyne formation other than bromine addition and double elimination can be pursued (see Figure 3.4). Preliminary results regarding the hydroboration of **5.15-5.20** indicate that the undesired regiochemistry is obtained and would make the requisite vinyl triflate or selenadiazole difficult to isolate. Dihydroxylation and oxidation of **5.15-5.20** could lead to a diketone that is also a suitable alkyne synthon. Efforts toward these strategies are underway.

Materials and Methods

General Experimental Procedure

All chemical reagents were purchased from Sigma-Aldrich, Acros, and TCI and used without purification unless noted otherwise. Anhydrous DMF and MeOH were purchased from Aldrich or Acros in sealed bottles; all other solvents were purified as described by Pangborn *et al.*¹⁶ In all cases, solvent was removed by reduced pressure with a Buchi Rotovapor R-114 equipped with a Welch self-cleaning dry vacuum. Products were further dried by reduced pressure with an Edwards RV5 high vacuum. Thin layer chromatography was performed with EMD 60 Å silica gel plates. Flash chromatography was performed using Silicycle® 60 Å 230-400 mesh silica. All ¹H and ¹³C NMR spectra are reported in ppm and referenced to solvent peaks. When mixtures of rotamers are present the minor rotamer is designated as “rot”. Spectra were obtained on Bruker AVQ-400, AVB-400, DRX-500, AV-500, or AV-600 instruments. Electron impact (EI) and electrospray ionization (ESI) mass spectra were obtained from the UC Berkeley Mass Spectrometry Facility. X-ray crystallography structures were obtained from the UC Berkeley X-Ray Crystallography Facility.

Experimental Procedures

tert-Butyl allyl((2R,3S,4R)-4-hydroxy-2,3-dimethoxyhex-5-enyl)carbamate (5.14). 6-Bromoglucopyranoside **3.9** (1.05 g, 3.66 mmol, 1.0 equiv.) was dissolved in 19:1 1-propanol/H₂O (140 mL). To this solution, allylamine (9.1 mL, 120 mmol, 34 equiv.), zinc (13.6 g, 209 mmol, 59 equiv.), and NaBH₃CN (1.1 g, 17 mmol, 4.9 equiv.) were added and the resulting mixture was heated to reflux for 2 h. After 2 h, the reaction mixture was cooled to rt, filtered through Celite and the filtrate was evaporated to dryness. The residue was dissolved in 6:4:1 CH₂Cl₂/MeOH/1.5 M HCl (95 mL) and stirred for 1 h checking to be sure that the solution remained acidic. The mixture was basified with 25% NaOH and extracted with CH₂Cl₂ (3 x 100 mL). The organics were dried with MgSO₄, decanted, and evaporated to dryness to result in crude divinylamine. The crude product was dissolved in

MeOH (60 mL, anhydrous) and *N,N*-diisopropylethyl amine (0.75 mL, 4.3 mmol, 1.2 equiv.) was added followed by di-*tert*-butyldicarbonate (2.0 g, 9.2 mmol, 2.6 equiv.). The mixture was stirred 3 h at rt, at which point it was evaporated to dryness and purified by silica gel chromatography with a hexane/ethyl acetate solvent system (10:1 to 2:1). This procedure resulted in 790 mg of pure **5.14** (2.5 mmol, 69%). $R_f = 0.5$ in 1:1 hexane/ethyl acetate. $^1\text{H NMR}$ (600 MHz, CDCl_3): δ 5.73-5.68 (m, 1H), 5.53 (ddt, $J = 15.7, 10.2, 5.1$ Hz, 1H), 5.09 (d, $J = 17.2$ Hz, 1H), 4.94- 4.84 (m, 3H), 4.07 (bs, 1H), 3.77- 3.70 (m, 1H), 3.60 (bs, 1H), 3.39 (bs, 1H), 3.32-2.98 (m, 9H), 2.89 (bs, 1H), 1.21 (s, 9H). $^{13}\text{C NMR}$ (150 MHz, CDCl_3): δ 155.3, 155.1 (rot), 138.1, 133.6, 115.9, 115.5 (rot), 115.2, 83.2, 79.8, 79.3 (bs), 71.8 (bs), 59.9 (bs), 58.8, 50.9, 50.2 (rot), 47.2 (bs), 28.0. HRMS (ESI): calcd. for $\text{C}_{16}\text{H}_{30}\text{O}_5\text{N}$ $[\text{M} + \text{H}]^+$, 316.2118; found, 316.212.

(5*R*,6*S*,7*S*,*Z*)-*tert*-Butyl 5-hydroxy-6,7-dimethoxy-5,6,7,8-tetrahydroazocine-1(2*H*)-carboxylate (5.13). Compound **5.14** (20 mg, 0.064 mmol, 1.0 equiv.) was dissolved in CH_2Cl_2 (5 mL, anhydrous), Grubb's 2nd generation catalyst (4 mg, 0.005 mmol, 8 mol%) was added and the mixture was heated to reflux. After 1.5 h TLC analysis indicated the reaction was complete. The mixture was cooled to rt, evaporated to dryness, and *immediately* purified by silica gel chromatography with a hexane/ethyl acetate solvent system (5:1, 3:1, 2:1). This procedure resulted in 18 mg of pure **5.13** (0.063 mmol, 97%) as a 0.6:0.4 mixture of rotamers. $R_f = 0.4$ in 1:1 hexane/ethyl acetate. $^1\text{H NMR}$ (600 MHz, CDCl_3): δ 5.39 (bs, 1H), 5.30-5.28 (m, 1H), 4.40 (d, $J = 17.4$ Hz, 0.6H, major rot), 4.24 (t, $J = 7.5$ Hz, 1H), 4.25-4.23 (m, 0.4H, minor rot), 3.58 (d, $J = 13.6$ Hz, 0.4H, minor rot), 3.45 (s, 4H), 3.35- 3.25 (m, 5H, 0.6H, minor rot), 2.77- 2.74 (m, 1H), 2.71-2.67 (m, 1H), 1.34 (s, 5.4H), 1.29 (s, 3.6H). $^{13}\text{C NMR}$ (150 MHz, CDCl_3): δ 155.2, 155.1 (rot), 133.9, 133.8 (rot), 125.0 (rot), 124.6, 86.0, 85.9 (rot), 82.9, 81.7 (rot), 80.3, 79.9 (rot), 67.0 (rot), 66.7, 61.4, 61.1 (rot), 57.8, 57.8 (rot), 47.0 (rot), 46.5, 45.4, 43.4 (rot), 28.4, 28.3 (rot). HRMS (ESI): calcd. for $\text{C}_{14}\text{H}_{26}\text{O}_5\text{N}$ $[\text{M} + \text{H}]^+$, 288.1805; found, 288.1808.

(5*R*,6*S*,7*S*,*Z*)-*tert*-Butyl 5-(benzoyloxy)-6,7-dimethoxy-5,6,7,8-tetrahydroazocine-1(2*H*)-carboxylate (5.15). Azacyclooctene **5.13** (18 mg, 0.063 mol, 1.0 equiv.) was dissolved in pyridine (0.5 mL, anhydrous) and cooled to 0 °C. Benzoyl chloride (10 μL , 0.085 mmol, 1.4 equiv.) was added dropwise and the mixture was allowed to warm to rt overnight. The following day the reaction was poured onto ice and extracted with CH_2Cl_2 (3 x 10 mL). The organics were combined and further washed with 6M HCl (10 mL), sat. NaHCO_3 (10 mL), and H_2O (10 mL). The organic layer was dried, decanted, evaporated to dryness, and purified by silica gel chromatography with a hexane/ethyl acetate solvent system (10:1, 8:1, 6:1, 4:1). This procedure yielded 14 mg of **5.15** (0.045 mmol, 71%) as a 1:0.7 mixture of rotamers. $R_f = 0.6$ in 1:1 hexane/ethyl acetate. $^1\text{H NMR}$ (500 MHz, CDCl_3): δ 8.07 (d, $J = 7.4$ Hz, 2H, 2rotH), 7.55 (t, $J = 7.2$ Hz, 1H, 1rotH), 7.44 (t, $J = 7.3$ Hz, 2H, 2rotH), 6.05-6.02 (m, 1H, 1rotH), 5.71-5.68 (m, 1H), 5.63-5.55 (bm, 1H, 2rotH), 4.65 (d, $J = 17.5$ Hz, 1H), 4.42 (d, $J = 17.5$ Hz, 1rotH), 3.92 (d, $J = 14.4$ Hz, 1rotH), 3.75 (d, $J = 14.2$ Hz, 1H), 3.66-3.60 (m, 1H, 2rotH), 3.52 (s, 6H), 3.48-3.43 (s, 1H, 6rotH), 3.32 (t, $J = 7.6$ Hz, 1rotH), 3.19 (t, $J = 8.4$ Hz, 1H), 3.06 (dd, $J = 14.1, 8.4$ Hz, 1rotH), 2.95 (dd, $J = 13.5, 11.5$ Hz, 1H), 1.55 (s, 9H), 1.51 (s, 9rotH). $^{13}\text{C NMR}$ (150 MHz, CDCl_3): δ 165.7

(rot), 165.6, 155.7, 155.6 (rot), 133.0, 133.0 (rot), 130.7 (rot), 130.6, 130.32, 129.8, 129.8 (rot), 129.7, 129.7 (rot), 128.6, 128.6 (rot), 127.5 (rot), 126.7, 85.7, 84.7 (rot), 82.0, 81.4 (rot), 81.1, 80.7 (rot), 72.1 (rot), 70.9, 61.6, 61.0 (rot), 59.1, 58.9 (rot), 47.28 (rot), 47.24, 46.7, 45.7 (rot), 28.7, 28.6 (rot). HRMS (ESI): calcd. for C₂₁H₂₉O₆NNa [M + Na]⁺: 414.1887; found: 414.1892.

(5R,6R,7S,Z)-tert-Butyl 5-(tert-butyldimethylsilyloxy)-6,7-dimethoxy-5,6,7,8-tetrahydroazocine-1(2H)-carboxylate (5.16). Azacyclooctene **5.13** (50 mg, 0.18 mmol, 1.0 equiv.) was dissolved in *N,N*-dimethylformamide (3 mL, anhydrous). To this solution *N,N*-disopropylethylamine (0.30 mL, 1.7 mmol, 9.4 equiv.) and *tert*-butyldimethylsilyltrifluoromethanesulfonate (0.12 mL, 0.53 mmol, 3.0 equiv.) were added and the mixture was stirred at rt overnight. The following morning the reaction was evaporated to dryness and purified by silica gel chromatography with a hexane/ethyl acetate solvent system (15:1, 12:1, 10:1) to yield 59 mg of **5.17** (0.15 mmol, 84%) as a 1:0.6 mixture of rotamers. R_f = 0.6 in 4:1 hexane/ethyl acetate. ¹H NMR (600 MHz, CDCl₃): δ 5.54-5.51 (m, 1H, 1rotH), 5.44-5.40 (m, 1H, 1rotH), 4.57 (t, *J* = 7.5 Hz, 1rotH), 4.52 (t, *J* = 7.9 Hz, 1H), 4.44 (d, *J* = 17.0 Hz, 1rotH), 4.23 (d, *J* = 17.0 Hz, 1H), 3.80 (apparent d, *J* = 12.0 Hz, 1rotH), 3.62 (dd, *J* = 14.9, 3.3 Hz, 1H), 3.59-3.56 (m, 1rotH), 3.53 (s, 3H), 3.51-3.43 (m, 4H, 8rotH), 3.41- 3.38 (m, 1H), 3.07- 2.94 (m, 2H, 2rotH), 1.50 (s, 9H), 1.46 (s, 9rotH), 0.95 (m, 9H, 9rotH), 0.63-0.56 (m, 6H, 6rotH). ¹³C NMR (150 MHz, CDCl₃): δ 155.6, 155.4 (rot), 136.4, 135.6 (rot), 124.9 (rot), 123.9, 86.6, 86.6 (rot), 82.6, 81.6 (rot), 80.5, 80.1 (rot), 70.5 (rot), 70.0, 61.4, 60.9 (rot), 58.8, 58.7 (rot), 46.9 (rot), 46.2, 45.7, 45.7 (rot), 28.69, 28.65 (rot), 7.0, 7.0 (rot), 5.1, 5.1 (rot). HRMS (ESI): calcd. for C₂₀H₄₀O₅NSi [M + H]⁺, 402.2670; found, 402.2674.

(5R,6R,7S,Z)-tert-Butyl 6,7-dimethoxy-5-(triethylsilyloxy)-5,6,7,8-tetrahydroazocine-1(2H)-carboxylate (5.17). Azacyclooctene **5.13** (50 mg, 0.18 mmol, 1.0 equiv.) was dissolved in *N,N*-dimethylformamide (3 mL, anhydrous). To this solution *N,N*-diisopropylethylamine (0.30 mL, 1.7 mmol, 9.4 equiv.) and triethylsilyltrifluoromethanesulfonate (0.12 mL, 0.53 mmol, 3.0 equiv.) were added and the mixture was stirred at rt overnight. The following morning the reaction was evaporated to dryness and purified by silica gel chromatography with a hexane/ethyl acetate solvent system (15:1, 12:1, 10:1) to yield 61 mg of **5.17** (0.16 mmol, 87%) as a 1:0.75 mixture of rotamers. R_f = 0.7 in 4:1 hexane/ethyl acetate. ¹H NMR (600 MHz, CDCl₃): δ 5.54-5.52 (m, 1H, 1rotH), 5.43-5.41 (m, 1H, 1rotH), 5.42 (d, *J* = 11.4 Hz, 1H), 4.55 (t, *J* = 7.5 Hz, 1rotH), 4.50 (t, *J* = 7.9 Hz, 1H), 4.43 (d, *J* = 17.0 Hz, 1H), 4.24 (d, *J* = 16.8 Hz, 1rotH), 3.83 (dd, *J* = 14.3, 2.4 Hz, 1rotH), 3.63 (dd, *J* = 14.5, 3.1 Hz, 1H), 3.57 (dd, *J* = 17.1, 5.2 Hz, 1rotH), 3.52 (s, 3H), 3.49-3.45 (m, 4H, 8rotH), 3.41- 3.38 (m, 1H), 3.04-2.93 (m, 2H, 2rotH), 1.50 (s, 9H), 1.46 (s, 9rotH), 0.88-0.89 (m, 9rotH), 0.11-0.03 (m, 6H, 6rotH). ¹³C NMR (150 MHz, CDCl₃): δ 155.6, 155.4 (rot), 136.3, 135.4 (rot), 124.9 (rot), 123.9, 86.64 (rot), 86.62, 82.6, 81.5 (rot), 80.5, 80.1 (rot), 70.7 (rot), 70.2, 61.5, 60.9 (rot), 58.8, 58.7 (rot), 47.0 (rot), 46.3, 45.71, 45.69 (rot), 28.72, 28.67 (rot), 26.1, 26.1 (rot), 18.5, 18.5 (rot), -4.5, -4.7. HRMS (ESI): calcd. for C₂₀H₄₀O₅NSi [M + H]⁺, 402.2670; found, 402.2675.

(5*R*,6*R*,7*S*,*Z*)-tert-Butyl 6,7-dimethoxy-5-(triisopropylsilyloxy)-5,6,7,8-tetrahydroazocine-1(2*H*)-carboxylate (5.18). Azacyclooctene **5.13** (50 mg, 0.18 mmol, 1.0 equiv.) was dissolved in *N,N*-dimethylformamide (0.1 mL, anhydrous). To this solution was added imidazole (31 mg, 0.46 mmol, 2.6 equiv.) and trisopropylsilyl chloride (60 μ L, 0.28 mmol, 1.6 equiv.). The mixture was stirred for 5 d at rt, at which point H₂O was added (10 mL) and the solution was extracted with CH₂Cl₂ (3 x 15 mL). The organics were combined, dried, decanted, and evaporated to dryness. The crude product was purified by silica gel chromatography with a hexane/ethyl acetate solvent system (20:1, 15:1, 10:1) to yield pure **5.18** (54 mg, 0.12 mmol, 70%) as a 1: 0.7 mixture of rotamers. ¹H NMR (500 MHz, CDCl₃): δ 5.58-5.55 (m, 1H, 1rotH), 5.45-5.42 (m, 1H, 1rotH), 4.69-4.63 (m, 1H, 1rotH), 4.47 (d, *J* = 17.0 Hz, 1H), 4.26 (d, *J* = 17.1 Hz, 1rotH), 3.75 (d, *J* = 14.2, 1.9 Hz, 1rotH), 3.63- 3.56 (m, 1H, 1rotH), 3.54 (s, 3H), 3.51-3.40 (m, 5H, 8rotH), 3.06-3.00 (m, 2rotH), 2.97-2.19 (m, 2H), 1.49 (s, 9H), 1.45 (s, 9rotH), 1.06 (bs, 21H, 21rotH). ¹³C NMR (125 MHz, CDCl₃): δ 155.5, 155.3 (rot), 137.1, 136.4 (rot), 124.5 (rot), 123.6, 87.3, 87.0 (rot), 82.6, 81.6 (rot), 80.5, 80.1 (rot), 70.5 (rot), 70.0, 61.6, 61.1 (rot), 58.9, 58.9 (rot), 46.9 (rot), 46.3, 46.0 (rot), 45.9, 28.7, 28.6 (rot), 18.24 (rot), 18.21, 12.5. HRMS (ESI): calcd. for C₂₃H₄₅O₅NSiNa [M + Na]⁺, 466.2959; found, 466.2963.

(5*R*,6*S*,7*S*,*Z*)-tert-Butyl 6,7-dimethoxy-5-((2-(trimethylsilyl)ethoxy)methoxy)-5,6,7,8-tetrahydroazocine-1(2*H*)-carboxylate (5.19). Azacyclooctene **5.13** (52 mg, 0.18 mmol, 1 equiv.) was dissolved in CH₂Cl₂ (0.12 mL, anhydrous) and *N,N*-diisopropylethyl amine (0.12 mL, 0.67 mmol, 3.9 equiv.) was added followed by 2-(trimethylsilyl)ethoxymethyl chloride (85 μ L, 0.48 mmol, 2.7 equiv.). The mixture was stirred at rt overnight. The following morning it was evaporated to dryness and purified by silica gel chromatography eluting with 10:1 and 8:1 hexane/ethyl acetate. This procedure yielded pure **5.19** (73 mg, 0.18 mmol, 96%) as a 1:0.8 mixture of rotamers. *R*_f = 0.5 in 4:1 hexane/ethyl acetate. ¹H NMR (600 MHz, CDCl₃): δ 5.56-5.51 (m, 2H, 2rotH), 4.73-4.70 (m, 2H, 2rotH), 4.51 (dd, *J* = 8.3, 6.5 Hz, 1rotH), 4.46 (dd, *J* = 9.0, 5.9 Hz, 1H), 4.37 (d, *J* = 17.1 Hz, 1H), 4.16 (d, *J* = 16.7 Hz, 1rotH), 3.82 (d, *J* = 14.4 Hz, 1rotH), 3.67-3.59 (m, 4H, 2rotH), 3.57-3.50 (m, 3H, 4rotH), 3.47-3.45 (m, 3H, 4rotH), 3.43-3.40 (m, 1H), 3.18-3.14 (m, 2rotH), 3.09 (dd, *J* = 9.0, 7.2 Hz, 1H), 3.05 (dd, *J* = 14.6, 9.3 Hz, 1H), 1.49 (s, 9H), 1.46 (s, 9rotH), 0.91 (t, *J* = 7.6 Hz, 2H, 2rotH), 0.01 (s, 9H, 9rotH). ¹³C NMR (150 MHz, CDCl₃): δ 155.7, 155.6 (rot), 133.0, 132.3 (rot), 127.1 (rot), 126.4 (rot), 94.24, 94.17 (rot), 86.0, 85.8 (rot), 82.6, 81.5 (rot), 80.5, 80.2 (rot), 74.6 (rot), 74.1, 65.2, 65.1 (rot), 60.8, 60.4 (rot), 58.8, 58.6 (rot), 46.8, 46.3 (rot), 45.8, 45.3 (rot), 28.7, 28.6 (rot), 18.1, 18.1 (rot), -1.2, -1.2 (rot). HRMS (ESI): calcd. for C₂₀H₄₀O₆NSi [M + H]⁺, 418.2619; found, 418.2624.

(5*R*,6*S*,7*S*,*Z*)-tert-Butyl 6,7-dimethoxy-5-(pivaloyloxy)-5,6,7,8-tetrahydroazocine-1(2*H*)-carboxylate (5.20). Azacyclooctene **5.13** (50 mg, 0.18 mmol, 1.0 equiv.) was dissolved in pyridine (3 mL, anhydrous). Pivoyl chloride (45 μ L, 0.37 mmol, 2.0 equiv.) was added and the mixture was stirred at rt overnight. The following morning it was evaporated to dryness and purified by silica gel chromatography using a hexane/ethyl acetate solvent system (10:1, 8:1). This procedure resulted in 44 mg of **5.20** (0.12 mmol, 65%) as a 1:0.7 mixture of rotamers. *R*_f = 0.4 in 4:1 hexane/ethyl acetate. ¹H NMR (600

MHz, CDCl₃) δ 5.69-5.67 (m, 1H, 1rotH), 5.53-5.48 (m, 2H, 1rotH), 5.43-5.40 (m, 1rotH), 4.55 (d, *J* = 17.7 Hz, 1H), 4.33 (d, *J* = 17.0 Hz, 1rotH), 3.84 (d, *J* = 14.6 Hz, 1rotH), 3.68 (dd, *J* = 14.5, 2.7 Hz, 1H), 3.60-3.55 (m, 2H, 1rotH), 3.52-3.48 (m, 6H, 7rotH), 3.18 (dd, *J* = 10.6, 6.7 Hz, 1rotH), 3.09-3.03 (m, 1H, 1rotH), 2.93 (dd, *J* = 14.4, 10.1 Hz, 1H), 1.53 (s, 9H), 1.48 (s, 9rotH), 1.22 (s, 9H, 9rotH). ¹³C NMR (150 MHz, CDCl₃) δ 177.3, 177.3 (rot), 155.7, 155.6 (rot), 130.4, 130.3 (rot), 127.4 (rot), 126.5, 85.2, 84.4 (rot), 82.4, 81.7 (rot), 81.0, 80.6 (rot), 71.0 (rot), 69.8, 61.6, 60.9 (rot), 58.9, 58.8 (rot), 47.0, 47.0 (rot), 46.4, 45.4 (rot), 38.9, 38.9 (rot), 28.7, 28.6 (rot), 27.8, 27.8 (rot). HRMS (ESI): calcd. for C₁₉H₃₃O₆NNa [M + Na]⁺, 394.2200; found, 394.2205.

(1*S*,5*R*,6*S*,7*S*,8*R*)-tert-Butyl 7-(benzyloxy)-6-bromo-8-methoxy-9-oxa-3-azabicyclo[3.3.1]nonane-3-carboxylate (5.21). Benzoate protected azacyclooctene **5.15** (4 mg, 0.009 mmol, 1 equiv.) was dissolved in CH₂Cl₂ (0.25 mL, anhydrous) and cooled to -20 °C. A solution of bromine in CH₂Cl₂ (70 μL of 100-fold dilution, 0.014 mmol, 1.5 equiv.) was added dropwise. The bromine color dispersed after each drop. Upon addition of all bromine, the reaction was quenched with 10% Na₂S₂O₃ and extracted with CH₂Cl₂ (3 x 5 mL). The CH₂Cl₂ was combined, dried, decanted, and evaporated to dryness to give pure **5.21** in quantitative yield with no additional purification necessary. R_f = 0.2 in 3:1 hexane/ethyl acetate. ¹H NMR (600 MHz, CDCl₃): δ 8.08 (d, *J* = 7.5 Hz, 2H), 7.58 (t, *J* = 7.4 Hz, 1H), 7.46 (t, *J* = 7.7 Hz, 2H), 5.92 (t, *J* = 9.7 Hz, 1H), 4.69 (bs, 1H), 4.36-4.04 (m, 4H), 3.64 (dd, *J* = 8.8, 5.9 Hz, 1H), 3.37 (s, 3H), 3.17-3.30 (m, 2H), 1.56 (s, 9H). ¹³C NMR (151 MHz, CDCl₃, peak assignments aided by HMQC data): δ 165.4, 154.1, 133.3, 130.3, 130.0, 128.6, 81.2, 81.1 (rot), 74.6, 72.0 (b), 69.8 (b), 59.5, 49.6 (b), 42.8 (b), 41.5 (b, rot), 40.3 (b), 28.6. HRMS (ESI): calcd for C₂₀H₂₆O₆NNa [M + Na]⁺, 478.0836; found, 478.0842.

Methyl 4,6-*O*-benzylidene-2,3-di-*O*-methyl- α ,D-mannopyranoside (5.23). Methyl 4,6-*O*-benzylidene- α ,D-mannopyranoside¹⁷ (200 mg, 0.71 mmol, 1.0 equiv.) was dissolved in toluene (7.5 mL, anhydrous) and potassium hydroxide (0.24 g, 4.3 mmol, 6.0 equiv.) was added followed by iodomethane (0.30 mL, 4.9 mmol, 6.8 equiv.). The reaction mixture was refluxed for 4 h, at which point it was cooled to rt. Additional toluene was added (25 mL) and the organics were washed with H₂O (3 x 15 mL). The organic layer was evaporated to dryness and chromatographed on silica gel using a hexane/ethyl acetate solvent system (8:1, 6:1, 4:1, 2:1). This procedure resulted in 198 mg of pure **5.23** (0.64 mmol, 90%). R_f = 0.7 in 1:1 hexane/ethyl acetate. ¹H NMR (600 MHz, CDCl₃): δ 7.47 (d, *J* = 7.5 Hz, 2H), 7.35-7.30 (m, 3H), 5.57 (s, 1H), 4.76 (s, 1H), 4.24 (dd, *J* = 10.1, 4.6 Hz, 1H), 4.05 (t, *J* = 9.6 Hz, 1H), 3.83 (t, *J* = 10.3 Hz, 1H), 3.76 (td, *J* = 9.9, 4.6 Hz, 1H), 3.70 (dd, *J* = 9.9, 3.2 Hz, 1H), 3.63-3.62 (m, 1H), 3.53 (s, 3H), 3.52 (s, 3H), 3.37 (s, 3H). ¹³C NMR (150 MHz, CDCl₃): δ 137.7, 128.9, 128.2, 126.2, 101.7, 99.5, 79.1, 78.7, 77.7, 68.9, 63.9, 59.7, 59.0, 55.0. HRMS (ESI): calcd. for C₁₆H₂₃O₆ [M + H]⁺, 311.1489; found, 311.1490.

Methyl 6-bromo-6-deoxy-2,3-di-*O*-methyl- α ,D-mannopyranoside (5.24). Mannopyranoside **5.23** (190 mg, 0.61 mmol, 1.0 equiv.) was dissolved in CCl₄ (7.0 mL,

anhydrous). Calcium carbonate (67 mg, 0.67 mmol, 1.1 equiv.) was added and the mixture was heated to reflux. Upon boiling, *N*-bromosuccinamide (122 mg, 0.69 mmol, 1.1 equiv., recrystallized) was added and the mixture immediately turned a brown/orange color. The mixture was refluxed until this color dissipated (approx. 1 h), at which point the mixture was cooled to rt and evaporated to dryness. The residue was dissolved in CH₂Cl₂ (20 mL) and washed with 10% Na₂S₂O₃ (10 mL) and sat. NaHCO₃ (10 mL). The aqueous layer were combined and extracted with CH₂Cl₂ (20 mL). The organics were combined, dried, decanted, and evaporated to dryness to yield crude Methyl 4-benzoate-6-bromo-6-deoxy-2,3-di-*O*-methyl- α ,*D*-mannopyranoside (199 mg). The benzoate group was immediately saponified by dissolving the crude product in methanol containing 1% NaOH (7.5 mL). The mixture was stirred at rt for 1 h, at which point it was neutralized with 3M HCl and evaporated to dryness. The residue was dissolved in H₂O (15 mL) and extracted with CH₂Cl₂ (3 x 10 mL). The organics were combined, dried, decanted, evaporated to dryness, and the crude product was purified by silica gel chromatography using a hexane/ethyl acetate solvent system (5:1, 3:1, 1:1). This procedure resulted in pure **5.24** (100 mg, 0.35 mmol, 58%). R_f = 0.5 in 1:1 hexane/ethyl acetate. ¹H NMR (400 MHz, CDCl₃): δ 4.82 (d, *J* = 1.4 Hz, 1H), 3.80- 3.75 (m, 1H), 3.71- 3.67 (m, 2H), 3.60-3.58 (m, 1H), 3.52- 3.47 (m, 1H), 3.45 (s, 3H), 3.44- 3.39 (m, 7H), 2.74 (bs, 1H). ¹³C NMR (100 MHz, CDCl₃): δ 98.5, 81.1, 75.7, 72.0, 69.0, 59.1, 57.2, 55.2. HRMS (ESI): calcd. for C₉H₁₇O₅BrNa [M + Na]⁺, 307.0152; found, 307.0155.

***tert*-Butyl allyl((2*S*,3*S*,4*R*)-4-hydroxy-2,3-dimethoxyhex-5-enyl)carbamate (5.25).** 6-Bromomannopyranoside **5.24** (95 mg, 0.32 mmol, 1.0 equiv.) was dissolved in 19:1 1-propanol/H₂O (14.3 mL). To this solution, allylamine (0.99 mL, 13 mmol, 41 equiv.), zinc (1.4 g, 22 mmol, 69 equiv.), and NaBH₃CN (1.1 g, 1.8 mmol, 5.6 equiv.) were added and the resulting mixture was heated to 80 °C 2 h. After 2 h, the reaction mixture was cooled to rt, filtered through Celite and the filtrate was evaporated to dryness. The residue was dissolved in 6:4:1 CH₂Cl₂/MeOH/1.5 M HCl (20 mL) and stirred for 45 min checking to be sure that the solution remained acidic. The mixture was basified with 10% NaOH and extracted with CH₂Cl₂ (3 x 20 mL). The organics were dried with MgSO₄, decanted, and evaporated to dryness to result in crude divinylamine. The crude product was dissolved in dioxane (1.5 mL) and triethylamine (20 μ L, 0.14 mmol, 0.4 equiv.) was added followed by di-*tert*-butyldicarbonate (60 g, 0.28 mmol, 0.90 equiv.). The mixture was stirred for 2 h at rt, at which point it was evaporated to dryness and purified by silica gel chromatography with a hexane/ethyl acetate solvent system (10:1 to 2:1; **5.25** elutes at 4:1). This procedure resulted in 31 mg of pure **5.25** (0.098 mmol, 31%). ¹H NMR (400 MHz, CDCl₃): δ 6.02-5.94 (m, 1H), 5.80 (ddd, *J* = 16.0, 10.6, 5.3 Hz, 1H), 5.44 (dt, *J* = 17.2, 1.5 Hz, 1H), 5.26 (d, *J* = 9.2 Hz, 1H), 5.21-5.11 (m, 2H), 4.28 (bs, 1H), 4.08-3.97 (m, 1H), 3.86 (dd, *J* = 16.0, 5.8 Hz, 1H), 3.67-3.58 (m, 1H), 3.50 (s, 3H), 3.44 (s, 3H), 3.32- 3.20 (m, 3H), 1.49 (s, 9H). ¹³C NMR (100 MHz, CDCl₃): δ 155.9, 138.0, 134.2, 116.4 (bs), 83.6 (bs), 81.4, 80.0 (bs), 71.7, 60.2, 59.1 (bs), 51.4, 50.6 (rot), 47.9, 28.6. HRMS (ESI): calcd. for C₁₆H₃₀O₅N [M + H]⁺, 316.2118; found, 316.2121.

(5R,6S,7R,Z)-tert-Butyl 5-hydroxy-6,7-dimethoxy-5,6,7,8-tetrahydroazocine-1(2H)-carboxylate (5.26). Compound **5.25** (30 mg, 0.095 mmol, 1.0 equiv.) and Grubbs 2nd generation catalyst (7 mg, 0.008 mmol, 10 mol%) were dissolved in CH₂Cl₂ (7.5 mL). The mixture was heated to reflux for 1.5 h, at which point it was evaporated to dryness and *immediately* purified by silica gel chromatography using a hexane/ethyl acetate solvent system (5:1, 3:1, 1:1). This procedure yielded 23 mg of pure **5.26** (0.080 mmol, 84%) as a 1: 0.8 mixture of rotamers ¹H NMR (600 MHz, CDCl₃): δ 5.51 (m, 2H, 2rotH), 4.65-4.61 (m, 1H, 1rotH), 4.41 (d, *J* = 17.8 Hz, 1H), 4.21-4.14 (m, 1H, 2rotH), 3.63 (s, 3H, 3rotH), 3.63-3.55 (m, 1H, 1rotH), 3.47- 3.39 (m, 5H, 5rotH), 3.03 (d, *J* = 12.8 Hz, 1H, 1rotH), 2.66 (s, 1rotH), 2.49 (s, 1H), 1.73 (s, 1H), 1.46 (s, 9H), 1.44 (s, 9rotH). ¹³C NMR (150 MHz, CDCl₃): δ 155.4, 155.3 (rot), 131.1 (rot), 130.9, 128.5, 128.2 (rot), 85.6 (rot), 84.8, 80.5, 80.3 (rot), 80.1, 79.9 (rot), 70.9, 70.1 (rot), 61.5 (rot), 61.40, 58.20 (rot), 58.17, 47.2, 47.2 (rot), 46.0, 44.6 (rot), 28.60, 28.6 (rot). HRMS (ESI): calcd. for C₁₄H₂₆O₅N [M + H]⁺, 288.1805; found, 288.1808.

(5R,6S,7R,Z)-tert-Butyl 5-(benzoyloxy)-6,7-dimethoxy-5,6,7,8-tetrahydroazocine-1(2H)-carboxylate (5.27). Azacyclooctene **5.26** (23 mg, 0.080 mmol, 1.0 equiv.) was dissolved in pyridine (0.5 mL, anhydrous) and cooled to 0 °C. Benzoyl chloride (10 μL, 0.085 mmol, 1.4 equiv.) was added dropwise and the mixture was allowed to warm to rt overnight. The following day the reaction was poured onto ice and extracted with CH₂Cl₂ (3 x 10 mL). The organics were combined and further washed with 6M HCl (10 mL), sat. NaHCO₃ (10 mL), and H₂O (10 mL). The organic layer was dried, decanted, evaporated to dryness, and purified by silica gel chromatography with a hexane/ethyl acetate solvent system (10:1, 8:1, 6:1, 4:1). This procedure yielded 23 mg of **5.27** (0.059 mmol, 69%) as a mixture of rotamers (1:1). R_f = 0.2 in 3:1 hexane/ethyl acetate. ¹H NMR (600 MHz, CDCl₃): δ 8.07 (d, *J* = 7.6 Hz, 1H), 7.56 (t, *J* = 7.2 Hz, 1H), 7.45 (t, *J* = 8.1 Hz, 2H), 6.05 (bs, 0.5H), 5.92 (bs, 0.5H), 5.67 (bs, 1H), 5.40 (bs, 1H), 4.56 (d, *J* = 18.0 Hz, 0.5H), 4.37 (d, *J* = 18.0 Hz, 0.5H), 4.28-4.24 (m, 1H), 3.87 (d, *J* = 8.3 Hz, 1H), 3.68 (dd, *J* = 29.2, 9.6 Hz, 1H), 3.58-3.53 (m, 3H), 3.48 (s, 3H), 3.15 (dd, *J* = 13.5, 3.1 Hz, 1H), 1.51 (s, 9H). HRMS (ESI): calcd. for C₂₁H₂₉O₆NNa [M + Na]⁺, 414.1887; found, 414.1892.

(1R,5R,6R,7S,8R)-tert-Butyl 7-(benzoyloxy)-5-bromo-8-methoxy-9-oxa-3-azabicyclo[4.2.1]nonane-3-carboxylate (5.29). Benzoate protected azacyclooctene **5.27** (4 mg, 0.009 mmol, 1 equiv.) was dissolved in CH₂Cl₂ (0.25 mL, anhydrous) and cooled to -20 °C. A solution of bromine in CH₂Cl₂ (70 μL of 100-fold dilution, 0.014 mmol, 1.5 equiv.) was added dropwise. After 15 min, the reaction was quenched with 10% Na₂S₂O₃ and extracted with CH₂Cl₂ (3 x 5 mL). The CH₂Cl₂ was combined, dried, decanted, and evaporated to dryness to give **5.29** as a 1:1 mixture of rotamers. R_f = 0.5 in 2.5:1 hexane/ethyl acetate. ¹H NMR (600 MHz, CDCl₃): δ 8.09 (t, *J* = 8.4 Hz, 2H), 7.61 (t, *J* = 7.3 Hz, 1H), 7.48 (t, *J* = 7.1 Hz, 2H), 5.94 (t, *J* = 8.3 Hz, 1H), 4.92 (dd, *J* = 7.4, 4.3 Hz, 1H), 4.50 (dd, *J* = 14.5, 5.1 Hz, 0.5H), 4.40-4.35 (m, 1.5H), 4.32-4.29 (m, 0.5H), 4.28-4.26 (m, 0.5H), 3.98 (s, 0.5H), 3.94 (s, 0.5H), 3.55- 3.49 (m, 1H), 3.46 (s, 1.5H), 3.42 (s, 1.5H), 3.11 (dd, *J* = 14.7, 4.0 Hz, 0.5H), 3.02 (dd, *J* = 17.8, 6.8 Hz, 0.5H), 1.48 (s, 4.5H), 1.46 (s, 4.5H). HRMS (ESI): calcd. for C₂₀H₂₆O₆NBrNa [M + Na]⁺, 478.0836; found, 478.0844.

X-Ray Crystallography

A colorless plate 0.05 x 0.05 x 0.02 mm in size was mounted on a Cryoloop with Paratone oil. Data were collected in a nitrogen gas stream at 100(2) K using phi and omega scans. Crystal-to-detector distance was 60 mm and exposure time was 10 seconds per frame using a scan width of 1.0°. Data collection was 99.5% complete to 67.00° in q . A total of 21596 reflections were collected covering the indices, $-16 \leq h \leq 16$, $-26 \leq k \leq 26$, $-7 \leq l \leq 6$. 3704 reflections were found to be symmetry independent, with an R_{int} of 0.0418. Indexing and unit cell refinement indicated a primitive, orthorhombic lattice. The space group was found to be P2(1)2(1)2 (No. 18). The data were integrated using the Bruker SAINT software program and scaled using the SADABS software program. Solution by direct methods (SIR-2008) produced a complete heavy-atom phasing model consistent with the proposed structure. All non-hydrogen atoms were refined anisotropically by full-matrix least-squares (SHELXL-97). All hydrogen atoms were placed using a riding model. Their positions were constrained relative to their parent atom using the appropriate HFIX command in SHELXL-97. Absolute stereochemistry was determined to be *R* at C2, C3, C5, and C6 and *S* at C4, respectively.

References

- (1) Massoud, T. F.; Gambhir, S. S. Molecular imaging in living subjects: Seeing fundamental biological processes in a new light. *Gene. Dev.* **2003**, *17*, 545-580.
- (2) Prescher, J. A.; Dube, D. H.; Bertozzi, C. R. Chemical remodelling of cell surfaces in living animals. *Nature* **2004**, *430*, 873-877.
- (3) Adams, K. E.; Ke, S.; Kwon, S.; Liang, F.; Fan, Z.; Lu, Y.; Hirschi, K.; Mawad, M.; E.; Barry, M. A.; Sevick-Muraca, E. M. Comparison of visible and near-infrared wavelength-excitable fluorescent dyes for molecular imaging of cancer. *J. Biomed. Opt.* **2007**, *12*, 024017.
- (4) Ntziachristos, V. Going deeper than microscopy: The optical imaging frontier in biology. *Nat. Methods* **2010**, *7*, 603-614.
- (5) Lemieux, G. A.; de Graffenried, C. L.; Bertozzi, C. R. A fluorogenic dye activated by the Staudinger ligation. *J. Am. Chem. Soc.* **2003**, *125*, 4708-4709.
- (6) Lin, F. L.; Hoyt, H. M.; van Halbeek, H.; Bergman, R. G.; Bertozzi, C. R. Mechanistic investigation of the Staudinger ligation. *J. Am. Chem. Soc.* **2005**, *127*, 2686-2695.
- (7) Hangauer, M. J.; Bertozzi, C. R. A FRET-based fluorogenic phosphine for live-cell imaging with the Staudinger ligation. *Angew. Chem. Int. Ed.* **2008**, *47*, 2394-2397.
- (8) Frangioni, J. V. In vivo near-infrared fluorescence imaging. *Curr. Opin. Chem. Biol.* **2003**, *7*, 626-634.
- (9) Chang, P. V. Chemical tools for imaging glycans in living systems, University of California, Berkeley: Berkeley, CA, 2010.

- (10) Prescher, J. A.; Contag, C. H. Guided by the light: Visualizing biomolecular processes in living animals with bioluminescence. *Curr. Opin. Chem. Biol.* **2010**, *14*, 80-89.
- (11) Cohen, A. S.; Dubikovskaya, E. A.; Rush, J. S.; Bertozzi, C. R. Real-time bioluminescence imaging of glycans on live cells. *J. Am. Chem. Soc.* **2010**, *132*, 8563-8565.
- (12) Denburg, J. L.; Lee, R. T.; McElroy, W. D. Substrate-binding properties of firefly luciferase: I. Luciferin-binding site. *Arch. Biochem. Biophys.* **1969**, *134*, 381-394.
- (13) Zhou, Z.; Fahrni, C. J. A fluorogenic probe for the copper(I)-catalyzed azide-alkyne ligation reaction: Modulation of the fluorescence emission via $3(n,\pi^*)-1(\pi,\pi^*)$ inversion. *J. Am. Chem. Soc.* **2004**, *126*, 8862-8863.
- (14) Bryden, C. C.; Reilley, C. N. Europium luminescence lifetimes and spectra for evaluation of 11 europium complexes as aqueous shift reagents for nuclear magnetic resonance spectrometry. *Anal. Chem.* **1982**, *54*, 610-615.
- (15) Sletten, E. M.; Liotta, L. J. A flexible stereospecific synthesis of polyhydroxylated pyrrolizidines from commercially available pyranosides. *J. Org. Chem.* **2006**, *71*, 1335-1343.
- (16) Pangborn, A. B.; Giardello, M. A.; Grubbs, R. H.; Rosen, R. K.; Timmers, F. J. Safe and convenient procedure for solvent purification. *Organometallics* **1996**, *15*, 1518-1520.
- (17) Tewson, T. J.; Soderlind, M. 1-Propenyl 4,6-O-benzylidene- β -D-mannopyranoside-2,3-cyclic sulfate: A substrate for the synthesis of [F-18] 2-deoxy-2-fluoro-D-glucose. *J. Carbohydrate Chem.* **1985**, *4*, 529-543.

Chapter 6

Cu-Free Click Chemistry as a Tool for Proteomics

Introduction to Proteomics

Imaging experiments are a major goal for bioorthogonal chemistries but they are not the only application in which bioorthogonal chemistries can excel. The covalent bond formed between a biomolecule of interest and a secondary reagent makes the bioorthogonal chemical reporter strategy ideally suited for the purification and identification of tagged biomolecules. The Staudinger ligation and traditional click chemistry have seen success regarding the identification of proteins post-translationally modified with glycans and lipids (via the metabolic incorporation of azido or alkynyl-analogues) through mass spectrometry based proteomics.^{1,2,3,4,5} Additionally, the Cravatt group has successfully used bioorthogonal chemistries in conjunction with activity-based protein profiling to identify new proteases.⁶ We looked to develop an experimental platform where Cu-free click chemistry could be used for the purification and identification of azido-biomolecules.

The identification of proteins from complex samples is done through mass spectrometry and relies on *de novo* peptide sequencing to obtain a protein identification.⁷ While mass spectrometry is a huge asset to this field and technology is rapidly advancing, identification is often very difficult, and cumbersome validation procedures are necessary to confirm results gained from mass spectrometry data.^{8,9} One of the major drawbacks of mass spectrometry based proteomics is that the instrumentation used for proteomic analysis have a dynamic range limited to 2-3 orders of magnitude.¹⁰ The consequence of this dynamic range is only the most abundant proteins in a sample are identified even if there are other more interesting low abundance proteins present. This limitation makes the purification of desired proteins from cell lysates and other complex protein samples imperative.

Affinity chromatography is a popular way of selecting for a desired set of proteins from a larger sample.¹¹ An ideal affinity purification will capture all of the desired protein subset, (*i.e.* proteins tagged with a chemical reporter group), wash away all unwanted proteins, and mildly, yet efficiently, elute all the captured proteins. This is a difficult task because it requires the affinity reagent to attach to the purification matrix very tightly so all proteins are captured and remain captured through washing, but at the same time, the affinity reagent must be easily and selectively removed from the column to allow for elution. To overcome this two-faced requirement, chemical biologists have recently looked to optimize the actual affinity reagent for capture and have engineered cleavable linkers into the affinity tag that facilitate elution. This strategy necessitates a reagent that has three components: affinity reagent, cleavable linker, and a reactive group.

Reagent Design

For Cu-free click chemistry based proteomics, the reactive group will be the cyclooctyne DIFO (**3.1**) and target azide-modified proteins.¹² When employing a cleavable linker strategy, the optimal affinity reagent binds the column matrix very tightly. While there are many affinity reagents employed in the literature, undoubtedly biotin fits this requirement best. The biotin-(strept)avidin bond is one of the strongest known non-covalent interactions with a K_d of 10^{-15} M and has been exploited for countless experiments at the interface of chemistry and biology.¹³ The essentially irreversible binding of biotin to (strept)avidin at physiological conditions makes it an ideal candidate for the affinity reagent.

While the biotin is fairly universal to all cleavable affinity tags, the method of cleavage is not. Ideally, a cleavage method will be mild, efficient, bioorthogonal and minimally perturbing. The basis for many of the cleavable linkers employed has come from linkers used in solid phase synthesis and can be grouped into four main categories: pH cleavable linkers,^{14,15,16} chemically cleavable linkers,^{17,18,19,20,21,22} photocleavable linkers,^{23,24,25} and enzymatically cleavable linkers.²⁶

At the onset of this project, we chose to use the disulfide bond popularized by the Gygi²¹ and Withers^{20,19} groups, because it allows elution under mild and neutral conditions with a simple and inexpensive small molecule reducing agent. Combining all of these component together, compound **6.1** became our target reagent for purification of azido-biomolecules (Figure 6.1). Compound **6.1** could come from the coupling of five components: activated biotin **6.2**, hydrophilic diamine **6.3**, succinic anhydride (**6.4**), cystamine (**6.5**) and activated DIFO **6.6**.

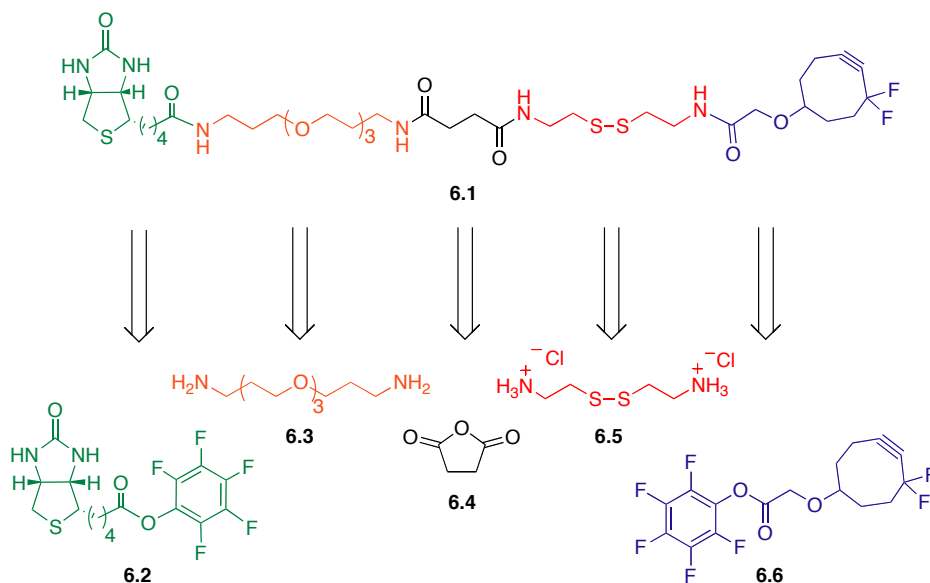
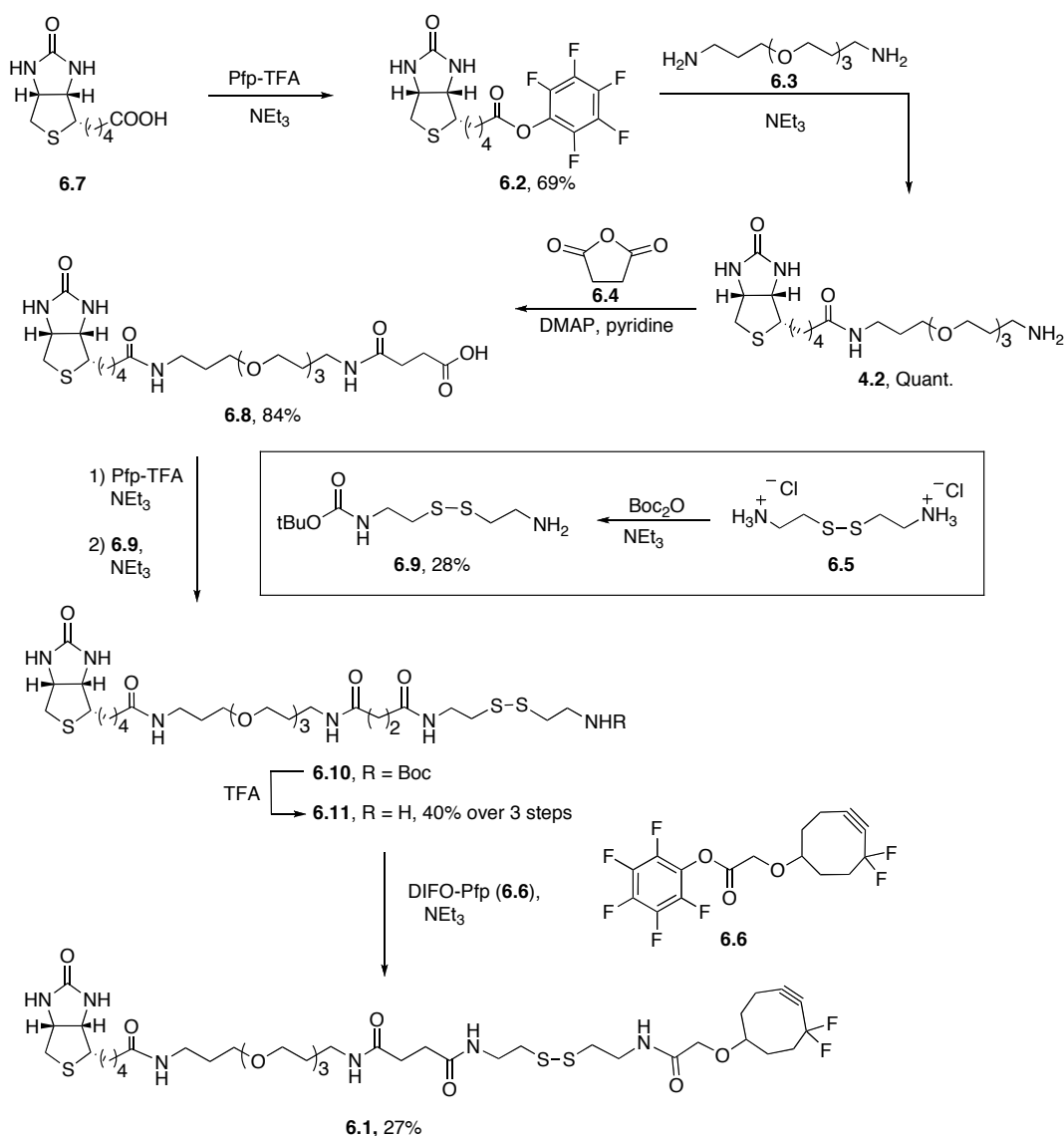


Figure 6.1. Target pull-down reagent for purification of azido-glycoproteins by Cu-free click chemistry.

Synthesis of Pull-Down Reagent

The carboxylic acid of D-Biotin (**6.7**) was activated as a pentafluorophenyl ester (**6.2**) and coupled to 4,7,10-trioxa-1,13-tridecanediamine (**6.3**) to yield **4.2**.²⁷ The resulting amine was combined with succinic anhydride in the presence of dimethylaminopyridine and pyridine to yield carboxylic acid containing compound **6.8**. Compound **6.8** was activated as a pentafluorophenyl ester and coupled with mono-Boc protected cystamine **6.9**, which was prepared from cystamine dihydrochloride (**6.5**). Following removal of the Boc group under standard acidic conditions (TFA) and coupling to DIFO (activated as a pentafluorophenyl ester **6.6**) the target pull-down reagent was obtained.

Scheme 6.1. Synthesis of target pull-down reagent.



Evaluation of Pull-Down Reagent

With the desired pull-down reagent in hand, we assessed its ability to capture and release an azide-labeled protein. For this, we used bovine serum albumin (BSA) that had been nonspecifically modified with the NHS ester of azidoacetic acid or wild-type BSA as a control. N₃-BSA (+) or BSA (-) were treated with compound **6.1** overnight. Excess reagent was removed and the labeled protein samples were subjected to NeutraAvidin beads. The beads were washed with PBS and elution was performed with either tris-(2-carboxyethyl) phosphine (TCEP) or dithiothreitol (DTT).²⁸ The efficiency and selectivity of capture and elution was analyzed by SDS-PAGE (Figure 6.2).

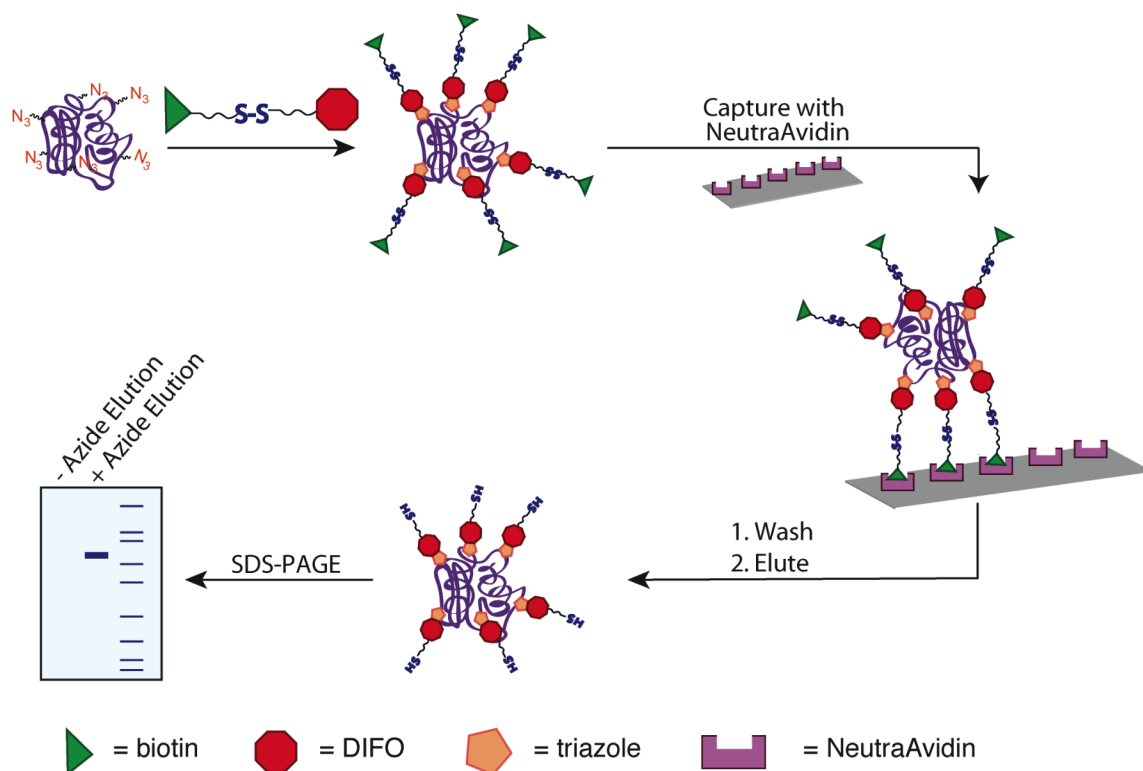


Figure 6.2. Experimental workflow for the capture, purification, and elution of azide-labeled proteins with pull-down reagent **6.1**.

Literature precedent for disulfide linkers involves cleavage with TCEP (30 mM at rt or 10 mM at 50 °C),^{19,20,21} however, TCEP did not appear to be effective at eluting the N₃-BSA from the NeutraAvidin. Fortunately, treatment with DTT successfully released the captured proteins, as evident by the significant BSA bands observed in the elution lanes for the N₃-BSA as compared to the faint band observed in the control BSA samples (Figure 6.3).

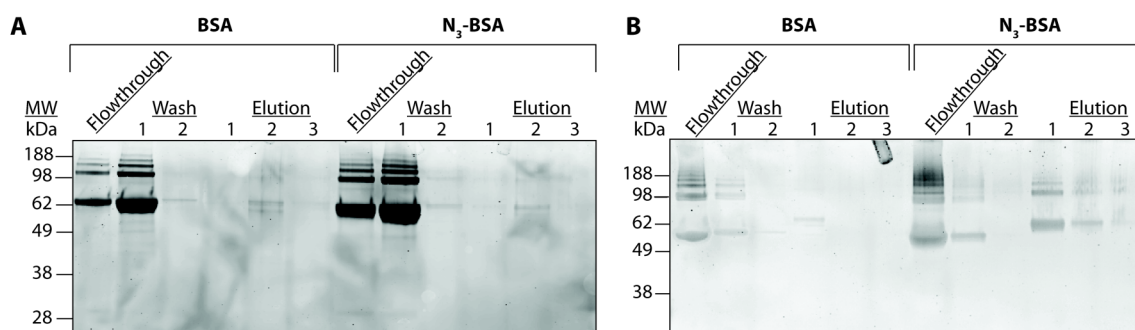


Figure 6.3. Pull-down reagent **6.1** allows for azide-specific capture and elution. BSA or N₃-BSA was combined with compound **6.1** (10 μM) overnight. The labeled protein was incubated with NeutrAvidin beads for 30 min. Protein not bound to the beads is evident in the flowthrough. The beads were washed with PBS then thrice treated with (A) TCEP or (B) DTT for 30 min. The presence of protein in the flowthrough, washes, and elutions was analyzed by SDS-PAGE staining with SyproOrange.

With encouraging results from this initial proof-of-principle experiment, N₃-BSA was doped into an H2^{V12} Ras cell lysate to show that only the desired protein was captured. The strong N₃-BSA bands and absence of other protein bands in elution lanes 1 and 2 of Figure 6.4 indicate that compound **6.1** enriches for azide-labeled proteins.

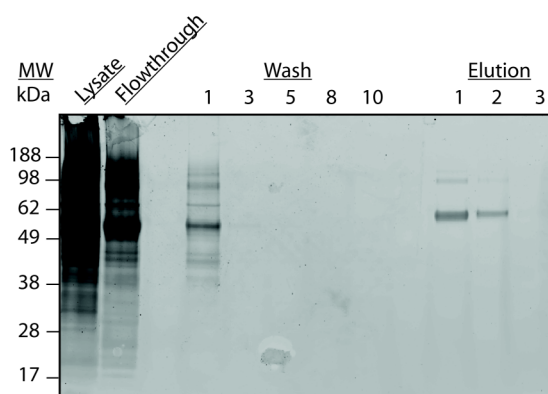


Figure 6.4. Pull-down reagent **6.1** enriches N₃-BSA from other proteins in a cell lysate. A mixture of N₃-BSA (250 μg) and H2 Ras lysate (750 μg) was treated with compound **6.1** (10 μM) overnight. The protein was incubated with NeutrAvidin beads for 30 min. Protein not bound to the beads is evident in the flowthrough. The beads were washed with PBS (x 10) then thrice treated with DTT (30 mM). The presence of protein in the flowthrough, washes, and elutions as compared to the original lysate was analyzed by SDS-PAGE staining with SyproOrange.

The next test for this pull-down reagent was to capture proteins, which were tagged with an azide through a metabolic incorporation strategy. H2 Ras cells were grown in the presence or absence of peracetylated N-azidoacetyl mannosamine (Ac₄ManNAz) for 3 days. Lysates were generated and subjected to the procedure outlined in Figure 6.2. The sample not treated with Ac₄ManNAz shows no signal in the elution bands while the ManNAz treated sample displays signal corresponding to eluted labeled glycoproteins indicating that compound **6.1** was able to selectively capture and elute azide-modified proteins (Figure 6.5).

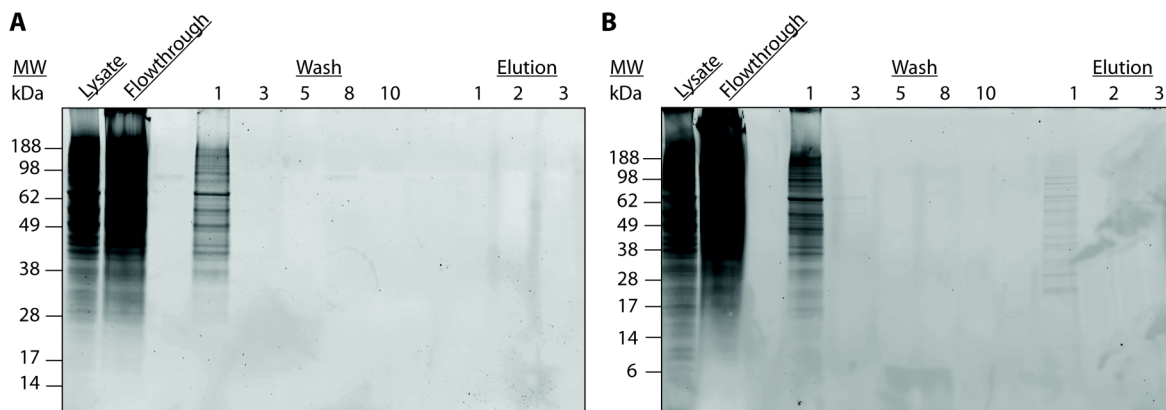


Figure 6.5. Pull-down reagent **6.1** enriches proteins from a cell lysate in an azide-dependent manner. H2 Ras cells were grown in the presence (B) or absence (A) of N-azidoacetyl mannosamine for 3 days. Lysates were generated and treated with **6.1** overnight. The labeled cell lysate was incubated with NeutrAvidin beads for 30 min. Protein not bound to the beads are evident in the flowthrough. The beads were washed with PBS (x 10) then treated with DTT for 30 min (x 3, elutions 1-3). The presence of protein in the flowthrough, washes, and elutions as compared to the original lysate was analyzed by SDS-PAGE staining with SyproOrange.

Conclusions and Future Directions for Cu-Free Click Chemistry Based Proteomics

While the results in Figure 6.5 are promising, they were not reproducible enough for this probe to be utilized for proteomics on complex samples. Initial multidimensional chromatography coupled to mass spectrometry on samples eluted with DTT did not yield promising results. At times, a significant amount of protein was evident in the control samples lanes that contained no azides. We attributed this to disulfide exchange of the pull-down reagent with cysteine residues in proteins,²⁹ which has since been identified as a major cause of background using disulfide cleavable linkers.³⁰ An exhaustive reduction and alkylation before treatment with compound **6.1** should solve this problem; however, this procedure was complicated by the fact that azides are susceptible to reduction. Thus, an alternative cleavable linker appears more suited toward Cu-free click chemistry. Work towards other cleavable pull-down reagents is underway by other members of the Bertozzi group.

Materials and Methods

General Experimental Procedure

Unless otherwise noted all reactions were performed while stirring under an atmosphere of N₂. All solvents were introduced to the reaction via a syringe unless otherwise noted. Anhydrous DMF, DMSO, and MeOH were purchased from Acros or Aldrich in sealed bottles. All other solvents were purified via packed columns as described by Pangborn *et al.*³¹ Unless otherwise noted, magnesium sulfate was used as a drying agent and solvent was removed with a rotary evaporator at reduced pressure. Thin layer chromatography was performed on 60 Å glass back silica gel plates and stained in the following manner: amines with ninhydrin, alkyne containing compounds with vanillin, all others in ceric ammonium molybdate. Reported R_f values are for the solvent system in which the reaction was monitored unless otherwise noted. Silica gel chromatography was performed using 60 Å 230-400 mesh silica gel unless otherwise noted. All NMR spectra are reported in ppm and standardized against solvent peaks. NMR spectra were obtained on Bruker AV-300, AVQ-400, AVB-400, DRX-500 or AV-500 instruments. IR spectra were obtained using thin films on NaCl plates. High-resolution fast atom bombardment (FAB) and electrospray ionization (ESI) mass spectra were obtained from the UC Berkeley Mass Spectrometry Facility.

Experimental Procedures

Biotin-pentafluorophenyl ester (6.2).³² D-Biotin **6.7** (2.1 g, 8.5 mmol, 1.0 equiv.) was suspended in DMF (40 mL, dry) and heated/sonicated until homogenous. Once the solution reached rt, NEt₃ (2.4 mL, 17 mmol, 2.0 equiv., anhydrous) was added followed by pentafluorophenol trifluoroacetate (2.3 mL, 13 mmol, 1.5 equiv.). The reaction was monitored by TLC (17:3:1 EtOAc/MeOH/H₂O) for the disappearance of **6.7** (R_f = 0.2), at which point (approx. 1.5 h) the reaction was evaporated to dryness. The residue was triturated with ether (50 mL) to yield white crystals of **6.2** (2.42 g, 5.90 mmol, 69%, R_f = 0.8). M.p. 190.0-191.5 °C (lit.³² 188-189 °C). ¹H NMR (400 MHz, DMSO): δ 6.49 (s, 1H), 6.40 (s, 1H), 4.32 (dd, *J* = 7.5, 5.3 Hz, 1H), 4.17-4.15 (m, 1H), 3.15-3.09 (m, 1H), 2.86-2.77 (m, 3H), 2.59 (d, *J* = 12.4 Hz, 1H), 1.74-1.63 (m, 3H), 1.57-1.35 (m, 3H). ¹³C NMR (100 MHz, DMSO): δ 170.0, 163.2, 142.3, 140.6, 139.8, 139.2, 138.1, 136.7, 61.5, 59.7, 55.7, 40.4, 32.8, 28.4, 28.2, 24.8. ¹⁹F NMR (376 MHz, DMSO): δ -153.58 (d, *J* = 21.8 Hz, 2F), -158.167 (t, *J* = 22.9 Hz, 1H), -162.66 (t, *J* = 20.1 Hz, 2H). IR: 3215, 2916, 2849, 2360, 1793, 1708, 1518, 1460, 1113, 1095, 1005, 987 cm⁻¹. HRMS (FAB): calcd. for C₁₆H₁₆N₂O₃SF₅⁺ [M+H]⁺, 411.0802; found, 411.0806.

N-(13-amino-4,7,10-trioxatridecanyl)biotinamide (4.2).²⁷ A 0 °C solution of compound **6.2** (2.38 g, 5.81 mmol, 1.0 equiv.) in *N,N*-dimethylformamide (30 mL, anhydrous) was added dropwise over 30 min using a syringe pump to a solution of 4,7,10-trioxa-1,13-tridecanediamine (14.5 mL, 66.1 mmol, 11.4 equiv., **6.3**) and NEt₃ (1.6 mL, 11 mmol, 1.9 equiv., anhydrous) in *N,N*-dimethylformamide (30 mL, anhydrous) at 0 °C. Upon addition

of **6.2**, the reaction was monitored by TLC (5:3:1 EtOAc/MeOH/H₂O) for the disappearance of **6.2** ($R_f = 0.9$), at which point (approx. 2.5 h) the solution was evaporated to dryness. The residue was suspended in ether (150 mL), stirred for 15 min in the dark, and decanted. This procedure was repeated twice to yield a sticky solid, which was further purified on silica gel using 5:3:1 EtOAc/MeOH/H₂O to yield pure **4.2** as a colorless hygroscopic wax (2.59 g, 5.81 mmol, 100%, $R_f = 0.2$). ¹H NMR (400 MHz, D₂O): δ 4.49 (dd, $J = 7.9, 4.8$ Hz, 1H), 4.31 (dd, $J = 4.4, 7.9$ Hz, 1H), 3.56-3.53 (m, 10H), 3.45 (t, $J = 6.3$ Hz, 2H), 3.22-3.19 (m, 1H), 3.13 (t, $J = 6.7$ Hz, 2H), 2.99 (t, $J = 7.1$ Hz, 2H), 2.87 (dd, $J = 16.1, 4.9$ Hz, 1H), 2.66 (d, $J = 13.0$ Hz, 1H), 2.13 (t, $J = 7.2$ Hz, 2H), 1.87-1.82 (m, 2H), 1.70-1.41 (m, 6H), 1.36-1.27 (m, 2H). ¹³C NMR (125 MHz, D₂O): δ 180.2, 165.1, 69.5 (2), 69.3 (2), 68.3, 68.2, 62.0, 60.2, 55.4, 39.7, 36.2, 35.5, 28.3, 28.0, 27.7, 26.5, 25.2, 22.8. IR: 3293, 3067, 2928, 2866, 1692, 1640, 1137 cm⁻¹. HRMS (FAB): calcd. for C₂₀H₃₉N₄O₅S⁺ [M+H]⁺, 447.2641; found, 447.2630.

3-[N-(D-biotinoyl)-13-amino-4,7,10-trioxatridecanylaminocarbonyl] propanoic acid (6.8).³³ Compound **4.2** (195 mg, 0.439 mmol, 1.0 equiv.) was dissolved in pyridine (16 mL, anhydrous) and *N,N*-dimethylaminopyridine (12 mg, 0.096 mmol, 0.22 equiv.) and succinic anhydride (99 mg, 0.99 mmol, 2.3 equiv., **6.4**) were added. The reaction was monitored by ESI-MS for the disappearance of **4.2** (approx. 3 h), at which point the reaction was evaporated to dryness and purified on silica gel eluting with 5:3:1 EtOAc/MeOH/H₂O with 1% AcOH. This procedure yield pure **6.8** as a white solid (202 mg, 0.369 mmol, 84%, $R_f = 0.5$ in 5:3:1 EtOAc/MeOH/H₂O). M.p. 144.2-144.9 °C. ¹H NMR (400 MHz, D₂O): δ 4.49 (dd, $J = 7.9, 4.8$ Hz, 1H), 4.32 (dd, $J = 7.9, 4.5$ Hz, 1H), 3.58-3.54 (m, 8H), 3.48-3.44 (m, 4H), 3.21-3.12 (m, 5H), 2.88 (dd, $J = 13.1, 5.0$ Hz, 1H), 2.66 (d, $J = 13.0$ Hz, 1H), 2.36 (dd, $J = 5.6, 4.3$ Hz, 4H), 2.14 (t, $J = 7.2$ Hz, 2H), 1.71-1.45 (m, 8H), 1.32-1.28 (m, 2H). ¹³C NMR (100 MHz, D₂O): δ 180.1, 176.5, 175.4, 165.2, 69.6 (br), 69.4, 69.3, 68.5, 68.4, 62.1, 60.2, 55.4, 39.7, 36.3, 35.5, 32.4, 32.0, 28.3 (2), 28.0, 27.7, 25.2, 22.6. IR: 3296, 2926, 2877, 2360, 1699, 1646, 1120 cm⁻¹. HRMS (FAB): calcd. for C₂₄H₄₂N₄O₈SN⁺ [M+Na]⁺, 569.2621; found, 569.2608.

***N*-tert-butylloxycarbonyl cystamine (6.9).**³⁴ Cystamine dihydrochloride (1.02 g, 4.54 mmol, 1.0 equiv., **6.5**), triethylamine (2.0 mL, 14 mmol, 3.1 equiv., anhydrous) and di-*tert*-butyldicarbonate (1.06 g, 4.80 mmol, 1.07 equiv.) were combined in methanol (50 mL, anhydrous) and allowed to stir at rt overnight. The following morning the mixture was evaporated to dryness, dissolved in pH 4 NaH₂PO₄ (20 mL) and washed with ether (2 x 12 mL). The pH of the aqueous layer was adjusted to 9 with 10% NaOH and the solution was extracted with ethyl acetate (5 x 10 mL). The ethyl acetate was combined, dried, decanted and evaporated to dryness to yield **6.9** as a slightly yellow oil (320 mg, 1.3 mmol, 28%). ¹H NMR (300 MHz, CDCl₃): δ 5.26 (bs, 1H), 3.33 (q, $J = 6.1$ Hz, 2H), 2.90 (t, $J = 6.1$ Hz, 2H), 2.67 (td, $J = 6.4, 2.7$ Hz, 4H), 1.61 (bs, 2H), 1.33 (s, 9H). ¹³C NMR (125 MHz, CDCl₃): 155.9, 79.3, 42.2, 40.3, 39.3, 38.3, 28.3 IR: 3350, 2975, 2930, 2360, 1698, 1521, 1170 cm⁻¹. HRMS (FAB): calcd. for C₉H₂₁N₂O₇S₂⁺ [M+H]⁺, 253.1045; found, 253.1038.

Compound 6.11. Compound **6.8** (68.9 mg, 0.126 mmol, 1.0 equiv.) was dissolved in *N,N*-dimethylformamide (2.0 mL, anhydrous). Triethylamine (37 μ L, 0.27 mmol, 2.1 equiv.,

anhydrous) was added, followed by pentafluorophenyl trifluoroacetate (45 μ L, 0.26 mmol, 2.1 equiv.) and the reaction was monitored by TLC (5:3:1 EtOAc/MeOH/H₂O 1% AcOH) for the disappearance of **6.8** (R_f = 0.2). More pentafluorophenyl trifluoroacetate was added if necessary (20 μ L). Upon completion, the mixture was evaporated to dryness and triturated with ether to yield a white solid containing the activated pentafluorophenyl ester of **6.8** (crude weight 120 mg). The product was dissolved in *N,N*-dimethylformamide (0.8 mL, anhydrous) and triethylamine (8 μ L, 0.06 mmol, anhydrous) were added. In a separate flask, *N-tert*-butyloxycarbonyl cystamine **6.9** (38.3 mg, 0.151 mmol) was dissolved in *N,N*-dimethylformamide (0.2 mL, anhydrous) and added to the above solution. The reaction was monitored by TLC (6:2:0.1 CH₂Cl₂/MeOH/NH₄OH) for the disappearance of the activated Pfp-ester (R_f = 0.5), at which point di-*tert*-butyldicarbonate (500 μ L of 1M solution) was added to quench unreacted **6.9**. The resulting mixture was stirred at rt for 2 h, evaporated to dryness, dissolved in H₂O and extracted with ether (3 x 2 mL) to remove *N,N*-di-*tert*-butyloxycarbonyl cystamine. The aqueous layer was evaporated to dryness to yield crude **6.10** (106 mg). Crude **6.10** was dissolved in a 20% TFA/CH₂Cl₂ solution (1 mL) and monitored by TLC (6:2:0.1 CH₂Cl₂/MeOH/NH₄OH) for the disappearance of **6.10** (R_f = 0.8), at which point (approx. 1 h) the mixture was evaporated to dryness and purified by reverse phase HPLC (CH₃CN/H₂O) to yield pure **6.11** as a colorless oil (34 mg, 0.050 mmol, 40%, R_f = 0.6). ¹H NMR (400 MHz, D₂O): δ 4.48 (dd, J = 7.9, 4.8 Hz, 1H), 4.30 (dd, J = 7.9, 4.5 Hz, 1H), 3.56-3.38 (m, 14H), 3.26-3.19 (m, 3H), 3.12 (q, J = 6.3 Hz, 4H), 2.89-2.84 (m, 3H), 2.37 (t, J = 6.3 Hz, 2H), 2.65 (d, J = 12.9 Hz, 1H), 2.40 (t, J = 3.2 Hz, 4H), 2.13 (t, J = 7.2 Hz, 2H), 1.73-1.41 (m, 8H), 1.32-1.28 (m, 2H). ¹³C NMR (125 MHz, D₂O): δ 181.7, 176.6, 174.7, 165.2, 69.5 (2), 69.3 (2), 68.4, 68.3, 62.0, 60.1, 55.3, 39.6, 37.8, 37.7, 36.3, 36.2, 36.1, 35.4, 33.6, 31.1, 28.2 (2), 27.9, 27.8, 27.6, 25.1. IR: 3292, 2926, 2867, 1703, 1692, 1678, 1123 cm⁻¹. HRMS (FAB): calcd. for C₂₈H₅₃N₆O₇S₃⁺ [M+H]⁺, 681.3138; found, 681.3132.

Compound 6.1. Compound **6.11** (9.1 mg, 0.013 mmol, 1.0 equiv.) and triethylamine (2 drops, anhydrous) were combined in *N,N*-dimethylformamide (1 mL, anhydrous). The resulting solution was added to **6.6** (10 mg, 0.028 mmol, 2.1 equiv.) and the reaction was stirred at rt and monitored by LC/MS for the disappearance of **6.11**. The reaction was no longer progressing after 18 h and it was evaporated to dryness. TLC (9:1 CH₂Cl₂/MeOH) indicated product with the expected R_f (green spot, R_f = 0.4). The crude mixture was HPLC purified (CH₃CN/H₂O) to yield pure **2** (2.2 mg, 2.5 μ mol, 43% brsm, 27% overall). ¹H NMR (400 MHz, D₂O): δ 4.48 (dd, J = 7.8, 5.1 Hz, 1H), 4.32 (dd, J = 7.8, 4.5 Hz, 1H), 3.95 (d, J = 3.1 Hz, 2H), 3.67-3.63 (m, 1H), 3.57-3.38 (m, 16H), 3.23-3.19 (m, 1H), 3.14-3.11 (m, 4H), 2.87 (dd, J = 13.1, 4.9 Hz, 1H), 2.78 (t, J = 6.1 Hz, 2H), 2.73 (t, J = 6.1 Hz, 2H), 2.66 (d, J = 13.0 Hz, 1H), 2.47-2.30 (m, 7H), 2.26-2.10 (m, 5H), 1.99 (dd, J = 16.5, 7.9 Hz, 1H), 1.93-1.87 (m, 1H), 1.68-1.42 (m, 8H), 1.33-1.23 (m, 2H). ¹⁹F NMR (376 MHz, D₂O): δ -86.6 (dddt, J = 259.0, 26.0, 12.8, 6.0 Hz, 1F), -88.6 (dm, J = 260.9 Hz, 1F). IR: 3274, 2922, 2851, 2285, 1734, 1650, 1642, 1631, 1489, 1441, 1260, 1099 cm⁻¹. HRMS (ESI): calcd. for C₃₈H₆₃N₆O₉S₃F₂⁺ [M+H]⁺, 881.3787; found, 881.3792.

N₃-BSA Pull-Down Assay

BSA (25 μ L of 8 mg/mL BSA solution), **6.1** (1 μ L of 1 mM solution), and PBS (74 μ L) were combined and reacted overnight at rt. N₃-BSA^a (16.7 μ L of 12 mg/mL solution), **6.1** (1 μ L of 1 mM solution), and PBS (82.3 μ L) were combined and reacted overnight. The following day the solutions were cleared of excess reagent by passage through a Bio-gel 6 size exclusion desalting column and the eluent was subsequently captured on NeutrAvidin from Pierce by incubating the eluent with resin (8 μ L) for 30 min. The flowthrough was collected and the NeutrAvidin was washed with three portions of 80 μ L of PBS. The elution was performed by incubating the washed NeutrAvidin with three portions of 80 μ L of 30 mM DTT for 30 min. All the eluents were concentrated to approximately 20 μ L with Microcon centrifugal devices (10 kDa MW cutoff) and analyzed by SDS-PAGE. The gel was stained with Sypro Orange according to the Bio-Rad specified procedure and the proteins were visualized on a Typhoon 9410 imaging system with excitation at 488 nm (450 V) and a 555 BP20 emission filter.

H2 Ras Pull-Down Assay

Protein (750 μ g) from a cell lysate^b generated from H2-Ras cells grown in the presence of absence of peracetylated N-azidoacetyl mannosamine was reacted with 10 μ M **6.1** in PBS overnight. Samples were purified from excess **6.1** by passage through a Bio-gel 6 size exclusion desalting column and captured on NeutrAvidin resin from Pierce (30 min incubation with 12 μ L NeutrAvidin). The flowthrough was collected, and the beads were washed ten times with 10 column volumes of PBS and eluted with three 30 minute incubations with 10 column volumes of 30 mM DTT. The collected flowthrough, washes, and elutions were concentrated to approximately 20 μ L, separated via SDS-PAGE, and visualized using the above procedure.

References

- (1) Kho, Y.; Kim, S. C.; Jiang, C.; Barma, D.; Kwon, S. W.; Cheng, J.; Jaunbergs, J.; Weinbaum, C.; Tamanoi, F.; Falck, J.; Zhao, Y. A tagging-via-substrate technology for detection and proteomics of farnesylated proteins. *Proc. Natl. Acad. Sci. U.S.A.* **2004**, *101*, 12479 -12484.
- (2) Dieterich, D. C.; Link, A. J.; Graumann, J.; Tirrell, D. A.; Schuman, E. M. Selective identification of newly synthesized proteins in mammalian cells using bioorthogonal noncanonical amino acid tagging (BONCAT). *Proc. Natl. Acad. Sci. U.S.A.* **2006**, *103*, 9482 -9487.

^a Prepared by Jeremy Baskin

^b Prepared by Sarah Hubbard

- (3) Hanson, S. R.; Hsu, T.-L.; Weerapana, E.; Kishikawa, K.; Simon, G. M.; Cravatt, B. F.; Wong, C.-H. Tailored glycoproteomics and glycan site mapping using saccharide-selective bioorthogonal probes. *J. Am. Chem. Soc.* **2007**, *129*, 7266-7267.
- (4) Boyce, M.; Carrico, I. S.; Ganguli, A. S.; Yu, S.-H.; Hangauer, M. J.; Hubbard, S. C.; Kohler, J. J.; Bertozzi, C. R. Metabolic cross-talk allows labeling of O-linked β -N-acetylglucosamine-modified proteins via the N-acetylgalactosamine salvage pathway. *Proc. Natl. Acad. Sci. U.S.A.* **2011**, *108*, 3141 -3146.
- (5) Nandi, A.; Sprung, R.; Barma, D. K.; Zhao, Y.; Kim, S. C.; Falck, J. R.; Zhao, Y. Global identification of O-GlcNAc-modified proteins. *Anal. Chem.* **2006**, *78*, 452-458.
- (6) Speers, A. E.; Adam, G. C.; Cravatt, B. F. Activity-based protein profiling in vivo using a copper(I)-catalyzed azide-alkyne [3 + 2] cycloaddition. *J. Am. Chem. Soc.* **2003**, *125*, 4686-4687.
- (7) Yates, J. R., 3rd Mass spectrometry and the age of the proteome. *J. Mass. Spectrom.* **1998**, *33*, 1-19.
- (8) Reinders, J.; Lewandrowski, U.; Moebius, J.; Wagner, Y.; Sickmann, A. Challenges in mass spectrometry-based proteomics. *Proteomics* **2004**, *4*, 3686-3703.
- (9) Aebersold, R.; Mann, M. Mass spectrometry-based proteomics. *Nature* **2003**, *422*, 198-207.
- (10) Qian, W.-J.; Jacobs, J. M.; Liu, T.; Camp, D. G.; Smith, R. D. Advances and challenges in liquid chromatography-mass spectrometry-based proteomics profiling for clinical applications. *Mol. Cell. Proteomics* **2006**, *5*, 1727-1744.
- (11) Arnau, J.; Lauritzen, C.; Petersen, G. E.; Pedersen, J. Current strategies for the use of affinity tags and tag removal for the purification of recombinant proteins. *Protein Expres. Purif.* **2006**, *48*, 1-13.
- (12) Baskin, J. M.; Prescher, J. A.; Laughlin, S. T.; Agard, N. J.; Chang, P. V.; Miller, I. A.; Lo, A.; Codelli, J. A.; Bertozzi, C. R. Copper-free click chemistry for dynamic in vivo imaging. *Proc. Natl. Acad. Sci. U.S.A.* **2007**, *104*, 16793 -16797.
- (13) Green, N. M. Avidin. In; Academic Press, 1975; Vol. 29, pp. 85-133.
- (14) Leitner, A.; Lindner, W. Chemistry meets proteomics: The use of chemical tagging reactions for MS-based proteomics. *Proteomics* **2006**, *6*, 5418-5434.
- (15) Fauq, A. H.; Kache, R.; Khan, M. A.; Vega, I. E. Synthesis of acid-cleavable light isotope-coded affinity tags (ICAT-L) for potential use in proteomic expression profiling analysis. *Bioconjugate Chem.* **2006**, *17*, 248-254.
- (16) van der Veken, P.; Dirksen, E. H. C.; Ruijter, E.; Elgersma, R. C.; Heck, A. J. R.; Rijkers, D. T. S.; Slijper, M.; Liskamp, R. M. J. Development of a novel chemical probe for the selective enrichment of phosphorylated serine- and threonine-containing peptides. *ChemBioChem* **2005**, *6*, 2271-2280.
- (17) Lin, W. C.; Morton, T. H. Two-step affinity chromatography. Model systems and an example using biotin-avidin binding and a fluoridolyzable linker. *J. Org. Chem.* **1991**, *56*, 6850-6856.
- (18) Ahmed, A. R.; Olivier, G. W.; Adams, G.; Erskine, M. E.; Kinsman, R. G.; Branch, S. K.; Moss, S. H.; Notarianni, L. J.; Pouton, C. W. Isolation and partial purification of a melanocyte-stimulating hormone receptor from B16 murine melanoma cells. A

- novel approach using a cleavable biotinylated photoactivated ligand and streptavidin-coated magnetic beads. *Biochem. J.* **1992**, *286*, 377-382.
- (19) Williams, S. J.; Hekmat, O.; Withers, S. G. Synthesis and testing of mechanism-based protein-profiling probes for retaining endo-glycosidases. *ChemBioChem* **2006**, *7*, 116-124.
- (20) Hekmat, O.; Kim, Y.-W.; Williams, S. J.; He, S.; Withers, S. G. Active-site peptide “fingerprinting” of glycosidases in complex mixtures by mass spectrometry. *J. Biol. Chem.* **2005**, *280*, 35126 -35135.
- (21) Gartner, C. A.; Elias, J. E.; Bakalarski, C. E.; Gygi, S. P. Catch-and-release reagents for broadscale quantitative proteomics analyses. *J. Proteome Res.* **2007**, *6*, 1482-1491.
- (22) Verhelst, S. H. L.; Fonović, M.; Bogyo, M. A mild chemically cleavable linker system for functional proteomic applications. *Angew. Chem. Int. Ed.* **2007**, *46*, 1284-1286.
- (23) Olejnik, J.; Sonar, S.; Krzymańska-Olejnik, E.; Rothschild, K. J. Photocleavable biotin derivatives: A versatile approach for the isolation of biomolecules. *Proc. Natl. Acad. Sci. U.S.A.* **1995**, *92*, 7590 -7594.
- (24) Piggott, A. M.; Karuso, P. Synthesis of a new hydrophilic o-nitrobenzyl photocleavable linker suitable for use in chemical proteomics. *Tetrahedron Lett.* **2005**, *46*, 8241-8244.
- (25) Kim, H.-Y. H.; Tallman, K. A.; Liebler, D. C.; Porter, N. A. An azido-biotin reagent for use in the isolation of protein adducts of lipid-derived electrophiles by streptavidin catch and photorelease. *Mol. Cell Proteomics* **2009**, *8*, 2080-2089.
- (26) Speers, A. E.; Cravatt, B. F. A tandem orthogonal proteolysis strategy for high-content chemical proteomics. *J. Am. Chem. Soc.* **2005**, *127*, 10018-10019.
- (27) Wilbur, D. S.; Hamlin, D. K.; Vessella, R. L.; Stray, J. E.; Buhler, K. R.; Stayton, P. S.; Klumb, L. A.; Pathare, P. M.; Weerawarna, S. A. Antibody fragments in tumor pretargeting. Evaluation of biotinylated Fab colocalization with recombinant streptavidin and avidin. *Bioconjugate Chem.* **1996**, *7*, 689-702.
- (28) Han, J. A procedure for quantitative determination of tris(2-carboxyethyl)phosphine, an odorless reducing agent more stable and effective than dithiothreitol. *Anal. Biochem.* **1994**, *220*, 5-10.
- (29) Gilbert, H. F. Thiol/disulfide exchange equilibria and disulfide bond stability. *Meth. Enzymol.* **1995**, *251*, 8-28.
- (30) Szychowski, J.; Mahdavi, A.; Hodas, J. J. L.; Bagert, J. D.; Ngo, J. T.; Landgraf, P.; Dieterich, D. C.; Schuman, E. M.; Tirrell, D. A. Cleavable biotin probes for labeling of biomolecules via azide-alkyne cycloaddition. *J. Am. Chem. Soc.* **2010**, *132*, 18351-18360.
- (31) Pangborn, A. B.; Giardello, M. A.; Grubbs, R. H.; Rosen, R. K.; Timmers, F. J. Safe and convenient procedure for solvent purification. *Organometallics* **1996**, *15*, 1518-1520.
- (32) Korshun, V. A.; Pestov, N. B.; Nozhevnikova, E. V.; Prokhorenko, I. A.; Gontarev, S. V.; Berlin, Y. A. Reagents for multiple non-radioactive labelling of oligonucleotides. *Synthetic Comm.* **1996**, *26*, 2531-2547.

- (33) Williams, S. J.; Hekmat, O.; Withers, S. G. Synthesis and testing of mechanism-based protein-profiling probes for retaining endo-glycosidases. *ChemBioChem* **2006**, *7*, 116-124.
- (34) Wang, C.; Leffler, S.; Thompson, D. H.; Hrycyna, C. A. A general fluorescence-based coupled assay for S-adenosylmethionine-dependent methyltransferases. *Biochem. Biophys. Res. Commun.* **2005**, *331*, 351-356.

Chapter 7

Towards a Tetrafluorinated Cyclooctyne

The Benefits of a Highly Reactive Cyclooctyne

The addition of two fluorine atoms at the propargylic position of a cyclooctyne, as in DIFO (**3.1**), caused a 60x rate enhancement of the 1,3-dipolar cycloaddition with azides.¹ While DIFO did not perform well in mice,² the first direct imaging experiment with bioorthogonal chemistry *in vivo* was achieved using Cu-free click chemistry with DIFO. DIFO-Alexa Fluor conjugates (DIFO-488, DIFO-555, etc.) successfully enabled the visualization of spatiotemporal changes in cell-surface glycosylation in *Caenorhabditis elegans*³ and in developing zebrafish⁴ (Figure 7.1). Using peracetylated N-azidoacetyl galactosamine (Ac₄GalNAz) as a metabolic label, glycoproteins were imaged during three stages of *C. elegans* development, and significant labeling was observed in the pharynx, vulva, and anus.³ In a similar manner, GalNAz-labeled glycoproteins in zebrafish embryos were imaged between 60 and 73 hours post fertilization (hpf), and dynamic labeling was monitored in the pectoral fins, olfactory pit, and jaw. Glycan trafficking between 60 and 72 hpf was further analyzed through pulse-chase experiments with spectrally-distinct DIFO conjugates.⁴ Glycans expressed during earlier stages of zebrafish embryogenesis could be detected by direct microinjection of GalNAz or the advanced metabolite UDP-GalNAz into the yolk of single-cell embryos. Using this technique, azidoglycans could be imaged as early as 7 hpf.⁵ These results could only be achieved with DIFO due to its rapid reaction kinetics, showcasing the benefits of a large second-order rate constant and leading us to imagine the opportunities available if an even more reactive cyclooctyne were to be synthesized.

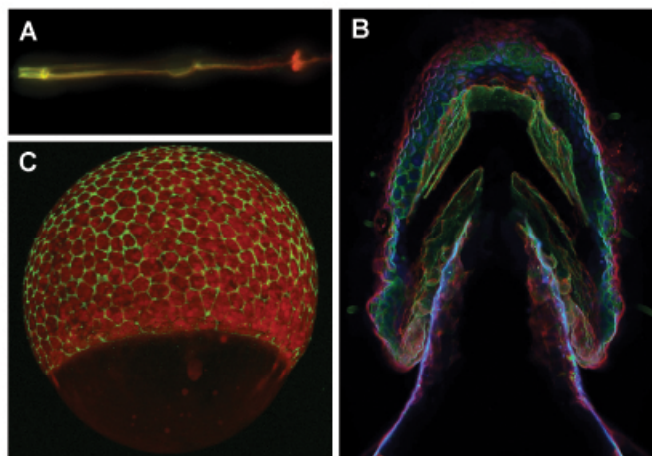


Figure 7.1. DIFO-Alexa Fluor conjugates label azides in higher organisms. A. *C. elegans* were grown in the presence of Ac₄GalNAz and reacted with DIFO-488 (100 μM) followed by DIFO-568 (100 μM) and imaged at their adult stage. B. Zebrafish embryos were metabolically labeled with Ac₄GalNAz from 3 to 60 hours post fertilization (hpf). The fish were sequentially incubated with 100 μM DIFO conjugated to Alexa Fluor 647 (DIFO-647, 60-61 hpf), DIFO-488 (62-63 hpf) and DIFO-555 (72-73 hpf) and imaged by confocal microscopy. During periods in which the zebrafish were not being labeled with DIFO, the fish were bathed in a solution of Ac₄GalNAz. Blue = DIFO-647, Green = DIFO-488, Red = DIFO-555. C. Zebrafish embryos were injected with UDP-GalNAz and a rhodamine-dextran tracer dye. At 7 hpf, the embryos were incubated with DIFO-488 (100 μM) for 1 h and imaged by confocal microscopy. Green = DIFO-488, Red = rhodamine-dextran.

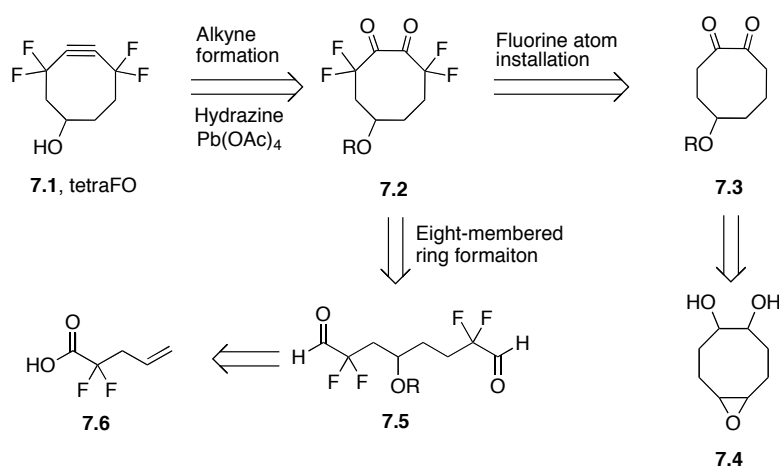
Design of a More Reactive Cyclooctyne

A logical strategy for further increasing the second-order rate constant of the cycloaddition between azides and cyclooctynes is to add two additional fluorine atoms to DIFO to result in a tetrafluorinated cyclooctyne (tetraFO, **7.1**, Scheme 7.1). We anticipated that the additional two fluorine atoms would further decrease the energy of the LUMO levels and dramatically increase the rate of the cycloaddition. Aided by DFT calculations, Houk and coworkers anticipated that this compound would be 25 times more reactive than DIFO.⁶

While a tetrafluorinated cyclooctyne was straightforward to propose, it posed a serious synthetic challenge. There are three key components in the synthesis of fluorinated cyclooctynes: strained alkyne formation, fluorine atom installation, and eight-membered ring formation. All syntheses require the former, which is generally the last hurdle within the preparation of a cyclooctyne; however, one of the other challenges can often be avoided by choosing a starting material, which already contains either the fluorine atoms or the eight-membered ring scaffold. For the synthesis of tetraFO, we envisioned alkyne formation could be achieved from tetrafluorinated diketone **7.2** by treatment with

hydrazine and lead tetraacetate (Scheme 7.1).⁷ Two synthetic pathways to diketone **7.2**, one necessitating fluorine group installation and the other requiring eight-membered ring formation (Scheme 7.1), were pursued. The installation of four fluorine atoms into diketone **7.3** could be achieved through alpha fluorination methods similar to those employed in the synthesis of DIFO,¹ and diketone **7.3** could be taken back to known cyclooctane diol **7.4**.⁸ Alternatively, compound **7.2** could be formed through the Pinacol coupling of tetrafluorinated dialdehyde **7.5**,^{9,10,11,12} which could be synthesized from known 2,2-difluoro-4-enoic acid (**7.6**).^{13,14}

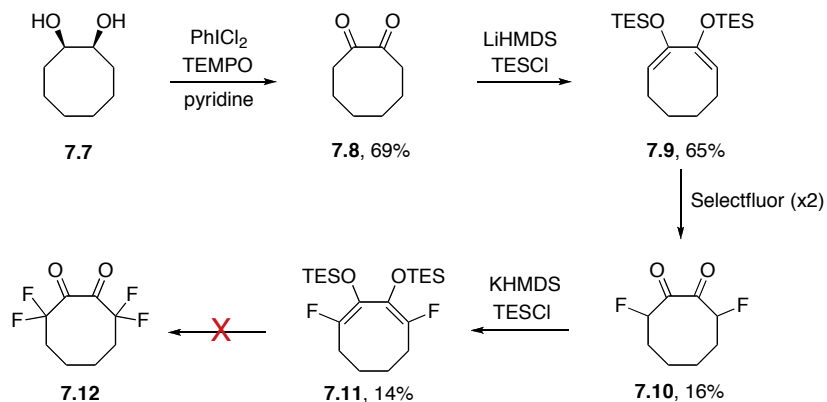
Scheme 7.1. Two approaches to tetrafluorinated cyclooctyne.



Initial Synthetic Attempts Toward TetraFO

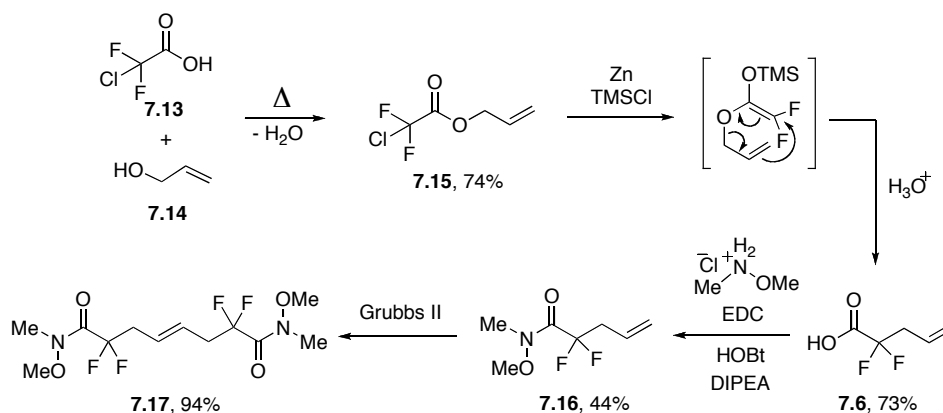
The viability of the fluorine installation route (**7.4** to **7.2**) was first assessed using the model compound 1,2-cyclooctadione (**7.8**) due to the commercial availability of the precursor *cis*-1,2-cyclooctanediol (**7.7**, Scheme 7.2). Oxidation of **7.7** to 1,2-cyclooctadione was achieved by TEMPO with iodobenzene dichloride as a stoichiometric oxidant.¹⁵ Bis(silyl enol ether) **7.9** was isolated by double deprotonation of **7.8** with LiHMDS followed by reaction with triethylsilyl chloride. When **7.9** was twice subjected to Selectfluor, low yields of difluorinated diketone **7.10** were isolated as a mixture of diastereomers and hydrates. This diketone could again be converted to the bis(silyl enol ether) by deprotonation with KHMDS and subsequent reaction with triethylsilyl chloride to yield **7.11**. Unfortunately, attempts to install two additional fluorine atoms on compound **7.11** to yield model tetrafluorinated diketone **7.12** proved unsuccessful. An array of fluorine peaks were apparent in the ¹⁹F-NMR spectrum when **7.11** was treated with Selectfluor.

Scheme 7.2. Efforts toward 3,3,8,8-tetrafluorocycloocta-1,2-dione.



With the fluorine installation strategy appearing difficult, we directed our attention toward the synthesis of tetrafluorinated dialdehyde **7.5**. The fluorine source for **7.5** was chlorodifluoroacetic acid (**7.13**), which upon esterification with allyl alcohol (**7.14**) gave **7.15** (Scheme 7.3). Compound **7.15** underwent a Reformatsky Claisen rearrangement to yield 2,2-difluoropent-4-enoic acid (**7.6**).¹³ Acid **7.6** was converted to Wienreb amide **7.16** using standard coupling conditions.¹⁶ Dimerization through an olefin cross metathesis reaction afforded compound **7.17**, which contained all the atoms necessary for the core of tetraFO.

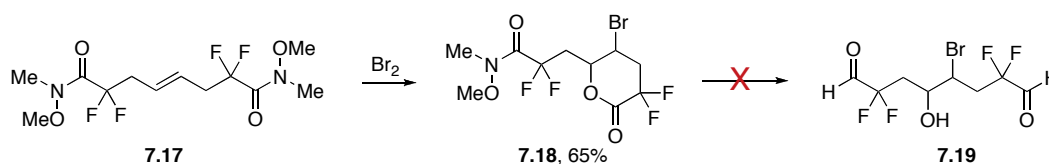
Scheme 7.3. Synthesis of tetrafluorinated alkene **7.17**.



The next step toward dialdehyde **7.5** was functionalization of the internal olefin so that a chemical handle was present for the conjugation of probe moieties, but the olefin in compound **7.17** proved to be frustratingly unreactive. An exhaustive list of hydroboration reagents yielded no promising results. Additionally, oxymercuration and thiol-ene chemistry did not result in desired product. Direct acid-catalyzed addition of water only gave a product with hydrolyzed amide bonds. Even more robust olefin functionalization methods such as epoxidation with mCPBA and dihydroxylation with OsO_4 did not yield

significant amounts of desired product. The only reagent that appeared sufficiently electrophilic for reaction with the olefin in **7.17** was bromine (Scheme 7.4). Treatment of **7.17** with bromine yielded bromolactone **7.18** in 70% yield. While this was not the anticipated transformation, dialdehyde **7.19** seemed accessible from **7.18**. Unfortunately, all attempts to reduce the lactone and Weinreb amide in **7.18** yielded only complex mixtures of products, most likely due to side reactivity of the resulting highly electrophilic aldehydes.

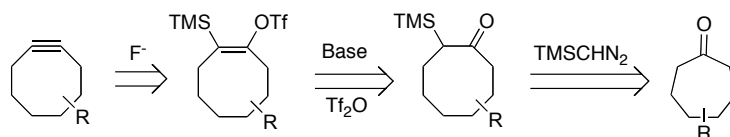
Scheme 7.4. Bromination of **7.17** to yield bromolactone **7.18**.



New Synthetic Strategy Toward TetraFO

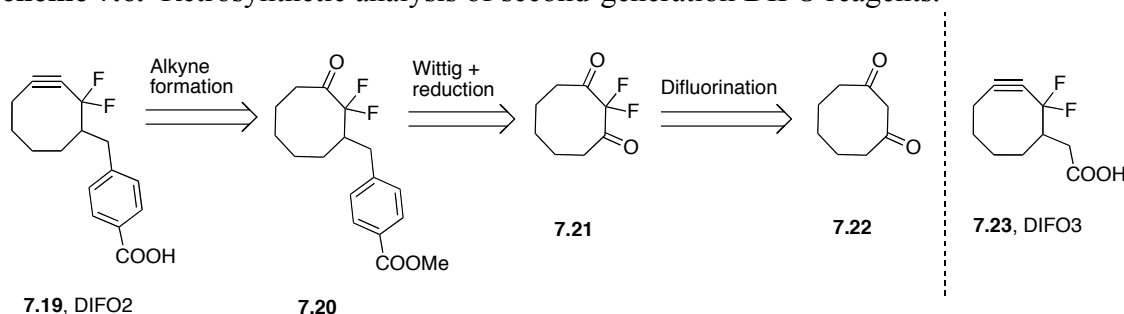
From the above results, neither synthetic pathway toward **7.2** appeared promising. At about this time, a paper by Moebius and Kingsbury reporting the $\text{Sc}(\text{OTf})_3$ catalyzed homologation of cycloalkanones with substituted diazomethanes inspired us to consider a ring expansion strategy.¹⁷ The options for commercially available cyclooctane containing compounds are rather limited, and the selection of starting materials would be greater if cycloheptane compounds could also be considered. A synthesis relying on a key ring-expansion became even more attractive when we recognized it could be coupled to a fluoride-mediated alkyne formation, similar to that commonly used for benzyne,¹⁸ if trimethylsilyldiazomethane (TMSCHN_2) was employed for the homologation reaction. Scheme 7.5 outlines the general retrosynthetic analysis for formation of a cyclooctyne by ring-expansion with TMSCHN_2 . The main challenge using this sequence would be maintaining the somewhat labile TMS group alpha to the ketone.¹⁹ Homologations with TMSCHN_2 are well-precedented;^{20,21,22} even for the synthesis of cyclooctynes.^{23,24} However, the TMS group was not retained for these syntheses, as trimethylsilyl diazomethane is usually chosen as a diazomethane surrogate on the basis of safety considerations and not because the silyl functionality is desired.^{25,26} At the conclusion of this work, Li and coworkers reported the homologation of aldehydes with TMSCHN_2 and further utilized the TMS functionality.²⁷

Scheme 7.5. A homologation strategy for the mild synthesis of cyclooctyne.



A homologation strategy could be key to solving two of the main challenges in cyclooctyne synthesis: eight-membered ring formation and strained-alkyne formation. However, for tetraFO, the task of introducing four fluorine atoms into a molecule was still daunting. In the synthesis of DIFO, each fluorine atom was installed in a two-step procedure where silyl enol ether formation was followed by treatment with Selectfluor. This was a tedious process and resulted in very low overall yields of DIFO. Work towards a more facile synthesis of DIFO yielded not only two new DIFO reagents (**7.19** and **7.23**, Scheme 7.6) in good overall yield, but a robust method for the simultaneous installation of two fluorine atoms in a 1,3-diketone.²⁸

Scheme 7.6. Retrosynthetic analysis of second-generation DIFO reagents.

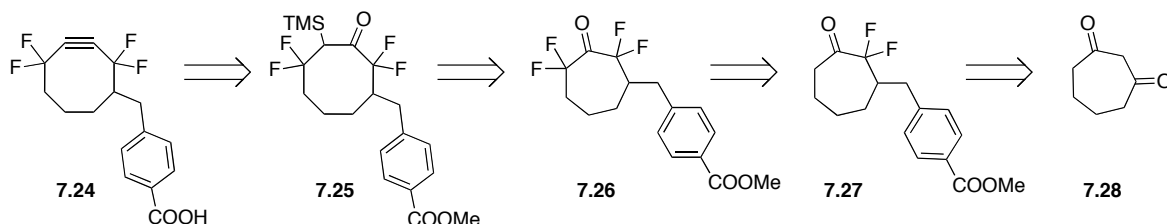


Synthesis of TetraFO using a Ring-Expansion Strategy

The retrosynthetic analysis of DIFO2 is shown in Scheme 7.6. This synthetic pathway combined with the homologation strategy outlined in Scheme 7.5, were key stepping-stones for the new approach toward tetraFO. The strained alkyne of DIFO2 was formed from ketone **7.20**. The linker group of **7.20** was installed by a mono-Wittig reaction on 2,2-difluoro-1,3-cyclooctadione (**7.21**). Compound **7.21** was obtained in high yield from known 1,3-cyclooctadione (**7.22**) by treatment with Cs_2CO_3 and Selectfluor. The synthesis of DIFO2 was much more facile than that of DIFO, but was limited by the scale in which 1,3-cyclooctadione could be produced due to the need for Na metal in the first step. Notably, since the report of DIFO2 there have been alternative methods developed for the preparation of 1,3-cyclooctadione, which are more suitable for large-scale synthesis.²⁹ Fortunately, 1,3-cycloheptadione, the requisite starting material if a homologation strategy was pursued, was readily available on large scales using robust, safe chemistry.³⁰

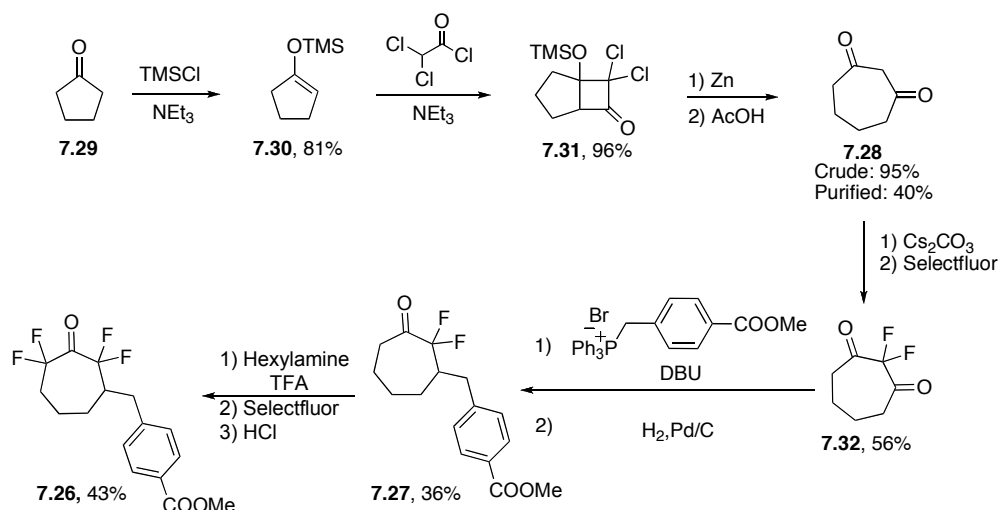
Scheme 7.7 depicts the proposed route to tetraFO **7.24** starting from 1,3-cycloheptadione (**7.28**). Alkyne formation could be achieved from **7.25** by vinyl triflate formation and treatment with a fluoride source. Compound **7.25** could come from the key homologation reaction of **7.26** and TMSCHN_2 . Tetrafluorinated ketone **7.26** could arise from compound **7.27**, which should be readily available following a sequence similar to that employed for the synthesis of DIFO2.

Scheme 7.7. Retrosynthetic analysis of tetraFO **7.24** by a homologation strategy.



1,3-Cycloheptadione (**7.28**) was prepared from cyclopentanone (**7.29**) by silyl enol ether formation (**7.30**) followed by a [2+2] cycloaddition reaction with *in situ* generated 2,2-dichloro ketene. The resulting bicycle **7.31** was dechlorinated and opened to desired diketone **7.28** according to previously reported procedures.³⁰ Purification of **7.28** proved to drastically decrease the yield and the 1,3-cycloheptadione was often used crude. Difluorination was accomplished through treatment with Cs_2CO_3 followed by Selectfluor. A mono-Wittig reaction between 2,2-difluoro-1,3-cycloheptadione (**7.32**) and (4-(methoxycarbonyl)benzyl)triphenylphosphonium bromide followed by hydrogenation of the resulting alkene yielded difluorinated ketone **7.27**. Installation of the final two fluorine atoms proceeded through imine formation with hexylamine and treatment with Selectfluor.³¹ The success of the second fluorination resulted in installation of all the fluorine atoms in only two synthetic steps (Scheme 7.8). At this point, tetraFO appeared only a homologation away.

Scheme 7.8. Synthesis of tetrafluorinated ketone **7.26**.



Homologation of ketone **7.26** proved to be a difficult synthetic transformation. Not only did TMSCHN₂ in combination with a variety of Lewis acids not afford desired compound **7.25**, but other diazo compounds also proved ineffective at facilitating the ring expansion (see Scheme 7.9 and Table 7.1).

Scheme 7.9. Attempted homologation of ketone **7.26**.

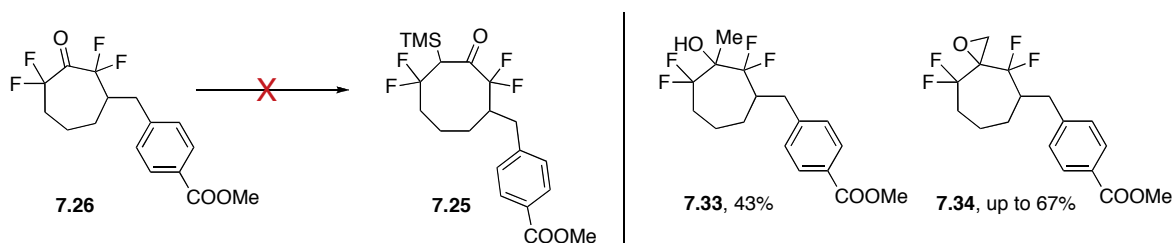


Table 7.1. Selected homologation attempts.

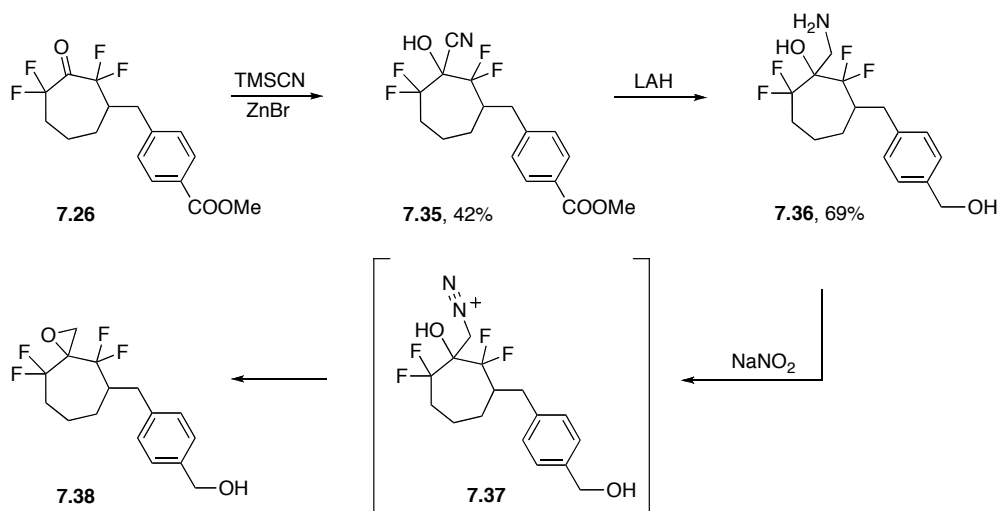
Entry	Diazo species	Lewis acid	Reaction conditions	Result
1	TMSCHN ₂	AlMe ₃	-78 °C, 3 min	Compound 7.33
2	TMSCHN ₂	BF ₃ ·OEt ₂	-78 °C, 2 h	Epoxide 7.34
3	TMSCHN ₂	MAD	0 °C, 2 h	Epoxide 7.34
4	TMSCHN ₂	TMSOTf	0 °C, 15 min	Epoxide 7.34
5	TMSCHN ₂	Sc(OTf) ₃	0 °C, 30 min	Epoxide 7.34
6	N ₂ CHCOOEt	AlMe ₃	Rt, overnight	No reaction
7	N ₂ CHCOOEt	BF ₃ ·OEt ₂	Rt, overnight	No reaction
8	N ₂ CHCOOEt	Sc(OTf) ₃	Rt, overnight	No reaction
9	N ₂ CHCOOEt	BF ₃ ·OEt ₂	60 °C, 1 week	Unknown
10	TMSCLiN ₂	N/A	40 °C, overnight	Epoxide 7.34
11	N ₂ CLiCOOEt	N/A	40 °C, 2 h	Decomposition
12	TMSCHN ₂	None	40 °C, overnight	Diazocompound (large IR stretch at 2090 nm)
13	TMSCHN ₂	None	Microwave, 10 min	Diazocompound
14	CH ₂ N ₂	AlMe ₃	0 °C, 1 h	Epoxide 7.34

The reaction of tetrafluorinated ketone **7.26** with trimethylsilyl diazomethane in the presence of a variety of Lewis acids favored epoxide formation (**7.34**) over homologation (Table 7.1, entries 2-5),^{17,20,21,26,32} the exception being when trimethylaluminum was employed as a Lewis acid. Instead of facilitating epoxide formation, AlMe₃ resulted in methyl addition to yield tertiary alcohol **7.33** (entry 1). Ethyldiazoacetate (N₂CHCOOEt), a diazo species commonly employed for homologation reactions when epoxide addition is competing with the desired transformation,^{33,34,35} proved unreactive under standard homologation conditions. Upon forcing conditions where **7.26** was combined with ethyldiazoacetate, unidentifiable products were produced. Further attempts at homologation with the more nucleophilic species TMSCLiN₂ (entry 10)³⁶ and

$\text{N}_2\text{CLiCOOEt}$ (entry 11)^{37,38} or TMSCHN_2 at elevated temperatures (entries 12-13) did not yield desired product. Lastly, even diazomethane yielded epoxide **7.33** (entry 14).

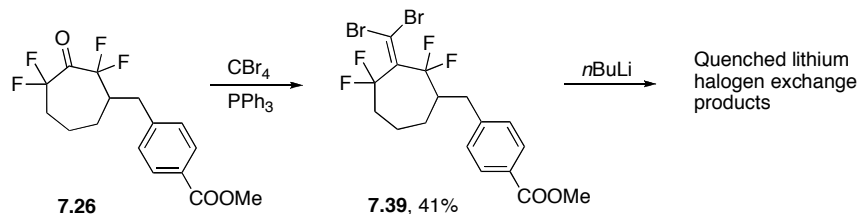
After many homologation attempts with diazo species, other ways to effect the same transformation were attempted. The desired diazo intermediate could also be formed though a multistep procedure. Cyanohydrin **7.35** was obtained through treatment of **7.26** with trimethylcyanide and zinc bromide. Reduction of **7.35** yielded amino-alcohol **7.36** and oxidation of **7.36** with NaNO_2 (Scheme 7.10) should then promote a Tiffeneau-Demjanov rearrangement.^{39,40,41} However, when this sequence was performed, we found that epoxide product **7.38** was again produced, suggesting the initial nucleophilic attack (which is often the rate-determining step in homologation reactions) was proceeding as desired and ring-expansion of **7.37** must not be a favorable process.

Scheme 7.10. Tiffeneau-Demjanov rearrangement of tetrafluorinated ketone **7.26**.



Another possible ring-expansion/alkyne formation strategy was the insertion of a carbene generated from an exocyclic olefin in a Corey-Fuchs type transformation (Scheme 7.11).⁴² Toward this end, tetrafluorinated ketone **7.26** was converted to **7.39** by treatment with CBr_4 and PPh_3 . Lithium halogen exchange of the dibromoalkene appeared to proceed but only protonated exocyclic olefin products were isolated.⁴³

Scheme 7.11. Corey-Fuchs alkyne formation from **7.26**.



Tetrafluorinated cyclooctyne **7.24** still remains elusive. Its possible that conditions for the desired homologation exist; however, based on the above results it seems unlikely that this transformation will proceed in high yield, and we directed our attention toward another reactive cyclooctyne containing a difluoro group and a fused aryl ring.

Materials and Methods

General Experimental Procedure

All chemical reagents were purchased from Sigma-Aldrich, Acros, and TCI and used without purification unless noted otherwise. Anhydrous DMF and MeOH were purchased from Aldrich or Acros in sealed bottles; all other solvents were purified as described by Pangborn *et al.*⁴⁴ In all cases, solvent was removed by reduced pressure with a Buchi Rotovapor R-114 equipped with a Welch self-cleaning dry vacuum. Products were further dried by reduced pressure with an Edwards RV5 high vacuum. Thin layer chromatography was performed with EMD 60 Å silica gel plates. Flash chromatography was performed using Silicycle® 60 Å 230-400 mesh silica. All ¹H, ¹³C, and ¹⁹F NMR spectra are reported in ppm and referenced to solvent peaks (¹H and ¹³C). Spectra were obtained on Bruker AV-300, AVQ-400, AVB-400, DRX-500, AV-500, or AV-600 instruments. Electron impact (EI) and electrospray ionization (ESI) mass spectra were obtained from the UC Berkeley Mass Spectrometry Facility.

Experimental Procedures

Cyclooctane-1,2-dione (7.8).¹⁵ A mixture containing 1,2-*cis*-octanediol **7.7** (735 mg, 5.10 mmol, 1.0 equiv.), (2,2,6,6-Tetramethylpiperidin-1-yl)oxyl (TEMPO, 137 mg, 0.878 mmol, 0.17 equiv.), iodobenzene dichloride¹⁵ (3.57 g, 13.0 mmol, 2.6 equiv.) and pyridine (2.6 mL, 32 mmol, 6.3 equiv.) in CH₂Cl₂ (50 mL, anhydrous) was heated to 50 °C overnight. The following morning the reaction mixture was diluted with CH₂Cl₂ (200 mL) and washed with sat. sodium sulfite (150 mL), 1M HCl (150 mL) and brine (200 mL). The organics were dried, decanted, and evaporated to dryness. The crude product was purified by on a Biotage 40M column using a hexane/CH₂Cl₂ solvent system (1:1 then 1:2 hexane/CH₂Cl₂) to yield 495 mg **7.8** (3.54 mmol, 69%). R_f = 0.6 in hexane/CH₂Cl₂. ¹H NMR (500 MHz, CDCl₃): δ 2.56-2.53 (m, 2H), 1.74 (dd, *J* = 3.7, 2.6 Hz, 2H), 1.60-1.57 (m, 2H). ¹³C NMR (125 MHz, CDCl₃): δ 210.2, 40.1, 26.5, 21.3.

(1E,3E)-2,3-Bis(triethylsilyloxy)cycloocta-1,3-diene (7.9). Lithium bis(trimethylsilyl)amide (4.8 mL of 1M in THF solution, 4.8 mmol, 2.1 equiv.) was further diluted in THF (28 mL, anhydrous) and cooled to -78 °C. 1,2-cyclooctadione (315 mg, 2.25 mmol, 1.0 equiv.) was dissolved in THF (8 mL, anhydrous) and added to the solution of base over 1 h. Upon addition of all diketone, the mixture was stirred for an additional 20 min at -78 °C, at which point triethylsilyl chloride (1.2 mL, 7.1 mmol, 3.2 equiv.) was added. The mixture was stirred 10 additional minutes at -78 °C, and warmed to rt. After

stirring 1.5 h at rt, the reaction was evaporated to dryness and the crude product was purified by silica gel chromatography on a Biotage 40M column with a hexane/ethyl acetate solvent system. This procedure yielded pure bis(silyl enol ether) **7.9** (540 mg, 1.5 mmol, 65%). $R_f = 0.3$ in hexane. $^1\text{H NMR}$ (400 MHz, CDCl_3): δ 5.08 (t, $J = 8.3$ Hz, 2H), 2.12 (bs, 2H), 1.96 (bs, 2H), 1.67 (bs, 2H), 1.27-1.11 (m, 2H), 0.98 (t, $J = 7.8$ Hz, 18H), 0.67 (q, $J = 7.8$ Hz, 12H). $^{13}\text{C NMR}$ (100 MHz, CDCl_3): δ 146.7, 112.2, 26.2, 25.0, 7.0, 5.2. HRMS (EI): cald. For $\text{C}_{20}\text{H}_{40}\text{O}_2\text{Si}_2^+ [\text{M}]^+$, 368.2567; found, 368.2575.

3,8-Difluorocyclooctane-1,2-dione (7.10). Bis(silyl enol ether) **7.9** (373 mg, 1.01 mmol, 1.0 equiv.) was dissolved in acetonitrile (70 mL, anhydrous). Selectfluor (1.62 g, 4.58 mmol, 4.5 equiv.) was added and the reaction was stirred at rt overnight. The reaction was monitored by TLC for disappearance of **7.9** ($R_f = 1$ in 2:1 hexane/ethyl acetate). When no more **7.9** was present the reaction mixture was quenched with water (100 mL) and extracted with ether (4 x 150 mL). The organics were combined, dried, decanted, and evaporated to dryness. The crude product was purified on a Biotage 40M silica gel column with a hexane/ethyl acetate solvent system (8:1 to 1:1). This procedure resulted in 28 mg of **7.10** (0.16 mmol, 16%) as a mixture of diastereomers and hydrates. $R_f = 0.2$ in 2:1 hexane/ethyl acetate. $^1\text{H NMR}$ (400 MHz, CDCl_3): δ 5.42 (ddd, $J = 46.4, 7.5, 3.8$ Hz, 1H), 5.23 (ddd, $J = 47.5, 8.3, 3.5$ Hz, 2H minor), 4.78 (ddd, $J = 44.9, 8.4, 3.1$ Hz, 1H), 2.58-2.39 (m, 1H), 2.23-1.98 (m, 1H, 2H minor), 1.95-1.80 (m, 1H, 2H minor), 1.75-1.45 (m, 2H, 2H minor), 1.36-1.03 (m, 3H, 2H minor). $^{19}\text{F NMR}$ (376 MHz, CDCl_3): δ -189.81 (ddd, $J = 45, 33, 12$ Hz, 1F), -193.36 - -193.57 (m, 2F minor), -195.19 (ddd, $J = 41, 28, 10$ Hz, 1F). HRMS (EI): cald. For $\text{C}_8\text{H}_{10}\text{O}_2\text{F}_2^+ [\text{M}]^+$, 176.0649; found, 176.0650.

((1Z,2Z)-3,8-difluorocycloocta-2,8-diene-1,2-diyl)bis(oxy)bis(trimethylsilane) (7.11). Potassium bis(trimethylsilyl)amide (0.7 mL of a 0.5 M solution in toluene, 0.35 mmol, 2.1 equiv.) was further diluted in THF (2.0 mL, anhydrous) and cooled to -78°C . Difluorodiketone **7.10** (30 mg, 0.17 mmol, 1.0 equiv.) was diluted in THF (1.0 mL, anhydrous) and added to the solution of base over 1 h. After an addition 2 h at -78°C , triethylsilyl chloride (0.10 mL, 0.59 mmol, 3.5 equiv.) was added. The mixture was stirred at -78°C for 45 min, warmed to rt, and stirred an additional 1.5 h at rt at which point the mixture was evaporated to dryness. The crude product was purified by silica gel chromatography with hexanes to yield 5 mg of **7.11** (0.012 mmol, 14%). $^1\text{H NMR}$ (500 MHz, CDCl_3): δ 2.50-2.42 (m, 2H), 2.28-2.16 (m, 2H), 1.73 (t, $J = 8.7$ Hz, 2H), 1.33 (t, $J = 10.7$ Hz, 2H), 0.97 (t, $J = 7.9$ Hz, 18H), 0.66 (q, $J = 7.9$ Hz, 12H). $^{19}\text{F NMR}$ (376 MHz, C_6D_6): δ -119.92 (dd, $J = 33, 20$ Hz, 2F).

Allyl 2-chloro-2,2-difluoroacetate (7.15).¹³ Chlorodifluoroacetic acid (**7.12**, 50 mL, 0.57 mol, 1.0 equiv.) and allyl alcohol (**7.14**, 52 mL, 0.77 mol, 1.3 equiv.) and hexanes (75 mL) were combined and heated to 90°C in a flask equipped with a Dean-Stark apparatus. When water ceased to be collected (~ 5 h), the product was purified by fractional distillation at ambient temperature with the product distilling at $\sim 100^\circ\text{C}$. This procedure resulted in 50 mL of pure **7.15** (72 g, 0.42 mol, 74%). $^1\text{H NMR}$ (500 MHz, CD_3CN): δ 6.00 (ddt, $J = 16.4, 10.7, 5.9$ Hz, 1H), 5.45 (dd, $J = 17.2, 1.2$ Hz, 1H), 5.37 (dd, $J = 10.5,$

0.9 Hz, 1H), 4.86 (d, $J = 5.9$ Hz, 2H). ^{13}C NMR (150 MHz, CDCl_3): δ 159.3 (t, $J = 35$ Hz), 129.8, 120.8, 117.1 (t, $J = 301$ Hz), 68.8. ^{19}F NMR (565 MHz, CDCl_3): δ -68.1 (3F).

2,2-Difluoropent-4-enoic acid (7.6).¹³ Allyl ester **7.15** (20.8 g, 124 mmol, 1.0 equiv.) was dissolved in acetonitrile (100 mL, anhydrous). Zinc (9.9 g, 150 mmol, 1.2 equiv.) and trimethylsilyl chloride (22 mL, 174 mmol, 1.4 equiv.) were added and the mixture was heated to reflux for 3 d. After 3 d, the reaction was still not complete and more zinc (2.0 g) and trimethylsilyl chloride (5 mL) was added. After an additional 2 d at reflux, the mixture was cooled to rt and quenched with 50 g of wet silica. This slurry was filtered and the filtrate was purified by fractional distillation to yield ~12 g of product (90 mmol, 73%). ^1H NMR (400 MHz, CDCl_3): δ 5.74 (ddt, $J = 17.3, 10.2, 7.1$ Hz, 1H), 5.28-5.22 (m, 2H), 2.82 (td, $J = 16.8, 7.1$ Hz, 2H). ^{13}C NMR (125 MHz, CDCl_3): δ 166.3 (t, $J = 32$ Hz), 128.5 (t, $J = 6$ Hz), 122.3, -116.8 (t, $J = 249$ Hz), 39.6 (t, $J = 24$ Hz). ^{19}F NMR (376 MHz, CD_3CN): δ -106.45 (t, $J = 17$ Hz). HRMS (ESI): calcd. for $\text{C}_5\text{H}_5\text{O}_2\text{F}_2^+$ [$\text{M}+\text{H}$] $^+$, 135.0263; found, 135.0261.

2,2-Difluoro-*N*-methoxy-*N*-methylpent-4-enamide (7.16). A solution containing acid **7.6** (1.0 g, 7.3 mmol, 1.0 equiv.), 1-hydroxybenzotriazole (HOBT, 1.5 g, 11 mmol, 1.5 equiv.), 1-ethyl-3-(3-dimethylaminopropyl)carbodiimide hydrochloride (EDC, 1.6 g, 10 mmol, 1.4 equiv.), *N,N*-diisopropylethyl amine (2.5 mL, 14 mmol, 2.0 equiv.), and *N,O*-dimethyl hydroxylamine hydrochloride (1.2 g, 12 mmol, 1.6 equiv.) in cold (0 °C) acetonitrile (60 mL, anhydrous) was prepared. The mixture was warmed to rt overnight. The following morning the reaction was evaporated to dryness and purified by silica gel chromatography with a hexane/ethyl acetate solvent system. This procedure yielded 580 mg of **7.16** (3.2 mmol, 44%). ^1H NMR (400 MHz, CDCl_3): δ 5.77-5.70 (m, 1H), 5.23-5.17 (m, 2H), 3.69 (s, 3H), 3.19 (s, 3H), 2.86 (td, $J = 17.1, 7.1$ Hz, 2H). ^{19}F NMR (376 MHz, CDCl_3): δ -102.23 (t, $J = 15$ Hz, 2F). HRMS (EI): calcd. for $\text{C}_7\text{H}_{11}\text{NO}_2\text{F}_2^+$ [M] $^+$, 179.0758; found, 179.0759.

(*E*)-2,2,7,7-Tetrafluoro-*N*¹,*N*⁸-dimethoxy-*N*¹,*N*⁸-dimethyloct-4-enediamide (7.17). Compound **7.16** (250 mg, 1.4 mmol, 1.0 equiv.) was dissolved in CH_2Cl_2 (10 mL, anhydrous) and Grubbs 2nd generation catalyst (93 mg, 0.11 mmol, 8 mol%) was added. The mixture was heated to 50 °C for 1 h, at which point it was cooled to rt, evaporated to a residue, and purified by silica gel chromatography using a hexane/ethyl acetate solvent system (10:1 to 1:1). This procedure yielded 220 mg of **7.17** (0.66 mmol, 94%). $R_f = 0.6$ in toluene/acetone. ^1H NMR (400 MHz, CDCl_3): δ 5.57 (bs, 2H), 3.66 (s, 6H), 3.17 (s, 6H), 2.84 (tdd, $J = 16.9, 3.6, 1.3$ Hz, 4H). ^{13}C NMR (101 MHz, CDCl_3): δ 163.3 (t, $J = 30$ Hz), 126.2, 116.9 (t, $J = 252$ Hz), 61.9, 38.1 (t, $J = 24$ Hz), 33.0 (t, $J = 24$ Hz). ^{19}F NMR (376 MHz, CDCl_3): δ -102.08 (s, 4F). HRMS (ESI): calcd. for $\text{C}_{12}\text{H}_{19}\text{N}_2\text{O}_4\text{F}_4^+$ [$\text{M}+\text{H}$] $^+$, 331.1275; found, 331.1280.

3-(3-Bromo-5,5-difluoro-6-oxotetrahydro-2H-pyran-2-yl)-2,2-difluoro-N-methoxy-N-methylpropanamide (7.18). Compound **7.17** (29 mg, 0.088 mmol, 1.0 equiv.) was dissolved in CH₂Cl₂ (0.75 mL, anhydrous) and cooled to 0 °C. To this solution, bromine (130 µL of a 1:10 dilution in CH₂Cl₂, 0.26 mmol, 2.9 equiv.) was added. After 3 h, the mixture was evaporated to dryness and purified by silica gel chromatography using a hexane/ethyl acetate solvent system (product elutes at 2:1). This procedure resulted in 21 mg of **7.18** (0.056 mmol, 65%). R_f = 0.7 in 1:1 hexane/ethyl acetate. ¹H NMR (400 MHz, CDCl₃): δ 4.74 (q, *J* = 6.7 Hz, 1H), 4.35 (bd, *J* = 6.2 Hz, 1H), 3.77 (s, 3H), 3.27 (s, 3H), 3.02-2.83 (m, 3H), 2.74-2.59 (m, 1H). ¹³C NMR (150 MHz, MeOD): δ 168.7 (t, *J* = 30 Hz), 168.6 (t, *J* = 29 Hz), 117.7 (t, *J* = 250 Hz), 117.4 (*J* = 250 Hz), 70.4 (q, *J* = 4 Hz), 61.90 (s), 51.7 (bs), 40.6 (t, *J* = 25 Hz), 40.1 (t, *J* = 24 Hz), 35.8. ¹⁹F NMR (565 MHz, CDCl₃): δ -103.75 (dt, *J* = 257, 14 Hz, 1F), -105.0 (dt, *J* = 255, 15 Hz, 1F), -106.8 (dt, *J* = 255, 16 Hz, 1F), -107.7 (ddd, *J* = 257, 21, 15 Hz, 1F). HRMS (ESI): calcd. for C₁₀H₁₃O₄NF₄Br⁺ [M+H]⁺, 365.9959; found, 365.9957.

2,2-Difluorocycloheptane-1,3-dione (7.32). 1,3-cycloheptadione³⁰ (**7.28**, 1.0 g, 7.9 mol, 1.0 equiv.) was dissolved in acetonitrile (44 mL, anhydrous). Cesium carbonate (4.05 g, 12 mmol, 1.6 equiv.) was added and the mixture was stirred at rt for 30 min. It was then cooled to 0 °C and Selectfluor (5.2 g, 15 mmol, 1.8 equiv.) was added. The mixture was warmed to rt and monitored by ¹⁹F-NMR for disappearance of Selectfluor. After 1.5 h the reaction was filtered to remove Cs₂CO₃. The filtrate was evaporated to dryness and pushed through a plus of silica gel eluting with 1:1 hexanes/ethyl acetate. This procedure yielded a mixture of **7.32** and hydrated **7.32** (760 mg, 4.5 mmol, 56%). ¹H NMR (600 MHz, CDCl₃): δ 3.65 (bs, 2H hydrate), 2.72-2.70 (m, 4H), 2.60 (t, *J* = 6.5 Hz, 2H hydrate), 2.01-1.99 (m, 4H, 2H hydrate), 1.84-1.83 (m, 2H hydrate), 1.68-1.65 (m, 2H hydrate). ¹³C NMR (150 MHz, CDCl₃): δ 198.9 (t, *J* = 23 Hz, hydrate), 197.7 (t, *J* = 25 Hz), 115.3 (t, *J* = 259 Hz, hydrate), 110.1 (t, *J* = 262 Hz), 94.8 (t, *J* = 26 Hz, hydrate), 39.8, 39.3 (hydrate), 37.5 (hydrate), 24.96, 22.6 (hydrate), 22.0 (hydrate). ¹⁹F NMR (565 MHz, CDCl₃): δ -115.84 (s, 2F), -120.09 (s, 2F, hydrate). HRMS (EI): calcd. for C₇H₈O₂F₂⁺ [M]⁺, 162.0492; found, 162.0496.

(E)-Methyl 4-((2,2-difluoro-3-oxocycloheptylidene)methyl)benzoate. 2,2-Difluorocycloheptane-1,3-dione (**7.32**, 366 mg, 2.26 mmol, 1.0 equiv.) and (4-(methoxycarbonyl)benzyl)triphenylphosphonium bromide (1.15 g, 2.34 mmol, 1.04 equiv.) were dissolved in THF (32 mL, anhydrous) and cooled to 0 °C. 1,8-Diazabicycloundec-7-ene (410 µL, 2.7 mmol, 1.2 equiv.) was added dropwise and the solution turned yellow in color. The mixture was stirred at 0 °C for 1.5 h, at which point it was quenched with methanol. The mixture was evaporated onto silica gel and further purified by silica gel chromatography using a mixture of 2:1 hexane/toluene with 0, 1, or 2% ethyl acetate. The product elutes with 2% ethyl acetate. This procedure yielded 241 mg of product (0.82 mmol, 36%). R_f = 0.7 in 2:1 hexane/ethyl acetate. ¹H NMR (600 MHz, CDCl₃): δ 8.04 (d, *J* = 8.3 Hz, 2H), 7.34 (d, *J* = 8.2 Hz, 2H), 7.10 (s, 1H), 3.92 (s, 3H), 2.70 (dd, *J* = 6.2, 6.2 Hz, 2H), 2.56 (dd, *J* = 5.9, 5.9 Hz, 2H), 1.94-1.92 (m, 2H), 1.84-1.82 (m, 2H). ¹³C NMR (100 MHz, CDCl₃): δ 199.4 (t, *J* = 29 Hz), 166.6, 139.7, 134.7 (t, *J* = 20 Hz), 131.1 (t, *J* =

9 Hz), 129.8, 129.6, 128.9, 115.5 (t, $J = 254$ Hz), 52.3, 39.3, 28.11, 27.1, 24.5. ^{19}F NMR (565 MHz, CDCl_3): δ -108.11 (s, 2F). HRMS (EI): calcd. for $\text{C}_{16}\text{H}_{16}\text{O}_3\text{F}_2^+ [\text{M}]^+$, 294.1068; found, 294.1064.

Methyl 4-((2,2-difluoro-3-oxocycloheptyl)methyl)benzoate (7.27). (*E*)-methyl 4-((2,2-difluoro-3-oxocycloheptylidene)methyl)benzoate (68 mg, 0.23 mmol, 1.0 equiv.) was dissolved in ethanol (1.5 mL) and flushed with nitrogen. Palladium hydroxide on carbon (20%, 7.5 mg) was added and solution was flushed with hydrogen. The reaction mixture was stirred under a hydrogen atmosphere for 1.5 h, at which point it was filtered through Celite, rinsed with ethanol, and evaporated to dryness to yield pure **7.27** (70 mg, 0.23 mmol, quant.). $R_f = 0.7$ in 2:1 hexane/ethyl acetate. ^1H NMR (600 MHz, CDCl_3): δ 7.95 (d, $J = 8.3$ Hz, 2H), 7.22 (d, $J = 8.2$ Hz, 2H), 3.87 (s, 3H), 3.18 (dd, $J = 13.8, 3.5$ Hz, 1H), 2.75 (dtd, $J = 15.2, 6.4, 3.0$ Hz, 1H), 2.63-2.58 (m, 1H), 2.46 (dd, $J = 13.8, 10.9$ Hz, 1H), 2.22-2.13 (m, 1H), 1.92-1.87 (m, 1H), 1.75-1.70 (m, 2H), 1.65-1.62 (m, 1H), 1.36-1.31 (m, 1H), 1.27-1.21 (m, 1H). ^{13}C NMR (150 MHz, CDCl_3): δ 201.9 (dd, $J = 29, 26$ Hz), 167.0, 144.4, 130.0, 129.4, 128.7, 119.5 (dd, $J = 256, 253$ Hz), 52.2, 44.5 (dd, $J = 22, 21$ Hz), 38.5, 33.6 (dd, $J = 6, 4$ Hz), 28.3 (dd, $J = 6, 2$ Hz), 25.1, 23.5. ^{19}F NMR (565 MHz, CDCl_3): δ -106.63 (d, $J = 245$ Hz, 1F), -120.51 (dd, $J = 245, 24$ Hz, 1F). HRMS (EI): calcd. for $\text{C}_{16}\text{H}_{18}\text{O}_3\text{F}_2^+ [\text{M}]^+$, 296.1224; found, 296.1228.

Methyl 4-((2,2,4,4-tetrafluoro-3-oxocycloheptyl)methyl)benzoate (7.26).

Difluoroketone **7.26** (595 mg, 2.1 mmol, 1.0 equiv.) was dissolved in cyclohexane (5 mL) in the presence of molecular sieves, trifluoroacetic anhydride (1 drop), and hexylamine (0.28 mL, 2.1 mmol, 1.0 equiv.). This mixture was heated to reflux for 10 h, at which point, it was cooled to rt, evaporated to dryness and the residue was dissolved in ether (75 mL). The ether solution was washed with saturated NaHCO_3 (50 mL) and brine (50 mL). The organics were dried, decanted, and evaporated to a residue containing the hexylimine of **7.26**. The residue was dissolved in acetonitrile (20 mL, anhydrous) and sodium sulfate (590 mg, 4.2 mmol, 2.0 equiv.) was added followed by Selectfluor (2.21 g, 6.2 mmol, 3.0 equiv.). The mixture was refluxed overnight. The following morning, 3M HCl (1 mL) was added and the mixture was heated for an additional 10 min. The solution was then cooled to rt and the acetonitrile was removed by evaporation. The residue was dissolved in ether (75 mL) was washed with saturated NaHCO_3 (50 mL) and brine (50 mL). The ether was dried, decanted, and evaporated to dryness. The crude product was purified by silica gel chromatography with a hexane/ethyl acetate solvent system (6:1 to 2:1). This procedure yielded 288 mg (0.87 mmol, 43%) as a mixture of ketone and hydrate. $R_f = 0.6$ in 3:1 toluene/acetone. ^1H NMR (600 MHz, CDCl_3): δ 8.01 (d, $J = 8.2$ Hz, 2H), 7.99 (d, $J = 8.4$ Hz, 2H hydrate), 7.29-7.26 (m, 2H, 2H hydrate), 4.02 (bs, 1H hydrate), 3.93 (s, 3H, 4H hydrate), 3.29 (d, $J = 9.5$ Hz, 1H hydrate), 3.25 (dd, $J = 13.8, 3.5$ Hz, 1H), 2.56-2.51 (m, 1H, 2H hydrate), 2.42-2.37 (m, 2H), 2.33-2.25 (m, 1H hydrate), 2.19-2.12 (m, 1H, 1H hydrate), 1.85-1.71 (m, 2H, 2H hydrate), 1.58-1.53 (m, 1H), 1.44-1.38 (m, 1H, 2H hydrate). ^{13}C NMR (150 MHz, CDCl_3): δ 189.02 (m), 167.3, 167.1 (hydrate), 145.1 (hydrate), 143.6, 130.2 (hydrate), 130.0, 129.5, 129.4 (hydrate), 129.1 (hydrate), 128.6, 121.7 (apparent t, $J = 254$ Hz), 121.2 (apparent t, $J = 250$ Hz, hydrate), 118.4 (apparent t, J

= 255 Hz, hydrate) 116.8 (t, $J = 252$ Hz) 94.8 (apparent dt, $J = 53$, 27 Hz, hydrate), 52.4 (hydrate), 52.3, 45.7 (t, $J = 23$ Hz, hydrate), 43.7 (t, $J = 25.1$ Hz), 35.0 (dd, $J = 7$, 5 Hz), 34.7 (t, $J = 24$ Hz, hydrate), 33.4 (apparent t, $J = 4$ Hz, hydrate), 32.7 (t, $J = 24$ Hz), 27.5 (d, $J = 5$ Hz, hydrate), 26.0 (d, $J = 8$ Hz), 20.2 (dd, $J = 8$, 3 Hz, hydrate), 19.5 (t, $J = 6$ Hz). ^{19}F NMR (565 MHz, CDCl_3): δ -98.01 (dq, $J = 268$, 11 Hz, 1F), -103.08 (dtd, $J = 259$, 20, 10 Hz, 1F hydrate), -104.20 (dm, $J = 260$ Hz, 1F), -105.55 (dddd, $J = 268$, 23, 13, 9 Hz, 1F), -107.64 (ddt, $J = 260$, 23, 10 Hz, 1F hydrate), -108.65 (dm, $J = 260.0$ Hz, 1F hydrate), -119.26 (ddd, $J = 260$, 24, 12 Hz, 1F), -121.66 (ddd, $J = 260$, 26, 20 Hz, 1F hydrate). HRMS (EI): calcd. for $\text{C}_{16}\text{H}_{16}\text{O}_3\text{F}_4^+$ $[\text{M}]^+$, 332.1036; found, 332.1039.

Methyl 4-((2,2,4,4-tetrafluoro-3-hydroxy-3-methylcycloheptyl)methyl)benzoate (7.33).

Tetrafluorinated ketone **7.26** (19 mg, 0.057 mmol, 1.0 equiv.) was dissolved in CH_2Cl_2 (0.5 mL) and cooled to 0 °C. Trimethylaluminum (35 μL of a 2M solution in toluene, 0.070 mmol, 1.2 equiv.) was added and the mixture was stirred for 20 min, at which point trimethylsilyl diazomethane (35 μL of a 2M solution in CH_2Cl_2 , 0.070 mmol, 1.2 equiv.) was added. After 5 min, TLC indicated the reaction was complete. The mixture was quenched with sat. aqueous Rochelle's salt and stirred until all aluminum was complexes. This solution was extracted with CH_2Cl_2 (3 x 5 mL). The organics were dried, decanted, evaporated to dryness and the crude product was purified by silica gel chromatography using a hexanes/ether solvent system (20:1 to 2:1). This procedure yielded 9 mg of **7.33** (0.026 mmol, 45%) as a mixture of diastereomers (~1:0.3). $R_f = 0.7$ in 3:1 hexane/ethyl acetate. ^1H NMR (600 MHz, CDCl_3 , major diastereomer only): δ 7.97 (d, $J = 7.2$ Hz, 2H), 7.27 (d, $J = 7.4$ Hz, 2H), 3.91 (s, 3H), 3.26 (dd, $J = 13.9$, 3.8 Hz, 1H), 2.80-2.70 (m, 1H), 2.50 (dd, $J = 13.8$, 10.5 Hz, 1H), 2.45-2.34 (m, 1H), 2.20 (s, 1H), 2.04-1.98 (m, 1H), 1.74-1.64 (m, 1H), 1.56-1.51 (m, 6H). ^{19}F NMR (565 MHz, CDCl_3): δ -99.07 (ddt, $J = 264$, 21, 7 Hz), -103.09 (ddd, $J = 255$, 35, 15 Hz), -105.93 (d, $J = 265$ Hz), -118.57 (ddd, $J = 264$, 29, 22 Hz). HRMS (EI): calcd. for $\text{C}_{17}\text{H}_{20}\text{O}_3\text{F}_4^+$ $[\text{M}]^+$, 348.1349; found, 348.1358.

Methyl 4-((4,4,9,9-tetrafluoro-1-oxaspiro[2.6]nonan-5-yl)methyl)benzoate (7.34). A solution of 0.09 M TMSCLiN_2 was generated by combining trimethylsilyldiazomethane (0.05 mL of a 2 M solution in CH_2Cl_2) with *n*butyllithium (0.06 mL of a 1.6 M solution in hexane) in THF (1.0 mL, anhydrous) at -78 °C. Tetrafluorinated ketone **7.26** (20 mg, 0.060 mmol, 1.0 equiv.) was dissolved in THF (1.5 mL, anhydrous) and cooled to 0 °C. The TMSCLiN_2 (0.67 mL, 0.060 mmol, 1.0 equiv.) was added and the mixture was warmed to rt. No significant reaction at rt and the mixture was heated to 40 °C overnight. The following morning the mixture was quenched with methanol and evaporated to dryness. The crude product was purified by silica gel chromatography with a hexanes/ether solvent system (40:1 to 10:1) to yield 14 mg of **7.34** (0.04 mmol, 67%). $R_f = 0.7$ in 3:1 hexane/ethyl acetate. ^1H NMR (400 MHz, CDCl_3): δ 8.0-7.96 (m, 2H major, 2H minor) 7.28-7.23 (m, 2H major, 2H minor), 3.91 (s, 3H minor), 3.91 (s, 3H major), 3.30-3.17 (m, 2H major, 2H minor), 3.14-3.10 (m, 1H major, 1H minor), 2.56-2.36 (m, 3H major, 3H minor), 2.18-2.04 (m, 1H major, 1H minor), 1.80-1.65 (m, 2H major, 2H minor), 1.62-1.46 (m, 1H major, 1H minor), 1.41-1.26 (m, 1H major, 1H minor). ^1H NMR (600 MHz, CDCl_3 , major only): δ 7.97 (d, $J = 8.2$ Hz, 2H), 7.24 (d, $J = 8.2$ Hz, 2H), 3.91

(d, $J = 3.1$ Hz, 3), 3.29 (t, $J = 5.6$ Hz, 1H), 3.23 (dt, $J = 14.1, 7.1$ Hz, 1H), 3.11 (t, $J = 5.9$ Hz, 1H), 2.55-2.38 (m, 3H), 2.17-2.04 (m, 1H), 1.75-1.69 (m, 2H), 1.52 (q, $J = 13.0$ Hz, 1H), 1.36 q, $J = 11.9$ Hz, 1H). ^{13}C NMR (150 MHz, CDCl_3): δ 167.1, 144.9, 130.1, 129.4, 128.7, 120.9 (ddd, $J = 254, 249, 4$ Hz), 120.0 (apparent td, $J = 246, 8$ Hz), 60.2-59.6 (m), 52.3, 46.8 (ddd, $J = 13, 5, 2$ Hz), 45.0 (t, $J = 23$ Hz), 36.8 (t, $J = 25$ Hz), 34.6 (dd, $J = 7, 6$ Hz), 29.4 (d, $J = 4$ Hz), 19.45 (d, $J = 9$ Hz). ^{19}F NMR (376 MHz, CDCl_3): δ -88.41 (d, $J = 261$ Hz, 1F major), -92.89 (dq, $J = 262, 5$ Hz, 1F minor), -97.46 (d, $J = 261$ Hz, 1F minor), -103.49 (d, $J = 261$ Hz, 1F major), -105.35 (dddd, $J = 30, 25, 19, 6$ Hz, 1F major), -107.00 (dm, $J = 214$ Hz, 1F minor), -118.04 (ddd, $J = 260, 28, 14$ Hz, 1F major), -120.62 (ddd, $J = 262, 24, 7$ Hz, 1F minor). HRMS (EI): calcd. for $\text{C}_{17}\text{H}_{18}\text{O}_3\text{F}_4^+ [\text{M}]^+$, 346.1192; found, 346.1195.

Methyl 4-((3-cyano-2,2,4,4-tetrafluoro-3-hydroxycycloheptyl)methyl)benzoate (7.35).

Tetrafluorinated ketone **7.26** (11 mg, 0.033 mmol, 1.0 equiv.) was dissolved in ether (0.25 mL, anhydrous). Zinc bromine (1 grain) and trimethylsilyl cyanide (~15 μL , 0.1 mmol, 3 equiv.) was added and the reaction mixture was stirred overnight at rt. The following morning the reaction was not complete and more trimethylsilyl cyanide (~15 μL) was added and the mixture was stirred at rt for an additional 24 h, at which point it was evaporated to dryness. The crude product was purified by silica gel chromatography using a hexanes/ethyl acetate solvent system (**7.35** elutes at 4:1). This procedure resulted in 5 mg of **7.35** as a 1:0.3 mixture of diastereomers (0.014 mmol, 42%). $R_f = 0.4$ in 3:1 hexane/ethyl acetate. ^1H NMR (600 MHz, CDCl_3): δ 8.00 (d, $J = 7.2$ Hz, 2H minor), 7.98 (d, $J = 8.3$ Hz, 2H major), 7.27-7.25 (m, 2H major, 2H minor), 4.66 (bs, 1H major), 4.39 (bs, 1H minor), 3.92 (s, 3H major, 3H minor), 3.27 (dd, $J = 13.7, 3.4$ Hz, 1H major, 1H minor), 2.73-2.64 (m, 1H major), 2.59-2.53 (m, 1H minor), 2.55 (dd, $J = 11.0, 13.9$ Hz, 1H major), 2.46-2.34 (m, 1H major, 2H minor), 2.24-2.09 (m, 1H major, 1H minor), 1.75-1.68 (m, 1H major, 1H minor), 1.58-1.50 (m, 3H major, 2H minor), 1.42-1.40 (m, 1H minor).

(4-((4,4,9,9-Tetrafluoro-1-oxaspiro[2.6]nonan-5-yl)methyl)phenyl)methanol (7.38).

Cyanohydrin **7.35** (5 mg, 0.014 mmol, 1.0 equiv.) was dissolved in ether (0.2 mL, anhydrous). This solution was added dropwise to a solution of lithium aluminum hydride (0.25 mL, 1M solution in THF, 0.25 mmol, 18 equiv.). The mixture was warmed to 50 $^\circ\text{C}$ and allowed to react overnight. The following morning it was quenched with sat. aqueous Rochelle's salt and extracted with ethyl acetate (3 x 15 mL). The organics were combined, dried, decanted, and evaporated to dryness to yield **7.36** (3 mg, 0.009 mmol, 69%; HRMS (ESI): calcd. for $\text{C}_{16}\text{H}_{22}\text{O}_2\text{NF}_4^+ [\text{M}+\text{H}]^+$, 336.1581; found, 336.1586). This crude product was dissolved in a mixture of water (80 μL) and acetic acid (80 μL). A separate solution of sodium nitrite (8 mg, 0.12 mmol, 13 equiv.) in water (160 μL) was prepared and added to the solution containing amino-alcohol **7.36**. The mixture was stirred at rt overnight. The following morning, additional water (2 mL) was added and the product was extracted with ether (3 x 5 mL). The organics were combined, dried, decanted, and evaporated to dryness to yield **7.38** as a mixture of diastereomers. ^1H NMR (600 MHz, CDCl_3): δ 7.32 (d, $J = 8.3$ Hz, 2H minor), 7.31 (d, $J = 8.3$ Hz, 2H major), 7.20 (d, $J = 7.9$ Hz, 1H), 7.17 (d, $J = 7.9$ Hz, 1H), 4.69 (s, 2H minor), 4.68 (s, 2H major), 3.29 (dd, $J = 14.7, 5.7$ Hz, 1H

major, 1H minor), 3.18-3.10 (m, 2H major, 2H minor), 2.49-2.40 (m, 3H major, 3H minor), 2.15-2.03 (m, 3H major, 2H minor), 1.86-1.22 (m, 3H major, 3H minor). ¹⁹F NMR (565 MHz, CDCl₃): δ -89.51 (dm, *J* = 259 Hz), -94.15 (dq, *J* = 256, 9 Hz), -98.45 (apparent d, *J* = 257 Hz), -104.71 (d, *J* = 259 Hz), -106.29 (dddd, *J* = 260, 30, 25, 18, 6 Hz), -107.96 (dm, *J* = 290 Hz), -118.96 (ddd, *J* = 261, 29, 14 Hz), -121.73 (ddd, *J* = 262, 24, 7 Hz). HRMS (EI): calcd. for C₁₆H₁₈O₂F₄⁺ [M]⁺, 318.1243; found, 318.1252.

Methyl 4-((3-(dibromomethylene)-2,2,4,4-tetrafluorocycloheptyl)methyl)benzoate (7.39). Tetrafluorinated ketone **7.26** (6 mg, 0.02 mmol, 1.0 equiv.) was dissolved in CH₂Cl₂ (0.5 mL) and cooled to 0 °C. Carbon tetrabromide (28 mg, 0.084 mmol, 4.2 equiv.) was added followed by triphenylphosphine (60 mg, 0.23 mmol, 11 equiv.). The mixture was stirred at rt overnight. The following morning, the mixture was evaporated to dryness and purified by silica gel chromatography using a hexanes/ethyl acetate solvent system. This procedure yielded 4 mg of **7.39** (0.008 mmol, 41%). R_f = 0.7 in 3:1 hexanes/ethyl acetate. ¹H NMR (600 MHz, CDCl₃): δ 7.98 (d, *J* = 7.9 Hz, 2H), 7.25 (d, *J* = 8.9 Hz, 2H), 3.91 (s, 3H), 3.25 (d, *J* = 10.4 Hz, 1H), 2.61- 2.452 (m, 2H), 2.33- 2.21 (m, 2H), 1.78-1.74 (m, 1H), 1.67-1.65 (m, 1H), 1.43- 1.34 (m, 2H). ¹³C NMR (150 MHz, CDCl₃): δ 167.1, 144.4, 135.5 (dd, *J* = 26, 25 Hz), 130.1, 129.4, 128.9, 122.3 (apparent t, *J* = 252 Hz), 120.8 (apparent t, *J* = 250 Hz), 101.2, 52.3, 47.8 (dd, *J* = 23, 23 Hz), 38.1 (apparent t, *J* = 26 Hz), 34.1 (d, *J* = 6 Hz), 27.6 (t, *J* = 3 Hz), 19.6 (dd, *J* = 7, 4 Hz). ¹⁹F NMR (565 MHz, CDCl₃): δ -82.92 (dq, *J* = 260, 13 Hz, 1F), -86.55 (dt, *J* = 258, 19 Hz, 1F), -88.09 (d, *J* = 259 Hz, 1F), -99.13 (dm, *J* = 262 Hz, 1F). HRMS (EI): calcd. for C₁₇H₁₆O₂Br₂F₄⁺ [M]⁺, 485.9453; found, 485.9453.

References

- (1) Baskin, J. M.; Prescher, J. A.; Laughlin, S. T.; Agard, N. J.; Chang, P. V.; Miller, I. A.; Lo, A.; Codelli, J. A.; Bertozzi, C. R. Copper-free click chemistry for dynamic in vivo imaging. *Proc. Natl. Acad. Sci. U.S.A.* **2007**, *104*, 16793 -16797.
- (2) Chang, P. V.; Prescher, J. A.; Sletten, E. M.; Baskin, J. M.; Miller, I. A.; Agard, N. J.; Lo, A.; Bertozzi, C. R. Copper-free click chemistry in living animals. *Proc. Natl. Acad. Sci. U.S.A.* **2010**, *107*, 1821-1826.
- (3) Laughlin, S. T.; Bertozzi, C. R. In vivo imaging of Caenorhabditis elegans glycans. *ACS Chem. Biol.* **2009**, *4*, 1068-1072.
- (4) Laughlin, S. T.; Baskin, J. M.; Amacher, S. L.; Bertozzi, C. R. In vivo imaging of membrane-associated glycans in developing zebrafish. *Science* **2008**, *320*, 664 -667.
- (5) Baskin, J. M.; Dehnert, K. W.; Laughlin, S. T.; Amacher, S. L.; Bertozzi, C. R. Visualizing enveloping layer glycans during zebrafish early embryogenesis. *Proc. Natl. Acad. Sci. U.S.A.* **2010**, *107*, 10360 -10365.
- (6) Schoenebeck, F.; Ess, D. H.; Jones, G. O.; Houk, K. N. Reactivity and regioselectivity in 1,3-dipolar cycloadditions of azides to strained alkynes and alkenes: A computational study. *J. Am. Chem. Soc.* **2009**, *131*, 8121-8133.

- (7) Leupin, W.; Wirz, J. Cyclooct-1-en-5-yne. Preparation, spectroscopic characteristics and chemical reactivity. *Helv. Chim. Acta* **1978**, *61*, 1663-1674.
- (8) Hodgson, D. M.; Galano, J.-M.; Christlieb, M. Synthesis of (-)-xialenon A by enantioselective α -deprotonation-rearrangement of a meso-epoxide. *Tetrahedron* **2003**, *59*, 9719-9728.
- (9) McMurry, J. E.; Rico, J. G. Synthesis of 1,2-cycloalkanediols by intramolecular titanium-induced pinacol coupling. *Tetrahedron Lett.* **1989**, *30*, 1169-1172.
- (10) Szymoniak, J.; Besançon, J.; Moïse, C. Pinacol coupling of aliphatic aldehydes promoted by niobium (III) reagent. *Tetrahedron* **1994**, *50*, 2841-2848.
- (11) Groth, U.; Jung, M.; Vogel, T. Intramolecular chromium(II)-catalyzed pinacol cross coupling of 2-methylene- α,ω -dicarbonyls. *Synlett* **2004**, 1054-1058.
- (12) Kato, N.; Kataoka, H.; Ohbuchi, S.; Tanaka, S.; Takeshita, H. Total synthesis of alibolic acid and ceroplastol II, 5-8-5-membered tricyclic insect sesterterpenoids, via a lactol-regulated silyloxy-Cope rearrangement. *J. Chem. Soc., Chem. Commun.* **1988**, 354-356.
- (13) Greuter, H.; Lang, R. W.; Romann, A. J. Fluorine-containing organozinc reagents. V.: The Reformatskii-Claisen reaction of chlorodifluoroacetic acid derivatives. *Tetrahedron Lett.* **1988**, *29*, 3291-3294.
- (14) Kolb, M.; Gerhart, F.; François, J.-P. Preparative flow techniques; 1. Low-temperature organometallic reactions: Synthesis of ethyl 2,2-difluoro-4-pentenoate. *Synthesis* **1988**, 469-470.
- (15) Zhao, X.-F.; Zhang, C. Iodobenzene dichloride as a stoichiometric oxidant for the conversion of alcohols into carbonyl compounds; Two facile methods for its preparation. *Synthesis* **2007**, 551-557.
- (16) Nahm, S.; Weinreb, S. M. N-Methoxy-N-methylamides as effective acylating agents. *Tetrahedron Lett.* **1981**, *22*, 3815-3818.
- (17) Moebius, D. C.; Kingsbury, J. S. Catalytic homologation of cycloalkanones with substituted diazomethanes. Mild and efficient single-step access to α -tertiary and α -quaternary carbonyl compounds. *J. Am. Chem. Soc.* **2009**, *131*, 878-879.
- (18) Himeshima, Y.; Sonoda, T.; Kobayashi, H. Fluoride-induced 1,2-elimination of o-trimethylsilylphenyl triflate to benzyne under mild conditions. *Chem. Lett.* **1983**, 1211-1214.
- (19) Sampson, P.; Wiemer, D. F. α -Trialkylsilylketones from α -bromoketones: Utilization of a 1,3-O to C silyl migration. *J. Chem. Soc., Chem. Commun.* **1985**, 1746-1747.
- (20) Maruoka, K.; Concepcion, A. B.; Yamamoto, H. Organoaluminum-promoted direct conversion of aldehydes to the homologous ketones or oxiranes with diazoalkanes. *Synlett* **1994**, 521-523.
- (21) Maruoka, K.; Concepcion, A. B.; Yamamoto, H. Selective homologation of ketones and aldehydes with diazoalkanes promoted by organoaluminum reagents. *Synthesis* **1994**, 1283-1290.
- (22) Shioiri, T.; Aoyama, T. Trimethylsilyldiazomethane: A useful reagent for generating alkylidene carbenes and its application to organic synthesis. *J. Syn. Org. Chem., Jpn.* **1996**, *54*, 918-928.

- (23) Brettreich, M.; Wudl, F.; Chaffins, S. An efficient synthesis of dibenzocycloocta-4a,6a,-diene-5,11-diyne and its precursors. *Synthesis* **2002**, 1191-1194.
- (24) Kornmayer, S.; Rominger, F.; Gleiter, R. Synthesis of 11,12-Didehydrodibenzo[a,e]cycloocten-5(6H)-one: A Strained Eight-Membered Alkyne. *Synthesis* **2009**, 2547-2552.
- (25) Hashimoto, N.; Aoyama, T.; Shioiri, T. New methods and reagents in organic synthesis. 10. Trimethylsilyldiazomethane(TMSCHN₂). A new, stable, and safe reagent for the homologation of ketones. *Tetrahedron Lett.* **1980**, *21*, 4619-4622.
- (26) Norio, H.; Toyohiko, A.; Takayuki, S. New Methods and Reagents in Organic Synthesis. 18. Homologation of Ketones with Trimethylsilyldiazomethane (TMSCHN₂). *Chem. Pharm. Bull.* **1982**, *30*, 119-124.
- (27) Li, J.; Sun, C.; Lee, D. Cyclopropenation of alkyldiene carbenes derived from α -silyl ketones. *J. Am. Chem. Soc.* **2010**, *132*, 6640-6641.
- (28) Codelli, J. A.; Baskin, J. M.; Agard, N. J.; Bertozzi, C. R. Second-generation difluorinated cyclooctynes for copper-free click chemistry. *J. Am. Chem. Soc.* **2008**, *130*, 11486-11493.
- (29) Sims, E. A.; DeForest, C. A.; Anseth, K. S. A mild, large-scale synthesis of 1,3-cyclooctanedione: expanding access to difluorinated cyclooctyne for copper-free click chemistry. *Tetrahedron Lett.* **2011**, *52*, 1871-1873.
- (30) Ragan, J. A.; Makowski, T. W.; am Ende, D. J.; Clifford, P. J.; Young, G. R.; Conrad, A. K.; Eisenbeis, S. A. A practical synthesis of cycloheptane-1,3-dione. *Org. Proc. Res. Dev.* **1998**, *2*, 379-381.
- (31) Pravst, I.; Zupan, M.; Stavber, S. Efficient synthesis of α,α -difluoro ketones using Selectfluor. *Synthesis* **2005**, 3140-3146.
- (32) Maruoka, K.; Concepcion, A. B.; Yamamoto, H. Organoaluminum-promoted homologation of ketones with diazoalkanes. *J. Org. Chem.* **1994**, *59*, 4725-4726.
- (33) Mock, W. L.; Hartman, M. E. Mechanism of the triethyloxonium ion catalyzed homologation of ketones with diazoacetic esters. *J. Org. Chem.* **1977**, *42*, 466-472.
- (34) Mock, W. L.; Hartman, M. E. Synthetic scope of the triethyloxonium ion catalyzed homologation of ketones with diazoacetic esters. *J. Org. Chem.* **1977**, *42*, 459-465.
- (35) Kanemasa, S.; Kanai, T.; Araki, T.; Wada, E. Lewis acid-catalyzed reactions of ethyl diazoacetate with aldehydes. Synthesis of alpha-formyl esters by a sequence of aldol reaction and 1,2-nucleophilic rearrangement. *Tetrahedron Lett.* **1999**, *40*, 5055-5058.
- (36) Miwa, K.; Aoyama, T.; Shioiri, T. Extension of the Colvin rearrangement using trimethylsilyldiazomethane. A new synthesis of alkynes. *Synlett* **1994**, 107-108.
- (37) Nagao, K.; Chiba, M.; Kim, S.-W. A new efficient homologation reaction of ketones via their lithiodiazoacetate adducts. *Synthesis* **1983**, 197-199.
- (38) Pellicciari, R.; Natalini, B. Ring expansion of thiochroman-4-one and isothiochroman-4-one with ethyl diazo(lithio)acetate to tetrahydrobenzothiepin beta-oxoesters. *J. Chem. Soc., Perkin Trans. 1* **1977**, 1822-1824.
- (39) McKinney, M. A.; Patel, P. P. Ring expansions. I. Diazomethane and Tiffeneau-Demjanov ring expansions of norcamphor and dehydronorcamphor. *J. Org. Chem.* **1973**, *38*, 4059-4064.

- (40) McKinney, M. A.; Patel, P. P. Ring expansions. II. Diazoethane ring expansion of norcamphor. *J. Org. Chem.* **1973**, *38*, 4064-4067.
- (41) Stern, A. G.; Nickon, A. Synthesis of brexan-2-one and ring-expanded congeners. *J. Org. Chem.* **1992**, *57*, 5342-5352.
- (42) Corey, E. J.; Fuchs, P. L. A synthetic method for formyl to ethynyl conversion. *Tetrahedron Lett.* **1972**, *13*, 3769-3772.
- (43) Curtin, D. Y.; Flynn, E. W. Reaction of 1,1-Diaryl-2-haloethylenes with butyllithium. *J. Am. Chem. Soc.* **1959**, *81*, 4714-4719.
- (44) Pangborn, A. B.; Giardello, M. A.; Grubbs, R. H. ;Rosen, R. K.; Timmers, F. J. Safe and convenient procedure for solvent purification. *Organometallics* **1996**, *15*, 1518-1520.

Chapter 8

Synthesis and Stabilization of Difluorobenzocyclooctyne

Fused Phenyl Rings Activate Cyclooctynes for Reaction with Azides

With the tetrafluorinated cyclooctyne appearing intangible (see previous chapter), we looked toward other methods to activate cyclooctynes for reactivity with azides. As the utility of Cu-free click chemistry became apparent to the chemical biology community, other groups joined the quest for more reactive cyclooctynes. In 2008, the Boons group reported a dibenzocyclooctyne (**8.1**, DIBO, Figure 8.1A) that displayed similar reactivity with azides to DIFO ($k = 0.057 \text{ M}^{-1}\text{s}^{-1}$ vs. $k = 0.076 \text{ M}^{-1}\text{s}^{-1}$ for DIBO and DIFO respectively).¹ By synthesizing DIBO-biotin (**8.2**) and performing a standard cell-surface labeling experiment (see Chapter 4), we confirmed that DIBO displayed comparable reactivity to DIFO on Jurkat cells treated with azidosugar (Figure 8.1B).

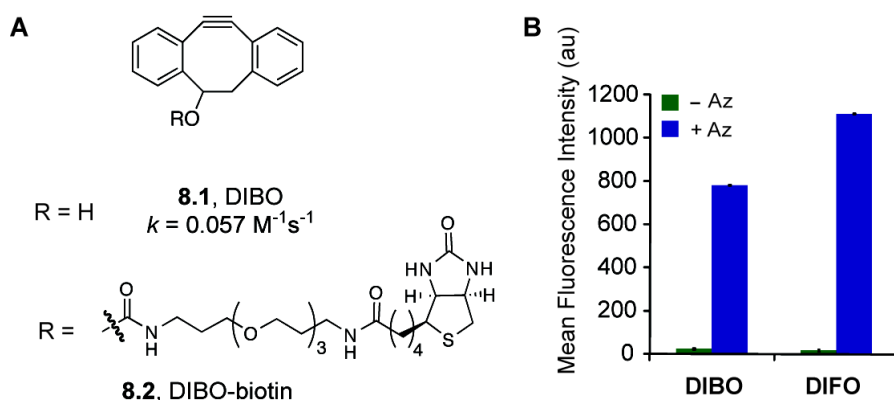


Figure 8.1. A. Dibenzocyclooctyne **8.1** and biotin conjugate **8.2**. B. Jurkat cells were incubated in the presence (+ Az, blue bars) or absence (– Az, green bars) of 25 μM Ac_4ManNAz for 3 d. Cells were reacted with 10 μM DIFO-biotin (**3.4**) or DIBO-biotin (**8.2**) for 1 h at rt, incubated with FITC-avidin, and analyzed by flow cytometry. The error bars represent standard deviations from three replicate samples. Au = arbitrary units.

In addition to other experimentalists becoming interested in the design and synthesis of new cyclooctyne reagents, many computational chemists have found Cu-free click chemistry an intriguing reaction. Theoretical work has been performed to understand the basis of DIFO and DIBO's rate enhancements compared to OCT.^{2,3,4,5} DFT-based methods have consistently predicted the rate-enhancing impact of fluorination, which has been attributed to its effects on transition state distortion/interaction energies.^{2,3} The fused

aryl rings of DIBO were proposed by Goddard and coworkers to exert two opposing effects on the rate of cycloaddition with azides.⁴ On the one hand, the aryl rings could promote the cycloaddition reaction by augmenting the cyclooctyne's ring strain. However, this effect was predicted to be tempered by unfavorable steric interactions (i.e., A-1,3 strain) between the azide's alkyl substituent and the *ortho* hydrogen atoms of the aryl rings. Goddard further speculated that removal of one aryl ring could enhance the cycloaddition rate compared to DIBO, at least for one triazole regioisomer.

Design of a More Reactive Difluorobenzocyclooctyne (DIFBO)

Motivated by this growing body of experimental and theoretical work, we proposed that compounds combining the rate-enhancing features of DIFO and DIBO might possess superior kinetics that are desirable for labeling azides in biological systems, while at the same time appearing more synthetically tractable than a tetrafluorinated cyclooctyne. Hence, we became interested in difluorobenzocyclooctyne (DIFBO) (**8.3**, Figure 8.2), a hybrid of DIFO and DIBO.

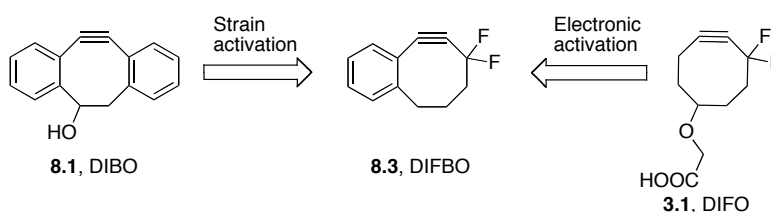


Figure 8.2. Difluorobenzocyclooctyne (DIFBO, **8.3**) is a hybrid of DIFO and DIBO.

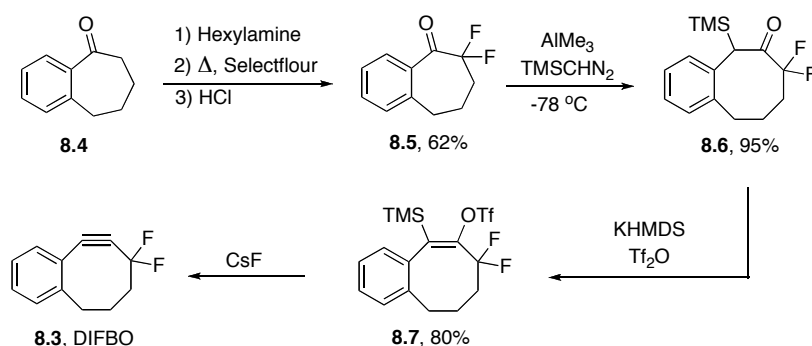
When designing the synthesis of DIFBO, we again looked to the homologation strategy outlined in Chapter 7 (Scheme 7.5). While the ring-expansion was unsuccessful for tetrafluorinated ketone **7.26**, the difluorinated ketone **7.27** was reactive with TMSCHN₂, providing precedent for the homologation of difluorinated ketones, such as **8.5**, which would be the necessary precursor for DIFBO. Compound **8.5** should be easily prepared by a method reported for difluorination of aryl ketones by Stavber and coworkers.⁶ Notably, DIFBO (**8.3**) does not contain a functional group for probe conjugation. We envisioned that a methyl-ester could easily be placed on the aryl ring if DIFBO appeared a promising reagent for Cu-free click chemistry.

Synthesis of DIFBO

Benzosuberone **8.4** was converted to 2,2-difluorobenzosuberone in 62% yield through imine formation with hexylamine followed by treatment of the imine with Selectfluor and hydrolysis back to the ketone with aqueous acid. Subjecting **8.5** to trimethylsilyldiazomethane (TMSCHN₂) with a stoichiometric amount of trimethyl

aluminum resulted in clean homologation to yield compound **8.6**, with the trimethylsilyl group intact alpha to the ketone. Immediate vinyl triflate formation by deprotonation with KHMDS followed by trapping of the enolate with trifluoromethane sulfonic anhydride yielded compound **8.7**. This intermediate was converted to DIFBO (**8.3**) by reaction with cesium fluoride (Scheme 8.1).⁷ The synthesis of DIFBO validated the homologation strategy for the facile synthesis of cyclooctynes. However, a complication arose in that the desired product could not be isolated in pure form. Rather, DIFBO underwent spontaneous homotrimerization upon concentration to form a mixture of two compounds, suggesting our initial hypothesis was correct and the combination of electronic and strain activation resulted in a highly reactive cyclooctyne.

Scheme 8.1. Synthesis of difluorobenzocyclooctyne.



After extensive NMR analysis (see appendix D) and further confirmation by X-ray crystallography (Figure 8.3), we determined that the two trimer products were asymmetric diastereomers **8.8** and **8.9** (Scheme 8.2). Interestingly, trimer product **8.10** that would be derived from three DIFBO molecules coming together in a C₃ symmetric manner was not observed. Trimerization is a well-established reaction pathway for highly strained cycloalkynes.^{8,9,10} However, the trimerization of DIFBO was a nearly quantitative process, and many of the precedented trimerization reactions are low yielding unless a metal is present.^{11,12}

To confirm that DIFBO had indeed been formed prior to trimerization, we added benzyl azide to the reaction of compound **8.3** with CsF and obtained a mixture of triazole products **8.11** and **8.12** (1:1.6 ratio, see appendix D) in 93% yield (Scheme 8.3). Thus, the rate of reaction of DIFBO with benzyl azide appeared to be faster than that of trimerization.

Scheme 8.2. Trimerization of DIFBO.

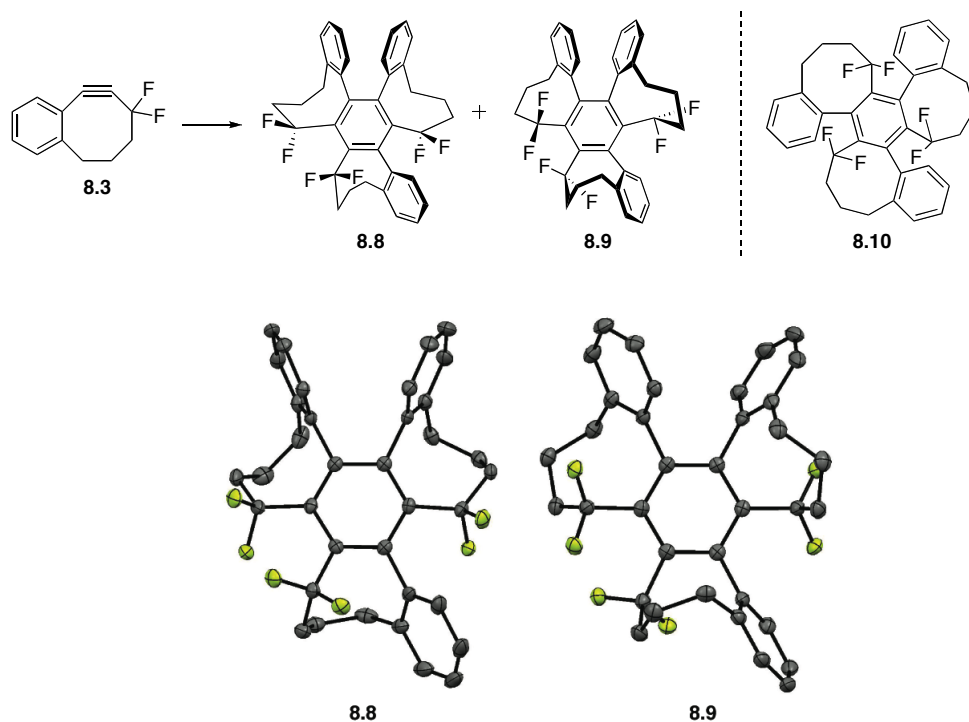
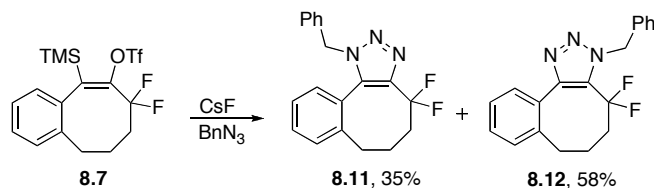


Figure 8.3. Crystal structures of trimer products. Thermal ellipsoid plots for trimer products **8.8** and **8.9** shown at 50% probability. Grey atoms correspond to carbon and green atoms correspond to fluorine. The hydrogen atoms have been removed for clarity.

Scheme 8.3. Isolation of cycloadducts between DIFBO and benzyl azide.



Stabilization of DIFBO

The trimerization reaction created several problems with regard to the characterization of DIFBO. The compound was impossible to isolate in pure form at convenient temperatures and could not be stored for future use. Thus, we sought a means to stabilize DIFBO for detailed spectroscopic and kinetic characterization. Cyclodextrins, cyclic oligomers of α -1,4 linked glucose, are well-known for their ability to bind small, non-polar molecules within their bowl-shaped cavities.^{13,14,15} The three commonly used cyclodextrins, α , β , and γ , comprising six, seven, and eight glucose residues, respectively, possess different cavity dimensions that can be selected to match the small molecule guest of interest (Figure 8.4). The inclusion complexes are stable in water and during freeze-drying but readily dissociate upon suspension in organic solvents. Cyclodextrin complexation has previously been exploited to enhance the stability of lipophilic drugs.^{16,17,18} Based on this precedent, we sought to test whether cyclodextrins would form stable inclusion complexes with DIFBO, thereby permitting long-term storage and facilitating kinetic characterization.

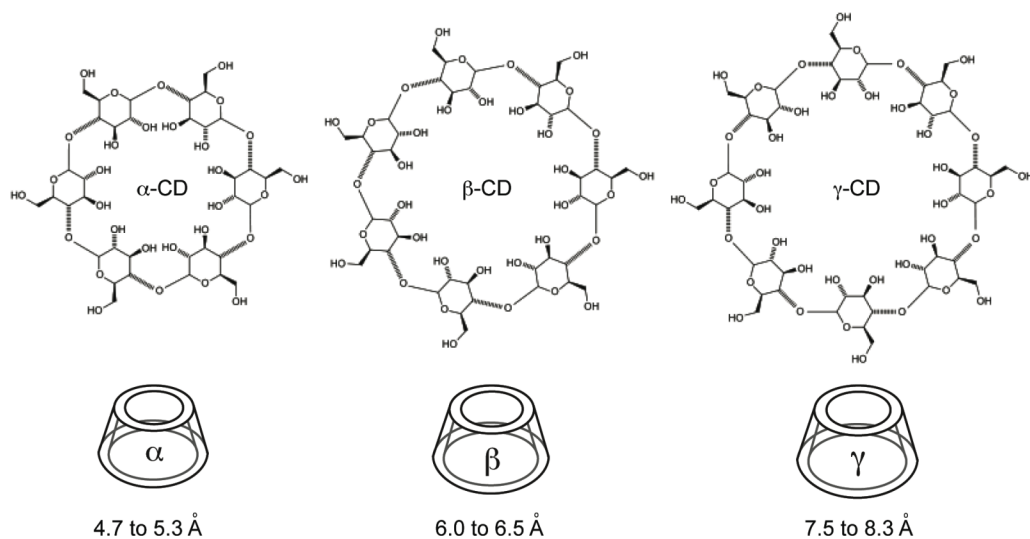
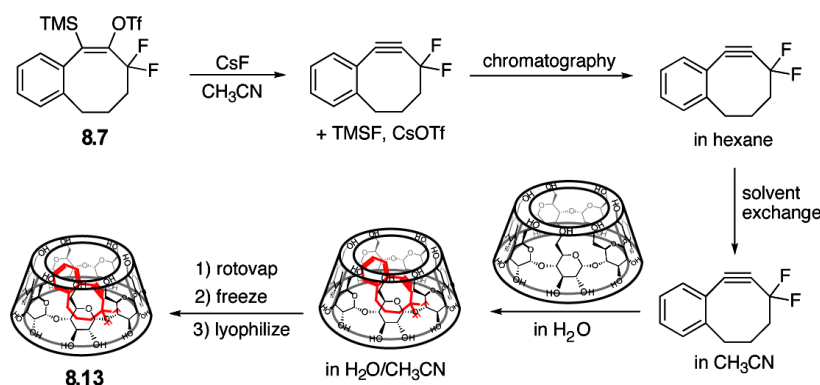


Figure 8.4. The three common cyclodextrin molecules, α , β , and γ containing 6, 7, and 8 glucose residues, respectively. Shown are the chemical structures (top), and the schematic which represents each structure (bottom) as well as the diameter of the cavity of each cyclodextrin host.

We combined a crude solution of DIFBO in acetonitrile, generated as shown in Scheme 8.1, with aqueous solutions of α -, β -, or γ -cyclodextrin. TLC and mass spectrometry analysis showed the persistence of DIFBO in the β -cyclodextrin-containing mixture, whereas side products were formed in the α - or γ -cyclodextrin-containing

mixtures. Encouraged by this observation, we developed a procedure for generating and isolating the DIFBO- β -cyclodextrin complex (Scheme 8.4). We found that the reaction solution in which DIFBO was generated could be directly loaded onto a silica gel column without concentration. Upon elution with hexanes, pure DIFBO was obtained. The DIFBO- β -cyclodextrin complex could not be formed in the presence of hexane, and consequently, we exchanged the solvent by dilution with acetonitrile followed by careful room temperature evaporation of the hexane. An aqueous solution of β -cyclodextrin was then added to the DIFBO/acetonitrile solution and immediately a white precipitate formed. This mixture was lyophilized to afford a white powder.

Scheme 8.4. Synthesis and purification of DIFBO- β -cyclodextrin complex **8.13**.



¹H NMR analysis of the powder dissolved in *d*₆-DMSO (Figure 8.5A) confirmed the presence of pure DIFBO, providing strong evidence for a successful complexation process. However, an inclusion complex of this type is expected to dissociate in DMSO,¹⁹ and indeed, our NMR analysis suggested that β -cyclodextrin and DIFBO were both free in solution (Figure 8.5A). To obtain direct spectral evidence of the DIFBO- β -cyclodextrin complex, we performed solid state CPMAS ¹³C NMR analysis of the lyophilized powder in comparison to pure β -cyclodextrin (Figure 8.5B). The resonance corresponding to the anomeric carbon of glucose in the putative DIFBO- β -cyclodextrin complex was shifted downfield from the corresponding resonance in pure β -cyclodextrin. In addition, all of the cyclodextrin ¹³C resonances were broadened in the putative complex. Both of these effects have been previously observed in CPMAS ¹³C-NMR spectra of β -cyclodextrin inclusion complexes,^{20,21} supporting our conclusion that DIFBO was indeed inside the β -cyclodextrin cavity.

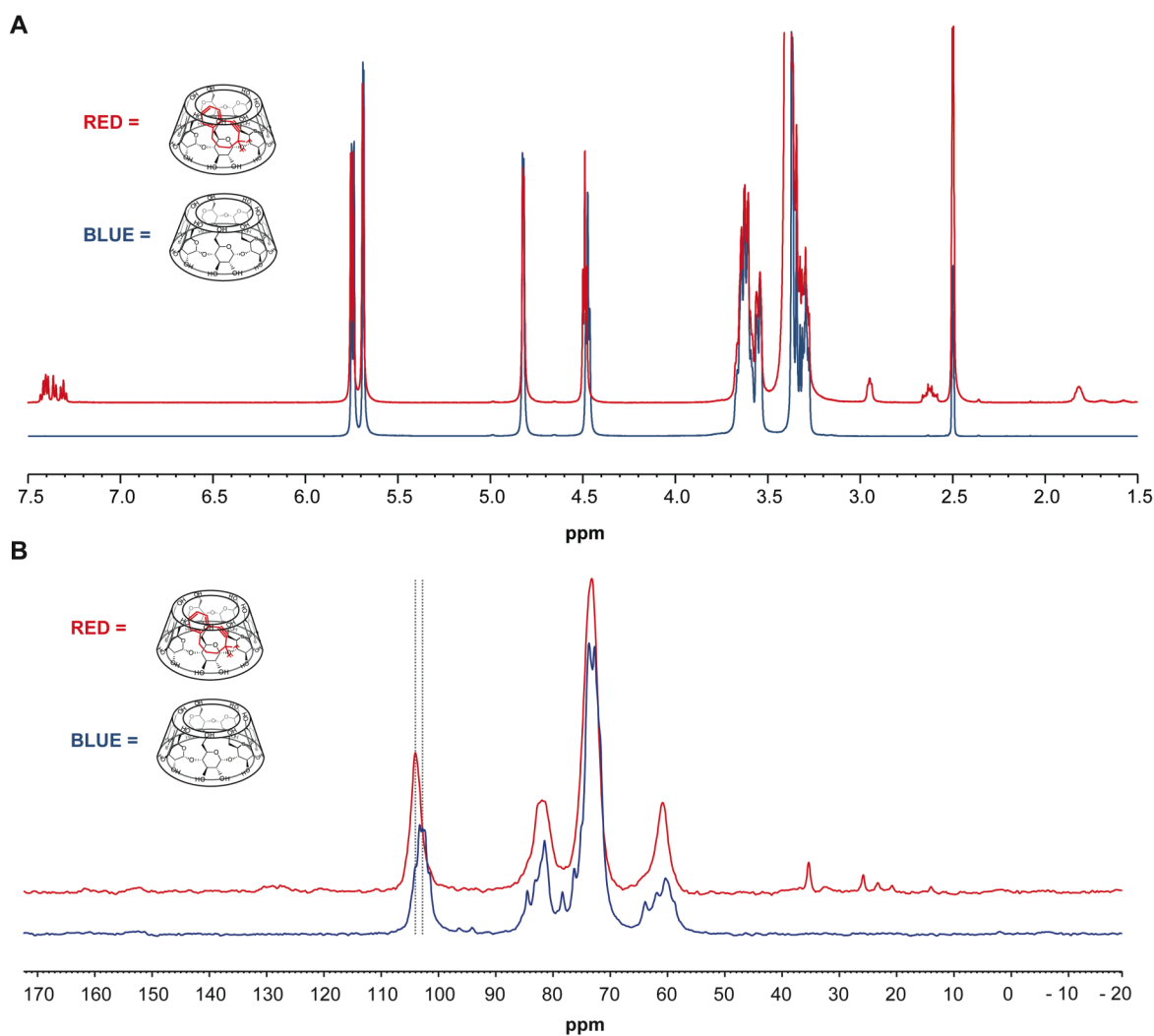


Figure 8.5. A. ^1H NMR spectrum in d_6 -DMSO of the β -cyclodextrin-DIFBO complex (red) and of β -cyclodextrin alone (blue). B. CPMAS ^{13}C NMR of the DIFBO- β -cyclodextrin complex (red) compared to β -cyclodextrin alone (blue).

Next a more detailed study of DIFBO's stability and reactivity with azides in the presence of β -cyclodextrin was performed. A solution of DIFBO in acetonitrile was combined with β -cyclodextrin and the aqueous mixtures were lyophilized. The resulting powders were resuspended in a solution of benzyl azide in acetonitrile and the products were analyzed by HPLC (Figure 8.6A) alongside synthetic standards (Figure 8.6B-E).

The reaction containing β -cyclodextrin produced two major products, which were identified as triazoles **8.11** and **8.12**, with only trace amounts of trimer isomers **8.8** and **8.9**. This result further confirms that β -cyclodextrin prevents trimerization of DIFBO. We then investigated the long-term stability of the DIFBO- β -cyclodextrin complex. The dry powder was periodically suspended in 1:1 acetonitrile/water containing benzyl azide and

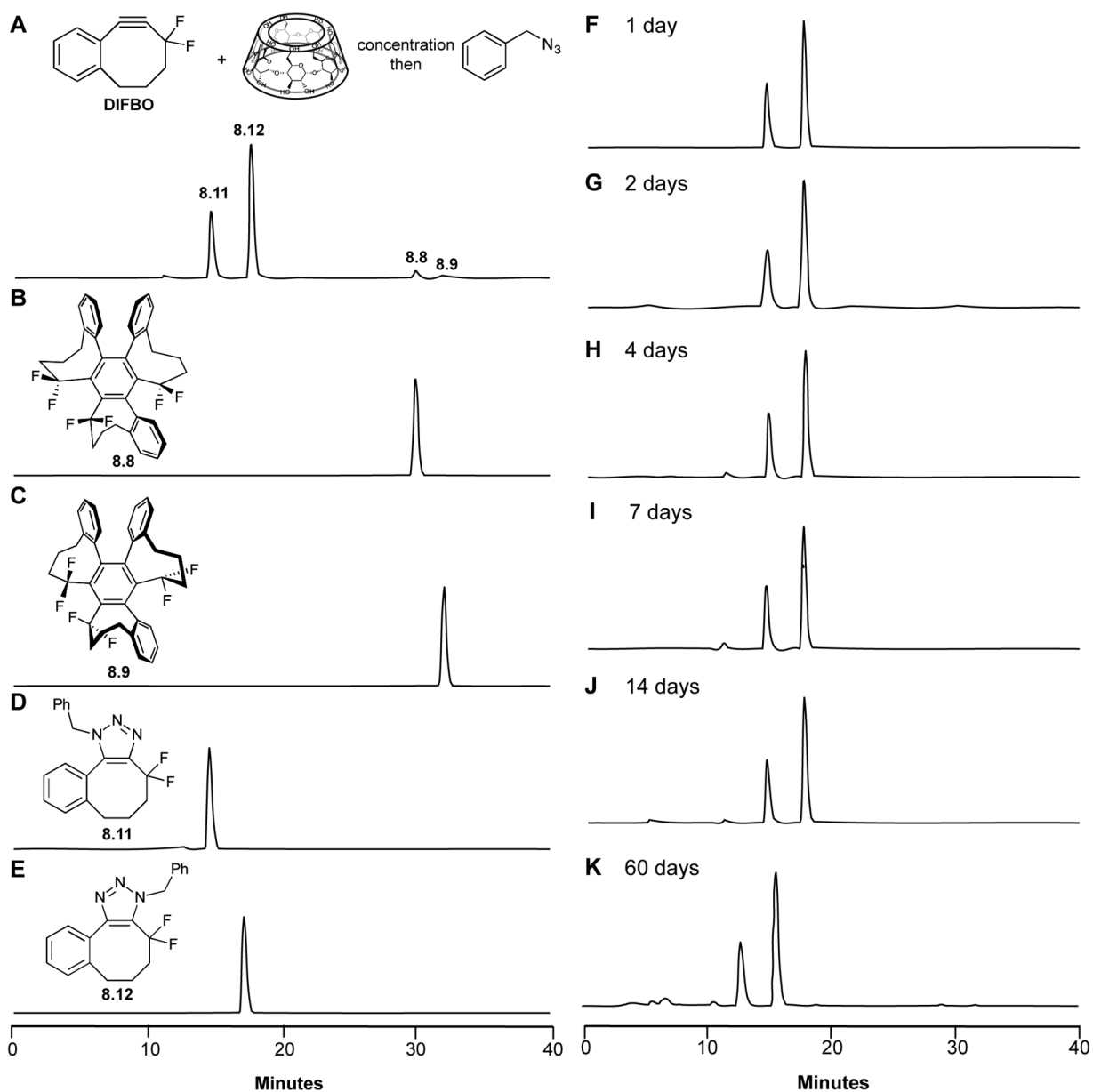


Figure 8.6. DIFBO is stable for 2 months as a β -cyclodextrin inclusion complex. A solution of DIFBO in acetonitrile was combined with β -cyclodextrin (1 equiv.) and concentrated. The resulting solid was resuspended in a 1:1 mixture of acetonitrile/water containing 1 equiv. of benzyl azide (final concentration of 600 μ M) immediately (A) or 1 (C), 2 (G), 4 (H), 7 (I), 14 (J), or 60 (K) days after preparation of the solid. The reaction mixtures were analyzed by reverse phase HPLC with detection by absorbance at 254 nm. Peak assignments were made through comparison to synthetic standards (B-E). The slight difference in retention times of the two triazole peaks in K as compared to F-J are attributed to a different HPLC column.

the integrity of DIFBO was determined indirectly by monitoring the formation of triazoles **8.11** and **8.12** as well as the absence of trimers **8.8** and **8.9**. No trimer formation, nor significant amounts of any other degradation products, were observed over the course of two months during storage on the benchtop at room temperature and open to air (Figure 8.6F-K). Therefore, β -cyclodextrin appears to be a convenient host for stabilization and storage of DIFBO. DIFBO can be readily extracted from the cyclodextrin by simply suspending the complex in organic solvent and removing the insoluble free cyclodextrin by filtration.

To ensure that the stability imparted on DIFBO was due to the correct matching of host and guest size, various additives were combined with DIFBO and subjected to the HPLC assay described above. These additives included all three cyclodextrins as well as monomeric glucose and water alone. In the absence of any additive (Figure 8.7A) or in the presence of water or glucose (Figure 8.7B/C), DIFBO formed trimers **8.8** and **8.9** prior to resuspension with benzyl azide. Similarly, addition of α -cyclodextrin had no stabilizing effect on DIFBO and only trimers were observed, indicating either that DIFBO cannot fit into the smaller cyclodextrin cavity or that its complex with α -cyclodextrin is relatively unstable (Figure 8.7D).

The products formed from the DIFBO/ γ -cyclodextrin mixture were more complicated (Figure 8.7F). Trimers **8.8** and **8.9** were the major species observed, though the presence of a small amount of triazoles **8.11** and **8.12** indicated that some DIFBO had been preserved through the lyophilization process, but this amount was minimal compared to the stabilization imparted by β -cyclodextrin (Figure 8.7E). More interestingly, multiple new peaks in the HPLC trace suggested that γ -cyclodextrin alters the reactivity of DIFBO. We isolated the two major new species (HPLC peaks designated with asterisks in Figure 8.7F) and, using mass spectrometry, NMR spectroscopy and X-ray crystallography, identified them as oxidized DIFBO dimers **8.14** and **8.15** (Figure 8.8). Both **8.14** and **8.15** comprise two DIFBO moieties as well as a molecule of oxygen, with **8.15** being hydrated as well.

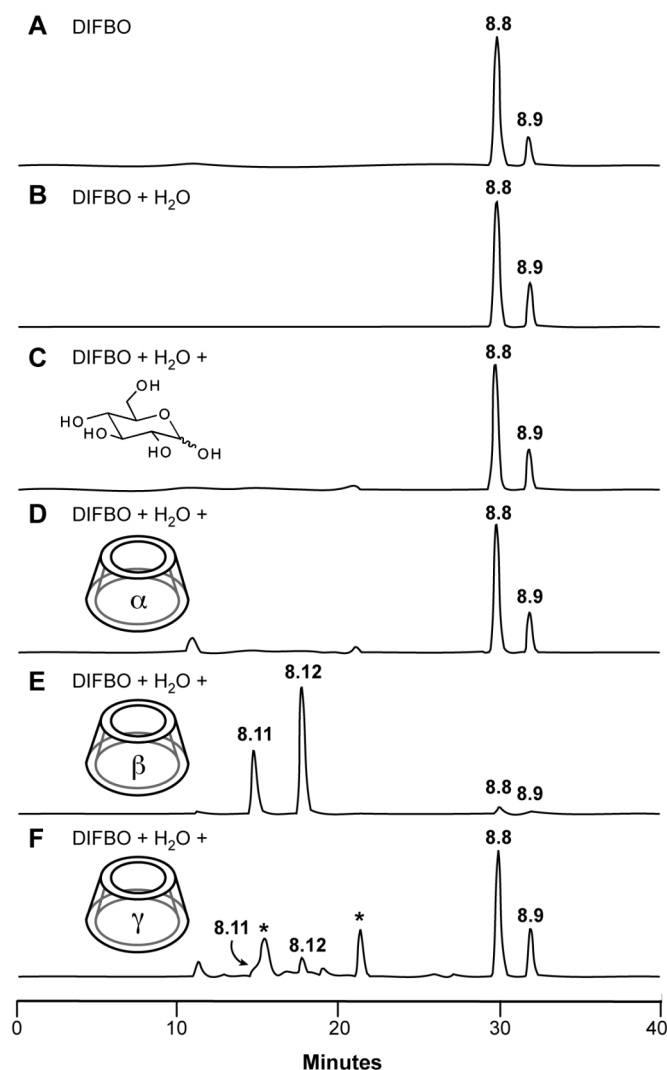


Figure 8.7. Only β -cyclodextrin prevents trimerization of DIFBO. Reverse phase HPLC analysis of lyophilized DIFBO mixtures treated with benzyl azide. A solution of DIFBO in acetonitrile was combined with no additive (A), water (B), glucose (C), α -cyclodextrin (D), β -cyclodextrin (E), or γ -cyclodextrin (F) and concentrated. The resulting solids were resuspended in a 1:1 mixture of acetonitrile/water containing 1 equiv. of benzyl azide (final concentration of 600 μ M). The reaction mixture was analyzed by reverse phase HPLC with detection by absorbance at 254 nm. Peak assignments were made through comparison to synthetic standards (Figure 8.6B-E).

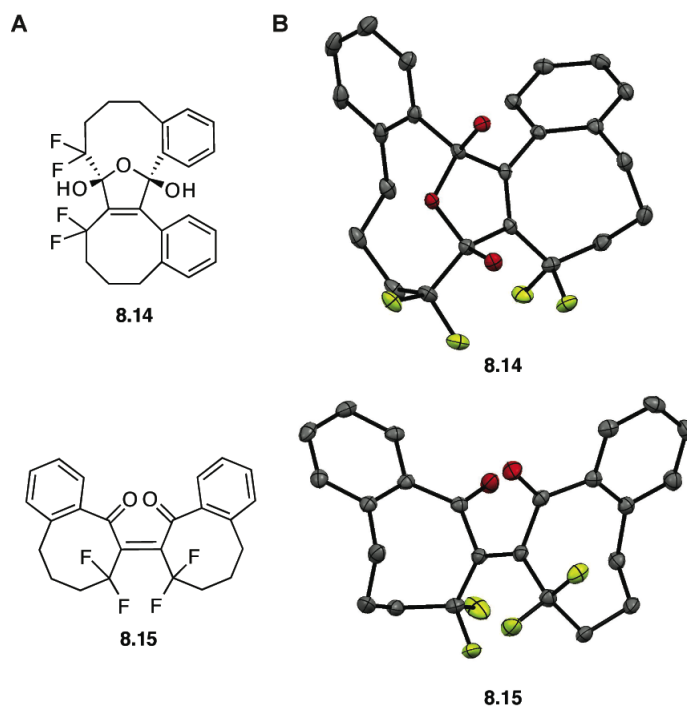
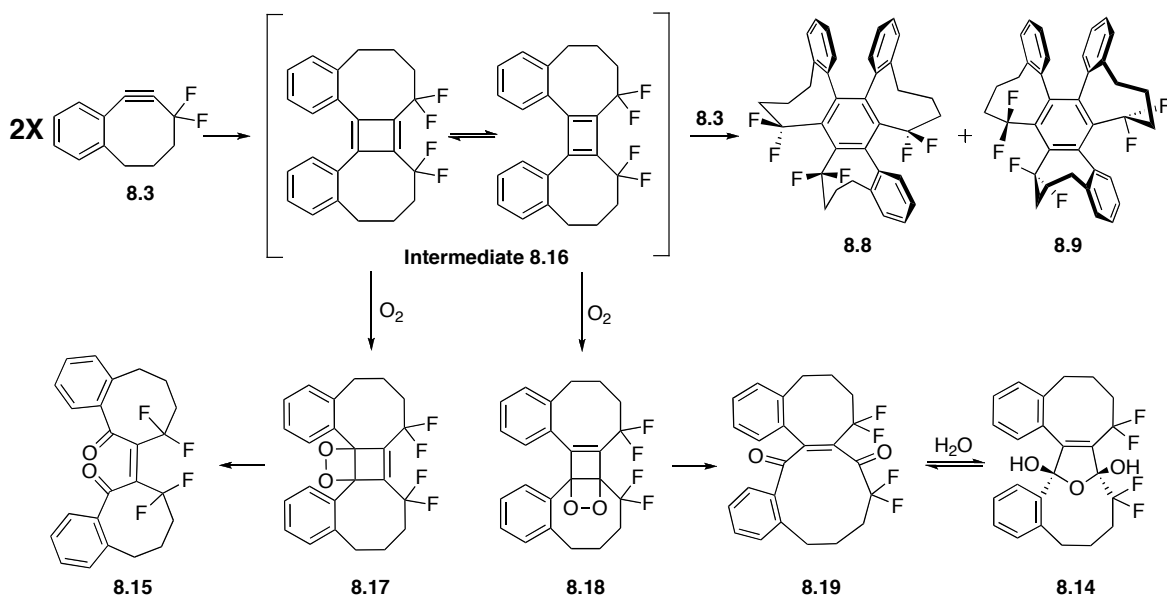


Figure 8.8. A. Chemical structures of dimers **8.14** and **8.15**. B. Thermal ellipsoids of dimers **8.14** and **8.15** shown with 50% probability. Grey atoms correspond to carbon, green atoms correspond to fluorine, and red atoms correspond to oxygen. The hydrogen atoms were removed for clarity.

We speculate that both **8.14** and **8.15** derive from a common intermediate, cyclobutadiene **8.16**, formed by dimerization of DIFBO (Scheme 8.5). This unstable antiaromatic intermediate presumably reacts rapidly with molecular oxygen to yield **8.17** or **8.18** depending on the automer of **8.16** which reacts with oxygen.^{22,23} C-C bond cleavage in either an exocyclic or endocyclic fashion with respect to the cyclooctyne rings leads to compound **8.15** or **8.19**, respectively. Compound **8.19** is readily hydrated due to the electrophilic α -fluorinated ketone. Compound **8.16** may also be an intermediate in the formation of trimers **8.8** and **8.9**, which constitute the two regioisomers formed by addition of another molecule of DIFBO. Indeed, rapid formation of **8.16** as the first step in the trimerization process would explain why C-3 symmetric trimer **8.10** is not observed.

Scheme 8.5. Proposed mechanism of DIFBO dimerization and trimerization.



The formation of dimers **8.14** and **8.15** only in the presence of γ -cyclodextrin raises an interesting question regarding the participation of this host molecule. It is possible that the γ -cyclodextrin cavity can accommodate two DIFBO molecules and thereby facilitate the dimerization reaction. Also, the host might uniquely bind intermediate **8.16**, thereby preventing its reaction with another large DIFBO molecule but not with molecular oxygen.

Precedent for Proposed Oligomerization Mechanism

Cyclobutadiene has a rich history as a guest molecule. The classic example of stabilization of cyclobutadiene in a host-guest complex is work from Cram's laboratory where unsubstituted cyclobutadiene was generated inside a hemicarcerand host, which sufficiently protected the cyclobutadiene for characterization by NMR (Figure 8.9).²⁴ More recent work has resulted in the first X-ray crystal structure of 1,3-dimethylcyclobutadiene, which was facilitated by complexation in a guanidinium-sulfonate-calixarene.²⁵

Additionally, there is considerable precedent for the dimerization of strained alkynes into cyclobutadiene. Cyclobutadiene **8.22**, the first cyclobutadiene that was stable at room temperature, was synthesized by Krebs and coworkers through the PdCl₂ mediated dimerization of 3,3,6,6-tetramethyl-1-thiacycloheptyne (**8.20**) through intermediate **8.21** (Scheme 8.6).^{26,27} Krebs has also hypothesized cyclobutadiene intermediates in the dimerization of highly strained 1,2-dehydrocyclooctatetraene.^{28,29} Furthermore, Wittig and coworkers have proposed cyclobutadiene intermediates in the trimer- and tetramerization of cyclohexyne.^{30,31}

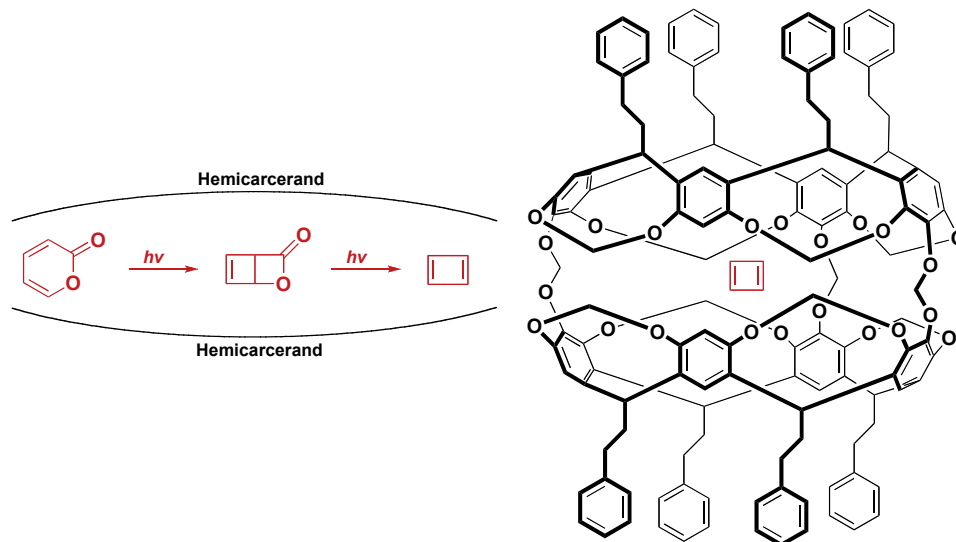
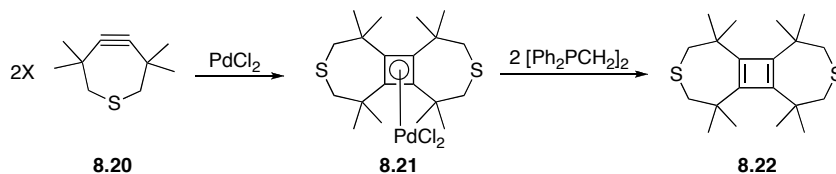


Figure 8.9. Work by Cram and coworkers where cyclobutadiene was generated inside a hemicarcerand host and characterized by NMR.

Scheme 8.6. Dimerization of thiacycloheptyne **8.20** to yield stable cyclobutadiene **8.22**.



Unexpected Lessons from DIFBO

Collectively, the data presented within this chapter lead us to believe that DIFBO's reactivity is rooted in its propensity to form a putatively antiaromatic compound. Thus, DIFBO offers a new tool to study the classical chemical principle of (anti)aromaticity that is still a topic of much discussion today.^{32,33} Additionally, the use of β -cyclodextrin to control the reactivity of DIFBO demonstrates a promising strategy to harness highly reactive small molecule components in bioconjugation reactions, opening the door for new, rapid bioorthogonal chemistries.

Materials and Methods

General Experimental Procedure

All chemical reagents were purchased from Sigma-Aldrich, Acros, and TCI and used without purification unless noted otherwise. Anhydrous DMF and MeOH were purchased from Aldrich or Acros in sealed bottles; all other solvents were purified as described by Pangborn *et al.*³⁴ In all cases, solvent was removed by reduced pressure with a Buchi Rotovapor R-114 equipped with a Welch self-cleaning dry vacuum. Products were further dried by reduced pressure with an Edwards RV5 high vacuum. Lyophilization was performed on a LABCONCO FreeZone[®] instrument equipped with an Edwards RV2 pump. Thin layer chromatography was performed with EMD 60 Å silica gel plates. Flash chromatography was performed using Silicycle[®] 60 Å 230-400 mesh silica. All ¹H, ¹³C, and ¹⁹F NMR spectra are reported in ppm and referenced to solvent peaks (¹H and ¹³C). Spectra were obtained on Bruker AVQ-400, AVB-400, DRX-500, AV-500, or AV-600 instruments. CPMAS ¹³C-NMR was performed on an AV-500 spectrometer (see below for further detail). Electron impact (EI) and electrospray ionization (ESI) mass spectra were obtained from the UC Berkeley Mass Spectrometry Facility. X-ray crystallography structures were obtained from the UC Berkeley X-ray Crystallography Facility.

Experimental Procedures

2,2-Difluoro-1-benzosuberone (8.5). Benzosuberone **8.4** (5, 1.0 mL, 6.7 mmol, 1 equiv.) was dissolved in cyclohexane (13.5 mL) and hexylamine (1.2 mL, 9.1 mmol, 1.4 equiv.) and trifluoroacetic acid (5 drops) were added. The reaction was heated to reflux overnight with azeotropic removal of water (Dean-Stark trap). The following morning the reaction mixture was evaporated to dryness, dissolved in ether (25 mL), washed with sat. NaHCO₃ (1 x 15 mL) and brine (1 x 15 mL). The organic solution was dried over MgSO₄ and evaporated to dryness. The resulting crude imine (1.8 g) was dissolved in acetonitrile (67 mL). To this solution Selectfluor[™] (5.01 g, 14.2 mmol, 2.1 equiv.) and Na₂SO₄ (680 mg, 4.9 mmol) were added. The reaction mixture was heated to reflux overnight. The following morning 3M HCl (4.5 mL) was added to hydrolyze the imine. After 10 min at reflux, the solution was cooled to rt and evaporated to dryness. The residue was dissolved in ether (25 mL), washed with sat. NaHCO₃ (1 x 15 mL) and brine (1 x 15 mL). The organic solution was dried over MgSO₄ and evaporated to dryness. The crude mixture was purified by flash chromatography with a hexane/ethyl acetate solvent system (30:1 to 15:1). This procedure yielded pure difluorobenzosuberone as a clear oil (0.92 g, 4.7 mmol, 70%). R_f = 0.4 in 4:1 hexane/ethyl acetate. ¹H NMR (400 MHz, CDCl₃): δ 7.72 (dd, *J* = 7.7, 1.3 Hz, 1H), 7.49 (td, *J* = 6.5, 1.4 Hz, 1H), 7.36 (td, *J* = 8.4, 0.9 Hz, 1H), 7.27 (dd, *J* = 7.7, 0.6 Hz, 1H), 3.04-3.07 (m, 2H), 2.35-2.46 (m, 2H), 2.04 (apparent quin, *J* = 6.4 Hz, 2H). ¹³C NMR (100 MHz, CDCl₃): δ 194.2 (t, *J* = 29 Hz), 141.7, 134.8, 133.0, 130.3, 129.9, 126.9, 119.0 (t, *J* = 250 Hz), 34.4 (t, *J* = 24 Hz), 33.6, 22.0 (t, *J* = 5 Hz). ¹⁹F NMR

(376 MHz, CDCl₃): δ -99.3 (t, J = 15 Hz, 2F). HRMS (EI): calcd. for C₁₁H₁₀OF₂⁺ [M]⁺, 196.0700; found, 196.0705.

7,7-difluoro-5-(trimethylsilyl)-7,8,9,10-tetrahydrobenzo[8]annulen-6(5H)-one (8.6).

Difluorobenzosuberone **8.4** (4.0 mmol, 1 equiv.) was dissolved in CH₂Cl₂ (50 mL) and cooled to -78 °C. To this solution, trimethylaluminum (2M solution in toluene, 2.0 mL, 4.0 mmol, 1 equiv.) was added. After 15 min, trimethylsilyl diazomethane (2M solution in hexanes, 2.0 mL, 4.0 mmol, 1 equiv.) was added. Five minutes later the reaction was quenched with sat. aqueous NH₄Cl and warmed to 0 °C. Rochelle's salt was added to complex the aluminum salts. This solution was stirred at rt for 15 min and then extracted with CH₂Cl₂ (3 x 75 mL). The organic layers were combined, dried with MgSO₄, decanted, and evaporated to dryness. This procedure resulted compound **7** with 33% toluene remaining (1.2 g, 3.9 mmol, 97%). R_f = 0.85 in 4:1 hexane/EtOAc. ¹H NMR (600 MHz, CDCl₃): δ 7.17-7.22 (m, 2H), 7.07 (dd, J = 6.8, 2.0 Hz, 1H), 7.04 (dd, J = 6.9, 1.9 Hz, 1H), 3.67 (s, 1H), 2.75 (dt, J = 14.7, 4.6 Hz, 1H), 2.45-2.51 (m, 1H), 2.04-2.12 (m, 1H), 1.90-1.97 (m, 1H), 1.64-1.76 (m, 1H), 1.56-1.63 (m, 1H), 0.12 (s, 9H). ¹³C NMR (150 MHz, CDCl₃): δ 201.8 (t, J = 27 Hz), 137.7, 135.1, 130.4, 130.1, 126.9, 126.7, 119.2 (t, J = 252 Hz), 48.6, 33.1 (t, J = 25 Hz), 30.2, 23.6 (t, J = 5 Hz), -1.6. ¹⁹F NMR (564 MHz, CDCl₃): δ -100.95 (apparent t, J = 17 Hz, 1F), -100.99 (dd, J = 23, 17 Hz, 1F). HRMS (EI): calcd. for C₁₅H₂₀OF₂Si⁺ [M]⁺, 282.1253; found, 282.1255.

7,7-difluoro-5-(trimethylsilyl)-7,8,9,10-tetrahydrobenzo[8]annulen-6-yl triflate (8.7).

A solution of compound **8.6** (8.5 mmol, 1 equiv) in THF (110 mL) was cooled to -78 °C and potassium bis(trimethylsilyl)amide (0.5 M solution in toluene, 20.4 mL, 10.2 mmol, 1.2 equiv.) was added and the solution turned a dark orange/brown. After 1 h, trifluoromethane sulfonic anhydride (Tf₂O, 2.07 mL, 10.2 mmol, 1.2 equiv.) was added and the solution turned a lighter yellow color. The solution was stirred for 3 hr, warming to ~ -45 °C, at which point it was quenched with methanol and evaporated to dryness. CAUTION: If a large XS of Tf₂O is used or this reaction is warmed to room temperature before quenching, a gel will form that is very difficult to separate compound **8.7** from. The crude product was purified via silica gel chromatography with a hexane/toluene solvent system (75:1, 50:1, 25:1). This procedure resulted in pure TMS vinyl triflate **8.7** in 80% yield (2.8 g, 6.8 mmol). R_f = 0.8 in 6:1 hexane/ethyl acetate. ¹H NMR (400 MHz, CDCl₃): δ 7.24-7.29 (m, 2H), 7.16-7.19 (m, 1H), 7.03-7.07 (m, 1H), 2.77 (dt, J = 13.1, 4.4 Hz, 1H), 2.56 (td, J = 5.3, 1.3 Hz, 1H), 1.91-2.13 (m, 2H), 1.49-1.69 (m, 2H), 0.19 (s, 9H). ¹³C NMR (100 MHz, CDCl₃): δ 144.9 (t, J = 28 Hz), 142.7 (t, J = 4 Hz), 136.2 (t, J = 3 Hz), 135.8, 128.7, 128.4, 126.7, 126.5, 119.0 (q, J = 321 Hz), 118.3 (dd, J = 246, 241 Hz), 32.6 (t, J = 25 Hz), 30.2, 23.9 (dd, J = 7, 3 Hz), -0.62. ¹⁹F NMR (376 MHz, CDCl₃): δ -70.1 (t, J = 13 Hz, 3F), -84.5 (dsex, J = 277, 11 Hz, 1F), -92.0 (dm, J = 278 Hz, 1F). HRMS (EI): calcd. for C₁₆H₁₉O₃F₅Si⁺ [M]⁺, 414.0744; found, 414.0642.

Difluorobenzocyclooctyne (DIFBO, 8.3). TMS vinyl triflate **8.7** (34 mg, 0.082 mmol, 1 equiv.) was dissolved in CD₃CN (3 mL) and CsF (75 mg, 0.50 mmol, 6 equiv.) was added. The reaction was stirred at rt for ~30 min (reaction mixture turns yellow and has a foul odor), at which point it was transferred directly onto a plug of silica gel and eluted with CD₃CN (0.75 mL). A portion of this solution was taken for NMR analysis. R_f = 0.75 in 4:1 hexane/ethyl acetate. ¹H NMR (500 MHz, CD₃CN): δ 7.38 (t, *J* = 8.1 Hz, 1H), 7.33 (t, *J* = 7.3 Hz, 1H), 7.26-7.31 (m, 2H), 2.97 (apparent t, *J* = 5.0 Hz, 2H), 2.57-2.65 (m, 2H), 1.89 (bs, 2H). Too unstable for ¹³C NMR. ¹⁹F NMR (564 MHz, CD₃CN): δ -87.5 (bs, 2F). HRMS (EI): calcd. for C₁₂H₁₀F₂⁺ [M]⁺, 192.0751; found, 192.0754.

Trimer 8.8. Elutes from reverse phase (C-18) HPLC at 29.7 min using CH₃CN/H₂O solvent system with a gradient of 50% to 100% CH₃CN over 25 min followed by 10 min of 100% CH₃CN. R_f = 0.45 in 4:1 hexane/ethyl acetate. ¹H NMR (500 MHz, CDCl₃): δ 7.51 (bs, 1H), 7.33 (td, *J* = 7.5, 0.9 Hz, 1H), 7.23 (*J* = 7.5, 1.0 Hz, 1H), 7.18 (d, *J* = 7.5, 1H), 7.00-7.09 (m, 4H), 6.83-6.89 (m, 3H), 6.68 (d, *J* = 7.3 Hz, 1H), 2.79-2.84 (m, 1H), 2.53-2.59 (m, 3H), 2.40 (apparent t, *J* = 6.4 Hz, 2H), 2.31 (td, *J* = 12.9, 5.6 Hz, 1H), 1.88-2.08 (m, 4H), 1.76-1.80 (m, 1H), 1.64-1.73 (m, 2H), 1.55-1.62 (m, 1H), 1.24-1.47 (m, 3H). ¹³C NMR (150 MHz, CDCl₃): δ 141.6 (dd, *J* = 5, 4 Hz), 141.02, 140.99, 139.9 (dd, *J* = 30, 22 Hz), 139.6 (t, *J* = 4 Hz), 138.9, 138.7 (apparent t, *J* = 3 Hz), 138.6 (d, *J* = 3 Hz), 138.3, 137.4, 136.8 (t, *J* = 23 Hz), 135.5 (dd, *J* = 33, 26 Hz), 133.4 (q, *J* = 5 Hz), 132.1, 131.2, 128.5, 128.08, 128.07, 128.01, 127.2, 127.1, 125.1 (dd, *J* = 247, 244 Hz), 125.0, 124.7, 124.1, 123.1 (dd, *J* = 247, 244 Hz), 122.8 (dd, *J* = 254, 240 Hz), 38.7 (td, *J* = 28, 7 Hz), 37.5 (t, *J* = 30 Hz), 35.8 (t, *J* = 28 Hz), 30.64, 30.61, 30.1, 24.0 (apparent q, *J* = 4 Hz), 23.6 (dd, *J* = 7, 3 Hz), 21.2 (d, *J* = 10 Hz). ¹⁹F NMR (564 MHz, CDCl₃): δ -59.1 (d, *J* = 255 Hz, 1F), -66.7 (d, *J* = 274 Hz, 1F), -70.0 (dd, *J* = 276, 71 Hz, 1F), -71.4 (dtt, *J* = 257, 70, 13 Hz, 1F), -75.8 (ddd, *J* = 275, 33, 10 Hz, 1F), -76.9 (dquin, *J* = 277, 30 Hz, 1F). HRMS (EI): calcd. for C₃₆H₃₀F₆⁺ [M]⁺, 576.2252; found, 576.2265.

Trimer 8.9. Elutes from reverse phase (C-18) HPLC at 31.7 min using CH₃CN/H₂O solvent system with a gradient of 50% to 100% CH₃CN over 25 min followed by 10 min of 100% CH₃CN. R_f = 0.55 in 4:1 hexane/ethyl acetate. ¹H-NMR (500 MHz, CDCl₃): δ 7.51-7.45 (m, 1H), 7.31 (td, *J* = 7.5, 1.2 Hz, 1H), 7.21 (td, *J* = 7.7, 1.1 Hz, 1H), 7.14 (d, *J* = 7.5 Hz, 1H), 6.96-7.05 (m, 4H), 6.72 (td, *J* = 7.4, 1.4 Hz, 1H), 6.66 (td, *J* = 7.7, 0.9 Hz, 1H), 6.47 (d, *J* = 7.6 Hz, 1H), 6.33 (d, *J* = 7.5 Hz, 1H), 2.67-2.82 (m, 4H), 2.52-2.65 (m, 2H), 2.45-2.51 (m, 1H), 2.33-2.39 (m, 1H), 2.05-2.20 (m, 3H), 1.87-1.98 (m, 2H), 1.76-1.84 (m, 1H), 1.59-1.71 (m, 3H), 1.48-1.58 (m, 1H). ¹³C NMR (125 MHz, CDCl₃): δ 141.2-141.3 (m), 140.6 (d, *J* = 7 Hz), 140.0 (d, *J* = 4 Hz), 139.7-139.8 (m), 139.5 (d, *J* = 5 Hz), 139.2-139.3 (m), 139.1 (d, *J* = 1 Hz), 138.2 (apparent q, *J* = 22 Hz), 137.1 (apparent t, *J* = 24 Hz), 133.7-133.8 (m), 130.5 (d, *J* = 3 Hz), 129.5, 128.2, 128.03, 127.99, 127.94, 127.2, 127.0, 125.7 (t, *J* = 245 Hz), 125.4, 124.6, 124.3 (apparent d, *J* = 245 Hz), 123.8, 123.3 (t, *J* = 246 Hz), 39.0 (td, *J* = 39, 27 Hz), 38.1 (td, *J* = 27, 11 Hz), 36.0 (t, *J* = 27 Hz), 31.1, 30.7, 30.2, 24.8-24.9 (m), 24.3 (apparent quin, *J* = 3 Hz), 23.6 (apparent q, *J* = 4 Hz). ¹⁹F NMR (564 Hz, CDCl₃): δ -62.2 (dt, *J* = 255, 16 Hz, 1F), -67.7 (dd, *J* = 270, 17 Hz, 1F), -69.1

(dd, $J = 255, 25$ Hz, 1F), -71.3 (dd, $J = 253, 81$ Hz, 1F), -72.6- -73.6 (m, 2F). HRMS (EI): calcd. for $C_{36}H_{30}F_6^+ [M]^+$, 576.2252; found, 576.2252.

Cycloadducts of benzyl azide and DIFBO (8.11, 8.12). Compound **8.7** (202 mg, 0.49 mmol, 1 equiv.) and CsF (440 mg, 2.9 mmol, 5.9 equiv.) were combined in CH_3CN (10 mL). After 15 minutes, benzyl azide (66 μ L, 0.53 mmol, 1.1 equiv.) was added. This mixture was let stir overnight at rt. The following morning the reaction mixture was evaporated to dryness and purified by silica gel chromatography (hexane/ethyl acetate system) to yield two triazole products (**8.11**, 55 mg, 0.17 mmol, 35%) and (**8.12**, 92 mg, 0.28 mmol, 58%). Compound **8.11**: $R_f = 0.2$ in 6:1 hexane/ethyl acetate. 1H NMR (600 MHz, CD_3CN): δ 7.48 (td, $J = 7.5, 1.5$ Hz, 1H), 7.44 (dd, $J = 7.7, 1.3$ Hz, 1H), 7.39 (apparent td, $J = 7.5, 1.3$ Hz, 1H), 7.30 (d, $J = 7.6$ Hz, 1H), 7.20-7.22 (m, 3H), 6.88-6.90 (m, 2H), 5.56 (apparent d, $J = 3.1$ Hz, 2H), 2.57 (apparent dd, $J = 13.4, 6.2$ Hz, 1H), 2.06-2.19 (m, 3H), 1.73-1.85 (m, 1H), 1.61-1.67 (m, 1H). ^{13}C NMR (150 MHz, CD_3CN): δ 143.1 (t, $J = 30$ Hz), 141.1, 136.6, 135.3 (t, $J = 6$ Hz), 132.0, 130.5, 130.0, 129.7, 129.1, 128.2, 127.9, 126.6, 119.1 (dd, $J = 235, 231$ Hz), 53.0, 31.9 (t, $J = 24$ Hz), 30.6, 25.9 (d, $J = 9$ Hz). ^{19}F NMR (564 MHz, CD_3CN): δ -91.8 (ddd, $J = 271, 34, 6$ Hz, 2F). HRMS (ESI): calcd. for $C_{19}H_{18}N_3F_2^+ [M+H]^+$, 326.1463; found, 326.1461. Compound **8.12**: $R_f = 0.6$ in 6:1 hexanes/ethyl acetate. 1H NMR (600 MHz, CD_3CN): δ 7.72 (dd, $J = 7.6, 1.3$ Hz, 1H), 7.45 (td, $J = 7.5, 1.5$ Hz, 1H), 7.36-7.41 (m, 3H), 7.32-7.35 (m, 4H), 5.80 (s, 2H), 2.50-2.68 (bm, 2H), 1.62-2.21 (bm, 4H). ^{13}C NMR (150 MHz, CD_3CN): δ 145.8 (t, $J = 6$ Hz), 139.5, 137.0, 131.5, 130.8, 130.7 (t, $J = 131$ Hz), 130.4, 130.2, 129.7, 129.2, 128.7, 127.8, 119.2 (t, $J = 235$ Hz), 54.5 (t, $J = 3$ Hz), 32.4 (t, $J = 24$ Hz), 30.8, 26.5 (t, $J = 5$ Hz). ^{19}F NMR (564 MHz, CD_3CN): δ -74.1 (d, $J = 270$ Hz, 1F), -89.8 (d, $J = 265$ Hz, 1F). HRMS (ESI): calcd. for $C_{19}H_{18}N_3F_2^+ [M+H]^+$, 326.1463; found, 326.1460.

Dimer 8.14. Elutes from reverse phase (C-18) HPLC at 15.3 min using CH_3CN/H_2O solvent system with a gradient of 50% to 100% CH_3CN over 25 min followed by 10 min of 100% CH_3CN . $R_f = 0.15$ in 4:1 hexane/ethyl acetate. In solution this compound sits as a mixture of isomers in a 3:1 ratio. Minor compound designated as H' (only major product tabulated for ^{13}C and ^{19}F NMR). 1H NMR (500 MHz, $CDCl_3$): δ 8.09 (d, $J = 7.9$ Hz, 1H'), 7.53 (d, $J = 7.9$ Hz, 1H), 7.34 (td, $J = 7.5, 1.2$ Hz, 1H), 7.18-7.28 (m, 4H, 3H'), 7.09-7.11 (m, 2H'), 7.04 (bs, 1H'), 6.94 (d, $J = 7.4$, 1H'), 6.85 (td, $J = 7.8, 1.0$ Hz, 1H), 6.15 (d, $J = 7.8$ Hz, 1H), 4.21 (bs, 1H'), 4.15 (bs, 1H), 4.04 (bs, 1H'), 3.36 (bs, 1H), 2.94-3.01 (m, 2H), 2.86 (apparent dd, $J = 14.5, 3.5$ Hz, 1H), 2.78 (apparent dd, $J = 13.3, 6.0$ Hz, 1H), 2.64-2.67 (m, 1H'), 2.51 (dt, $J = 14, 3.5$ Hz, 1H'), 2.21-2.39 (m, 2H, 5H'), 1.93-2.19 (m, 4H, 1H'), 1.70-1.83 (m, 1H, 3H'), 1.55-1.61 (m, 1H, 1H'). ^{13}C NMR (150 MHz, $CDCl_3$): δ 146.7 (t, $J = 8.4$ Hz), 141.8, 140.1 (d, $J = 3$ Hz), 135.6, 133.8 (t, $J = 30$ Hz), 131.5, 130.3, 129.9, 128.9, 128.5, 126.9, 126.7, 125.8, 121.6 (dd, $J = 256, 250$ Hz), 120.0 (dd, $J = 240, 232$ Hz), 110.3, 107.0 (dd, $J = 33, 25$ Hz), 36.6 (apparent td, $J = 25, 6$ Hz), 34.4, 32.2 (t, $J = 26$ Hz), 30.4, 24.9 (d, $J = 9$ Hz), 23.1 (d, $J = 11$ Hz). ^{19}F NMR (564 MHz, $CDCl_3$): δ -74.8 (d, $J = 270$ Hz, 1F), -93.6 (d, $J = 287$ Hz, 1F), -99.1 (d, $J = 259$ Hz, 1F), -110.2 (d, $J = 260$ Hz, 1F). HRMS (ESI): calcd. for $C_{24}H_{22}F_4O_3Na^+ [M+Na]^+$, 457.1403; found, 457.1413.

Dimer 8.15. Elutes from reverse phase (C-18) HPLC at 21.3 min using CH₃CN/H₂O solvent system with a gradient of 50% to 100% CH₃CN over 25 min followed by 10 min of 100% CH₃CN. R_f = 0.4 in 4:1 hexane/ethyl acetate. ¹H NMR (500 MHz, CDCl₃): δ 7.90 (dd, *J* = 8.0, 1.4 Hz, 1H), 7.52 (td, *J* = 7.5, 1.5 Hz, 1H), 7.30 (td, *J* = 6.7, 1.2 Hz, 1H), 7.25 (d, *J* = 9.2 Hz, 1H), 3.42 (bs, 2H), 2.33 (bs, 2H), 2.01 (bs, 2H). ¹³C NMR (125 MHz, CDCl₃): δ 193.3 (d, *J* = 3 Hz), 145.1-145.6 (m), 143.0, 135.6, 134.8, 131.8, 129.9, 127.1, 120.4 (ddd, *J* = 253, 246, 8 Hz), 35.8-36.0 (m), 31.3, 23.3 (t, *J* = 2 Hz). ¹⁹F NMR (564 MHz, CDCl₃): δ -86.5 (bs, 2F). HRMS (ESI): calcd. for C₂₄H₂₀O₂F₄Na⁺ [M+Na]⁺, 439.1292; found, 439.1270.

DIFBO-β-cyclodextrin complex (8.13). DIFBO precursor **8.7** (256 mg, 0.618 mmol, 1 equiv.) was dissolved in acetonitrile (26 mL) and CsF (573 mg, 3.77 mmol, 6.1 equiv.) was added. This mixture was allowed to stir at rt until all **8.7** was converted into DIFBO (~25 min, turns slightly yellow in color and has a foul odor). This solution was directly loaded onto silica gel and eluted with hexane. The fractions containing DIFBO were combined with ~75 mL acetonitrile and the hexane was removed by careful rotary evaporation at rt. The remaining DIFBO/acetonitrile solution was added to a solution of β-cyclodextrin (recrystallized, 702 mg, 0.618 mmol, 1 equiv, in 50 mL DI H₂O). The solution becomes cloudy. The acetonitrile was removed by rotary evaporation and the resulting aqueous solution was flash-frozen in liquid N₂ and lyophilized to a white powder (688 mg, 0.518 mmol, 84%).

CPMAS ¹³C NMR Procedure

Solid-state NMR measurements of β-cyclodextrin and β-cyclodextrin-DIFBO complex were taken at rt on a 11.75 T Bruker Avance NMR spectrometer equipped with a double resonance magic angle spinning (MAS) probe. Samples were spun at 10 kHz using zirconia rotors of 4 mm outer diameter and 80 μL sample volume. The 1-D ¹³C cross-polarization (CP) experiments were conducted using a ¹H 90° pulse of 4.2 μs, a 59 kHz ¹H-decoupling field, 2 ms contact time, 2 s recycle delay and 1800-4000 scans. The ¹³C chemical shifts were referenced against the adamantane ¹³C signals at 29.45 and 38.48 ppm.

Analysis of DIFBO-Cyclodextrin Complexes

DIFBO was generated, purified, and transferred into acetonitrile as described above. The resulting DIFBO-acetonitrile solution was divided into six portions (A-F) that were treated in different manners. Portion A was evaporated to dryness and placed on the lyophilizer. Portion B was combined with water (4 mL), the acetonitrile was removed by rotary evaporation and the resulting aqueous solution was flash-frozen and lyophilized. Portion C was combined with 1 equiv. of glucose in water (4 mL) and treated in the same manner as portion B. Portion D, E and F were treated in the same manner as portion C

except the glucose was replaced by β -cyclodextrin, α -cyclodextrin, or γ -cyclodextrin respectively.

For HPLC analysis of the resulting products, 0.6 μmol of each powder was dissolved in $\text{CH}_3\text{CN}/\text{H}_2\text{O}$ (1 mL, 1:1 ratio). To this solution, 1 equiv. of benzyl azide (15 μL of 0.04 mM solution in 1:1 $\text{CH}_3\text{CN}/\text{H}_2\text{O}$) was added and the mixture was let react overnight. The following morning 150 nmol (250 μL) was analyzed by reverse phase HPLC (C-18 column) using a gradient of 50% $\text{CH}_3\text{CN}/50\%$ H_2O to 100% CH_3CN over 25 min followed by isocratic elution with 100% CH_3CN for 10 min before re-equilibration to 50% $\text{CH}_3\text{CN}/50\%$ H_2O . The chromatography was monitored by absorbance at 210 and 254 nm.

X-Ray Crystallography

Major Trimer 8.8. A colorless prism 0.12 x 0.08 x 0.04 mm in size was mounted on a Cryoloop with Paratone oil. Data were collected in a nitrogen gas stream at 100(2) K using phi and omega scans. Crystal-to-detector distance was 60 mm and exposure time was 5 seconds per frame using a scan width of 1.0° . Data collection was 99.9% complete to 67.00° in q . A total of 12405 reflections were collected covering the indices, $-10 \leq h \leq 10$, $-15 \leq k \leq 14$, $-14 \leq l \leq 14$. 4349 reflections were found to be symmetry independent, with an R_{int} of 0.0149. Indexing and unit cell refinement indicated a primitive, monoclinic lattice. The space group was found to be P2(1) (No. 4). The data were integrated using the Bruker SAINT software program and scaled using the SADABS software program. Solution by direct methods (SIR-2008) produced a complete heavy-atom phasing model consistent with the proposed structure. All non-hydrogen atoms were refined anisotropically by full-matrix least-squares (SHELXL-97). All hydrogen atoms were placed using a riding model. Their positions were constrained relative to their parent atom using the appropriate HFIX command in SHELXL-97.

Minor trimer 8.9. A colorless rod 0.20 x 0.20 x 0.20 mm in size was mounted on a Cryoloop with Paratone oil. Data were collected in a nitrogen gas stream at 100(2) K using phi and omega scans. Crystal-to-detector distance was 60 mm and exposure time was 5 seconds per frame using a scan width of 1.0° . Data collection was 97.5% complete to 67.00° in q . A total of 46641 reflections were collected covering the indices, $-13 \leq h \leq 13$, $-13 \leq k \leq 13$, $-26 \leq l \leq 29$. 9620 reflections were found to be symmetry independent, with an R_{int} of 0.0356. Indexing and unit cell refinement indicated a primitive, triclinic lattice. The space group was found to be P-1 (No. 2). The data were integrated using the Bruker SAINT software program and scaled using the SADABS software program. Solution by direct methods (SIR-2008) produced a complete heavy-atom phasing model consistent with the proposed structure. All non-hydrogen atoms were refined anisotropically by full-matrix least-squares (SHELXL-97). All hydrogen atoms were placed using a riding model. Their positions were constrained relative to their parent atom using the appropriate HFIX command in SHELXL-97.

Dimer 8.14. A colorless prism 0.12 x 0.10 x 0.06 mm in size was mounted on a Cryoloop with Paratone oil. Data were collected in a nitrogen gas stream at 100(2) K using phi and omega scans. Crystal-to-detector distance was 60 mm and exposure time was 5 seconds per frame using a scan width of 1.0°. Data collection was 97.9% complete to 67.00° in q. A total of 38046 reflections were collected covering the indices, $-13 \leq h \leq 13$, $-13 \leq k \leq 17$, $-18 \leq l \leq 18$. 7750 reflections were found to be symmetry independent, with an R_{int} of 0.0245. Indexing and unit cell refinement indicated a primitive, triclinic lattice. The space group was found to be P-1 (No. 2). The data were integrated using the Bruker SAINT software program and scaled using the SADABS software program. Solution by direct methods (SIR-2008) produced a complete heavy-atom phasing model consistent with the proposed structure. All non-hydrogen atoms were refined anisotropically by full-matrix least-squares (SHELXL-97). All hydrogen atoms, except for the water hydrogen atoms H8x and H8y, were placed using a riding model. Their positions were constrained relative to their parent atom using the appropriate HFIX command in SHELXL-97. The hydrogen atoms H8x and H8y were located from the Fourier difference map and their distances were restrained to the parent oxygen atom O8.

Dimer 8.15. A colorless prism 0.12 x 0.10 x 0.05 mm in size was mounted on a Cryoloop with Paratone oil. Data were collected in a nitrogen gas stream at 100(2) K using phi and omega scans. Crystal-to-detector distance was 60 mm and exposure time was 5 seconds per frame using a scan width of 1.0°. Data collection was 97.7% complete to 67.00° in q. A total of 16000 reflections were collected covering the indices, $-9 \leq h \leq 9$, $-10 \leq k \leq 10$, $-17 \leq l \leq 16$. 3374 reflections were found to be symmetry independent, with an R_{int} of 0.0180. Indexing and unit cell refinement indicated a primitive, triclinic lattice. The space group was found to be P-1 (No. 2). The data were integrated using the Bruker SAINT software program and scaled using the SADABS software program. Solution by direct methods (SIR-2008) produced a complete heavy-atom phasing model consistent with the proposed structure. All non-hydrogen atoms were refined anisotropically by full-matrix least-squares (SHELXL-97). All hydrogen atoms were placed using a riding model. Their positions were constrained relative to their parent atom using the appropriate HFIX command in SHELXL-97.

Cell Culture

Jurkat (human T cell lymphoma) cells were maintained in a 5% CO₂, water-saturated atmosphere and grown in RPMI 1640 media supplemented with 10% FBS, penicillin (100 units/ml), and streptomycin (0.1 mg/ml). Cell densities were maintained between 1×10^5 and 2×10^6 cells per mL.

Cell-Surface Azide Labeling and Detection

Jurkat cells were incubated in untreated media or media containing 25 μM Ac₄ManNAz. After 3 d, the cells were twice concentrated (500 x g, 3 min, 4 °C) and

resuspended in 10 mL FACS buffer (PBS containing 1% FCS, 2 x 10 mL) and cells (approx. 500,000 per a well) were placed in a 96 well V-bottom plate. The cells were concentrated by centrifugation (2500 x g, 3 min, 4 °C), resuspended in 200 µL cold FACS buffer, and again concentrated by centrifugation (2500 x g, 3 min, 4 °C). The cells were then reacted for 1 h at rt with the specified reagent DIBO-biotin or DIFO-biotin (10 µM). After 1 h, the cells were thrice concentrated by centrifugation (2500 x g, 3 min, 4 °C) and resuspended in 200 µL cold FACS buffer. Following an additional concentration by centrifugation (2500 x g, 3 min, 4 °C), cells were resuspended in FACS buffer (100 µL) containing FITC-avidin (1:200 dilution of 1 mg/mL stock, Sigma-Aldrich) and incubated in the dark at 4 °C for 15 min. Following the incubation, cells were concentrated by centrifugation, resuspended in 200 µL cold FACS buffer, concentrated by centrifugation, and another FITC-avidin incubation was performed. After the second FITC-avidin labeling, the cells were thrice concentrated by centrifugation (2500 x g, 3 min, 4 °C) and resuspended in 200 µL cold FACS buffer. The cells were then diluted to 400 µL for flow cytometry analysis. Flow cytometry was performed on a BD Biosciences FACSCalibur flow cytometer equipped with a 488-nm argon laser. All flow cytometry experiments were performed with three replicate samples.

References

- (1) Ning, X.; Guo, J.; Wolfert, M. A.; Boons, G.-J. Visualizing metabolically labeled glycoconjugates of living cells by copper-free and fast Huisgen cycloadditions. *Angew. Chem. Int. Ed.* **2008**, *47*, 2253-2255.
- (2) Schoenebeck, F.; Ess, D. H.; Jones, G. O.; Houk, K. N. Reactivity and regioselectivity in 1,3-dipolar cycloadditions of azides to strained alkynes and alkenes: A computational study. *J. Am. Chem. Soc.* **2009**, *131*, 8121-8133.
- (3) Ess, D. H.; Jones, G. O.; Houk, K. N. Transition states of strain-promoted metal-free click chemistry: 1,3-Dipolar cycloadditions of phenyl azide and cyclooctynes. *Org. Lett.* **2008**, *10*, 1633-1636.
- (4) Chenoweth, K.; Chenoweth, D.; Goddard III, W. A. Cyclooctyne-based reagents for uncatalyzed click chemistry: A computational survey. *Org. Biomol. Chem.* **2009**, *7*, 5255-5258.
- (5) Bach, R. D. Ring strain energy in the cyclooctyl system. The effect of strain energy on [3 + 2] cycloaddition reactions with azides. *J. Am. Chem. Soc.* **2009**, *131*, 5233-5243.
- (6) Pravst, I.; Zupan, M.; Stavber, S. Efficient synthesis of α,α -difluoro ketones using Selectfluor. *Synthesis* **2005**, 3140-3146.
- (7) Atanes, N.; Escudero, S.; Pérez, D.; Guitián, E.; Castedo, L. Generation of cyclohexyne and its Diels-Alder reaction with α -pyrones. *Tetrahedron Lett.* **1998**, *39*, 3039-3040.
- (8) Bühl, H.; Gugel, H.; Kolshorn, H.; Meier, H. Eine verbesserte cyclooctyn-synthese. *Synthesis* **1978**, 536-537.

- (9) Wittig, G.; Krebs, A. Zur Existenz niedergliedriger Cycloalkyne, I. *Chem. Ber.* **1961**, *94*, 3260-3275.
- (10) Krebs, A.; Wilke, J. Angle strained cycloalkynes. In *Wittig Chemistry*; Springer-Verlag: Berlin/Heidelberg, **1983**; Vol. 109, pp. 189-233.
- (11) Iglesias, B.; Peña, D.; Pérez, D.; Guitián, E.; Castedo, L. Palladium-catalyzed trimerization of strained cycloalkynes: Synthesis of decacyclene. *Synlett* **2002**, 486-488.
- (12) Meier, H.; Voigt, E. Bildung und fragmentierung von cycloalkeno-1,2,3-selenadiazolen. *Tetrahedron* **1972**, *28*, 187-198.
- (13) Dodziuk, H. *Cyclodextrins and their complexes: Chemistry, analytical methods, applications*; 1st ed. Wiley VHC: Weinheim, 2006; Vol. 1.
- (14) Saenger, W. Cyclodextrin inclusion compounds in research and industry. *Angew. Chem. Int. Ed.* **1980**, *19*, 344-362.
- (15) Wenz, G. Cyclodextrins as building blocks for supramolecular structures and functional units. *Angew. Chem. Int. Ed.* **1994**, *33*, 803-822.
- (16) Brewster, M. E.; Loftsson, T. Cyclodextrins as pharmaceutical solubilizers. *Adv. Drug Deliver. Rev.* **2007**, *59*, 645-666.
- (17) Uekama, K. Design and evaluation of cyclodextrin-based drug formulation. *Chem. Pharm. Bull.* **2004**, *52*, 900-915.
- (18) Uekama, K.; Hirayama, F.; Irie, T. Cyclodextrin drug carrier systems. *Chem. Rev.* **1998**, *98*, 2045-2076.
- (19) Taraszewska, J. Complexes of β -cyclodextrin with chloronitrobenzenes and with solvents in water and organic solvent mixtures. *J. Incl. Phenom. Macrocycl. Chem.* **1991**, *10*, 69-78.
- (20) Koontz, J. L.; Marcy, J. E.; O'Keefe, S. F.; Duncan, S. E. Cyclodextrin inclusion complex formation and solid-state characterization of the natural antioxidants α -tocopherol and quercetin. *J. Arg. Food Chem.* **2009**, *57*, 1162-1171.
- (21) Pietrzaka, M.; Oodziuka, H. CPDAS study of ring inversion of cis-decalin in the solid state when complexed with β -cyclodextrin. *Aust. J. Chem.* **2010**, *63*, 709-711.
- (22) Maier, G. The cyclobutadiene problem. *Angew. Chem. Int. Ed.* **1974**, *13*, 425-438.
- (23) Bally, T.; Masamune, S. Cyclobutadiene. *Tetrahedron* **1980**, *36*, 343-370.
- (24) Cram, D. J.; Tanner, M. E.; Thomas, R. The taming of cyclobutadiene. *Angew. Chem. Int. Ed.* **1991**, *30*, 1024-1027.
- (25) Legrand, Y.-M.; van der Lee, A.; Barboiu, M. Single-crystal X-ray structure of 1,3-dimethylcyclobutadiene by confinement in a crystalline matrix. *Science* **2010**, *329*, 299-302.
- (26) Krebs, A.; Kimling, H.; Kemper, R. Synthese und eigenschaften eines durch sterische effekte stabilisierten cyclobutadiens. *Justus Liebigs Ann. Chem.* **1978**, *1978*, 431-439.
- (27) Kimling, H.; Krebs, A. Synthesis of a cyclobutadiene stabilized by steric effects. *Angew. Chem. Int. Ed.* **1972**, *11*, 932-933.
- (28) Krebs, A.; Byrd, D. Dehydroannulene mittlerer ringgröße, II. Über das intermediäre auftreten von 1.2-dehydro-cyclooctatetraen. *Justus Liebigs Ann. Chem.* **1967**, *707*, 66-74.

- (29) Krebs, A. Intermediate occurrence of 1,2-dehydrocyclooctatetraene. *Angew. Chem. Int. Ed.* **1965**, *4*, 953-954.
- (30) Wittig, G.; Weinlich, J. Zur existenz niedergliederiger cycloalkine, VII. Über das tetramere cyclohexin und seine valenzisomeren. *Chem. Ber.* **1965**, *98*, 471-479.
- (31) Wittig, G.; Mayer, U. Zur existenz niedergliederiger cycloalkine, IV Über die tetramerisation des cyclohexins. *Chem. Ber.* **1963**, *96*, 342-348.
- (32) Bally, T. Cyclobutadiene: The antiaromatic paradigm? *Angew. Chem. Int. Ed.* **2006**, *45*, 6616-6619.
- (33) Alabugin, I. V.; Gold, B.; Shatruk, M.; Kovnir, K. Comment on "Single-crystal X-ray structure of 1,3-dimethylcyclobutadiene by confinement in a crystalline matrix." *Science* **2010**, *330*, 1047.
- (34) Pangborn, A. B.; Giardello, M. A.; Grubbs, R. H.; Rosen, R. K.; Timmers, F. J. Safe and convenient procedure for solvent purification. *Organometallics* **1996**, *15*, 1518-1520.

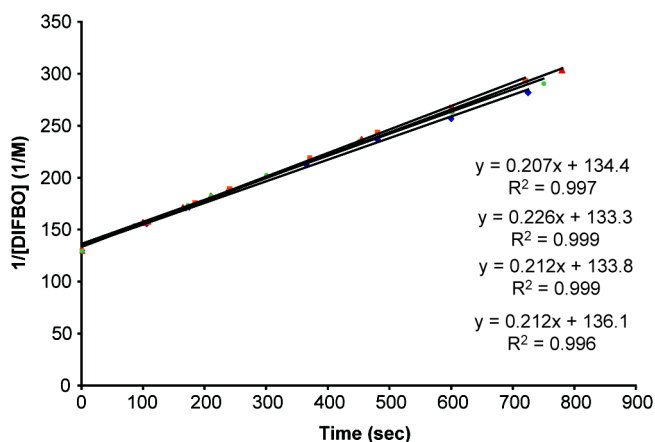
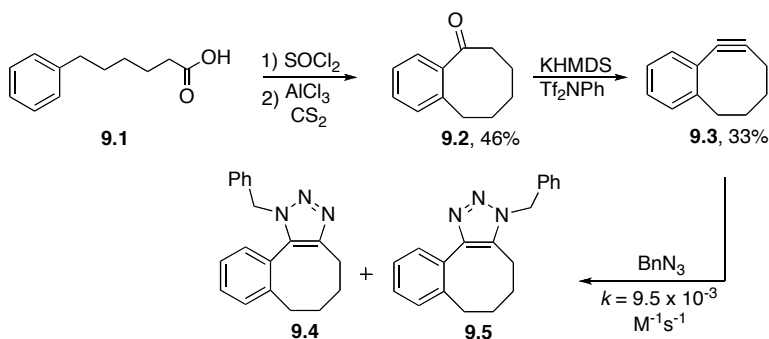


Figure 9.1. Plot of $1/[DIFBO]$ vs. time for the reaction of DIFBO with benzyl azide in CD_3CN at rt. The slope of the line represents the second-order rate constant for the reaction.

These results demonstrated that fusion of an aryl ring to the DIFO scaffold enhanced its reactivity with azides by a significant margin and suggested that addition of electron withdrawing groups to the DIBO scaffold would augment its reactivity as well. However, DIFBO and DIBO cannot be directly compared; according to Goddard's proposal (as discussed in Chapter 8), the second aryl ring in DIBO may actually retard the reaction rate due to unfavorable steric interactions between its *ortho* hydrogen atom and the azide substrate in the transition state.⁴ Thus, we synthesized monobenzocyclooctyne **9.3** (MOBO),⁵ as it was the ideal substrate against which to judge the relative contribution of fluorination to DIFBO's reactivity. Starting from 6-phenylhexanoic acid (**9.1**), an intramolecular Friedel Crafts acylation yielded ketone **9.2**⁶ followed by vinyl triflate formation and elimination to the alkyne (MOBO, Scheme 9.2). Unlike DIFBO, MOBO was readily isolable and displayed only minimal decomposition upon extended storage. We found the rate constant of its cycloaddition reaction with benzyl azide, forming cycloadducts **9.4** and **9.5** (1:2 ratio), to be $0.0095 \pm 0.0003 \text{ M}^{-1}\text{s}^{-1}$ (Scheme 9.2, Figure 9.2).

Scheme 9.2. Synthesis of MOBO and reactivity with benzyl azide.



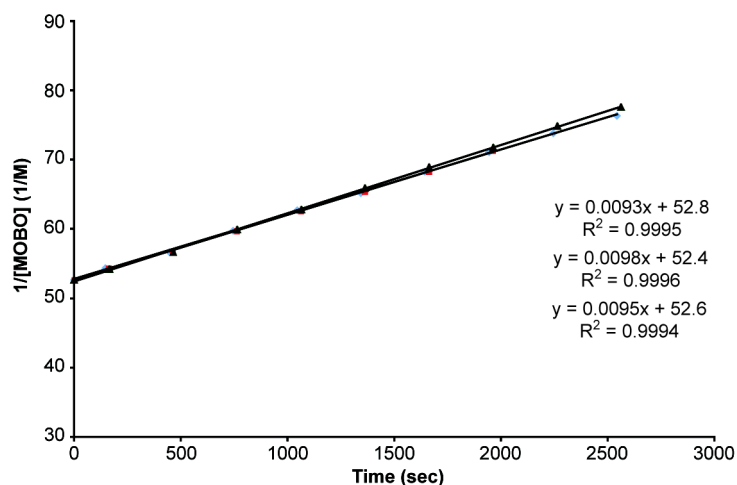


Figure 9.2. Plot of $1/[\text{MOBO}]$ vs. time for the reaction of MOBO with benzyl azide in CD_3CN at rt. The slope of the line represents the second-order rate constant for the reaction.

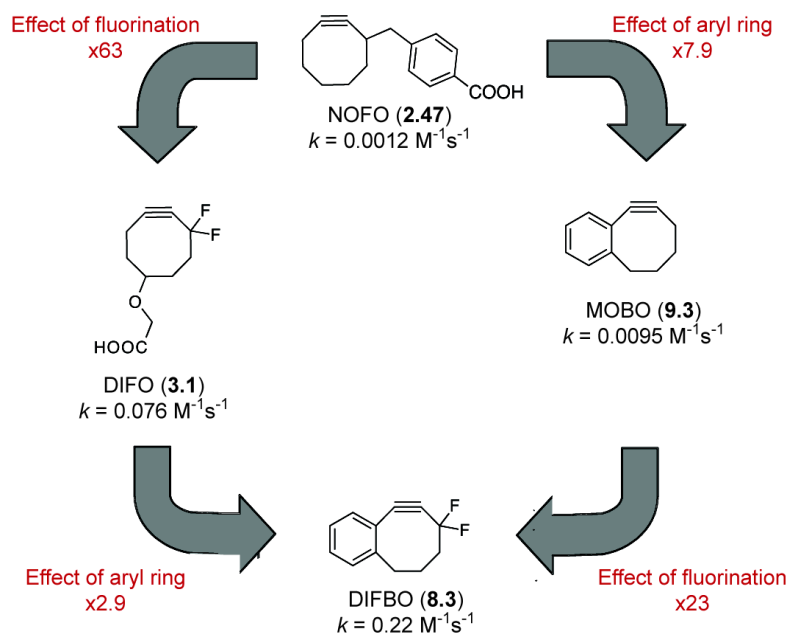


Figure 9.3. Comparison of NOFO (2.47), MOBO (9.3), DIFO (3.1), and DIFBO (8.3) illustrating that electronic effects of the *gem*-difluoro group provide more rate enhancement than a fused aryl ring.

The second-order rate constant for MOBO is 23-fold lower than that observed for DIFBO and also almost an order of magnitude lower than those of DIFO or DIBO.²³ This result confirms that both the electronic effects of fluorination and the enhanced ring strain created by the fused aryl ring contribute to DIFBO's reactivity, though the electronic effects seem to predominate (Figure 9.3). These results suggest that tetraFO (**7.1**) would display even more rapid reactivity with azides than DIFBO. Also of note is that DIBO reacts with benzyl azide considerably faster than MOBO, contrary to the previous DFT-based predictions, suggesting that the steric effects of an *ortho*-hydrogen do not significantly hinder the transition-state geometry necessary for the cycloaddition to proceed.⁴

Reactivity of DIFBO in a Biological Setting

DIFBO gave us valuable information regarding the two established methods of rate-enhancement for Cu-free click chemistry. However, DIFBO was unstable and, while its reactivity with benzyl azide appeared faster than its rate of trimerization, it did not display selective reactivity with protein-associated azides as judged by a Western blot competition experiment (Figure 9.4).

Jurkat cells were grown in the presence of peracetylated N-azidoacetyl mannosamine for 3 days and lysates were generated. These lysates were first treated with protected DIFBO **8.13** in phosphate buffered saline (PBS) and then reacted with Phos-FLAG (**2.11**) overnight. The degree of Staudinger ligation product was analyzed by Western blot probing with an α -FLAG antibody. Signal from the Western blot is representative of the number of azide groups present in the lysate. No difference in signal intensity was observed between cell lysate treated with or without DIFBO, suggesting that DIFBO was either not selective for azides or stays contained within the β -cyclodextrin in aqueous solution. The latter explanation is unlikely, as model reactions with **8.13** and 2-azidoethanol in water appear to proceed with kinetics comparable to free DIFBO (**8.3**). Evidence for the former explanation is observed when lysate that was not treated with azide is analyzed. Upon overexposure of the blot, more nonspecific background binding of the α -FLAG antibody to cell lysate that was treated with DIFBO was evident, likely due to the additional hydrophobicity DIFBO imparts on a protein.

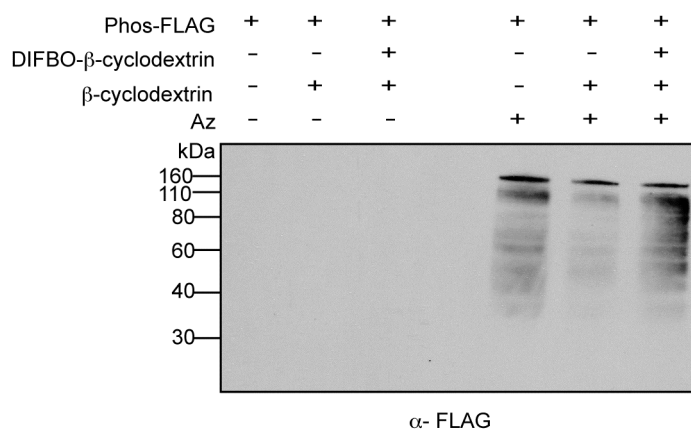


Figure 9.4. Western blot competition experiment between DIFBO and Phos-FLAG. Lysate (25 μ g) from Jurkat cells grown in the presence or absence of Ac₄ManNAz (25 μ M) for 3 days was treated with DIFBO- β -cyclodextrin (150 μ M), free β -cyclodextrin (150 μ M), or no reagent for 4 h. Phos-FLAG (250 μ M) was added to all samples and the Staudinger ligation proceeded overnight. The following day the lysate was analyzed by Western blot probing with α -FLAG-HRP.

Efforts to Stabilize DIFBO^b

Clearly strategies to increase the reactivity of cyclooctynes have been the main focus of Cu-free click chemistry, but the results of DIFBO demonstrated that the optimal cyclooctyne for labeling azides in living systems can only be designed if we understand *both* factors that *activate* and *stabilize* cyclooctynes. Thus, we turned our attention to using DIFBO as a scaffold to study stabilizing factors. Through the synthesis of MOBO, we had already demonstrated that decreasing the electronic activation (removal of the *gem*-difluoro group) resulted in a stable, yet slow cyclooctyne. Additionally, DIFO is a stable molecule and hence, decreasing the ring-strain should be a successful method of stabilization for DIFBO. We proposed decreasing the ring-strain by expanding the ring size of DIFBO to result in cyclononyne **9.6**. These two stabilization methods are simply reversions of the activation methods and result in a net thermodynamic stabilization, which will most likely bring about a significant decrease in reactivity with azides (Figure 9.4).

A more promising strategy is the kinetic stabilization of DIFBO through structural changes rather than the kinetic stabilization from a non-covalent interaction (*i.e.* encapsulation inside β -cyclodextrin). Physical organic chemists have spent considerable effort synthesizing highly strained molecules that are able to persist due to kinetic stability.^{7,8,9,10} Considering the main degradation product of DIFBO was a trimer, we envisioned that steric protection of the alkyne through an appropriately placed methyl group at the *ortho*-position on the aryl ring (compound **9.7**) or the addition of methyl

^b Hitomi Nakamura contributed to work in this section.

groups at the propargylic position (compounds **9.8** and **9.9**) would result in a more stable cyclooctyne (Figure 9.4). Because steric protection of the alkyne at the propargylic position required removal of the activating fluorine atoms, we envisioned methyl-DIFBO **9.7** with steric protection off the aryl ring was the best candidate for a reactive yet stable DIFBO species.

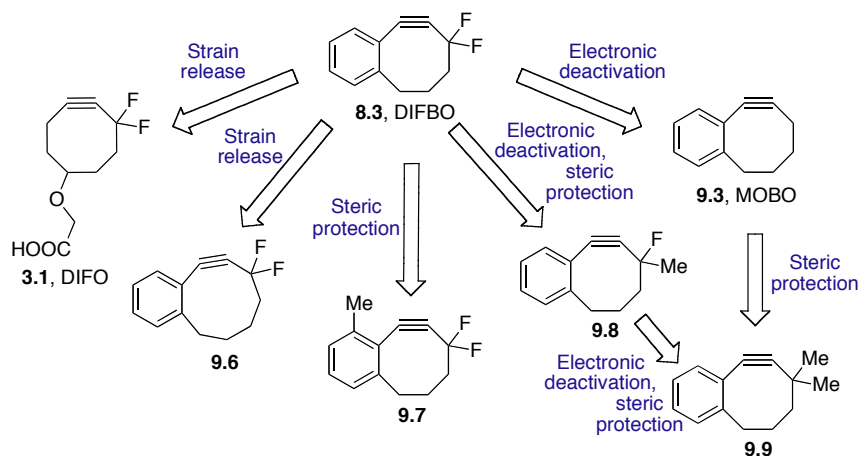
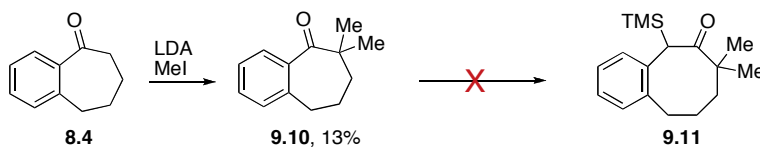


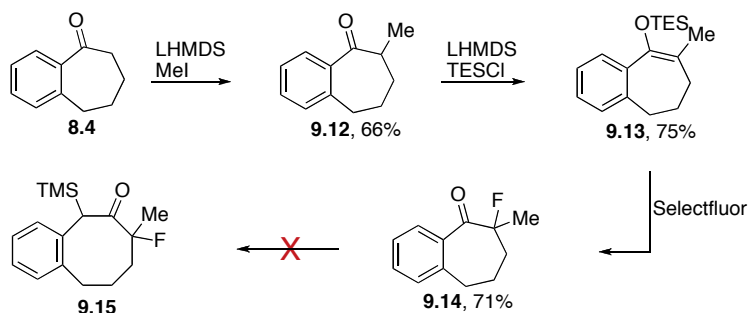
Figure 9.5. A variety of methods to stabilize DIFBO.

We envisioned all these monobenzocycloalkynes (**9.6-9.9**) could be synthesized through the homologation strategy employed for DIFBO. The substituted benzosuberone precursors for cyclooctyne **9.8** and **9.9** (**9.14** and **9.10**, respectively) were synthesized by standard alkylation and for the case of **9.8** fluorination methods (Schemes 9.3 and 9.4). 2,2-dimethyl benzosuberone (**9.10**) was synthesized in one step through dialkylation of **8.4** with MeI.¹¹ 2-Fluoro-2-methyl benzosuberone (**9.14**) was obtained through monoalkylation with MeI (**9.12**) followed by silyl enol ether formation (**9.13**) and treatment with Selectfluor. Unfortunately, all attempts to homologate ketone **9.14** and **9.10** did not yield desired α -silyl ketones **9.11** or **9.15**, nor any ring-expansion product. It appeared that the ketones of **9.10** and **9.14** were not electrophilic enough for this transformation, as addition of trimethylsilyl cyanide¹² and dithionate^{13,14} also did not proceed efficiently.

Scheme 9.3. Synthesis and attempted homologation of 2,2-dimethylbenzosuberone **9.10**.

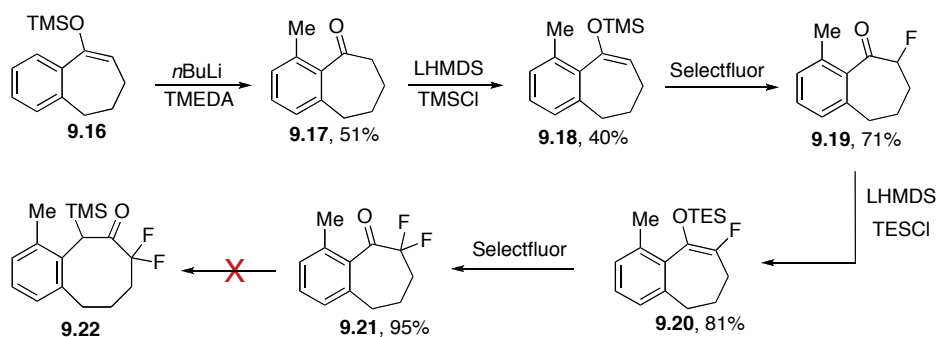


Scheme 9.4. Synthesis and attempted homologation of 2-fluoro-2-methyl benzosuberone.



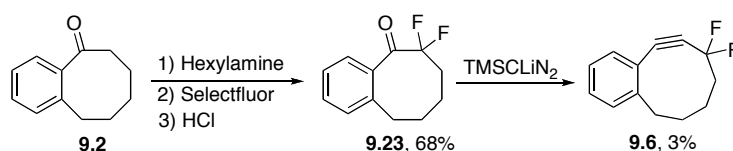
Fortunately, the ketone necessary for the synthesis of methyl-DIFBO **9.7** contains the same *gem*-difluoro group as difluorobenzosuberone (**8.5**), which readily underwent homologation with trimethylsilyl diazomethane. As was the case for DIFBO, the synthesis of **9.7** began with benzosuberone (**8.4**), which was converted to silyl enol ether **9.16**. Treatment of **9.16** with 2 equivalents of *n*BuLi and TMEDA and quenching with MeI yielded methylated benzosuberone **9.17**.¹⁵ The additional methyl group prevented imine formation with hexylamine, presumably due to unfavorable steric interactions between the *ortho*-methyl group and alkyl chain of hexylamine, so the simple procedure of Stavber and coworkers for direct addition of two fluorine atoms was not feasible.¹⁶ Hence, the two fluorine atoms were installed via a four-step process involving silyl enol ether formation and treatment with Selectfluor (Scheme 9.5) to yield ketone **9.21**. After screening many combinations of Lewis acids and diazo species,^{17,18,19,20,21,22} we were unable to form **9.22** or any product containing the requisite eight-membered ring scaffold, which could lead to **9.7**. This result demonstrated that the homologation strategy is highly substrate dependent and even small structural differences can lead to large differences in reactivity. For the case of ketone **9.21**, we suspect that the *ortho*-methyl group prevents the transition-state geometry required for homologation from being obtained.

Scheme 9.5. Synthesis and attempted homologation of difluorinated benzosuberone **9.21**.



We next directed our efforts toward cyclononyne **9.6** (Scheme 9.6). Ketone **9.2** employed in the synthesis of MOBO was converted to the hexylamine imine and treated with Selectfluor.¹⁶ Following imine hydrolysis, difluoroketone **9.23** was obtained in 68% yield. However, as with the other DIFBO analogues, ketone **9.23** did not readily undergo homologation with TMSCHN₂. We could unreliably form a small amount of cyclononyne **9.6** through treatment of **9.23** with TMSCLiN₂.²³ The small amount of **9.6** isolated appeared stable but reacted very slowly with azides ($k \sim 10^{-5} \text{ M}^{-1}\text{s}^{-1}$). This result demonstrated that while ring-expansion was an effective stabilizing method, the addition of an extra carbon significantly decreased ring-strain and was not a practical strategy for Cu-free click chemistry.

Scheme 9.6. Synthesis of difluorobenzocyclononyne **9.6**.

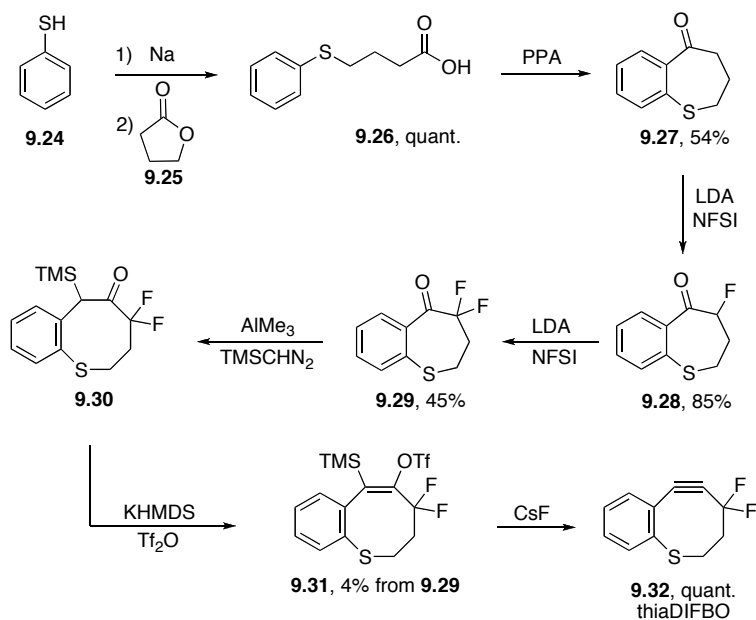


A More Subtle Strain-Release Strategy^c

At this point, we became interested in a more subtle method of ring-expansion: the addition of a sulfur atom. A canonical C(*sp*³)-C(*sp*³) bond length is 1.54 Å whereas a C(*sp*³)-S(*sp*³) bond length is closer to 1.81 Å, a significant difference, but much more conservative than expanding the ring size. Our target compound became cyclooctyne **9.32**, deemed thiaDIFBO. The synthesis of thiaDIFBO again relied on a ring expansion strategy. Ketone **9.27** was prepared from thiophenol (**9.24**) and γ -butyric lactone (**9.25**) though an S_N2 reaction to yield **9.26**, which was cyclized with polyphosphoric acid to give **9.27**.²⁴ The installation of fluorine atoms in ketone **9.27** was complicated by the fact that Selectfluor is able to fluorinate sulfides, which then results in a Pummerer type transformation.²⁵ Thus, the less activated electrophilic fluorinating agent N-fluorobenzenesulfonimide (NFSI) was employed for fluorination alpha to the ketone. Ketone **9.29** was obtained in 37% yield after two iterations of deprotonation with LDA and quenching with NFSI. Treatment of **9.29** with trimethylaluminum and TMSCHN₂, the conditions employed for homologation of 2,2-difluorobenzosuberone (**8.5**), resulted in α -silyl ketone **9.30**. The homologation product was immediately converted to vinyl triflate **9.31** through enolate formation with NaHMDS and trapping with trifluoromethane sulfonic anhydride. Cesium fluoride quantitatively converted **9.31** into thiaDIFBO **9.32**, which, unlike DIFBO, was stable to concentration and no trimer products were observed even upon long-term storage.

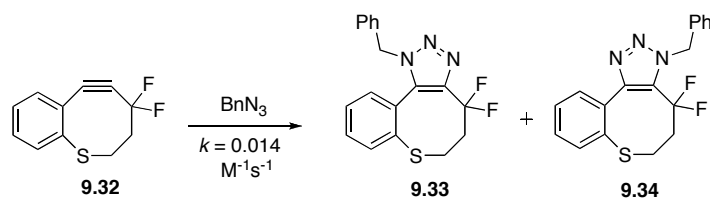
^c Gabriela de Almeida contributed to work in this section.

Scheme 9.7. Synthesis of thiaDIFBO.



With ring-expansion by replacement of a carbon with an endocyclic sulfur atom appearing to be a successful stabilization strategy, we investigated the effect the decrease in ring strain had on the rate of cycloaddition with benzyl azide. ThiaDIFBO was combined with one equivalent of benzyl azide and the reaction to yield triazole products **9.33** and **9.34** was monitored by NMR. We found that thiaDIFBO had a second-order rate constant of $0.014 \text{ M}^{-1}\text{s}^{-1}$, almost twenty-fold slower than DIFBO ($k = 0.22 \text{ M}^{-1}\text{s}^{-1}$) and on par with the reactivity of MOBO ($k = 0.0095 \text{ M}^{-1}\text{s}^{-1}$).

Scheme 9.8. Reactivity of thiaDIFBO with benzyl azide.



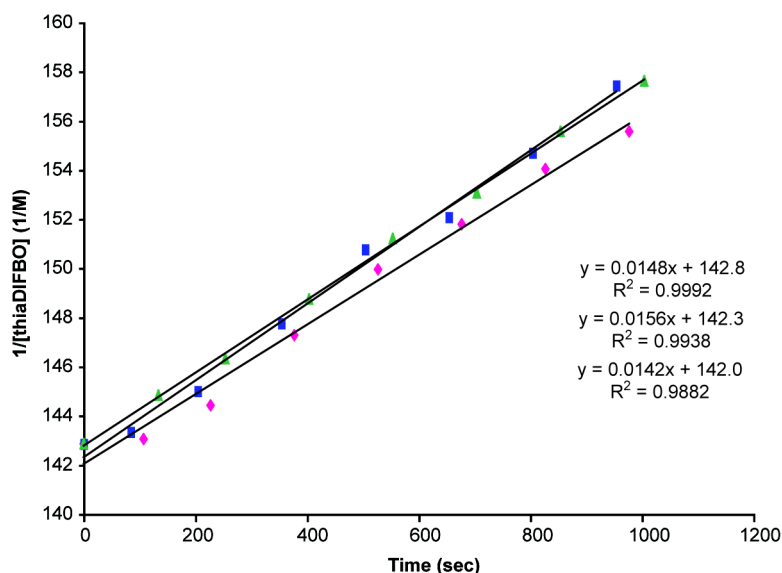


Figure 9.6. Plot of $1/[\text{thiaDIFBO}]$ vs. time for the reaction of thiaDIFBO with benzyl azide in CD_3CN at rt. The slope of the line represents the second-order rate constant for the reaction.

Clearly, the addition of a sulfur atom has a substantial affect on the rate of Cu-free click chemistry even when an activating propargylic *gem*-difluoro group is present. At this point, we realized that if the stabilization imparted by the addition of a sulfur atom could be coupled with the more traditional stabilization methods of steric protection of the alkyne, the dramatic activating effect of decreasing the ring size to a seven-membered ring could be explored for Cu-free click reagents for the first time. A stable thiacycloheptyne, 3,3,6,6 tetramethylthiacycloheptyne (TMTH) **8.20**, was known in the literature, although its rate of reactivity with azides had not been determined. We were interested in a monobenzo version of TMTH, which contained a fused aryl ring on one side of the alkyne and a *gem*-dimethyl group on the other side (thiacycloheptyne **9.35**).

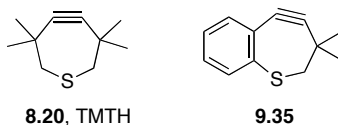
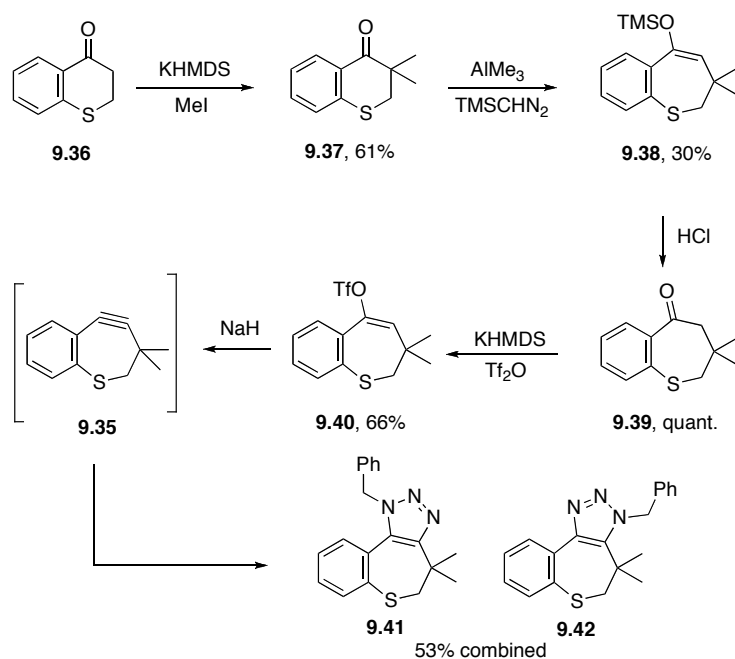


Figure 9.7. Thiacycloheptynes.

As for the case of DIFBO and thiaDIFBO, the synthesis of thiacycloheptyne **9.35** was facilitated by a homologation reaction (Scheme 9.9). Commercially available benzothiacyclohexanone **9.36** was dimethylated by treatment with KHMDS and methyl iodide to produce **9.37**. Subjecting dimethylcyclohexanone **9.37** to AlMe_3 and TMSCHN_2 resulted in a successful ring expansion, but we obtained silyl enol ether **9.38** rather than the

anticipated α -silyl ketone. This result prevented the mild-fluoride mediated alkyne formation from being employed; however, the seven-membered ring scaffold was in place and ketone **9.39** was revealed by treatment with acid and transformed to vinyl triflate **9.40** under standard conditions. Unexpectedly, treatment of **9.40** with lithium diisopropylamide and other amide bases often employed for alkyne formation from vinyl triflate species proved to be ineffective for accessing **9.35** from **9.40**, perhaps due to steric hindrance between these large bases and the *gem*-dimethyl group adjacent to the vinyl proton. Only sodium hydride led to depletion of starting material, but, disappointingly, no desired alkyne or other small molecule could be recovered. However, if **9.40** was treated with sodium hydride in the presence of benzyl azide, triazole cycloadducts **9.41** and **9.42** were obtained, suggesting that **9.35** was formed *in situ*.

Scheme 9.9. Synthesis and trapping of monobenzothiacycloheptyne **9.35**.



Cu-Free Click Chemistry Conclusions

The quest for a highly reactive cyclooctyne for Cu-free click chemistry seems to be one that necessitates walking the narrow balance beam between reactivity and stability. We have learned a great deal regarding factors that activate and stabilize cycloalkynes, but dramatic increases in the second-order rate constant appear unlikely at this point. Cu-free click chemistry is reaching the end of its kinetic modifications and it is time for the development of new bioorthogonal chemistries.

Materials and Methods

General Experimental Procedure

All chemical reagents were purchased from Sigma-Aldrich, Acros, and TCI and used without purification unless noted otherwise. Anhydrous DMF and MeOH were purchased from Aldrich or Acros in sealed bottles; all other solvents were purified as described by Pangborn *et al.*²⁶ In all cases, solvent was removed by reduced pressure with a Buchi Rotovapor R-114 equipped with a Welch self-cleaning dry vacuum. Products were further dried by reduced pressure with an Edwards RV5 high vacuum.

Lyophilization was performed on a LABCONCO FreeZone[®] instrument equipped with an Edwards RV2 pump. Thin layer chromatography was performed with EMD 60 Å silica gel plates. Flash chromatography was performed using Silicycle[®] 60 Å 230-400 mesh silica. All ¹H, ¹³C, and ¹⁹F NMR spectra are reported in ppm and referenced to solvent peaks (¹H and ¹³C). Spectra were obtained on Bruker AVQ-400, AVB-400, DRX-500, AV-500, or AV-600 instruments. Electron impact (EI) and electrospray ionization (ESI) mass spectra were obtained from the UC Berkeley Mass Spectrometry Facility.

Experimental Procedures

7,8,9,10-tetrahydrobenzo[8]anulen-5(6H)-one (9.2).⁶ One drop of *N,N*-dimethylformamide (anhydrous) was added 6-phenyl hexanoic acid (2.0 mL, 11 mmol, 1.0 equiv.). To this solution oxalyl chloride (1.2 mL, 13 mmol, 1.2 equiv.) was added dropwise and bubbling was observed. After bubbling ceased, the reaction was stirred an additional 15 min and evaporated to dryness to yield the 6-phenyl hexanoic acid chloride. The acid chloride was dissolved in carbon disulfide (50 mL). This solution was added to a refluxing mixture of aluminum chloride (5.1 g, 38 mmol, 3.5 equiv.) in carbon disulfide (90 mL) at a rate of 1.5 mL/h. After 3 d at reflux, the reaction was evaporated to dryness, redissolved in CH₂Cl₂ (200 mL) and again evaporated to dryness. The crude product was purified by silica gel chromatography using a hexane/ethyl acetate solvent system (product elutes at 10:1 hexane/ethyl acetate) to yield 870 mg (5.0 mmol, 46%) of **9.2**. *R*_f = 0.8 in 3:1 hexane/ethyl acetate. ¹H NMR (500 MHz, CDCl₃): δ 7.63 (dd, *J* = 7.7, 1.2 Hz, 1H), 7.36 (td, *J* = 7.5, 1.4 Hz, 1H), 7.24 (td, *J* = 7.4, 0.8 Hz, 1H), 7.15 (d, *J* = 7.6 Hz, 1H), 3.01 (dd, *J* = 6.5, 6.5 Hz, 2H), 2.89 (dd, *J* = 6.9, 6.9 Hz, 2H), 1.83-1.74 (m, 4H), 1.52- 1.47 (m, 2H). ¹³C NMR (100 MHz, CDCl₃): δ 207.6, 140.1, 140.0, 131.7, 131.1, 127.7, 126.5, 44.3, 34.5, 28.0, 25.3, 24.2. HRMS (EI): calcd. for C₁₂H₁₄O⁺ [*M*]⁺, 174.1045; found, 174.1049.

Monobenzocyclooctyne (9.3).⁵ 7,8,9,10-tetrahydrobenzo[8]anulen-5(6H)-one (**9.2**)⁶ (100 mg, 0.57 mmol, 1.0 equiv.) was dissolved in THF (3 mL, anhydrous) and cooled to -78 °C. To this solution, potassium bis(trimethylsilyl)amide (0.5 M solution in toluene, 2.28 mL, 1.14 mmol, 2.0 equiv.) was added and the mixture was stirred at -78 °C. After 1 h, *N*-phenyl-bis(trifluoromethanesulfonimide) (234 mg, 0.66 mmol, 1.1 equiv. in 5 mL THF) was added. The reaction mixture was allowed to warm to 0 °C. After 1 h at 0 °C, the reaction was quenched with MeOH and evaporated to dryness to result in crude

monobenzocyclooctyne **9.3**. Silica gel chromatography eluting with hexane yielded monobenzocyclooctyne **9.3** as a volatile, foul smelling oil (30 mg, 0.19 mmol, 33%). $R_f = 0.9$ in 4:1 hexane/EtOAc. $^1\text{H NMR}$ (600 MHz): δ 7.14-7.20 (m, 4H), 2.80 (bs, 2H), 2.58 (t, $J = 6.8$ Hz, 2H), 2.13 (bs, 2H), 1.76 (bs, 2H). $^{13}\text{C NMR}$ (150 MHz): δ 151.6, 128.9, 127.1, 126.1, 125.8, 124.3, 112.8, 93.8, 39.2, 33.8, 25.7, 20.5. HRMS (EI): calcd. for $\text{C}_{12}\text{H}_{12}^+$ $[\text{M}]^+$, 156.0939; found, 156.0940.

2,2-Dimethyl-1-benzosuberone (9.10). A 0.5 M solution of LDA was prepared (2.5 ml 1.4 M nBuLi, 4.0 mL THF, 0.70 mL diisopropylamine combined at -78 °C and let stir for 30 min) and benzosuberone (**8.4**, 0.50 mL, 3.4 mmol, 1 equiv) was added. After this mixture was stirred for 1 h at -78 °C, MeI (0.60 mL, 9.6 mmol, 2.8 equiv) was added. The resulting yellow solution was warmed to rt overnight. The following day the reaction mixture was quenched with aqueous sat. NH_4Cl (7 mL) and the product was extracted into CH_2Cl_2 (3 x 10 mL). The organics were combined, dried with MgSO_4 , decanted and evaporated to dryness. The crude mixture was purified by silica gel chromatography, eluting with 20:1 hexane/ethyl acetate to yield **9.1** (80 mg, 0.43 mmol, 13%) as well as a mixture of mono- and dimethylated benzosuberones. $R_f = 0.6$ in 9:1 hexane/EtOAc. $^1\text{H NMR}$ (400 MHz): δ 7.33-7.36 (m, 1H), 7.25-7.28 (m, 2H), 7.11 (d, $J = 7.4$, 1H), 2.77 (t, $J = 6.7$ Hz, 2H), 1.91 (quin, $J = 6.6$ Hz, 2H), 1.66-1.69 (m, 2H), 1.18 (s, 6H). $^{13}\text{C NMR}$ (150 MHz): δ 215.1, 141.5, 137.4, 130.8, 128.7, 127.2, 126.7, 46.1, 37.8, 33.2, 25.9, 23.4. HRMS (EI): calcd. for $\text{C}_{13}\text{H}_{16}\text{O}^+$ $[\text{M}]^+$, 188.1201; found, 188.1201.

2-Methyl-1-benzosuberone (9.12). Lithium bis(trimethylsilyl)amide (1M solution in THF, 0.80 mL, 0.80 mmol, 1.2 equiv.) and THF were cooled to -78 °C. To this solution, benzosuberone (**8.4**, 100 μL , 0.68 mmol, 1.0 equiv.) was added dropwise. This solution was stirred for 1.5 h at which point methyl iodide (210 μL , 3.4 mmol, 5.0 equiv.) was added. The reaction was warmed to rt over 4 h and then quenched with methanol. The mixture was evaporated to dryness and the crude oil was purified by silica gel chromatography (35:1 hexane/ethyl acetate). This procedure yielded **9.12** as a clear oil (79 mg, 0.45 mmol, 66%). $R_f = 0.6$ in 9:1 hexane/ethyl acetate. $^1\text{H NMR}$ (600 MHz): δ 7.44 (d, $J = 7.7$ Hz, 1H), 7.35 (t, $J = 7.1$ Hz, 1H), 7.25 (t, $J = 7.6$ Hz, 1H), 7.19 (d, $J = 7.3$ Hz, 1H), 2.88-3.01 (m, 3H), 2.03-2.06 (m, 1H), 1.84-1.91 (m, 1H), 1.64-1.68 (m, 2H), 1.21 (d, $J = 6.5$ Hz, 3H). $^{13}\text{C NMR}$ (150 MHz): δ 207.9, 142.0, 139.8, 131.4, 129.9, 128.5, 126.5, 44.3, 33.8, 32.1, 25.7, 16.6. HRMS (EI): calcd. for $\text{C}_{12}\text{H}_{14}\text{O}^+$ $[\text{M}]^+$, 174.1045; found, 174.1042.

Compound 9.13. 2-Methyl-1-benzosuberone (**9.12**, 318 mg, 1.8 mmol, 1.0 equiv.) was dissolved in THF (31 mL) and cooled to -78 °C. Lithium bis(trimethylsilyl)amide (1M solution in THF, 2.0 mL, 2.0 mmol, 1.1 equiv.) was added to this solution. After 1 hr, TESCOI (490 μL , 2.9 mmol, 1.6 equiv.) was added and the reaction mixture was warmed to rt overnight. The following morning the reaction was quenched with water (1 mL) and evaporated to dryness. The crude product was extracted with Et_2O (3 x 10 mL, 15 mL H_2O). The organic extracts were combined, dried with MgSO_4 , decanted, and evaporated to dryness. The product was purified by silica gel chromatography with hexane/ethyl

acetate (100% hexane to 100:1 hexane/ethyl acetate) to yield 394 mg of silyl enol ether **9.13**. (1.4 mmol, 75%). $R_f = 0.9$ in 9:1 hexane/ethyl acetate. $^1\text{H NMR}$ (500 MHz): δ 7.46 (d, $J = 8.0$ Hz, 1H), 7.23-7.28 (m, 1H), 7.17-7.21 (m, 2H), 2.62 (t, $J = 7.1$ Hz, 2H), 2.13 (apparent quin, $J = 7.2$ Hz, 2H), 1.96 (s, 3H), 1.84 (t, $J = 7.1$ Hz, 2H), 0.94 (t, $J = 7.9$ Hz, 9H), 0.57 (q, $J = 8.0$ Hz, 6H). $^{13}\text{C NMR}$ (150 MHz): δ 143.2, 140.2, 140.1, 128.6, 127.1, 126.9, 125.8, 117.3, 33.8, 32.7, 30.0, 17.8, 6.9, 5.4. HRMS (EI): calcd. for $\text{C}_{18}\text{H}_{28}\text{OSi}^+ [\text{M}]^+$, 288.1909; found, 288.1913.

2-Fluoro-2-methyl-1-benzosuberone (9.14). Selectfluor (533 mg, 1.5 mmol, 1.5 equiv) was dissolved in DMF (20 mL) and cooled to 0 °C. Compound **9.13** (294 mg, 1.0 mmol, 1 equiv.) was dissolved in DMF (15 mL) and this solution was added to the SelectfluorTM solution over 30 min. After addition of **9.13**, the reaction mixture was warmed to rt and stirred for an additional 30 min. The reaction was then quenched with H_2O (20 mL) and extracted with ether (2 x 40 mL). The ether extracts were combined, dried with MgSO_4 , decanted and evaporated to dryness. The crude product was purified by silica gel chromatography eluting with 15:1 hexane/ethyl acetate. This procedure resulted in 139 mg of pure **9.14** (0.72 mmol, 71%). $R_f = 0.4$ in 9:1 hexane/ethyl acetate. $^1\text{H NMR}$ (600 MHz): δ 7.52 (dd, $J = 7.6, 1.1$ Hz, 1H), 7.40 (td, $J = 7.5, 1.3$ Hz, 1H), 7.30 (t, $J = 7.4$ Hz, 1H), 7.21 (d, $J = 7.6$ Hz, 1H), 3.14 (dd, $J = 15.9, 10.7$ Hz, 1H), 2.91 (dd, $J = 16.1, 8.3$ Hz, 1H), 2.20-2.28 (m, 1H), 2.10-2.16 (m, 1H), 2.04 (dtd, $J = 32.2, 14.5, 5.1$ Hz, 1H), 1.78-1.85 (m, 1H), 1.59 (d, $J = 21.6$ Hz, 3H). $^{13}\text{C NMR}$ (150 MHz): δ 204.6 (d, $J = 29$ Hz), 141.1, 137.7, 131.5, 129.7, 128.9, 126.5, 100.8 (d, $J = 178$ Hz), 38.3 ($J = 23$ Hz), 34.5, 24.1 ($J = 2$ Hz), 23.5 (d, $J = 24$ Hz). $^{19}\text{F-NMR}$ (564 MHz): δ -144.9- -144.6 (m, 1F). HRMS (EI): calcd. for $\text{C}_{12}\text{H}_{13}\text{OF}^+ [\text{M}]^+$, 192.0950; found, 192.0952.

9-Methyl-1-benzosuberone (9.17). 9-Methyl-1-benzosuberone (**9.17**) was prepared as described by R. McCague.¹⁵ Briefly, TMS-enol ether of benzosuberone **9.16** (2.55 g, 11 mmol, 1.0 equiv.) was dissolved in hexanes (32 mL, dried over molecular sieves overnight). To this solution, tetramethylethylenediamine (4.0 mL, 27 mmol, 2.5 equiv., freshly distilled) was added followed by $n\text{BuLi}$ (1.42 M solution in hexanes, 16.0 mL, 23.0 mmol, 2.1 equiv.). The resulting orange mixture was heated to reflux. After 2 h, methyl iodide (0.87 mL, 14 mmol, 1.3 equiv) in hexanes (5.1 mL) was added and the reaction was immediately quenched with water (25 mL). Upon cooling to rt, the product was extracted into hexane (3 x 50 mL). The organics were combined, dried with MgSO_4 , decanted and evaporated to dryness. The crude product was purified by silica gel chromatography in a hexane/ether solvent system (40:1 to 30:1). This procedure yielded desired product **9.17** (980 mg, 5.6 mmol, 51%) plus some recovered benzosuberone and 2,9-dimethyl benzosuberone. $R_f = 0.5$ in 5:1 hexane/ethyl acetate. $^1\text{H NMR}$ (500 MHz): δ 7.14 (d, $J = 7.6$ Hz, 1H), 7.02 (d, $J = 7.6$ Hz, 1H), 6.90 (d, $J = 7.5$ Hz, 1H), 2.69 (t, $J = 6.6$ Hz, 2H), 2.53-2.55 (m, 2H), 2.27 (s, 3H), 1.67-1.76 (m, 4H). $^{13}\text{C NMR}$ (125 MHz): δ 210.3, 139.5, 138.0, 135.3, 129.9, 129.0, 126.3, 42.0, 32.3, 25.5, 22.3, 19.7. HRMS (ESI): calcd. for $\text{C}_{12}\text{H}_{15}\text{O}^+ [\text{M}+\text{H}]^+$, 175.1117; found, 175.1115.

Trimethyl(1-methyl-6,7-dihydro-5H-benzo[7]annulen-9-yloxy)silane (9.18). 9-Methyl-1-benzosuberone (**9.17**, 440 mg, 2.5 mmol, 1.0 equiv.) was dissolved in THF (44 mL, anhydrous) and cooled to -78 °C. Lithium bis(trimethylsilyl)amide (1 M solution in THF, 4.7 mL, 4.7 mmol, 1.9 equiv.) was added and the resulting mixture was stirred at -78 °C. After 1.5 h, TMSCl (1.07 mL, 8.4 mmol, 3.4 equiv) was added and the reaction was warmed to 0 °C. Upon reaching 0 °C, the reaction was quenched with methanol and evaporated to dryness. The crude product was purified by silica gel chromatography eluting with hexane to yield **9.18** (255 mg, 1.0 mmol, 40%). $R_f = 0.9$ in 4:1 hexane/ethyl acetate. $^1\text{H NMR}$ (600 MHz): δ 7.13 (t, $J = 7.5$ Hz, 1H), 7.08 (d, $J = 7.3$ Hz, 1H), 7.03 (d, $J = 7.5$ Hz, 1H), 5.45 (t, $J = 7.7$ Hz, 1H), 2.62 (t, $J = 7.0$ Hz, 2H), 2.39 (s, 3H), 1.98 (apparent quin, $J = 7.0$ Hz, 2H), 1.73 (bs, 2H), 0.17 (s, 9H). $^{13}\text{C NMR}$: 150.3, 140.6, 137.2, 136.7, 128.8, 127.7, 126.2, 108.4, 34.0, 32.7, 22.1, 21.0, 0.3. HRMS (EI): calcd. for $\text{C}_{15}\text{H}_{22}\text{OSi}^+ [\text{M}]^+$, 246.1440; found, 246.1440.

2-Fluoro-9-methyl-1-benzosuberone (9.19). Selectfluor (475 mg, 1.3 mmol, 1.3 equiv) was dissolved in *N,N*-dimethylformamide (25 mL, anhydrous) and cooled to 0 °C. Compound **9.18** (255 mg, 1.0 mmol, 1.0 equiv) was dissolved in *N,N*-dimethylformamide (12 mL, anhydrous) and this solution was added to the Selectfluor solution over 30 min at 0 °C. After addition of **9.18** was complete, the reaction mixture was warmed to rt and stirred for an additional 1.5 h. The reaction was then quenched with water (25 mL) and extracted with ether (2 x 50 mL). The ether extracts were combined, dried with MgSO_4 , decanted and evaporated to dryness. The crude product was purified by silica gel chromatography eluting with 40:1 hexanes/ether. This procedure resulted in 142 mg of pure **9.19** (0.74 mmol, 71%). $R_f = 0.7$ in 3:1 hexane/ethyl acetate. $^1\text{H NMR}$ (600 MHz): δ 7.17 (t, $J = 7.7$ Hz, 1H), 7.07 (d, $J = 7.6$ Hz, 1H), 6.96 (d, $J = 7.5$ Hz, 1H), 5.07 (ddd, $J_F = 50.5$ Hz, portion at 5.11 apparent t, $J = 5.8$ Hz, portion at 5.03 dd, $J = 7.6, 4.1$ Hz, 1H), 2.74-2.76 (m, 2H), 2.26 (s, 3H), 2.13-2.17 (m, 2H), 1.99-2.05 (m, 1H), 1.78-1.84 (m, 1H). $^{13}\text{C NMR}$ (150 MHz): δ 206.3 (d, $J = 24$ Hz), 138.1, 137.9, 135.9, 130.2, 129.0, 127.0, 94.9 (d, $J = 183$ Hz), 35.2, 33.7 (d, $J = 22$ Hz), 23.2 (d, $J = 6$ Hz), 19.6. $^{19}\text{F NMR}$ (564 MHz): δ -101.2 (t, $J = 11$ Hz, 1F). HRMS (EI): Calcd. for $\text{C}_{12}\text{H}_{13}\text{OF}^+ [\text{M}]^+$, 192.0950; found, 192.0954.

Triethyl(8-fluoro-1-methyl-6,7-dihydro-5H-benzo[7]annulen-9-yloxy)silane (9.20). 2-Fluoro-9-methyl-1-benzosuberone (**9.19**, 114 mg, 0.59 mmol, 1.0 equiv.) was dissolved in THF (10 mL, anhydrous) and cooled to -78 °C. Lithium bis(trimethylsilyl)amide (1M solution in THF, 1.1 mL, 1.1 mmol, 1.9 equiv.) was added. The reaction mixture was stirred for 30 min at -78 °C at which point TMSCl (0.33 mL, 2.0 mmol, 3.4 equiv.) was added. The reaction was warmed to rt. After 10 min at rt, the reaction was quenched with methanol, evaporated to dryness, and chromatographed on silica gel eluting with hexane/ethyl acetate (20:1). This procedure resulted in pure **9.20** (147 mg, 0.48 mmol, 81%). $R_f = 0.95$ in 3:1 hexane/ethyl acetate. $^1\text{H NMR}$ (500 MHz): δ 7.10 (apparent t, $J = 7.4$ Hz, 1H), 7.05 (d, $J = 7.2$ Hz, 1H), 6.98 (d, $J = 7.4$ Hz, 1H), 2.65 (bs, 2H), 2.39 (s, 3H), 2.07-2.15 (bm, 4H), 0.89 (t, $J = 7.9$ Hz, 9H), 0.60 (q, $J = 7.9$ Hz, 6H). $^{13}\text{C NMR}$ (125 MHz): δ 148.8 (d, $J = 255$ Hz), 139.9, 138.2 (d, $J = 4$ Hz), 135.5 (d, $J = 4$ Hz), 129.8 (d, J

= 14 Hz), 129.1, 127.8, 126.4, 33.4, 32.5, 25.3 (d, $J = 25$ Hz), 21.0, 5.3, 5.2. ^{19}F NMR (564 MHz): δ -126.1 (t, $J = 23$ Hz, 1F). HRMS (EI): calcd. for $\text{C}_{18}\text{H}_{27}\text{FOSi}^+ [\text{M}]^+$, 306.1815; found.

2,2-Difluoro-9-methyl-1-benzosuberone (9.21). Selectfluor (121 mg, 0.34 mmol, 1.6 equiv.) was dissolved in *N,N*-dimethylformamide (6 mL, anhydrous). Compound **9.20** (64 mg, 0.21 mmol, 1.0 equiv.) was dissolved in *N,N*-dimethylformamide (3 mL, anhydrous) and this solution was added to the Selectfluor solution over 30 min. After addition of **9.20** was complete, the reaction was stirred for an additional 30 min, at which point water (5 mL) was added and the product was extracted with ether (2 x 15 mL). The ether extracts were combined, dried with MgSO_4 , decanted and evaporated to dryness. The crude product was purified by silica gel chromatography (hexane/ethyl acetate). This procedure resulted in 42 mg of pure **9.21** (0.20 mmol, 95%). $R_f = 0.7$ in 3:1 hexane/ethyl acetate. ^1H -NMR (500 MHz): δ 7.25 (t, $J = 7.6$ Hz, 1H), 7.13 (d, $J = 7.7$ Hz, 1H), 7.00 (d, $J = 7.7$ Hz, 1H), 2.79-2.81 (m, 2H), 2.30 (s, 3H), 2.26-2.33 (m, 2H), 1.94-1.98 (m, 2H). ^{13}C -NMR (125 MHz): δ 198.5 (t, $J = 30$ Hz), 138.2, 137.0, 136.2, 131.0 (apparent d, $J = 12$ Hz), 129.3 (apparent d, $J = 19$ Hz), 127.1 (apparent d, $J = 18$ Hz), 118.1 (t, $J = 250$ Hz), 35.8 (t, $J = 24$ Hz), 34.3, 22.5 (bs), 19.7. ^{19}F -NMR (564 MHz): δ -106.0 (apparent t, $J = 11$ Hz, 2F). HRMS (EI): calcd. for $\text{C}_{12}\text{H}_{12}\text{OF}_2^+ [\text{M}]^+$, 210.0856; found, 210.0860.

Compound 9.23. Ketone **9.2**⁶ (88 mg, 0.51 mmol, 1 equiv) was dissolved in cyclohexane (12 mL) and hexylamine (90 μL , 0.68 mmol, 1.3 equiv) and trifluoroacetic acid (1 drop) were added. The reaction was heated to reflux overnight. The following morning the reaction mixture was washed with sat. NaHCO_3 (1 x 15 mL) and brine (1 x 15 mL). The organic solution was dried over MgSO_4 and evaporated to dryness. The resulting crude imine (155 mg) was dissolved in acetonitrile (5 mL). To this solution Selectfluor (354 g, 1.0 mmol, 2.0 equiv) and Na_2SO_4 (50.3 mg, 0.35 mmol) were added. The reaction mixture was heated to reflux overnight. The following morning 3M HCl was added to hydrolyze the imine. After 10 min at reflux, the solution was cooled to rt and evaporated to dryness. The residue was dissolved in ether (10 mL), washed with sat. NaHCO_3 (1 x 5 mL) and brine (1 x 5 mL). The organic solution was dried over MgSO_4 and evaporated to dryness. The crude mixture was purified by flash chromatography with a hexane/ethyl acetate solvent system (96:4 hexane/EtOAc). This procedure yielded pure **9.23** (72 mg, 0.34 mmol, 68%). $R_f = 0.8$ in 3:1 hexane/ethyl acetate). ^1H NMR (600 MHz): δ 7.41 (td, $J = 7.6, 1.4$ Hz, 1H), 7.30 (td, $J = 7.5, 1.0$ Hz, 1H), 7.23 (dd, $J = 7.6, 1.0$ Hz, 1H), 7.21 (dd, $J = 7.7, 0.2$ Hz, 1H), 2.73-2.75 (m, 2H), 2.14-2.21 (m, 2H), 1.78 (apparent quin, $J = 6.2$ Hz, 2H), 1.61 apparent quin, $J = 5.3$ Hz, 2H). ^{13}C NMR (150 MHz): δ 198.3 (t, $J = 29$ Hz), 137.8, 137.0, 130.9, 129.7, 126.5, 126.3, 119.1 (t, $J = 251$ Hz), 33.1 (t, $J = 24$ Hz), 31.4, 28.9, 19.0 (t, $J = 6$ Hz). ^{19}F -NMR (564 MHz): δ -105.1 (t, $J = 16$ Hz, 2F). HRMS (EI): calcd. for $\text{C}_{12}\text{H}_{12}\text{OF}_2^+ [\text{M}]^+$, 210.0856; found, 210.0859.

Difluorobenzocyclononyne 9.6. A solution of 0.09 M TMSCLiN_2 was generated by combining trimethylsilyldiazomethane (0.1 mL of a 2 M solution in CH_2Cl_2) with *n*butyllithium (0.12 mL of a 1.6 M solution in hexane) in THF (2.0 mL, anhydrous) at -78

°C. This solution was stirred for 20 min at -78 °C. Difluoroketone **9.23** (15 mg, 0.071 mmol, 1.0 equiv.) was dissolved in THF (1.0 mL, anhydrous) and cooled to 0 °C. TMSCLiN₂ (0.8 mL, 0.07 mmol, 1.0 equiv.) was added. The mixture was stirred for 30 min at 0 °C, at which point it was quenched with methanol and evaporated to dryness. It was purified by silica gel chromatography to yield 0.5 mg of **9.6** (0.002 mmol, 3%). This procedure was very unreliable and often did not yield any cyclononyne product. R_f = 0.9 in 3:1 hexane/ethyl acetate. ¹H NMR (400 MHz, CDCl₃): δ 7.86 (bs, 1H), 7.26-7.11 (m, 3H), 4.23 (bs, 1H), 3.47 (bs, 1H), 2.76 (bs, 1H), 2.31-2.15 (m, 1H), 2.02-1.88 (m, 2H), 1.81-1.55 (m, 2H). ¹⁹F NMR (376 MHz, CDCl₃): δ -92.06 (d, *J* = 183.7 Hz), -109.52 (d, *J* = 239.7 Hz).

4-(phenylthio)butanoic acid (9.26).²⁴ Na metal (1.6 g, 70 mmol, 1.1 equiv.) was added portionwise to ethanol (19 mL) cooled to 0 °C. Upon addition of all Na, thiophenol (**9.24**, 6.52 mL, 64 mmol, 1 equiv.) was added dropwise. Upon addition of all thiophenol, the Na was completely dissolved. γ -Butyrolactone (**9.25**, 5.1 mL, 67 mmol, 1.1 equiv.) and the solution was heated to reflux for 4 h, with lots of white precipitate forming. The reaction mixture was quenched with wet ethanol and evaporated to a white solid. The solid was dissolved in water and filtered. The filtrate was acidified with 1M HCl and precipitate formed. The precipitate was recrystallized from hexanes (1L) to yield **9.26** (8.9 g, 64 mmol, quant.) ¹H NMR (600 MHz, CDCl₃): δ 7.35 (d, *J* = 7.9 Hz, 2H), 7.29 (t, *J* = 7.6 Hz, 2H), 7.19 (t, *J* = 7.3 Hz, 1H), 2.98 (t, *J* = 7.1 Hz, 2H), 2.53 (t, *J* = 7.2 Hz, 2H), 1.96 (p, *J* = 7.1 Hz, 2H).

3,4-dihydrobenzo[*b*]thiepin-5(2*H*)-one (9.27).²⁴ Acid **9.26** (2.6 g, 13 mmol, 1.0 equiv.) was dissolved in polyphosphoric acid (38 g) and heated to 100 °C for 2 h. The reaction mixture was poured onto ice and extracted with toluene (3 x 150 mL). The organics were dried, decanted, and evaporated to dryness. The crude product was purified by silica gel chromatography using a hexane/ethyl acetate solvent system (15:1 to 10:1). This procedure yielded pure **9.27** (1.3 g, 7.1 mmol, 54%). R_f = 0.5 in 5:1 hexane/ethyl acetate. ¹H NMR (500 MHz, CDCl₃): δ 7.83 (dd, *J* = 7.8, 1.3 Hz, 1H), 7.45 (d, *J* = 7.8 Hz, 1H), 7.31 (td, *J* = 7.4, 0.9 Hz, 1H), 7.24 (td, *J* = 7.4, 0.9 Hz, 1H), 3.04 (t, *J* = 6.7 Hz, 2H), 2.97 (t, *J* = 6.8 Hz, 2H), 2.26 (p, *J* = 6.7 Hz, 2H). ¹³C NMR (150 MHz, CDCl₃): δ 202.7, 142.1, 138.2, 130.9, 130.2, 130.1, 125.9, 40.1, 34.9, 29.9. HRMS (EI): calcd. for C₁₀H₁₀OS⁺ [M]⁺, 178.0452; found, 178.0457.

4-fluoro-3,4-dihydrobenzo[*b*]thiepin-5(2*H*)-one (9.28). A flame-dried flask was charged with 3,4-dihydrobenzo[*b*]thiepin-5(2*H*)-one **9.27** (1.2 g, 6.6 mmol, 1.0 equiv.). The flask was evacuated and backfilled with nitrogen twice. THF (33 mL, anhydrous) was added to the flask and the solution cooled to -78 °C. Lithium diisopropylamide (4.0 mL of 2M solution in heptane/THF/ ethylbenzene, 8.0 mmol, 1.2 equiv) was added and the solution warmed to 0 °C and allowed to stir for 1 h. Separately, a dry flask was charged with *N*-fluorobenzenesulfonimide (NFSI) (2.7 g, 8.6 mmol, 1.3 equiv) and evacuated and backfilled with nitrogen twice. THF (30 mL, anhydrous) was added and the solution cooled to -78 °C. The solution of **9.27** was slowly added to the NFSI solution over 12 min

via syringe and the mixture was allowed to warm to rt over 30 min, at which point it was quenched with saturated ammonium chloride (50 mL). The organic layer was separated and the aqueous layer extracted with ethyl acetate (2 x 100 mL). The organic layers were combined, dried with sodium sulfate, filtered, and concentrated under reduced pressure. The crude oil was purified using silica gel chromatography (93:7 hexanes/ethyl acetate) to yield 1.1 g (5.6 mmol, 85%) of **9.28** as a yellow oil. $R_f = 0.5$ in 9:1 hexane/ethyl acetate. ^1H NMR (300 MHz, CDCl_3): δ 8.02-7.98 (dd, $J = 7.6, 1.5$ Hz, 1H), 7.47-7.44 (d, $J = 7.8$ Hz, 1H), 7.41-7.7.36 (td, $J = 7.5, 1.5$ Hz, 1H), 7.33-7.28 (t, $J = 7.1$ Hz, 1H), 5.81-5.76 (dd, $J = 7.2, 9$ Hz, 0.5 Hz), 5.65-5.60 (dd, $J = 7.2, 9$ Hz, 0.5H), 3.24-3.16 (m, 1H), 2.89-2.70 (m, 1H), 2.52-2.37 (m, 1H). ^{13}C NMR (130 MHz, CDCl_3): δ 197.5-197.4 (d, $J = 16.6$), 141.7, 134.9, 131.8, 131.1, 130.1, 126.2, 93.8-92.5 (d, $J = 185$), 36.4-36.3 (d, $J = 24$), 29.7 (d, $J = 12$). ^{19}F NMR (375 MHz, CDCl_3): δ -189.4 (dt, $J_f = 4, 45$ Hz, 1F). HRMS (EI): calcd. for $\text{C}_{10}\text{H}_9\text{FOS}^+ [\text{M}]^+$, 196.0358; found, 196.0357.

4,4-difluoro-3,4-dihydrobenzo[b]thiepin-5(2H)-one (9.29). A flame-dried flask was charged with 4-fluoro-3,4-dihydrobenzo[b]thiepin-5(2H)-one **9.28** (800 mg, 4.1 mmol, 1.0 equiv.). The flask was evacuated and backfilled with nitrogen twice. THF (20 mL, anhydrous) was added to the flask and the solution cooled to -78 °C. LDA (2.5 mL of 2 M solution in heptane/ THF/ ethylbenzene, 4.9 mmol, 1.2 equiv.) was added and the solution warmed to 0 °C and allowed to stir for 1 h. Separately, a dry flask was charged with NFSI (1.7 g, 5.3 mmol, 1.3 equiv.) and evacuated and backfilled with nitrogen twice. THF (20 mL, anhydrous) was added and the solution cooled to -78 °C. The solution of base was slowly added to the NFSI solution over 10 min via syringe and the reaction then allowed to warm to rt. Saturated ammonium chloride (40 mL) was added to the reaction followed by ethyl acetate (50 mL). The organic layer was separated and the aqueous layer extracted with ethyl acetate (2 x 50 mL). The organic layers were combined, dried over sodium sulfate, filtered, and concentrated under reduced pressure. The crude oil was purified using silica gel chromatography (93:7 hexanes/EtOAc) to yield 390 mg (1.8 mmol, 45%) of **9.29** as a light yellow oil that solidified upon cooling. $R_f = 0.6$ in 9:1 hexane/ethyl acetate. ^1H NMR (500 MHz, CDCl_3): δ 7.65-7.63 (d, $J = 7.8$, 1H), 7.39-7.30 (m, 2H), 7.26-7.24 (t, $J = 8$ Hz, 1H), 3.05-3.03 (t, $J = 6$ Hz, 2H), 2.76-2.68 (m, 2H). ^{13}C NMR (150 MHz, CDCl_3): δ 193, 138.5, 135.0, 132.0, 131.2, 130.0, 126.4, 118.6 (t, $J = 243$ Hz), 39.6 (t, $J = 25$ Hz), 28.0. ^{19}F NMR (375 MHz, CDCl_3): δ -99 (t, $J = 19$ Hz, 1F). HRMS (EI): calcd. for $\text{C}_{10}\text{H}_8\text{F}_2\text{OS}^+ [\text{M}]^+$, 214.0264; found, 214.0270.

(Z)-4,4-difluoro-6-(trimethylsilyl)-3,4-dihydro-2H-benzo[b]thiocin-5-yl trifluoromethanesulfonate (9.31). A flame-dried flask was charged with 4,4-difluoro-3,4-dihydrobenzo[b]thiepin-5(2H)-one **9.29** (214 mg, 1.00 mmol, 1.0 equiv.) and evacuated and backfilled with nitrogen twice. Dichloromethane (12.5 mL, anhydrous) was added and the solution cooled to 0 °C. Trimethylsilyl diazomethane (TMSCHN_2) (600 μL of 2M solution in dichloromethane, 1.2 mmol, 1.2 equiv.) was added via syringe immediately followed by trimethylaluminum (AlMe_3) (600 μL of 2M solution in toluene, 1.2 mmol, 1.2 equiv.). The reaction was stirred at 0 °C for 10 min, at which point the reaction was quenched with saturated ammonium chloride (5 mL) followed by saturated

Rochelle's salt (5 mL). The mixture was extracted with CH₂Cl₂ (3 x 25 mL). The organic layers were combined, dried over sodium sulfate, filtered, and concentrated to an oil that still contained 4,4-difluoro-6-(trimethylsilyl)-3,4-dihydro-2*H*-benzo[*b*]thiocin-5(6*H*)-one (**9.30**) and toluene was obtained. The oil was transferred to a dry flask that was evacuated and backfilled with nitrogen twice. THF (10 mL, anhydrous) was added and the reaction cooled to -78 °C. NaHMDS (600 μL of 2M solution in THF, 1.2 mmol, 1.2 equiv.) was added and the reaction stirred for 2 h at -78 °C. Trifluoromethane sulfonic anhydride (200 μL, 1.2 mmol, 1.2 equiv.) was then added and the reaction stirred for 1 h at -78 °C. Methanol (1 mL) was added and the reaction was then allowed to warm to rt and concentrated. The oily solid was taken up in dichloromethane and filtered. The filtrate was concentrated and purified via HPLC on a 100 Å C₁₈ column, (70% to 100% acetonitrile in water over 30 minutes). The desired product eluted at 17 minutes. Concentration of desired fraction yielded 16 mg (0.037 mmol, 4%) of (*Z*)-4,4-difluoro-6-(trimethylsilyl)-3,4-dihydro-2*H*-benzo[*b*]thiocin-5-yl trifluoromethanesulfonate **9.31** as a clear oil. R_f = 0.8 in 9:1 hexane/ethyl acetate. ¹H NMR (500 MHz, CDCl₃): δ 7.67-7.65 (d, *J* = 8, 1H), 7.40-7.37 (t, *J* = 7.5, 1H), 7.29-7.26 (m, 1H), 7.16-7.14 (d, *J* = 7.5 Hz, 1H), 3.00-2.96 (m, 1H), 2.83-2.76 (m, 1H), 2.35-2.23 (m, 1H), 2.12-2.05 (m, 1H), 0.019 (s, 9H). ¹³C NMR (125 MHz, CDCl₃): δ 144.1 (t, *J* = 30), 143 (d, *J* = 24), 136.6, 130.3, 129.3, 128.2, 126.5, 122.6, 120, 119.9, 117.5, 116, 34.2 (t, *J* = 26.3 Hz), 29.8 (t, *J* = 5 Hz), -1.3. ¹⁹F NMR (375 MHz, CDCl₃): δ -70 (t, *J* = 19 Hz, 3F), -90 (dp, *J*_F = 262, 22.5 Hz, 1H), -92 (bd, *J* = 274 Hz, 1H). HRMS (EI): calcd. for C₁₅H₁₇F₅O₃S₂Si⁺ [M]⁺, 432.0309; found, 432.0316.

ThiaDIFBO (9.32). (*Z*)-4,4-difluoro-6-(trimethylsilyl)-3,4-dihydro-2*H*-benzo[*b*]thiocin-5-yl trifluoromethanesulfonate **9.31** (16 mg, 0.037 mmol, 1.0 equiv.) was dissolved in deuterated acetonitrile (1 mL) and cesium fluoride (34 mg, 0.22 mmol, 6.0 equiv.) was added. The reaction was stirred for 1 h at rt. It was then filtered, and the filtrate concentrated and purified by silica gel chromatography (99:1 hexanes/ EtOAc) to yield 8 mg (0.04 mmol, 99%) of the desired product as a clear oil. R_f = 0.9 in 9:1 hexane/ethyl acetate. ¹H NMR (600 MHz, CD₃CN): δ 7.56-7.54 (d, *J* = 9 Hz, 1H), 7.47-7.45 (d, *J* = 8 Hz, 1H), 7.42-7.39 (t, *J* = 7.2 Hz, 1H), 7.35-7.33 (t, *J* = 7.5 Hz, 1H), 3.17-2.16 (m, 1H), 2.86- 2.79 (m, 1H). ¹³C NMR (125 MHz, CD₃CN): δ 148, 131.4, 130.9, 128.8, 127.4, 122.4, 120.6, 119.9, 106.3 (t, *J* = 9 Hz), 46.1 (t, *J* = 27.5 Hz), 28.8 (t, *J* = 3.8 Hz). ¹⁹F NMR (375 MHz, CD₃CN): -86 (bt, 2F). HRMS (EI): calcd. for C₁₁H₈F₂⁺ [M]⁺, 210.0315; found, 210.0321.

3-methylthiochroman-4-one. THF (5.5 mL, anhydrous) and LiHMDS (3.61 mL of 1 M solution in THF, 3.61 mmol, 1.2 equiv.) were combined and cooled to -78 °C. Thiochromanone **9.36** (502 mg, 3.05 mmol, 1.0 equiv.) was dissolved in THF (2.0 mL, anhydrous) and added to the solution of base over 1 h at -78 °C. After stirring for an additional hour at -78 °C, methyl iodide (0.93 mL, 15 mmol, 4.9 equiv.) was added and the mixture was warmed to rt over 3 h at which point, the reaction was quenched with methanol (2 mL) and evaporated to dryness. Silica gel chromatography (35:1 hexane/ethyl acetate) resulted in pure desired compound (400 mg, 2.24 mmol, 73%). R_f = 0.45 in 6:1 hexane/ethyl acetate. ¹H NMR (600 MHz, CDCl₃): δ 8.05 (dd, *J* = 7.2, 1.0, 1H), 7.33-7.30

(m, 1H), 7.19 (dd, $J = 7.9, 0.7$ Hz, 1H), 7.13-7.10 (m, 1H), 3.09 (s, 1H), 3.08 (d, $J = 3.1$ Hz, 1H), 2.88 (dp, $J = 8.7, 6.8$ Hz, 1H), 1.30 (d, $J = 6.8$ Hz, 3H). ^{13}C NMR (150 MHz, CDCl_3): δ 196.5, 141.9, 133.0, 130.5, 129.6, 127.4, 124.9, 42.2, 33.1, 15.1. HRMS (EI): calcd. for $\text{C}_{10}\text{H}_{10}\text{OS}^+ [\text{M}]^+$, 178.0452; found, 178.0452.

3,3-dimethylthiochroman-4-one (9.37). THF (1.0 mL, anhydrous) and LiHMDS (0.96 mL of 1 M solution in THF, 0.96 mmol, 1.2 equiv.) were combined and cooled to -78 °C. 3-methylthiochroman-4-one (144 mg, 0.809 mmol, 1.0 equiv.) was dissolved in THF (1.0 mL, anhydrous) and added to the solution of base over 1 h at -78 °C. After stirring for an additional hour at -78 °C, methyl iodide (0.25 mL, 4.0 mmol, 4.9 equiv) was added and the mixture was warmed to rt over 3 h, at which point the reaction was quenched with MeOH (1 mL) and evaporated to dryness. Silica gel chromatography (40:1 hexanes/ EtOAc) resulted in pure **9.37** (129 mg, 0.672 mmol, 83%). $R_f = 0.55$ in 6:1 hexane/ethyl acetate. ^1H NMR (500 MHz, CDCl_3): δ 8.08 (dd, $J = 8.0, 1.2$ Hz, 1H), 7.33 (ddd, $J = 8.0, 7.2, 1.5$ Hz, 1H), 7.20 (dd, $J = 8.0, 0.8$ Hz, 1H), 7.14 (ddd, $J = 8.2, 7.2, 1.2$ Hz, 1H), 3.07 (s, 2H), 1.32 (s, 6H). ^{13}C NMR (125 MHz, CDCl_3): δ 198.5, 141.6, 132.9, 130.3, 129.7, 127.3, 124.9, 41.1, 39.3, 23.7. HRMS (EI): calcd. for $\text{C}_{11}\text{H}_{12}\text{OS}^+ [\text{M}]^+$, 192.0609; found, 192.0604.

(3,3-dimethyl-2,3-dihydrobenzo[b]thiepin-5-yloxy)trimethylsilane (9.38). 3,3-dimethylthiochroman-4-one **9.37** (365 mg, 1.90 mmol, 1.0 equiv.) was dissolved in CH_2Cl_2 (10 mL, anhydrous) and cooled to -78 °C. AlMe_3 (1.14 mL of 2M solution in toluene, 2.28 mmol, 1.2 equiv.) was added and the solution was stirred for 15 min at which point, TMSCHN_2 (1.14 mL of 2M solution in CH_2Cl_2 , 2.28 mmol, 1.2 equiv.) was added. The solution was warmed to rt overnight. The mixture was quenched with aqueous Rochelle's salt (5 mL) and stirred until two layers formed. The quenched solution was extracted with dichloromethane (3 x 10 mL). The organic layers were combined, dried with MgSO_4 , decanted, and evaporated to dryness. Silica gel chromatography (150:1 hexane/ethyl acetate) resulted in pure **9.38** (160 mg, 0.576 mmol, 30%). $R_f = 0.9$ in 6:1 hexane/ethyl acetate. ^1H NMR (600 MHz, CDCl_3): δ 7.38 (d, $J = 7.6$ Hz, 1H), 7.14-7.11 (m, 2H), 7.00 (t, $J = 7.1$ Hz, 1H), 5.81 (s, 1H), 2.77 (s, 2H), 1.28 (s, 6H), 0.30 (s, 9H). ^{13}C NMR (125 MHz, CDCl_3): δ 162.3, 137.4, 137.1, 131.5, 131.0, 126.6, 124.8, 110.1, 46.1, 44.2, 28.0, 0.8. HRMS (EI): calcd. for $\text{C}_{15}\text{H}_{22}\text{OSSi}^+ [\text{M}]^+$, 278.1161; found, 278.1163.

3,3-dimethyl-3,4-dihydrobenzo[b]thiepin-5(2H)-one (9.39). Silyl enol ether **9.38** (90 mg, 0.32 mmol, 1 equiv.) was dissolved in methanol and 12M HCl (1 drop) was added. The mixture was stirred for 30 min at rt and then quenched with saturated sodium bicarbonate (until bubbling ceased). The methanol was removed by rotary evaporation and the resulting aqueous solution was extracted with dichloromethane (3 x 10 mL). The organic layers were combined, dried with MgSO_4 , decanted, and evaporated to dryness. This procedure resulted in pure ketone **9.39** (65 mg, 0.31 mol, 97% yield). $R_f = 0.5$ in 4:1 hexane/ethyl acetate. ^1H NMR (400 MHz, CDCl_3): δ 7.46 (dd, $J = 7.5, 1.1$ Hz, 1H), 7.29 (d, $J = 7.3$ Hz, 1H), 7.20 (td, $J = 7.5, 1.4$ Hz, 1H), 7.14 (td, $J = 7.5, 1.4$ Hz, 1H), 4.03 (s, 2H), 2.83 (s, 2H), 1.32 (s, 6H). ^{13}C NMR (150 MHz, CDCl_3): δ 209.3, 138.2, 136.8, 132.7,

130.6, 128.6, 127.5, 49.3, 47.2, 46.2, 24.3. HRMS (EI): calcd. for $C_{12}H_{14}OS^+$ $[M]^+$, 206.0765; found, 206.0764.

3,3-dimethyl-2,3-dihydrobenzo[*b*]thiepin-5-yl trifluoromethanesulfonate (9.40).

Ketone **9.39** (62 mg, 0.30 mmol, 1 equiv.) was dissolved in THF (4.5 mL, anhydrous) and cooled to $-78\text{ }^{\circ}\text{C}$. KHMDS (0.72 mL of 0.5 M solution in toluene, 0.36 mmol, 1.2 equiv.) was added and the solution was stirred for 2 h at $-78\text{ }^{\circ}\text{C}$ at which point trifluoromethane sulfonic anhydride (70 μL , 0.42 mmol, 1.4 equiv.) was added and the reaction was warmed to $0\text{ }^{\circ}\text{C}$ over 2 h. The reaction mixture was quenched with methanol (1 mL) and evaporated to dryness. Silica gel chromatography with hexanes/ethyl acetate (150:1) resulted in pure **9.40** (66 mg, 0.20 mmol, 66%). $R_f = 0.9$ in 4:1 hexane/ethyl acetate. ^1H NMR (500 MHz, CDCl_3): δ 7.47 (dd, $J = 7.6, 1.4$ Hz, 1H), 7.30-7.24 (m, 2H), 7.20 (td, $J = 7.4, 1.7$ Hz, 1H), 6.62 (s, 1H), 2.86 (s, 2H), 1.42 (s, 6H). ^{13}C NMR (150 MHz, CDCl_3): δ 158.3, 139.2, 133.9, 132.9, 131.5, 128.2, 127.2, 122.0, 118.7 (q, $J = 320$ Hz), 45.5, 44.5, 27.3. ^{19}F NMR (565 MHz, CDCl_3): δ -75.63. HRMS (EI): calcd. for $C_{13}H_{13}O_3S_2F_3^+$ $[M]^+$, 338.0258; found, 338.0262.

Triazole products (9.41 and 9.42). Vinyl triflate **9.40** (10 mg, 0.030 mmol, 1.0 equiv.) was dissolved in THF (1.0 mL, anhydrous). NaH (10 mg, 60% in mineral oil, 0.26 mmol, 8.7 equiv.) was added to this solution followed by benzyl azide (15 μL , 0.12 mmol, 4.0 equiv.). The mixture was allowed to stir overnight. The following day the reaction was quenched with methanol (0.25 mL) and evaporated to dryness. The crude reaction mixture was purified by silica gel chromatography (6:1, 4:1, 1:1 hexanes/ethyl acetate). This procedure resulted in 5 mg of pure **9.41** and **9.42** (0.016 mmol, 53%) in a 1:0.6 ratio. $R_f = 0.3$ in 4:1 hexane/ethyl acetate. ^1H NMR (600 MHz, MeOD): δ 8.21 (d, $J = 7.8$ Hz, 1H), 7.60 (d, $J = 7.8$ Hz, 1H'), 7.56 (d, $J = 7.8$ Hz, 1H'), 7.52 (d, $J = 7.7$ Hz, 1H), 7.39-7.35 (m, 3H, 2H'), 7.31-7.22 (m, 2H, 3H'), 7.08 (d, $J = 7.7$ Hz, 2H), 6.96 (d, $J = 6.8$ Hz, 2H'), 5.92 (s, 2H), 5.69 (s, 2H'), 2.96 (s, 2H), 2.90 (s, 2H'), 1.50 (s, 6H'), 1.46 (s, 6H). ^{13}C NMR (150 MHz, MeOD): δ 154.0, 143.5, 143.0, 142.1, 139.5, 138.2, 137.4, 134.8, 134.5, 133.1, 132.4, 131.5, 131.1, 130.2, 130.0, 129.9, 129.9, 129.1, 129.0, 128.8, 128.6, 128.6, 127.8, 127.54, 127.52, 55.0, 54.1, 51.6, 51.2, 49.7, 39.5, 39.0, 30.4, 28.4. HRMS (ESI): calcd. for $C_{19}H_{20}N_3S^+$ $[M+H]^+$, 322.1372; found, 322.1374.

Kinetics

DIFBO (8.3). β -cyclodextrin-DIFBO complex (~200 mg, **8.13**) was dissolved in CD_3CN (~4 mL) and the β -cyclodextrin was removed by filtration. The white solid was washed with CD_3CN (~1.5 mL). The resulting eluent was transferred to NMR tubes (600 μL each). A 59 mM solution of BnN_3 in CD_3CN was prepared. To the first NMR tube containing DIFBO, an approximate amount of BnN_3 solution was added. Using integration, the amount of BnN_3 necessary for an exact 1:1 mixture of BnN_3 :DIFBO to be obtained was calculated. This amount (90-100 μL) was added to the remaining DIFBO solutions and each reaction was monitored by ^1H NMR over 15 min. The concentration of each sample was determined relative to the amount of BnN_3 added. A plot of $1/[\text{DIFBO}]$

(M^{-1}) vs. time (sec) resulted in a linear regression (Figure 9.1) whose slope was the second-order rate constant. This procedure was repeated four times with a concentration of 7-8 mM, to yield a second-order rate constant of $0.22 \pm 0.01 M^{-1}s^{-1}$.

Monobenzocyclooctyne (9.3). A solution of monobenzocyclooctyne (24 mM) in CD_3CN with a small amount of hexamethyldisilane was prepared. A solution of BnN_3 (146 mM) was also prepared using the same solution of CD_3CN containing a small amount of hexamethyldisilane. 1H -NMR spectra of each of these solutions were obtained, and using the ratio of BnN_3 or **9.3** to hexamethyldisilane the appropriate amount of each solution necessary for a 1:1 mixture of BnN_3 :**9.3** was calculated. The correct amount of BnN_3 was added to **9.3** and the reaction was monitored by 1H NMR over 45 min. The concentration of each sample was determined based on the concentration of the initial monobenzocyclooctyne solution. A plot of $1/[9.3]$ (M^{-1}) vs. time (sec) resulted in a linear regression whose slope was the second-order rate constant (Figure 9.2). This procedure was repeated three times with a concentration of 19 mM to yield a second-order rate constant of $0.0095 \pm 0.0003 M^{-1}s^{-1}$.

ThiaDIFBO (9.32). ThiaDIFBO **9.32** and BnN_3 were separately dissolved in CD_3CN and mixed together in a 1: 1 ratio at a concentration of 7 mM. The reaction was monitored by 1H NMR for 20 min at rt. The percent conversion was calculated by the disappearance of thiaDIFBO and BnN_3 relative to the formation of product as determined by integration. The triazole isomers were formed in approximately a 3:1 ratio. The second-order rate constant was determined by plotting $1/[9.32]$ versus time. The plot was fit to a linear regression and the slope corresponds to the second-order rate constant. Shown are data from three replicate experiments (Figure 9.6). The three lines had an average slope of $0.015 \pm 0.001 M^{-1}s^{-1}$.

Western Blot Analysis of β -Cyclodextrin-DIFBO Treated Lysates

Jurkat cells were grown in media supplemented with or without 25 μM $Ac_4ManNAz$ (+Az or -Az respectively) for 3 d. The cells were concentrated ($500 \times g$, 3 min) and washed three times by sequential resuspension with 10 mL chilled PBS and concentration. The cell pellet was resuspended in lysis buffer (150 mM NaCl, 20 mM Tris, 1% NP-40 substitute (Sigma-Aldrich), pH 7.4; 500 μL buffer per 2.8×10^7 cells) containing protease inhibitors (Roche) and disrupted by sonication with one 30 s 6 W pulse. Following sonication, insoluble debris were removed by centrifugation ($20000 \times g$, 10 min) and the supernatant was kept. The protein concentration of each lysate was determined using the Bio-RAD[®] D_c protein assay.

Twenty-five micrograms of total protein from each lysate was reacted with 150 μM β -cyclodextrin-DIFBO complex (**8.13**), β -cyclodextrin alone, or no reagent for 4 h at rt. Phos-FLAG (250 μM) was added to each of the samples and they were incubated overnight at rt. The following morning, SDS-PAGE loading buffer (4X, BioRAD) was added to each sample and the proteins were separated via electrophoresis and transferred to a nitrocellulose membrane. Equal protein loading and successful transfer were confirmed

by visualizing the proteins with Ponceau S. The membrane was blocked with 5-10% BSA in PBST (PBS pH 7.4 containing 0.1% Tween 20) for 2 h at rt. The membrane was incubated with horseradish peroxidase-conjugated α -FLAG (1:5,000 dilution, Sigma) in PBST for 1 h. The membrane was washed with PBST (3 x 15 min). Detection was performed by chemiluminescence using Pierce SuperSignal West Pico Chemiluminescent Substrate.

References

- (1) Sletten, E. M.; Nakamura, H.; Jewett, J. C.; Bertozzi, C. R. Difluorobenzocyclooctyne: Synthesis, reactivity, and stabilization by β -cyclodextrin. *J. Am. Chem. Soc.* **2010**, *132*, 11799-11805.
- (2) Baskin, J. M.; Prescher, J. A.; Laughlin, S. T.; Agard, N. J.; Chang, P. V.; Miller, I. A.; Lo, A.; Codelli, J. A.; Bertozzi, C. R. Copper-free click chemistry for dynamic in vivo imaging. *Proc. Natl. Acad. Sci. U.S.A.* **2007**, *104*, 16793 -16797.
- (3) Mbua, N. E.; Guo, J.; Wolfert, M. A.; Steet, R.; Boons, G. Strain-promoted alkyne-azide cycloadditions (SPAAC) reveal new features of glycoconjugate biosynthesis. *ChemBioChem* **2011**, *12*, 1912-1921.
- (4) Chenoweth, K.; Chenoweth, D.; Goddard III, W. A. Cyclooctyne-based reagents for uncatalyzed click chemistry: A computational survey. *Org. Biomol. Chem.* **2009**, *7*, 5255-5258.
- (5) Meier, H.; Layer, M.; Zetzche, A. 7,8,9,10-Tetrahydro-5,6-dehydrobenzocyclooctene. Cycloalkyne with high ring tension. *Chem-Ztg.* **1974**, *98*, 460.
- (6) Huisgen, R.; Rapp, W. Mittlere ringe, I. Mitteil.: 1.2-Benzo-cycloocten-(1)-on-(3). *Chem. Ber.* **1952**, *85*, 826-835.
- (7) Maier, G. Tetrahedrane and cyclobutadiene. *Angew. Chem. Int. Ed.* **1988**, *27*, 309-332.
- (8) Liebman, J. F.; Greenberg, A. A survey of strained organic molecules. *Chem. Rev.* **1976**, *76*, 311-365.
- (9) Tokitoh, N. Synthesis of aromatic species containing a heavier group 14 element by taking advantage of kinetic stabilization. *Bull. Chem. Soc. Jpn.* **2004**, *77*, 429-441.
- (10) Tsuji, T.; Ohkita, M.; Kawai, H. Preparation and kinetic stabilization of highly strained paracyclophanes. *Bull. Chem. Soc. Jpn.* **2002**, *75*, 415-433.
- (11) Coumbarides, G. S.; Eames, J.; Weerasooriya, N. The synthesis and characterization of 2-Trideuteriomethyl and 2,2-di(trideuteriomethyl) aryl ketones. *J. Labelled Compd. Rad.* **2002**, *45*, 935-942.
- (12) Kim, S. S.; Rajagopal, G.; Song, D. H. Mild and efficient silylcyanation of ketones catalyzed by cesium fluoride. *J. Organomet. Chem.* **2004**, *689*, 1734-1738.
- (13) Seebach, D.; Corey, E. J. Generation and synthetic applications of 2-lithio-1,3-dithianes. *J. Org. Chem.* **1975**, *40*, 231-237.

- (14) Ranu, B. C.; Jana, U. A new redundant rearrangement of aromatic ring fused cyclic α -hydroxydithiane derivatives. Synthesis of aromatic ring fused cyclic 1,2-diketones with one-carbon ring expansion. *J. Org. Chem.* **1999**, *64*, 6380-6386.
- (15) McCague, R. An analogue of the antioestrogen tamoxifen of sufficient rigidity to exist as distinct enantiomers: Synthesis and conformational dynamics studies. *Tetrahedron-Asymmetr.* **1990**, *1*, 97-110.
- (16) Pravst, I.; Zupan, M.; Stavber, S. Efficient synthesis of α,α -difluoro ketones using Selectfluor. *Synthesis* **2005**, 3140-3146.
- (17) Nagao, K.; Chiba, M.; Kim, S.-W. A new efficient homologation reaction of ketones via their lithiodiazoacetate adducts. *Synthesis* **1983**, 197-199.
- (18) Moebius, D. C.; Kingsbury, J. S. Catalytic homologation of cycloalkanones with substituted diazomethanes. Mild and efficient single-step access to α -tertiary and α -quaternary carbonyl compounds. *J. Am. Chem. Soc.* **2009**, *131*, 878-879.
- (19) Mock, W. L.; Hartman, M. E. Mechanism of the triethyloxonium ion catalyzed homologation of ketones with diazoacetic esters. *J. Org. Chem.* **1977**, *42*, 466-472.
- (20) Maruoka, K.; Concepcion, A. B.; Yamamoto, H. Organoaluminum-promoted homologation of ketones with diazoalkanes. *J. Org. Chem.* **1994**, *59*, 4725-4726.
- (21) Hashimoto, N.; Aoyama, T.; Shioiri, T. New methods and reagents in organic synthesis. 10. Trimethylsilyldiazomethane(TMSCHN₂). A new, stable, and safe reagent for the homologation of ketones. *Tetrahedron Lett.* **1980**, *21*, 4619-4622.
- (22) Shioiri, T.; Aoyama, T. Trimethylsilyldiazomethane: A useful reagent for generating alkylidene carbenes and its application to organic synthesis. *J. Syn. Org. Chem., Jpn.* **1996**, *54*, 918-928.
- (23) Miwa, K.; Aoyama, T.; Shioiri, T. Extension of the Colvin rearrangement using trimethylsilyldiazomethane. A new synthesis of alkynes. *Synlett* **1994**, 107-108.
- (24) Traynelis, V. J.; Love, R. F. Seven-membered heterocycles. I. Synthesis of benzo[b]thiepin 1,1-dioxide and 1-phenylsulfonyl-4-phenyl-1,3-butadiene. *J. Org. Chem.* **1961**, *26*, 2728-2733.
- (25) Lal, G. S. Site-selective fluorination of organic compounds using 1-alkyl-4-fluoro-1,4-diazabicyclo[2.2.2]octane salts (Selectfluor reagents). *J. Org. Chem.* **1993**, *58*, 2791-2796.
- (26) Pangborn, A. B.; Giardello, M. A.; Grubbs, R. H.; Rosen, R. K.; Timmers, F. J. Safe and convenient procedure for solvent purification. *Organometallics* **1996**, *15*, 1518-1520.

Chapter 10

The Road to a New Bioorthogonal Reaction

A Guide to Bioorthogonal Reaction Development

The process of bioorthogonal reaction development and optimization is a journey that requires a critical understanding of mechanistic chemistry, biochemistry, and for *in vivo* applications, pharmacology and metabolism. The effort begins with an analysis of those functionalities and reaction types that are not represented among nature's repertoire. From this abiotic chemical space, a prototype reaction among functional groups with inherent stability toward biological moieties – nucleophiles, reductants, and of course, water – is identified (Figure 10.1, step 1). Bioorthogonal reactions for the azide have demonstrated that the chemical literature from the early to mid 20th century is fertile ground for unearthing prototype reactions. During this period, physical organic chemists were intrigued by the properties of exotic structures outside the mainstream of organic synthesis, and the practical utility of some of these mechanistic oddities was generally not of primary importance. Understanding the fundamental behaviors of organic molecules – how structure relates to reactivity – was sufficient justification for such mechanistic explorations, a testament to a time when society was more forgiving of curiosity-driven science.

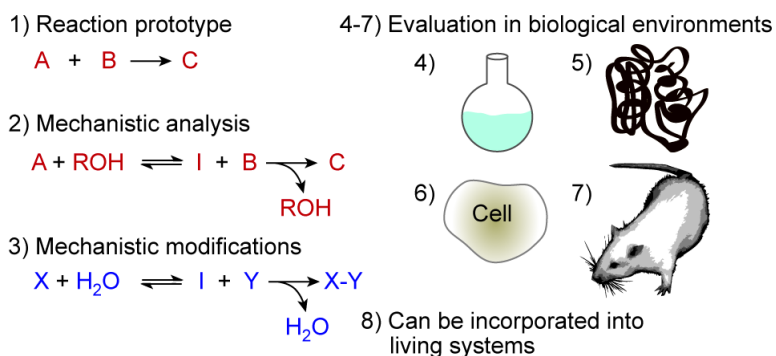


Figure 10.1. A step-by-step guide to bioorthogonal reaction development.

Once a prototype reaction is selected, an in-depth mechanistic analysis is essential to guide the requisite adaptations for use in biological systems and to anticipate potential pitfalls (Figure 10.1, step 2). Each elementary step of the reaction must be compatible with water and the large excess of nucleophilic functionalities found in nature (*e.g.* amines, thiols, hydroxy groups). These elementary steps must proceed at reasonable rates under physiological conditions. In practice, reactions with a second-order rate constant smaller than $10^{-4} \text{ M}^{-1}\text{s}^{-1}$ will be too slow for practical use when reagents are held at the low

concentrations necessary to label biomolecules with minimal background. For this reason, rate enhancement is a common initial goal (step 3) in transforming a prototype reaction into a *bona fide* bioorthogonal transformation.

The next step (Figure 10.1, step 3) is to modify the reagents, and in some cases the overall mechanism, to solve whatever problems are revealed in step 2. Adjustments might include the addition of steric bulk for protection from biological nucleophiles, exchange of heteroatoms to promote optimal orbital interactions, or activation of the reagents by strain enhancement or electronic perturbation. The mechanistic modifications are the most difficult part of the reaction development process, and chemists often find themselves pursuing numerous iterations of a reaction along the way.

Once the optimized candidate reaction proceeds efficiently in a flask (*i.e.* an effective chemical reaction from a synthetic chemist's perspective), it must be tested against the standards of bioorthogonality in environments of increasing complexity (Figure 10.1, steps 4-7). The first test is whether the reaction proceeds reliably in aqueous media alongside biological metabolites such as amino acids and sugars (step 4). Next, the reaction must be evaluated on biomolecules (step 5), in live cells (step 6), and ultimately in model organisms such as zebrafish or mice (step 7). Not all bioorthogonal reactions developed to date have succeeded in live animals, or even in live cells, but these decisive measures of bioorthogonality should always be considered a central goal.

The final criterion of a superior bioorthogonal reaction is that at least one of its participating functional groups can be incorporated into biomolecules in living systems (Figure 10.1, step 8). In reality, step 8 is often pursued in parallel to steps 6 and 7. Numerous methods for installing unnatural functional groups within proteins, glycans, lipids, nucleic acids and other metabolites have been developed. The functional groups with access to the most extensive array of biomolecules – typically the smallest functional groups – are those whose bioorthogonal reactions will ultimately be the most useful.

The success of the azide as a chemical reporter group for biomolecules makes the development of a new bioorthogonal reaction a daunting task. The azide is only three atoms and not present in living systems, yet it is stable to biological milieu and undergoes selective reaction with phosphines, cyclooctynes, and copper-(or ruthenium)-acetylides.¹² However, a major goal in our laboratory is to study the dynamic interactions of several types of biomolecules simultaneously, which will require parallel use of a collection of bioorthogonal reactions (Figure 10.2) that are mutually orthogonal to each other. While this is a common experimental platform using antibodies, to achieve this goal using covalent chemistries the development of both a new, efficient, chemical reporter group and a secondary reagent which undergoes selective reactivity with only the chemical reporter group of interest is necessary.

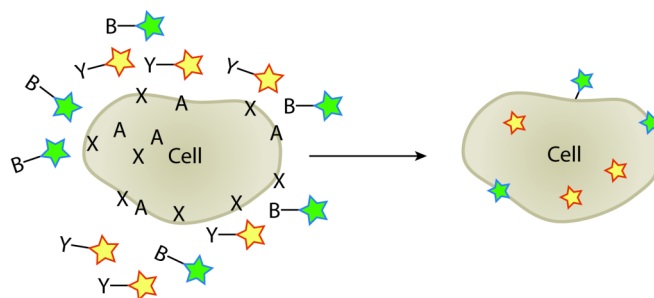
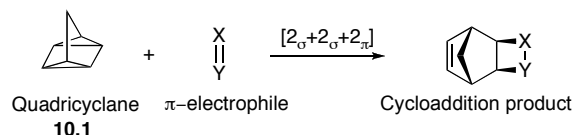


Figure 10.2. Schematic for a double labeling experiment with mutually orthogonal bioorthogonal chemistries. Chemical reporter group A selectively reacts with secondary reagent B while chemical reporter group X selectively reacts with secondary reagent Y.

A New Chemical Reporter Group

In an effort to develop new bioorthogonal reactions that are themselves orthogonal to the current cohort, we sought to explore unrepresented reactivity space. The bioorthogonal transformations discussed thus far can fall into three categories: 1,3-dipolar cycloadditions (Cu-free click chemistry),³ metal-catalyzed couplings (Cu or Ru catalyzed azide-alkyne cycloaddition; cross-coupling with aryl halides),^{4,5,6,7,8} and nucleophilic additions (Staudinger ligation and oxime or hydrazone formation).^{9,10} Outside of this space lies the [2+2+2] cycloaddition reaction, a popular choice for the rapid assembly of functionalized ring systems.^{11,12} In practice, such reactions are typically metal catalyzed as a means to overcome an otherwise significant entropic barrier. However, the highly strained hydrocarbon quadricyclane (**10.1**) directly undergoes [2+2+2] cycloaddition with specific types of π systems (Scheme 10.1).¹³

Scheme 10.1. A generic $[2_{\sigma}+2_{\sigma}+2_{\pi}]$ reaction between quadricyclane and π -electrophiles to yield a norbornene cycloaddition product.



Quadricyclane possesses many qualities that render it a promising chemical reporter group. First, it is abiotic, and we envisioned that quadricyclane's all sp^3 -hybridized carbon system would provide little functionality capable of reacting with native biomolecules. Second, although quadricyclane contains seven non-hydrogen atoms rather than the three of the azide, the molecule is relatively compact.^{14,15} In fact, all the C-C bond lengths are shorter than the canonical $C(sp^3)-C(sp^3)$ bond length of 1.54 Å except for the two bonds which connect the cyclopropyl rings (Figure 10.3). A molecule of this size

should be amenable to metabolic incorporation into biomolecules, most likely through the sialic acid salvage pathway¹⁶ or through unnatural amino acid incorporation.^{17,18}

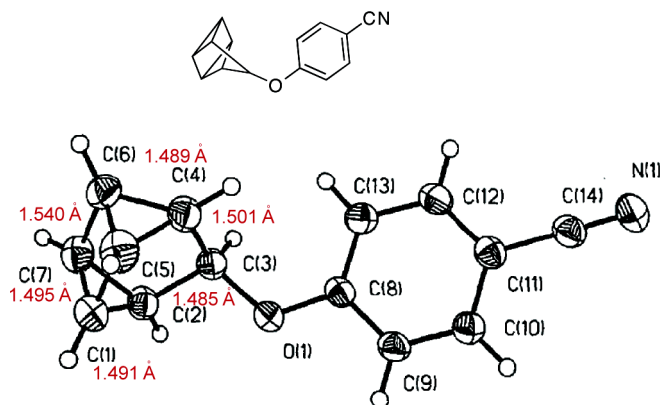


Figure 10.3. Crystal structure of 3-(*p*-cyanophenoxy) quadricyclane reported by Watson and Tavanaiepour. Figure modified from *Acta Crystallogr.* **1987**, *C43*, 1356.¹⁵

Third, quadricyclane is highly strained (80 kcal/mol)¹⁹ and displays intriguing reactivity with a variety of electrophilic reagents including diazodicarboxylates²⁰ and other electron-deficient π systems (Figure 10.4).^{21,22,23} By contrast, quadricyclane is highly stable to nucleophiles under physiological conditions, and additionally, does not react readily with simple alkenes, alkynes or even cyclooctynes employed for other bioorthogonal chemistries.¹³ Lastly, [2+2+2] cycloadditions with quadricyclane have been used to study the “on water” effect both through empirical and theoretical work.^{24,25,26} These studies have reported a dramatic rate increase in water and stabilization of the transition state by 7 kcal/mol.²⁷

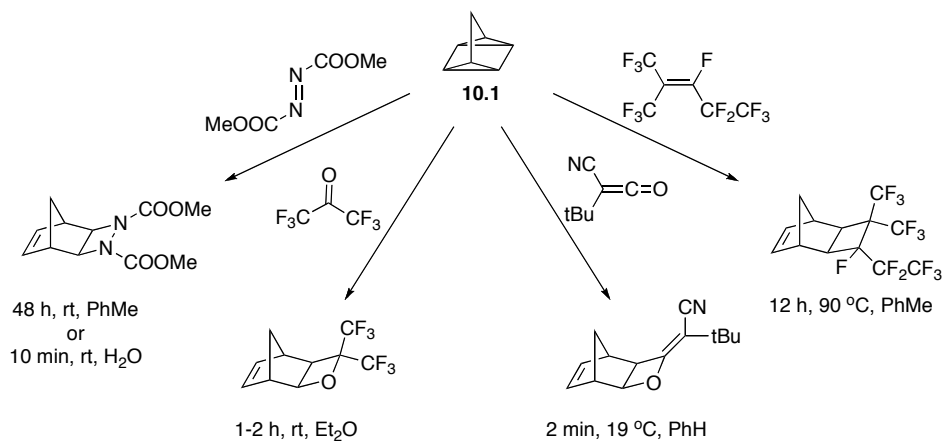
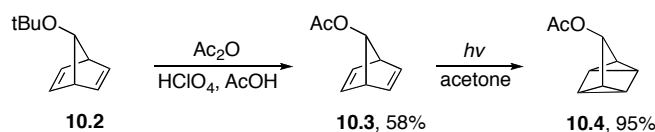


Figure 10.4. Selected [2+2+2] cycloaddition reactions with quadricyclane.

Before embarking on the quest for a reaction partner for quadricyclane, we wanted to ensure that quadricyclane was indeed stable enough for use as a chemical reporter group in living systems. A substituted quadricyclane, 7-acetoxy quadricyclane (**10.4**, Scheme 10.2), was prepared from 7-*tert*-butyl [2,5]norbornadiene (**10.2**).^{28,29} Acid cleavage of the *tert*-butyl ether in the presence of acetic anhydride gave 7-acetoxy [2,5]norbornadiene (**10.3**), which was converted to quadricyclane **10.4** in a photoinitiated intramolecular [2+2] cycloaddition. Acetone was employed as a triplet sensitizer for this transformation. It should be noted that while norbornadiene is considerably less strained than quadricyclane, the isomerization of quadricyclane to norbornadiene is a Woodward-Hoffman forbidden process and consequently has a large half-life ($t_{1/2} = 14$ h at 140 °C).³⁰

Scheme 10.2. Synthesis of 7-acetoxy quadricyclane.



Compound **10.4** was found to be stable to phosphate buffered saline (PBS, pH 7.4) with no degradation at room temperature after more than 2 months (Figure 10.5A). We also found **10.4** to be unreactive with sugars, a variety of oxidants, and free amino acids, most notably cysteine (Figure 10.5B). Furthermore, quadricyclane was stable in the presence of bovine serum albumin (BSA) and cell culture media under conditions emulating those necessary for metabolic labeling experiments. Our findings are consistent with most published reports regarding the stability of quadricyclane in aqueous solutions.^{31,32,33}

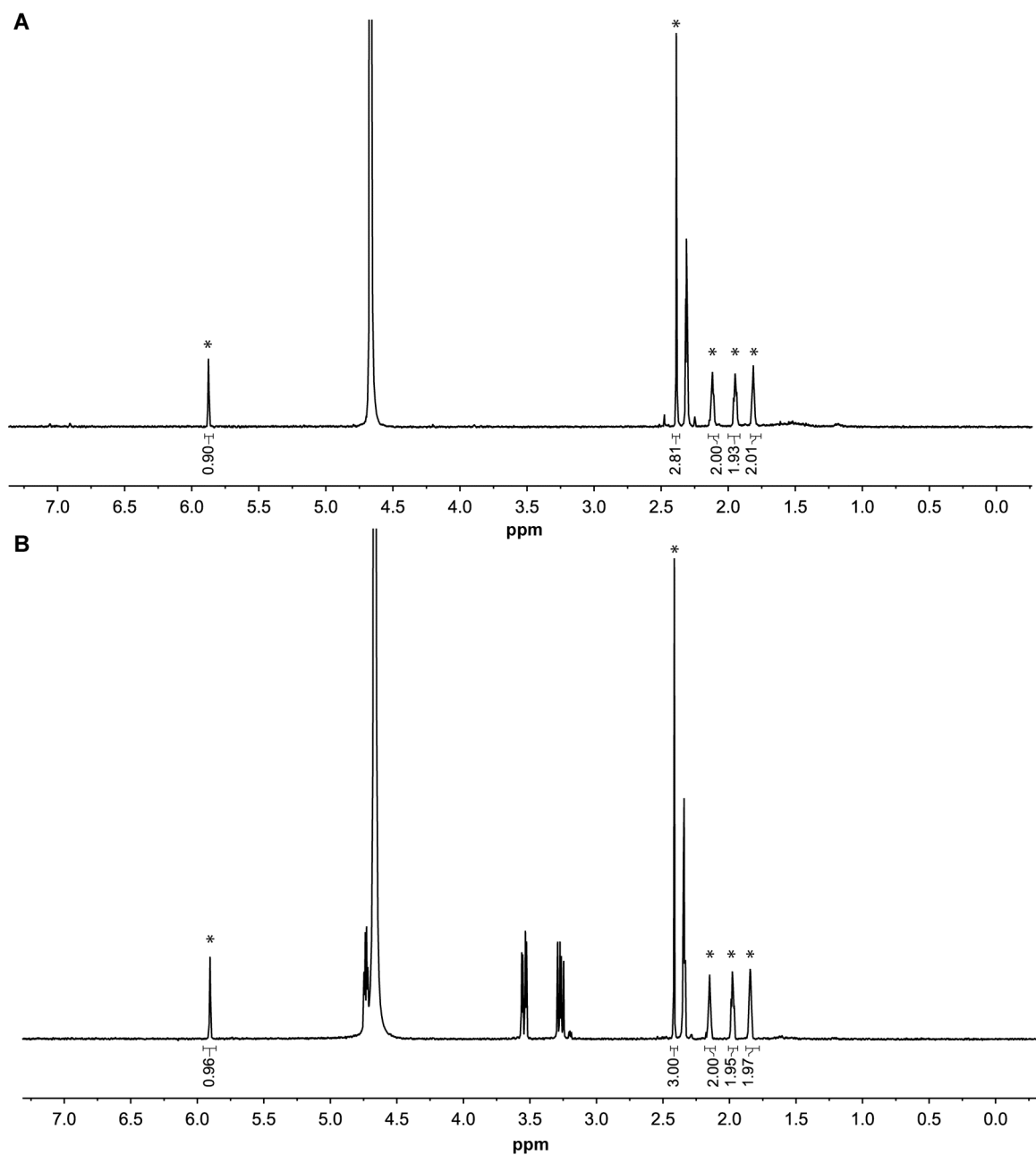
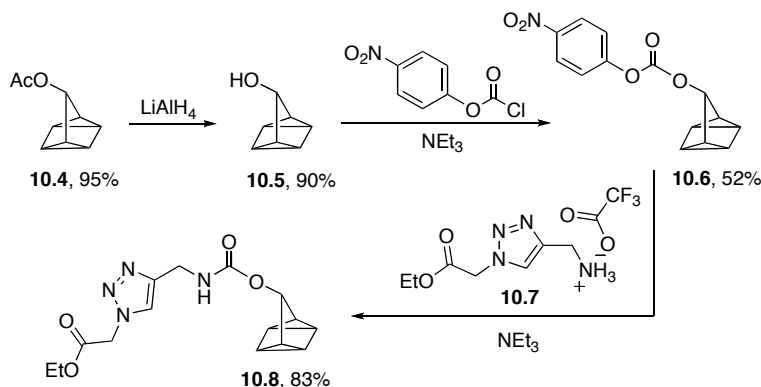


Figure 10.5. Quadricyclane is stable to phosphate buffered saline (PBS, pH 7.4) and cysteine. A. 7-acetoxy quadricyclane (**10.4**) was dissolved in a mixture of deuterated PBS and CD₃CN (1:1 ratio). The NMR spectrum above was taken 2.5 months after the solution was prepared. B. 7-acetoxy quadricyclane (**10.4**) and cysteine were dissolved at approximately equimolar amounts in a mixture of deuterated PBS and CD₃CN (1:1 ratio). The NMR spectrum was taken 2.5 months after the described solution was prepared. A/B. Peaks corresponding to 7-acetoxy quadricyclane are designated with an asterisk (*).

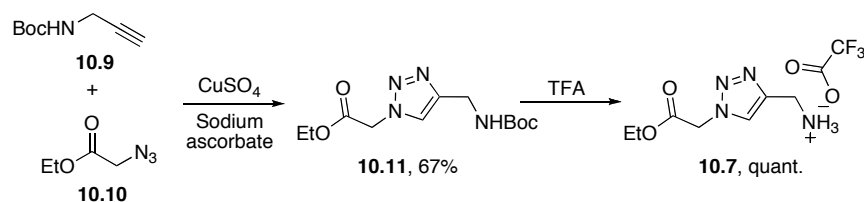
Finding a Reaction Partner for Quadricyclane

At this point, quadricyclane appeared to possess the qualities necessary for a chemical reporter group if a selective reaction could be developed. To identify a bioorthogonal reaction partner for quadricyclane, we prepared a triazole-functionalized quadricyclane (**10.8**, Scheme 10.3), which had advantageous ionization properties for electrospray mass spectrometry. Briefly, quadricyclane **10.8** was prepared by reduction of the acetoxy group in **10.4** with lithium aluminum hydride to yield **10.5**, which was activated as a *p*-nitrophenyl carbonate (**10.6**). Activated carbonate **10.6** was treated with triazole **10.7** to yield quadricyclane **10.8**. Triazole **10.7** was prepared through the CuAAC of Boc-protected propargyl amine (**10.9**) and ethyl azidoacetate **10.10** to yield **10.11**, which was deprotected with TFA to give **10.7** (Scheme 10.4).

Scheme 10.3. Synthesis of triazole-functionalized quadricyclane.

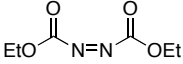
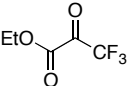
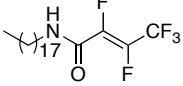
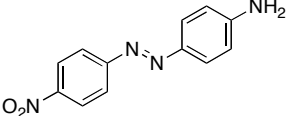
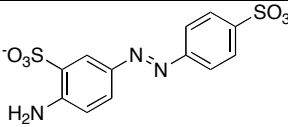
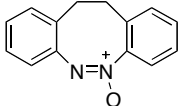
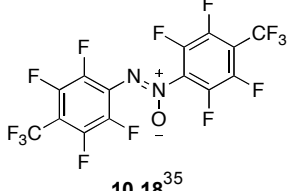
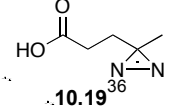
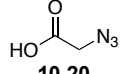


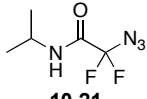
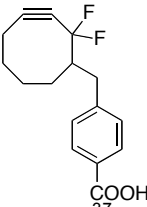
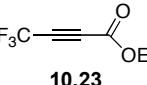
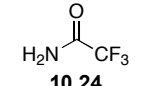
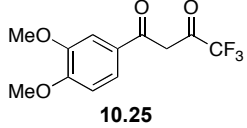
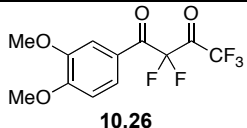
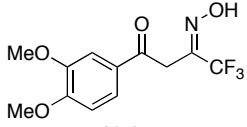
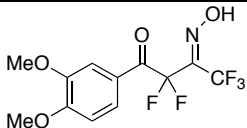
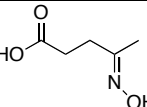
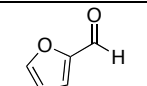
Scheme 10.4. Synthesis of triazole linker **10.7**.

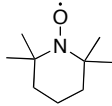
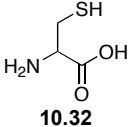
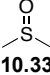
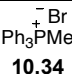

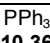
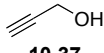
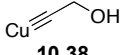
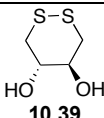
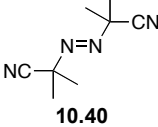
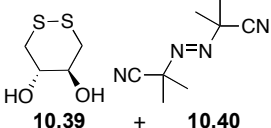
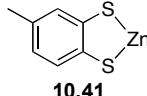
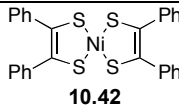


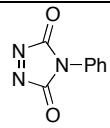
An initial screen with quadricyclane **10.8** and potential reaction partners (Table 10.1) was performed and monitored by TLC and mass spectrometry over the course of a week. Any reaction partners that appeared promising by the TLC/MS assay were further analyzed by NMR.

Table 10.1. Compounds screened for reactivity with quadricyclane.

Entry	Compound	Comments
1	 10.12	12.5 mM 10.8 + 125 mM 10.12 in 3:1 MeOH/H ₂ O; product evident by LCMS and TLC but multiple products appear present. ¹ H-NMR analysis of 10.4 (5 mg) and 10.12 (7 mg) in DCM (0.2 mL) only yielded a small amount of product after 3 d at 37 °C. When performed in polar protic solvent (MeOH or H ₂ O) degradation of 10.12 is apparent.
2	 10.13	12.5 mM 10.8 + 125 mM 10.13 in 3:1 MeOH/H ₂ O; nothing promising by LCMS or TLC over multiple days at rt.
3	 10.14	12.5 mM 10.8 + 125 mM 10.14 in 3:1 MeOH/H ₂ O; nothing promising by LCMS or TLC over multiple days at rt.
4	 10.15	12.5 mM 10.8 + 125 mM 10.15 in 3:1 MeOH/H ₂ O; nothing promising by LCMS or TLC over multiple days at rt.
5	 10.16	12.5 mM 10.8 + 125 mM 10.16 in 3:1 MeOH/H ₂ O; nothing promising by LCMS or TLC over multiple days at rt.
6	 10.17 ³⁴	12.5 mM 10.8 + 125 mM 10.17 in 3:1 MeOH/H ₂ O; Promising peak by LCMS. ¹ H-NMR assay indicated no reaction with 50 mM 10.17 and 50 mM 10.5 in 4:1:1 MeOD/D ₂ O/CDCl ₃ .
7	 10.18 ³⁵	12.5 mM 10.8 + 125 mM 10.18 in 3:1 MeOH/H ₂ O; nothing promising by LCMS or TLC over multiple days at rt.
8	 10.19 ³⁶	12.5 mM 10.8 + 125 mM 10.19 in 3:1 MeOH/H ₂ O; nothing promising by LCMS or TLC over multiple days at rt.
9	 10.20	12.5 mM 10.8 + 125 mM 10.20 in 3:1 MeOH/H ₂ O; nothing promising by LCMS or TLC over multiple days at rt.

10	 10.21	12.5 mM 10.8 + 125 mM 10.21 in 3:1 MeOH/H ₂ O; nothing promising by LCMS or TLC over multiple days at rt.
11	 10.22 ³⁷	12.5 mM 10.8 + 125 mM 10.22 in 3:1 MeOH/H ₂ O; nothing promising by LCMS or TLC over multiple days at rt.
12	 10.23	12.5 mM 10.8 + 125 mM 10.23 in 3:1 MeOH/H ₂ O; product observed but polymerization/stability of product appeared problematic. The reaction was also monitored by ¹ H-NMR with 50 mM 10.23 and 50 mM 10.5 in 4:1:1 MeOD/D ₂ O/CDCl ₃ . There was still starting material after 5 d at rt.
13	 10.24	12.5 mM 10.8 + 125 mM 10.24 in 3:1 MeOH/H ₂ O; nothing promising by LCMS or TLC over multiple days at rt.
14	 10.25	12.5 mM 10.8 + 125 mM 10.25 in 3:1 MeOH/H ₂ O; Promising peak by LCMS. However, no reaction by ¹ H-NMR with 50 mM 10.25 and 50 mM 10.5 . The solvent mixture was 4:1:1 MeOD/D ₂ O/CDCl ₃ .
15	 10.26	12.5 mM 10.8 + 125 mM 10.26 in 3:1 MeOH/H ₂ O; nothing promising by LCMS or TLC over multiple days at rt.
16	 10.27	12.5 mM 10.8 + 125 mM 10.27 in 3:1 MeOH/H ₂ O; nothing promising by LCMS or TLC over multiple days at rt.
17	 10.28	12.5 mM 10.8 + 125 mM 10.28 in 3:1 MeOH/H ₂ O; nothing promising by LCMS or TLC over multiple days at rt.
18	 10.29	12.5 mM 10.8 + 125 mM 10.29 in 3:1 MeOH/H ₂ O; nothing promising by LCMS or TLC over multiple days at rt.
19	 10.30	12.5 mM 10.8 + 125 mM 10.30 in 3:1 MeOH/H ₂ O; nothing promising by LCMS or TLC over multiple days at rt.

20	 10.31	12.5 mM 10.8 + 125 mM 10.31 in 3:1 MeOH/H ₂ O; nothing promising by LCMS or TLC over multiple days at rt.
21	 10.32	12.5 mM 10.8 + 125 mM 10.32 in 3:1 MeOH/H ₂ O; nothing promising by LCMS or TLC over multiple days at rt.
22	 10.33	12.5 mM 10.8 + 125 mM 10.33 in 3:1 MeOH/H ₂ O; nothing promising by LCMS or TLC over multiple days at rt.
23	 10.34	12.5 mM 10.8 + 125 mM 10.34 in 3:1 MeOH/H ₂ O; nothing promising by LCMS or TLC over multiple days at rt.
24	 10.35	12.5 mM 10.8 + 125 mM 10.35 in 3:1 MeOH/H ₂ O; nothing promising by LCMS or TLC over multiple days at rt.
25	 10.36	12.5 mM 10.8 + 125 mM 10.36 in 3:1 MeOH/H ₂ O; nothing promising by LCMS or TLC over multiple days at rt.
26	 10.37	12.5 mM 10.8 + 125 mM 10.37 in 3:1 MeOH/H ₂ O; nothing promising by LCMS or TLC over multiple days at rt.
27	 10.38	12.5 mM 10.8 + 125 mM 10.38 in 3:1 MeOH/H ₂ O; nothing promising by LCMS or TLC over multiple days at rt.
28	 10.39	12.5 mM 10.8 + 125 mM 10.39 in 3:1 MeOH/H ₂ O; A small amount of DTT adduct was evident by LCMS after multiple days.
29	 10.40	12.5 mM 10.8 + 125 mM 10.40 in 3:1 MeOH/H ₂ O; nothing promising by LCMS or TLC over multiple days at rt.
30	 10.39 + 10.40	12.5 mM 10.8 + 125 mM 10.39 and 10.40 in 3:1 MeOH/H ₂ O; A small amount of DTT adduct was evident by LCMS after multiple days.
31	 10.41	12.5 mM 10.8 + 125 mM 10.41 in 3:1 MeOH/H ₂ O; nothing promising by LCMS or TLC over multiple days at rt.
32	 10.42	12.5 mM 10.8 + 125 mM 10.42 in 3:1 MeOH/H ₂ O; Product peak observed. Also product formation observed by ¹ H NMR when 10.42 and 10.4 were combined in CDCl ₃ . The very limited solubility of 10.42 prevented the

		analysis of this reaction by $^1\text{H-NMR}$ in other, more relevant solvents.
33	 <p>10.43</p>	Reaction between 10.4 and 10.43 was clean by $^1\text{H-NMR}$ in CDCl_3 and CD_3CN . (LCMS assay not performed on this compound).

Of the initial hits, 4-phenyl-1,2,4-triazole-3,5-dione (**10.43**, PTAD, Table 10.1 entry 33)³⁸ appeared most promising as it was a fairly polar, organic compound which reacted with quadricyclane to yield adduct **10.44** (Scheme 10.5). The rate constant for this reaction was measured in CDCl_3 and CD_3CN and found to be comparable to the rate constant of the Staudinger ligation and the original cyclooctynes synthesized for Cu-free click chemistry (Figure 10.6).^{9,39,40}

Scheme 10.5. 7-acetoxy quadricyclane reacts with PTAD to yield norbornene product **10.44**.

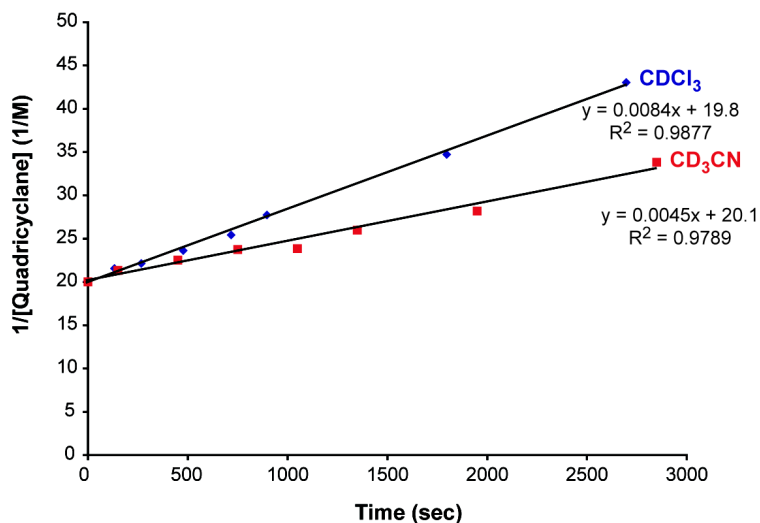
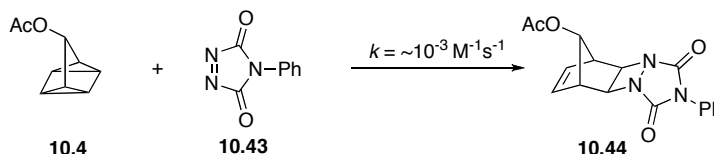
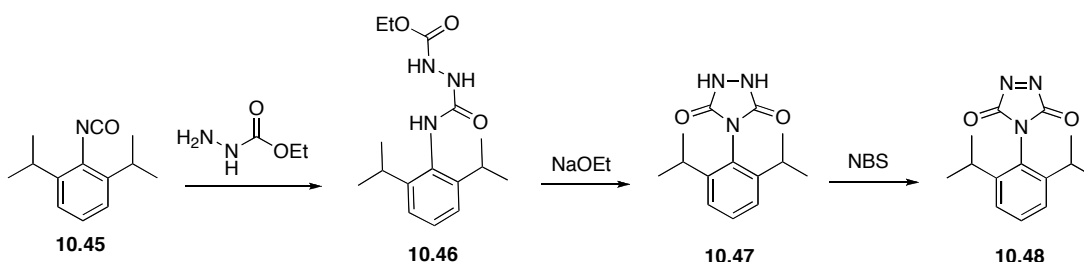


Figure 10.6. Plot of $1/[\text{quadricyclane}]$ vs. time for the reaction of 7-acetoxy quadricyclane with N-phenyl-1,2,4-triazole-3,5-dione in CDCl_3 (blue) or CD_3CN (red) at rt. The slope of the line represents the second-order rate constant for the reaction.

However, upon placement in protic solvent (including water) the PTAD appeared to be unstable. At first, this was a surprising result as Barbas and coworkers have recently reported PTAD as a method for bioconjugation to tyrosine residues through a formal ene reaction (see Chapter 13, Figure 13.2).⁴¹ Their work indicated that a specific solvent combination was necessary to achieve this transformation; however, in our hands, even these buffers resulted in substantial degradation of PTAD. Our results were supported by a 1983 report by Van Nice and coworkers where the half-life of PTAD **10.43** in 9:1 acetone/water was measured to be 1 min.⁴² In an effort to “develop water soluble TADs that were sufficiently stable in water to allow a Diels-Alder reaction to compete successfully without decomposition” Van Nice and coworkers reported bis(isopropyl) PTAD **10.48**, which had a half-life nine times that of PTAD. We prepared bis(isopropyl) PTAD from isocyanate **10.45** by nucleophilic addition of ethyl carbazate to yield **10.46**, followed by base mediated cyclization and oxidation of **10.47** with NBS to yield PTAD **10.48** (Scheme 10.6). Unfortunately, experiments in aqueous solution revealed that while **10.48** was indeed more stable than PTAD, it was not nearly stable enough for use as a bioorthogonal reagent.

Other initially promising reagents including α -fluoroketones and fluorinated alkenes and alkynes reacted with quadricyclane too slowly for practical utility (Table 10.1, entries 2-3, 11-17). Reagents that are prone to radical chemistry also did not appear reactive with quadricyclane (Table 10.1, entries 20, 29-30).

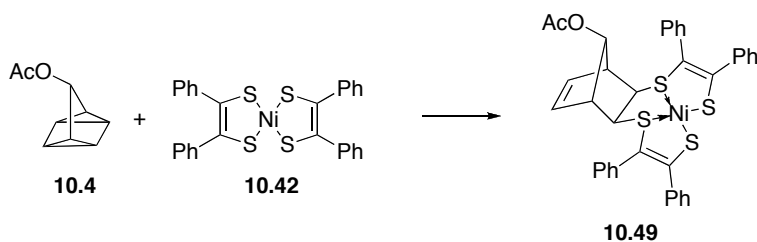
Scheme 10.6. Synthesis of bis(isopropyl) PTAD **10.48**.



A Prototype Reaction

It wasn't until we expanded our screen to include organometallic reagents that we found a lead, which could be developed into a selective reaction for quadricyclane (Table 10.1, entry 32). That lead was bis(dithiobenzil)nickel(II) **10.42**, a Ni bis(dithiolene) complex which reacted cleanly with 7-acetoxy quadricyclane **10.4** to give adduct **10.49** (Scheme 10.7). Our results were consistent with a 1986 report by Sugimori and coworkers that highlighted the rapid reactivity of **10.42** with quadricyclane through stopped-flow kinetics experiments.⁴³

Scheme 10.7. Reaction of 7-acetoxy quadricyclane with bis(dithiobenzil)nickel(II).



Further mining the literature regarding this reaction revealed that norbornadiene also reacts with **10.42** to form an identical complex but at much slower reaction rates.⁴⁴ The reactivity of **10.42** with norbornadiene first was noted by Schrauzer and coworkers in the early 1960s,⁴⁵ soon after they first reported Ni bis(dithiolene) reagents.^{46,47} However, neither the structure of the product nor the reactivity with quadricyclane was elucidated until work by Okamura and coworkers in 1970.⁴⁸ During these early studies, it was also reported that the addition product was light sensitive and degraded to **10.42** plus norbornadiene,^{43,44,45} a potential liability that we needed to address for this reaction to be successful as a bioorthogonal chemical ligation strategy. Since their initial report, Ni bis(dithiolene) complexes have found far reaching applications including: purification of olefins,⁴⁹ singlet oxygen quenchers,⁵⁰ components of magnets,⁵¹ media for optical recording devices,⁵² semiconductors,⁵³ catalysts for photo-oxidation of water,⁵⁴ Q switching lasers,^{55,56} infrared dyes,⁵⁷ and liquid crystals.⁵⁸ We aimed to add bioorthogonal chemistry to this list.

Materials and Methods

General Experimental Procedure

All chemical reagents were purchased from Sigma-Aldrich, Acros or TCI and used without purification unless noted otherwise. Anhydrous DMF and MeOH were purchased from Aldrich or Acros in sealed bottles; all other solvents were purified as described by Pangborn *et al.*⁵⁹ In all cases, solvent was removed by reduced pressure with a Buchi Rotovapor R-114 equipped with a Welch self-cleaning dry vacuum. Non-volatile products were further dried by reduced pressure with an Edwards RV5 high vacuum. Thin layer chromatography was performed with EMD 60 Å silica gel plates. Flash chromatography was performed using Silicycle[®] 60 Å 230-400 mesh silica. All ¹H and ¹³C spectra are reported in ppm and referenced to solvent peaks. Spectra were obtained on Bruker AVQ-400, AVB-400, DRX-500, AV-500, or AV-600 instruments. Electron impact (EI) and electrospray ionization (ESI) mass spectra were obtained from the UC Berkeley Mass Spectrometry Facility.

Experimental Procedures

7-acetoxy-2,5-norbornadiene (10.3).²⁸ 7-*tert*-Butoxy-2,5-norbornadiene **10.2**^{60,61} (1.7 g, 10 mmol, 1.0 equiv.) was combined with acetic anhydride (3.4 mL, 36 mmol, 3.6 equiv.) and acetic acid (16.9 mL) at 0 °C. This solution was poured into precooled perchloric acid (2.3 mL, 60%). The yellow reaction mixture was stirred for 1 min at 0 °C and then poured onto ice water (~50 mL). Additional water was added until no yellow color remained. The aqueous solution was extracted with dichloromethane (3 x 50 mL). The organic layers were combined, dried, decanted, and evaporated to dryness. The crude product was purified by silica gel chromatography eluting with 25:1 hexanes/ether. This procedure resulted in 910 mg pure **10.3** as a colorless oil (6.1 mmol, 58%). $R_f = 0.5$ in 10:1 hexanes/ethyl acetate. ¹H NMR (600 MHz, CDCl₃): δ 6.63 (s, 2H), 6.50 (s, 2H), 4.50 (s, 1H), 3.53 (s, 2H), 1.89 (s, 3H). ¹³C NMR (100 MHz, CDCl₃): δ 171.2, 140.4, 137.9, 99.4, 52.5, 21.3. HRMS (EI): calcd. for C₉H₁₀O₂⁺ [M]⁺, 150.0681; found, 150.0638.

7-acetoxy quadricyclane (10.4).²⁹ 7-acetoxy-2,5-norbornadiene **10.3** (400 μL, 3.9 mmol, 1.0 equiv.) was dissolved in hexane (150 mL, degassed) and placed in a quartz round bottom flask containing a small amount of acetone (~0.5 mL). The mixture was irradiated with a 450W Mercury Arc lamp for 5 h. Throughout the irradiation process, the reaction was kept under a nitrogen atmosphere. Following irradiation, sat AgNO₃ (5 mL) was added and the mixture was vigorously stirred in the dark for 15 min to complex any remaining **4**. The hexane was removed and the aqueous solution was filtered and extracted with hexanes (2 x 10 mL). The hexanes were combined, dried, decanted, and evaporated to dryness to result in pure **10.4** as a wet, colorless solid (560 mg, 3.7 mmol, 95%). $R_f = 0.7$ in 5:1 hexane/ethyl acetate. ¹H NMR (400 MHz, CDCl₃): δ 5.62 (t, $J = 1.7$ Hz, 1H), 2.11 (s, 3H), 1.83-1.80 (m, 2H), 1.62- 1.59 (m, 2H), 1.53- 1.51 (m, 2H). ¹³C NMR (125 MHz, CDCl₃): δ 171.9, 82.4, 25.8, 21.5, 16.1, 14.8. HRMS (EI): calcd. for C₉H₁₀O₂⁺ [M]⁺, 150.0681; found, 150.0638.

7-hydroxy quadricyclane (10.5).²⁹ 7-acetoxy quadricyclane **10.4** (325 mg, 2.2 mmol, 1.0 equiv.) was dissolved ether (1.0 mL, anhydrous). This solution was added to lithium aluminum hydride (1.2 mL, 1.2 mmol, 0.55 equiv., 1 M in diethyl ether) precooled to 0 °C. The mixture was warmed to rt and stirred for 15 min, at which point the reaction was quenched with aqueous Rochelle's salt (~ 5 mL). The mixture was stirred until the aluminum was sufficiently complexed and two layers formed in the flask. The aqueous layer was extracted with ether (3 x 20 mL) and the organic layers were combined, dried with MgSO₄, filtered, and evaporated to dryness. This procedure resulted in ~90% pure **10.5** as a volatile, colorless oil (210 mg, 1.8 mmol, 80% yield). Note: If this compound is purified by silica gel chromatography and aldehyde byproduct is formed resulting in a less pure product than that obtained from the crude reaction. $R_f = 0.2$ in 5:1 hexane/ethyl acetate. ¹H NMR (400 MHz, CDCl₃): δ 4.87 (t, $J = 1.8$ Hz, 1H), 1.77-1.74 (m, 2H), 1.56-1.53 (m, 2H), 1.38-1.36 (m, 2H). ¹³C NMR (125 MHz, CDCl₃): δ 79.5, 29.0, 15.9, 14.9. HRMS (EI): calcd. for C₇H₈O⁺ [M]⁺, 108.0575; found, 108.0574.

***p*-Nitrophenyl carbonate quadricyclane 10.6.** 7-hydroxy quadricyclane **10.5** (20 mg, 0.19 mmol, 1.0 equiv.) was dissolved in dichloromethane (7 mL, anhydrous) and cooled to 0 °C. Pyridine (90 µL, 1.1 mmol, 5.8 equiv., anhydrous) was added followed by *p*-nitrophenyl chloroformate (87 mg, 0.44 mmol, 2.3 equiv.). The reaction mixture was warmed to rt over 3 h, at which point it was quenched with water and extracted with dichloromethane (3 x 15 mL). The organic layers were combined, dried with MgSO₄, decanted, and evaporated to dryness. The crude product was purified by silica gel chromatography with hexanes/ether (9:1, 4:1, 2:1). This procedure resulted in 27 mg of pure **10.6** as a white solid (0.010 mmol, 52%). R_f = 0.7 in 7:1 hexane/ethyl acetate. ¹H NMR (600 MHz, CDCl₃): δ 8.28 (d, *J* = 9.0 Hz, 2H), 7.43 (d, *J* = 9.0 Hz, 2H), 5.71 (s, 1H), 1.93-1.91 (m, 2H), 1.70-1.68 (m, 2H), 1.65-1.64 (m, 2H). ¹³C NMR (150 MHz, CDCl₃): δ 155.9, 152.9, 145.5, 125.5, 122.0, 88.0, 25.8, 16.4, 15.3. HRMS (EI): calcd. for C₁₄H₁₁O₅N⁺ [M]⁺, 273.0637; found, 273.0634.

Ethyl 2-(4-((*tert*-butoxycarbonylamino)methyl)-1*H*-1,2,3-triazol-1-yl)acetate (10.11). Ethyl azidoacetate **10.10** (120 mg, 0.930 mmol, 1.00 equiv.) and *N*-*boc* propargyl amine **10.9** (146 mg, 0.942 mmol, 1.02 equiv.) were dissolved in a mixture of ethanol (1.8 mL) and water (1.8 mL). To this solution, CuSO₄ (2 mg, 0.01 mmol, 0.1 equiv.) and sodium ascorbate (50 µL of 2M solution in water, 0.1 mmol, 1 equiv.) were added. The mixture was stirred overnight at rt. The following morning, the ethanol was removed by evaporation and the product was extracted into ethyl acetate (3 x 50 mL). The ethyl acetate was dried with MgSO₄, filtered and evaporated to dryness. The crude product was purified by silica gel chromatography with hexanes/ethyl acetate (5:1, 3:1, 1:1, 1:2). This procedure resulted in 178 mg of pure **10.11** (0.627 mmol, 67%). R_f = 0.7 in ethyl acetate. ¹H NMR (600 MHz, CDCl₃): δ 7.61 (s, 1H), 5.34 (s, 1H), 5.08 (s, 2H), 4.34 (d, *J* = 6.0 Hz, 2H), 4.19 (q, *J* = 7.1 Hz, 2H), 1.37 (s, 9H), 1.23 (t, *J* = 7.1 Hz, 3H). ¹³C NMR (150 MHz, CDCl₃): δ 166.3, 155.9, 145.9, 123.4, 79.5, 62.3, 50.8, 36.0, 28.3, 14.0. HRMS (ESI): calcd. for C₇H₁₃O₂N₄ [M+H]⁺, 185.1039; found, 185.1033.

(1-(2-ethoxy-2-oxoethyl)-1*H*-1,2,3-triazol-4-yl)methanaminium 2,2,2-trifluoroacetate (10.7). *Boc*-protected triazole **10.11** (178 mg, 0.627 mmol, 1 equiv.) was dissolved in dichloromethane (8 mL, anhydrous). Trifluoroacetic acid (2 mL) was added and this mixture was stirred for 1 h at rt, at which point the reaction mixture was evaporated to dryness to yield pure **10.7** (200 mg, 0.67 mmol, quant.). R_f = 0.7 in 5:3:1 ethyl acetate/methanol/water. ¹H NMR (600 MHz, MeOD): δ 8.15 (s, 1H), 5.34 (s, 2H), 4.31 (s, 2H), 4.23 (q, *J* = 7.1 Hz, 2H), 1.27 (t, *J* = 7.1 Hz, 3H). ¹³C NMR (151 MHz, MeOD): δ 168.6, 161.3 (q, *J* = 38.3 Hz), 141.5, 127.4, 117.2 (q, *J* = 287.3 Hz), 63.6, 52.0, 35.6, 14.4. HRMS (ESI): calcd. for C₁₂H₂₁O₄N₄ [M+H]⁺, 285.1563; found, 285.1556.

Quadricyclane 10.8. Triazole **10.7** (45 mg, 0.15 mmol, 1.5 equiv.) and *N,N*-diisopropylethylamine (165 µL, 0.95 mmol, 10 equiv.) were combined in dichloromethane (2 mL, anhydrous) and cooled to 0 °C. *p*-Nitrophenyl carbonate quadricyclane **10.6** (27 mg, 0.099 mmol, 1.0 equiv.) was dissolved in dichloromethane (1 mL, anhydrous) and added to the solution containing triazole **10.7**. The reaction mixture was warmed to rt overnight. The

following morning, the mixture was evaporated to dryness and purified by silica gel chromatography to yield **10.7** (26 mg, 0.082 mmol, 83%). $R_f = 0.1$ in 1:1 hexane/ethyl acetate. $^1\text{H NMR}$ (400 MHz, CDCl_3): δ 7.69 (s, 1H), 5.60 (s, 1H), 5.39 (bs, 1H), 5.13 (s, 2H), 4.50 (d, $J = 6.3$ Hz, 2H), 4.26 (q, $J = 7.1$ Hz, 2H), 1.79-1.77 (m, 2H), 1.58 (bs, 2H), 1.49 (bs, 2H), 1.29 (t, $J = 7.1$ Hz, 3H). $^{13}\text{C NMR}$ (100 MHz, CDCl_3): δ 166.4, 157.1, 145.8, 123.7, 83.1, 62.7, 51.1, 36.6, 26.0, 16.1, 14.8, 14.3. HRMS (ESI): calcd. for $\text{C}_{15}\text{H}_{19}\text{O}_4\text{N}_4$ $[\text{M}+\text{H}]^+$, 319.1401; found, 319.1404.

2-azido-2,2-difluoro-*N*-isopropylacetamide (10.21). Known ethyl 2-azido-2,2-difluoroacetate⁶² (250 mg, 1.5 mmol, 1.0 equiv.) was dissolved in *N,N*-dimethylformamide (3 mL, anhydrous) and cooled to 0 °C. Isopropylamine (133 μL , 1.6 mmol, 1.1 equiv.) was added and the mixture was stirred for 1.5 h. The reaction was quenched with H_2O (5 mL) and extracted with Et_2O (3 x 8 mL). The Et_2O was combined, dried, decanted, and carefully concentrated to ~ 1 mL. The resulting solution was purified by Khughl Rhor distillation. The product distilled over at 90 °C (2 mTorr) to yield pure **10.21** (34 mg, 0.19 mmol, 12%) as a clear liquid. $^1\text{H NMR}$ (400 MHz, CDCl_3): δ 6.07 (s, 1H), 4.11 (dq, $J = 13.5, 6.8$ Hz, 1H), 1.24 (d, $J = 6.6$ Hz, 6H). $^{19}\text{F NMR}$ (376 MHz, CDCl_3): δ -83.68 (s, 2F).

Complex 10.49. Bis(dithiobenzil)nickel(II) (**10.42**, 50 mg, 0.092 mmol, 1.0 equiv.) was combined with 7-acetoxy quadricyclane **10.4** (30 mg, 0.20 mmol, 2.2 equiv.) in dichloromethane (1 mL) for 5 days in the dark. The reaction was evaporated to ~200 mL and methanol (1 mL) was added. This mixture was placed in the fridge until brown precipitate formed. The precipitate was collected and washed with minimal amounts of methanol to yield 40 mg of **10.49** (0.058 mmol, 63%) Some product was left in the mother liquor. The crude $^1\text{H NMR}$ showed ~90% conversion of **10.42** to **10.49**. $R_f = 0.1$ in 1:3 hexane/dichloromethane. $^1\text{H NMR}$ (600 MHz, CDCl_3): δ 7.28-7.26 (m, 4H), 7.19-7.10 (m, 16H), 5.63 (s, 2H), 4.97 (s, 1H), 4.04 (s, 2H), 2.43 (apparent q, $J = 1.7$ Hz, 2H), 1.97 (s, 3H). $^{13}\text{C NMR}$ (125 MHz, CDCl_3): δ 170.8, 162.2, 140.1, 137.4, 133.0, 129.9, 129.1, 128.7, 128.4, 128.1, 127.5, 118.0, 85.4, 62.0, 53.6, 49.5, 21.1. HRMS (EI): calcd. for $\text{C}_{37}\text{H}_{20}\text{O}_2\text{NiS}_4$ $[\text{M}]^+$, 692.0482; found, 692.0485.

Kinetics

The reaction in Scheme 10.5 was monitored by $^1\text{H NMR}$. 7-acetoxy quadricyclane (**10.4**) and *N*-phenyl-1,2,4-triazole-3,5-dione (**10.43**) were separately dissolved in CDCl_3 or CD_3CN and mixed together in a 1:1 ratio at a concentrations of 50 mM (CDCl_3 experiment) or 20 mM (CD_3CN experiment). The percent conversion was calculated by the disappearance of **10.4** relative to the appearance of product **10.44** as determined by integration. No product other than **10.44** was apparent by $^1\text{H NMR}$. The second-order rate constant was determined by plotting $1/[\text{10.44}]$ versus time. The plot was fit to a linear regression and the slope corresponds to the second-order rate constant.

References

- (1) Sletten, E. M.; Bertozzi, C. R. Bioorthogonal chemistry: Fishing for selectivity in a sea of functionality. *Angew. Chem. Int. Ed.* **2009**, *48*, 6974-6998.
- (2) Debets, M. F.; van der Doelen, C. W. J.; Rutjes, F. P. J. T.; van Delft, F. L. Azide: A unique dipole for metal-free bioorthogonal ligations. *ChemBioChem* **2010**, *11*, 1168-1184.
- (3) Jewett, J. C.; Bertozzi, C. R. Cu-free click cycloaddition reactions in chemical biology. *Chem. Soc. Rev.* **2010**, *39*, 1272-1279.
- (4) Rostovtsev, V. V.; Green, L. G.; Fokin, V. V.; Sharpless, K. B. A stepwise Huisgen cycloaddition process: Copper(I)-catalyzed regioselective "ligation" of azides and terminal alkynes. *Angew. Chem. Int. Ed.* **2002**, *41*, 2596-2599.
- (5) Tornøe, C. W.; Christensen, C.; Meldal, M. Peptidotriazoles on solid phase: [1,2,3]-Triazoles by regiospecific copper(I)-catalyzed 1,3-dipolar cycloadditions of terminal alkynes to azides. *J. Org. Chem.* **2002**, *67*, 3057-3064.
- (6) Zhang, L.; Chen, X.; Xue, P.; Sun, H. H. Y.; Williams, I. D.; Sharpless, K. B.; Fokin, V. V.; Jia, G. Ruthenium-catalyzed cycloaddition of alkynes and organic azides. *J. Org. Chem.* **2005**, *127*, 15998-15999.
- (7) Kodama, K.; Fukuzawa, S.; Nakayama, H.; Kigawa, T.; Sakamoto, K.; Yabuki, T.; Matsuda, N.; Shirouzu, M.; Takio, K.; Tachibana, K.; Yokoyama, S. Regioselective carbon-carbon bond formation in proteins with palladium catalysis; New protein chemistry by organometallic chemistry. *ChemBioChem* **2006**, *7*, 134-139.
- (8) Kodama, K.; Fukuzawa, S.; Nakayama, H.; Sakamoto, K.; Kigawa, T.; Yabuki, T.; Matsuda, N.; Shirouzu, M.; Takio, K.; Yokoyama, S.; Tachibana, K. Site-specific functionalization of proteins by organopalladium reactions. *ChemBioChem* **2007**, *8*, 232-238.
- (9) Saxon, E.; Bertozzi, C. R. Cell surface engineering by a modified Staudinger reaction. *Science* **2000**, *287*, 2007-2010.
- (10) Rose, K. Facile synthesis of homogeneous artificial proteins. *J. Am. Chem. Soc.* **1994**, *116*, 30-33.
- (11) Chopade, P. R.; Louie, J. [2+2+2] Cycloaddition reactions catalyzed by transition metal complexes. *Adv. Syn. Catal.* **2006**, *348*, 2307-2327.
- (12) Domínguez, G.; Pérez-Castells, J. Recent advances in [2+2+2] cycloaddition reactions. *Chem. Soc. Rev.* **2011**, *40*, 3430-3444.
- (13) Petrov, V. A.; Vasil'ev, N. V. Synthetic chemistry of quadricyclane. *Curr. Org. Syn.* **2006**, *3*, 215-259.
- (14) Mizuno, K.; Fukuyama, T.; Kuchitsu, K. Molecular structure of quadricyclane (tetracyclo[3.2.0.0²,7.0⁴,6] heptane) studied by gas electron diffraction. *Chem. Lett.* **1972**, 249-254.
- (15) Watson, W. H.; Tavanaiepour, I.; Marchand, A. P.; Dave, P. R. 3-(p-Cyanophenoxy)quadricyclane and a redetermination of the structure of a hexachloroquadricyclane dicarboxylate. *Acta Crystallogr. C* **1987**, *43*, 1356-1359.
- (16) Luchansky, S. J.; Goon, S.; Bertozzi, C. R. Expanding the diversity of unnatural cell-surface sialic acids. *ChemBioChem* **2004**, *5*, 371-374.

- (17) Wang, L.; Schultz, P. G. Expanding the genetic code. *Angew. Chem. Int. Ed.* **2005**, *44*, 34-66.
- (18) Link, A. J.; Mock, M. L.; Tirrell, D. A. Non-canonical amino acids in protein engineering. *Curr. Opin. Biotechnol.* **2003**, *14*, 603-609.
- (19) Kabakoff, D. S.; Buenzli, J. C. G.; Oth, J. F. M.; Hammond, W. B.; Berson, J. A. Enthalpy and kinetics of isomerization of quadricyclane to norbornadiene. Strain energy of quadricyclane. *J. Am. Chem. Soc.* **1975**, *97*, 1510-1512.
- (20) Rieber, N.; Alberts, J.; Lipsky, J. A.; Lemal, D. M. delta-1-1,2-Diazetines. *J. Am. Chem. Soc.* **1969**, *91*, 5668-5669.
- (21) Petrov, V. A.; Davidson, F.; Smart, B. E. Quadricyclane-thermal cycloaddition to polyfluorinated carbonyl compounds: A simple synthesis of polyfluorinated 3-oxatricyclo[4.2.1.0 2,5]non-7-enes. *J. Fluorine Chem.* **2004**, *125*, 1543-1552.
- (22) Gheorghiu, M. D.; Parvulescu, L.; Popescu, A.; Cimpoia, R. A. The reaction of ketene with carbon-carbon sigma bonds. The case of Moore's ketene. *J. Org. Chem.* **1990**, *55*, 3713-3714.
- (23) Petrov, V. A.; Davidson, F.; Krusic, P. J.; Marchione, A. A.; Marshall, W. J. Cycloaddition reaction of quadricyclane and fluoroolefins. *J. Fluorine Chem.* **2005**, *126*, 599-608.
- (24) Jung, Y.; Marcus, R. A. On the theory of organic catalysis "on water." *J. Am. Chem. Soc.* **2007**, *129*, 5492-5502.
- (25) Narayan, S.; Muldoon, J.; Finn, M. G.; Fokin, V. V.; Kolb, H. C.; Sharpless, K. B. "On Water": Unique reactivity of organic compounds in aqueous suspension. *Angew. Chem. Int. Ed.* **2005**, *44*, 3275-3279.
- (26) Jung, Y.; Marcus, R. A. Protruding interfacial OH groups and "on-water" heterogeneous catalysis. *J. Phys.: Condens. Matter* **2010**, *22*, 284117.
- (27) Domingo, L. R.; Saez, J. A.; Zaragoza, R. J.; Arnó, M. Understanding the participation of quadricyclane as nucleophile in polar $[2\sigma + 2\sigma + 2\pi]$ cycloadditions toward electrophilic π molecules. *J. Org. Chem.* **2008**, *73*, 8791-8799.
- (28) Story, P. R.; Fahrenholtz, S. R. 7-Quadricyclo [2.2.1.0 2,6O3,5]heptanone (Quadricyclanone). *J. Am. Chem. Soc.* **1964**, *86*, 1270-1271.
- (29) Gassman, P. G.; Patton, D. S. Acid-catalyzed rearrangement of quadricyclanone and quadricyclanone dimethyl ketal. Product dependency on carbon protonation versus oxygen protonation. *J. Am. Chem. Soc.* **1968**, *90*, 7276-7282.
- (30) Hammond, G. S.; Turro, N. J.; Fischer, A. Photosensitized cycloaddition reactions. *J. Am. Chem. Soc.* **1961**, *83*, 4674-4675.
- (31) Tamiaki, H.; Maruyama, K. A water-stable quadricyclane derivative. *Chem. Lett.* **1988**, 1875-1876.
- (32) Hill, W. E.; Szechi, J.; Hofstee, C.; Dane, J. H. Fate of a highly strained hydrocarbon in aqueous soil environment. *Environ. Sci. Technol.* **1997**, *31*, 651-655.
- (33) Stauffer, T. B.; Antworth, C. P.; Burr, E. M.; Macintyre, W. G. Quadricyclane hydration kinetics in natural waters. *Environ. Toxicol. Chem.* **1999**, *18*, 2237-2242.
- (34) Smith, M. A.; Weinstein, B.; Greene, F. D. Cyclic azo dioxides. Synthesis and properties of bis(o-nitrosobenzyl) derivatives. *J. Org. Chem.* **1980**, *45*, 4597-4602.

- (35) Korobeinicheva, I. K.; Fugaeva, O. M.; Furin, G. G. Effect of fluorine substitution on stretching vibrations of the azoxy group in azoxybenzenes. *J. Fluorine Chem.* **1988**, *39*, 373-384.
- (36) Bond, M. R.; Zhang, H.; Vu, P. D.; Kohler, J. J. Photocrosslinking of glycoconjugates using metabolically incorporated diazirine-containing sugars. *Nat. Protocols* **2009**, *4*, 1044-1063.
- (37) Codelli, J. A.; Baskin, J. M.; Agard, N. J.; Bertozzi, C. R. Second-generation difluorinated cyclooctynes for copper-free click chemistry. *J. Am. Chem. Soc.* **2008**, *130*, 11486-11493.
- (38) LeBlanc, B. F.; Sheridan, R. S. Photochemical generation and direct observation of 7-norbornadienone. *J. Am. Chem. Soc.* **1985**, *107*, 4554-4556.
- (39) Agard, N. J.; Prescher, J. A.; Bertozzi, C. R. A strain-promoted [3 + 2] azide-alkyne cycloaddition for covalent modification of biomolecules in living systems. *J. Am. Chem. Soc.* **2004**, *126*, 15046-15047.
- (40) Agard, N. J.; Baskin, J. M.; Prescher, J. A.; Lo, A.; Bertozzi, C. R. A comparative study of bioorthogonal reactions with azides. *ACS Chem. Biol.* **2006**, *1*, 644-648.
- (41) Ban, H.; Gavriluk, J.; Barbas Tyrosine bioconjugation through aqueous ene-type reactions: A click-like reaction for tyrosine. *J. Am. Chem. Soc.* **2010**, *132*, 1523-1525.
- (42) Keana, J. F. W.; Guzikowski, A. P.; Ward, D. D.; Morat, C.; Van Nice, F. L. Potent hydrophilic dienophiles. Synthesis and aqueous stability of several 4-aryl- and sulfonated 4-aryl-1,2,4-triazoline-3,5-diones and their immobilization on silica gel. *J. Org. Chem.* **1983**, *48*, 2654-2660.
- (43) Kajitani, M.; Kohara, M.; Kitayama, T.; Asano, Y.; Sugimori, A. Photosensitive 1:1 adduct between bis(1,2-diphenyl-1,2-ethylenedithiolato)nickel(0) and quadricyclane. *Chem. Lett.* **1986**, 2109-2112.
- (44) Kajitani, M.; Kohara, M.; Kitayama, T.; Akiyama, T.; Sugimori, A. Formation of 1:1 adducts between bis(1,2-diaryl-1,2-ethylenedithiolato)metal(0) (metal = Ni, Pd, and Pt) and quadricyclane and their photodissociation. *J. Phys. Org. Chem.* **1989**, *2*, 131-145.
- (45) Schrauzer, G. N.; Mayweg, V. P. Preparation, reactions, and structure of bisdithio- α -diketone complexes of nickel, palladium, and platinum. *J. Am. Chem. Soc.* **1965**, *87*, 1483-1489.
- (46) Schrauzer, G. N.; Mayweg, V. Reaction of diphenylacetylene with nickel sulfides. *J. Am. Chem. Soc.* **1962**, *84*, 3221.
- (47) Schrauzer, G. N. Coordination compounds with delocalized ground states. Transition metal derivatives of dithiodiketones and ethylene-1,2-dithiolates (metal dithienes). *Acc. Chem. Res.* **1969**, *2*, 72-80.
- (48) Wing, R. M.; Tustin, G. C.; Okamura, W. H. Oxidative cycloaddition of metal dithiolenes to olefins. Synthesis and characterization of norbornadiene-bis-cis-(1,2-perfluoromethylethene-1,2-dithiolato)nickel. *J. Am. Chem. Soc.* **1970**, *92*, 1935-1939.
- (49) Wang, K.; Stiefel, E. I. Toward separation and purification of olefins using dithiolene complexes: An electrochemical approach. *Science* **2001**, *291*, 106-109.

- (50) Shiozaki, H.; Nakazumi, H.; Takamura, Y.; Kitao, T. Mechanisms and rate constants for the quenching of singlet oxygen by nickel complexes. *Bull. Chem. Soc. Jpn.* **1990**, *63*, 2653-2658.
- (51) Robertson, N.; Cronin, L. Metal bis-1,2-dithiolene complexes in conducting or magnetic crystalline assemblies. *Coordin. Chem. Rev.* **2002**, *227*, 93-127.
- (52) Winter, C. S.; Oliver, S. N.; Manning, R. J.; Rush, J. D.; Hill, C. A. S.; Underhill, A. E. Non-linear optical studies of nickel dithiolene complexes. *J. Mater. Chem.* **1992**, *2*, 443-447.
- (53) Cho, J.-Y.; Domercq, B.; Jones, S. C.; Yu, J.; Zhang, X.; An, Z.; Bishop, M.; Barlow, S.; Marder, S. R.; Kippelen, B. High electron mobility in nickel bis(dithiolene) complexes. *J. Mater. Chem.* **2007**, *17*, 2642-2647.
- (54) Lyris, E.; Argyropoulos, D.; Mitsopoulou, C.-A.; Katakis, D.; Vrachnou, E. New catalysts in the photo-oxidation of water. *J. Photochem. Photobiol. A* **1997**, *108*, 51-54.
- (55) Mueller-Westerhoff, U. T.; Vance, B.; Ihl Yoon, D. The synthesis of dithiolene dyes with strong near-IR absorption. *Tetrahedron* **1991**, *47*, 909-932.
- (56) Qing, D.; Feng, C. X.; Hong, C.; Xing, G.; Ping, Z. X.; Zhusheng, C. Synthesis and laser application of the dithiolene nickel complex compounds. *Supramol. Sci.* **1998**, *5*, 531-536.
- (57) Kuramoto, N.; Asao, K. The syntheses and crystal structures of some bis(1,2-diaryl-1,2-ethylenedithiolato)nickel complexes and their photostabilizing efficiency to organic dyes. *Dyes Pigments* **1990**, *12*, 65-76.
- (58) Marshall, K. L.; Painter, G.; Lotito, K.; Noto, A. G.; Chang, P. Transition metal dithiolene near-IR dyes and their applications in liquid crystal devices. *Mol. Cryst. Liq. Cryst.* **2006**, *454*, 47-79.
- (59) Pangborn, A. B.; Giardello, M. A.; Grubbs, R. H.; Rosen, R. K.; Timmers, F. J. Safe and convenient procedure for solvent purification. *Organometallics* **1996**, *15*, 1518-1520.
- (60) Story, P. R.; Fahrenholtz, S. R. 7-t-Butoxynorbornadiene. *Org. Syn.* **1964**, *44*, 12.
- (61) Baxter, A. D.; Binns, F.; Javed, T.; Roberts, S. M.; Sadler, P.; Scheinmann, F.; Wakefield, B. J.; Lynch, M.; Newton, R. F. Synthesis and use of 7-substituted norbornadienes for the preparation of prostaglandins and prostanoids. *J. Chem. Soc., Perkin Trans. 1* **1986**, 889-900.
- (62) Koppes, W. M.; Chaykovsky, M. Preparation of 2-azido-2,2-difluoroethanol. US Patent 5276171, **1994**.

Chapter 11

Mechanistic Investigation and Modifications of Quadricyclane-Ni bis(dithiolene) Chemistry

Mechanistic Investigation

Molecular Orbital Analysis

Having selected the reaction between quadricyclane and Ni bis(dithiolene) reagents as our prototype reaction, we needed to further understand the mechanism of this transformation and optimize the reaction for utility in biological systems. The literature regarding this reaction is limited and it is not clear whether the ligation product is formed through a charge-transfer mechanism or a true concerted cycloaddition reaction. However, a simple molecular orbital analysis of Ni bis(dithiolene), quadricyclane, and norbornadiene provides insight into why norbornadiene reacts much more slowly with Ni bis(dithiolene) species than quadricyclane does and suggests a concerted transition state for the reaction with quadricyclane (Figure 11.1).¹

The LUMO of a Ni bis(dithiolene) species, which is relatively low lying,² is in phase to directly combine with quadricyclane through the sulfur atoms on separate ligands of the Ni bis(dithiolene) species. Conversely, norbornadiene does not contain the proper symmetry for a direct interligand reaction. Norbornadiene must first interact with the sulfur atoms on one ligand and then undergo rearrangement to the more stable product. Evidence for this two-step process with norbornadiene comes from isolation of dihydrodithin byproduct **11.4** (Scheme 11.1).¹

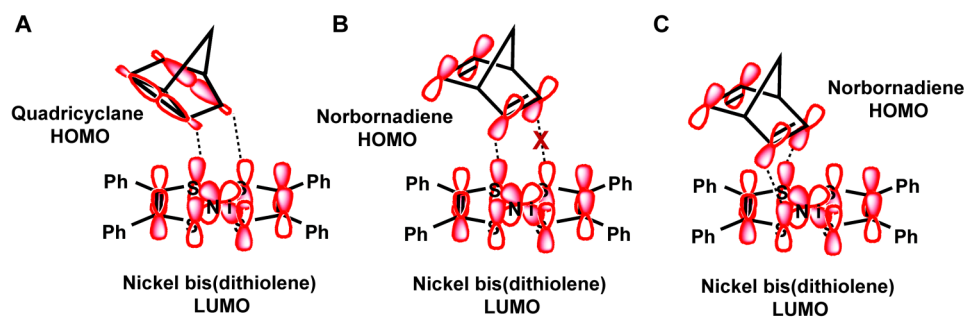
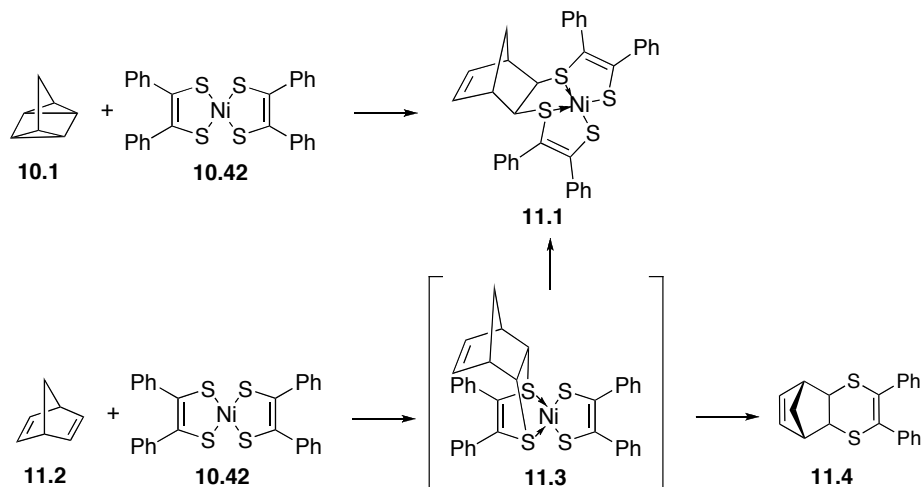


Figure 11.1. Molecular orbital interaction diagrams for the LUMO of Ni bis(dithiolene) and the HOMO of quadricyclane (A) or norbornadiene (B/C).

Scheme 11.1. Reactivity of Ni bis(dithiolene) with quadricyclane (top) and norbornadiene (bottom).



Kinetic Analysis

We aimed to determine the second-order rate constant for the reaction of quadricyclane and Ni bis(dithiolene) **10.42**. Compound **10.42** has a large absorption band centered at 855 nm that is absent in the product (Figure 11.2), which allows for facile kinetic measurements by UV/Vis/NIR spectroscopy.

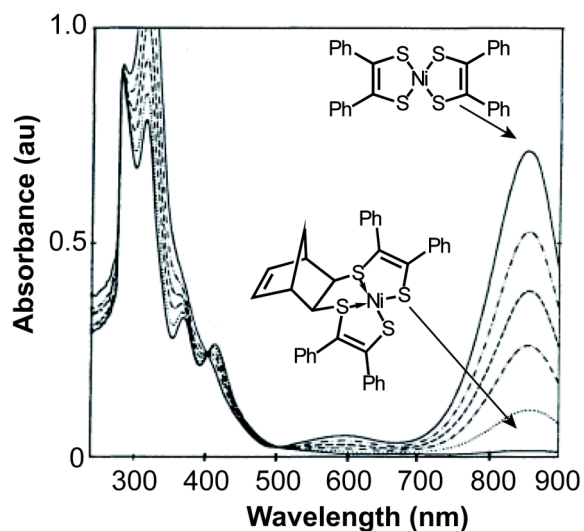
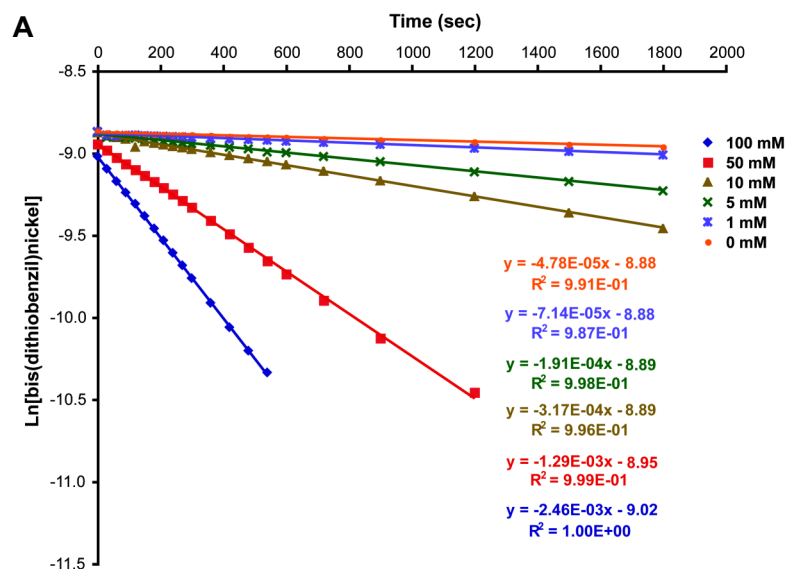
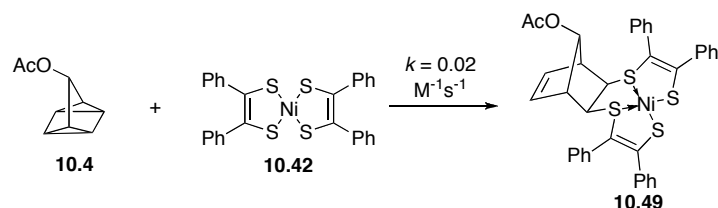


Figure 11.2. UV/Vis/NIR spectra of Ni bis(dithiolene) **10.42** and product **11.1** (labeled) as well as spectra containing a mixture of the two species (dotted lines). The peak at 855 nm indicates the presence of **10.42**. Figure modified from *Chem. Lett.* **1986**, 2109.³

Unfortunately, even at the low concentrations necessary for absorbance measurements, the only polar solvent Ni bis(dithiolene) **10.42** was soluble in was DMSO. Using pseudo-first order kinetics, we found that the second-order rate constant in DMSO for the reaction between 7-acetoxy quadricyclane (**10.4**) and Ni bis(dithiolene) **10.42** at room temperature was $0.02 \text{ M}^{-1}\text{s}^{-1}$, a rate constant comparable to those measured for other bioorthogonal chemical reactions (Scheme 11.2, Figure 11.3).^{4,5} The kinetic data for the reaction between **10.4** and **10.42** adequately fit the analysis necessary for a second-order reaction, which provides further evidence for a bimolecular rate-determining step.

Scheme 11.2. Reaction between 7-acetoxy quadricyclane and bis(dithiobenzil)nickel(II).



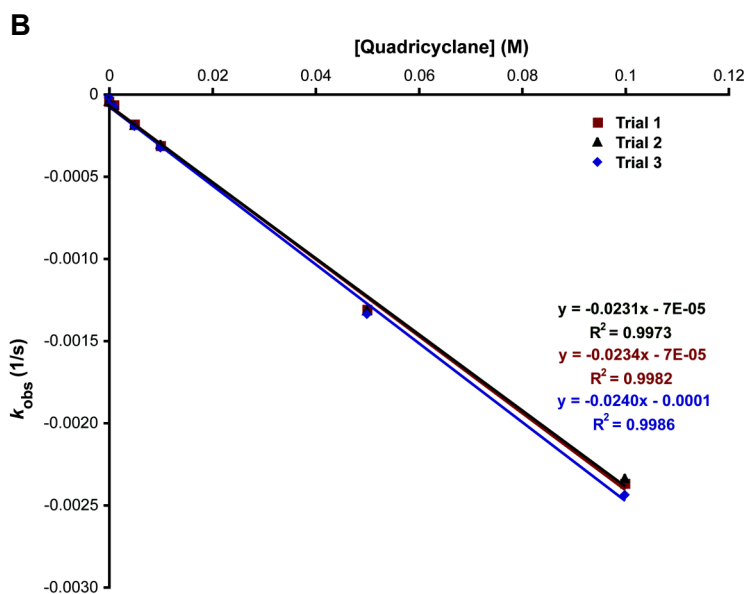


Figure 11.3. The second-order rate constant for the reaction of **10.4** and **10.42** was determined using pseudo-first order kinetics. A solution of 400 μM **10.42** in PBS was combined with various solutions of quadricyclane **10.4** (20 mM, 16 mM, 12 mM, 8 mM, 4 mM, or 0 mM in EtOH) in a 1:1 ratio (total volume = 100 μL). The reactions were monitored by the absorbance at 850 nm for 30 min. The absorbance values were correlated to the concentration of **10.42** using a standard curve. A plot of $\text{Ln}[\mathbf{10.42}]$ verses time resulted in a series of first-order rate constants (k_{obs}). Plotting each k_{obs} value vs. $[\mathbf{10.4}]$ yields a linear regression with the slope of the line indicating the second-order rate constant. The average of three trials gave a second-order rate constant of $0.023 \pm 0.001 \text{ M}^{-1}\text{s}^{-1}$. A. A representative plot to determine k_{obs} . B. Plot of k_{obs} vs. $[\mathbf{10.4}]$ for each trial.

Stability Analysis of Ni bis(dithiolene) and Ligation Product

With the prototype reaction exhibiting encouraging kinetics, we proceeded to assess the stability of the Ni bis(dithiolene) and the ligation product (**10.42** and **10.49**, respectively). A thorough study of the stability of **10.42** was precluded by its extremely limited solubility in polar solvents, but an initial screen of biological metabolites in dichloromethane was promising. Additionally, a literature search suggested that due to the 10 electron aromatic system present in Ni bis(dithiolene) complexes,⁶ **10.42** is significantly more stable than most organometallic species. A major concern regarding the use of organometallic complexes in biological systems is the stability of the metal-ligand bond in the presence of the hard nucleophiles abundant in biological milieu; however, the literature suggests that this will not be a problem for **10.42** because exchange of the dithiolene ligands necessitates high temperatures and bidentate species.⁷

With the requisite reaction partners appearing stable to biological environments, we directed our attention to the stability of product **10.49**, which was reported to be photolabile.^{1,3} Indeed we found that **10.49**, if left out in ambient light, reverts to **10.42** and **10.3**

with a half-life of about 35 h in CDCl₃ (Scheme 11.3, Figure 11.4), a degree of instability that would be problematic for many biological labeling applications. Using an NMR assay, degradation of **10.49** over the first few hours is not evident (Figure 11.4). However, using UV/Vis/NIR spectroscopy, which has greater sensitivity than NMR, the formation of **10.42** from **10.49** is evident at early timepoints (Figure 11.5).

Scheme 11.3. Photodegradation of **10.49** into norbornadiene **10.3** and Ni bis(dithiolene) **10.42**. Addition of diethyldithiocarbamate (**11.5**) prevents this photodegradation.

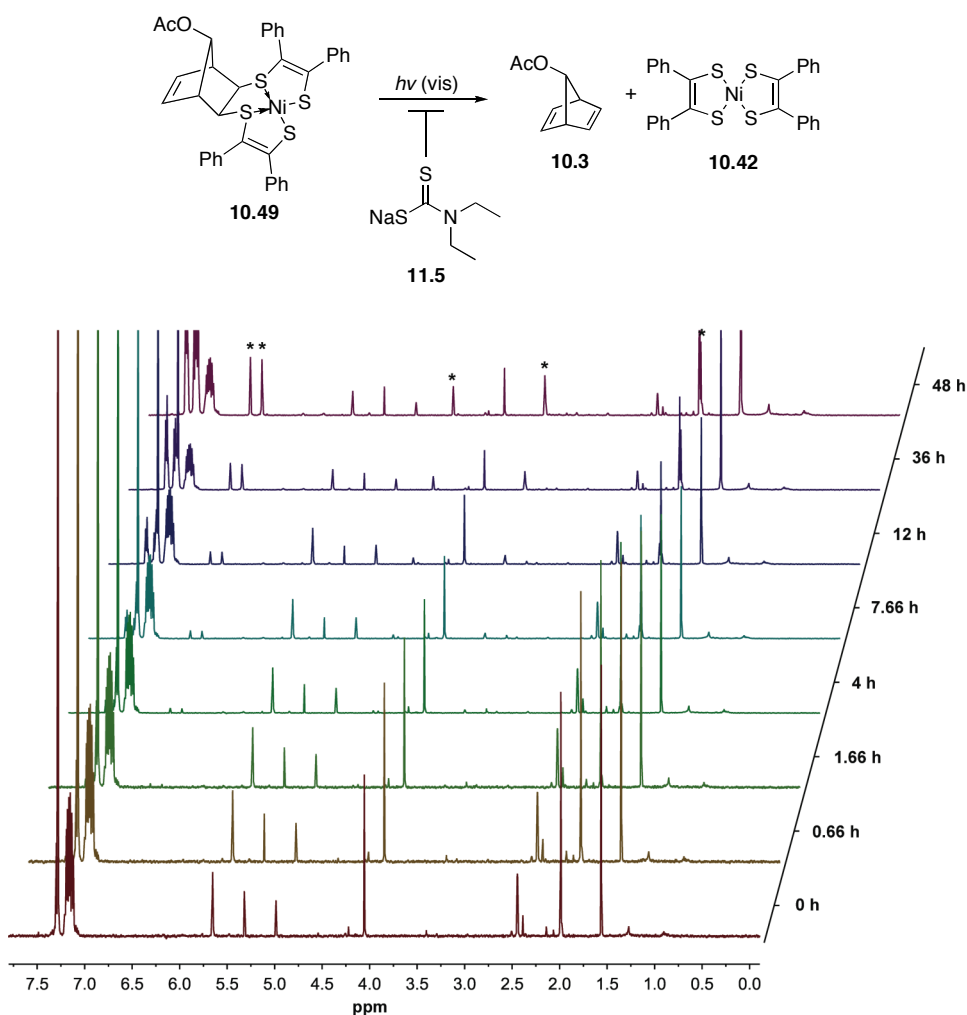


Figure 11.4. Complex **10.49** is photo-labile. Complex **10.49** was dissolved in CDCl₃ and placed in an NMR tube on the bench continually exposed to ambient light. NMR spectra were periodically obtained. The asterisks indicate the chemical shifts for 7-acetoxy norbornadiene (**10.3**). At the 36 h time point, there is a 1:1.1 ratio of **10.49**:**10.3** as judged by integration of the olefin peaks. The calculated half-life based on all integration data is 34.8 h.

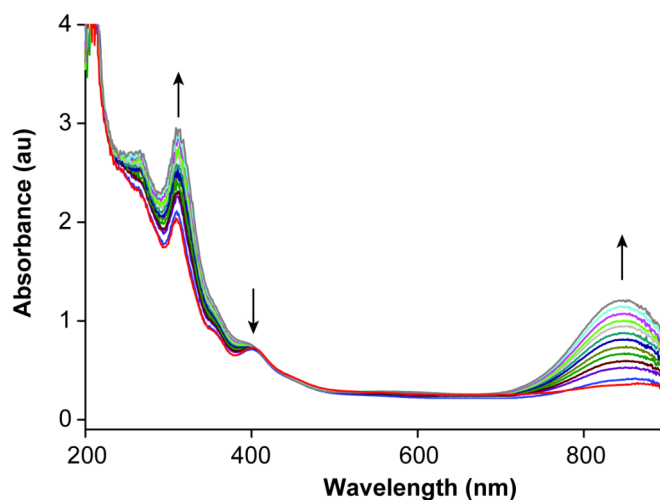


Figure 11.5. Complex **10.49** is photo-labile. A solution of **10.49** was prepared in CH₃CN and left in ambient light. A UV/Vis/NIR spectrum was collected every 15 min. The NIR absorption band at 850 nm is characteristic of **10.42** is growing in, while the small hump centered at ~400 nm characteristic of the product is becoming less defined.³ The absorption band at 350 nm is also increasing in intensity.

The mechanism of the photochemical reversion is not well understood, but we presumed the reaction could be inhibited by removing Ni from the product using a metal chelator. A variety of additives were tested to prevent photodegradation of complex **10.49** (Table 11.1). A solution containing 200 μ M **10.49** and 1.25 mM additive in 3:1 CH₃CN/H₂O was left in ambient light and monitored for formation of **10.42** by UV/Vis/NIR spectroscopy. As discussed above, compound **10.42** has poor solubility properties and immediately crashed out of the 3:1 CH₃CN/H₂O mixture. However, some additives were able to reduce compound **10.42** to the anionic state (**11.6**, scheme 11.4) as evident by a peak centered at ~900 nm in the UV/Vis/NIR spectra. Thus, the loss of absorbance over time or the presence of a peak at ~900 nm in the UV/Vis/NIR spectrum indicates photodegradation of complex **10.49**.

Scheme 11.4. Reduction of neutral Ni bis(dithiolene) to the anionic species.

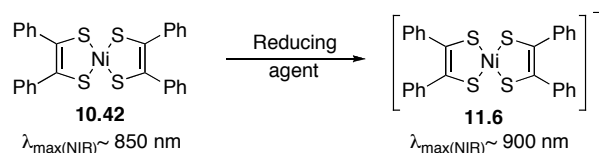


Table 11.1. Screen for additives that inhibit the photodegradation of **10.49**.

Entry	Compound	Result
1	No additive	Photodegradation; 10.42 precipitates from solution. See Figure 11.6.
2 ⁸	1,2-diaminocyclohexane tetraacetate	Photodegradation; 10.42 precipitates from solution.
3	Triphenylphosphine	Photodegradation and reduction to 11.6 (abs band ~ 900 nm).
4	Histidine	Photodegradation and some reduction to 11.6 but also some precipitate observed.
5	Ethylenediamine tetraacetate	Photodegradation; 10.42 precipitates from solution.
6 ⁸	Diethyldithiocarbamate	Complex 10.49 present after 20 h in light. See Figure 11.6.
7	Cysteine	Photodegradation and reduction of 10.42 to 11.6 (abs band ~ 900 nm). See Figure 11.6B.
8	Dithiothreitol	Photodegradation and reduction to 11.6 (abs band ~ 900 nm).
9 ⁹	Methyl iodide*	Photodegradation; 10.42 precipitates from solution.

* Methyl iodide experiment performed in 100% CH₃CN

Fortunately, diethyldithiocarbamate prevented the photodegradation entirely (Figure 11.6). The mechanism of this transformation is unknown as there doesn't seem to be a change in the absorption spectrum, which would be expected if the nickel was removed from the product. Additionally, if **10.49** is removed from the solution of diethyldithiocarbamate, photodegradation is restored, which also suggests the nickel is still intact. The current hypothesis is that diethyldithiocarbamate acts as an additional ligand for nickel in product **10.49** but is not strong enough to remove the nickel from the chelation sphere of the four sulfur atoms in **10.49**.

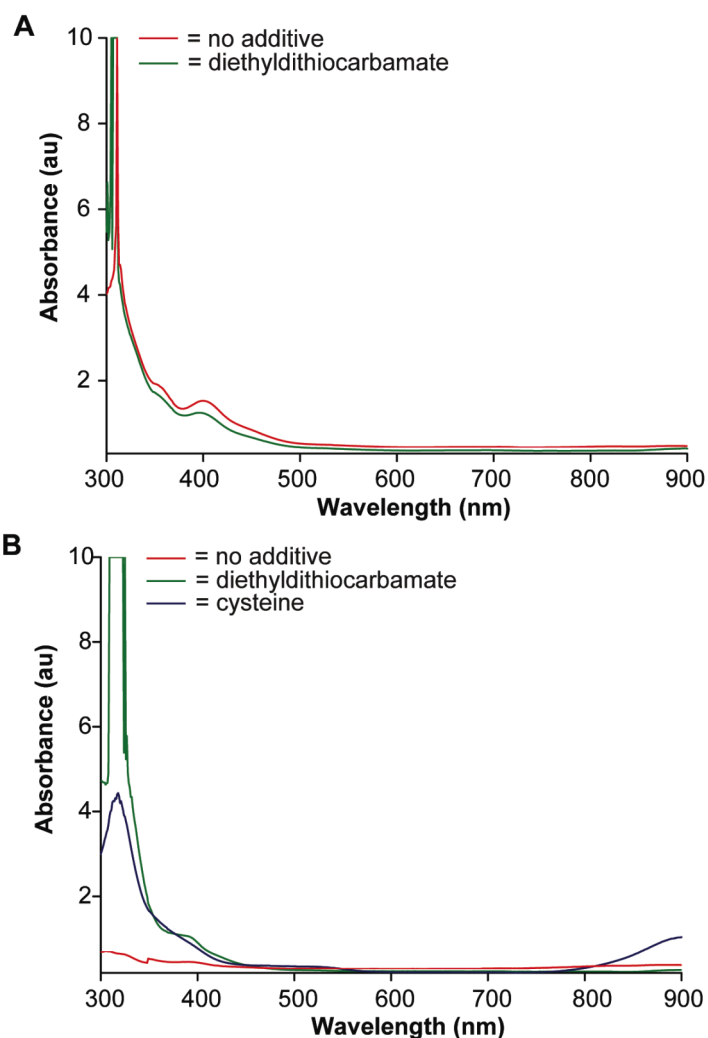


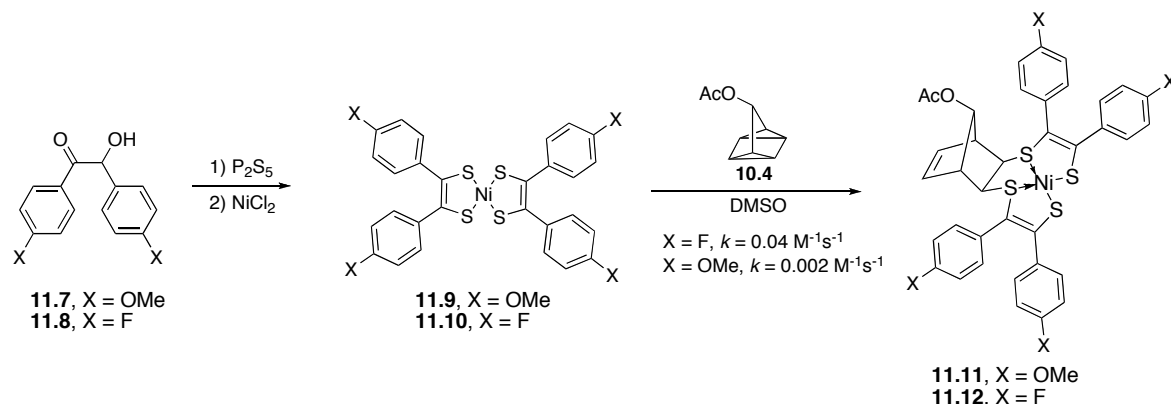
Figure 11.6. Diethyldithiocarbamate (**11.5**) prevents the photodegradation of complex **10.49**. A solution containing 200 μM **10.49** and 0 (red) or 1.25 (green) mM **11.5** in 3:1 $\text{CH}_3\text{CN}/\text{H}_2\text{O}$ was prepared and left in ambient light continually. A. UV/Vis/NIR spectra of the described solutions taken before being exposed to light. B. UV/Vis/NIR spectra of the described solutions taken after 20 h of exposure to light. The red line displays little absorbance due to the low solubility of **10.42** in acetonitrile/water. If **10.42** is reduced to the anionic state by cysteine (1.25 mM, blue line) to give **11.6**, solubility in acetonitrile is improved and evidence of photodegradation can be seen. The diethyldithiocarbamate treated sample remains unaltered after exposure to light indicating no photodegradation occurred.

Mechanistic Modifications

Rate Enhancement

We hypothesized that the reaction between Ni bis(dithiolene) **10.42** and quadricyclane is a concerted cycloaddition process involving the HOMO of quadricyclane and the LUMO of the nickel complex (see Figure 11.1) and thus, modifications to the LUMO of the Ni bis(dithiolene) should alter the reaction rate in a rational manner. Using the method of Schrauzer and coworkers,¹⁰ we prepared substituted Ni bis(dithiolene) complexes **11.11** and **11.12** from benzoin precursors **11.7** and **11.8**, respectively. Upon kinetic analysis, we found that an electron withdrawing *para* substituent (fluorine, complex **11.12**) accelerated the rate ($k = 0.04 \text{ M}^{-1}\text{s}^{-1}$), while an electron donating methoxy group at the *para* position (complex **11.11**) significantly retarded the reaction ($k = 0.002 \text{ M}^{-1}\text{s}^{-1}$) (Scheme 11.5). These kinetics experiments were performed in DMSO using pseudo-first order kinetics in an analogous manner to the parent aryl system (Figure 11.3). These results are consistent with our molecular orbital hypothesis as well as results from Sugimori and coworkers.¹

Scheme 11.5. Preparation and kinetic analysis of substituted Ni bis(dithiolene) complexes.



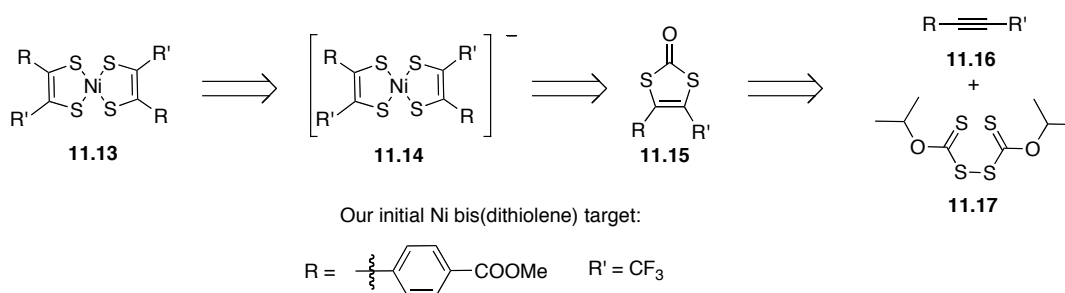
Solubility Enhancement Coupled with Rate Enhancement

At this point, the major limitation of the reaction between quadricyclane and Ni bis(dithiolene) complexes was the very limited solubility of these reagents in polar protic and aqueous solvents. These complexes, with their extended aryl rings and square planar geometry, are large flat, rigid structures and removal of the aryl groups appeared to be a logical and facile strategy to increase their solubility. Additionally, based on the above results, we hypothesized that exchange of an aryl ring for an electron withdrawing group would impart even more favorable reaction kinetics to this putative bioorthogonal chemical reaction.

Removal of one or both aryl rings from the Ni bis(dithiolene) necessitated a new synthetic pathway. Fortunately, a more contemporary method for the synthesis of a variety of Ni bis(dithiolene) species (**11.13**) had been developed, which involves treatment of dithiol-2-one ligand precursors (**11.15**) with nucleophilic base and NiCl₂.¹¹ This procedure yields an anionic Ni bis(dithiolene) (**11.14**) which must be oxidized to the neutral state to give a reagent which can undergo reaction with quadricyclane (Scheme 11.6).

A number of preparations for dithiol-2-one precursors exist.¹¹ We ultimately chose the method of Gareau and Beauchemin, which involves the radical addition of diisopropyl xanthogen disulfide (**11.17**) to an alkyne (**11.16**) due to the flexibility it would give for varying the R groups on **11.13**.¹² The major limitation with this method of dithiol-2-one formation is it proceeds best when the R group is able to stabilize the radical intermediate. Optimal yields were reported when the alkyne substituents were monosubstituted with an aryl ring or other *sp*² hybridized functionality. Based on these results, we selected an aryl ring with a methyl ester at the *para* position for the R group. The methyl ester is electron withdrawing, which is favorable from a reaction kinetics standpoint. In addition, it can provide a point of attachment for a probe moiety to facilitate detection of the ligation product in biological systems.

Scheme 11.6. Retrosynthesis of Ni bis(dithiolene) complex via a dithiol-2-one ligand precursor.



Next, we turned our attention to the selection of the R' group. We wanted the R' group to be sufficiently hydrophilic but also electron withdrawing. The literature indicates that the obvious candidates of cyano and methyl ester groups are not ideal, as tetracyano Ni bis(dithiolene) **11.18** and tetramethylester Ni bis(dithiolene) **11.19** are not isolable as neutral complexes (Figure 11.7).^{13,14} However, the tetratrifluoromethyl Ni bis(dithiolene) **11.20** is stable in its neutral form. In fact, it was this Ni bis(dithiolene) complex that was first reported to react with quadricyclane in the 1970s.¹⁵ More recently, compound **11.20** has resurfaced as a means to purify ethylene from crude olefin streams.¹⁶ Based on these results, we choose the CF₃ group for R'.

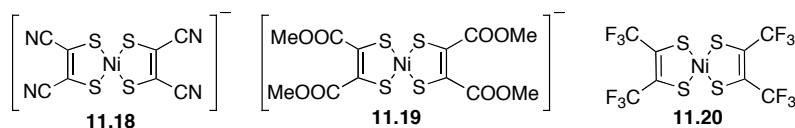
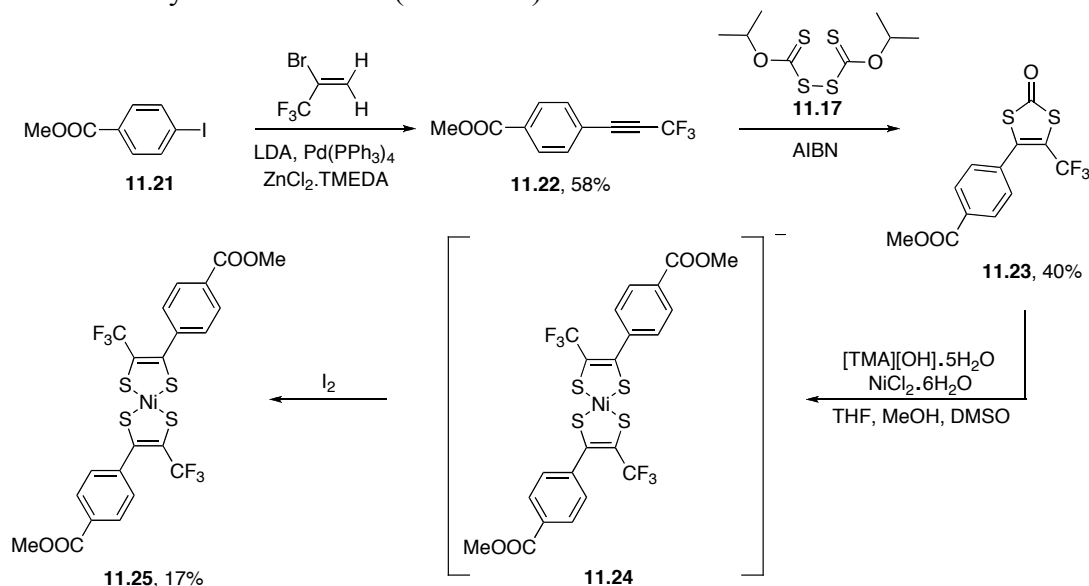


Figure 11.7. Known Ni bis(dithiolene) complexes with electron withdrawing substituents.

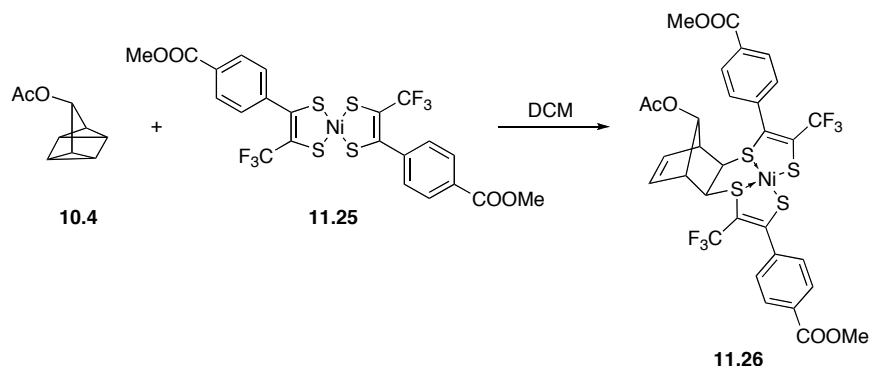
The requisite alkyne, methyl 4-(3,3,3-trifluoroprop-1-ynyl)benzoate **11.22**, was obtained through *in situ* generation of a trifluoromethyl zinc acetylide followed by cross-coupling with methyl 4-iodobenzoate (**11.21**).¹⁷ Treatment of alkyne **11.22** with isopropyl xanthogen disulfide (**11.17**)¹⁸ and the radical initiator azobisisobutyronitrile (AIBN) yielded desired dithiol-2-one ligand **11.23** in 40% yield.¹² Compound **11.23** was converted to anionic Ni bis(dithiolene) **11.24** through reaction with tetramethylammonium hydroxide and NiCl_2 .¹⁹ The anionic species was immediately oxidized with iodine to yield desired Ni bis(dithiolene) **11.25** (Scheme 11.7).

Scheme 11.7. Synthesis of Ni bis(dithiolene) **11.25**.



With the desired nickel complex **11.25** in hand, we analyzed its reactivity with 7-acetoxy quadricyclane (**10.4**) and found that this complex underwent rapid ligation with quadricyclane (Scheme 11.8). As with the aryl Ni (bis)dithiolene species, UV/Vis/NIR spectroscopy was employed to find a rate-constant for the reaction. Compound **11.25** displays a large absorption band at 750 nm (100 nm blue-shifted from **10.42** due to the removal of two aryl groups), which is absent in product **11.26**. Using pseudo-first order kinetics, we found that the second-order rate constant for this reaction in dichloromethane is $5.3 \text{ M}^{-1}\text{s}^{-1}$.

Scheme 11.8. Reaction between quadricyclane **10.4** and Ni bis(dithiolene) **11.25**.



In order to compare the reactivity of Ni bis(dithiolene) **11.25** to the parent reaction with bis(dithiobenzil)nickel(II) (**10.42**), we aimed to perform the kinetic experiment in DMSO. However we did not observe any reaction between **11.25** and 7-acetoxycycloheptatriene (**10.4**) in DMSO. This is evident in Figure 11.8, which shows UV/Vis/NIR absorption spectra taken every 30 sec after the addition of quadricyclane to a solution of **11.25** in dichloromethane and DMSO. A rapid decrease in the band at 750 nm is evident when **11.25** is subjected to quadricyclane in dichloromethane (Figure 11.8A), but no reaction is apparent when the same two species are combined in DMSO (Figure 11.8B). Further, in DMSO, the NIR absorption band is significantly red-shifted and smaller. These features are both indicative of reduction to anionic Ni bis(dithiolene) **11.24**, as the anionic species does not react with quadricyclane and also has a characteristic red shift.^{1,20}

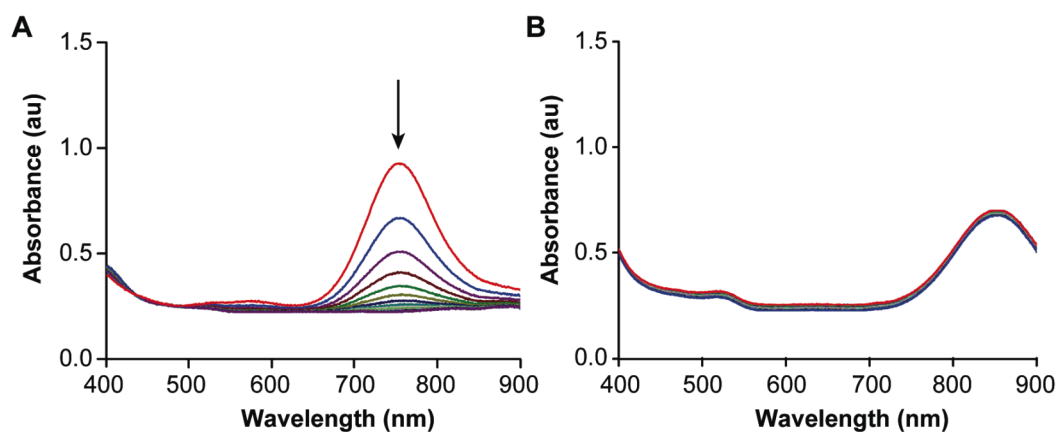


Figure 11.8. UV/Vis/NIR spectra taken every 30 sec following addition of 7-acetoxycycloheptatriene (**10.4**) to a solution of Ni bis(dithiolene) **11.25** in (A) dichloromethane or (B) DMSO. The final concentrations of species were 1 mM quadricyclane and 50 μ M Ni bis(dithiolene).

It is conceivable that DMSO is acting as a reducing agent for **11.25**. In fact, further inspection of the raw kinetic data from the aryl Ni bis(dithiolene) complexes (particularly **10.42** and **11.2**) suggest they also slowly undergo reduction in DMSO. In an effort to find a solvent that does not readily reduce compound **11.25** to **11.24** (Scheme 11.9), we monitored **11.25** in a variety of solvents by UV/Vis/NIR spectroscopy (Figure 11.9). The results from this experiment indicate that most solvents promote the reduction of **11.25** to **11.24**.²¹ These data are surprising as many of the solvents that appear to reduce **11.25** do not have high oxidation potentials. It has been proposed that reduction is actually a function of ligand displacement in more nucleophilic solvents and a net disproportionation reaction occurs to yield a mixture of the reduced species, free ligand, and Ni(II) coordinated to solvent and/or other counterions present in solution.²²

Scheme 11.9. Reduction of Ni bis(dithiolene) **11.25** to anionic species **11.24**.

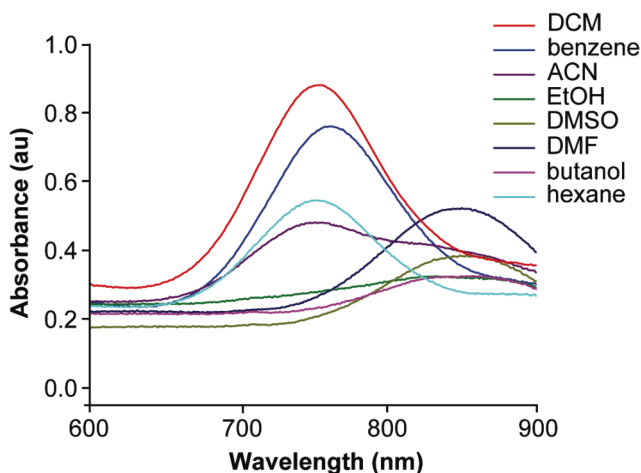
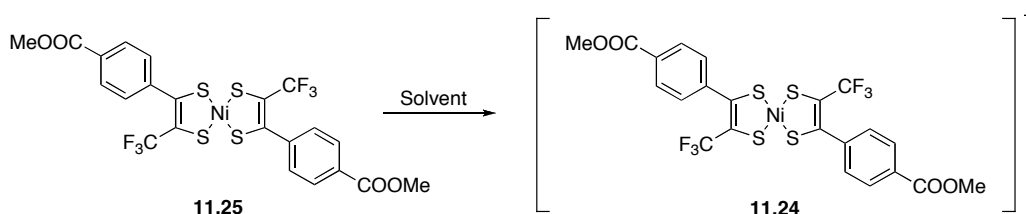


Figure 11.9. Ni bis(dithiolene) **11.25** is reduced by polar solvents. The NIR band of the UV/Vis/NIR spectrum of **11.25** taken in a variety of solvents. A peak around 750 nm indicates the neutral species (**11.25**) is present while a peak around 850 nm is representative of the reduced form (**11.24**).

Stability Enhancement

Through the synthesis of Ni bis(dithiolene) **11.25**, we succeeded in synthesizing a new complex with enhanced reaction kinetics and somewhat improved solubility properties, but this compound proved to be too electron deficient to persist in the correct oxidation state in polar solvents. Another round of modifications was necessary for this prototype reaction to be useful as a bioorthogonal reaction.

We embarked on the synthesis of a series of diaryl Ni bis(dithiolene) species that were not as electron deficient as compound **11.25** (Figure 11.10). Two strategies were employed to alter the electronics of the nickel complexes: removal of the trifluoromethyl group and removal of the electron withdrawing aryl methyl ester. Using one (compounds **11.27** or **11.28**) or both (compound **11.29**) of these strategies, we hoped to obtain a nickel complex with adequate reactivity and stability in polar solvents.

The synthesis of these three new Ni bis(dithiolene) reagents proceeded in a manner analogous to **11.25**. Compound **11.27** was synthesized from methyl 4-iodobenzoate (**11.21**) which underwent Sonogashira coupling with 3-methoxyprop-1-yne (**11.30**) to yield alkyne **11.31**. The alkyne was subjected to isopropyl xantogen disulfide and AIBN to give the dithiol-2-one ligand precursor functionality (**11.32**) in 56% yield. Treatment of **11.32** with tetramethyl ammonium hydroxide, NiCl₂ and I₂ produced desired Ni bis(dithiolene) **11.27** (Scheme 11.10).

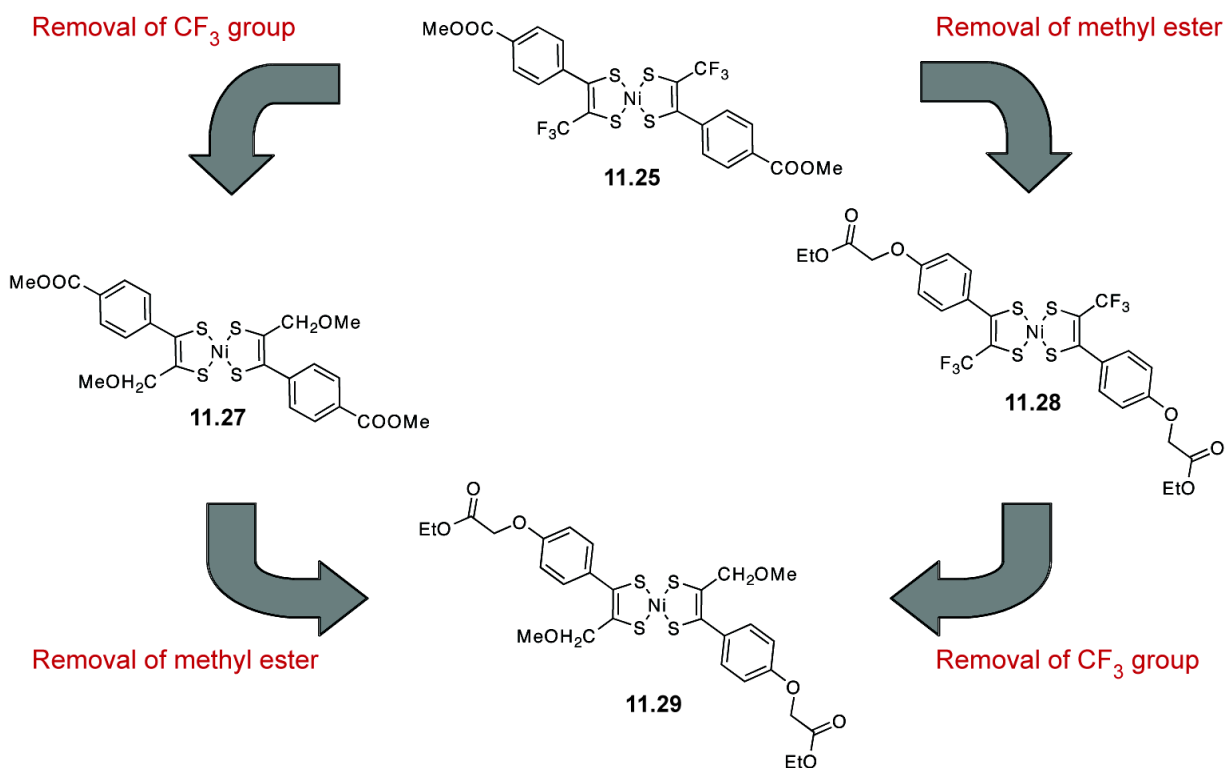
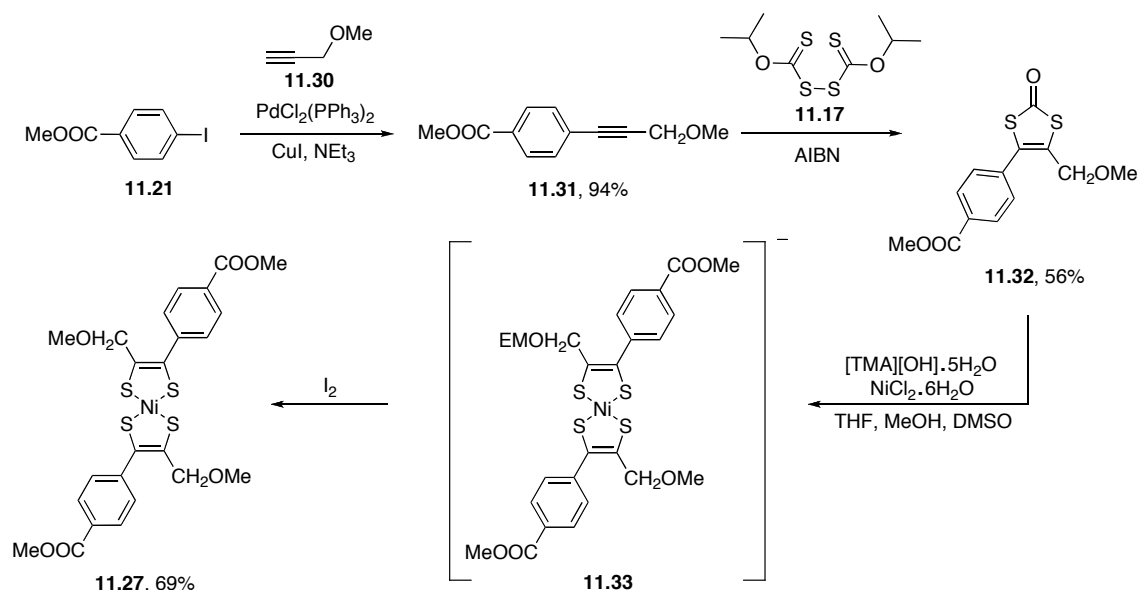


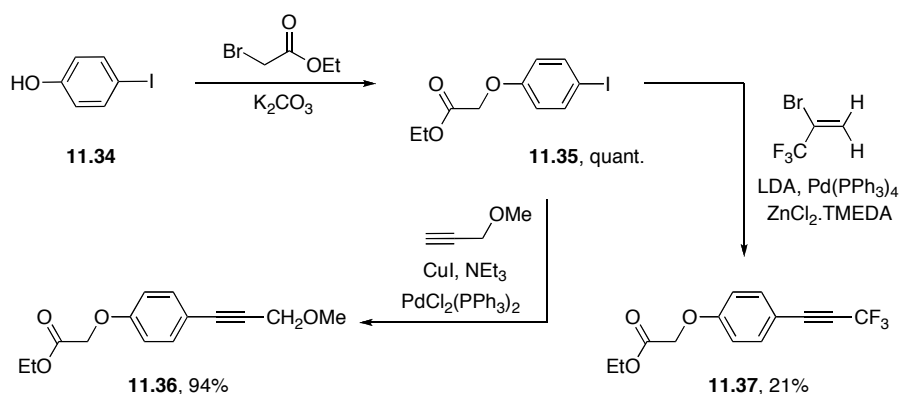
Figure 11.10. Sequential electronic deactivation of Ni bis(dithiolene) **11.25** by removal of the trifluoromethyl group or removal of the methyl ester.

Scheme 11.10. Synthesis of Ni bis(dithiolene) **11.27**.

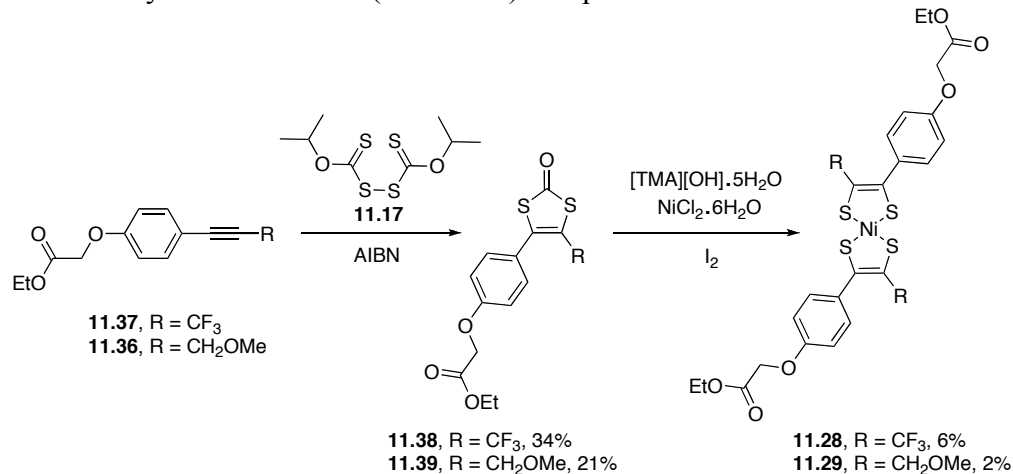


For the synthesis of Ni bis(dithiolene) compounds **11.28** and **11.29**, 4-iodo-phenol (**11.34**) was alkylated with ethyl bromoacetate to yield **11.35** which underwent Sonogashira coupling with 3-methoxyprop-1-yne or cross-coupling with *in situ* generated trifluoromethyl zinc acetylide to yield alkynes **11.36** and **11.37**, respectively (Scheme 11.11). These alkynes underwent radical reaction with xanthogen disulfide **11.17** to yield **11.38** and **11.39**, followed by transformation to the desired Ni bis(dithiolene) complexes **11.28** or **11.29** (Scheme 11.12).

Scheme 11.11. Synthesis of alkynes **11.36** and **11.37**.



Scheme 11.12. Synthesis of Ni bis(dithiolene) complexes **11.28** and **11.29**.



None of the diaryl nickel complexes appeared as promising of reagents as the initial bis(dithiobenzil)nickel(II) lead. The complexes which did not contain the trifluoromethyl group (**11.27**, **11.29**) were considerably more stable than **11.25** in polar solvent; however, they reacted with quadricyclane very slowly. Conversely, **11.28** displayed adequate reaction kinetics with quadricyclane, but this compound was still too susceptible to reduction for use as a bioorthogonal reagent.

Further Mechanistic Modifications

We gained valuable insight into the behavior of the Ni bis(dithiolene) species through the first rounds of mechanistic modifications. Taking all the newly acquired knowledge, we returned our attention to the tetraaryl scaffold which displays good reaction kinetics and much better stability than the trifluoromethylated Ni bis(dithiolene) complexes. The major problem with the tetraaryl scaffold was the lack of solubility in polar solvents. Thus, we looked to employ other methods for enhancing the water-solubility. Sulfonate groups appeared the obvious choice as they are commonly used to decrease hydrophobic interactions of dye molecules and they have significant electron withdrawing character ($\sigma_{\text{para}} = 0.38$).²³

We obtained sulfonated Ni bis(dithiolene) **11.44** using the same synthetic pathway employed for the diaryl nickel complexes (Scheme 11.13). Alkyne **11.40** was prepared by Sonogashira reaction of phenyl acetylene and methyl 4-iodobenzoate (**11.21**). Treatment of alkyne **11.40** with xanthogen disulfide **11.17** in the presence of the radical initiator 1,1'-azobis(cyclohexanecarbonitrile) yielded **11.41**. The dithiocarbonate in **11.41** proved to be highly acid stable, and heating **11.41** overnight in fuming sulfuric acid installed a single sulfonate group and also hydrolyzed the methyl ester to produce **11.42** in good yield. Standard amide bond coupling conditions were used to conjugate isopropyl amine to the acid moiety on **11.43**, which was then converted to Ni bis(dithiolene) **11.44** by treatment

Scheme 11.14. Reaction between 7-acetoxo quadricyclane (**10.4**) and Ni bis(dithiolene) **11.44**.

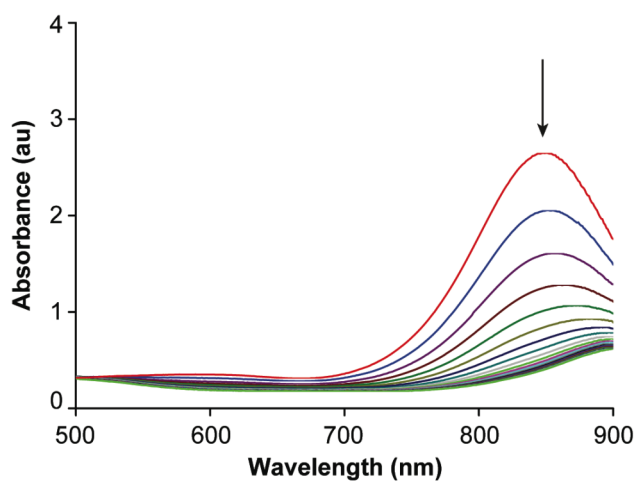
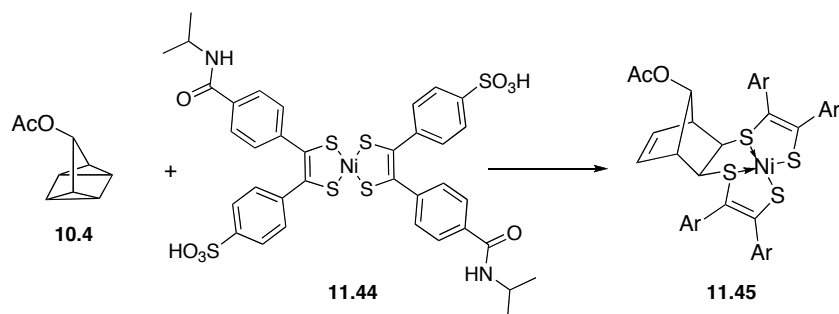


Figure 11.11. A series of UV/Vis/NIR spectra taken as the reaction between quadricyclane **10.4** and **11.44** is proceeding. A solution of **11.44** (400 μ M in PBS) was combined with **10.4** (20 mM in EtOH) and a UV/Vis/NIR spectrum was obtained every 30 seconds.

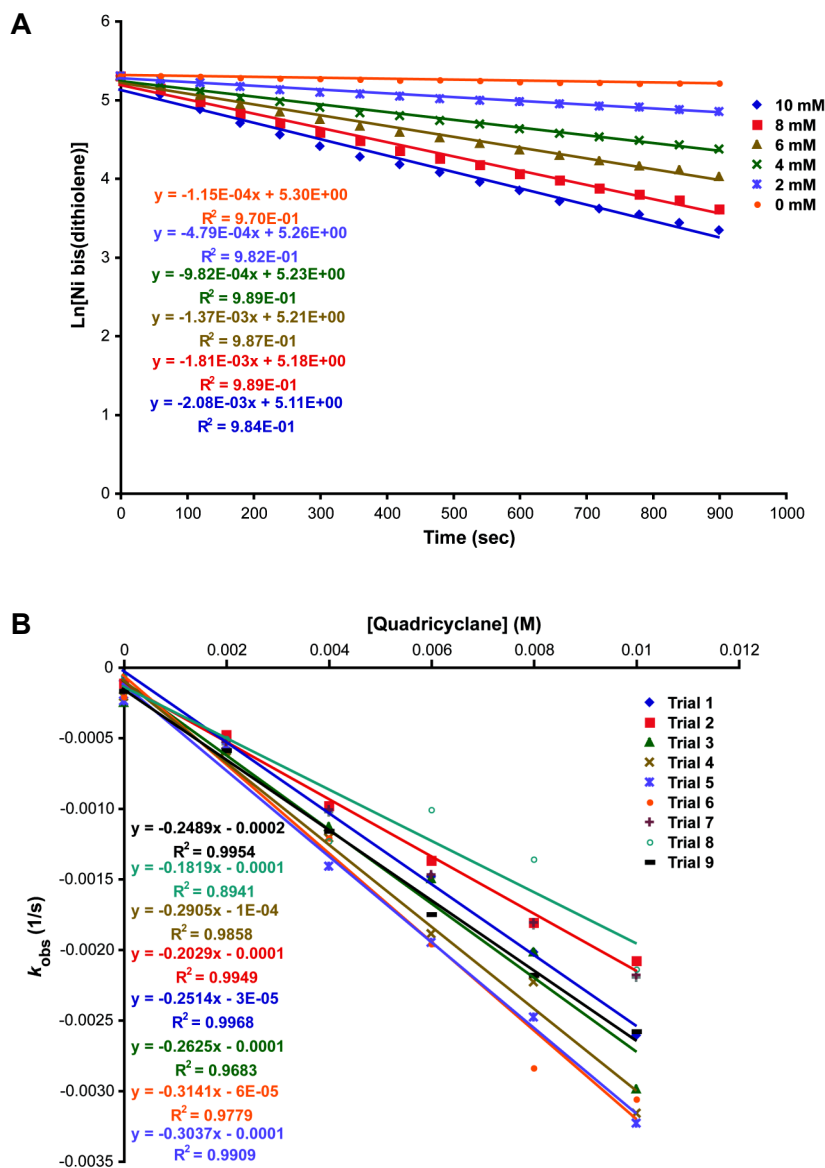


Figure 11.12. The second-order rate constant for the reaction of **10.4** and **11.44** was determined using pseudo-first order kinetics. A solution of $400 \mu\text{M}$ **11.44** in PBS was combined with various solutions of quadracycline **10.4** (20 mM, 16 mM, 12 mM, 8 mM, 4 mM, or 0 mM in EtOH) in a 1:1 ratio (total volume = $100 \mu\text{L}$). The reaction was monitored by the absorbance at 850 nm for 15 min. The absorbance values were correlated to the concentration of **11.44** using a standard curve. A plot of $\text{Ln}[\text{11.44}]$ versus time resulted in a series of first-order rate constants (k_{obs}). Plotting each k_{obs} value vs. $[\text{10.4}]$ yields a linear regression with the slope of the line indicating the second-order rate constant. The average of nine trials resulted in a second-order rate constant of $0.25 \pm 0.05 \text{ M}^{-1}\text{s}^{-1}$. A. A representative plot to determine k_{obs} . B. Plot of k_{obs} vs. $[\text{10.4}]$ for each trial.

It was also determined that this reaction has similar reaction kinetics in DMSO, suggesting that the sulfonate groups are sufficiently electron withdrawing to have a significant rate-enhancement when compared to parent Ni bis(dithiolene) complex **10.42** ($k = 0.023 \text{ M}^{-1}\text{s}^{-1}$). The reaction kinetics do not display a drastic pH difference as the rate constant in 1:1 MES (pH = 6.1)/EtOH is $0.28 \pm 0.01 \text{ M}^{-1}\text{s}^{-1}$ at room temperature. We also confirmed that the reaction of **11.44** with 7-acetoxy norbornadiene (**10.3**) is several orders of magnitude slower than the reaction between 7-acetoxy quadricyclane and **11.44** ($k = (7.2 \pm 0.9) \times 10^{-3} \text{ M}^{-1}\text{s}^{-1}$ in 1:1 PBS/EtOH at room temperature).

Stability Analysis of Ni bis(dithiolene) 11.44

The stability of **11.44** was also investigated by monitoring the NIR absorption band. Absorption at 850 nm remained essentially unaltered when **11.44** was incubated in PBS for 20 h (Figure 11.13). In addition, incubation with 125-fold excess amino acids had either no effect or a minimal effect on the absorption intensity over 2 h (Figure 11.14). A marked exception was cysteine, which even at 1 molar equivalent caused an immediate reduction in the intensity of the 850 nm absorption band and concomitant appearance of a new band at ~900 nm (Figure 11.15A). This transformation is consistent with reduction of **11.44** to **11.46** (Scheme 11.15)^{26,27} and treatment of **11.44** with other reducing agents yields similar results (Figure 11.15B-D). The disappearance of the band at 900 nm when 100 equivalents of reducing agent is present is likely due to further reduction of the anionic species (overall charge = -2).¹⁹

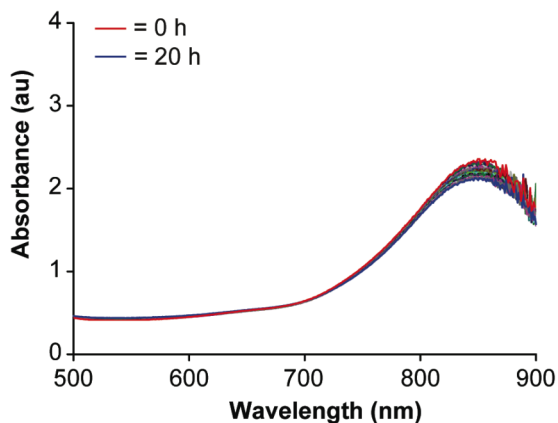


Figure 11.13. Ni bis(dithiolene) **11.44** is stable to PBS. Ni bis(dithiolene) **11.44** was dissolved in PBS and the absorption of the NIR band was monitored for changes over 20 h. A UV/Vis/NIR spectrum was taken every hour. Only slight reduction in signal is evident.

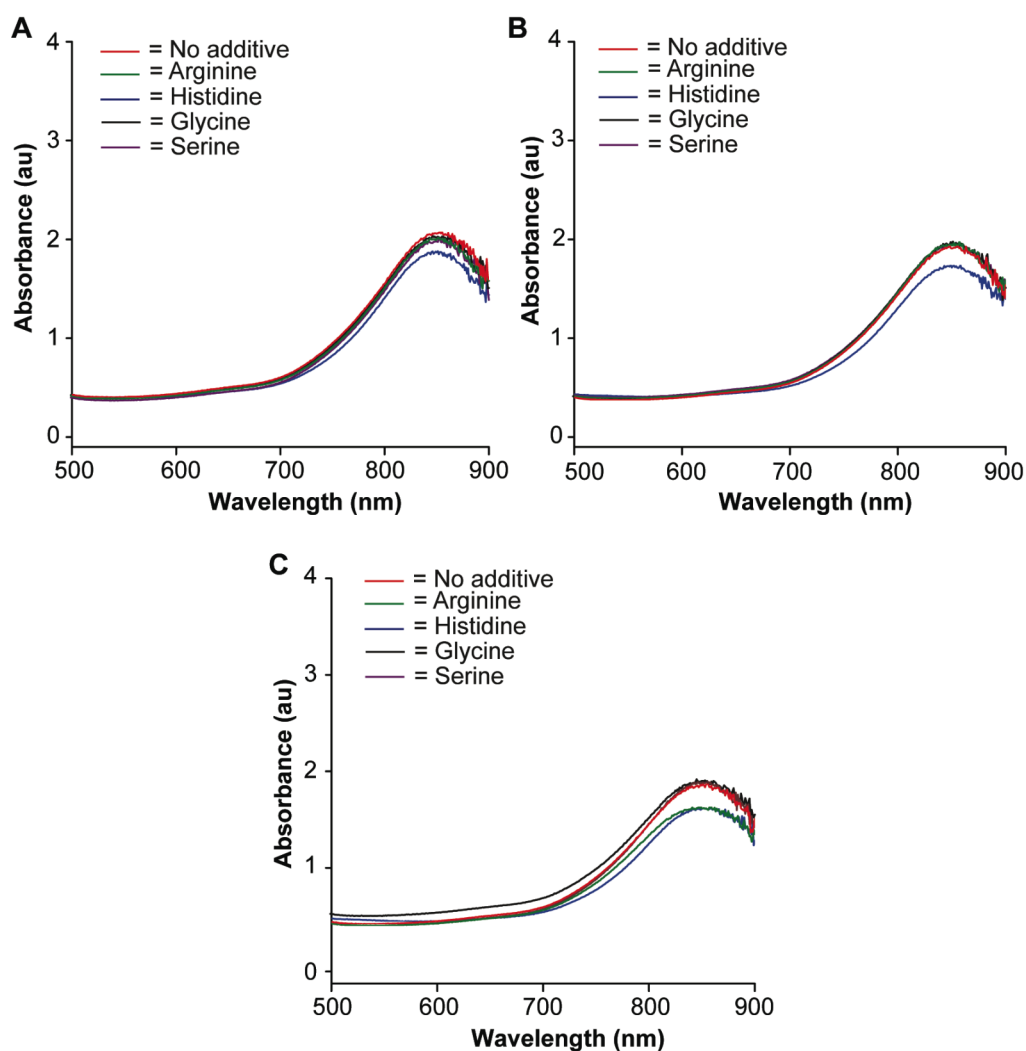


Figure 11.14. Ni bis(dithiolene) **11.44** is moderately stable to an excess of free amino acids. A solution of 400 μM **11.44** in PBS was combined with 50 mM solutions of the indicated amino acid in a 1:1 ratio. The absorbance of each solution was monitored over time. A. The UV/Vis/NIR spectra taken after approximately 15 min. B. The UV/Vis/NIR spectra taken after 1 h. C. The UV/Vis/NIR spectra taken after 2 h. Red = no amino acid present. Green = arginine. Blue = histidine. Black = glycine. Purple = serine.

Scheme 11.15. Reduction of **11.44** to anionic species **11.46**.

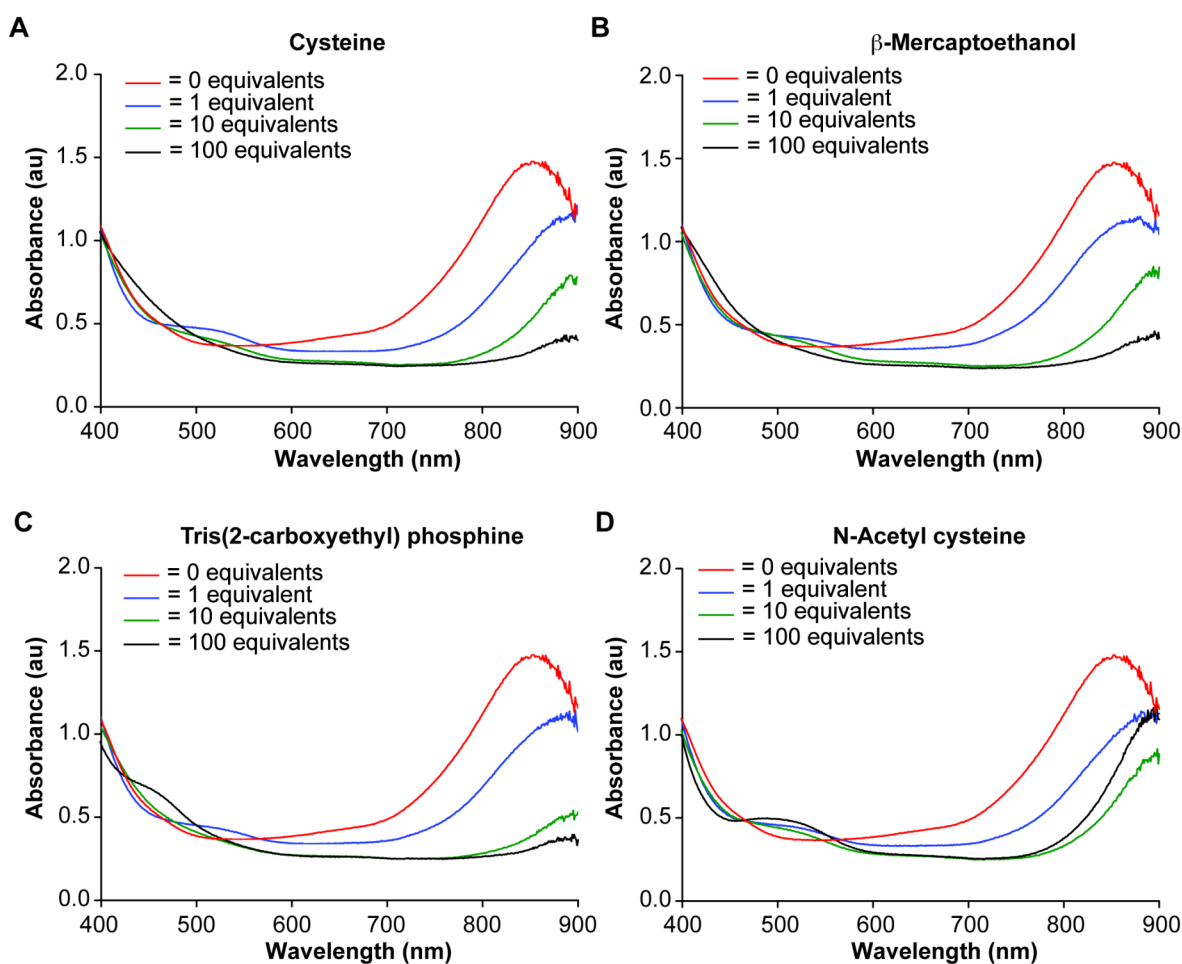
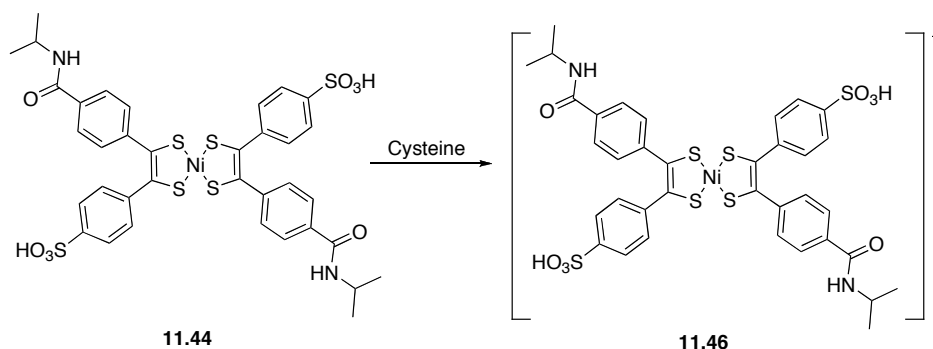


Figure 11.15. UV/Vis/NIR analysis of the reaction between **11.44** and reducing agents. A solution of 125 μM **11.44** in PBS was prepared with 0 (red), 1 (blue), 10 (green) or 100 (black) equivalents of reducing agent. All the mixtures instantly turned orange upon addition of reducing agent and displayed the UV/Vis/NIR spectra shown above. A smaller, red-shifted NIR absorption band is consistent with reduction of **11.44**. A.

Reduction by cysteine. B. Reduction by β -mercaptoethanol. C. Reduction by tris(2-carboxyethyl)phosphine. D. Reduction by N-acetyl cysteine.

The neutral complex can be restored by addition of potassium ferricyanide ($\text{K}_3\text{Fe}(\text{CN})_6$) as judged by the reappearance of the absorption band at 850 nm and restoration of reactivity with **10.4** (Figures 11.16). This restoration can only be achieved if a mild excess of reducing agent is used (1 to 10-fold). When a large excess of reducing agent is present, further reduction to the dianionic species or decomposition of **11.44** might be occurring.^{19,22}

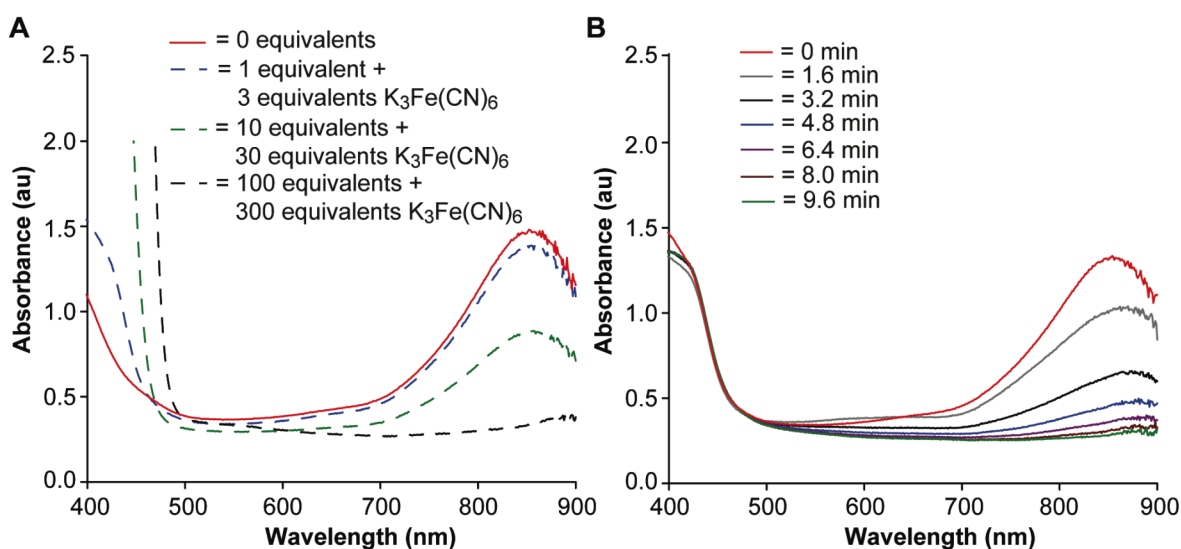


Figure 11.16. Ni bis(dithiolenes) **11.44** can be rescued by addition of $\text{K}_3\text{Fe}(\text{CN})_6$. A. A solution of $125 \mu\text{M}$ **11.44** in PBS was treated with 1, 10, or 100 equivalents of cysteine followed by 3, 30, or 300 equivalents of $\text{K}_3\text{Fe}(\text{CN})_6$, respectively (blue, green, black dashed lines). After 1 h, UV/Vis/NIR spectra were collected. The red line represents $125 \mu\text{M}$ **11.44** with no treatment. B. Ni bis(dithiolenes) **11.44** rescued by the addition of $\text{K}_3\text{Fe}(\text{CN})_6$ reacts with quadricyclane. A solution of $125 \mu\text{M}$ **11.44** in PBS was treated with 1 equivalent of cysteine followed by 3 equivalents of $\text{K}_3\text{Fe}(\text{CN})_6$. Quadricyclane was added and a UV/Vis/NIR spectrum was immediately recorded (red line). UV/Vis/NIR spectra were then collected every 1 min and 40 sec. The observed reduction in signal is indicative of reaction with quadricyclane.

Concerned that the presence of cysteine residues within proteins would undermine the reactivity of **11.44**, we monitored the stability of **11.44** in the presence of oxidized insulin, BSA, thioredoxin (Trx), and glutathione-S-transferase (GST). Compound **11.44** is stable to 1.2 equivalents of oxidized insulin (Figure 11.17), which contained no free sulfhydryl groups, for 5 h. BSA, which possesses a solvent-exposed reduced cysteine side chain,²⁸ is able to reduce **11.44** but at a much slower rate than free cysteine (even with 12 equivalents present), indicating that the reduction should not be competitive with the reaction with quadricyclane (Figure 11.18). However, **11.44** is highly susceptible to reduction by Trx and GST (Figure 11.19), both enzymes with active site cysteine residues.^{29,30} Thus, the stability of **11.44** appeared adequate for protein labeling, but its redox stability will need to be improved for general utility with proteins that readily undergo oxidation state changes.

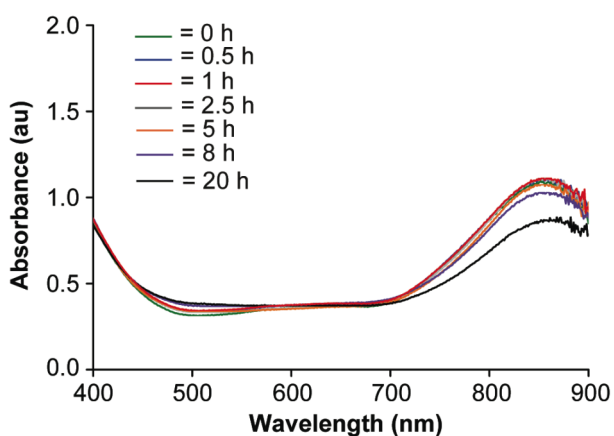


Figure 11.17. Ni bis(dithiolene) **11.44** is stable to oxidized insulin over multiple hours. A solution containing **11.44** (100 μ M) and oxidized insulin (1.2 equivalents) was monitored by UV/Vis/NIR spectroscopy at various timepoints over 20 h. UV/Vis/NIR spectra were normalized to each other at 650 nm.

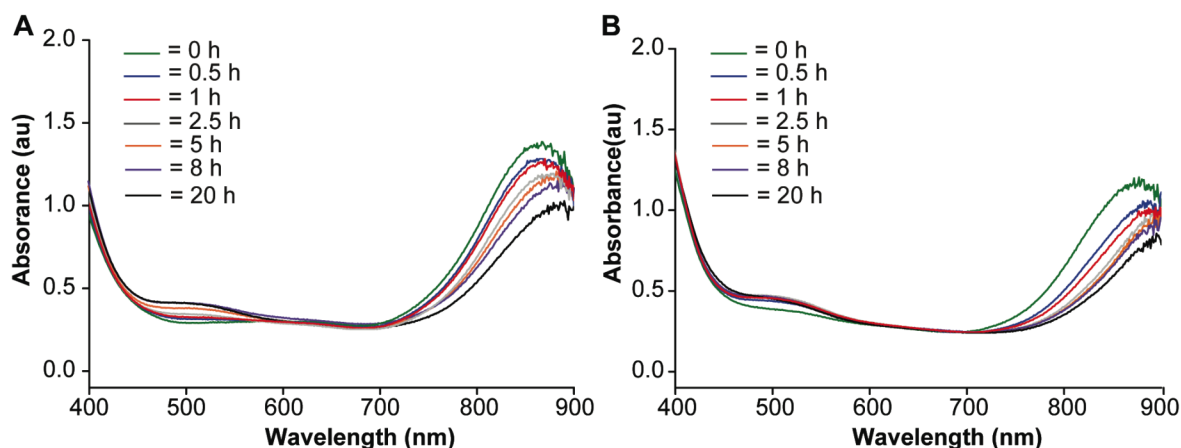


Figure 11.18. Ni bis(dithiolene) **11.44** is reduced by bovine serum albumin (BSA). A solution containing **11.44** (100 μ M) and BSA (1.2 equivalents (A) or 12 equivalents (B)) was monitored by UV/Vis/NIR spectroscopy at various timepoints over 20 h. UV/Vis/NIR spectra were normalized to each other at 650 nm. An Ellman's test for sulfhydryl groups indicated 30-40% of the predicted free cysteine residues on commercial BSA were available for disulfide exchange.

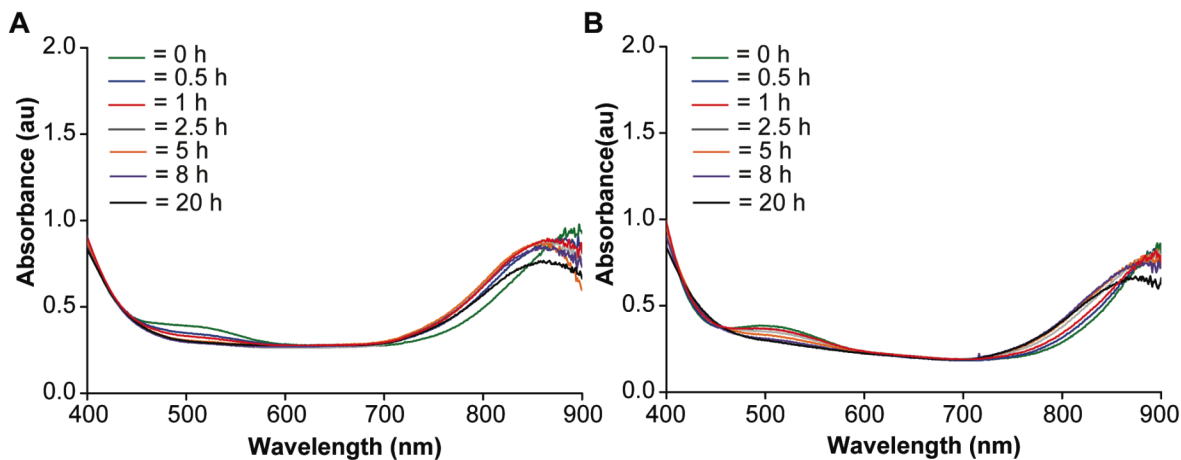


Figure 11.19. Ni bis(dithiolene) **11.44** is reduced by thioredoxin (Trx) and glutathione S-transferase (GST). A solution containing **11.44** (100 μ M) and Trx (A, 1.2 equivalents) or GST (B, 1.2 equivalents) was monitored by UV/Vis/NIR spectroscopy at various timepoints over 20 h. UV/Vis/NIR spectra were normalized to each other at 650 nm.

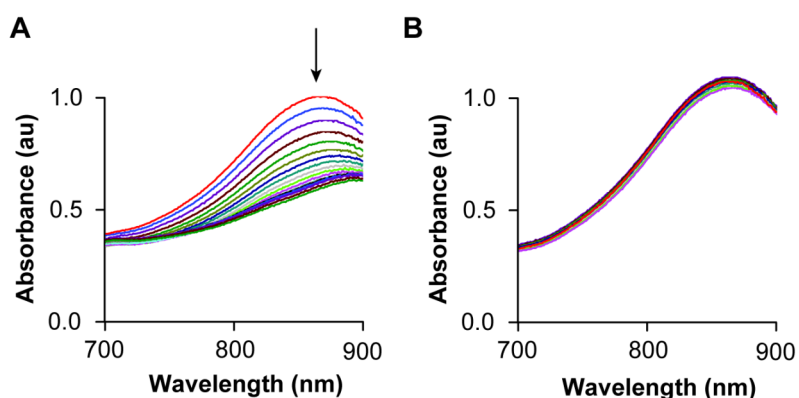


Figure 11.20. Ni bis(dithiolene) **11.44** reacts with quadricyclane **10.5** in the presence of live Jurkat cells. Jurkat cells in RPMI media were combined with 200 μM **11.44**. The UV/Vis/NIR absorption spectrum was monitored for changes in the presence (A) or absence (B) of **10.5**. Shown are spectra taken every 30 sec.

Collectively, the reaction kinetics and reagent stability for the reaction between quadricyclane and Ni bis(dithiolene) reagents appeared sufficient for a bioorthogonal reaction. Before embarking on the synthesis of a Ni bis(dithiolene) which could be detected in biological milieu, we further analyzed the bioorthogonality of **11.44** by combining **11.44** with RPMI media containing live Jurkat cells and monitoring the NIR absorption band in the presence and absence of 7-hydroxy quadricyclane (**10.5**) (Figure 11.19). Gratifyingly, the absorption band centered at 850 nm decreased only in a quadricyclane dependent manner, suggesting that biomolecules appended with quadricyclane should be able to be selectively modified.

Summary of Mechanistic Modifications

Clearly, a number of mechanistic modifications were necessary for a suitable Ni bis(dithiolene) species to be obtained. While the stability of the ligation product as well as the propensity for the Ni bis(dithiolene) complexes to undergo reduction, are not ideal, we thought that complex **11.44** was suitable to test in more complex systems. Thus, for a first generation bioorthogonal reaction we deemed the mechanistic modifications complete (Figure 10.1, step 3) and proceeded to protein and live cell labeling experiments (Figure 10.1, steps 4-5). The results of these experiments would indicate how crucial further mechanistic modifications would be.

Materials and Methods

General Experimental Procedure

All chemical reagents were purchased from Sigma-Aldrich, Acros or TCI and used without purification unless noted otherwise. Anhydrous DMF and MeOH were purchased from Aldrich or Acros in sealed bottles; all other solvents were purified as described by Pangborn *et al.*³¹ In all cases, solvent was removed by reduced pressure with a Buchi Rotovapor R-114 equipped with a Welch self-cleaning dry vacuum. Products were further dried by reduced pressure with an Edwards RV5 high vacuum. Lyophilization was performed on a LABCONCO FreeZone[®] instrument equipped with an Edwards RV2 pump. Thin layer chromatography was performed with EMD 60 Å silica gel plates. Flash chromatography was performed using Silicycle[®] 60 Å 230-400 mesh silica. All ¹H, ¹³C and ¹⁹F NMR spectra are reported in ppm and referenced to solvent peaks (¹H and ¹³C). Spectra were obtained on Bruker AVQ-400, AVB-400, DRX-500, AV-500, or AV-600 instruments. UV/Vis/NIR spectra were acquired on a CARY 100 Bio UV-Visible Spectrophotometer with a range of 200-900 nm. Electron impact (EI) and electrospray ionization (ESI) mass spectra were obtained from the UC Berkeley Mass Spectrometry Facility. HPLC was performed on a Varian Pro Star or Varian Prep Star instrument with a C18 column.

Experimental Procedures

Methyl 4-(3,3,3-trifluoroprop-1-ynyl)benzoate (11.22). Lithium diisopropylamide was generated by combining diisopropylamine (3.5 mL, 25 mmol, 3.2 equiv.) and *n*-butyllithium (15.7 mL of 1.6M solution in hexane, 25 mmol, 3.2 equiv.) in THF (22.8 mL, anhydrous) at -78 °C. Upon stirring for 30 min, 2-bromo-3,3,3-trifluoroprop-1-ene (1.14 mL, 11.1 mmol, 1.4 equiv.) was added dropwise followed by a zinc chloride tetramethylethylenediamine complex (ZnCl₂·TMEDA, 3.17 g, 12.7 mmol, 1.7 equiv.). The mixture was stirred for 30 min at -78 °C and 30 min at rt, at which point methyl 4-iodobenzoate (**11.21**, 1.96 g, 7.48 mmol, 1.0 equiv.) and tetrakis(triphenylphosphine) palladium (466 mg, 0.40 mmol, 5 mol%) were added. The reaction was heated to reflux overnight. The following morning the mixture was quenched with aqueous ammonium chloride and extracted with ethyl acetate (3 x 100 mL). The organics were combined, dried, decanted, and evaporated to dryness. The crude product was purified by silica gel chromatography using a hexane/toluene solvent system (8:1, 5:1, 3:1, 2:1). This procedure resulted in pure **11.22** (992 mg, 4.35 mmol, 58%). R_f = 0.6 in 1:1 hexane/toluene. ¹H NMR (600 MHz, CDCl₃): δ 8.03 (d, *J* = 8.3 Hz, 2H), 7.59 (d, *J* = 8.3 Hz, 2H), 3.92 (s, 3H). ¹³C NMR (150 MHz, CDCl₃): δ 165.9, 132.5, 132.3, 129.8, 122.9, 114.85 (q, *J* = 257.3 Hz), 85.33 (q, *J* = 6.3 Hz), 77.83 (q, *J* = 52.0 Hz), 52.4. ¹⁹F NMR (565 MHz, CDCl₃): δ -51.50 (s, 3F). HRMS (EI): calcd. for C₁₁H₇O₂⁺ [M]⁺, 228.0398; found, 228.0400.

Methyl 4-(2-oxo-5-(trifluoromethyl)-1,3-dithiol-4-yl)benzoate (11.23). Alkyne **11.22** (285 mg, 1.25 mmol, 1.0 equiv.) was dissolved in benzene (11.4 mL, degassed). Isopropyl xanthogen disulfide **11.17** (385 mg, 1.42 mmol, 1.1 equiv.) and azobisisobutyronitrile (AIBN, 123 mg, 0.75 mmol, 0.6 equiv.) were added and the mixture was heated to 80 °C for 2 d. After 2 d, the reaction was cooled to rt, evaporated to dryness, and purified by silica gel chromatography using a hexane/toluene solvent system (product elutes at 1:1 hexane/toluene). This procedure resulted in 161 mg of pure **11.23** (0.51 mmol, 40%). $R_f = 0.3$ in 3:2 toluene/hexane. $^1\text{H NMR}$ (600 MHz, CDCl_3): δ 8.11 (d, $J = 8.2$ Hz, 2H), 7.49 (d, $J = 8.2$ Hz, 2H), 3.95 (s, 3H). $^{13}\text{C NMR}$ (150 MHz, CDCl_3): δ 186.5, 166.2, 138.6 (q, $J = 3.6$ Hz), 133.8, 132.2, 130.2, 129.3 (q, $J = 1.6$ Hz), 119.92 (q, $J = 273.9$ Hz), 118.15 (q, $J = 36.2$ Hz), 52.7. $^{19}\text{F NMR}$ (565 MHz, CDCl_3): δ -53.13 (s, 3F). HRMS (EI): calcd. for $\text{C}_{12}\text{H}_7\text{O}_3\text{F}_3\text{S}_2^+ [\text{M}]^+$, 319.9789; found, 319.9796.

Ni bis(dithiolene) 11.25. Ligand **11.23** (50 mg, 0.16 mmol, 1.0 equiv.) was dissolved in THF (1.5 mL, anhydrous). A solution of methanolic tetramethylammonium hydroxide ([TMA][OH]) was prepared by dissolving [TMA][OH]·5H₂O (60 mg, 0.33 mmol, 2.1 equiv.) in MeOH (75 μL). This solution was added to the solution of **11.23** and stirred at rt for 5 min, at which point NiCl₂·6H₂O (19 mg, 0.08 mmol, 0.5 equiv.) in a solution of DMSO (150 μL) and MeOH (75 μL) was added. This mixture was stirred at rt for 6 h, at which point iodine (20 mg, 0.16 mmol, 1.0 equiv) was added and the solution turned blue. This mixture was stirred at rt overnight. The following morning it was evaporated to dryness and the Ni bis(dithiolene) was purified by silica gel chromatography using a hexane/CH₂Cl₂ solvent system (product elutes at 1:1 hexane/CH₂Cl₂). This procedure yielded 9 mg of **11.25** as a dark blue solid (0.014 mmol, 17%). $R_f = 0.8$ in CH₂Cl₂. $^1\text{H NMR}$ (600 MHz, CDCl_3): δ 8.13 (dd, $J = 23.5, 10.9$ Hz, 4H), 7.59 (d, $J = 8.2$ Hz, 4H), 3.99 (s, 6H). UV/Vis/NIR (CH₂Cl₂): 753 nm (0.9 au), 572 nm (0.3 au), 349 nm (0.8 au), 277 nm (1.6 au), 236 nm (1.8 au), 215 nm (1.2 au). HRMS (EI): calcd. for $\text{C}_{22}\text{H}_{14}\text{O}_4\text{S}_4\text{F}_6\text{Ni}^+ [\text{M}]^+$, 641.9033; found, 641.9036.

Methyl 4-(3-methoxyprop-1-ynyl)benzoate (11.31). Methyl 4-iodobenzoate (**11.21**, 1.0 g, 3.8 mmol, 1.0 equiv.) and methyl propargyl ether (**11.30**, 0.5 mL, 5.9 mmol, 1.5 equiv.) were dissolved in THF (30 mL, anhydrous). To this solution, bis(triphenylphosphine) palladium chloride (150 mg, 0.21 mmol, 5.6 mol%), copper iodide (100 mg, 0.52 mmol, 14 mol%), and triethylamine (2.0 mL, 14 mmol, 3.7 equiv.) were added. The mixture turned dark brown upon addition of triethylamine. After 1 h, the brown color had dispersed and the reaction was complete. It was quenched with aqueous ammonium chloride and extracted with ethyl acetate (3 x 100 mL). The organics were combined, dried, decanted and evaporated to dryness. The crude product was purified by silica gel chromatography with 25:1 hexane/ethyl acetate. This procedure resulted in pure **11.31** (725 mg, 3.6 mmol, 94%). $^1\text{H NMR}$ (400 MHz, CDCl_3): δ 7.87 (d, $J = 8.4$ Hz, 2H), 7.39 (d, $J = 8.4$ Hz, 2H), 4.22 (s, 2H), 3.79 (s, 3H), 3.34 (s, 3H). $^{13}\text{C NMR}$ (100 MHz, CDCl_3): δ 166.2, 131.5, 129.7, 129.4, 127.3, 88.1, 85.5, 60.2, 57.5, 52.0. HRMS (EI): calcd. for $\text{C}_{12}\text{H}_{11}\text{O}_3^+ [\text{M}]^+$, 203.0708; found, 203.0712.

Methyl 4-(5-(methoxymethyl)-2-oxo-1,3-dithiol-4-yl)benzoate (11.32). Alkyne **11.31** (350 mg, 1.7 mmol, 1.0 equiv.) was dissolved in benzene (17 mL). Isopropyl xanthate disulfide **11.17** (522 mg, 1.9 mmol, 1.1 equiv.) and azobisisobutyronitrile (AIBN, 280 mg, 1.7 mmol, 1.0 equiv.) were added and the mixture was heated to 80 °C for 3 d. After 3 d, additional **11.17** (500 mg) and AIBN (100 mg) were added. The mixture was heated to 80 °C for another 4 d, at which point it was evaporated to dryness and purified by silica gel chromatography using a hexane/ethyl acetate solvent system. This procedure resulted in 280 mg of pure **11.32** (0.95 mmol, 56%) in addition to 285 mg recovered alkyne **11.31**. ¹H NMR (500 MHz, CDCl₃): δ 7.92 (d, *J* = 8.5 Hz, 2H), 7.45 (d, *J* = 8.4 Hz, 2H), 4.28 (s, 2H), 3.85 (s, 3H), 3.40 (s, 3H). ¹³C NMR (125 MHz, CDCl₃): δ 190.7, 166.3, 135.4, 131.0, 130.7, 130.3, 129.4, 129.1, 67.7, 58.6, 52.5. HRMS (EI): calcd. for C₁₂H₁₂O₄S₂⁺ [M]⁺, 296.0177; found, 296.0182.

Ni bis(dithiolene) 11.27. Ligand **11.32** (10 mg, 0.034 mmol, 1.0 equiv.) was dissolved in THF (0.3 mL, anhydrous). To this solution, tetramethylammonium hydroxide (12 mg, 0.066 mmol, 1.9 equiv.) in MeOH (30 μL) was added. The mixture was stirred at rt for 5 min, at which point NiCl₂ (4 mg, 0.015 mmol, 0.5 equiv.) in MeOH (30 μL) was added. This mixture was stirred at rt for 6 h, at which point iodine (4 mg, 0.031 mmol, 0.9 equiv.) was added and the reaction proceeded at rt overnight. The following day, the mixture was evaporated to dryness and purified by silica gel chromatography eluting with 1:3 hexane/CH₂Cl₂. This procedure resulted in 7 mg of **11.27** (0.012 mmol, 69%). ¹H NMR (500 MHz, CDCl₃): δ 8.15 (bs, 4H), 7.72 (bs, 4H), 4.49 (s, 4H), 3.97 (s, 6H), 3.48 (s, 6H). UV/Vis/NIR (CH₂Cl₂): 786 nm (1.0 au), 575 nm (0.4 au), 349 nm (0.9 au), 311 nm (1.7 au), 228 nm (1.8 au).

Ethyl 2-(4-iodophenoxy)acetate (11.35). Iodophenol (**11.34**, 5.0 g, 23 mmol, 1.0 equiv.) was dissolved in acetone (500 mL) and K₂CO₃ (15.7 g, 114 mmol, 5.0 equiv.) was added followed by ethylbromoacetate (4.0 mL, 36 mmol, 1.6 equiv.). The mixture was stirred at rt overnight at which point excess K₂CO₃ was removed by filtration and the filtrate was evaporated to dryness. The crude product was purified by silica gel chromatography with 10:1 hexane/ethyl acetate. This procedure resulted in pure **11.35** in quantitative yield (6.98 g, 22.8 mmol). ¹H NMR (600 MHz, CDCl₃): δ 7.54 (apparent d, *J* = 8.9 Hz, 2H), 6.66 (apparent d, *J* = 8.6 Hz, 2H), 4.56 (s, 2H), 4.23 (q, *J* = 7.1 Hz, 2H), 1.26 (t, *J* = 7.1 Hz, 3H). ¹³C NMR (150 MHz, CDCl₃): δ 168.5, 157.8, 138.4, 117.1, 84.1, 65.4, 61.5, 14.3. HRMS (EI): calcd. for C₁₀H₁₁O₃I⁺ [M]⁺, 305.9753; found, 305.9759.

Ethyl 2-(4-(3,3,3-trifluoroprop-1-ynyl)phenoxy)acetate (11.37). Lithium diisopropylamide was generated by combining diisopropylamine (0.265 mL, 1.9 mmol, 3.3 equiv.) and *n*-butyllithium (1.74 mL of 1.6M solution in hexane, 2.8 mmol, 4.9 equiv.) in THF (2.0 mL, anhydrous) at -78 °C. Upon stirring for 30 min, 2-bromo-3,3,3-trifluoroprop-1-ene (100 μL, 0.97 mmol, 1.7 equiv.) was added dropwise followed by a zinc chloride tetramethylethylenediamine complex (ZnCl₂ TMEDA, 0.24 g, 0.95 mmol, 1.7 equiv.). The mixture was stirred for 30 min at -78 °C and 30 min at rt, at which point aryl iodide **11.35** (175 mg, 0.57 mmol, 1.0 equiv.) and tetrakis(triphenylphosphine) palladium

(40 mg, 0.034 mmol, 6 mol%) were added. The reaction was heated to reflux overnight. The following morning the mixture was quenched with methanol, evaporated onto silica gel and the crude product was purified by silica gel chromatography using a hexane/ethyl acetate solvent system (25:1, 20:1, 15:1). This procedure resulted in pure **11.37** (32 mg, 0.12 mmol, 21%). $R_f = 0.4$ in 4:1 hexane/ethyl acetate. $^1\text{H NMR}$ (600 MHz, CDCl_3): δ 7.49 (d, $J = 8.7$ Hz, 2H), 6.90 (d, $J = 8.7$ Hz, 2H), 4.65 (s, 2H), 4.27 (q, $J = 7.1$ Hz, 2H), 1.29 (t, $J = 7.1$ Hz, 3H). $^{13}\text{C NMR}$ (150 MHz, CDCl_3): δ 168.4, 159.9, 134.4, 115.17 (q, $J = 260.8$ Hz), 115.15, 111.7, 86.8 (q, $J = 6.5$ Hz), 75.23 (q, $J = 52.5$ Hz), 65.4, 61.8, 14.3. $^{19}\text{F NMR}$ (565 MHz, CDCl_3): δ -50.48 (s, 3F). HRMS (EI): calcd. for $\text{C}_{13}\text{H}_{11}\text{O}_3\text{F}_3^+ [\text{M}]^+$, 272.0660; found, 272.0664.

Ethyl 2-(4-(2-oxo-5-(trifluoromethyl)-1,3-dithiol-4-yl)phenoxy)acetate (11.38). Alkyne **11.37** (32 mg, 0.12 mmol, 1.0 equiv.) was dissolved in benzene (1.2 mL). To this solution diisopropyl xanthate **11.17** (36 mg, 0.13 mmol, 1.1 equiv.) and azobisisobutyronitrile (12 mg, 0.073 mmol, 1.8 equiv.) were added and the solution was heated to 80 °C for 5 d. After 5 d, the mixture was evaporated to dryness and purified by silica gel chromatography using a hexane/ethyl acetate solvent system (product elutes at 20:1 to 15:1 hexanes/ethyl acetate). This procedure resulted in 15 mg of **11.38** (0.041 mmol, 34%). $^1\text{H NMR}$ (600 MHz, CDCl_3): δ 7.35 (d, $J = 8.6$ Hz, 2H), 6.95 (d, $J = 8.6$ Hz, 2H), 4.66 (s, 2H), 4.29 (q, $J = 7.1$ Hz, 2H), 1.30 (t, $J = 7.1$ Hz, 3H). $^{13}\text{C NMR}$ (150 MHz, CDCl_3): δ 187.1, 168.5, 159.6, 139.7, 130.7, 122.6, 120.1 (q, $J = 273.6$ Hz), 116.8 (q, $J = 35.9$ Hz), 115.2, 65.5, 61.9, 14.4. $^{19}\text{F NMR}$ (565 MHz, CDCl_3): δ -52.99 (s, 3F). HRMS (EI): calcd. for $\text{C}_{14}\text{H}_{11}\text{O}_4\text{F}_3\text{S}_2^+ [\text{M}]^+$, 364.0051; found, 364.0051.

Ni bis(dithiolene) 11.28. Ligand **11.38** (13 mg, 0.036 mmol, 1.0 equiv.) was dissolved in THF (0.36 mL) and tetramethylammonium chloride (14 mg, 0.077 mmol, 2.1 equiv.) in methanol (35 μL) was added. The mixture was stirred for 5 min, at which point $\text{NiCl}_2 \cdot 6\text{H}_2\text{O}$ (4.3 mg, 0.018 mmol, 0.5 equiv.) was added in methanol (35 μL). This mixture was stirred for 6 h, at which point iodine (4 mg, 0.031 mmol, 0.9 equiv.) was added. This solution was stirred overnight and the following morning it was evaporated to dryness and purified by silica gel chromatography using a hexane/ CH_2Cl_2 solvent system. This procedure yielded 0.8 mg of **11.28** (0.001 mmol, 6%). UV/Vis/NIR (CH_2Cl_2): 779 nm (1.2 au), 543 nm (0.3 au), 292 nm (3.0 au), 231 nm (3.0 au). HRMS (EI): calcd. for $\text{C}_{26}\text{H}_{22}\text{F}_6\text{O}_6\text{S}_4\text{Ni}^+ [\text{M}]^+$, 729.9557; found, 729.8195.

Ethyl 2-(4-(3-methoxyprop-1-ynyl)phenoxy)acetate (11.36). Aryl iodide **11.35** (500 mg, 1.6 mmol, 1.0 equiv.) and methyl propargyl ether (0.2 mL, 2.4 mmol, 1.5 equiv.) were dissolved in THF (15 mL, anhydrous). To this solution, bis(triphenylphosphine) palladium chloride (120 mg, 0.17 mmol, 11 mol%), copper iodide (100 mg, 0.52 mmol, 33 mol%), and triethylamine (0.8 mL, 5.6 mmol, 3.5 equiv.) were added. The mixture turned dark brown upon addition of triethylamine. After 1 h, the reaction was quenched with aqueous ammonium chloride and extracted with ethyl acetate (3 x 100 mL). The organics were combined, dried, decanted and evaporated to dryness. The crude product was purified by

silica gel chromatography with a hexane/ethyl acetate solvent system. This procedure resulted in pure **11.36** (375 mg, 1.5 mmol, 94%). ¹H NMR (500 MHz, CDCl₃): δ 7.36 (apparent d, *J* = 8.5 Hz, 2H), 6.81 (apparent d, *J* = 9.0 Hz, 2H), 4.58 (s, 2H), 4.26 (s, 2H), 4.22 (q, *J* = 7.1 Hz, 2H), 3.40 (s, 3H), 1.25 (t, *J* = 7.1 Hz, 3H). ¹³C NMR (125 MHz, CDCl₃): δ 168.6, 158.0, 133.3, 115.9, 114.7, 86.0, 84.0, 65.3, 61.5, 60.5, 57.7, 14.2.

Ethyl 2-(4-(5-(methoxymethyl)-2-oxo-1,3-dithiol-4-yl)phenoxy)acetate (11.39). Alkyne **11.36** (375 mg, 1.5 mmol, 1.0 equiv.) was dissolved in benzene (15 mL) and isopropyl xanthogen disulfide **11.17** (450 mg, 1.7 mmol, 1.1 equiv.) was added followed by azobisisobutyronitrile (150 mg, 0.91 mmol, 0.61 equiv.). This mixture was heated to 80 °C for 10 d, at which point it was evaporated to dryness and purified by silica gel chromatography. This procedure resulted in pure **11.39** (106 mg, 0.31 mmol, 21%) plus recovered **11.36** (245 mg, 0.99 mmol, 66%). ¹H NMR (500 MHz, CDCl₃): δ 7.30-7.27 (m, 2H), 6.99-6.92 (m, 2H), 4.65 (s, 2H), 4.30-4.26 (m, 4H), 3.34 (s, 3H), 1.30 (t, *J* = 7.1 Hz, 3H). ¹³C NMR (125 MHz, CDCl₃): δ 191.4, 168.6, 158.7, 131.7, 130.8, 127.2, 124.4, 115.2, 67.7, 65.5, 61.7, 58.5, 14.3. HRMS (ESI): calcd. for C₁₅H₁₇O₅S₂⁺ [M+H]⁺, 341.0512; found, 341.0508.

Ni bis(dithiolene) 11.29. Ligand **11.36** (34 mg, 0.10 mmol, 1.0 equiv.) was dissolved in THF (1.0 mL) and tetramethylammonium chloride (39 mg, 0.22 mmol, 2.2 equiv.) in methanol (100 μL) was added. The mixture was stirred for 5 min, at which point NiCl₂·6H₂O (12 mg, 0.05 mmol, 0.5 equiv.) was added in methanol (100 μL). This mixture was stirred for 6 h, at which point iodine (12 mg, 0.05 mmol, 1.0 equiv.) was added. This solution was stirred overnight. The following morning the color of the solution was still very brown (not blue indicating the desired product) and more iodine was added (~5 mg). After an additional hour, there was no change in the color of the reaction mixture. The reaction mixture was evaporated to dryness and purified by silica gel chromatography using a hexane/CH₂Cl₂/MeOH solvent system (product elutes at 40:1 CH₂Cl₂/MeOH) to yield a small amount of product (0.6 mg, 0.002 mmol, 2%). R_f = 0.8 in 9:1 CH₂Cl₂/MeOH. UV/Vis/NIR (CH₂Cl₂): 834 nm (0.8 au), 322 nm (2.7 au), 254 nm (2.8 au), 231 nm (3.1 au).

Methyl 4-(phenylethynyl)benzoate (11.40). Phenyl acetylene (1.5 mL, 14 mmol, 1.3 equiv.) and methyl-4-iodobenzoate (3.0 g, 11 mmol, 1.0 equiv., **11.21**) were dissolved in THF (90 mL, anhydrous). To this solution, CuI (300 mg, 1.5 mmol, 0.14 equiv.), PdCl₂(PPh₃)₂ (450 mg, 0.64 mmol, 0.06 equiv.), and triethylamine (6.0 mL, 43 mmol, 3.9 equiv.) were added. Upon triethylamine addition, the reaction mixture turned dark black. The mixture was stirred at rt until the solution was no longer dark (~ 2 h), at which point the reaction was quenched with methanol (25 mL), evaporated to dryness, and purified by silica gel chromatography with hexane/ethyl acetate (200:1, 100:1, 50:1, 25:1, 10:1, 8:1, 6:1). This procedure yielded pure **11.40** in 99% yield (2.7 g, 11 mmol). R_f = 0.5 in 8:1 hexanes/ethyl acetate. ¹H NMR (400 MHz, CDCl₃): δ 8.02 (d, *J* = 8.1 Hz, 2H), 7.59 (d, *J* = 8.4 Hz, 2H), 7.56-7.54 (m, 2H), 7.38-7.36 (m, 3H), 3.93 (s, 3H). ¹³C NMR (100 MHz,

CDCl₃): δ 166.8, 131.9, 131.7, 129.7, 129.7, 129.0, 128.6, 128.2, 122.9, 92.6, 88.8, 52.4. HRMS (EI): calcd. for C₁₆H₁₂O₂⁺ [M]⁺, 236.0837; found, 236.0841.

Methyl 4-(2-oxo-5-phenyl-1,3-dithiol-4-yl)benzoate (11.41). Methyl 4-(phenylethynyl)benzoate **11.40** (250 mg, 1.1 mmol, 1.0 equiv.) was combined with diisopropyl xanthogen disulfide **11.17** (290 mg, 1.1 mmol, 1.0 equiv.) and 1,1'-azobis(cyclohexanecarbonitrile) (110 mg, 0.48 mmol, 0.45 equiv.) in *m*-xylene (2.2 mL, anhydrous). The mixture was heated to reflux for 20 h, at which point the reaction mixture was evaporated to dryness and **11.41** was purified by silica gel chromatography eluting with hexanes/ethyl acetate (40:1). This procedure resulted in 130 mg of **11.41** (0.40 mmol, 37%). R_f = 0.5 in 6:1 hexanes/ethyl acetate. ¹H NMR (600 MHz, CDCl₃): δ 7.91 (d, *J* = 7.1 Hz, 2H), 7.31-7.30 (m, 1H), 7.29-7.26 (m, 4H), 7.20-7.19 (m, 2H), 3.90 (s, 3H). ¹³C NMR (150 MHz, CDCl₃): δ 190.2, 166.5, 136.5, 131.6, 131.0, 130.4, 130.2, 129.8, 129.7, 129.4, 129.2, 127.6, 52.5. HRMS (EI): calcd. for C₁₇H₁₂O₃S₂⁺ [M]⁺, 328.0228; found, 328.0222.

4-(2-oxo-5-(4-sulfophenyl)-1,3-dithiol-4-yl)benzoic acid (11.42). Compound **11.41** (700 mg, 2.1 mmol, 1.0 equiv.) was dissolved in sulfuric acid (8 mL, 18 M) and fuming sulfuric acid (80 μL, 20% in H₂SO₄) was added. This mixture was heated to 90 °C overnight. The following day it was cooled to rt, neutralized with NaOH and NaHCO₃ and evaporated. The resulting solid was subjected to methanol (~100 mL) and sonicated. This solution was then filtered and the filtrate was evaporated to dryness. The remaining solid was purified by silica gel chromatography with an acetonitrile/methanol solvent system (15:1, 10:1) to result in 620 mg of pure **11.42** (1.6 mmol, 74%). R_f = 0.5 in 9:1 acetonitrile/water. ¹H NMR (600 MHz, MeOD): δ 7.93 (d, *J* = 8.4 Hz, 2H), 7.76 (d, *J* = 8.4 Hz, 2H), 7.35 (dd, *J* = 13.9, 8.4 Hz, 4H). ¹³C NMR (150 MHz, MeOD): δ 190.9, 169.2, 147.1, 137.1, 134.6, 132.9, 131.3, 130.9, 130.85, 130.4, 130.0, 127.8. HRMS (ESI): calcd. for C₁₆H₉O₆S₃⁻ [M-H]⁻, 392.9567; found 392.9565.

4-(5-(4-(isopropylcarbamoyl)phenyl)-2-oxo-1,3-dithiol-4-yl)benzenesulfonic acid (11.43). Compound **11.42** (130 mg, 0.33 mmol, 1.0 equiv.) was dissolved in dimethylformamide (5 mL, anhydrous). To this solution, isopropyl amine (30 μL, 0.037 mol, 1.1 equiv.), 1-ethyl-3-(3-dimethylaminopropyl)carbodiimide hydrochloride (EDC·HCl, 96 mg, 0.50 mmol, 1.5 equiv.), hydroxybenzotriazole hydrate (HOBt, 65 mg, 0.42 mmol, 1.3 equiv.), and triethylamine (90 μL, 0.65 mmol, 1.9 equiv.) were added. The mixture was stirred at rt for 5 h, at which point it was evaporated to dryness. Compound **11.43** was purified by HPLC using a water/methanol solvent system with a gradient of 30-95% methanol over 25 min. The desired product elutes at 14 min. This procedure resulted in pure **11.43** (56 mg, 0.13 mmol, 39 %). ¹H NMR (600 MHz, MeOD): δ 7.75-7.72 (m, 4H), 7.34-7.31 (m, 4H), 4.17 (sep, *J* = 6.6 Hz, 1H), 1.22 (d, *J* = 6.6 Hz, 6H). ¹³C NMR (150 MHz, MeOD): δ 191.0, 168.5, 147.3, 136.8, 135.8, 134.7, 131.0, 130.9, 130.3, 130.1, 129.1, 127.8, 43.4, 22.6. HRMS (ESI): calcd. for C₁₉H₁₆O₅N₁S₃⁻ [M-H]⁻ 434.0196; found, 434.0193.

Ni bis(dithiolene) 11.44. 4-(5-(4-(isopropylcarbamoyl)phenyl)-2-oxo-1,3-dithiol-4-yl)benzenesulfonic acid **11.43** (45 mg, 0.10 mmol, 1.0 equiv.) was dissolved in a mixture of THF/MeOH (1 mL/0.7 mL). Tetramethyl ammonium hydroxide pentahydrate (40 mg, 0.22 mmol, 2.2 equiv.) was dissolved in MeOH (0.2 mL) and added to the solution with compound **11.43**. The mixture turned a light orange color. After 30 min, NiCl₂·6H₂O (12 mg, 0.050 mmol, 0.50 equiv.) was added and the mixture turned dark red. This mixture was stirred at rt overnight. The following morning, iodine (12 mg, 0.047 mmol, 0.051 equiv.) was added and the mixture became dark blue. After 2 h stirring at rt, the mixture was evaporated to dryness and purified by silica gel chromatography eluting with acetonitrile/water (25:1, 10:1, 5:1). This procedure resulted in 40 mg of **11.44** as a blue solid (0.046 mmol, 90%). R_f = 0.2 in 9:1 acetonitrile/water. ¹H NMR (600 MHz, MeOD): δ 7.88 (d, *J* = 6.4 Hz, 4H), 7.68 (d, *J* = 7.8 Hz, 4H), 7.54 (d, *J* = 7.1 Hz, 4H), 7.22 (s, 4H), 4.32- 4.11 (m, 3H), 1.30 (d, *J* = 6.5 Hz, 12H). The NMR was taken in the presence of I₂ to keep all of **11.44** in the neutral oxidation state. The anionic form is paramagnetic which prevents a spectrum from being obtained. Due to this difficulty we have characterized the sulfonated Ni bis(dithiolene) complexes by UV/Vis/NIR, HRMS, and HPLC instead of NMR. UV/Vis/NIR (water): 851 nm (1.2 au), 638 nm (0.4 au), 312 nm (3.1 au), 282 nm (3.3 au), 209 nm (5.1 au), 206 nm (4.7 au). HRMS (ESI): calcd. for C₃₆H₃₂O₈N₂NiS₆⁻² [M - 2H]⁻², 434.9924; found, 434.9918.

Kinetics

All kinetics experiments were performed under pseudo-first order conditions using absorbance measurements, which were acquired on a Molecular Devices SpectraMax M3 plate reader (for DMSO, EtOH, or aqueous solutions) or a CARY 100 Bio UV-Visible Spectrophotometer (for CH₂Cl₂). Absorbance values were correlated to the concentration of the Ni bis(dithiolene) reagents through a standard curve containing six points. Six pseudo-first order rate constants were measured for the reaction between Ni bis(dithiolene) and quadricyclane using a 5- to 1000-fold excess of quadricyclane. The reactions were monitored for changes in the absorbance of the NIR band for 10-30 min recording a measurement every 30-60 sec. Pseudo-first order rate constants were calculated by plotting Ln[Ni bis(dithiolene)] vs. time (sec). The slope of the line indicated the pseudo-first order rate constant (*k*_{obs}). The second-order rate constant was determined by plotting *k*_{obs} vs. [quadricyclane]. The slope of the line represented the second-order rate constant.

Kinetics experiments for Ni bis(dithiolene) compound **10.42**, **11.11**, and **11.12** were performed with 100 μM Ni bis(dithiolene) and 0, 1, 5, 10, 50, or 100 mM quadricyclane **10.4** in a total volume of 100 μL DMSO. Kinetics experiments for compound **11.25** were performed with 50 μM **11.25** and 0, 0.25, 0.5, 0.75, 1, or 1.25 mM quadricyclane **10.4** in a total volume of 0.5 mL. Kinetics experiments for sulfonated Ni bis(dithiolene) **11.44** were performed with 200 μM **11.44** and 0, 2, 4, 6, 8, or 10 mM quadricyclane **10.4** in a total volume of 100 μL (50 μL ethanol, 50 μL buffer). To determine the rate constant for the reaction of **11.44** and norbornadiene, 200 μM **11.44** and 0, 20, 40, 60, 80, or 100 mM norbornadiene **10.3** were used in a total volume of 100 μL.

Stability Analysis of **11.44**

All UV/Vis/NIR spectra were obtained on a CARY 100 Bio UV-Visible Spectrophotometer with a range of 200-900 nm. The concentration of **11.44** was between 100 and 400 μM for all experiments with a total volume of 0.3 to 1.5 mL of solution. For Figures 11.17-11.19, all proteins were purchased from Sigma or New England Biolabs. For figure 11.20, Jurkat (human T cell lymphoma) cells were maintained in a 5% CO_2 , water-saturated atmosphere and grown in RPMI 1640 media supplemented with 10% FBS, penicillin (100 units/ml), and streptomycin (0.1 mg/ml). Cell densities within the cuvette were $\sim 10^6$ cells per mL.

References

- (1) Kajitani, M.; Kohara, M.; Kitayama, T.; Akiyama, T.; Sugimori, A. Formation of 1:1 adducts between bis(1,2-diaryl-1,2-ethylenedithiolato)metal(0) (metal = Ni, Pd, and Pt) and quadricyclane and their photodissociation. *J. Phys. Org. Chem.* **1989**, *2*, 131-145.
- (2) Watanabe, E.; Fujiwara, M.; Yamaura, J.-I.; Kato, R. Synthesis and properties of novel donor-type metal–dithiolene complexes based on 5,6-dihydro-1,4-dioxine-2,3-dithiol (edo) ligand. *J. Mater. Chem.* **2001**, *11*, 2131-2141.
- (3) Kajitani, M.; Kohara, M.; Kitayama, T.; Asano, Y.; Sugimori, A. Photosensitive 1:1 adduct between bis(1,2-diphenyl-1,2-ethylenedithiolato)nickel(0) and quadricyclane. *Chem. Lett.* **1986**, 2109-2112.
- (4) Agard, N. J.; Baskin, J. M.; Prescher, J. A.; Lo, A.; Bertozzi, C. R. A comparative study of bioorthogonal reactions with azides. *ACS Chem. Biol.* **2006**, *1*, 644-648.
- (5) Baskin, J. M.; Prescher, J. A.; Laughlin, S. T.; Agard, N. J.; Chang, P. V.; Miller, I. A.; Lo, A.; Codelli, J. A.; Bertozzi, C. R. Copper-free click chemistry for dynamic in vivo imaging. *Proc. Natl. Acad. Sci. U.S.A.* **2007**, *104*, 16793 -16797.
- (6) Cui, Y.-H.; Tian, W. Q.; Feng, J.-K.; Li, W.-Q.; Liu, Z.-Z. Aromaticity of Ni bis-dithiolenes complexes. *J. Mol. Struct. THEOCHEM.* **2009**, *897*, 61-65.
- (7) Miller, T. R.; Dance, I. G. Reactions of dithiolene complexes with amines. II. Formation and properties of mixed-ligand dithiolene alpha-diimine complexes of nickel. *J. Am. Chem. Soc.* **1973**, *95*, 6970-6979.
- (8) Dwivedi, P. P.; Athar, M.; Hasan, S. K.; Srivastava, R. C. Removal of nickel by chelating drugs from the organs of nickel poisoned rats. *Chemosphere* **1986**, *15*, 813-821.
- (9) Schrauzer, G. N.; Ho, R. K. Y.; Murillo, R. P. Structure, alkylation, and macrocyclic derivatives of bicyclo[2.2.1]hepta-2,5-diene adducts of metal dithiolenes. *J. Am. Chem. Soc.* **1970**, *92*, 3508-3509.
- (10) Schrauzer, G. N.; Mayweg, V. P. Preparation, reactions, and structure of bisdithio- α -diketone complexes of nickel, palladium, and platinum. *J. Am. Chem. Soc.* **1965**, *87*, 1483-1489.

- (11) Dalgleish, S.; Robertson, N. Electropolymerisable dithiolene complexes. *Coordin. Chem. Rev.* **2010**, *254*, 1549-1558.
- (12) Gareau, Y.; Beauchemin, A. Free radical reaction of diisopropyl xanthogen disulfide with unsaturated systems. *Heterocycles* **1998**, *48*, 2003-2017.
- (13) Geiger, W. E.; Barrière, F.; LeSuer, R. J.; Trupia, S. On the electrochemical preparation of the neutral complexes $M[S_4C_4(CN)_4]$, $M(mnt)_2$, $M = Ni, Pd, Pt$. *Inorg. Chem.* **2001**, *40*, 2472-2473.
- (14) Nomura, M.; Okuyama, R.; Fujita-Takayama, C.; Kajitani, M. New synthetic methods for η^5 -cyclopentadienyl nickel(III) dithiolene complexes derived from nickelocene. *Organometallics* **2005**, *24*, 5110-5115.
- (15) Wing, R. M.; Tustin, G. C.; Okamura, W. H. Oxidative cycloaddition of metal dithiolenes to olefins. Synthesis and characterization of norbornadiene-bis-cis-(1,2-perfluoromethylethene-1,2-dithiolato)nickel. *J. Am. Chem. Soc.* **1970**, *92*, 1935-1939.
- (16) Wang, K.; Stiefel, E. I. Toward separation and purification of olefins using dithiolene complexes: An electrochemical approach. *Science* **2001**, *291*, 106-109.
- (17) Konno, T.; Chae, J.; Kanda, M.; Nagai, G.; Tamura, K.; Ishihara, T.; Yamanaka, H. Facile syntheses of various per- or polyfluoroalkylated internal acetylene derivatives. *Tetrahedron* **2003**, *59*, 7571-7580.
- (18) Jamir, L.; Yella, R.; Patel, B. K. Efficient one-pot preparation of bis alkyl xanthogen disulfides from alcohols. *J. Sulfur Chem.* **2009**, *30*, 128-134.
- (19) Dalgleish, S.; Robertson, N. A stable near IR switchable electrochromic polymer based on an indole-substituted nickel dithiolene. *Chem. Commun.* **2009**, *45*, 5826-5828.
- (20) Harrison, D. J.; Nguyen, N.; Lough, A. J.; Fekl, U. New insight into reactions of $Ni(S_2C_2(CF_3)_2)_2$ with simple alkenes: Alkene adduct versus dihydrodithiin product selectivity is controlled by $[Ni(S_2C_2(CF_3)_2)_2]^-$ anion. *J. Am. Chem. Soc.* **2006**, *128*, 11026-11027.
- (21) Davison, A.; Edelstein, N.; Holm, R. H.; Maki, A. H. The preparation and characterization of four-coordinate complexes related by electron-transfer reactions. *Inorg. Chem.* **1963**, *2*, 1227-1232.
- (22) Dance, I. G.; Miller, T. R. Ready displacement of dithiolene ligands from electron-poor dithiolene complexes by weak nucleophiles. *J. Chem. Soc., Chem. Commun.* **1976**, 112-113.
- (23) Jaffé, H. H. A reëxamination of the Hammett equation. *Chem. Rev.* **1953**, *53*, 191-261.
- (24) Ning, X.; Guo, J.; Wolfert, M. A.; Boons, G.-J. Visualizing metabolically labeled glycoconjugates of living cells by copper-free and fast Huisgen cycloadditions. *Angew. Chem. Int. Ed.* **2008**, *47*, 2253-2255.
- (25) Debets, M. F.; van Berkel, S. S.; Schoffelen, S.; Rutjes, F. P. J. T.; van Hest, J. C. M.; van Delft, F. L. Aza-dibenzocyclooctynes for fast and efficient enzyme PEGylation via copper-free (3+2) cycloaddition. *Chem. Commun.* **2010**, *46*, 97-99.

- (26) Nakazumi, H.; Hamada, E.; Ishiguro, T.; Shiozaki, H.; Kitao, T. The influence of dithiolato nickel complexes on the light fastness of a thin layer of a near-infra-red absorbing cyanine dye. *J. Soc. Dyers Colour.* **1989**, *105*, 26-29.
- (27) Nomura, M.; Takayama, C.; Kajitani, M. Electrochemical behavior of S,S'-bridged adducts of square planar metalladithiolene complexes $[M(S_2C_2Ph_2)_2]$ (M=Ni, Pd, and Pt). *Inorg. Chim. Acta* **2004**, *357*, 2294-2300.
- (28) Clark, M. L. Albumin structure, function and uses. *Gut* **1978**, *19*, 159-159.
- (29) Collet, J.-F.; Messens, J. Structure, function, and mechanism of thioredoxin proteins. *Antioxid. Redox Signal.* **2010**, *13*, 1205-1216.
- (30) Angelucci, F.; Baiocco, P.; Brunori, M.; Gourlay, L.; Morea, V.; Bellelli, A. Insights into the catalytic mechanism of glutathione S-transferase: The lesson from *Schistosoma haematobium*. *Structure* **2005**, *13*, 1241-1246.
- (31) Pangborn, A. B.; Giardello, M. A.; Grubbs, R. H.; Rosen, R. K.; Timmers, F. J. Safe and convenient procedure for solvent purification. *Organometallics* **1996**, *15*, 1518-1520.

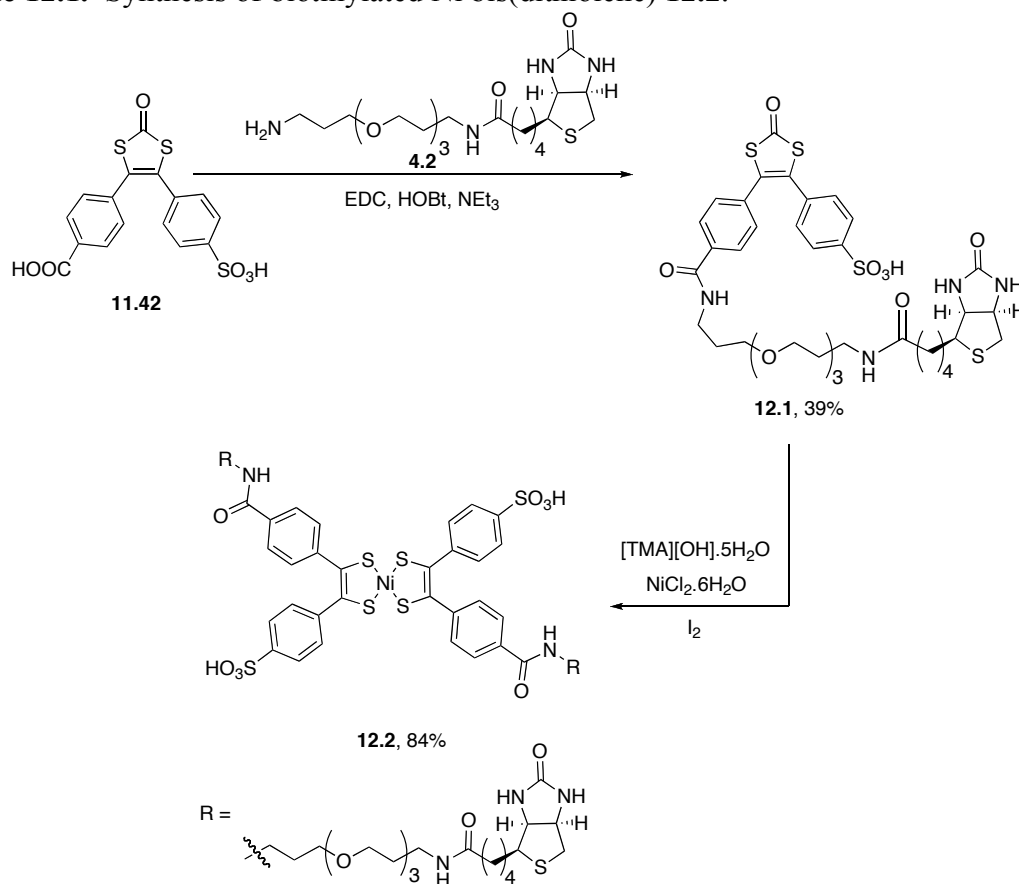
Chapter 12

A Bioorthogonal Quadricyclane Ligation

Selective Protein Modification with the Quadricyclane Ligation

The extensive UV/Vis/NIR analysis performed to assess the stability and reactivity of the Ni bis(dithiolene) complexes and quadricyclane strongly indicated that this ligation reaction– the “quadricyclane ligation” –is bioorthogonal. However, the first true test of bioorthogonality is selective protein labeling. In order for the ligation product to be identified on proteins, biotin was appended to the dithiol-2-one ligand precursor by coupling biotin amine **4.2**¹ to the acid of **11.42**. Biotinylated compound **12.1** was then converted to the Ni bis(dithiolene) by treatment with tetramethyl ammonium hydroxide and NiCl₂ followed by oxidation with iodine. Gratifyingly, when only 0.5 equivalents of iodine were used, no oxidation of biotin’s thioether group was observed (Scheme 12.1).

Scheme 12.1. Synthesis of biotinylated Ni bis(dithiolene) **12.2**.



To initially test the bioorthogonality of the quadricyclane ligation, we modified lysine residues on the model protein bovine serum albumin (BSA) with quadricyclane *p*-nitrophenyl carbonate **10.6** (Figure 12.1). We then treated the quadricyclane-BSA (QC-BSA) with Ni bis(dithiolene) **12.2** under a variety of conditions to analyze the scope of the bioorthogonality of this reaction (Figure 12.2).

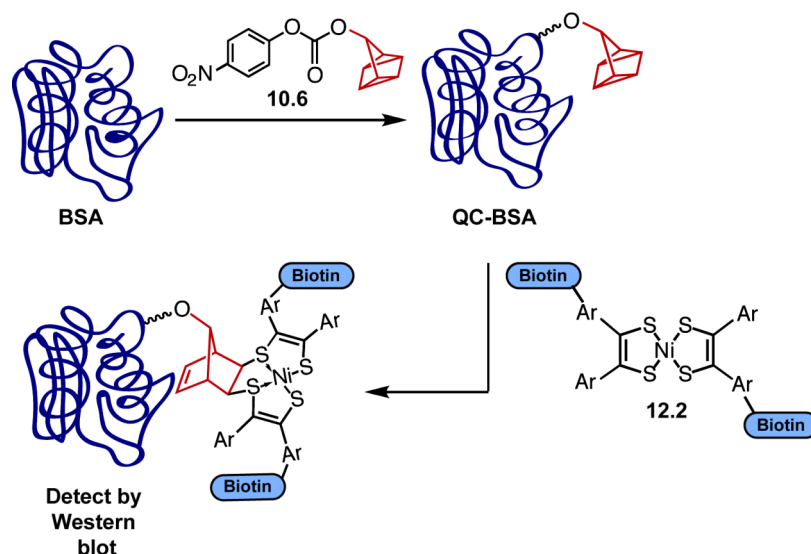


Figure 12.1. General schematic for protein labeling with Ni bis(dithiolene) **12.2**. Modification of the lysine residues of bovine serum albumin (BSA) proceeds by treatment with the activated carbonate of quadricyclane. The resulting protein is labeled with Ni bis(dithiolene) reagent **12.2** and the product is detected by Western blot.

First, we treated QC-BSA or native BSA with 50 μM **12.2** for various amounts of time and, after quenching with excess quadricyclane **10.4** and diethyldithiocarbamate (**11.5**), assayed the products by Western blot probing with an α -biotin antibody conjugated to horse-radish peroxidase (α -biotin-HRP). We were excited to find that **12.2** selectively labeled QC-BSA in a time-dependent manner with very little background labeling of unmodified BSA, even upon prolonged exposure of the Western blot (Figure 12.2A). Similarly, when the reaction time was held constant (30 min) and the concentration of **12.2** was varied, dose-dependent labeling was observed, again with minimal nonspecific reactivity (Figure 12.2B).

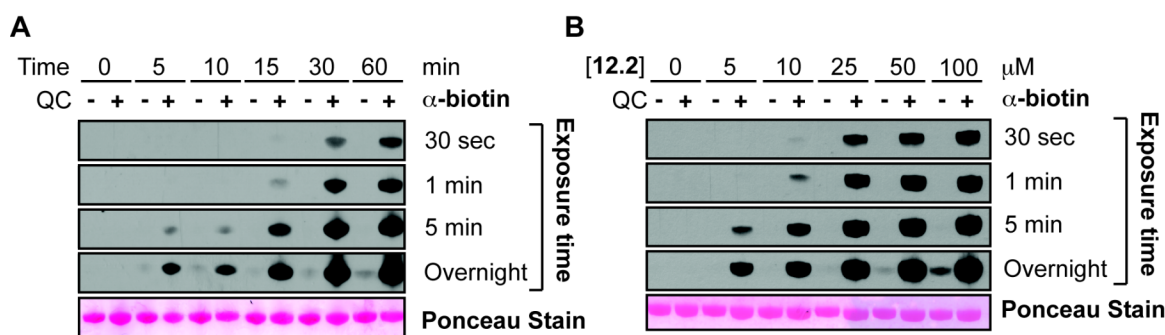
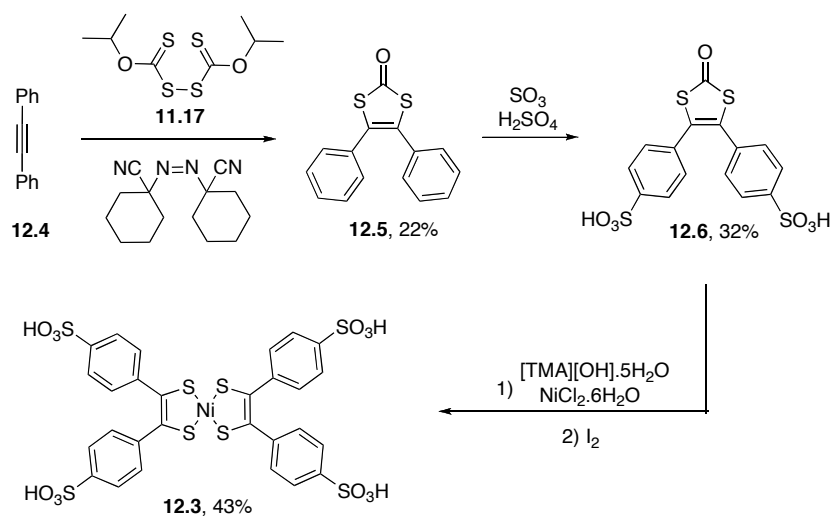


Figure 12.2. Ni bis(dithiolene) **12.2** selectively labels quadricyclane-modified BSA. BSA (-) or QC-BSA (+) (5 μ g) was treated with 50 μ M **12.2** for various amounts of time (A) or various concentrations of **12.2** for 30 min (B). The reactions were quenched with quadricyclane **10.4** and diethyldithiocarbamate (**11.5**), and the presence of product was detected by Western blot using α -biotin-HRP. Equal protein loading was confirmed by Ponceau stain.

We also performed a competition experiment where QC-BSA was pretreated with an unlabeled Ni bis(dithiolene), tetrasulfonated Ni bis(dithiolene) **12.3**, to analyze whether the signal obtained from reaction with **12.2** could be decreased. We synthesized **12.3** from diphenylacetylene **12.4**, which was combined with isopropyl xanthogen disulfide **11.17**² and 1,1'-azobis(cyclohexanecarbonitrile) to yield 4,5-diphenyl-1,3-dithiol-2-one (**12.5**). Heating **12.5** in the presence of fuming sulfuric acid overnight installed two sulfonate groups to give **12.6**, which could be converted to the Ni bis(dithiolene) using the standard conditions of tetramethyl ammonium hydroxide, NiCl₂, and oxidation with iodine (Scheme 12.2).³

Scheme 12.2. Synthesis of tetrasulfonated Ni bis(dithiolene) **12.3**.



QC-BSA or BSA (5 μg) was treated with various amounts of **12.3** (0 to 500 μM) for 30 min, at which point, 50 μM of biotinylated Ni bis(dithiolene) **12.2** was added. After an additional 30 min, the reaction was quenched with excess quadricyclane and diethyldithiocarbamate. The degree of labeling was probed by Western blot with α -biotin-HRP (Figure 12.3). As expected, pretreatment of QC-BSA with tetrasulfonated Ni bis(dithiolene) **12.3** quenched the protein-bound quadricyclane moiety, and resulted in decreased or abolished α -biotin signal.

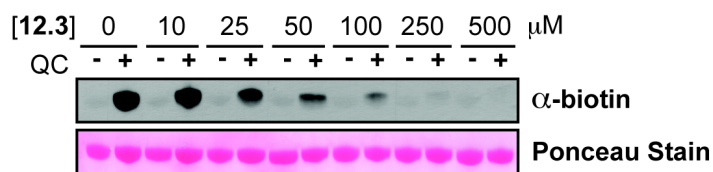


Figure 12.3. Reaction of **12.2** with QC-BSA can be prevented by pretreatment with tetrasulfonated Ni bis(dithiolene) **12.3**. BSA (-) or QC-BSA (+) (5 μg) was treated with varying amounts of **12.3** for 30 min followed by 50 μM of **12.2** for 30 min. The reactions were quenched with quadricyclane and diethyldithiocarbamate and the samples were analyzed by Western blot probing with α -biotin-HRP. Equal protein loading was confirmed by Ponceau stain.

To determine whether the quadricyclane ligation possessed the heightened selectivity required to label target biomolecules within more complex samples, we combined 1.5 μg of QC-BSA (or unmodified BSA) with 25 μg of *E. coli* lysate. This mixture was treated with 50 μM **12.2** for 30 min, quenched and analyzed by Western blot. Selective labeling of QC-BSA was observed but the signal was weak (Figure 12.4, lanes 7-8), particularly when compared to the signal from an endogenously biotinylated protein (marked with asterisk). We hypothesized that the diminished signal was due to reduction of **12.2** by a species present in the lysate. Gratifyingly, when we added the water-soluble oxidizing agent potassium ferricyanide ($\text{K}_3\text{Fe}(\text{CN})_6$, 1 mM) to the reaction mixture, robust and selective labeling of QC-BSA was observed (Figure 12.4, lanes 9-10). Notably, the signal from the lysate is still not as intense as that observed for BSA alone. This suggests that some of **12.2** is still in the anionic form, or underwent disproportionation, and cannot undergo reaction with QC-BSA.⁴

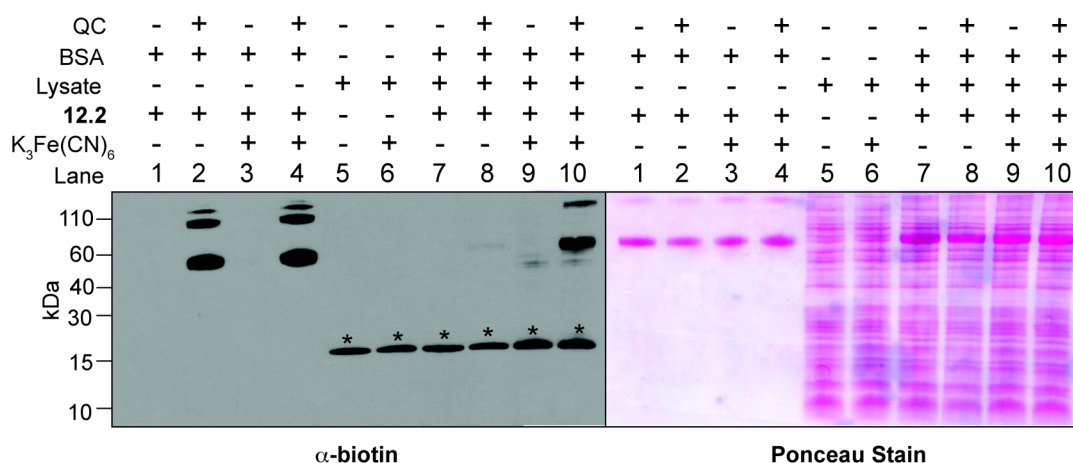


Figure 12.4. Oxidizing agent increases the efficiency of labeling of QC-BSA by **12.2** in a mixture of proteins. BSA (1.5 μ g, lanes 1,3) or QC-BSA (1.5 μ g, lanes 2,4) were combined with **12.2** (50 μ M) for 30 min in the presence (lanes 3-4) or absence (lanes 1-2) of 1 mM K₃Fe(CN)₆. Lysate from *E. coli* (25 μ g) was combined with (lane 6) or without (lane 5) 1 mM K₃Fe(CN)₆ for 30 min. Lysate (25 μ g) and BSA (1.5 μ g, lanes 7,9) or QC-BSA (1.5 μ g, lanes 8,10) were combined with **12.2** (50 μ M) for 30 min in the presence (lanes 9,10) or absence (lanes 7,8) of 1 mM K₃Fe(CN)₆. After 30 min, all reaction mixtures were quenched with excess 7-acetoxy quadricyclane (**10.4**) and diethyldithiocarbamate (**11.5**) and analyzed by Western blot probing with α -biotin-HRP. Protein loading was verified by Ponceau Stain. The bands denoted with an asterisk represent an endogenously biotinylated *E. coli* protein.

The Quadricyclane Ligation is Orthogonal to Existing Bioorthogonal Reactions

New additions to the bioorthogonal reaction compendium are most powerful when they can be used in conjunction with other bioorthogonal chemistries. We therefore aimed to determine whether the quadricyclane ligation can be performed simultaneously with two established bioorthogonal reactions, Cu-free click chemistry and oxime formation, which are already known to be mutually compatible.⁵ A mixture containing equal amounts of QC-BSA (MW \sim 66 kDa), azidohomoalanine-containing dihydrofolate reductase (Az-DHFR, MW \sim 23 kDa),⁶ and aldehyde-tagged maltose binding protein (CHO-MBP, MW \sim 42 kDa)⁷ was treated with nickel complex **12.2**, a dimethoxyazacyclooctyne conjugated to fluorescein (DIMAC-fluor),⁸ and an aminoxy-functionalized FLAG peptide (H₂NO-FLAG)⁷ (Figure 12.5A). After incubation for 3 h, the mixture was separated into 3 portions and each was analyzed by Western blot probing with one of the following antibodies: α -biotin-HRP, α -fluorescein-HRP, or α -FLAG-HRP (Figure 12.5B). In parallel, each protein was combined with its appropriate reaction partner (Figure 12.5C,E,G) and analyzed by Western blot (Figure 12.5D,F,H) to control for the banding

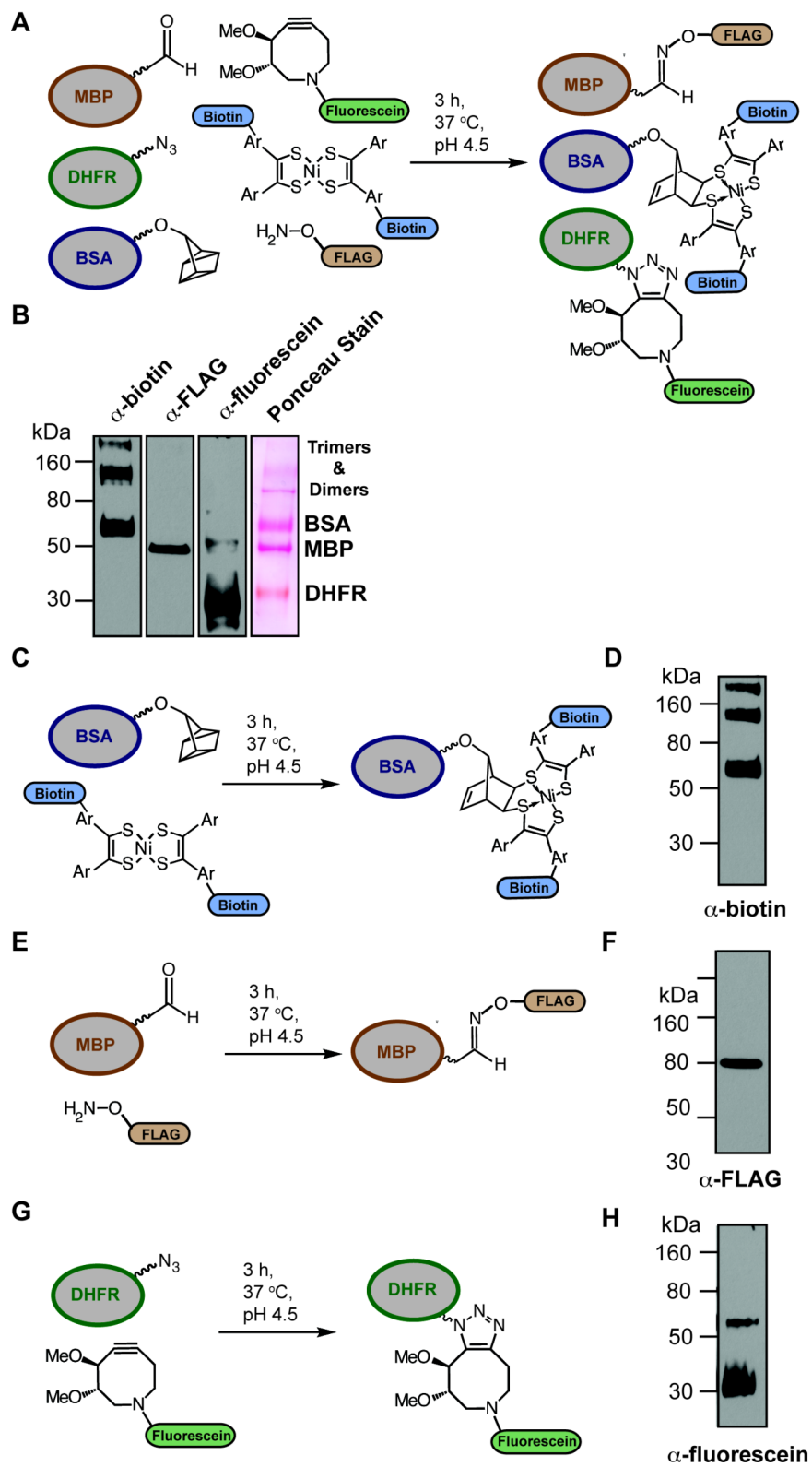


Figure 12.5. The quadricyclane ligation is orthogonal to Cu-free click chemistry and the oxime ligation. A. A mixture of 8 μg of QC-BSA, Az-DHFR, and CHO-MBP was treated with **12.2** (150 μM), DIMAC-fluor (250 μM), and $\text{H}_2\text{NO-FLAG}$ (1 mM) for 3 h at 37 $^\circ\text{C}$, pH 4.5. B. This mixture was basified with 850 mM tris buffer and quenched with excess 7-acetoxy quadricyclane, diethyldithiocarbamate, and 2-azidoethanol. It was then separated into 3 portions and each portion was analyzed by Western blot probing with a different antibody: α -biotin-HRP (quadricyclane ligation), α -fluorescein-HRP (Cu-free click chemistry) or α -FLAG-HRP (oxime ligation). The Ponceau stain indicates all three proteins were present. Oligomer bands are observed for BSA and DHFR. C-H. Controls for the banding patterns observed in part B. C. QC-BSA (8 μg) and **12.2** (150 μM) were combined at 37 $^\circ\text{C}$, pH 4.5. D. After 3 h, this mixture was basified and quenched (as in part B) and analyzed by Western blot probing with an α -biotin-HRP. E. CHO-MBP (8 μg) and $\text{H}_2\text{NO-FLAG}$ (1 mM) were combined at 37 $^\circ\text{C}$, pH 4.5. F. After 3 h, this mixture was basified, quenched, and analyzed by Western blot probing with an α -FLAG-HRP antibody. G. Az-DHFR (8 μg) and DIMAC-fluor (250 μM) were combined at 37 $^\circ\text{C}$, pH 4.5. H. After 3 h, this mixture was basified, quenched, and analyzed by Western blot probing with an α -fluorescein-HRP antibody.

patterns observed in the multiplexed labeling experiment. As evident from Figure 12.5B, each chemical probe, including **12.2**, reacted only with its complementary bioorthogonal functional group. Like the cyclooctyne and aminoxy probes, compound **12.2** showed no significant labeling of proteins lacking its partner (quadricyclane), nor did it interfere with the other bioorthogonal reactions. Notably, the conditions of this multiplexed reaction (i.e., pH (4.5), temperature (37 $^\circ\text{C}$) and time (3 h)) were tuned to accommodate the oxime ligation, the most sluggish of the three transformations.⁹ The quadricyclane ligation was quite tolerant of these conditions.

Live Cell Labeling with the Quadricyclane Ligation

The protein labeling data indicates that the quadricyclane ligation is a promising bioorthogonal reaction, which can proceed alongside other popular bioorthogonal chemistries. The two reaction partners reliably form their covalent adduct in environs as complex as cell lysate. The next challenge for the quadricyclane ligation is application to live cell labeling. Before proceeding to live cell labeling, we needed to ensure that the Ni bis(dithiolene) complexes are non-toxic.

We performed toxicity studies on Jurkat cells (human T-cell lymphoma cells) using 7-Aminoactinomycin D (7-AAD) and Annexin V to stain for dead (compromised membranes) and apoptotic (early apoptosis epitopes) cells, respectively.^{10,11} The degree of labeling with 7-AAD and Annexin V was quantified by flow cytometry. The viability of cells treated with Ni bis(dithiolene) **12.3** and the QC-**12.3** adduct were assayed alongside NiCl_2 and Cu(I) at concentrations ranging from 0-500 μM for a 1 h reaction; these conditions emulate those anticipated for live cell labeling experiments. No significant loss

of viability was observed for any of the nickel containing compounds; however, Cu(I) displayed a dramatic loss of viability between 100 and 250 μM (Figure 12.6). These results indicate that Ni bis(dithiolene) reagents should be suitable for live cell labeling experiments.

With these encouraging results, we aimed to perform a live cell labeling experiment where cell-surface lysine residues were modified with quadricyclane using activated carbonate **10.6** (Figure 12.8A). Treatment of these cells with **12.2** followed by FITC-avidin and detection by flow cytometry gave insight regarding the quadricyclane ligation's ability to label live cells. Unfortunately, no quadricyclane dependent labeling was observed (Figure 12.8B). Further investigation of these results showed that there was a significant amount of cell death, even when cells were not treated with Ni bis(dithiolene) (Figure 12.8C). We hypothesize that this toxicity was derived from altering the polarity of the cells' surfaces due to capping charged lysine residues with the considerably hydrophobic quadricyclane moiety.

Thus, we attempted an alternate strategy for attaching quadricyclane onto the cell-surface. From the orthogonal labeling Western blot experiment (Figure 12.5), we know that the quadricyclane ligation is orthogonal to Cu-free click chemistry and envisioned that Cu-free click chemistry on cells treated with azidosugar could lead to quadricyclane-modified cells. Toward this end, we synthesized a dimethoxyazacyclooctyne-quadricyclane conjugate (DIMAC-QC, **12.9**, Scheme 12.3). DIMAC **3.35**⁸ was coupled to Boc-protected amine **12.7** using HATU as a coupling agent. The Boc protecting group was removed by quick treatment with TFA, as previously our group and others have found cyclooctynes to be unstable to TFA.^{12,13} Gratifyingly, we found the free amine could be obtained in quantitative yield and coupled to activated quadricyclane **10.6** to yield DIMAC-QC **12.9**.

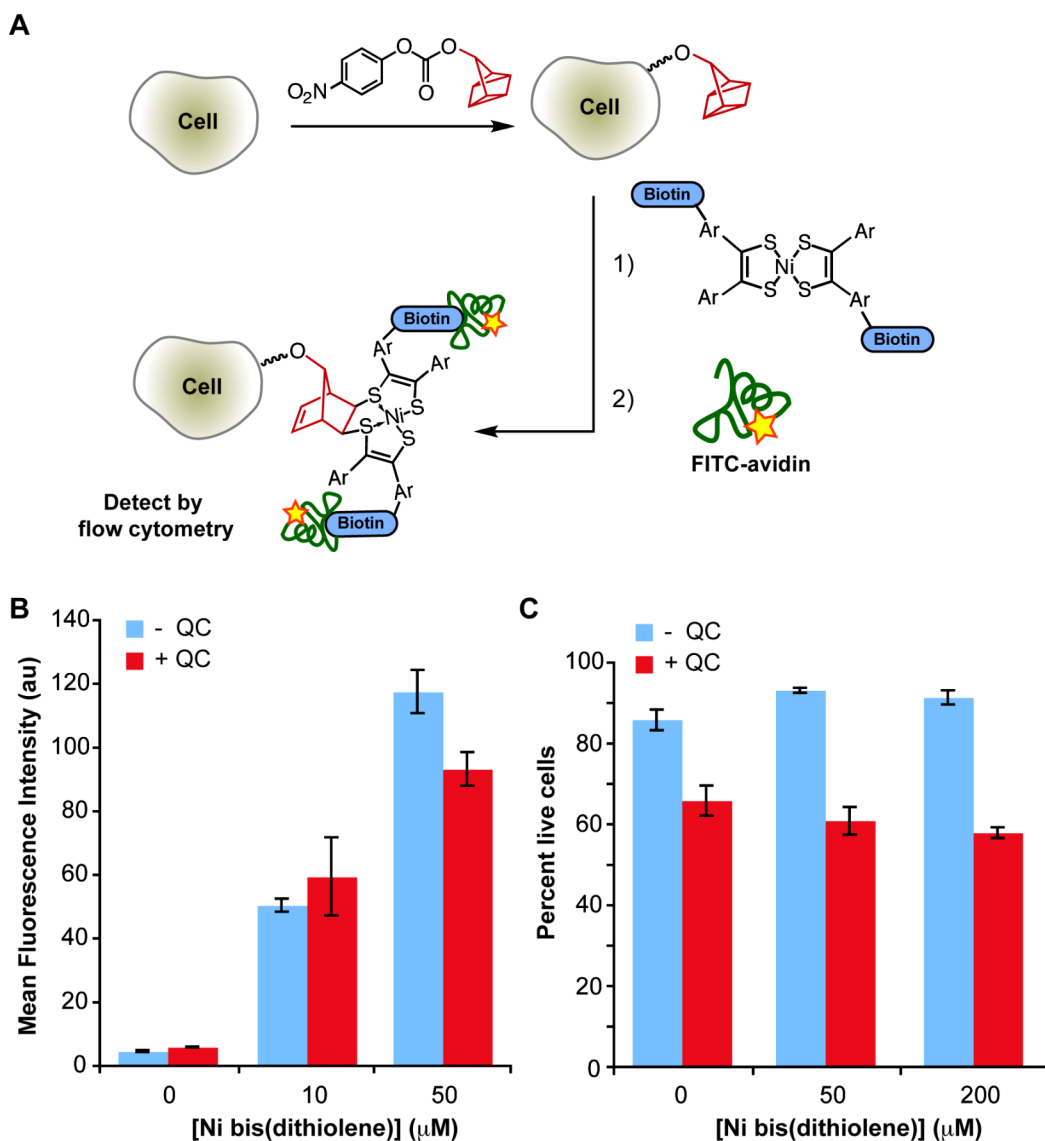
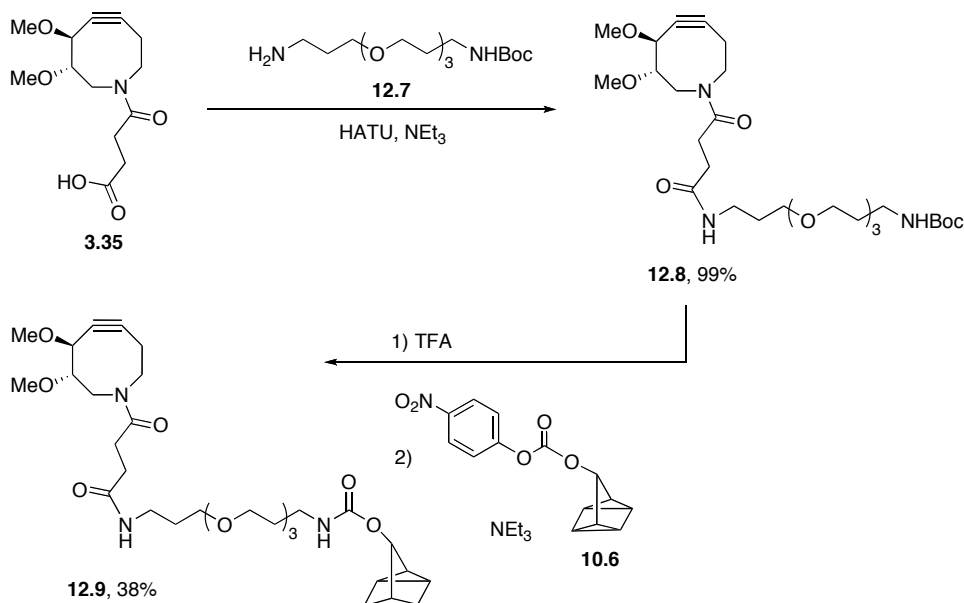


Figure 12.7. Modification of cell-surfaces with quadricyclane and subsequent labeling with Ni bis(dithiolene) **12.2**. A. Schematic outlining the cell labeling experiment. B/C. Jurkat cells were incubated with quadricyclane **10.6** (250 μM) in PBS containing 1% serum and 1% DMSO for 1 h at 37 °C. The cells were treated with varying concentrations of **12.2** for 30 min, twice incubated with a fluorescent avidin protein (FITC-avidin), stained with 7-AAD and analyzed by flow cytometry. Plotted are the average mean fluorescence intensities from the fluorescein signal (B) and the average number of live cells as determined by staining with 7-AAD (C). The error bars represent the standard deviation of three replicate samples.

Scheme 12.3. Synthesis of dimethoxyazacyclooctyne-quadracyclane (DIMAC-QC).



To employ the Cu-free click chemistry strategy to label cells with quadracyclane, Jurkat cells were grown in the presence of Ac₄ManNAz for three days.¹⁴ After washing away excess azidosugar, the cells were incubated with DIMAC-QC **12.9** for 1 h. Following another series of washes to remove the DIMAC-QC, the cells were treated with Ni bis(dithiolene) **12.2** under a variety of conditions. The degree of labeling was assayed by treatment with FITC-avidin followed by flow cytometry (Figure 12.8).

Initially, time- and dose-dependent labeling with Ni bis(dithiolene) **12.2** was performed. Unlike the case with lysine modification, the viability of the cells treated with DIMAC-QC was no different than that observed for untreated cells. When the quadracyclane-modified cells were treated with nickel complex **12.2** significant labeling over background was achieved, although the signal was weaker than we anticipated based on the kinetics of the reaction. The signal above background did increase with additional reaction times (Figure 12.9A) or higher concentrations of Ni bis(dithiolene) **12.2** (Figure 12.9B) suggesting that the signal is in fact due to the quadracyclane ligation occurring on live cells. Additionally, the cell viability, even after treating with complex **12.2**, appeared encouraging with only slight loss of viability evident in a reaction-dependent manner when long labeling times or high concentrations of nickel complex are employed (Figure 12.9C/D). This reaction-dependent toxicity could be due to delivery of Ni(II) directly to the cell-surface, although further experiments are necessary to make any conclusions regarding the mechanism of the cytotoxicity.

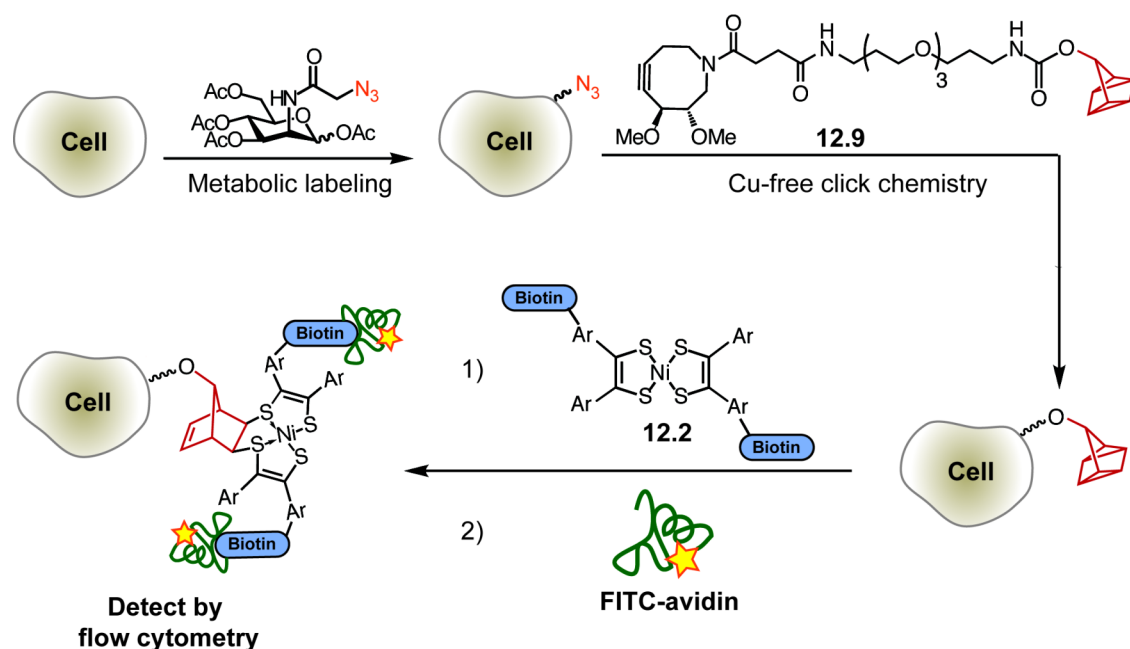
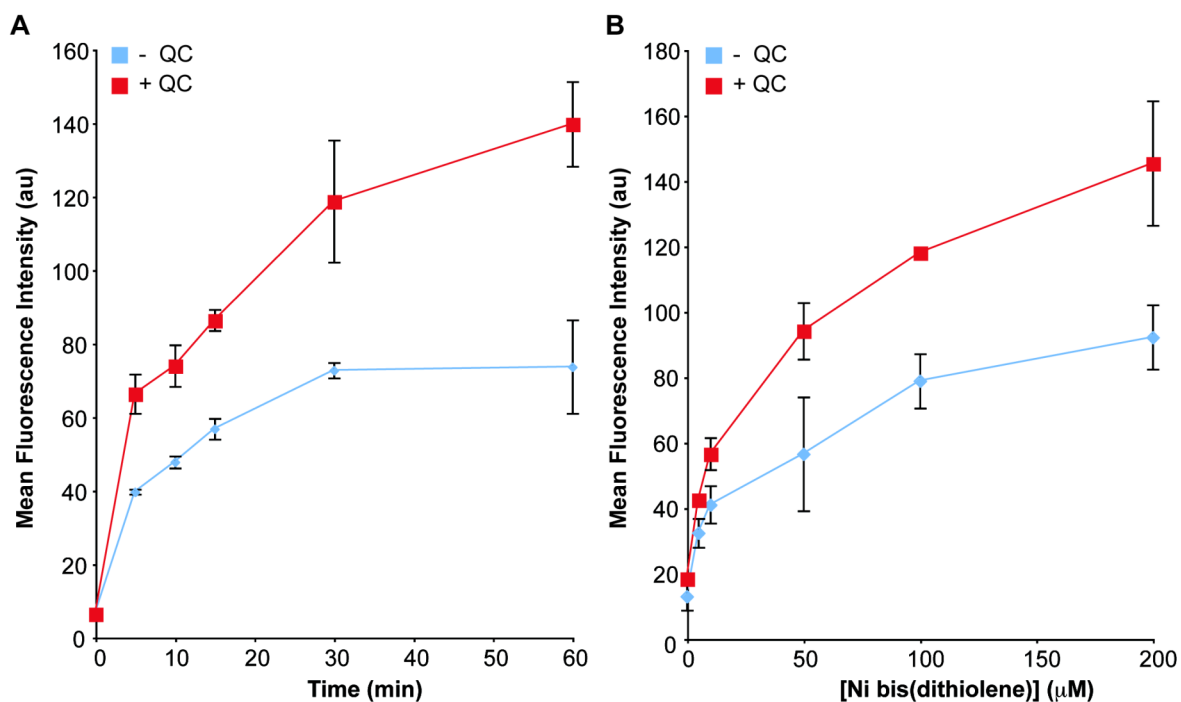


Figure 12.8. Work-flow of the live cell labeling experiments. DIMAC-QC **12.9** is employed to deliver quadricyclane to live cells. The quadricyclane modified cells are then labeled with Ni bis(dithiolene) **12.2** and stained with FITC-avidin. The degree of fluorescence was analyzed by flow cytometry.



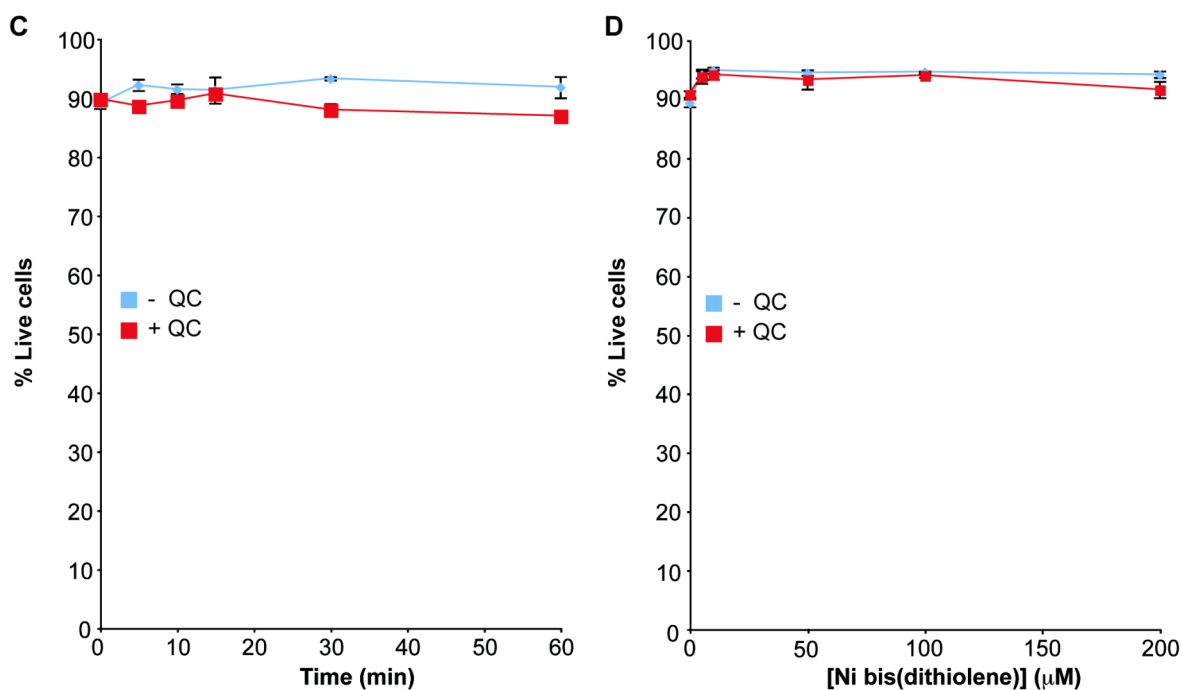


Figure 12.9. Labeling of quadricyclane-modified cells with Ni bis(dithiolene) **12.2**. Jurkat cells were grown in the presence or absence of peracetylated N-azidoacetyl mannosamine (Ac₄ManNAz, 25 μM) for 3 d. The cells were incubated for 1 h at 37 °C with 250 μM DIMAC conjugated to quadricyclane (**12.9**). The cells were treated with 150 μM **12.2** for various amounts of time (A/C) or various concentrations of Ni bis(dithiolene) **12.2** for 30 min (B/D). The cells were twice treated with FITC-avidin, stained with 7-AAD and analyzed by flow cytometry. Plotted are average mean fluorescence intensities from the fluorescein signal (A/B) and the average number of live cells as determined by staining with 7-AAD (C/D). The error bars represent the standard deviation of three replicate samples. Au = arbitrary units.

The signal observed from the quadricyclane ligation on live cell surfaces was significantly less than anticipated. We envisioned this could be due to a competing photodegradation pathway as the experimental procedure for the live cell labeling is quite lengthy. Diethyldithiocarbamate (**11.5**) was added at millimolar concentrations in the protein labeling experiments to prevent photodegradation and we aimed to see if this small organic molecule would be compatible with mammalian cells at similar concentrations. An experiment analogous to the one employed to assess the toxicity of **12.2** was performed using diethyldithiocarbamate. There was no significant loss of viability upon treating cells with diethyldithiocarbamate for 1 h at all concentrations tested (0-5 mM, Figure 12.10).

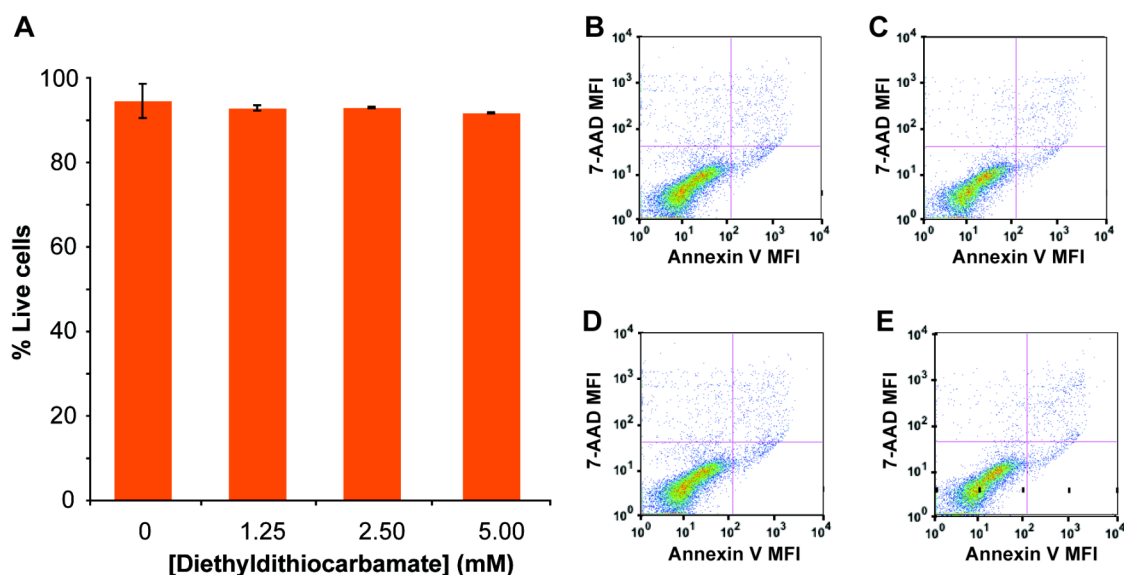


Figure 12.10. Cytotoxicity of diethyldithiocarbamate (**11.5**). Jurkat cells were treated with 0, 1.25, 2.5, or 5.0 mM diethyldithiocarbamate in PBS with 1% serum for 1 h. The cells were washed, stained with 7-AAD and Annexin V-PE, and analyzed by flow cytometry (FL2 vs. FL3). A. Plotted is the percentage of cells that do not stain with either 7-AAD or Annexin V-PE. The error bars represent the standard deviation of three replicate samples. B-E. Representative dot plots from cells treated with 0 (B), 1.25 (C), 2.5 (D), or 5 (E) mM diethyldithiocarbamate. The percentage of cells in the bottom left quadrant is what is plotted in part A. MFI = mean fluorescence intensity (arbitrary units).

Thus, we performed another live cell experiment where we first labeled cells with DIMAC-QC and then with Ni bis(dithiolene) **12.2**. All washes and incubations following the quadricyclane ligation reaction contained diethyldithiocarbamate (5 mM). Unfortunately, it did not appear that diethyldithiocarbamate increased the signal on live cells from the quadricyclane ligation, which suggests that photodegradation is not the cause of the low signal observed. However, the diethyldithiocarbamate treatment did appear to reduce overall background signal. The background signal is another concern, as there appears to be significant background reactivity of the Ni bis(dithiolene) complexes which also displays dose- and time-dependence. Efforts to decrease this background, preferably in a quadricyclane ligation dependent manner, will be important for the optimization of the quadricyclane ligation on live cells.

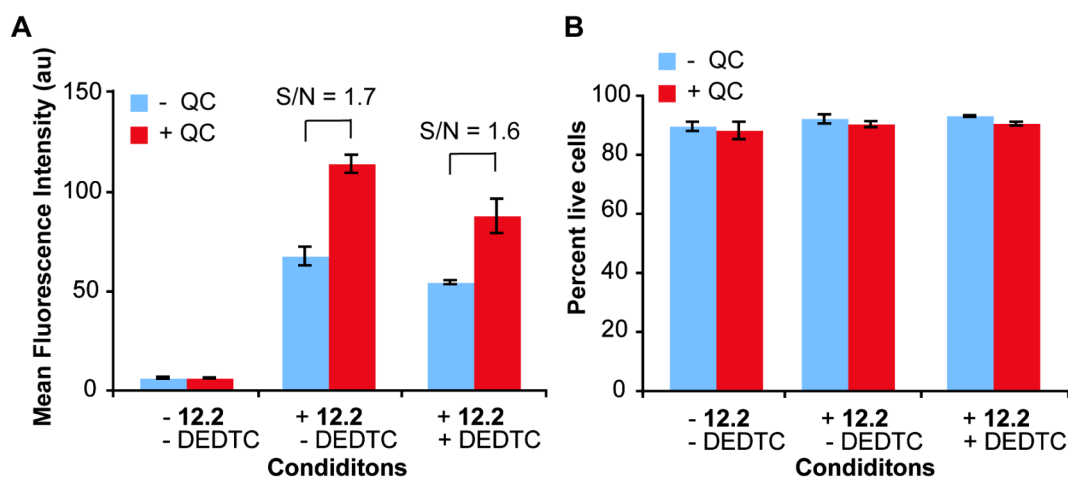


Figure 12.11. Comparison of live cell labeling of quadricyclane modified cells with Ni bis(dithiolene) **12.2** treated with or without diethyldithiocarbamate (**11.5**, DEDTC). Jurkat cells were grown in the presence or absence of peracetylated N-azidoacetyl mannosamine (25 μ M) for 3 d. The cells were incubated for 1 h at 37 $^{\circ}$ C with (red bars) or without (blue bars) 250 μ M DIMAC conjugated to quadricyclane. The cells were treated with (+) or without (-) 150 μ M **12.2** for 30 min. Following treatment with **12.2**, all washes and incubations were performed with FACS buffer (1% FBS in PBS, - DEDTC) or FACS buffer with 5 mM diethyldithiocarbamate (+ DEDTC). The cells were twice treated with FITC-avidin, stained with 7-AAD and analyzed by flow cytometry. Plotted are the average mean fluorescence intensity from the fluorescein signal (A) and the average number of live cells as determined by staining with 7-AAD (B). The error bars represent the standard deviation of three replicate samples. Au = arbitrary units. S/N = signal-to-noise ratio.

Future Directions for the Quadricyclane Ligation

Clearly, the quadricyclane ligation needs improvement for utility on live cells. The origin of the high background reactivity needs to be addressed. A screen of different cell lines might provide some insight into the cause of the quadricyclane-independent cell labeling. Ultimately, additional mechanistic modifications of one or both reaction components might be necessary to increase the signal to noise of the quadricyclane ligation on live cells and beyond.

Additional avenues to pursue regarding the quadricyclane ligation surround the incorporation of quadricyclane into a biomolecule. As mentioned in Chapter 10, the sialic acid salvage pathway¹⁵ and unnatural amino acid incorporation^{16,17} appear to be the most promising strategies for introduction of quadricyclane into biomolecules. Figure 12.12 shows some initial target quadricyclane-modified metabolites. The synthesis and evaluation of these compounds is an important step for the success and widespread use of the quadricyclane ligation.

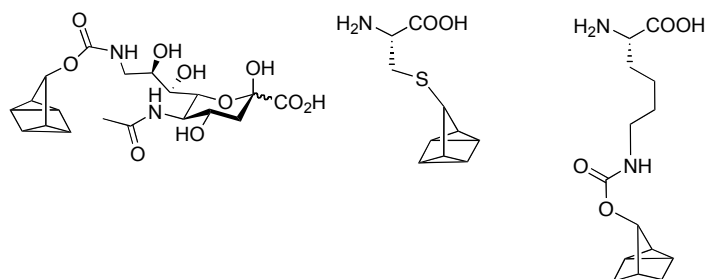


Figure 12.12. Proposed quadricyclane-modified metabolites.

Materials and Methods

General Experimental Procedure

All chemical reagents were purchased from Sigma-Aldrich, Acros or TCI and used without purification unless noted otherwise. Anhydrous DMF and MeOH were purchased from Aldrich or Acros in sealed bottles; all other solvents were purified as described by Pangborn *et al.*¹⁸ In all cases, solvent was removed by reduced pressure with a Buchi Rotovapor R-114 equipped with a Welch self-cleaning dry vacuum. Products were further dried by reduced pressure with an Edwards RV5 high vacuum. Lyophilization was performed on a LABCONCO FreeZone[®] instrument equipped with an Edwards RV2 pump. Thin layer chromatography was performed with EMD 60 Å silica gel plates. Flash chromatography was performed using Silicycle[®] 60 Å 230-400 mesh silica. All ¹H and ¹³C spectra are reported in ppm and referenced to solvent peaks. Spectra were obtained on Bruker AVQ-400, AVB-400, DRX-500, AV-500, or AV-600 instruments. UV/Vis/NIR spectra were acquired on a CARY 100 Bio UV-Visible Spectrophotometer with a range of 200-900 nm. Electron impact (EI) and electrospray ionization (ESI) mass spectra were obtained from the UC Berkeley Mass Spectrometry Facility. HPLC was performed on a Varian Pro Star or Varian Prep Star instrument with a C18 column.

Experimental Procedures

Compound 12.1. 4-(2-oxo-5-(4-sulfophenyl)-1,3-dithiol-4-yl)benzoic acid **11.42** (20 mg, 0.046 mmol, 1 equiv.) was dissolved in dimethylformamide (1 mL, anhydrous). To this solution, biotin-(PEG)₃-amine **4.2**¹ (23 mg, 0.056 mmol, 1.1 equiv.), 1-ethyl-3-(3-dimethylaminopropyl)carbodiimide hydrochloride (EDC·HCl, 15 mg, 0.078 mmol, 1.7 equiv.), hydroxybenzotriazole (HOBt, 10 mg, 0.065 mmol, 1.4 equiv.), and NEt₃ (15 μL, 0.11 mmol, 2.0 equiv.) were added. The mixture was stirred at rt overnight. The following morning the mixture was evaporated to dryness and purified by HPLC using water/methanol solvent system. Compound **12.1** eluted at 32 min when a gradient of 0 to 100% methanol over 45 min was used. This procedure resulted in pure **12.1** (17 mg, 0.021 mol, 45%). R_f = 0.4 in 4:1 acetonitrile/methanol. ¹H NMR (500 MHz, CDCl₃): δ 7.71 (d, J = 7.9 Hz, 4H), 7.31 (t, J = 7.6 Hz, 4H), 4.53- 4.50 (m, 1H), 4.34- 4.32 (m, 1H), 3.57- 3.52

(m, 8H), 3.49-3.48 (m, 2H), 3.42 (dd, $J = 10.2, 5.9$ Hz, 4H), 3.23-3.16 (m, 4H), 3.11-3.07 (m, 1H), 2.89 (dd, $J = 12.8, 4.8$ Hz, 1H), 2.69 (d, $J = 12.8$ Hz, 1H), 2.18 (t, $J = 7.3$ Hz, 2H), 1.83-1.81 (m, 2H), 1.72-1.58 (m, 6H), 1.41-1.37 (m, 2H). ^{13}C NMR (125 MHz, CDCl_3): δ 190.8, 176.4, 167.0, 166.0, 147.3, 136.4, 135.9, 134.7, 131.1, 131.0, 130.3, 130.0, 129.1, 127.8, 71.6, 71.4, 71.3, 70.4, 70.0, 64.0, 62.4, 57.0, 50.0, 43.5, 41.0, 39.0, 38.2, 36.7, 30.4, 29.9, 29.5, 27.0. HRMS (ESI): calcd. For $\text{C}_{36}\text{H}_{45}\text{O}_{10}\text{N}_4\text{S}_4^-$ [M-H] $^-$, 821.2024; found, 821.2036.

Ni bis(dithiolene) 12.2. Ligand precursor **12.1** (24 mg, 0.029 mmol, 1.0 equiv.) was dissolved in a mixture of THF/ H_2O (0.4 mL/0.4 mL). Tetramethyl ammonium hydroxide pentahydrate (11 mg, 0.061 mmol, 2.1 equiv.) in MeOH (60 μL) was added to the solution with compound **12.1**. The mixture turned a yellow/orange color. After 30 min, $\text{NiCl}_2 \cdot 6\text{H}_2\text{O}$ (3.5 mg, 0.015 mmol, 0.50 equiv.) was added and the solution turned a dark reddish brown. This mixture was stirred at rt overnight. The following morning, iodine (3.5 mg, 0.014 mmol, 0.48 equiv.) was added and the mixture turned dark blue in color. After 3 h stirring at rt, the mixture was purified by silica gel chromatography eluting with acetonitrile/water (10:1, 5:1, 2:1). This procedure resulted in 20 mg of **12.2** as a blue solid (0.024 mmol, 84%). $R_f = 0.3$ in 3:1 acetonitrile/water. UV/Vis/NIR (water): 868 nm (0.6 au), 349 nm (0.9 au), 315 nm (1.5 au), 276 nm (1.7 au), 201 nm (3.9 au). HRMS (ESI): calcd. for $\text{C}_{70}\text{H}_{90}\text{O}_{18}\text{N}_8\text{NiS}_8^{2-}$ [M-2H] $^{2-}$, 822.1752; found, 822.1749.

4,5-diphenyl-1,3-dithiol-2-one (12.5). Diphenylacetylene **12.4** (2.5 g, 13.9 mmol, 1.0 equiv.) was combined with 1,1'-azobis(cyclohexane)carbonitrile (1.5 g, 6.1 mmol, 0.44 equiv.), diisopropyl xanthogen disulfide **11.17** (4.3 g, 15.9 mmol, 1.1 equiv.) in *m*-xylene (30 mL, anhydrous). The reaction mixture was heated to reflux overnight. The following day, the reaction mixture was cooled to rt, evaporated to dryness, and purified by silica gel chromatography with a hexane/toluene solvent system (10:1, 8:1, 6:1). This procedure resulted in 830 mg of **12.5** (3.1 mmol, 22% yield). $R_f = 0.6$ in 10:1 hexanes/ethyl acetate. ^1H NMR (400 MHz, CDCl_3): δ 7.35- 7.25 (m, 10H). ^{13}C NMR (100 MHz, CDCl_3): δ 190.7, 131.8, 129.6, 128.93, 128.89, 128.8. HRMS (EI): calcd. for $\text{C}_{15}\text{H}_{10}\text{OS}_2^+$ [M] $^+$, 270.0173; found, 270.0179.

4,4'-(2-oxo-1,3-dithiole-4,5-diyl)dibenzenesulfonic acid (12.6). 4,5-diphenyl-1,3-dithiol-2-one **12.5** (830 mg, 3.1 mmol, 1.0 equiv.) was dissolved in sulfuric acid (10 mL, 18 M). Fuming sulfuric acid (150 μL , 20% in sulfuric acid) was added and the reaction mixture was heated to 90 $^\circ\text{C}$ overnight. The following morning the mixture was cooled to 0 $^\circ\text{C}$ and neutralized first with NaOH then with NaHCO_3 . Once neutral, methanol (100 mL) was added, the solution was filtered, and the filtrate evaporated to dryness. The solid was again dissolved in methanol (100 mL), filtered, and the filtrate evaporated to dryness. The residue was then dissolved in water (50 mL) and washed with hexane (3 x 50 mL). The water layer was evaporated to dryness and the crude product was purified by HPLC on a C18 column with a water/acetonitrile solvent system (0 to 30% acetonitrile over 30 min). The product elutes at 10 min. This procedure resulted in 430 mg of pure **12.5** (1.0 mmol, 32% yield). ^1H NMR (600 MHz, MeOD): δ 7.76 (d, $J = 8.3$ Hz, 4H), 7.33 (d, $J = 8.4$ Hz,

4H). ^{13}C NMR (150 MHz, MeOD): δ 191.0, 147.1, 134.6, 130.8, 130.1, 127.8. HRMS (ESI): calcd. for $\text{C}_{15}\text{H}_9\text{O}_7\text{S}_4^-$ [M-H] $^-$, 428.9237; found, 428.9238.

Ni bis(dithiolene) 12.3. 4,4'-(2-oxo-1,3-dithiole-4,5-diyl)dibenzenesulfonic acid **12.6** (33 mg, 0.075 mmol, 1.0 equiv.) was dissolved in a mixture of methanol (0.5 mL), THF (0.7 mL), and water (0.75 mL). Tetramethyl ammonium hydroxide pentahydrate (28 mg, 0.15 mmol, 2.1 equiv.) was dissolved in MeOH (0.15 mL) and added to the solution with compound **12.6**. The mixture turned a yellow color. After 30 min, $\text{NiCl}_2 \cdot 6\text{H}_2\text{O}$ (8.5 mg, 0.036 mmol, 0.48 equiv.) was added and stirred for 6 h, at which point iodine (8.5 mg, 0.033 mmol, 0.45 equiv.) was added and the blue mixture was stirred overnight at rt. The following morning, TLC indicated that some reduced complex may be present and more iodine (5 mg, 0.020 mmol, 0.26 equiv.) was added. After stirring for an additional 30 min, the reaction was evaporated to dryness and purified by silica gel chromatography eluting with acetonitrile/water (25:1, 9:1). This procedure resulted in 28 mg of **12.3** (0.033 mmol, 43% yield). UV/Vis/NIR: 832 nm (1.1 au), 591 nm (0.3 au), 349 nm (1.0 au), 315 nm (2.0 au), 272 nm (1.7 au). HRMS (ESI): calcd. for $\text{C}_{28}\text{H}_{16}\text{O}_{12}\text{NiS}_8^{4+}$ [M-4H] $^{4+}$, 214.4446; found, 214.4447.

DIMAC-fluorescein. DIMAC 8 (**3.35**, 8.0 mg, 0.030 mmol, 1.0 equiv.) was dissolved in CH_3CN (1 mL, anhydrous) and cooled to 0 $^\circ\text{C}$. DIPEA (10 μL , 0.057 mmol, 1.9 equiv.) was added and the mixture was stirred for 10 min, at which point pentafluorophenyltrifluoroacetate (15 μL , 0.087 mmol, 2.9 equiv.) was added. The reaction was warmed to rt and stirred for 1.5 h. It was then evaporated to dryness and purified by silica gel chromatography eluting with toluene/ether (7:1, 5:1, 3:1, anhydrous solvents used for chromatography). This procedure resulted in DIMAC-pentafluorophenyl ester (13 mg, 0.030 mmol, quant.). Half of the DIMAC-pentafluorophenyl ester (6.5 mg, 0.015 mmol, 1.0 equiv.) was dissolved in dimethylformamide (0.5 mL, anhydrous). In a separate flask, fluorescein-piperazine 19 (11 mg, 0.028 mmol, 1.8 equiv.) was dissolved in dimethylformamide (0.5 mL, anhydrous) and DIPEA (~10 μL , 0.06 mmol, 4 equiv.). The DIMAC solution was added to the fluorescein-piperazine solution at 0 $^\circ\text{C}$. The reaction was warmed to rt over 5 h, at which point it was evaporated to dryness and purified first by silica gel chromatography (5:3:1 EtOAc/MeOH/ H_2O) then by HPLC (C18 column, with methanol/water, 40-100% methanol over 25 min, elutes at 15 min). This procedure resulted in pure DIMAC-fluorescein (3 mg, 0.005 mmol, 31% yield). $R_f = 0.7$ in 5:3:1 ethyl acetate/methanol/water. HRMS (ESI): calcd. for $\text{C}_{37}\text{H}_{37}\text{O}_8\text{N}_3\text{Na}$ [M+Na] $^+$, 674.2473; found, 674.2478.

Compound 12.8. DIMAC 8 **3.35** (10 mg, 0.37 mmol, 1 equiv.) was dissolved in acetonitrile (1.0 mL, anhydrous). To the solution, *N,N*-diisopropylethyl amine (40 μL , 0.23 mmol, 6.2 equiv.) and *N*-Boc(4,7,10-trioxa-1,3-tridecanediamine) 20 **12.7** (20 mg, 0.063 mmol, 1.7 equiv.) were added. The solution was cooled to 0 $^\circ\text{C}$ and 2-(1H-7-Azabenzotriazol-1-yl)-1,1,3,3-tetramethyl uronium hexafluorophosphate (HATU, 17 mg, 0.45 mmol, 1.2 equiv.) was added. The mixture was warmed to rt. After 1 h, the reaction was evaporated to dryness and purified by silica gel chromatography using a

toluene/acetone solvent system (3:1, 1:1, 1:2). This procedure resulted in pure **12.8** (21 mg, 0.037 mmol, 99%) as 1:0.2 mixture of rotamers. ^1H NMR (600 MHz, MeOD): δ 4.29 (dd, $J = 12.7, 3.7$ Hz, 1rotH), 4.18 (dd, $J = 14.8, 5.4$ Hz, 1H, 1rotH), 4.07-4.04 (m, 2H), 3.96 (d, $J = 15.9$ Hz, 1rotH), 3.74-3.71 (m, 1rotH), 3.70 (t, $J = 8.7$ Hz, 1H), 3.65-3.63 (m, 4H, 4rotH), 3.60-3.57 (m, 7H, 7rotH), 3.52 (dt, $J = 12.1, 6.2$ Hz, 4H, 4rotH), 3.39 (dd, $J = 15.9, 9.1$ Hz, 1rotH), 3.34 (s, 2rotH), 3.32-3.19 (m, 4H), 3.14-3.01 (m, 2H, 2rotH), 2.97 (td, $J = 12.4, 3.9$ Hz, 1rotH), 2.91 (dd, $J = 14.0, 9.0$ Hz, 1H), 2.88-2.72 (m, 2H, 2rotH), 2.68-2.48 (m, 3H, 3rotH), 2.25 (dt, $J = 16.8, 3.6$ Hz, 1H), 2.17 (apparent d, $J = 14.3$ Hz, 1rotH), 1.78- 1.70 (m, 4H, 4rotH), 1.43 (s, 9H, 9rotH). HRMS (ESI): calcd. for $\text{C}_{28}\text{H}_{50}\text{O}_9\text{N}_3$ $[\text{M} + \text{H}]^+$, 572.3542; found, 572.3549.

DIMAC-Quadricyclane 12.9. Compound **12.8** (20 mg, 0.035 mmol, 1.0 equiv.) was dissolved in CH_2Cl_2 (300 μL , anhydrous) and cooled to 0 $^\circ\text{C}$. Trifluoroacetic acid (100 μL) was added and the mixture was stirred for 10 min, at which point it was evaporated to dryness and further azeotroped with toluene (5 mL) to yield an ammonium trifluoroacetate salt (16 mg, 0.027 mmol, 78%). This product was immediately coupled with *p*-nitrophenyl carbonate quadricyclane **10.6**. The ammonium trifluoroacetate salt (16 mg, 0.027 mmol, 1.0 equiv.) and **10.6** (8 mg, 0.029 mmol, 1.1 equiv.) were combined in CH_2Cl_2 (1.0 mL, anhydrous). Triethylamine (20 μL , 0.15 mmol, 5.5 equiv.) was added and the mixture was stirred overnight at rt. The following morning the reaction was evaporated to dryness and purified by silica gel chromatography using a toluene/acetone solvent system. This procedure resulted in 6 mg of **12.9** with a small amount of norbornadiene impurity (0.010 mmol, 38%) as a 1:0.2 mixture of rotamers. $R_f = 0.1$ in ethyl acetate. ^1H NMR (500 MHz, MeOD, rotamer not tabulated): δ 5.49 (s, 1H), 4.18 (dd, $J = 14.8, 5.3$ Hz, 1H), 4.07-4.03 (m, 2H), 3.69 (apparent t, $J = 8.1$ Hz, 1H), 3.65- 3.51 (m, 17H), 3.34-3.20 (m, 6H), 2.91 (dd, $J = 13.9, 8.9$ Hz, 1H), 2.83- 2.75 (m, 2H), 2.62- 2.51 (m, 3H), 2.25 (ddd, $J = 16.4, 3.5, 3.1$ Hz, 1H), 1.78-1.74 (m, 6H), 1.59 (bs, 2H), 1.48 (bs, 2H). HRMS (ESI): calcd. for $\text{C}_{31}\text{H}_{48}\text{O}_9\text{N}_3$ $[\text{M}+\text{H}]^+$, 606.3385; found, 606.3382.

Preparation of QC-BSA

Bovine serum albumin (100 mg, Sigma) was dissolved in PBS (5 mL). Quadricyclane *p*-nitrophenyl carbonate **10.6** (5 mg, 0.02 mmol) was dissolved in DMSO (300 μL) with a small amount of DMF (60 μL). A portion of the BSA solution (0.5 mL) was combined with the quadricyclane solution (100 μL) and DMSO (200 μL). The mixture instantly turned yellow indicating release of *p*-nitrophenol. After 3 h, the protein was purified on a NAP-5 column. The column was pre-equilibrated with PBS (10 mL). A portion of the protein mixture (350 μL) was added to the column and eluted with PBS (500 μL per fraction). Four fractions were collected with the second fraction containing the most protein. Protein concentrations were assayed by a NanoDrop2000 (Thermo Scientific) and a BioRAD D_c assay.

Western Blot Procedures

Figures 12.2-12.4. The described protein mixtures were quenched with diethyldithiocarbamate (**11.5**) and 7-acetoxy-quadracycline (**10.4**) (3-15 mM). 4X SDS-loading buffer (with BME) was added and the protein mixtures were loaded onto a 12% BisTris gel (BioRAD, Criterion). The gel was run at 200 V in MES buffer. Proteins were transferred to nitrocellulose (0.45 μ m, BioRAD) over 90 min at 75 V. The nitrocellulose was then treated with Ponceau stain and incubated in blocking buffer (5% BSA in PBS with 0.1% Tween 20) for 2 h at rt. Anti-biotin conjugated to horse-radish peroxidase (α -biotin-HRP, Jackson Labs) was added to the blocking buffer (1:100,000 dilution) and incubated at rt for 1 h. The blot was washed with PBST (PBS with 0.1% Tween 20, 3 x 10 min) and detection was performed by chemiluminescence using Pierce SuperSignal West Pico Chemiluminescent Substrate.

Figure 12.5. The described protein mixtures were quenched with diethyldithiocarbamate **11.5** (9.6 mM), quadracycline **10.4** (9.6 mM), 2-azidoethanol (14.5 mM), and excess 850 mM tris buffer pH 7.2 until the pH was neutralized. 4X SDS loading buffer (with BME) was added and the mixture was separated into three equal portions and loaded onto a 4-12% BisTris gel (BioRAD, Criterion). The gel was run at 150 V in MES buffer. Proteins were transferred to nitrocellulose (0.45 μ m, BioRAD) over 120 min at 50 V. The nitrocellulose was then treated with Ponceau stain and separated into three sections. Two sections were incubated in BSA blocking buffer (5% BSA in PBST) and the third was incubated with milk blocking buffer (5% non-fat milk in PBST) for 2 h at rt. One BSA-blocked blot was incubated with α -biotin-HRP (1:100,000, Jackson Laboratories). The other BSA-blocked blot was incubated with α -fluorescein-HRP (1:100,000, Invitrogen) and the milk-blocked blot was incubated with α -FLAG-HRP (1:100,000, Sigma, M2 monoclonal). All incubations were performed for 1 h at rt and followed by washing with PBST (3 x 10 min). Detection was performed by chemiluminescence using Pierce SuperSignal West Pico Chemiluminescent Substrate.

Cell Culture

Jurkat (human T cell lymphoma) cells were maintained in a 5% CO₂, water-saturated atmosphere and grown in RPMI 1640 media supplemented with 10% FBS, penicillin (100 units/ml), and streptomycin (0.1 mg/ml). Cell densities were maintained between 1 x 10⁵ and 2 x 10⁶ cells per mL.

Cell-Surface Labeling and Detection

Figure 12.6. Jurkat cells were washed twice with FACS buffer (PBS with 1% FBS) and placed in a 96-well plate with ~400,000 cells/well (pellet 2500 x g, 3 min, 4 °C). The cells were treated with at 0, 10, 25, 50, 100, 250, or 500 μM of **12.3**, the product of **12.3** and **10.4**, NiCl_2 , or CuSO_4 in the presence of 1 mM TCEP for 1 h. The cells were washed three times by resuspension in FACS buffer (200 μL) followed by concentration by centrifugation (2500 x g, 3 min, 4 °C). Following the third wash, the cells were resuspended in 100 μL of 1X binding buffer containing 5 μL of 7-AAD and 5 μL of FITC-Annexin V (buffer and reagents from BD Pharmingen). The cells were incubated at rt in the dark for 15 min, diluted to 500 μL with binding buffer and analyzed by flow cytometry (FL1 vs. FL3) on a BD Biosciences FACSCalibur flow cytometer equipped with a 488-nm argon laser. Plotted is the percentage of cells that do not stain with either 7-AAD or FITC-Annexin V. The error bars represent the standard deviation of three replicate samples.

Figure 12.7. Jurkat cells were concentrated (500 x g, 3 min, 4 °C) and resuspended in 10 mL FACS buffer (PBS containing 1% FCS, 2 x 10 mL) and cells were incubated with or without **10.6** (250 μM in FACS buffer with 1% DMSO) for 1 h at 37 °C. The cells were transferred to a 96-well plate (approx. 750,000 cells per well) and concentrated by centrifugation (2500 x g, 3 min, 4 °C) and washed three times by resuspension in 200 μL cold FACS buffer, and a concentrated by centrifugation (2500 x g, 3 min, 4 °C). The cells were then reacted for 30 min at rt in the dark with the **12.2** (0, 10 or 50 μM in FACS buffer). After 30 h, the cells were thrice concentrated by centrifugation (2500 x g, 3 min, 4 °C) and resuspended in 200 μL cold FACS buffer. Following an additional concentration by centrifugation (2500 x g, 3 min, 4 °C), cells were resuspended in FACS buffer (100 μL) containing FITC-avidin (1:200 dilution of 1 mg/mL stock, Sigma-Aldrich) and incubated in the dark at 4 °C for 15 min. Following the incubation, cells were concentrated by centrifugation, resuspended in 200 μL cold FACS buffer, concentrated by centrifugation, and another FITC-avidin incubation was performed. After the second FITC-avidin labeling, the cells were thrice concentrated by centrifugation (2500 x g, 3 min, 4 °C) and resuspended in 400 μL cold FACS buffer with 7.5 μL of 7-AAD (BD Pharmingen) present. Flow cytometry was performed on a BD Biosciences FACSCalibur flow cytometer equipped with a 488-nm argon laser. All flow cytometry experiments were performed with three replicate samples.

Figure 12.9. Jurkat cells were grown in the presence 25 μM peracetylated N-azidoacetyl mannosamine for 3 d. The cells were washed three times with FACS buffer (PBS with 1% FBS), placed in a 96-well plate with ~500,000 cells/well, and incubated for 1 h at 37 °C with 250 μM DIMAC conjugated to quadricyclane. The cells were washed three times with FACS buffer (pellet 2500 x g, 3 min, 4 °C) and were treated with 100 μM **12.2** for various amounts of time (A) or various concentrations of Ni bis(dithiolene) **12.2** for 30 min (B). The cells were washed three times by resuspension in FACS buffer followed by concentration by centrifugation (2500 x g, 3 min, 4 °C). Following the third wash, the cells

were incubated with a fluorescent avidin protein (FITC-avidin, 1:200 Sigma stock) for 15 min at 0 °C. The cells were washed once and again incubated with FITC-avidin for 15 min at 0 °C. The cells were then washed three times and resuspended in 400 µL FACS buffer containing diethyldithiocarbamate (5 mM) and 7.5 µL of 7-AAD (BD Pharmingen) for analysis by flow cytometry. Flow cytometry was performed on a BD Biosciences FACSCalibur flow cytometer equipped with a 488-nm argon laser (FL1 vs. FL3) The error bars represent the standard deviation of three replicate samples. Au = arbitrary units.

Figure 12.10. Jurkat cells were washed twice with FACS buffer (PBS with 1% FBS) and placed in a 96-well plate with ~500,000 cells/well (pellet 2500 x g, 3 min, 4 °C). The cells were treated with 0, 1.25, 2.5, or 5.0 mM of diethyldithiocarbamate (**11.5**) for 1 h. The cells were washed three times by resuspension in FACS buffer (200 µL) followed by concentration by centrifugation (2500 x g, 3 min, 4 °C). Following the third wash, the cells were resuspended in 100 µL of 1X binding buffer and 7.5 µL of 7-AAD and 5 µL of Annexin V-PE were added (buffer and reagents from BD Pharmingen). The cells were incubated at rt in the dark for 15 min, diluted to 500 µL with binding buffer and analyzed by flow cytometry (FL2 vs. FL3) on a BD Biosciences FACSCalibur flow cytometer equipped with a 488-nm argon laser.

Figure 12.11. Jurkat cells were grown in the presence 25 µM peracetylated N-azidoacetyl mannosamine for 3 d. The cells were washed three times with FACS buffer (PBS with 1% FBS), placed in a 96-well plate with ~500,000 cells/well, and incubated for 1 h at 37 °C with 250 µM DIMAC conjugated to quadricyclane. The cells were washed three times with FACS buffer (pellet 2500 x g, 3 min, 4 °C) and were treated with 0 or 150 µM **12.2** 30 min. The cells were washed three times by resuspension in FACS buffer containing 5 mM diethyldithiocarbamate (200 µL) followed by concentration by centrifugation (2500 x g, 3 min, 4 °C). At this point, all washes and incubations were either performed with FACS buffer or FACS buffer containing 5 mM diethyldithiocarbamate. Following the third wash, the cells were incubated with a fluorescent avidin protein (FITC-avidin, 1:200 Sigma stock) for 15 min at 0 °C. The cells were washed once and again incubated with FITC-avidin for 15 min at 0 °C. The cells were then washed three times and resuspended in 400 µL FACS buffer containing diethyldithiocarbamate (5 mM) and 7.5 µL of 7-AAD (BD Pharmingen) for analysis by flow cytometry. Flow cytometry was performed on a BD Biosciences FACSCalibur flow cytometer equipped with a 488-nm argon laser (FL1 vs. FL3) The error bars represent the standard deviation of three replicate samples. Au = arbitrary units.

References

- (1) Wilbur, D. S.; Hamlin, D. K.; Vessella, R. L.; Stray, J. E.; Buhler, K. R.; Stayton, P. S.; Klumb, L. A.; Pathare, P. M.; Weerawarna, S. A. Antibody fragments in tumor pretargeting. Evaluation of biotinylated Fab colocalization with recombinant streptavidin and avidin. *Bioconjugate Chem.* **1996**, *7*, 689-702.
- (2) Jamir, L.; Yella, R.; Patel, B. K. Efficient one-pot preparation of bis alkyl xanthogen disulfides from alcohols. *J. Sulfur Chem.* **2009**, *30*, 128-134.
- (3) Dalgleish, S.; Robertson, N. Electropolymerisable dithiolene complexes. *Coordin. Chem. Rev.* **2010**, *254*, 1549-1558.
- (4) Dance, I. G.; Miller, T. R. Ready displacement of dithiolene ligands from electron-poor dithiolene complexes by weak nucleophiles. *J. Chem. Soc., Chem. Commun.* **1976**, 112-113.
- (5) Chang, P. V.; Prescher, J. A.; Hangauer, M. J.; Bertozzi, C. R. Imaging cell surface glycans with bioorthogonal chemical reporters. *J. Am. Chem. Soc.* **2007**, *129*, 8400-8401.
- (6) Kiick, K. L.; Saxon, E.; Tirrell, D. A.; Bertozzi, C. R. Incorporation of azides into recombinant proteins for chemoselective modification by the Staudinger ligation. *Proc. Natl. Acad. Sci. U.S.A.* **2002**, *99*, 19-24.
- (7) Carrico, I. S.; Carlson, B. L.; Bertozzi, C. R. Introducing genetically encoded aldehydes into proteins. *Nat. Chem. Biol.* **2007**, *3*, 321-322.
- (8) Sletten, E. M.; Bertozzi, C. R. A hydrophilic azacyclooctyne for Cu-free click chemistry. *Org. Lett.* **2008**, *10*, 3097-3099.
- (9) Jencks, W. P. Studies on the mechanism of oxime and semicarbazone formation. *J. Am. Chem. Soc.* **1959**, *81*, 475-481.
- (10) Lecoeur, H.; de Oliveira-Pinto, L. M.; Gougeon, M.-L. Multiparametric flow cytometric analysis of biochemical and functional events associated with apoptosis and oncosis using the 7-aminoactinomycin D assay. *J. Immunol. Methods* **2002**, *265*, 81-96.
- (11) Watanabe, M.; Hitomi, M.; van der Wee, K.; Rothenberg, F.; Fisher, S. A.; Zucker, R.; Svoboda, K. K. H.; Goldsmith, E. C.; Heiskanen, K. M.; Nieminen, A.-L. The pros and cons of apoptosis assays for use in the study of cells, tissues, and organs. *Microsc. Microanal.* **2002**, *8*, 375-391.
- (12) Chang, P. V.; Prescher, J. A.; Sletten, E. M.; Baskin, J. M.; Miller, I. A.; Agard, N. J.; Lo, A.; Bertozzi, C. R. Copper-free click chemistry in living animals. *Proc. Natl. Acad. Sci. U.S.A.* **2010**, *107*, 1821-1826.
- (13) Kele, P.; Mezö, G.; Achatz, D.; Wolfbeis, O. S. Dual labeling of biomolecules by using click chemistry: A sequential approach. *Angew. Chem. Int. Ed.* **2009**, *48*, 344-347.
- (14) Laughlin, S. T.; Agard, N. J.; Baskin, J. M.; Carrico, I. S.; Chang, P. V.; Ganguli, A. S.; Hangauer, M. J.; Lo, A.; Prescher, J. A.; Bertozzi, C. R. Metabolic labeling of glycans with azido sugars for visualization and glycoproteomics. *Meth. Enzymol.* **2006**, *415*, 230-250.

- (15) Luchansky, S. J.; Goon, S.; Bertozzi, C. R. Expanding the diversity of unnatural cell-surface sialic acids. *ChemBioChem* **2004**, *5*, 371-374.
- (16) Wang, L.; Schultz, P. G. Expanding the genetic code. *Angew. Chem. Int. Ed.* **2005**, *44*, 34-66.
- (17) Link, A. J.; Mock, M. L.; Tirrell, D. A. Non-canonical amino acids in protein engineering. *Curr. Opin. Biotechnol.* **2003**, *14*, 603-609.
- (18) Pangborn, A. B.; Giardello, M. A.; Grubbs, R. H.; Rosen, R. K.; Timmers, F. J. Safe and convenient procedure for solvent purification. *Organometallics* **1996**, *15*, 1518-1520.
- (19) Hangauer, M. J.; Bertozzi, C. R. A FRET-based fluorogenic phosphine for live-cell imaging with the Staudinger ligation. *Angew. Chem. Int. Ed.* **2008**, *47*, 2394-2397.
- (20) Trester-Zedlitz, M.; Kamada, K.; Burley, S. K.; Fenyő, D.; Chait, B. T.; Muir, T. W. A modular cross-linking approach for exploring protein interactions. *J. Am. Chem. Soc.* **2003**, *125*, 2416-2425.

Chapter 13

The growth of a field

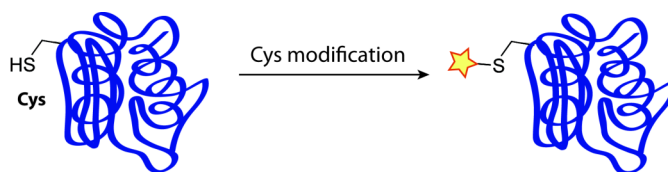
There has been an explosion of interest in bioorthogonal chemistry over the past five years both in terms of reaction development and biological applications. This concluding chapter highlights all the advances that have been made within the field during my tenure in graduate school. Its contents parallel that of the first two chapters with new sections added as deemed appropriate.

Protein Modification

Canonical Residue Modification

The development of new methods to modify the canonical amino acids continues to be a significant area of research, with the focus primarily remaining on cysteine, lysine and tyrosine residues. Davis and coworkers have developed a two-step method for cysteine modification (Figure 13.1, entry 1).¹ The first step in this procedure is the transformation of cysteine into dehydroalanine via treatment with O-mesitylenesulfonylhydroxylamine under basic conditions. The dehydroalanine residues then undergo a Michael addition with thiol reagents to yield a thioether linkage. The Michael addition is not stereospecific and, thus, a diastereomeric mixture of modified proteins is produced. Davis has reported that a direct displacement reaction can be used to form allyl sulfides from cysteine residues (Figure 13.1, entry 2), although in this report, the authors note that particularly nucleophilic lysine residues are also prone to alkylation.² A more elegant and selective method for formation of allyl sulfides was developed by drawing inspiration from work of Baldwin,³ Sharpless⁴ and Crich.⁵ This method employed a reductive sigmatropic rearrangement of the Se-allyl selenenyl sulfide of cysteine (Figure 13.1, entry 3).² The allyl sulfides can then be modified by cross-metathesis with Hoveyda-Grubbs 2nd generation catalyst. The Davis group has determined that allyl sulfides are a privileged structure for cross-metathesis⁶ and has successfully modified allyl sulfide containing proteins with glycosylated and PEGylated allyl ethers.⁷ In fact, work by the Davis group regarding protein-compatible cross-metathesis has led to the incorporation of alkene-containing amino acids into proteins.⁸

Another emerging cysteine modification technique that yields a thioether linkage is thiol-ene chemistry,⁹ which involves the addition of a thiol across an alkene through a radical-based mechanism (Figure 13.1, entry 4).¹⁰ The radical species can be generated by standard radical initiators or through irradiation with light,⁹ with the latter method displaying greater functional group tolerance and shorter reaction times.¹¹ Thiol-ene chemistry has been performed on proteins modified with either thiols¹² or alkenes¹³ or more recently, on native cysteine residues¹⁴ and on alkenes incorporated into proteins through the introduction of the unnatural amino acid homoallylglycine.¹⁵ The corresponding reaction with alkynes– thiol-yne chemistry– is another potential option for



Entry	Residue	Reagents/Catalyst	pH	Product
1	Cys	1) 2) HS-★	10-11	 (stereochemistry of cysteine is not preserved)
2	Cys		8	(★) ^a
3	Cys		8	(★) ^a
4	Cys	 <i>hv</i> or AIBN	7.4	
5	Cys		7-9	
6	Cys		7	
7	Cys	 X = CH ₂ , NH, O	7-9	 X = CH ₂ , NH, O
8	Cys or Lys		5-8	 X = S, NH

^a Probe is inserted through a subsequent chemical labeling step.

Figure 13.1. New methods for the modification of cysteine residues. Cys is modified through a two-step labeling procedure, which involves formation of dehydroalanine and subsequent Michael addition of a thiol (entry 1). Cys can be converted to an allyl sulfide for further elaboration via cross-metathesis by direct alkylation with allylchloride (entry 2) or, more selectively, through a sigmatropic rearrangement of a Se-allyl selenenyl sulfide (entry 3). The radical-based thiol-ene reaction is suitable for modification of Cys with terminal alkene reagents (entry 4). Variations on the classic Michael addition using bromomaleimides, oxanorbornadienes, electron-deficient alkynes, or vinyl sulfones (entries 5-8, respectively) provide additional methods of cysteine modification, some which contain opportunities for further functionalization.

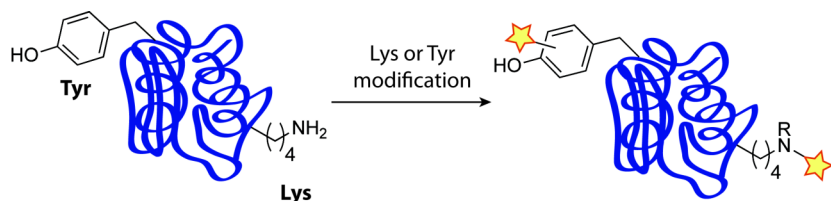
the modification of cysteine residues, although the fact that double addition products are obtained complicates the utility of this reaction.^{16,17}

New variations on the classic Michael addition have also been reported recently. Barker and coworkers have employed bromomaleimides as reagents for cysteine modification, which result in protein-associated thiomaleimides (Figure 13.1, entry 5).¹⁸ The resulting thiomaleimides can either be further modified with a thiol probe, cleaved to dehydroalanine by treatment with base (although yields are poor in aqueous solution), or released to yield the initial cysteine residue. Dibromomaleimides can lead to similar transformations.¹⁹ Finn and coworkers have used the oxanorbornadiene scaffold as a reactive partner for thiols (Figure 13.1, entry 6).²⁰ When coupled with a Dansyl group, a fluorogenic thiol-reactive reagent is obtained, which can be further modified with chemical probes as well. The oxanorbornadiene reagents also have additional modes of reactivity that can be employed for selective reagent release or further modification of the alkylated thiol. Electron deficient alkynes (alkynones, alkynoic esters and alkynoic amides) have also been employed for cysteine modification recently (Figure 13.1, entry 7).²¹ Terminal alkynones rapidly react with cysteine residues; however, this ligation could be cleaved by treatment with reducing agent. Shui and coworkers demonstrated the utility of this reversibility by treating a mixture of peptides with a biotin-alkynone, subjecting the labeled peptides to streptavidin beads, and then eluting the captured peptides with excess reducing agent.²¹ Notably, this was only effective with alkynones, as alkynoic esters and amides resulted in stable cysteine adducts. Vinyl sulfone groups have also been recognized as suitable Michael acceptors for cysteine as well as lysine residues (Figure 13.1, entry 7). Santoyo-Gonzalez and coworkers have developed a strategy for synthesizing vinyl sulfone containing probes, and further non-specific modification of lysine and cysteine residues on proteins.²²

A new selective lysine modification method is the condensation of lysine with (*E*)-ester aldehydes followed by electrocyclization of the resulting azatriene Schiff base (Figure 13.2, entry 1). This reaction is surprisingly fast and selective for unhindered lysine residues and has even been performed inside living mice for PET imaging with ¹⁸F modified (*E*)-ester aldehydes.^{23,24} The van Hest group has developed a protein-compatible diazotransfer reaction, which employs imidazole-1-sulfonyl azide as a reagent for the conversion of lysine-associated amines into azides (Figure 13.2, entry 2). The initial report necessitated high pH and Cu(II);²⁵ however, more recent work has eliminated the need for Cu(II) and developed conditions for selective diazotransfer to the N-terminus.²⁶ The azides can then be modified using any of the available bioorthogonal chemistries for this versatile chemical reporter group.

Tanaka and coworkers have built upon the Mannich-type modification of tyrosine residues originally reported by Francis and coworkers (Figure 1.2, entry 3).²⁷ In the original version of this reaction, the requisite imine was formed *in situ*. However, if a stable cyclic imine is employed as the reactive partner, the transformation proceeds readily at a wide range of pHs.^{28,29} Work from the same group has also produced fluorogenic amines for use in the three component version of this reaction.³⁰ Another new tyrosine modification has been reported by the Barbas group. In this transformation, tyrosine

residues are covalently modified by a cyclic diazodicarboxamide through a formal ene reaction (entry 4).³¹



Entry	Residue	Reagents/Catalyst	pH	Product
1	Lys		7.4	
2	Lys		8.5-11	
3	Tyr		2-10	
4	Tyr		7.4	

^a Probe is inserted through a subsequent chemical labeling step.

Figure 13.2. New methods for the modification of lysine and tyrosine residues. Lys residues are modified by Schiff base formation with an (*E*)-carboxyester aldehyde, which undergoes a spontaneous electrocyclization to yield a ligation product (entry 1). The aqueous compatible diazotransfer reagent imidazole-1-sulfonyl azide converts Lys residues into azides for further modification with terminal or strained alkynes (entry 2). Tyr can be modified through a Mannich reaction with stable, cyclic imines (entry 3) or through a formal ene reaction with cyclic diazodicarboxamide reagents (entry 4).

N-Terminal Modification

The major advancement regarding N-terminal modification is the cyanobenzothiazole condensation for proteins containing an N-terminal cysteine residue (Figure 13.3). The condensation of cyanobenzothiazole and cysteine is the last step in the synthesis of luciferin and has been known for a half a century;³² however, its high selectivity and speed has only been realized in the past few years. Rao and coworkers employed fluorescent and biotinylated cyanobenzothiazoles to label luciferase or a cyan fluorescent protein, which were engineered via a TEV protease to contain N-terminal cysteine residues.³³ This reaction is highly selective and could even be performed on live cell-surfaces where free cysteine is not present to interfere with the condensation reaction. Rao and coworkers have since utilized this reaction to control polymerization in pH, redox, and enzymatic sensitive manners *in vitro* and inside mammalian cells.³⁴ In lysate samples, it was noted that condensation with free cysteine was observed; however, inside cells the reaction with free cysteine would simply prevent polymer formation and did not complicate their experimental results.³⁴ The utility of this transformation mirrors native chemical ligation in the sense that 1,2-aminothiols are naturally occurring; however, their abundance in nature is minimal enough that this reaction can be performed in living systems under certain conditions. A significant advantage that the cyanobenzothiazole condensation has over native chemical ligation is that it is very fast ($k = 9 \text{ M}^{-1}\text{s}^{-1}$).³⁵ This large second-order rate constant, coupled with the oxidizing environment of the cell-surface, could make this a valuable bioorthogonal reaction for studying extracellular events (similar to the utility of carbonyl chemistry).

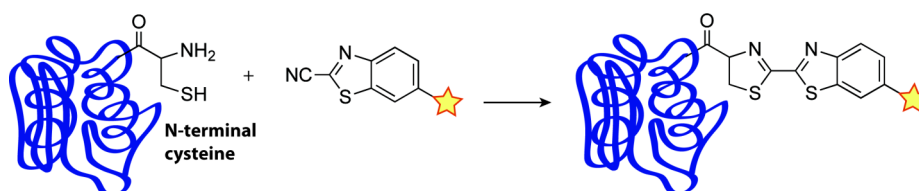


Figure 13.3. The condensation between cyanobenzothiazole and a protein containing an N-terminal cysteine residue.

In efforts to extend the cyanobenzothiazole ligation to the labeling of proteins at locations other than the N-terminus, Chin and coworkers have recently evolved a tRNA synthetase/tRNA_{CUA} pair to incorporate protected 1,2-aminothiol containing amino acid **13.1** (Figure 13.4).³⁵ This amino acid can be deprotected with O-methyl hydroxylamine under denaturing conditions (6M guanadimum chloride pH 4, 4 h) and then rapidly condensed with a functionalized cyanobenzothiazole. The Chin group has also site-specifically incorporated aminothiol **13.2** and protected version **13.3** for modification of proteins by native chemical ligation.³⁶

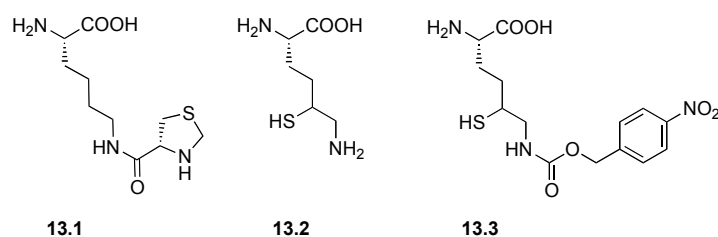
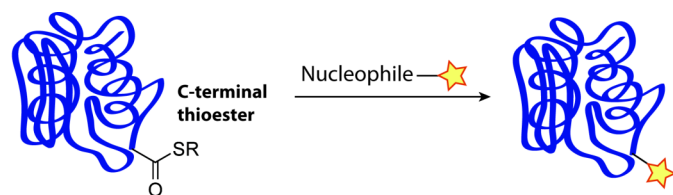


Figure 13.4. Unnatural amino acids containing 1,2-aminothiols for further modification by the cyanobenzothiazole condensation or native chemical ligation.

Aside from the cyanobenzothiazole condensation³² and selective diazotransfer to the N-terminus,²⁶ recent advancements regarding methods to modify the N-terminus of proteins have been minimal. However, native chemical ligation still plays a prominent role in chemical biology. Some recent highlights from research that was facilitated by native chemical ligation are: semisynthesis of ion channels,³⁷ analysis of histone acetylation,³⁸ synthesis of D-peptides for protein-protein interaction inhibitors,³⁹ semisynthesis of an enzyme,^{40,41,42} and the study of glycosylphosphatidylinositol anchors⁴³ and GTPases⁴⁴. From the chemical perspective, many groups have attempted to perform native chemical ligation at residues other than cysteine including valine,^{45,46} phenylalanine,⁴⁷ leucine,⁴⁸ lysine⁴⁹ and proline.⁵⁰ The Wong group has even employed a glycan to assist in chemical ligation.^{51,52}

C-Terminal Modification

In contrast to the relatively few advances for N-terminal modification in recent years, site-specific protein modification at the C-terminus has been explored by a variety of groups. Generally, all the non-enzymatic C-terminal modification methods rely on trapping the C-terminal thioester generated through expressed protein ligation (Figure 1.4B) with a nucleophile other than cysteine. This strategy was first pioneered by Raines and coworkers who used a hydrazine linked to an azide to create a stable protein with a C-terminal azide (Figure 13.5, entry 1).⁵³ Other nucleophiles enhanced by the alpha effect have been utilized for reaction with a C-terminal thioester including free hydrazine (Figure 13.5, entry 2)⁵⁴ and amino-oxy groups (Figure 13.5, entry 3).⁵⁵ In a more creative approach, Liu and coworkers employed sulfonazides for the modification of C-terminal thioesters through a thioacid/azide amidation reaction (Figure 13.5, entry 4).⁵⁶



Entry	Nucleophile	Product
1		
2	1) $\text{H}_2\text{N-NH}_2$ 2)	
3	$\text{H}_2\text{N-O-CH}_2\text{-CH}_2\text{-O-NH}_2$	
4	1) Na_2S 2)	

^a Probe is inserted through a subsequent chemical labeling step.

Figure 13.5. Methods for functionalization of the C-terminus involve modification of the C-terminal thioester produced by expressed protein ligation. The thioester can be modified with nucleophiles enhanced by the alpha-effect such as hydrazine and aminoxy reagents (entries 1-3). Additionally, the free thioacid can be modified through a thioacid/azide amidation reaction (entry 4).

Selective Protein Modification through Protein and Peptide Fusions

The green fluorescent protein still remains the workhorse of many molecular and cell biology experiments as evidenced by the 2008 Nobel Prize in Chemistry being awarded to Osamu Shimomura,⁵⁷ Martin Chalfie,⁵⁸ and Roger Tsien⁵⁹ for the discovery, utility, and engineering of fluorescent proteins. However, the need for smaller perturbations to a protein of interest is still valid⁶⁰ and many research groups have directed their efforts to developing new methods for selective protein modification through peptide fusions.

Bisboronic Acid Reagents

In a system that conceptually parallels Tsien and coworkers bisarsenical dyes which bind the tetracysteine motif, Schepartz and coworkers have reported a bisboronic acid rhodamine-based dye (RhoBo, Figure 13.6) that binds to tetraserine motifs with a

nanomolar K_d .⁶¹ Like bisarsenical dyes FIAsh and ReAsH, RhoBo is fluorogenic and cell-permeable, yet RhoBo does not employ the cytotoxic element arsenic nor does it suffer background fluorescence due to thiol exchange. RhoBo was initially developed as a tool for monosaccharide detection,⁶² but it binds monosaccharides with a significantly higher K_d compared to peptides with SSPGSS motifs, allowing RhoBo to selectively label proteins in the presence of carbohydrates.⁶¹ However, some endogenous proteins contain SSXXSS-like sequences that might lead to off-target labeling in cell-based systems. Schepartz and coworkers have also extended the use of the tetracysteine motif in recent years to study protein folding, aggregation, and protein-protein interactions.⁶³

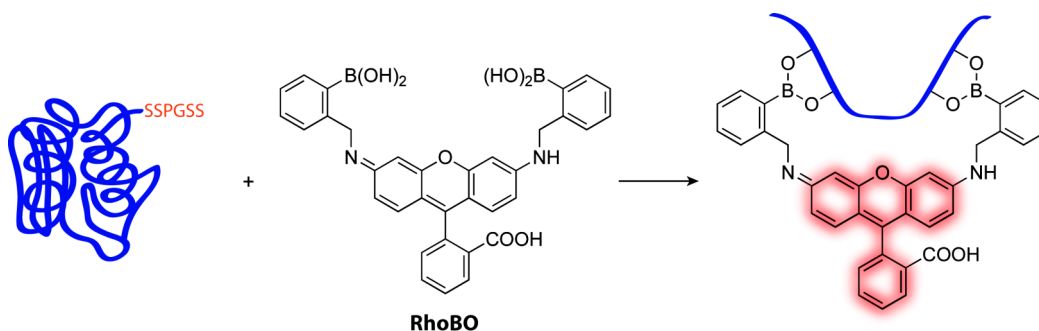
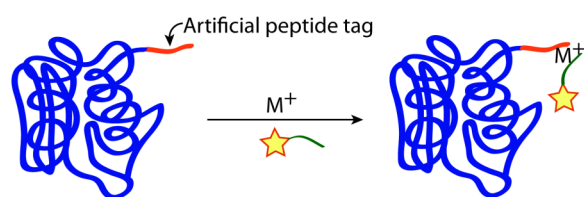


Figure 13.6. A fluorogenic bisboronic acid rhodamine reagent for labeling proteins containing tetraserine motifs.

Peptide Tags Detected Through Chelation of Transition Metals

New metal chelation strategies have been developed for the modification of peptide tags. In addition to the nickel-nitrilotriacetate (Ni-NTA) probes which bind hexahistidine peptides, Hauser and Tsien have developed a Zn(II) mediated chelation strategy. The fluorescent tag termed HisZiFit (Figure 13.7, entry 1) was designed to bind His₆ in a Zn(II) dependent manner, and fluorescence is only obtained upon binding. This reagent was used to investigate the stromal interaction molecule STIM1.⁶⁴ The report of HisZiFit prompted a variety of other probes for polyhistidine sequences that undergo spectral changes in response to binding. Most of these probes are based on the standard Ni-NTA scaffold;^{65,66} however, Higuchi and coworkers determined that Ni(II) could be replaced by Co(II) (Figure 13.7, entry 2).⁶⁷ More recently, Yamamoto and coworkers developed a macrocycle, which binds to hexahistidine sequences with comparable affinities to the NTA scaffold (Figure 13.7, entry 3). The nickel-binding macrocycle was tethered to dichlorofluorescein to create a turn-on probe for detection of His-tagged proteins.⁶⁸

Hamachi and coworkers have also exploited Zn(II) in the development of chelating probes that recognize tetraaspartate sequences (Figure 13.7, entry 4).⁶⁹ Multinuclear zinc complexes (Zn-DpaTyrs) were synthesized, conjugated to fluorescein and cyanine dyes, and used to image the muscarinic acetylcholine receptor in Chinese hamster ovary (CHO) cells. Two strategies to engineer fluorescence activation of Zn-DpaTyrs upon protein



Entry	Peptide	Metal	Reagent ^a
1	HHHHHH	Zn ²⁺	
2	HHHHHH	Co ²⁺	
3	HHHHHH	Ni ²⁺	
4	DDDD	Zn ²⁺	

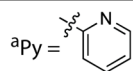


Figure 13.7. Metal-assisted detection of peptide tags. Zinc, cobalt, or nickel can be employed to promote the binding of polyhistidine sequences to either a fluorogenic HisZiFit dye, a NTA functionalized probe, or a dichlorofluorescein conjugated to an Ni-binding macrocycle, respectively (entries 1-3). Tetraaspartate peptides can be detected with multinuclear zinc complexes (entry 4).

binding were explored. The first involved the use of an Asp₄GlyAsp₄ tag and a pyrene chromophore. When both tetraaspartate motifs were chelated to Zn-DpaTyr_s, the pyrenes created an excimer complex with altered fluorescent properties.⁷⁰ The second method employed a fluorophore that undergoes a spectroscopic change as a function of pH. The tetraaspartate motif created a local acidic environment that was reflected in the fluorescence of the bound dye.⁷¹ A further advance regarding this methodology was a Zn-DpaTyr_s reagent bearing a chloroacetamide group that alkylated a cysteine residue positioned near the tetraaspartate motif.⁷² This reagent extended the use of the dye to

Western blotting and affinity purification applications, which require more robust protein conjugation chemistries. Recently, this binding-promoted alkylation was employed to visualize G-protein coupled receptors on live cells tagged with tandem tetraaspartate motifs.⁷³

Binding-Promoted Covalent Modification

Binding promoted selective protein modifications using proteins that naturally have high specificity for a particular structure have become increasingly popular over the past five years. Hamachi and coworkers have utilized this concept to selectively alkylate carbonic anhydrase *in vivo* with phenylsulfonate probes.⁷⁴ Cornish and coworkers have exploited the high binding affinity of trimethoprim and dihydrofolate reductase (DHFR) to promote a specific Michael addition of a cysteine residue on proteins fused with DHFR.⁷⁵ Fukase and coworkers have also utilized this method to specifically label human serum albumin with a coumarin directed (*E*)-carboxyester aldehyde.²⁴ A coiled-coil interaction has been used to direct modification of tryptophan or tyrosine residues using a peptide-associated rhodium carbenoid.⁷⁶

Enzymatic Modification of Peptide Tags

The enzyme-mediated modification of peptide tags has continued to be a fruitful area of research. The Ting group remains a major player in this field and they have expanded the scope of unnatural functional groups tolerated by the ligase enzymes by the use of mutated enzymes and enzymes from different species. Through a screen of biotin ligases from nine different organisms, Ting and coworkers found that azidodesthiobiotin or alkynyl-modified biotin could be ligated to the acceptor peptide if BirA from the proper species was employed (Figure 13.8, entries 1-2).⁷⁷ Previous to this screen, the only unnatural substrate known to be accepted by BirA was keto-biotin (Figure 1.7, entry 1). The original version of the biotin ligase system continues to be employed for biological assays as exemplified by recent work from the Ting group where protein-protein interactions were probed by fusing the BirA acceptor peptide to one protein of interest and the BirA enzyme to the other protein of interest. Biotinylation of the acceptor peptide suggested a protein-protein interaction occurred.⁷⁸

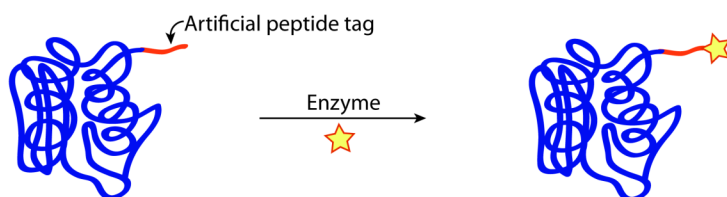
The majority of the work from Ting group is currently focused on the enzyme lipoic acid ligase. The natural lipoic acid ligase from *E. coli* will accept a short-chain azido fatty acid and modify an appropriately tagged protein (Figure 13.8, entry 3).⁷⁹ The azide can then be detected in live mammalian cells using cyclooctyne-based probes. Lipoic acid can also be used in conjunction with biotin ligase to orthogonally label two different proteins. Mutations to lipoic acid ligase have allowed for large substrates to be utilized including an aryl azide for photocrosslinking applications⁸⁰ or the direct addition of a coumarin⁸¹ (Figure 13.8, entries 4-5). Ting and coworkers have termed the direct addition of a coumarin to proteins tagged with the appropriate acceptor peptide PRIME (PProbe Incorporation Mediated by Enzymes). Since the original report of PRIME, the coumarin dye has been optimized.⁸²

Some posttranslational modifications have intrinsic orthogonal reactivity that allows for direct protein labeling at the modification site. This is the case for the aldehyde-containing formylglycine (fGly) residue formed by the action of the formylglycine-generating enzyme (FGE).^{83,84} FGE recognizes a six-residue motif in which a cysteine residue is oxidized to fGly. Normally found in type I sulfatases, the motif can be cloned into heterologous proteins where it is nonetheless recognized by FGE. The Bertozzi group has exploited the FGE consensus as a genetically encoded aldehyde tag for site-specific protein modification (Figure 13.8, entry 6).^{85,86,87} Coexpression of the tagged protein alongside FGE directly produces the aldehyde-functionalized protein. The aldehyde can be detected using a variety of methods, such as condensations with aminoxy or hydrazide probes.⁸⁵ While most organisms have endogenous FGE activity, it was determined that conversion of cysteine to fGly is enhanced if FGE is overexpressed. The aldehyde tag has been employed to modify proteins expressed in *E. coli* as well as in mammalian cells, including secreted, cytosolic, and membrane-associated proteins.⁸⁸

The Sortag and SNAP tag have both continued to be extensively used over the past five years. In 2007, Ploegh and coworkers reported the first sortase modification of proteins on live cells.⁸⁹ In their report, a MHC H-2K^b protein was modified with a variety of oligoglycine probes containing biotin, fluorescein, tetramethylrhodamine, an aryl azide, and an *o*-nitrophenyl group. In later work, Nagamune and coworkers employed SrtA on live cells to label the extracellular C-terminus of a membrane protein, ODF, with biotin and Alexa Fluor 488. The ligation of GFP to ODF was also demonstrated using SrtA.⁹⁰ The benefit of sortase tagging is that there is no observed limitation to the size of the modification introduced, eliminating the need for two-step strategies. Transglutaminase has also recently been employed as an antibody modification strategy.⁹¹

The SNAP tag has become the most widely used enzyme chimera for covalent labeling of a protein with small molecules. An orthogonal enzyme that recognizes alkylated cytosine rather than alkylated guanosine has been engineered and is referred to as a CLIP tag (Figure 13.8, entry 7).⁹² The SNAP and CLIP technologies have been commercialized by New England Biolabs, which has allowed the community easy access to labeled proteins. Consequently, many applications have been reported including organelle specific sensing of ions^{93,94} and metabolites,⁹⁵ optical FRET-based switches,⁹⁶ chromophores-assisted laser inactivation of proteins,⁹⁷ the study of protein-protein interactions by FRET⁹⁸ and crosslinking,⁹⁹ time-resolved FRET imaging,¹⁰⁰ live cell stochastic optical reconstruction microscopy (STORM),¹⁰¹ and semisynthetic fluorescent sensor proteins.¹⁰² Recently, SNAP and CLIP tagged proteins have been extended to higher organisms including zebrafish¹⁰³ and mice.¹⁰⁴ In addition, the Johnson group in collaboration with New England Biolabs is working toward enhancing the activity of the SNAP enzyme and developing fluorogenic benzylguanosine probes.¹⁰⁵

Two new additions to enzyme-protein chimeras that enable covalent modification of target proteins have been reported recently. These include the HaloTag and the serine esterase cutinase. Promega has also developed the HaloTag, where a protein of interest is fused to a bacterial haloalkane dehalogenase (DhaA) that has been mutated at the catalytic site to trap the covalent intermediate. The protein of interest can then be tagged using alkyl chloride probes (Figure 13.8, entry 8).¹⁰⁶ The protease cutinase is a moderate



Entry	Enzyme	Small Molecule	Product
1	BirA (yeast)		
2	BirA (<i>P. horikoshii</i>)		
3	LplA	$\text{HOOC}-(\text{CH}_2)_7\text{N}_3$	
4	mutated LplA		
5	mutated LplA		
6	FGE	N/A	
7	mutated hAGT ^b		
8	mutated DhaA ^b	$\text{Cl}-(\text{CH}_2)_{60}\text{CH}_2\text{CH}_2\text{O}-\text{S}-\text{Star}$	
9	cutinase ^b		
10	PFTase		

^a Probe is inserted through a subsequent chemical labeling step.

^b Enzyme is fused to the protein of interest and no peptide tag is employed.

Figure 13.8. Site-specific modification of proteins with small molecules by enzymatic elaboration of a peptide tag. The biotin ligase enzyme (BirA) from yeast and *P. horikoshii* recognize azido- and alkynyl- biotin derivatives, respectively (entries 1-2). Lipoic acid ligase (LplA) or mutated versions of LplA catalyze the attachment of alkyl (entry 3) or aryl (entry 4) azido-lipoic acid derivatives or a coumarin lipoic acid derivative (entry 5) to proteins tagged with the appropriate acceptor peptide. The formylglycine-generating enzyme (FGE) catalyzes the transformation of a Cys into a formylglycine in proteins that contain the motif CXPXR (entry 6). A protein recombinantly expressed as a fusion with a mutated version of the human repair protein O⁶-alkylguanine-DNA alkyltransferase (hAGT) can be alkylated by modified O-benzylcytosine probes (entry 7). A protein recombinantly expressed as a fusion with an engineered haloalkane dehalogenase (DhaA) can be modified by alkyl chloride probes (entry 8). A protein recombinantly expressed as a fusion with the serine protease cutinase can be labeled using derivatives of *p*-nitrophenyl phosphonate suicide inhibitors (entry 9). Proteins containing the C-terminal sequence CVIA can be labeled with an alkynyl farnesyl group using a protein farnesyltransferase (PFTase) enzyme (entry 10).

sized enzyme (22 kDa) and can be inserted into loop regions of the target protein. Covalent modification of cutinase can be achieved by the introduction of derivatized *p*-nitrophenyl phosphonate probes (Figure 13.8, entry 9).¹⁰⁷

Distefano and coworkers have also reported a new peptide tag for enzymatic modification based on farnesylation. Protein farnesyltransferases (PFTase) catalyze the addition of farnesyl groups onto C-terminal CVIA sequences through modification of the cysteine residue. The PFTase enzymes will accept alkynyl substrates, which can be further modified with Cu-catalyzed click chemistry (Figure 13.8, entry 10).¹⁰⁸

Bioorthogonal Chemistry for the Carbonyl

Oxime and hydrazone formation still remains a popular strategy for the selective labeling of carbonyl groups on proteins and live cells. One of the main limitations of this chemistry is its relatively sluggish reaction kinetics at neutral pH;¹⁰⁹ however, Dawson and coworkers have overcome this limitation by reporting that the kinetics of oxime formation can be enhanced through aniline catalysis.¹¹⁰ Aniline catalysis is also effective for hydrazone formation.^{111,112} An elegant demonstration of the effects of aniline catalysis was performed by Paulson and coworkers, where aldehydes were introduced into sialic acid residues by mild periodate oxidation. The modified glycoproteins were then detected by reaction with an aminoxy containing biotin reagent in the presence of aniline followed by labeling with a fluorescent streptavidin (Figure 13.9).¹¹³ This technique has since been used by our lab to visualize sialylated glycans on zebrafish, although due to toxicity concerns most experiments were performed without aniline.¹¹⁴ Recently, Meijler and coworkers have reported that aniline catalysis (in addition to stringent washing) allows for selective oxime formation inside bacteria, despite the fact that many intracellular metabolites contain carbonyl functionality.¹¹⁵ This is an exciting development for oxime ligation chemistry.

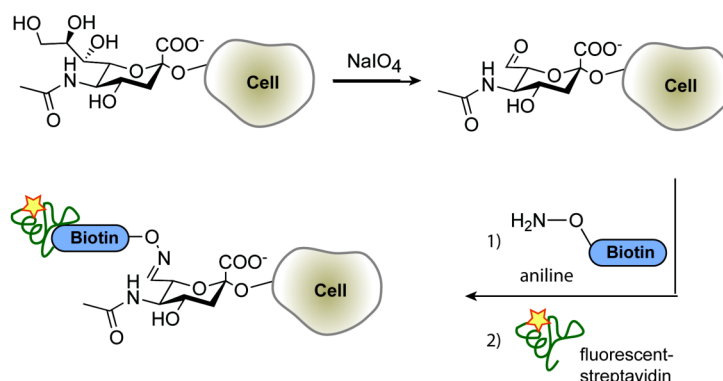


Figure 13.9. Mammalian cells containing sialylated glycans are treated with sodium periodate to oxidize the 1,2-diol moieties to an aldehyde. The aldehydes are detected through aniline-catalyzed oxime formation with an aminoxy-derivatized biotin followed by incubation with a fluorescent streptavidin. The degree of labeling is significantly enhanced by the use of aniline.

The other potential disadvantage of the condensation chemistry employed for modification of ketones and aldehydes is that an irreversible linkage is not obtained¹¹⁶ and hydrolysis could be problematic for certain applications.¹¹⁷ New chemistries for the aldehyde have recently been developed which lead to carbon-carbon bond formation. Loh and coworkers reported the modification of N-terminal aldehydes by a Mukaiyama aldol reaction (Figure 13.10A). Multiple ketene acetals were able to selectively modify peptide-associated aldehydes, although direct introduction of epitope tags or fluorophores has not been achieved using this reaction.¹¹⁸

The reactivity of the carbonyl group has also recently been converted from an electrophile into a 1,3 dipole such as a nitron or nitrile oxide for further modification through a cycloaddition reaction. The reactivity of nitrones with cyclooctynes was first reported by Pezacki and coworkers who demonstrated that the kinetics of this cycloaddition reaction were similar to or better than that for the azide-cyclooctyne reaction ($k = 0.088$ to $1.5 \text{ M}^{-1}\text{s}^{-1}$ vs. $0.062 \text{ M}^{-1}\text{s}^{-1}$ for the reaction with a variety of nitrones or benzyl azide, respectively).¹¹⁹ In their report, Pezacki and coworkers speculated that this could be a valuable bioorthogonal reaction; however, it was the Boons group in collaboration with van Delft and coworkers who first utilized this transformation to label a protein (Figure 13.10B).¹²⁰ Using a multistep procedure involving oxidation of the N-terminal serine residue in interleukin-8 to an aldehyde with sodium periodate, quenching of excess periodate with *p*-methoxybenzenethiol and condensation of the aldehyde with N-methylhydroxylamine in the presence of a *p*-anisidine gave a nitron. Finally, treatment with a PEGylated dibenzocyclooctyne yielded a selectively modified protein as determined by mass spectrometry.¹²⁰ Considering all the additives necessary for this transformation, deemed the strain-promoted azide-nitron cycloaddition (SPANC), it is most likely best suited for *in vitro* protein modification.

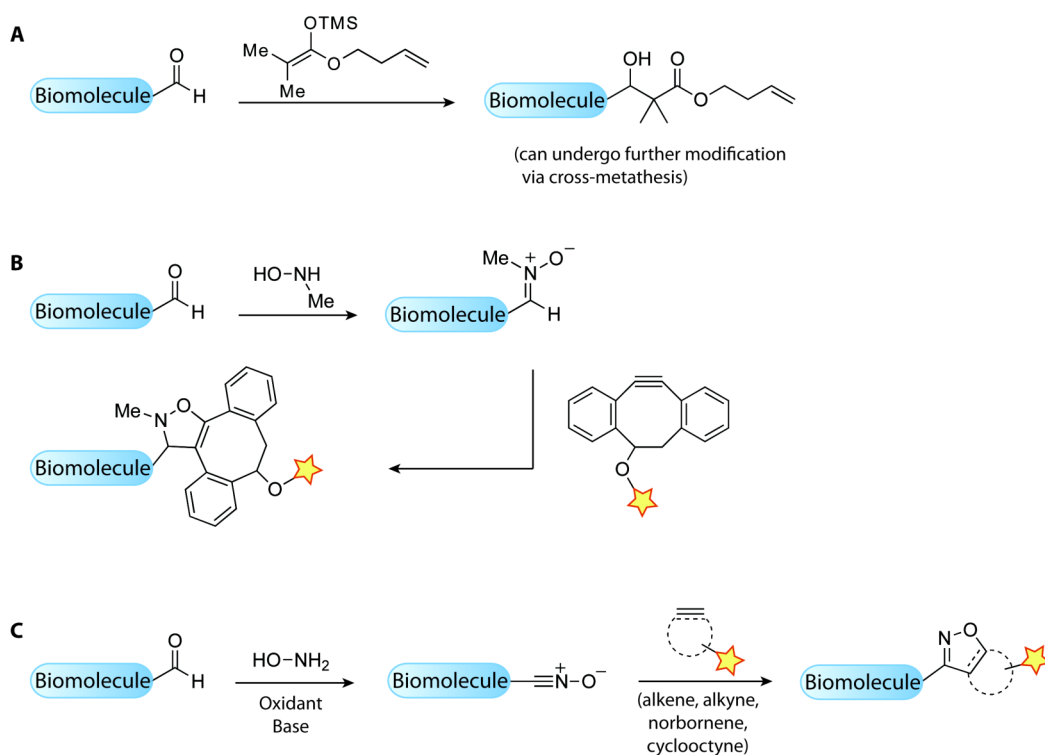


Figure 13.10. New chemistries for the aldehyde which form irreversible linkages. A. Biomolecule-associated aldehydes can be modified through a Mukaiyama aldol condensation with silyl ketene acetal reagents. B. Aldehydes can be converted to nitrones by condensation with N-methylhydroxylamine. The nitrones then undergo 1,3-dipolar cycloaddition with cyclooctyne reagents. C. Aldehydes can be converted to nitrile oxides by condensation with hydroxylamine followed by oxidation. The nitrile oxides can then undergo reaction with a variety of alkene or alkyne dipolarophiles, with strained reagents resulting in superior reaction rates.

Aldehydes have also been converted to nitrile oxides by condensation with hydroxylamine, oxidation with N-chlorosuccinamide, chloramine T, [bis(acetoxy)iodo]benzene, or phenyliodine bis(trifluoroacetate) and, for the case of chlorine oxidation, treatment with a mild base. The resulting nitrile oxide can undergo cycloaddition reaction with alkene or alkyne dipolarophiles (Figure 13.10C). This reaction has mainly been utilized for functionalization of oligonucleotides.^{121,122,123,124} The cycloaddition reaction with terminal alkenes and alkynes is relatively sluggish; however, the Carell and Heany group have modified norbornene or cyclooctyne functionalized DNA, respectively, with good efficiencies due to the increased ring strain of these dipolarophiles.^{125,126} The van Delft group has also modified nucleoside-associated cyclooctynes with nitrile oxides generated from aldehydes and hypervalent iodine species.¹²⁷ More recently, the Boons and Popik groups have done a thorough study regarding the rates of 1,3-dipolar cycloaddition between dibenzocyclooctyne **8.1** and various 1,3 dipoles including azides, nitrones, nitrile oxides, and diazocarbonyl species.

Through this study they have found that nitrile oxides are the most reactive partner for cyclooctynes ($k = 3.4 \text{ M}^{-1}\text{s}^{-1}$) followed by azides ($k = 0.059 \text{ M}^{-1}\text{s}^{-1}$), then diazocarbonyl species ($k = 0.031 \text{ M}^{-1}\text{s}^{-1}$) and nitrones ($k = 0.024 \text{ M}^{-1}\text{s}^{-1}$).¹²⁸

The Staudinger Ligation

The Staudinger ligation, now over a decade old, still has its place as the optimal bioorthogonal reaction for some applications. As highlighted in Chapter 4, it is the reaction of choice for labeling azides in mice. Brindle, Leeper and coworkers have recently performed a two-step *in vivo* labeling procedure where tumor-bearing mice containing azidosialoglycans were injected with Phos-biotin (**2.10**) followed by a fluorescent or radiolabeled NeutrAvidin protein. Azide-dependent labeling of the tumor was evident by optical and SPECT imaging techniques, although no azide-dependent labeling was observed in the remainder of the mouse.¹²⁹ Contrary to our results and those from the Brindle group, is recently published work regarding the application of the Staudinger ligation to labeling pretargeted antibodies *in vivo*. The Vugts group synthesized a number of triarylphosphine probes with applications for MRI, SPECT, and PET imaging. The pharmacokinetics of these reagents were analyzed in mice and the probes were cleared from the serum within an hour, a timescale that should allow for some Staudinger ligation to occur if high doses of the reagent are employed. However, when the probes were injected into mice containing azide-labeled antibody, no Staudinger ligation product was observed, most likely due to the slow kinetics of this bioorthogonal reaction and the potentially rapid clearance times of the pretargeted antibody. The authors concluded that the Staudinger ligation could not proceed in mouse serum due to nonspecific reactivity of the phosphine probes.

Despite the results from the Vugts group, the Staudinger ligation still remains the preferred bioorthogonal reaction for the azide in situations where selectivity is imperative, such as proteomic and activity-based profiling experiments.^{130,131} Many groups have used the Staudinger ligation to aid in azido-protein identification.^{132,133,134,135} Notably, the Bertozzi group has recently used Staudinger ligation aided proteomics to determine that N-azidoacetyl galactosamine (**2.17**) enables superior labeling of O-GlcNAcylated proteins than N-azidoacetyl glucosamine (**2.18**) does.¹³⁶ The Staudinger ligation has also been used as a method for immobilizing proteins to surfaces.^{137,138}

The traceless Staudinger ligation has seen modification over the past five years. Raines and coworkers have explored electronic, steric, and coulombic effects on the traceless Staudinger ligation^{139,140} and synthesized more water-soluble phosphine reagents.¹⁴¹ Additionally, progress toward solving the major liability of phosphine oxidation has been made. Toward this end, phosphine reagents can be protected as boranes and deprotected *in situ* prior to reaction with azides.¹⁴²

New applications of the traceless Staudinger ligation have been reported. Peptide cyclization has been achieved using a peptide with an N-terminal azidoacetate group and a C-terminal phosphine containing thioester (Figure 13.11).¹⁴³ The borane protecting group proved advantageous in this study. The traceless Staudinger ligation was employed to

append “reverse” N-linked glycans to model proteins, and surprisingly, this represents one of the first reports of this version of the Staudinger ligation on a whole protein.¹⁴⁴ The advantages of native amide bond formation using the traceless Staudinger ligation have also been employed for the preparation of ¹⁸F labeled metabolites for PET imaging.¹⁴⁵ As with the cyclic peptide synthesis, this study was aided by a borane-protected phosphine reagent.

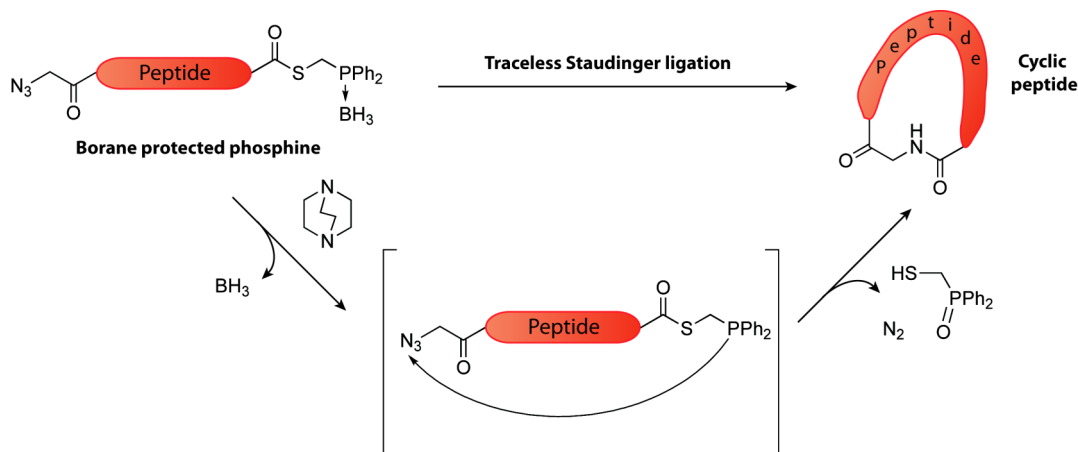


Figure 13.11. A peptide containing a C-terminal azide and N-terminal thioester appended with a borane-protected diarylphosphine readily undergoes cyclization by the traceless Staudinger ligation when the borane is deprotected with base.

Finally, the Hackenberger group has developed another modification of the Staudinger ligation: the Staudinger-phosphite ligation.¹⁴⁶ In this transformation, the azide undergoes nucleophilic attack by a phosphite reagent, following loss of nitrogen and hydrolysis, a stable phosphoramidite product is obtained. This reaction was first employed to modify protein-associated aryl azides to mimic phosphotyrosine residues.¹⁴⁶ Since the inaugural report, proteins have been PEGylated¹⁴⁷ and biotinylated¹⁴⁸ using appropriately functionalized phosphite reagents.

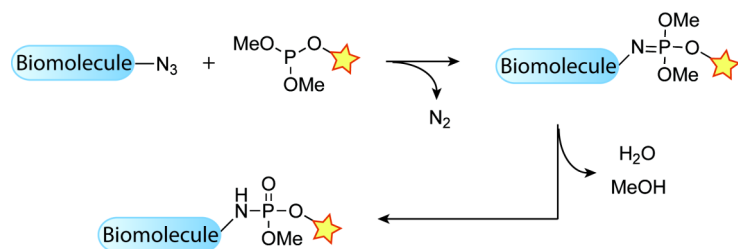


Figure 13.12. The Staudinger-phosphite ligation reaction. A labeled phosphite reagent can attack a biomolecule-associated azide to yield an azaylide intermediate which upon hydrolysis gives a stable phosphoramidite ligation product.

Cu-Catalyzed Azide-Alkyne Cycloaddition

An entire chapter could be composed of just applications of Cu-catalyzed click chemistry over the past few years. A number of recent reviews nicely summarize the advances click chemistry has made in chemical biology related fields.^{149,150,151,152,153,154,155,156,157,158,159} Many new alkynyl- and azido- metabolites have been developed to study biomolecules of interest by click chemistry methods. A selection of metabolites are shown in Figures 13.13-13.17 and range from amino acids, lipids, glycans, nucleic acids, fatty acids, acetyl groups, and cofactors. Additionally, the Cravatt group continues to use CuAAC to probe a variety of classes of enzymes through activity-based protein profiling.^{160,161,162,163}

Monosaccharides containing terminal alkyne residues such as alkynyl fucose (**13.4**)¹⁶⁴ and alkynyl N-acetyl mannosamine (**13.5**, alkynyl ManNAc)¹⁶⁴ have been shown to be well-tolerated by mammalian cells as evidenced by decreased toxicity of **13.4** compared to the azido analogue **13.6**.¹⁶⁵ Additionally, the incorporation of alkynyl ManNAc is superior when compared to N-azidoacetyl mannosamine (ManNAZ, **2.12**) *in vitro* and *in vivo*.¹⁶⁶ The disadvantage of these alkynyl sugars is the only bioorthogonal reaction available for their modification is Cu-catalyzed click chemistry, which limits their use for live cell labeling experiments. An excellent example of the utility of these alkynyl metabolites was a glycoproteomic study by Wong and coworkers, where sialylated glycoproteins labeled with alkynes due to alkynyl ManNAc incorporation were purified and identified using a CuAAC-mediated enrichment. The alkyne-associated glycans were tagged with biotin through CuAAC with an azide-biotin probe and captured on streptavidin-conjugated beads. Direct digestion of the proteins off the beads with trypsin and mass spectrometry analysis led to the identification of over 200 glycoproteins.¹⁶⁷

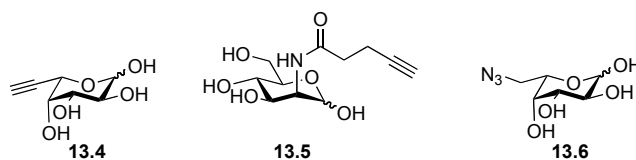


Figure 13.13. Recent alkynyl- and azidosugars employed for metabolic labeling of glycans.

Click chemistry continues to be a valuable readout for proteins containing alkynyl and azido unnatural amino acids. Homopropargylglycine (**2.35**) containing proteins in mammalian cells¹⁶⁸ and rat hippocampal neurons¹⁶⁹ have been visualized with CuAAC. Additionally, sequential labeling with homopropargylglycine and azidohomoalanine (**2.19**) has allowed distinct populations of proteins to be visualized simultaneously.^{169,170} These double-labeling experiments gave temporal information regarding globally synthesized proteins; however, imaging of a specific cell-type or species could not be performed. In order to achieve further selectivity, the Tirrell group utilized azidonorleucine (**13.7**) as their unnatural metabolite and engineered specific cells to express the appropriate amino acyl tRNA synthetase so that this unnatural amino acid would be selectively incorporated.¹⁷¹

Using a similar strategy, Hang and coworkers have employed 2-amino-octynoic acid (**13.8**) to tag bacterial proteins in mammalian hosts.¹⁷² This method represents a promising strategy for the study of infection. Additionally, a variety of new azido- and alkynyl-amino acids have been used for the site-specific modification of proteins by amber stop codon techniques. These amino acids include carbamylated lysine residues **13.9** and **13.10** and well as pyrrolysine derivative **13.11**.^{173,174}

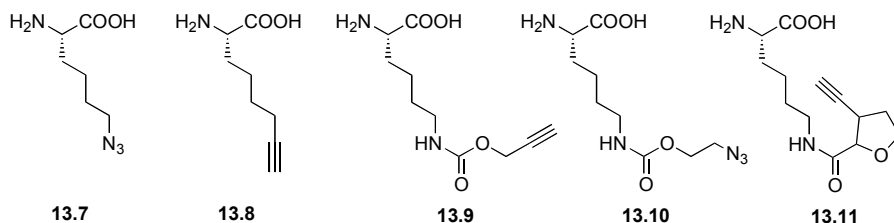


Figure 13.14. Azido- and alkynyl-derivatized unnatural amino acids.

Hang and coworkers have also made significant contributions toward the study of fatty acid acylation using bioorthogonal chemistries. In an early study, Hang *et al.* demonstrated that azide-labeled fatty acid **13.12** is converted *in situ* to the CoA analog and transferred to sites of myristoylation on endogenous proteins. The longer chain fatty acids **13.13-13.15**, by contrast, were attached to proteins at sites normally modified by palmitoylation.¹⁷⁵ Since this initial study, primarily alkynyl-fatty acids have been employed for protein lipidation studies in both mammalian¹⁷⁶ and bacterial systems.¹⁷⁷ Recently, the Hang group has focused on studying S-palmitoylation using alkynyl probes **13.16-13.18**.^{178,179} The dynamics of this system have been analyzed using a combination of unnatural amino acid incorporation (azidohomoalanine) and alkynyl fatty acids.¹⁸⁰ A similar strategy was used by Yao and coworkers to globally examine the dynamics of posttranslational modifications on newly synthesized proteins.¹⁸¹

Protein prenylation has also been analyzed using CuAAC. Toward this end, Distefano and coworkers synthesized azido and alkynyl isoprenoid analogues (**13.19-13.22**) and analyzed their abilities to be incorporated into proteins using in-gel fluorescence assays including 2D gels of proteins from mammalian cell lysates. Recently, Neef and Schultz have extended the bioorthogonal chemical reporter strategy to study the dynamics of phospholipids in bilayers.¹⁸² Alkyne-modified phosphatidic acids **13.23** and **13.24** were synthesized and introduced to mammalian cells. The S-acetylthioethyl (SATE) groups facilitated penetration of the cell membrane and were cleaved by esterases once inside the cytosol. Terminal alkyne-functionalized phospholipid **13.23** and nonhydrolyzable version **13.24** were visualized on fixed cells using CuAAC with an azidocoumarin dye.

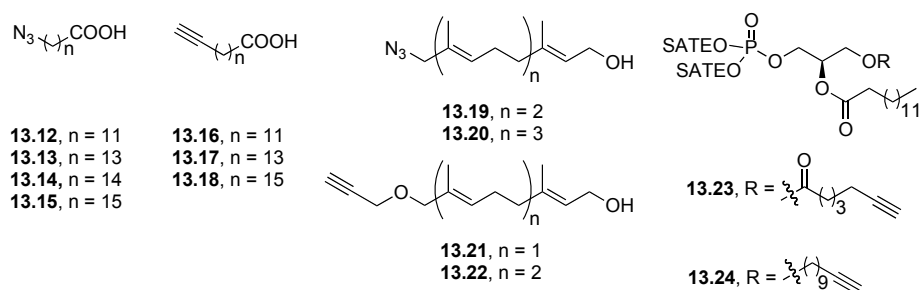


Figure 13.15. A selection of azido and alkynyl fatty acids, isoprenoids, and phospholipids employed for studying protein acylation, farnesylation or geranylation as well as the global dynamics of phospholipids. SATE = S-acetylthioethyl.

Choline phospholipids have also been visualized using a bioorthogonal chemical reporter strategy (Figure 13.16). In this case, propargyl choline **13.25** was introduced to mammalian cells and metabolically incorporated into phospholipid **13.26** with good efficiency on the hour timescale.¹⁸³ Furthermore, when injected into mice, click chemistry with a fluorescent azide performed on organ sections indicated incorporation of the propargyl group into lipid bilayers.

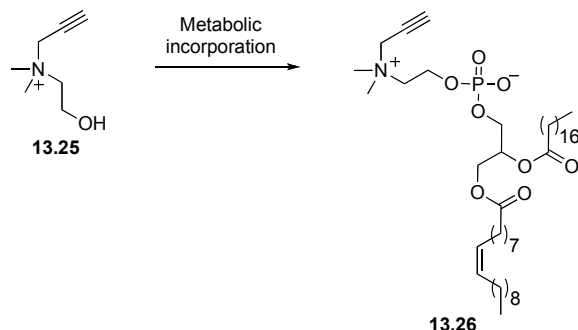


Figure 13.16. Propargyl choline **13.25** is elaborated into choline phospholipids by endogenous enzymes. Further elaboration by CuAAC allows for visualization of the phospholipids.

A significant breakthrough regarding click chemistry over the past five years is its use for visualizing DNA synthesis. Salic and Mitchison have reported that 5-ethynyl-2'-deoxyuridine (**13.27**, EdU) can be metabolically incorporated into DNA during replication and subsequently detected with an azido-fluorophore reagent through CuAAC. The alkynes can be detected on live cells if a cell-permeable fluorophore is employed, although the viability of cells is compromised after exposure to Cu(I). Using this procedure, newly synthesized DNA can be visualized quickly, with good sensitivity under milder conditions than the traditional method using 5-bromo-2'-deoxyuridine (BrdU) and a corresponding antibody.^{184,185} EdU is even effective for visualizing cells undergoing DNA synthesis in mice. More recently, RNA synthesis has been imaged using 5-ethynyluridine (**13.28**, EU) and fluorescent azides in an analogous method.¹⁸⁶ The azido analog of EdU, 5-azido-2'-

Arguably, the biggest advance for Cu-catalyzed click chemistry in the past five years has not been the array of biological processes probed using this chemistry but the chemical advances toward minimizing the toxic side effects of this reaction. Finn and coworkers have analyzed the cause of Cu(I) toxicity to be from the propensity to form reactive oxygen species. Using additives to combat these reactive oxygen species- mainly hydroxylated tris(triazolylmethyl)amine ligand **13.31** (THPTA, Figure 13.18), as opposed to the more traditional aryl containing TBTA ligand (**2.37**, Figure 2.13), and amino-guanidine (**13.32**) Cu-click chemistry was successfully performed on live HeLa, Chinese hamster ovary (CHO), and Jurkat cells.¹⁹⁸ Wu and coworkers have also directed their efforts toward developing reaction conditions and ligands for Cu-click chemistry which facilitate live cell labeling, primarily due to the increased reaction kinetics which minimize exposure times to Cu(I). Through ligand screens, the Wu group has identified two new tris(triazole) ligands for CuAAC: bis(*tert*-butyltriazolyl) ligand **13.33** (BTES)¹⁹⁹ and **13.34** (BTAA)²⁰⁰, which contain sulfonate and acetate solubilizing groups respectively. BTAA proved to be the most reactive of the catalysts for CuAAC and allowed for labeling of alkyne containing glycoproteins on live cells and zebrafish.²⁰⁰ A significant rate increase for CuAAC has also been obtained by using 1-iodoalkynes. These alkynes have not been used for biological labeling experiments, perhaps due to the large atomic radius of iodine, but, nevertheless, represents an interesting avenue of future research.²⁰¹

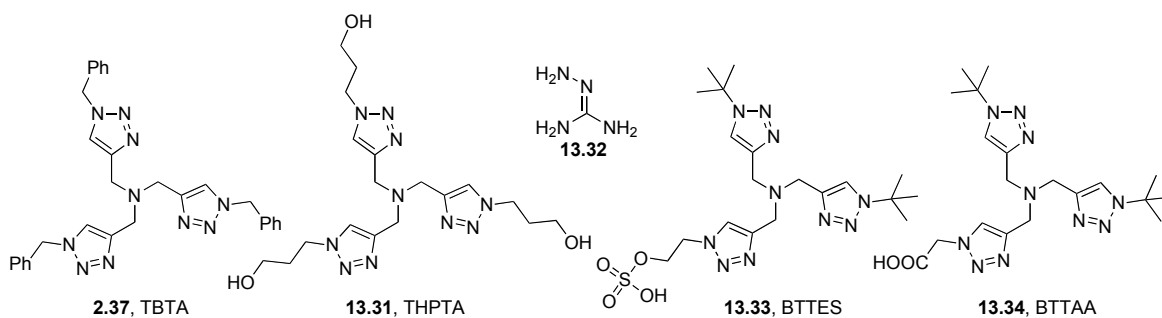


Figure 13.18. Ligands and additives for Cu-catalyzed azide-alkyne cycloaddition.

Cu-Free Click Chemistry

Cu-free click chemistry has undergone substantial improvements over the past five years, a significant portion of which has been outlined through Chapters 3-9. Many groups have joined the quest for highly reactive yet bioorthogonal cyclooctyne reagents. All the cyclooctynes synthesized for Cu-free click chemistry that contain a functional handle for probe conjugation appear in Figure 13.19. In addition to DIMAC and the early generation cyclooctynes described in Chapter 2, another monofluorinated cyclooctyne with similar kinetics but a more facile synthesis has been reported (MOFO2, Figure 13.19, **13.35**).²⁰² This is also the case for DIFO, as Leeper and coworkers recently reported a new, Selectfluor-free synthesis of difluorinated cyclooctyne **13.36**, which contains an alcohol for further conjugation to an epitope tag.²⁰³

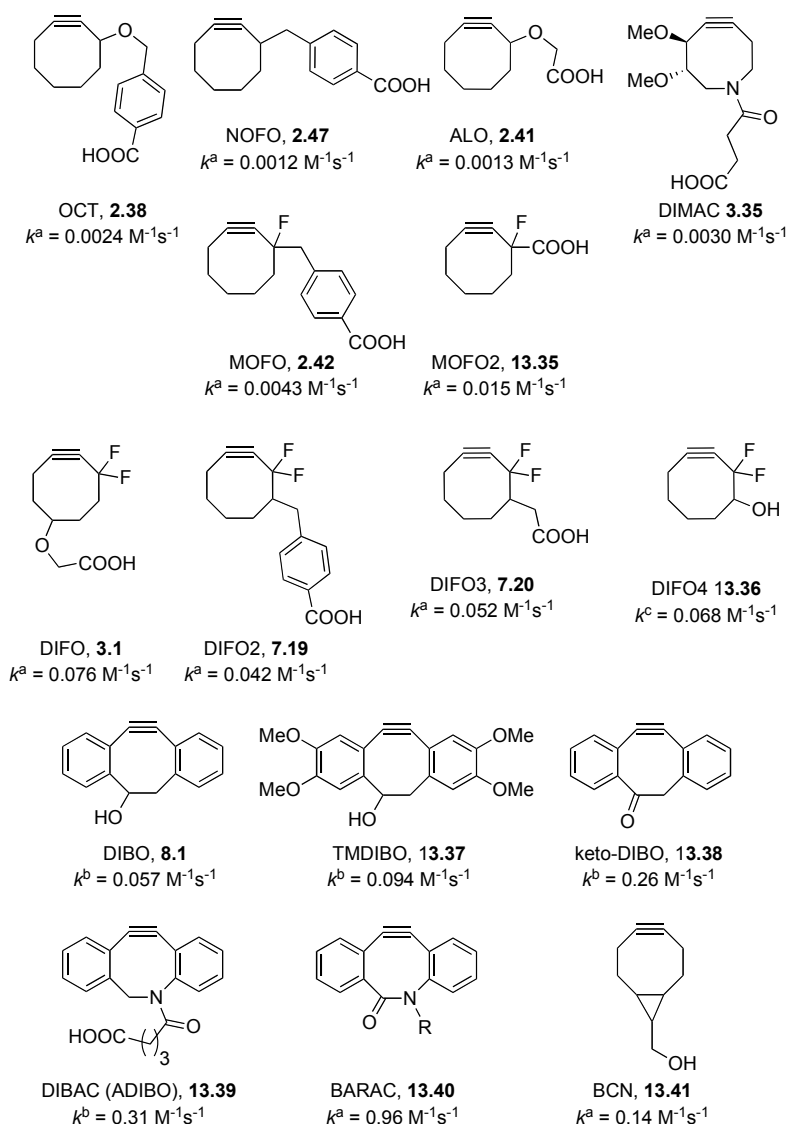


Figure 13.19. Cyclooctynes for Cu-free click chemistry and their second-order rate constants for reaction with benzyl azide measured in (a) CD_3CN , (b) MeOD , or (c) CDCl_3 .

Activation by increased ring strain through fused phenyl rings has become a lucrative means to obtain highly reactive yet stable cyclooctynes. DIBO marked the first cyclooctyne of this nature used for Cu-free click chemistry,²⁰⁴ but since then variations on DIBO have been synthesized. In the same account as the fourth generation DIFO molecule, a tetramethoxy version of DIBO (TMDIBO, **13.37**) was reported, which had slightly enhanced kinetics, stability, and solubility properties as compared to DIBO.²⁰³ The alcohol of DIBO has also been oxidized to a ketone (keto-DIBO, **13.38**) and probes can be conjugated to this molecule through oxime or hydrazone formation. Interestingly,

keto-DIBO undergoes spectral changes upon reaction with an azide as the initial cyclooctyne is fluorescent but the triazole products are dark.²⁰⁵ Unfortunately, this spectral change is not nearly as useful as one where fluorescence is obtained upon reaction with an azide (as discussed in Chapter 5). Keto-DIBO also had improved reaction kinetics over DIBO ($k = 0.26 \text{ M}^{-1}\text{s}^{-1}$), demonstrating that an additional sp^2 center adds a significant amount of strain to the cyclooctyne. Also noteworthy was this report contained an improved synthesis of DIBO, which relies on a homologation ring-expansion strategy.

An additional sp^2 center has also been added to the DIBO through the addition of an amide in either an exocyclic or endocyclic fashion. Compound **13.39**, reported by the van Delft²⁰⁶ and Popik²⁰⁷ groups and named DIBAC or ADIBO respectively, contains an exocyclic amide and has a second order rate constant of $0.31 \text{ M}^{-1}\text{s}^{-1}$, over two orders of magnitude faster than the original cyclooctynes. DIBAC is now commercially available and many groups are beginning to employ this reagent to label azides in biological systems. While the Popik and van Delft groups were working toward DIMAC/ADIBO, we were developing a biarylazacyclooctynone (BARAC, **13.40**), which contains an endocyclic amide, resulting in additional unsaturation within the cyclooctyne ring.²⁰⁸ BARAC proved to be the fastest cyclooctyne developed for Cu-free click chemistry to date with a second-order rate constant of $0.96 \text{ M}^{-1}\text{s}^{-1}$. This rate constant was readily translated to live cells and a timecourse comparison experiment between DIFO, DIBO, and BARAC (Figure 13.20A) showcases the superior reaction kinetics BARAC displays. In fact, BARAC was so reactive that azide-dependent cell-surface labeling could be observed without washing away excess reagent (Figure 13.20B).

We have since performed a thorough analysis of BARAC's structure and reactivity aided by X-ray crystallography, DFT calculations (in collaboration with the Houk group), and experimental data from BARAC analogues. The results from these studies suggest that increased ring strain, which results in decreased distortion energy necessary to reach the transition state for the cycloaddition reaction,²⁰⁹ dominates the electronic effects from the addition of electron withdrawing (or donating) substituents.²¹⁰

The other exciting advance BARAC has enabled is the synthesis of the first fluorogenic cyclooctyne. One of the aryl rings of BARAC was converted into a coumarin to yield coumBARAC **13.42** (Figure 13.21).²¹¹ This compound displays a 10-fold increase in fluorescence upon reaction with azides; however, its spectral properties will need to be tuned for widespread use. In its current form, the desired excitation wavelength is 305 nm, which is higher in energy than is compatible with standard microscopes.

Another intriguing cyclooctyne structure is the bicyclononyne (BCN, **13.41**) reported by the van Delft group.²¹² This cyclooctyne contains a fused cyclopropane ring across from the alkyne which leads to a surprising rate-enhancement ($k = 0.14 \text{ M}^{-1}\text{s}^{-1}$, 58-fold over OCT) most likely due to a combination of increased strain from the ring fusion and decreased steric interactions during the cycloaddition transition state. It does appear that this cyclooctyne is more prone to side-reactivity in biological labeling experiments, which could stem from the decreased steric protection of the alkyne. BCN has recently seen application as a method of surface functionalization for ELISA assays.²¹³

Hosoya and coworkers have used dibenzocyclooctadiyne **13.43** as a “converter” to facilitate labeling of azido-proteins with dyes conjugated to azides (Figure 13.22).²¹⁴ With dibenzocyclooctadiyne the first Cu-free click reaction is slower than the second cycloaddition. Surprisingly, Hosoya only characterized a small amount of protein dimerization when combining **13.43** with an azido-fluorophore and model azide-labeled protein.

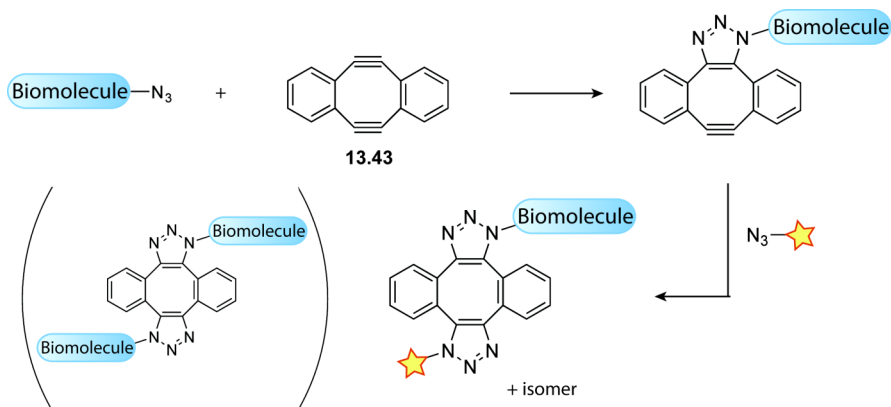


Figure 13.22. A strategy for labeling azide-modified biomolecules with azide-probes by employing dibenzocyclooctadiyne as a linker molecule.

In a collaborative effort, the Popik and Boons groups have developed a photo-caged version of DIBO, compound **13.44**, where the alkyne is masked as a cyclopropenone (Figure 13.23).²¹⁵ Irradiation with 355 nm light prompted formation of the dibenzocyclooctyne scaffold (**13.45**). Thus, this reagent should allow for spatiotemporal control of Cu-free click chemistry in biological systems. In the initial report of this molecule, labeling of azido-glycans was demonstrated, but photo-caged DIBO has since seen use for surface functionalization and patterning.²¹⁶

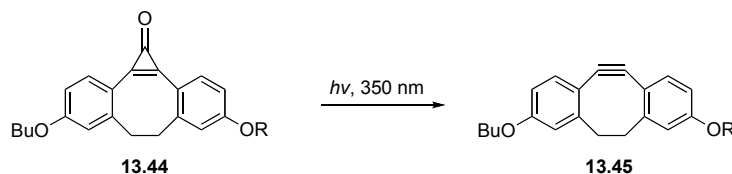


Figure 13.23. A photo-caged dibenzocyclooctyne for spatiotemporal labeling of azides.

Many of the above cyclooctynes have been used to label azide-tagged glycans. Boons and coworkers have used keto-DIBO in conjunction with lectin staining to study the relative amounts of O- and N-sialylated and galactosylated glycans in mammalian cells with altered glycans.²⁰⁵ As described throughout the text of this thesis, we have labeled azido-glycans in a variety of organisms using DIFO-reagents.^{217,218,219,220} Zebrafish have

been particularly lucrative higher organisms for imaging azide-associated glycans.^{114,219} The most recent additions include imaging of azido-fucose²²¹ and azido-sialic acid through the course of zebrafish development. Texier and coworkers have conjugated the early generation cyclooctyne ALO (**2.41**) to quantum dots and shown that the advantageous spectral properties of quantum dots allow for this cyclooctyne with slow reaction kinetics to be employed for imaging of azides on cell-surface glycans.²²² We also used DIFO probes to detect incorporation of an azidosugar which was uncaged only in the presence of the protease prostate specific antigen.²²³ This study represents our initial efforts toward selective incorporation of azidosugars.

Proteins containing azides through either metabolic or enzymatic incorporation have been detected with cyclooctyne reagents. Tirrell and coworkers have used OCT, MOFO, and DIFO reagents to globally label proteins modified with azides.^{169,224,225} Through this work, the Tirrell group discovered that when conjugated to coumarin²²⁴ or bodipy²²⁵ dyes, the cyclooctynes are rendered cell-permeable. Ting and coworkers have also employed a variety of cyclooctyne probes to label proteins tagged with azides by lipoic acid ligase.⁷⁹

Cu-free click chemistry, in conjunction with cleavable linker strategies, has also been used for the purification and identification of azide-labeled proteins, in an approach analogous to that proposed in Chapter 6. De Koster and coworkers have employed the nonfluorinated cyclooctyne (NOFO, **2.47**) connected to a disulfide linker to purify *E. coli* proteins labeled with azidohomoalaine.²²⁶ Recent work from the van Hest group has employed BCN conjugated to a sterically hindered ester, which is readily cleaved by hydrazine, to isolate a model azide-modified protein.²²⁷

The highly selective and rapid nature of the azide-cyclooctyne cycloaddition reaction has resulted in its implementation for functionalization of oligonucleotides, peptides, and polymers. Oligonucleotides have been adorned with cyclooctyne probes to facilitate conjugation to other more chemically sensitive moieties, which are not amenable to standard methods for solid phase DNA or RNA synthesis.^{228,229,230,231,232} Heemstra and coworkers have used a split-aptamer system for the detection of cocaine where one half of the aptamer was modified with an azide and the other with the cyclooctyne ALO (**2.41**).²³³ MOFO2 (**13.35**) has been employed for the synthesis of DOTA-conjugates^{202,234,235} and spin labels.²³⁶ In addition, MOFO2 has been applied to a liposome quantification assay.²³⁷ Cyclooctynes have been used to functionalize polymers and dendrimers labeled with azides.^{238,239,240,241} Other materials applications for Cu-free click chemistry include the formation of biofriendly hydrogels^{242,243} and photodegradable polymeric materials.²⁴⁴

Despite their large size, cyclooctynes are also beginning to make their way into biomolecules as chemical reporter groups (Figure 13.24). Neef and Schultz were the first to integrate a cyclooctyne into a biomolecule for a cell-based study by appending it to a phospholipid (compound **13.46**) and visualizing the dynamics of lipid bilayers on live cells.¹⁸² A cyclooctyne SAM analogue (**13.47**)²⁴⁵ as well as a DIFO2 modified nucleotide (**13.48**)²³² have been reported, although they have yet to be used in living systems. Burkhart and coworkers have used DIFO2-functionalized pantetheine probe **13.49** in conjunction with an azidopantetheine probe to study protein-protein interactions in non-ribosomal peptide synthesis.²⁴⁶ Finally, in an impressive demonstration of unnatural amino

acid incorporation, Lemke and coworkers have incorporated cyclooctyne amino acids **13.51** and **13.52** in a site-specific manner into proteins in *E. coli*.²⁴⁷ These proteins were then detected with fluorogenic azido-coumarin **2.34** in an experiment similar to that reported by Beatty *et. al* (Figure 2.13), except no Cu-catalyst was necessary.

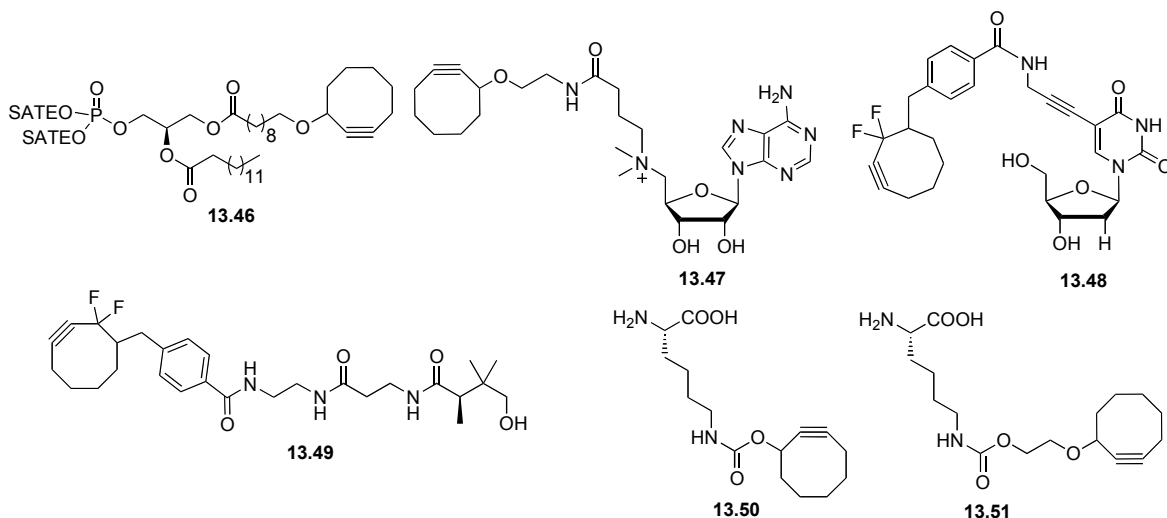


Figure 13.24. Metabolites adorned with cyclooctyne reagents for use in the bioorthogonal chemical reporter strategy. SATE = S-acetylthioethyl.

The Tetrazine Ligation

A major advance in the field of bioorthogonal chemistry over the past five years has been the tetrazine ligation. This reaction is an inverse-electron demand Diels-Alder reaction between a strained alkene and tetrazine (Figure 13.25). The initial alkene-tetrazine reaction yields cycloadduct **13.52**, which readily loses nitrogen to produce dihydropyridazine **13.53** that tautomerizes to final ligation product **13.54**. Three groups independently reported this reaction in late 2008 to early 2009.^{248,249,250}

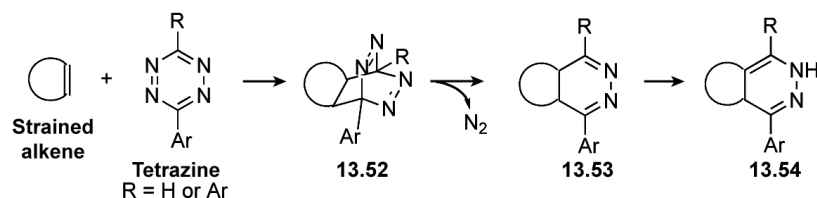


Figure 13.25. The tetrazine ligation: An inverse-electron demand Diels-Alder reaction between tetrazines and strained alkenes.

Fox and coworkers developed the reaction of *trans*-cyclooctene **13.55** with bipyridyl tetrazine **13.56** to yield **13.57** and its isomers (Scheme 13.26A).²⁴⁸ At the time, this reaction was the fastest bioorthogonal chemical reaction reported to date ($k \sim 10^3 \text{ M}^{-1}\text{s}^{-1}$). In simple biological systems, which lack thiols, tetrazine **13.56** was very effective at selectively modifying *trans*-cyclooctene, as demonstrated by the reaction of *trans*-cyclooctene-functionalized thioredoxin and bipyridyl tetrazine **13.56**. However, tetrazine **13.56**, which had been optimized for reaction kinetics, displayed some background reactivity with amines, thiols, and water.²⁴⁸

Hilderbrand, Weissleder and coworkers developed a norbornene-tetrazine ligation and used it to label antibodies on live cells. The Hilderbrand version of the tetrazine ligation (Scheme 13.26B) involved the reaction of norbornene **13.58** and mono-aryl tetrazine **13.59** to yield ligation product **13.60** (and isomers).²⁴⁹ This reaction is slower ($k \sim 1 \text{ M}^{-1}\text{s}^{-1}$) than the reaction reported by Fox and coworkers but still as rapid as the fastest cyclooctyne reagent for Cu-free click chemistry. The bioorthogonality of this reaction was tested by the conjugation of norbornene and rhodamine to a monoclonal antibody. The doubly labeled antibody was introduced to cells expressing the corresponding antigen. After allowing time for clearing of excess antibody, the cells were incubated with tetrazine **13.59** linked to a near IR dye (VT680). The cells were imaged and robust colocalization between the rhodamine and VT680 was observed, indicating that the tetrazine ligation is selective for norbornene on live cells.²⁴⁹

The third version of the tetrazine ligation was developed by Pipkorn and coworkers as a method to ligate a peptide to the drug candidate temozolomide (TMZ). This ligation involved the Diels-Alder reaction of cyclobutene **13.61** and biaryltetrazine **13.62** to form product **13.63** and its tautomer (Scheme 13.26C).²⁵⁰ The kinetics and selectivity of the ligation reaction were not analyzed in this report. However, the reaction is compatible with aqueous solution containing amines and disulfides. Since their initial report, Pipkorn and coworkers have continued to use this system to ligate TMZ to various molecules that promote selective delivery of this chemotherapeutic.^{251,252,253,254}

Since these three initial reports Weissleder, Hilderbrand and coworkers have elegantly demonstrated the bioorthogonality and potential of this rapid ligation reaction. The *trans*-cyclooctene (**13.55**) reported by Fox has become the strained alkene of choice due to its rapid reactivity with tetrazine reagents and its pairing with the monoaryl tetrazine (**13.59**) results in a rapid bioorthogonal reaction ($k = 6000 \text{ M}^{-1}\text{s}^{-1}$) where both partners are reasonably stable in biological systems.²⁵⁵ Using a *trans*-cyclooctene modified EGFR antibody and fluorescent VT680-tetrazine **13.64**, Weissleder and coworkers imaged A549 cancer cells and showed that washing steps were not necessary to give ample signal-to-noise (Figure 13.27A).²⁵⁵ Additionally, Robillard and coworkers quickly adopted this bioorthogonal reaction for use *in vivo*.²⁵⁶ In 2010, just two years after the introduction of this reaction, a tetrazine-DOTA conjugate **13.65** was used for SPECT imaging of *trans*-cyclooctene modified CC49 antibodies in living mice (Figure 13.27B).²⁵⁶ This successful study is in stark contrast to the results from Vugts and coworkers who attempted a similar pretargeted antibody strategy *in vivo* with the Staudinger ligation and highlights the advantages of rapid reaction kinetics.

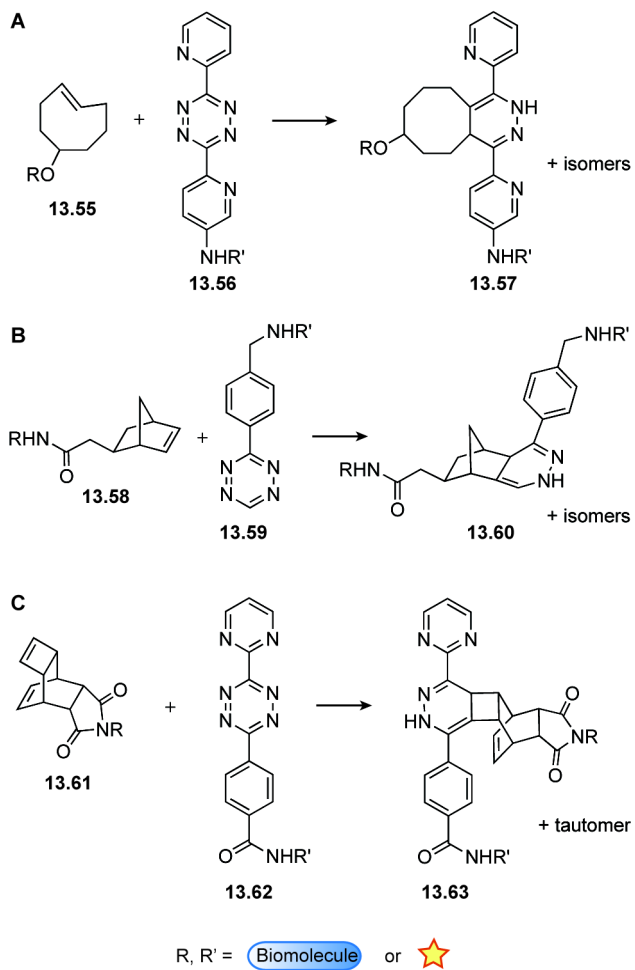


Figure 13.26. The three variations of the tetrazine ligation, which were independently developed by the (A) Fox, (B) Hilderbrand/Weissleder, and (C) Pipkorn groups.

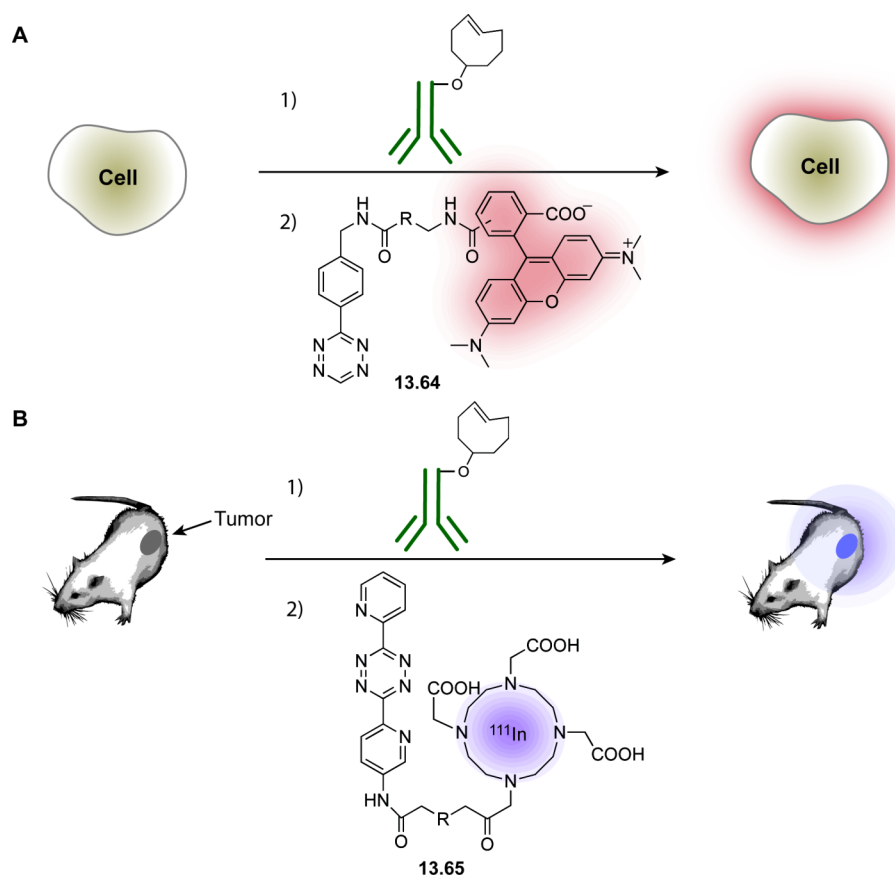


Figure 13.27. Applications of the tetrazine ligation to detection of pretargeted antibodies on (A) live cells and (B) in living mice. A. Anti-EGFR was modified with a *trans*-cyclooctene and introduced to cancer cells. The cells were then incubated with VT680-tetrazine **13.64**. Fluorescence was observed for cells which expressed EGFR on their cell-surfaces. The labeling was so effective that washing away excess **13.64** was not necessary. B. An anti-CC49 antibody was modified with a *trans*-cyclooctene and injected into tumor bearing mice, where CC49 was expressed within the tumor. A DOTA-conjugated tetrazine was loaded with ^{111}In (**13.65**) and injected into the mice containing tumors and labeled-antibodies. Robust SPECT signal was evident from the tumors when both reaction components were present. In **13.64** and **13.65** R represents a linker group.

There have been a number of reports for the use of the tetrazine ligation to prepare antibodies and small molecules for PET imaging with ^{18}F probes.^{257,258,259,260} The kinetics of the tetrazine ligation reaction are well suited for use with ^{18}F due to the very short half-life (~110 min) of this radionuclide, and we anticipate *in vivo* PET imaging that was facilitated by the tetrazine ligation will be reported in the near future.

The tetrazine ligation is also applicable for intracellular labeling. When conjugated to a bodipy dye (**13.66**) the tetrazine was not only rendered cell-permeable but the tetrazine moiety quenched the fluorescence of the bodipy serendipitously creating a fluorogenic

reagent (Figure 13.28).²⁶¹ Weissleder and coworkers elegantly used this fluorogenic tetrazine to visualize taxol-induced microtubule stabilization by treatment of cells with a *trans*-cyclooctene modified taxol followed by the fluorogenic tetrazine reagent.²⁶¹ Efforts are also underway by the Weissleder group to employ the tetrazine ligation for nanoparticle targeting to aid both extra- and intracellular biomarker detection.^{262,263}

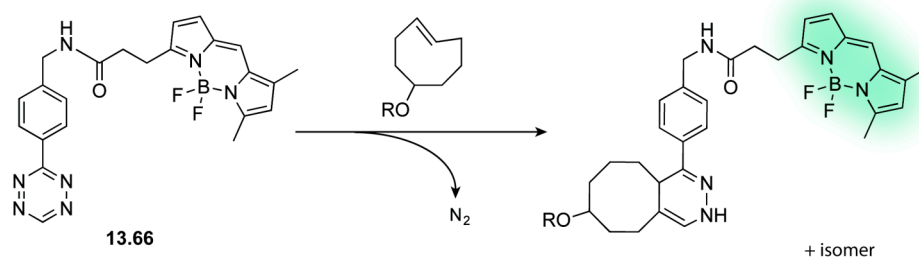


Figure 13.28. A fluorogenic and cell-permeable tetrazine for intracellular labeling of *trans*-cyclooctenes. If R = Taxol microtubule formation can be visualized.

As was the case with Cu-free click chemistry, the tetrazine ligation is beginning to be used for applications other than imaging living systems. Jaschke and coworkers have recently reported the functionalization of norbornene-containing DNA using this ligation,²⁶⁴ while Pipkorn and coworkers have used their version of the reaction to modify peptide nucleic acids.^{265,266} Bawendi, in collaboration with Hilderbrand and Weissleder, have prepared norbornene-modified quantum dots for use with the tetrazine ligation.²⁶⁷ Norbornene-containing polymers have also recently been functionalized through reaction with modified tetrazines.²⁶⁸

Despite the impressive kinetics of this bioorthogonal reaction, efforts have been directed toward further increasing the speed of the ligation. The Fox group has increased the second-order rate constant of the tetrazine an order of magnitude ($k = 22000 \text{ M}^{-1}\text{s}^{-1}$) through the fusion of a cyclopropyl group across the ring from the *trans*-alkene²⁶⁹ (**13.67**, Figure 13.29A), in a manner similar to that employed for the rate enhancement of Cu-free click chemistry with BCN (**13.41**).²¹² The Fox group was aided by DFT calculation in the design of *trans*-bicyclononyne **13.67**, and demonstrated that the fusion of a cyclopropyl group to this position prevents the *trans*-cyclooctene from sitting in the most stable “crown” confirmation.²⁶⁹ Perhaps a similar effect can be attributed to the rate-enhancement in BCN. It should be noted that this sizeable second-order rate constant is for the reaction with dipyrindyl tetrazine **13.68**, which suffers background reactivity in biological milieu.

Leeper and coworkers have also contributed to *trans*-cyclooctene reagent development. They prepared a *trans-trans*-1,5-cyclooctadiene **13.69** (Figure 13.29B), which can undergo ligation reactions with tetrazine **13.68** ($k = 8,900 \text{ M}^{-1}\text{s}^{-1}$) to yield **13.70** or **13.71** if excess tetrazine is employed (second Diels-Alder reaction has a rate constant of $450 \text{ M}^{-1}\text{s}^{-1}$). Additionally, **13.69** undergoes cycloaddition reaction with azides, although with at a slower rate ($k = 0.02 \text{ M}^{-1}$).²⁷⁰ The azide cycloaddition product **13.72** can be

isolated, and the resulting functionalized *trans*-cyclooctene can undergo tetrazine ligation to yield **13.73**. Thus, the *trans,trans*-1,5-cyclooctadiene represents a strategy for the preparation of modified *trans*-cyclooctenes.

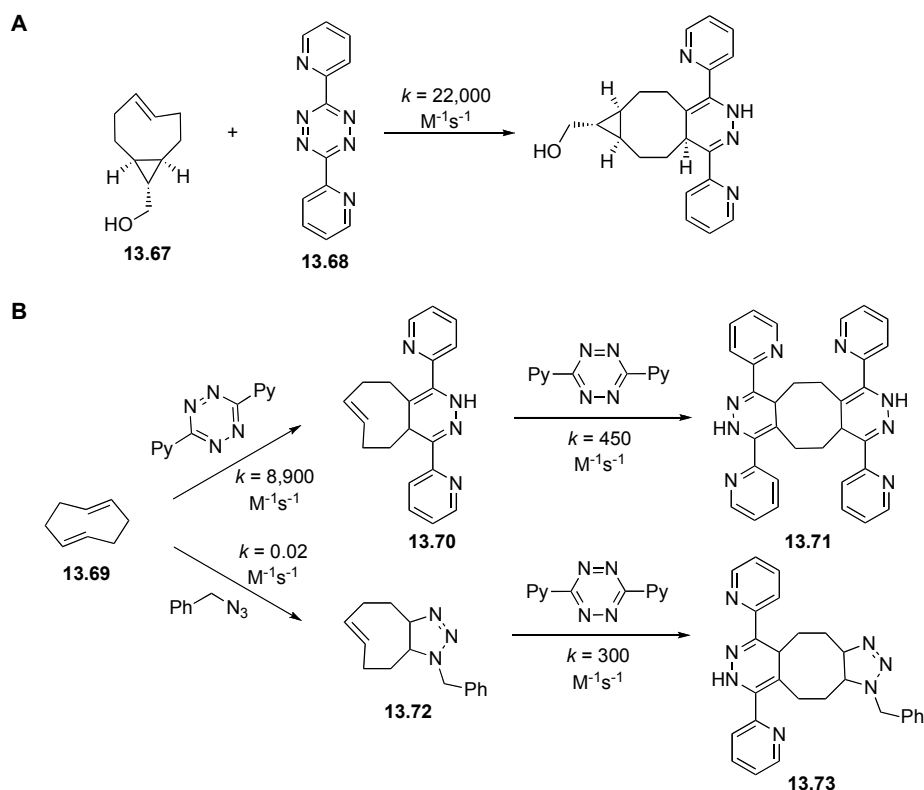


Figure 13.29. New *trans*-cyclooctene reagents for the tetrazine ligation. A. A cyclopropyl fused *trans*-cyclooctene exhibits remarkably fast reaction kinetics when combined with tetrazines. B. *Trans, trans*-1,5-cyclooctadiene readily reacts with tetrazine reagents to yield mono- or diaddition products. The *trans, trans*-1,5-cyclooctadiene is also sufficiently strained to undergo cycloaddition reaction with azide reagents and triazoline **13.72** can be isolated and further reacted with tetrazine reagents.

Currently, the main limitation of the tetrazine ligation is that neither the *trans*-cyclooctene or the tetrazine appear to be stable or small enough to withstand metabolic incorporation, and thus, cannot be effectively used as a chemical reporter group. The stability appears to be the major factor as relatively large groups, such as cyclooctyne, have recently been incorporated into proteins. While not as activated of a reaction partner, norbornene should be stable enough for metabolic incorporation and could be an avenue for use of the bioorthogonal chemical reporter strategy with this impressive ligation reaction.

Photoclick Chemistry

Another bioorthogonal chemical reaction that has made great strides over just a few years is photoclick chemistry. This bioorthogonal reaction was developed by the Lin group and involves the cycloaddition of alkenes and nitrile imines, which are generated *in situ* by UV irradiation of tetrazoles.²⁷¹ In the inaugural report of this reaction, nitrile imine **13.74**, generated from irradiation of tetrazole **13.75** with 290 nm light, was reacted with alkene **13.76** to yield pyrazoline **13.77** (Figure 13.30).²⁷¹ The formation of the dipole **13.74** is fast ($k \sim 10^{-1} \text{ s}^{-1}$), as is the cycloaddition ($k \sim 10^1 \text{ M}^{-1} \text{ s}^{-1}$) with activated alkene **13.76**. However, **13.76** is also a good Michael acceptor and not suitable for use as a chemical reporter group. An advantage of the alkene-tetrazole reaction is that the resulting pyrazoline cycloadducts are fluorescent, facilitating direct detection of the reaction within a biological system.

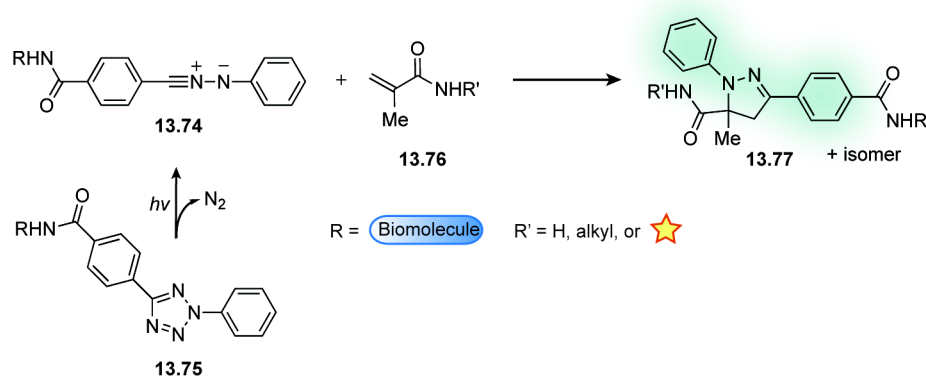


Figure 13.30. The initial report of photoclick chemistry involving *in situ* generation of a nitrile imine dipole from a tetrazole and subsequent cycloaddition with activated alkene **13.76**.

The tetrazole reagents have been modified with efforts toward increasing the rate of the cycloaddition with unactivated alkenes (Figure 13.31). Electron donating groups were most effective at enhancing the rate of the cycloaddition, with tetrazole **13.78** having a rate-constant of $0.79 \text{ M}^{-1} \text{ s}^{-1}$ for reaction with a terminal alkene.²⁷² Macrocyclic tetrazoles such as **13.79** were also employed in attempt to add distortion to the *in situ* generated nitrile imine dipole.²⁷³ A variety of tetrazole reagents were prepared to screen for dipole formation upon irradiation with lower energy light, as the original 290 nm light is not particularly friendly to living systems.^{274,275} Through these studies tetrazole **13.80** was found which produced a nitrile imine dipole when subjected to 365 nm light.²⁷⁵ Biotinylated and bodipy-conjugated tetrazoles have also been synthesized for use in biological labeling experiments.²⁷⁶

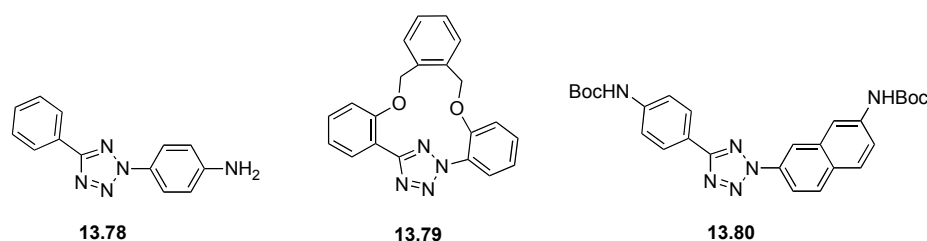


Figure 13.31. Selected optimized tetrazoles for photoclick chemistry.

Since photoclick chemistry does not require a large, strained alkene, it is more easily employed for the labeling of metabolically modified biomolecules through the bioorthogonal chemical reporter strategy. Toward this end, Lin and coworkers site-specifically incorporated O-allyl tyrosine (**13.81**) using amber stop codon techniques (*i.e.* Schultz method) into a Z-domain protein in *E. coli*.²⁷⁷ Upon treatment with tetrazole **13.82** and 302 nm light overnight, alkene-modified *E. coli* were selectively labeled (Figure 13.32A). The success of photoclick chemistry in bacteria prompted a move toward mammalian cells. In this study, the amino acid homoallylglycine (**13.83**) was metabolically incorporated into all proteins in place of methionine (*i.e.* Tirrell method).²⁷⁶ Using tetrazole **13.84** alkene-dependent labeling was evident by microscopy and flow cytometry (Figure 13.32B), although background labeling was considerable during flow cytometry analysis, perhaps due to reaction with alkene-containing metabolites in the cytosol. In this same study, Lin and coworkers also showed that selective irradiation could lead to spatiotemporal imaging of homoallylglycine-labeled proteins.²⁷⁶

In order to prevent background reaction with intracellular metabolites and increase the reaction kinetics of the cycloaddition by employing more activated alkenes, Lin and coworkers have looked to use tetrazoles as chemical reporter groups. They have synthesized tetrazole containing amino acids²⁷⁸ and, in collaboration with the Wang group, have site-specifically incorporated tetrazole amino acid **13.83** into myoglobin in *E. coli*.²⁷⁹ The tetrazole containing proteins were detected in cell lysate with an activated alkene conjugated to fluorescein (**13.86**). It should be noted that this is not the first report of a photoactivatable group being incorporated into proteins as diazirines,^{280,281,282} aryl azides,²⁸³ and ketones²⁸⁴ have all been employed for photocrosslinking studies.

The Lin group has also incorporated a tetrazole amino acid into the enhanced green fluorescent protein eGFP by native chemical ligation methods.²⁸⁵ The tetrazole was then functionalized with a lipid to yield a model for protein lipidation. Microtubule formation has also been visualized through conjugation of a tetrazole and alkene to taxol in a manner similar to that first performed by Weissleder and coworkers with the tetrazine ligation,²⁶¹ except that with photoclick chemistry an intramolecular, photoinduced, fluorogenic reaction is employed.²⁸⁶ Photoclick chemistry has also been recently used to create stapled peptides.^{287,288}

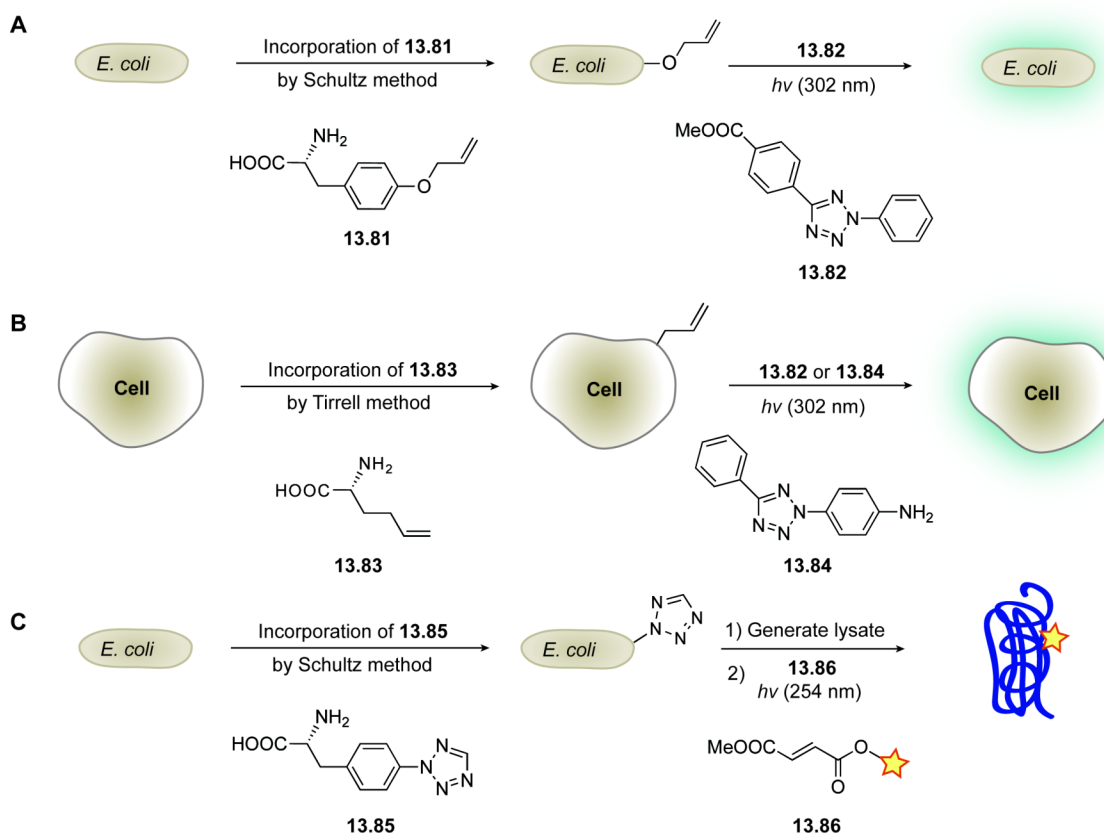


Figure 13.32. Photoclick chemistry is effective for labeling alkenes or tetrazoles metabolically installed into proteins. **A.** The amino acid O-allyl tyrosine (**13.81**) can be site-specifically installed into a Z-domain protein in *E. coli* and labeled with tetrazine **13.82**. **B.** Homoallylglycine (**13.83**) can be globally incorporated into newly synthesized proteins in mammalian cells as a methionine surrogate and the live cells can be labeled with tetrazine **13.84**. **C.** Tetrazole amino acid **13.85** can be incorporated into myoglobin in *E. coli* and detected in cell lysates through photoclick chemistry with activated alkene **13.86**.

Overall photoclick chemistry is a promising new bioorthogonal reaction, with both reaction components able to function as chemical reporter groups. Additionally, the alkene is quite small and should be readily incorporated into a variety of metabolites to probe biomolecules other than proteins. The photoinducibility of this reaction is advantageous in that further temporal or spatial control of the bioorthogonal ligation reaction is possible. As eluded to above, the main limitation of this reaction is the presence of alkenes in lipids and metabolites, which most likely leads to background reactivity. Also the moderate reaction kinetics of the cycloaddition reaction make it likely that a large amount of nitrile imine dipole is quenched, which necessitates high concentrations of reagent. Nevertheless, the Lin group has shown that this reaction is well-suited to the study of living systems and should soon be adopted by other chemical biologists.

Emerging Bioorthogonal Chemical Reactions

Azirine Ligation

The Lin group has also made progress on another photo-induced bioorthogonal ligation that they have termed the azirine ligation (Figure 13.33).²⁸⁹ In this transformation an azirine (**13.87**) is irradiated with light to create a nitrile ylide *in situ* (**13.88**), which undergoes cycloaddition with activated alkenes (**13.86**) to yield pyrroline products (**13.89**). Nitrile ylides are more reactive than the nitrile imines generated with tetrazole precursors, and thus, this reaction should have superior kinetics. Indeed, it appears that the rate-limiting step in this reaction is the formation of the dipole. Lin and coworkers have demonstrated using mass spectrometry of azirine functionalized lysozyme that selective PEGylation can be achieved via this bioorthogonal reaction.²⁸⁹ We anticipate further modification and applications of this reaction will be reported in due course.

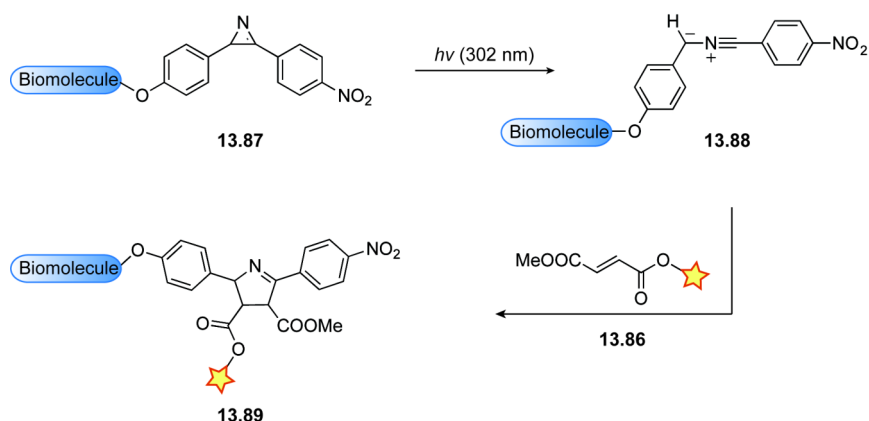


Figure 13.33. The azirine ligation. Azirines are irradiated with light to generate nitrile ylides, which undergo cycloaddition with activated alkenes.

Light-Induced Hetero-Diels-Alder Reaction

Popik and coworkers have explored the cycloaddition of *in situ* generated *ortho*-quinone methides and vinyl ethers to yield benzochroman products for development as a bioorthogonal reaction (Figure 13.34).²⁹⁰ *Ortho*-quinone methide **13.90** can be generated from 3-hydroxyl-2-naphthalenemethanol **13.91** by irradiation with 300 or 350 nm light. The resulting heterodiene (**13.90**) is very reactive and in aqueous solution it appears that a significant amount is quenched by water; however, this just results in regenerated starting material. A screen of dienophiles showed that **13.90** displays selective reactivity with vinyl ethers (**13.92** or **13.93**), and the reaction has a second-order rate constant of $\sim 5 \times 10^4 \text{ M}^{-1}\text{s}^{-1}$, reactivity that approaches the tetrazine ligation. A complication of this reaction, which will most likely prevent it from being truly bioorthogonal, is the background

reaction with thiols to yield **13.94**. The reaction between **13.90** and thiols displays a second-order rate constant of $2 \times 10^5 \text{ M}^{-1}\text{s}^{-1}$, which is more rapid than the desired cycloaddition reaction, although Popik and coworkers have found that thiol adduct **13.94** can be reactivated to the *ortho*-quinone methide by additional treatment with 300 nm light.²⁹⁰

The reaction proceeds well with ethers functionalized with a tyrosine residue at either the oxygen or carbon of the vinyl ether. Additionally, PEGylated or biotinylated 3-hydroxyl-2-naphthalenemethanol reagents have been prepared, and thus far, been used for surface patterning applications,²⁹¹ although other protein- and cell-labeling applications are eluded to at the conclusion of the original report.²⁹⁰ A unique feature of this reaction is that the choice of vinyl ether dictates the stability of the ligation product. If a probe is attached to the dienophile through an oxygen linkage (**13.92**) the resulting benzochroman (**13.95**) contains an acetal linkage between the biomolecule and probe. Subjecting **13.95** to acidic conditions results in hydrolysis of the acetal and reversal of the ligation product. This will be advantageous for applications such as the elution of captured proteins from (strept)avidin resin. Conversely, if an irreversible ligation product is desired, functionalization off the carbon of the vinyl ether (**13.93**) will result in carbon-carbon bond formation between the biomolecule and probe (**13.97**), which remains intact after acid treatment (**13.98**).^{290,291} As with the other emerging bioorthogonal reactions, future reports demonstrating the bioorthogonality of this reaction are anticipated.

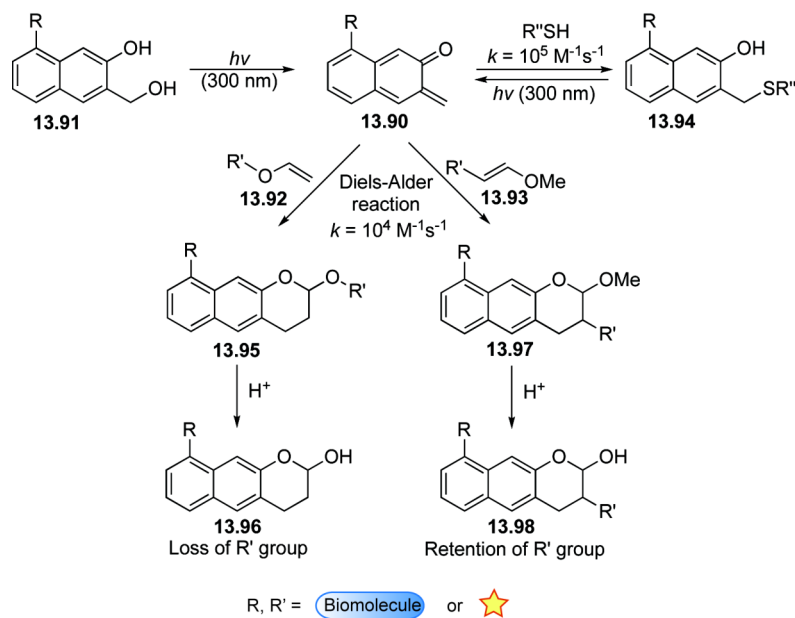


Figure 13.34. The photo-induced hetero-Diels-Alder reaction between *ortho*-quinone methides (**13.90**) and vinyl ethers (**13.92** or **13.93**). The connectivity of the probe to the vinyl ether (O- or C-linked) dictates the stability of the final ligation product (**13.95**, **13.97**), which could be advantageous for applications where cleavable linkages are desired. An additional complication of this reaction is the propensity for *ortho*-quinone methides to react with thiols (**13.94**).

Oxanorbornadiene-Azide Cycloaddition

In 2007, the Rutjes group reported that the reaction between azides and electron-deficient oxanorbornadienes reagent (**13.99**) was bioorthogonal and produced stable triazole products (Figure 13.35). Strained alkenes are well-known to react with azides in cycloaddition reactions; however, their triazoline products are significantly less stable than the aromatic triazole and, consequently, are not ideal for bioconjugation reactions where stability of the ligation product is crucial. By employing oxanorbornadiene reagents as a dipolarophile for the azide, Rutjes and coworkers artfully engineered a strained alkene to result in a stable triazole product. Upon cycloaddition with an azide, the intermediate triazoline **13.100** readily extrudes furan through a retro-Diels-Alder reaction to yield triazole product **13.101**.

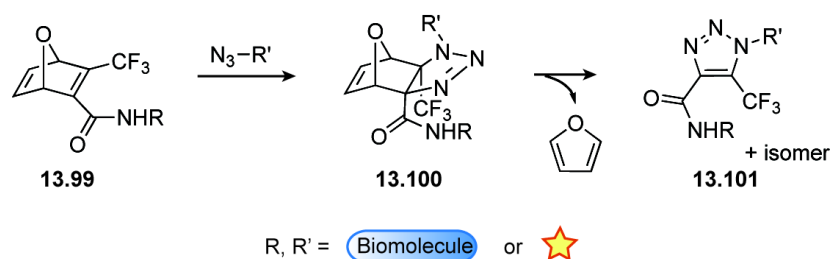


Figure 13.35. The reaction between oxanorbornadienes and azides to yield stable triazole products.

Using this metal-free triazole formation, Rutjes and coworkers have selectively labeled oxanorbornadiene-functionalized proteins with PEG groups and functionalized an azido-cyclic RGD peptide with a DTPA chelator. Upon chelation with ¹¹¹In, the RGD peptide was found to have increased affinity for tissue expressing $\alpha_v\beta_3$, the anticipated target of RGD.²⁹² This cycloaddition reaction has also been used to functionalize polymersomes for targeted delivery of proteins to specific organelles.²⁹³ The requisite oxanorbornadiene reagents are easy to synthesize; however, the reaction kinetics of the cycloaddition are quite slow ($k \sim 10^{-4} \text{ M}^{-1}\text{s}^{-1}$) which have limited the use of this bioorthogonal reaction.

Boronic Acids

Boronic acids have been recognized as a suitable chemical reporter group although a covalent bioorthogonal ligation reaction for this unnatural functionality has not been identified yet. As discussed earlier in this chapter, Schepartz and coworkers have elegantly used boronic acids for the detection of tetraserine motifs (Figure 13.6).²⁹⁴ Jaffery and coworkers have also successfully used a boronate ester forming reaction to assemble ligands *in situ* (Figure 13.36A).²⁹⁵ The Jaffery system employs a salicylhydroxamic acid

(**13.102**) instead of a diol as a partner for the boronic acid (**13.103**), which results in a more stable adduct (**13.104**) than a simple boronic ester. The authors make note that this could be used as a bioorthogonal reaction; however, modification of a biomolecule was not performed in this study.

The classic use of boronic acids to form an irreversible linkage is as a partner in a Suzuki reaction, and biomolecule-associated boronic acids have been modified in this manner (Figure 13.36B). In fact, *p*-boronophenylalanine **13.105** was site-specifically incorporated into a Z-domain protein and labeled with a bodipy dye through Pd-mediated coupling of **13.106**, although elevated temperatures were necessary for moderate conversion.²⁹⁶ Recently, Davis and coworkers have discovered a water-soluble palladium catalyst (**13.107**, Figure 13.36C) for Suzuki coupling on proteins²⁹⁷ and have shown that artificially incorporated aryl halides can be modified with boronic acids in high yield under physiological conditions.²⁹⁸

An additional application of boronic esters, which deserves mention, is their use in sensing hydrogen peroxide. Chang and coworkers have elegantly synthesized a variety of hydrogen peroxide sensors by employing a boronate ester as a quenching moiety for fluorescence, bioluminescence, or lanthanide luminescence.²⁹⁹ Hydrogen peroxide, in preference to all other reactive oxygen species, selectively cleaves the boronate ester to a phenol and generates a fluorogenic probe. Figure 13.36D contains an example of one of the initial hydrogen peroxide sensors (**13.108**).³⁰⁰ Using these probes, the Chang group has studied hydrogen peroxide biology in many systems, including inside living mice.³⁰¹

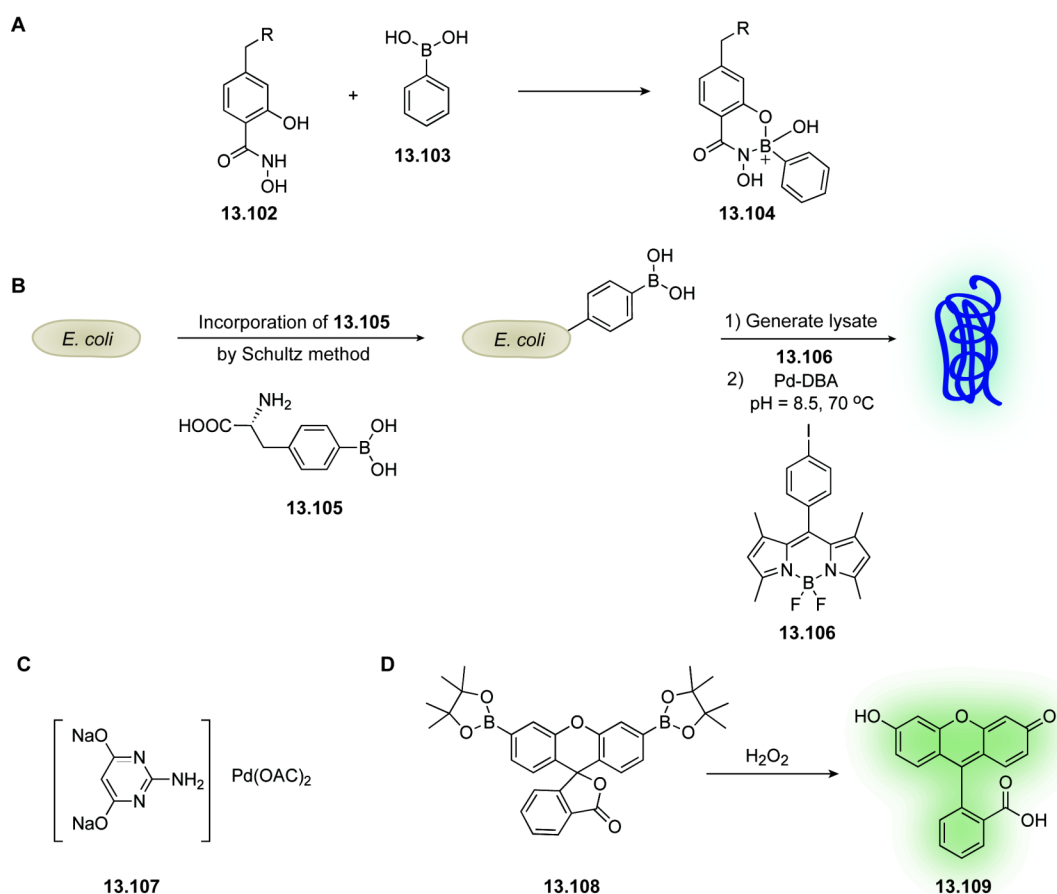


Figure 13.36. Utility of boronic acids as bioorthogonal reagents. A. The association of salicylhydroxamic acid and a boronic acid occurs in biological settings. B. The site-specific incorporation of an aryl boronic acid into a Z-domain protein in *E. coli* and further elaboration through Suzuki coupling. C. A water-soluble catalyst for Suzuki coupling. D. A hydrogen peroxide sensor based on the cleavage of boronate esters.

Pyrroline-Carboxy-Lysine Condensation

Very recently, the reaction of 2-amino-benzaldehydes (**13.111**) with pyrroline-carboxy-lysine (**13.110**) was reported by Geierstanger and coworkers to be a selective bioorthogonal protein modification reaction (Figure 13.37).³⁰² This reaction relies upon a cascade of condensations beginning with attack of the aniline in **13.111** at the pyrroline-carboxy-lysine imine to yield **13.112**, which is positioned for intramolecular condensation of the pyrroline amine and the aldehyde. This transformation yields iminium **13.113**, which is sufficiently electrophilic for intramolecular reaction with the amide nitrogen to yield polycyclic product **13.114**. To enhance the stability of the product, Geierstanger and coworkers reduced **13.114** to **13.115** with sodium cyanoborohydride; however, the authors

state that reduction was only required for 2-amino-acetophenone reagents, which were also employed in this study. A second-order rate constant for this reaction was not reported, but based on reaction concentrations and times employed for protein modification, it appears this reaction has comparable kinetics to the oxime and hydrazone ligations.

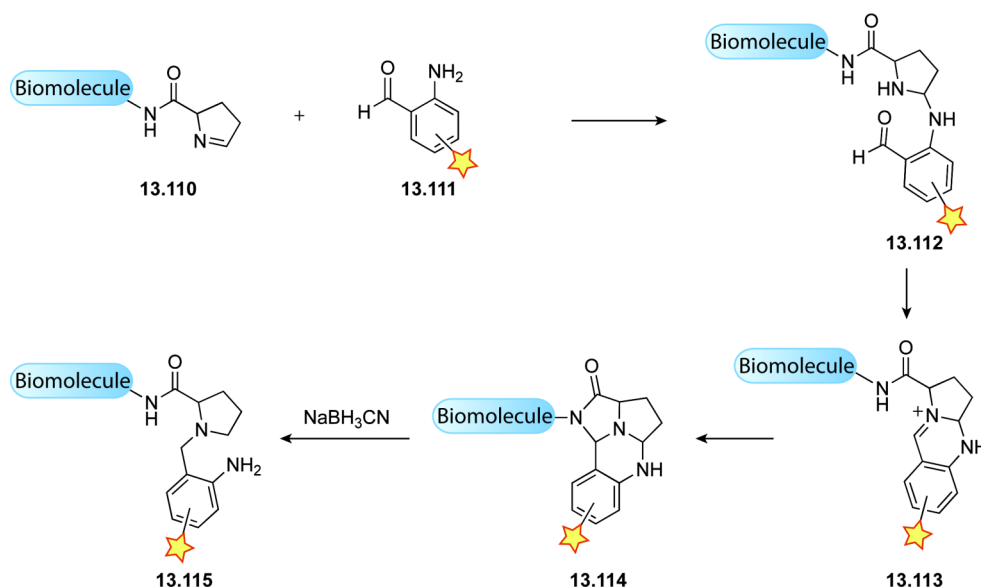


Figure 13.37. The multi-step condensation cascade of pyrroline-carboxy-lysine associated biomolecules and 2-aminobenzaldehyde reagents to yield tetracyclic ligation product **13.114** which can be reduced to **13.115** for enhanced stability.

Pyrroline-carboxy-lysine corresponds to a demethylated pyrrolysine. Pyrrolysine, also known as the 22nd amino acid, is naturally encoded at TAG codons in methanogenic archaea.³⁰³ Pyrroline-carboxy-lysine is accepted by the enzymes in the pyrrolysine pathway, which results in a much simpler incorporation procedure for this unnatural amino acid when compared to those usually employed for amber stop codon mutagenesis experiments. The biosynthetic machinery for synthesis of pyrrolysine tRNA (*PlyC*, *PlyD*, *PlyS RS*, and *PltT tRNA*) from the methanogenic archaea was engineered into *E. coli*,³⁰⁴ and upon introduction of the metabolic precursor *D*-ornithine³⁰⁵ and transformation of the mutated gene for the protein interest, pyrroline-carboxy-lysine was site-specifically incorporated into proteins (Figure 13.38). These modified proteins were then elaborated with a variety of 2-amino-benzaldehydes functionalized with PEG, biotin, fluorescein, disaccharides, dinitrophenyl, or peptides.³⁰² This procedure was even effective for proteins in mammalian cells, something that is generally a challenge for amber stop codon mutagenesis techniques and highlights the advantages of the pyrrolysine biosynthetic pathway.³⁰⁶

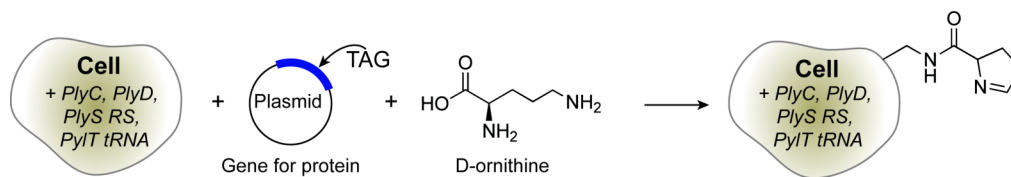


Figure 13.38. The incorporation of pyrroline-carboxy-lysine into proteins using *E. coli* or mammalian cells that contain the genes necessary for pyrrolysine biosynthesis and tRNA synthesis. D-ornithine is accepted by these enzymes and results in incorporation of pyrroline-carboxy-lysine instead of pyrrolysine.

The discovery that pyrrolysine-loaded tRNA naturally recognizes the amber stop codon and the pyrrolysine-tRNA synthetase is orthogonal to both bacterial and mammalian amino acyl tRNA synthetases represents a huge advancement for site-specific noncanonical amino acid incorporation. In only a few years, many unnatural amino acids have been incorporated using mutated versions of the pyrrolysine-tRNA synthetase including **13.1-13.3** and **13.9-13.11**. Additionally, the pyrrolysine-tRNA synthetase has facilitated extension of unnatural amino acid incorporation to a higher organism for the first time. Chin and coworkers successfully introduced a Boc-protected lysine as well as carbamylated lysine **13.9** into the mCherry protein in *C. elegans*.³⁰⁷ Robust fluorescence was observed from the worms treated with the Boc-protected lysine suggesting complete mCherry synthesis; however, when the unnatural amino acid was not present, no fluorescence was observed corresponding to early termination of protein biosynthesis due to the amber stop codon. Treating *C. elegans* with **13.9** and further reaction of lysates with a biotin-azide by CuAAC, biotinylated mCherry was detected by Western blot only when the worms were treated with **13.9**.³⁰⁷ This is an exciting advance for selective protein modification and the bioorthogonal chemical reporter strategy.

Conclusion

Bioorthogonal chemistry has grown immensely over the past five years and it has been an exciting time to be a part of this field. When I began graduate school, there were relatively few groups working on bioorthogonal reaction development and only four known bioorthogonal reactions (carbonyl chemistry, Staudinger ligation, Cu-catalyzed azide-alkyne cycloaddition, and strain-promoted azide-alkyne cycloaddition). Further, only four cyclooctynes had been synthesized for applications in labeling azido-biomolecules. Today, there are at least 15 reactions, which could be deemed bioorthogonal, including the quadricyclane ligation (Chapters 10-12), my contribution to the field. As for cyclooctyne reagents, there are now 16 differentially functionalized cyclooctynes that have been employed for Cu-free click chemistry. This count does not include the difluorobenzocyclooctyne that I synthesized and found to be unstable (Chapter 8) or the monobenzocyclooctyne analogues, which were created to explore factors that activate and stabilize strained cycloalkynes (Chapter 9). However, I did contribute one cyclooctyne to

the 16 employed for Cu-free click chemistry: a hydrophilic dimethoxyazacyclooctyne, DIMAC (Chapter 3). DIMAC was able to label cell-surface glycans on cultured mammalian cells as well as in living mice with decreased background labeling as compared to other more hydrophobic (and more reactive) cyclooctyne reagents (Chapter 4). Since its creation, DIMAC has been employed by a handful of groups for labeling azides in biological systems.

At the rate this field is progressing it's hard to imagine where it will be in another five to ten years. The move toward performing bioorthogonal chemistries in higher organisms is clear. We have directed considerable effort toward methods to label azides in zebrafish and living mice. Others have also used *C. elegans*, zebrafish, and mice to showcase the utility of bioorthogonal chemistries; however, a genuine biological discovery has yet to be made using covalent chemistries in these higher organisms. The stage has been set for such a study and a report where the bioorthogonal chemical reporter strategy allows for a key biological breakthrough would serve to fully validate this rapidly expanding field.

References

- (1) Bernardes, G. J. L.; Chalker, J. M.; Errey, J. C.; Davis, B. G. Facile conversion of cysteine and alkyl cysteines to dehydroalanine on protein surfaces: Versatile and switchable access to functionalized proteins. *J. Am. Chem. Soc.* **2008**, *130*, 5052-5053.
- (2) Chalker, J. M.; Lin, Y. A.; Boutureira, O.; Davis, B. G. Enabling olefin metathesis on proteins: Chemical methods for installation of S-allyl cysteine. *Chem. Commun.* **2009**, *45*, 3714-3716.
- (3) Hoefle, G.; Baldwin, J. E. Thiosulfoxides. Intermediates in rearrangement and reduction of allylic disulfides. *J. Am. Chem. Soc.* **1971**, *93*, 6307-6308.
- (4) Sharpless, K. B.; Lauer, R. F. Facile thermal rearrangements of allyl selenides and diselenides. [1,3] and [2,3] Shifts. *J. Org. Chem.* **1972**, *37*, 3973-3974.
- (5) Crich, D. Brebion, F.; Krishnamurthy, V. Allylic disulfide rearrangement and desulfurization: Mild, electrophile-free thioether formation from thiols. *Org. Lett.* **2006**, *8*, 3593-3596.
- (6) Lin, Y. A.; Chalker, J. M.; Floyd, N.; Bernardes, G. J. L.; Davis, B. G. Allyl sulfides are privileged substrates in aqueous cross-metathesis: Application to site-selective protein modification. *J. Am. Chem. Soc.* **2008**, *130*, 9642-9643.
- (7) Lin, Y. A.; Chalker, J. M.; Davis, B. G. Olefin cross-metathesis on proteins: Investigation of allylic chalcogen effects and guiding principles in metathesis partner selection. *J. Am. Chem. Soc.* **2010**, *132*, 16805-16811.
- (8) Ai, H.; Shen, W.; Brustad, E.; Schultz, P. G. Genetically encoded alkenes in yeast. *Angew. Chem. Int. Ed.* **2010**, *49*, 935-937.
- (9) Dondoni, A. The emergence of thiol-ene coupling as a click process for materials and bioorganic chemistry. *Angew. Chem. Int. Ed.* **2008**, *47*, 8995-8997.

- (10) Triola, G.; Brunsveld, L.; Waldmann, H. Racemization-free synthesis of S-alkylated cysteines via thiol-ene reaction. *J. Org. Chem.* **2008**, *73*, 3646-3649.
- (11) Campos, L. M.; Killops, K. L.; Sakai, R.; Paulusse, J. M. J.; Damiron, D.; Drockenmuller, E.; Messmore, B. W.; Hawker, C. J. Development of thermal and photochemical strategies for thiol-ene click polymer functionalization. *Macromolecules* **2008**, *41*, 7063-7070.
- (12) Wittrock, S.; Becker, T.; Kunz, H. Synthetic vaccines of tumor-associated glycopeptide antigens by immune-compatible thioether linkage to bovine serum albumin. *Angew. Chem. Int. Ed.* **2007**, *46*, 5226-5230.
- (13) Jonkheijm, P.; Weinrich, D.; Köhn, M.; Engelkamp, H.; Christianen, P. C. M.; Kuhlmann, J.; Maan, J. C.; Nüsse, D.; Schroeder, H.; Wacker, R.; Breinbauer, R.; Niemeyer, C. M.; Waldmann, H. Photochemical surface patterning by the thiol-ene reaction. *Angew. Chem. Int. Ed.* **2008**, *47*, 4421-4424.
- (14) Dondoni, A.; Massi, A.; Nanni, P.; Roda, A. A new ligation strategy for peptide and protein glycosylation: Photoinduced thiol-ene coupling. *Chem. Eur. J.* **2009**, *15*, 11444-11449.
- (15) Floyd, N.; Vijayakrishnan, B.; Koeppe, J. R.; Davis, B. G. Thiyl glycosylation of olefinic proteins: S-Linked glycoconjugate synthesis. *Angew. Chem. Int. Ed.* **2009**, *48*, 7798-7802.
- (16) Lo Conte, M.; Pacifico, S.; Chambery, A.; Marra, A.; Dondoni, A. Photoinduced addition of glycosyl thiols to alkynyl peptides: Use of free-radical thiol-yne coupling for post-translational double-glycosylation of peptides. *J. Org. Chem.* **2010**, *75*, 4644-4647.
- (17) Hoogenboom, R. Thiol-yne chemistry: A powerful tool for creating highly functional materials. *Angew. Chem. Int. Ed.* **2010**, *49*, 3415-3417.
- (18) Tedaldi, L. M.; Smith, M. E. B.; Nathani, R. I.; Baker, J. R. Bromomaleimides: New reagents for the selective and reversible modification of cysteine. *Chem. Commun.* **2009**, *45*, 6583-6585.
- (19) Smith, M. E. B.; Schumacher, F. F.; Ryan, C. P.; Tedaldi, L. M.; Papaioannou, D.; Waksman, G.; Caddick, S.; Baker, J. R. Protein modification, bioconjugation, and disulfide bridging using bromomaleimides. *J. Am. Chem. Soc.* **2010**, *132*, 1960-1965.
- (20) Hong, V.; Kislukhin, A. A.; Finn, M. G. Thiol-selective fluorogenic probes for labeling and release. *J. Am. Chem. Soc.* **2009**, *131*, 9986-9994.
- (21) Shiu, H.; Chan, T.; Ho, C.; Liu, Y.; Wong, M.; Che, C. Electron-deficient alkynes as cleavable reagents for the modification of cysteine-containing peptides in aqueous medium. *Chem. Eur. J.* **2009**, *15*, 3839-3850.
- (22) Morales-Sanfrutos, J.; Lopez-Jaramillo, J.; Ortega-Muñoz, M.; Megia-Fernandez, A.; Perez-Balderas, F.; Hernandez-Mateo, F.; Santoyo-Gonzalez, F. Vinyl sulfone: A versatile function for simple bioconjugation and immobilization. *Org. Biomol. Chem.* **2010**, *8*, 667-675.
- (23) Tanaka, K.; Masuyama, T.; Hasegawa, K.; Tahara, T.; Mizuma, H.; Wada, Y.; Watanabe, Y.; Fukase, K. A submicrogram-scale protocol for biomolecule-based PET imaging by rapid 6π -azaelectrocyclization: Visualization of sialic acid

- dependent circulatory residence of glycoproteins. *Angew. Chem. Int. Ed.* **2008**, *47*, 102-105.
- (24) Tanaka, K.; Fujii, Y.; Fukase, K. Site-selective and nondestructive protein labeling through azaelectrocyclization-induced cascade reactions. *ChemBioChem* **2008**, *9*, 2392-2397.
- (25) van Dongen, S. F. M.; Teeuwen, R. L. M.; Nallani, M.; van Berkel, S. S.; Cornelissen, J. J. L. M.; Nolte, R. J. M.; van Hest, J. C. M. Single-step azide introduction in proteins via an aqueous diazo transfer. *Bioconjugate Chem.* **2009**, *20*, 20-23.
- (26) van Berkel, S. S.; Dirks, A. (Ton) J.; Debets, M. F. van Delft, F. L.; Cornelissen, J. J. L. M.; Nolte, R. J. M.; Rutjes, F. P. J. T. Metal-free triazole formation as a tool for bioconjugation. *ChemBioChem* **2007**, *8*, 1504-1508.
- (27) Joshi, N. S.; Whitaker, L. R.; Francis, M. B. A three-component Mannich-type reaction for selective tyrosine bioconjugation. *J. Am. Chem. Soc.* **2004**, *126*, 15942-15943.
- (28) Minakawa, M.; Guo, H.-M.; Tanaka, F. Imines that react with phenols in water over a wide pH range. *J. Org. Chem.* **2008**, *73*, 8669-8672.
- (29) Guo, H.-M.; Minakawa, M.; Ueno, L.; Tanaka, F. Synthesis and evaluation of a cyclic imine derivative conjugated to a fluorescent molecule for labeling of proteins. *Bioorg. Med. Chem. Lett.* **2009**, *19*, 1210-1213.
- (30) Guo, H.-M.; Minakawa, M.; Tanaka, F. Fluorogenic imines for fluorescent detection of Mannich-type reactions of phenols in water. *J. Org. Chem.* **2008**, *73*, 3964-3966.
- (31) Ban, H.; Gavriluk, J.; Barbas Tyrosine bioconjugation through aqueous ene-type reactions: A click-like reaction for tyrosine. *J. Am. Chem. Soc.* **2010**, *132*, 1523-1525.
- (32) White, E. H.; McCapra, F.; Field, G. F.; McElroy, W. D. The structure and synthesis of firefly luciferin. *J. Am. Chem. Soc.* **1961**, *83*, 2402-2403.
- (33) Ren, H.; Xiao, F.; Zhan, K.; Kim, Y.; Xie, H.; Xia, Z.; Rao, J. A biocompatible condensation reaction for the labeling of terminal cysteine residues on proteins. *Angew. Chem. Int. Ed.* **2009**, *48*, 9658-9662.
- (34) Liang, G.; Ren, H.; Rao, J. A biocompatible condensation reaction for controlled assembly of nanostructures in living cells. *Nat. Chemistry* **2010**, *2*, 54-60.
- (35) Nguyen, D. P.; Elliott, T.; Holt, M.; Muir, T. W.; Chin, J. W. Genetically encoded 1,2-aminothiols facilitate rapid and site-specific protein labeling via a bio-orthogonal cyanobenzothiazole condensation. *J. Am. Chem. Soc.* **2011**, *133*, 11418-11421.
- (36) Virdee, S.; Kapadnis, P. B.; Elliott, T.; Lang, K.; Madrzak, J.; Nguyen, D. P.; Riechmann, L.; Chin, J. W. Traceless and site-specific ubiquitination of recombinant proteins. *J. Am. Chem. Soc.* **2011**, *133*, 10708-10711.
- (37) Focke, P. J.; Valiyaveetil, F. I. Studies of ion channels using expressed protein ligation. *Curr. Opin. Chem. Biol.* **2010**, *14*, 797-802.

- (38) Shimko, J. C.; North, J. A.; Bruns, A. N.; Poirier, M. G.; Ottesen, J. J. Preparation of fully synthetic histone H3 reveals that acetyl-lysine 56 facilitates protein binding within nucleosomes. *J. Mol. Biol.* **2011**, *408*, 187-204.
- (39) Liu, M.; Li, C.; Pazgier, M.; Li, C.; Mao, Y.; Lv, Y.; Gu, B.; Wei, G.; Yuan, W.; Zhan, C.; Lu, W.-Y.; Lu, W. D-peptide inhibitors of the p53-MDM2 interaction for targeted molecular therapy of malignant neoplasms. *Proc. Natl. Acad. Sci. U.S.A.* **2010**, *107*, 14321-14326.
- (40) Piontek, C.; Ring, P.; Harjes, O.; Heinlein, C.; Mezzato, S.; Lombana, N.; Pöhner, C.; Püttner, M.; Varón Silva, D.; Martin, A.; Schmid, F. X.; Unverzagt, C. Semisynthesis of a homogeneous glycoprotein enzyme: Ribonuclease C: Part 1. *Angew. Chem. Int. Ed.* **2009**, *48*, 1936-1940.
- (41) Piontek, C.; Varón Silva, D.; Heinlein, C.; Pöhner, C.; Mezzato, S.; Ring, P.; Martin, A.; Schmid, F. X.; Unverzagt, C. Semisynthesis of a homogeneous glycoprotein enzyme: Ribonuclease C: Part 2. *Angew. Chem. Int. Ed.* **2009**, *48*, 1941-1945.
- (42) Mandal, K.; Kent, S. B. H. Total chemical synthesis of biologically active vascular endothelial growth factor. *Angew. Chem. Int. Ed.* **2011**, *50*, 8029-8033.
- (43) Paulick, M. G.; Forstner, M. B.; Groves, J. T.; Bertozzi, C. R. A chemical approach to unraveling the biological function of the glycosylphosphatidylinositol anchor. *Proc. Natl. Acad. Sci. U.S.A.* **2007**, *104*, 20332-20337.
- (44) Wu, Y.-W.; Oesterlin, L. K.; Tan, K.-T.; Waldmann, H.; Alexandrov, K.; Goody, R. S. Membrane targeting mechanism of Rab GTPases elucidated by semisynthetic protein probes. *Nat. Chem. Biol.* **2010**, *6*, 534-540.
- (45) Haase, C.; Rohde, H.; Seitz, O. Native chemical ligation at valine. *Angew. Chem. Int. Ed.* **2008**, *47*, 6807-6810.
- (46) Chen, J.; Wan, Q.; Yuan, Y.; Zhu, J.; Danishefsky, S. J. Native chemical ligation at valine: A contribution to peptide and glycopeptide synthesis. *Angew. Chem. Int. Ed.* **2008**, *47*, 8521-8524.
- (47) Crich, D.; Banerjee, A. Native chemical ligation at phenylalanine. *J. Am. Chem. Soc.* **2007**, *129*, 10064-10065.
- (48) Harpaz, Z.; Siman, P.; Kumar, K. S. A.; Brik, A. Protein synthesis assisted by native chemical ligation at leucine. *ChemBioChem* **2010**, *11*, 1232-1235.
- (49) Yang, R.; Pasunooti, K. K.; Li, F.; Liu, X.-W.; Liu, C.-F. Dual native chemical ligation at lysine. *J. Am. Chem. Soc.* **2009**, *131*, 13592-13593.
- (50) Shang, S.; Tan, Z.; Dong, S.; Danishefsky, S. J. An advance in proline ligation. *J. Am. Chem. Soc.* **2011**, *133*, 10784-10786.
- (51) Brik, A.; Yang, Y.-Y.; Ficht, S.; Wong, C.-H. Sugar-assisted glycopeptide ligation. *J. Am. Chem. Soc.* **2006**, *128*, 5626-5627.
- (52) Yang, Y.-Y.; Ficht, S.; Brik, A.; Wong, C.-H. Sugar-assisted ligation in glycoprotein synthesis. *J. Am. Chem. Soc.* **2007**, *129*, 7690-7701.
- (53) Kalia, J.; Raines, R. T. Reactivity of intein thioesters: Appending a functional group to a protein. *ChemBioChem* **2006**, *7*, 1375-1383.

- (54) Thom, J.; Anderson, D.; McGregor, J.; Cotton, G. Recombinant protein hydrazides: Application to site-specific protein PEGylation. *Bioconjugate Chem.* **2011**, *22*, 1017-1020.
- (55) Yi, L.; Sun, H.; Wu, Y.; Triola, G.; Waldmann, H.; Goody, R. S. A highly efficient strategy for modification of proteins at the C-terminus. *Angew. Chem. Int. Ed.* **2010**, *49*, 9417-9421.
- (56) Zhang, X.; Li, F.; Lu, X.-W.; Liu, C.-F. Protein C-terminal modification through thioacid/azide amidation. *Bioconjugate Chem.* **2009**, *20*, 197-200.
- (57) Shimomura, O. Discovery of green fluorescent protein (GFP). *Angew. Chem. Int. Ed.* **2009**, *48*, 5590-5602.
- (58) Chalfie, M. GFP: Lighting up life. *Angew. Chem. Int. Ed.* **2009**, *48*, 5603-5611.
- (59) Tsien, R. Y. Constructing and exploiting the fluorescent protein paintbox. *Angew. Chem. Int. Ed.* **2009**, *48*, 5612-5626.
- (60) Werner, J. N.; Chen, E. Y.; Guberman, J. M.; Zippilli, A. R.; Irgon, J. J.; Gitai, Z. Quantitative genome-scale analysis of protein localization in an asymmetric bacterium. *Proc. Natl. Acad. Sci. U.S.A.* **2009**, *106*, 7858-7863.
- (61) Halo, T. L.; Appelbaum, J.; Hobert, E. M.; Balkin, D. M.; Schepartz, A. Selective recognition of protein tetraserine motifs with a cell-permeable, pro-fluorescent bis-boronic acid. *J. Am. Chem. Soc.* **2009**, *131*, 438-439.
- (62) Kim, K. K.; Escobedo, J. O.; St. Luce, N. N.; Rusin, O.; Wong, D.; Strongin, R. M. Postcolumn HPLC detection of mono- and oligosaccharides with a chemosensor. *Org. Lett.* **2003**, *5*, 5007-5010.
- (63) Scheck, R. A.; Schepartz, A. Surveying protein structure and function using bis-arsenical small molecules. *Acc. Chem. Res.* **2011**, *44*, 654-665.
- (64) Hauser, C. T.; Tsien, R. Y. A hexahistidine-Zn²⁺-dye label reveals STIM1 surface exposure. *Proc. Natl. Acad. Sci. U.S.A.* **2007**, *104*, 3693-3697.
- (65) Soh, N.; Seto, D.; Nakano, K.; Imato, T. Methodology of reversible protein labeling for ratiometric fluorescent measurement. *Mol. BioSyst.* **2006**, *2*, 128-131.
- (66) Kamoto, M.; Umezawa, N.; Kato, N.; Higuchi, T. Turn-on fluorescent probe with visible light excitation for labeling of hexahistidine tagged protein. *Bioorg. Med. Chem. Lett.* **2009**, *19*, 2285-2288.
- (67) Kamoto, M.; Umezawa, N.; Kato, N.; Higuchi, T. Novel probes showing specific fluorescence enhancement on binding to a hexahistidine tag. *Chem. Eur. J.* **2008**, *14*, 8004-8012.
- (68) Taki, M.; Asahi, F.; Hirayama, T.; Yamamoto, Y. Design and synthesis of fluorescent probe for polyhistidine tag using macrocyclic nickel(II) complex and fluorescein conjugate. *Bull. Chem. Soc. Jpn.* **2011**, *84*, 386-394.
- (69) Ojida, A.; Honda, K.; Shinmi, D.; Kiyonaka, S.; Mori, Y.; Hamachi, I. Oligo-Asp tag/Zn(II) complex probe as a new pair for labeling and fluorescence imaging of proteins. *J. Am. Chem. Soc.* **2006**, *128*, 10452-10459.
- (70) Honda, K.; Fujishima, S.; Ojida, A.; Hamachi, I. Pyrene excimer-based dual-emission detection of an oligoaspartate tag-fused protein by using a Zn^{II}-DpaTyr probe. *ChemBioChem* **2007**, *8*, 1370-1372.

- (71) Honda, K.; Nakata, E.; Ojida, A.; Hamachi, I. Ratiometric fluorescence detection of a tag fused protein using the dual-emission artificial molecular probe. *Chem. Commun.* **2006**, *42*, 4024-4026.
- (72) Nonaka, H.; Tsukiji, S.; Ojida, A.; Hamachi, I. Non-enzymatic covalent protein labeling using a reactive tag. *J. Am. Chem. Soc.* **2007**, *129*, 15777-15779.
- (73) Nonaka, H.; Fujishima, S.-H.; Uchinomiya, S.-H.; Ojida, A.; Hamachi, I. Selective covalent labeling of tag-fused GPCR proteins on live cell surface with a synthetic probe for their functional analysis. *J. Am. Chem. Soc.* **2010**, *132*, 9301-9309.
- (74) Tsukiji, S.; Miyagawa, M.; Takaoka, Y.; Tamura, T.; Hamachi, I. Ligand-directed tosyl chemistry for protein labeling in vivo. *Nat. Chem. Biol.* **2009**, *5*, 341-343.
- (75) Gallagher, S. S.; Sable, J. E.; Sheetz, M. P.; Cornish, V. W. An in vivo covalent TMP-tag based on proximity-induced reactivity. *ACS Chem. Biol.* **2009**, *4*, 547-556.
- (76) Popp, B. V.; Ball, Z. T. Structure-selective modification of aromatic side chains with dirhodium metallopeptide catalysts. *J. Am. Chem. Soc.* **2010**, *132*, 6660-6662.
- (77) Slavoff, S. A.; Chen, I.; Choi, Y.-A.; Ting, A. Y. Expanding the substrate tolerance of biotin ligase through exploration of enzymes from diverse species. *J. Am. Chem. Soc.* **2008**, *130*, 1160-1162.
- (78) Fernández-Suárez, M.; Chen, T. S.; Ting, A. Y. Protein–protein interaction detection in vitro and in cells by proximity biotinylation. *J. Am. Chem. Soc.* **2008**, *130*, 9251-9253.
- (79) Fernandez-Suarez, M.; Baruah, H.; Martinez-Hernandez, L.; Xie, K. T.; Baskin, J. M.; Bertozzi, C. R.; Ting, A. Y. Redirecting lipoic acid ligase for cell surface protein labeling with small-molecule probes. *Nat. Biotech.* **2007**, *25*, 1483-1487.
- (80) Baruah, H.; Puthenveetil, S.; Choi, Y.; Shah, S.; Ting, A. Y. An engineered aryl azide ligase for site-specific mapping of protein–protein interactions through photo-cross-linking. *Angew. Chem. Int. Ed.* **2008**, *47*, 7018-7021.
- (81) Uttamapinant, C.; White, K. A.; Baruah, H.; Thompson, S.; Fernández-Suárez, M.; Puthenveetil, S.; Ting, A. Y. A fluorophore ligase for site-specific protein labeling inside living cells. *Proc. Natl. Acad. Sci. U.S.A.* **2010**, *107*, 10914 -10919.
- (82) Jin, X.; Uttamapinant, C.; Ting, A. Y. Synthesis of 7-aminocoumarin by Buchwald–Hartwig cross coupling for specific protein labeling in living Cells. *ChemBioChem* **2011**, *12*, 65-70.
- (83) Dierks, T.; Schmidt, B.; Borissenko, L. V.; Peng, J.; Preusser, A.; Mariappan, M.; von Figura, K. Multiple sulfatase deficiency is caused by mutations in the gene encoding the human C α -formylglycine generating enzyme. *Cell* **2003**, *113*, 435-444.
- (84) Carlson, B. L.; Ballister, E. R.; Skordalakes, E.; King, D. S.; Breidenbach, M. A.; Gilmore, S. A.; Berger, J. M.; Bertozzi, C. R. Function and structure of a prokaryotic formylglycine-generating enzyme. *J. Biol. Chem.* **2008**, *283*, 20117 -20125.
- (85) Carrico, I. S.; Carlson, B. L.; Bertozzi, C. R. Introducing genetically encoded aldehydes into proteins. *Nat. Chem. Biol.* **2007**, *3*, 321-322.

- (86) Dierks, T.; Lecca, M. R.; Schlotterhose, P.; Schmidt, B.; von Figura, K. Sequence determinants directing conversion of cysteine to formylglycine in eukaryotic sulfatases. *EMBO J.* **1999**, *18*, 2084-2091.
- (87) Rush, J. S.; Bertozzi, C. R. New aldehyde tag sequences identified by screening formylglycine generating enzymes in vitro and in vivo. *J. Am. Chem. Soc.* **2008**, *130*, 12240-12241.
- (88) Wu, P.; Shui, W.; Carlson, B. L.; Hu, N.; Rabuka, D.; Lee, J.; Bertozzi, C. R. Site-specific chemical modification of recombinant proteins produced in mammalian cells by using the genetically encoded aldehyde tag. *Proc. Natl. Acad. Sci. U.S.A.* **2009**, *106*, 3000-3005.
- (89) Popp, M. W.; Antos, J. M.; Grotenbreg, G. M.; Spooner, E.; Ploegh, H. L. Sortagging: A versatile method for protein labeling. *Nat. Chem. Biol.* **2007**, *3*, 707-708.
- (90) Tanaka, T.; Yamamoto, T.; Tsukiji, S.; Nagamune, T. Site-specific protein modification on living cells catalyzed by sortase. *ChemBioChem* **2008**, *9*, 802-807.
- (91) Jeger, S.; Zimmermann, K.; Blanc, A.; Grünberg, J.; Honer, M.; Hunziker, P.; Struthers, H.; Schibli, R. Site-specific and stoichiometric modification of antibodies by bacterial transglutaminase. *Angew. Chem. Int. Ed.* **2010**, *49*, 9995-9997.
- (92) Gautier, A.; Juillerat, A.; Heinis, C.; Corrêa Jr., I. R.; Kindermann, M.; Beaufils, F.; Johnsson, K. An engineered protein tag for multiprotein labeling in living cells. *Chem. Biol.* **2008**, *15*, 128-136.
- (93) Tomat, E.; Nolan, E. M.; Jaworski, J.; Lippard, S. J. Organelle-specific zinc detection using Znpyr-labeled Fusion Proteins in live cells. *J. Am. Chem. Soc.* **2008**, *130*, 15776-15777.
- (94) Bannwarth, M.; Correa, I. R.; Sztretye, M.; Pouvreau, S.; Fellay, C.; Aebischer, A.; Royer, L.; Ríos, E.; Johnsson, K. Indo-1 derivatives for local calcium sensing. *ACS Chem. Biol.* **2009**, *4*, 179-190.
- (95) Srikun, D.; Albers, A. E.; Nam, C. I.; Iavarone, A. T.; Chang, C. J. Organelle-targetable fluorescent probes for imaging hydrogen peroxide in living cells via SNAP-tag protein labeling. *J. Am. Chem. Soc.* **2010**, *132*, 4455-4465.
- (96) Mao, S.; Benninger, R. K. P.; Yan, Y.; Petchprayoon, C.; Jackson, D.; Easley, C. J.; Piston, D. W.; Marriott, G. Optical lock-in detection of FRET using synthetic and genetically encoded optical switches. *Biophys. J.* **2008**, *94*, 4515-4524.
- (97) Keppler, A.; Ellenberg, J. Chromophore-assisted laser inactivation of α - and γ -tubulin SNAP-tag fusion proteins inside living cells. *ACS Chem. Biol.* **2009**, *4*, 127-138.
- (98) Maurel, D.; Comps-Agrar, L.; Brock, C.; Rives, M.-L.; Bourrier, E.; Ayoub, M. A.; Bazin, H.; Tinel, N.; Durroux, T.; Prezeau, L.; Trinquet, E.; Pin, J.-P. Cell-surface protein-protein interaction analysis with time-resolved FRET and snap-tag technologies: Application to GPCR oligomerization. *Nat. Methods* **2008**, *5*, 561-567.

- (99) Gautier, A.; Nakata, E.; Lukinavicius, G.; Tan, K.-T.; Johnsson, K. Selective cross-linking of interacting proteins using self-labeling tags. *J. Am. Chem. Soc.* **2009**, *131*, 17954-17962.
- (100) Alvarez-Curto, E.; Ward, R. J.; Pediani, J. D.; Milligan, G. Ligand regulation of the quaternary organization of cell surface M3 muscarinic acetylcholine receptors analyzed by fluorescence resonance energy transfer (FRET) imaging and homogeneous time-resolved FRET. *J. Biol. Chem.* **2010**, *285*, 23318-23330.
- (101) Klein, T.; Loschberger, A.; Proppert, S.; Wolter, S.; van de Linde, S.; Sauer, M. Live-cell dSTORM with SNAP-tag fusion proteins. *Nat. Methods* **2011**, *8*, 7-9.
- (102) Brun, M. A.; Tan, K.-T.; Nakata, E.; Hinner, M. J.; Johnsson, K. Semisynthetic fluorescent sensor proteins based on self-labeling protein tags. *J. Am. Chem. Soc.* **2009**, *131*, 5873-5884.
- (103) Campos, C.; Kamiya, M.; Banala, S.; Johnsson, K.; González-Gaitán, M. Labelling cell structures and tracking cell lineage in zebrafish using SNAP-tag. *Dev. Dynam.* **2011**, *240*, 820-827.
- (104) Bojkowska, K.; Santoni de Sio, F.; Barde, I.; Offner, S.; Verp, S.; Heinis, C.; Johnsson, K.; Trono, D. Measuring in vivo protein half-life. *Chem. Biol.* **2011**, *18*, 805-815.
- (105) Sun, X.; Zhang, A.; Baker, B.; Sun, L.; Howard, A.; Buswell, J.; Maurel, D.; Masharina, A.; Johnsson, K.; Noren, C. J.; Xu, M.; Corrêa Jr., I. R. Development of SNAP-tag fluorogenic probes for wash-free fluorescence imaging. *ChemBioChem* **2011**, *12*, 2217-2226.
- (106) Los, G. V.; Encell, L. P.; McDougall, M. G.; Hartzell, D. D.; Karassina, N.; Zimprich, C.; Wood, M. G.; Learish, R.; Ohana, R. F.; Urh, M.; Simpson, D.; Mendez, J.; Zimmerman, K.; Otto, P.; Vidugiris, G.; Zhu, J.; Darzins, A.; Klaubert, D. H.; Bulleit, R. F.; Wood, K. V. HaloTag: A novel protein labeling technology for cell imaging and protein analysis. *ACS Chem. Biol.* **2008**, *3*, 373-382.
- (107) Bonasio, R.; Carman, C. V.; Kim, E.; Sage, P. T.; Love, K. R.; Mempel, T. R.; Springer, T. A.; von Andrian, U. H. Specific and covalent labeling of a membrane protein with organic fluorochromes and quantum dots. *Proc. Natl. Acad. Sci. U.S.A.* **2007**, *104*, 14753 -14758.
- (108) Duckworth, B. P.; Zhang, Z.; Hosokawa, A.; Distefano, M. D. Selective labeling of proteins by using protein farnesyltransferase. *ChemBioChem* **2007**, *8*, 98-105.
- (109) Jencks, W. P. Studies on the mechanism of oxime and semicarbazone formation. *J. Am. Chem. Soc.* **1959**, *81*, 475-481.
- (110) Dirksen, A.; Hackeng, T. M.; Dawson, P. E. Nucleophilic catalysis of oxime ligation. *Angew. Chem.* **2006**, *118*, 7743-7746.
- (111) Dirksen, A.; Dawson, P. E. Rapid oxime and hydrazone ligations with aromatic aldehydes for biomolecular labeling. *Bioconjugate Chem.* **2008**, *19*, 2543-2548.
- (112) Bhat, V. T.; Caniard, A. M.; Luksch, T.; Brenk, R.; Campopiano, D. J.; Greaney, M. F. Nucleophilic catalysis of acylhydrazone equilibration for protein-directed dynamic covalent chemistry. *Nat. Chemistry* **2010**, *2*, 490-497.

- (113) Zeng, Y.; Ramya, T. N. C.; Dirksen, A.; Dawson, P. E.; Paulson, J. C. High-efficiency labeling of sialylated glycoproteins on living cells. *Nat. Methods* **2009**, *6*, 207-209.
- (114) Baskin, J. M.; Dehnert, K. W.; Laughlin, S. T.; Amacher, S. L.; Bertozzi, C. R. Visualizing enveloping layer glycans during zebrafish early embryogenesis. *Proc. Natl. Acad. Sci. U.S.A.* **2010**, *107*, 10360-10365.
- (115) Rayo, J.; Amara, N.; Krief, P.; Meijler, M. M. Live cell labeling of native intracellular bacterial receptors using aniline-catalyzed oxime ligation. *J. Am. Chem. Soc.* **2011**, *133*, 7469-7475.
- (116) Kalia, J.; Raines, R. T. Hydrolytic stability of hydrazones and oximes. *Angew. Chem. Int. Ed.* **2008**, *47*, 7523-7526.
- (117) Kalia, J.; Raines, R. T. Advances in bioconjugation. *Curr. Org. Chem.* **2010**, *14*, 138-147.
- (118) Alam, J.; Keller, T. H.; Loh, T.-P. Functionalization of peptides and proteins by Mukaiyama aldol reaction. *J. Am. Chem. Soc.* **2010**, *132*, 9546-9548.
- (119) McKay, C. S.; Moran, J.; Pezacki, J. P. Nitrones as dipoles for rapid strain-promoted 1,3-dipolar cycloadditions with cyclooctynes. *Chem. Commun.* **2010**, *46*, 931-933.
- (120) Ning, X.; Temming, R. P.; Dommerholt, J.; Guo, J.; Ania, D. B.; Debets, M. F.; Wolfert, M. A.; Boons, G.-J.; van Delft, F. L. Protein modification by strain-promoted alkyne-nitrone cycloaddition. *Angew. Chem. Int. Ed.* **2010**, *49*, 3065-3068.
- (121) Singh, I.; Heaney, F. Metal free, “click and click–click” conjugation of ribonucleosides and 2'-OMe oligoribonucleotides on the solid phase. *Org. Biomol. Chem.* **2010**, *8*, 451-456.
- (122) Algay, V.; Singh, I.; Heaney, F. Nucleoside and nucleotide analogues by catalyst free Huisgen nitrile oxide–alkyne 1,3-dipolar cycloaddition. *Org. Biomol. Chem.* **2010**, *8*, 391-397.
- (123) Singh, I.; Vyle, J. S.; Heaney, F. Fast, copper-free click chemistry: A convenient solid-phase approach to oligonucleotide conjugation. *Chem. Commun.* **2009**, *45*, 3276-3278.
- (124) Gutmiedl, K.; Fazio, D.; Carell, T. High-density DNA functionalization by a combination of Cu-catalyzed and Cu-free click chemistry. *Chem. Eur. J.* **2010**, *16*, 6877-6883.
- (125) Gutmiedl, K.; Wirges, C. T.; Ehmke, V.; Carell, T. Copper-free “click” modification of DNA via nitrile oxide–norbornene 1,3-dipolar cycloaddition. *Org. Lett.* **2009**, *11*, 2405-2408.
- (126) Singh, I.; Heaney, F. Solid phase strain promoted “click” modification of DNA via [3+2]-nitrile oxide–cyclooctyne cycloadditions. *Chem. Commun.* **2011**, *47*, 2706-2708.
- (127) Jawalekar, A. M.; Reubsæet, E.; Rutjes, F. P. J. T.; van Delft, F. L. Synthesis of isoxazoles by hypervalent iodine-induced cycloaddition of nitrile oxides to alkynes. *Chem. Commun.* **2011**, *47*, 3198-3200.

- (128) Sanders, B. C.; Friscourt, F.; Ledin, P. A.; Mbua, N. E.; Arumugam, S.; Guo, J.; Boltje, T. J.; Popik, V. V.; Boons, G.-J. Metal-free sequential [3 + 2]-dipolar cycloadditions using cyclooctynes and 1,3-dipoles of different reactivity. *J. Am. Chem. Soc.* **2011**, *133*, 949-957.
- (129) Neves, A. A.; Stockmann, H.; Harmston, R. R.; Pryor, H. J.; Alam, I. S.; Ireland-Zecchini, H.; Lewis, D. Y.; Lyons, S. K.; Leeper, F. J.; Brindle, K. M. Imaging sialylated tumor cell glycans in vivo. *FASEB J.* **2011**, *25*, 2528-2537.
- (130) van der Linden, W. A.; Li, N.; Hoogendoorn, S.; Ruben, M.; Verdoes, M.; Guo, J.; Boons, G.-J.; van der Marel, G. A.; Florea, B. I.; Overkleeft, H. S. Two-step bioorthogonal activity-based proteasome profiling using copper-free click reagents: A comparative study. *Bioorg. Med. Chem. Lett.* **2011**, *0*.
- (131) Vellucci, D.; Kao, A.; Kaake, R. M.; Rychnovsky, S. D.; Huang, L. Selective enrichment and identification of azide-tagged cross-linked peptides using chemical ligation and mass spectrometry. *J. Am. Soc. Mass. Spectrom.* **2010**, *21*, 1432-1445.
- (132) Geurink, P. P.; Florea, B. I.; Van der Marel, G. A.; Kessler, B. M.; Overkleeft, H. S. Probing the proteasome cavity in three steps: Bio-orthogonal photo-reactive suicide substrates. *Chem. Commun.* **2010**, *46*, 9052-9054.
- (133) Verdoes, M.; Florea, B. I.; Hillaert, U.; Willems, L. I.; van der Linden, W. A.; Sae-Heng, M.; Filippov, D. V.; Kisselev, A. F.; van der Marel, G. A.; Overkleeft, H. S. Azido-BODIPY acid reveals quantitative Staudinger-Bertozzi ligation in two-step activity-based proteasome profiling. *ChemBioChem* **2008**, *9*, 1735-1738.
- (134) Reddie, K. G.; Seo, Y. H.; Muse III, W. B.; Leonard, S. E.; Carroll, K. S. A chemical approach for detecting sulfenic acid-modified proteins in living cells. *Mol. Biosyst.* **2008**, *4*, 521-531.
- (135) Hubbard, S. C.; Boyce, M.; McVaugh, C. T.; Peehl, D. M.; Bertozzi, C. R. Cell surface glycoproteomic analysis of prostate cancer-derived PC-3 cells. *Bioorg. Med. Chem. Lett.* **2011**, *21*, 4945-4950.
- (136) Boyce, M.; Carrico, I. S.; Ganguli, A. S.; Yu, S.-H.; Hangauer, M. J.; Hubbard, S. C.; Kohler, J. J.; Bertozzi, C. R. Metabolic cross-talk allows labeling of O-linked β -N-acetylglucosamine-modified proteins via the N-acetylgalactosamine salvage pathway. *Proc. Natl. Acad. Sci. U.S.A.* **2011**, *108*, 3141 -3146.
- (137) Kalia, J.; Abbott, N. L.; Raines, R. T. General method for site-specific protein immobilization by Staudinger ligation. *Bioconjugate Chem.* **2007**, *18*, 1064-1069.
- (138) Köhn, M. Immobilization strategies for small molecule, peptide and protein microarrays. *J. Pept. Sci.* **2009**, *15*, 393-397.
- (139) Tam, A.; Soellner, M. B.; Raines, R. T. Electronic and steric effects on the rate of the traceless Staudinger ligation. *Org. Biomol. Chem.* **2008**, *6*, 1173-1175.
- (140) Tam, A.; Raines, R. T. Coulombic effects on the traceless Staudinger ligation in water. *Bioorg. Med. Chem. Lett.* **2009**, *17*, 1055-1063.
- (141) Tam, A.; Soellner, M. B.; Raines, R. T. Water-soluble phosphinothiols for traceless Staudinger ligation and integration with expressed protein ligation. *J. Am. Chem. Soc.* **2007**, *129*, 11421-11430.
- (142) Mühlberg, M.; Jaradat, D. M. M.; Kleineweischede, R.; Papp, I.; Dechtrirat, D.; Muth, S.; Broncel, M.; Hackenberger, C. P. R. Acidic and basic deprotection

- strategies of borane-protected phosphinothioesters for the traceless Staudinger ligation. *Bioorg. Med. Chem. Lett.* **2010**, *18*, 3679-3686.
- (143) Kleineweischede, R.; Hackenberger, C. P. R. Chemoselective peptide cyclization by traceless Staudinger ligation. *Angew. Chem. Int. Ed.* **2008**, *47*, 5984-5988.
- (144) Bernardes, G. J. L.; Linderoth, L.; Doores, K. J.; Boutureira, O.; Davis, B. G. Site-selective traceless Staudinger ligation for glycoprotein synthesis reveals scope and limitations. *ChemBioChem* **2011**, *12*, 1383-1386.
- (145) Carroll, L.; Boldon, S.; Bejot, R.; Moore, J. E.; Declerck, J.; Gouverneur, V. The traceless Staudinger ligation for indirect ¹⁸F-radiolabelling. *Org. Biomol. Chem.* **2011**, *9*, 136-140.
- (146) Serwa, R.; Wilkening, I.; Del Signore, G.; Mühlberg, M.; Claußnitzer, I.; Weise, C.; Gerrits, M.; Hackenberger, C. P. R. Chemoselective Staudinger-phosphite reaction of azides for the phosphorylation of proteins. *Angew. Chem. Int. Ed.* **2009**, *48*, 8234-8239.
- (147) Serwa, R.; Majkut, P.; Horstmann, B.; Swiecicki, J.-M.; Gerrits, M.; Krause, E.; Hackenberger, C. P. R. Site-specific PEGylation of proteins by a Staudinger-phosphite reaction. *Chem. Sci.* **2010**, *1*, 596-602.
- (148) Böhrsch, V.; Serwa, R.; Majkut, P.; Krause, E.; Hackenberger, C. P. R. Site-specific functionalization of proteins by a Staudinger-type reaction using unsymmetrical phosphites. *Chem. Commun.* **2010**, *46*, 3176-3178.
- (149) Lutz, J. 1,3-Dipolar cycloadditions of azides and alkynes: A universal ligation tool in polymer and materials science. *Angew. Chem. Int. Ed.* **2007**, *46*, 1018-1025.
- (150) Special issue: Click chemistry. *QSAR Comb. Sci.* **2007**, *26*, 1111-1323.
- (151) Wu, P.; Fokin, V. V. Catalytic azide—alkyne cycloaddition: Reactivity and applications. *Aldrichim. Acta* **2007**, *40*, 7-17.
- (152) Tron, G. C.; Pirali, T.; Billington, R. A.; Canonico, P. L.; Sorba, G.; Genazzani, A. A. Click chemistry reactions in medicinal chemistry: Applications of the 1,3-dipolar cycloaddition between azides and alkynes. *Med. Res. Rev.* **2008**, *28*, 278-308.
- (153) Fokin, V. V. Click imaging of biochemical processes in living systems. *ACS Chem. Biol.* **2007**, *2*, 775-778.
- (154) Fournier, D.; Hoogenboom, R.; Schubert, U. S. Clicking polymers: A straightforward approach to novel macromolecular architectures. *Chem. Soc. Rev.* **2007**, *36*, 1369-1380.
- (155) El-Sagheer, A. H.; Brown, T. Click chemistry with DNA. *Chem. Soc. Rev.* **2010**, *39*, 1388-1405.
- (156) Mamidyala, S. K.; Finn, M. G. In situ click chemistry: Probing the binding landscapes of biological molecules. *Chem. Soc. Rev.* **2010**, *39*, 1252-1261.
- (157) Wängler, C.; Schirmacher, R.; Bartenstein, P.; Wängler, B. Click-chemistry reactions in radiopharmaceutical chemistry: Fast and easy introduction of radiolabels into biomolecules for in vivo imaging. *Curr. Med. Chem.* **2010**, *17*, 1092-1116.

- (158) van Dijk, M.; Rijkers, D. T. S.; Liskamp, R. M. J.; van Nostrum, C. F.; Hennink, W. E. Synthesis and applications of biomedical and pharmaceutical polymers via click chemistry methodologies. *Bioconjugate Chem.* **2009**, *20*, 2001-2016.
- (159) Lutz, J.-F.; Zarafshani, Z. Efficient construction of therapeutics, bioconjugates, biomaterials and bioactive surfaces using azide-alkyne “click” chemistry. *Adv. Drug Deliver. Rev.* **2008**, *60*, 958-970.
- (160) Barglow, K. T.; Cravatt, B. F. Activity-based protein profiling for the functional annotation of enzymes. *Nat. Methods* **2007**, *4*, 822-827.
- (161) Nomura, D. K.; Dix, M. M.; Cravatt, B. F. Activity-based protein profiling for biochemical pathway discovery in cancer. *Nat. Rev. Cancer* **2010**, *10*, 630-638.
- (162) Simon, G. M.; Cravatt, B. F. Activity-based proteomics of enzyme superfamilies: Serine hydrolases as a case study. *J. Biol. Chem.* **2010**, *285*, 11051-11055.
- (163) Cravatt, B. F.; Wright, A. T.; Kozarich, J. W. Activity-based protein profiling: From enzyme chemistry to proteomic chemistry. *Annu. Rev. Biochem* **2008**, *77*, 383-414.
- (164) Sawa, M.; Hsu, T.-L.; Itoh, T.; Sugiyama, M.; Hanson, S. R.; Vogt, P. K.; Wong, C.-H. Glycoproteomic probes for fluorescent imaging of fucosylated glycans in vivo. *Proc. Natl. Acad. Sci. U.S.A.* **2006**, *103*, 12371 -12376.
- (165) Rabuka, D.; Hubbard, S. C.; Laughlin, S. T.; Argade, S. P.; Bertozzi, C. R. A chemical reporter strategy to probe glycoprotein fucosylation. *J. Am. Chem. Soc.* **2006**, *128*, 12078-12079.
- (166) Chang, P. V.; Chen, X.; Smyrniotis, C.; Xenakis, A.; Hu, T.; Bertozzi, C. R.; Wu, P. Metabolic labeling of sialic acids in living animals with alkynyl sugars. *Angew. Chem. Int. Ed.* **2009**, *48*, 4030-4033.
- (167) Hanson, S. R.; Hsu, T.-L.; Weerapana, E.; Kishikawa, K.; Simon, G. M.; Cravatt, B. F.; Wong, C.-H. Tailored glycoproteomics and glycan site mapping using saccharide-selective bioorthogonal probes. *J. Am. Chem. Soc.* **2007**, *129*, 7266-7267.
- (168) Beatty, K. E.; Liu, J. C.; Xie, F.; Dieterich, D. C.; Schuman, E. M.; Wang, Q.; Tirrell, D. A. Fluorescence visualization of newly synthesized proteins in mammalian cells. *Angew. Chem. Int. Ed.* **2006**, *45*, 7364-7367.
- (169) Dieterich, D. C.; Hodas, J. J. L.; Gouzer, G.; Shadrin, I. Y.; Ngo, J. T.; Triller, A.; Tirrell, D. A.; Schuman, E. M. In situ visualization and dynamics of newly synthesized proteins in rat hippocampal neurons. *Nat. Neurosci.* **2010**, *13*, 897-905.
- (170) Beatty, K. E.; Tirrell, D. A. Two-color labeling of temporally defined protein populations in mammalian cells. *Bioorg. Med. Chem. Lett.* **2008**, *18*, 5995-5999.
- (171) Ngo, J. T.; Champion, J. A.; Mahdavi, A.; Tanrikulu, I. C.; Beatty, K. E.; Connor, R. E.; Yoo, T. H.; Dieterich, D. C.; Schuman, E. M.; Tirrell, D. A. Cell-selective metabolic labeling of proteins. *Nat. Chem. Biol* **2009**, *5*, 715-717.
- (172) Grammel, M.; Zhang, M. M.; Hang, H. C. Orthogonal alkynyl amino acid reporter for selective labeling of bacterial proteomes during infection. *Angew. Chem. Int. Ed.* **2010**, *49*, 5970-5974.
- (173) Nguyen, D. P.; Lusic, H.; Neumann, H.; Kapadnis, P. B.; Deiters, A.; Chin, J. W. Genetic encoding and labeling of aliphatic azides and alkynes in recombinant

- proteins via a pyrrolysyl-tRNA synthetase/tRNACUA pair and click chemistry. *J. Am. Chem. Soc.* **2009**, *131*, 8720-8721.
- (174) Fekner, T.; Li, X.; Lee, M. M.; Chan, M. K. A pyrrolysine analogue for protein click chemistry. *Angew. Chem. Int. Ed.* **2009**, *48*, 1633-1635.
- (175) Hang, H. C.; Geutjes, E.-J.; Grotenbreg, G.; Pollington, A. M.; Bijlmakers, M. J.; Ploegh, H. L. Chemical probes for the rapid detection of fatty-acylated proteins in mammalian cells. *J. Am. Chem. Soc.* **2007**, *129*, 2744-2745.
- (176) Charron, G.; Zhang, M. M.; Yount, J. S.; Wilson, J.; Raghavan, A. S.; Shamir, E.; Hang, H. C. Robust fluorescent detection of protein fatty-acylation with chemical reporters. *J. Am. Chem. Soc.* **2009**, *131*, 4967-4975.
- (177) Rangan, K. J.; Yang, Y.-Y.; Charron, G.; Hang, H. C. Rapid visualization and large-scale profiling of bacterial lipoproteins with chemical reporters. *J. Am. Chem. Soc.* **2010**, *132*, 10628-10629.
- (178) Wilson, J. P.; Raghavan, A. S.; Yang, Y.-Y.; Charron, G.; Hang, H. C. Proteomic analysis of fatty-acylated proteins in mammalian cells with chemical reporters reveals S-acylation of histone H3 variants. *Mol. Cell. Proteomics* **2011**, *10*, M110.0011981-15.
- (179) Yount, J. S.; Moltedo, B.; Yang, Y.-Y.; Charron, G.; Moran, T. M.; López, C. B.; Hang, H. C. Palmitoylome profiling reveals S-palmitoylation-dependent antiviral activity of IFITM3. *Nat. Chem. Biol.* **2010**, *6*, 610-614.
- (180) Zhang, M. M.; Tsou, L. K.; Charron, G.; Raghavan, A. S.; Hang, H. C. Tandem fluorescence imaging of dynamic S-acylation and protein turnover. *Proc. Natl. Acad. Sci. U.S.A.* **2010**, *107*, 8627-8632.
- (181) Liu, K.; Yang, P.; Na, Z.; Yao, S. Q. Dynamic monitoring of newly synthesized proteomes: Up-regulation of myristoylated protein kinase A during butyric acid induced apoptosis. *Angew. Chem. Int. Ed.* **2011**, *50*, 6776-6781.
- (182) Neef, A. B.; Schultz, C. Selective fluorescence labeling of lipids in living cells. *Angew. Chem. Int. Ed.* **2009**, *48*, 1498-1500.
- (183) Jao, C. Y.; Roth, M.; Welti, R.; Salic, A. Metabolic labeling and direct imaging of choline phospholipids in vivo. *Proc. Natl. Acad. Sci. U.S.A.* **2009**, *106*, 15332 - 15337.
- (184) Salic, A.; Mitchison, T. J. A chemical method for fast and sensitive detection of DNA synthesis in vivo. *Proc. Natl. Acad. Sci. U.S.A.* **2008**, *105*, 2415 -2420.
- (185) Gratzner, H. Monoclonal antibody to 5-bromo- and 5-iododeoxyuridine: A new reagent for detection of DNA replication. *Science* **1982**, *218*, 474 -475.
- (186) Jao, C. Y.; Salic, A. Exploring RNA transcription and turnover in vivo by using click chemistry. *Proc. Natl. Acad. Sci. U.S.A.* **2008**, *105*, 15779 -15784.
- (187) Gramlich, P. M. E.; Wirges, C. T.; Manetto, A.; Carell, T. Postsynthetic DNA modification through the copper-catalyzed azide-alkyne cycloaddition reaction. *Angew. Chem. Int. Ed.* **2008**, *47*, 8350-8358.
- (188) Burley, G. A.; Gierlich, J.; Mofid, M. R.; Nir, H.; Tal, S.; Eichen, Y.; Carell, T. Directed DNA metallization. *J. Am. Chem. Soc.* **2006**, *128*, 1398-1399.

- (189) Gierlich, J.; Burley, G. A.; Gramlich, P. M. E.; Hammond, D. M.; Carell, T. Click chemistry as a reliable method for the high-density postsynthetic functionalization of alkyne-modified DNA. *Org. Lett.* **2006**, *8*, 3639-3642.
- (190) Gramlich, P. M. E.; Warncke, S.; Gierlich, J.; Carell, T. Click–click–click: Single to triple modification of DNA. *Angew. Chem. Int. Ed.* **2008**, *47*, 3442-3444.
- (191) Seela, F.; Xiong, H.; Leonard, P.; Budow, S. 8-Aza-7-deazaguanine nucleosides and oligonucleotides with octadiynyl side chains: Synthesis, functionalization by the azide-alkyne “click” reaction and nucleobase specific fluorescence quenching of coumarin dye conjugates. *Org. Biomol. Chem.* **2009**, *7*, 1374-1387.
- (192) Sirivolu, V. R.; Chittepu, P.; Seela, F. DNA with branched internal side chains: Synthesis of 5-tripropargylamine-dU and conjugation by an azide-alkyne double click reaction. *ChemBioChem* **2008**, *9*, 2305-2316.
- (193) Seela, F.; Sirivolu, V. R. Pyrrolo-dC oligonucleotides bearing alkynyl side chains with terminal triple bonds: Synthesis, base pairing and fluorescent dye conjugates prepared by the azide–alkyne “click” reaction. *Org. Biomol. Chem.* **2008**, *6*, 1674-1687.
- (194) Weisbrod, S. H.; Marx, A. A nucleoside triphosphate for site-specific labelling of DNA by the Staudinger ligation. *Chem. Commun.* **2007**, *43*, 1828-1830.
- (195) Binda, O.; Boyce, M.; Rush, J. S.; Palaniappan, K. K.; Bertozzi, C. R.; Gozani, O. A chemical method for labeling lysine methyltransferase substrates. *ChemBioChem* **2011**, *12*, 330-334.
- (196) Yang, Y.-Y.; Ascano, J. M.; Hang, H. C. Bioorthogonal chemical reporters for monitoring protein acetylation. *J. Am. Chem. Soc.* **2010**, *132*, 3640-3641.
- (197) Meier, J. L.; Mercer, A. C.; Rivera, H.; Burkart, M. D. Synthesis and evaluation of bioorthogonal pantetheine analogues for in vivo protein modification. *J. Am. Chem. Soc.* **2006**, *128*, 12174-12184.
- (198) Hong, V.; Steinmetz, N. F.; Manchester, M.; Finn, M. G. Labeling live cells by copper-catalyzed alkyne–azide click chemistry. *Bioconjugate Chem.* **2010**, *21*, 1912-1916.
- (199) Soriano del Amo, D.; Wang, W.; Jiang, H.; Besanceney, C.; Yan, A. C.; Levy, M.; Liu, Y.; Marlow, F. L.; Wu, P. Biocompatible copper(I) catalysts for in vivo imaging of glycans. *J. Am. Chem. Soc.* **2010**, *132*, 16893-16899.
- (200) Besanceney-Webler, C.; Jiang, H.; Zheng, T.; Feng, L.; Soriano del Amo, D.; Wang, W.; Klivansky, L. M.; Marlow, F. L.; Liu, Y.; Wu, P. Increasing the efficacy of bioorthogonal click reactions for bioconjugation: A comparative study. *Angew. Chem. Int. Ed.* **2011**, *50*, 8051-8056.
- (201) Hein, J. E.; Tripp, J. C.; Krasnova, L. B.; Sharpless, K. B.; Fokin, V. V. Copper(I)-catalyzed cycloaddition of organic azides and 1-iodoalkynes. *Angew. Chem. Int. Ed.* **2009**, *48*, 8018-8021.
- (202) Schultz, M. K.; Parameswarappa, S. G.; Pigge, F. C. Synthesis of a DOTA–biotin conjugate for radionuclide chelation via Cu-free click chemistry. *Org. Lett.* **2010**, *12*, 2398-2401.

- (203) Stöckmann, H.; Neves, A. A.; Stairs, S.; Ireland-Zecchini, H.; Brindle, K. M.; Leeper, F. J. Development and evaluation of new cyclooctynes for cell surface glycan imaging in cancer cells. *Chem. Sci.* **2011**, *2*, 932-936.
- (204) Ning, X.; Guo, J.; Wolfert, M. A.; Boons, G.-J. Visualizing metabolically labeled glycoconjugates of living cells by copper-free and fast Huisgen cycloadditions. *Angew. Chem. Int. Ed.* **2008**, *47*, 2253-2255.
- (205) Mbua, N. E.; Guo, J.; Wolfert, M. A.; Steet, R.; Boons, G. Strain-promoted alkyne-azide cycloadditions (SPAAC) reveal new features of glycoconjugate biosynthesis. *ChemBioChem* **2011**, *12*, 1912-1921.
- (206) Debets, M. F.; van Berkel, S. S.; Schoffelen, S.; Rutjes, F. P. J. T.; van Hest, J. C.; M.; van Delft, F. L. Aza-dibenzocyclooctynes for fast and efficient enzyme PEGylation via copper-free (3+2) cycloaddition. *Chem. Commun.* **2010**, *46*, 97-99.
- (207) Kuzmin, A.; Poloukhine, A.; Wolfert, M. A.; Popik, V. V. Surface functionalization using catalyst-free azide-alkyne cycloaddition. *Bioconjugate Chem.* **2010**, *21*, 2076-2085.
- (208) Jewett, J. C.; Sletten, E. M.; Bertozzi, C. R. Rapid Cu-free click chemistry with readily synthesized biarylazacyclooctynones. *J. Am. Chem. Soc.* **2010**, *132*, 3688-3690.
- (209) Ess, D. H.; Jones, G. O.; Houk, K. N. Transition states of strain-promoted metal-free click chemistry: 1,3-Dipolar cycloadditions of phenyl azide and cyclooctynes. *Org. Lett.* **2008**, *10*, 1633-1636.
- (210) Gordon, C. G.; Mackey, J.; Jewett, J. C.; Sletten, E. M.; Houk, K. N.; Bertozzi, C. R. Reactivity of biarylazacyclooctynones in copper-free click chemistry. *Manuscript in preparation.*
- (211) Jewett, J. C.; Bertozzi, C. R. Synthesis of a fluorogenic cyclooctyne activated by Cu-free click chemistry. *Org. Lett.* Submitted.
- (212) Dommerholt, J.; Schmidt, S.; Temming, R.; Hendriks, L. J. A.; Rutjes, F. P. J. T.; van Hest, J. C. M.; Lefeber, D. J.; Friedl, P.; van Delft, F. L. Readily accessible bicyclononynes for bioorthogonal labeling and three-dimensional imaging of living cells. *Angew. Chem. Int. Ed.* **2010**, *49*, 9422-9425.
- (213) Canalle, L. A.; Vong, T.; Adams, P. H. H. M.; van Delft, F. L.; Raats, J. M. H.; Chirivi, R. G. S.; van Hest, J. C. M. Clickable enzyme-linked immunosorbent assay. *Biomacromolecules* **2011**, *12*, 3692-3697.
- (214) Kii, I.; Shiraishi, A.; Hiramatsu, T.; Matsushita, T.; Uekusa, H.; Yoshida, S.; Yamamoto, M.; Kudo, A.; Hagiwara, M.; Hosoya, T. Strain-promoted double-click reaction for chemical modification of azido-biomolecules. *Org. Biomol. Chem.* **2010**, *8*, 4051-4055.
- (215) Poloukhine, A. A.; Mbua, N. E.; Wolfert, M. A.; Boons, G.-J.; Popik, V. V. Selective labeling of living cells by a photo-triggered click reaction. *J. Am. Chem. Soc.* **2009**, *131*, 15769-15776.
- (216) Orski, S. V.; Poloukhine, A. A.; Arumugam, S.; Mao, L.; Popik, V. V.; Locklin, J. High density orthogonal surface immobilization via photoactivated copper-free click chemistry. *J. Am. Chem. Soc.* **2010**, *132*, 11024-11026.

- (217) Baskin, J. M.; Prescher, J. A.; Laughlin, S. T.; Agard, N. J.; Chang, P. V.; Miller, I. A.; Lo, A.; Codelli, J. A.; Bertozzi, C. R. Copper-free click chemistry for dynamic in vivo imaging. *Proc. Natl. Acad. Sci. U.S.A.* **2007**, *104*, 16793-16797.
- (218) Laughlin, S. T.; Bertozzi, C. R. In vivo imaging of *Caenorhabditis elegans* glycans. *ACS Chem. Biol.* **2009**, *4*, 1068-1072.
- (219) Laughlin, S. T.; Baskin, J. M.; Amacher, S. L.; Bertozzi, C. R. In vivo imaging of membrane-associated glycans in developing zebrafish. *Science* **2008**, *320*, 664-667.
- (220) Chang, P. V.; Prescher, J. A.; Sletten, E. M.; Baskin, J. M.; Miller, I. A.; Agard, N. J.; Lo, A.; Bertozzi, C. R. Copper-free click chemistry in living animals. *Proc. Natl. Acad. Sci. U.S.A.* **2010**, *107*, 1821-1826.
- (221) Dehnert, K. W.; Beahm, B. J.; Huynh, T. T.; Baskin, J. M.; Laughlin, S. T.; Wang, W.; Wu, P.; Amacher, S. L.; Bertozzi, C. R. Metabolic labeling of fucosylated glycans in developing zebrafish. *ACS Chem. Biol.* **2011**, *6*, 547-552.
- (222) Bernardin, A.; Cazet, A.; Guyon, L.; Delannoy, P.; Vinet, F.; Bonnaffé, D.; Texier, I. Copper-free click chemistry for highly luminescent quantum dot conjugates: Application to in vivo metabolic imaging. *Bioconjugate Chem.* **2010**, *21*, 583-588.
- (223) Chang, P. V.; Dube, D. H.; Sletten, E. M.; Bertozzi, C. R. A strategy for the selective imaging of glycans using caged metabolic precursors. *J. Am. Chem. Soc.* **2010**, *132*, 9516-9518.
- (224) Beatty, K. E.; Fisk, J. D.; Smart, B. P.; Lu, Y. Y.; Szychowski, J.; Hangauer, M. J.; Baskin, J. M.; Bertozzi, C. R.; Tirrell, D. A. Live-cell imaging of cellular proteins by a strain-promoted azide-alkyne cycloaddition. *ChemBioChem* **2010**, *11*, 2092-2095.
- (225) Beatty, K. E.; Szychowski, J.; Fisk, J. D.; Tirrell, D. A. A BODIPY-cyclooctyne for protein imaging in live cells. *ChemBioChem* **2011**, *12*, 2137-2139.
- (226) Nessen, M. A.; Kramer, G.; Back, J.; Baskin, J. M.; Smeenk, L. E. J.; de Koning, L. J.; van Maarseveen, J. H.; de Jong, L.; Bertozzi, C. R.; Hiemstra, H.; de Koster, C. G. Selective enrichment of azide-containing peptides from complex mixtures. *J. Proteome Res.* **2009**, *8*, 3702-3711.
- (227) Temming, R. P.; van Scherpenzeel, M.; te Brinke, E.; Schoffelen, S.; Gloerich, J.; Lefeber, D. J.; van Delft, F. L. Protein enrichment by capture-release based on strain-promoted cycloaddition of azide with bicyclononyne (BCN). *Bioorg. Med. Chem. Lett.* **2011**.
- (228) Jayaprakash, K. N.; Peng, C. G.; Butler, D.; Varghese, J. P.; Maier, M. A.; Rajeev, K. G.; Manoharan, M. Non-nucleoside building blocks for copper-assisted and copper-free click chemistry for the efficient synthesis of RNA conjugates. *Org. Lett.* **2010**, *12*, 5410-5413.
- (229) van Delft, P.; Meeuwenoord, N. J.; Hoogendoorn, S.; Dinkelaar, J.; Overkleeft, H. S.; van der Marel, G. A.; Filippov, D. V. Synthesis of oligoribonucleic acid conjugates using a cyclooctyne phosphoramidite. *Org. Lett.* **2010**, *12*, 5486-5489.
- (230) Shelbourne, M.; Chen, X.; Brown, T.; El-Sagheer, A. H. Fast copper-free click DNA ligation by the ring-strain promoted alkyne-azide cycloaddition reaction. *Chem. Commun.* **2011**, *47*, 6257-6259.

- (231) Marks, I. S.; Kang, J. S.; Jones, B. T.; Landmark, K. J.; Cleland, A. J.; Taton, T. A. Strain-promoted “click” chemistry for terminal labeling of DNA. *Bioconjugate Chem.* **2011**, *22*, 1259-1263.
- (232) Dai, C.; Wang, L.; Sheng, J.; Peng, H.; Draganov, A. B.; Huang, Z.; Wang, B. The first chemical synthesis of boronic acid-modified DNA through a copper-free click reaction. *Chem. Commun.* **2011**, *47*, 3598-3600.
- (233) Sharma, A. K.; Heemstra, J. M. Small-molecule-dependent split aptamer ligation. *J. Am. Chem. Soc.* **2011**, *133*, 12426-12429.
- (234) Martin, M. E.; Parameswarappa, S. G.; O’Dorisio, M. S.; Pigge, F. C.; Schultz, M. K. A DOTA-peptide conjugate by copper-free click chemistry. *Bioorg. Med. Chem. Lett.* **2010**, *20*, 4805-4807.
- (235) Baumhover, N. J.; Martin, M. E.; Parameswarappa, S. G.; Kloeping, K. C.; O’Dorisio, M. S.; Pigge, F. C.; Schultz, M. K. Improved synthesis and biological evaluation of chelator-modified α -MSH analogs prepared by copper-free click chemistry. *Bioorg. Med. Chem. Lett.* **2011**, *21*, 5757-5761.
- (236) Kálai, T.; Fleissner, M. R.; Jeko, J.; Hubbell, W. L.; Hideg, K. Synthesis of new spin labels for Cu-free click conjugation. *Tetrahedron Lett.* **2011**, *52*, 2747-2749.
- (237) Jølcck, R. I.; Sun, H.; Berg, R. H.; Andresen, T. L. Catalyst-free conjugation and in situ quantification of nanoparticle ligand surface density using fluorogenic Cu-free click chemistry. *Chem. Eur. J.* **2011**, *17*, 3326-3331.
- (238) Ornelas, C.; Lodescar, R.; Durandin, A.; Canary, J. W.; Pennell, R.; Liebes, L. F.; Weck, M. Combining aminocyanine dyes with polyamide dendrons: A promising strategy for imaging in the near-infrared region. *Chem. Eur. J.* **2011**, *17*, 3619-3629.
- (239) Huang, B.; Desai, A.; Zong, H.; Tang, S.; Leroueil, P.; Baker Jr., J. R. Copper-free click conjugation of methotrexate to a PAMAM dendrimer platform. *Tetrahedron Lett.* **2011**, *52*, 1411-1414.
- (240) Ornelas, C.; Broichhagen, J.; Weck, M. Strain-promoted alkyne azide cycloaddition for the functionalization of poly(amide)-based dendrons and dendrimers. *J. Am. Chem. Soc.* **2010**, *132*, 3923-3931.
- (241) Ledin, P. A.; Friscourt, F.; Guo, J.; Boons, G. Convergent assembly and surface modification of multifunctional dendrimers by three consecutive click reactions. *Chem. Eur. J.* **2011**, *17*, 839-846.
- (242) DeForest, C. A.; Polizzotti, B. D.; Anseth, K. S. Sequential click reactions for synthesizing and patterning three-dimensional cell microenvironments. *Nat. Materials* **2009**, *8*, 659-664.
- (243) DeForest, C. A.; Sims, E. A.; Anseth, K. S. Peptide-functionalized click hydrogels with independently tunable mechanics and chemical functionality for 3D cell culture. *Chem. Mater.* **2010**, *22*, 4783-4790.
- (244) Johnson, J. A.; Baskin, J. M.; Bertozzi, C. R.; Koberstein, J. T.; Turro, N. J. Copper-free click chemistry for the in situ crosslinking of photodegradable star polymers. *Chem. Commun.* **2008**, *42*, 3064-3066.
- (245) Joce, C.; Caryl, J.; Stockley, P. G.; Warriner, S.; Nelson, A. Identification of stable S-adenosylmethionine (SAM) analogues derivatised with bioorthogonal tags:

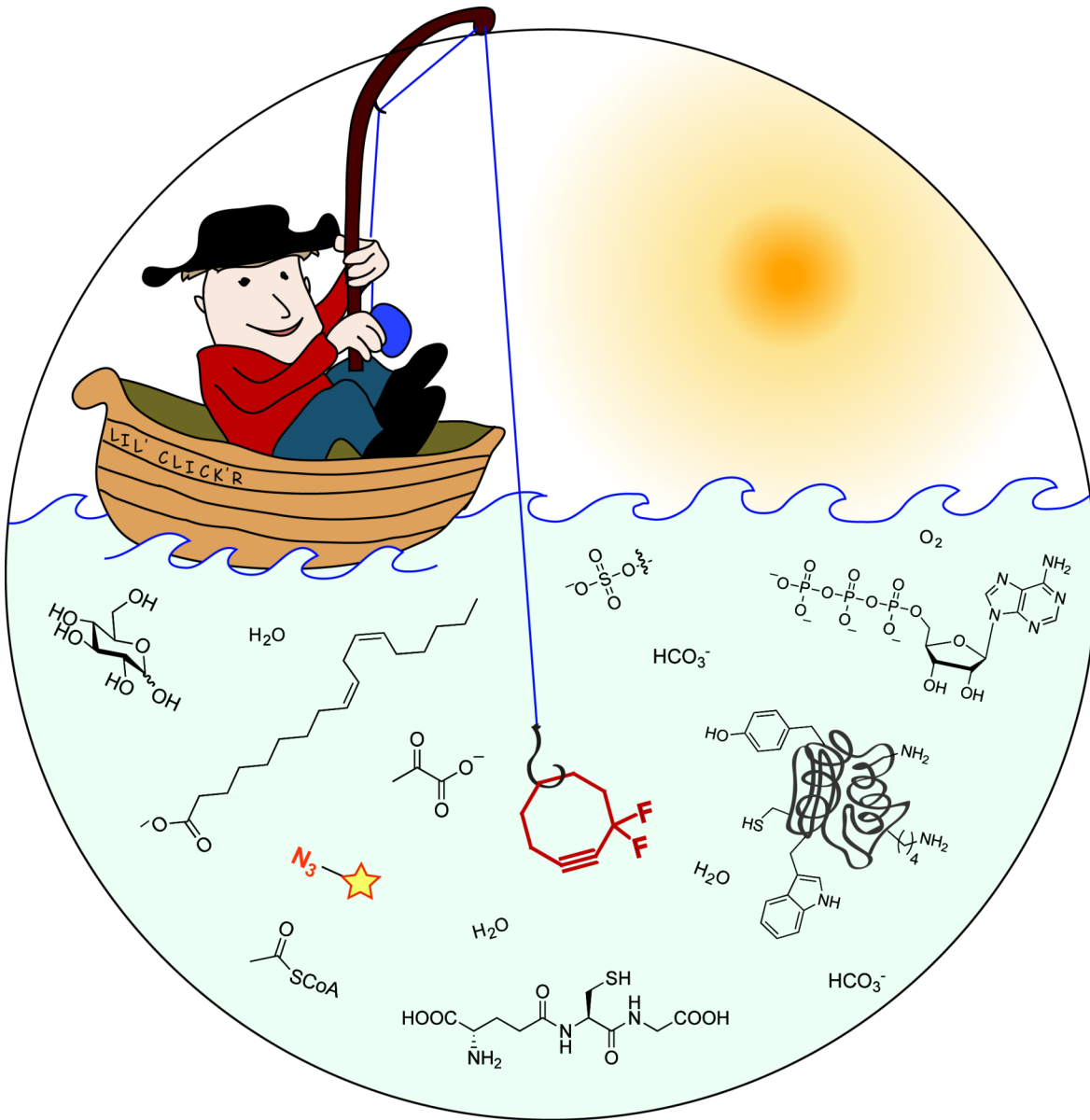
- Effect of ligands on the affinity of the E. coli methionine repressor, MetJ, for its operator DNA. *Org. Biomol. Chem.* **2009**, *7*, 635-638.
- (246) Hur, G. H.; Meier, J. L.; Baskin, J.; Codelli, J. A.; Bertozzi, C. R.; Marahiel, M. A.; Burkart, M. D. Crosslinking studies of protein-protein interactions in monribosomal peptide biosynthesis. *Chem. Biol.* **2009**, *16*, 372-381.
- (247) Plass, T.; Milles, S.; Koehler, C.; Schultz, C.; Lemke, E. A. Genetically encoded copper-free click chemistry. *Angew. Chem. Int. Ed.* **2011**, *50*, 3878-3881.
- (248) Blackman, M. L.; Royzen, M.; Fox, J. M. Tetrazine ligation: Fast bioconjugation based on inverse-electron-demand Diels–Alder reactivity. *J. Am. Chem. Soc.* **2008**, *130*, 13518-13519.
- (249) Devaraj, N. K.; Weissleder, R.; Hilderbrand, S. A. Tetrazine-based cycloadditions: Application to pretargeted live cell imaging. *Bioconjugate Chem.* **2008**, *19*, 2297-2299.
- (250) Pipkorn, R.; Waldeck, W.; Diding, B.; Koch, M.; Mueller, G.; Wiessler, M.; Braun, K. Inverse-electron-demand Diels-Alder reaction as a highly efficient chemoselective ligation procedure: Synthesis and function of a BioShuttle for temozolomide transport into prostate cancer cells. *J. Pept. Sci.* **2009**, *15*, 235-241.
- (251) Braun, K. Treatment of glioblastoma multiform cells with temozolomide-BioShuttle ligated by the inverse Diels-Alder ligation chemistry. *Drug Des. Dev. Ther.* **2009**, *6*, 289-301.
- (252) Braun, K.; Ehemann, V.; Wiessler, M.; Pipkorn, R.; Diding, B.; Mueller, G.; Waldeck, W. High-resolution flow cytometry: A suitable tool for monitoring aneuploid prostate cancer cells after TMZ and TMZ-BioShuttle treatment. *Int. J. Med. Sci.* **2009**, *6*, 338-347.
- (253) Wiessler, M.; Waldeck, W.; Kliem, C.; Pipkorn, R.; Braun, K. The Diels-Alder-reaction with inverse-electron-demand, a very efficient versatile click-reaction concept for proper ligation of variable molecular partners. *Int. J. Med. Sci.* **2009**, *7*, 19-28.
- (254) Braun, K.; Wiessler, M.; Pipkorn, R.; Ehemann, V.; Bäuerle, T.; Fleischhacker, H.; Müller, G.; Lorenz, P.; Waldeck, W. A cyclic-RGD-BioShuttle functionalized with TMZ by DARinv “Click Chemistry” targeted to $\alpha v \beta 3$ integrin for therapy. *Int. J. Med. Sci.* **2010**, *7*, 326-339.
- (255) Devaraj, N. K.; Upadhyay, R.; Haun, J. B.; Hilderbrand, S. A.; Weissleder, R. Fast and sensitive pretargeted labeling of cancer cells through a tetrazine- *trans*-cyclooctene cycloaddition. *Angew. Chem. Int. Ed.* **2009**, *48*, 7013-7016.
- (256) Rossin, R.; Renart Verkerk, P.; van den Bosch, S. M.; Vuldere, R. C. M.; Verel, I.; Lub, J.; Robillard, M. S. In vivo chemistry for pretargeted tumor imaging in live mice. *Angew. Chem. Int. Ed.* **2010**, *49*, 3375-3378.
- (257) Keliher, E. J.; Reiner, T.; Turetsky, A.; Hilderbrand, S. A.; Weissleder, R. High-yielding, two-step ^{18}F labeling strategy for ^{18}F -PARP1 inhibitors. *ChemMedChem* **2011**, *6*, 424-427.
- (258) Li, Z.; Cai, H.; Hassink, M.; Blackman, M. L.; Brown, R. C. D.; Conti, P. S.; Fox, J. M. Tetrazine-*trans*-cyclooctene ligation for the rapid construction of ^{18}F labeled probes. *Chem. Commun.* **2010**, *46*, 8043-8045.

- (259) Zeglis, B. M.; Mohindra, P.; Weissmann, G. I.; Divilov, V.; Hilderbrand, S. A.; Weissleder, R.; Lewis, J. S. A modular strategy for the construction of radiometallated antibodies for positron emission tomography based on inverse electron demand Diels-Alder click chemistry. *Bioconjugate Chem.* **2011**, DOI: 10.1021/bc200288d.
- (260) Selvaraj, R.; Liu, S.; Hassink, M.; Huang, C.-W.; Yap, L.-P.; Park, R.; Fox, J. M.; Li, Z.; Conti, P. S. Tetrazine-trans-cyclooctene ligation for the rapid construction of integrin α vs. β 3 targeted PET tracer based on a cyclic RGD peptide. *Bioorg. Med. Chem. Lett.* **2011**, *21*, 5011-5014.
- (261) Devaraj, N. K.; Hilderbrand, S.; Upadhyay, R.; Mazitschek, R.; Weissleder, R. Bioorthogonal turn-on probes for imaging small molecules inside living cells. *Angew. Chem. Int. Ed.* **2010**, *49*, 2869-2872.
- (262) Haun, J. B.; Devaraj, N. K.; Hilderbrand, S. A.; Lee, H.; Weissleder, R. Bioorthogonal chemistry amplifies nanoparticle binding and enhances the sensitivity of cell detection. *Nat. Nanotechnol.* **2010**, *5*, 660-665.
- (263) Haun, J. B.; Devaraj, N. K.; Marinelli, B. S.; Lee, H.; Weissleder, R. Probing intracellular biomarkers and mediators of cell activation using nanosensors and bioorthogonal chemistry. *ACS Nano.* **2011**, *5*, 3204-3213.
- (264) Schoch, J.; Wiessler, M.; Jaschke, A. Post-synthetic modification of DNA by inverse-electron-demand Diels-Alder reaction. *J. Am. Chem. Soc.* **2010**, *132*, 8846-8847.
- (265) Wiessler, M.; Waldeck, W.; Pipkorn, R.; Kliem, C.; Lorenz, P.; Fleischhacker, H.; Hafner, M.; Braun, K. Extension of the PNA world by functionalized PNA monomers eligible candidates for inverse Diels-Alder click chemistry. *Int. J. Med. Sci.* **2010**, *7*, 213-223.
- (266) Pipkorn, R.; Wiessler, M.; Waldeck, W.; Lorenz, P.; Muehlhausen, U.; Fleischhacker, H.; Koch, M.; Braun, K. Enhancement of the click chemistry for the inverse Diels-Alder technology by functionalization of amide-based monomers. *Int. J. Med. Sci.* **2011**, *8*, 387-396.
- (267) Han, H.-S.; Devaraj, N. K.; Lee, J.; Hilderbrand, S. A.; Weissleder, R.; Bawendi, M. G. Development of a bioorthogonal and highly efficient conjugation method for quantum dots using tetrazine-norbornene cycloaddition. *J. Am. Chem. Soc.* **2010**, *132*, 7838-7839.
- (268) Hansell, C. F.; Espeel, P.; Stamenović, M. M.; Barker, I. A.; Dove, A. P.; Du Prez, F. E.; O'Reilly, R. K. Additive-free clicking for polymer functionalization and coupling by tetrazine-norbornene chemistry. *J. Am. Chem. Soc.* **2011**, *133*, 13828-13831.
- (269) Taylor, M. T.; Blackman, M. L.; Dmitrenko, O.; Fox, J. M. Design and synthesis of highly reactive dienophiles for the tetrazine-trans-cyclooctene ligation. *J. Am. Chem. Soc.* **2011**, *133*, 9646-9649.
- (270) Stöckmann, H.; Neves, A. A.; Day, H. A.; Stairs, S.; Brindle, K. M.; Leeper, F. J. (*E,E*)-1,5-Cyclooctadiene: A small and fast click-chemistry multitalent. *Chem. Commun.* **2011**, *47*, 7203-7205.

- (271) Song, W.; Wang, Y.; Qu, J.; Madden, M. M.; Lin, Q. A photoinducible 1,3-dipolar cycloaddition reaction for rapid, selective modification of tetrazole-containing proteins. *Angew. Chem. Int. Ed.* **2008**, *47*, 2832-2835.
- (272) Wang, Y.; Song, W.; Hu, W. J.; Lin, Q. Fast alkene functionalization in vivo by photoclick chemistry: HOMO lifting of nitrile imine dipoles. *Angew. Chem. Int. Ed.* **2009**, *48*, 5330-5333.
- (273) Yu, Z.; Lim, R. K.; V.; Lin, Q. Synthesis of macrocyclic tetrazoles for rapid photoinduced bioorthogonal 1,3-dipolar cycloaddition reactions. *Chem. Eur. J.* **2010**, *16*, 13325-13329.
- (274) Wang, Y.; Hu, W. J.; Song, W.; Lim, R. K. V.; Lin, Q. Discovery of long-wavelength photoactivatable diaryltetrazoles for bioorthogonal 1,3-dipolar cycloaddition reactions. *Org. Lett.* **2008**, *10*, 3725-3728.
- (275) Yu, Z.; Ho, L. Y.; Wang, Z.; Lin, Q. Discovery of new photoactivatable diaryltetrazoles for photoclick chemistry via 'scaffold hopping'. *Bioorg. Med. Chem. Lett.* **2011**, *21*, 5033-5036.
- (276) Song, W.; Wang, Y.; Yu, Z.; Vera, C. I. R.; Qu, J.; Lin, Q. A metabolic alkene reporter for spatiotemporally controlled imaging of newly synthesized proteins in mammalian cells. *ACS Chem. Biol.* **2010**, *5*, 875-885.
- (277) Song, W.; Wang, Y.; Qu, J.; Lin, Q. Selective functionalization of a genetically encoded alkene-containing protein via "photoclick chemistry" in bacterial cells. *J. Am. Chem. Soc.* **2008**, *130*, 9654-9655.
- (278) Wang, Y.; Lin, Q. Synthesis and evaluation of photoreactive tetrazole amino acids. *Org. Lett.* **2009**, *11*, 3570-3573.
- (279) Wang, J.; Zhang, W.; Song, W.; Wang, Y.; Yu, Z.; Li, J.; Wu, M.; Wang, L.; Zang, J.; Lin, Q. A biosynthetic route to photoclick chemistry on proteins. *J. Am. Chem. Soc.* **2010**, *132*, 14812-14818.
- (280) Suchanek, M.; Radzikowska, A.; Thiele, C. Photo-leucine and photo-methionine allow identification of protein-protein interactions in living cells. *Nat. Methods* **2005**, *2*, 261-268.
- (281) Nakashima, H.; Hashimoto, M.; Sadakane, Y.; Tomohiro, T.; Hatanaka, Y. Simple and versatile method for tagging phenyldiazirine photophores. *J. Am. Chem. Soc.* **2006**, *128*, 15092-15093.
- (282) MacKinnon, A. L.; Garrison, J. L.; Hegde, R. S.; Taunton, J. Photo-leucine incorporation reveals the target of a cyclodepsipeptide inhibitor of cotranslational translocation. *J. Am. Chem. Soc.* **2007**, *129*, 14560-14561.
- (283) Chin, J. W.; Santoro, S. W.; Martin, A. B.; King, D. S.; Wang, L.; Schultz, P. G. Addition of p-azido-l-phenylalanine to the genetic code of Escherichia coli. *J. Am. Chem. Soc.* **2002**, *124*, 9026-9027.
- (284) Chin, J. W.; Martin, A. B.; King, D. S.; Wang, L.; Schultz, P. G. Addition of a photocrosslinking amino acid to the genetic code of Escherichia coli. *Proc. Natl. Acad. Sci. U.S.A.* **2002**, *99*, 11020 -11024.
- (285) Song, W.; Yu, Z.; Madden, M. M.; Lin, Q. A bioorthogonal chemistry strategy for probing protein lipidation in live cells. *Mol. BioSyst.* **2010**, *6*, 1576-1578.

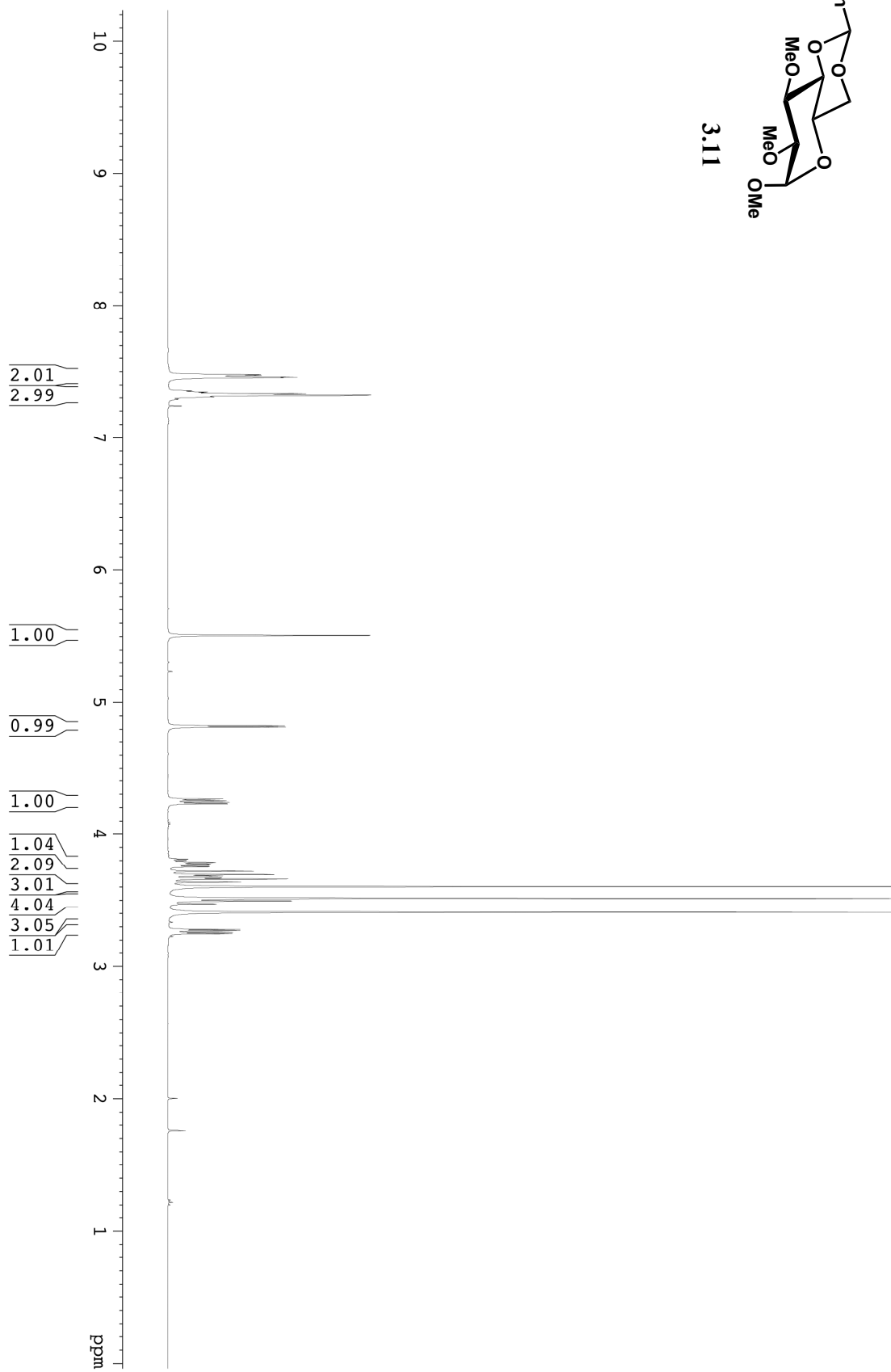
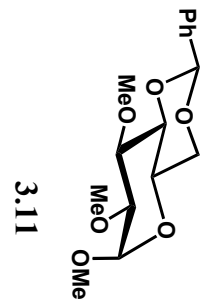
- (286) Yu, Z.; Ho, L. Y.; Lin, Q. Rapid, photoactivatable turn-on fluorescent probes based on an intramolecular photoclick reaction. *J. Am. Chem. Soc.* **2011**, *133*, 11912-11915.
- (287) Madden, M. M.; Rivera Vera, C. I.; Song, W.; Lin, Q. Facile synthesis of stapled, structurally reinforced peptide helices via a photoinduced intramolecular 1,3-dipolar cycloaddition reaction. *Chem. Commun.* **2009**, *45*, 5588-5590.
- (288) Madden, M. M.; Muppidi, A.; Li, Z.; Li, X.; Chen, J.; Lin, Q. Synthesis of cell-permeable stapled peptide dual inhibitors of the p53-Mdm2/Mdmx interactions via photoinduced cycloaddition. *Bioorg. Med. Chem. Lett.* **2011**, *21*, 1472-1475.
- (289) Lim, R. K. V.; Lin, Q. Azirine ligation: Fast and selective protein conjugation via photoinduced azirine-alkene cycloaddition. *Chem. Commun.* **2010**, *46*, 7993-7995.
- (290) Arumugam, S.; Popik, V. V. Light-induced hetero-Diels-Alder cycloaddition: A facile and selective photoclick reaction. *J. Am. Chem. Soc.* **2011**, *133*, 5573-5579.
- (291) Arumugam, S.; Popik, V. V. Patterned surface derivatization using Diels-Alder photo-click reaction. *J. Am. Chem. Soc.* **2011**, *0*.
- (292) Laverman, P.; Meeuwissen, S. A.; van Berkel, S. S.; Oyen, W. J. G.; van Delft, F. L.; Rutjes, F. P. J. T.; Boerman, O. C. In-depth evaluation of the cycloaddition-retro-Diels-Alder reaction for in vivo targeting with ¹¹¹In-DTPA-RGD conjugates. *Nucl. Med. Biol.* **2009**, *36*, 749-757.
- (293) van Dongen, S. F. M.; Verdurmen, W. P. R.; Peters, R. J. R. W.; Nolte, R. J. M.; Brock, R.; van Hest, J. C. M. Cellular integration of an enzyme-loaded polymersome nanoreactor. *Angew. Chem. Int. Ed.* **2010**, *49*, 7213-7216.
- (294) Halo, T. L.; Appelbaum, J.; Hobert, E. M.; Balkin, D. M.; Schepartz, A. Selective recognition of protein tetraserine motifs with a cell-permeable, pro-fluorescent bis-boronate ester. *J. Am. Chem. Soc.* **2009**, *131*, 438-439.
- (295) Shin, S. B. Y.; Almeida, R. D.; Gerona-Navarro, G.; Bracken, C.; Jaffrey, S. R. Assembling ligands in situ using bioorthogonal boronate ester synthesis. *Chem. Biol.* **2010**, *17*, 1171-1176.
- (296) Brustad, E.; Bushey, M. L.; Lee, J. W.; Groff, D.; Liu, W.; Schultz, P. G. A genetically encoded boronate-containing amino acid. *Angew. Chem. Int. Ed.* **2008**, *47*, 8220-8223.
- (297) Chalker, J. M.; Wood, C. S. C.; Davis, B. G. A convenient catalyst for aqueous and protein Suzuki-Miyaura cross-coupling. *J. Am. Chem. Soc.* **2009**, *131*, 16346-16347.
- (298) Spicer, C. D.; Davis, B. G. Palladium-mediated site-selective Suzuki-Miyaura protein modification at genetically encoded aryl halides. *Chem. Commun.* **2011**, *47*, 1698-1700.
- (299) Lippert, A. R.; Van de Bittner, G. C.; Chang, C. J. Boronate oxidation as a bioorthogonal reaction approach for studying the chemistry of hydrogen peroxide in living systems. *Acc. Chem. Res.* **2011**, *44*, 793-804.
- (300) Chang, M. C. Y.; Pralle, A.; Isacoff, E. Y.; Chang, C. J. A selective, cell-permeable optical probe for hydrogen peroxide in living cells. *J. Am. Chem. Soc.* **2004**, *126*, 15392-15393.

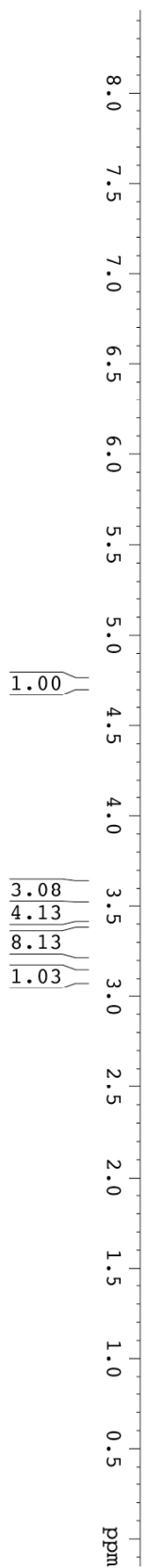
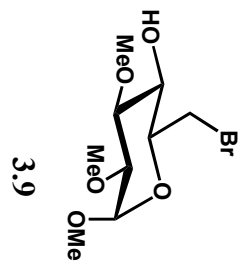
- (301) Van de Bittner, G. C.; Dubikovskaya, E. A.; Bertozzi, C. R.; Chang, C. J. In vivo imaging of hydrogen peroxide production in a murine tumor model with a chemoselective bioluminescent reporter. *Proc. Natl. Acad. Sci. U.S.A.* **2010**, *107*, 21316-21321.
- (302) Ou, W.; Uno, T.; Chiu, H.-P.; Grünewald, J.; Cellitti, S. E.; Crossgrove, T.; Hao, X.; Fan, Q.; Quinn, L. L.; Patterson, P.; Okach, L.; Jones, D. H.; Lesley, S. A.; Brock, A.; Geierstanger, B. H. Site-specific protein modifications through pyrroline-carboxy-lysine residues. *Proc. Natl. Acad. Sci. U.S.A.* **2011**, *108*, 10437-10442.
- (303) Zhang, Y.; Baranov, P. V.; Atkins, J. F.; Gladyshev, V. N. Pyrrolysine and selenocysteine use dissimilar decoding strategies. *J. Biol. Chem.* **2005**, *280*, 20740-20751.
- (304) Longstaff, D. G.; Larue, R. C.; Faust, J. E.; Mahapatra, A.; Zhang, L.; Green-Church, K. B.; Krzycki, J. A. A natural genetic code expansion cassette enables transmissible biosynthesis and genetic encoding of pyrrolysine. *Proc. Natl. Acad. Sci. U.S.A.* **2007**, *104*, 1021-1026.
- (305) Cellitti, S. E.; Ou, W.; Chiu, H.-P.; Grünewald, J.; Jones, D. H.; Hao, X.; Fan, Q.; Quinn, L. L.; Ng, K.; Anfora, A. T.; Lesley, S. A.; Uno, T.; Brock, A.; Geierstanger, B. H. D-Ornithine coopts pyrrolysine biosynthesis to make and insert pyrroline-carboxy-lysine. *Nat. Chem. Biol.* **2011**, *7*, 528-530.
- (306) Chen, P. R.; Groff, D.; Guo, J.; Ou, W.; Cellitti, S.; Geierstanger, B. H.; Schultz, P. G. A facile system for encoding unnatural amino acids in mammalian cells. *Angew. Chem. Int. Ed.* **2009**, *48*, 4052-4055.
- (307) Greiss, S.; Chin, J. W. Expanding the genetic code of an animal. *J. Am. Chem. Soc.* **2011**, *133*, 14196-14199.

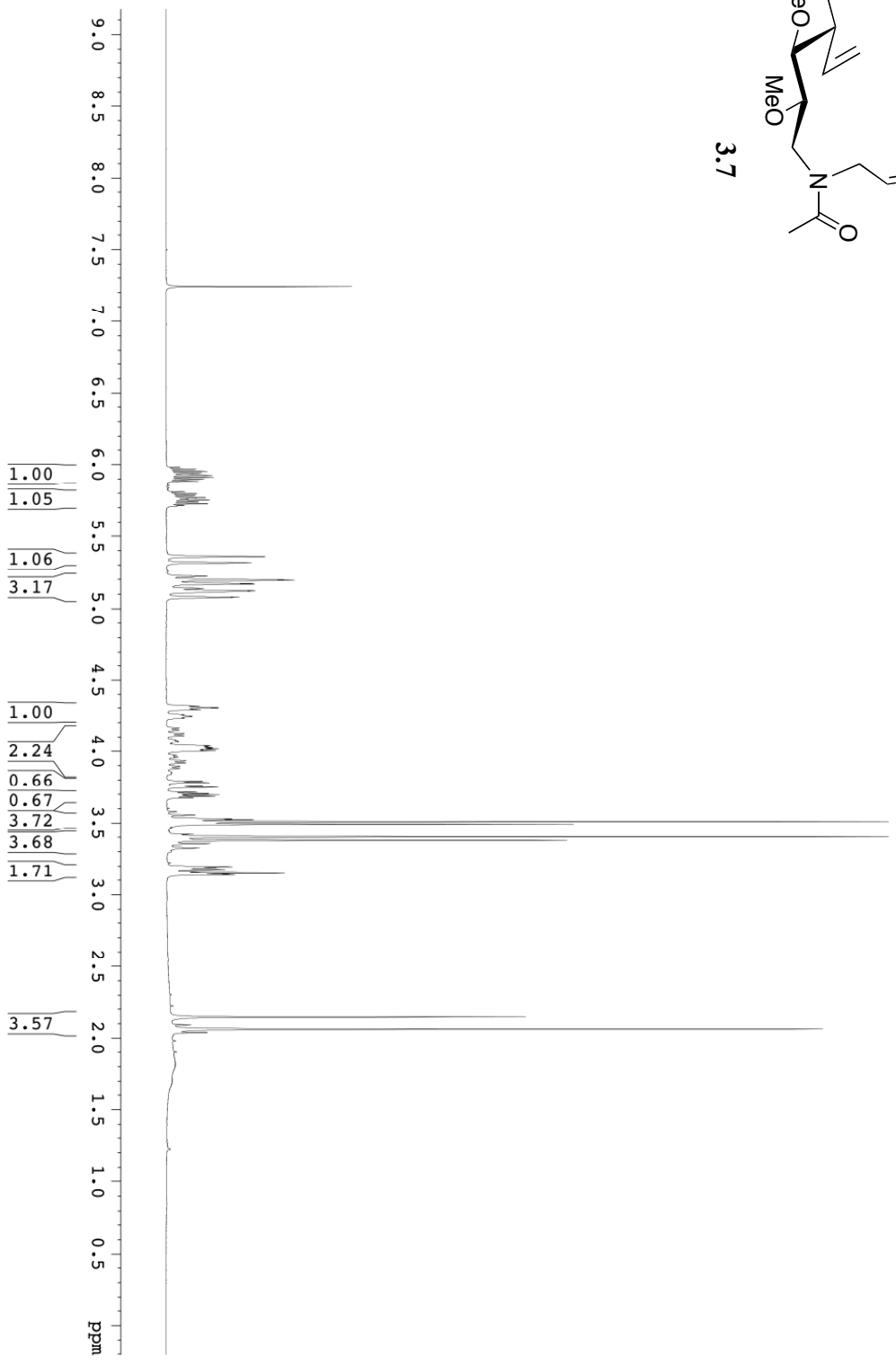
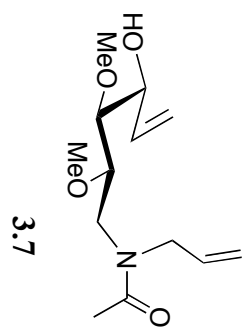


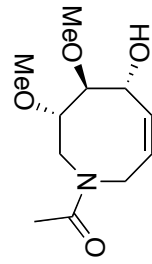
Appendix A

^1H NMR Spectra

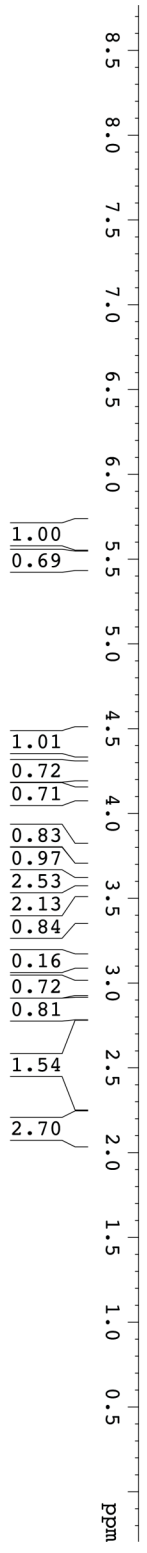


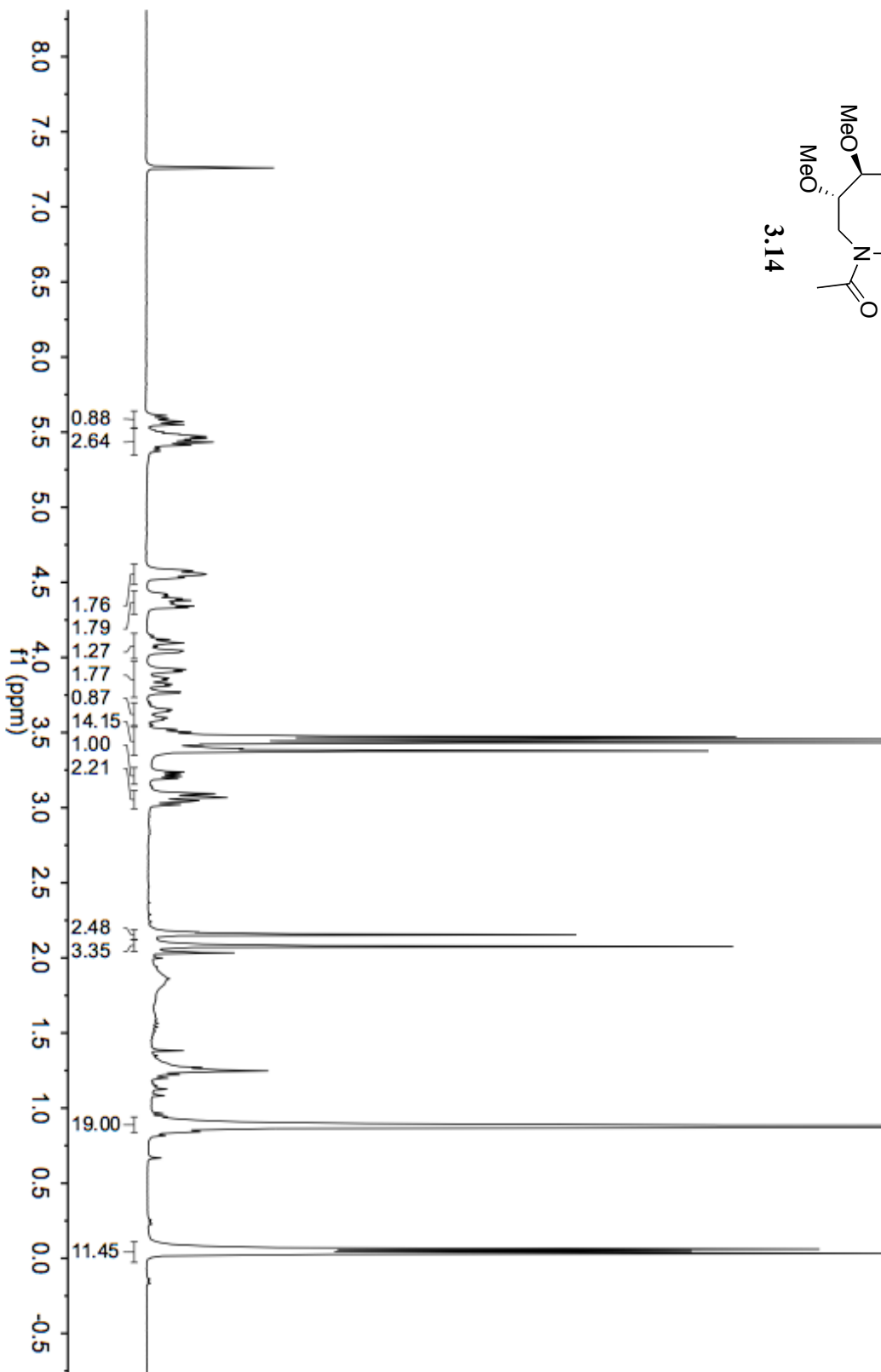
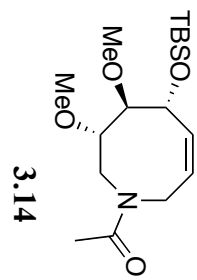


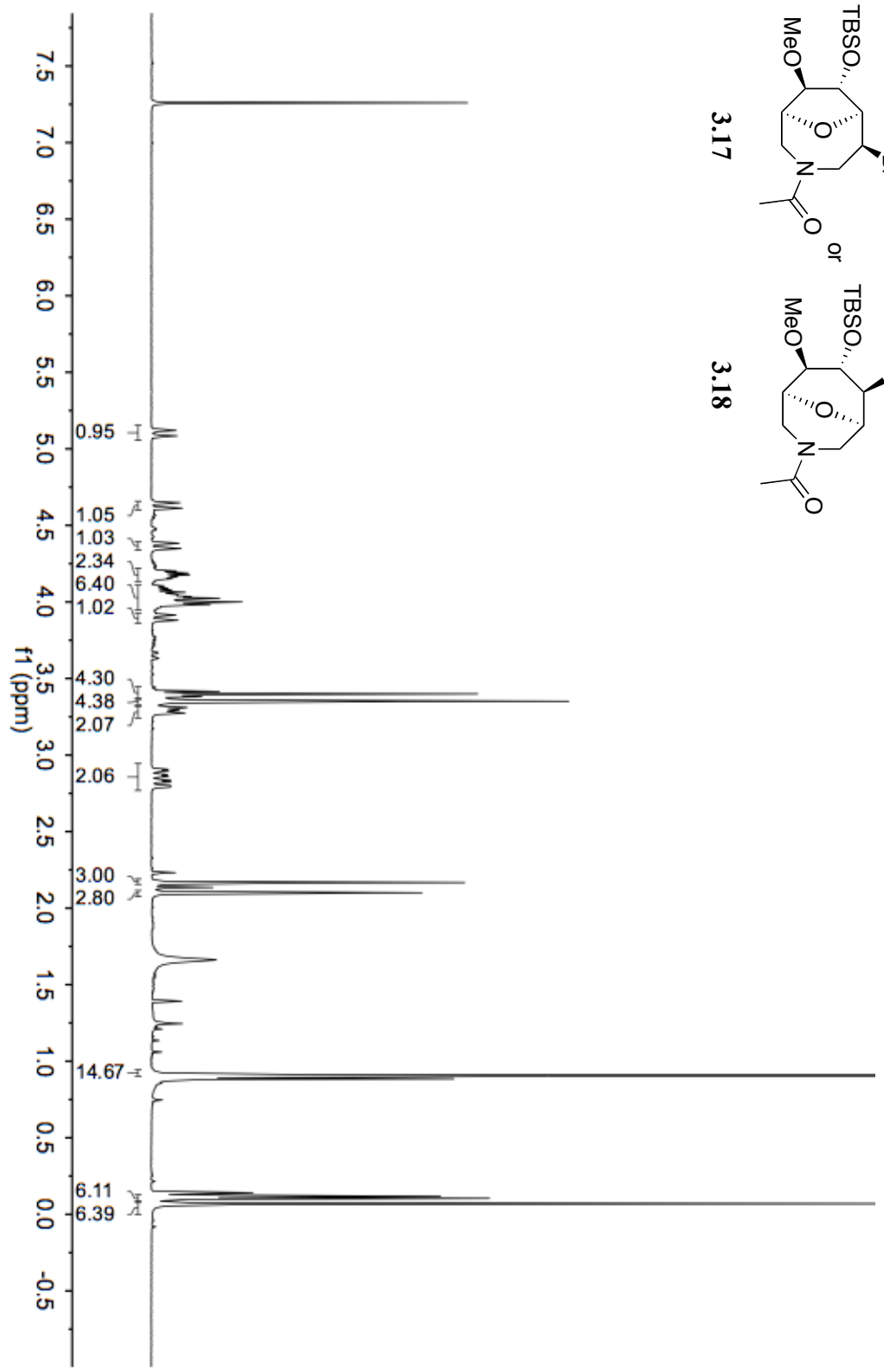
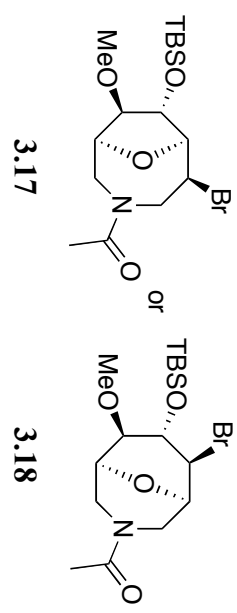


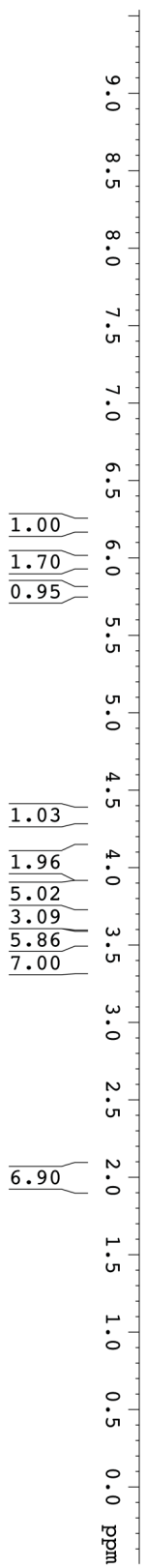
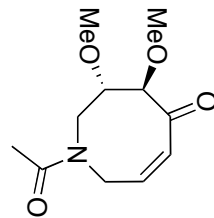


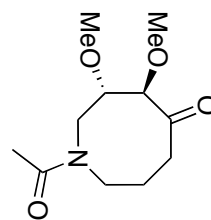
3.6



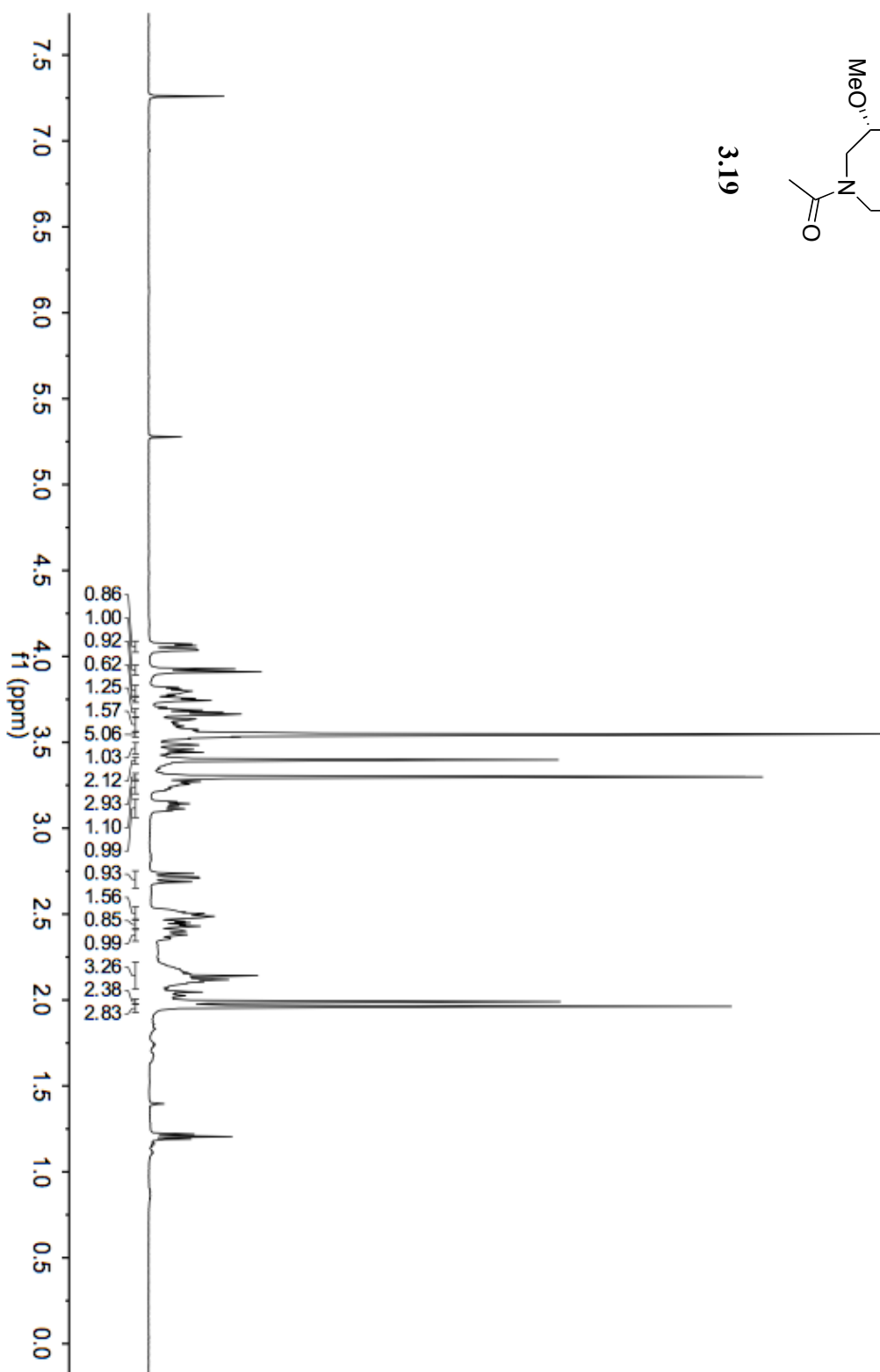


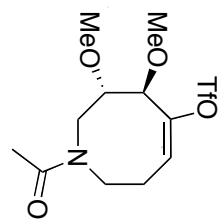




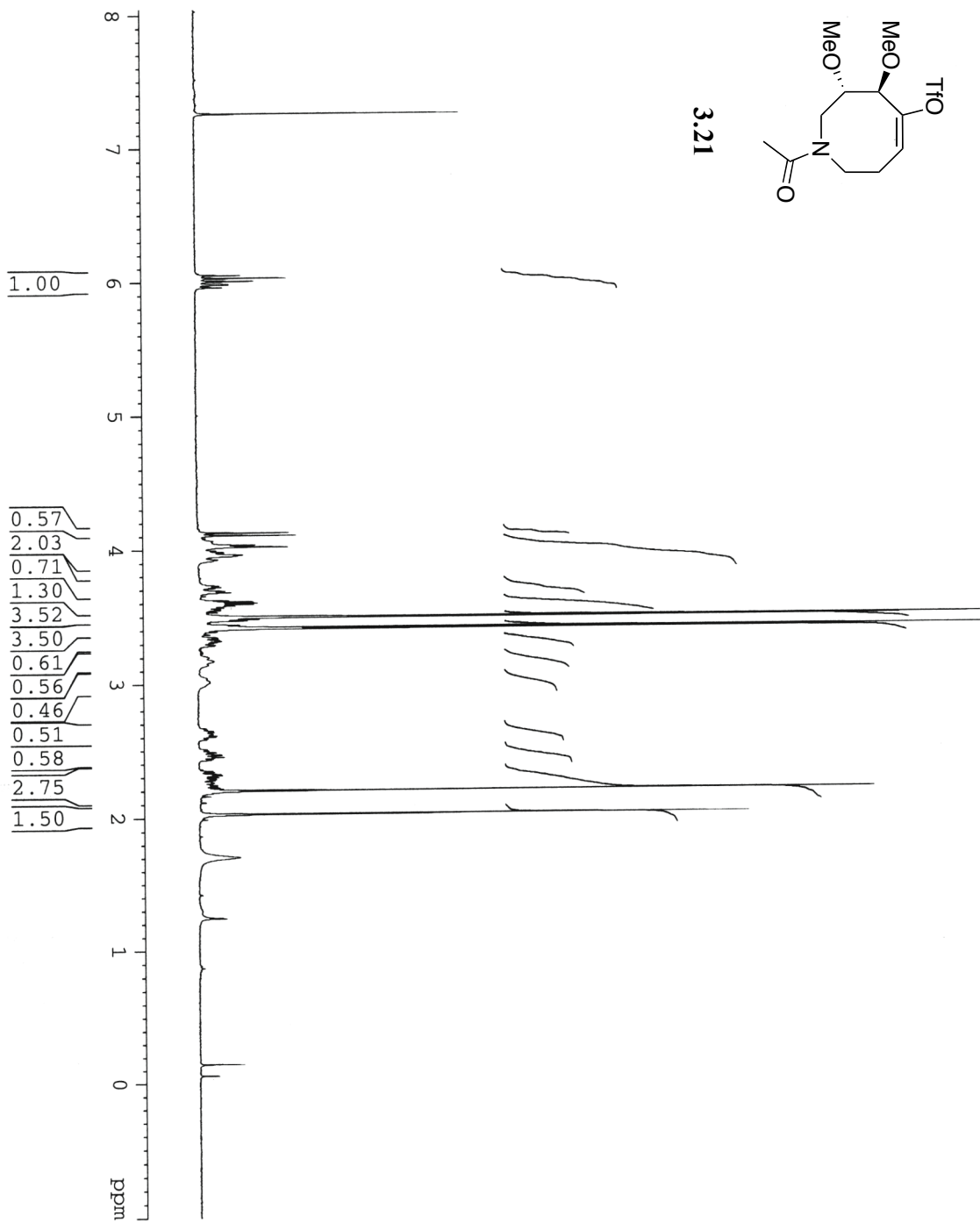


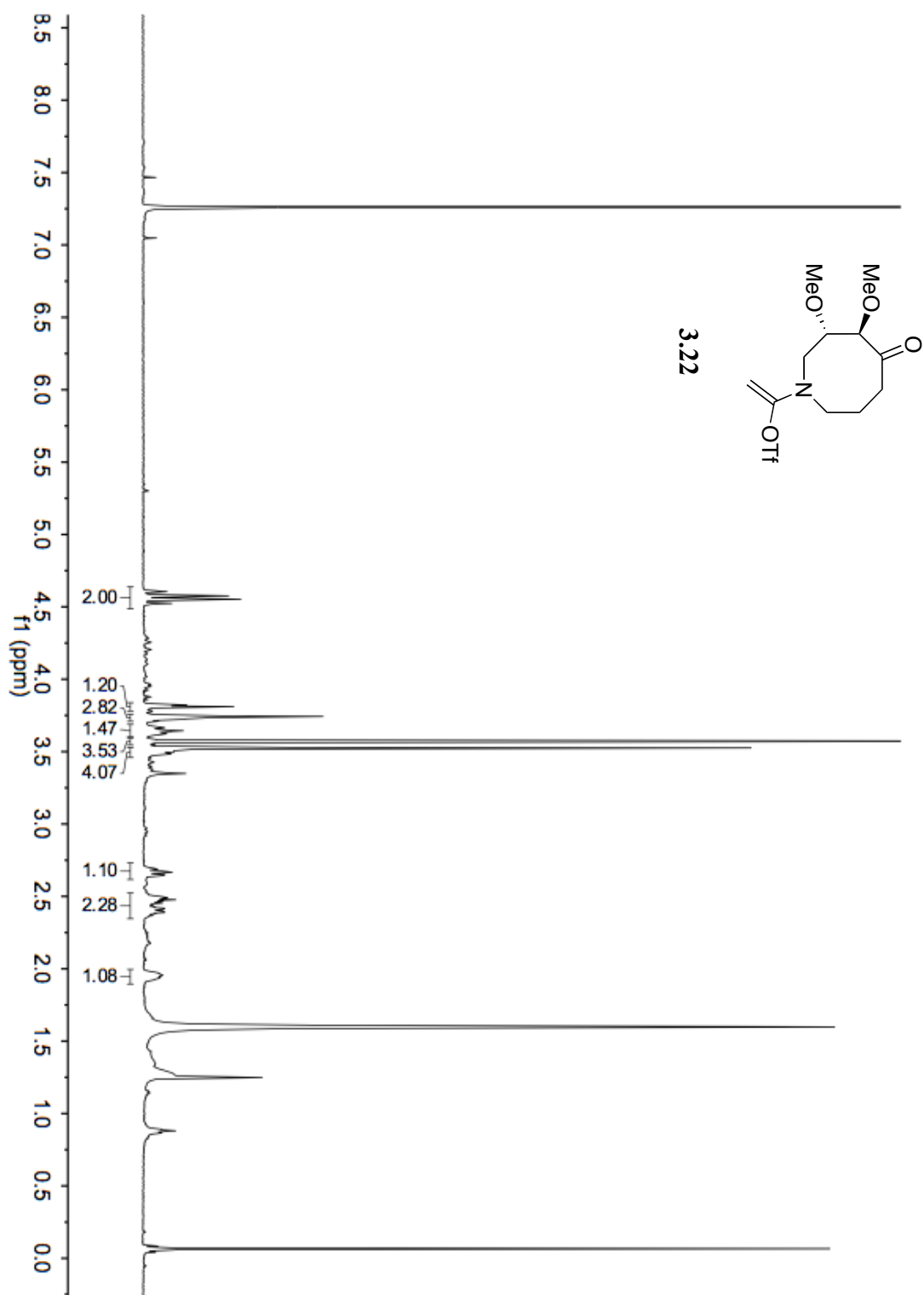
3.19

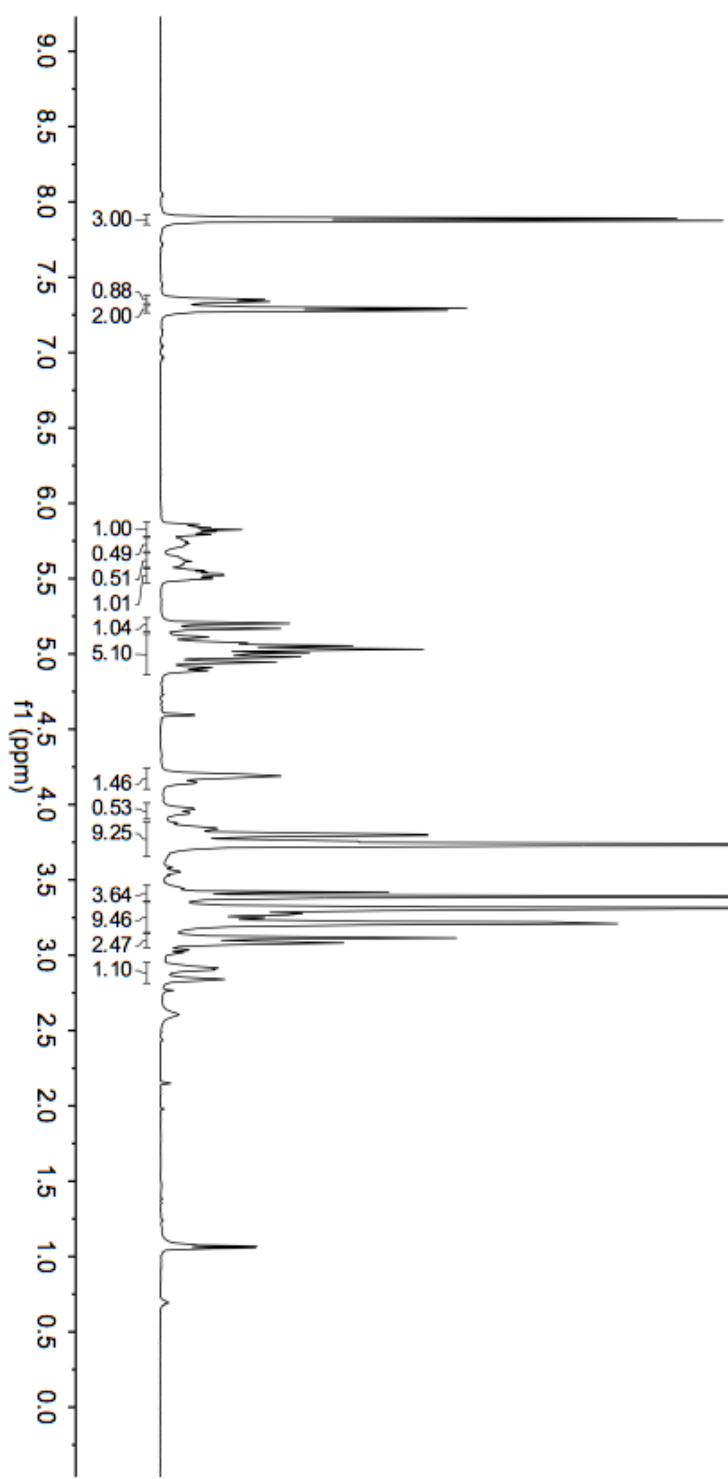
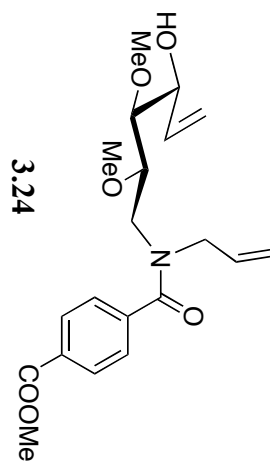


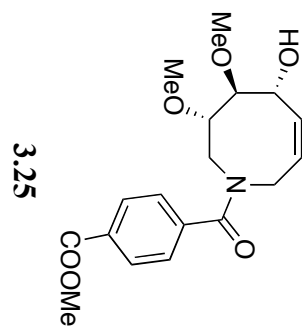


3.21

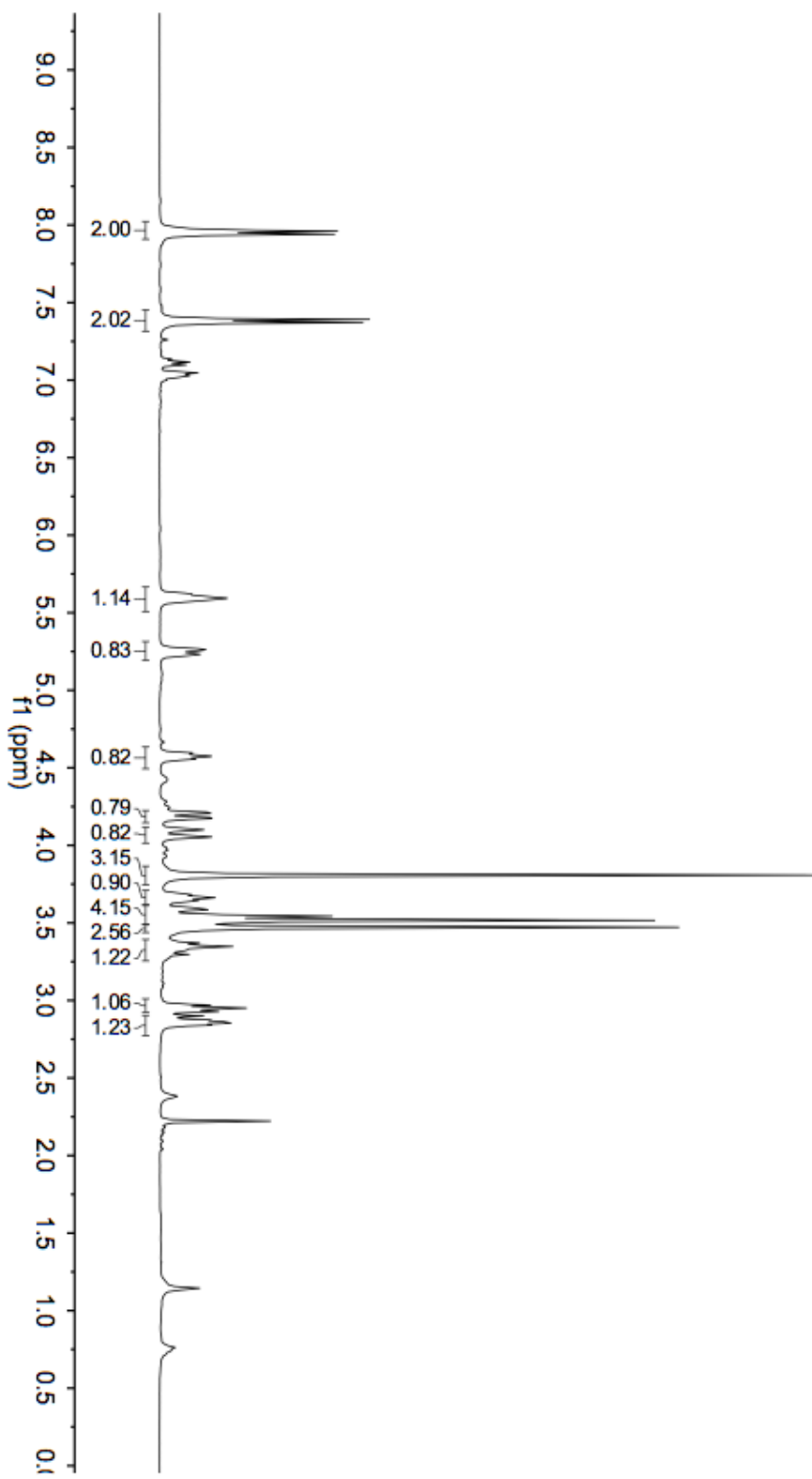


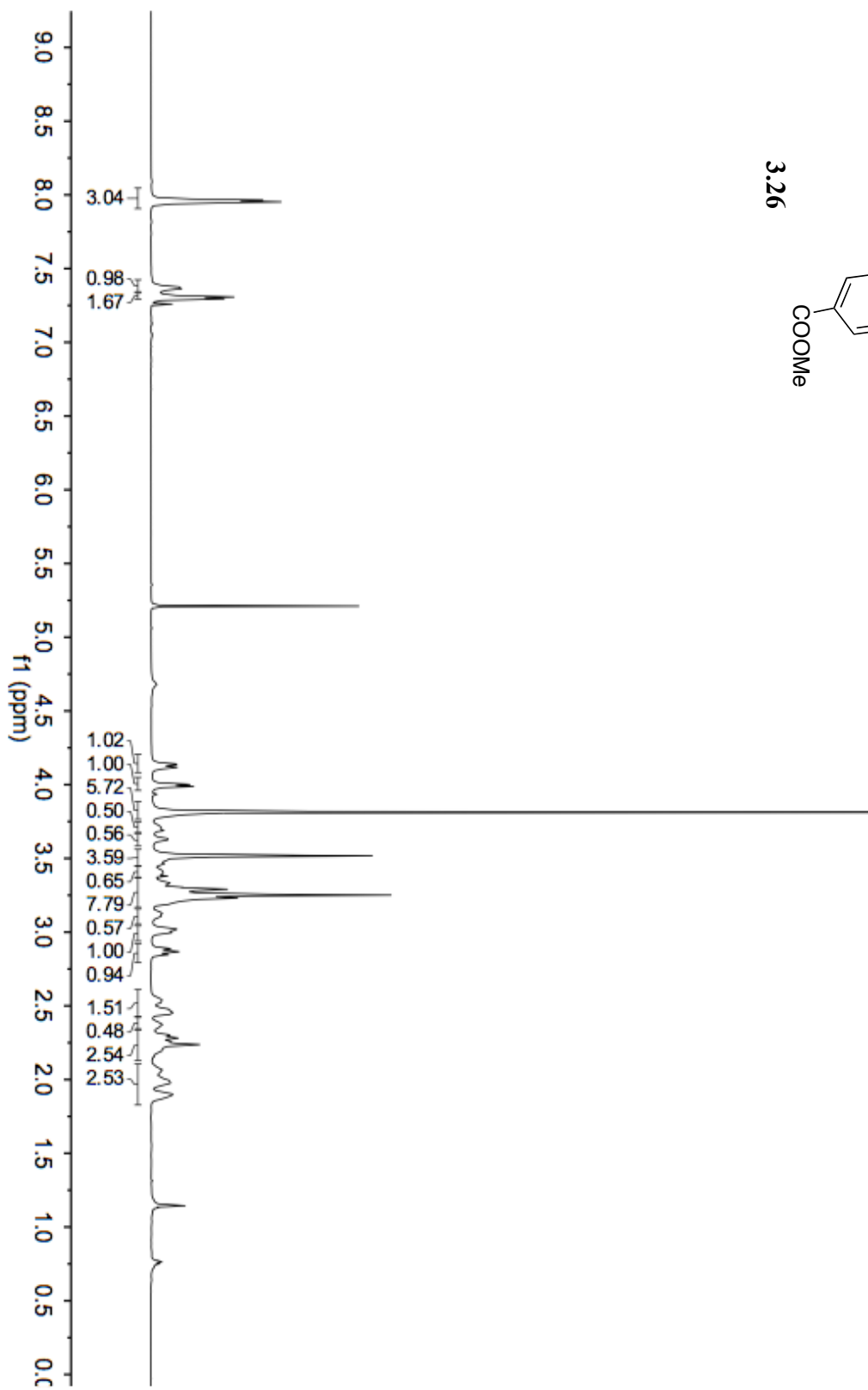
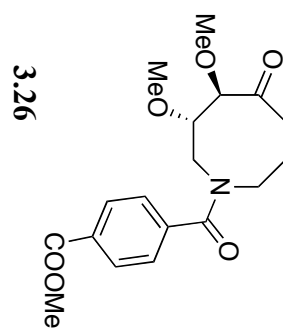


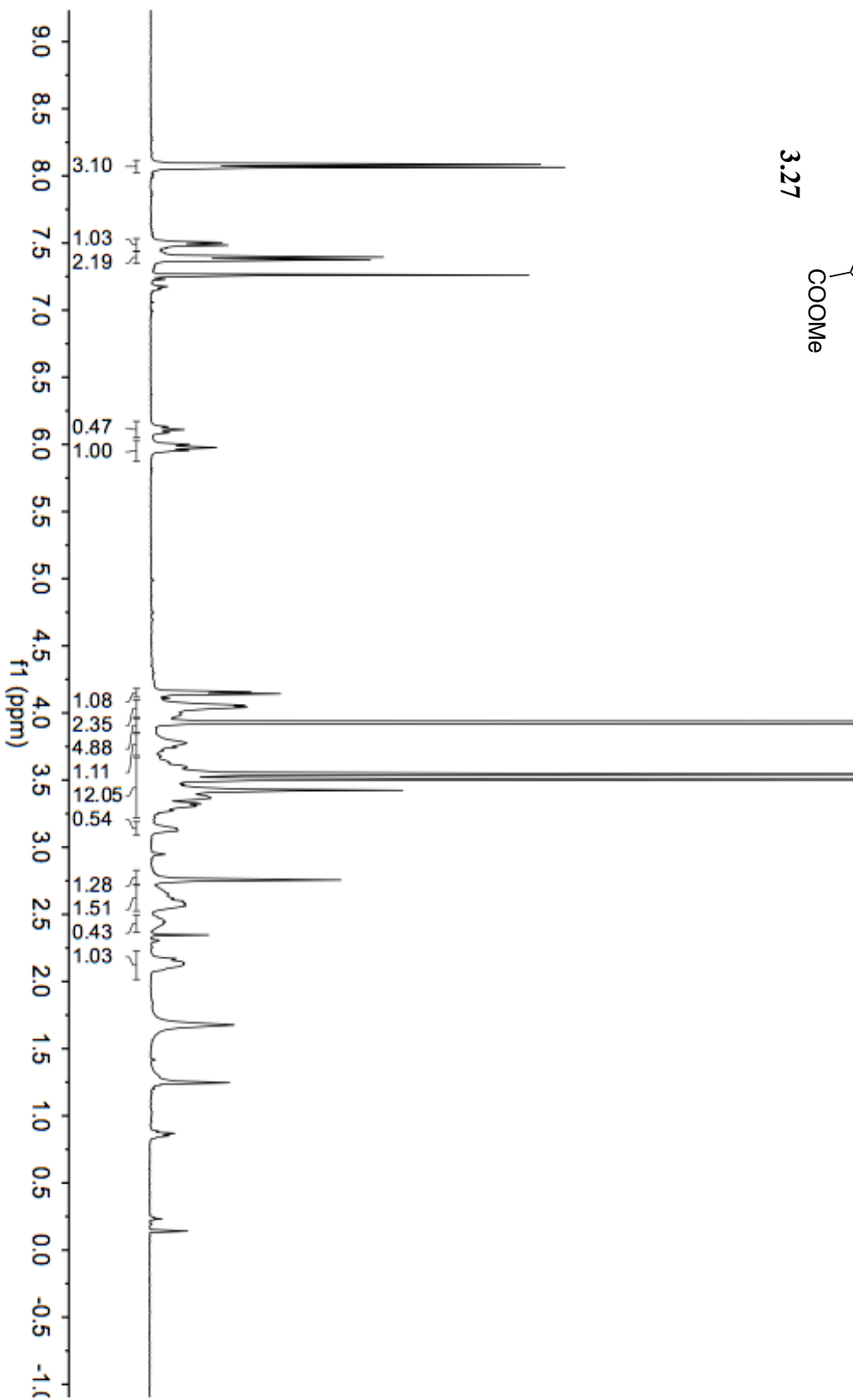
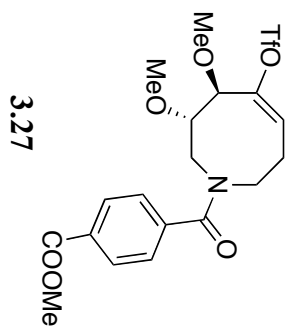


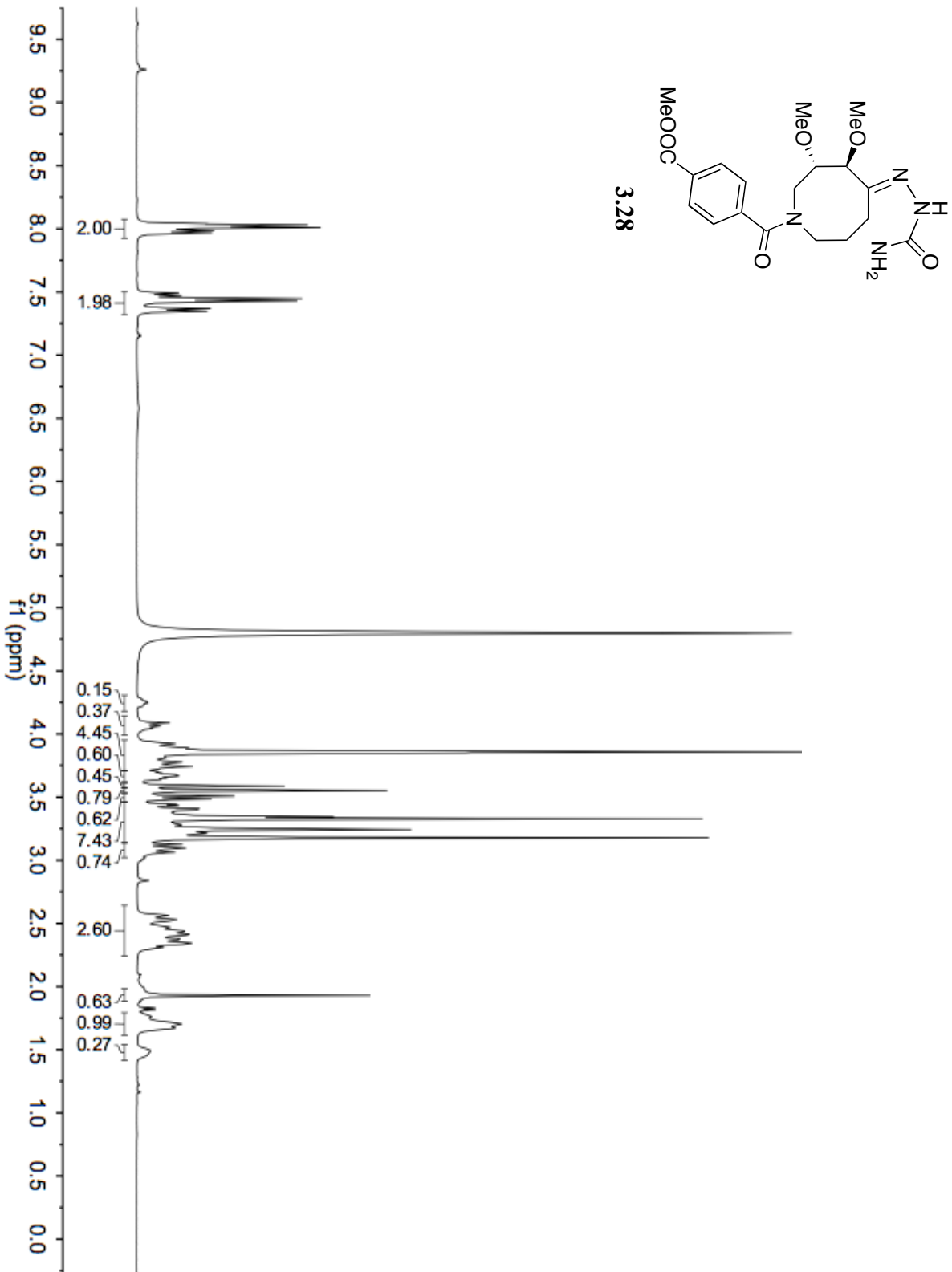


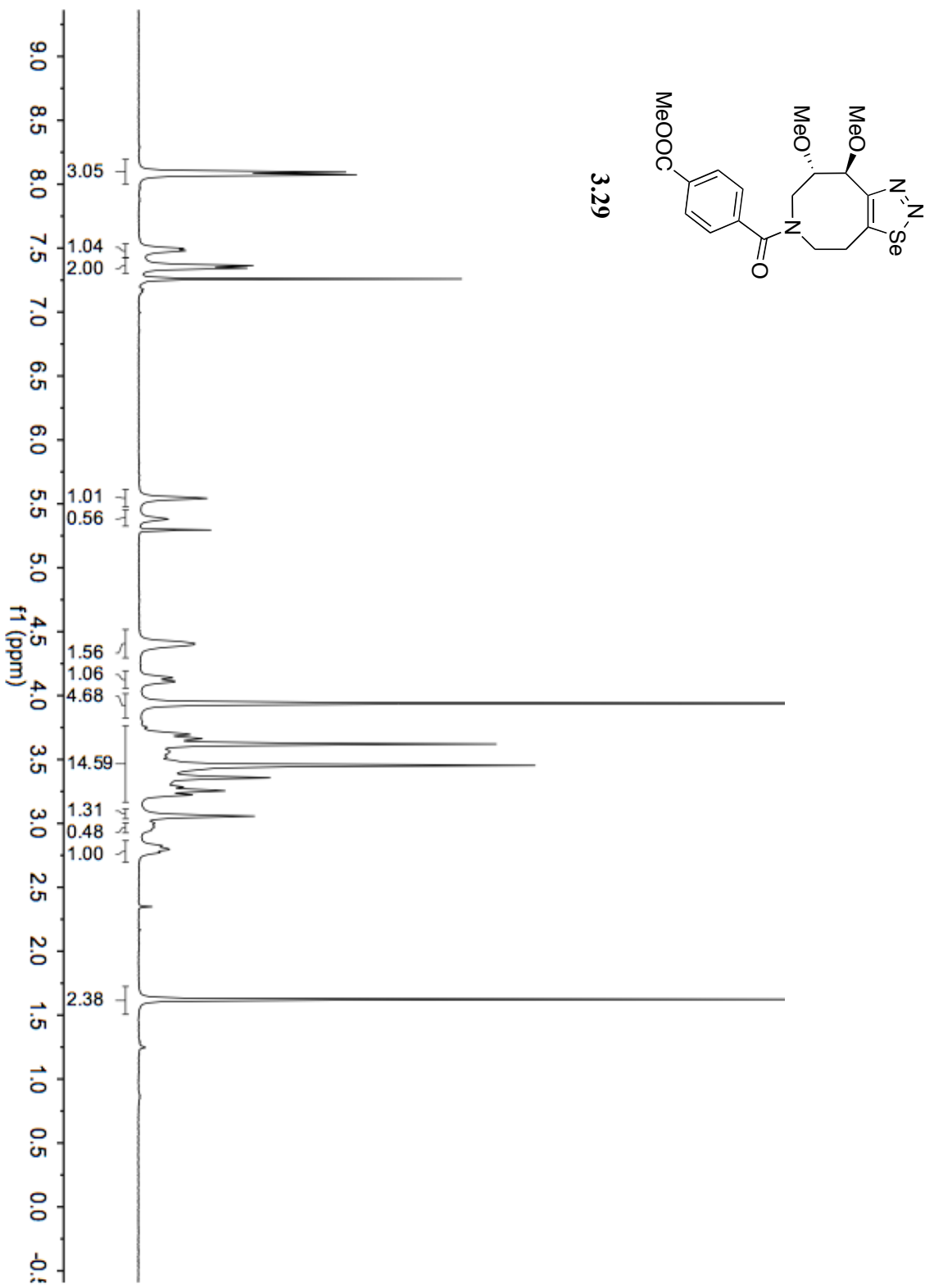
3.25

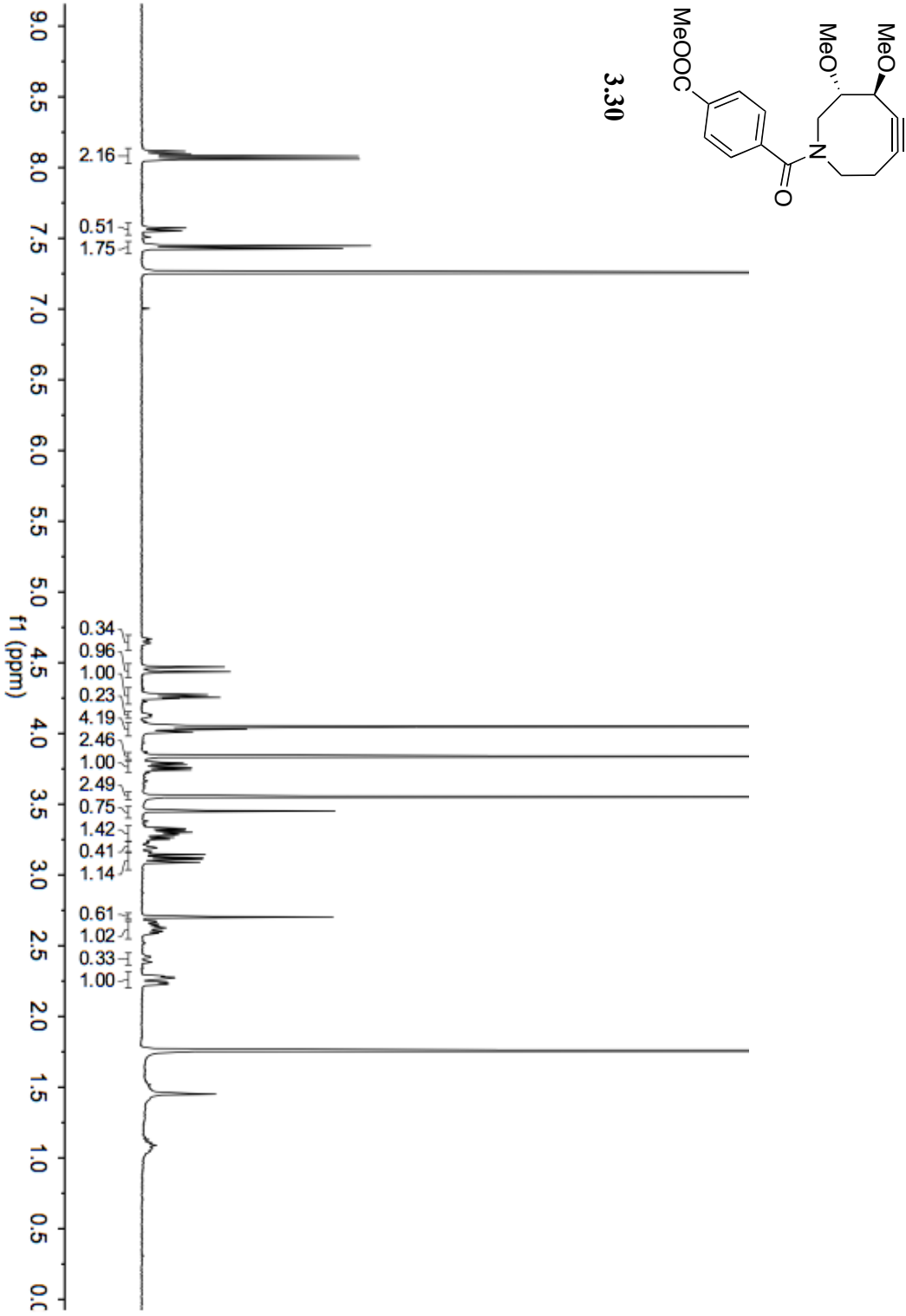


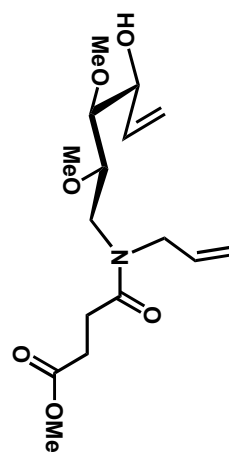




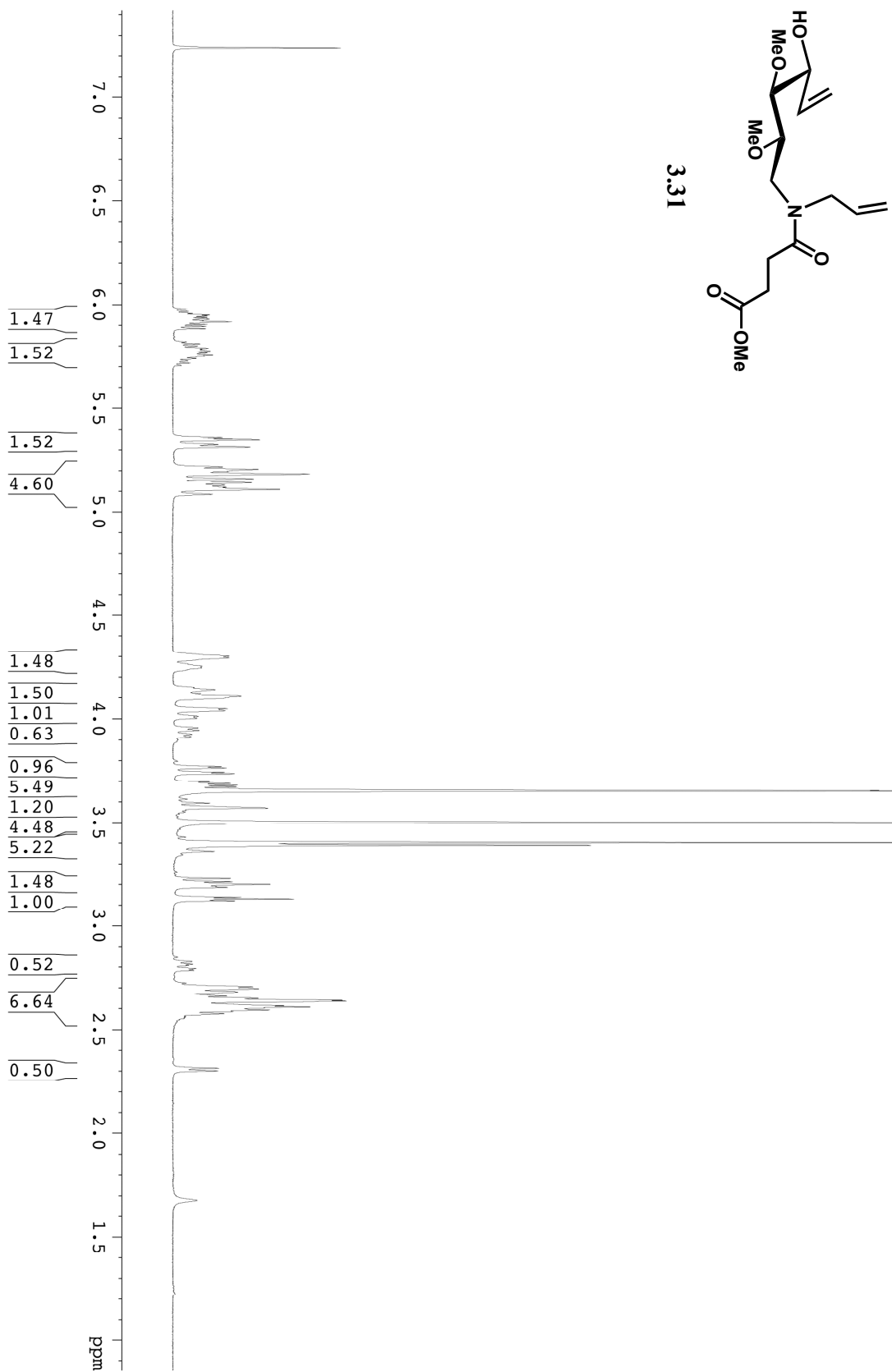


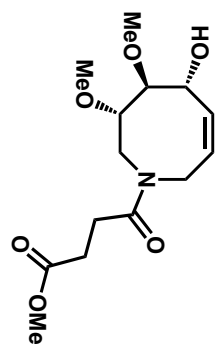




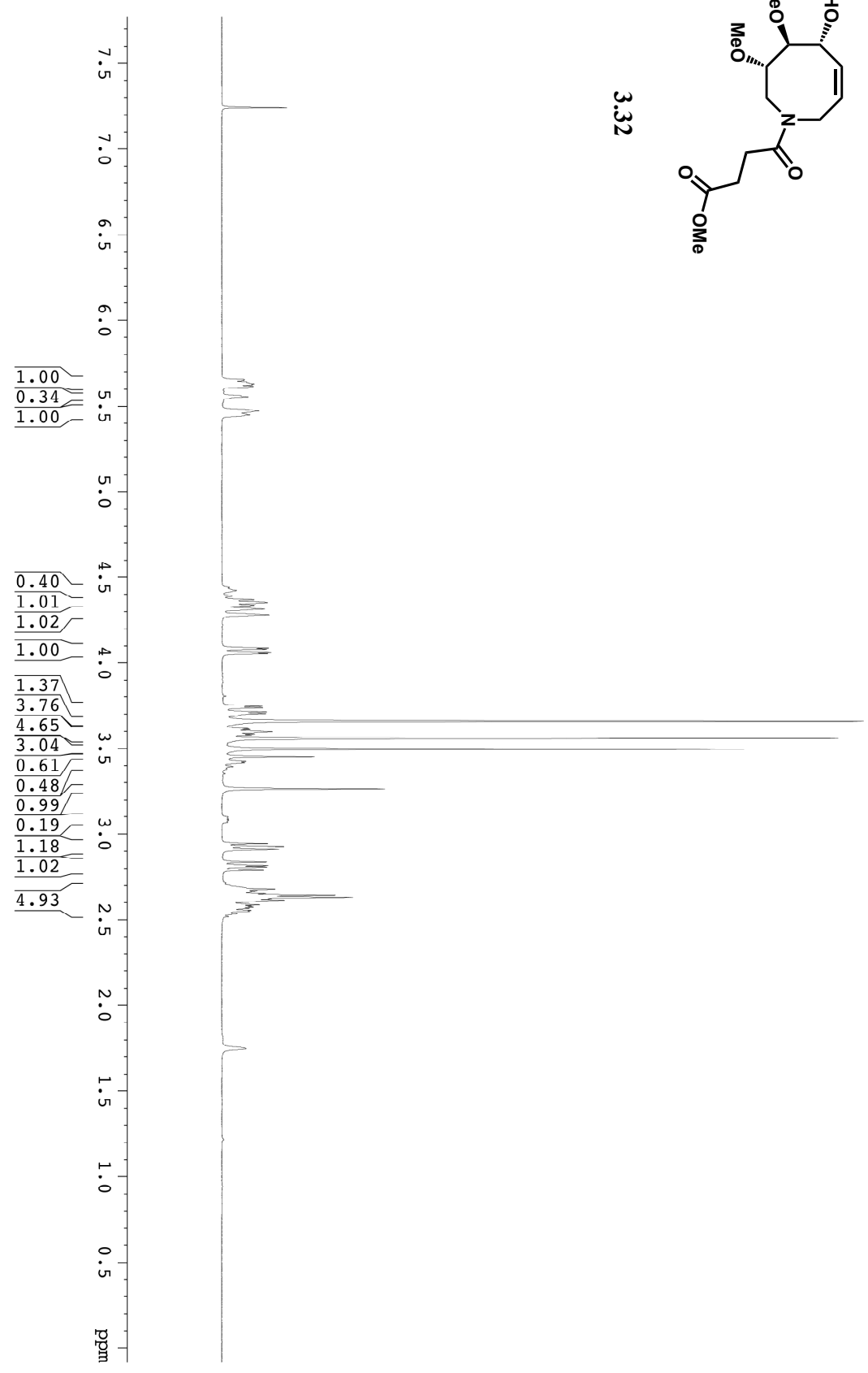


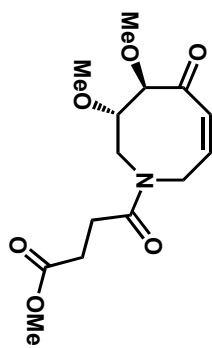
3.31



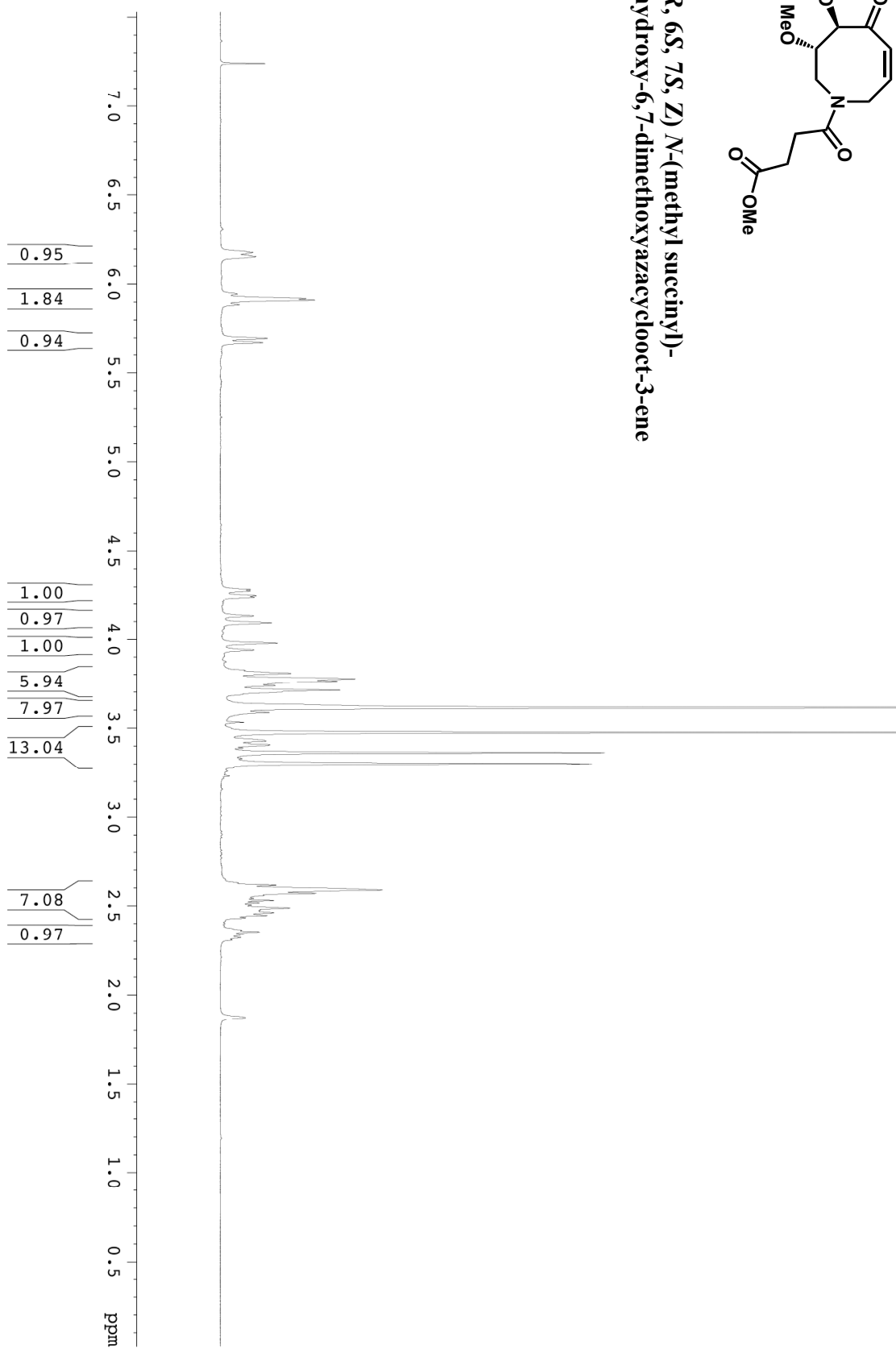


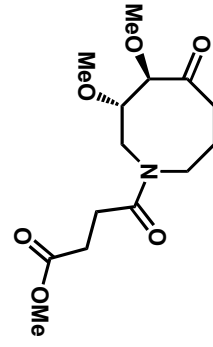
3.32



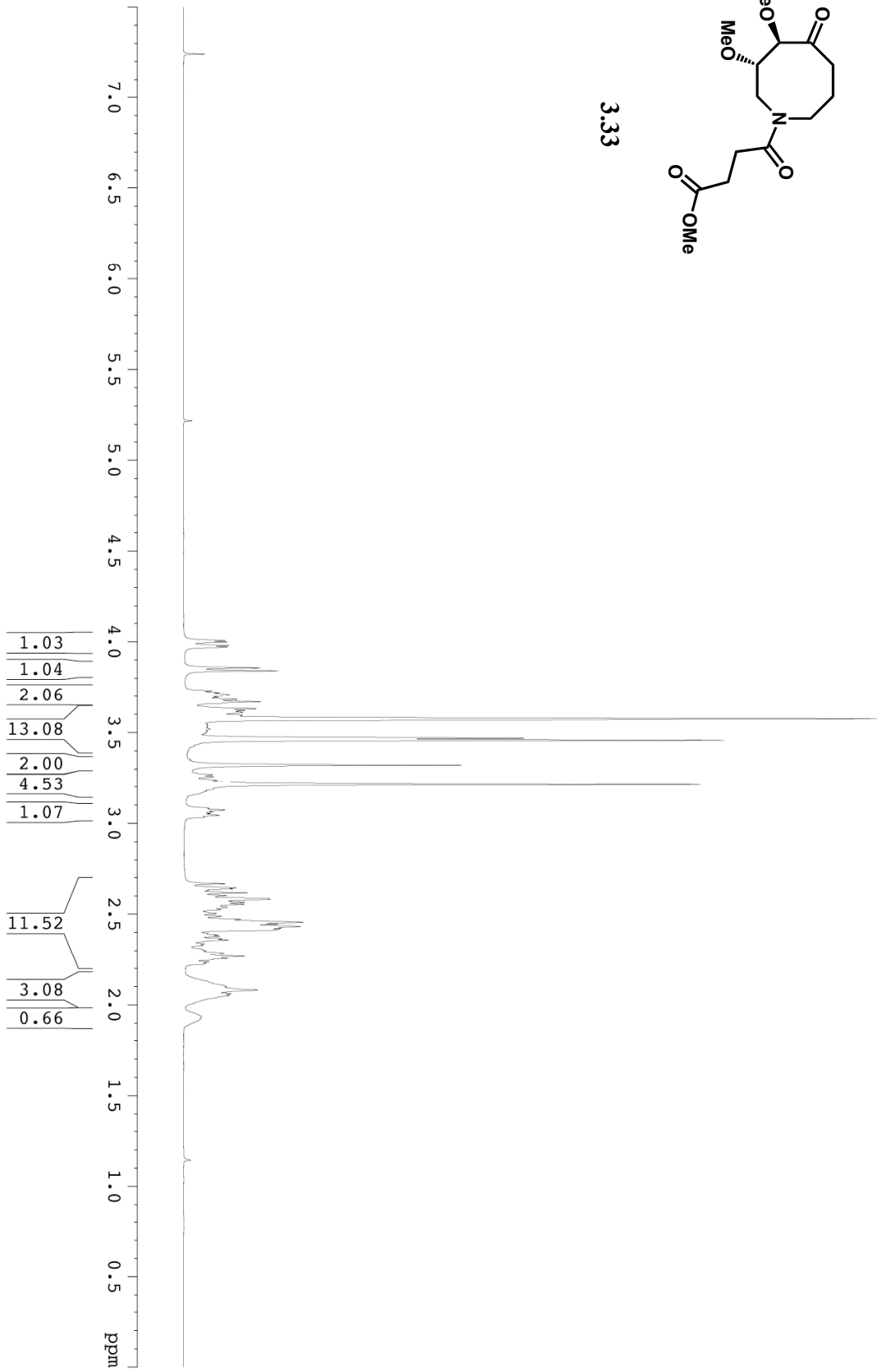


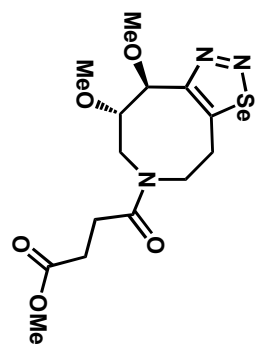
(5*R*, 6*S*, 7*S*, *Z*) *N*-(methyl succinyl)-5-hydroxy-6,7-dimethoxyazacyclooct-3-ene



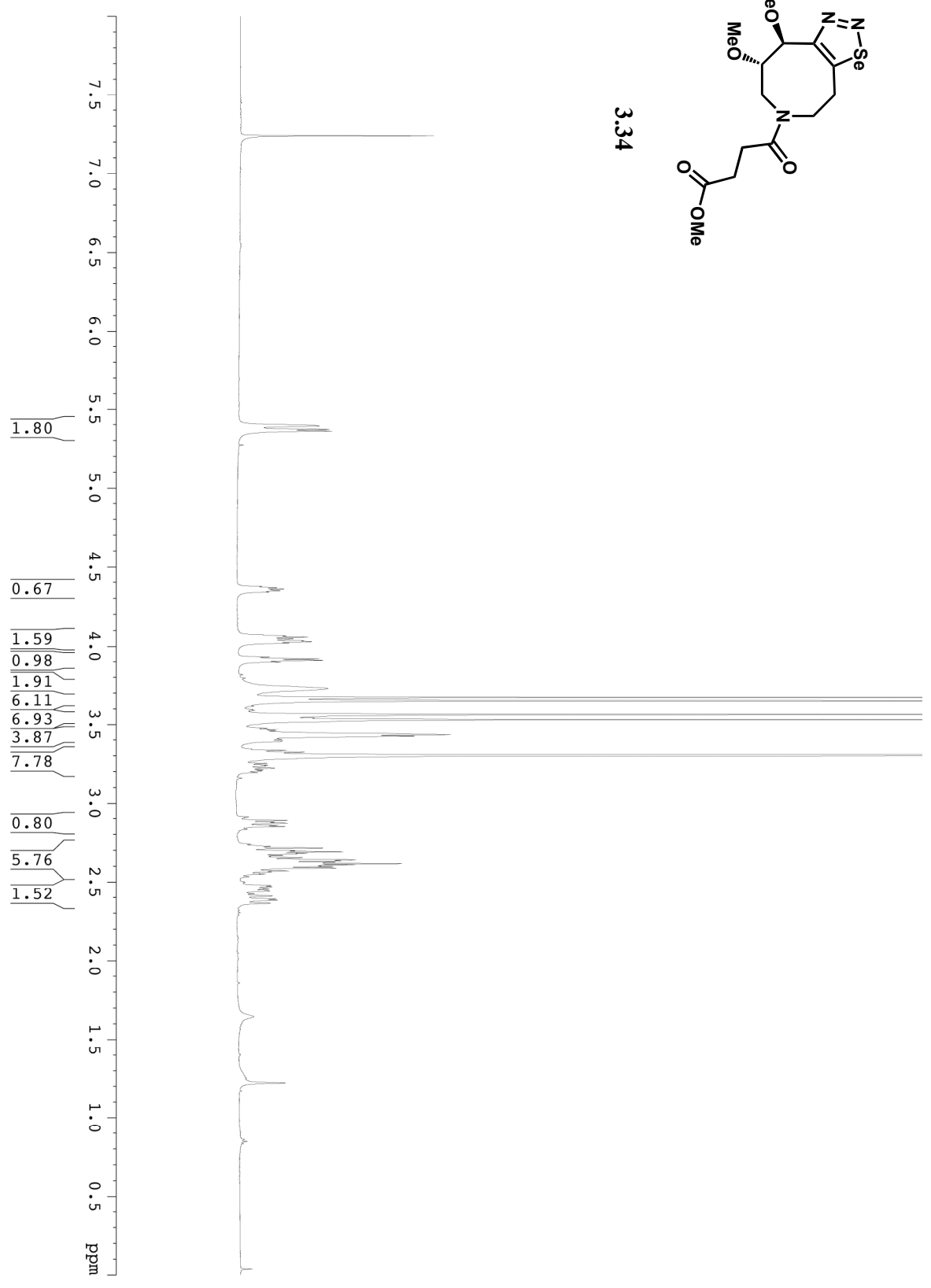


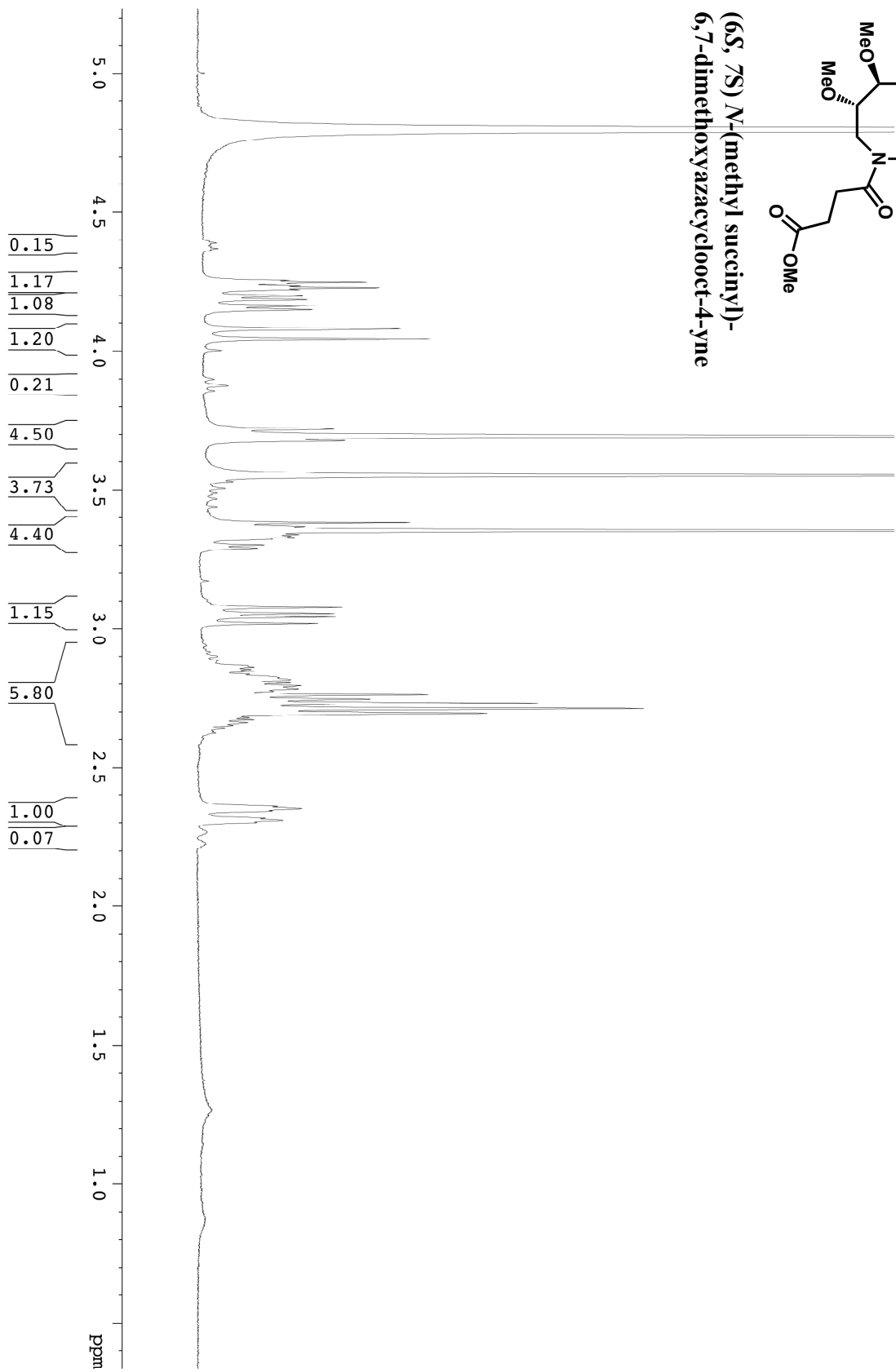
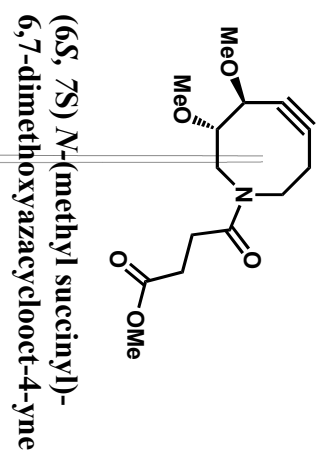
3.33

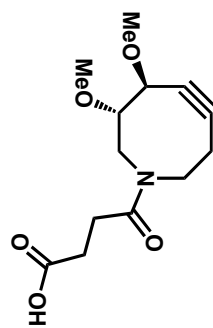




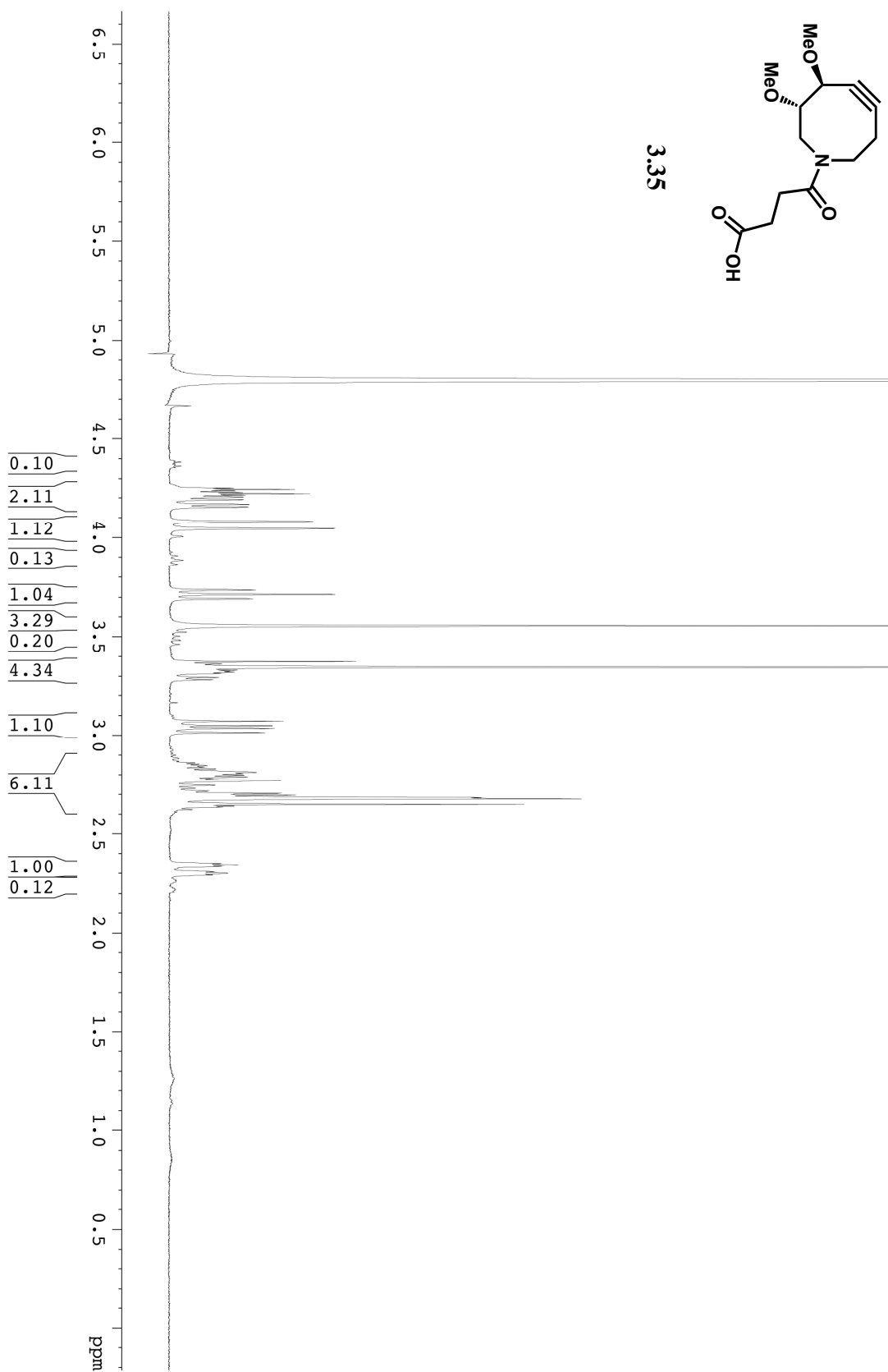
3.34

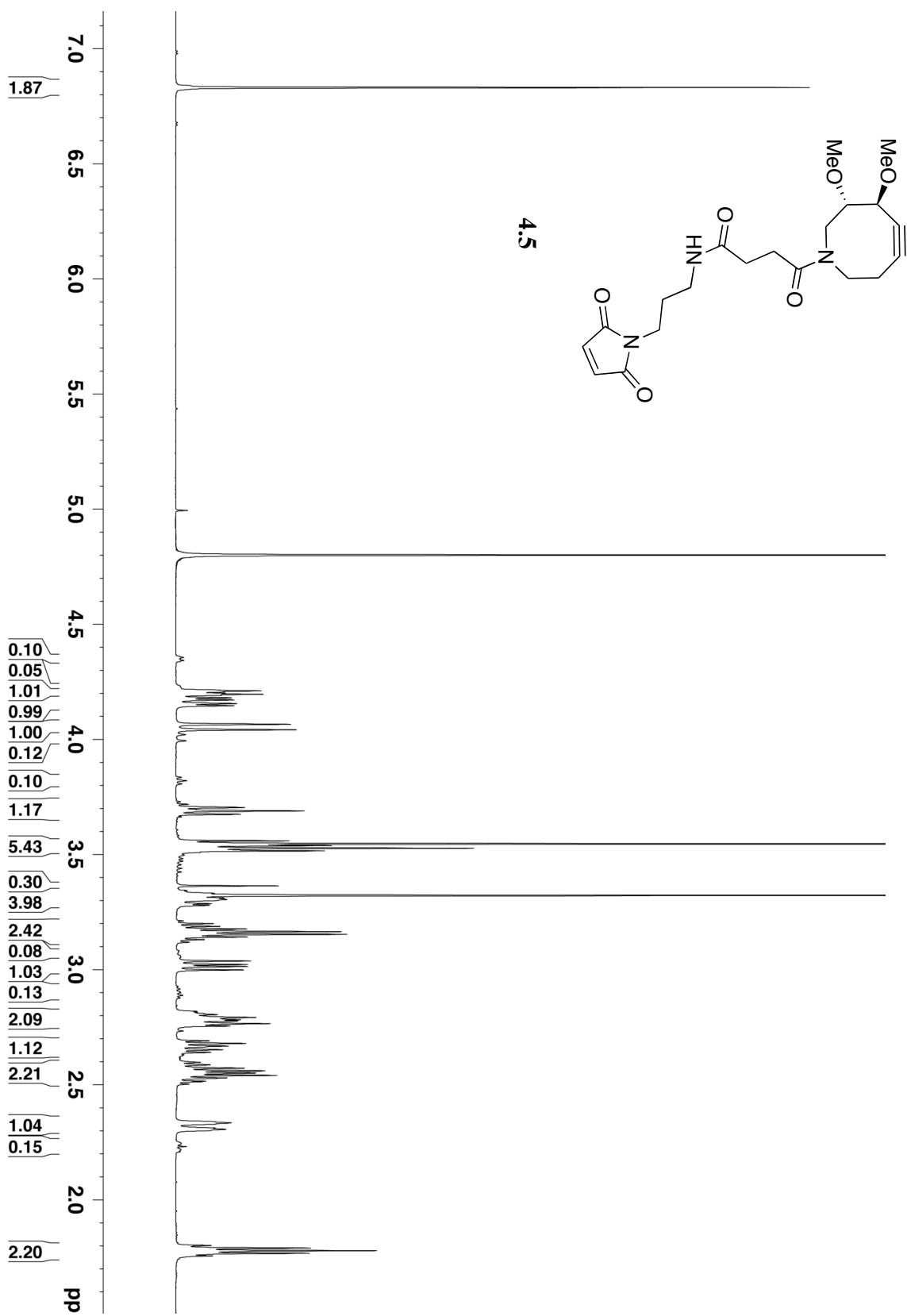


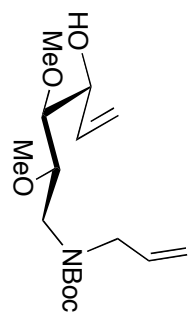




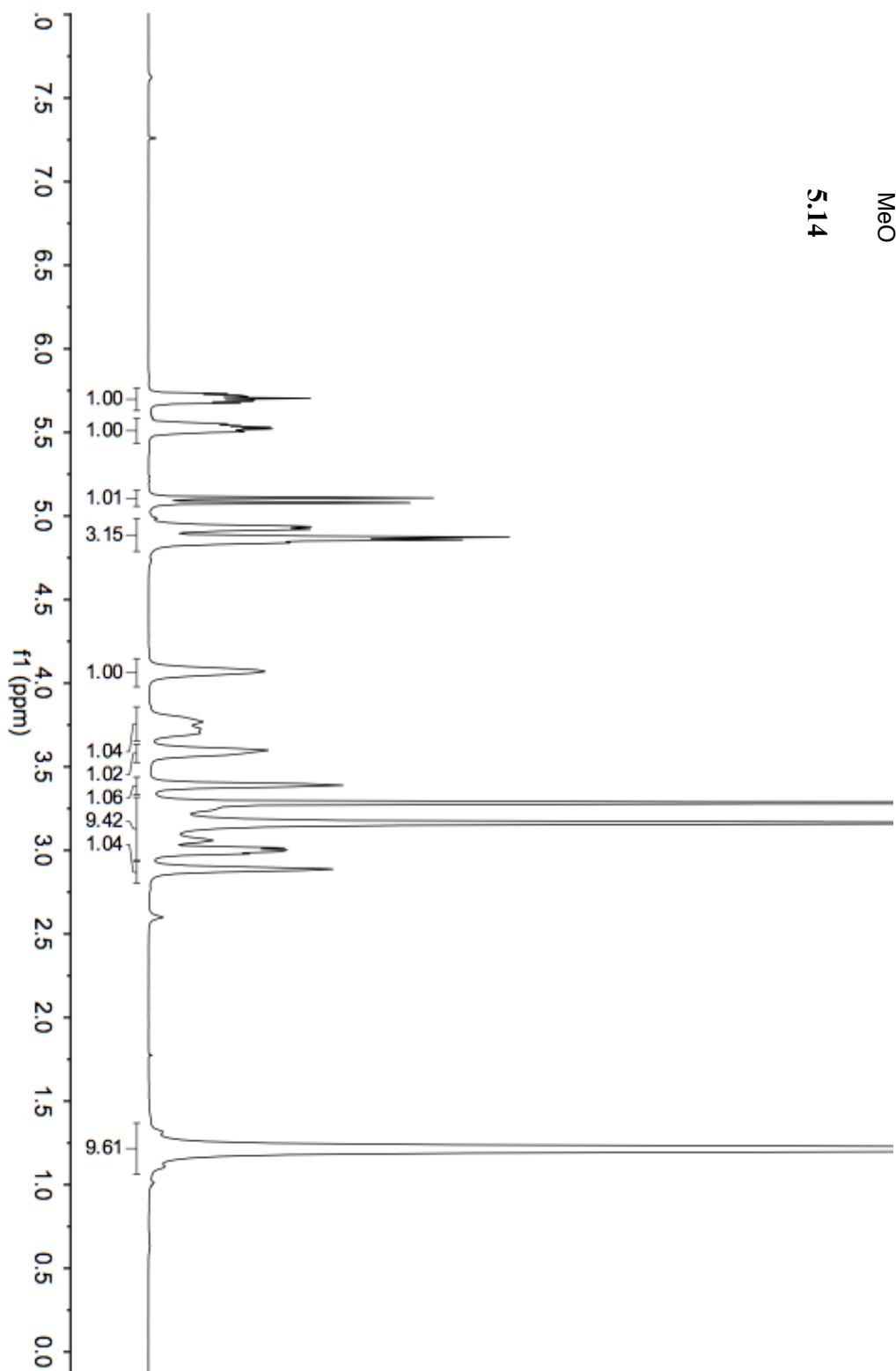
3.35

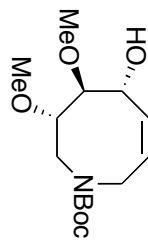




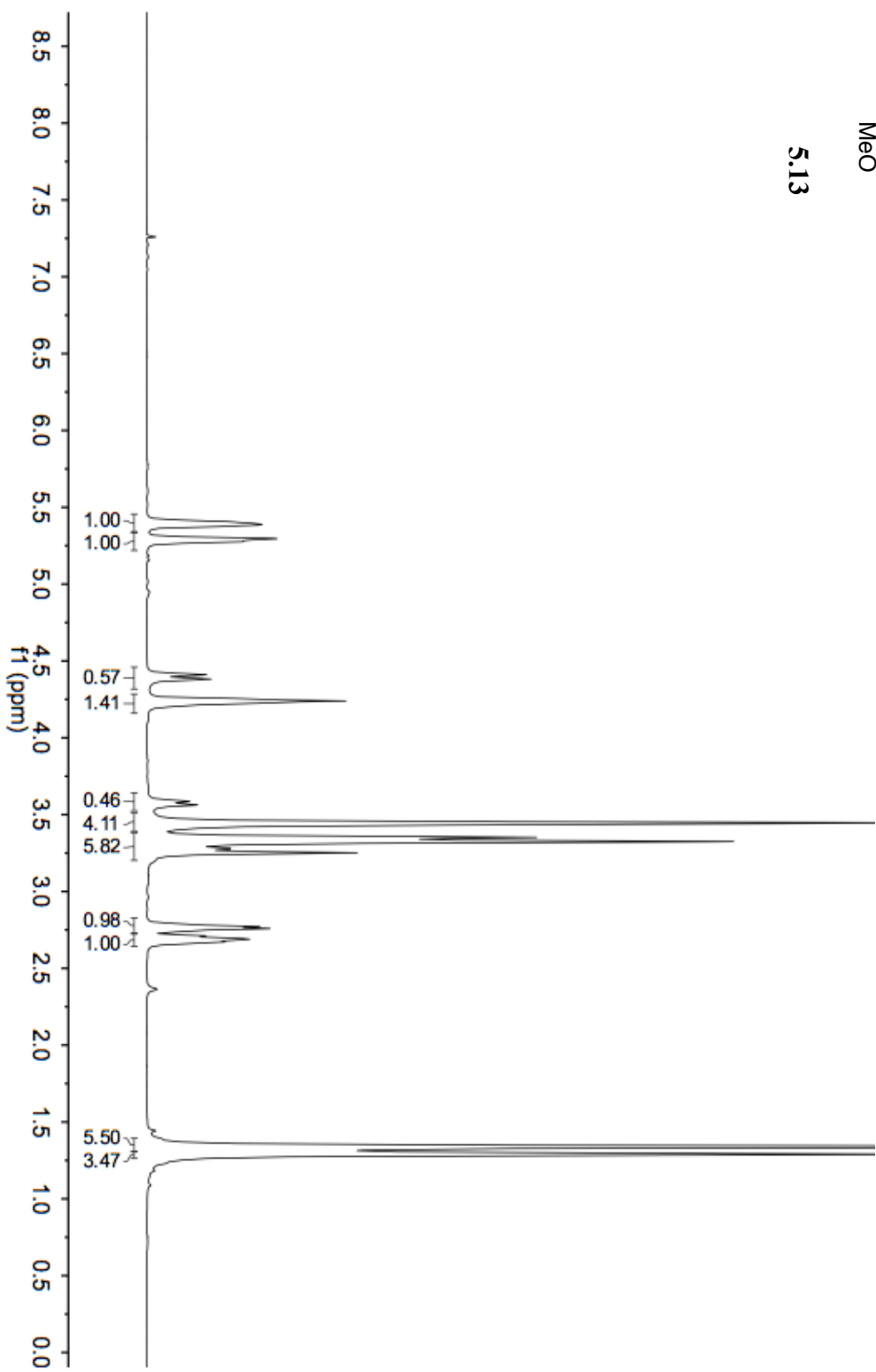


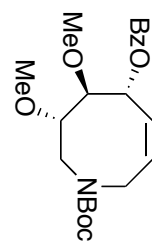
5.14



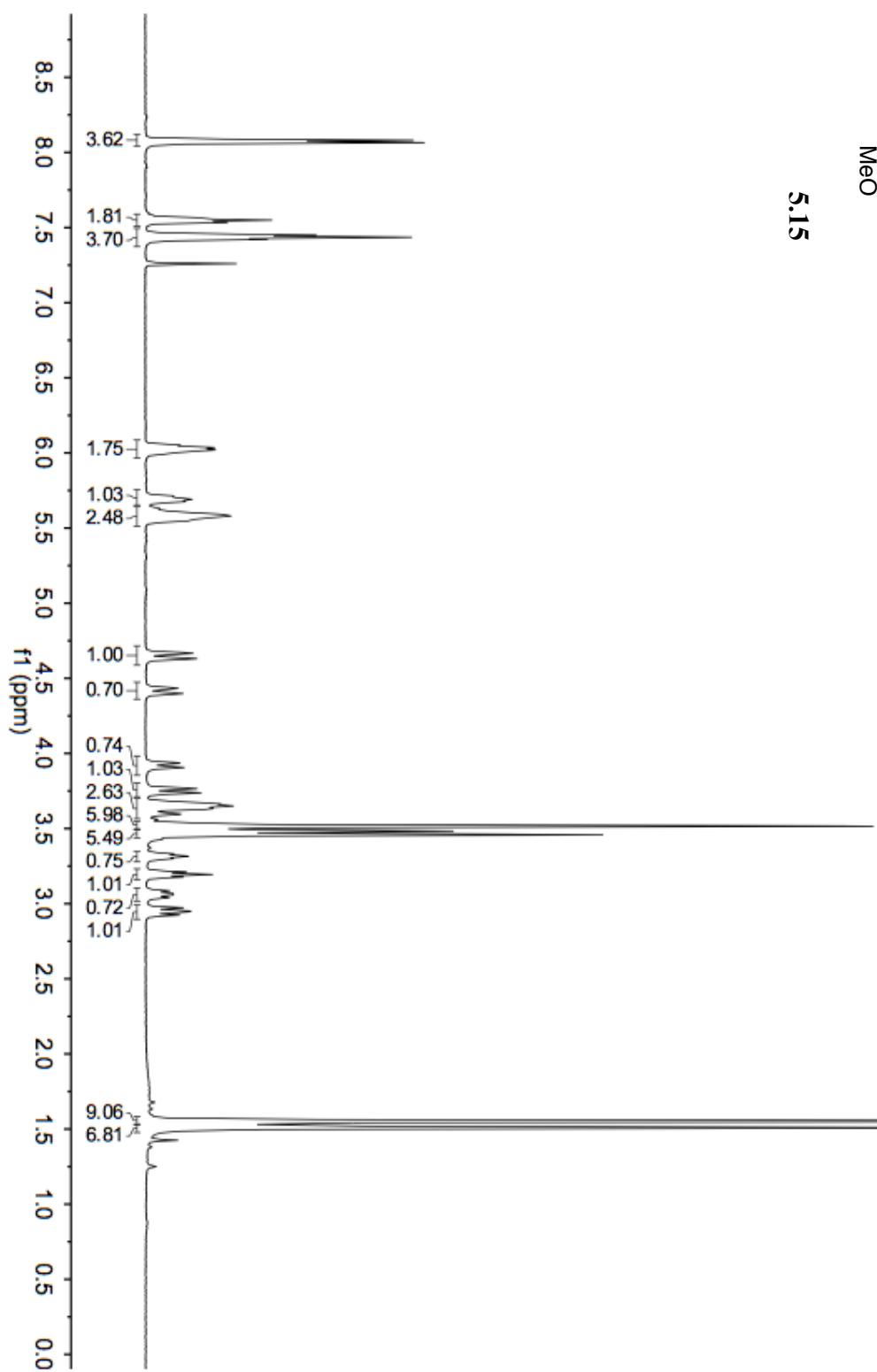


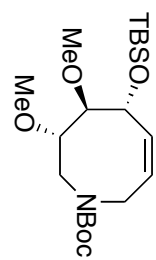
5.13



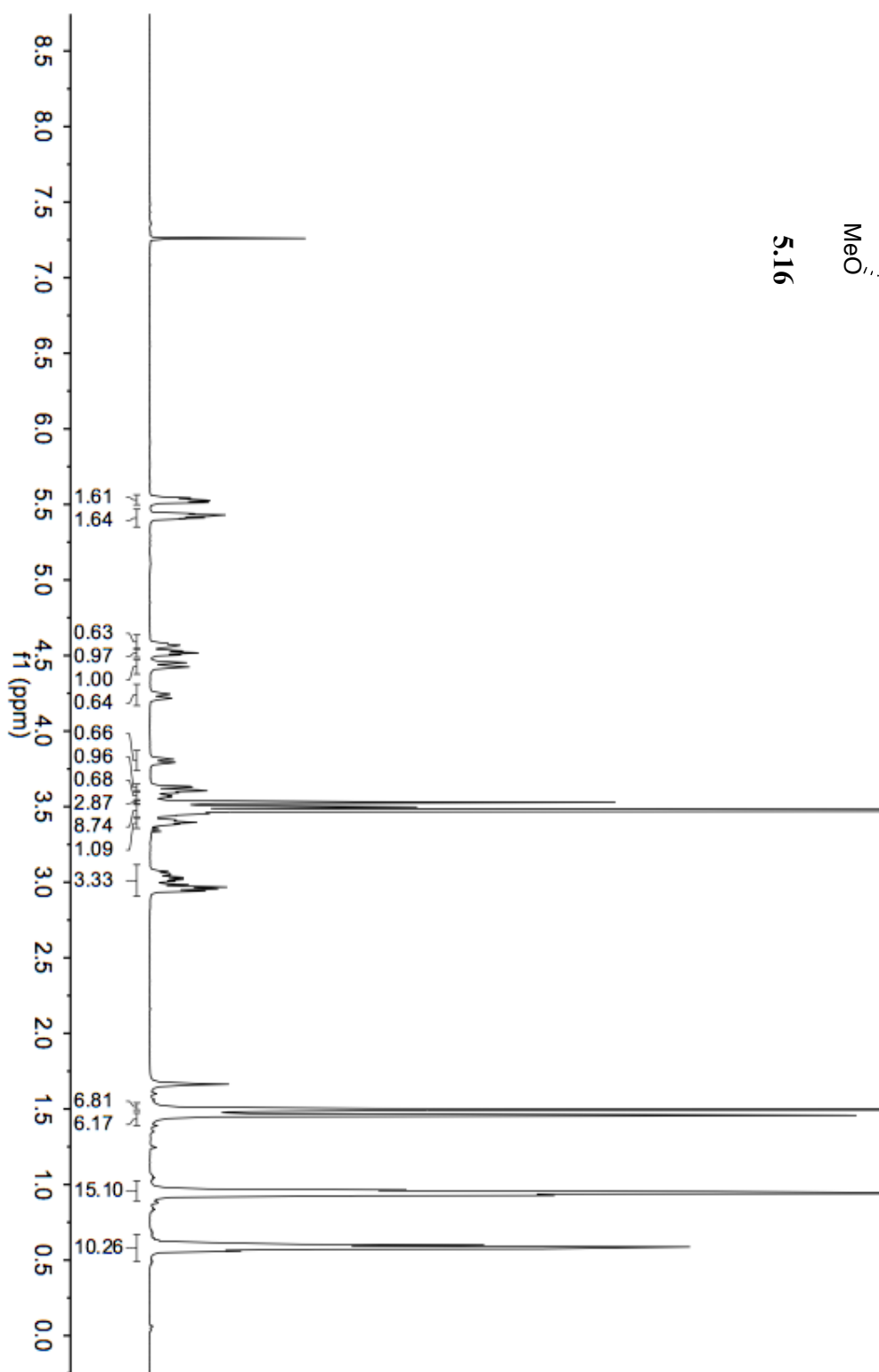


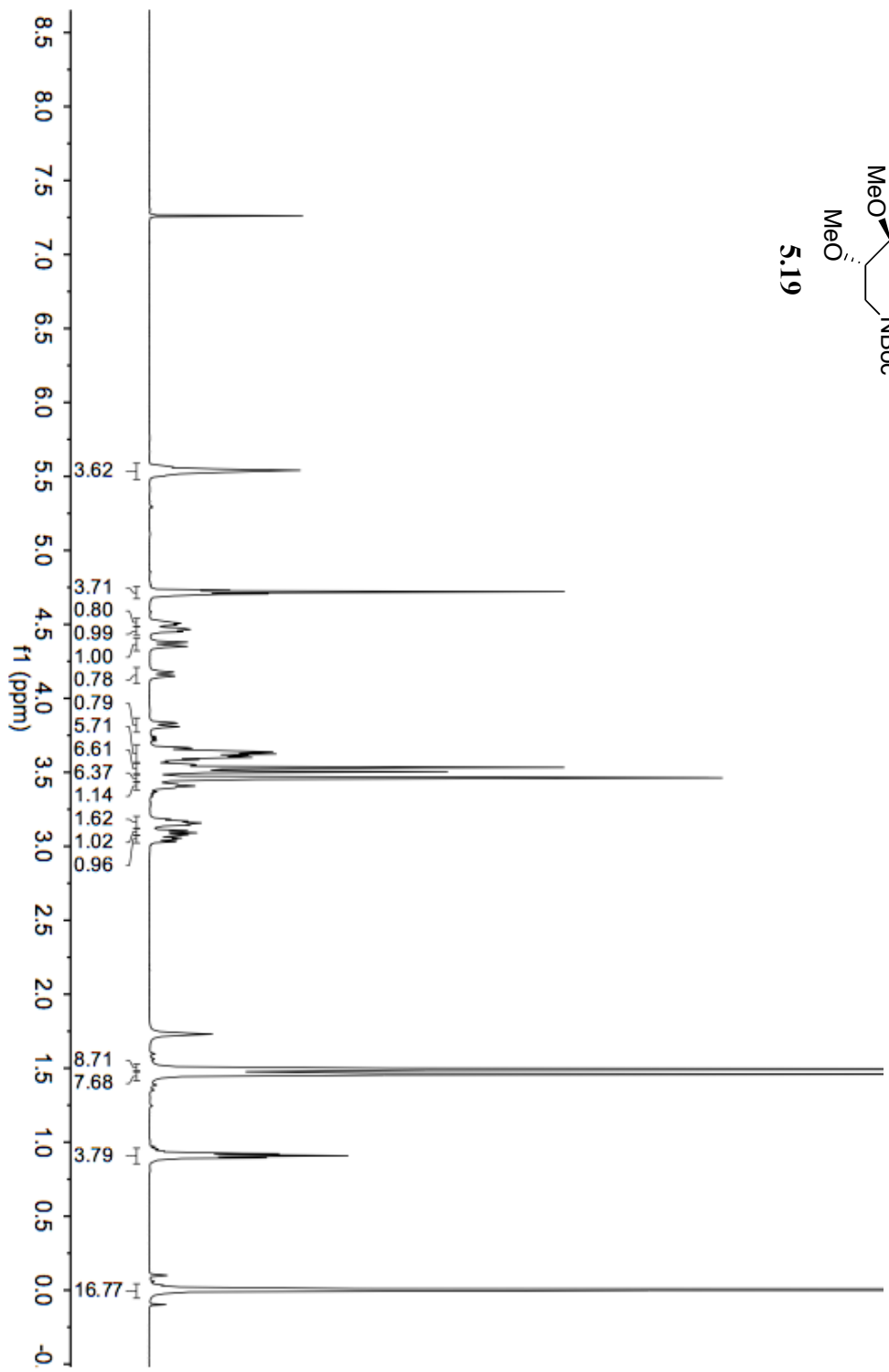
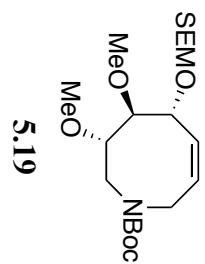
5.15

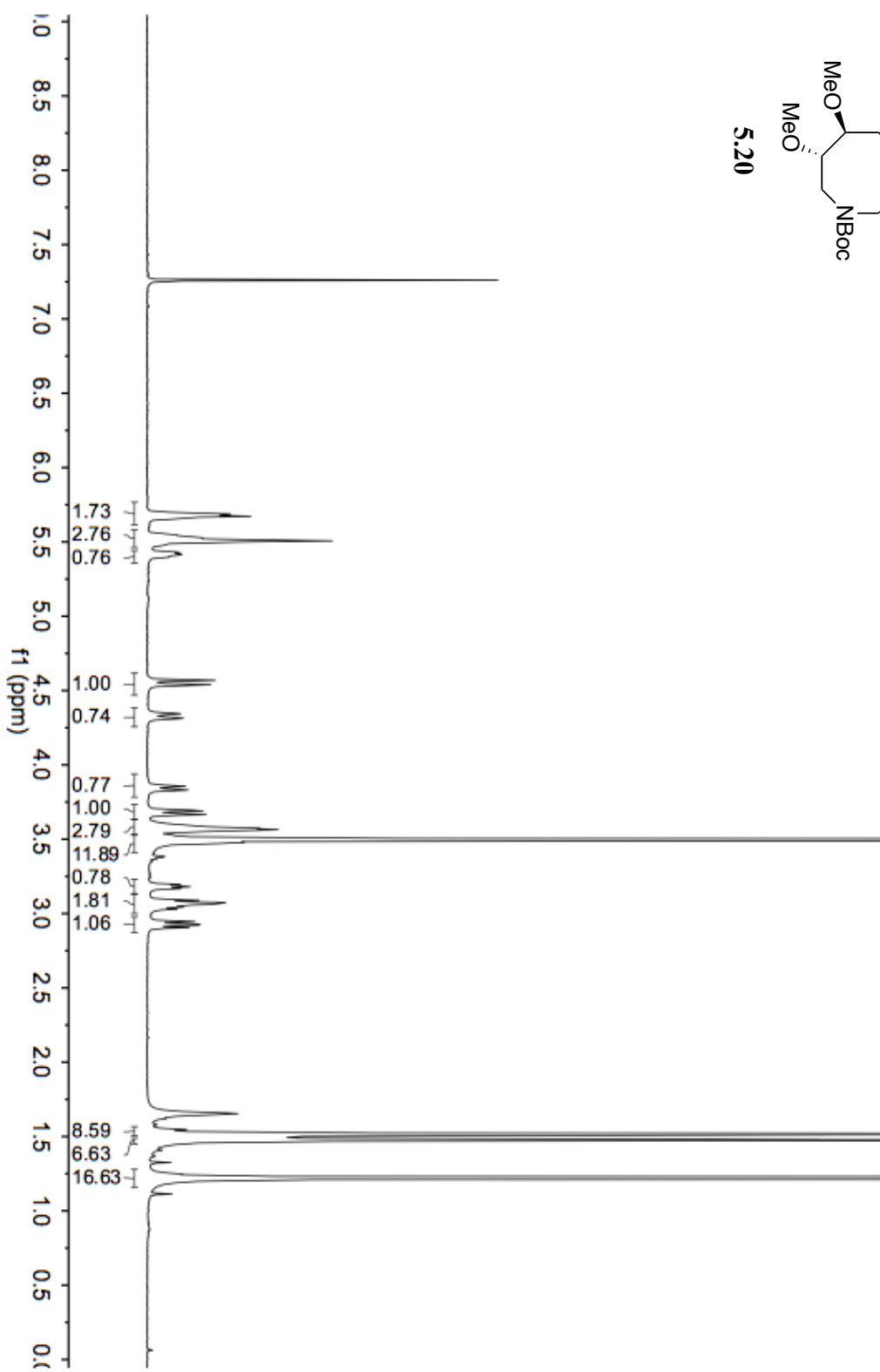
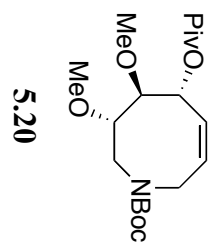


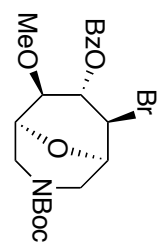


5.16

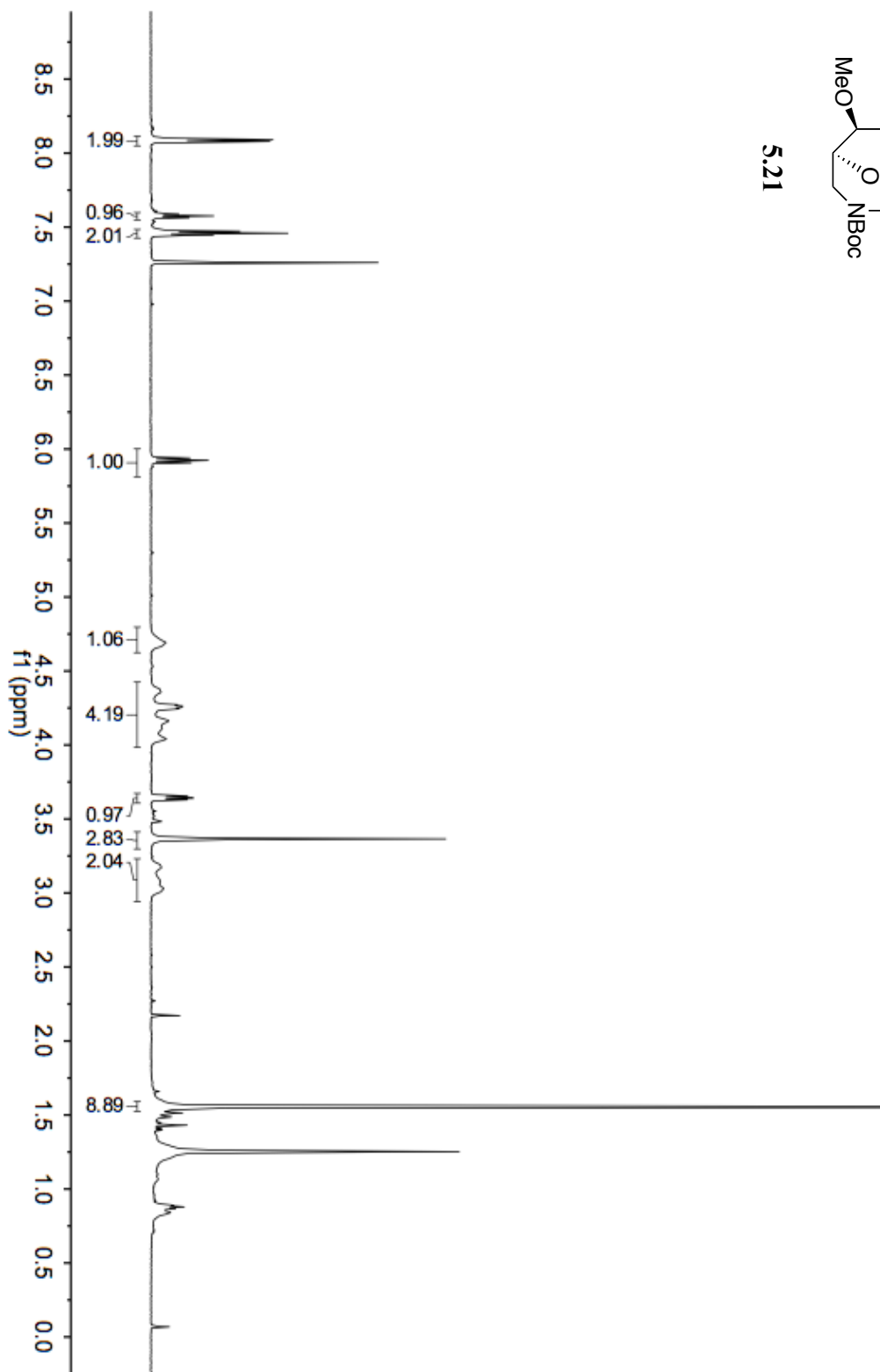


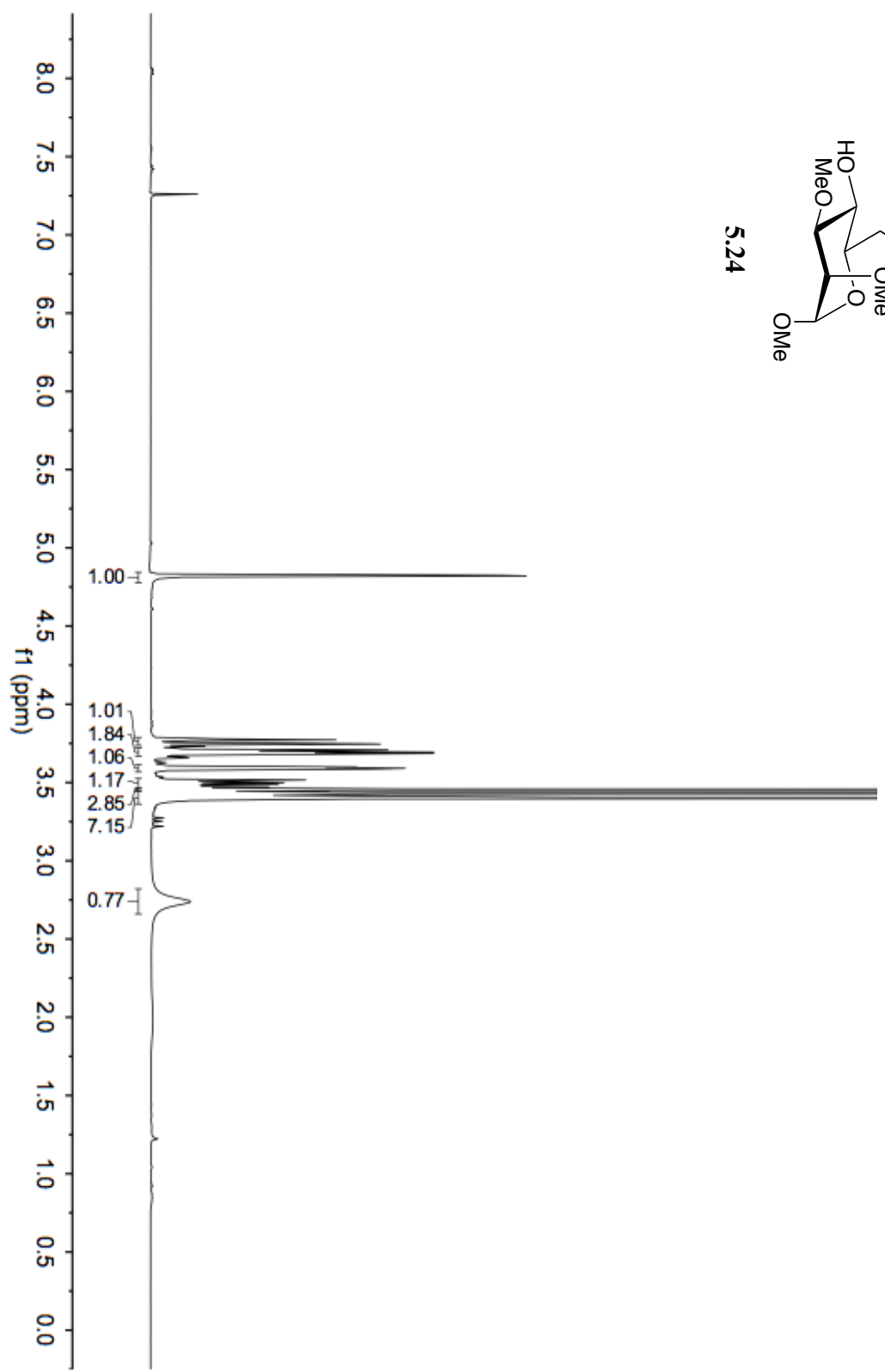
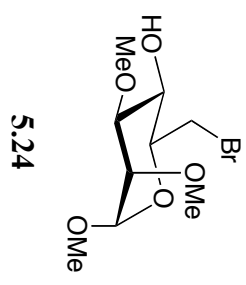


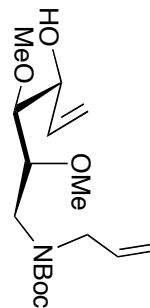




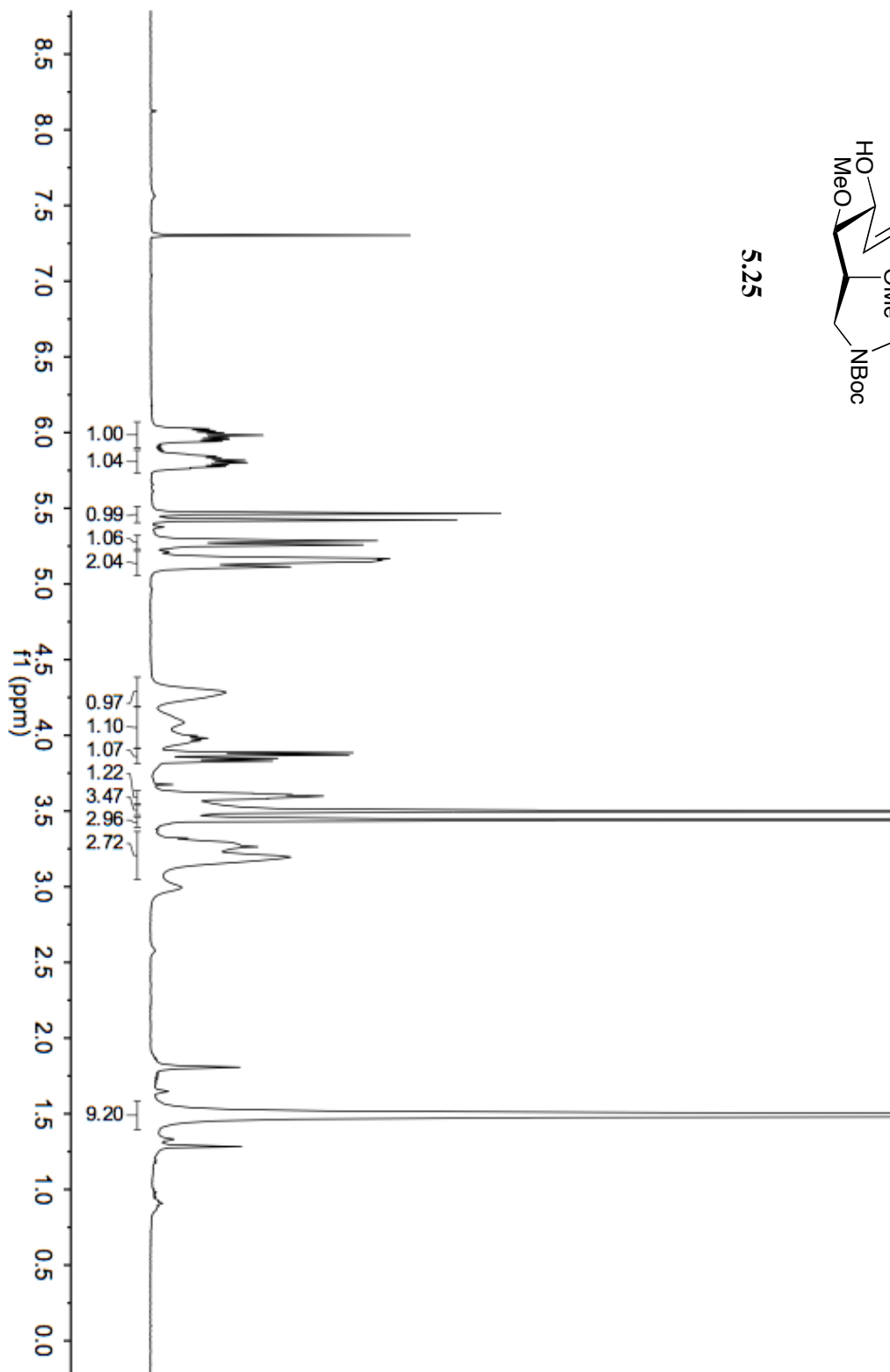
5.21

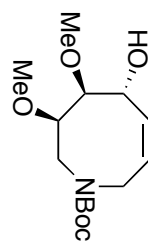




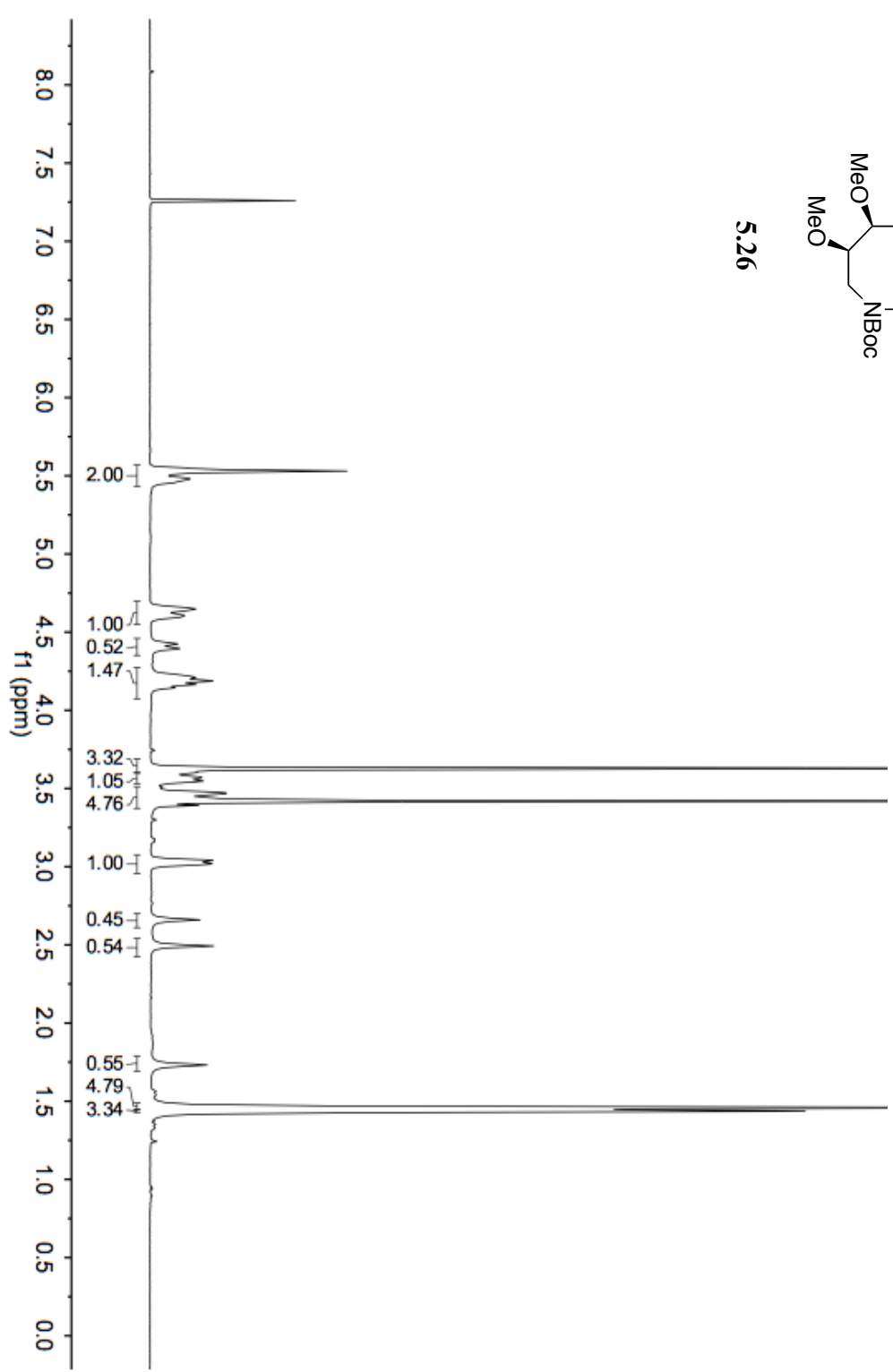


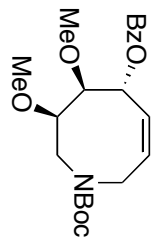
5.25



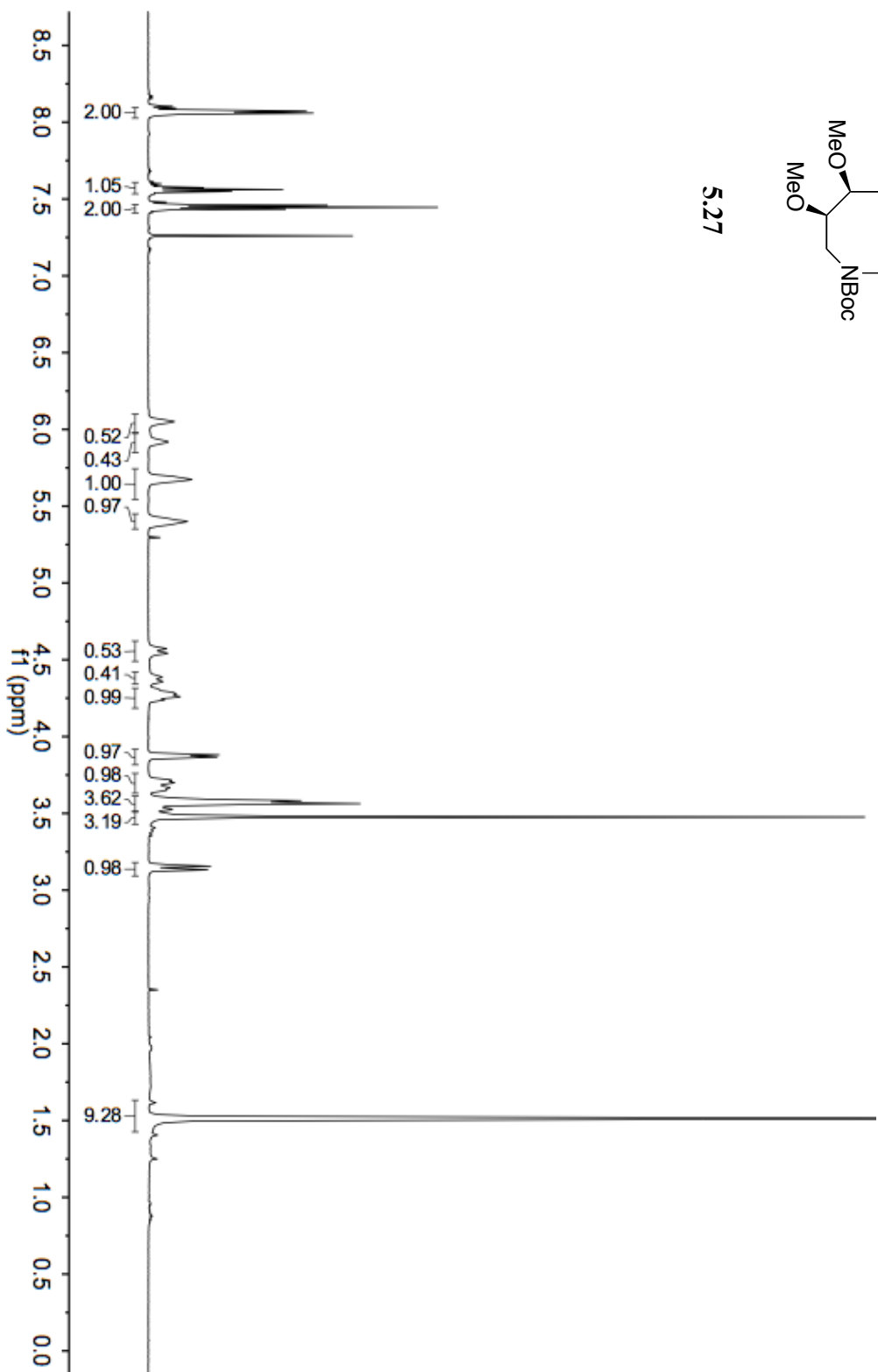


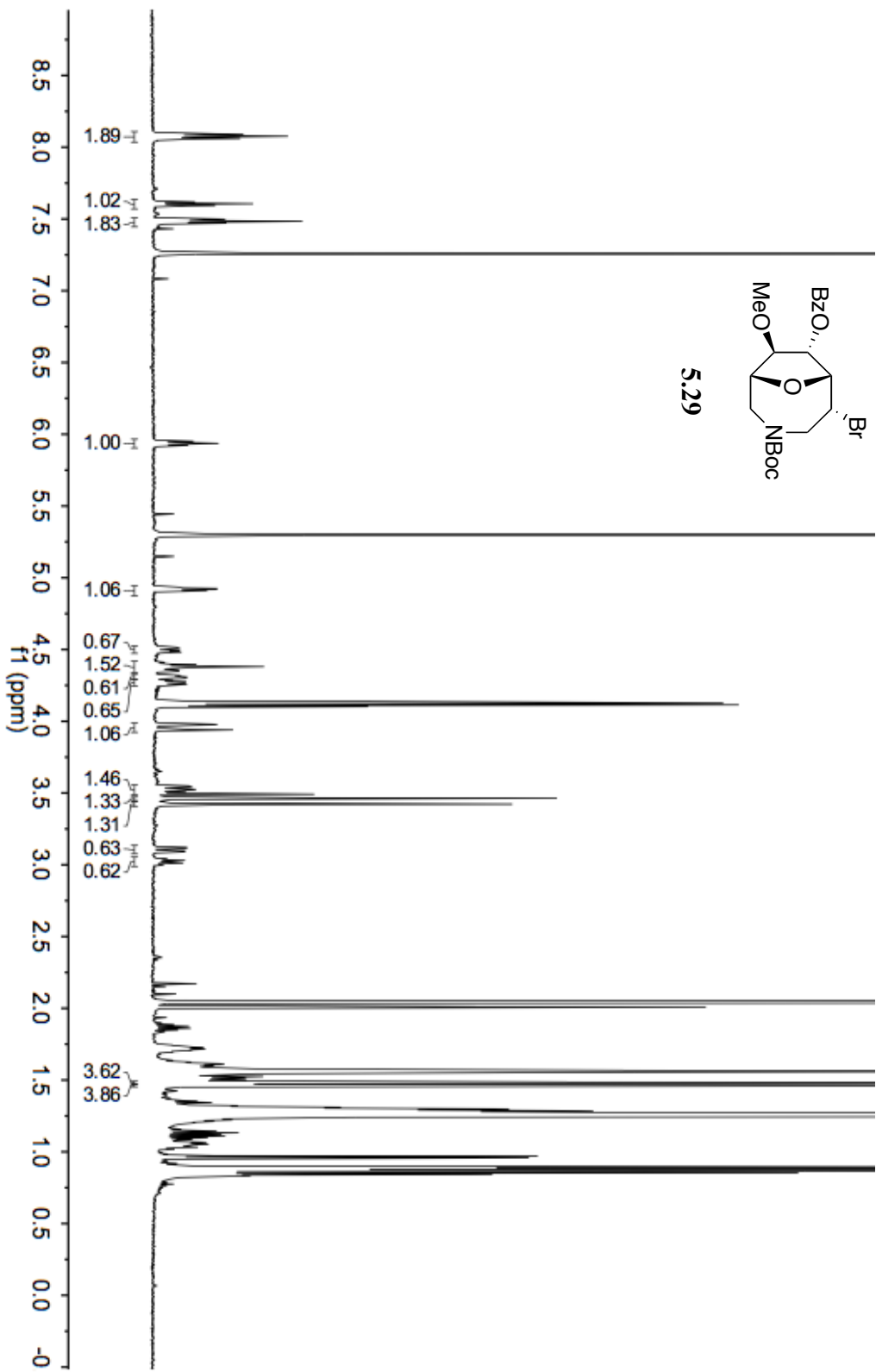
5.26

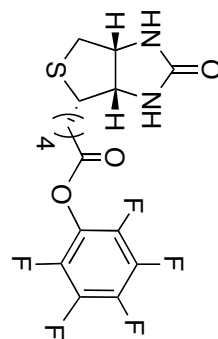




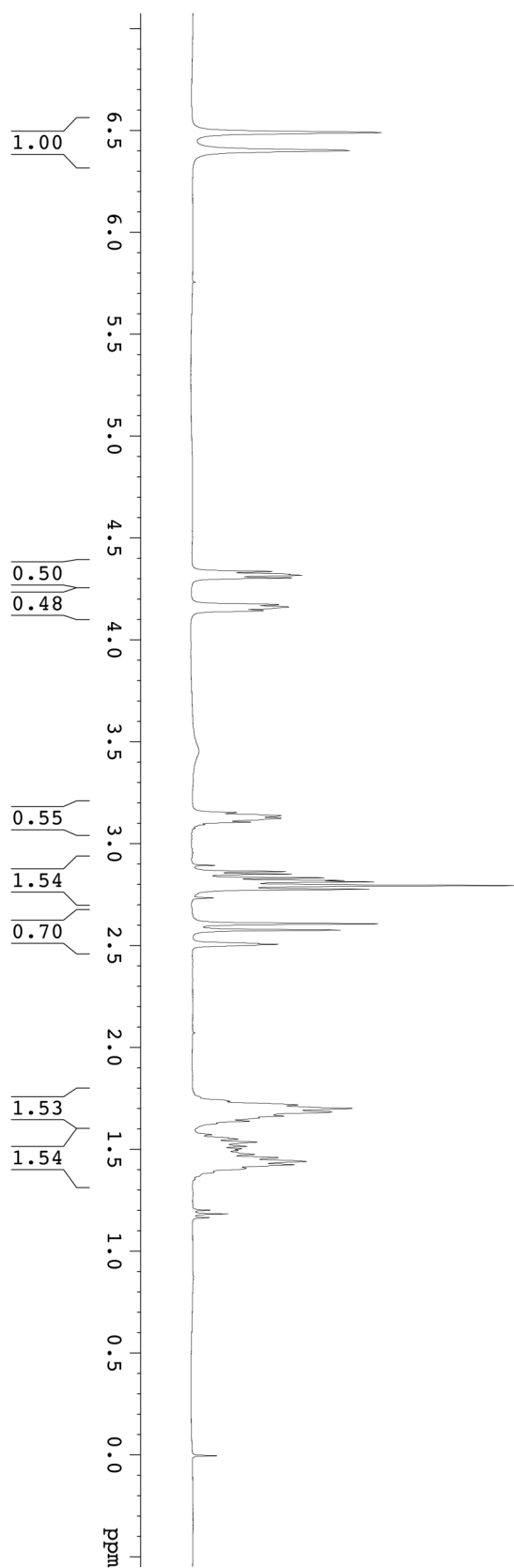
5.27

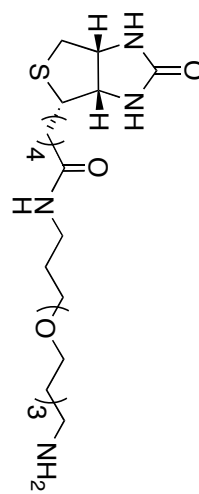




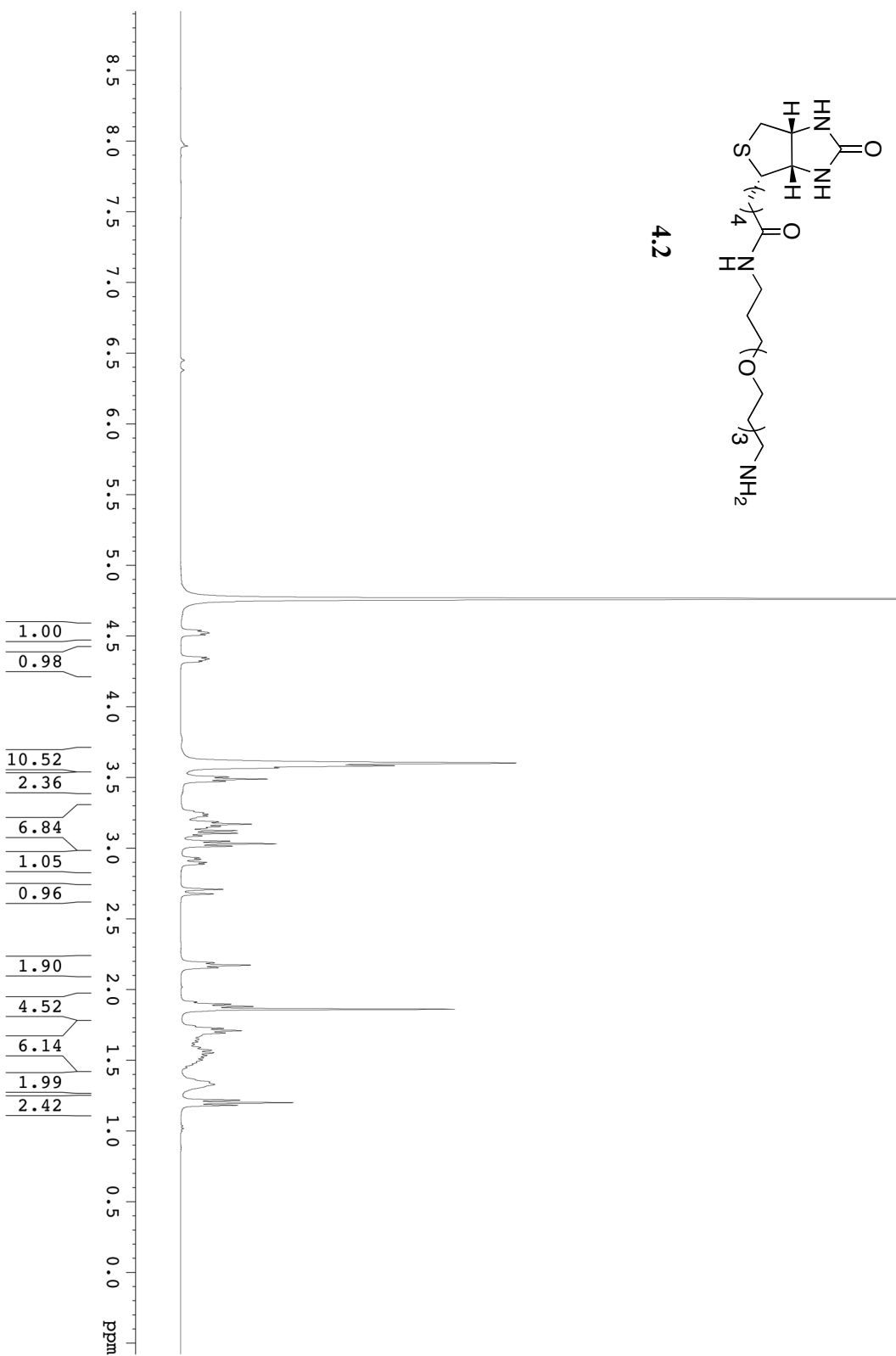


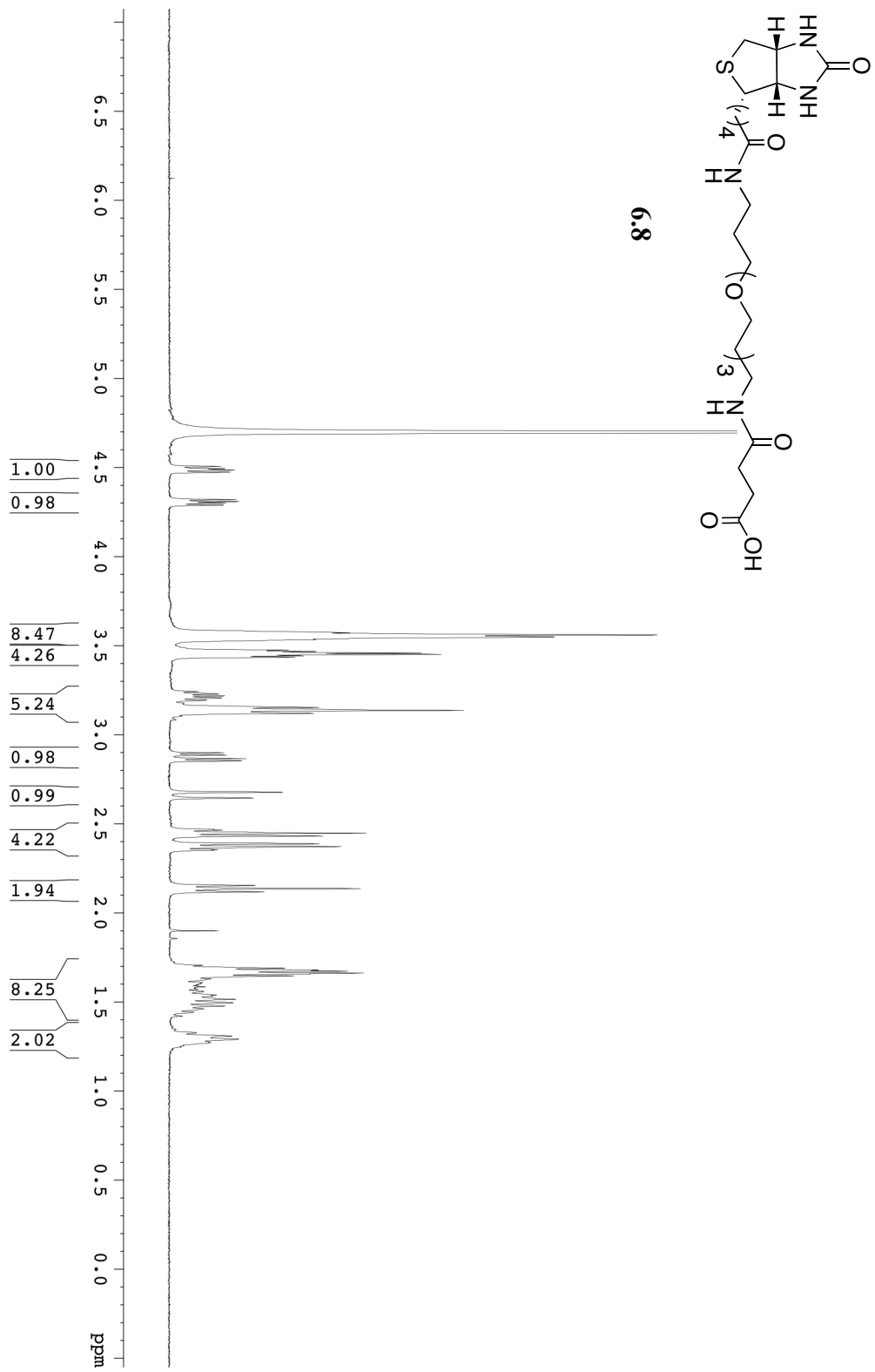
6.2

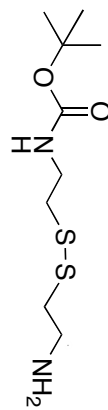




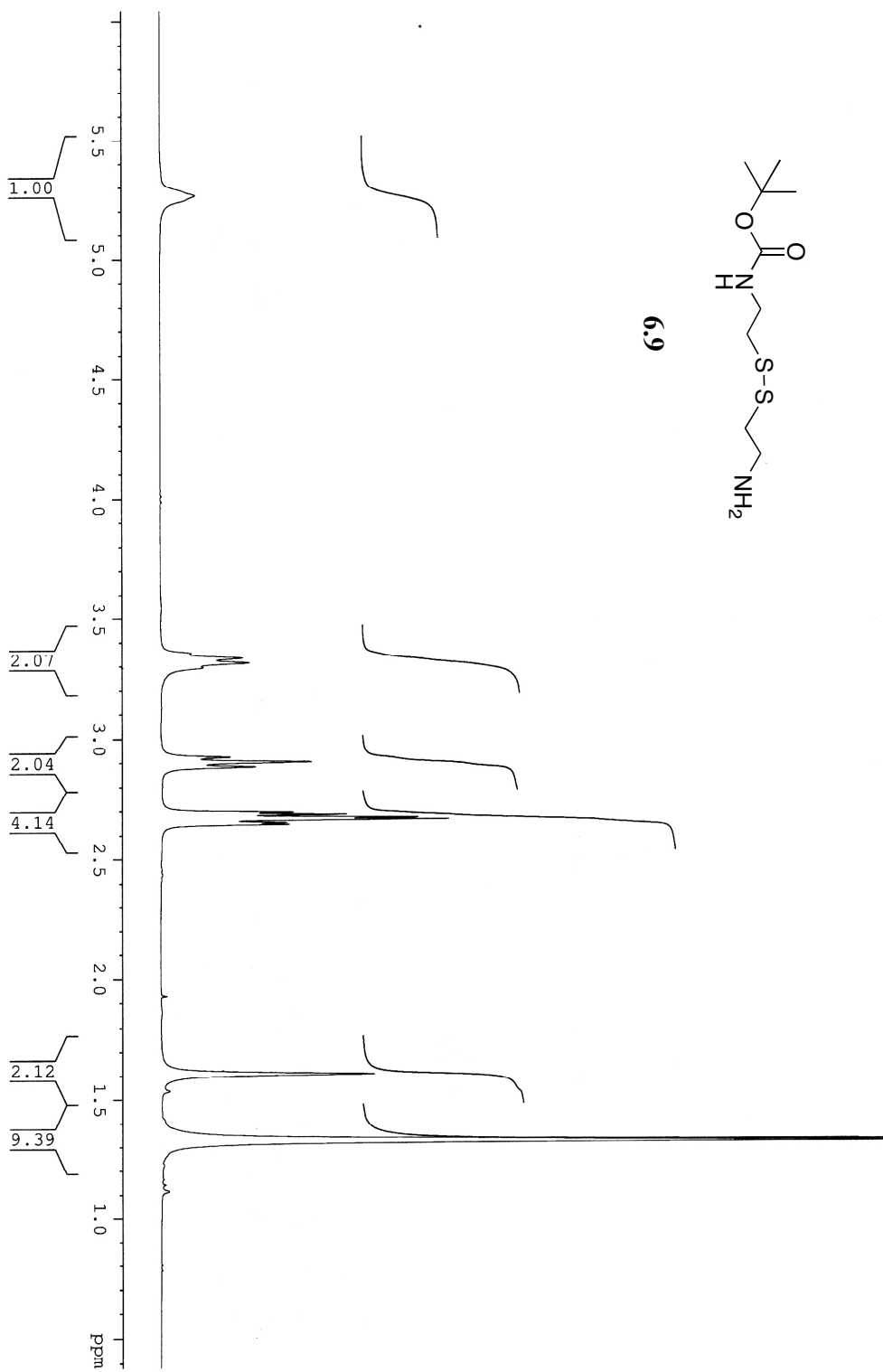
4.2

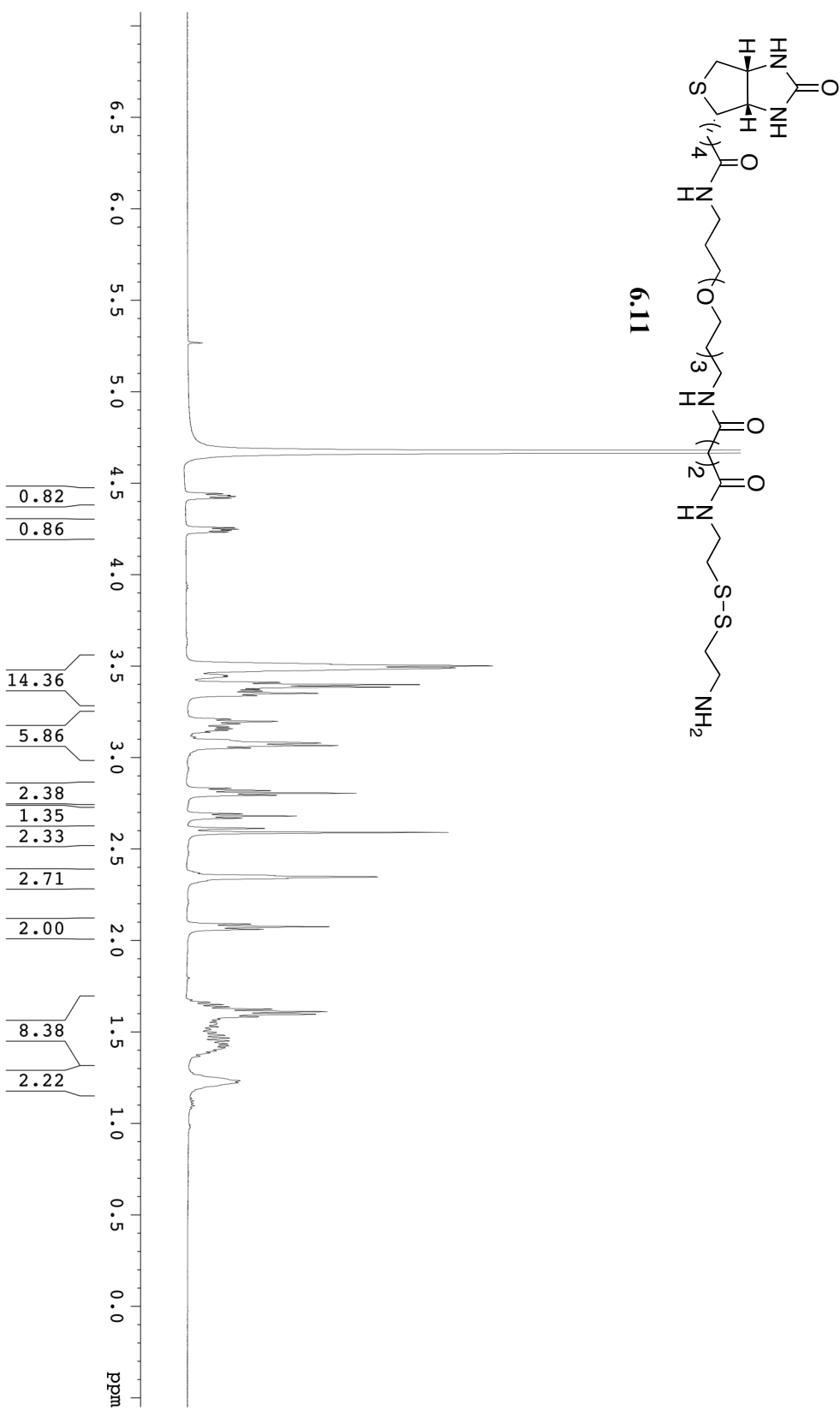


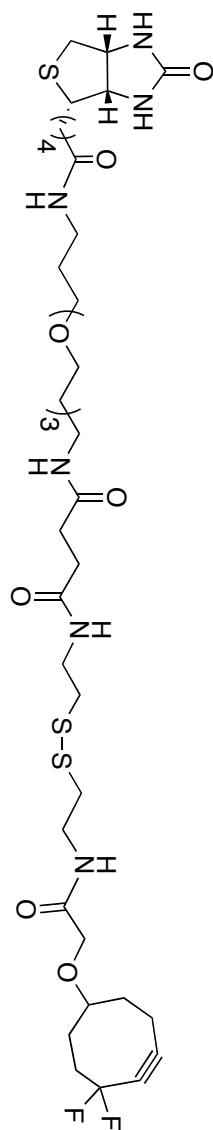




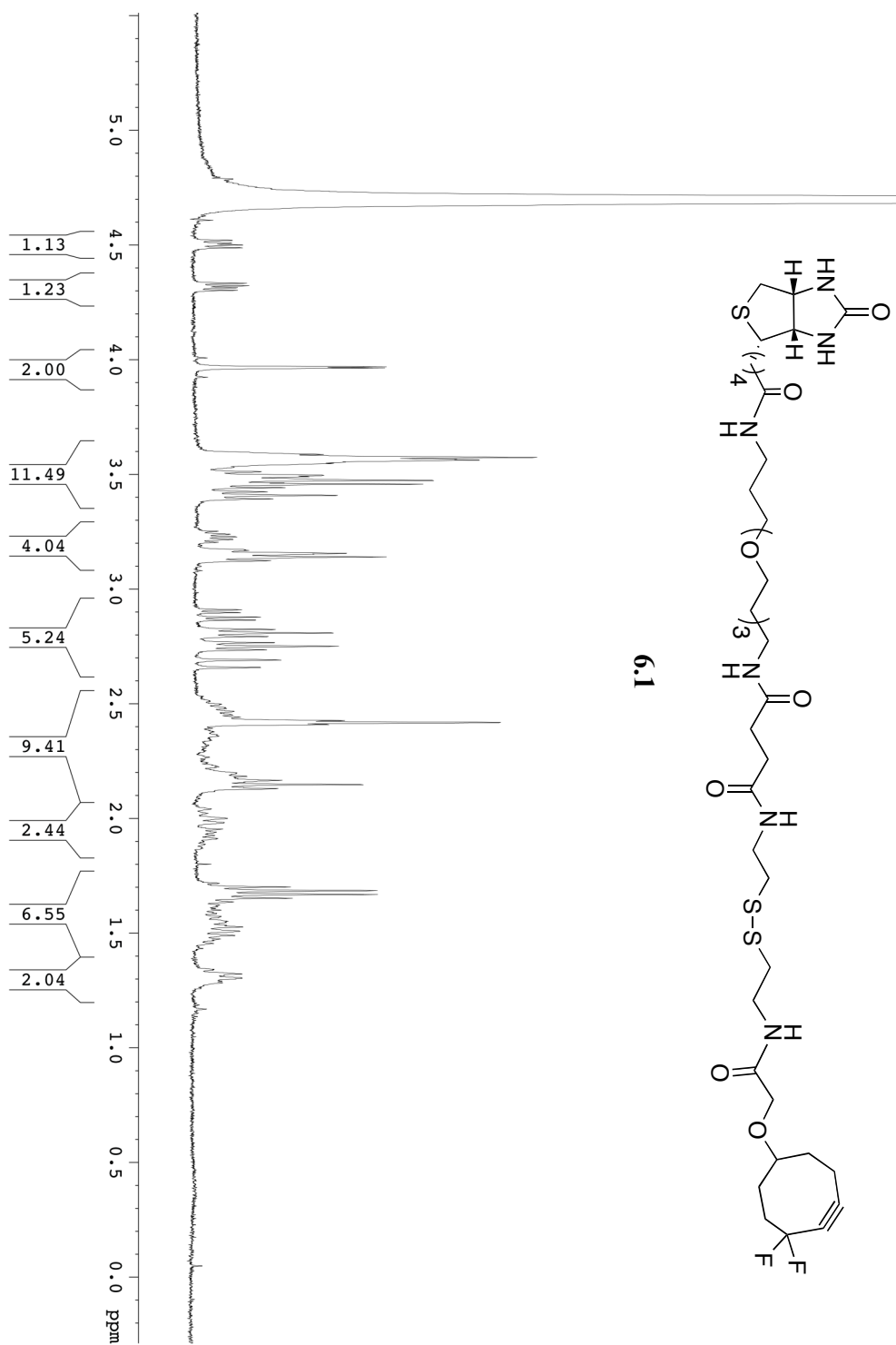
6.9

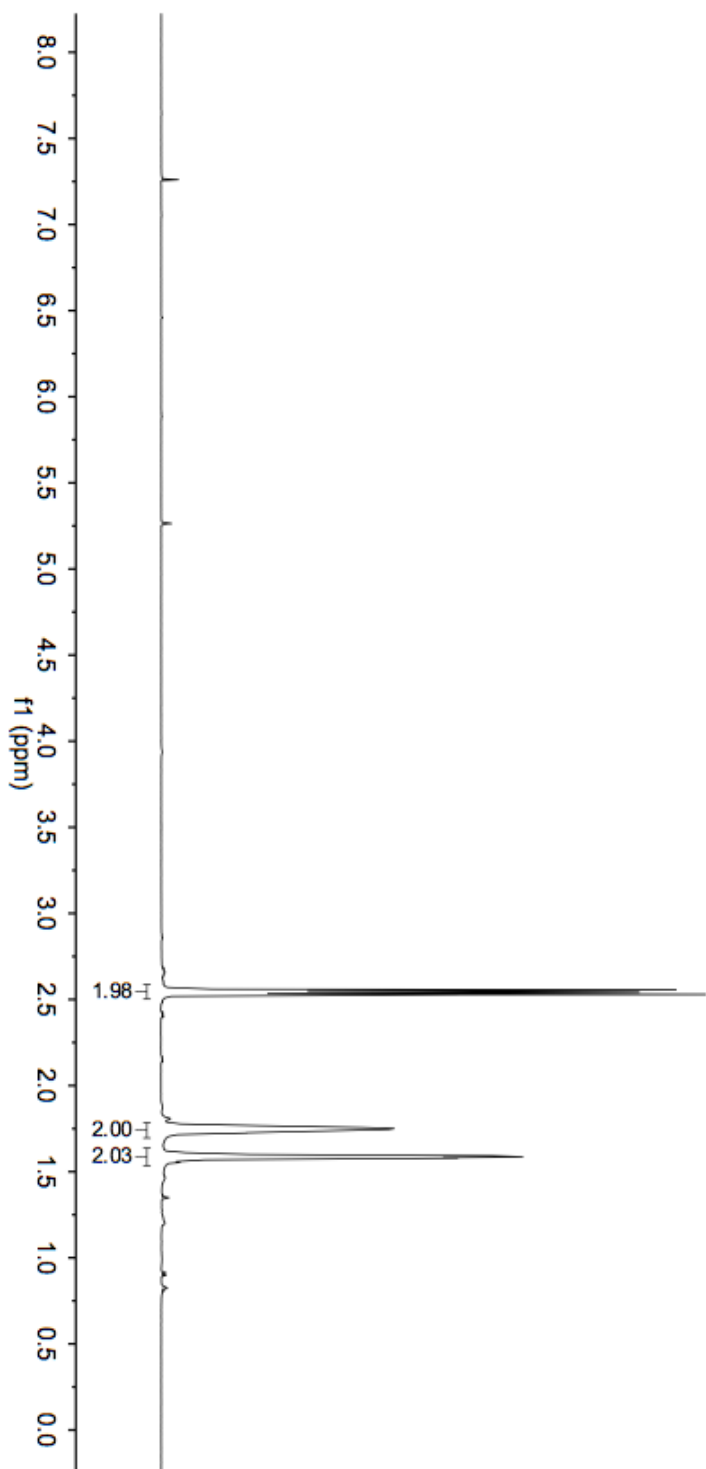
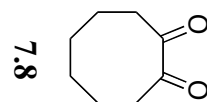


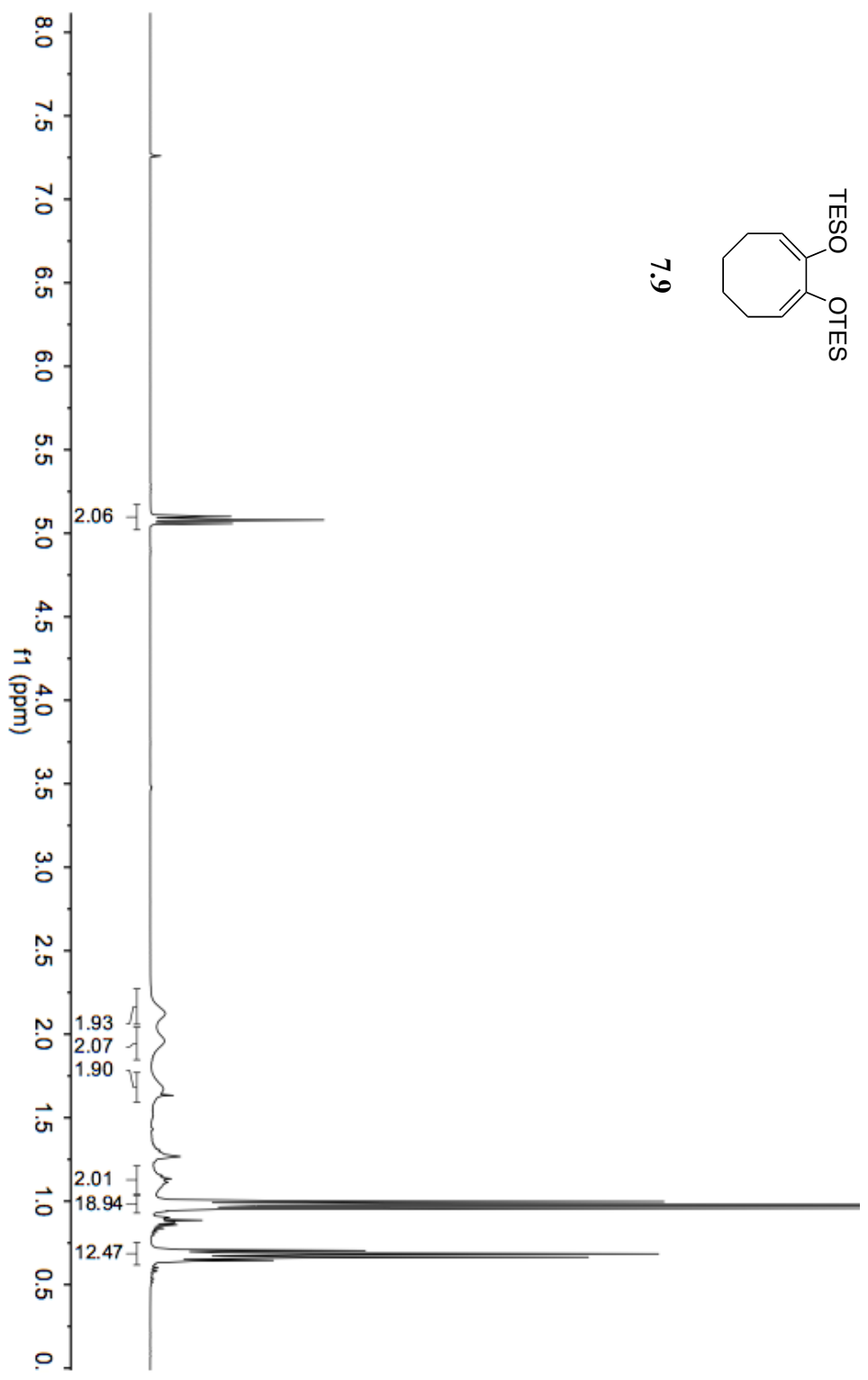


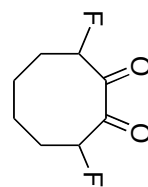


6.1

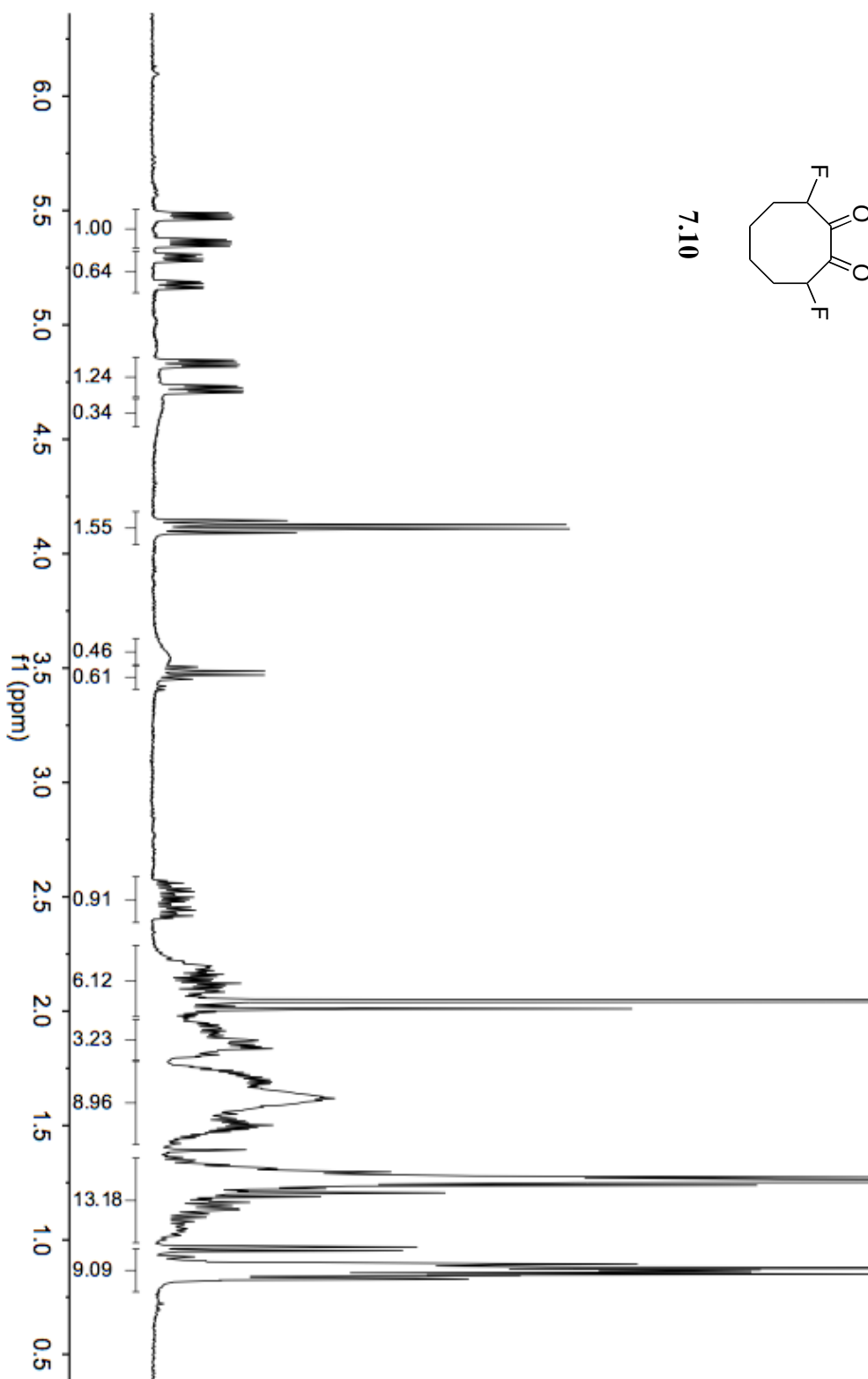


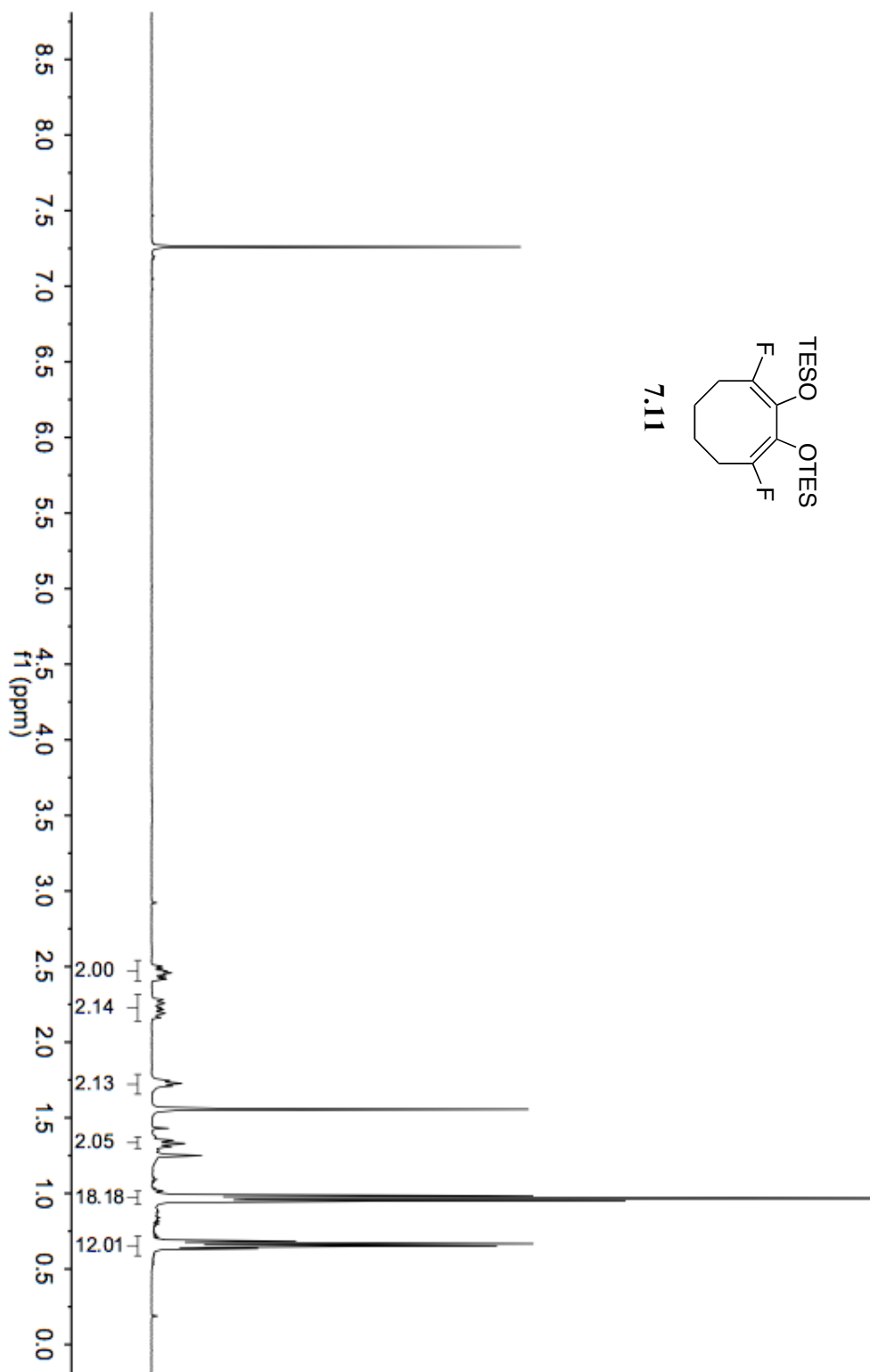
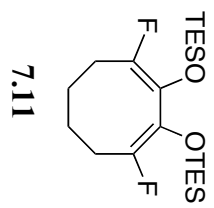


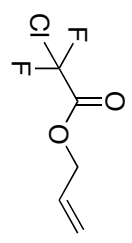




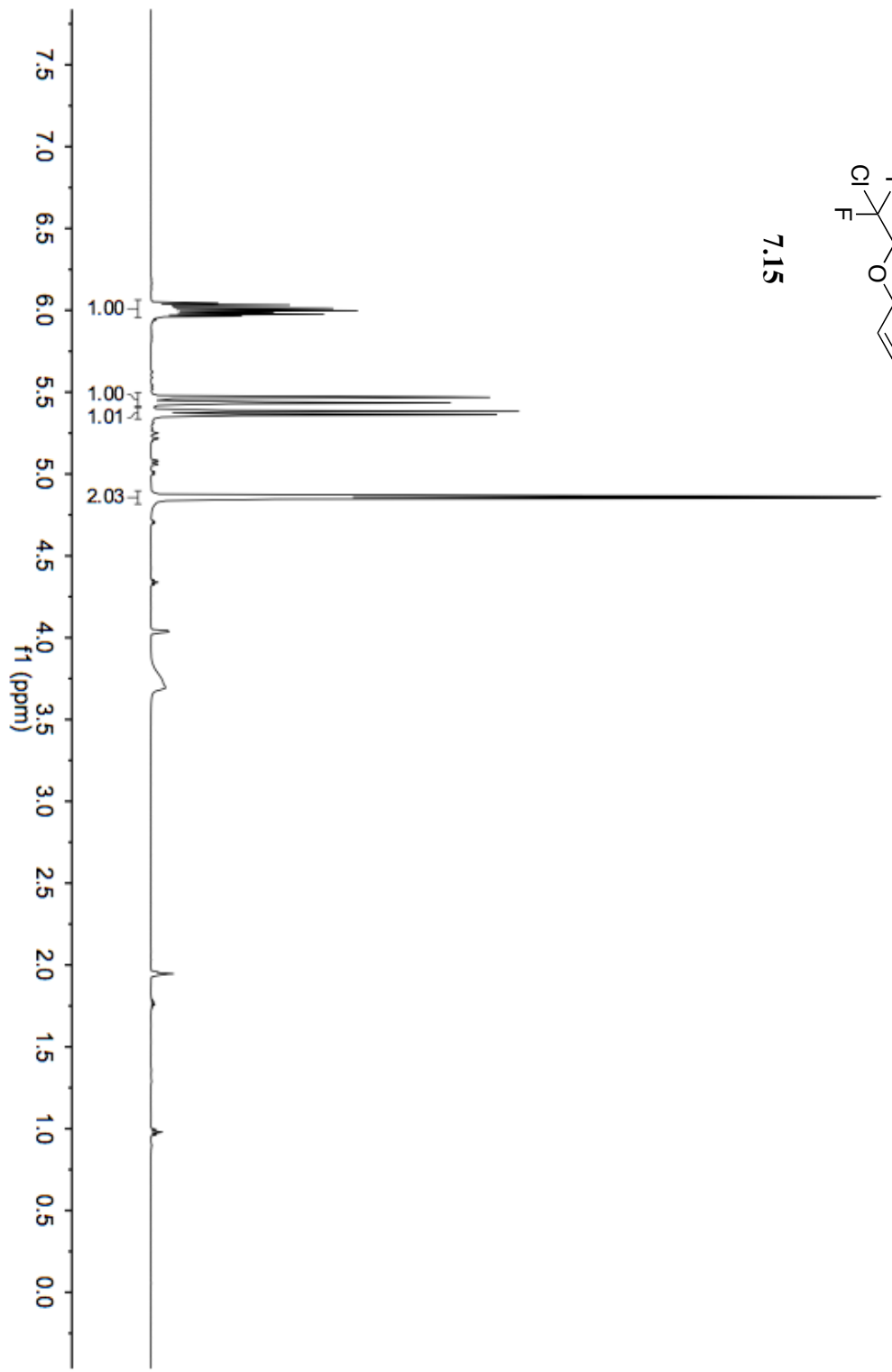
7.10

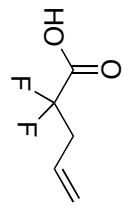




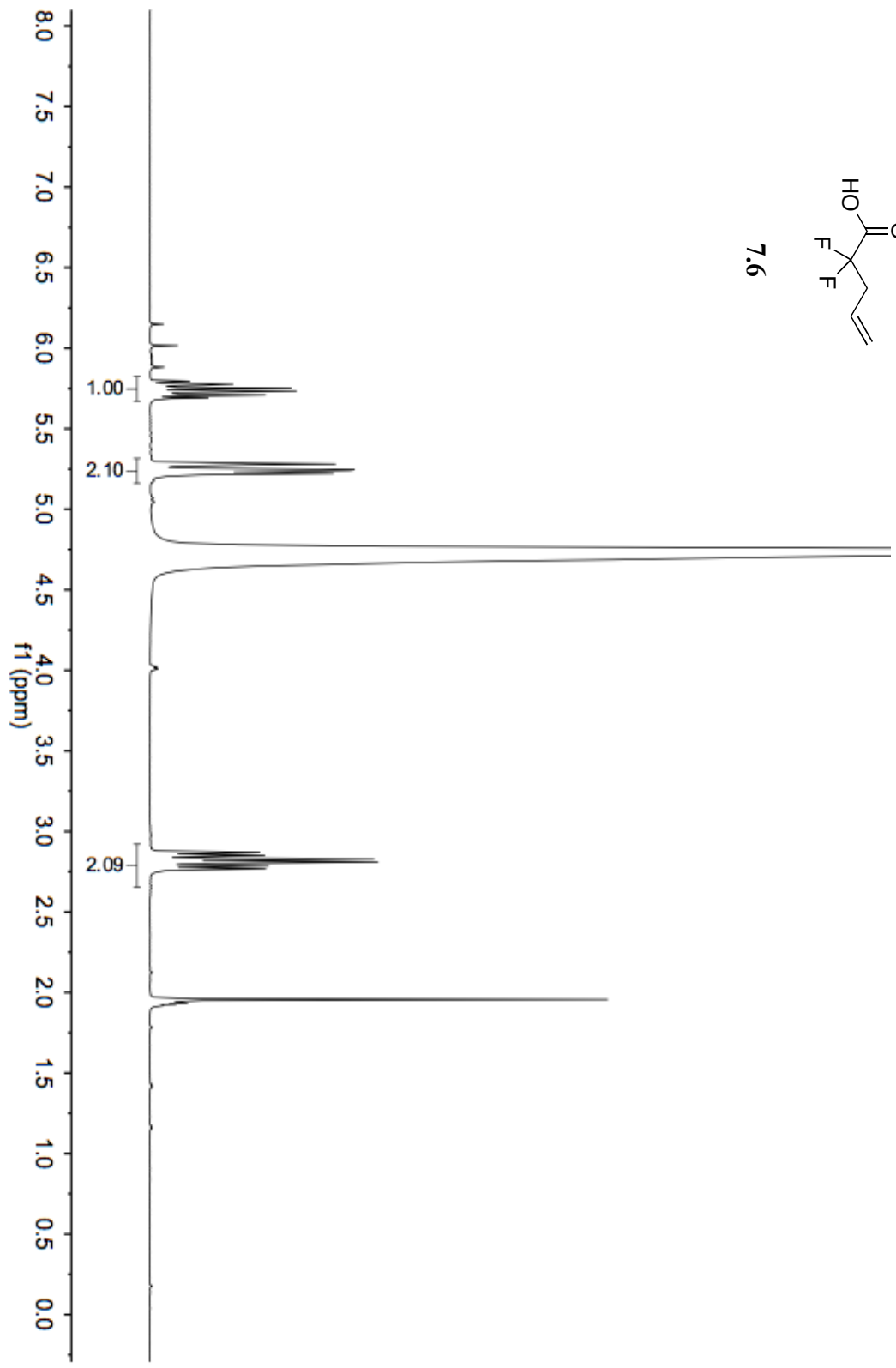


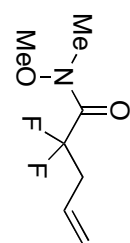
7.15



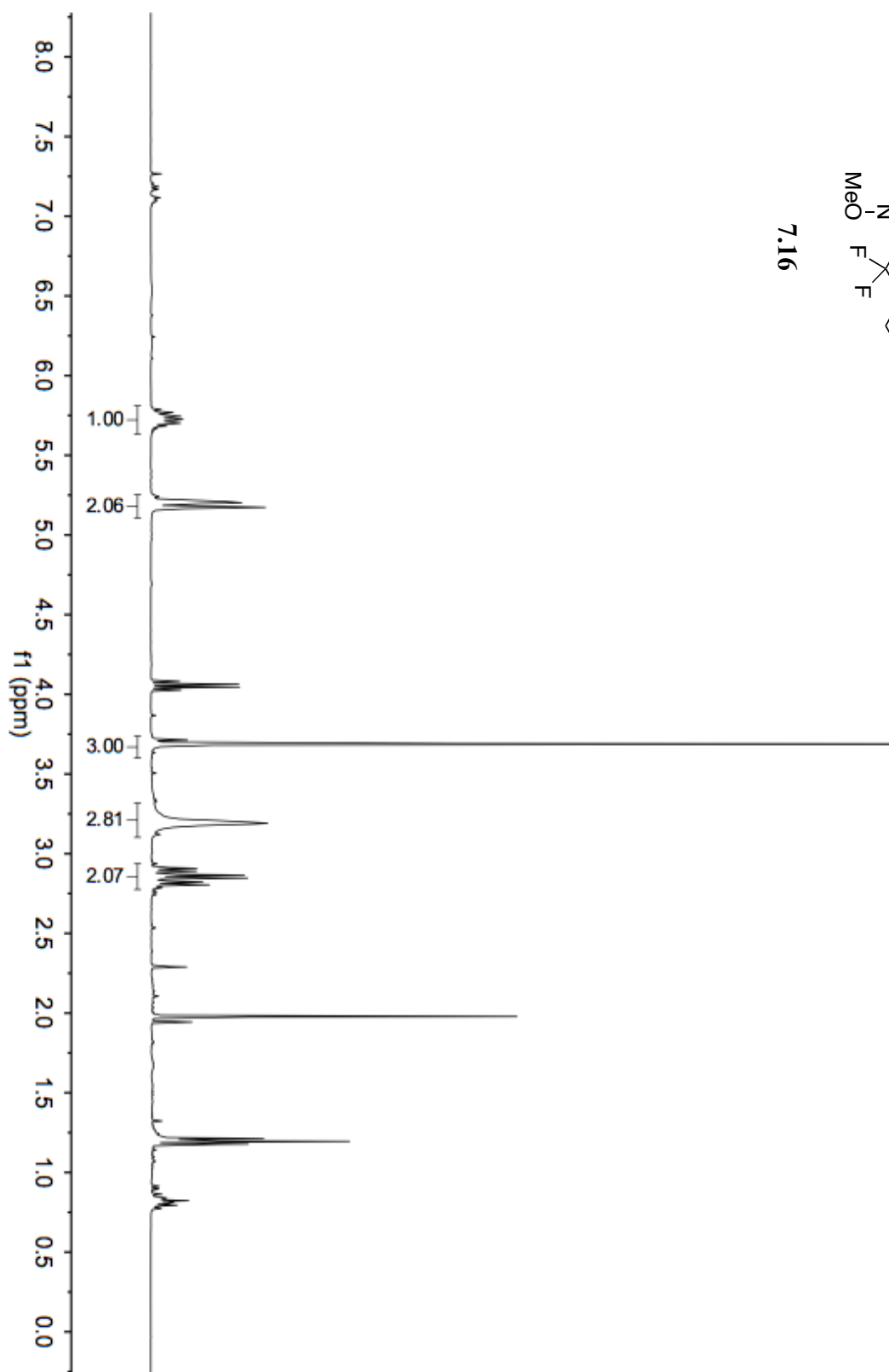


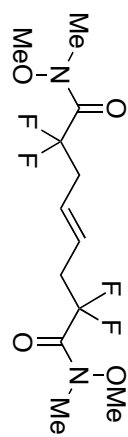
7.6



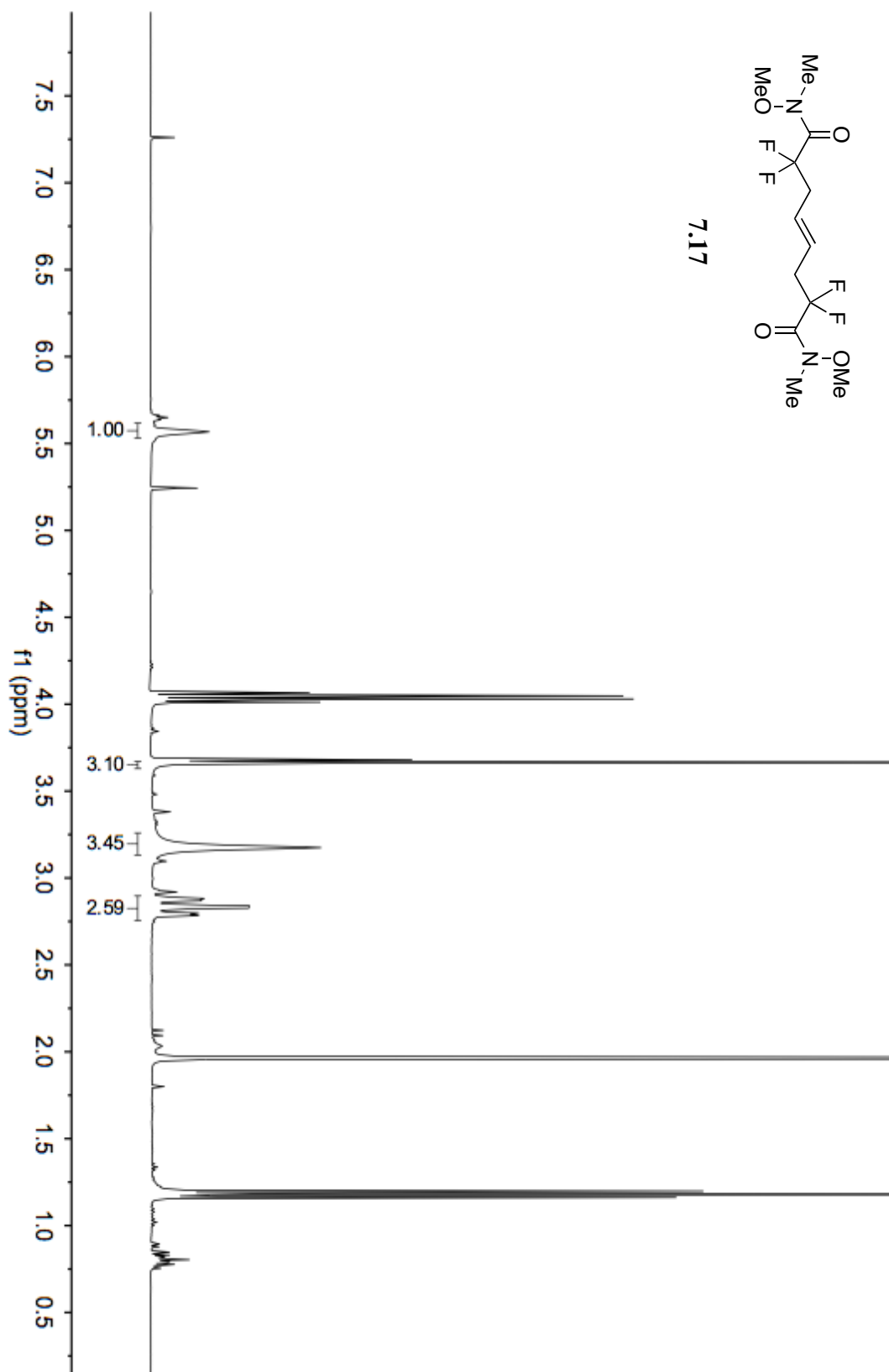


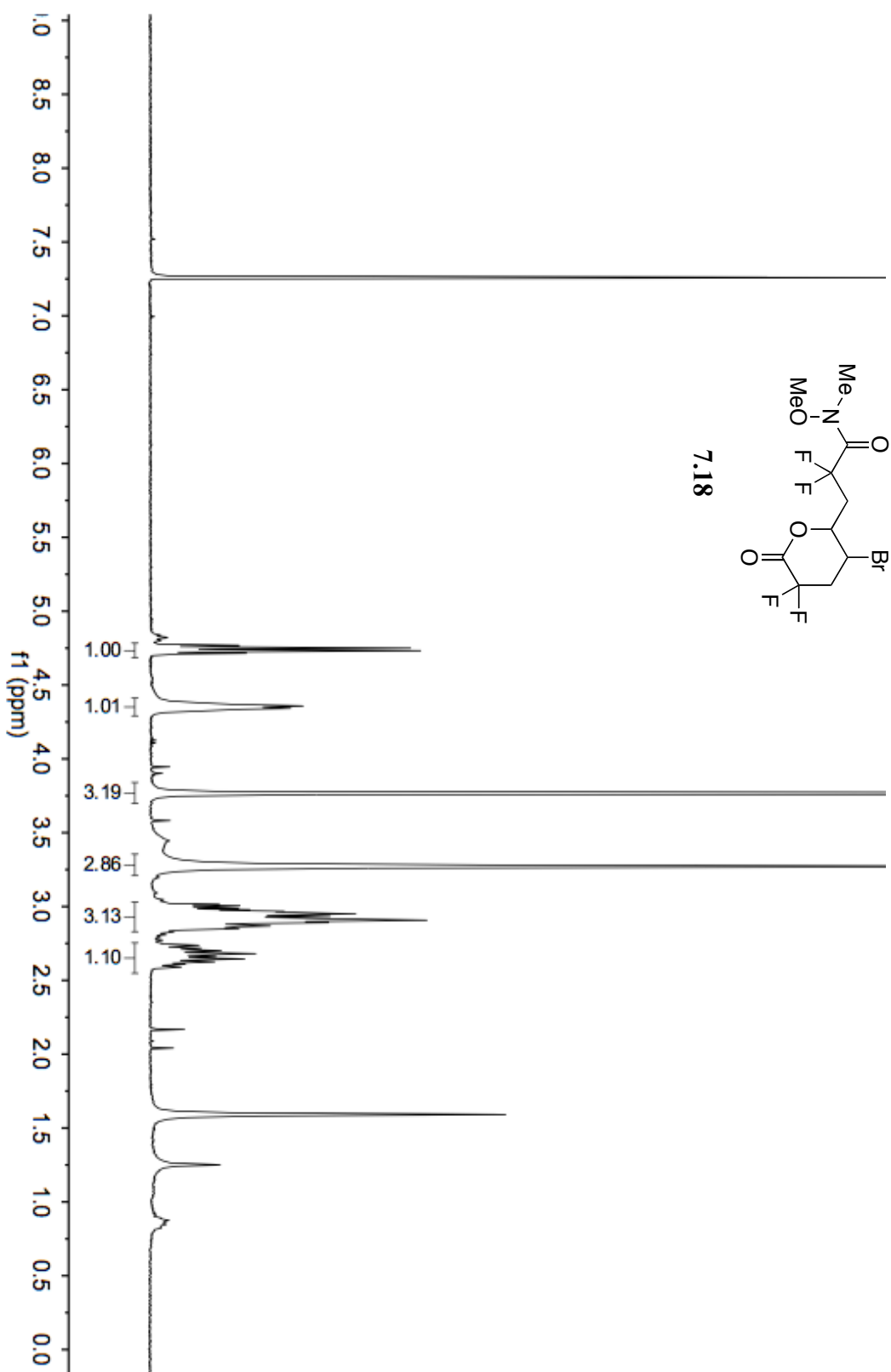
7.16

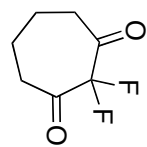




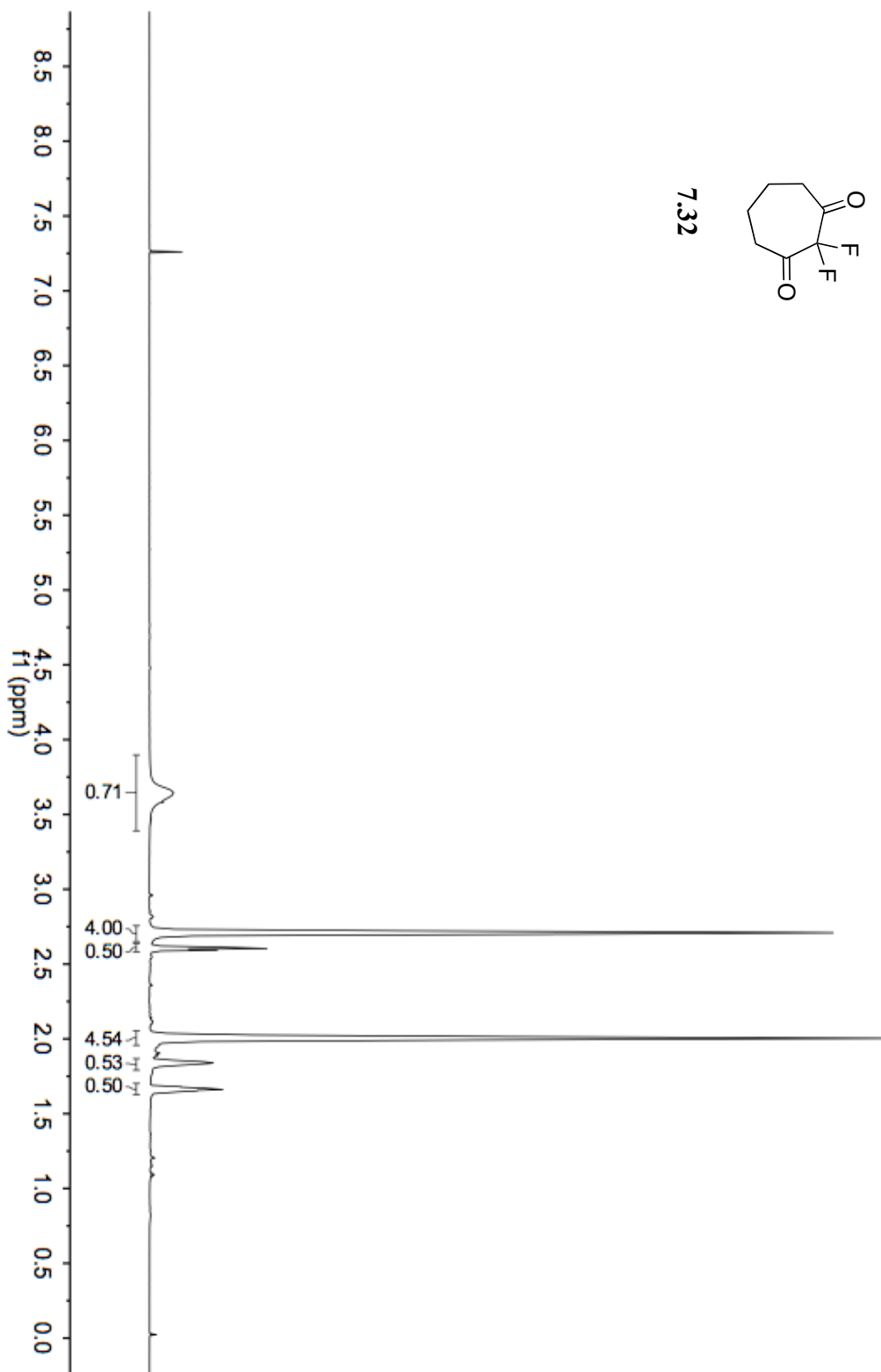
7.17

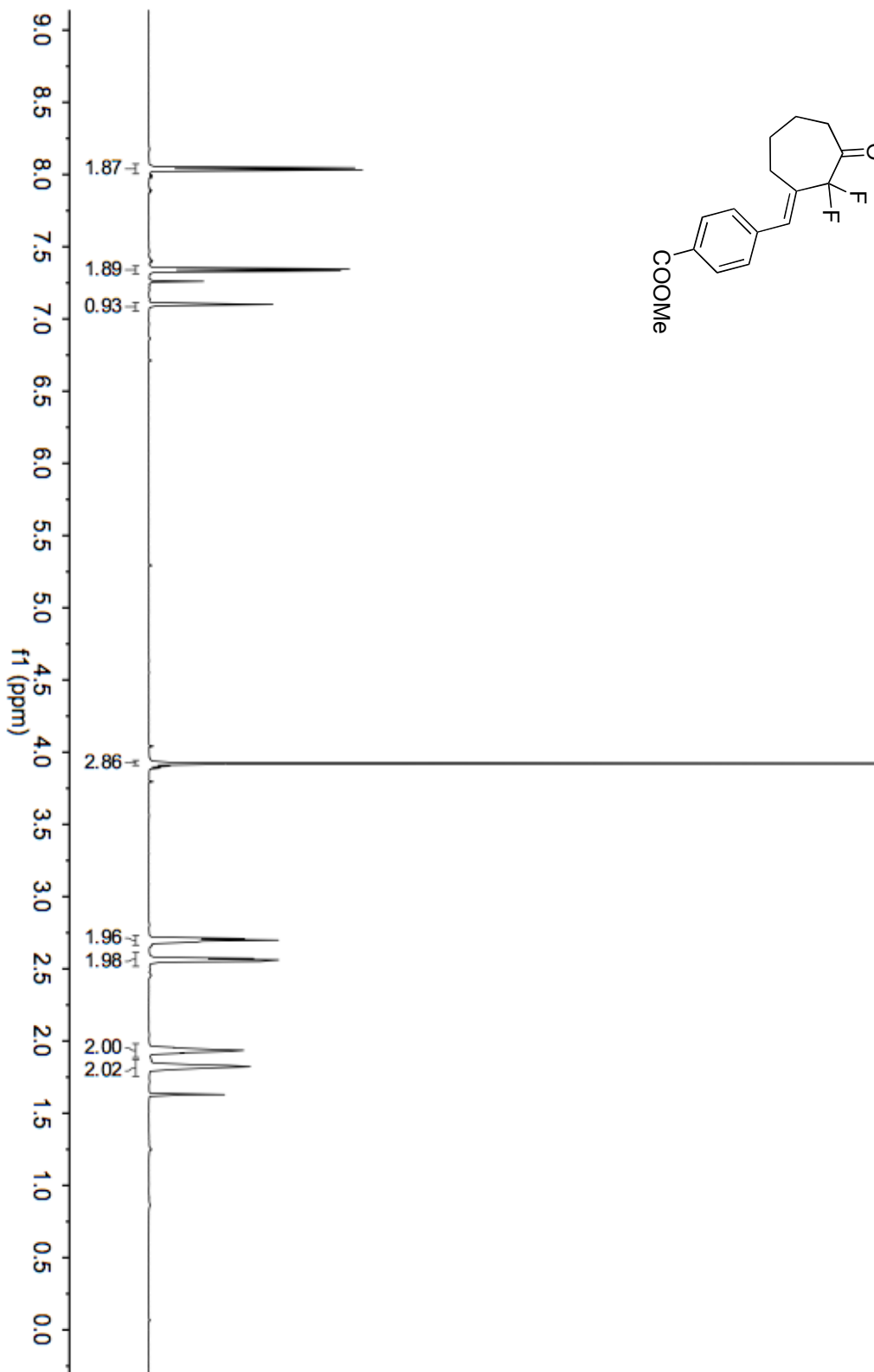
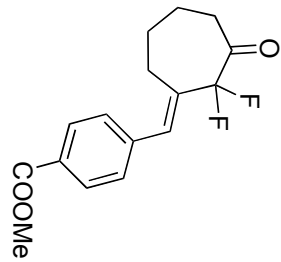


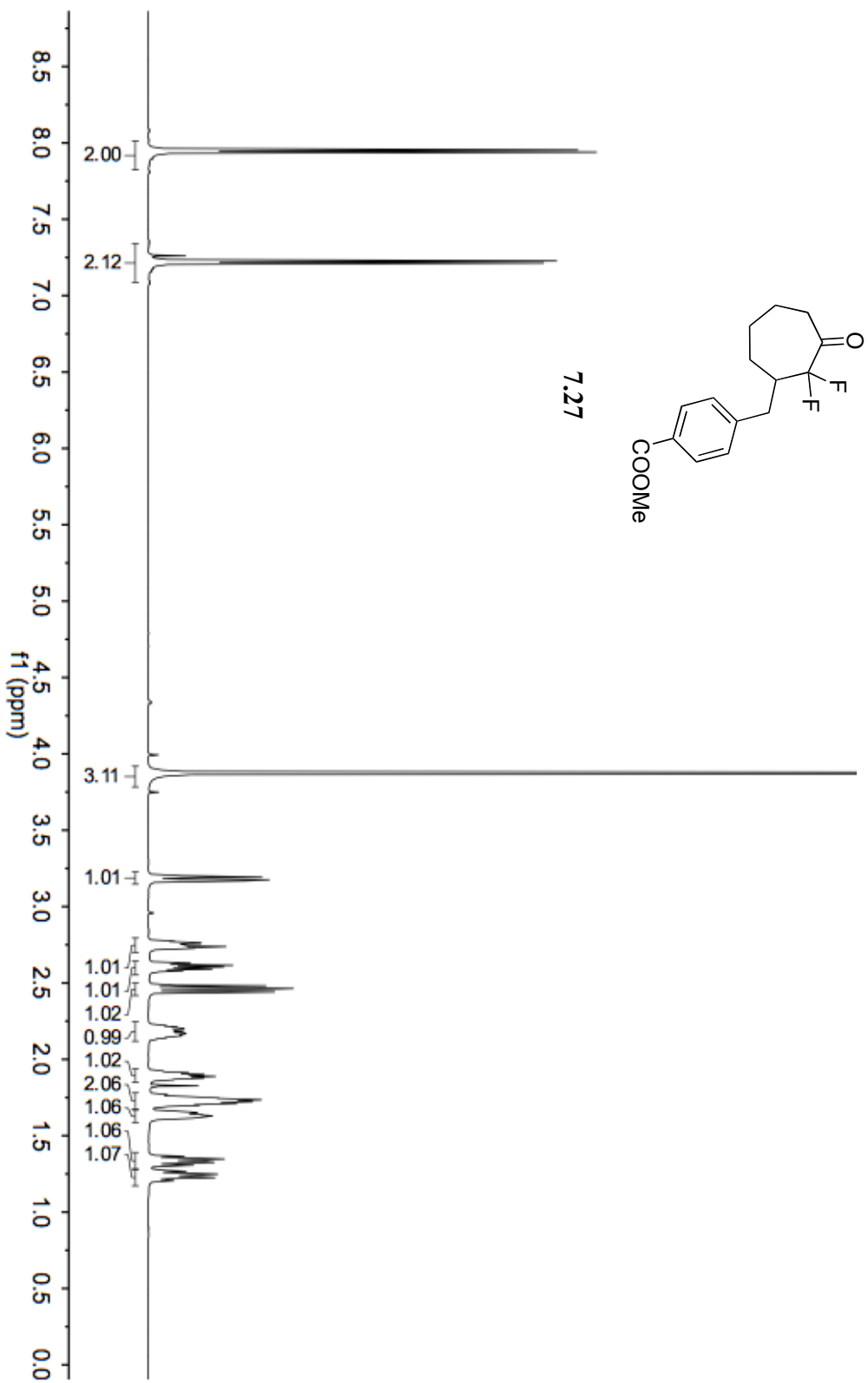


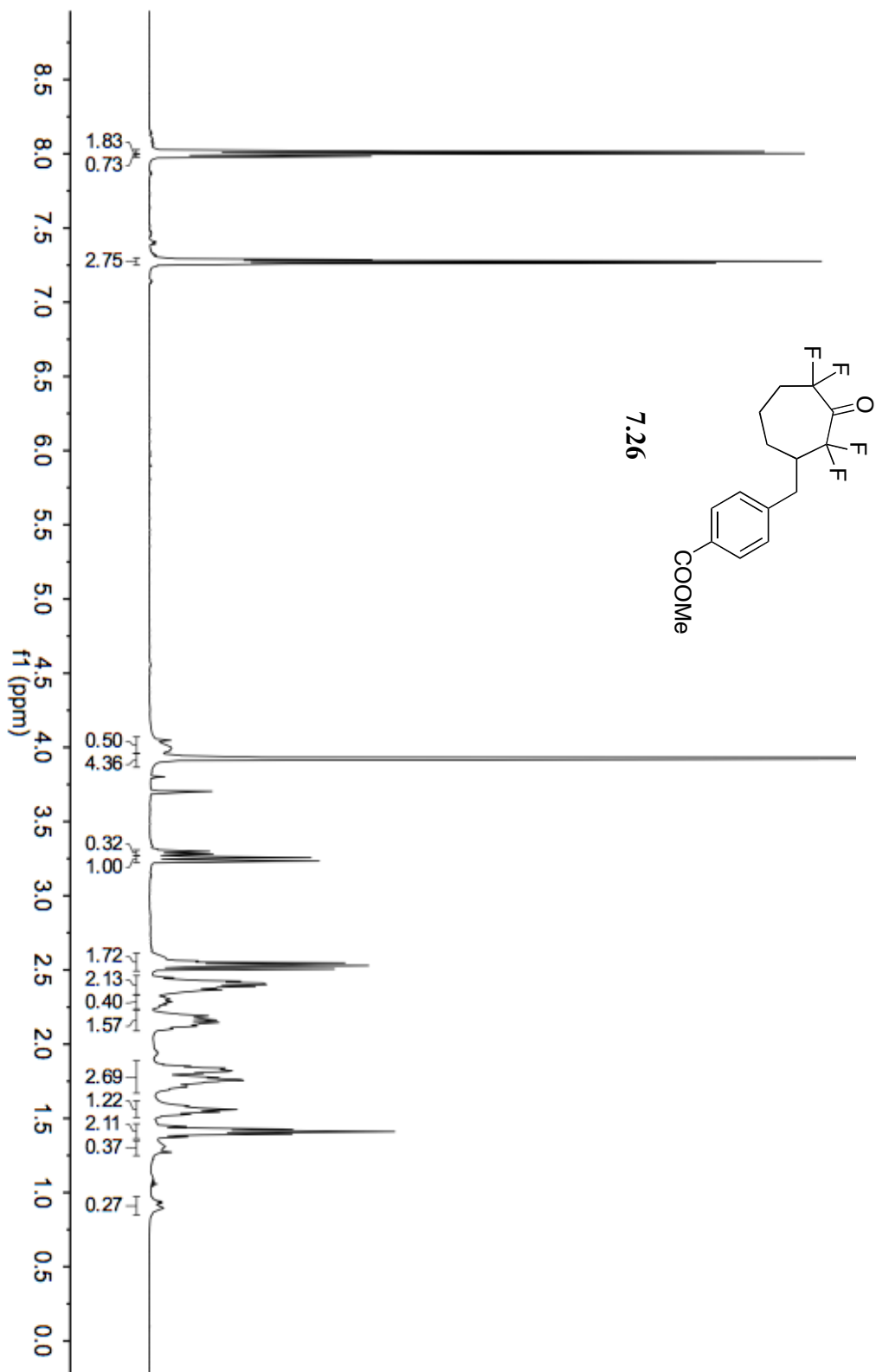


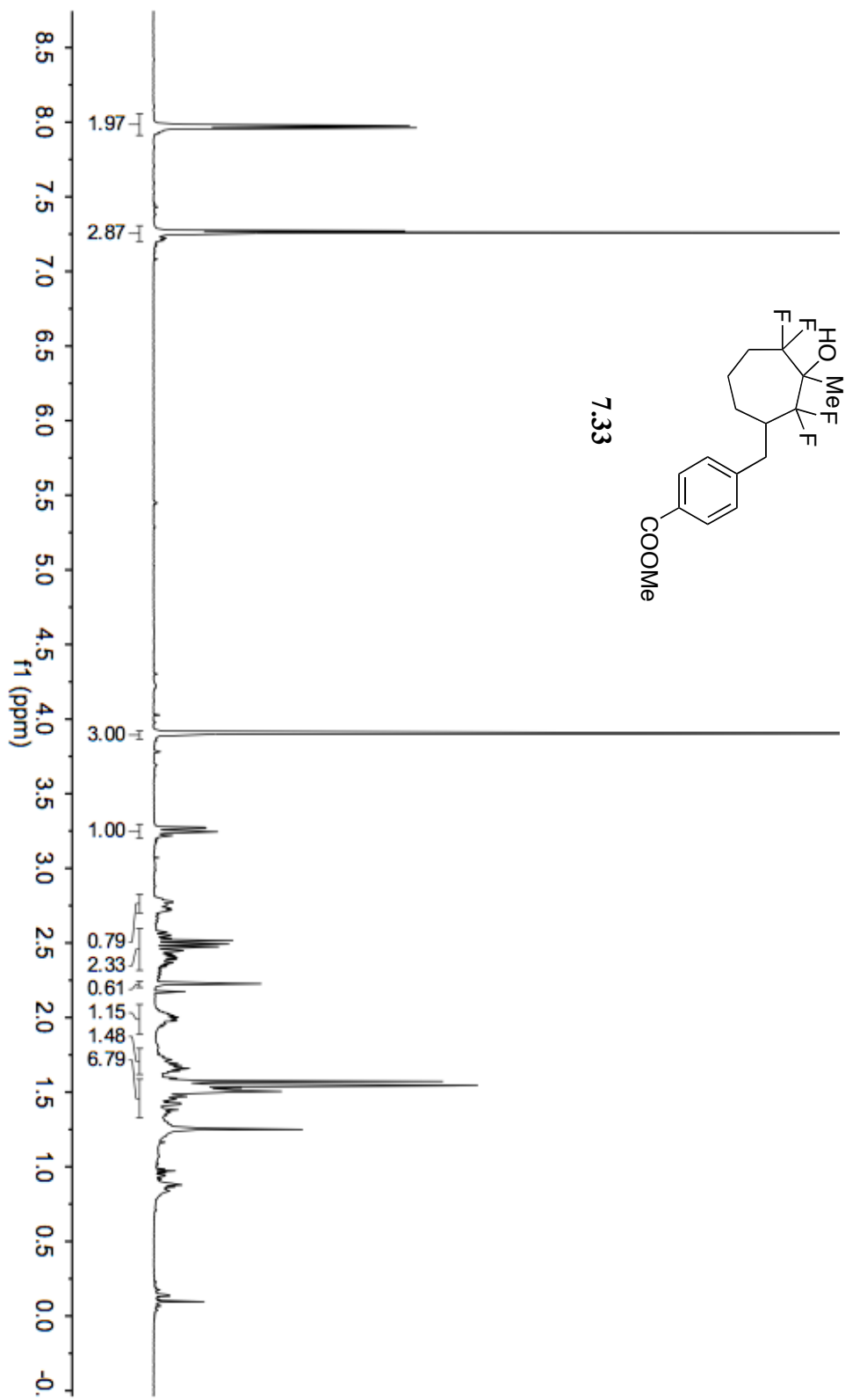
7.32

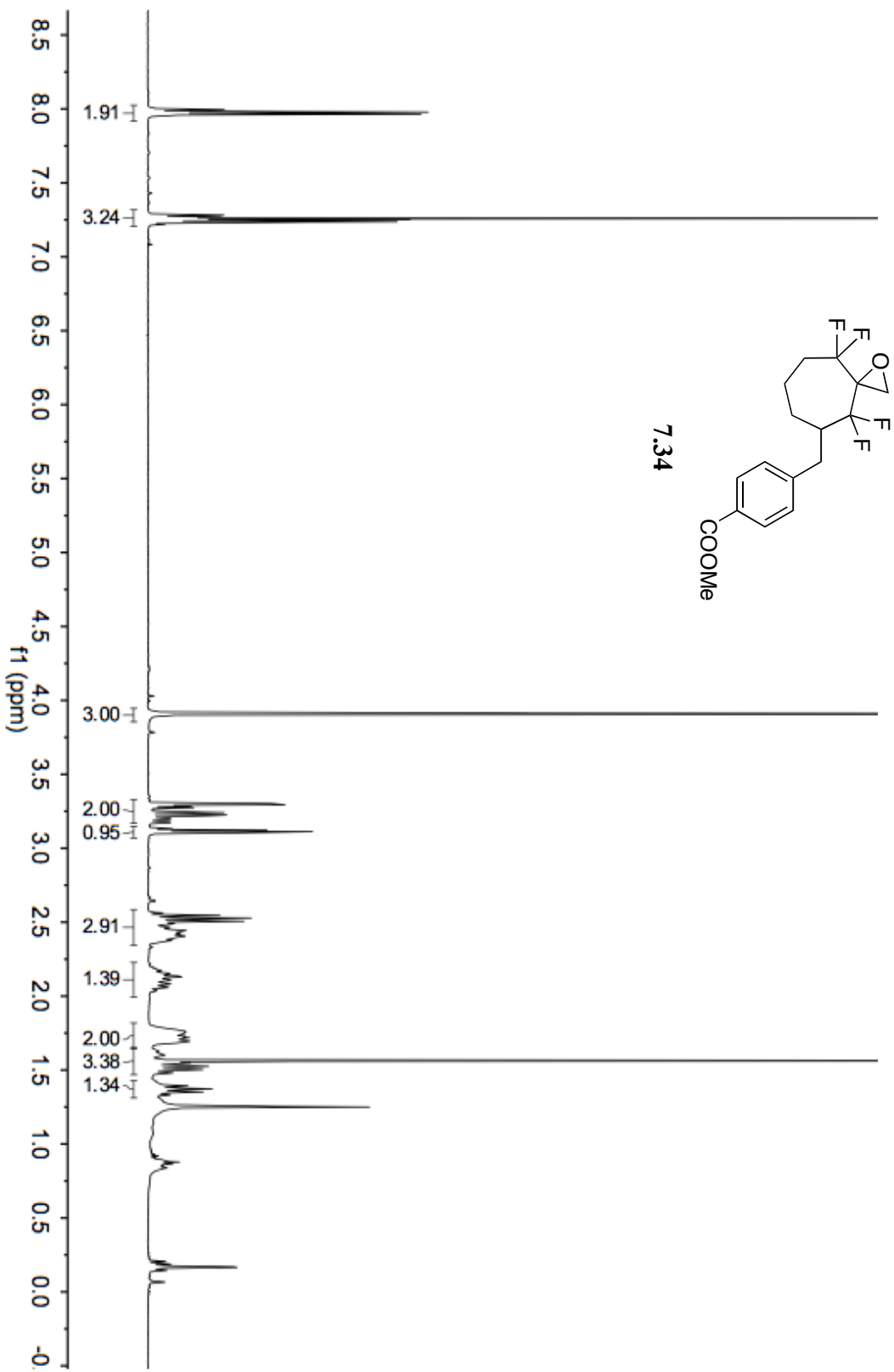


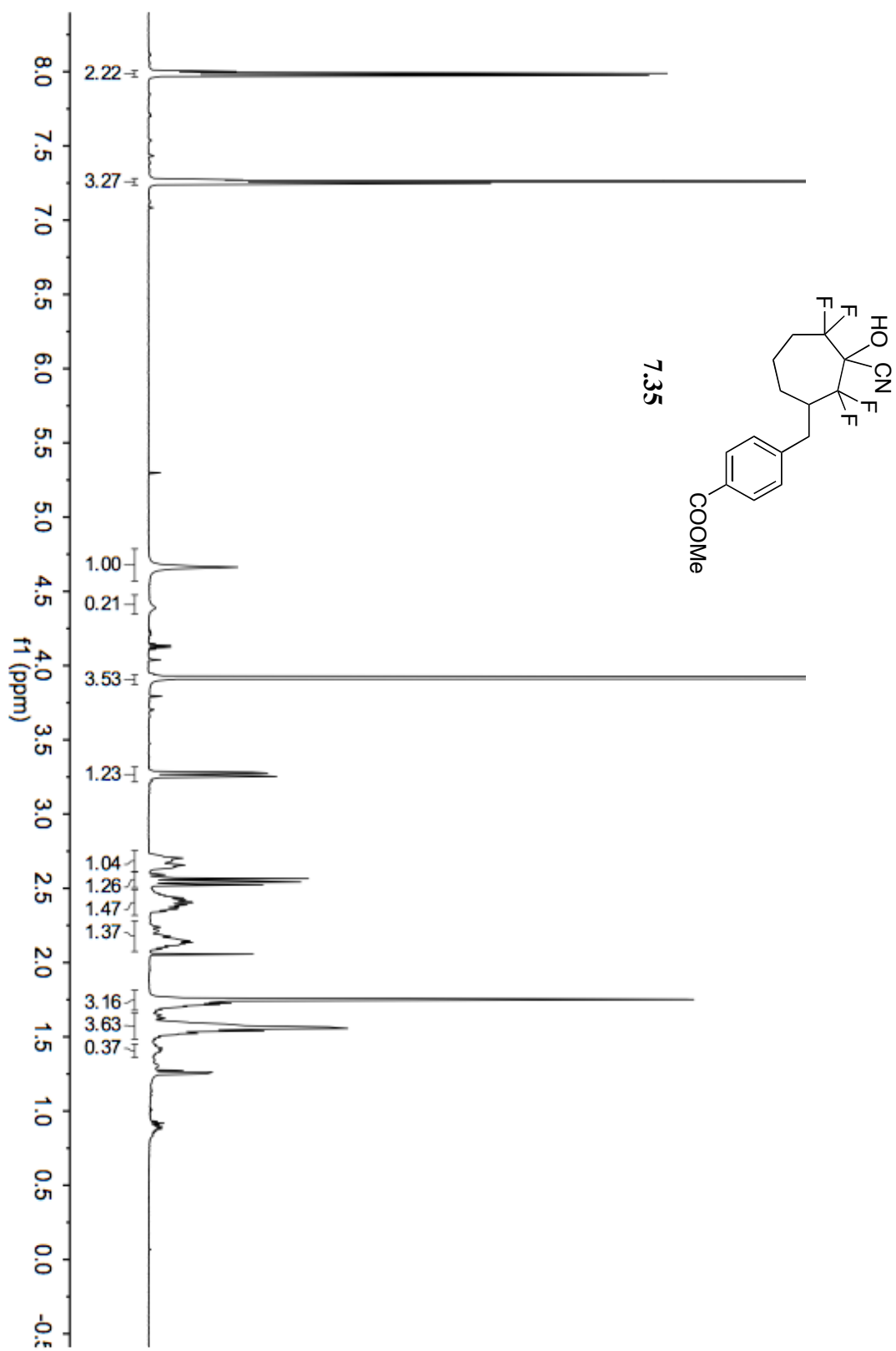


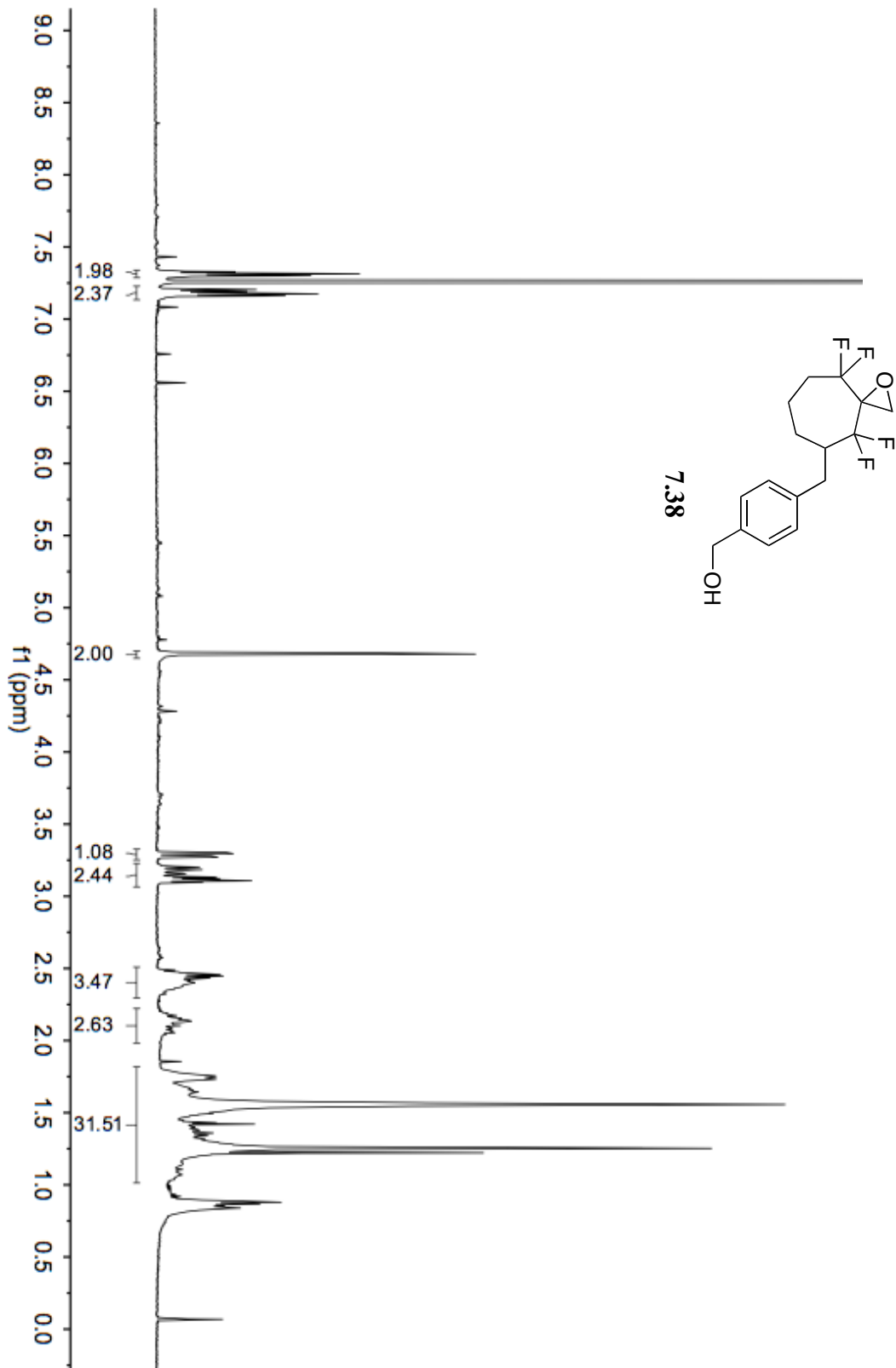


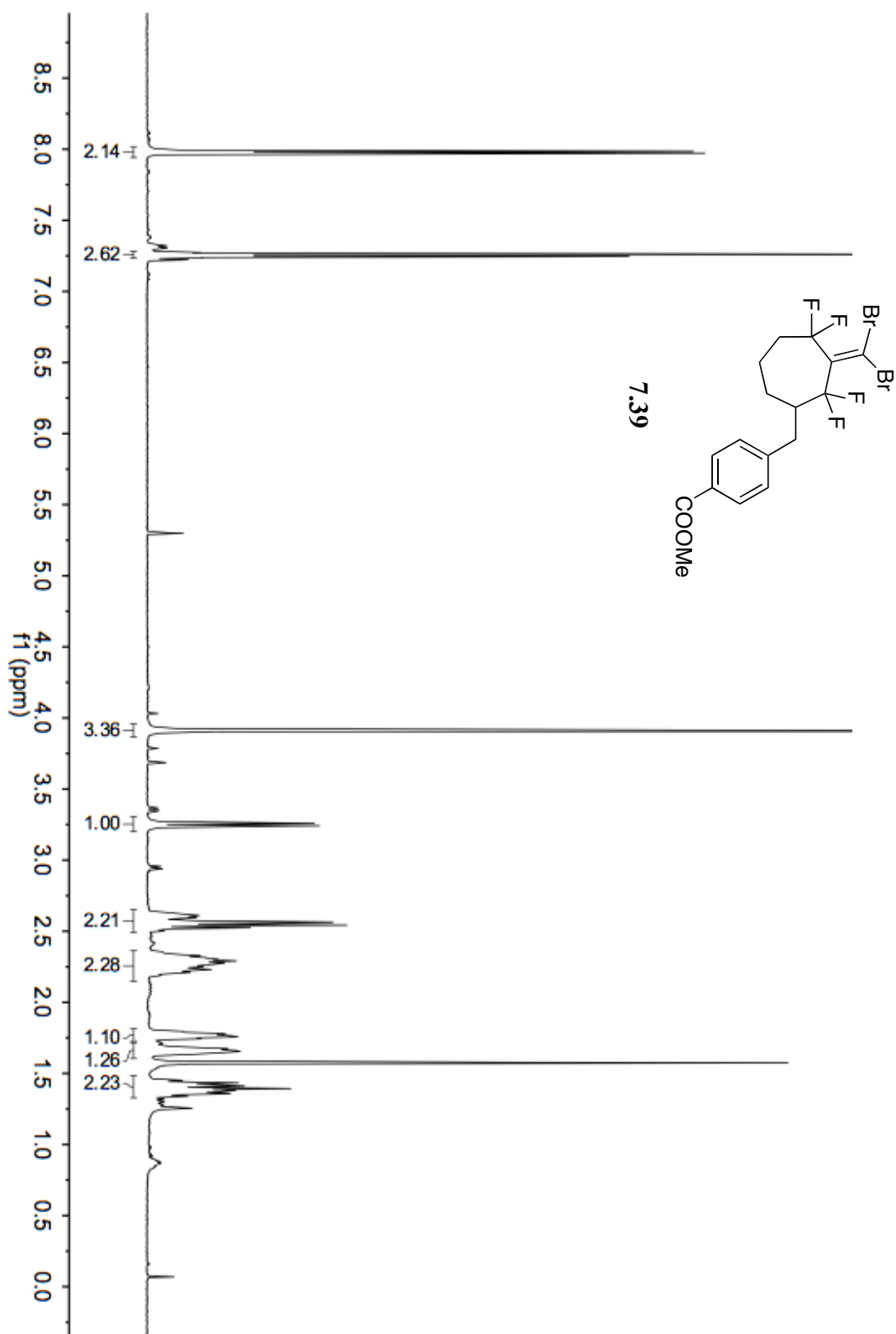


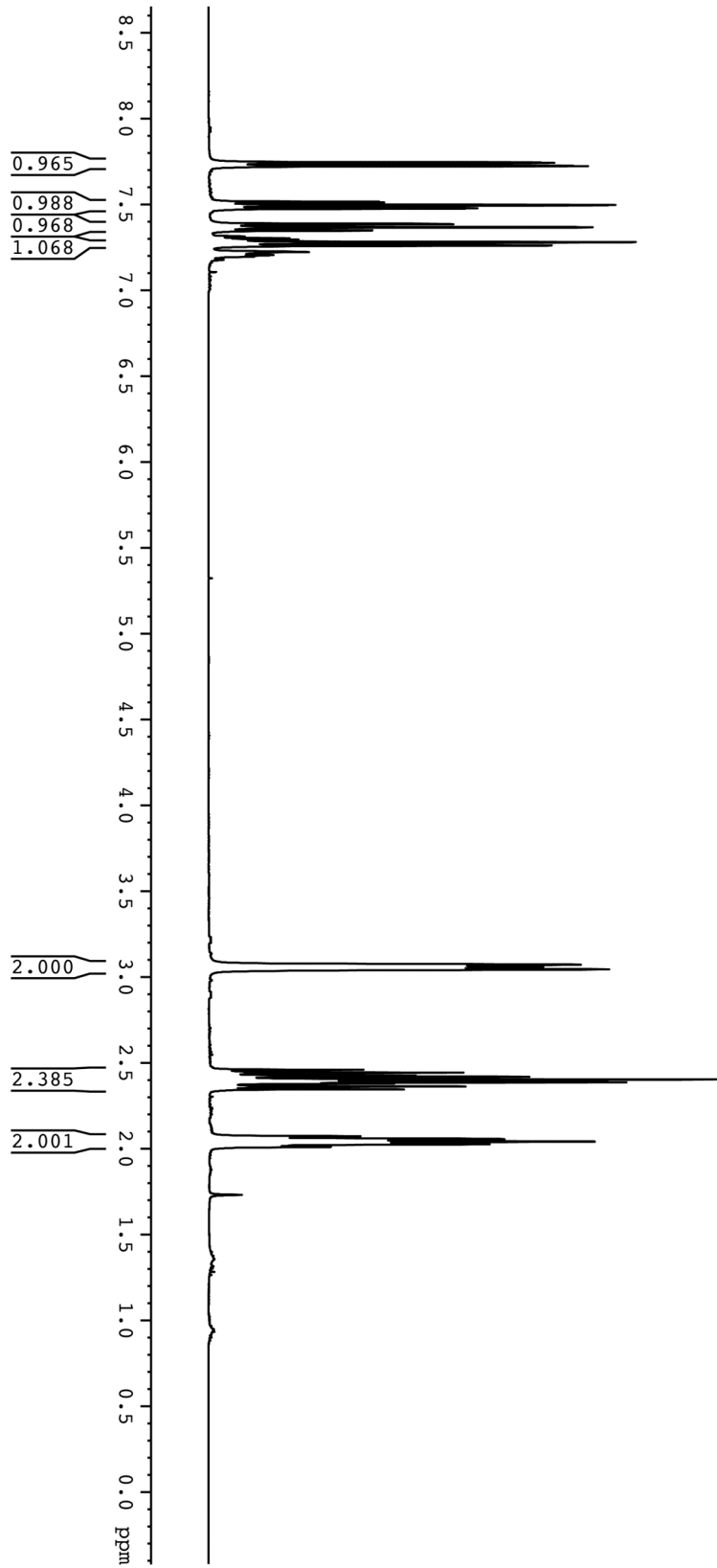




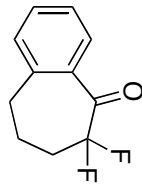


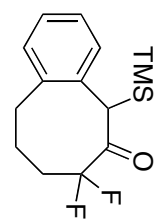




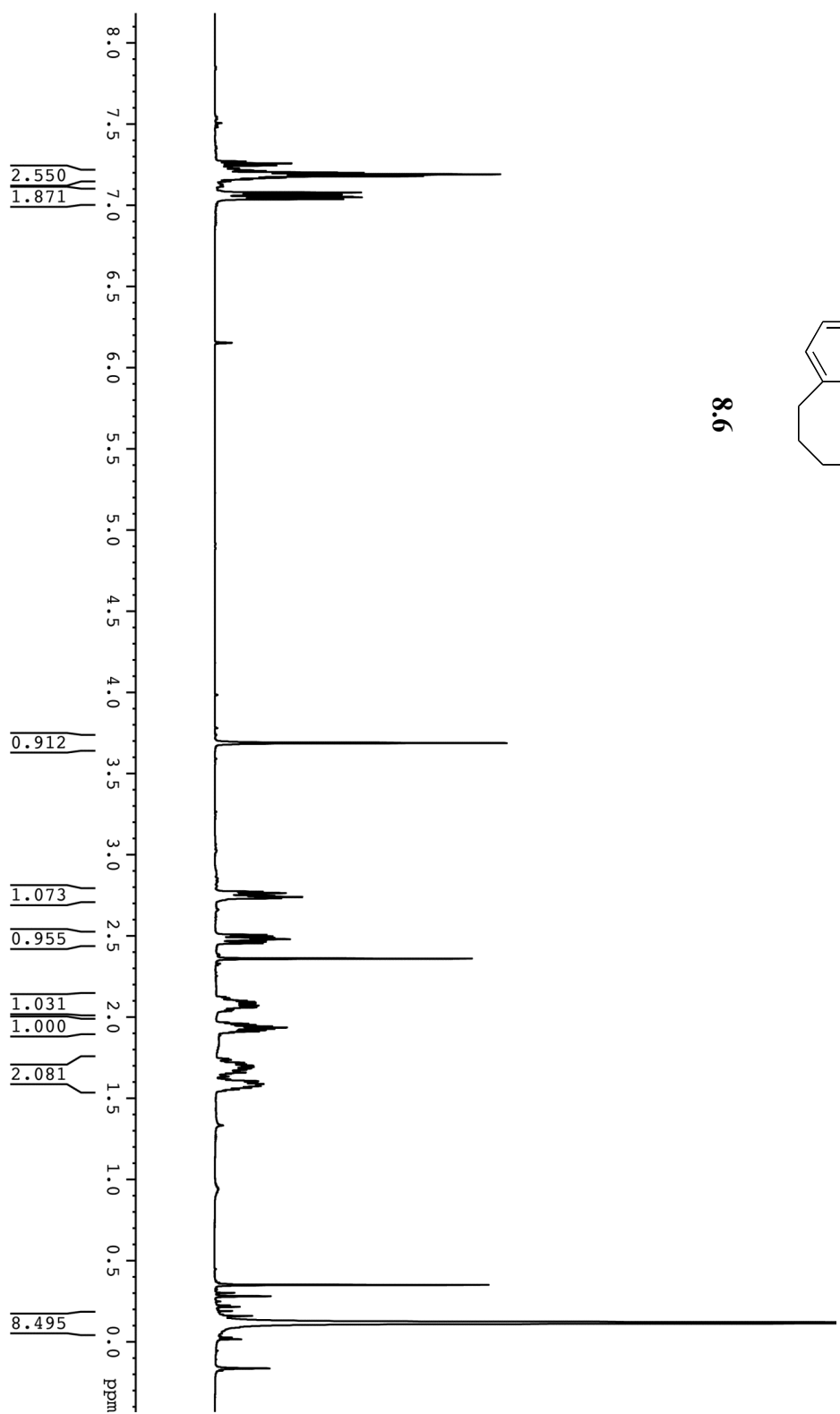


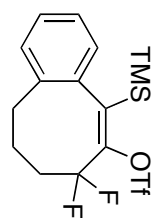
8.5



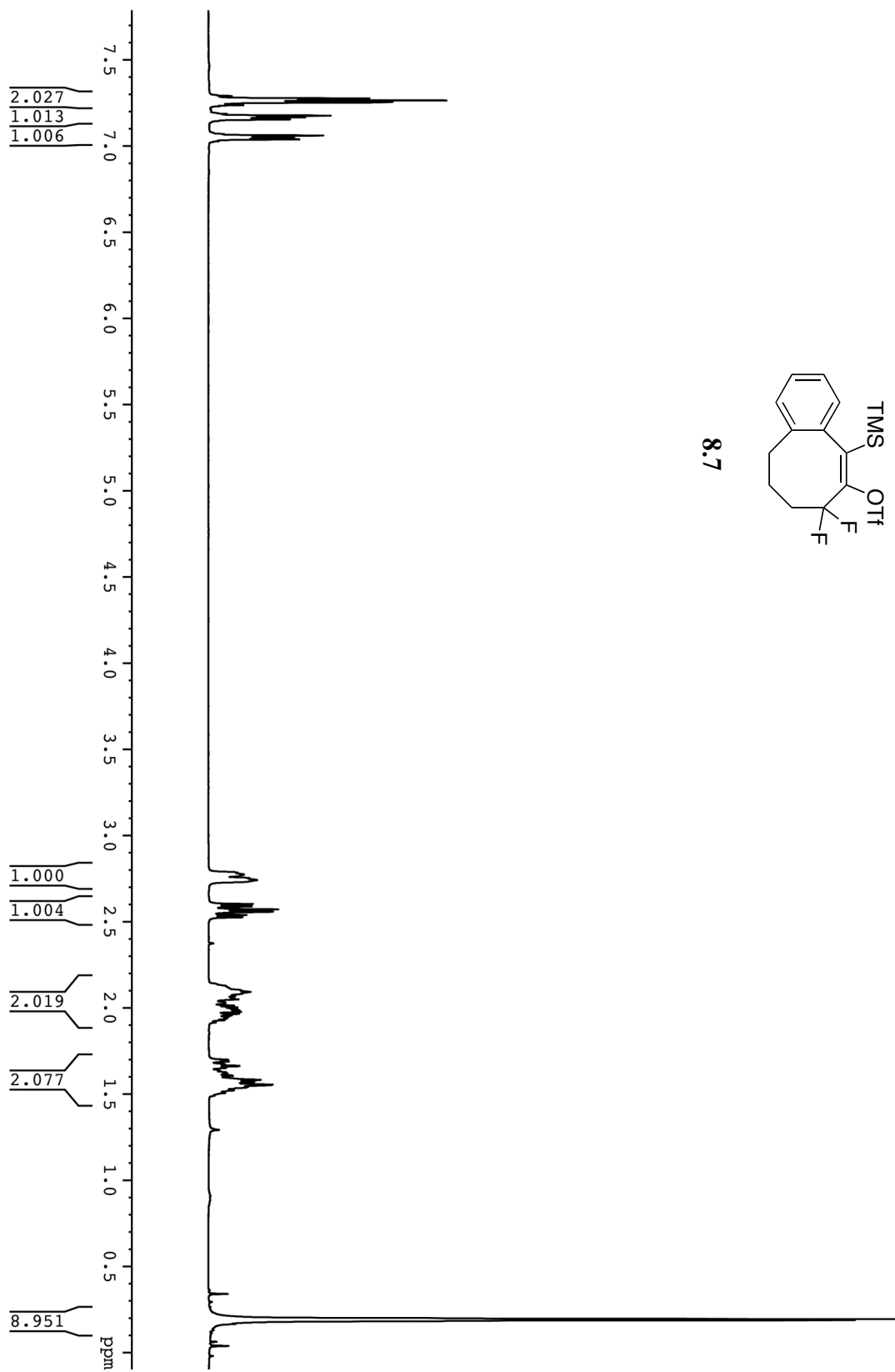


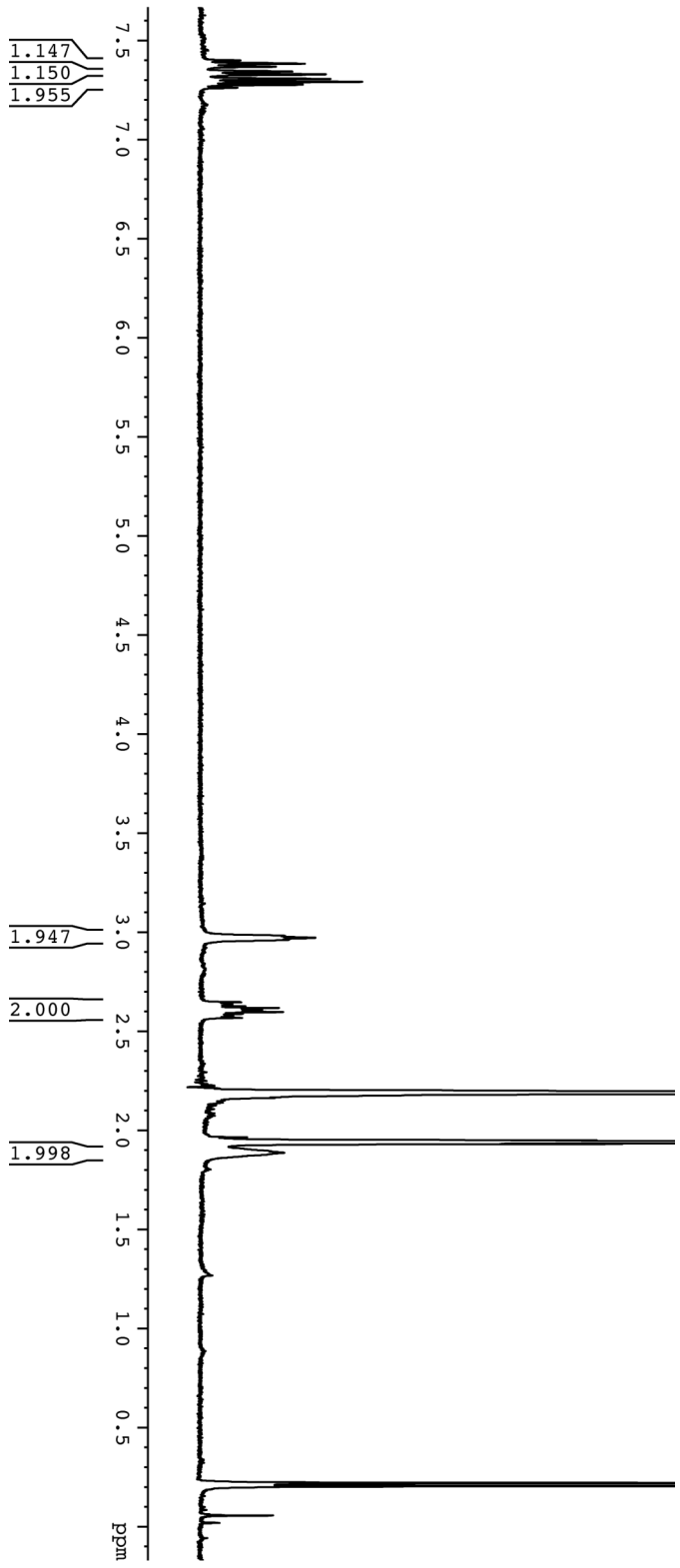
8.6



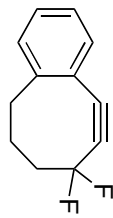


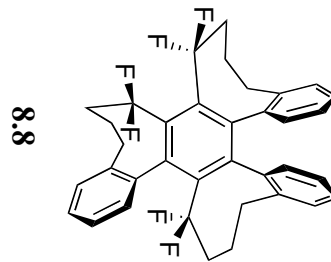
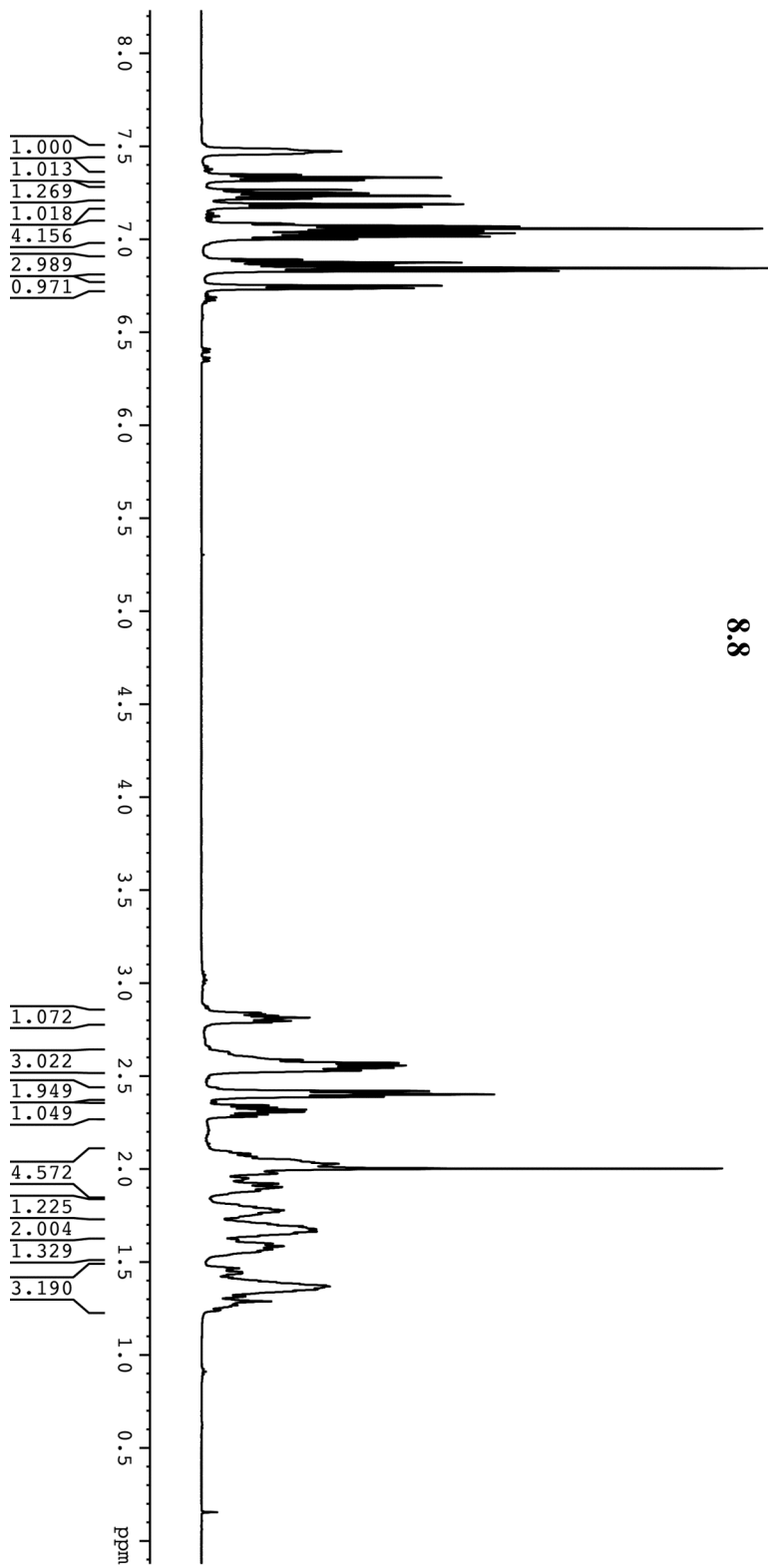
8.7

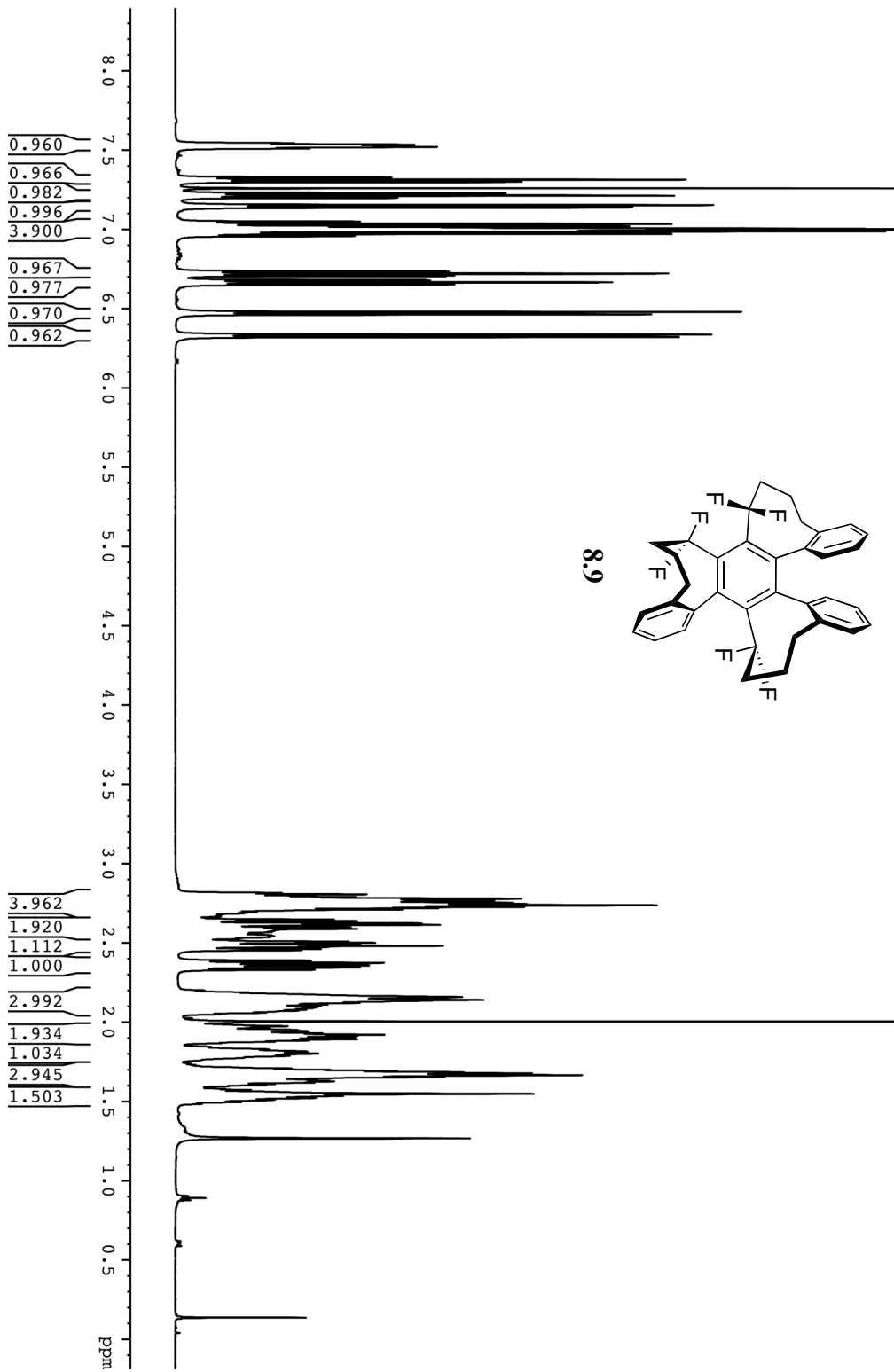


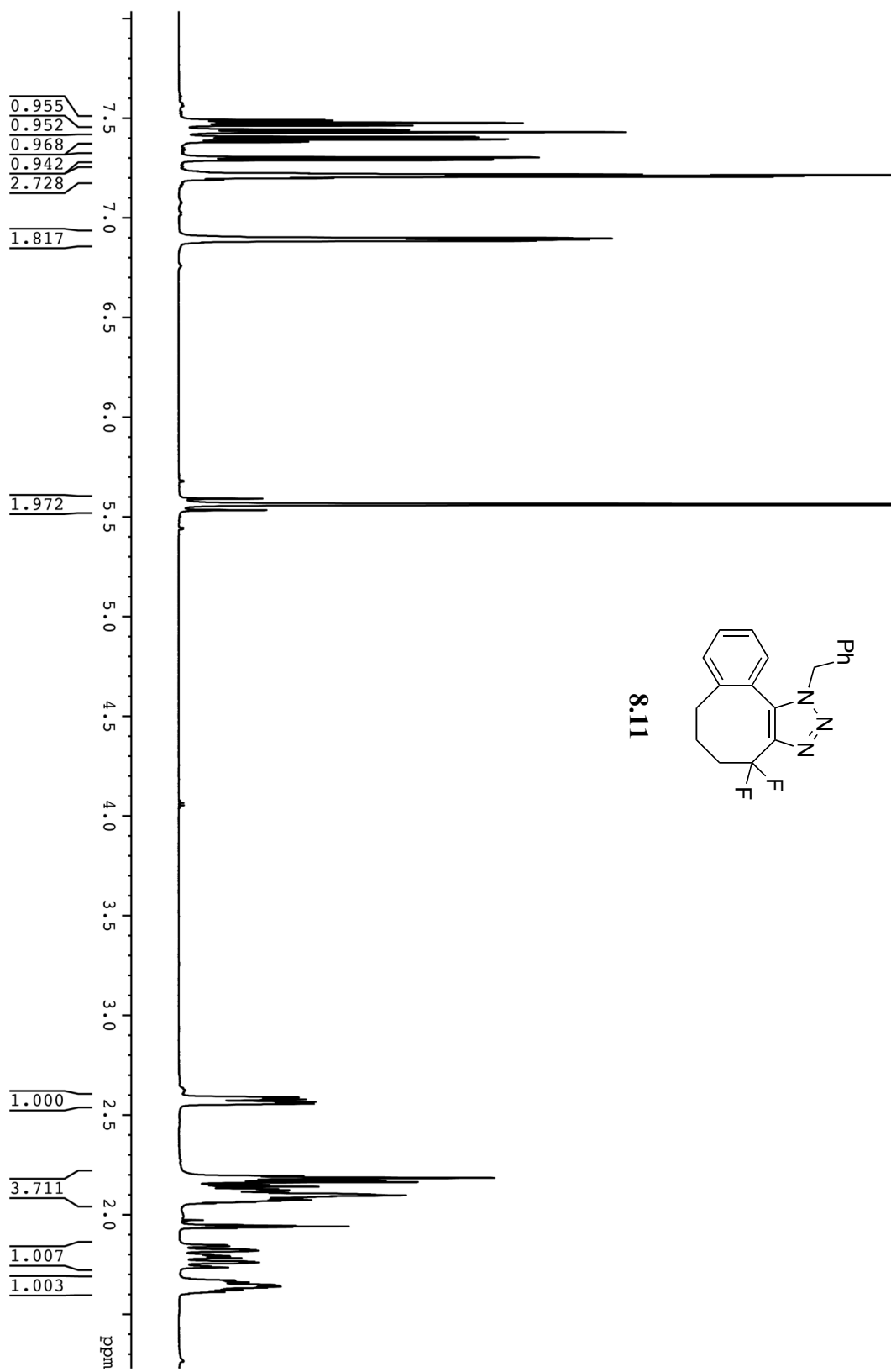


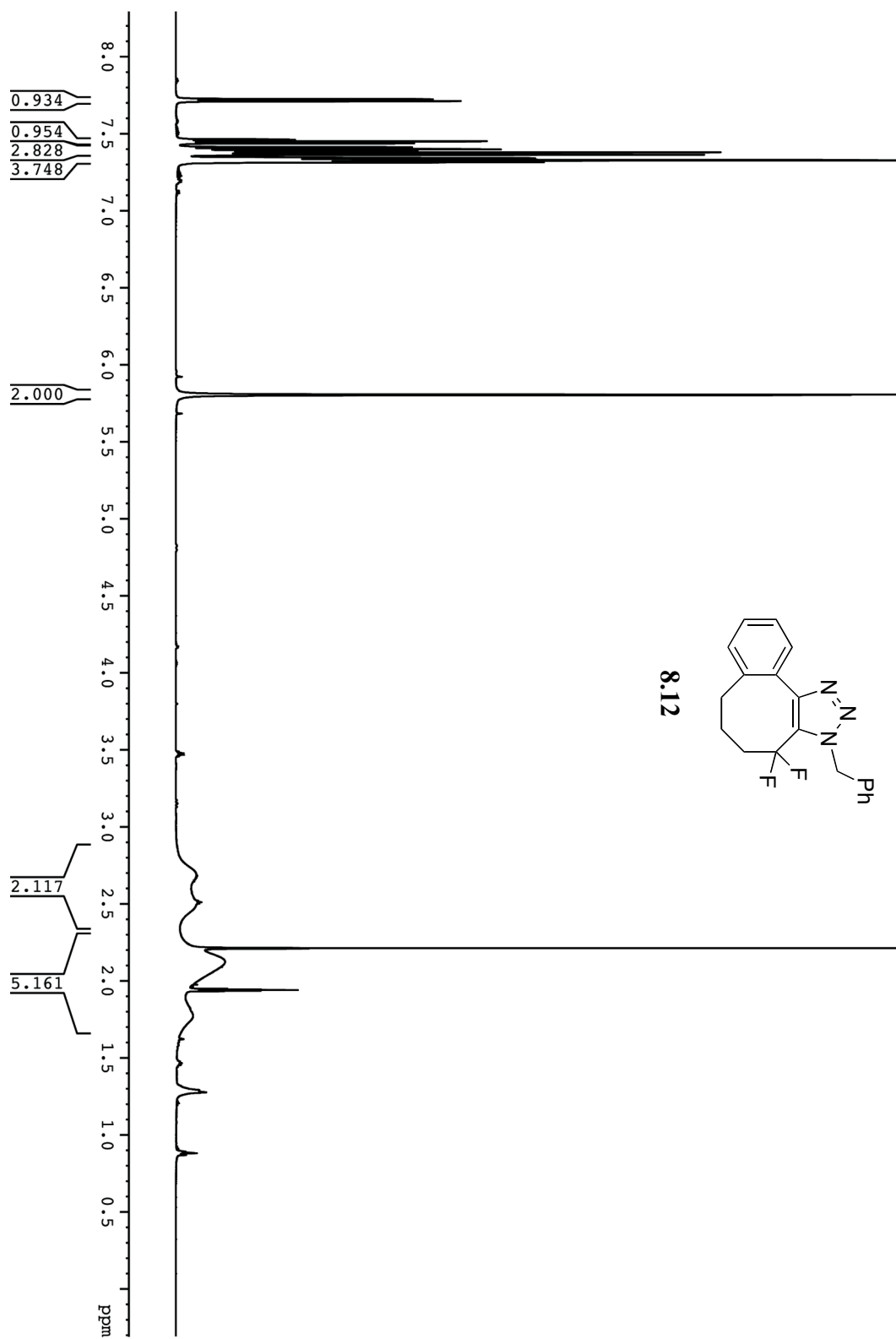
8.3

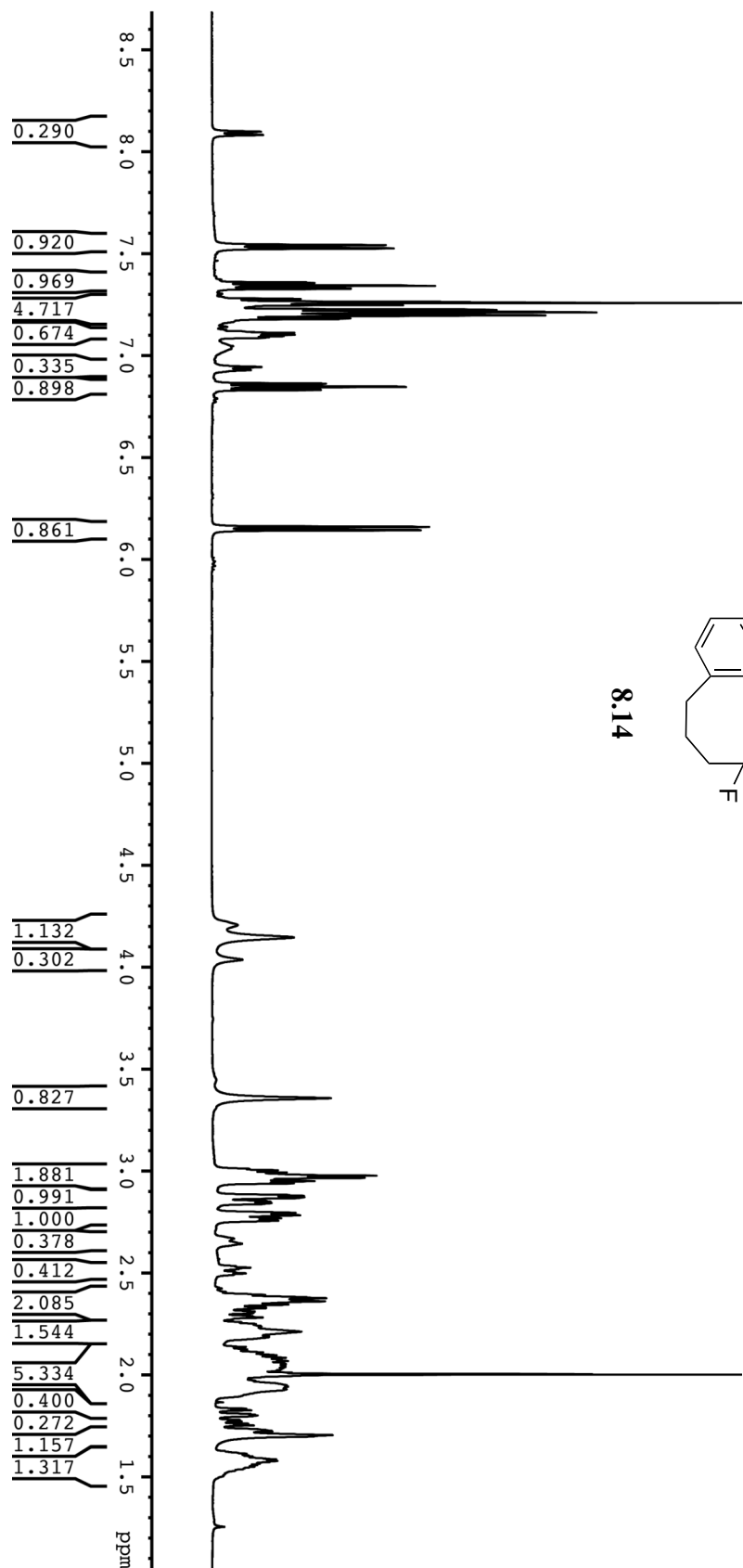


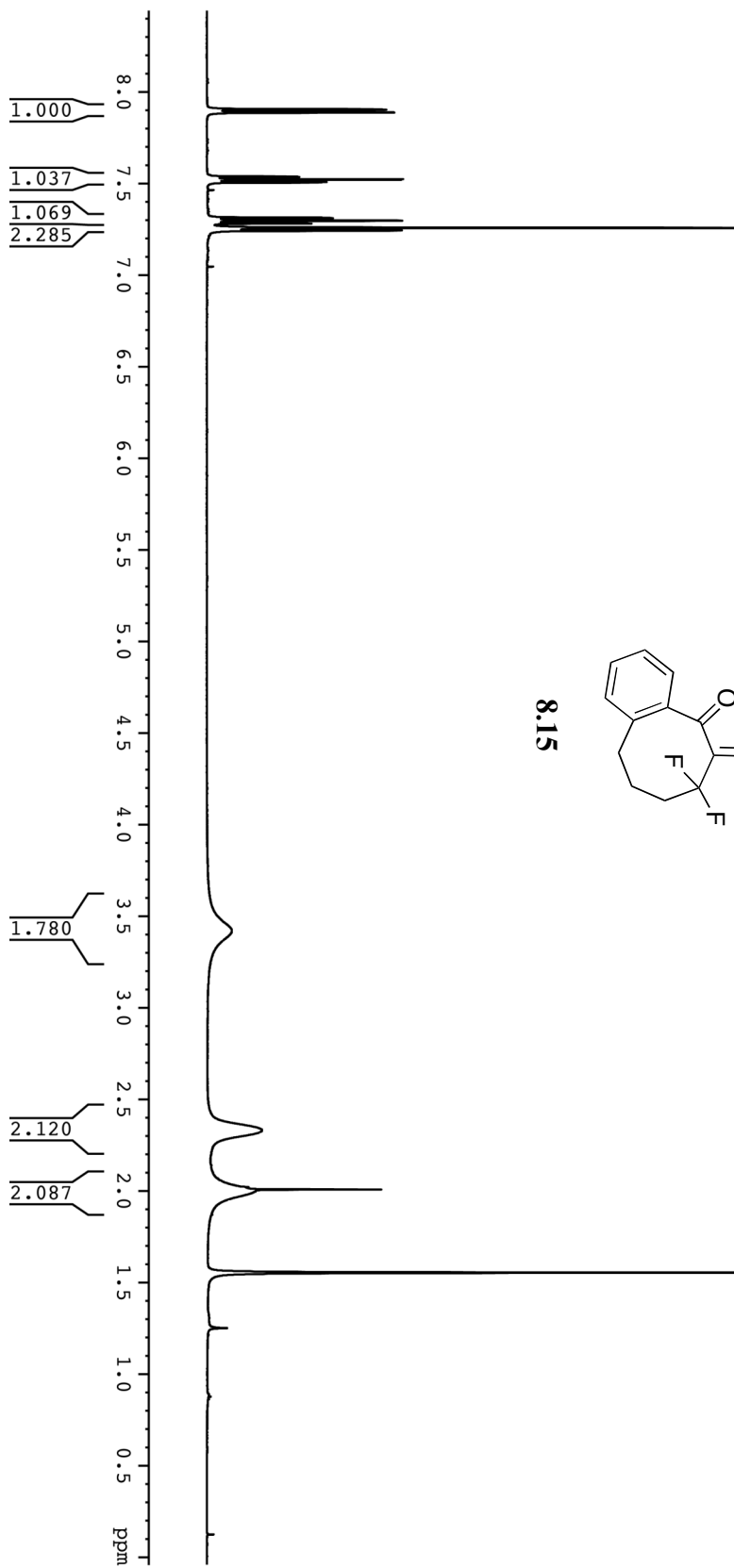


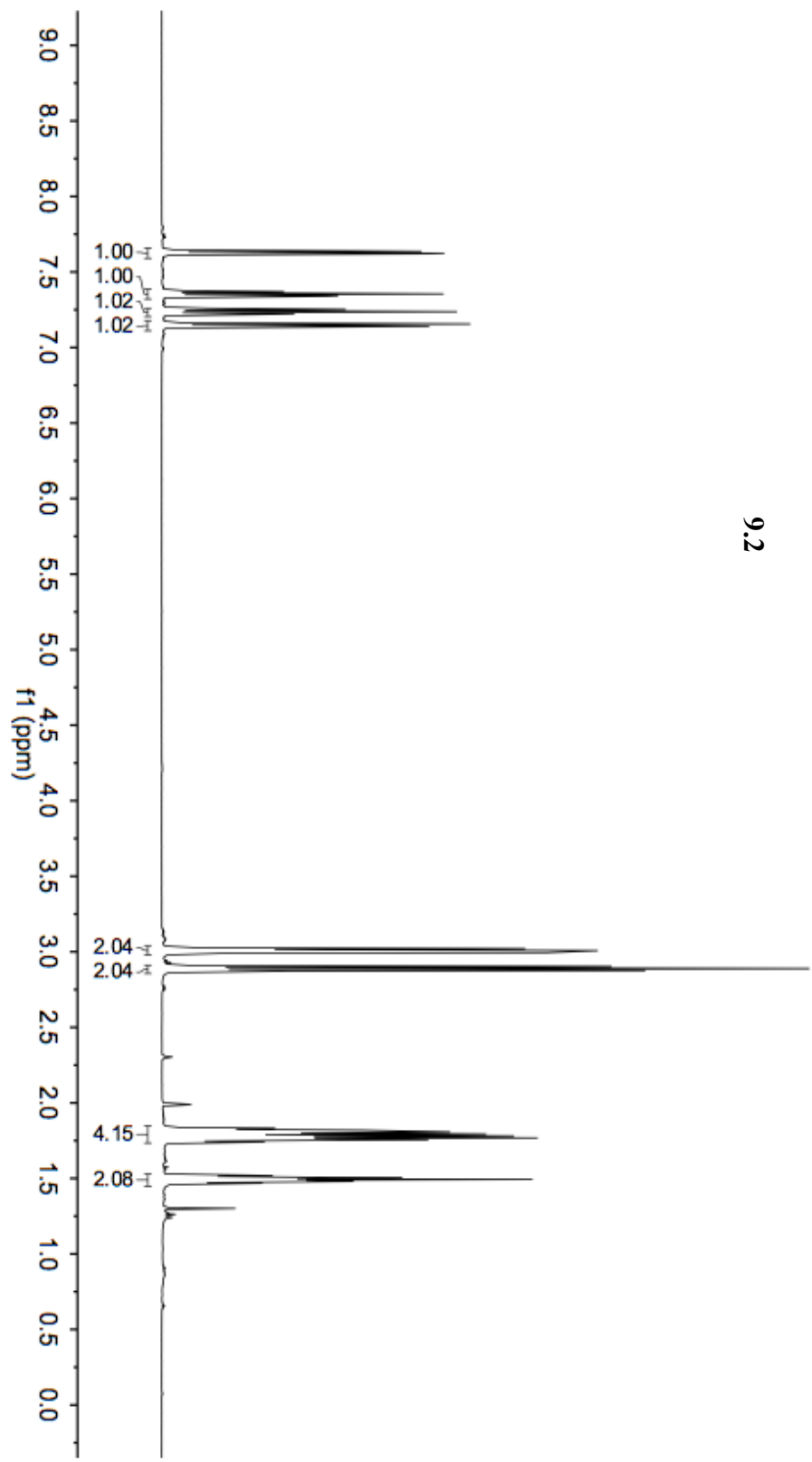
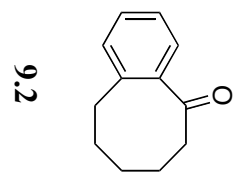


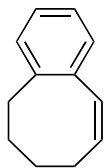




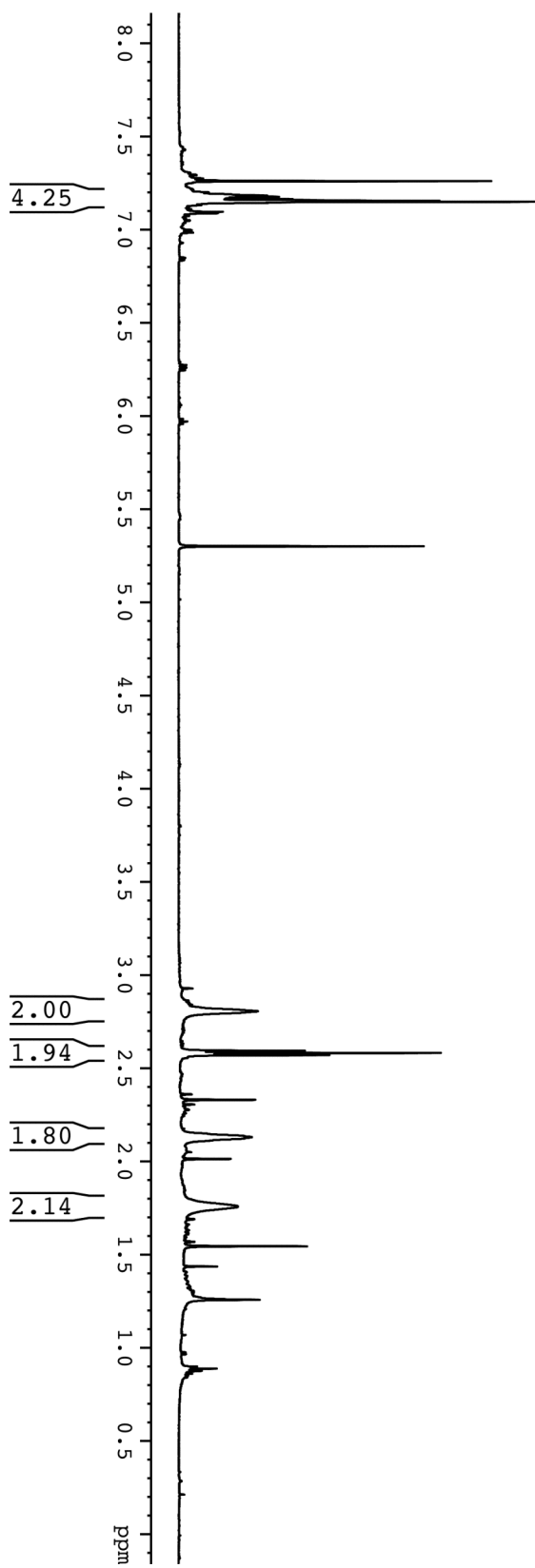


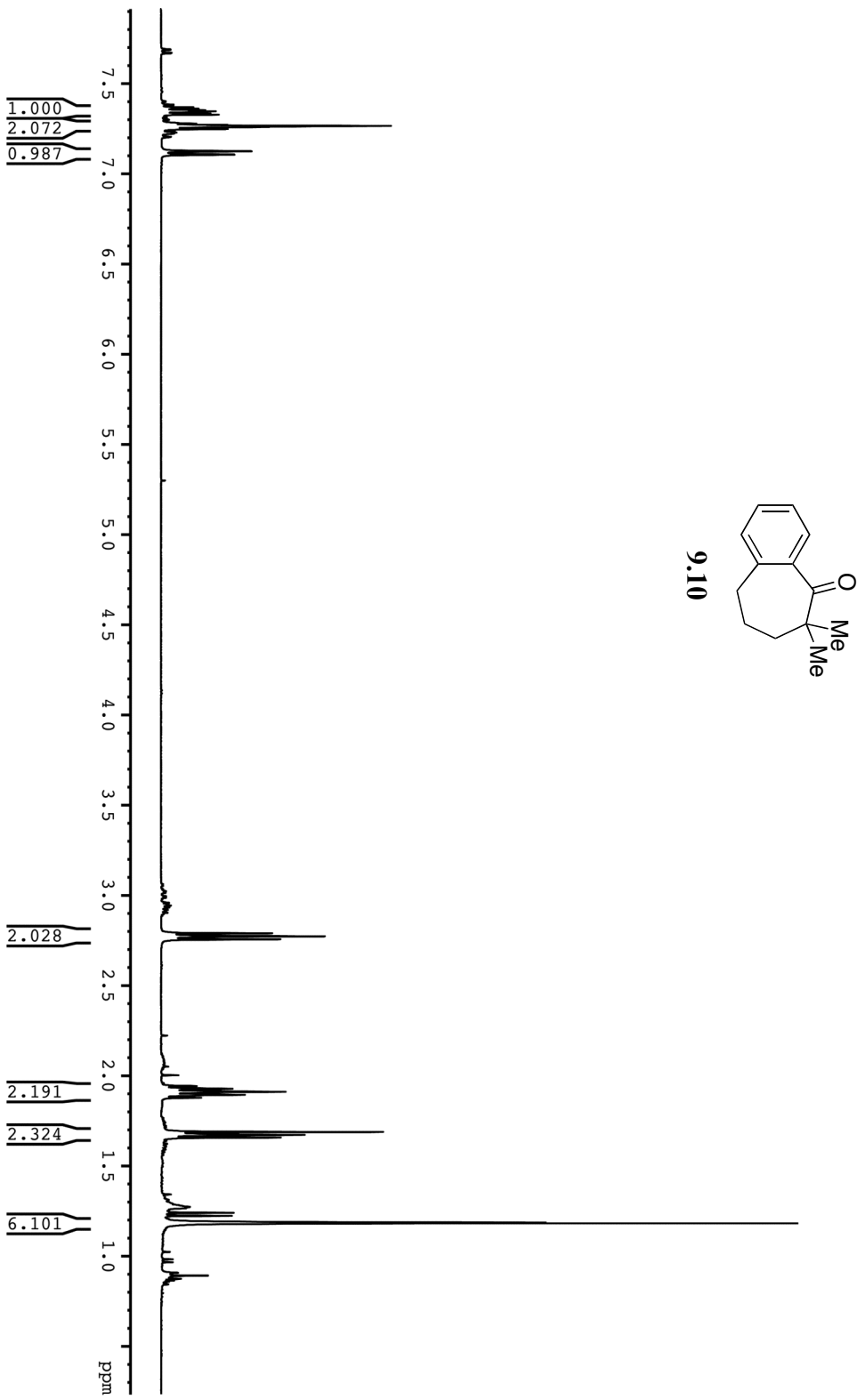


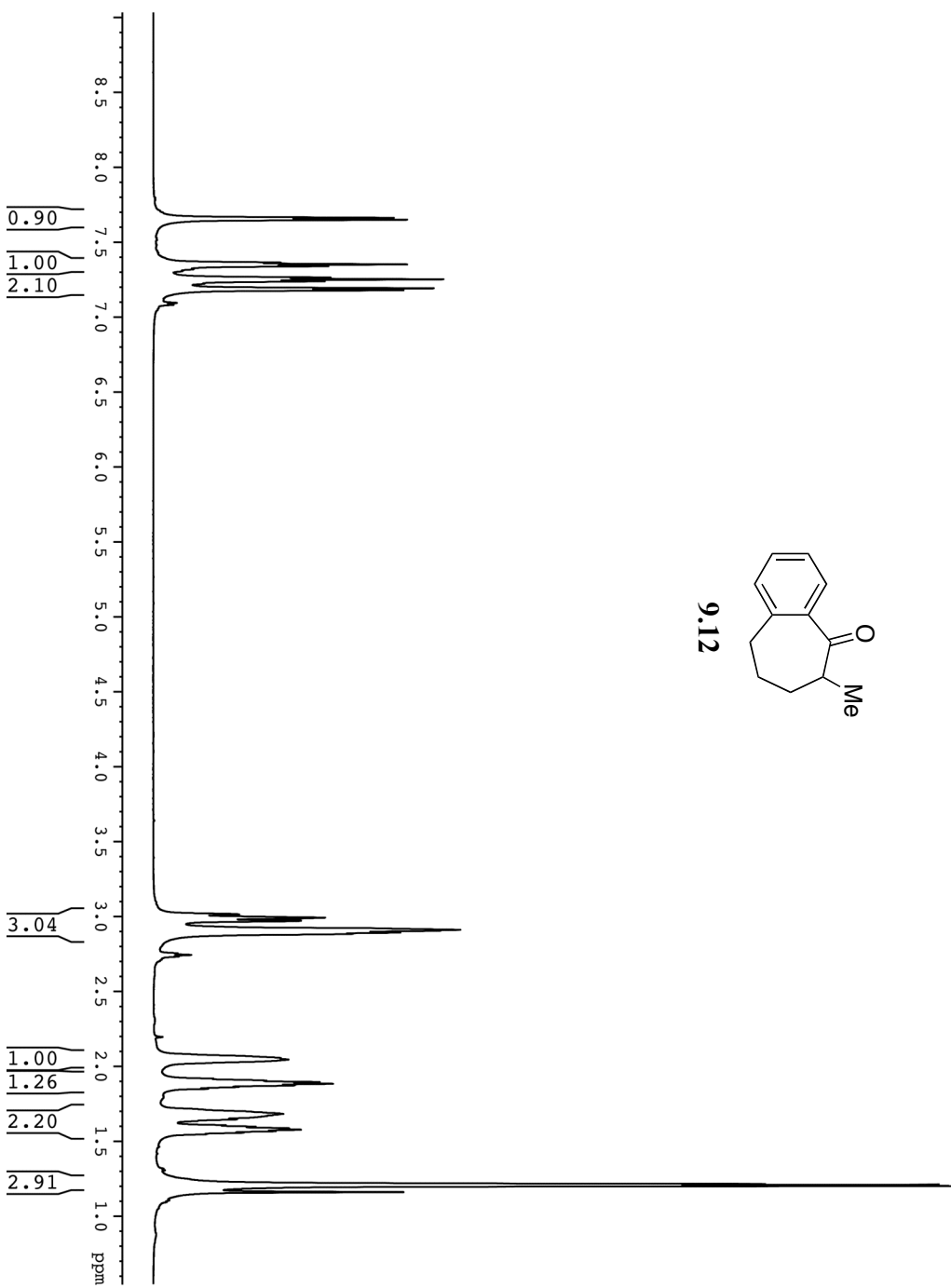
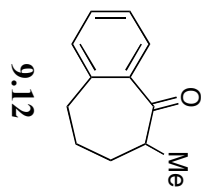


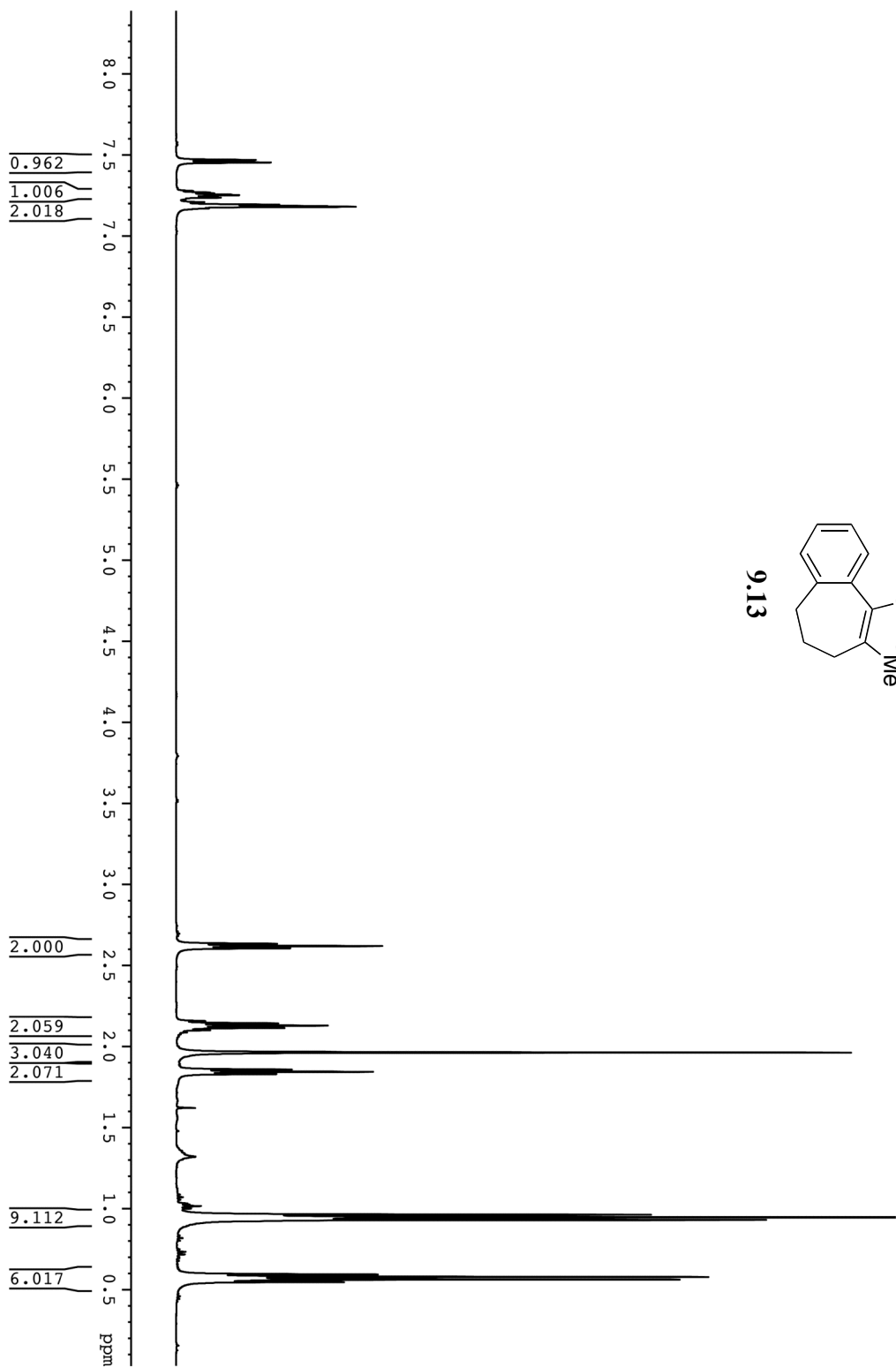
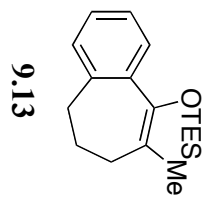


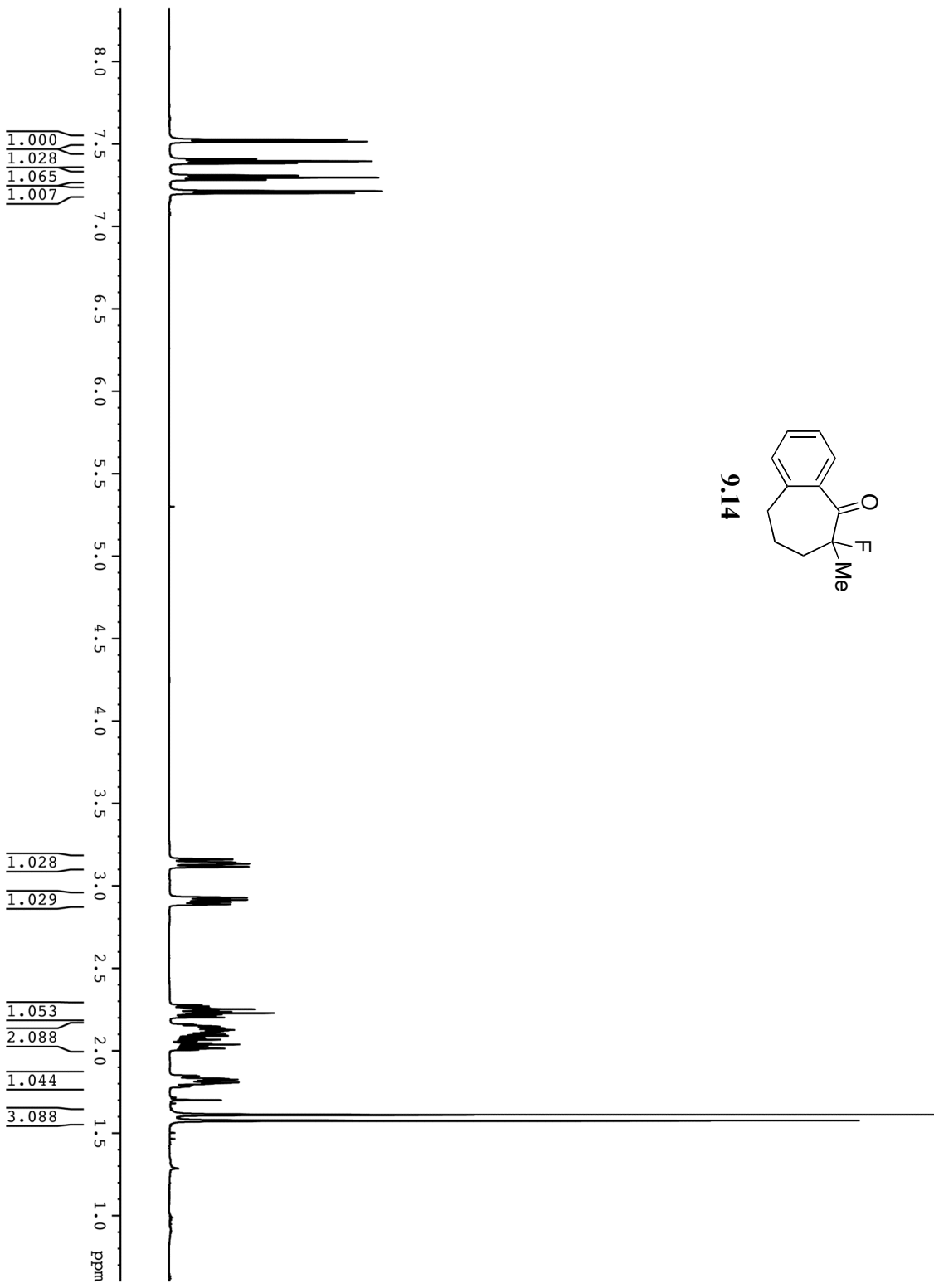
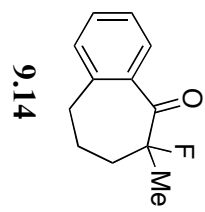
9.3

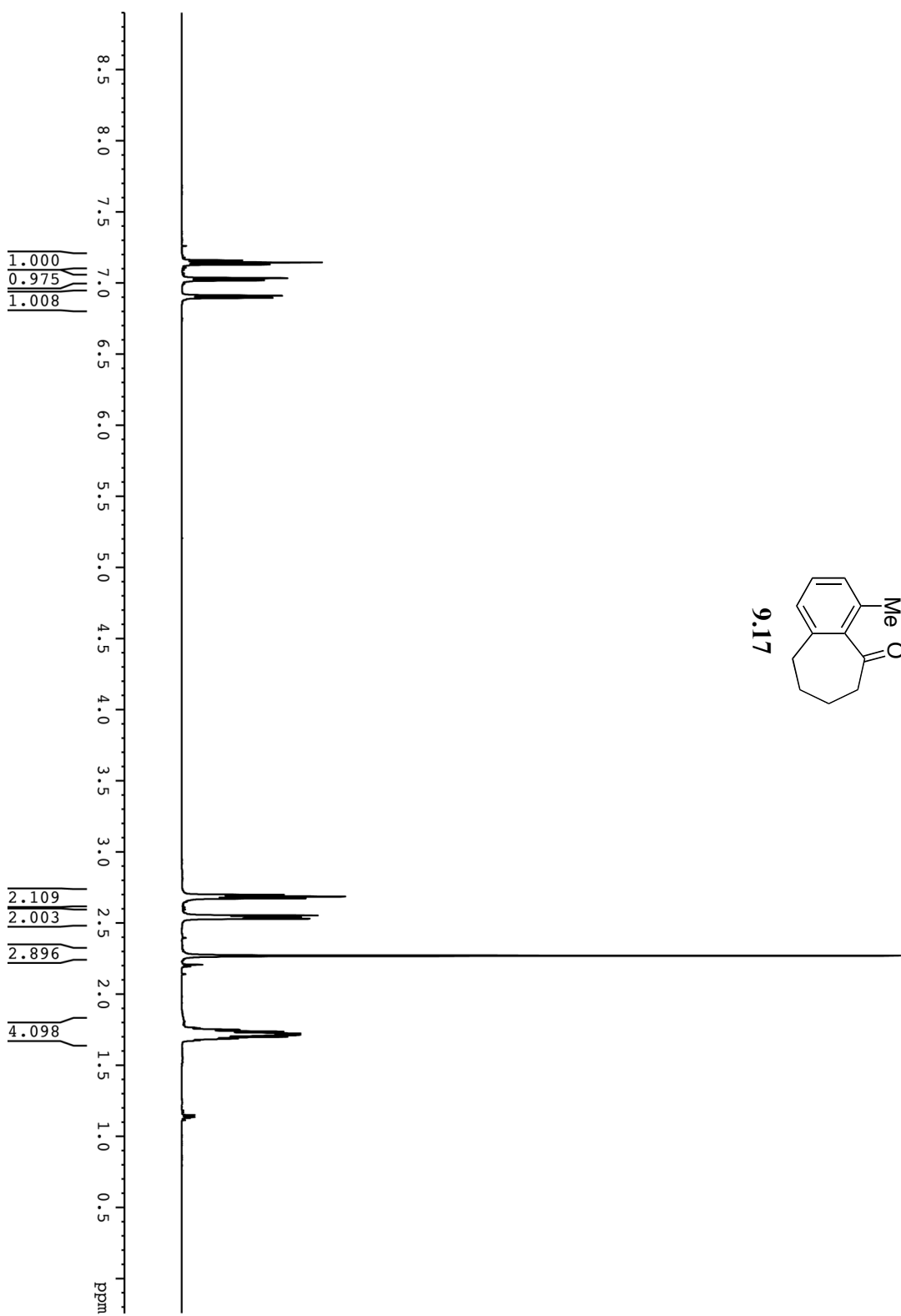
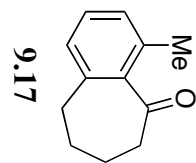


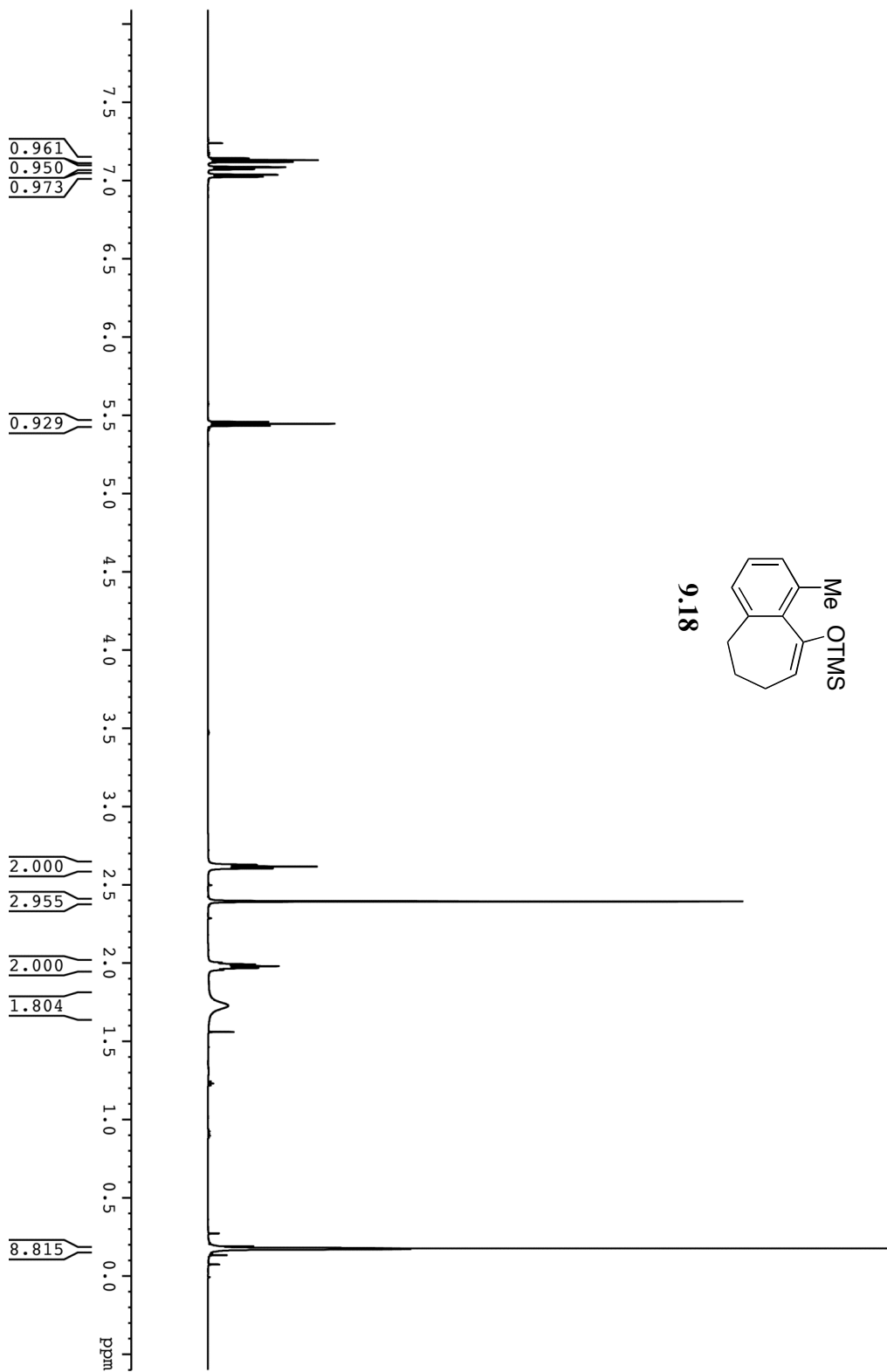


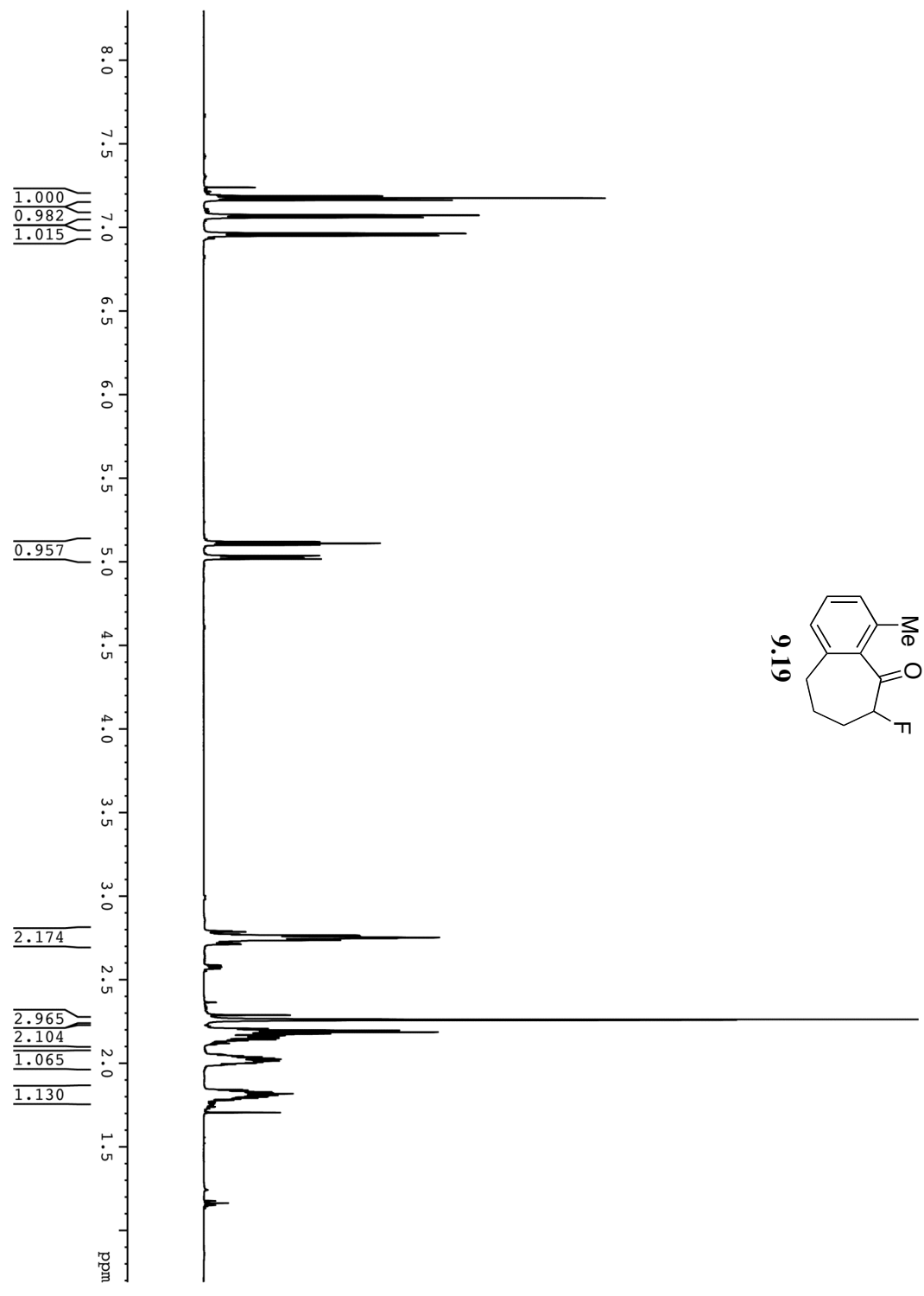


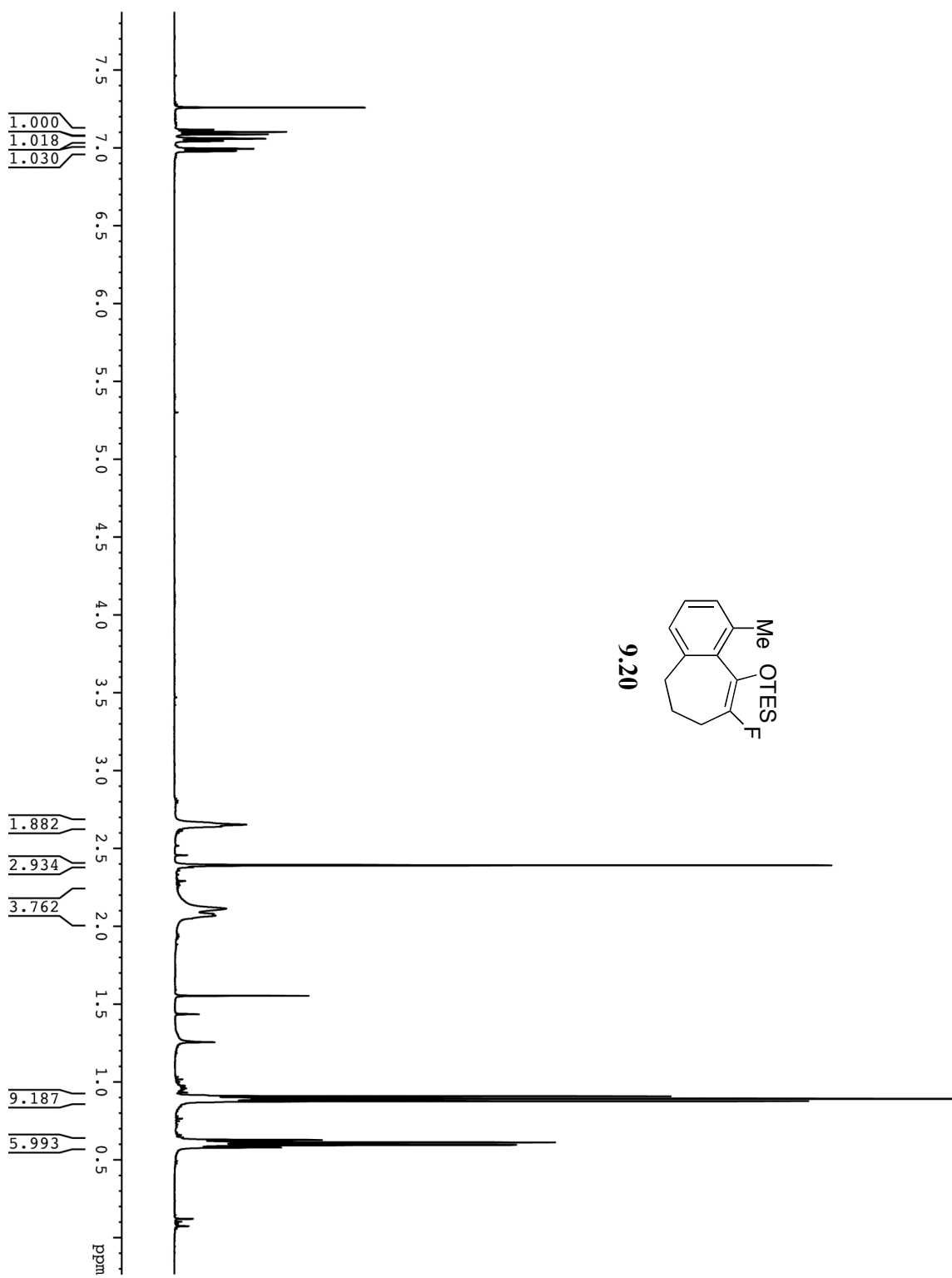


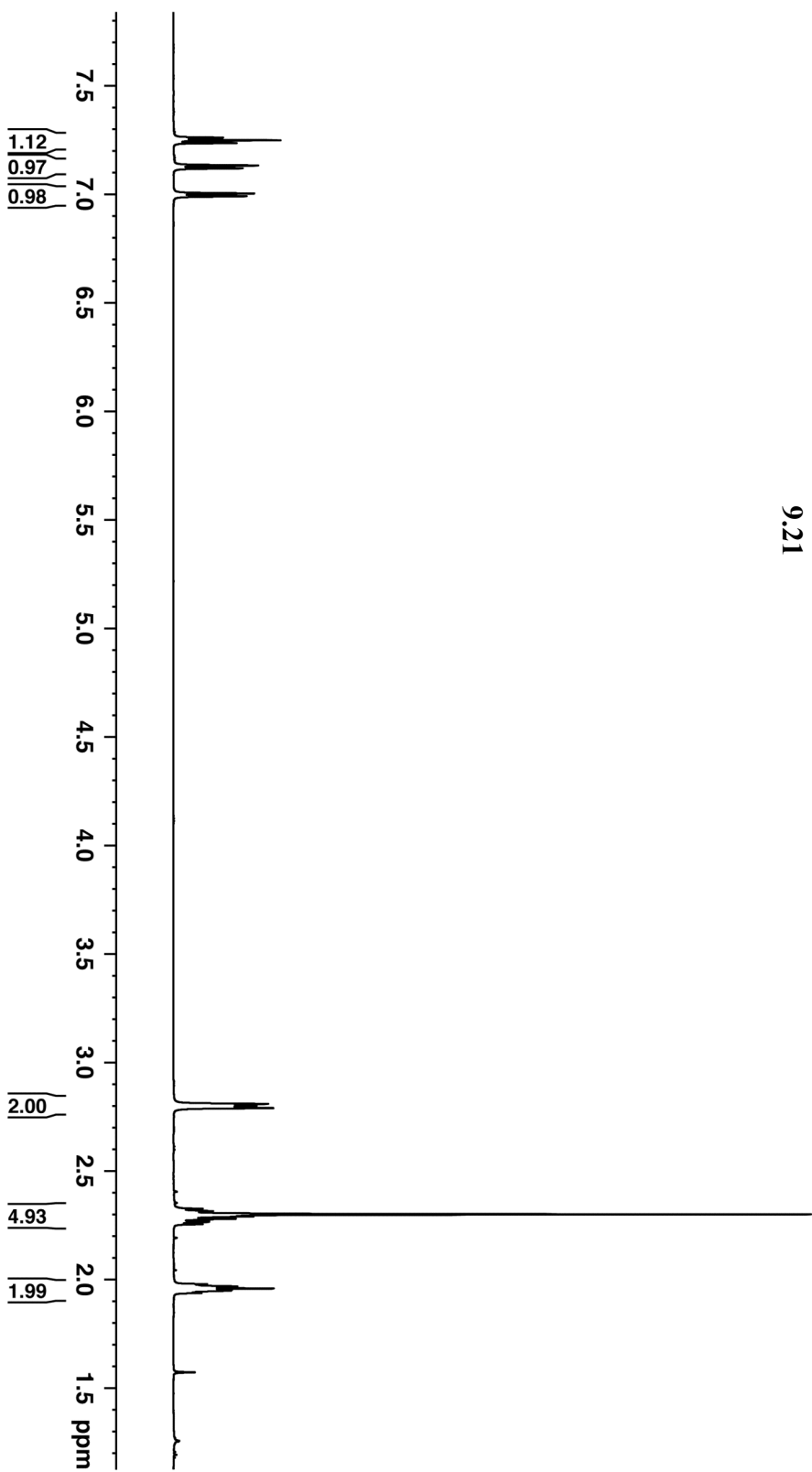
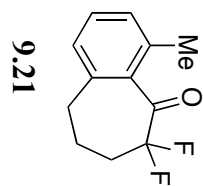


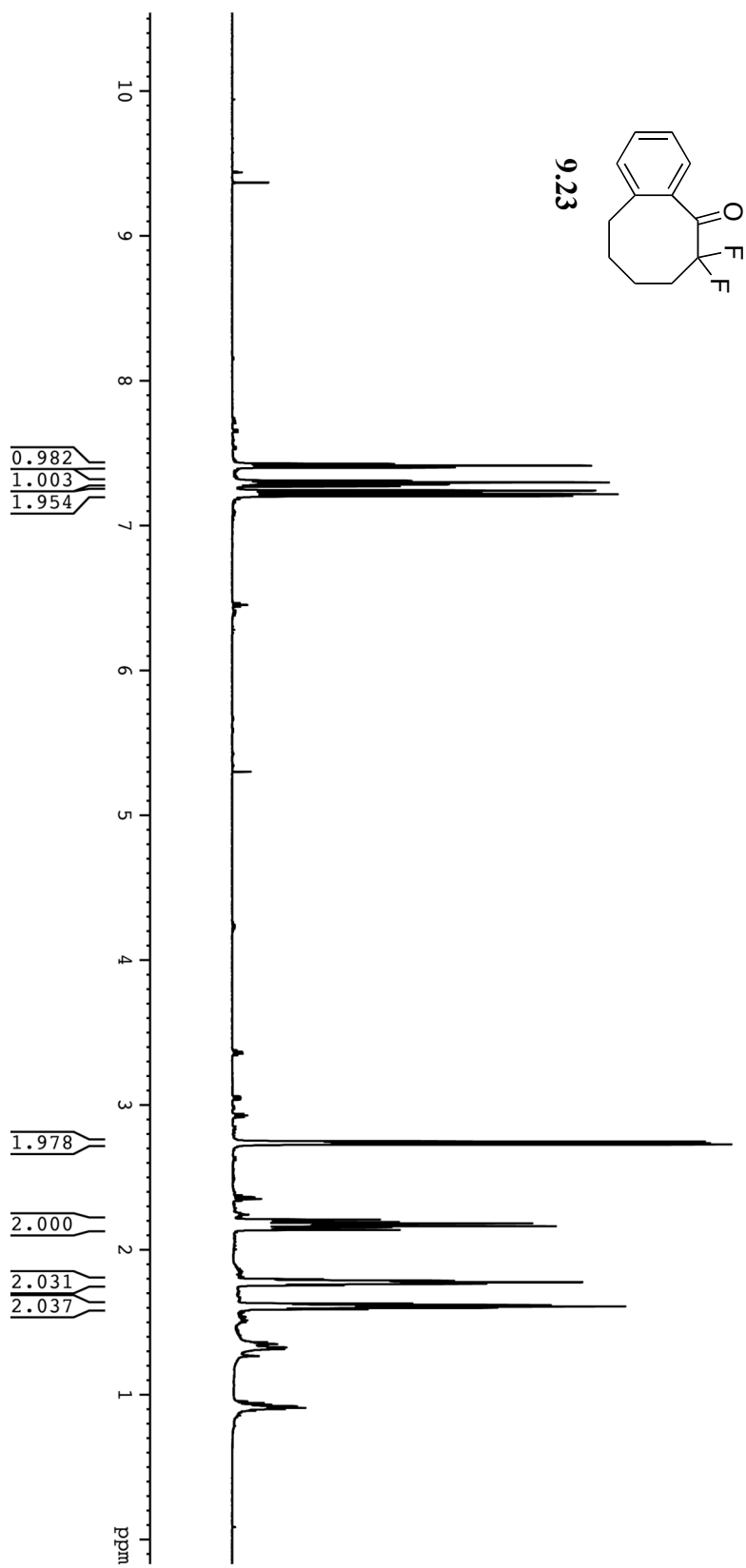


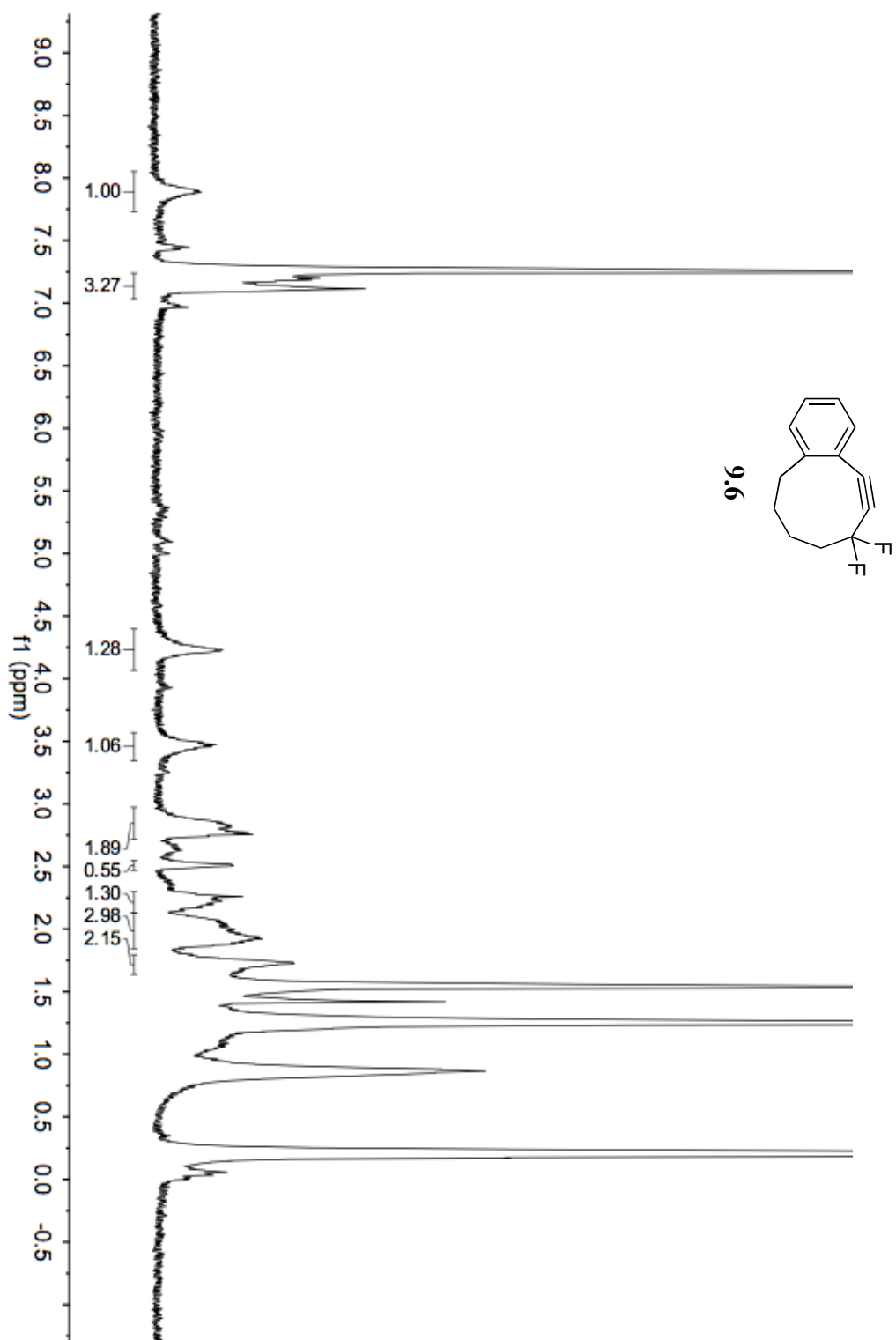


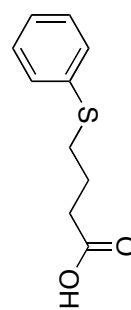




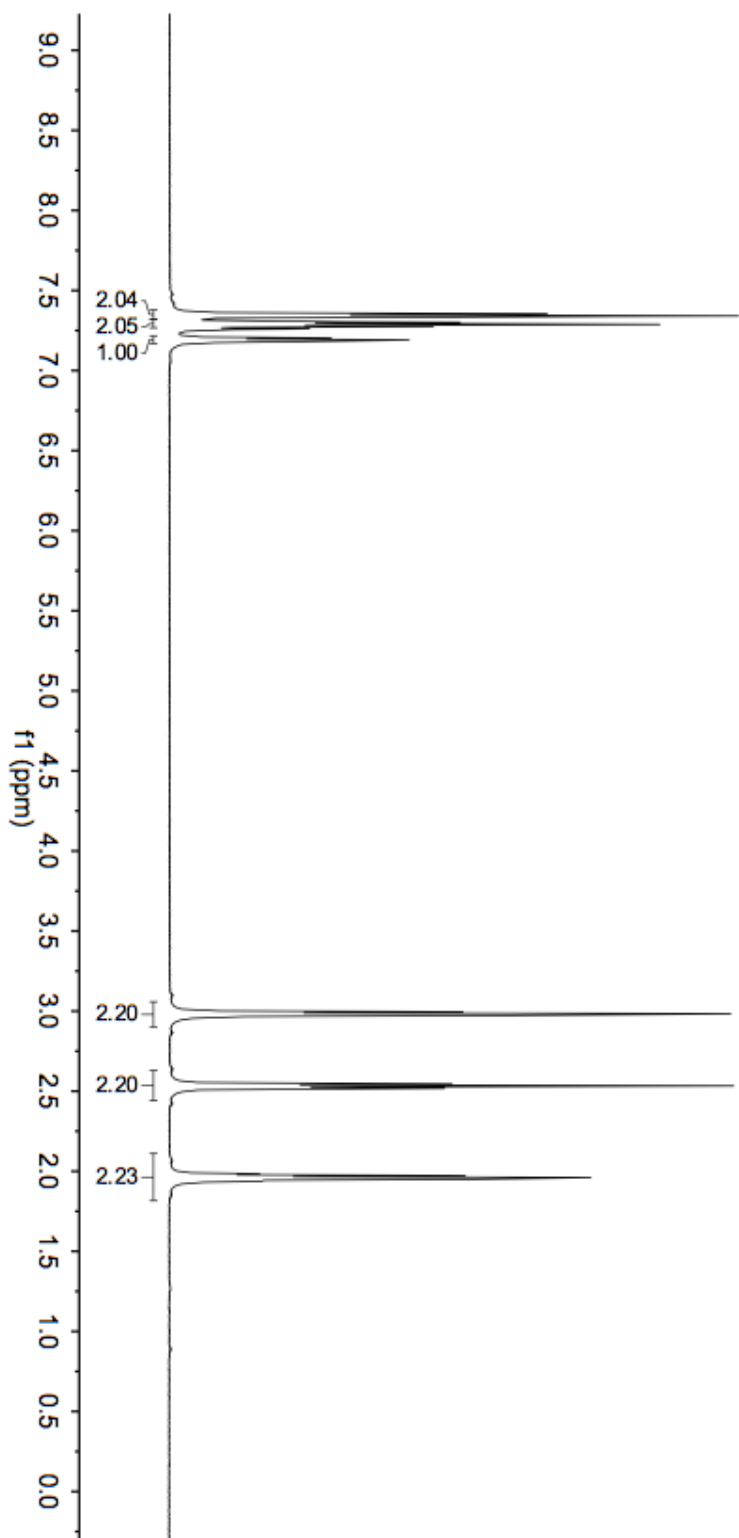


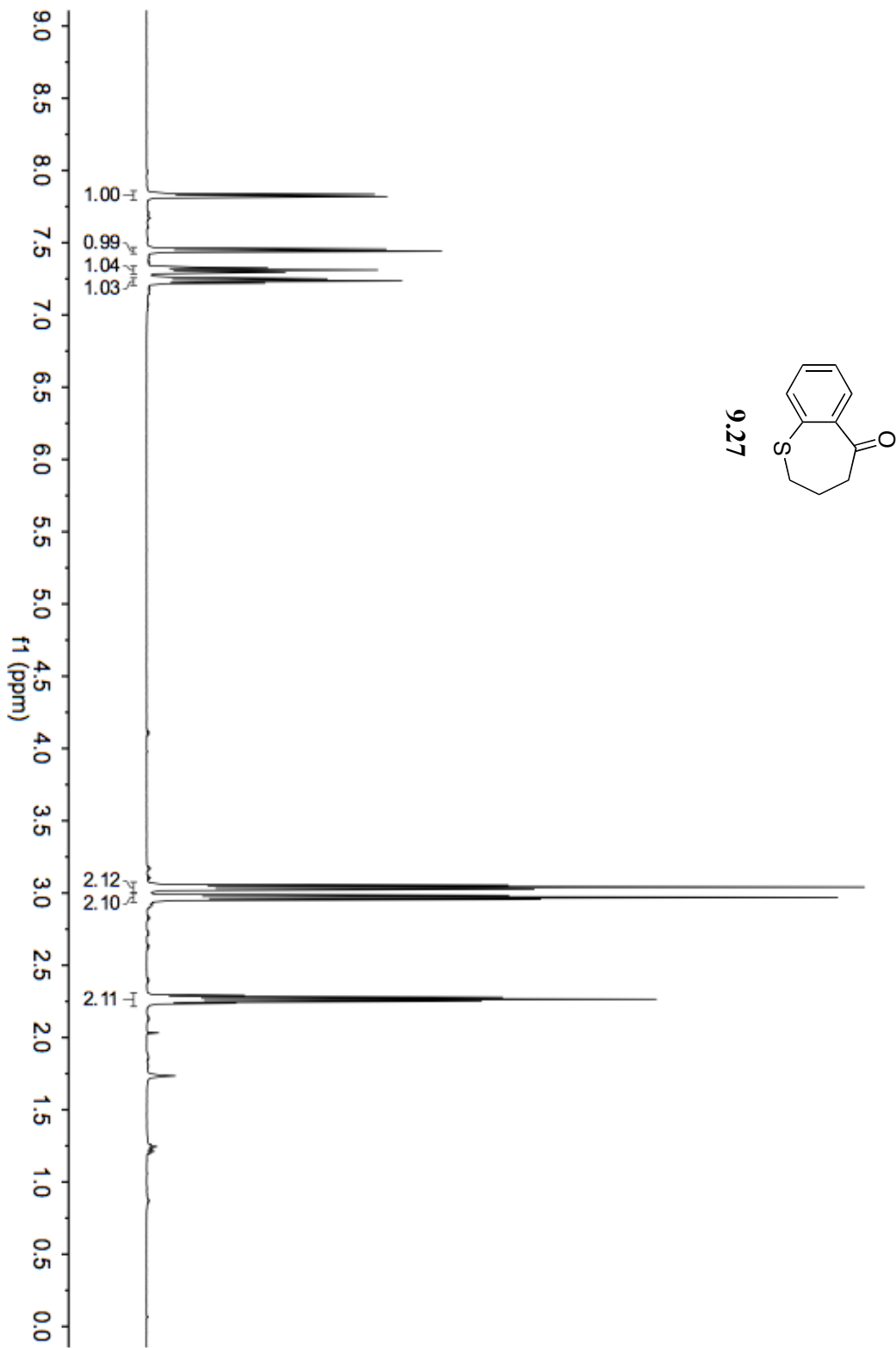


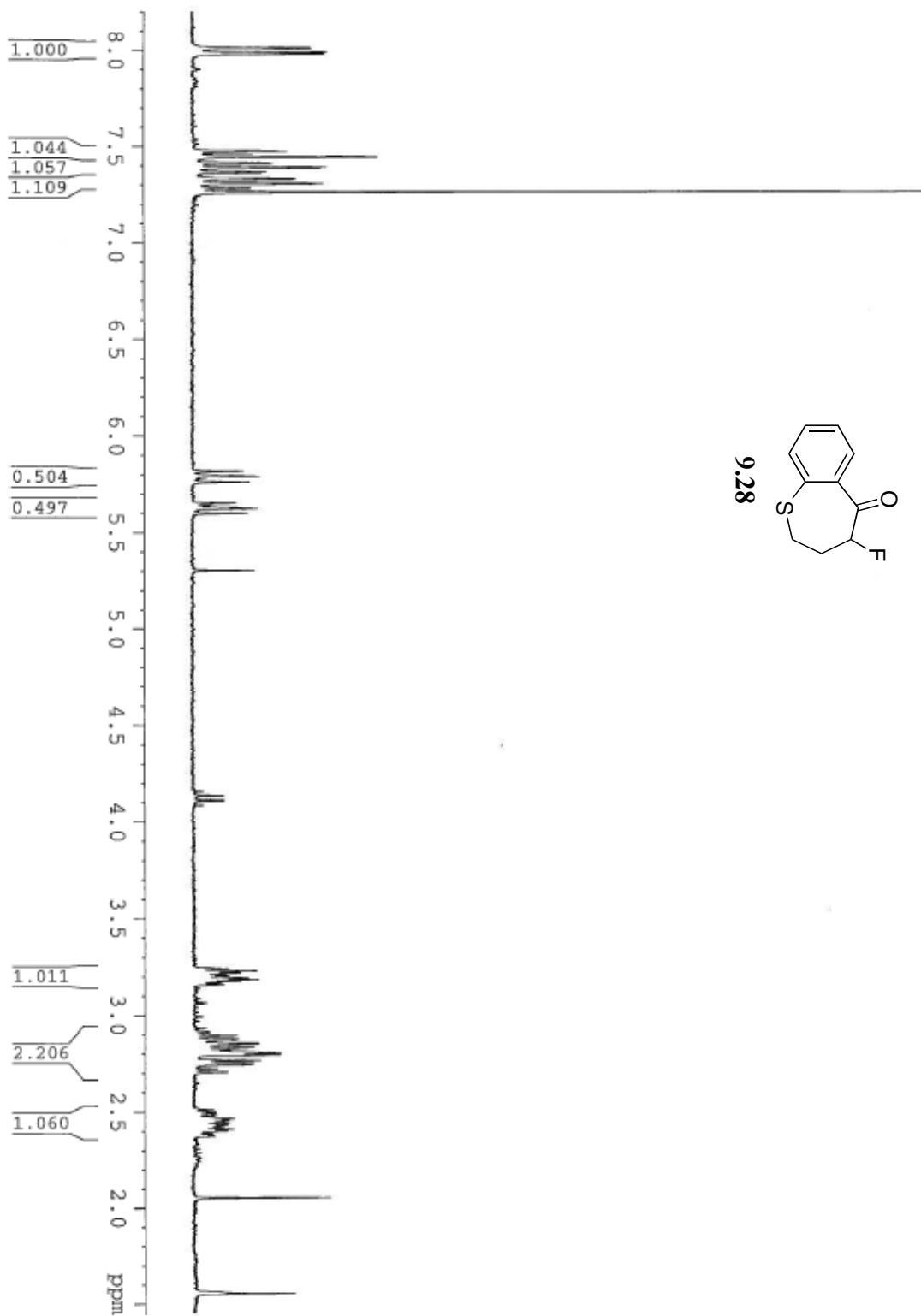


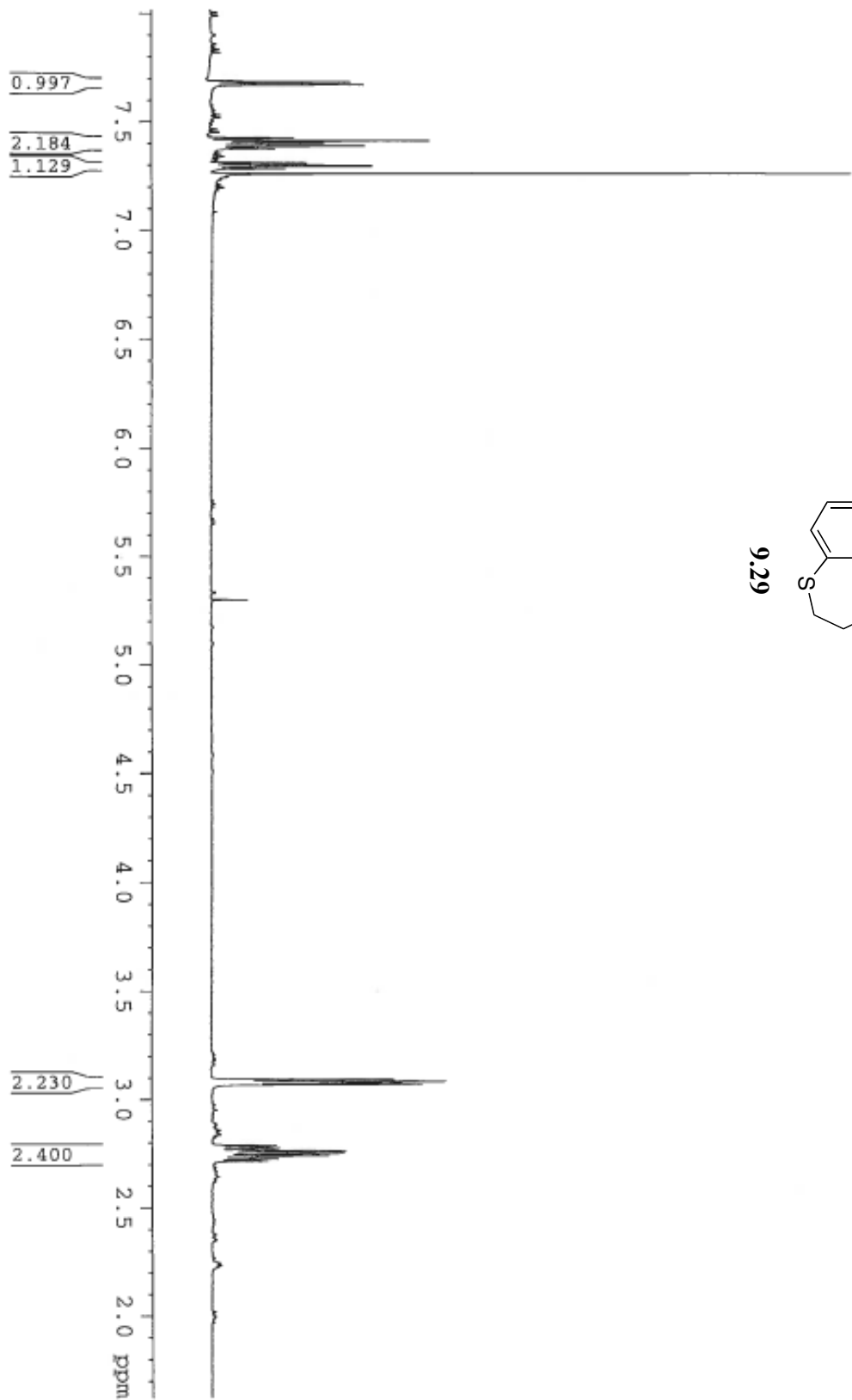
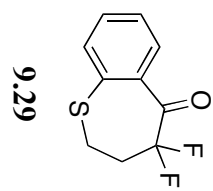


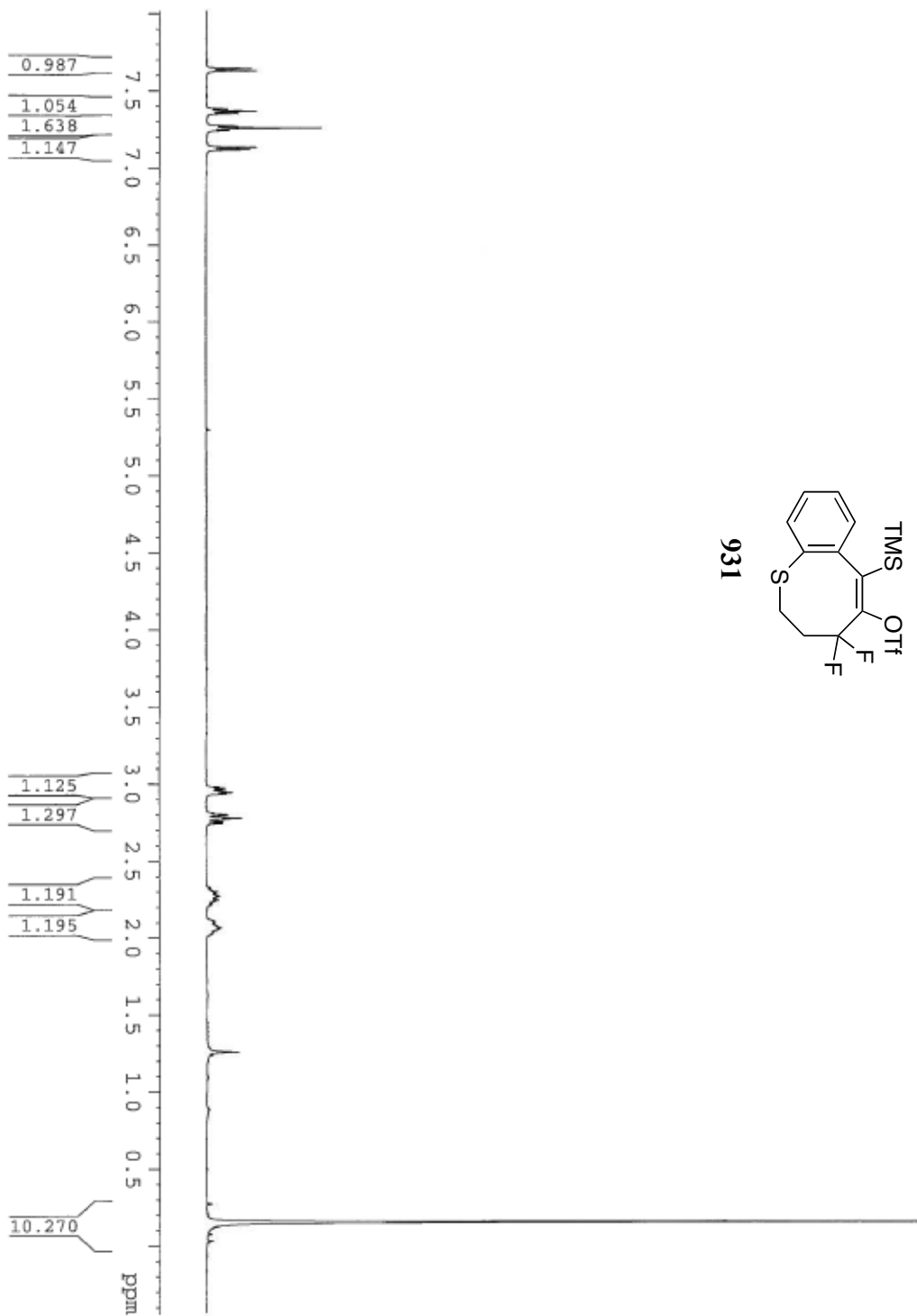
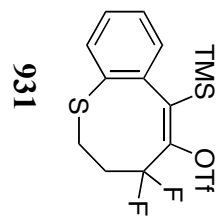
9.26

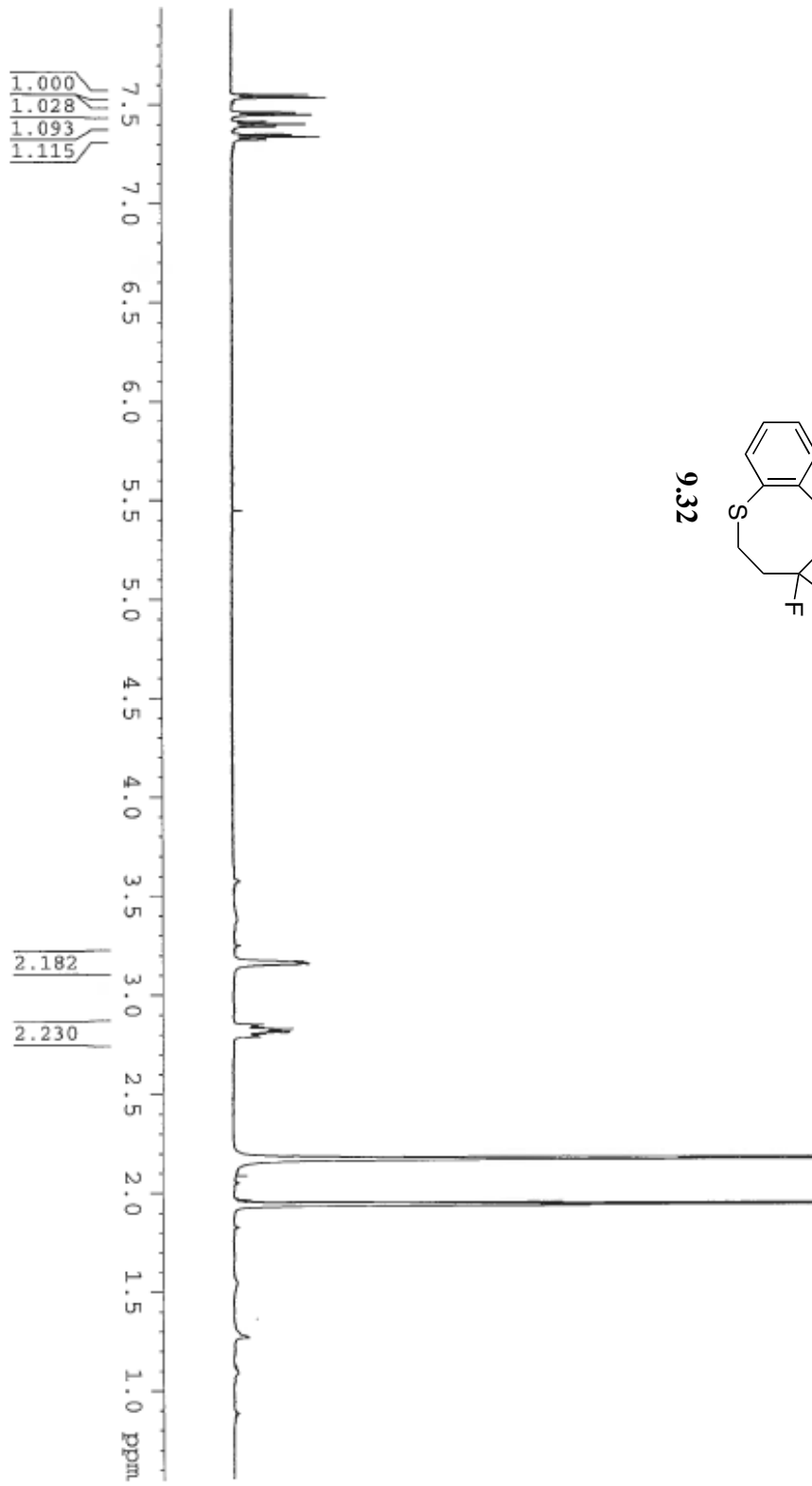
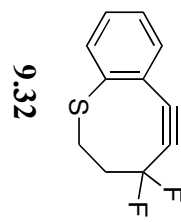


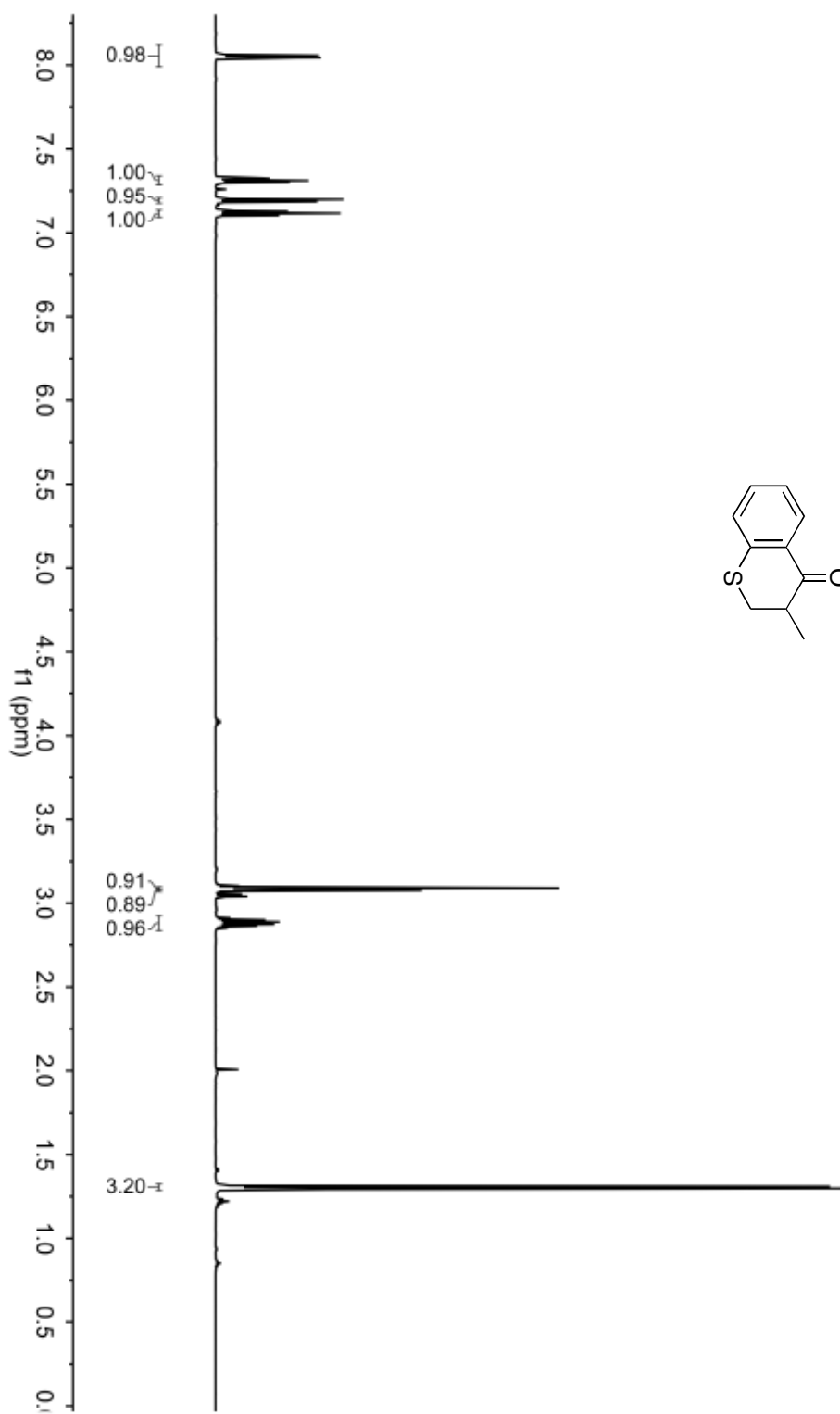
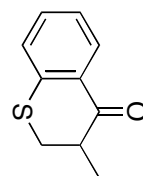


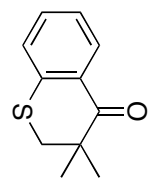




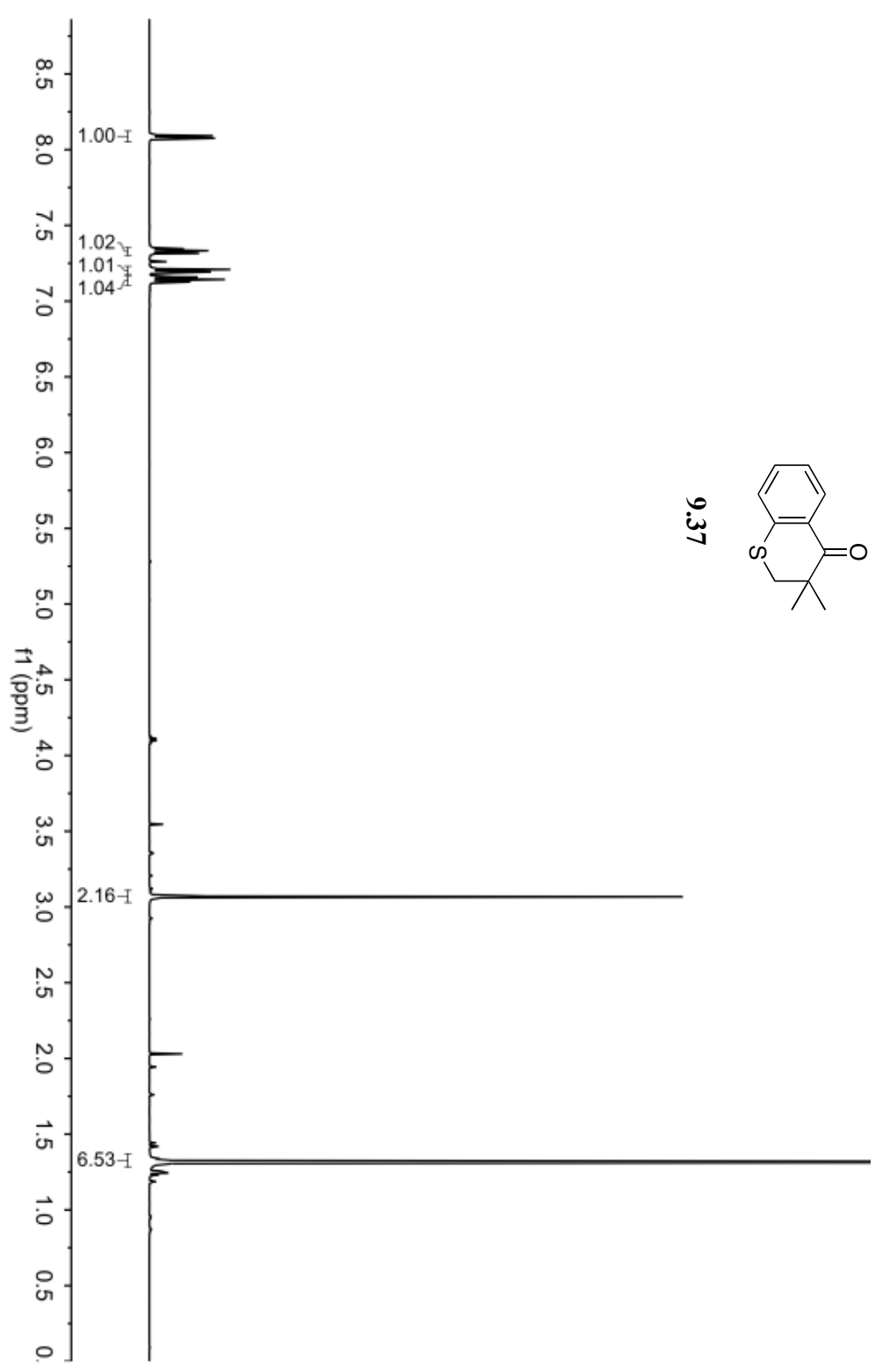


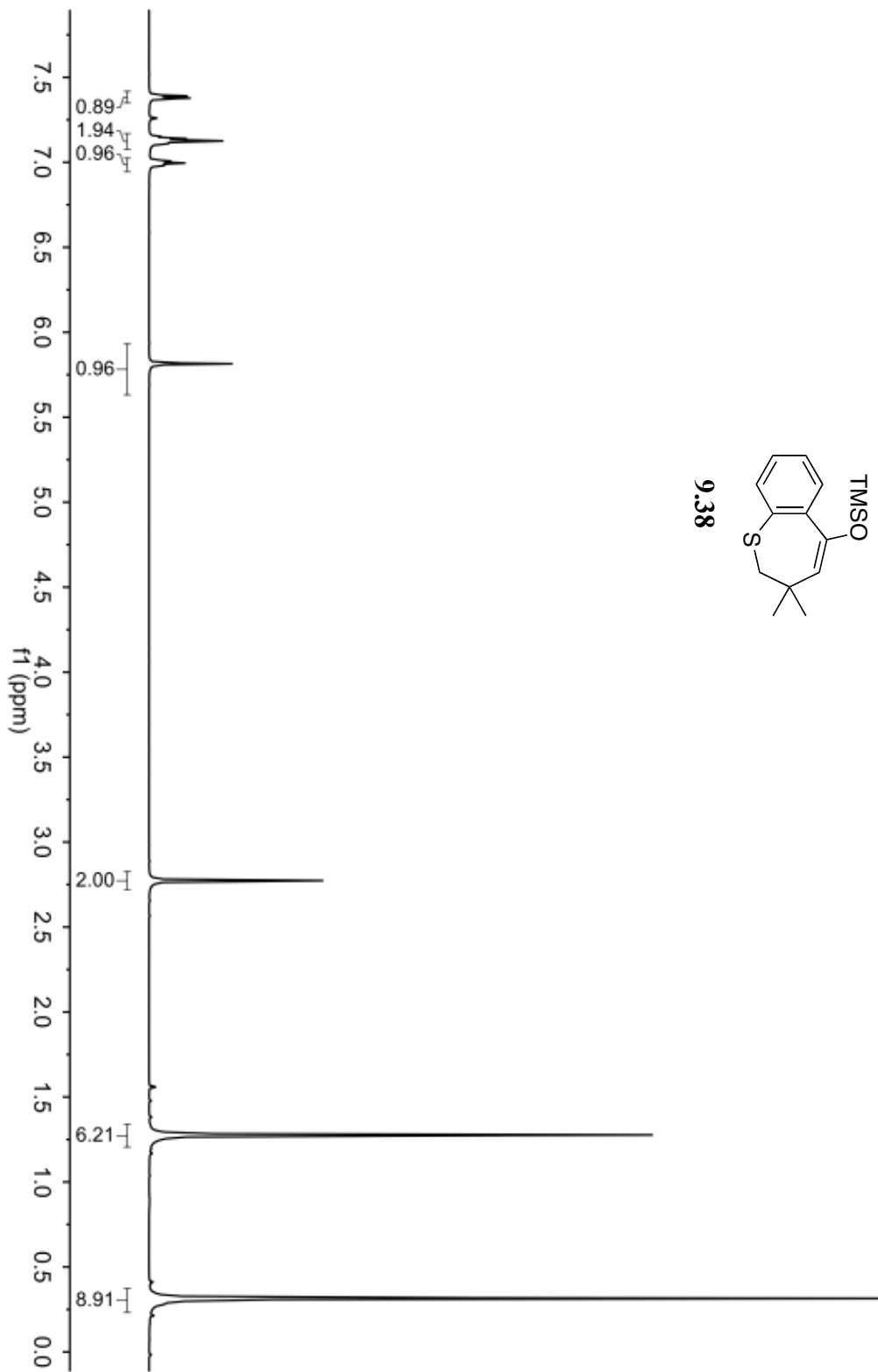


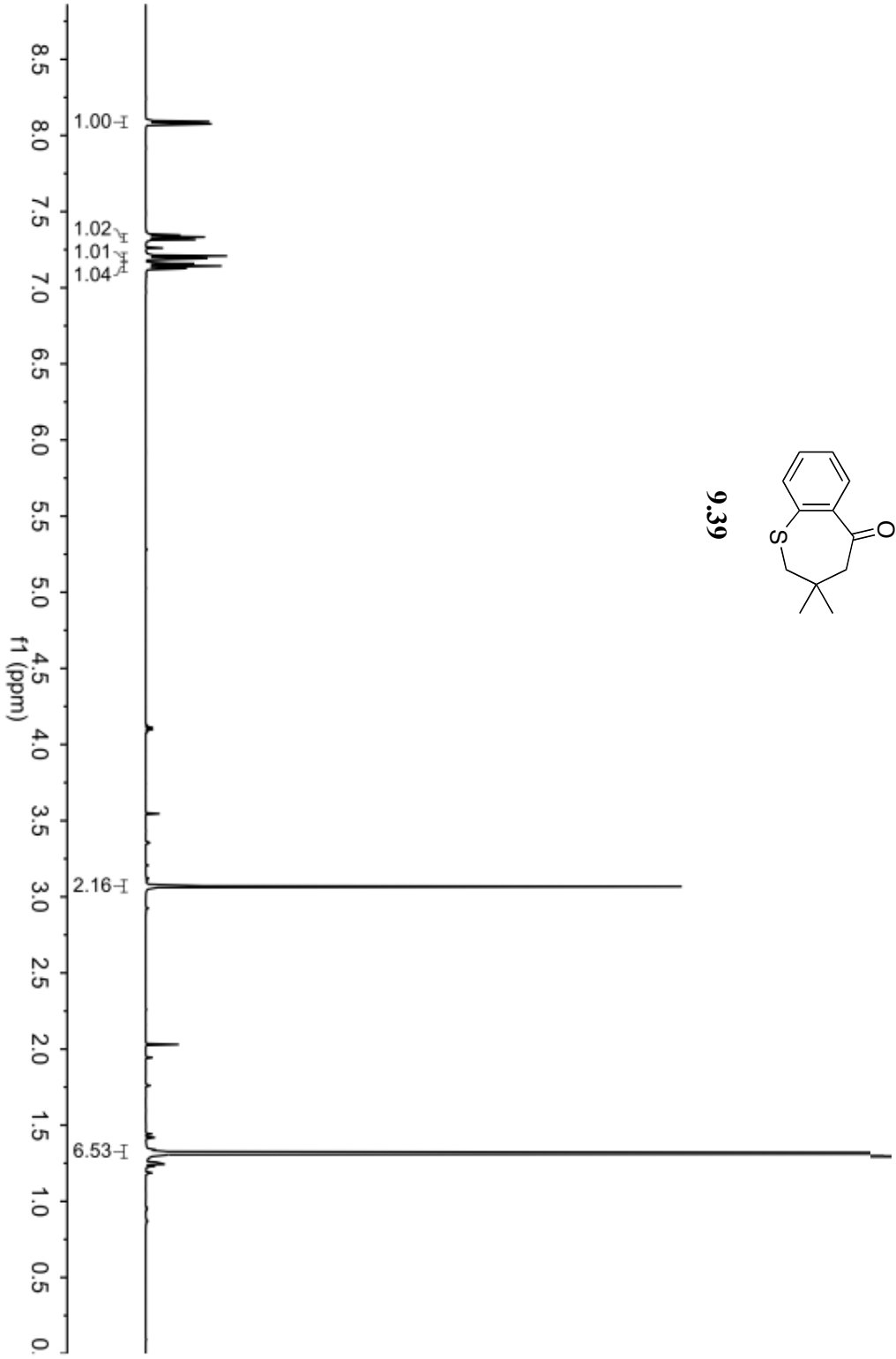


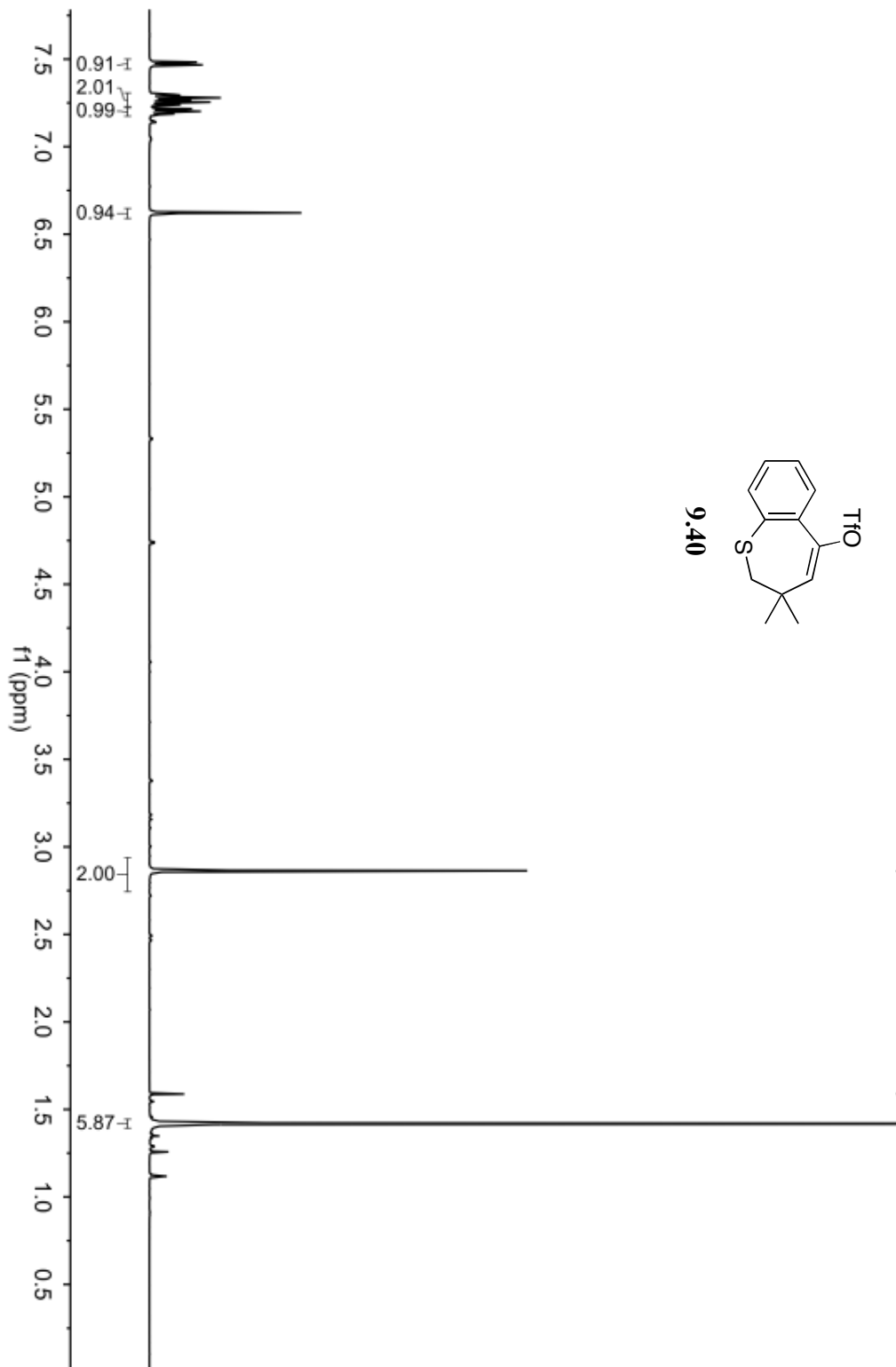


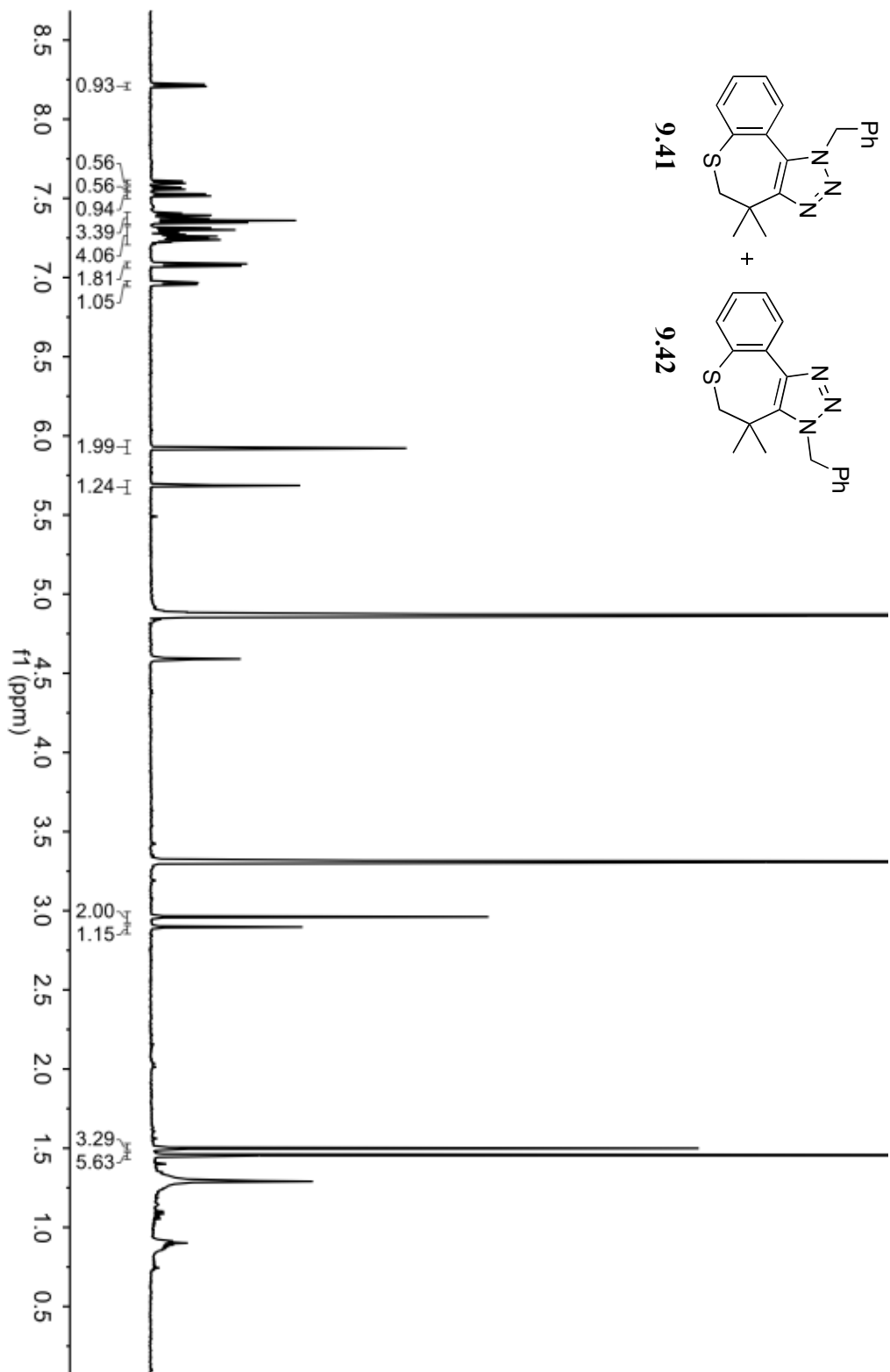
9.37

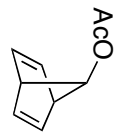




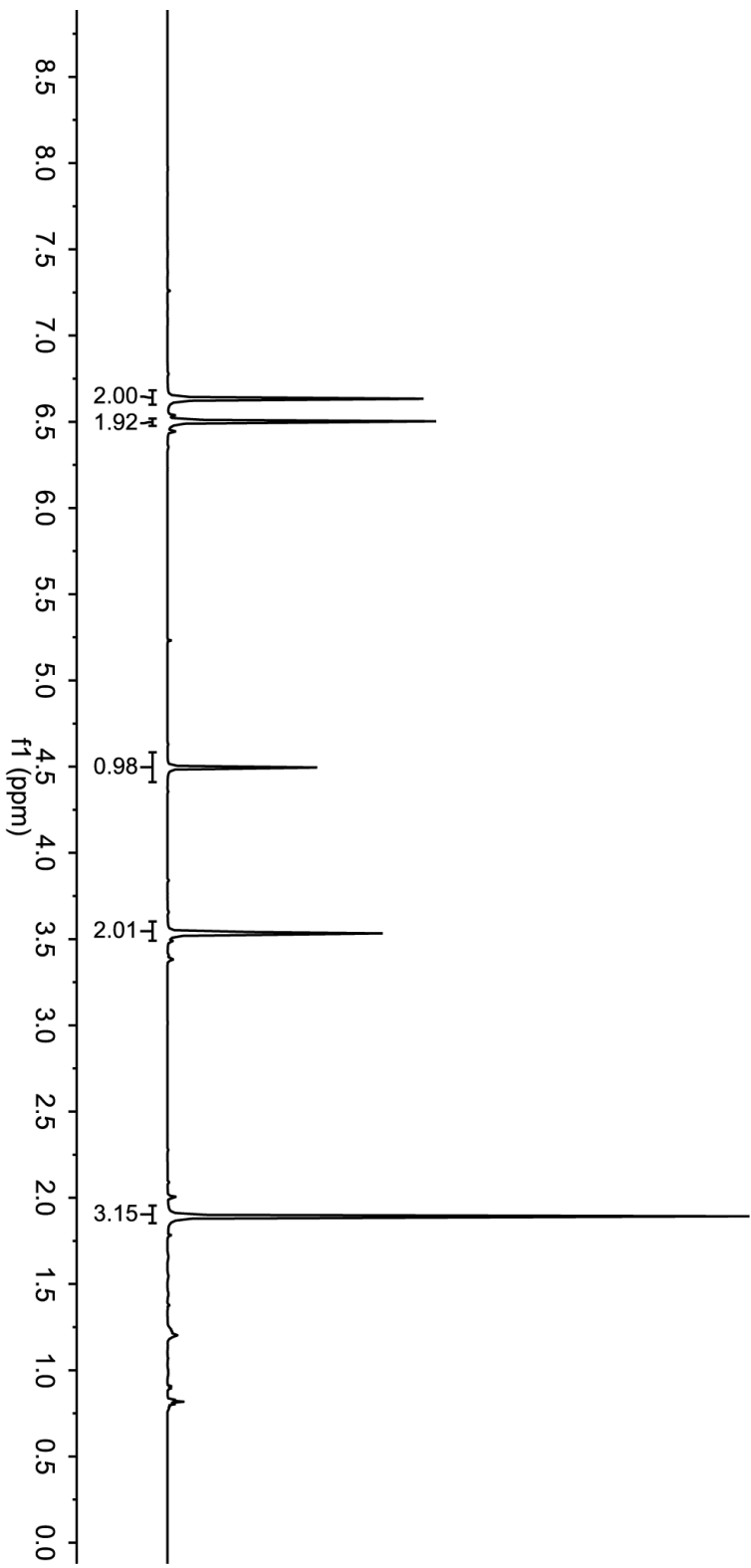


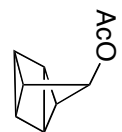




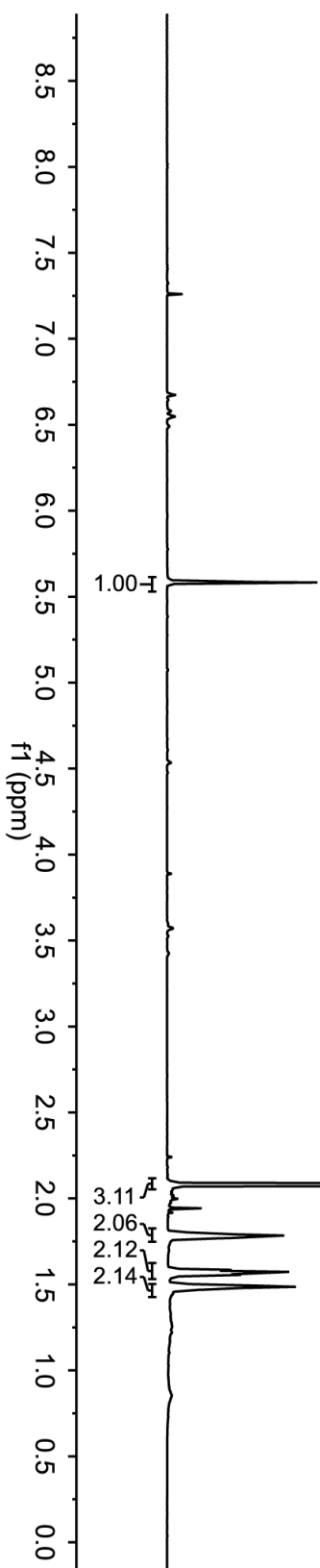


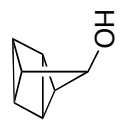
10.3



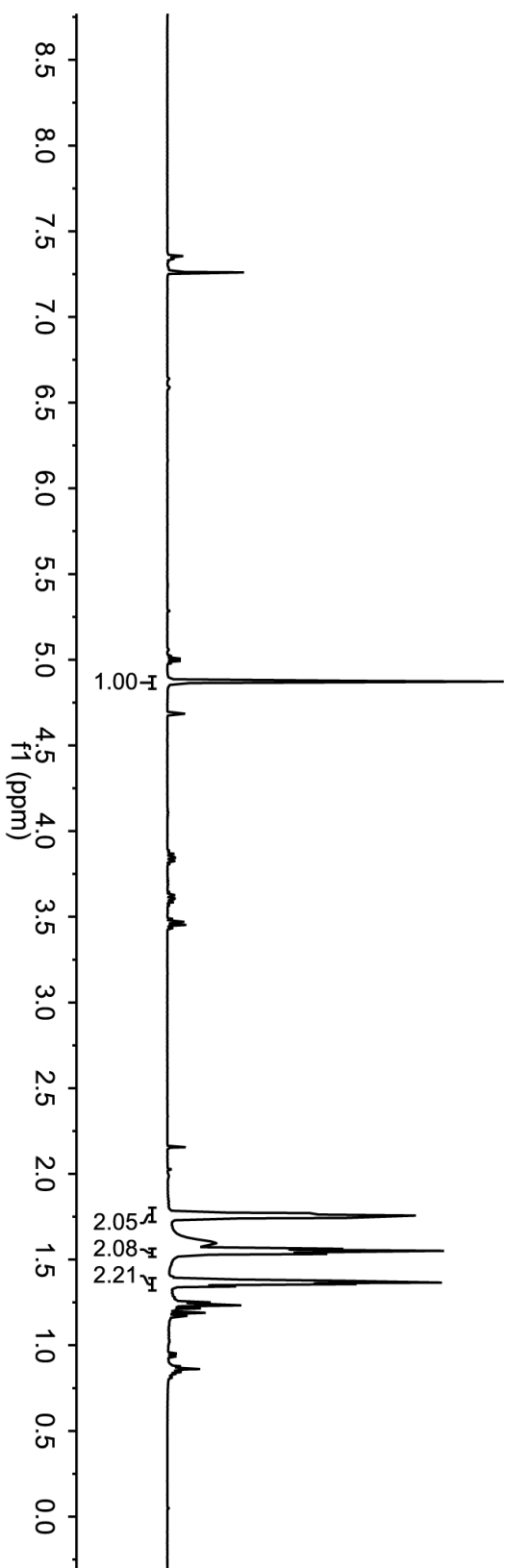


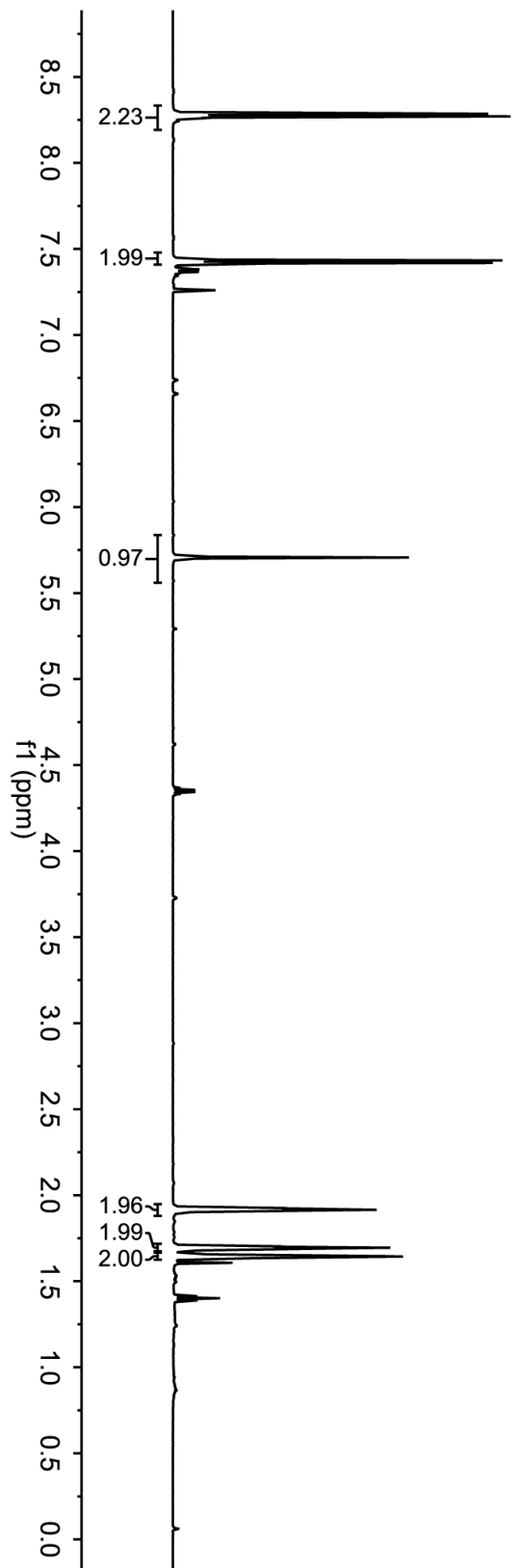
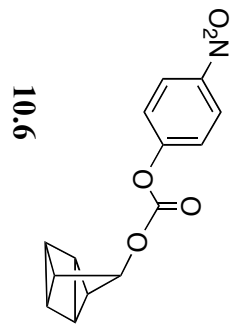
10.4

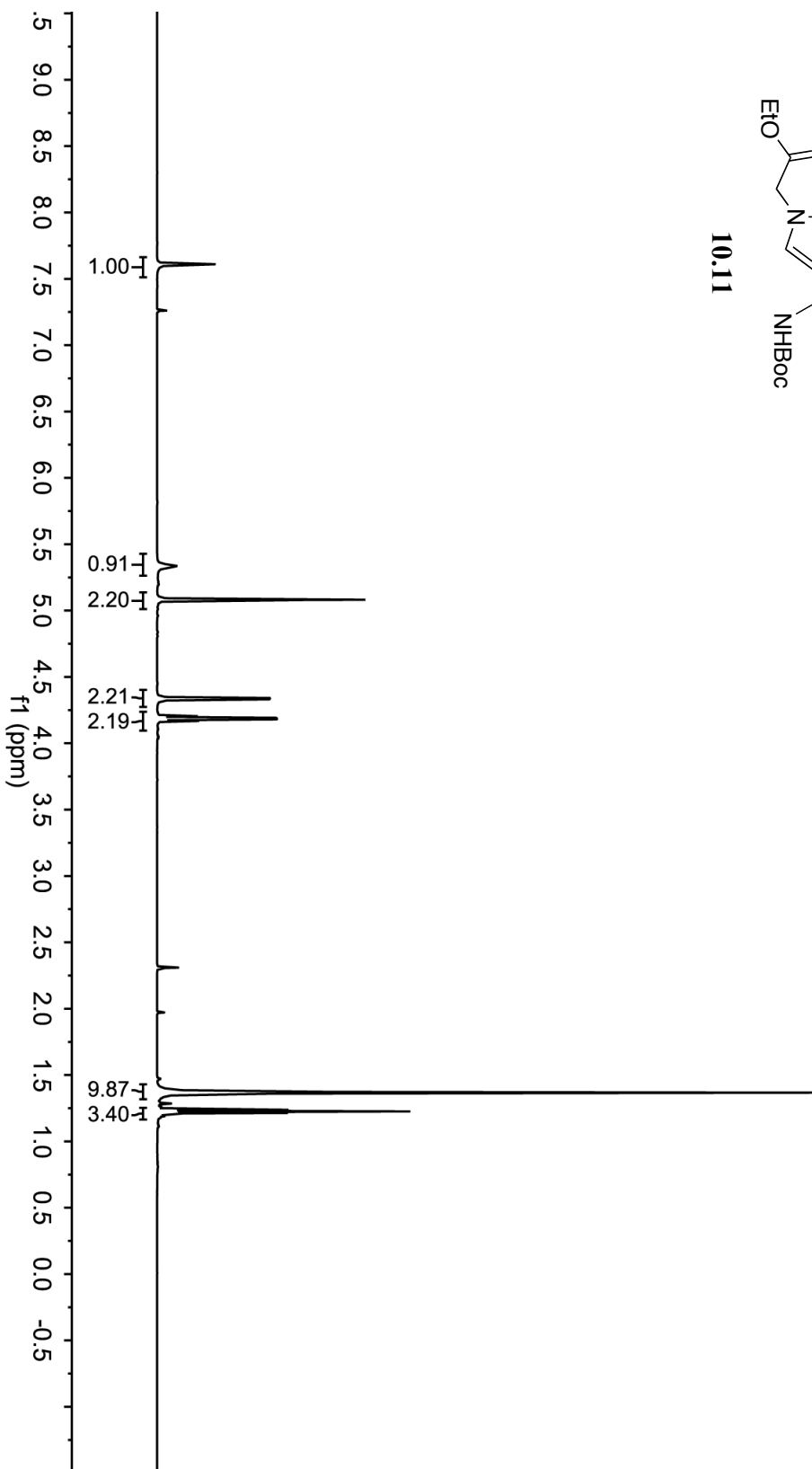
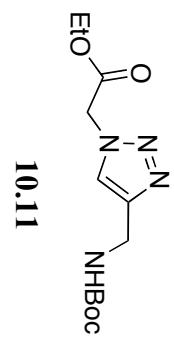


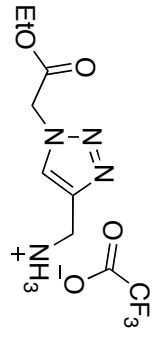


10.5

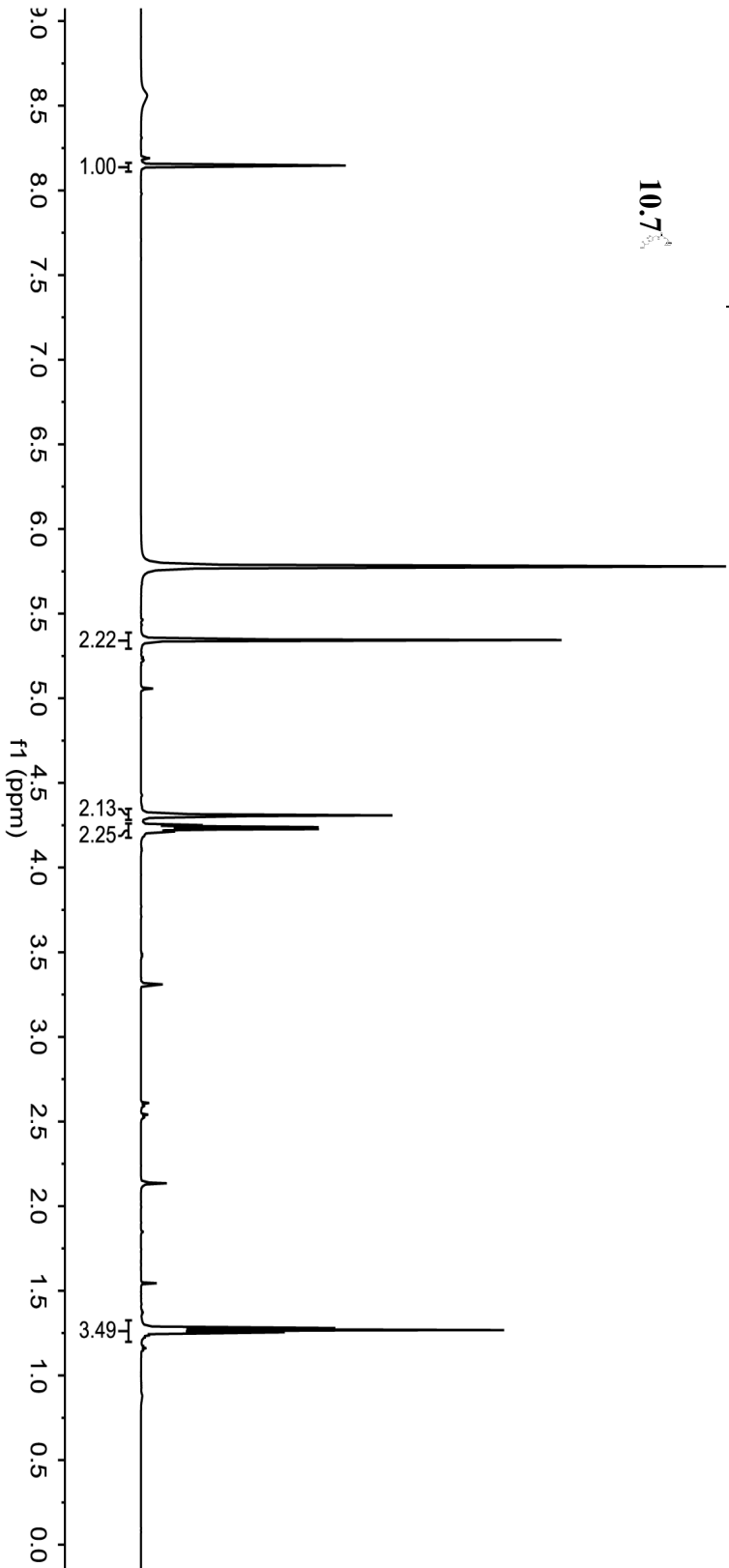


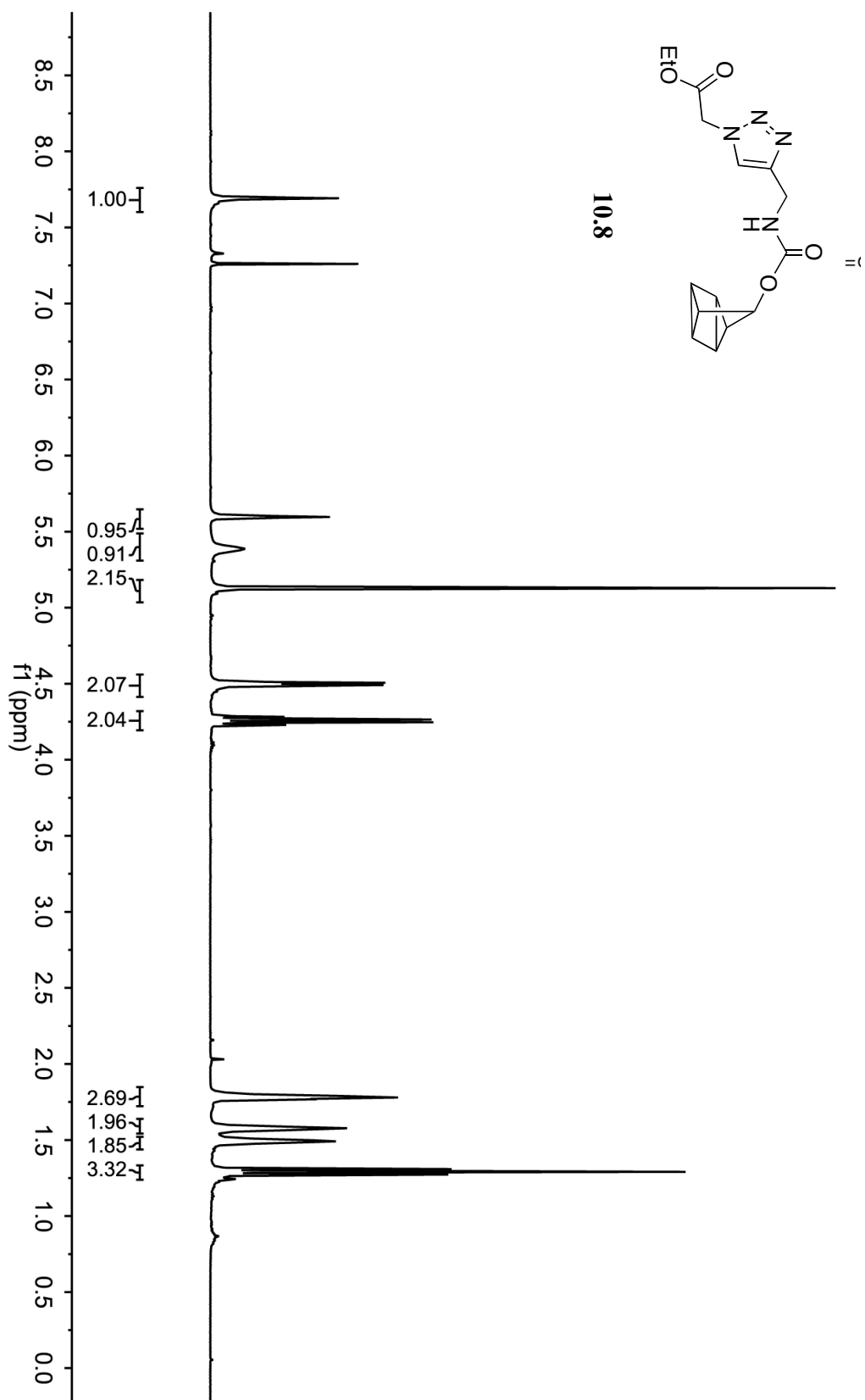


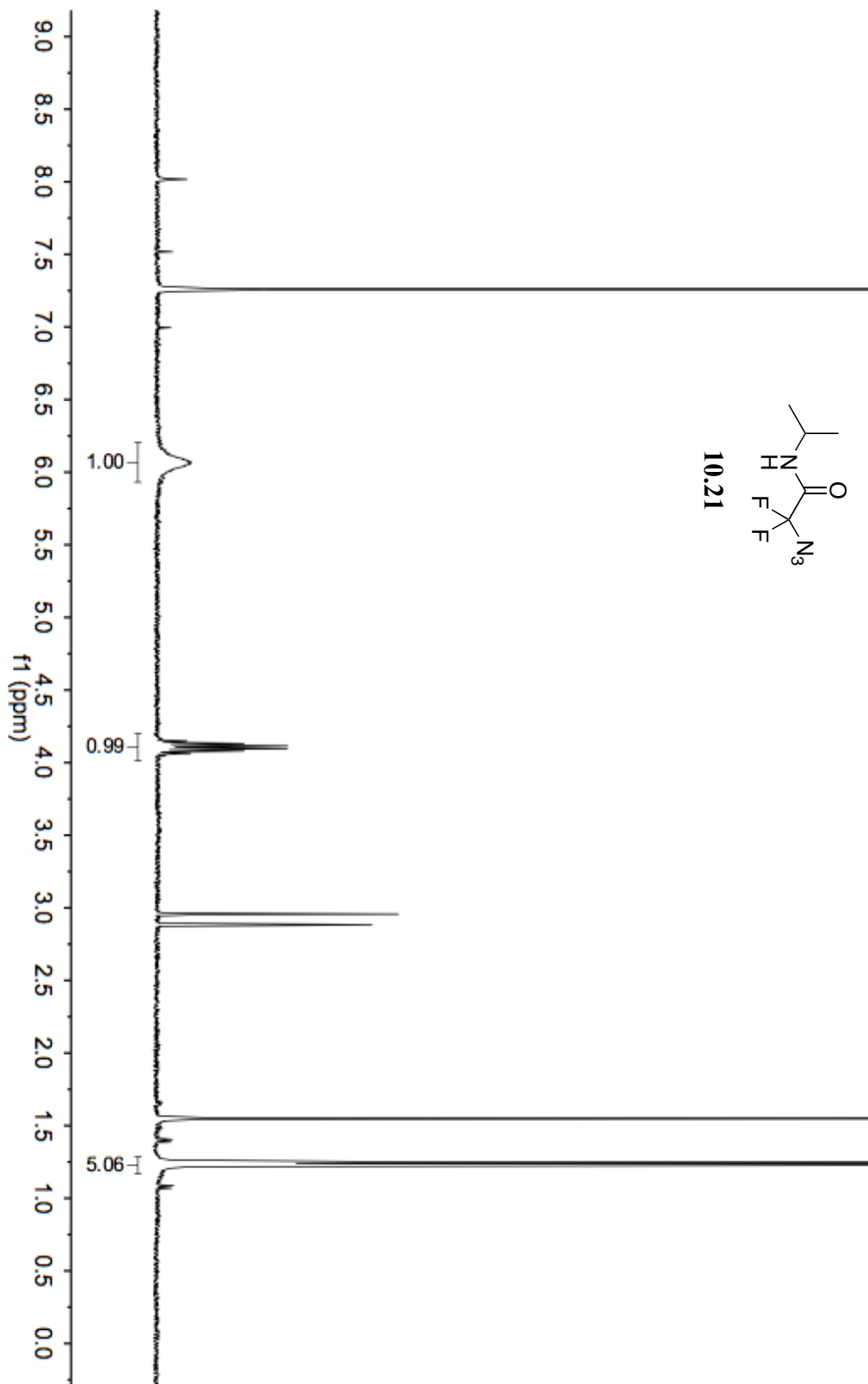


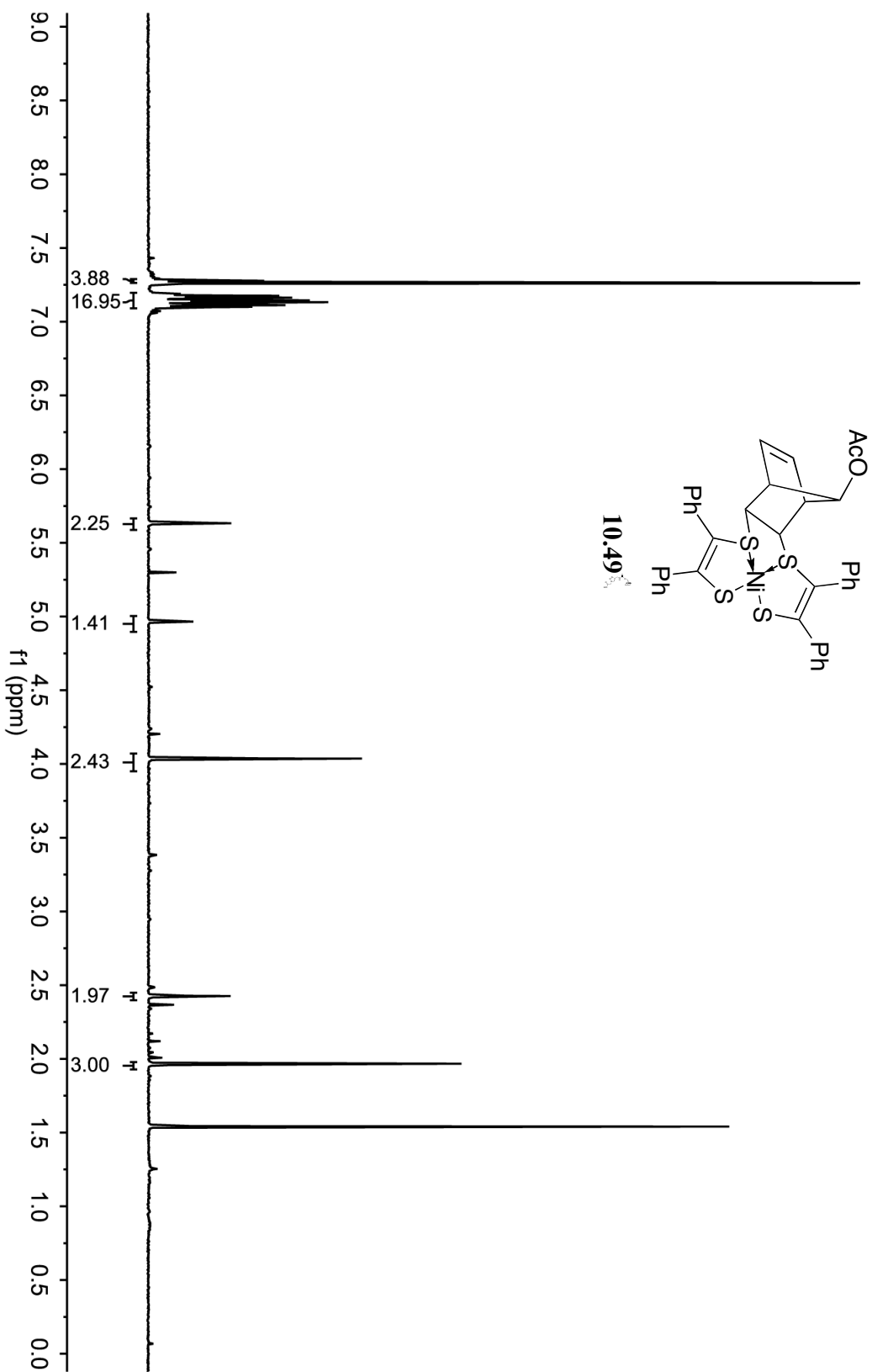


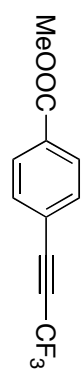
10.7



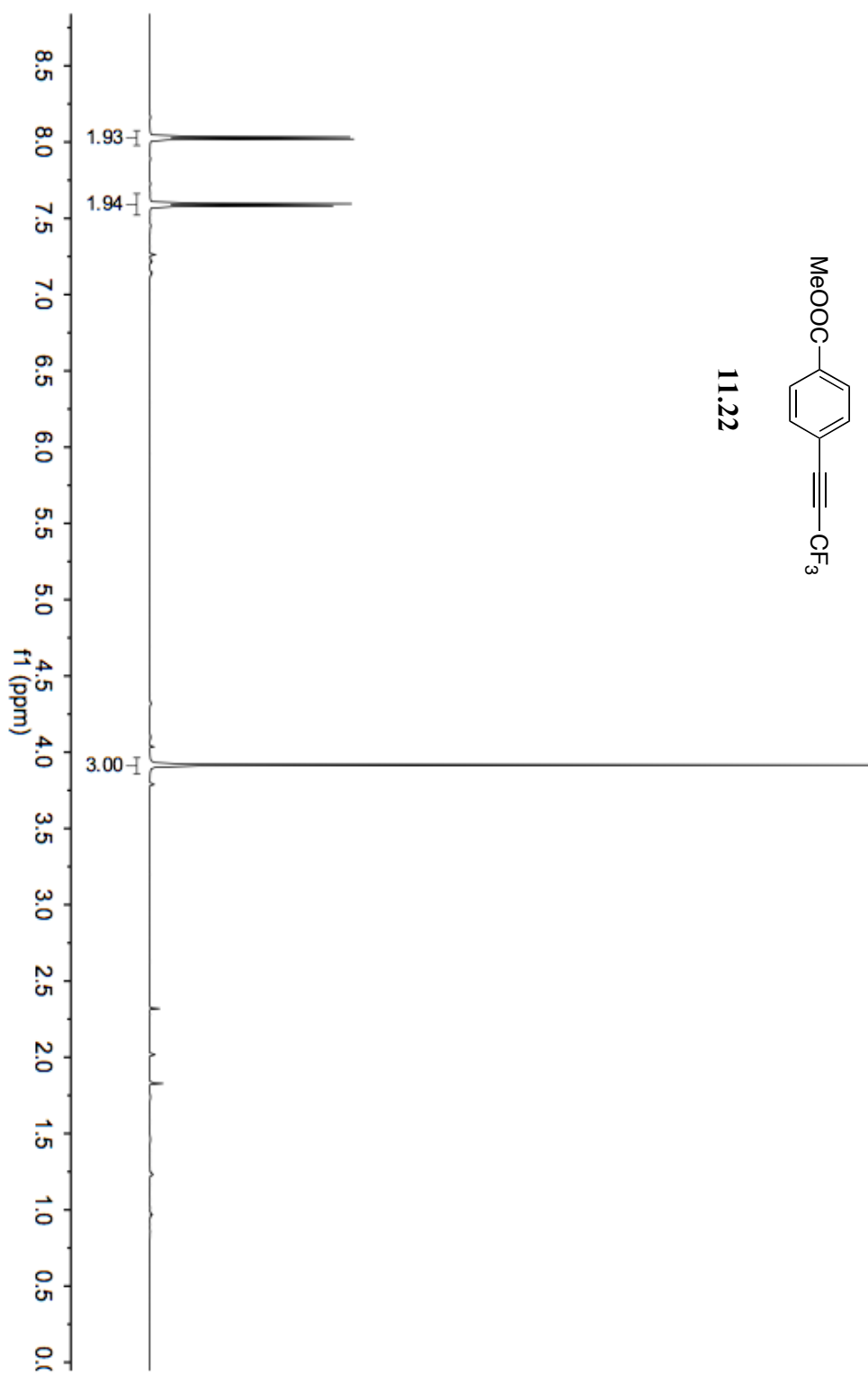


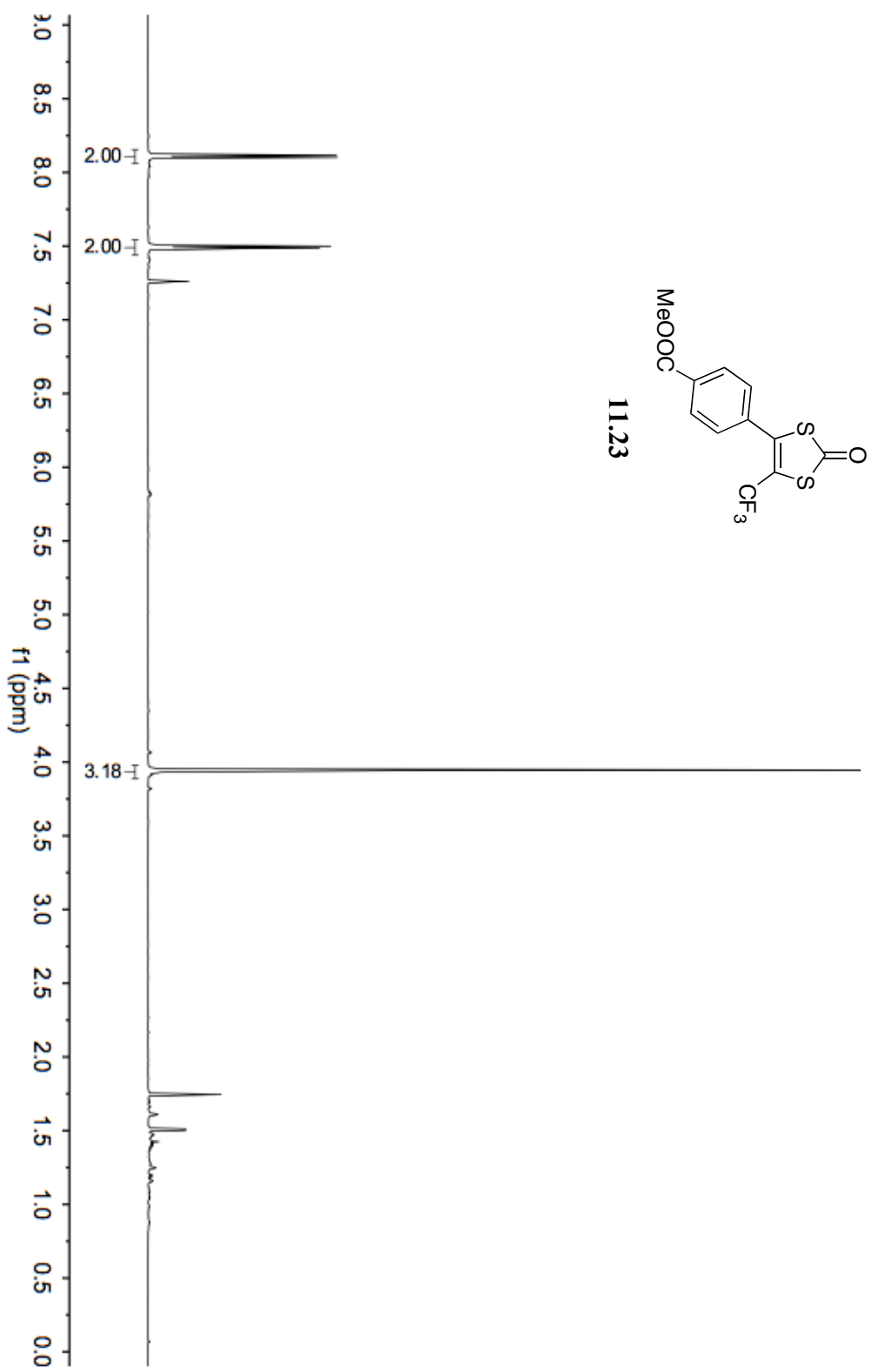


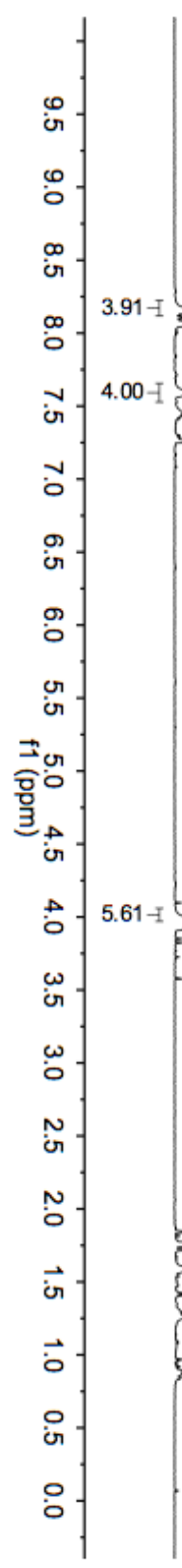
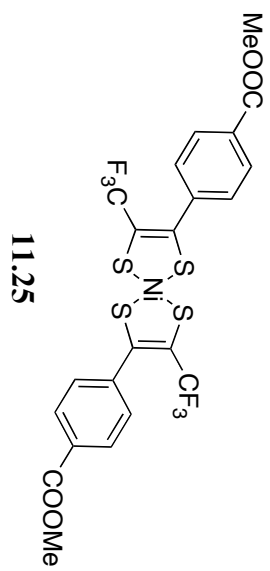


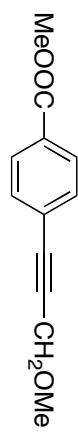


11.22

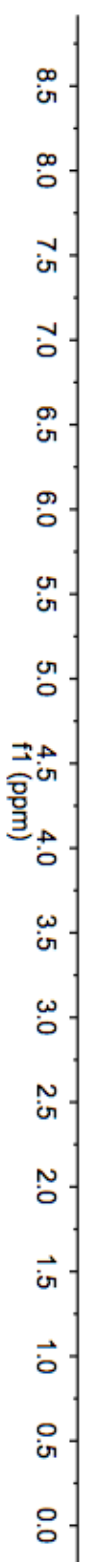


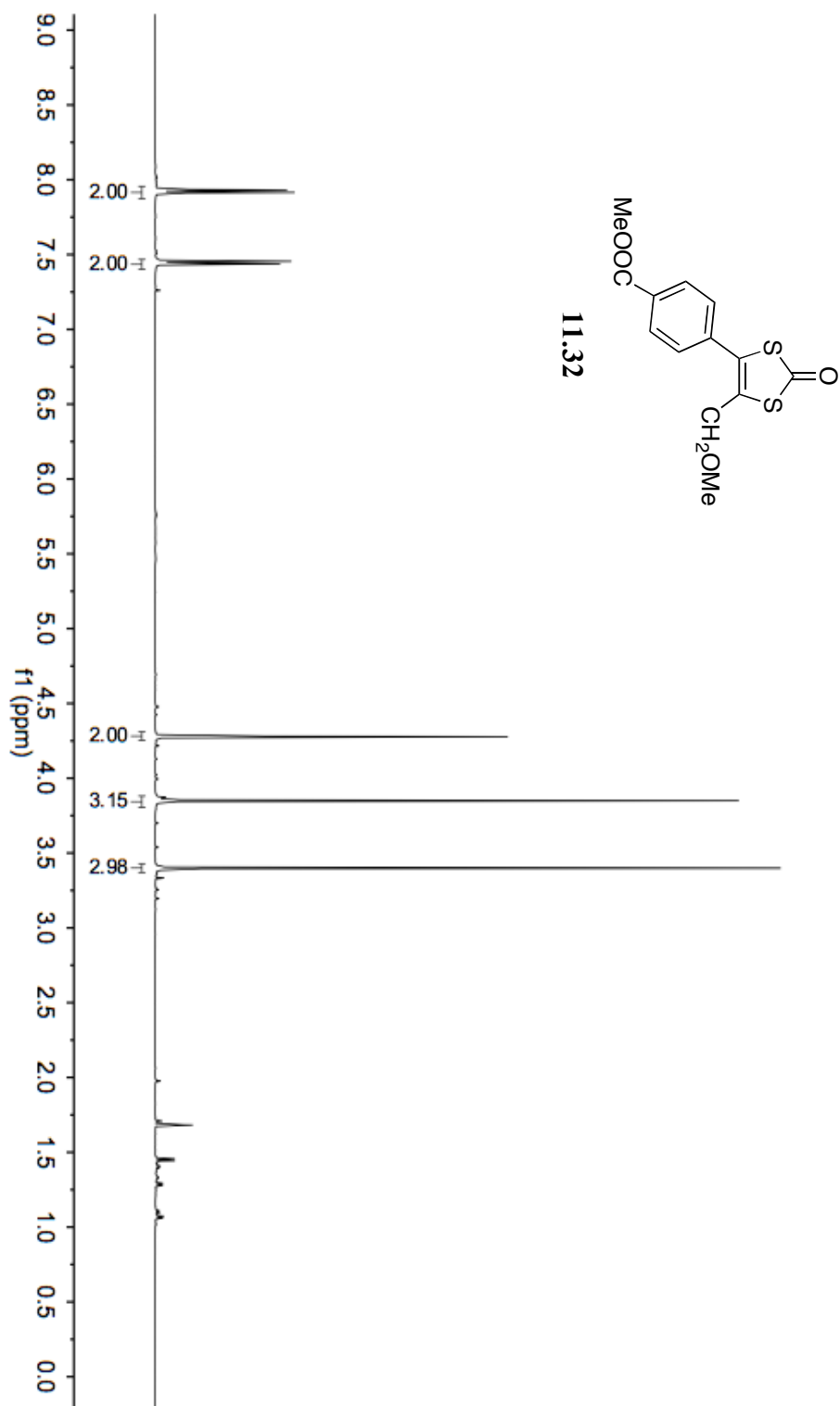


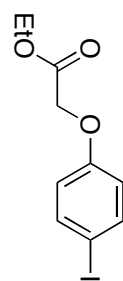




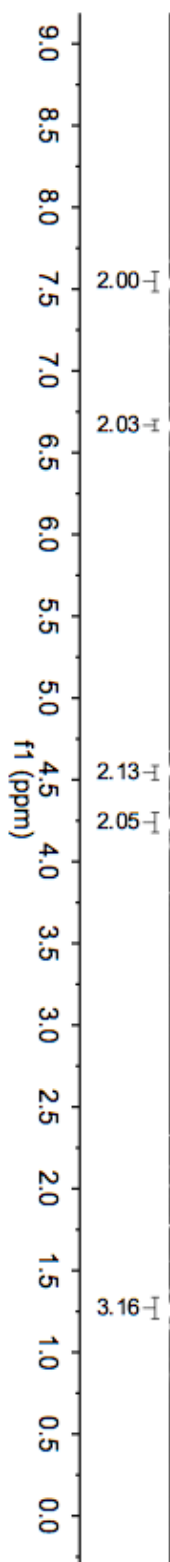
11.31

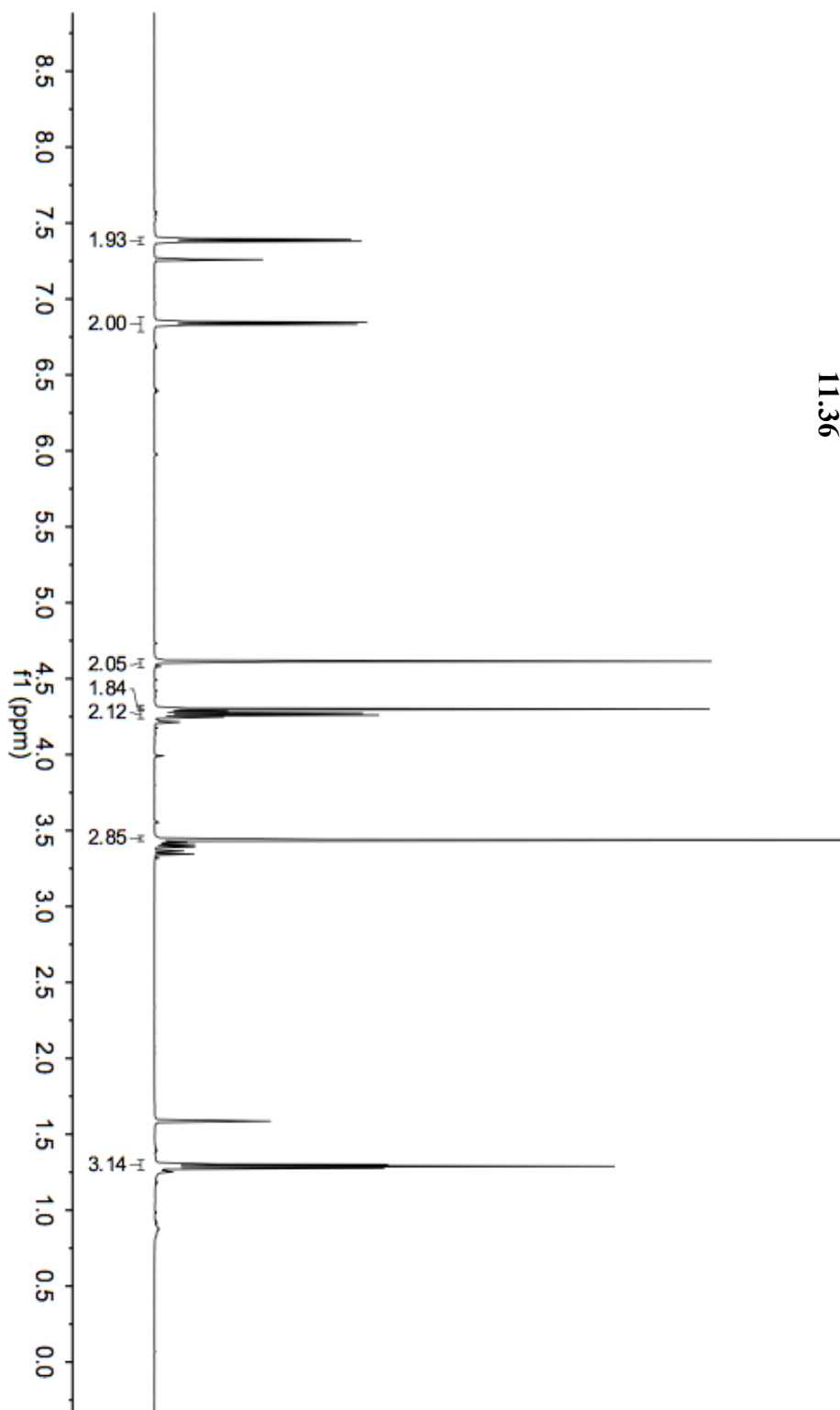
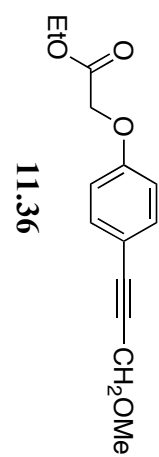


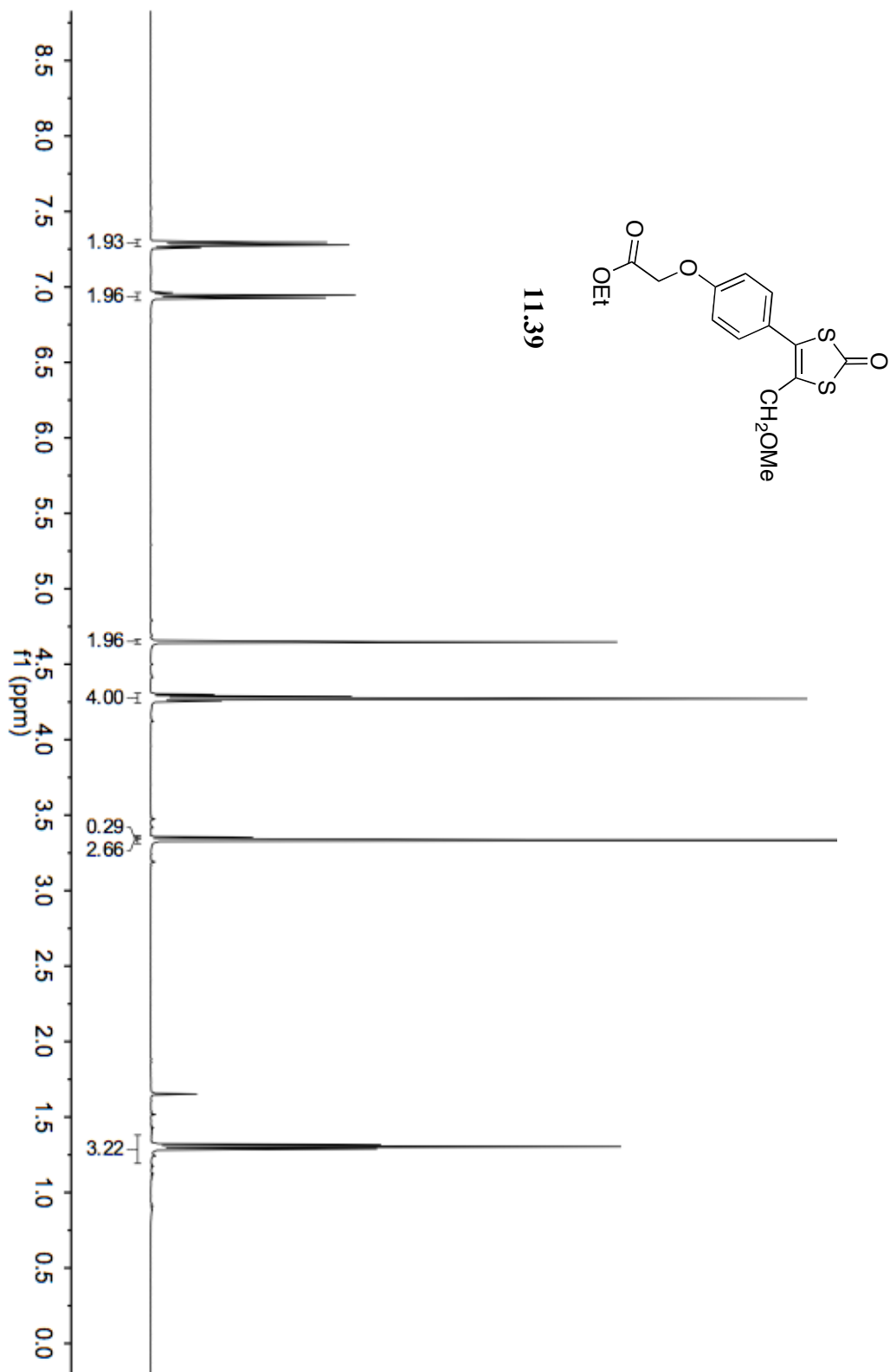


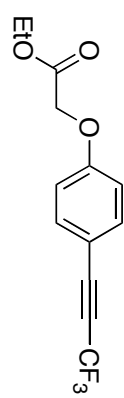


11.35

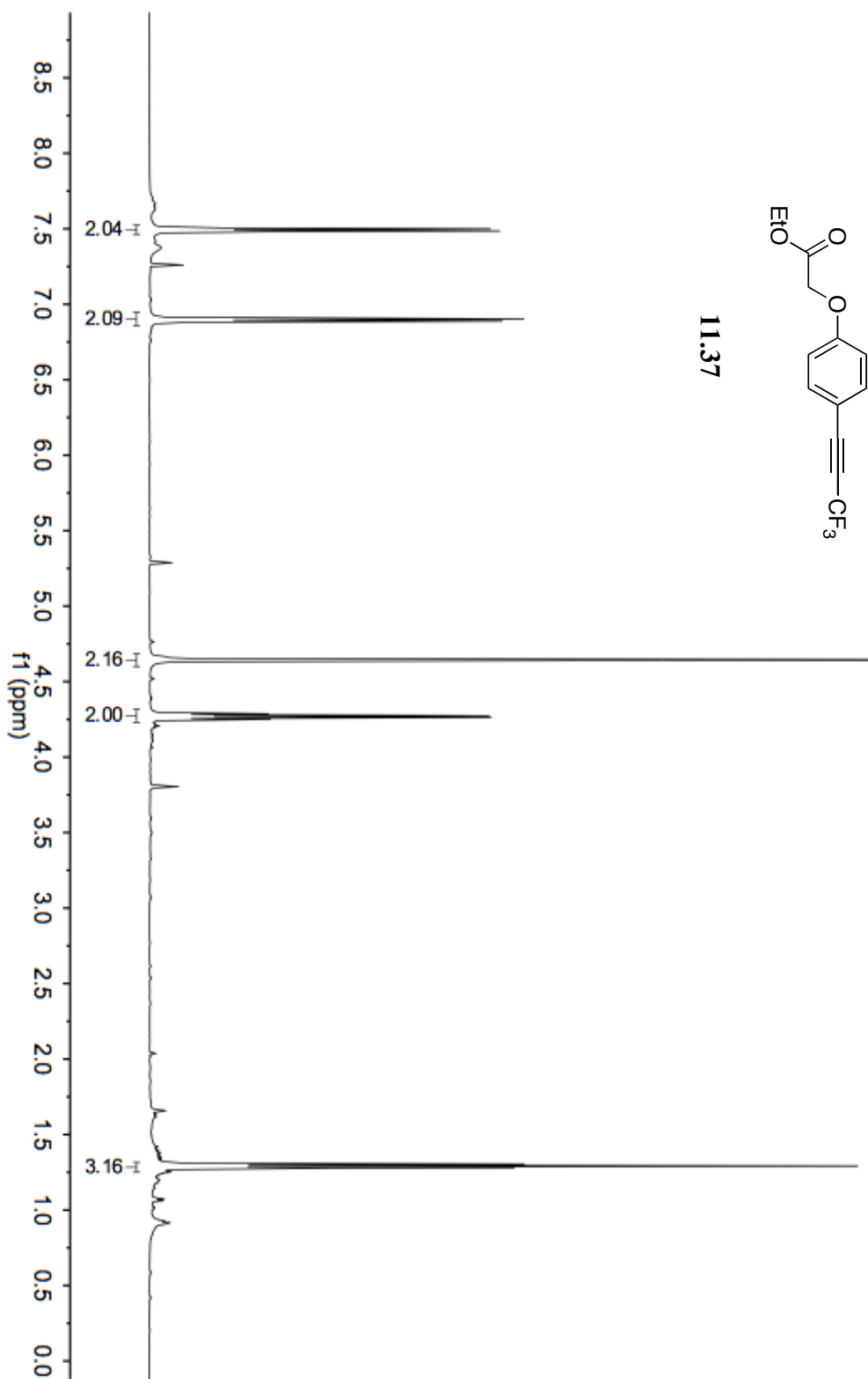


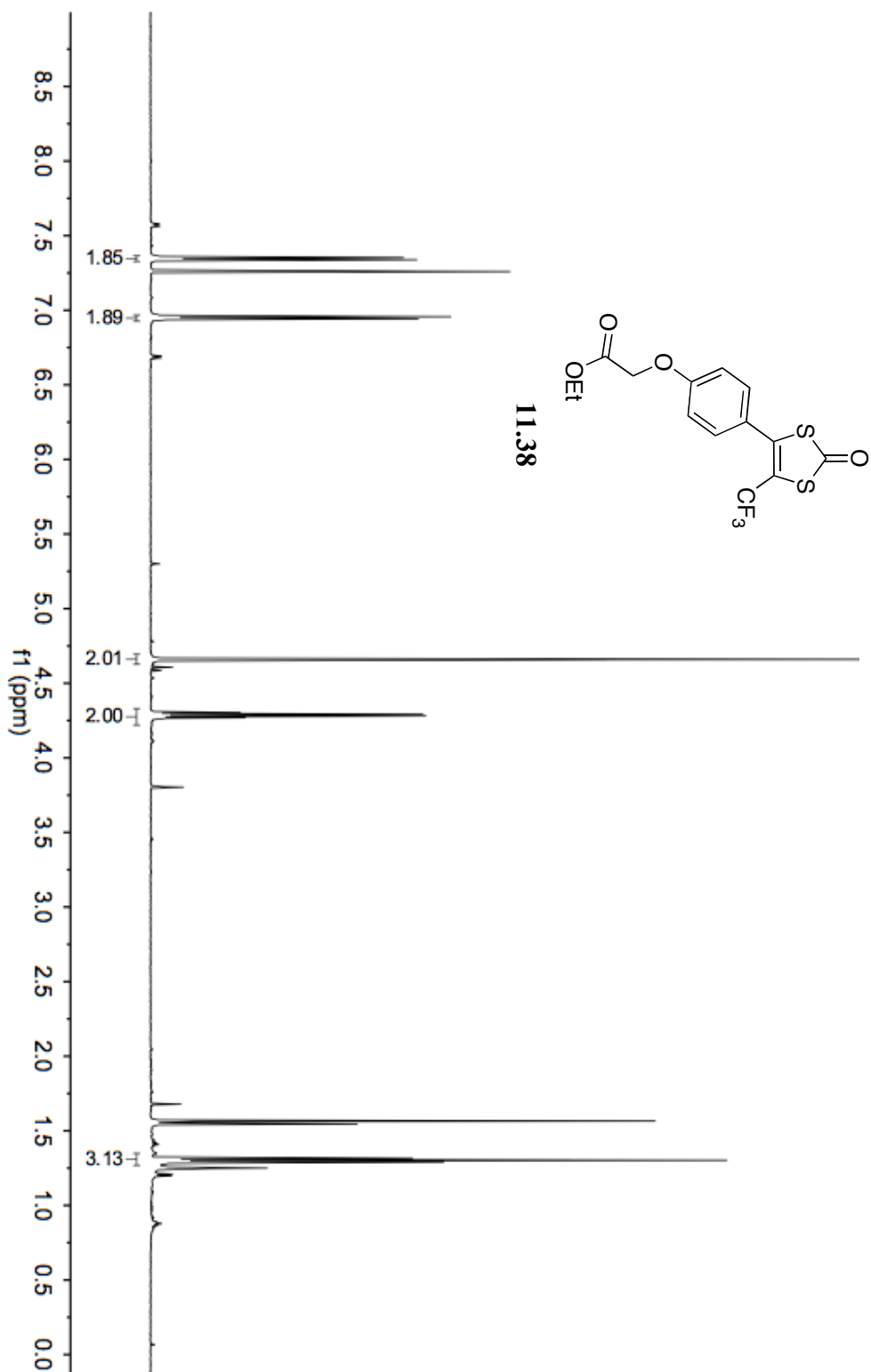


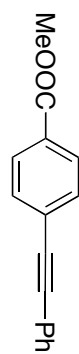




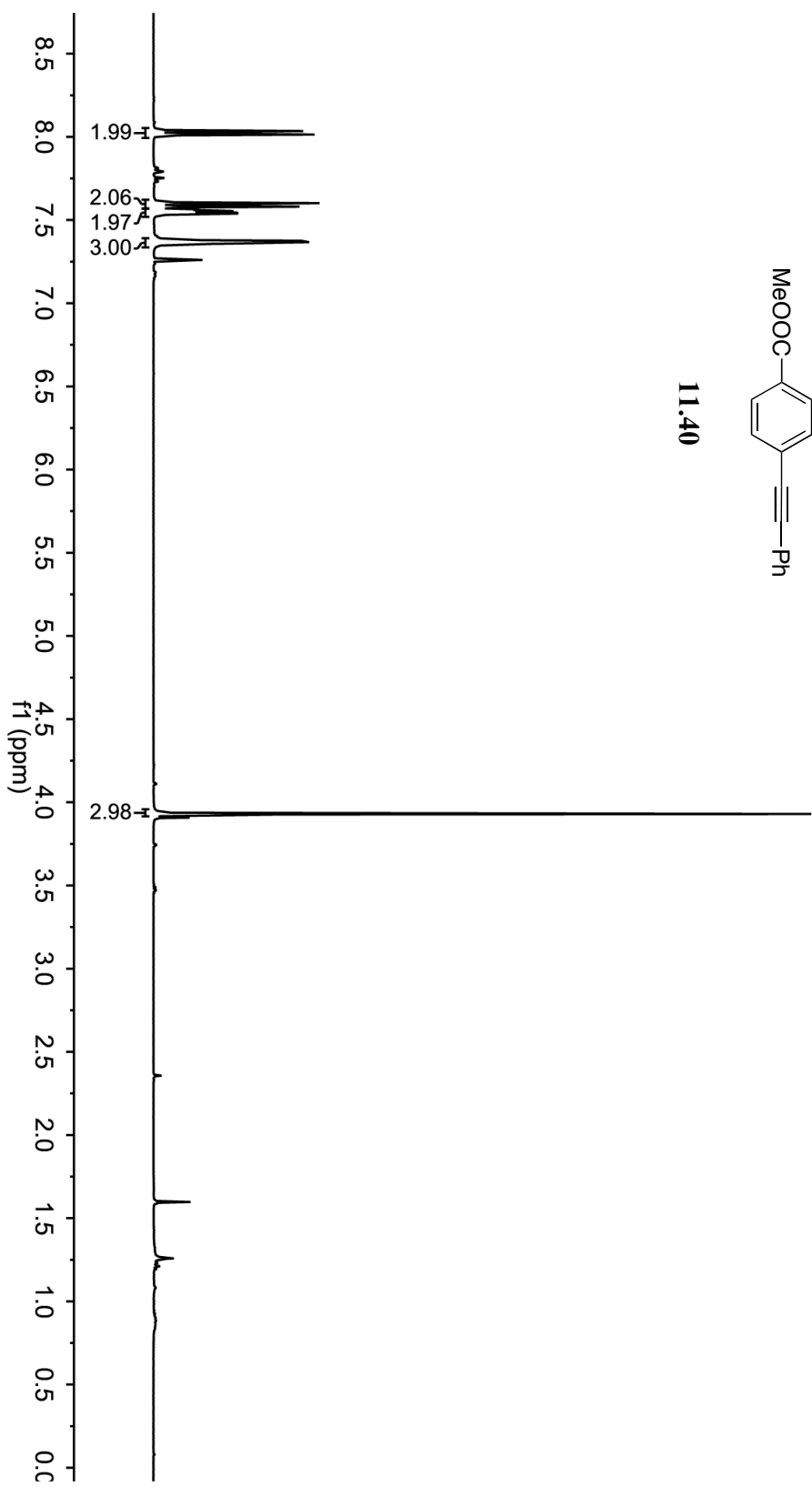
11.37

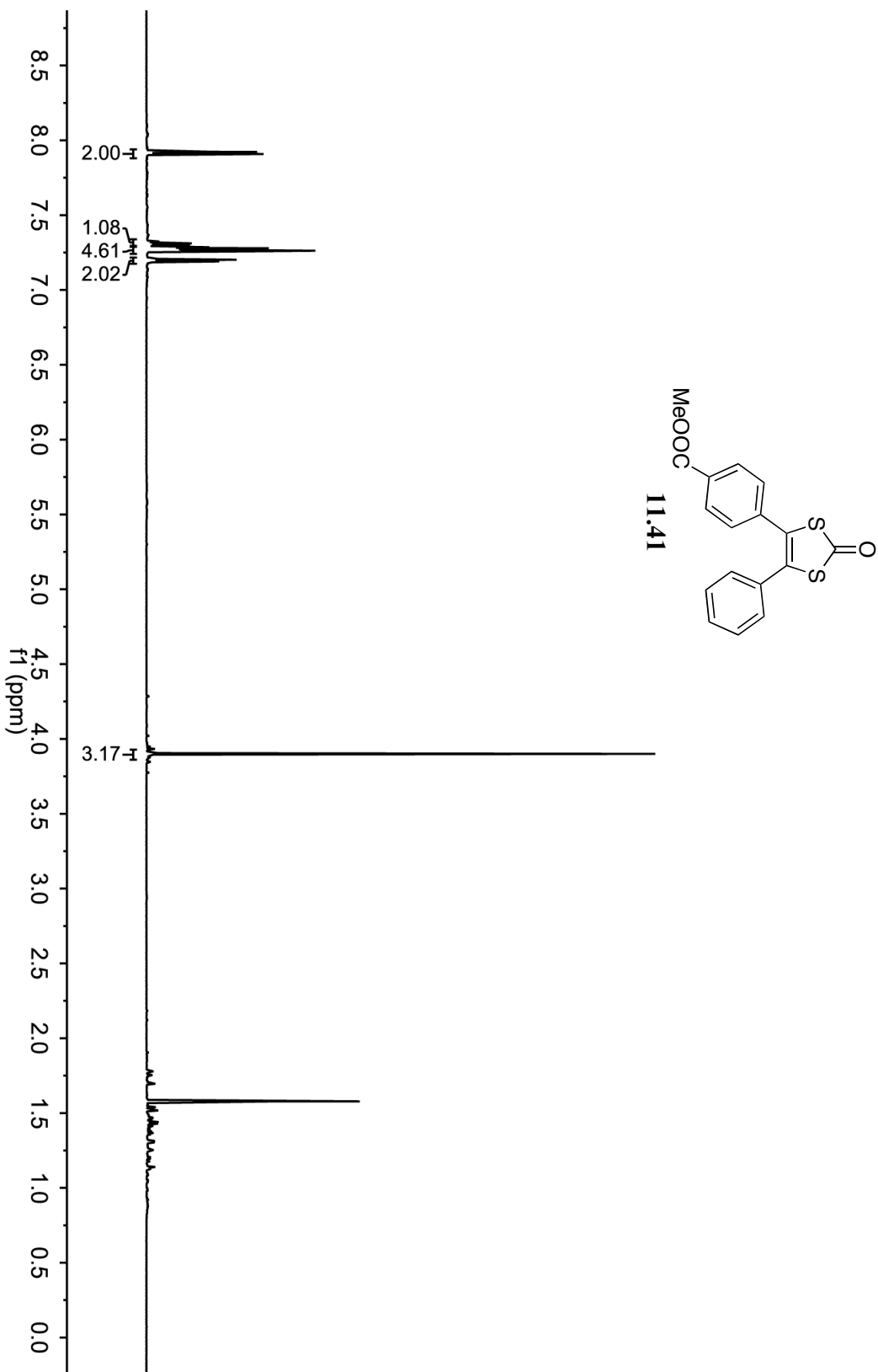


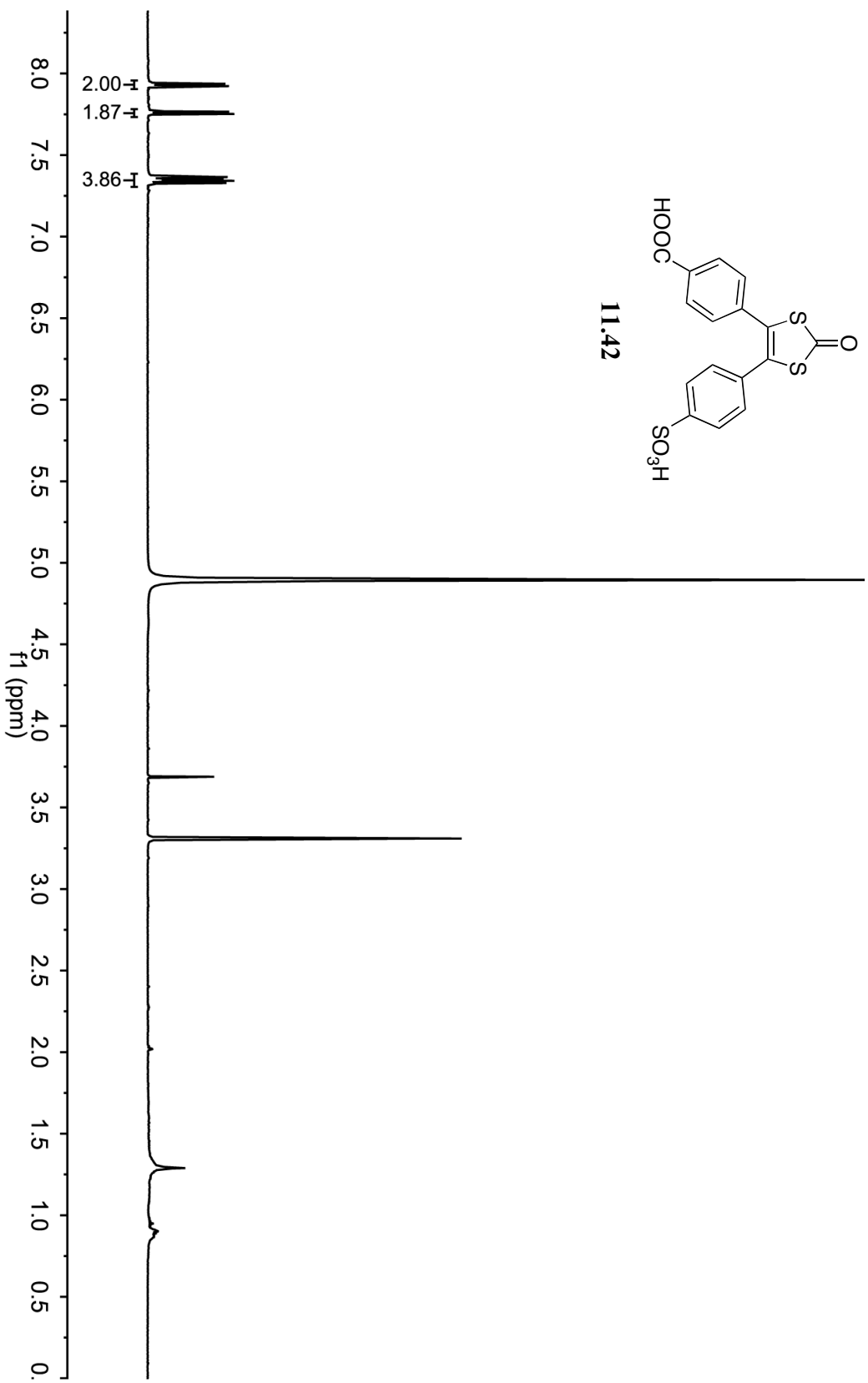


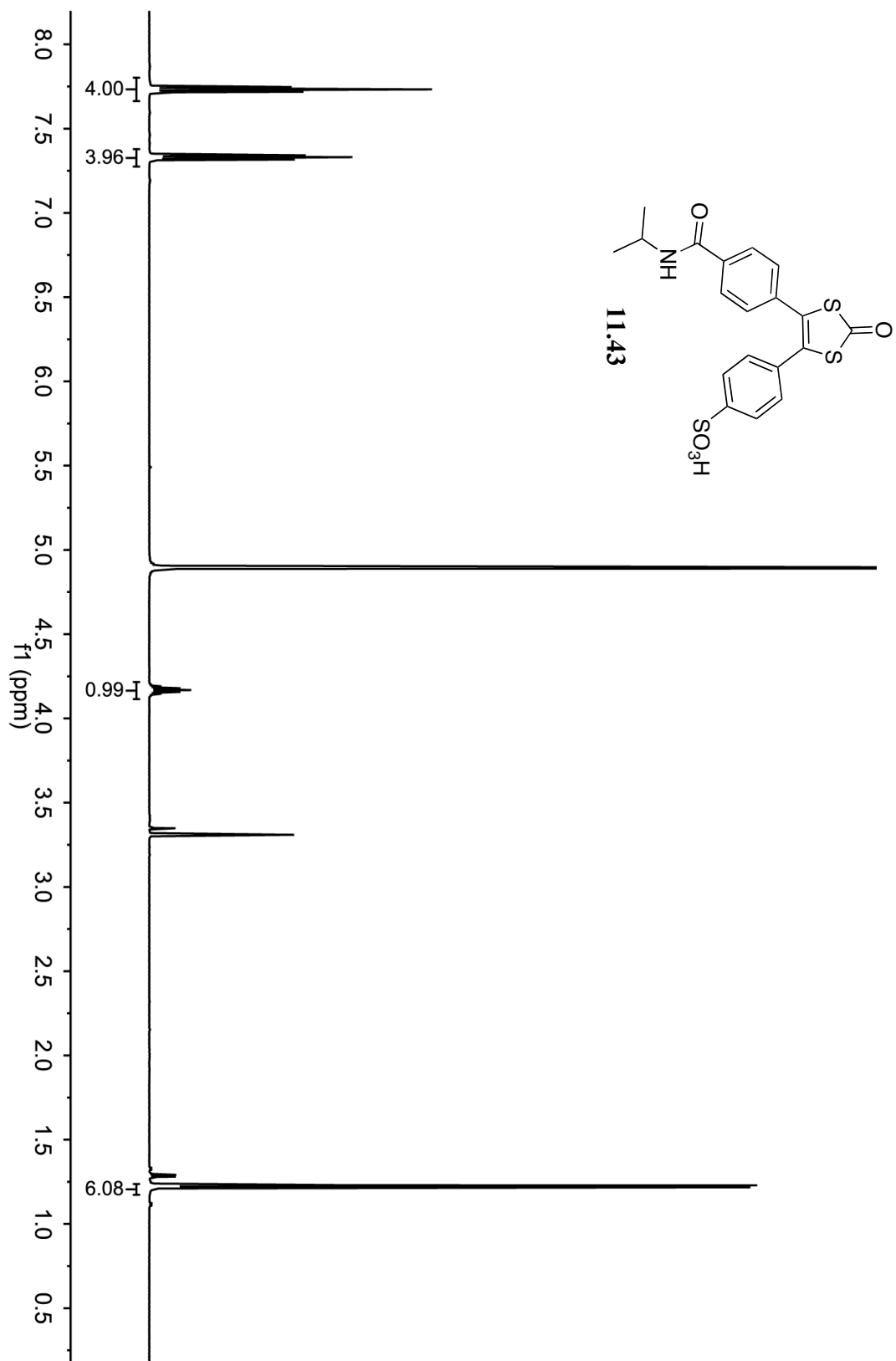


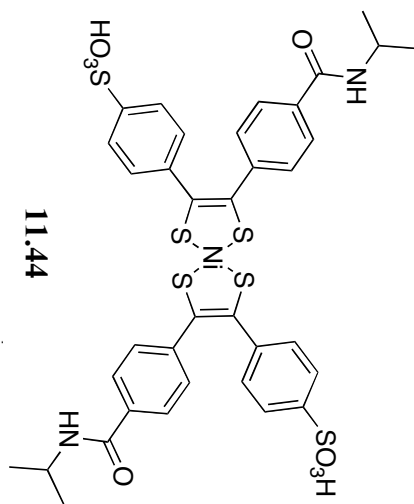
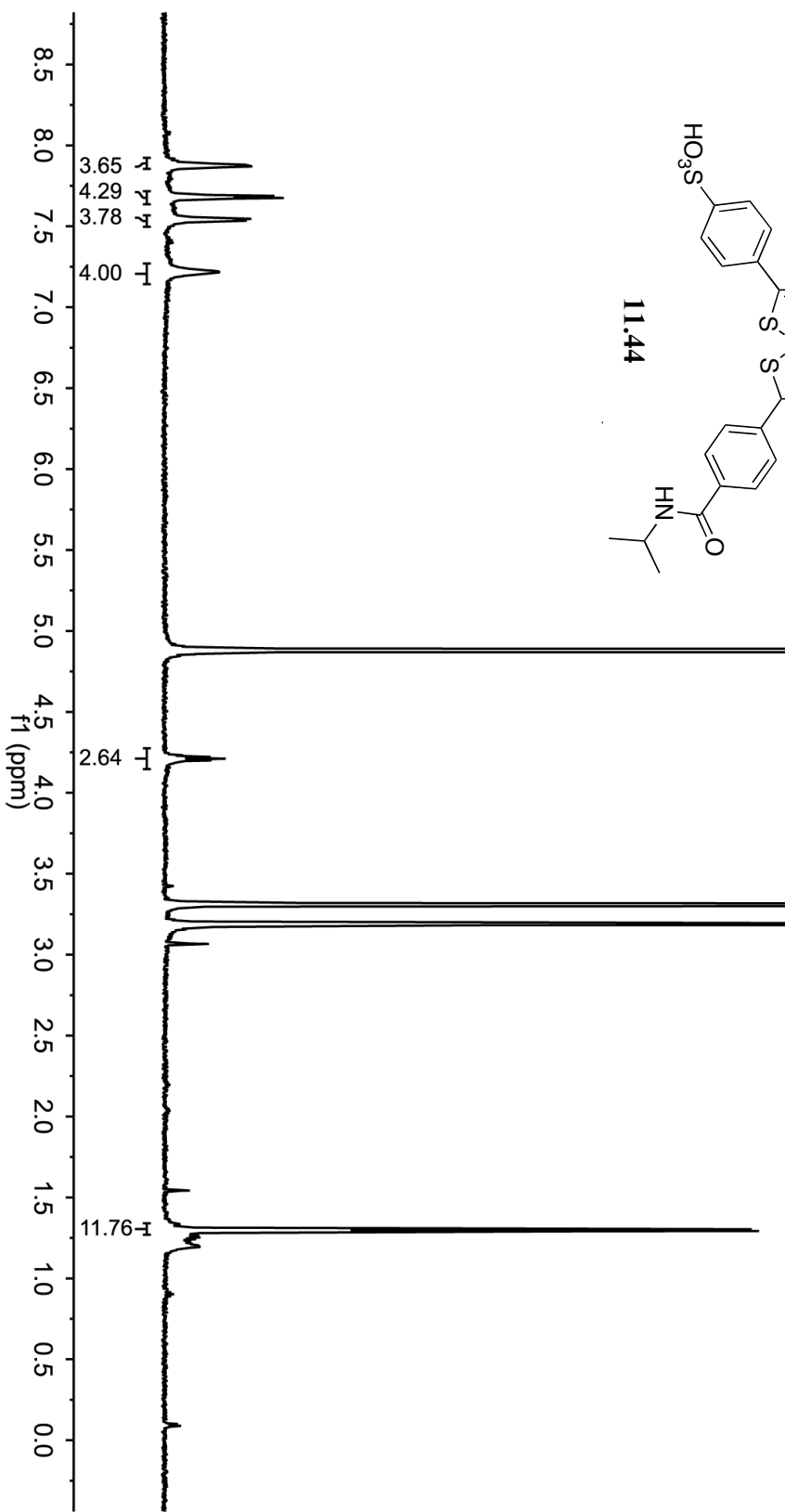
11.40

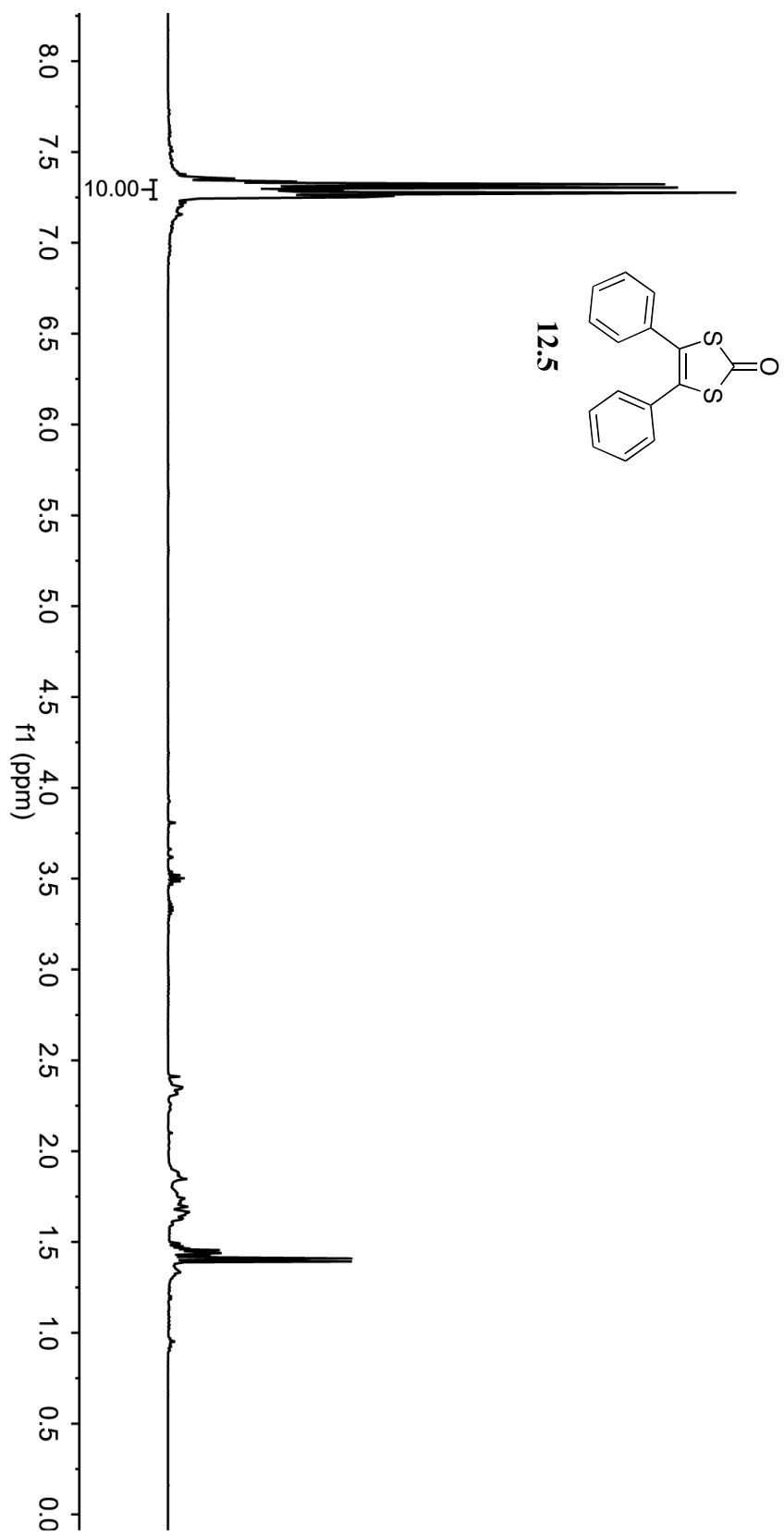


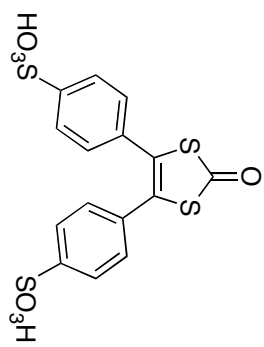




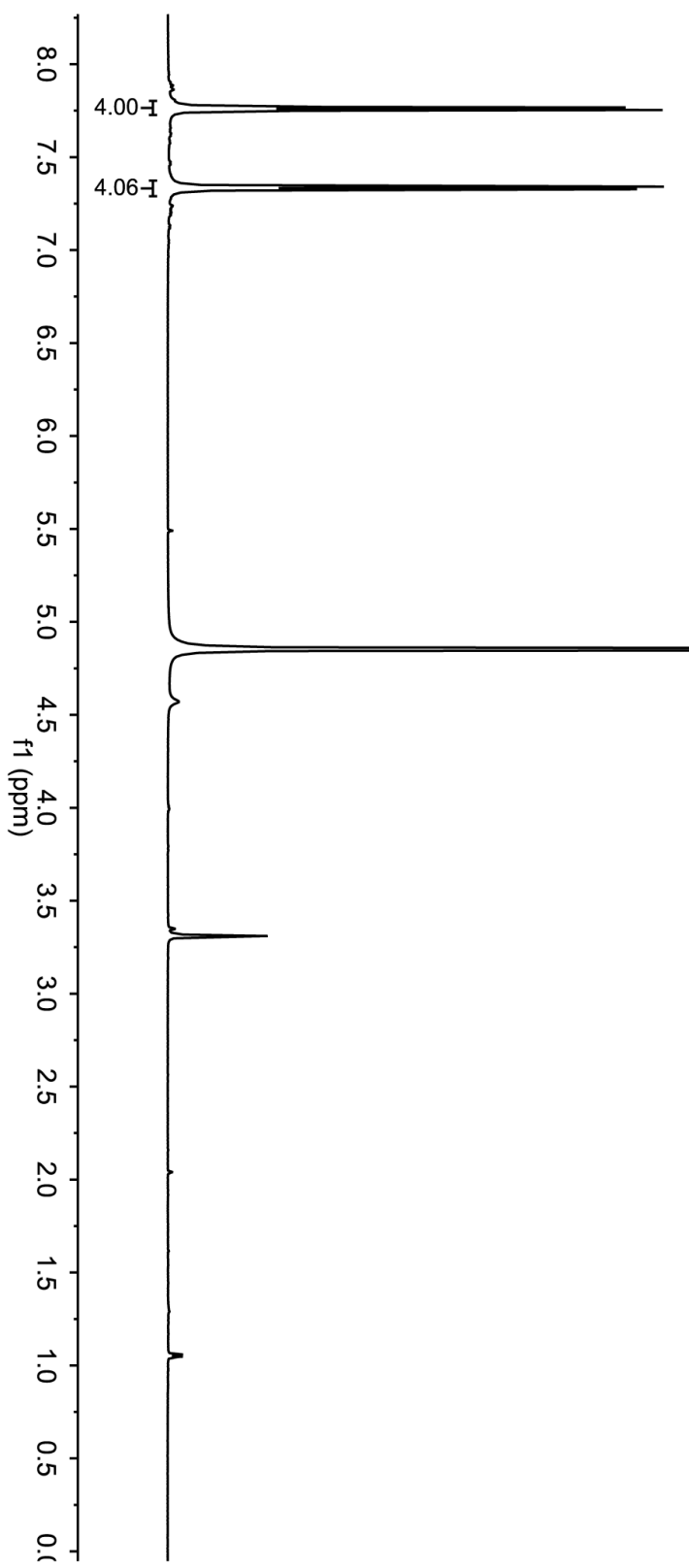


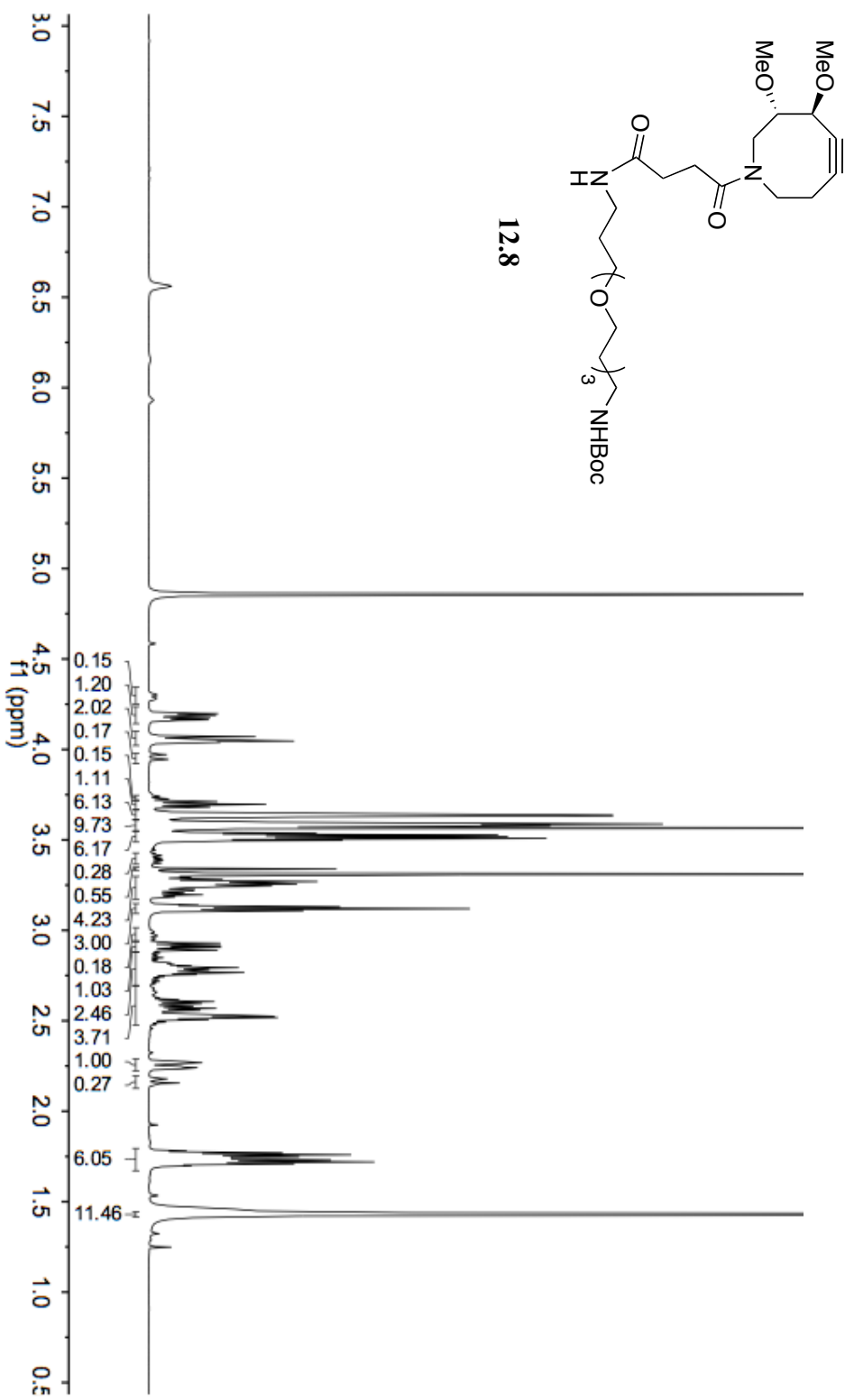


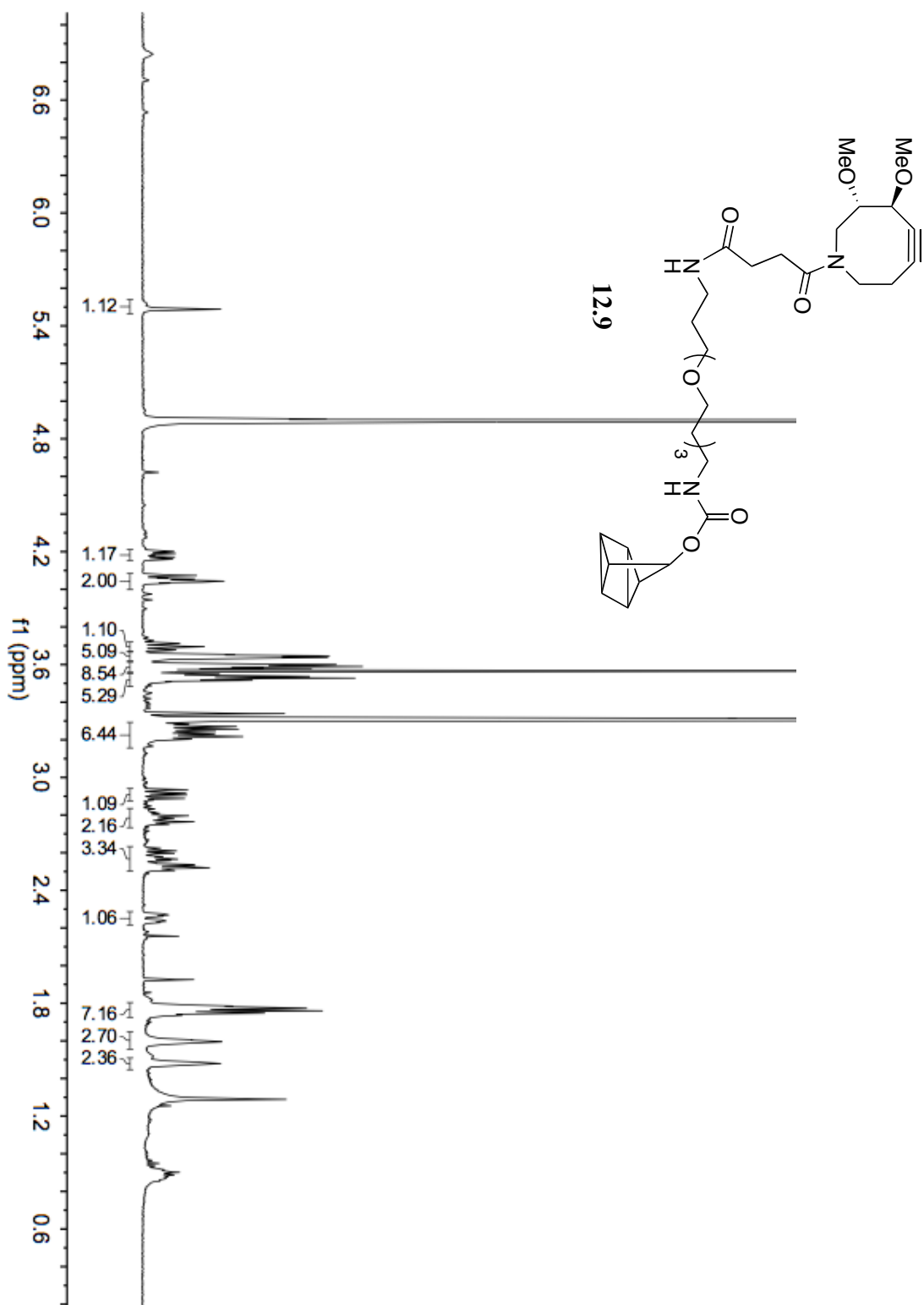




12.6

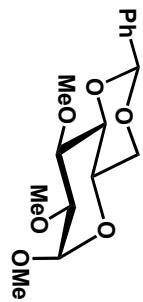




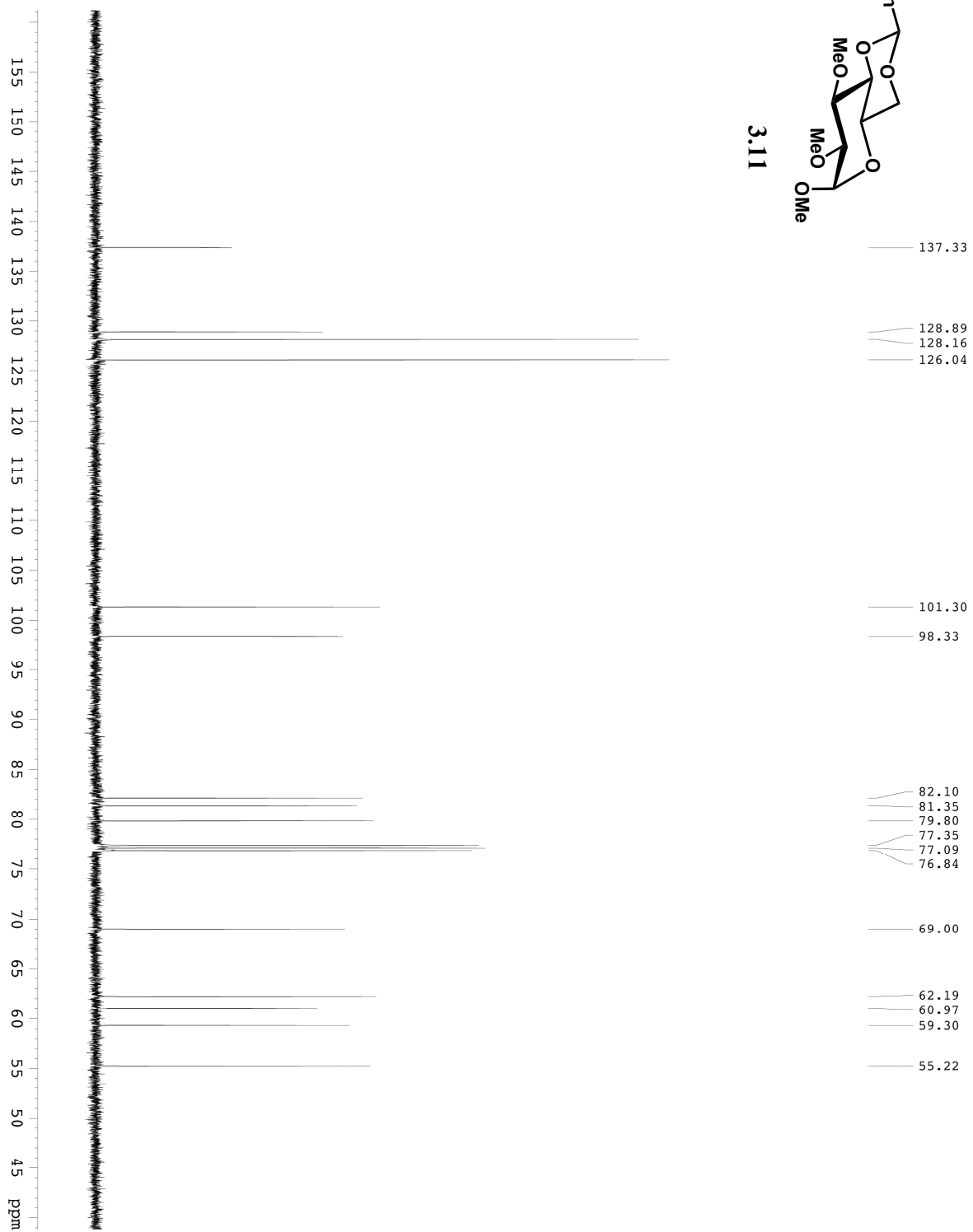


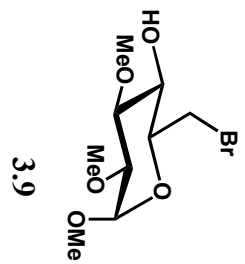
Appendix B

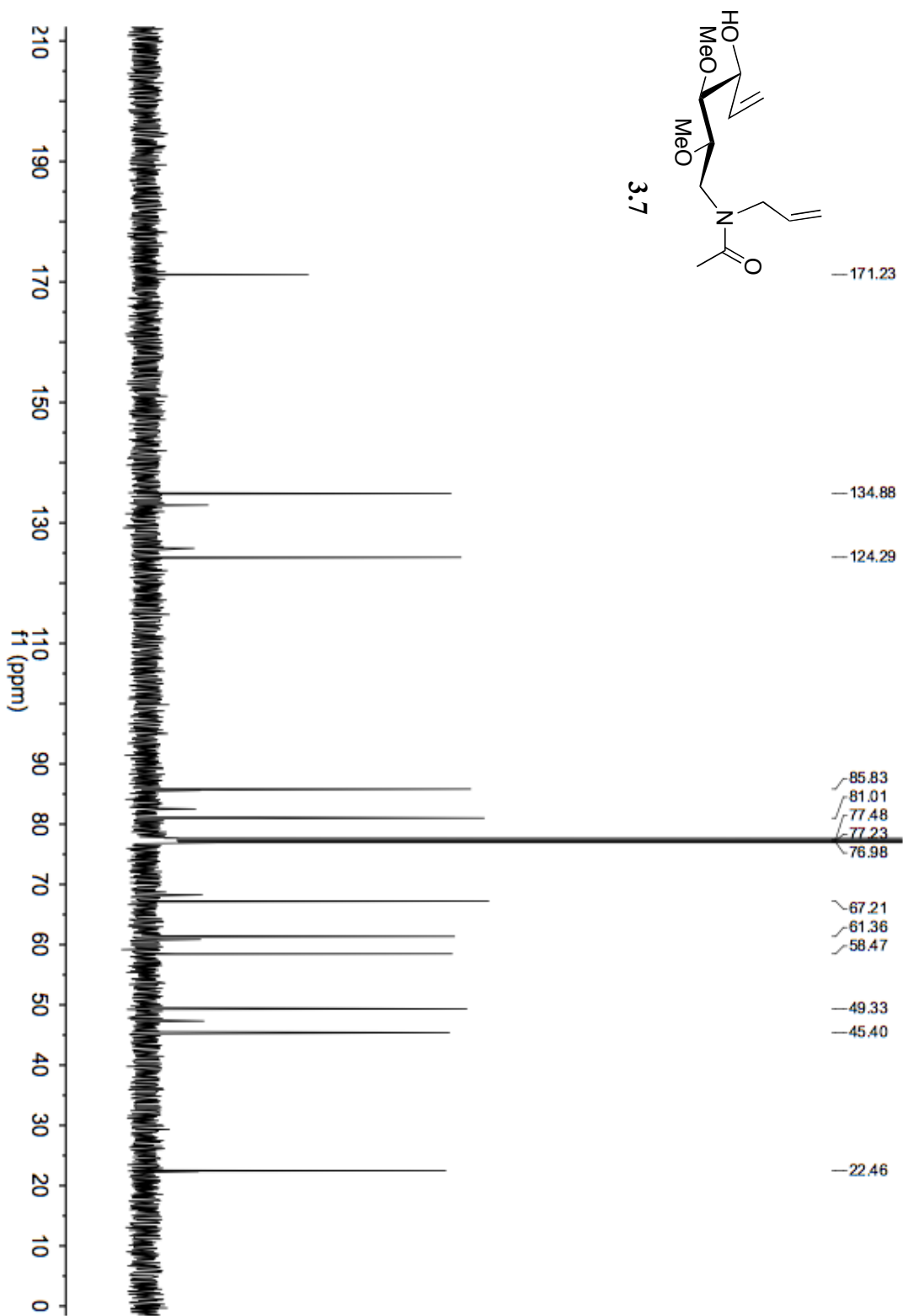
¹³C NMR Spectra

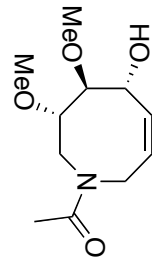


3.11

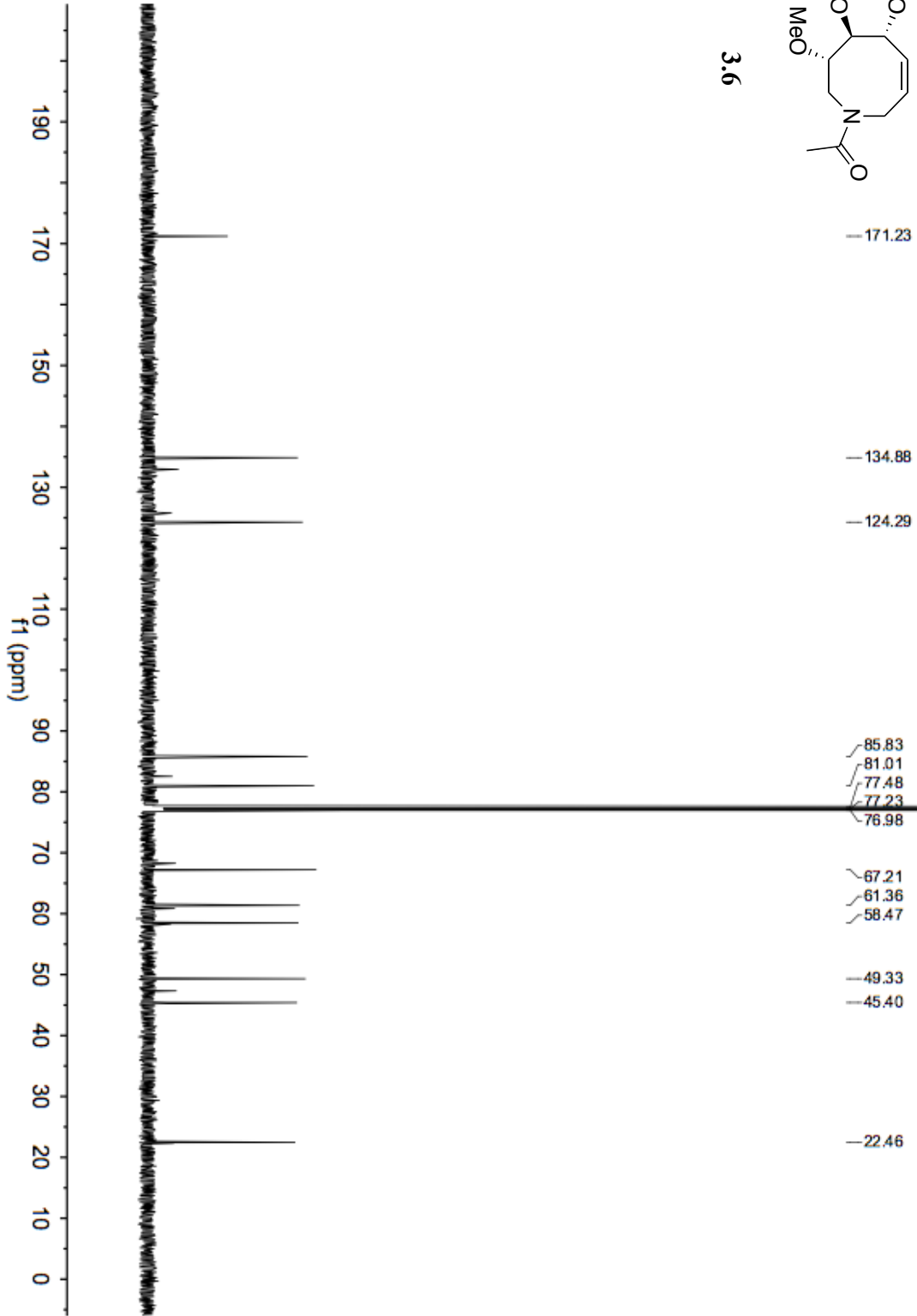


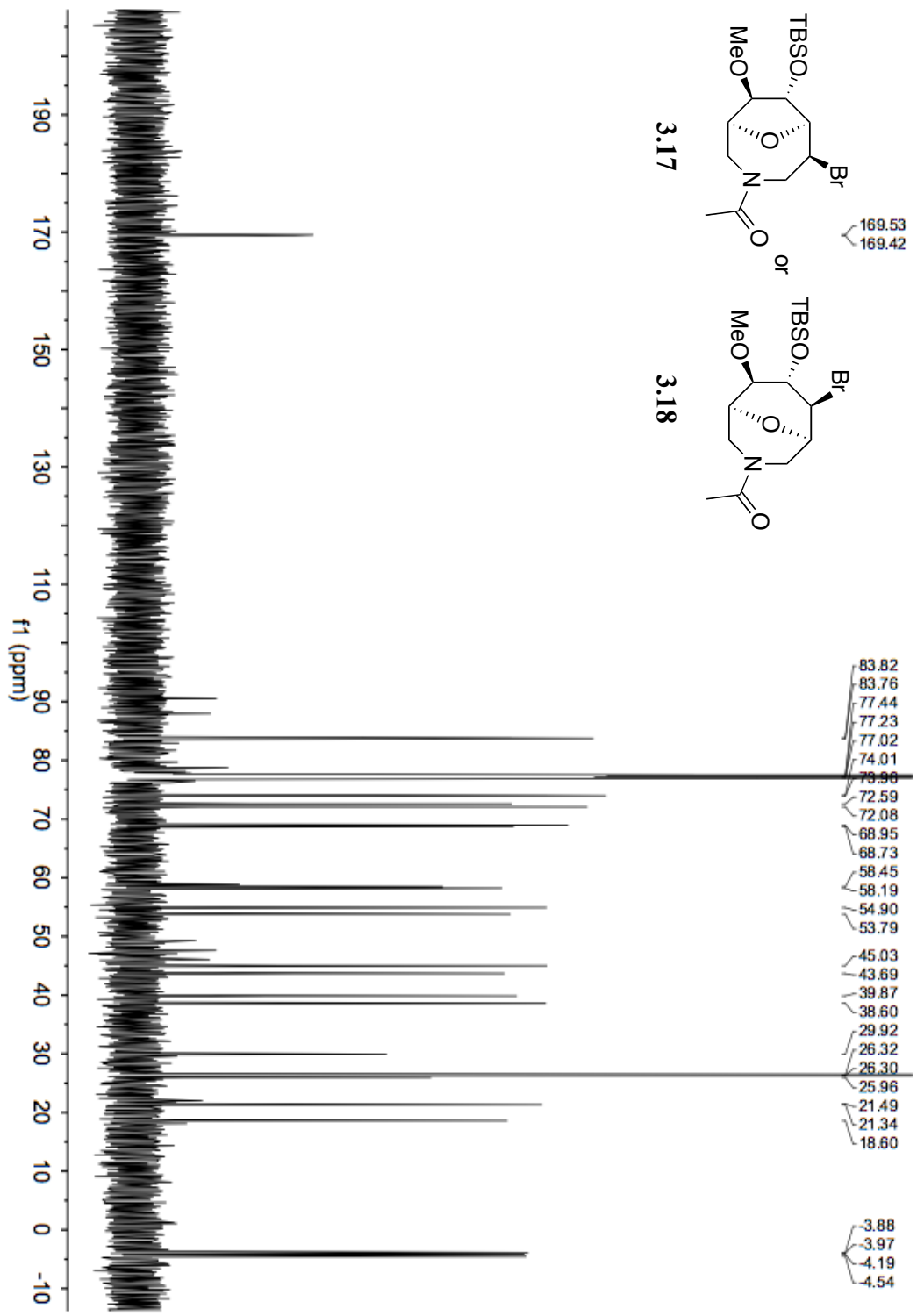


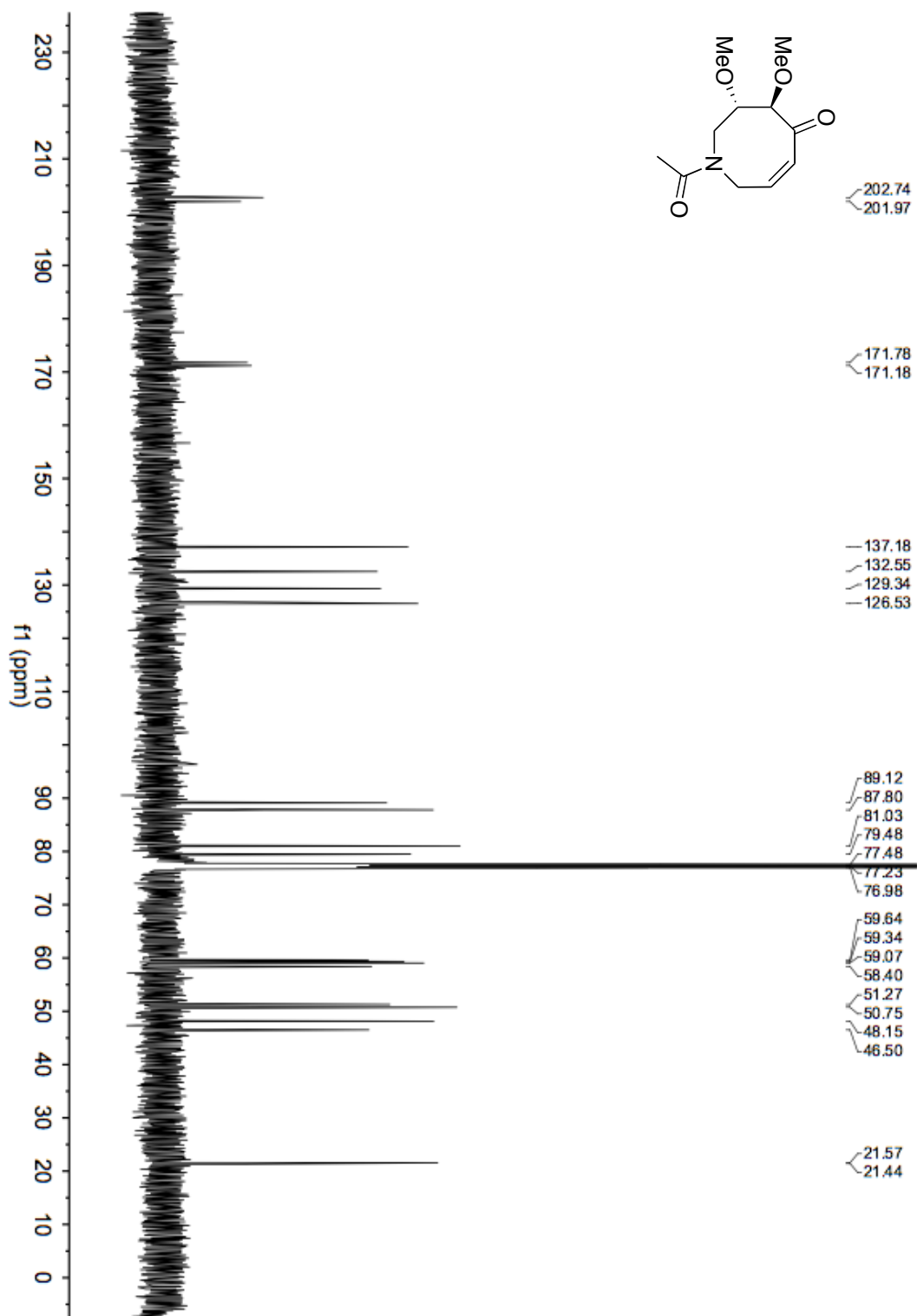


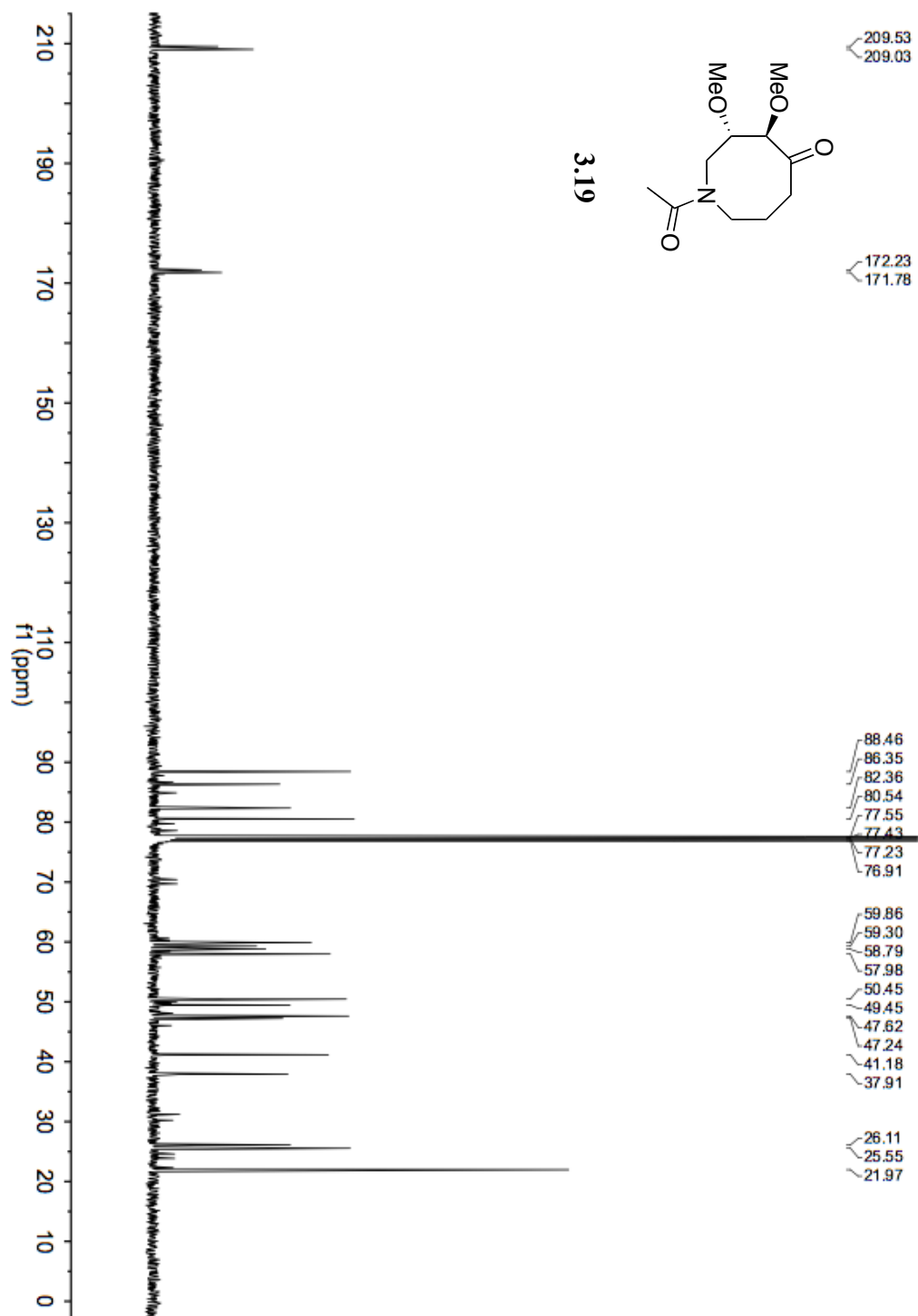


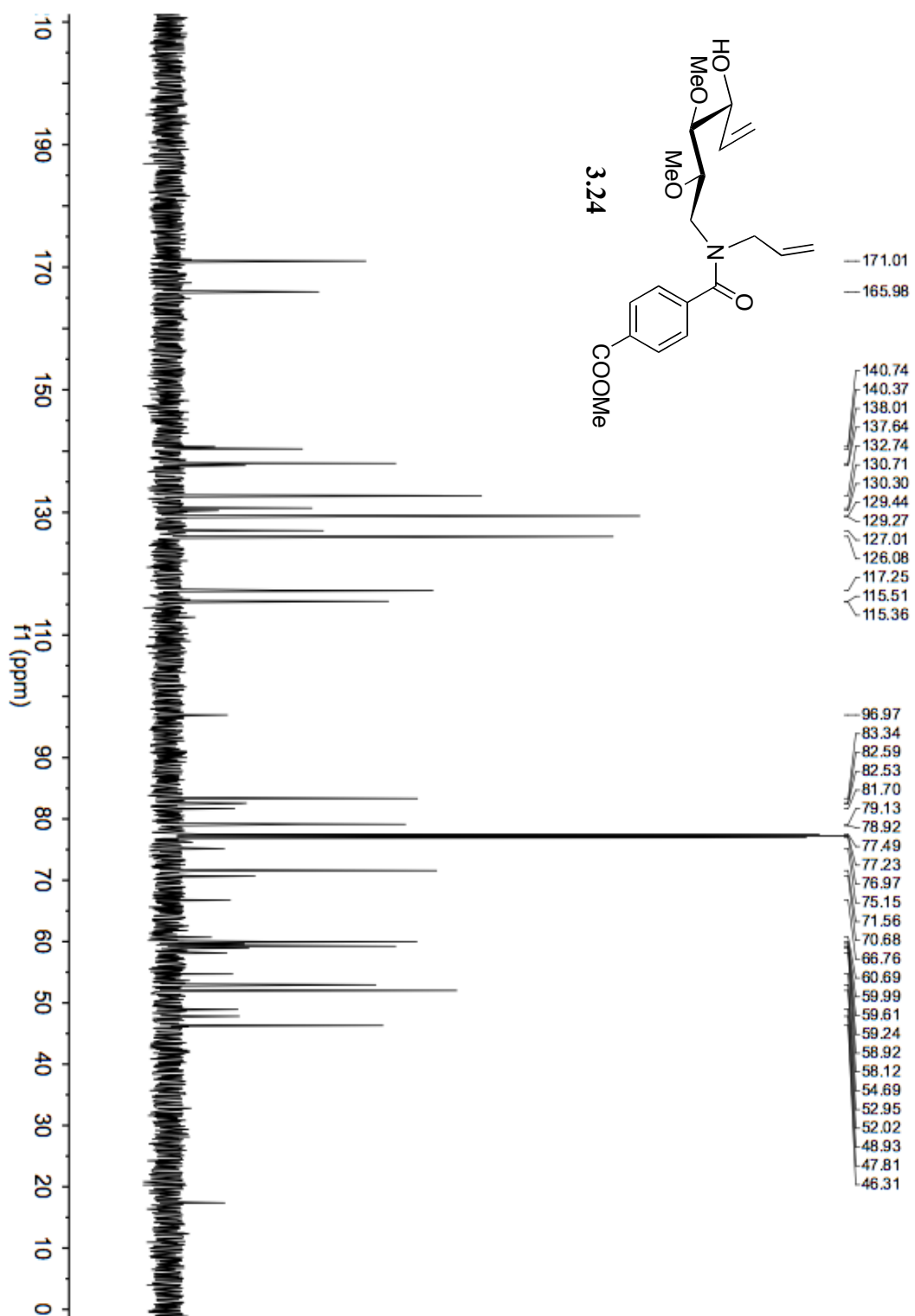
3.6

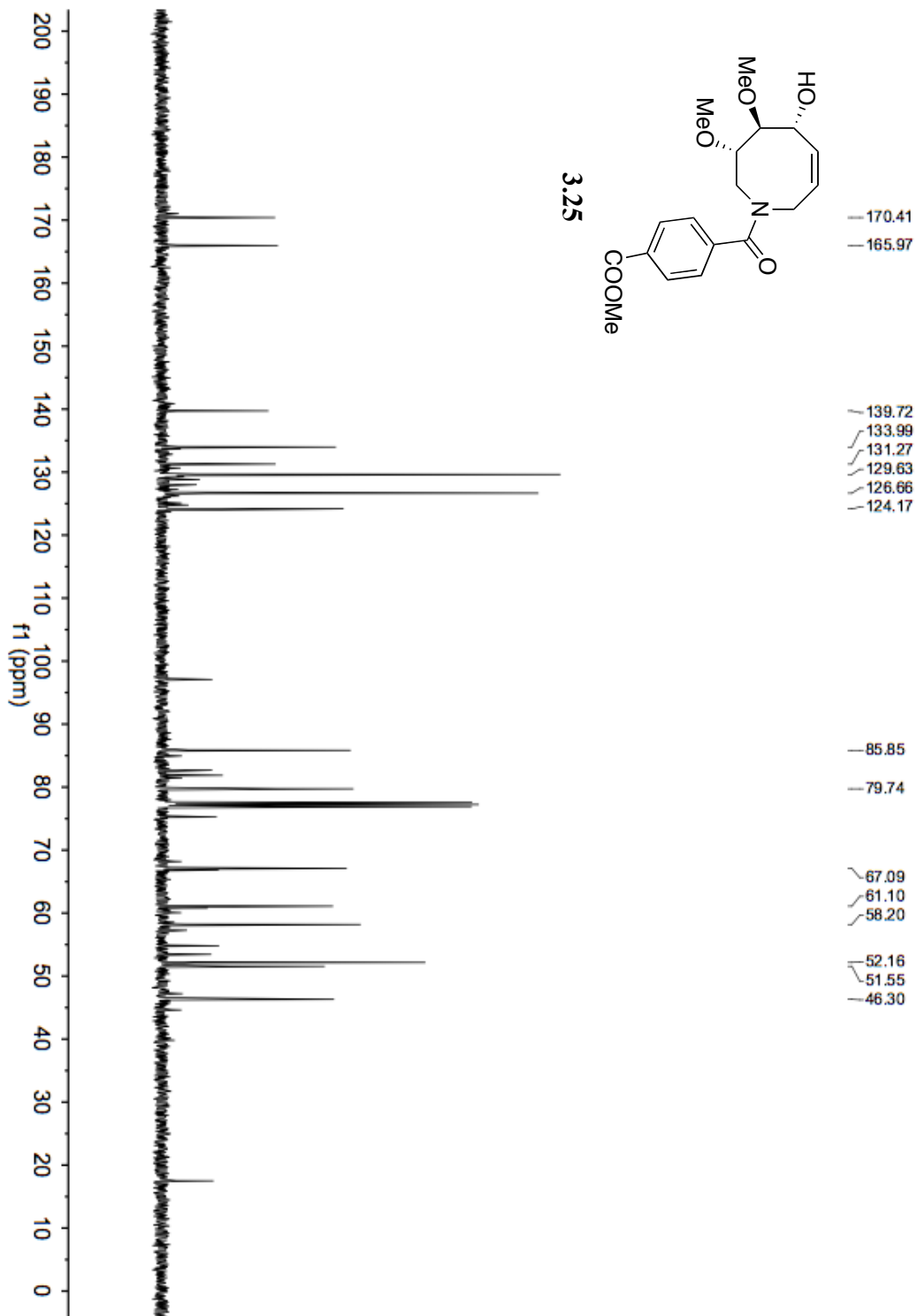


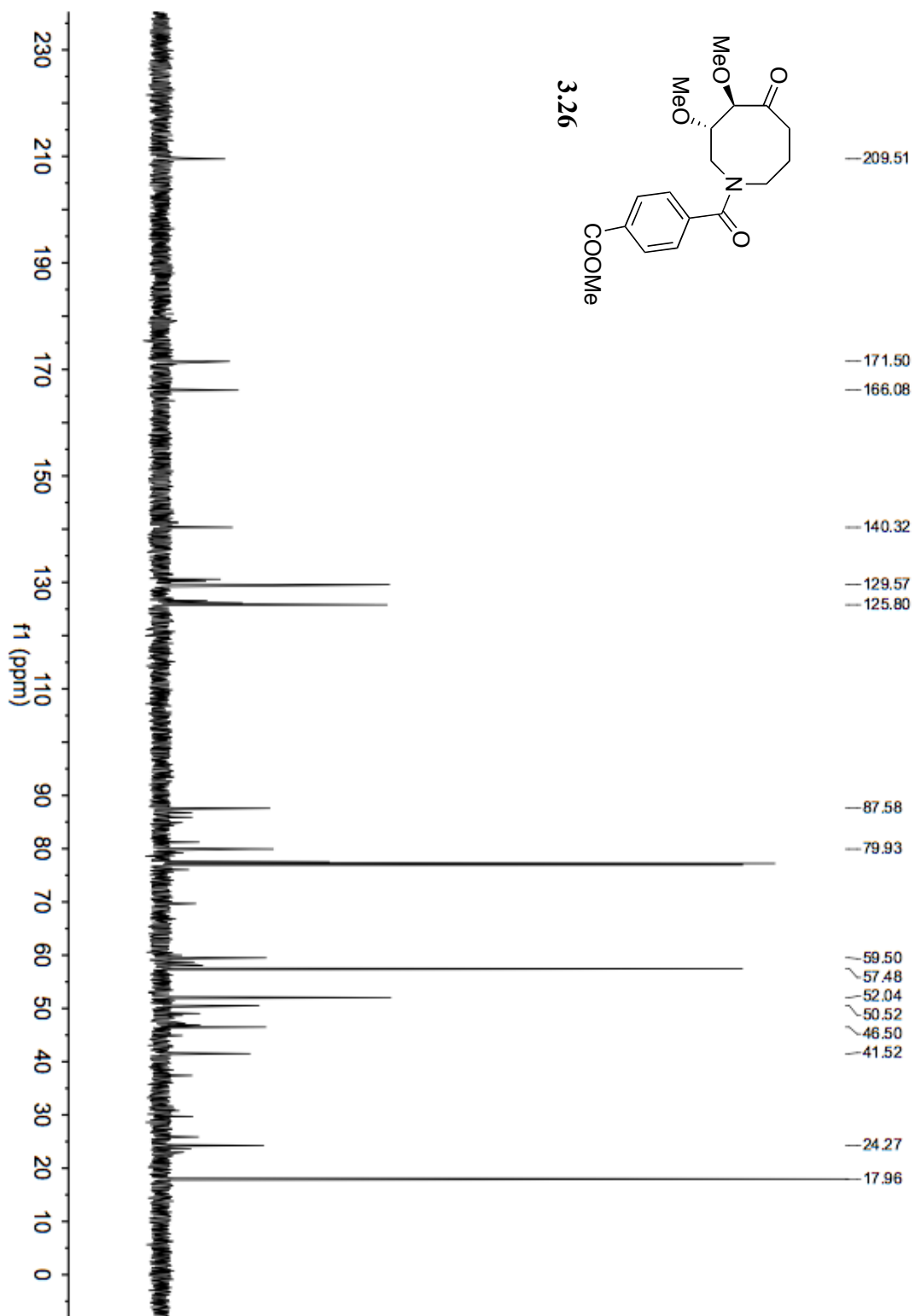


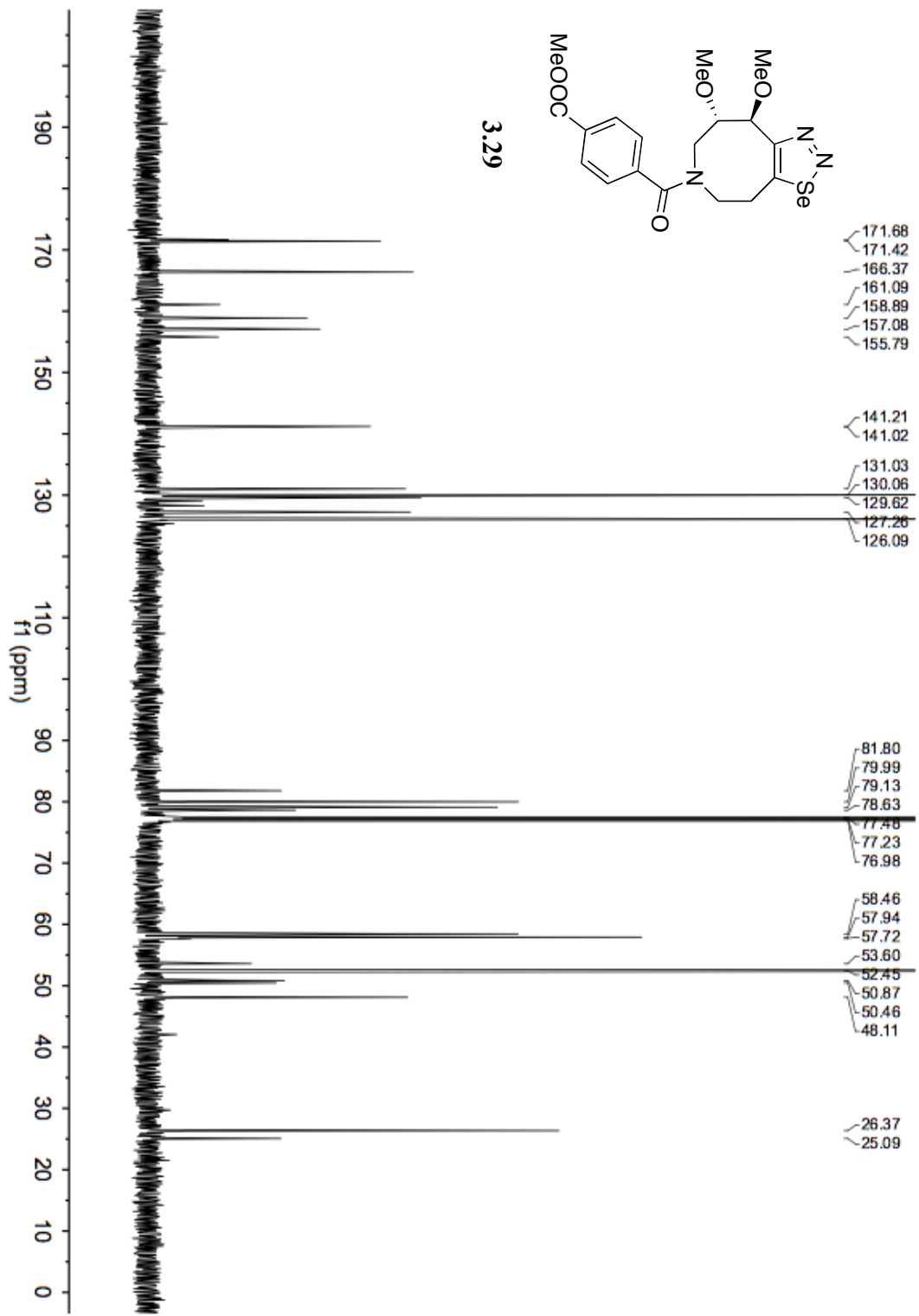


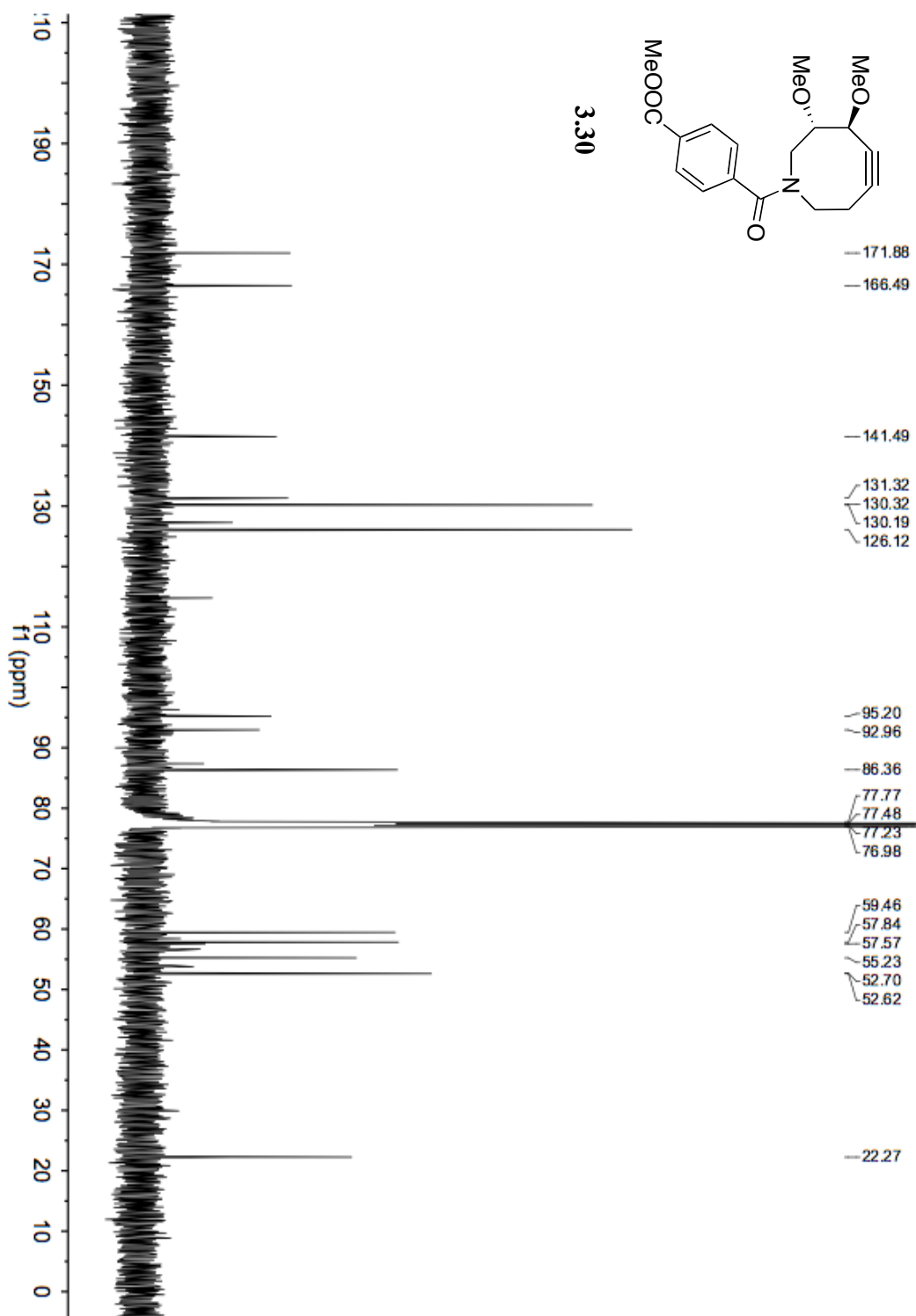


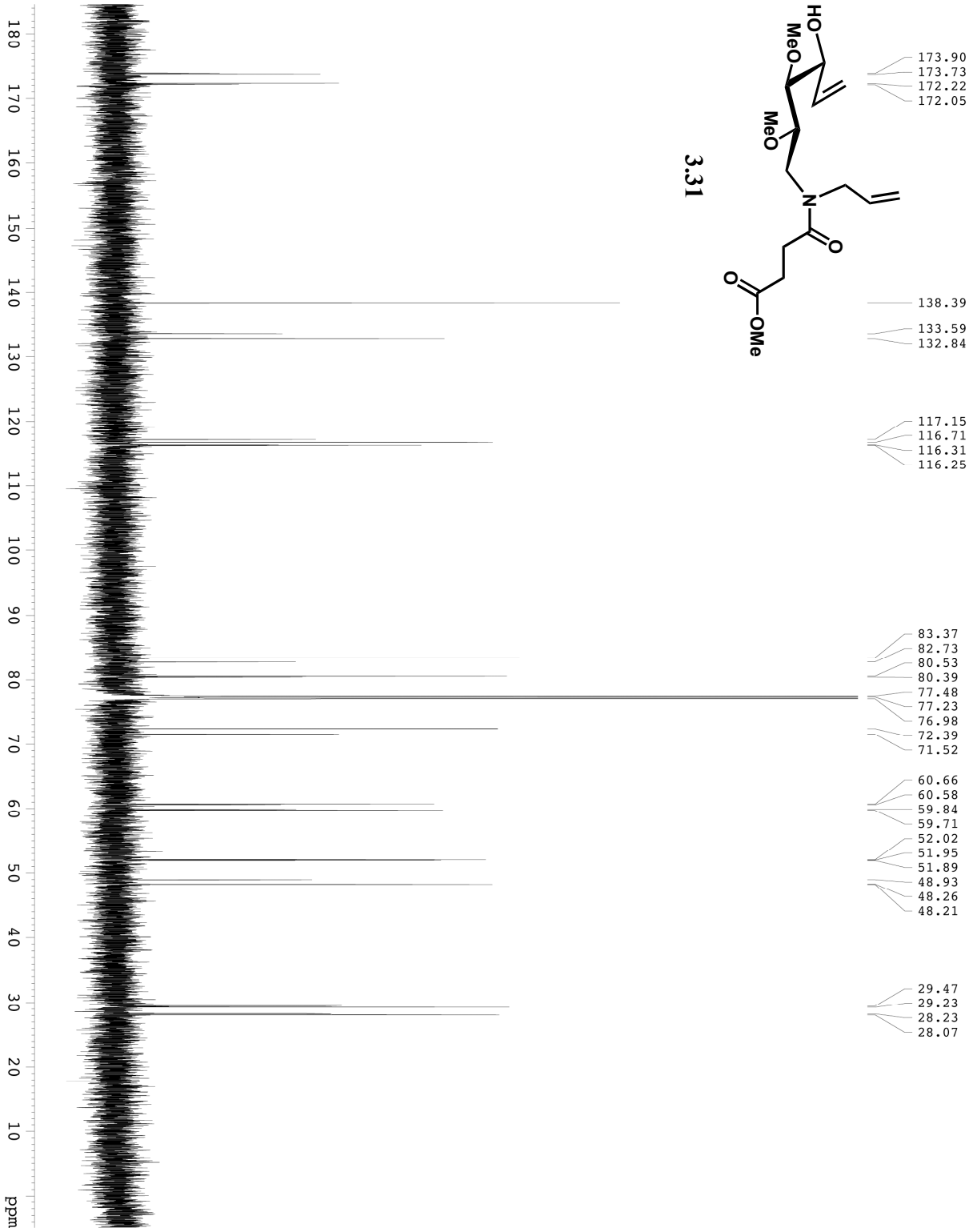


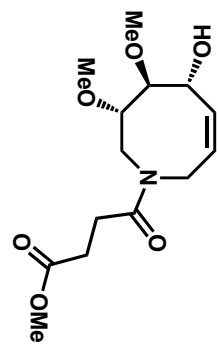




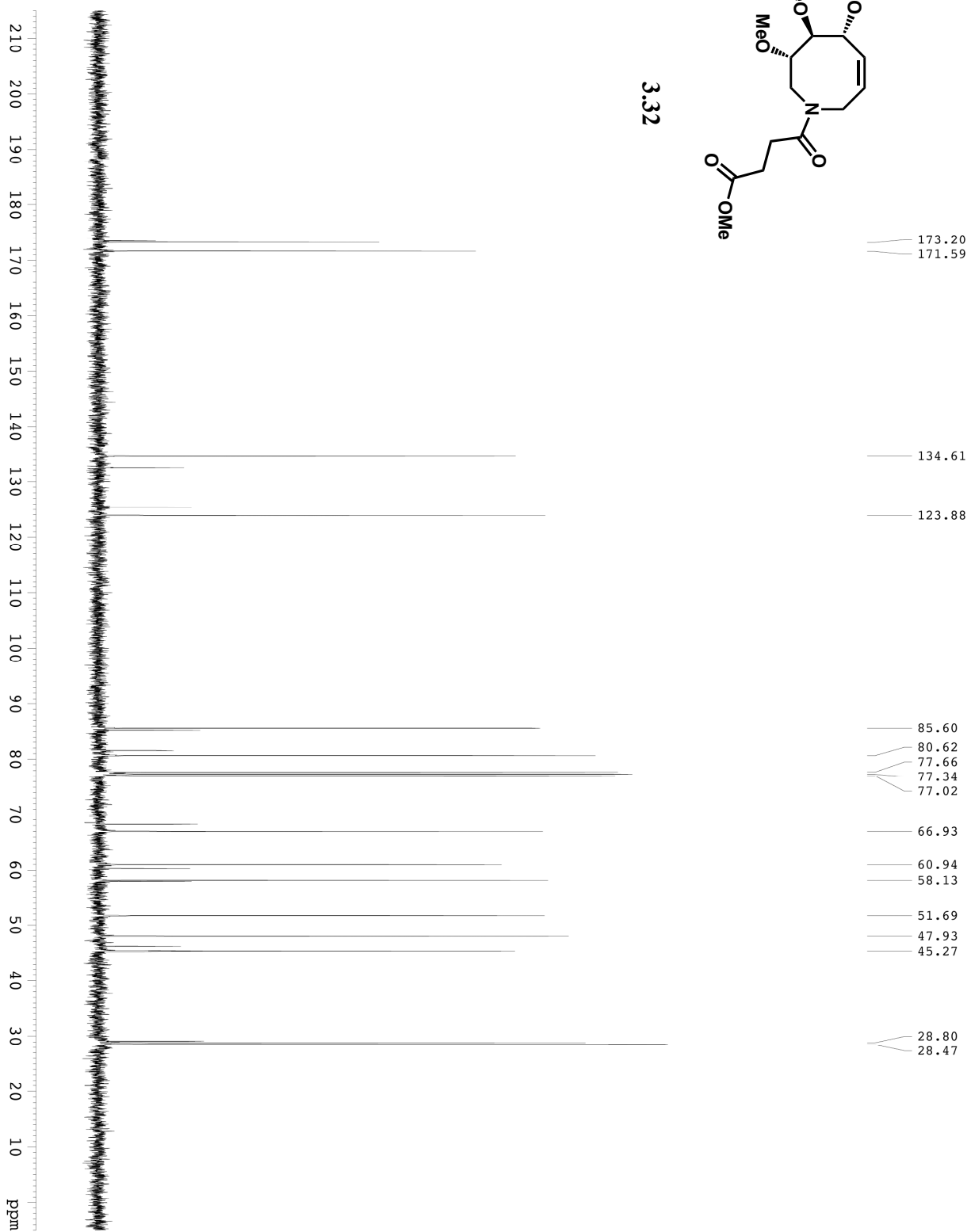




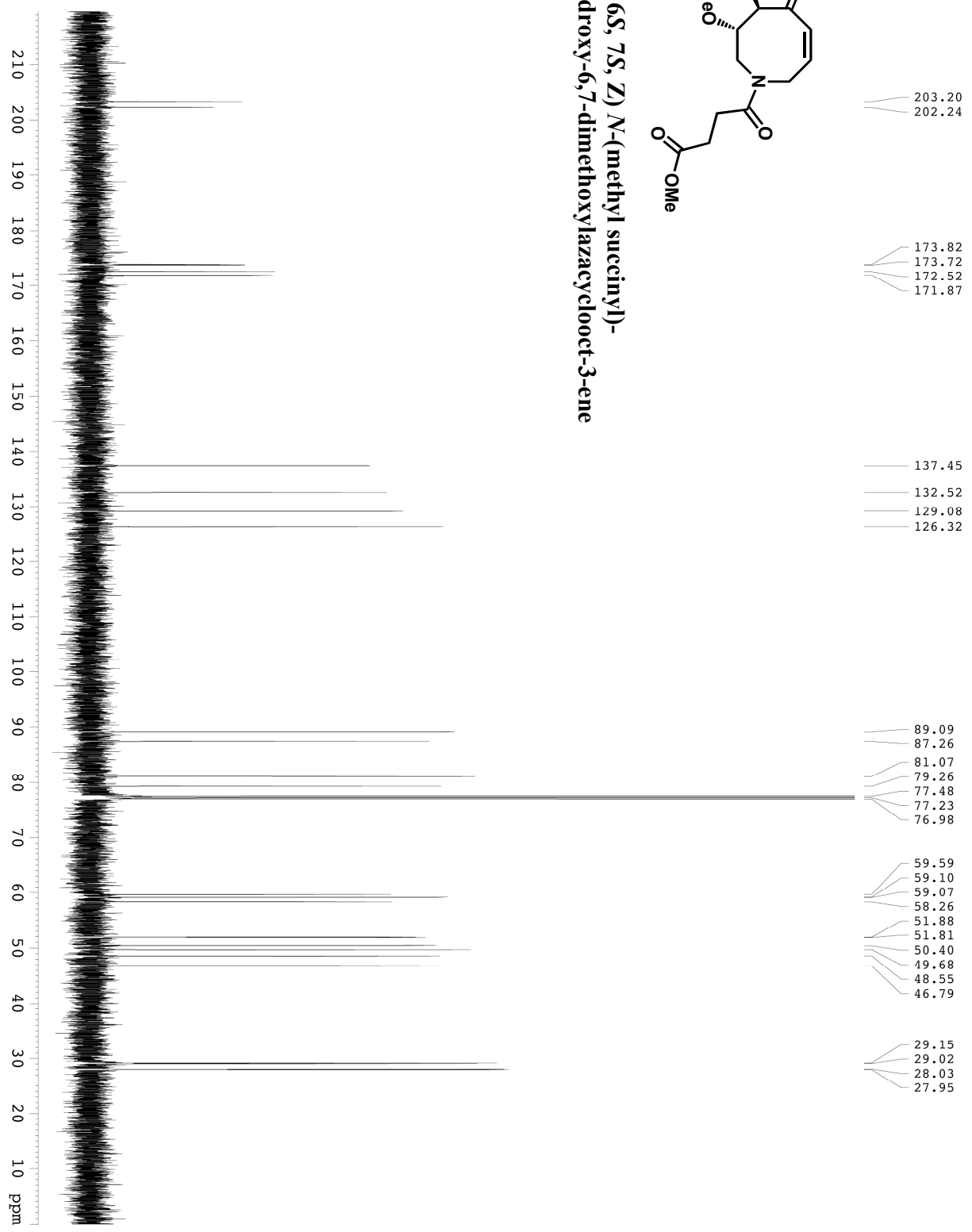
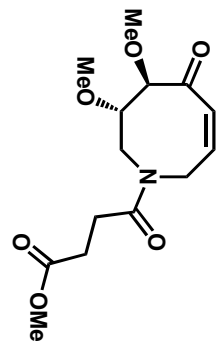


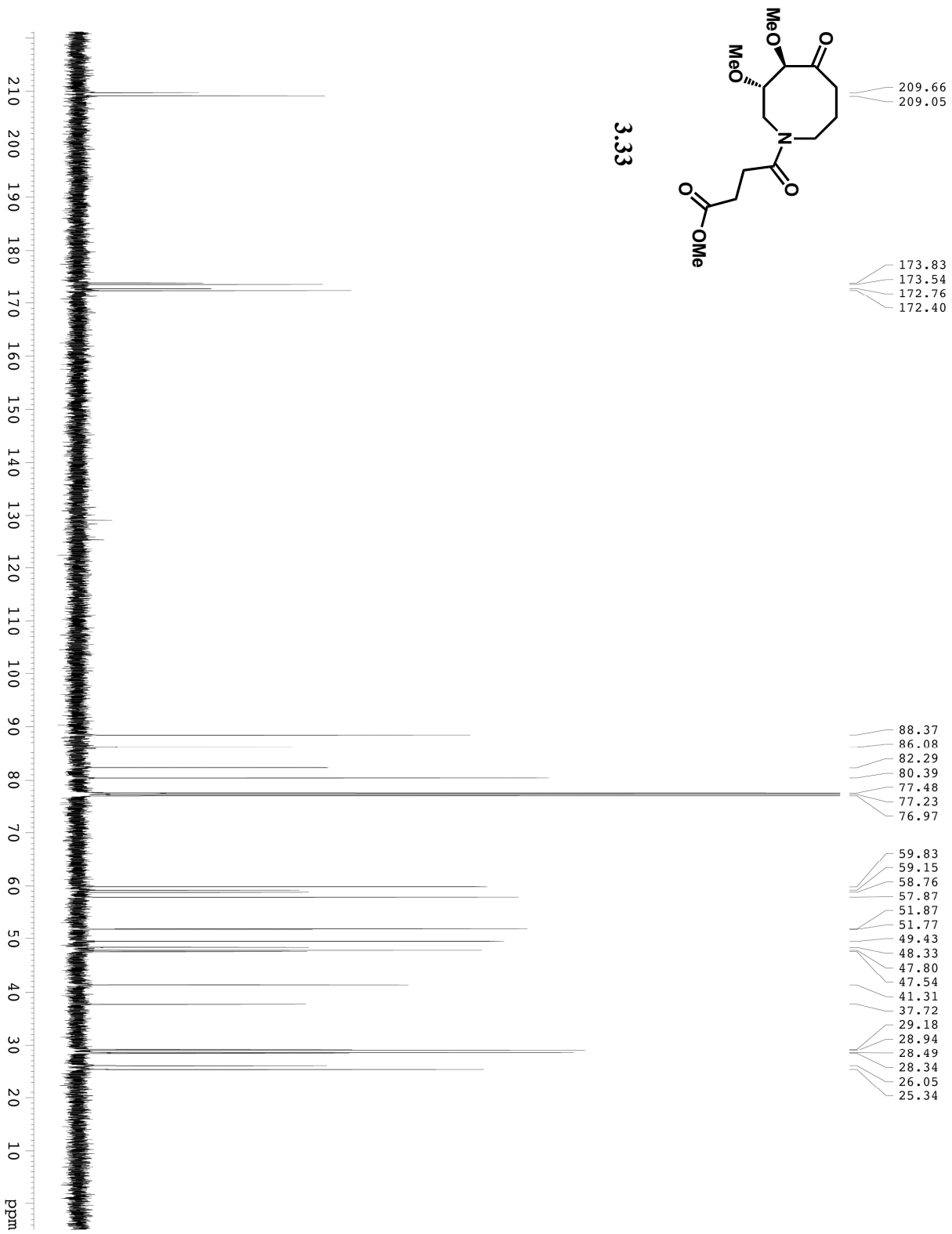


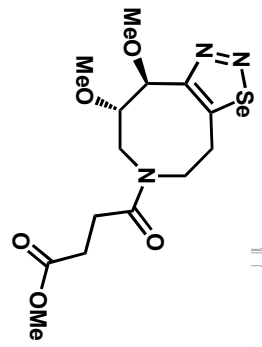
3.32



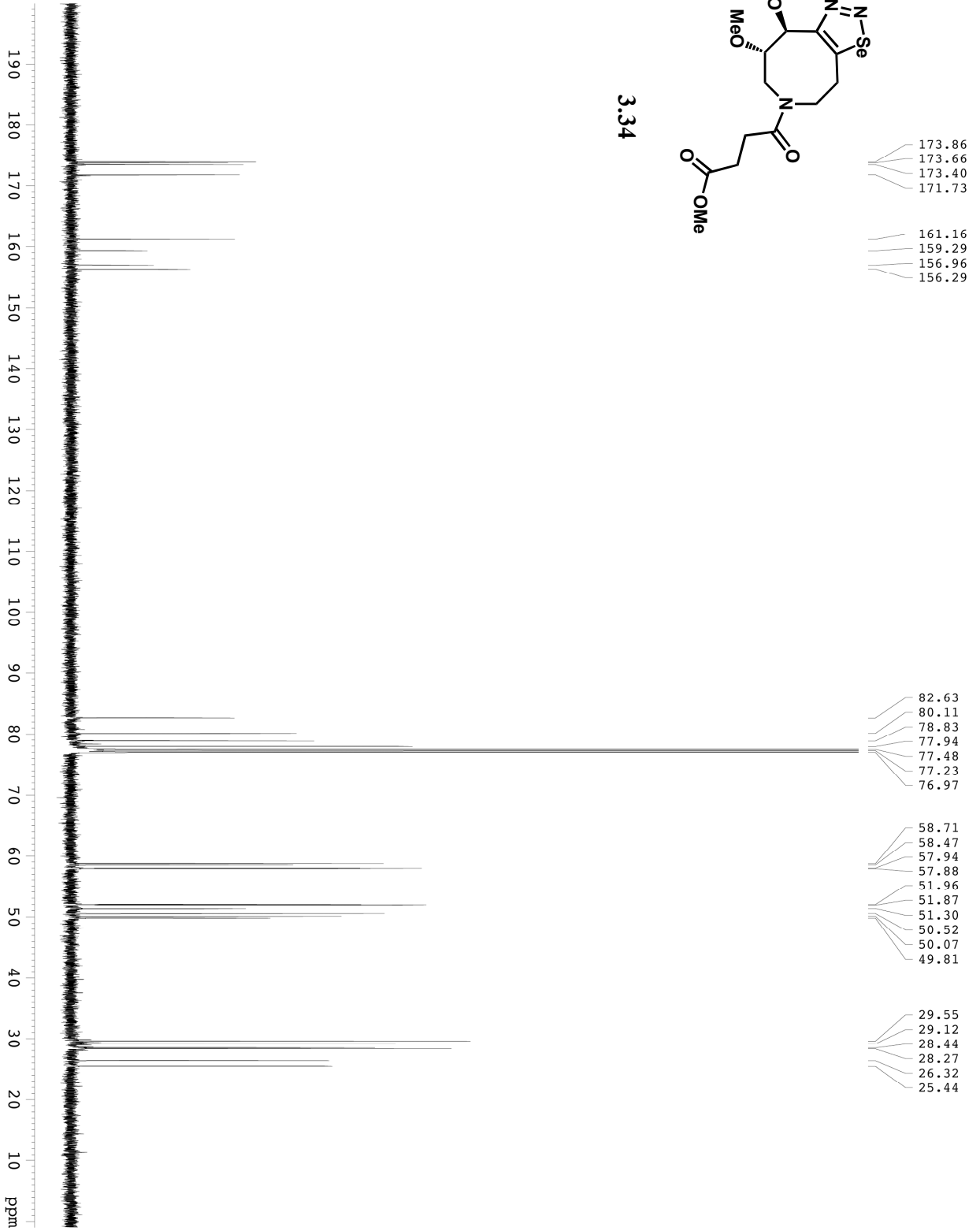
**(5*R*, 6*S*, 7*S*, 2*Z*) *N*-(methyl succinyl)-
5-hydroxy-6,7-dimethoxylazacyclooct-3-ene**

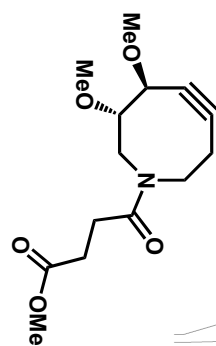






3.34



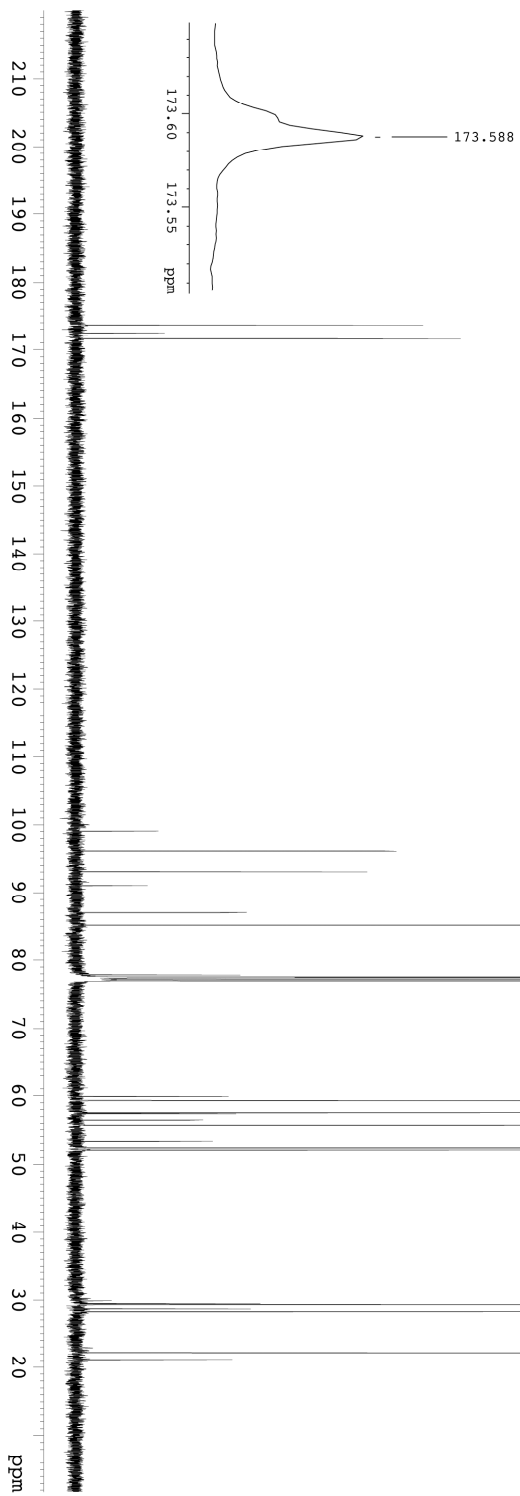


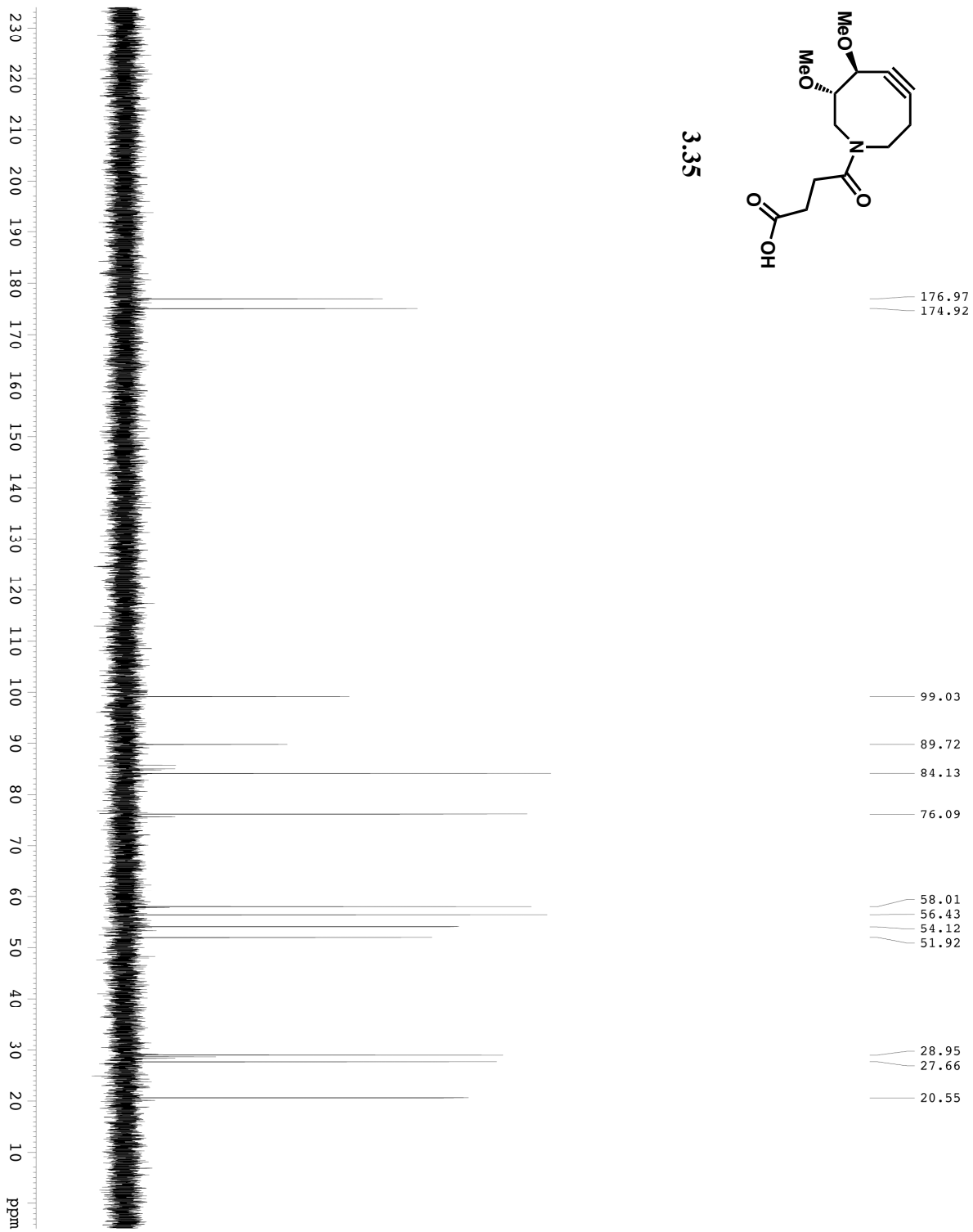
**(6*S*, 7*S*) *N*-(methyl succinyl)-
6,7-dimethoxyazacyclooct-4-yne**

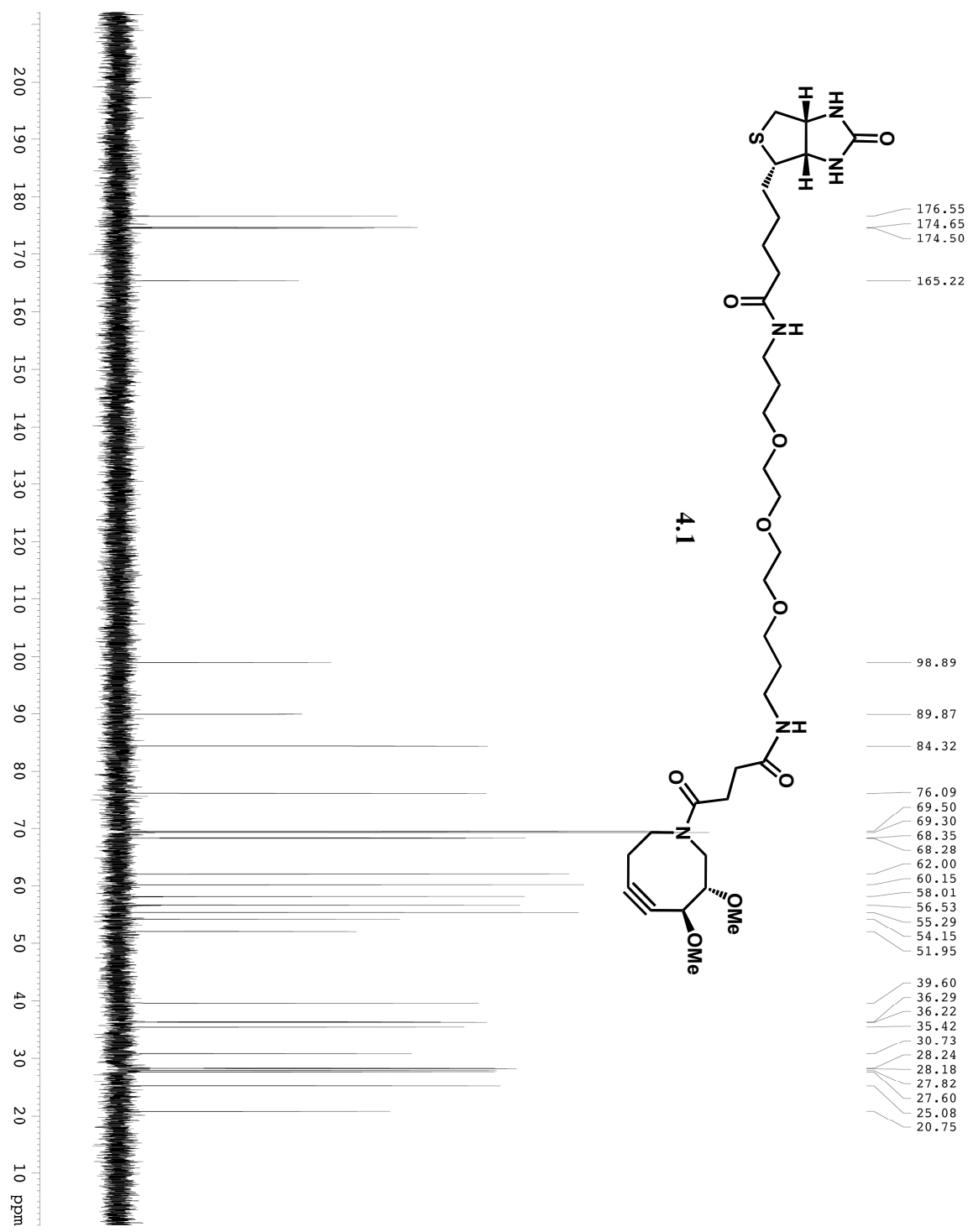
173.59
172.45
171.58

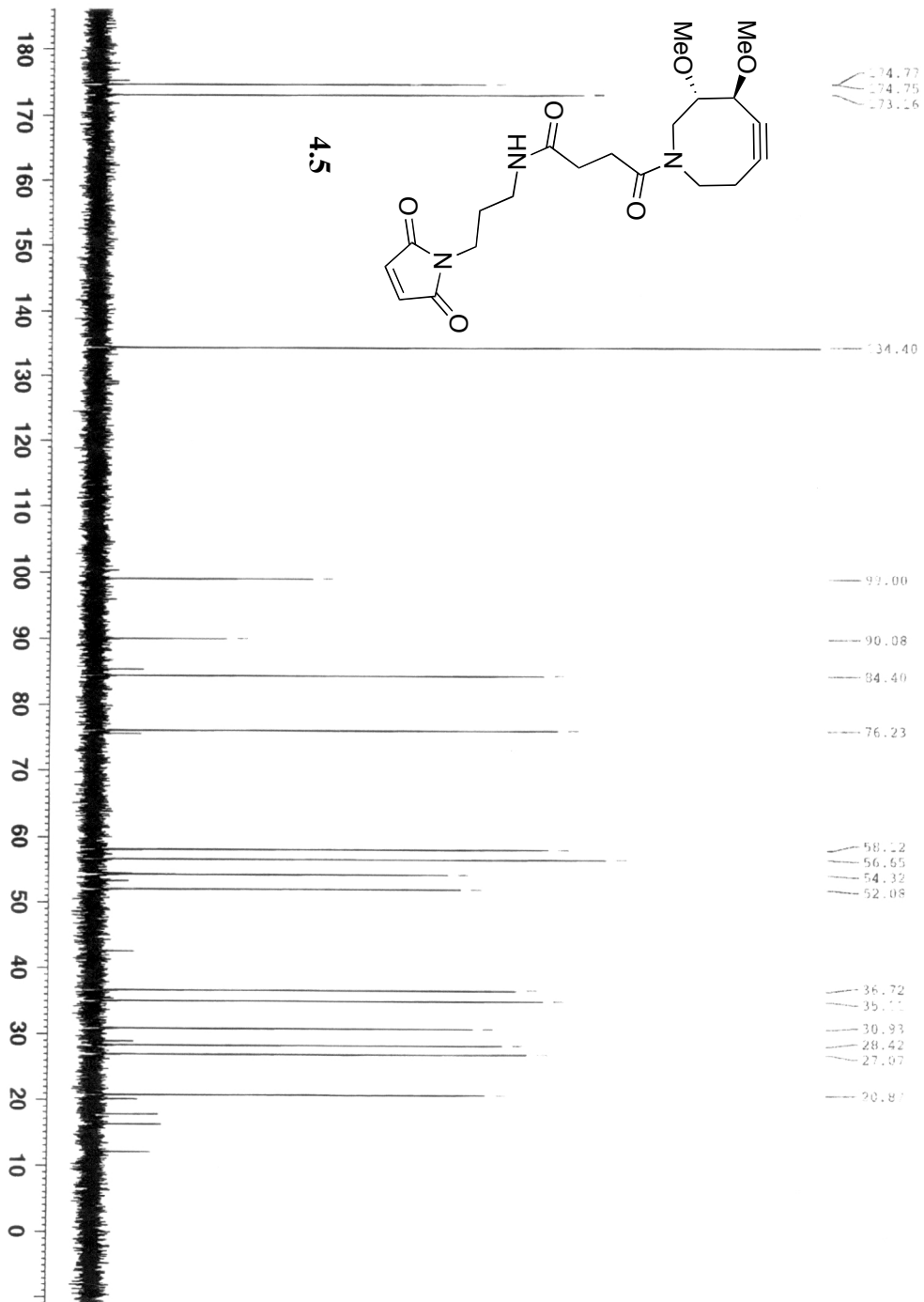
99.03
95.99
93.02
91.03
87.00
85.15
77.79
77.48
77.43
77.23
76.98
59.81
59.26
57.50
57.36
56.45
55.71
53.25
52.32
52.02
51.99

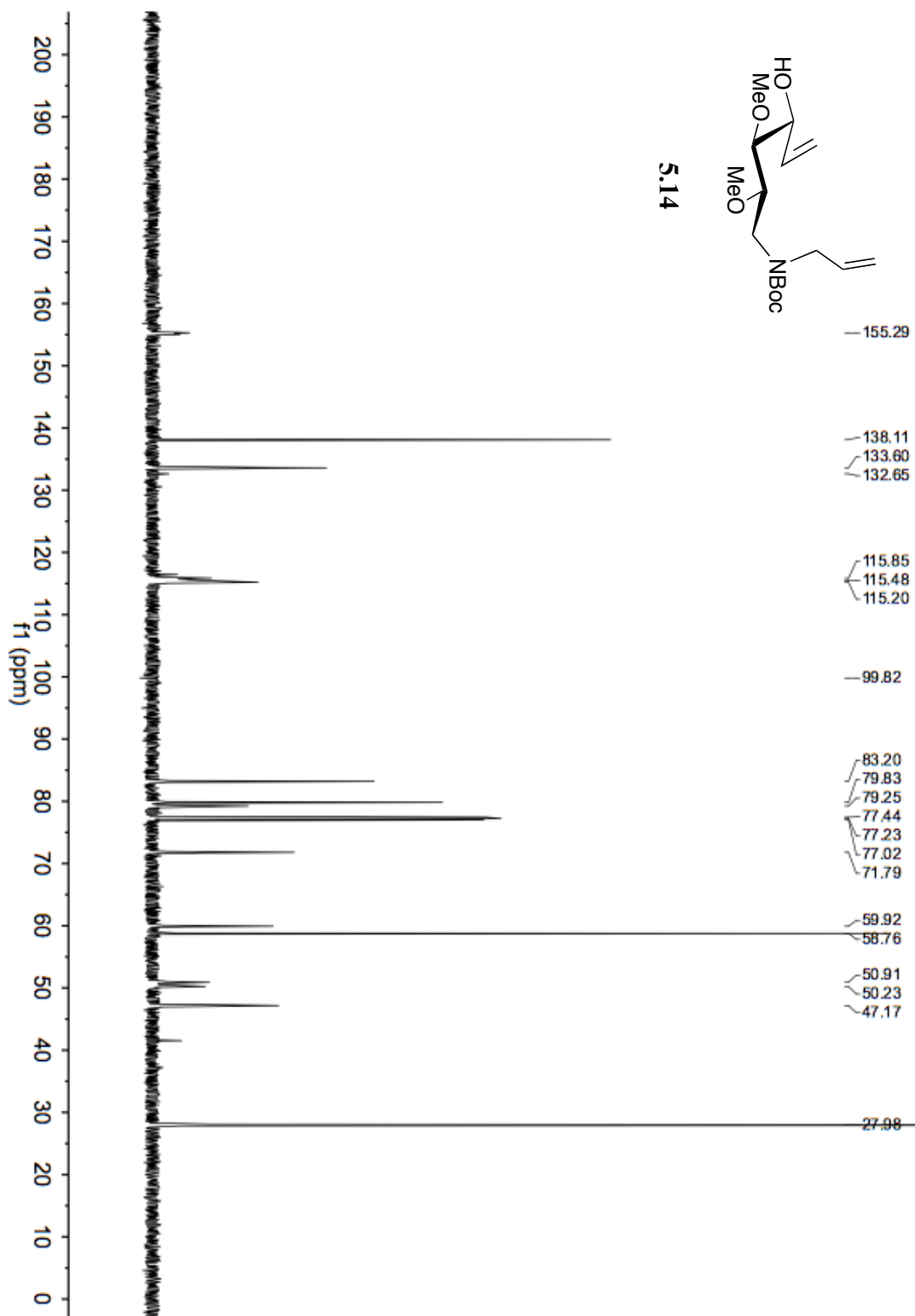
29.47
29.31
28.70
28.31
22.11
21.10

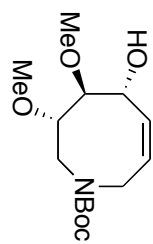




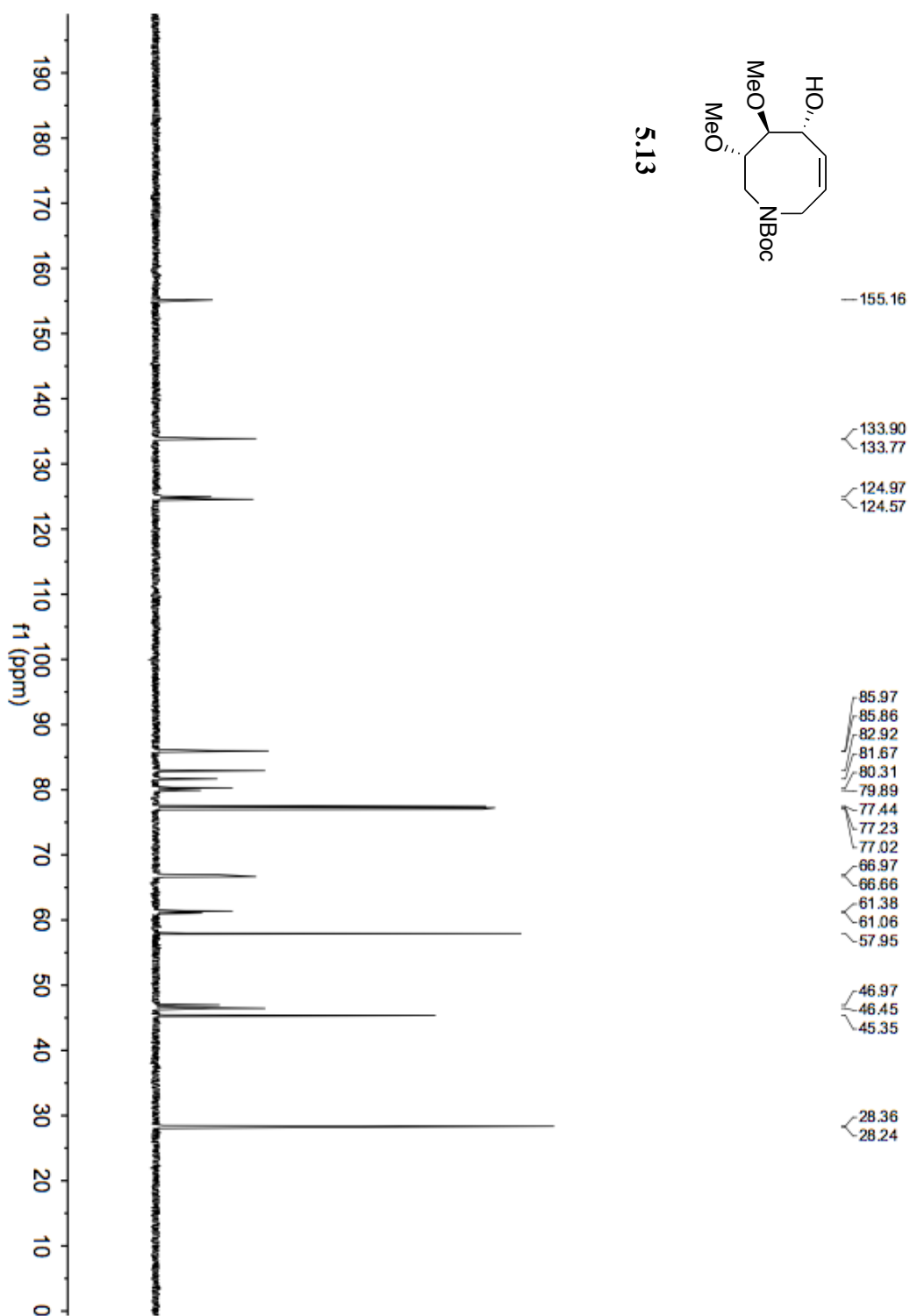


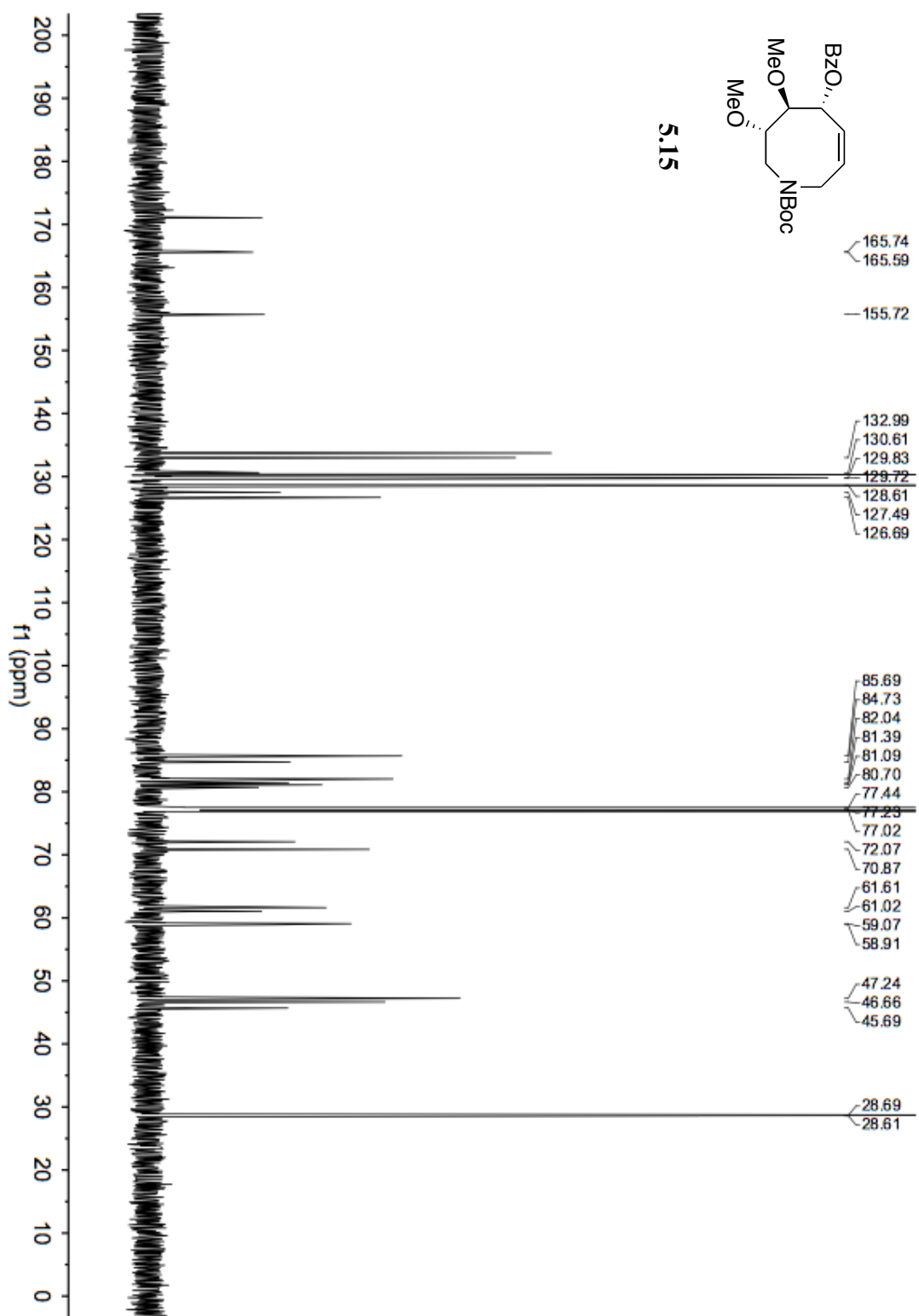


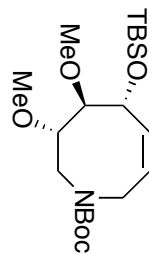




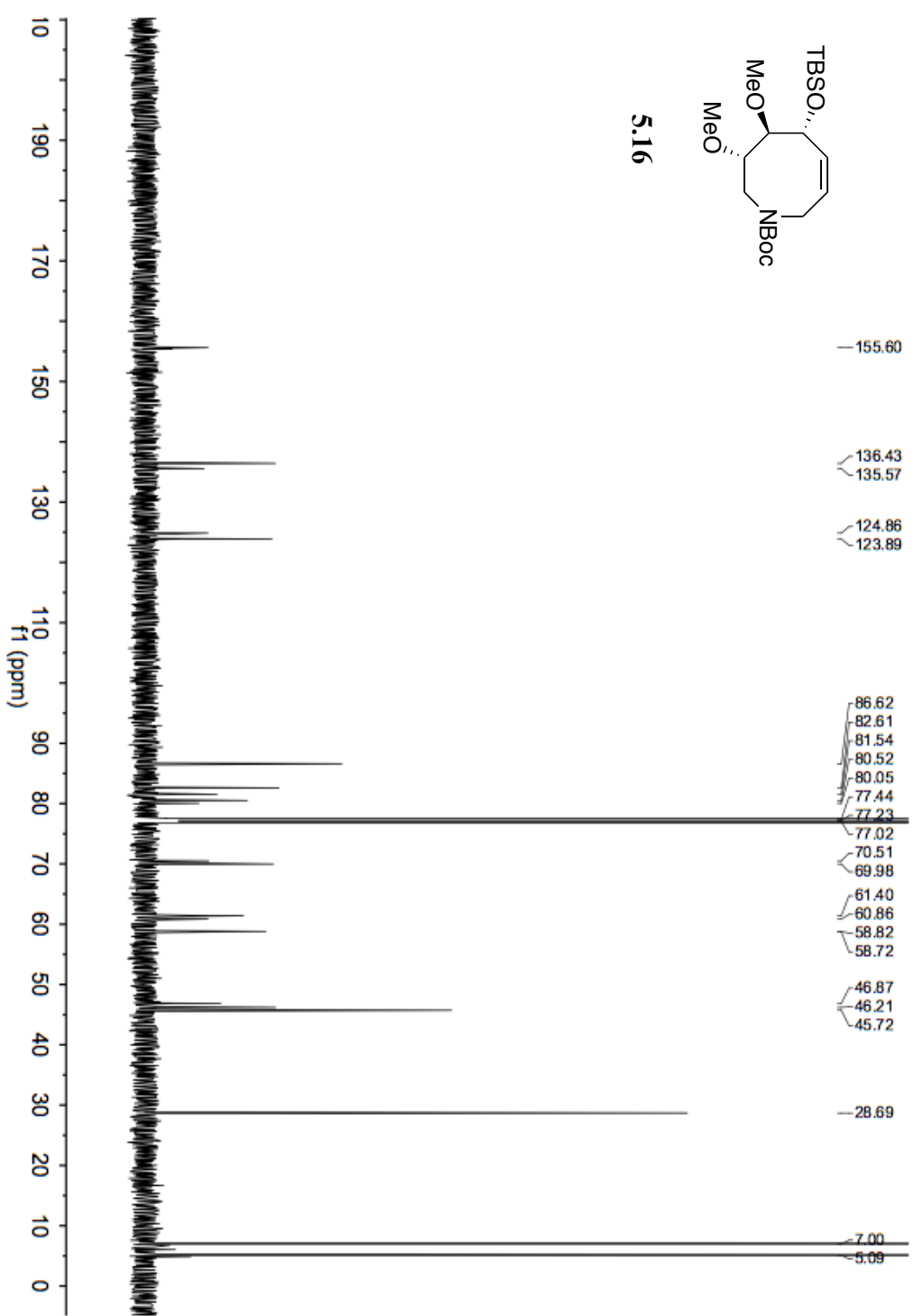
5.13

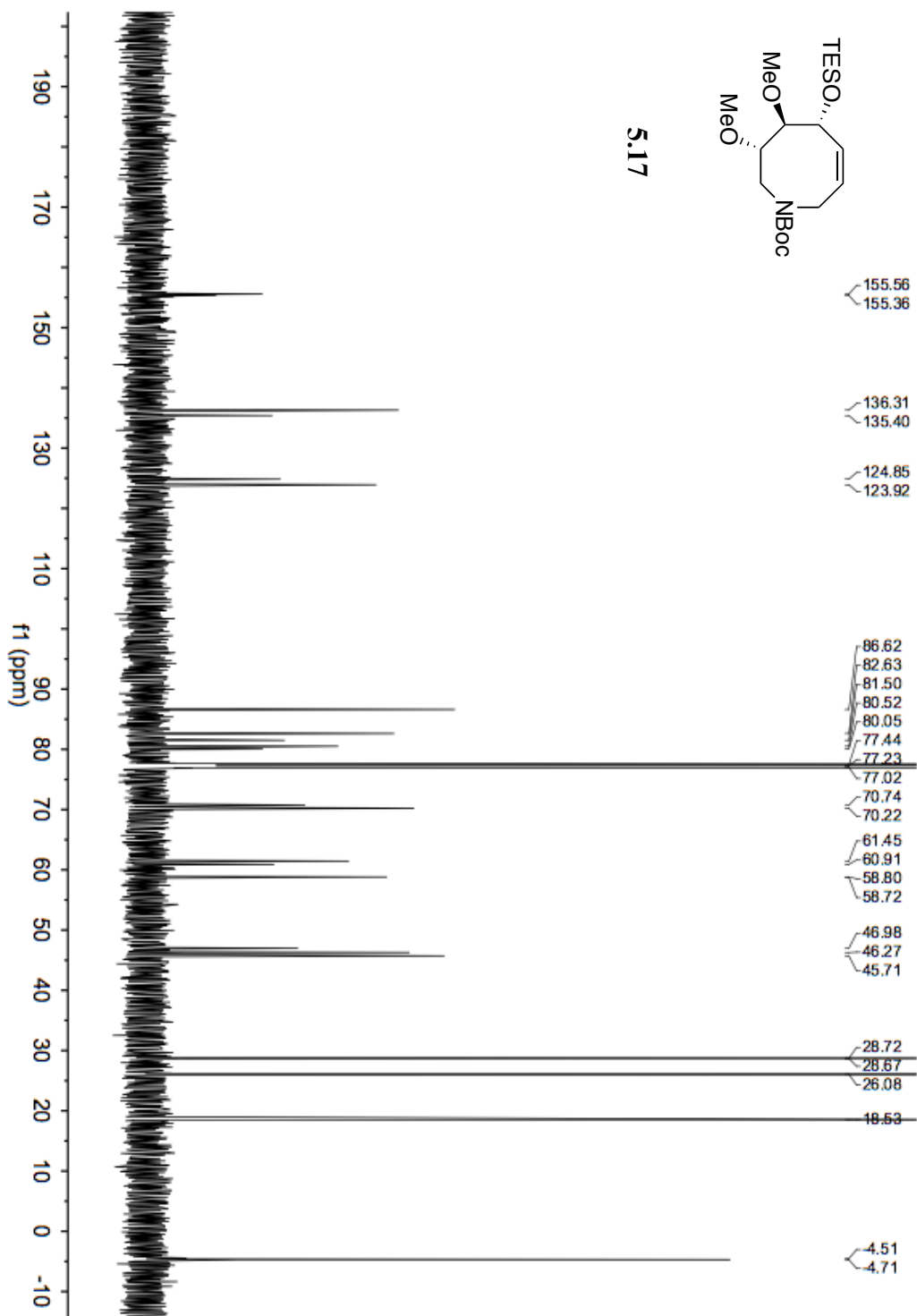


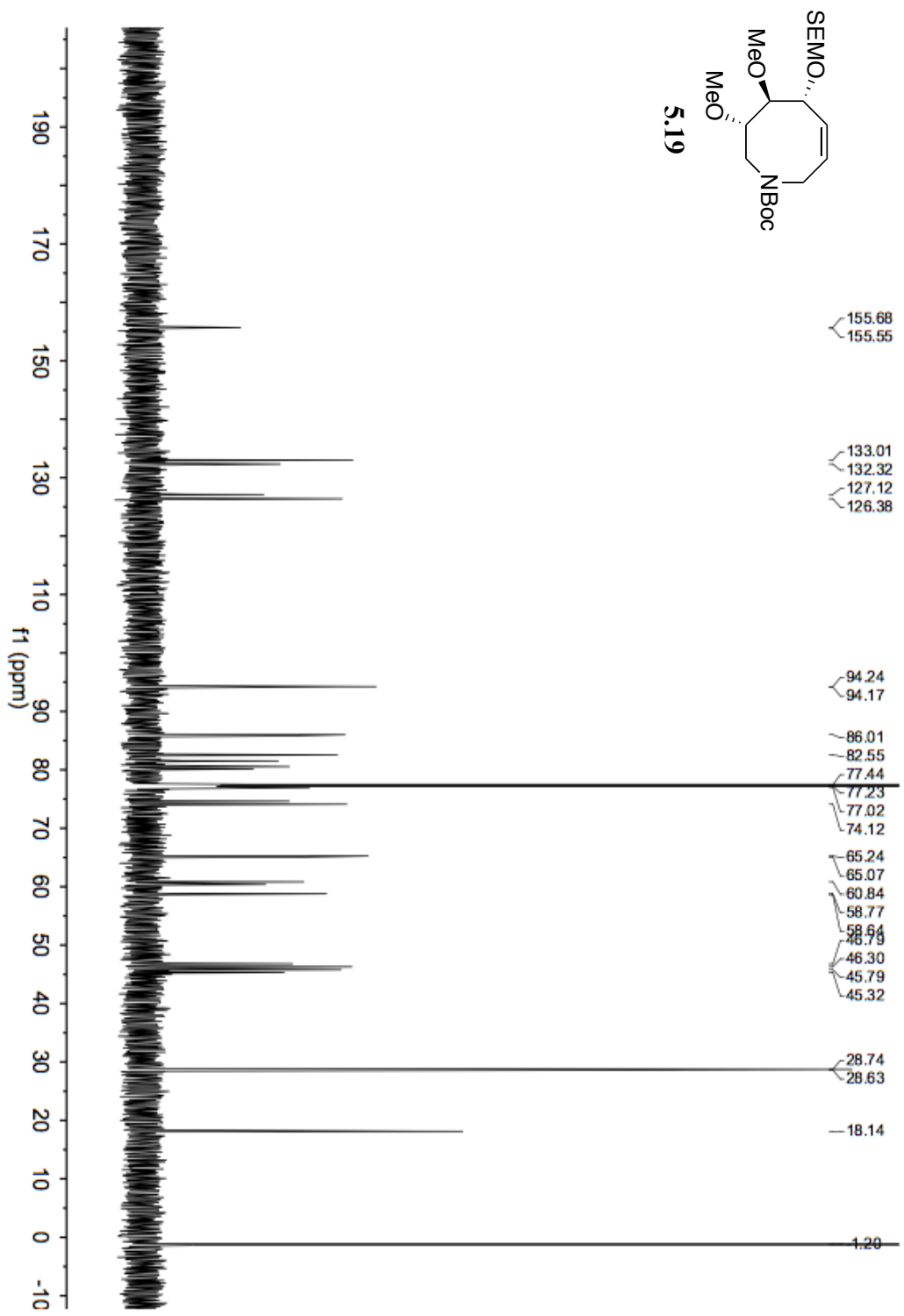


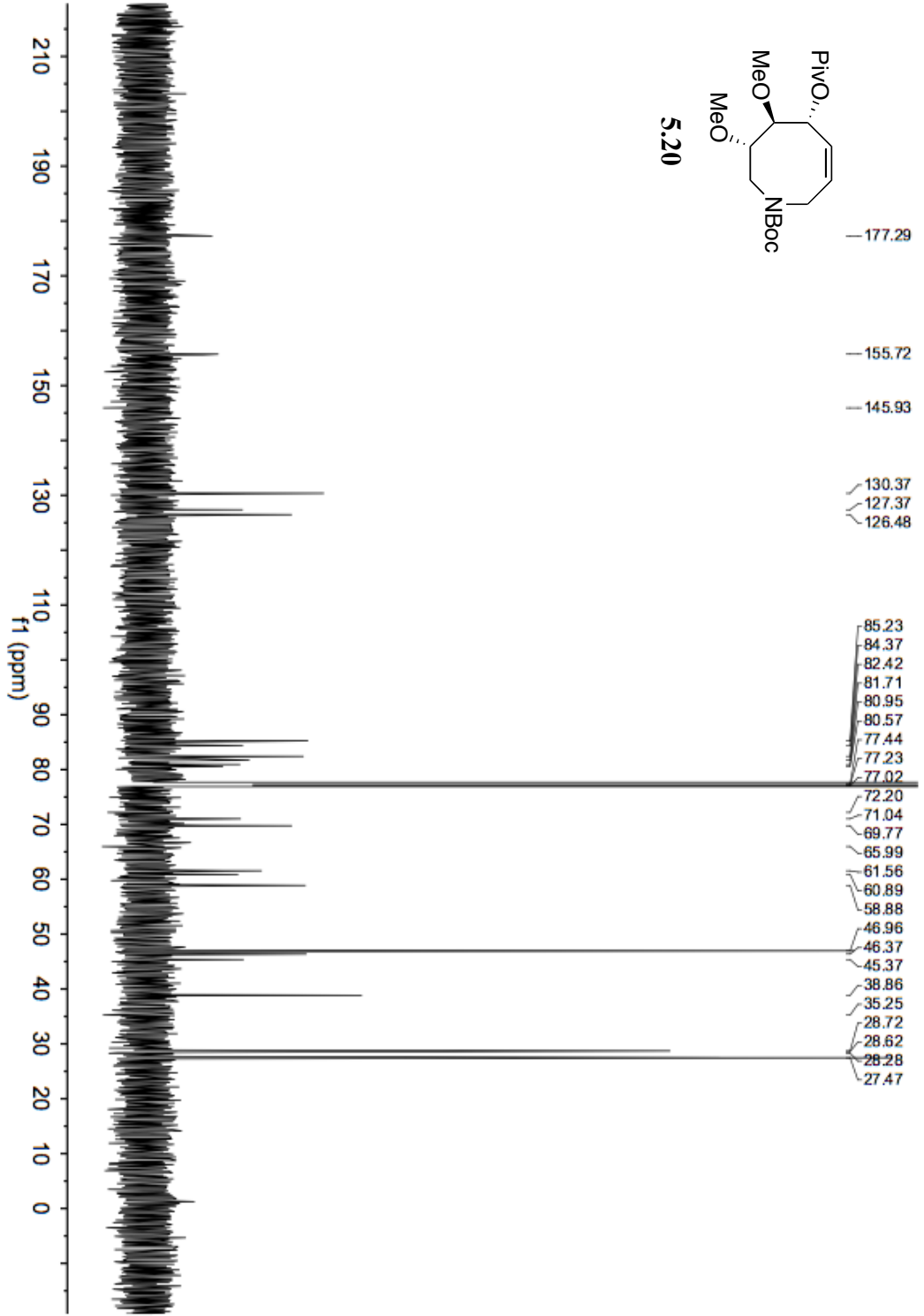


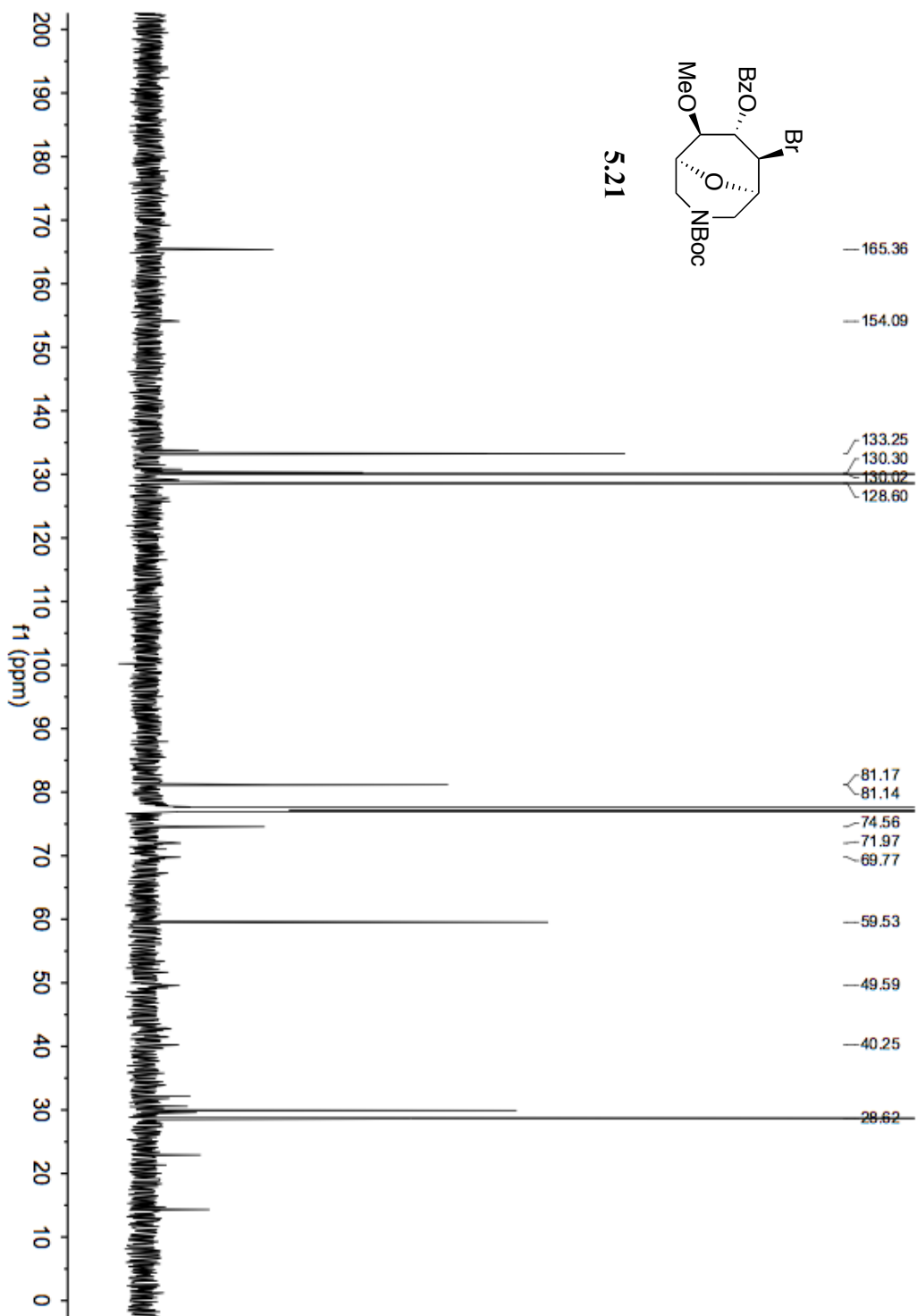
5.16

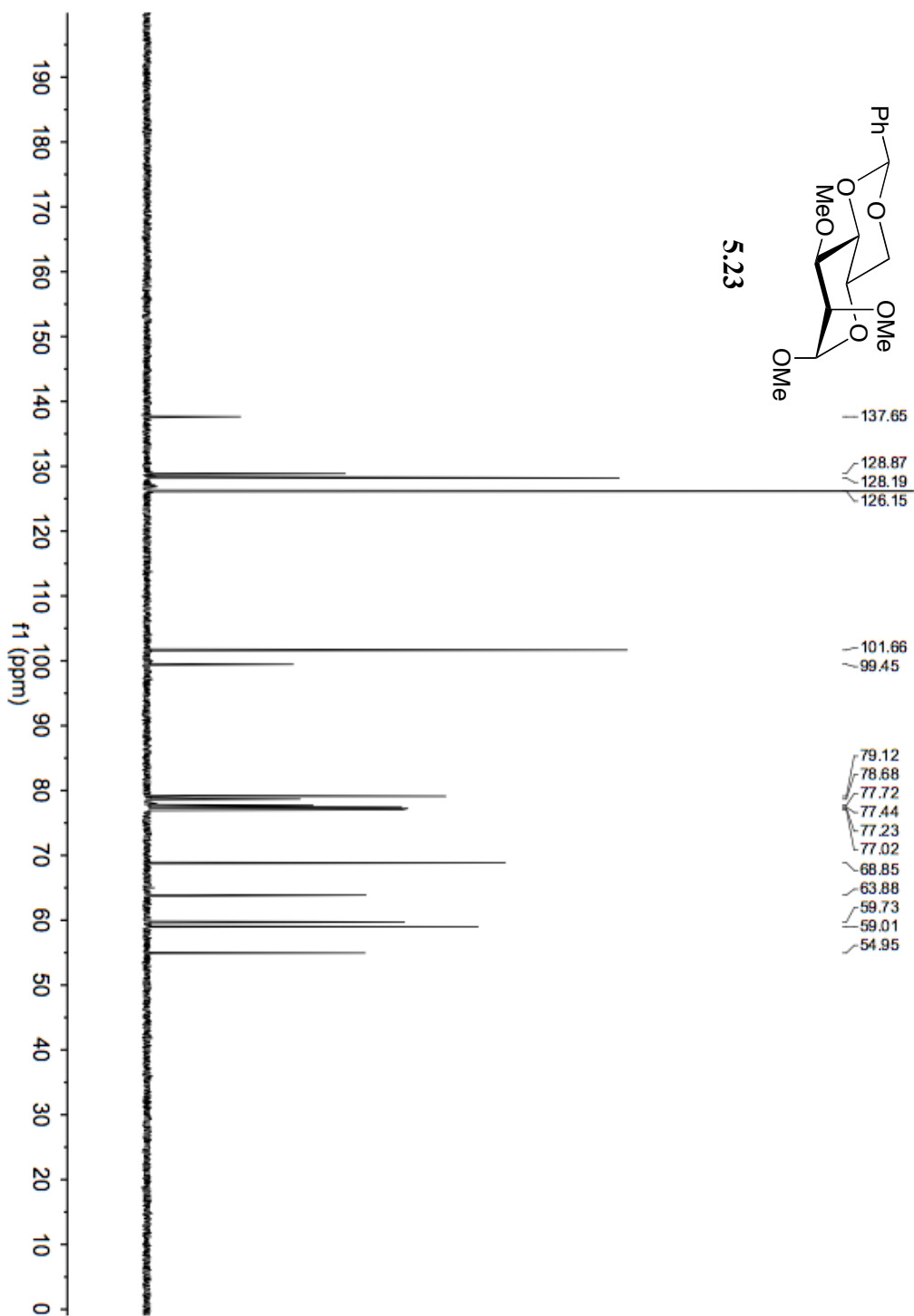


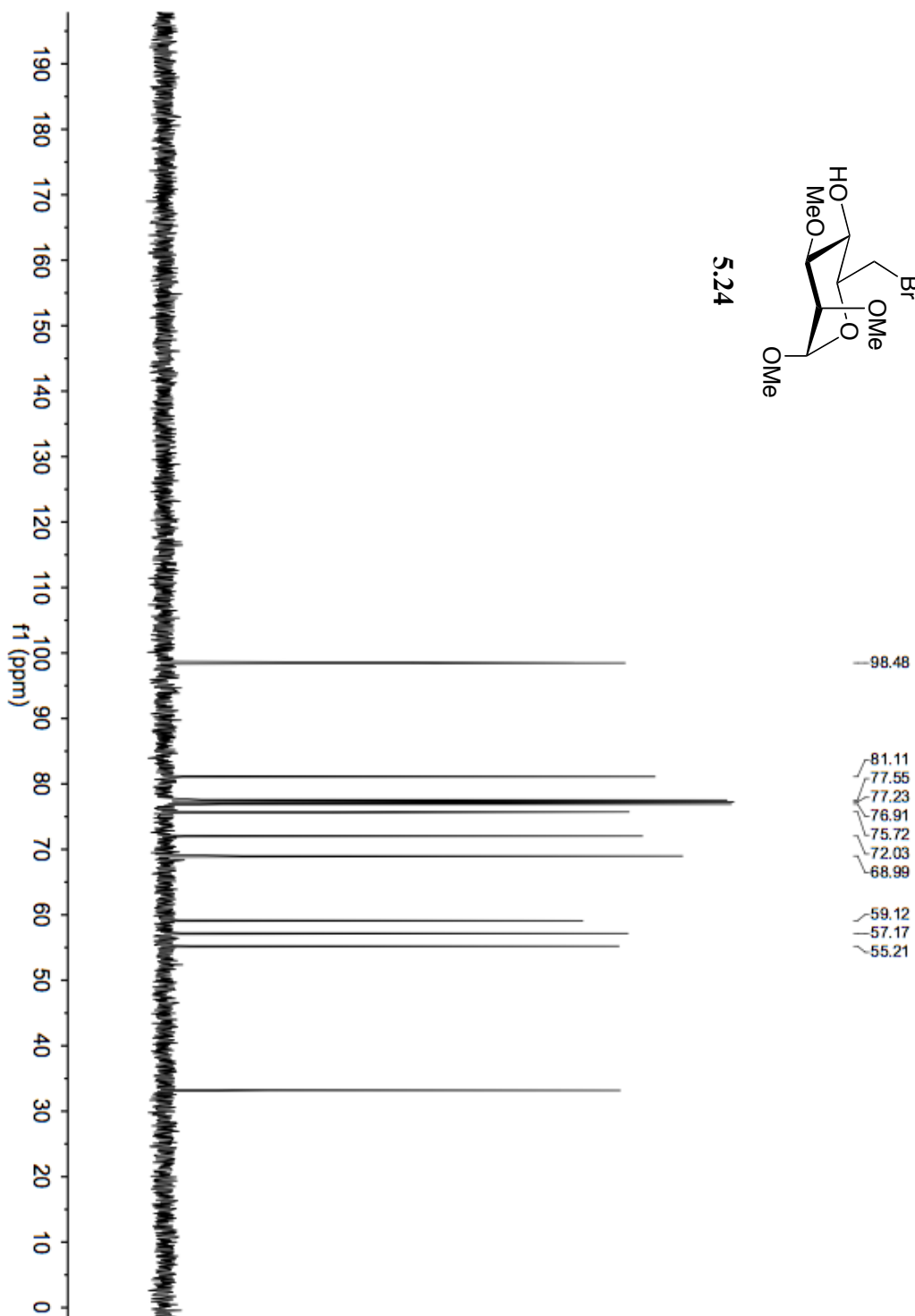
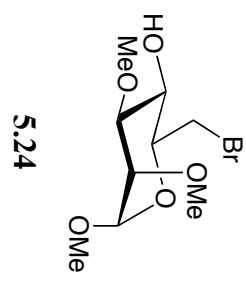


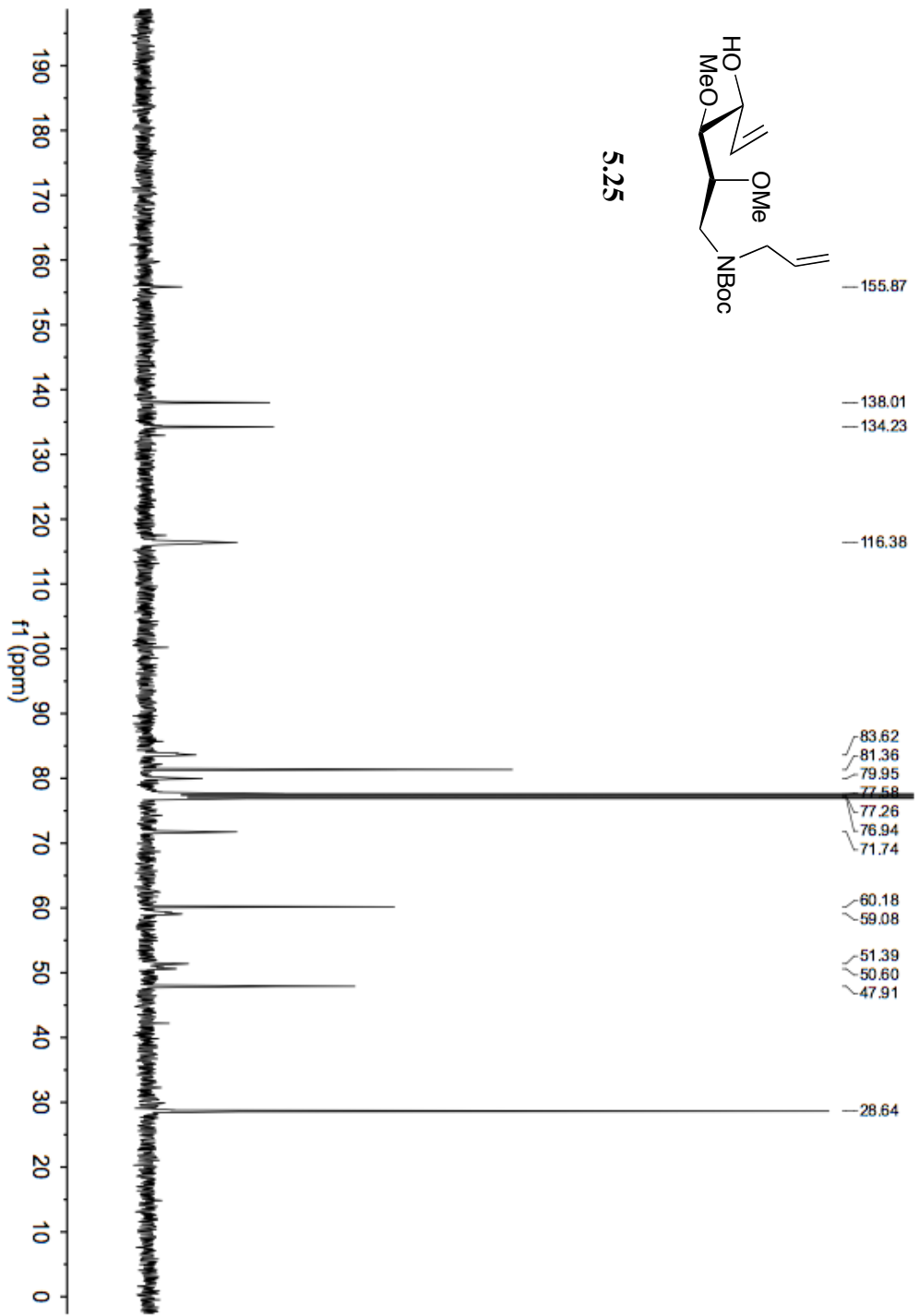




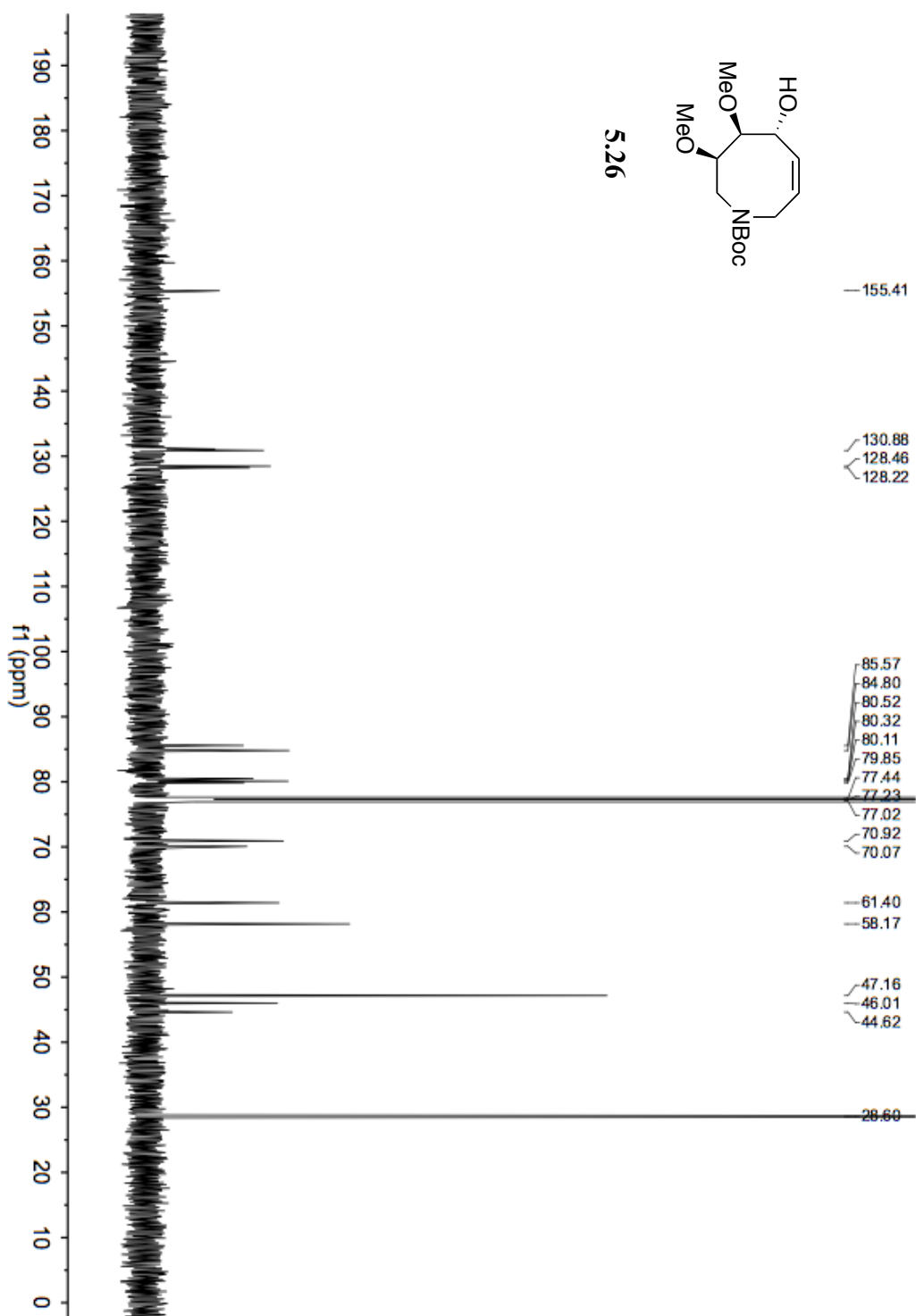


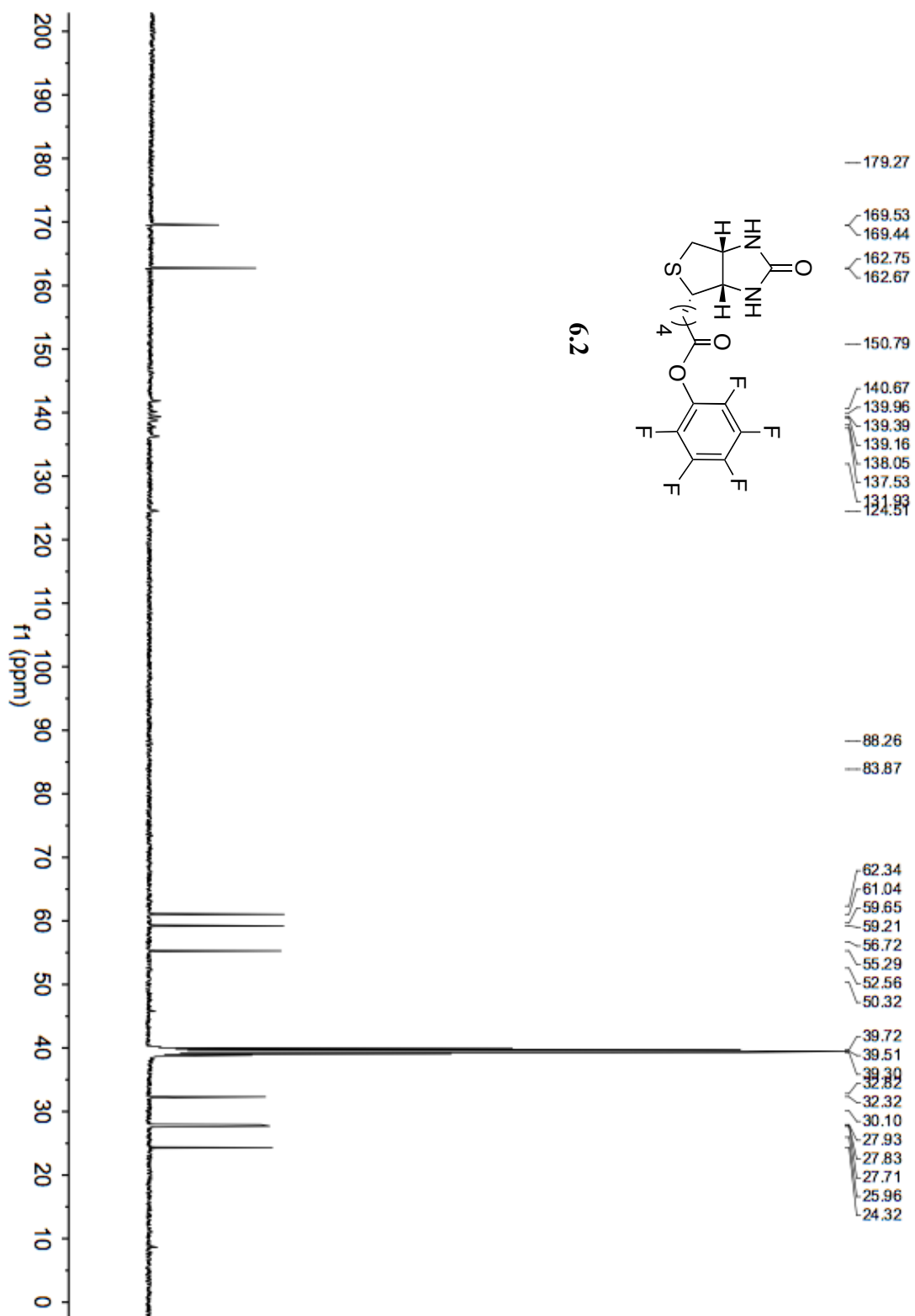


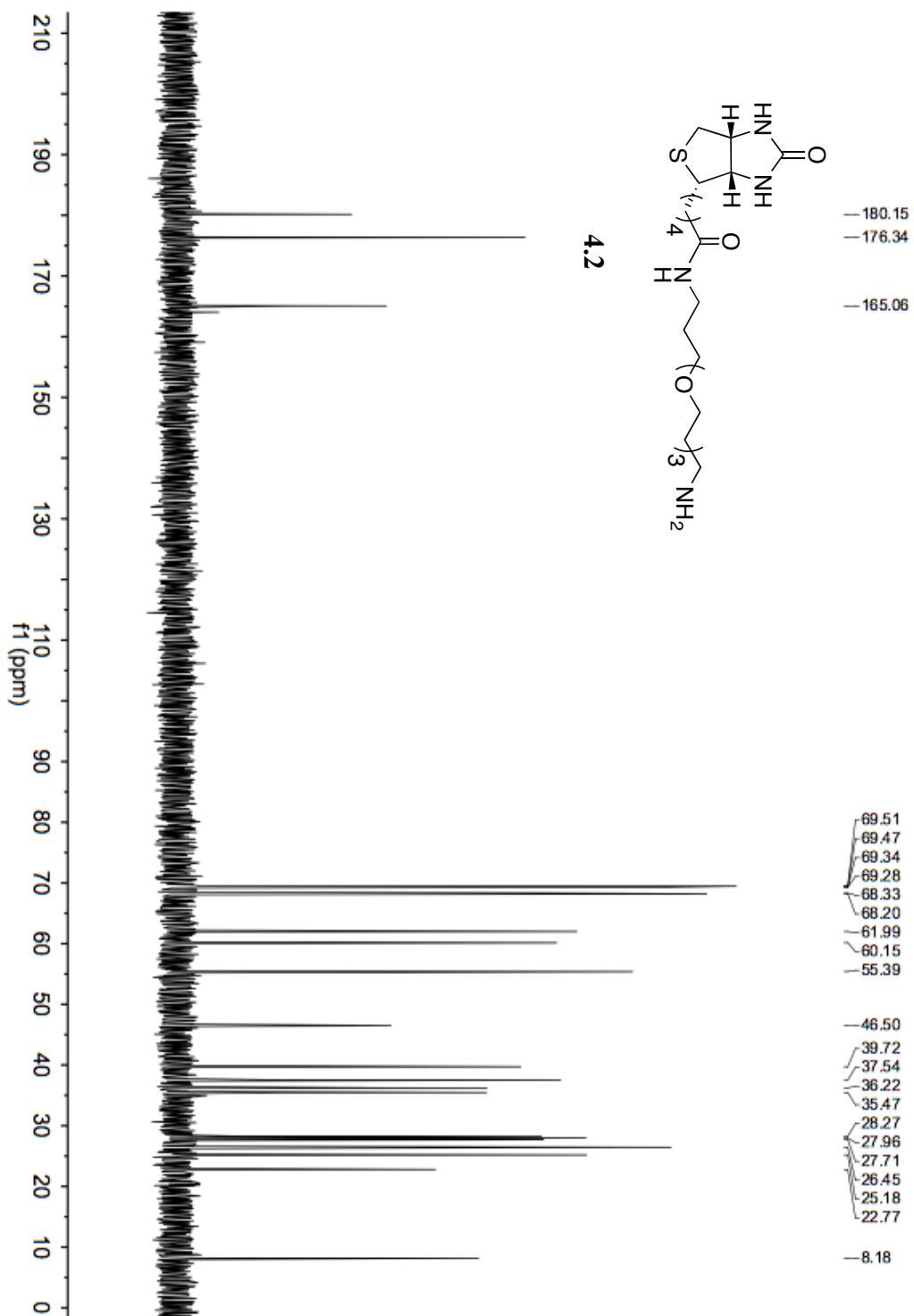


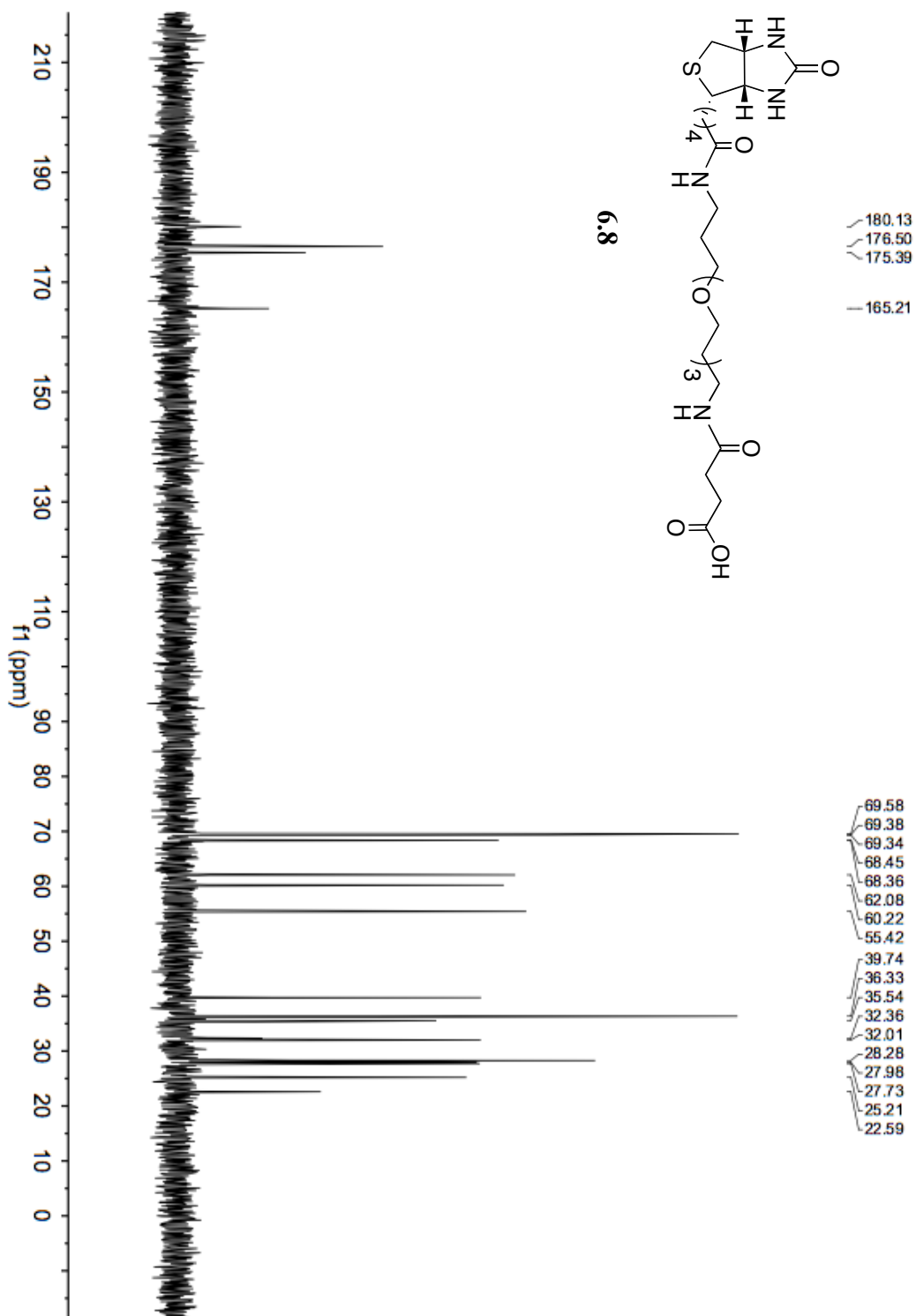


5.25

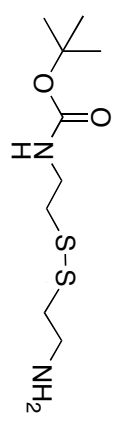




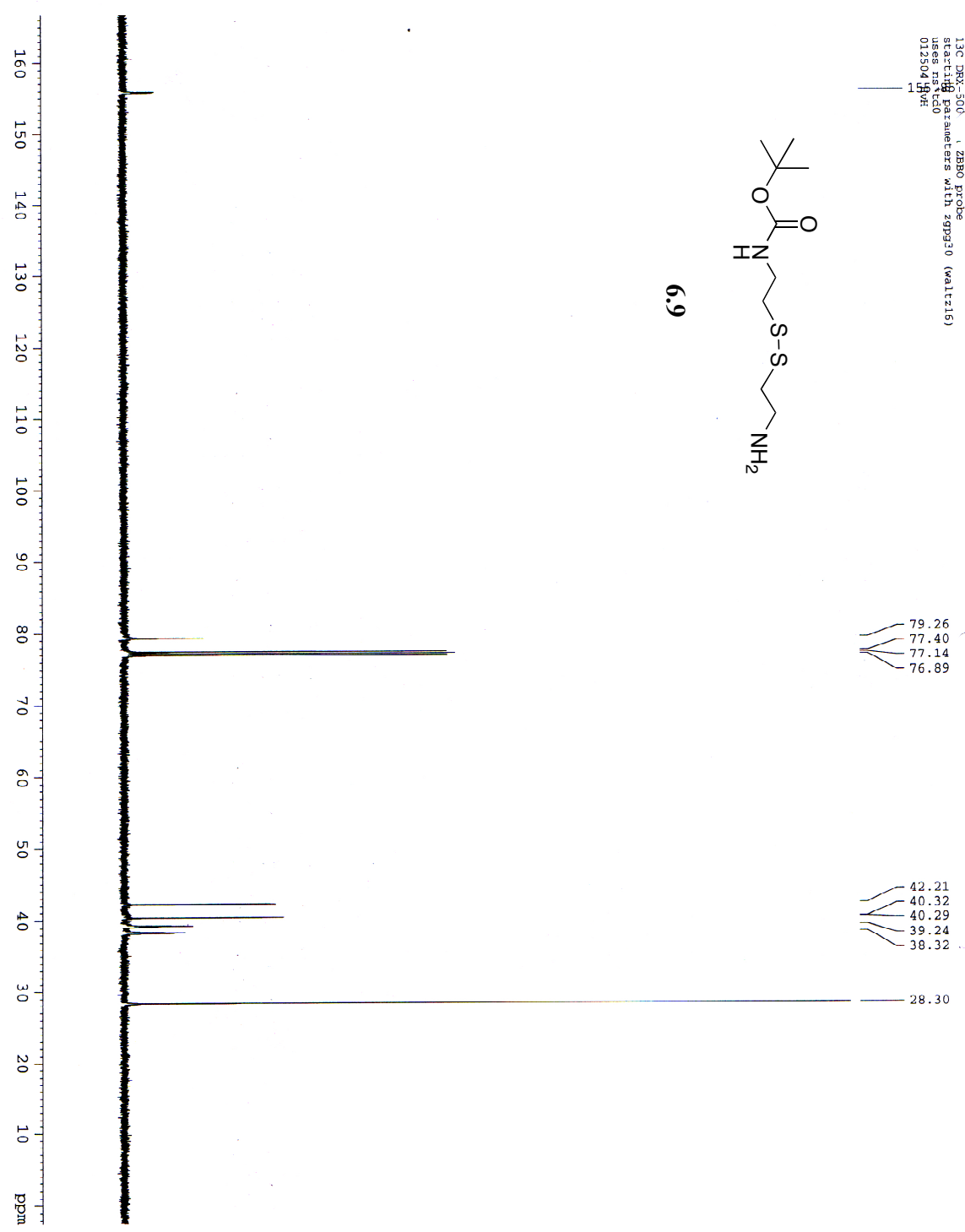


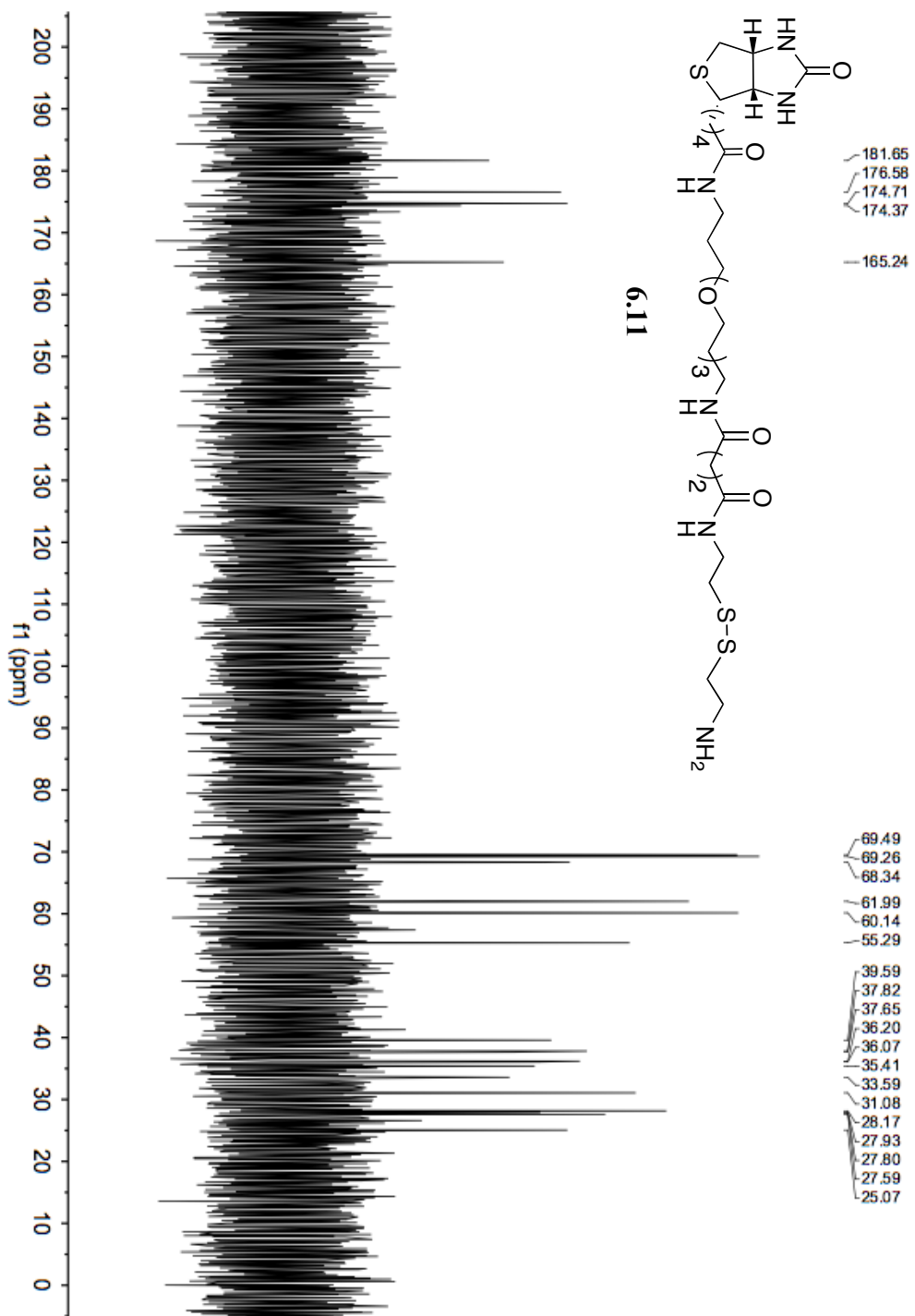


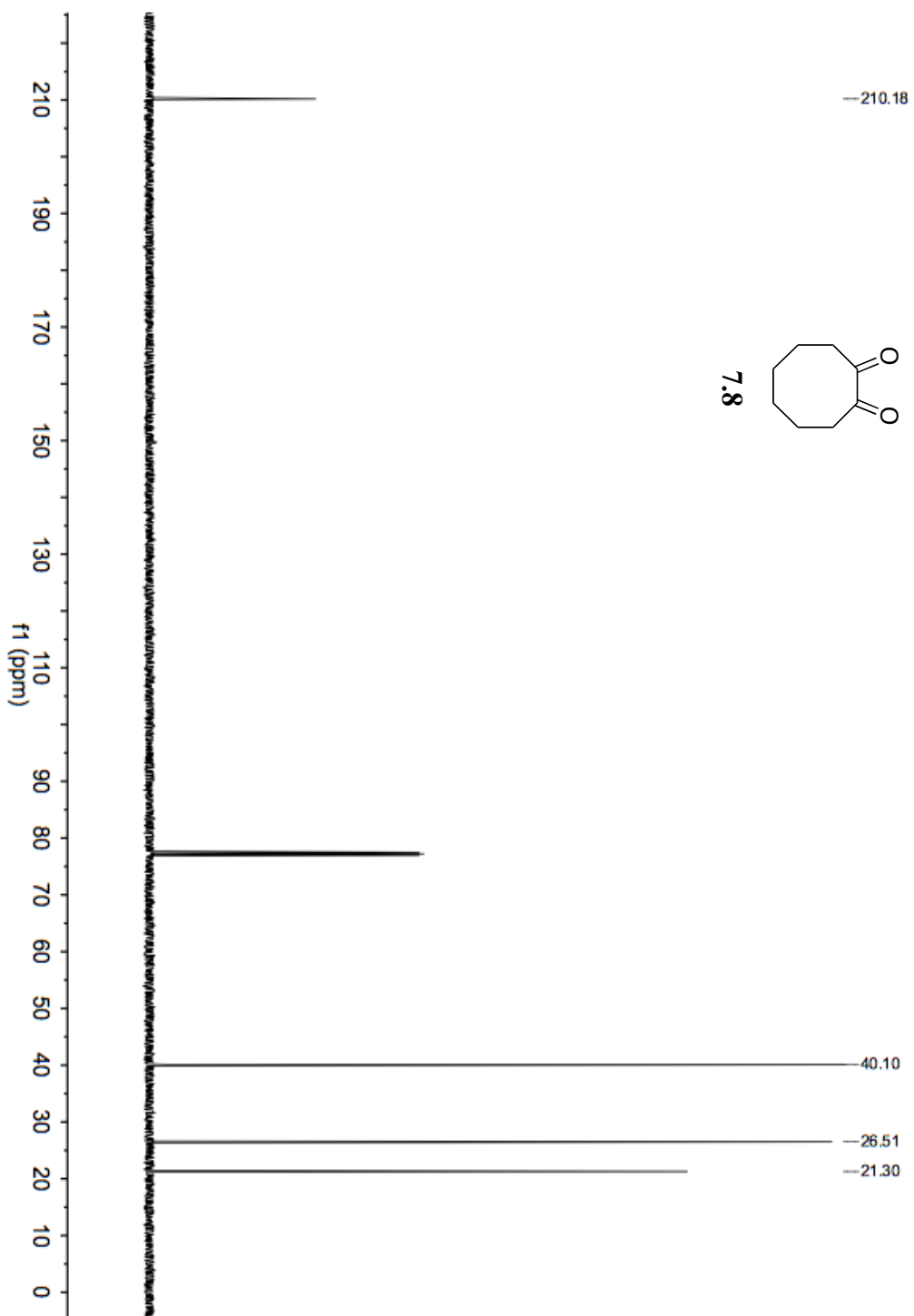
13C DEX-500 Z80 probe
Stacking parameters with zgpg30 (wall-15)
012504 19H

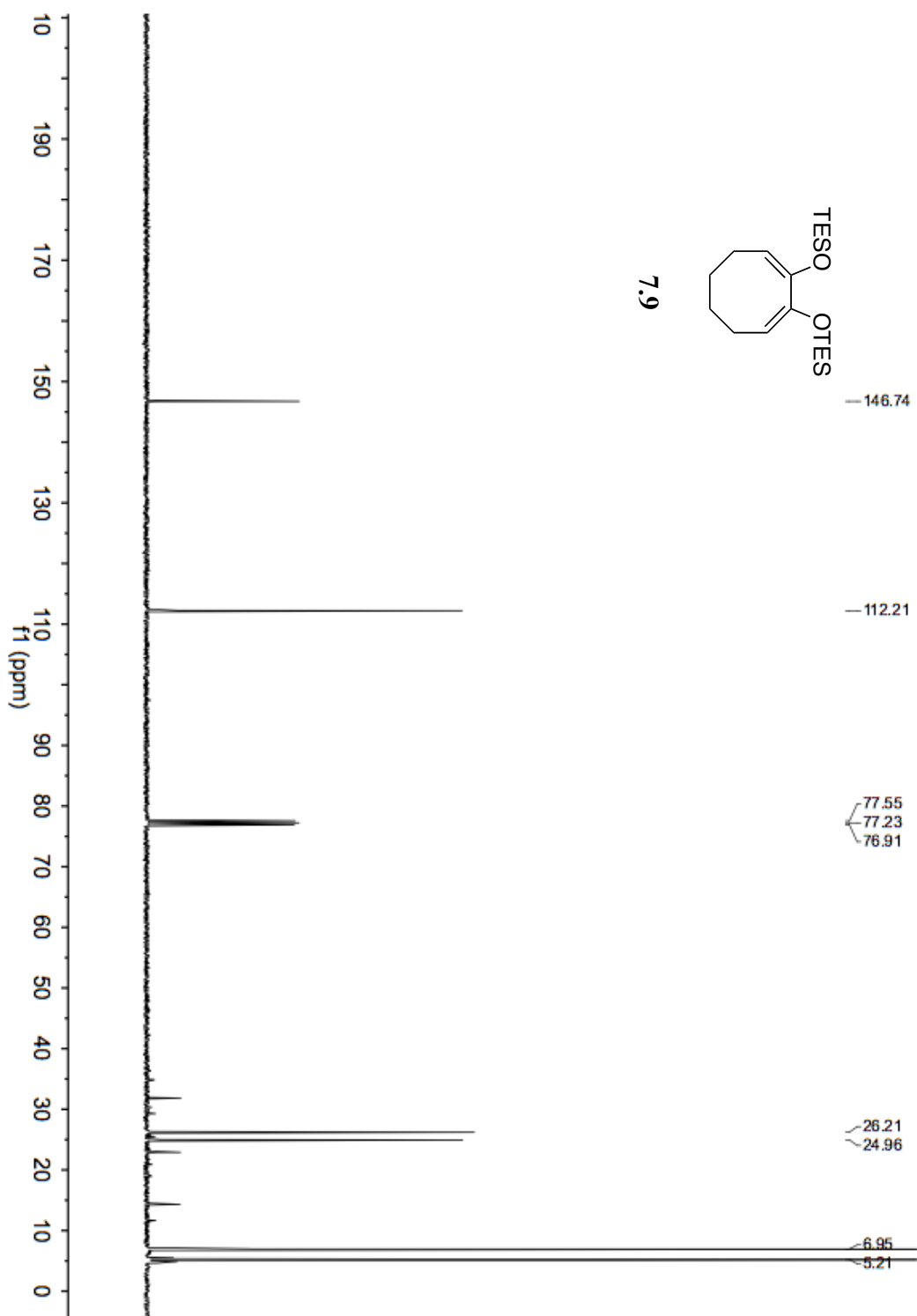


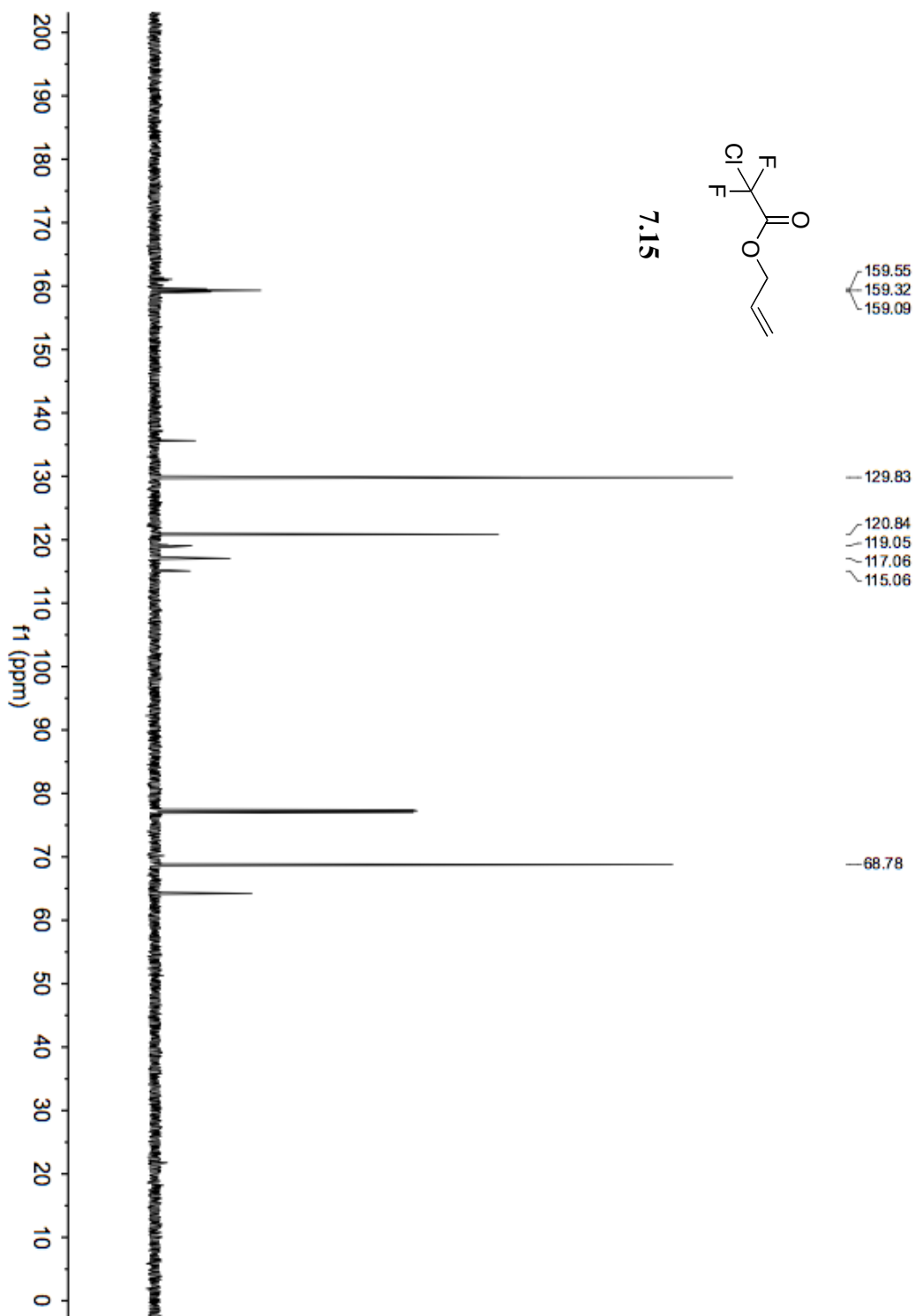
6.9

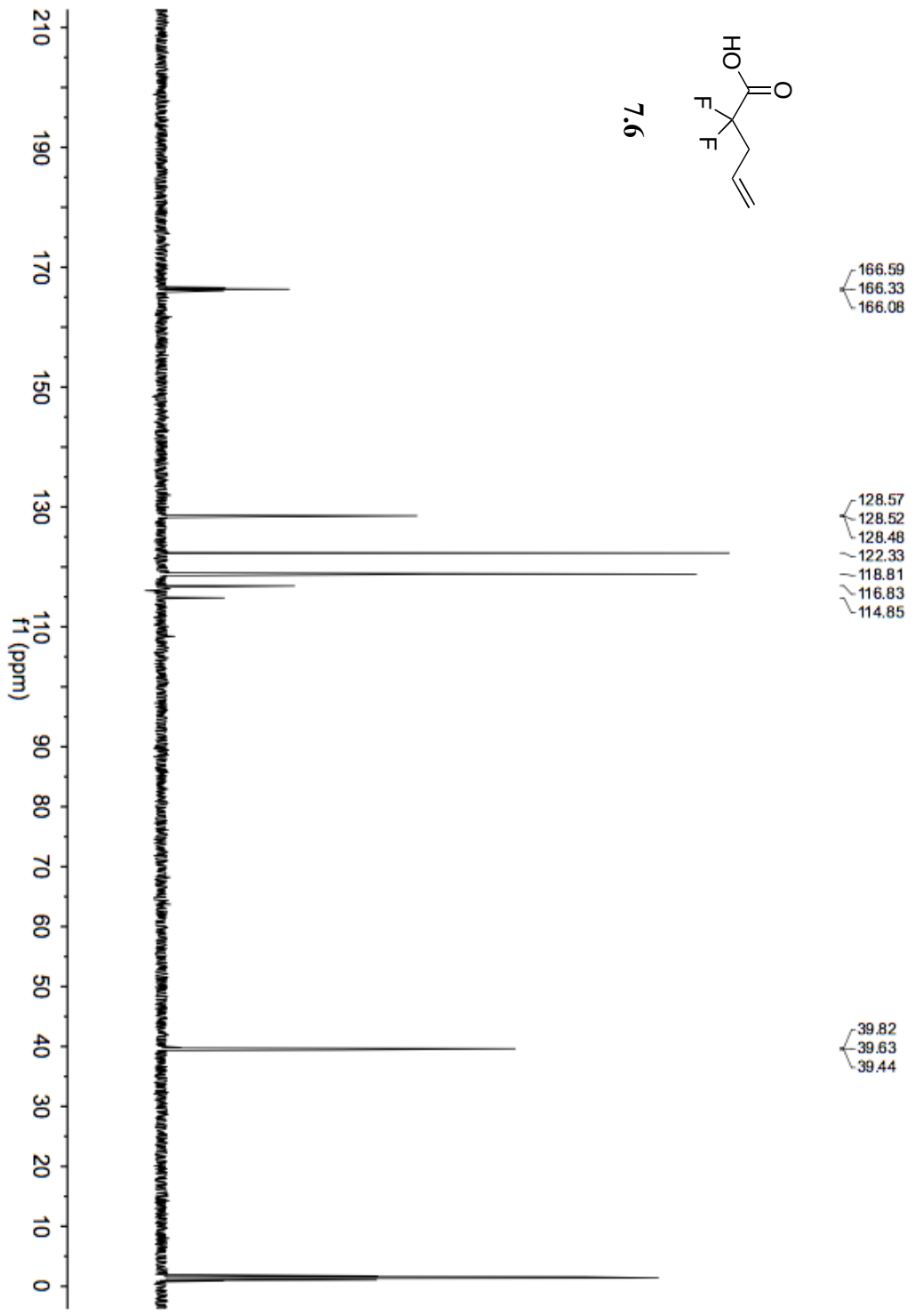
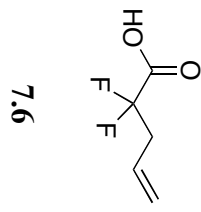


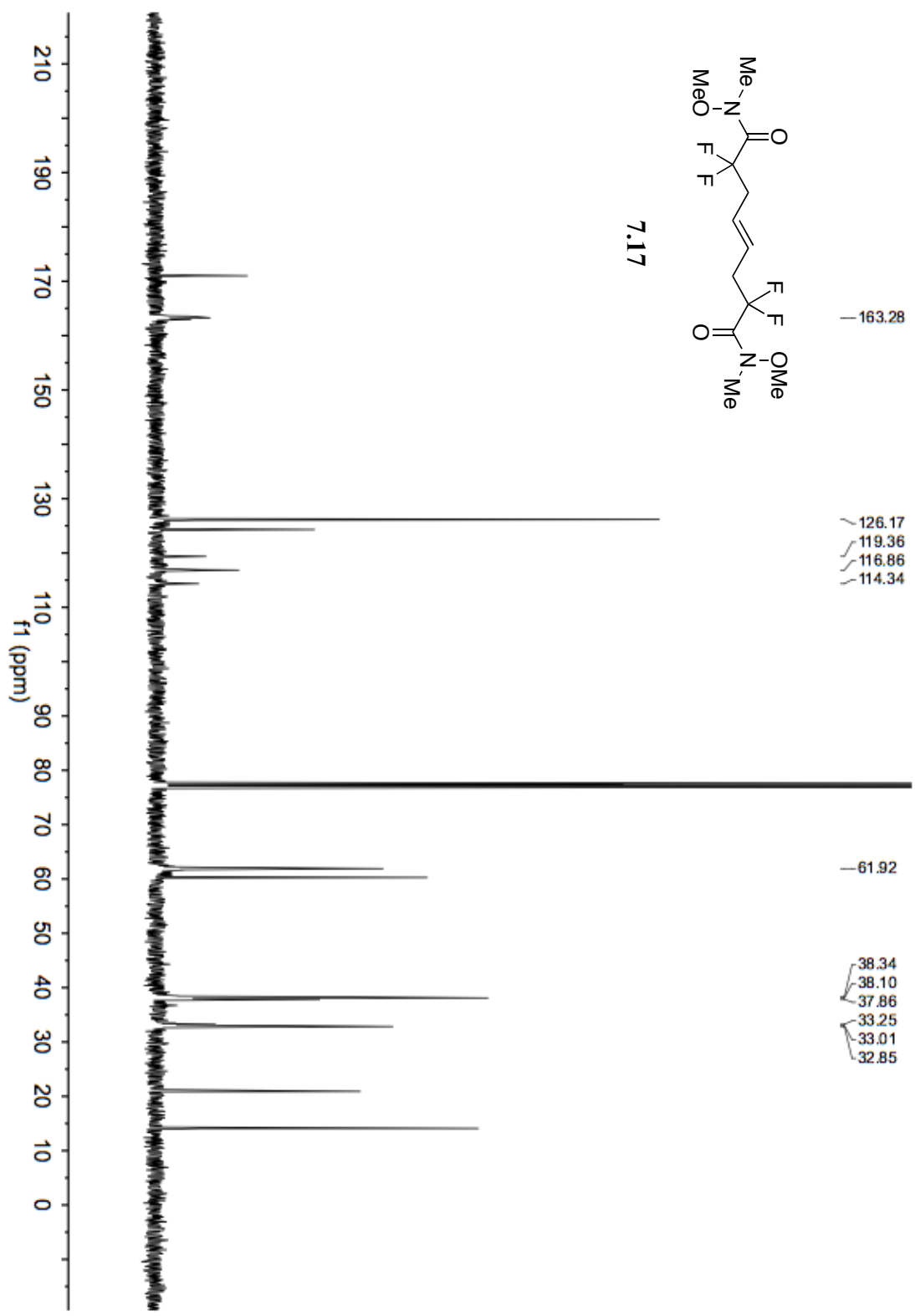


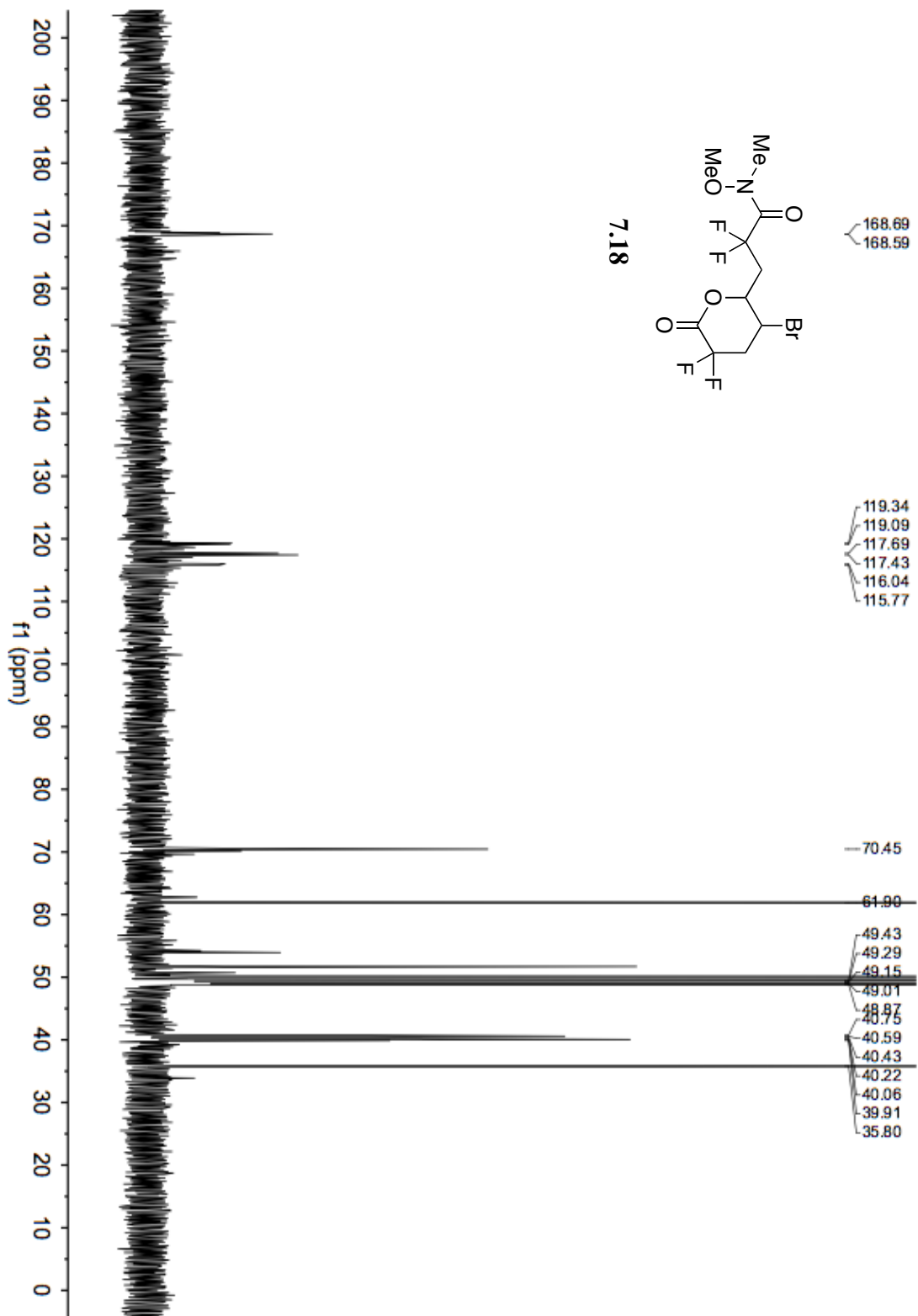


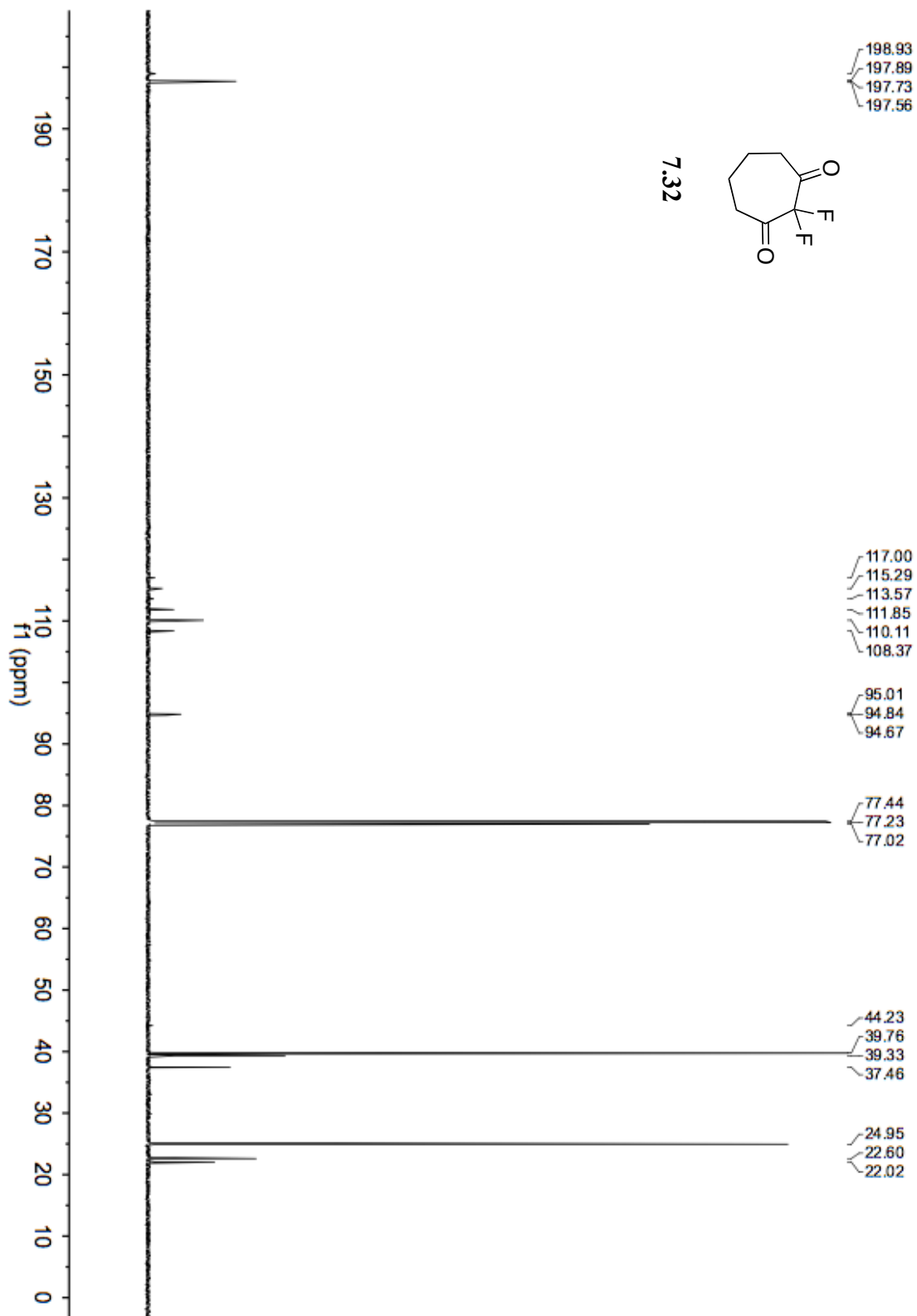


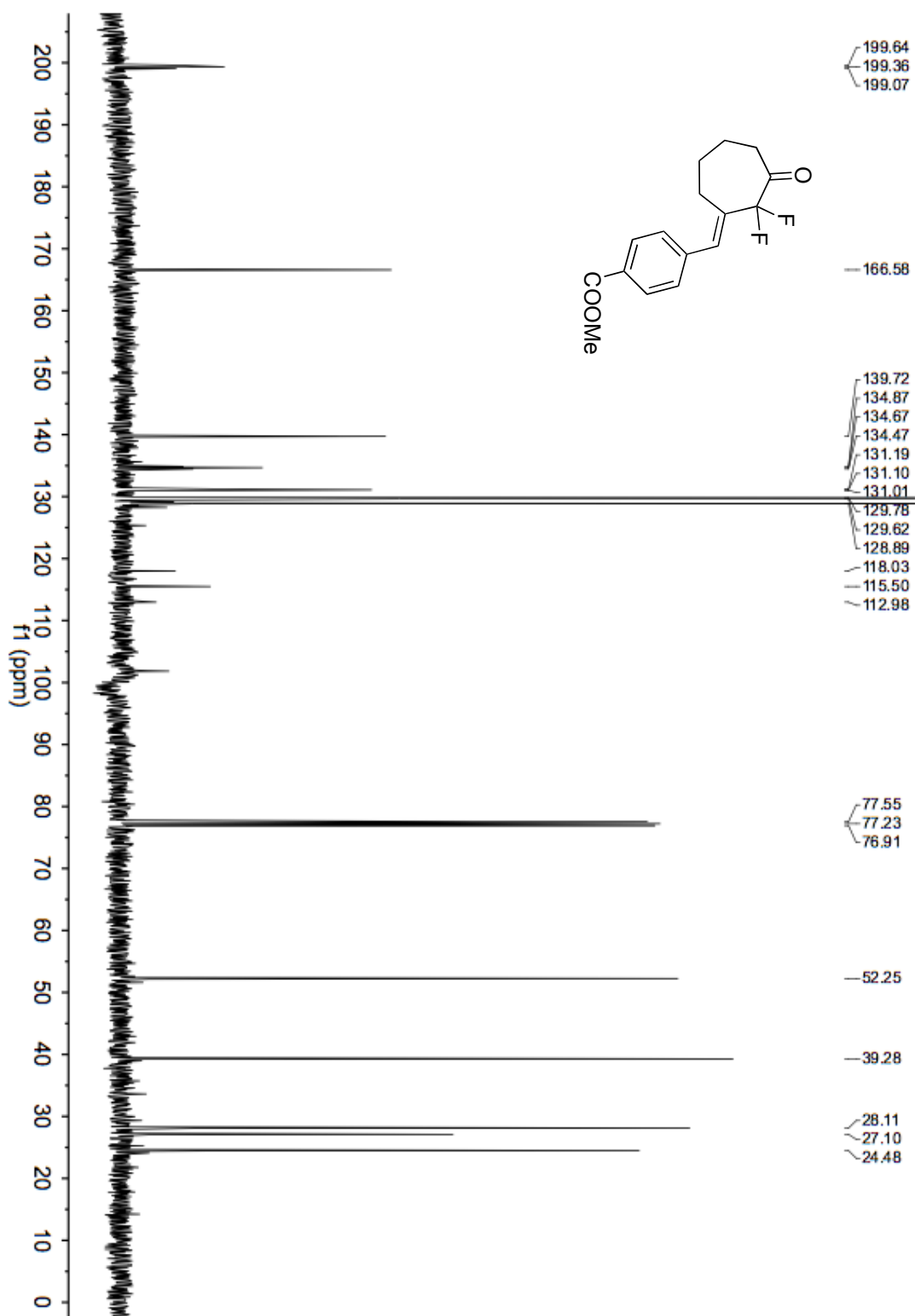


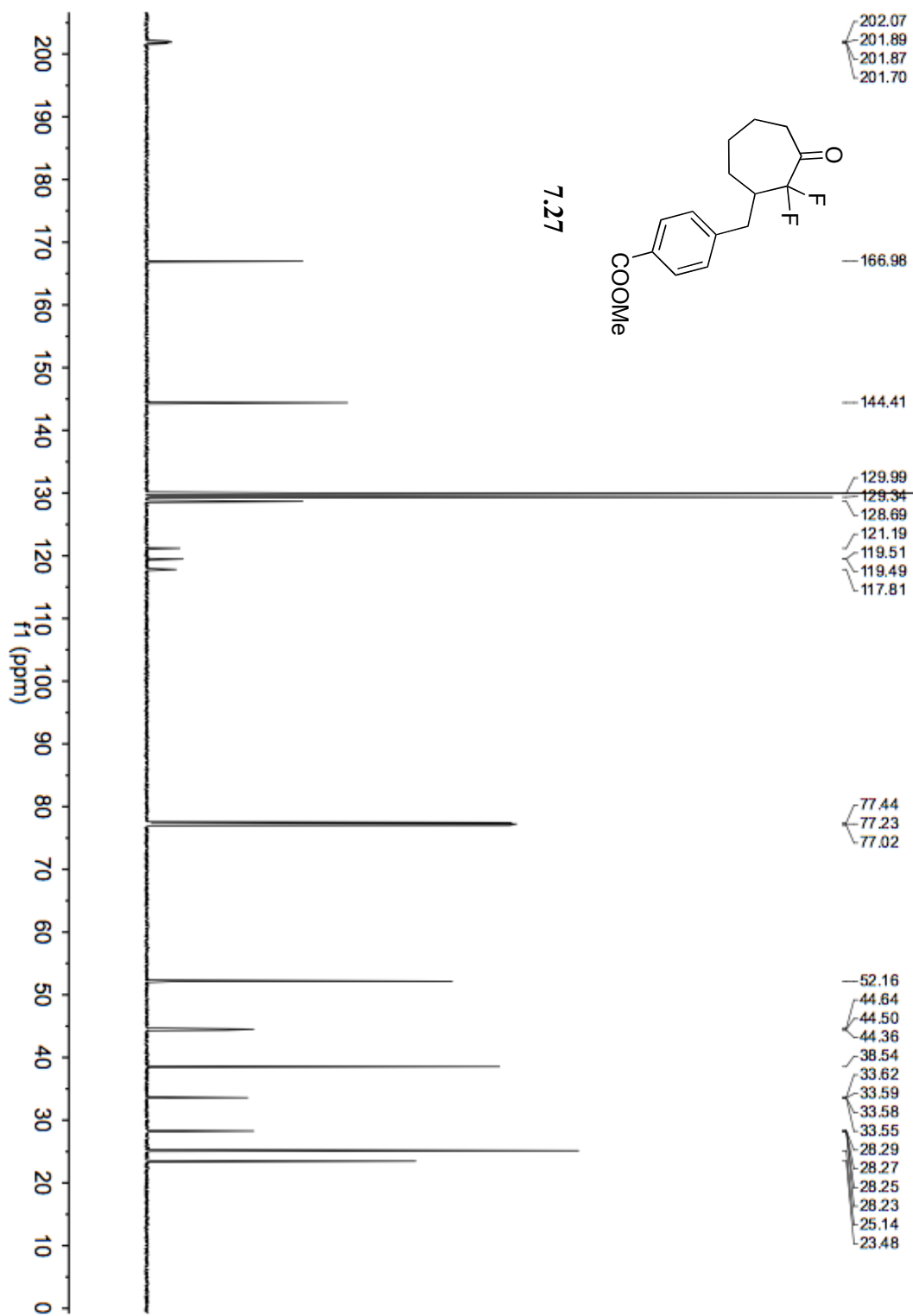


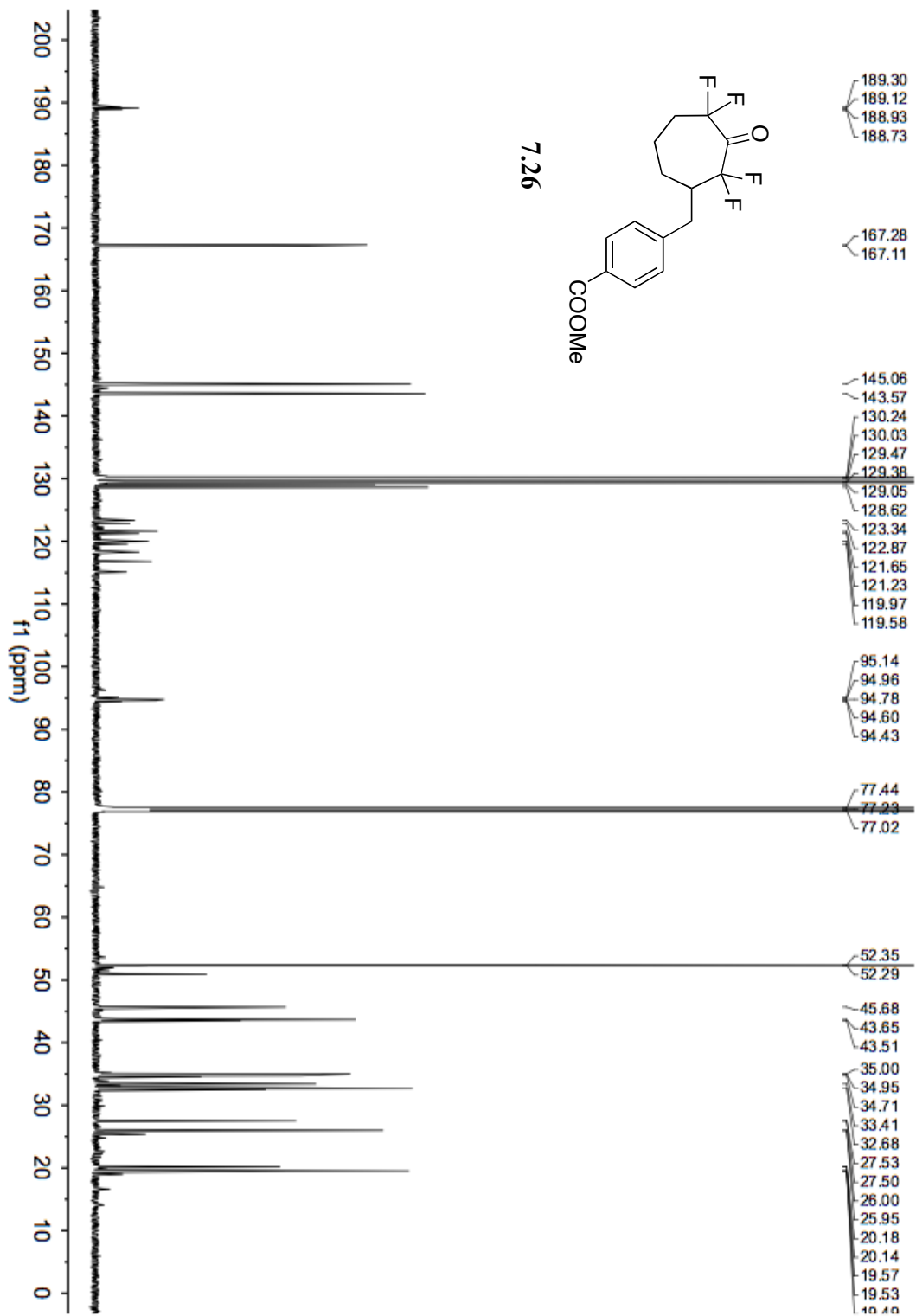


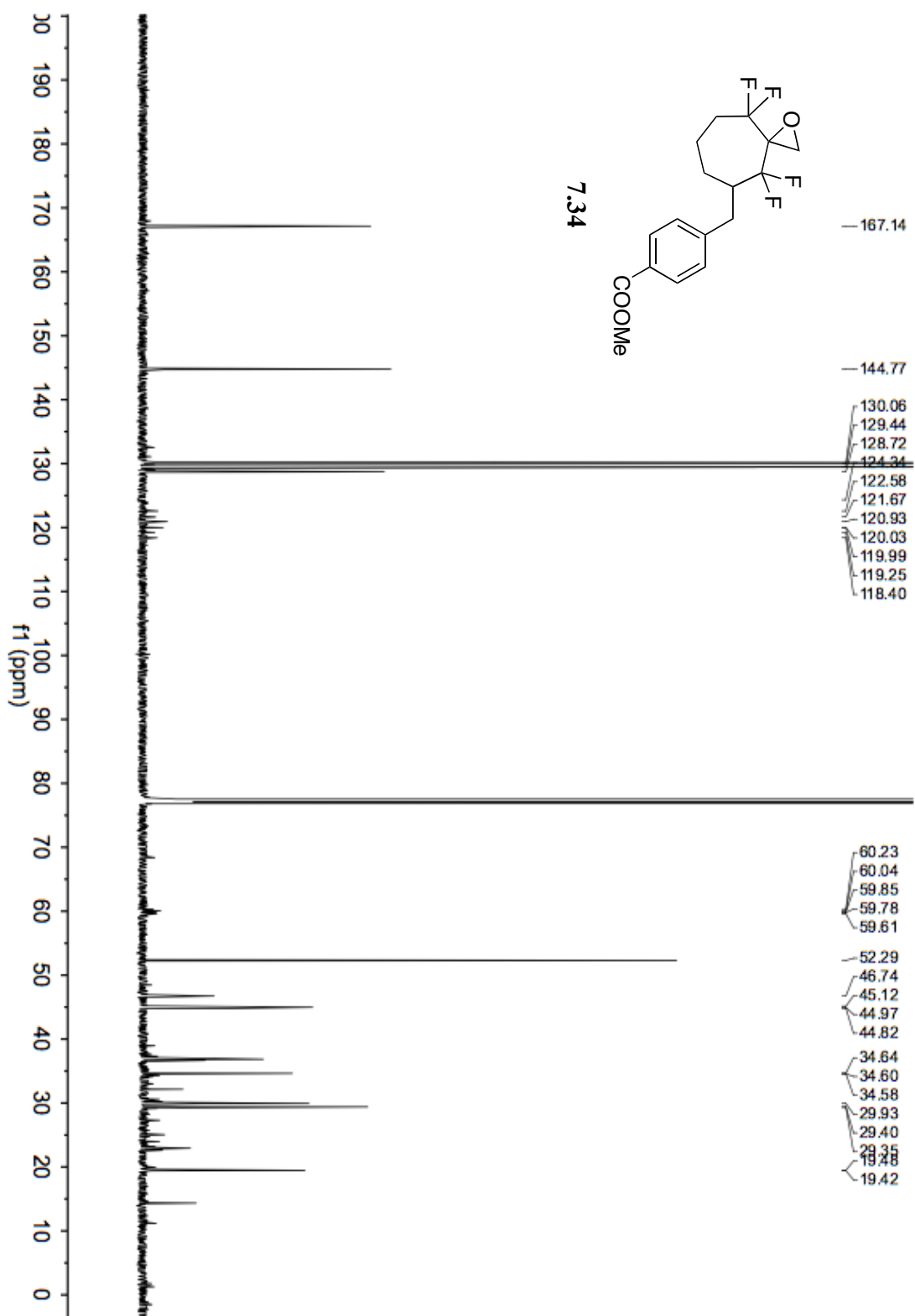


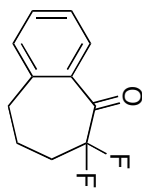






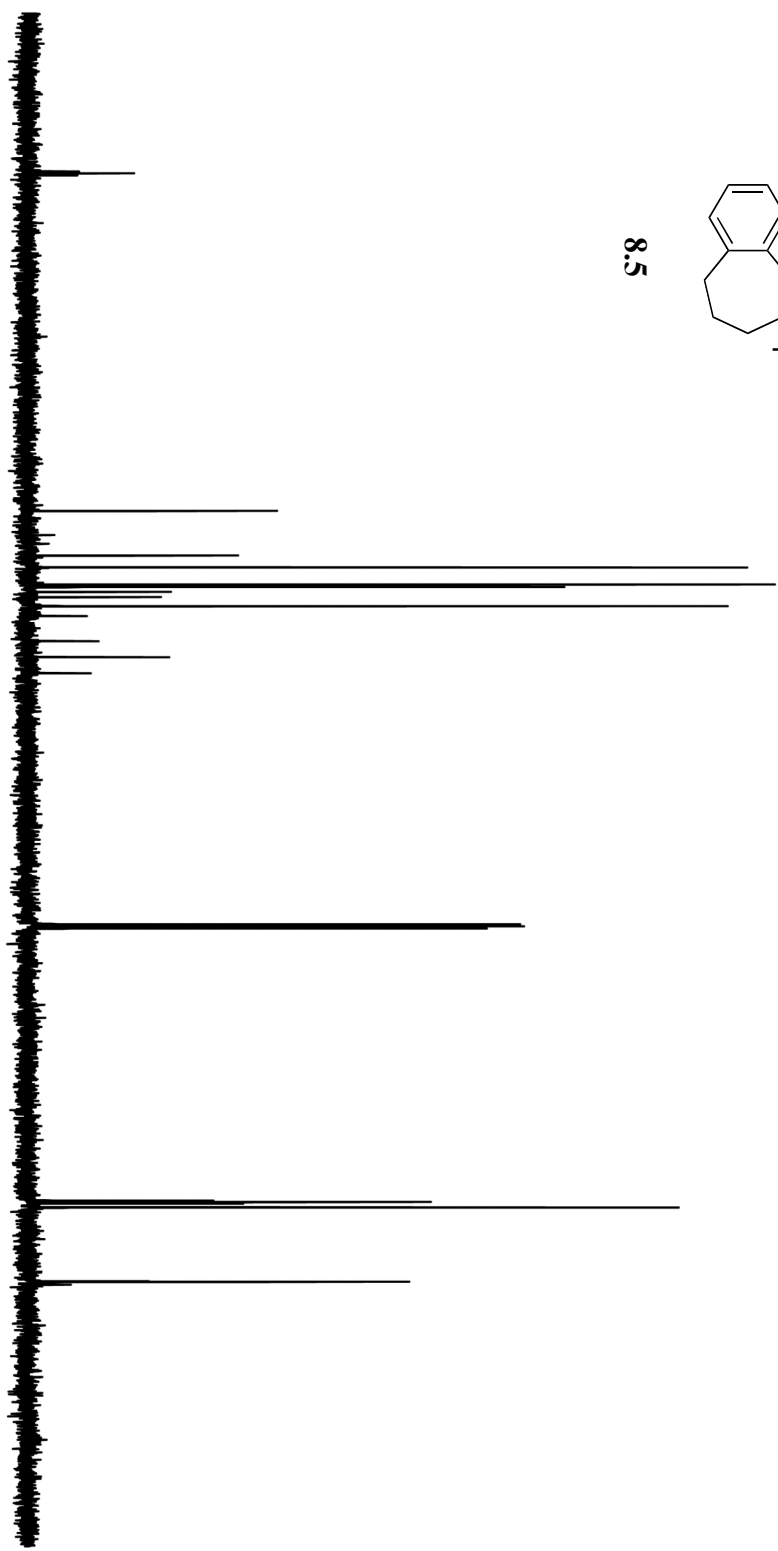


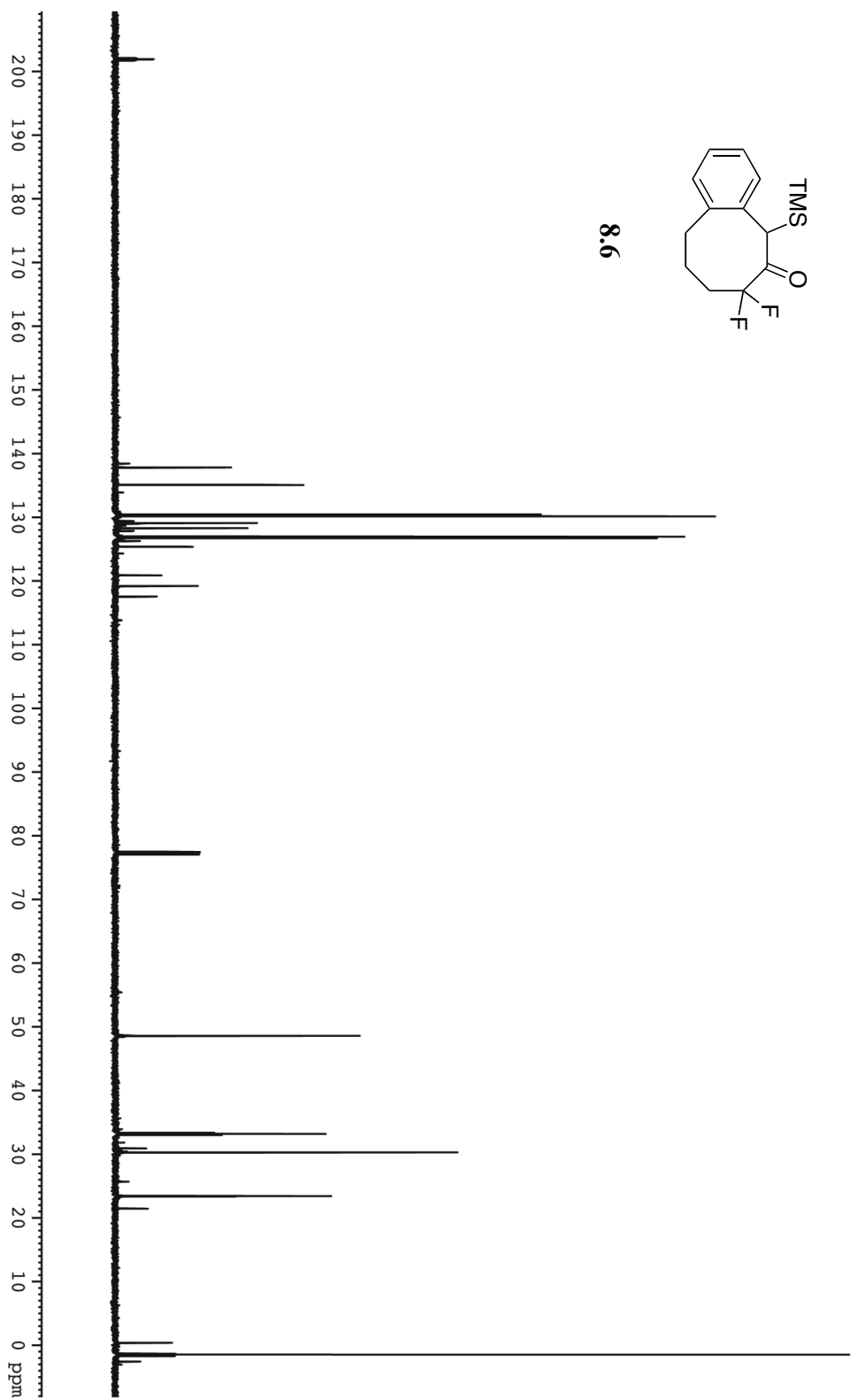


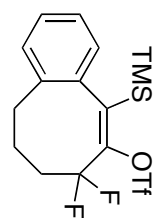


8.5

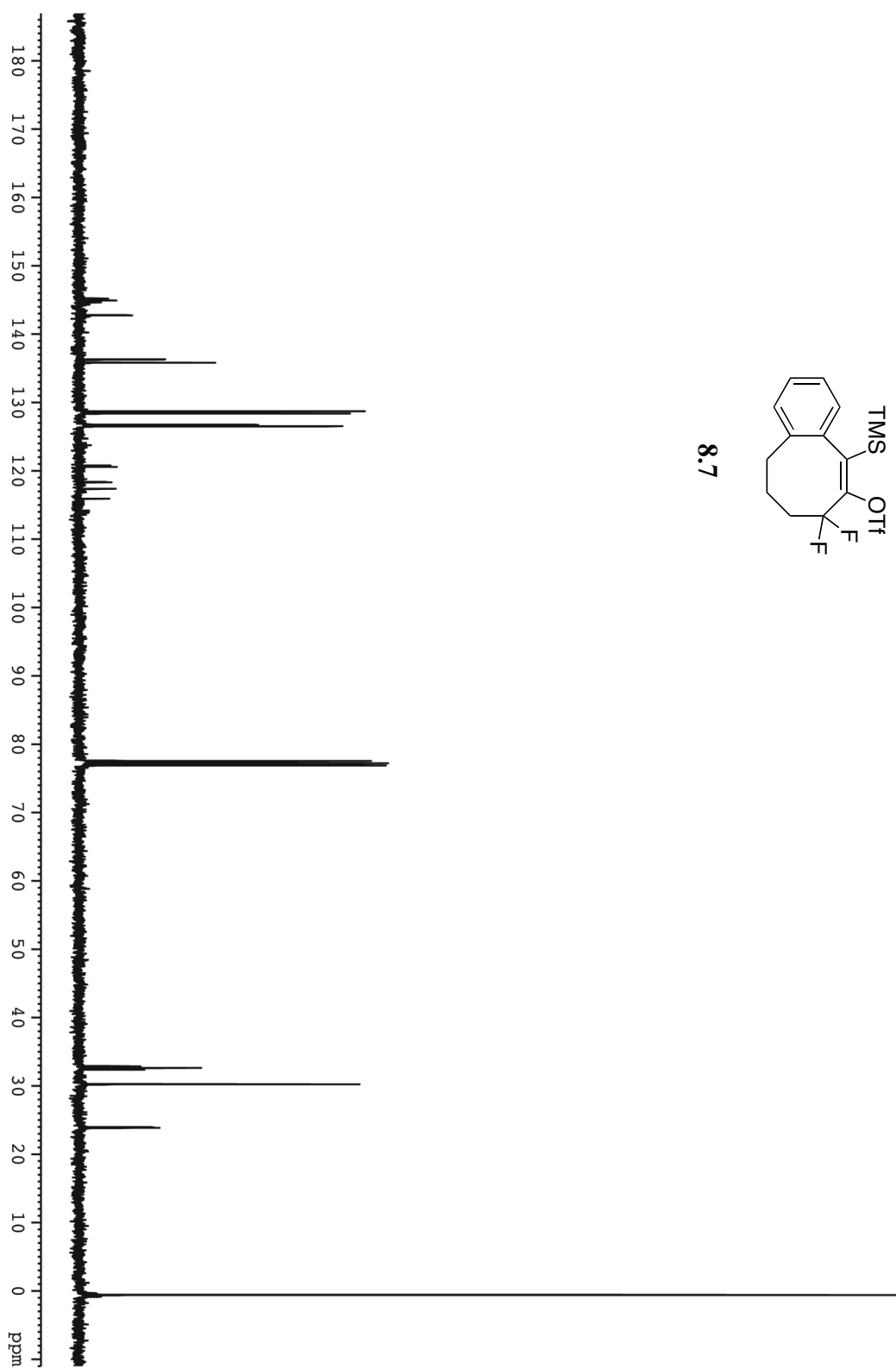
210 200 190 180 170 160 150 140 130 120 110 100 90 80 70 60 50 40 30 20 10 0 ppm

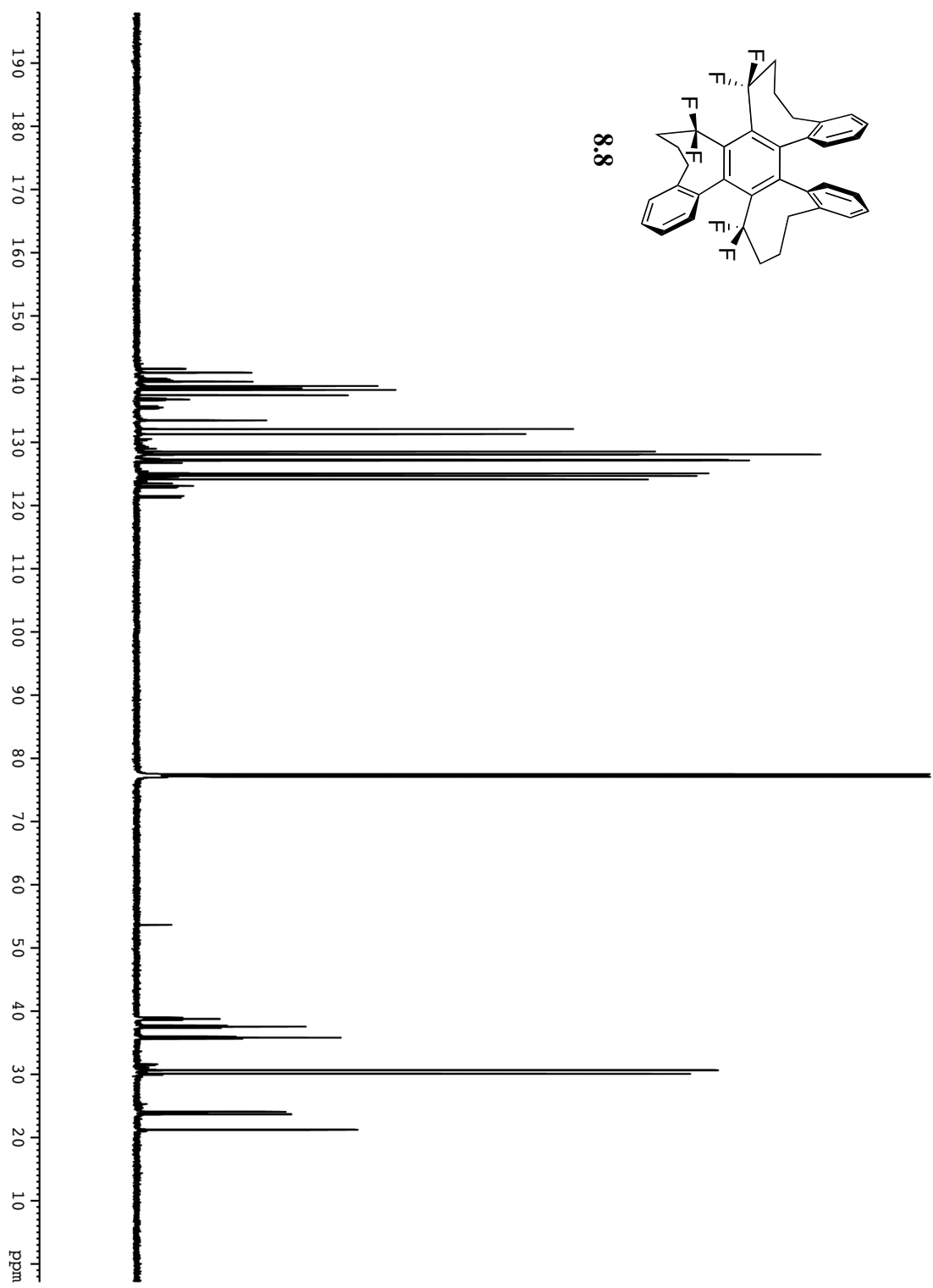
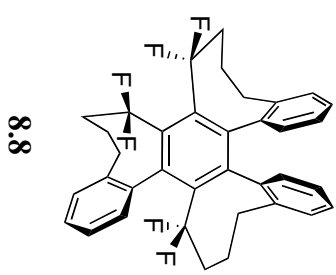


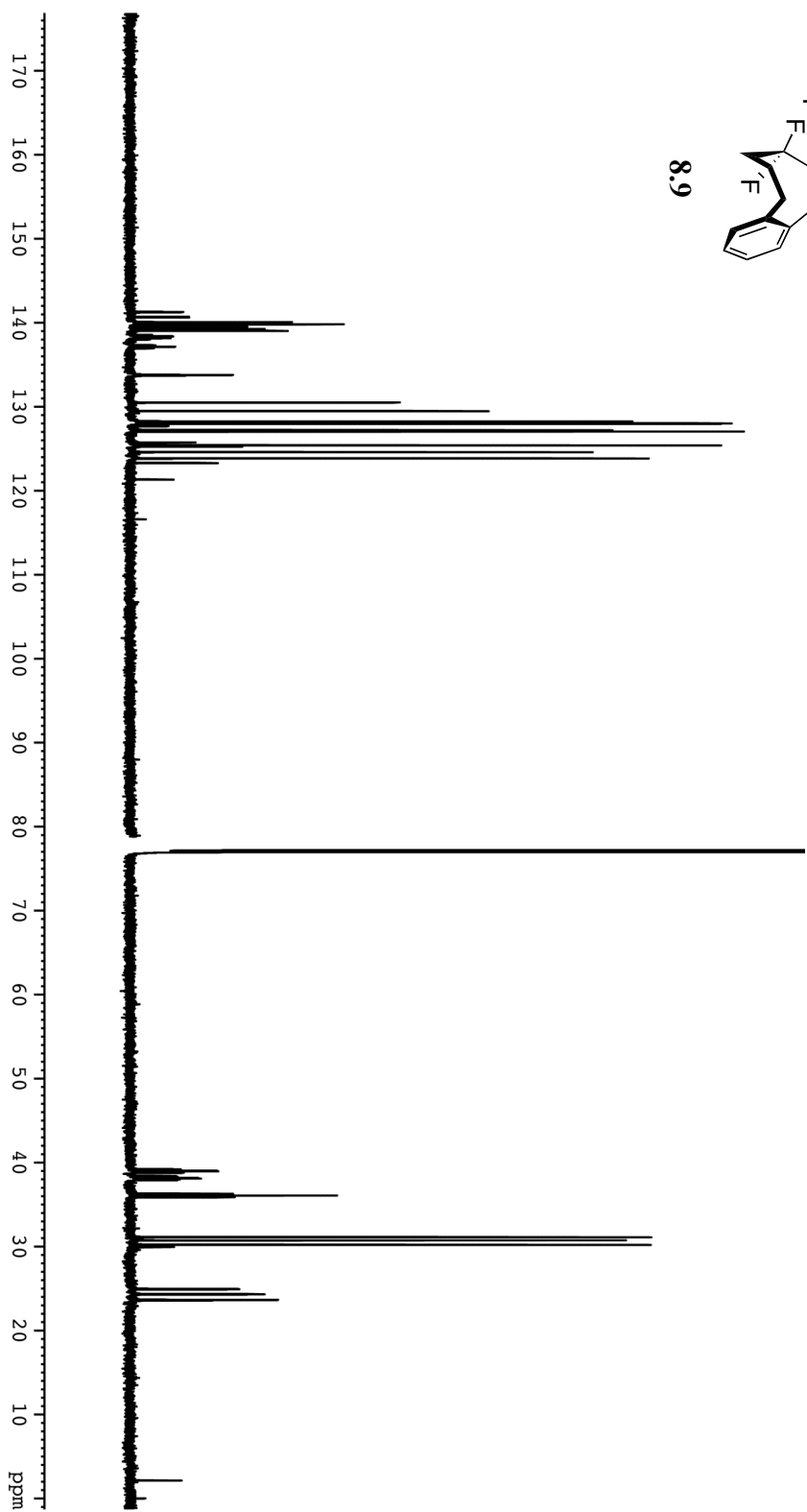
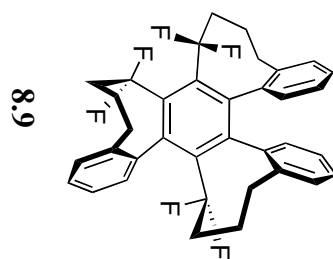


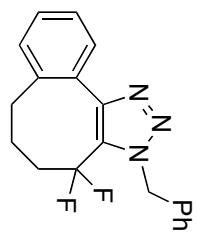


8.7

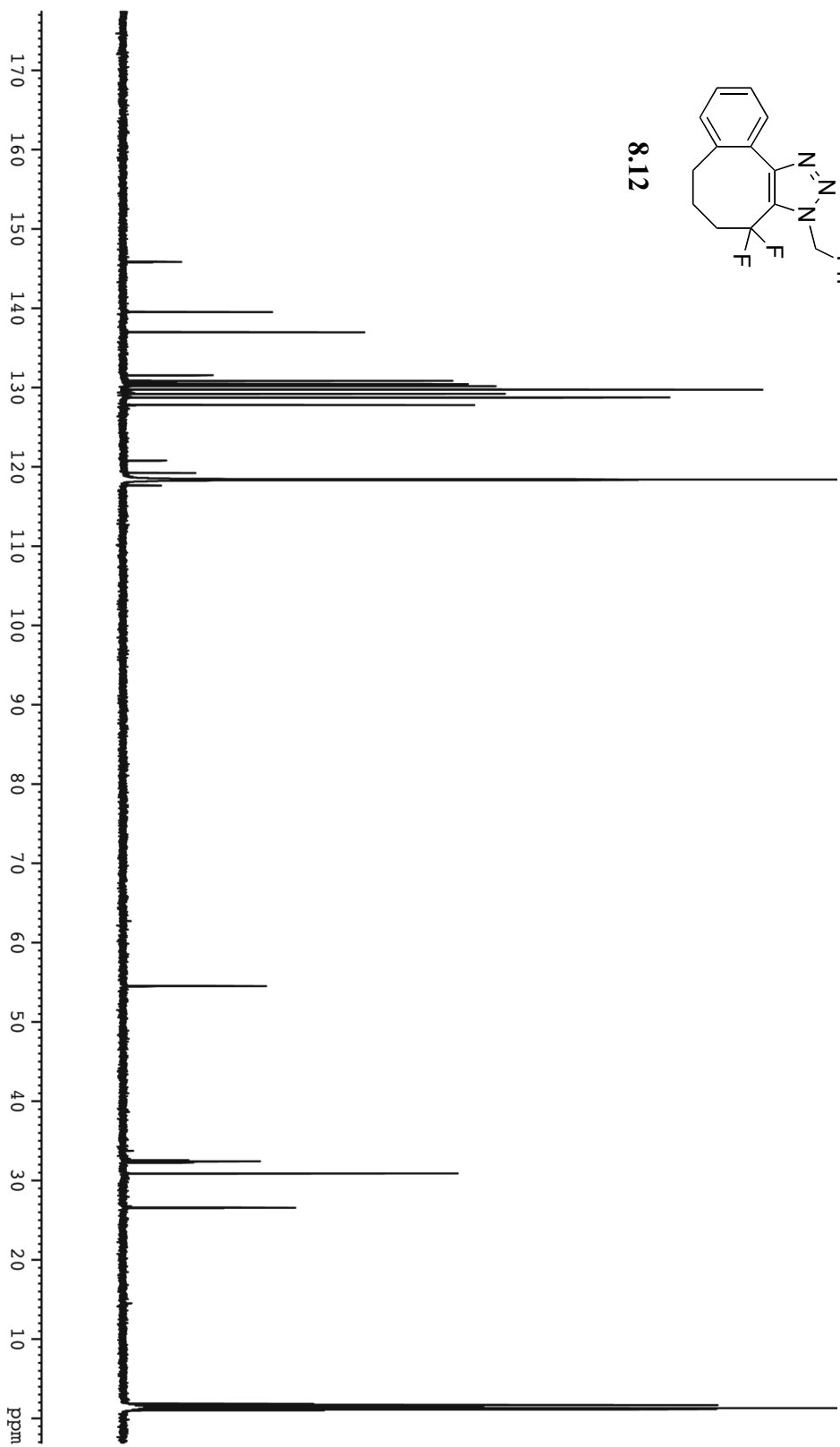


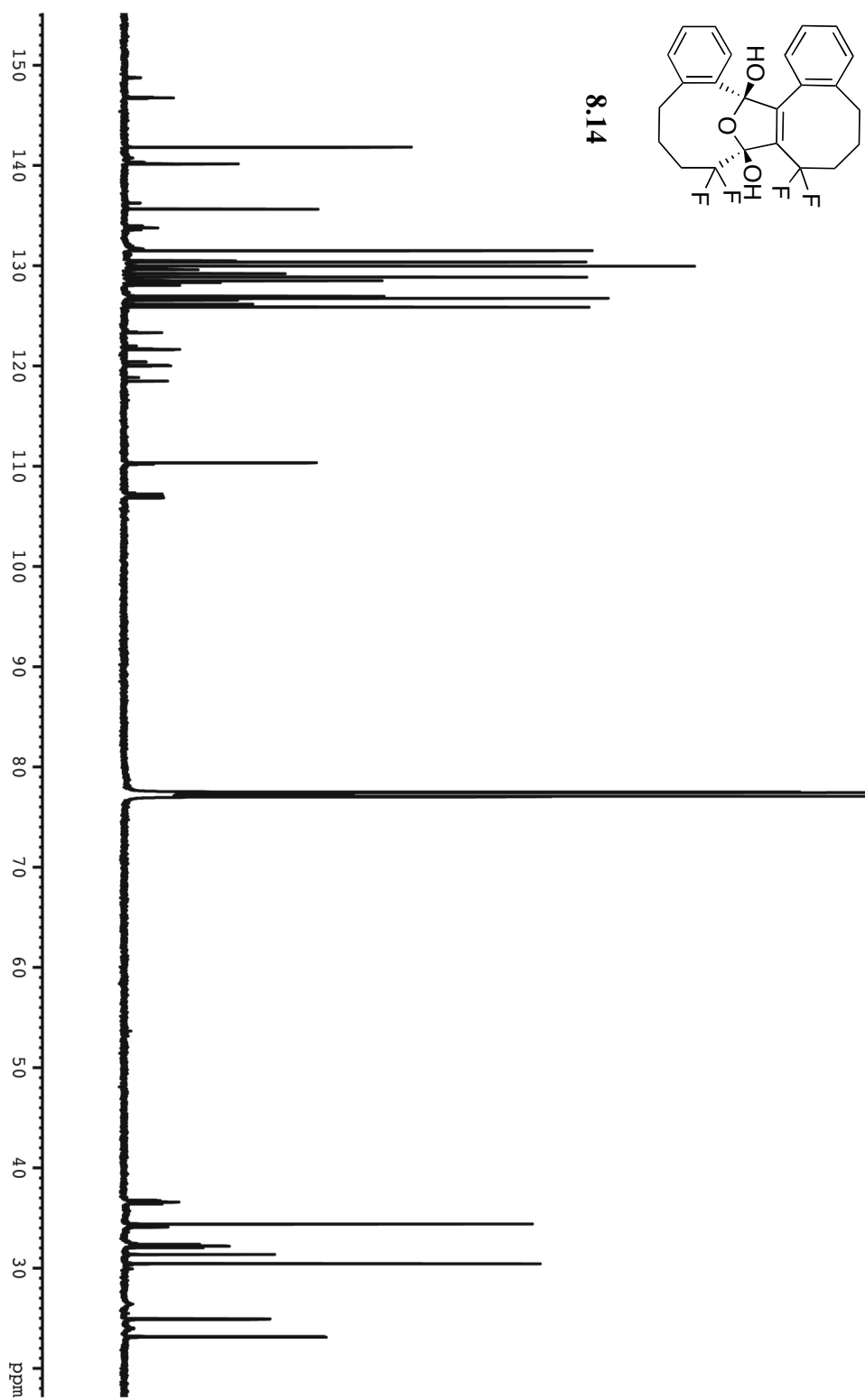


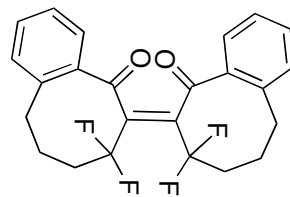




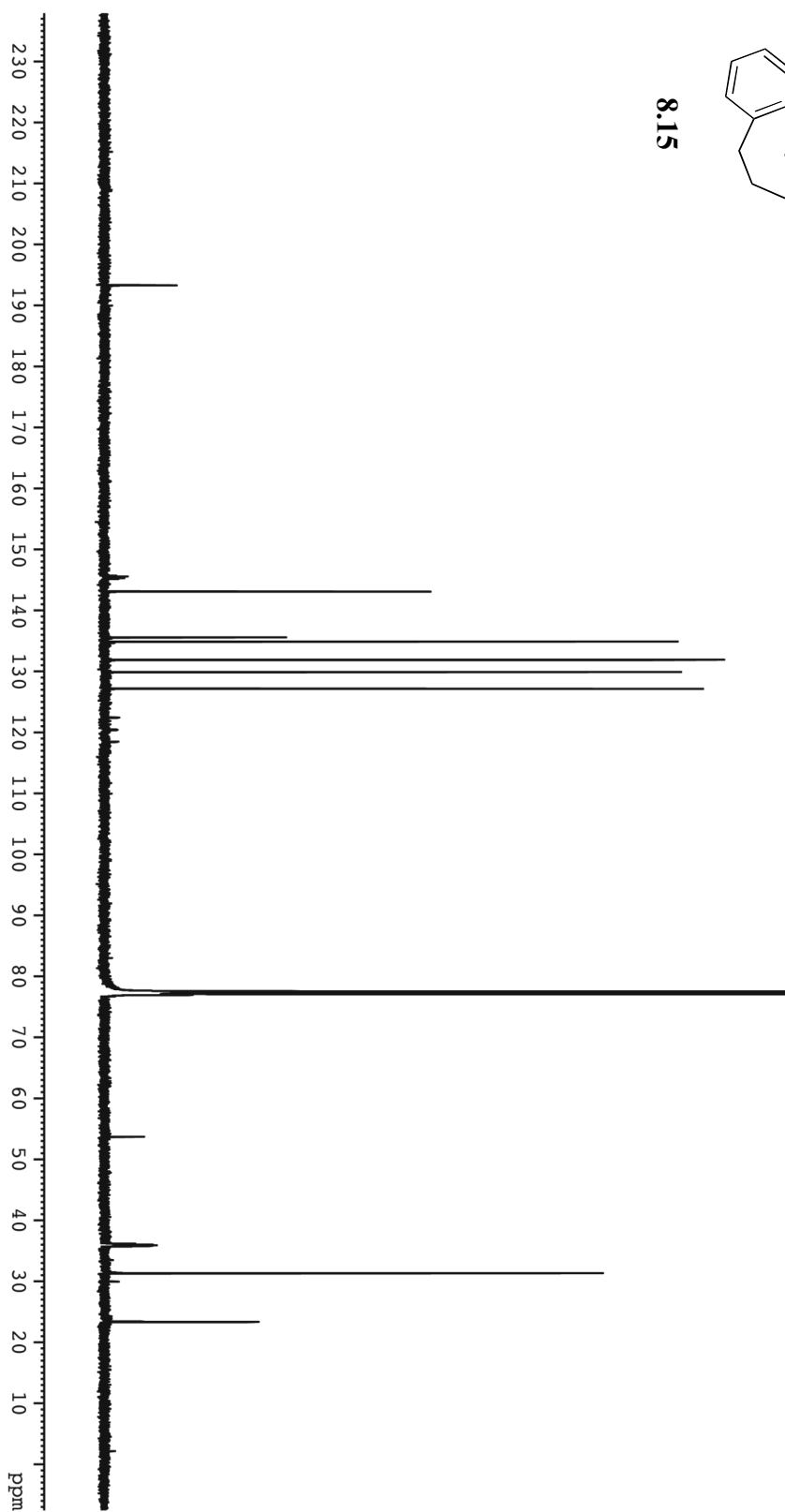
8.12

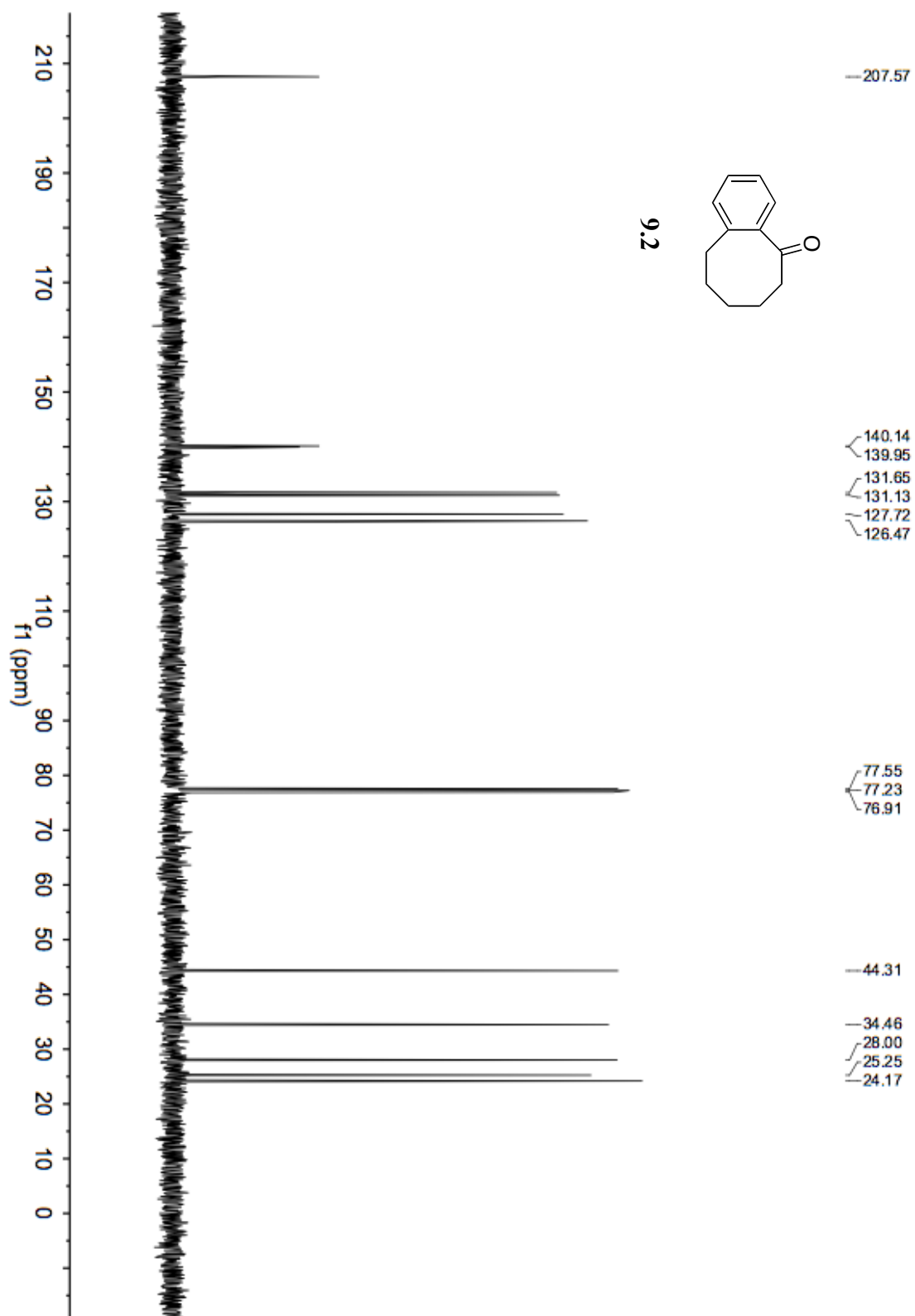


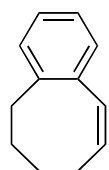




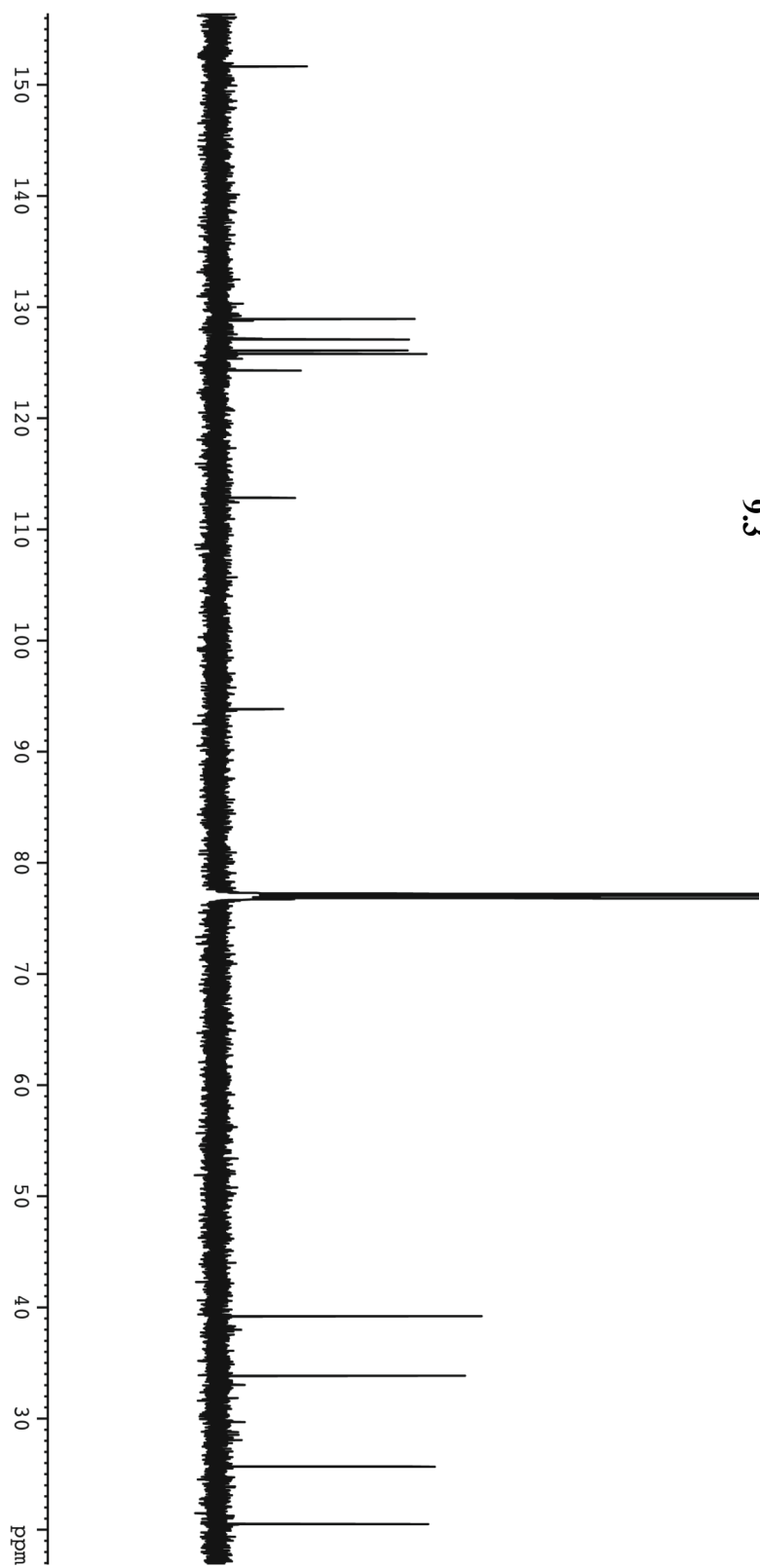
8.15

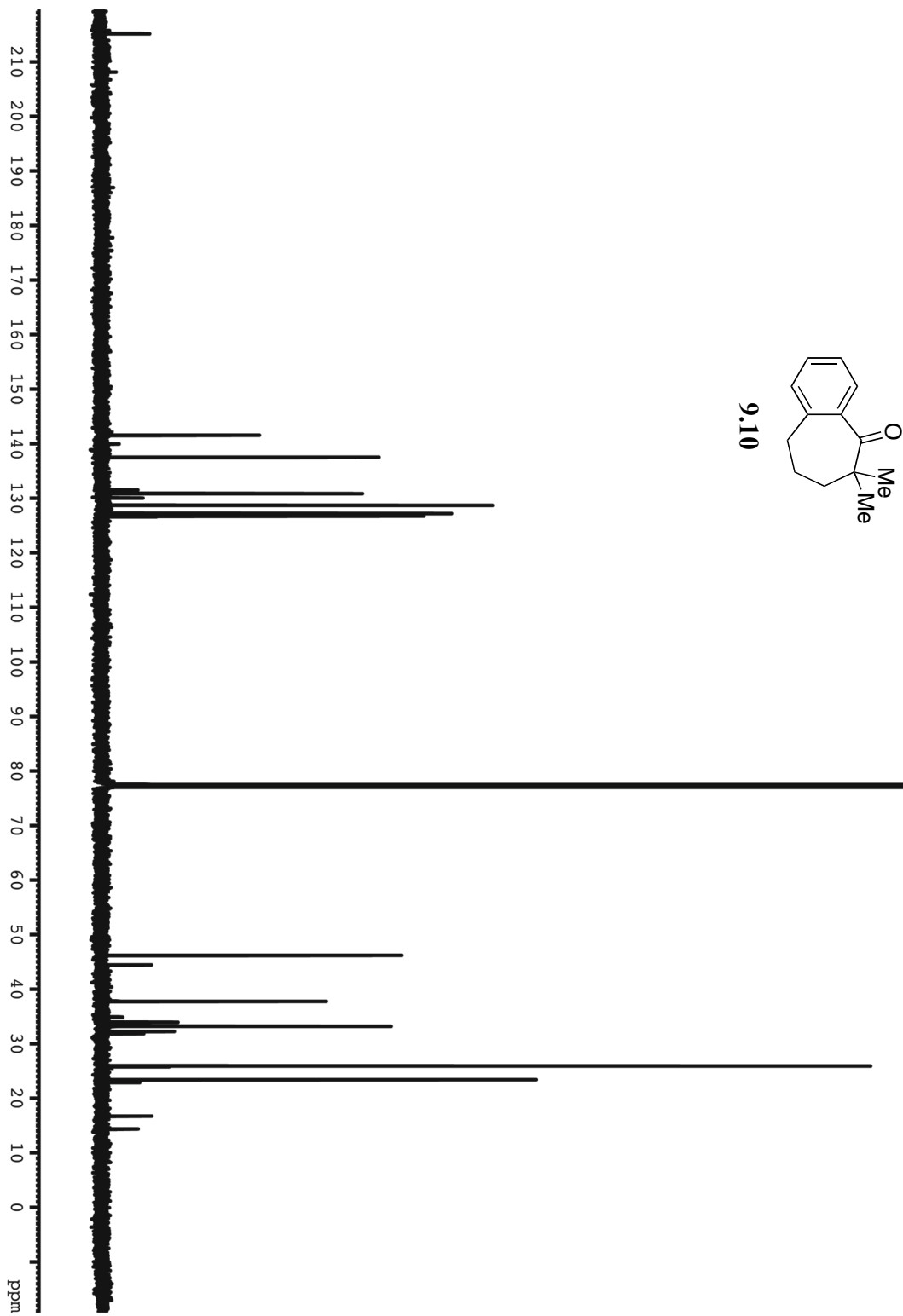
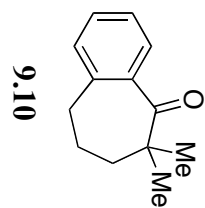


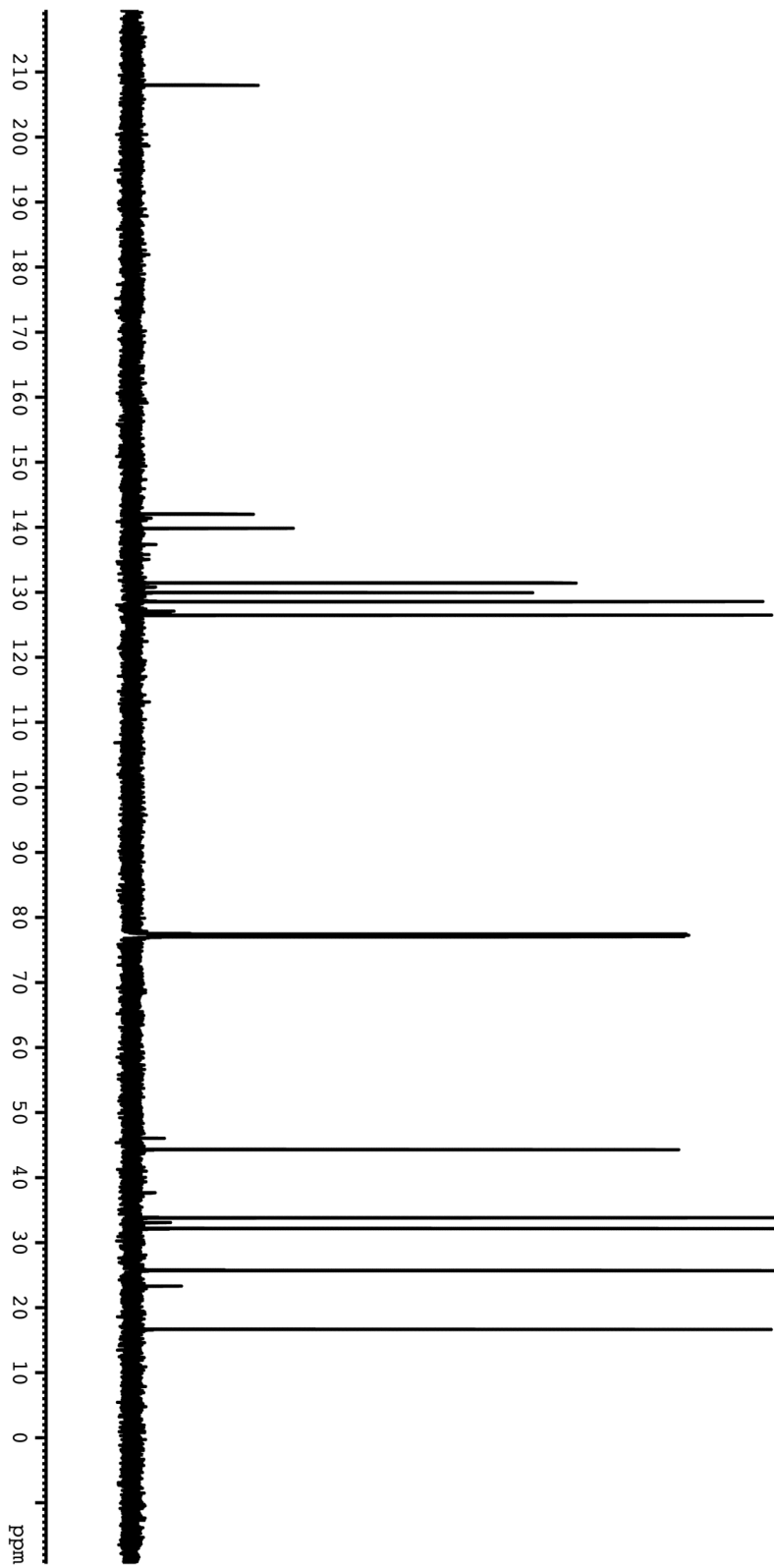
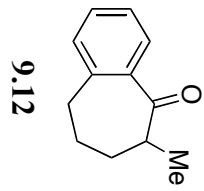


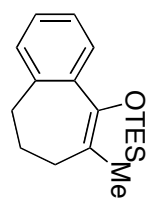


9.3

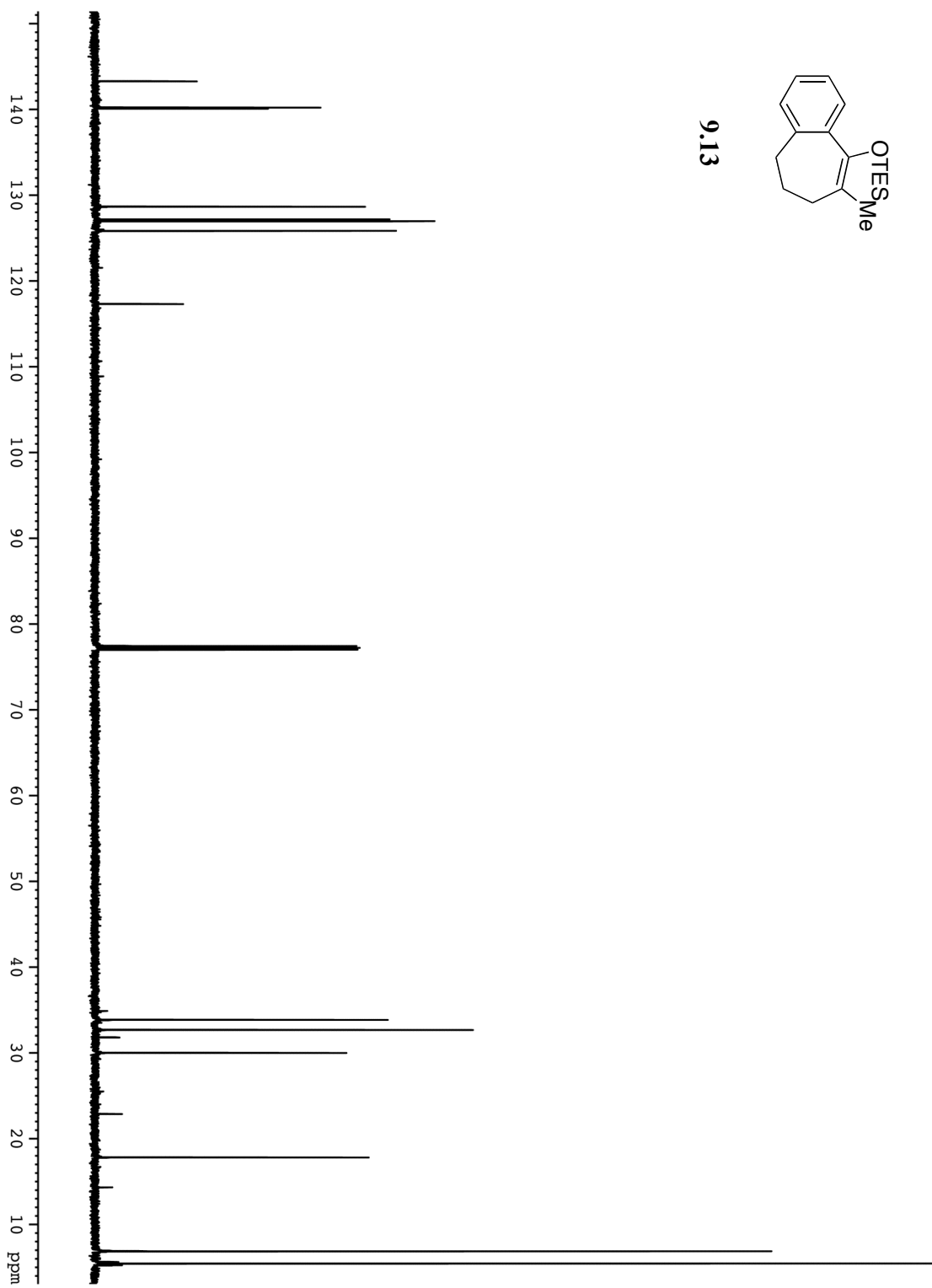


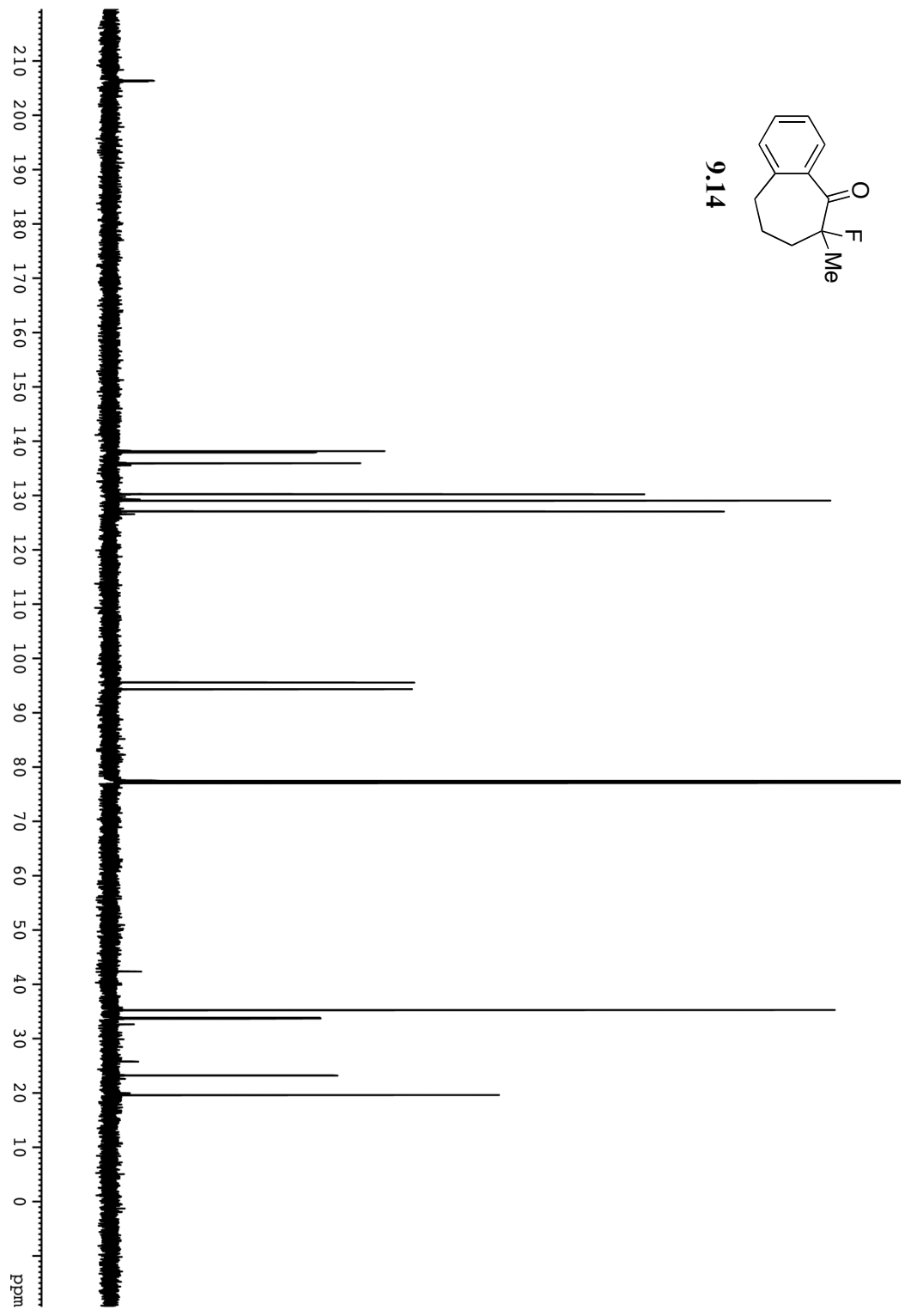
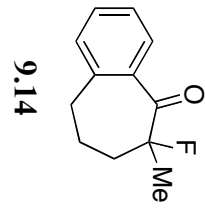


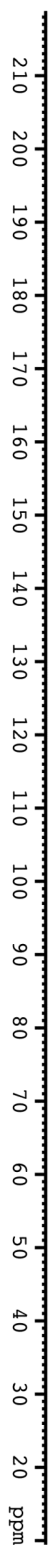
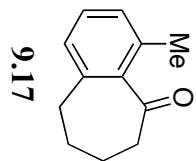


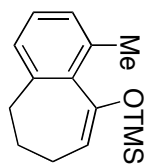


9.13

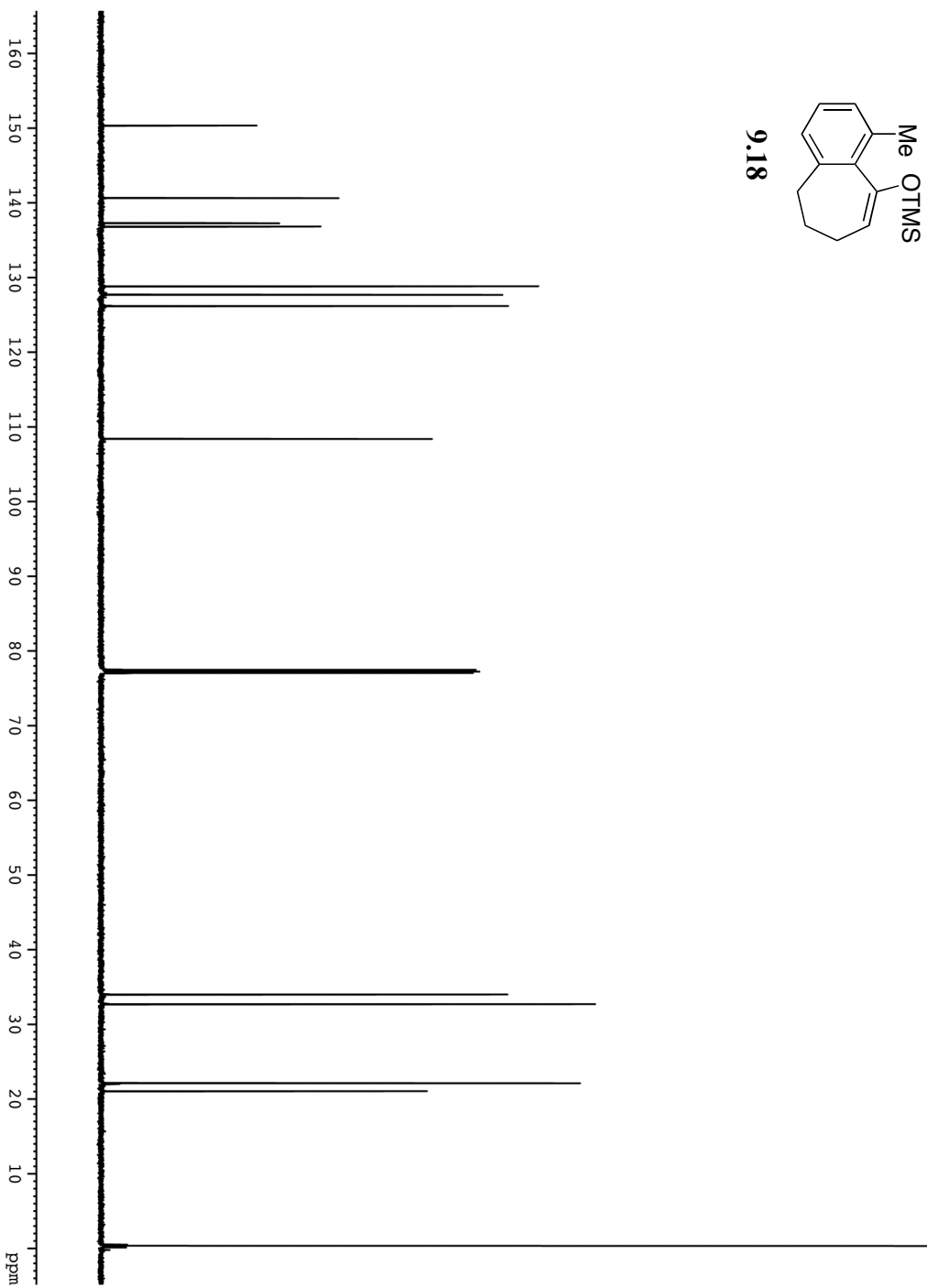


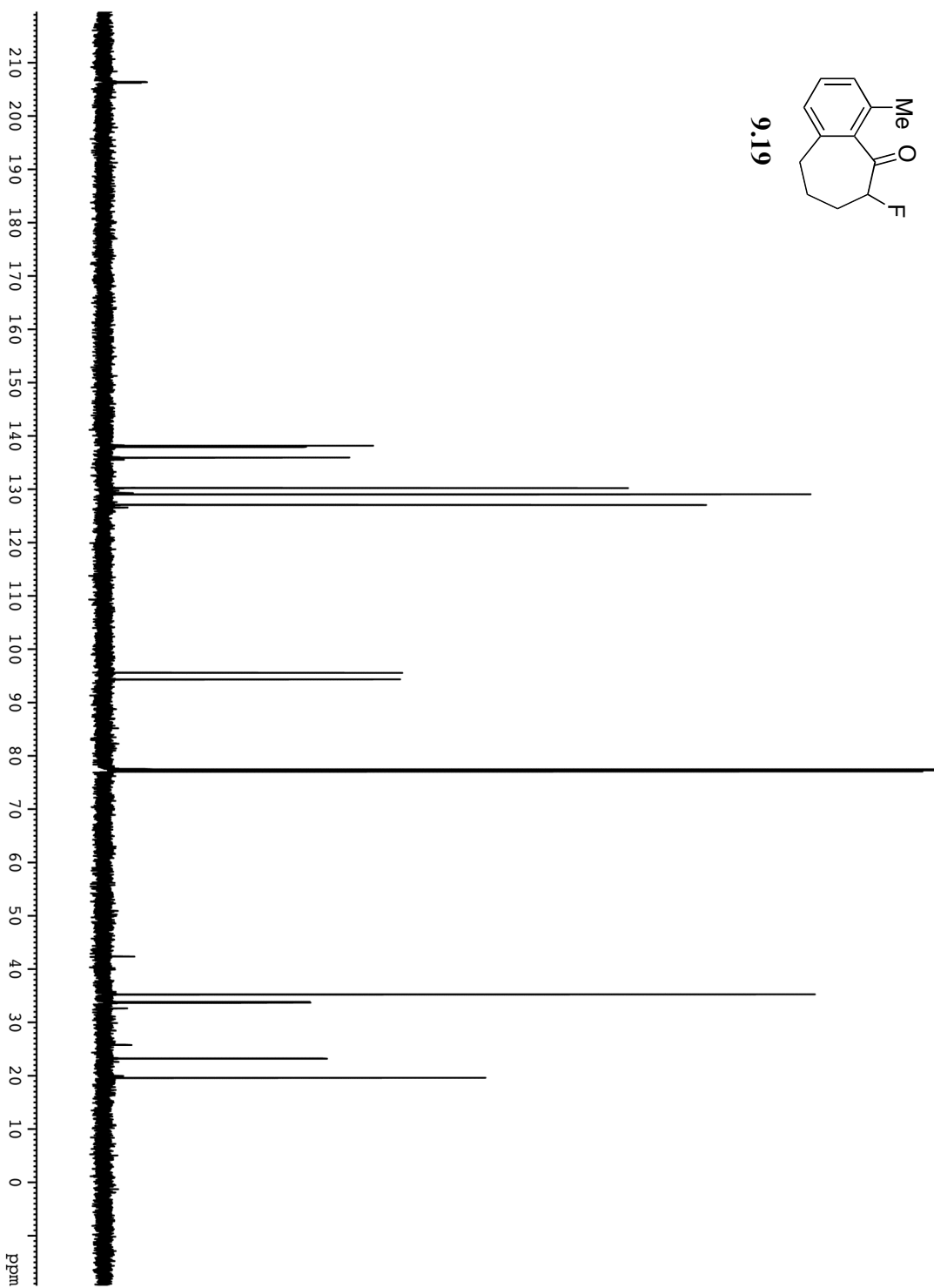
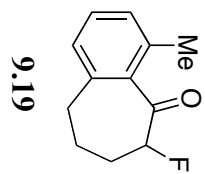


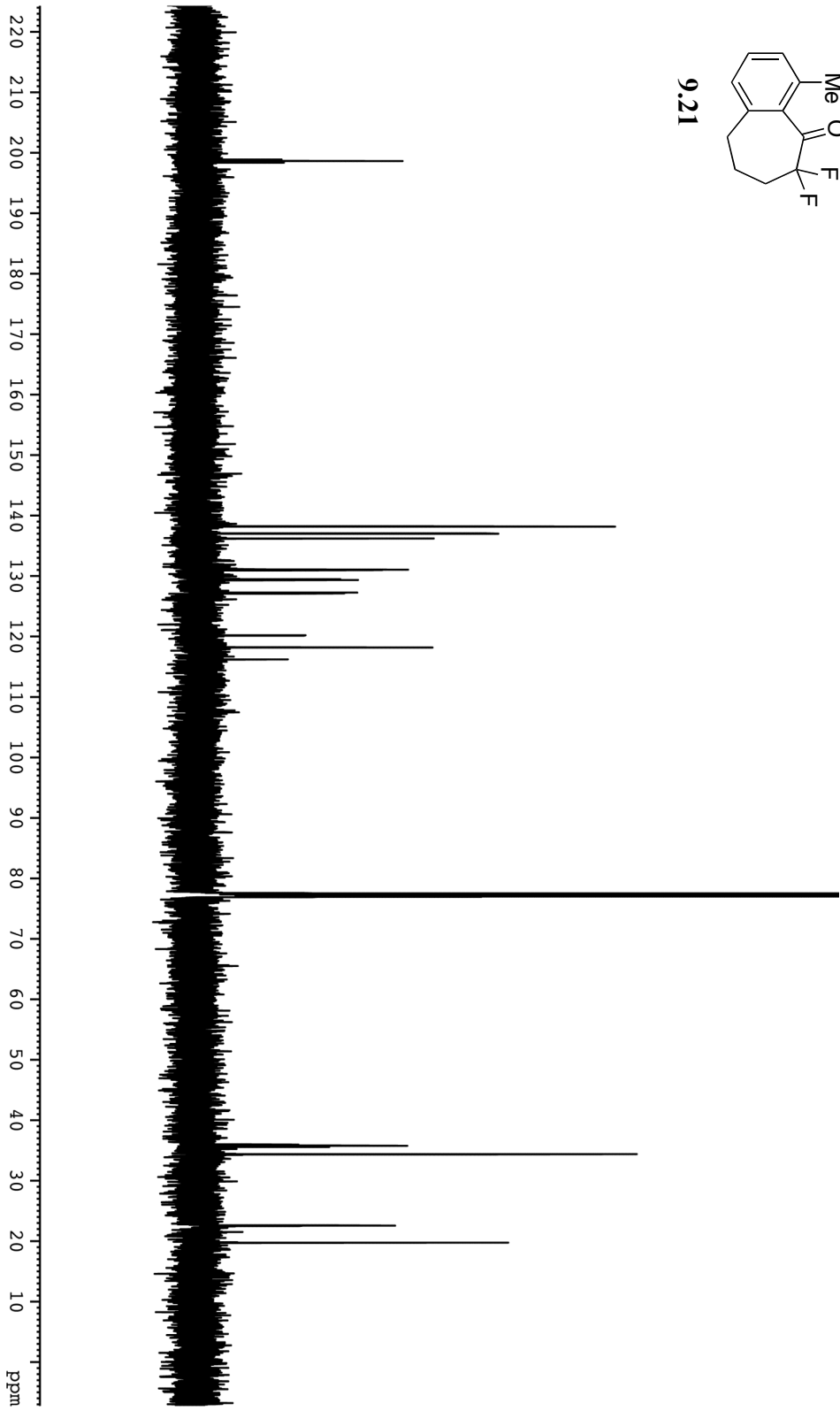
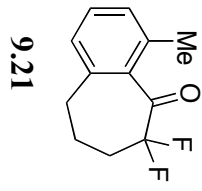


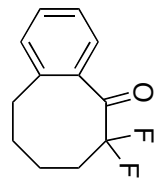


9.18

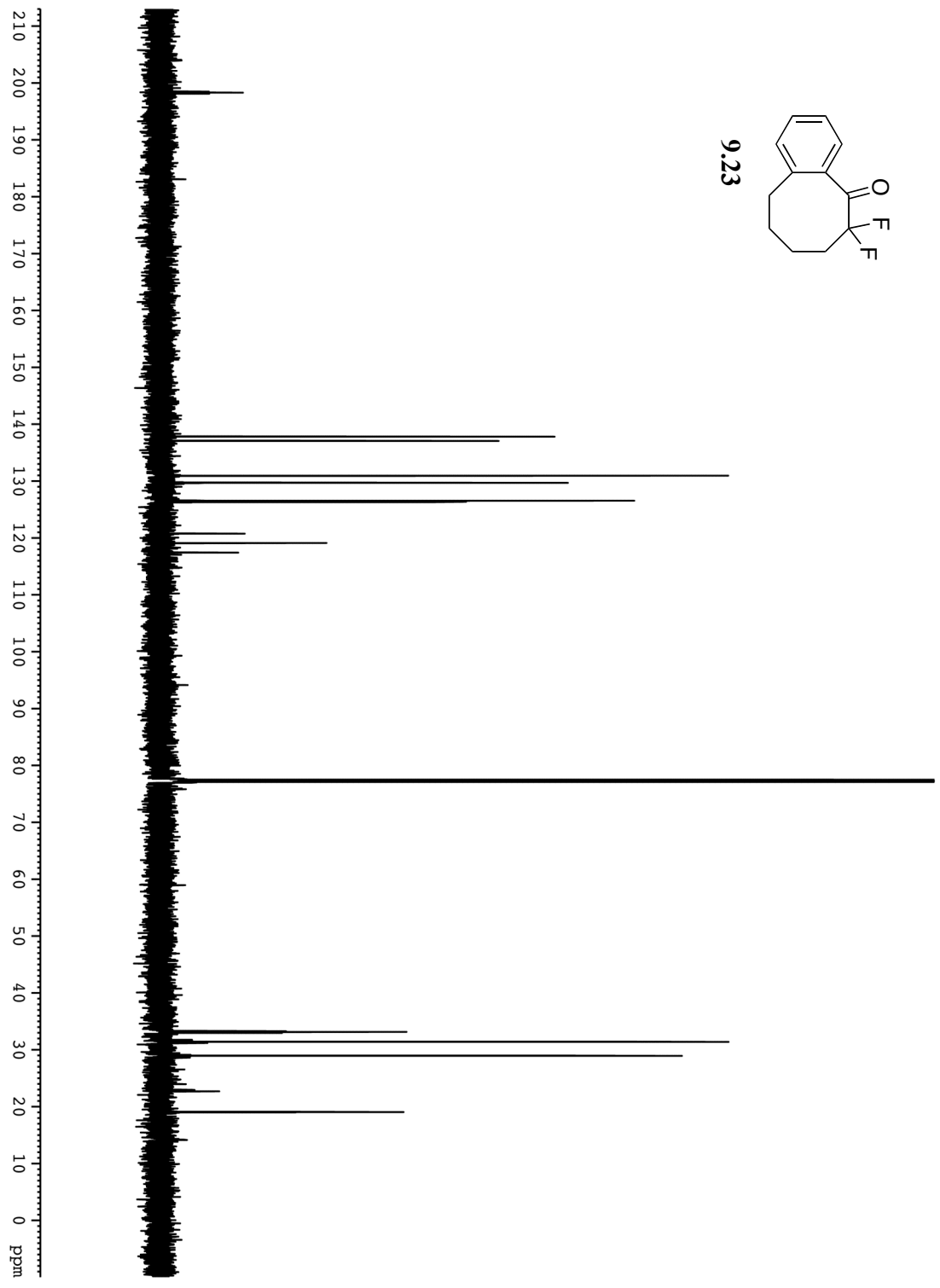


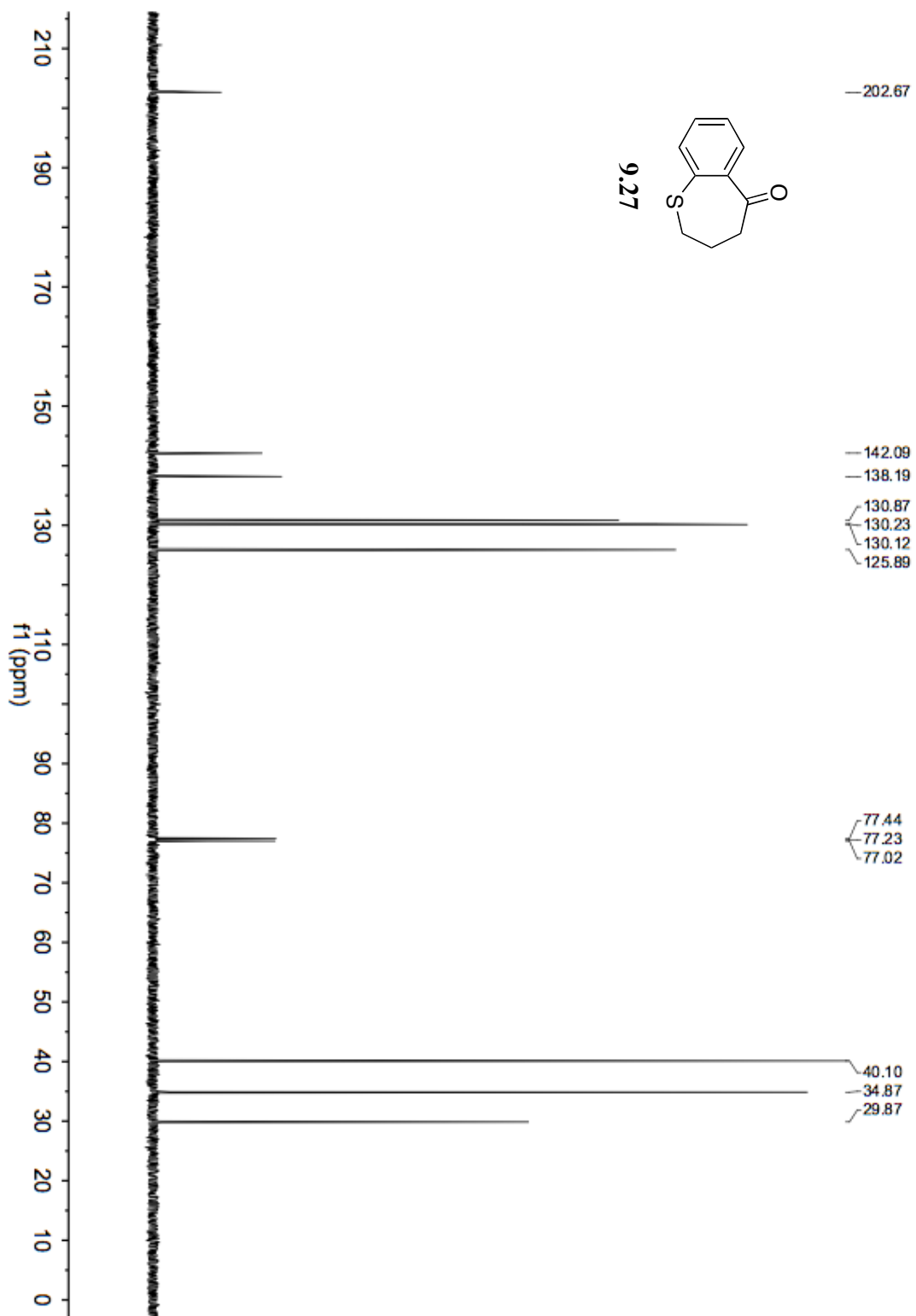


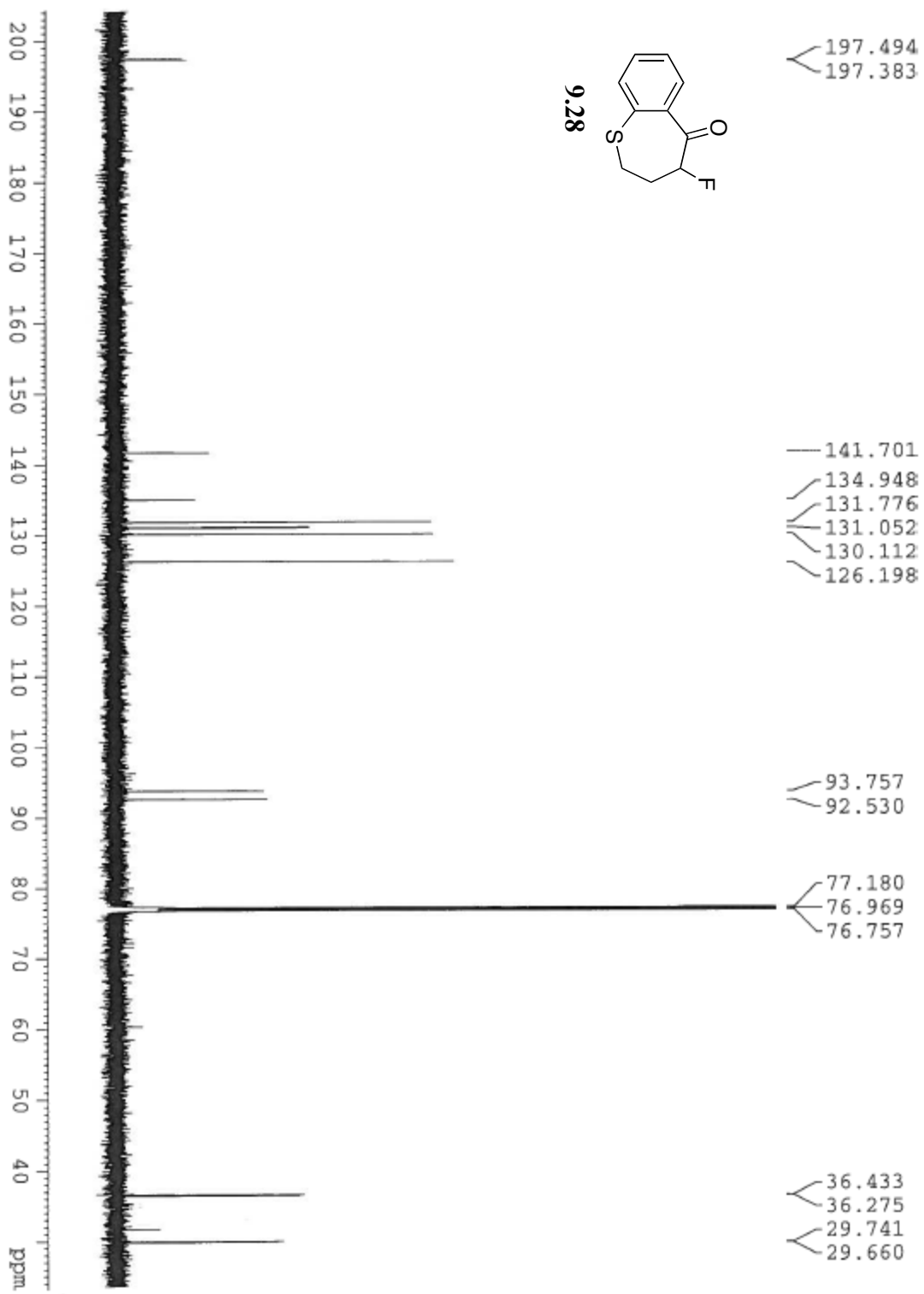


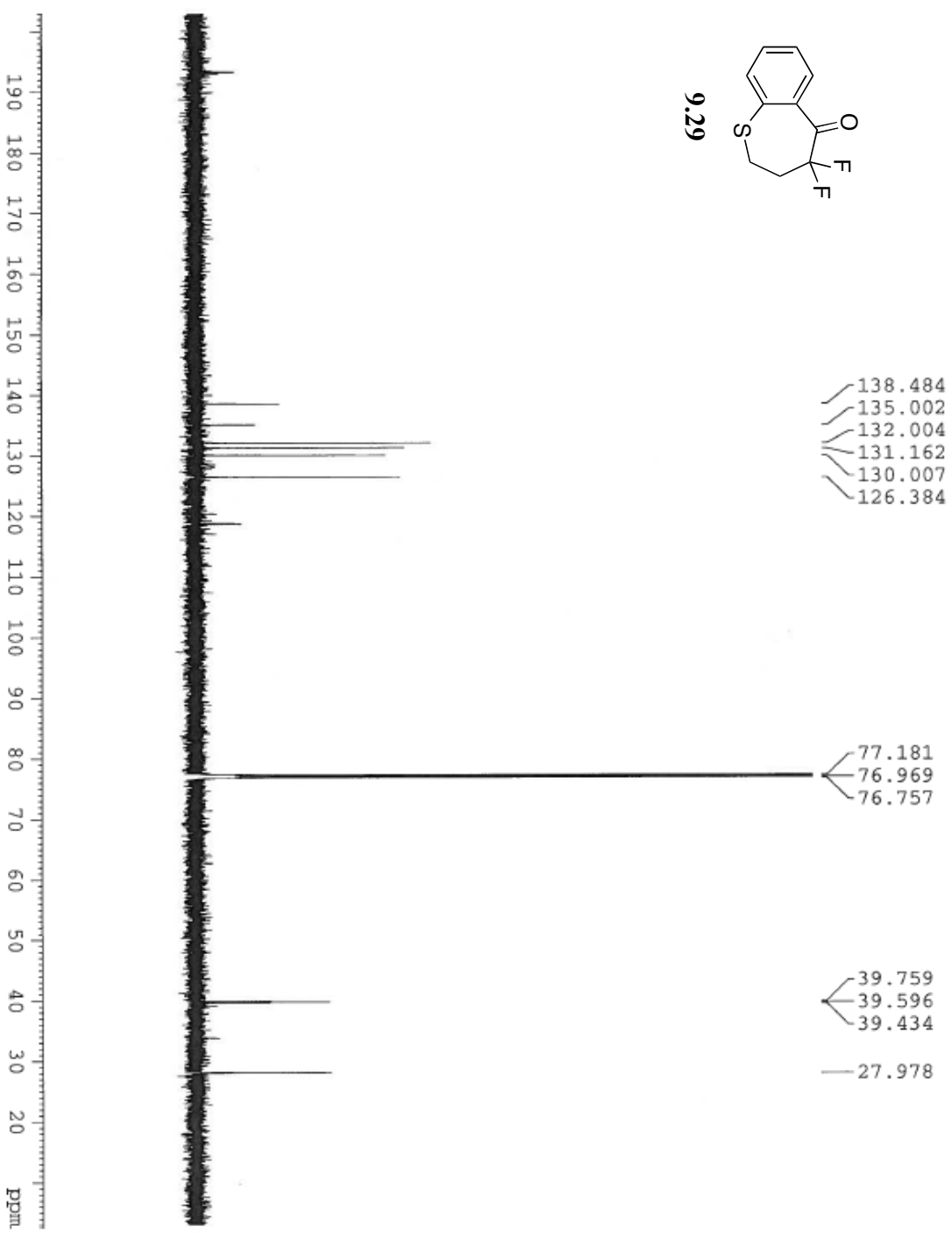
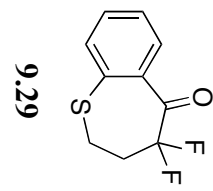


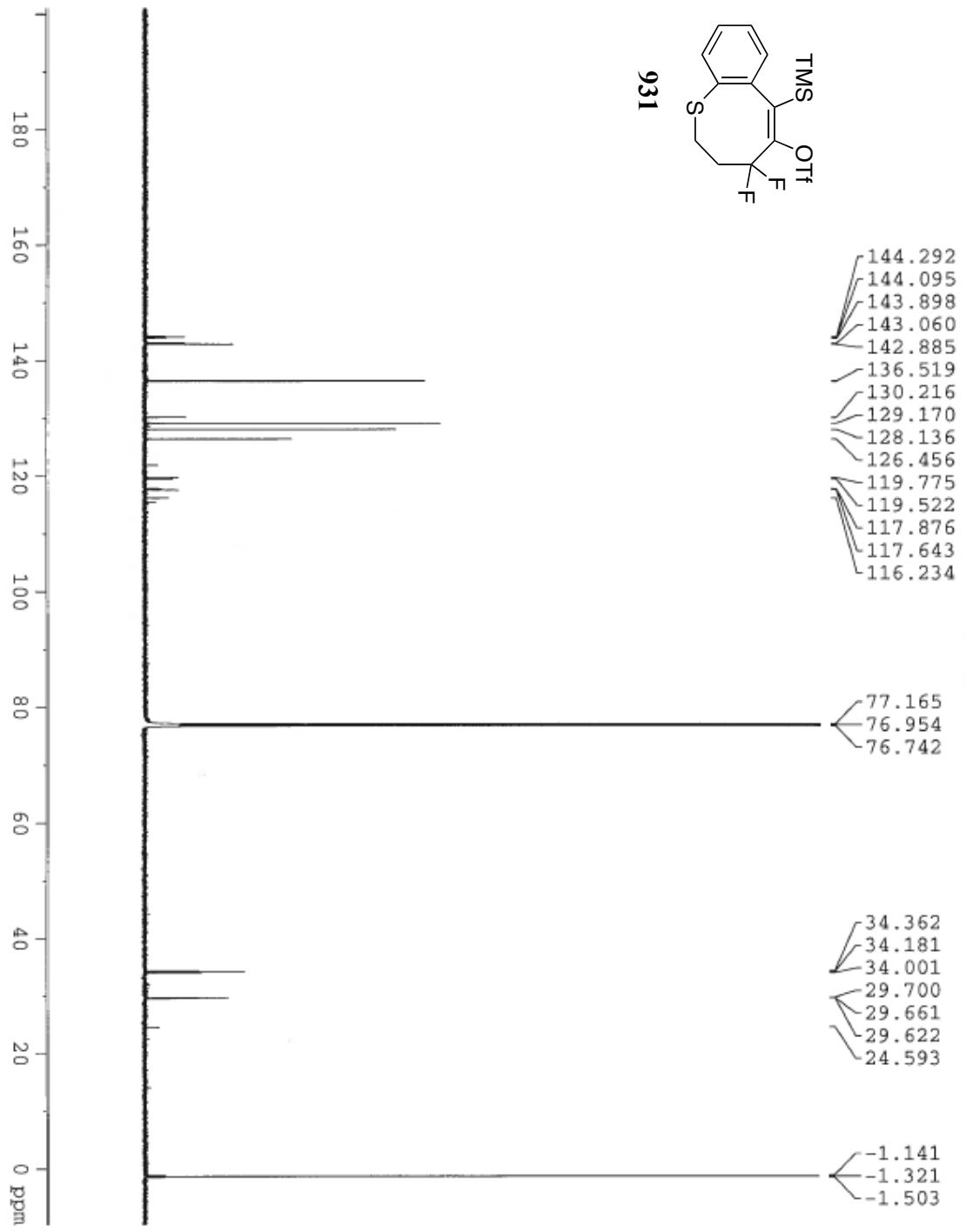
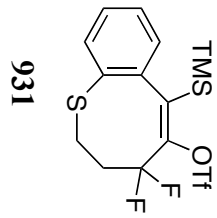
9.23

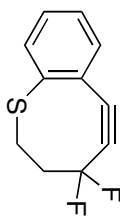




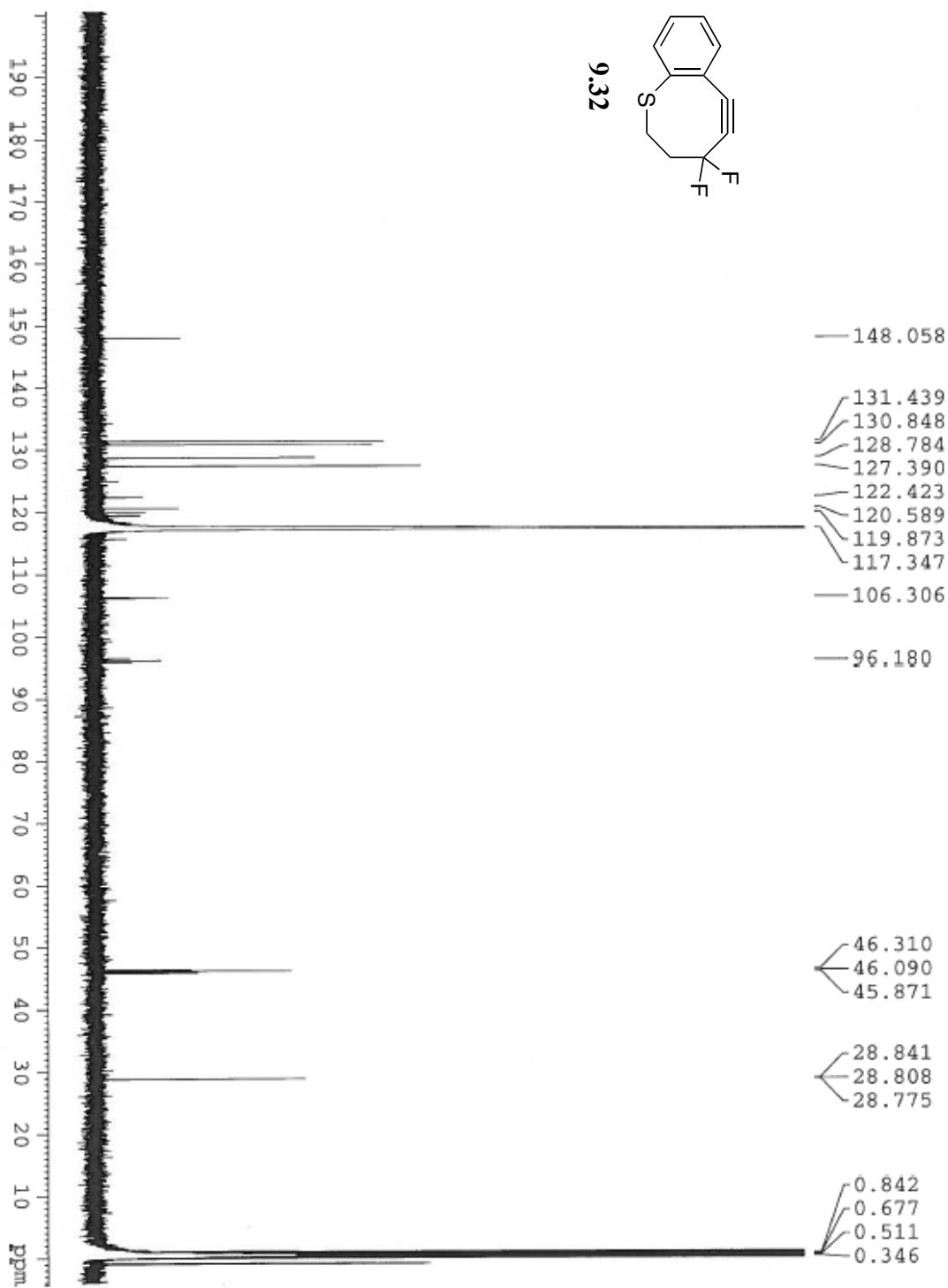


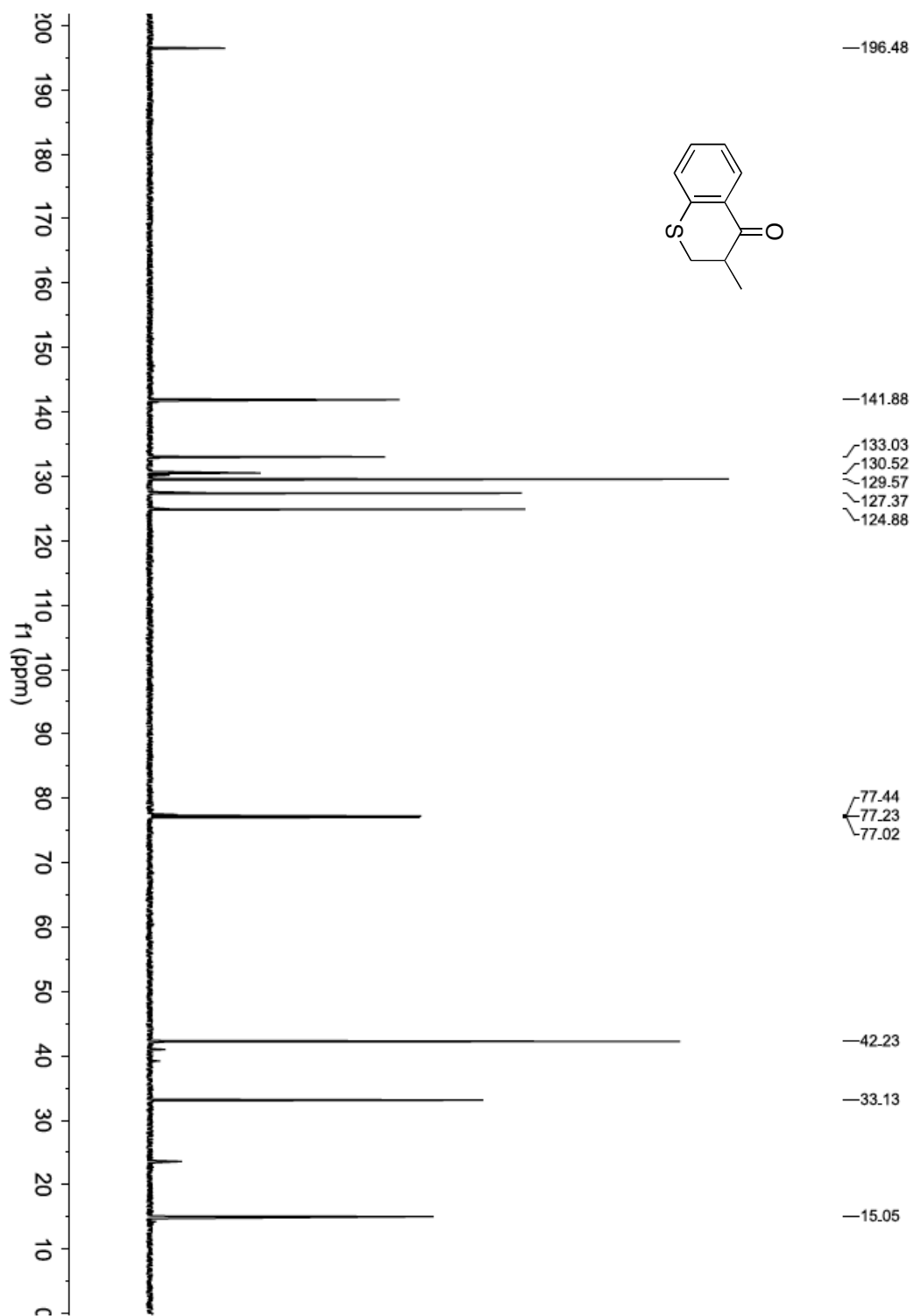


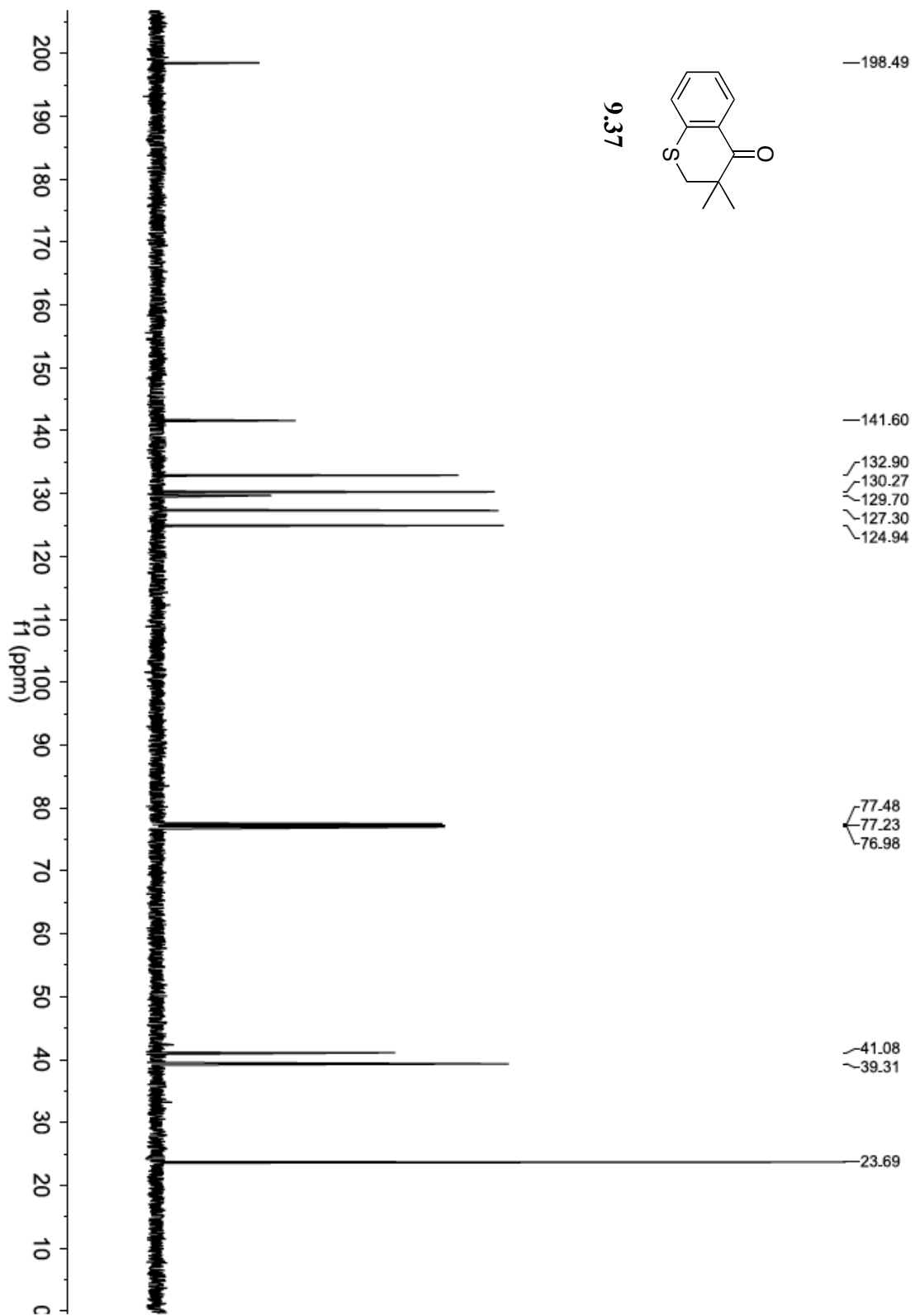
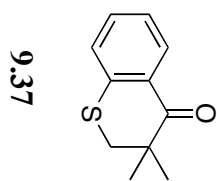


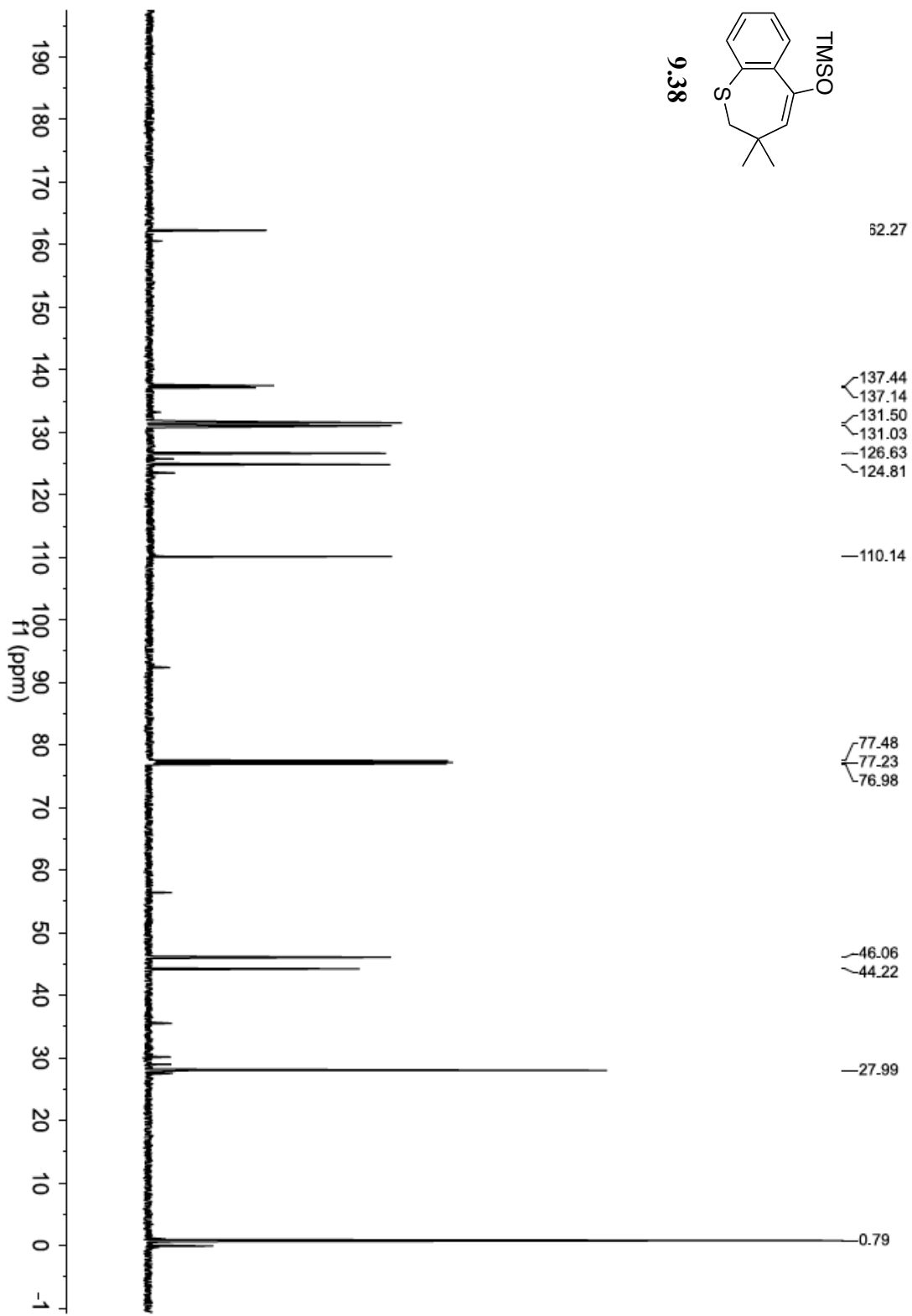
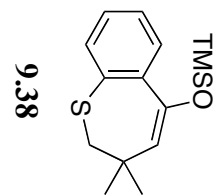


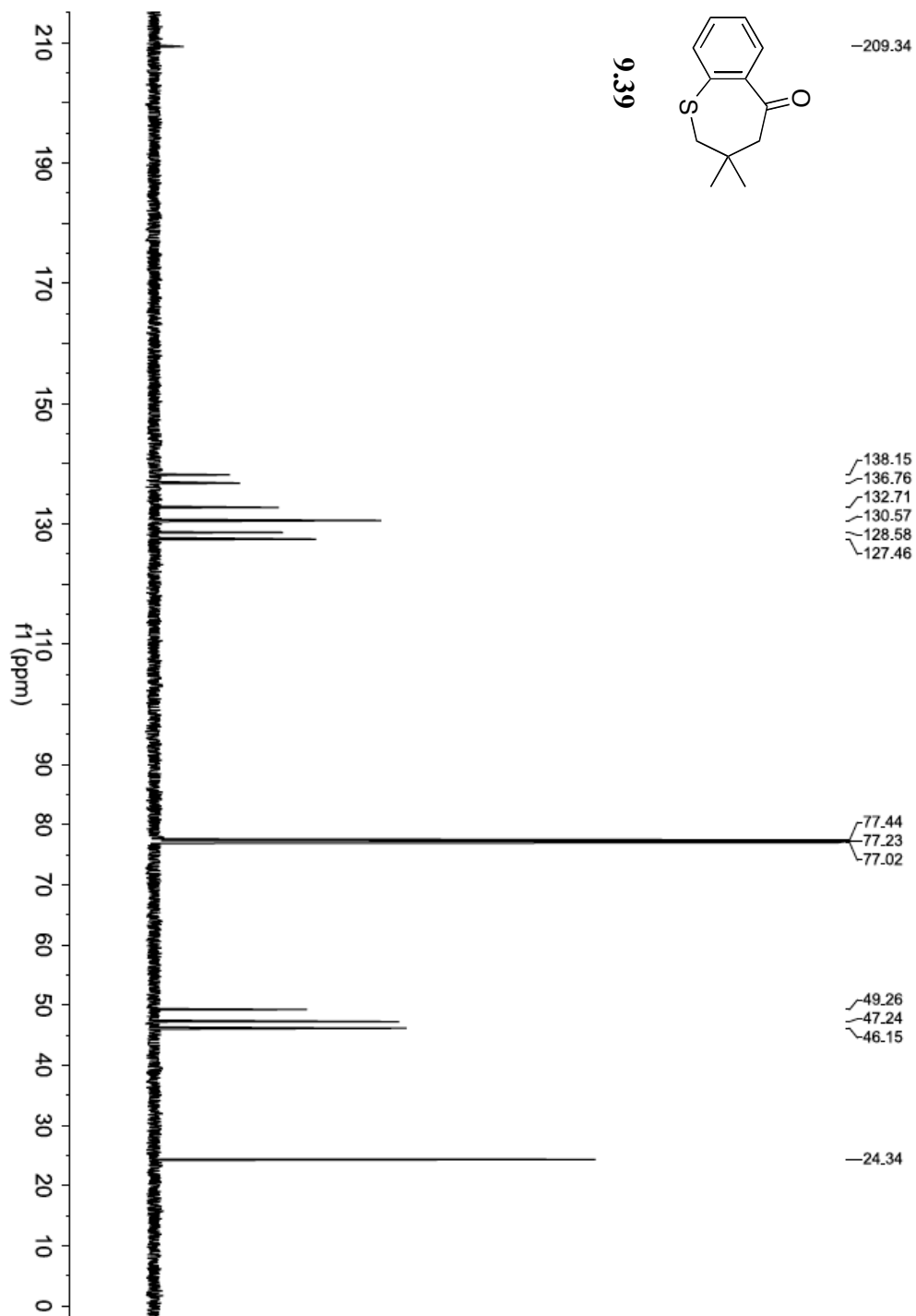
9.32

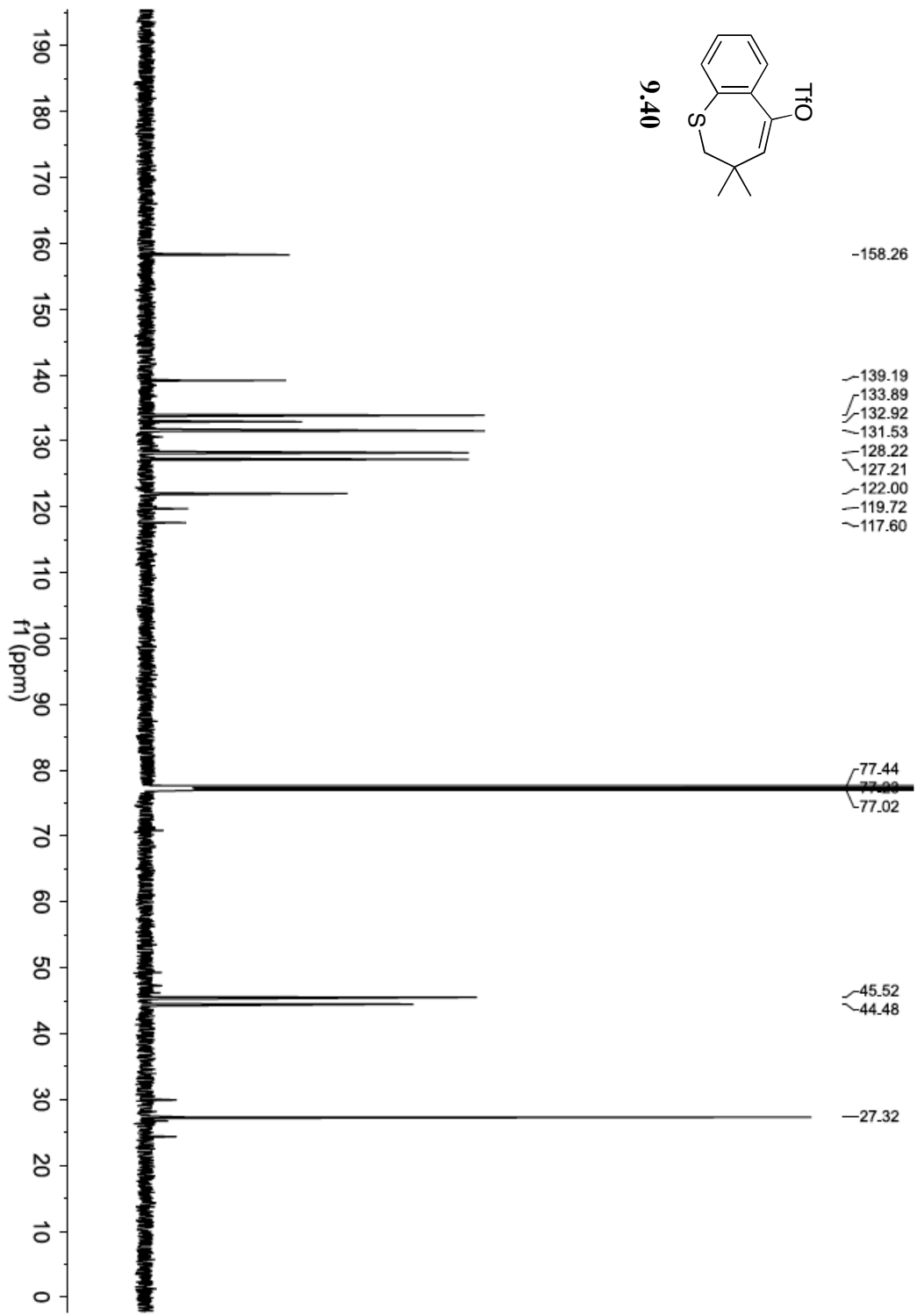


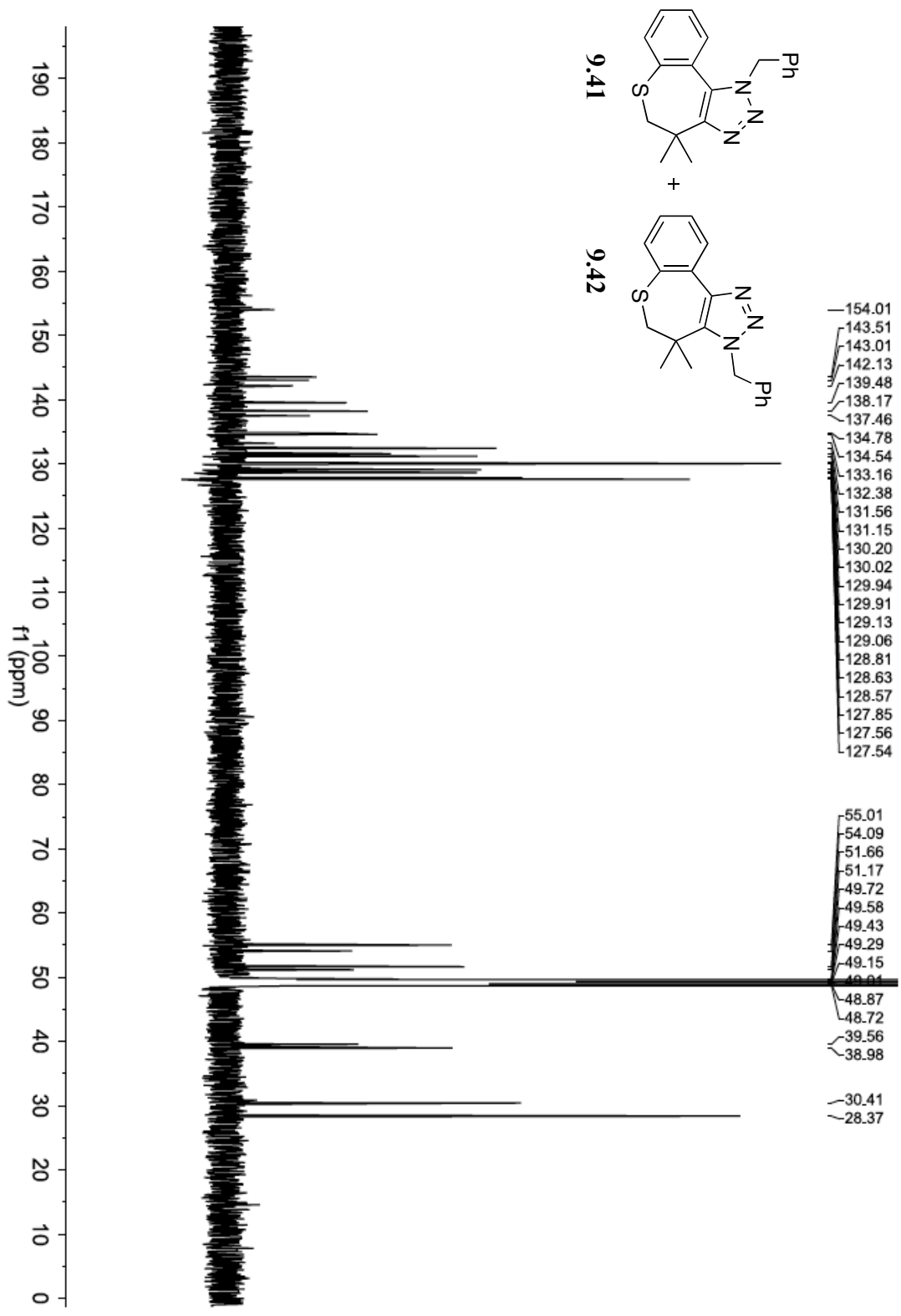


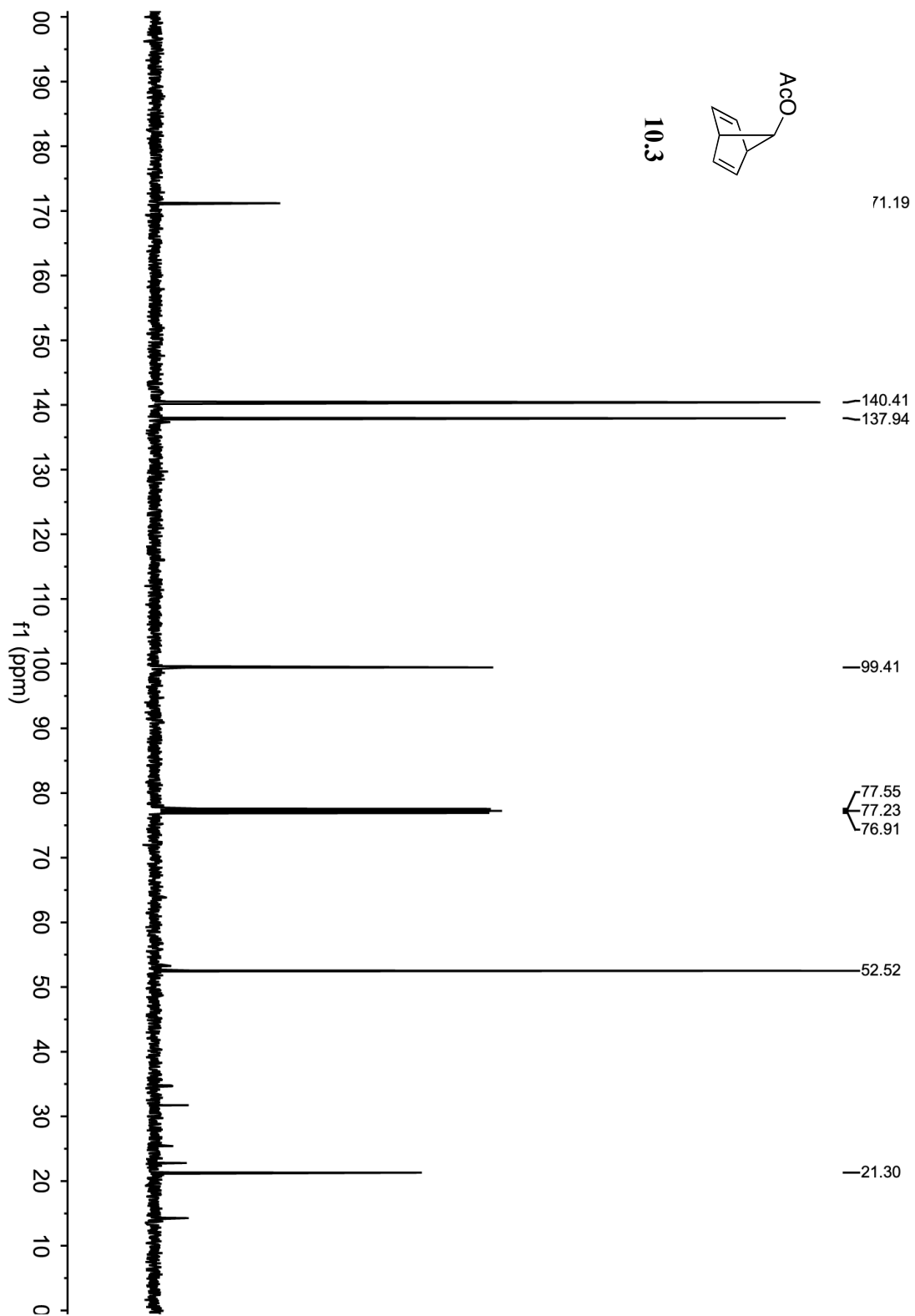


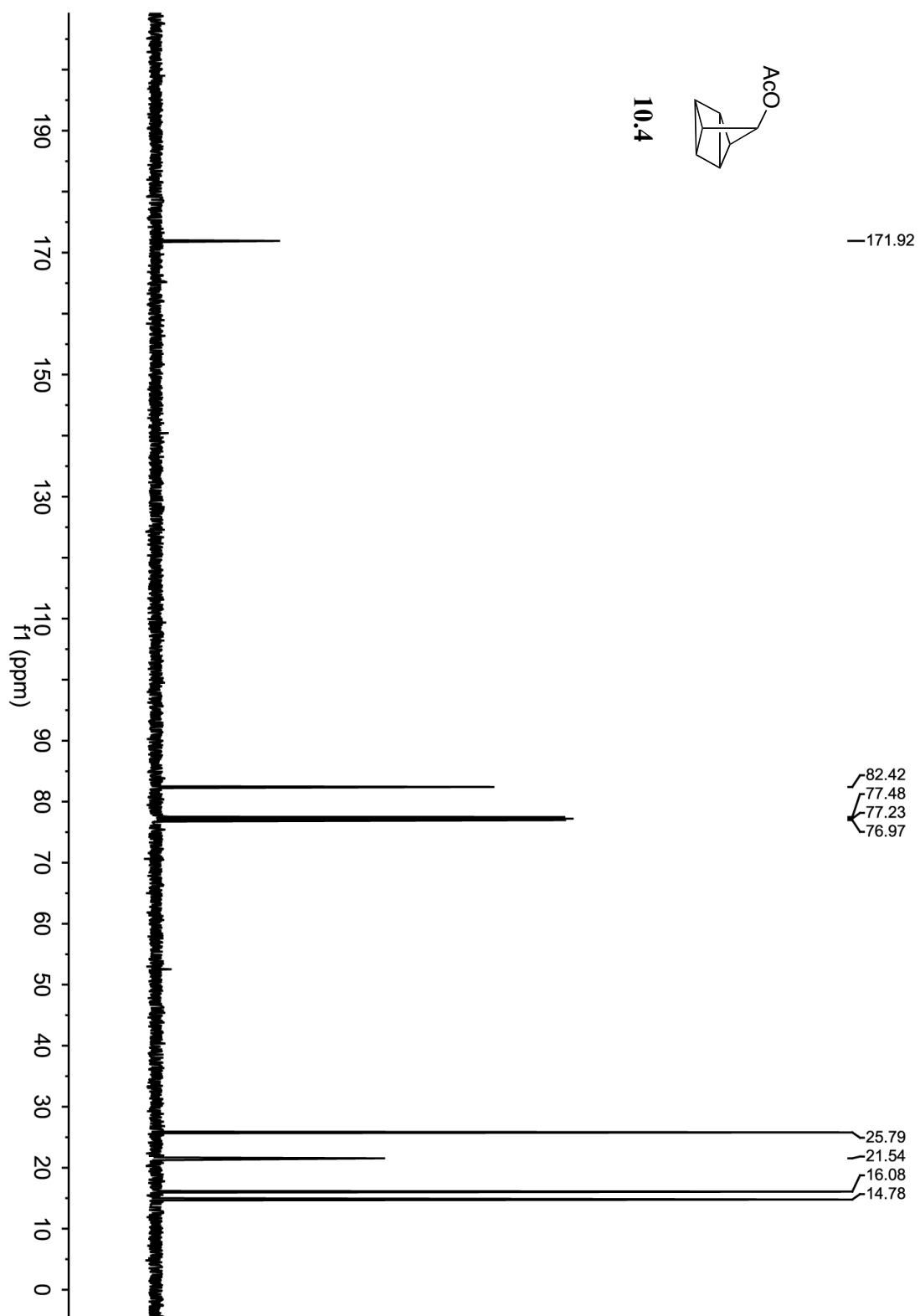


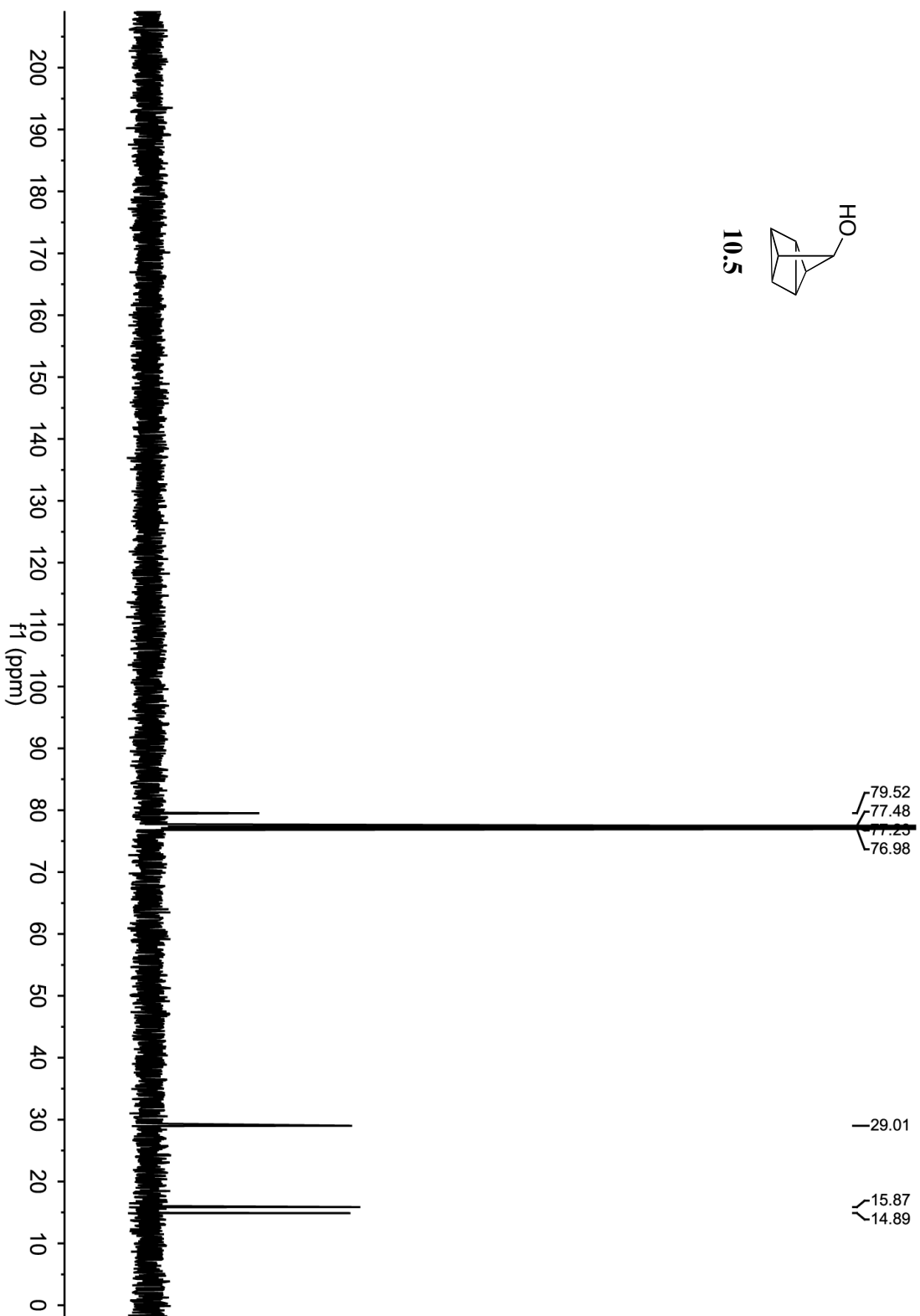


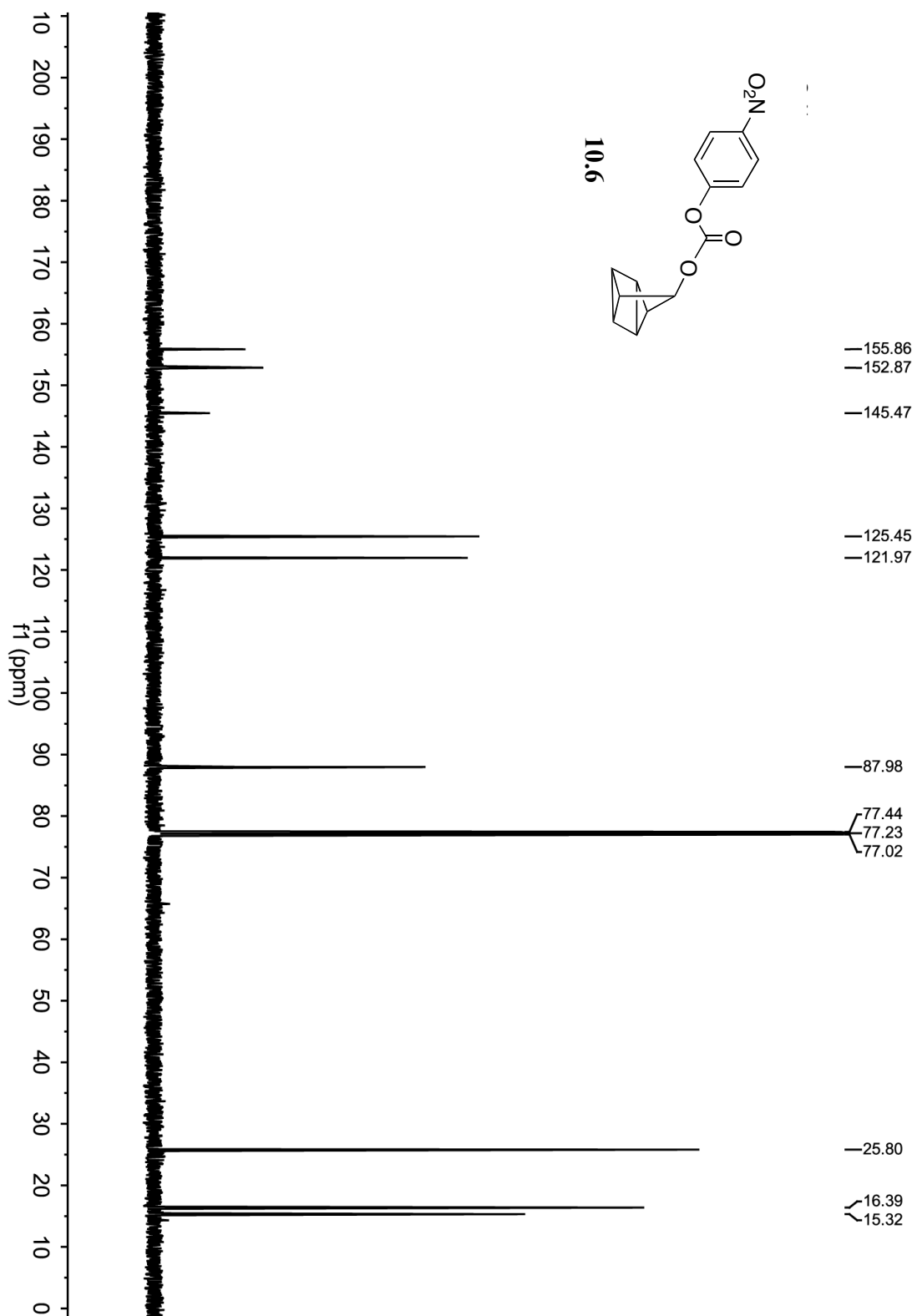


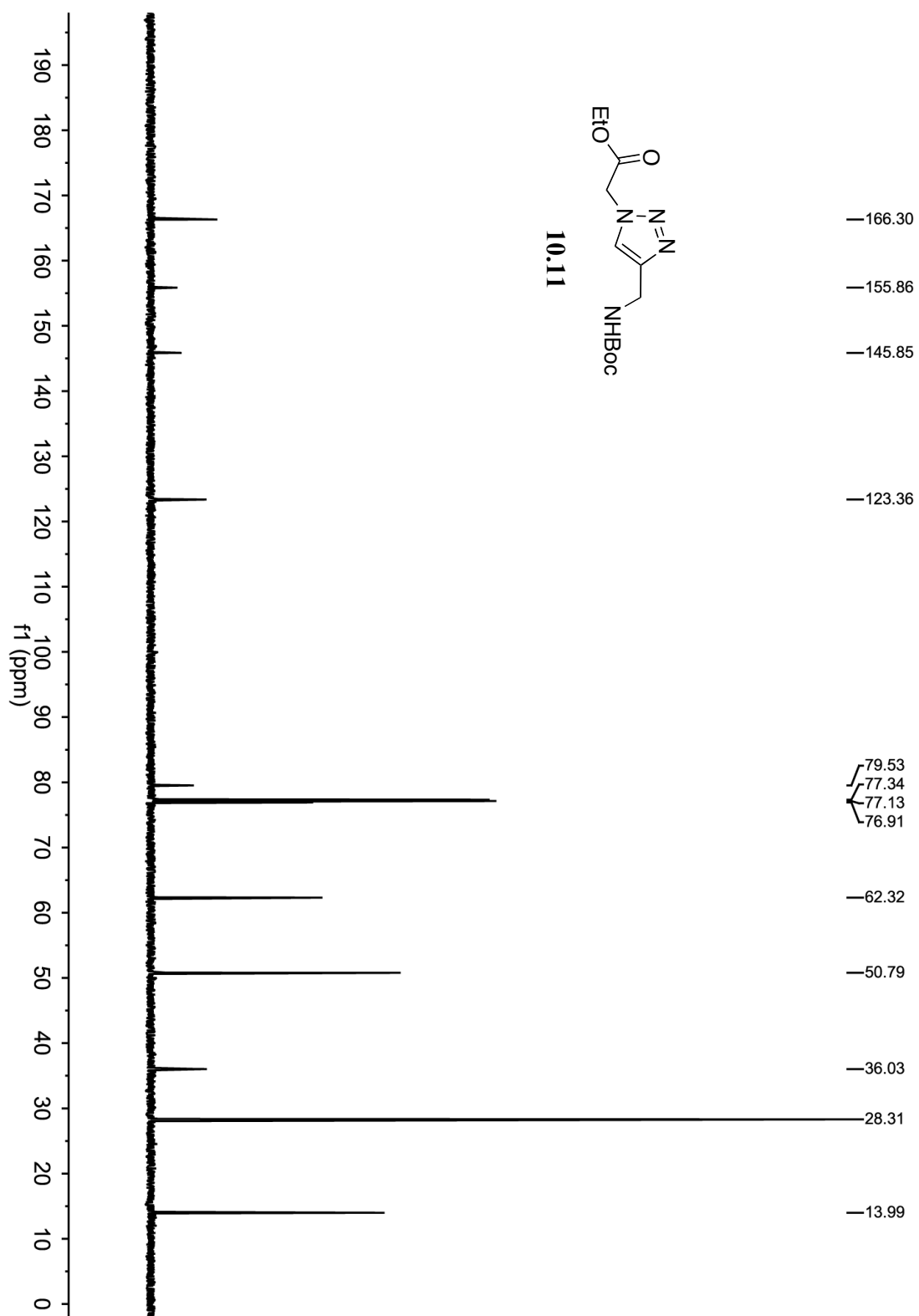


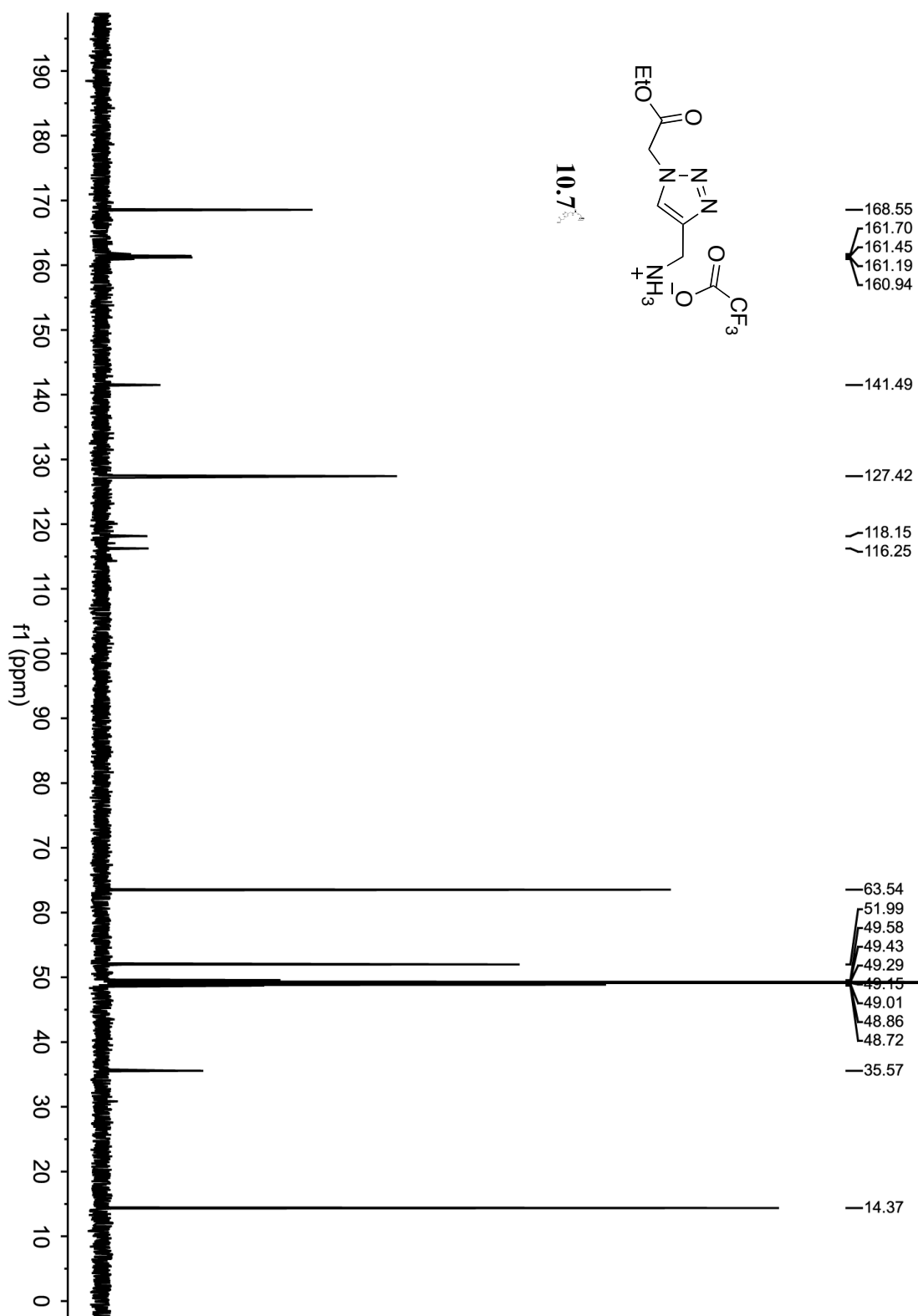


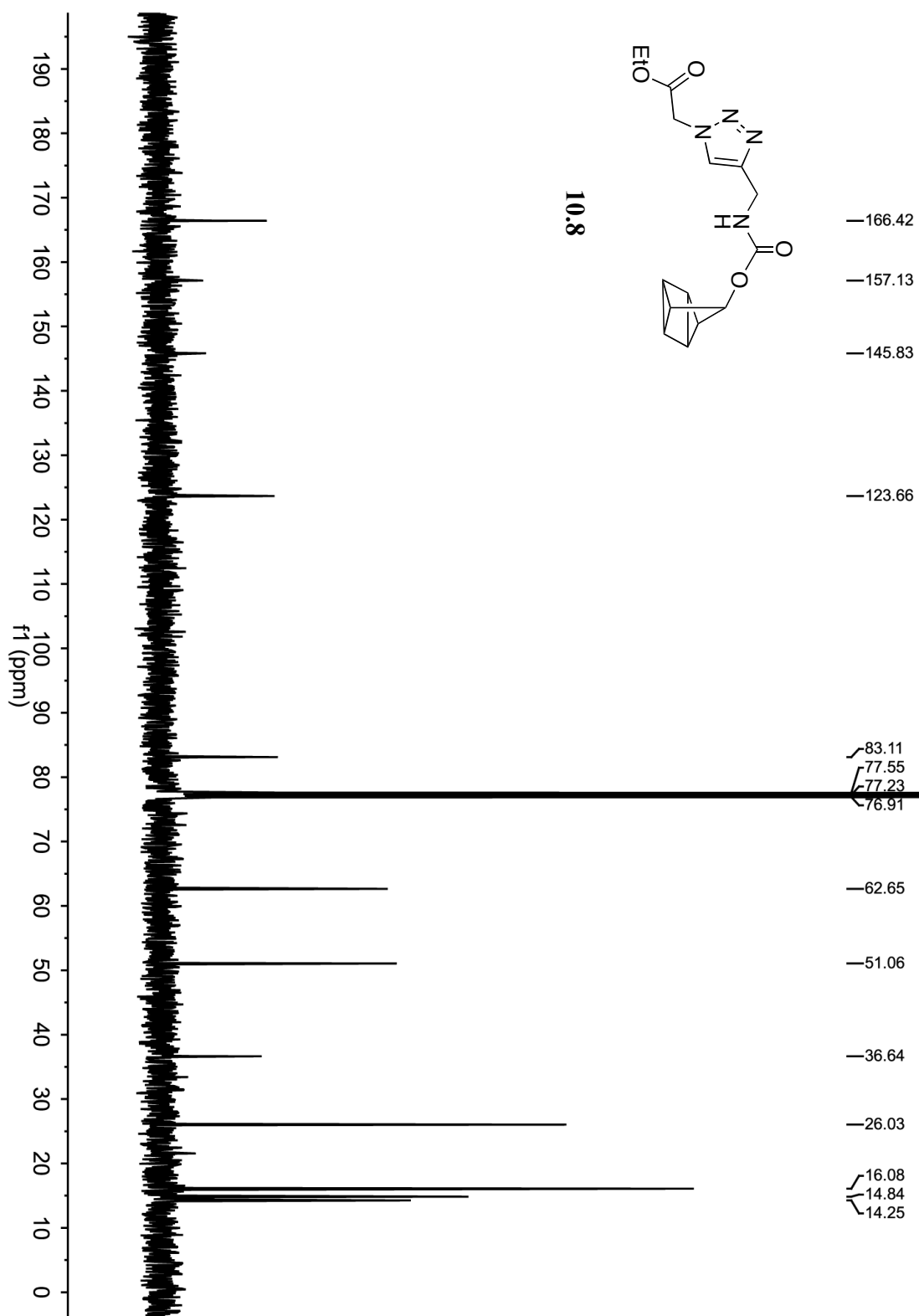


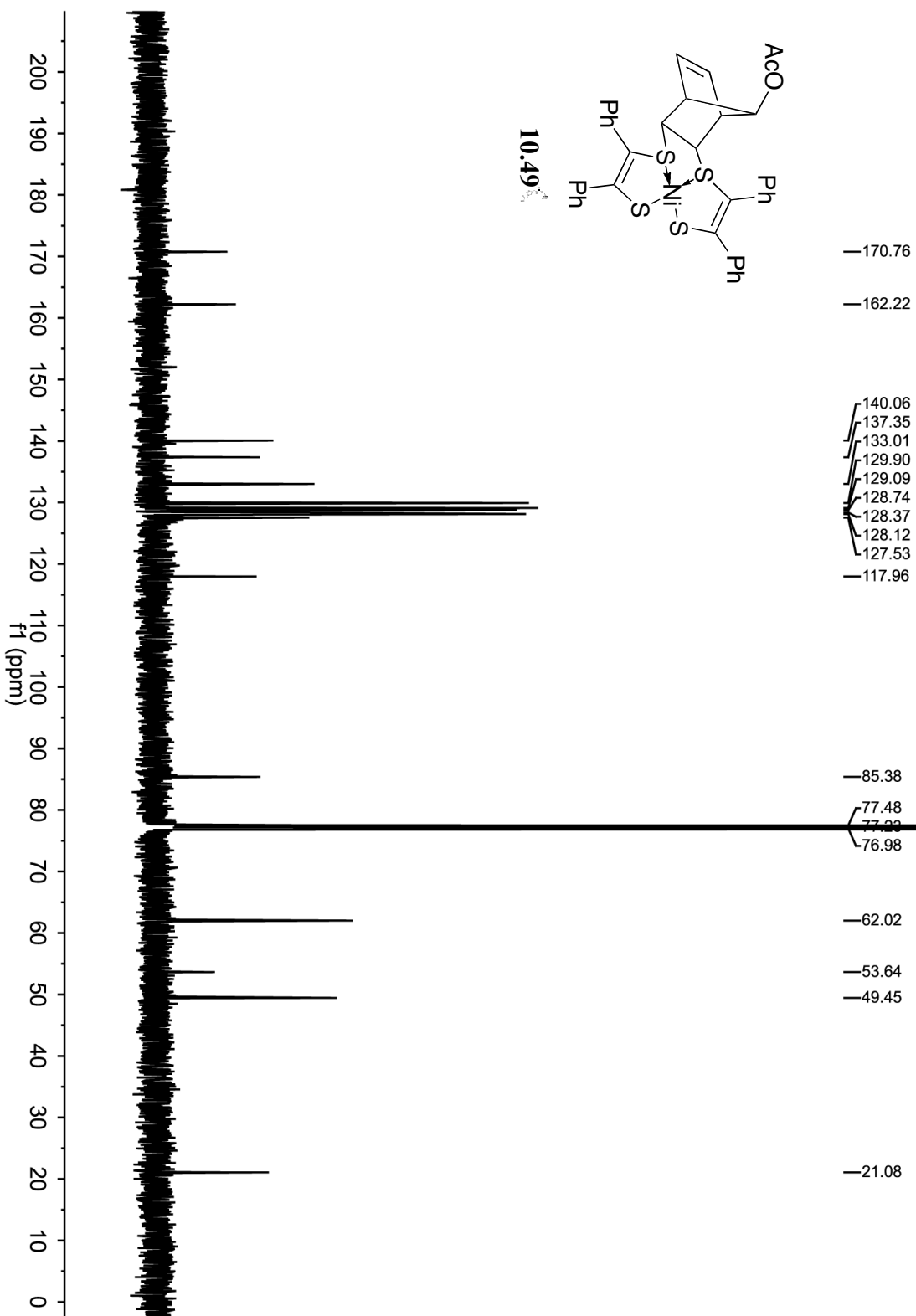


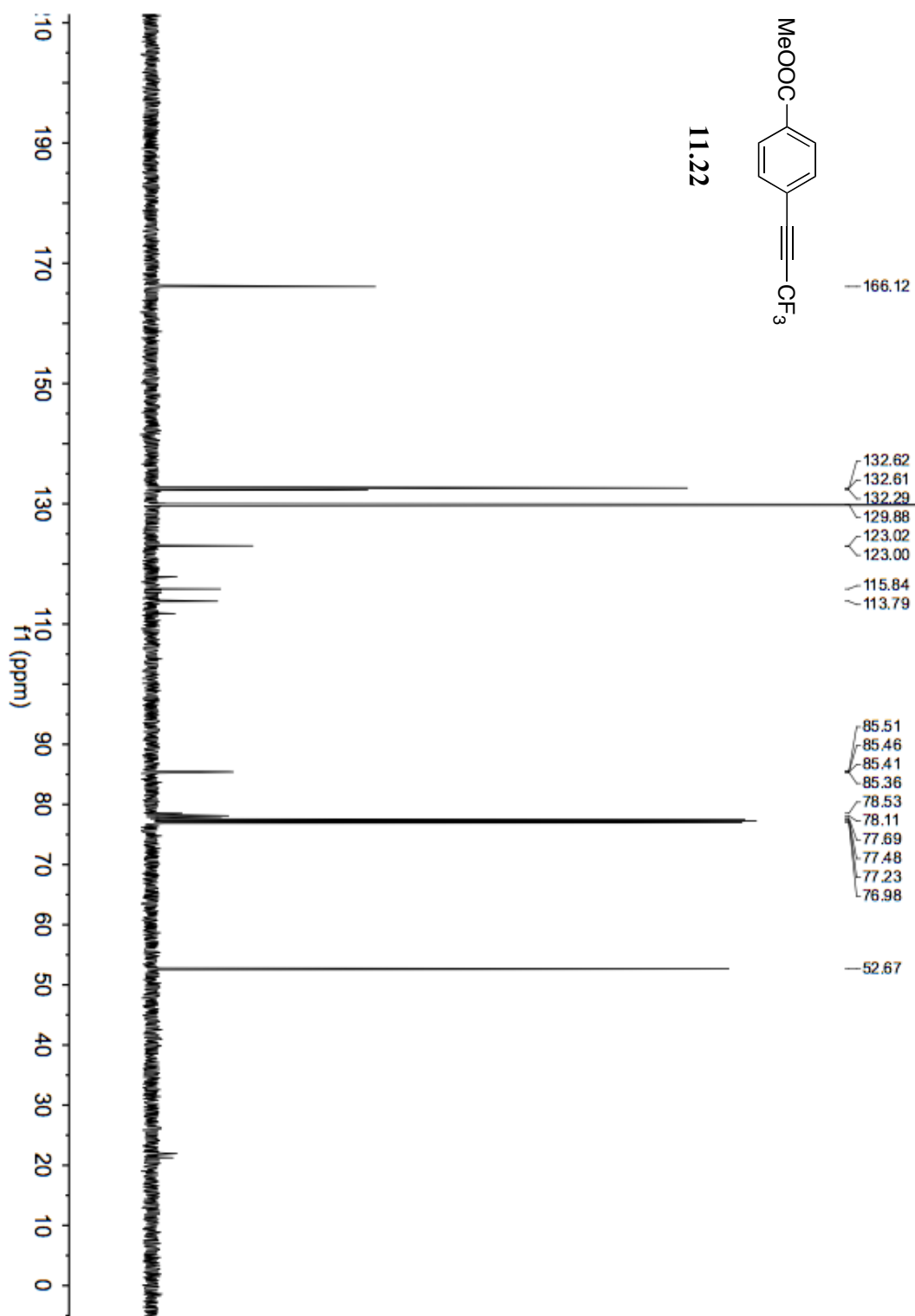


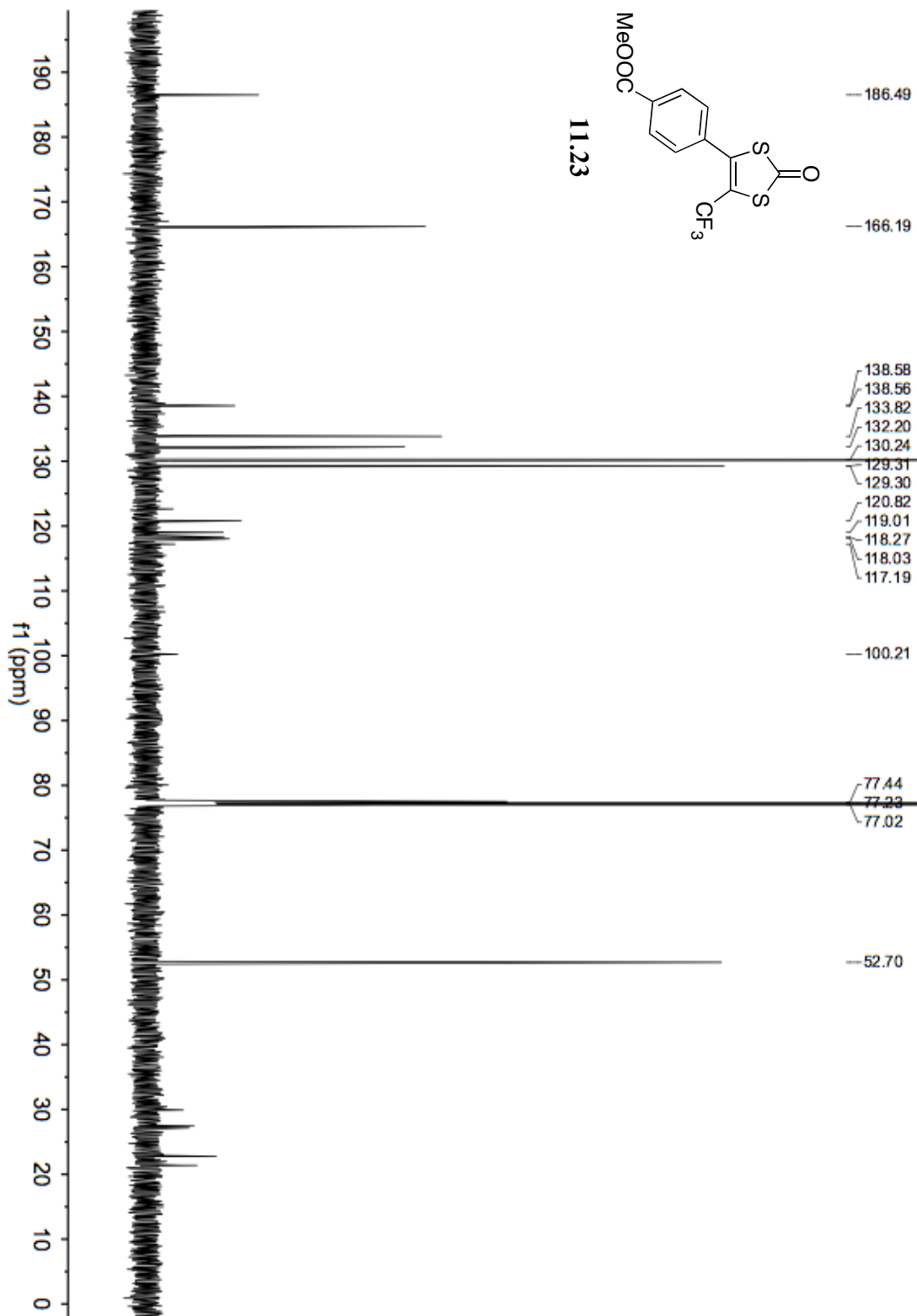


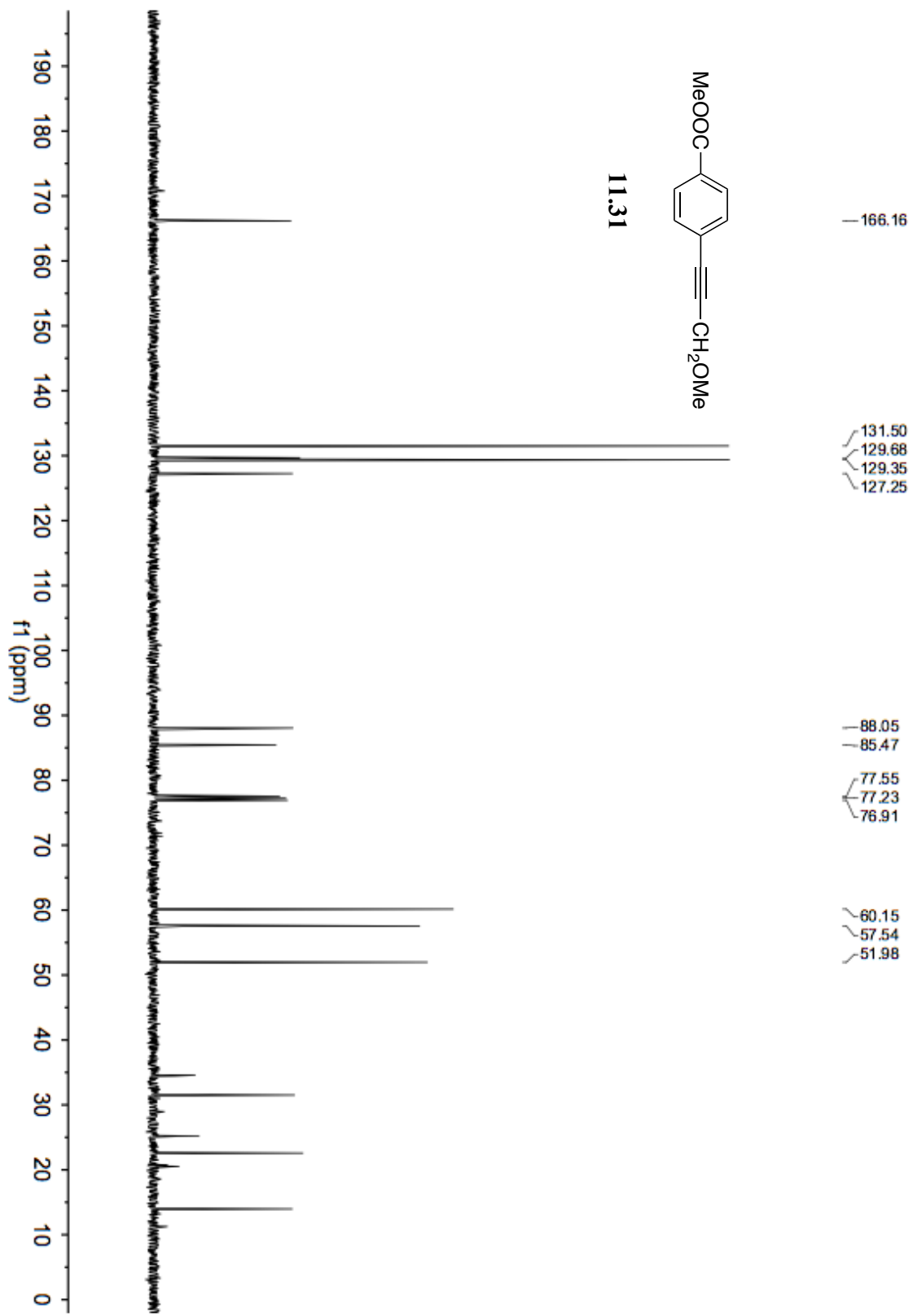


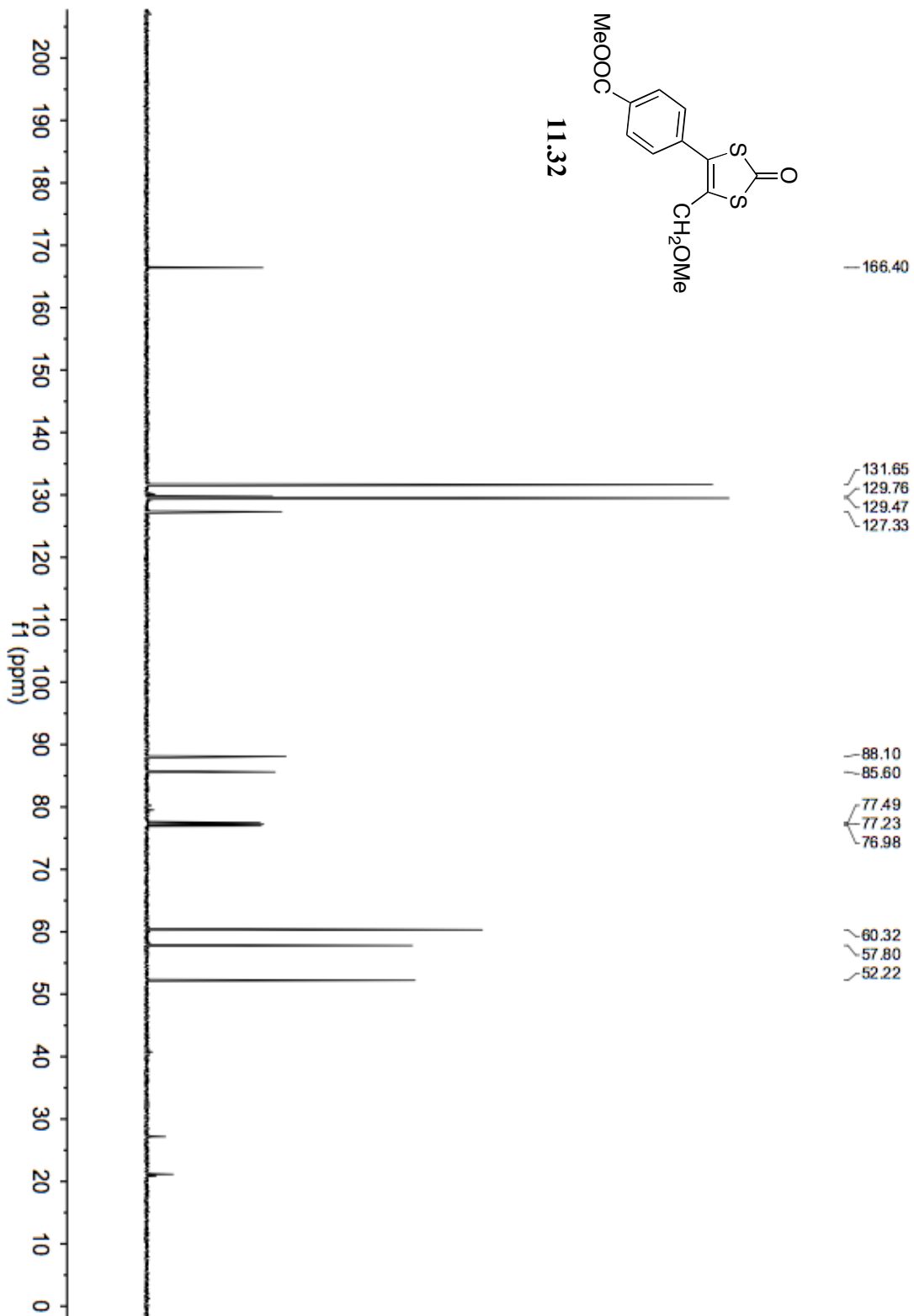


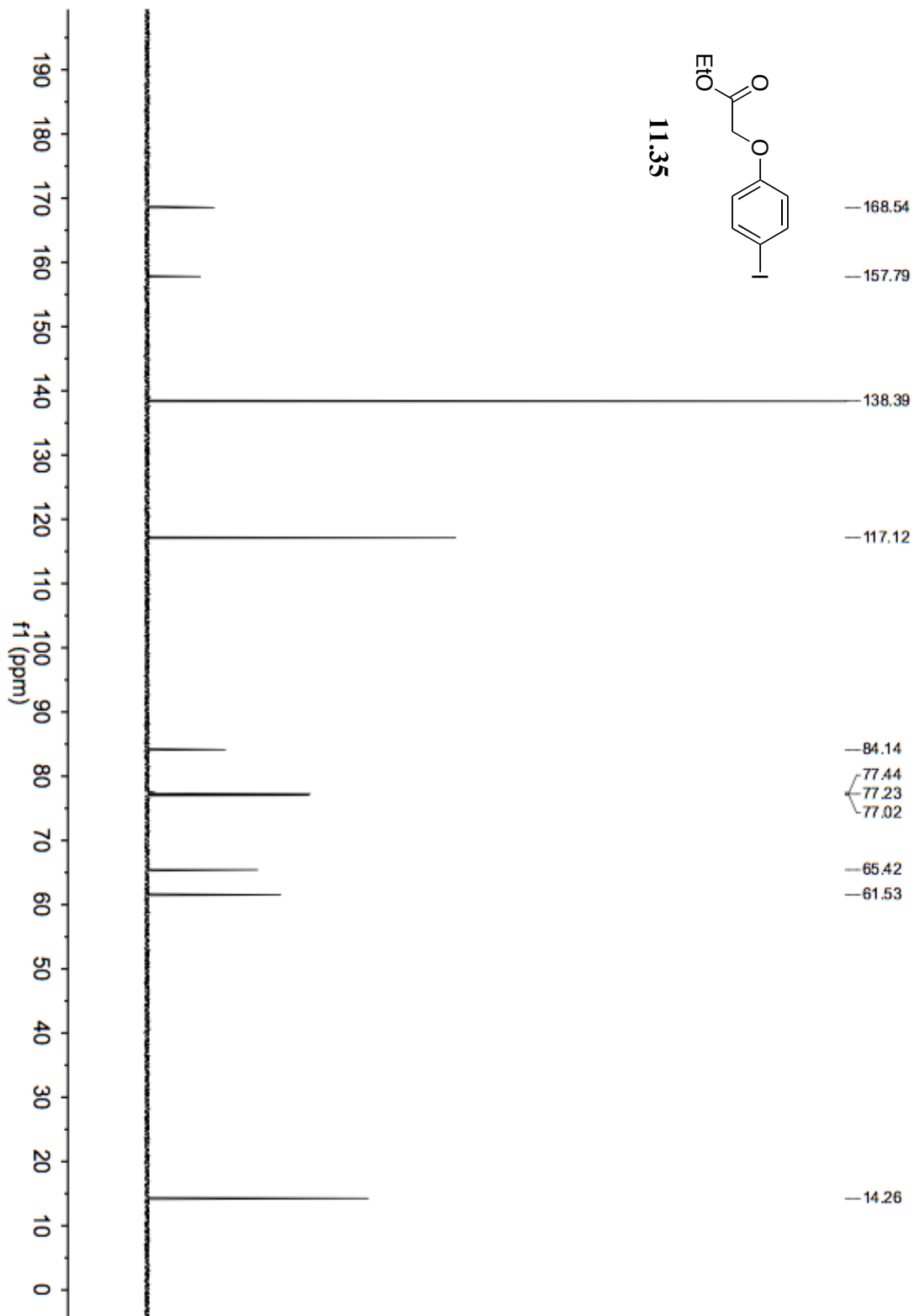


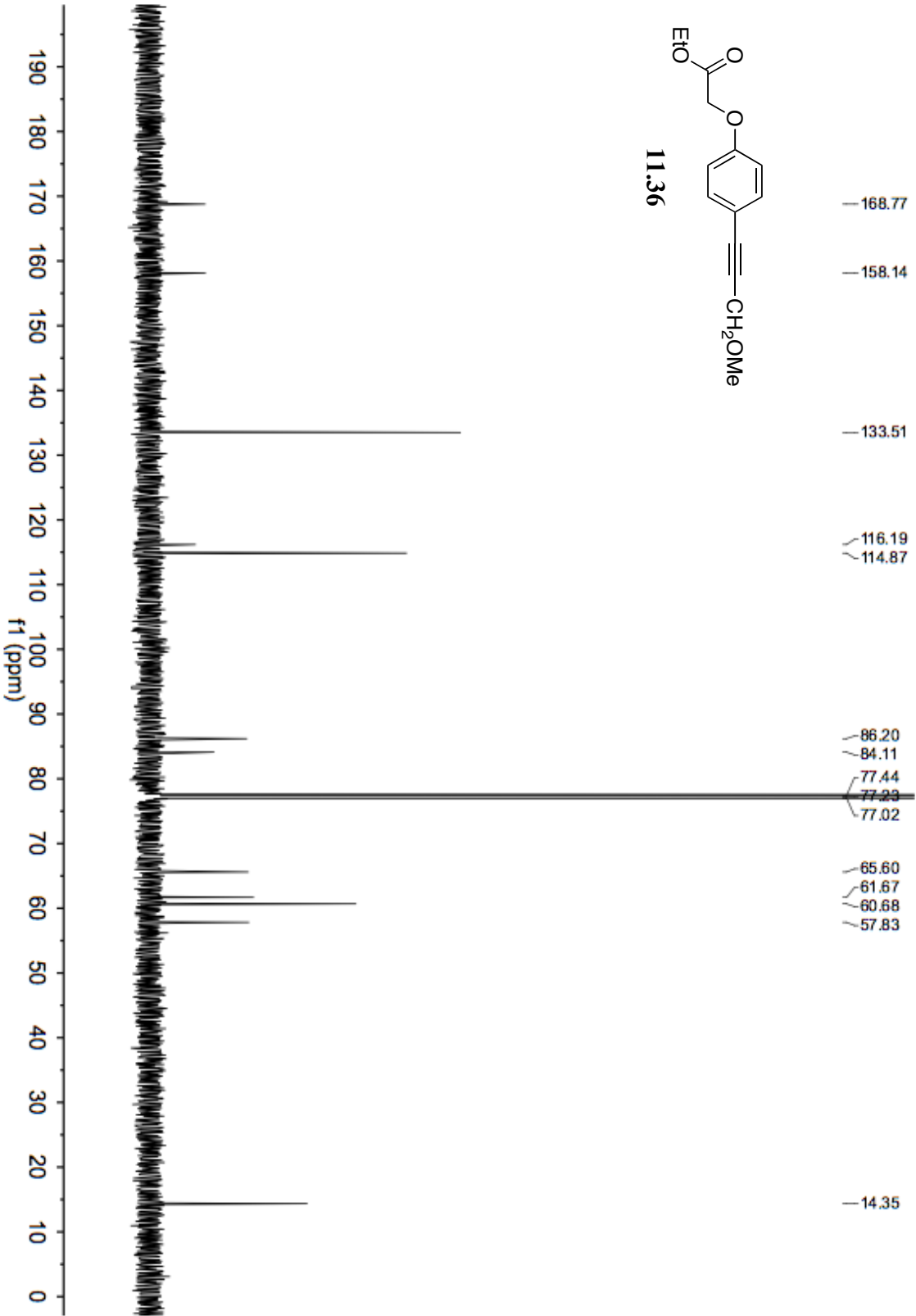


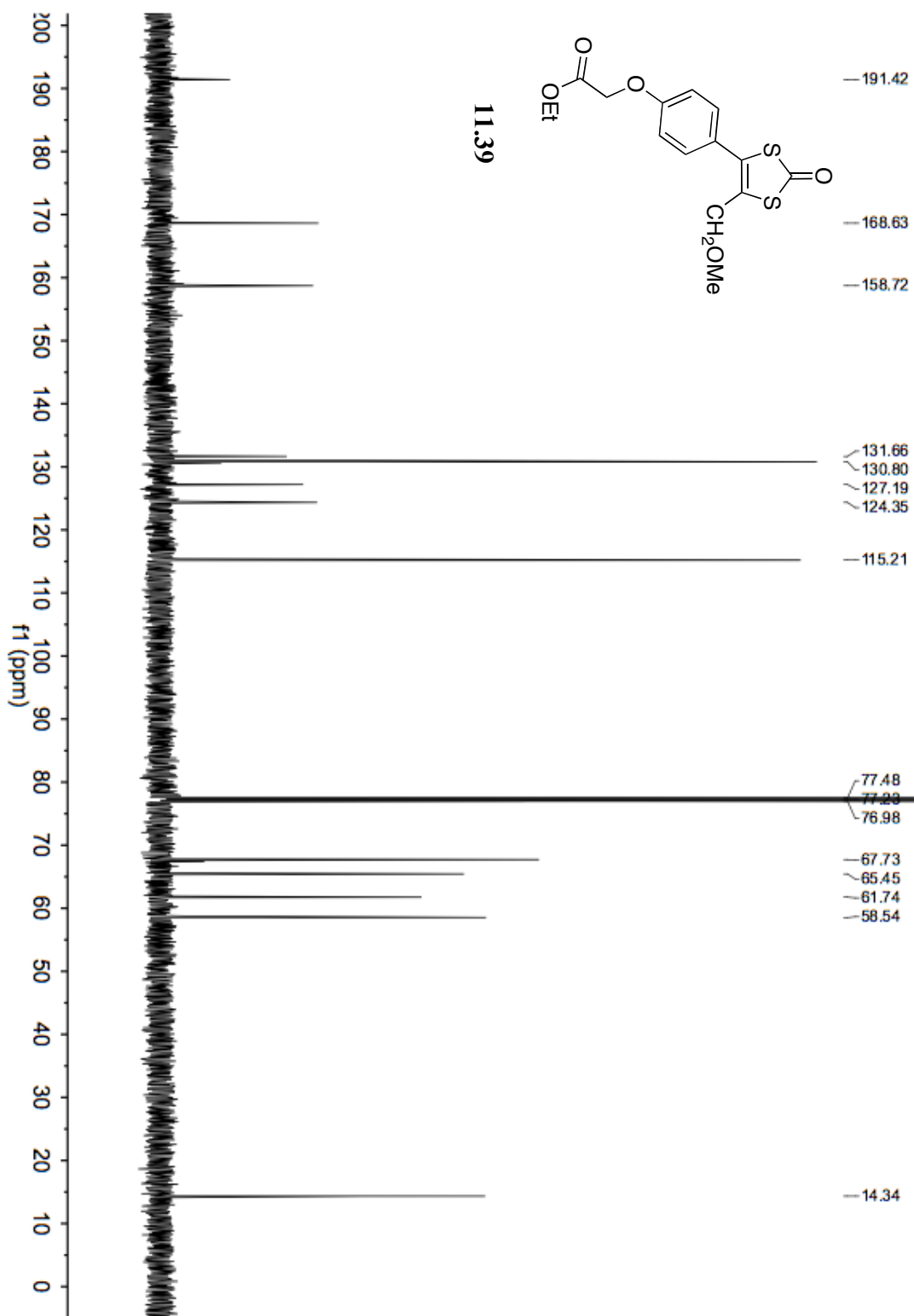


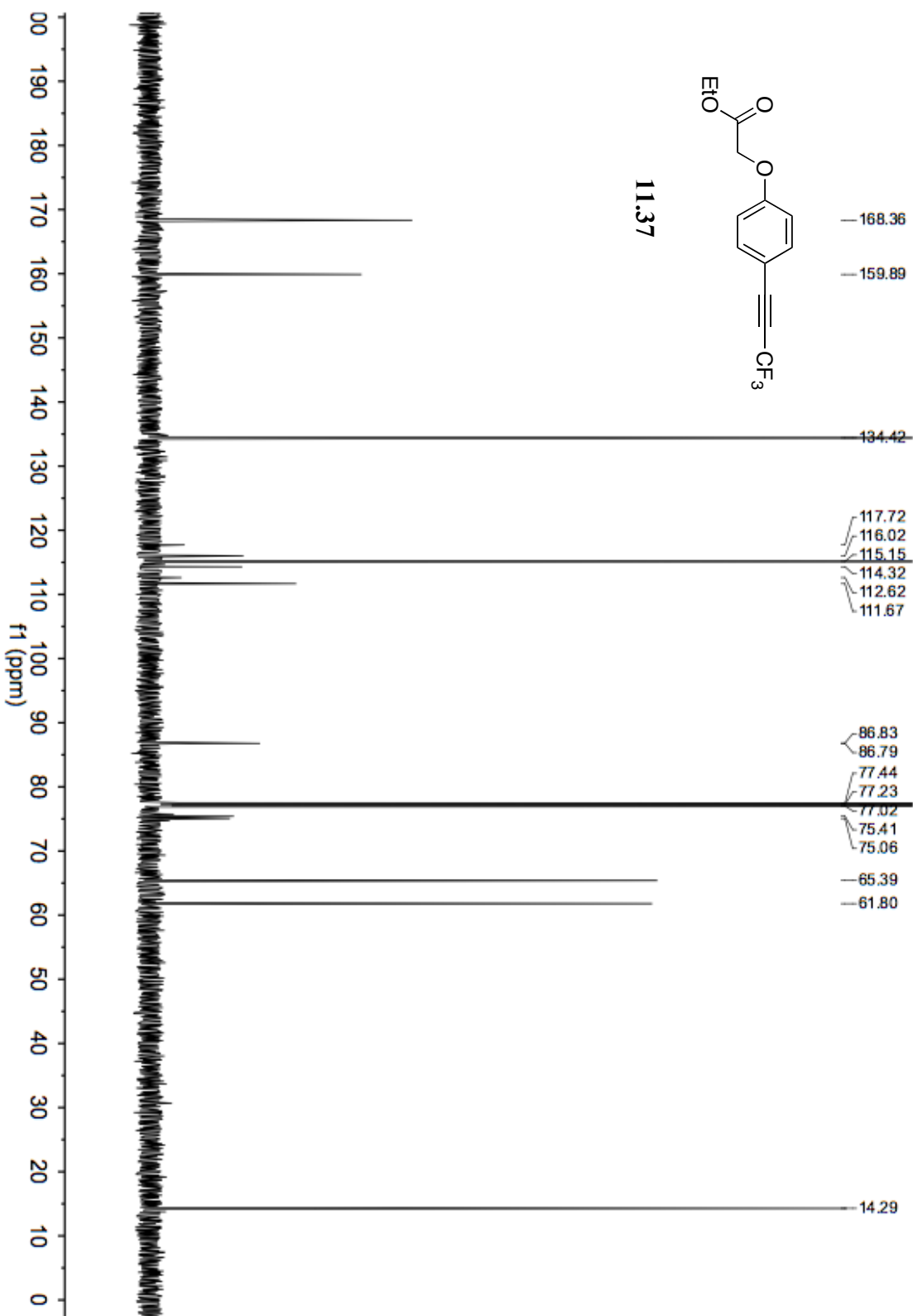


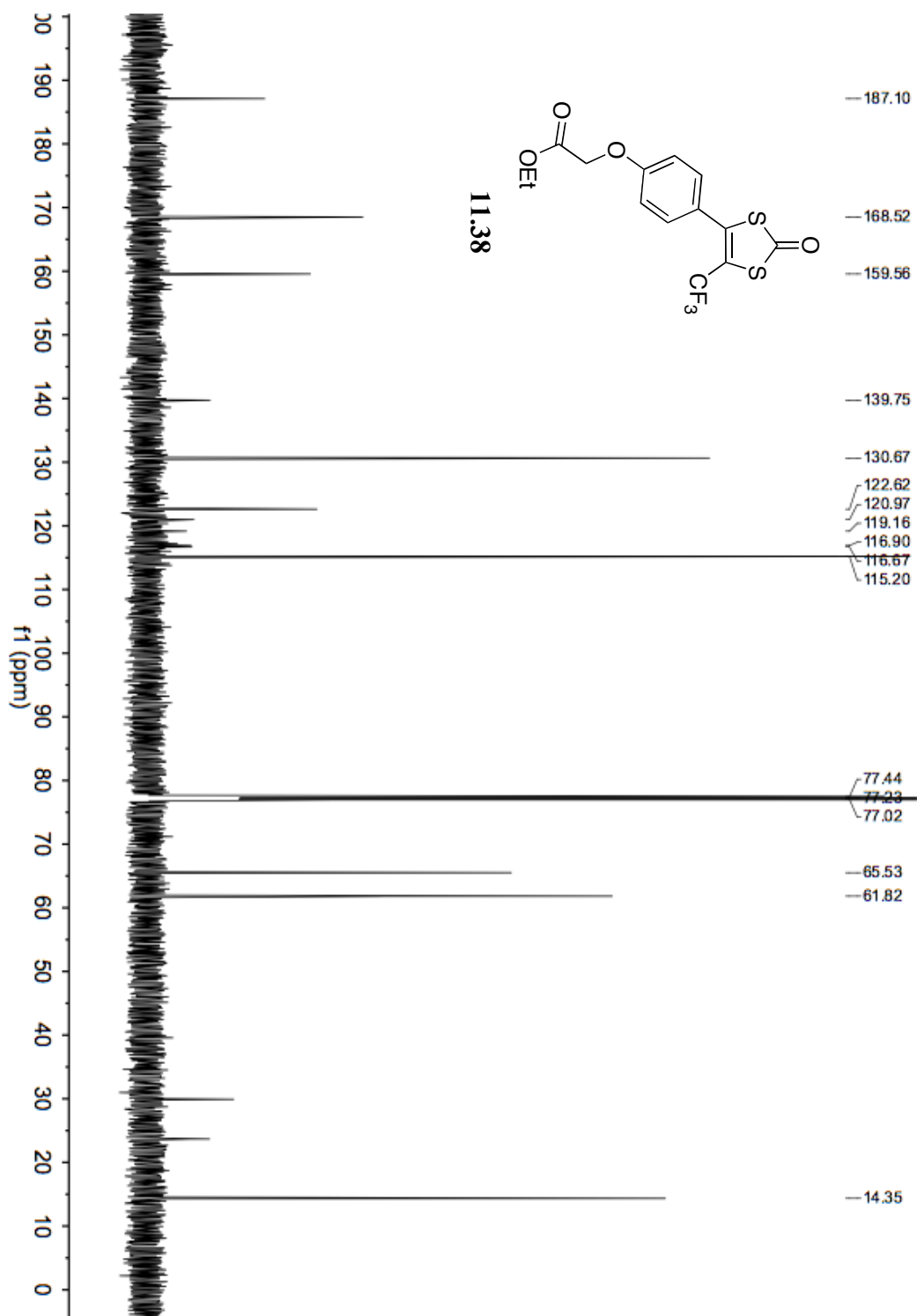


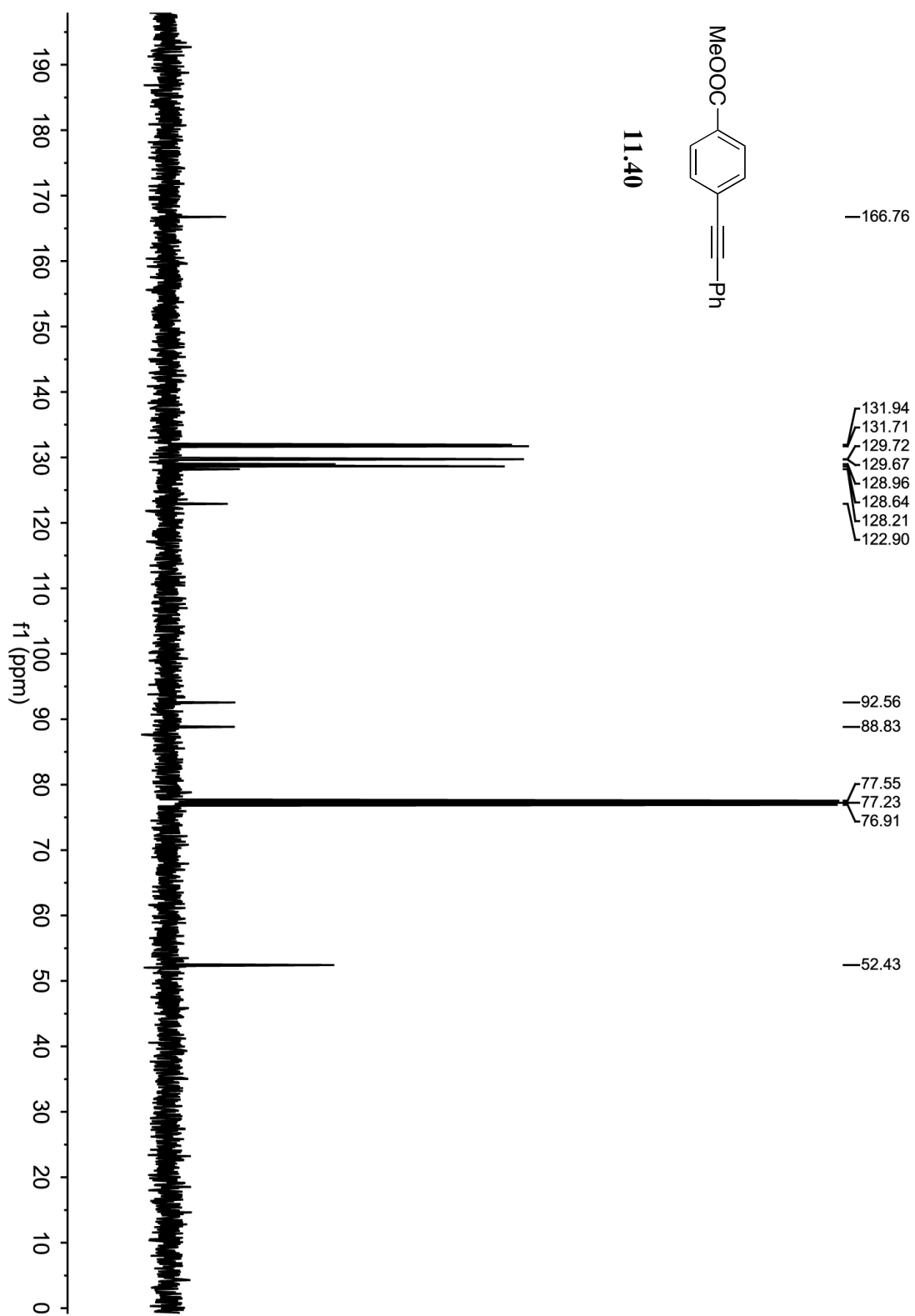


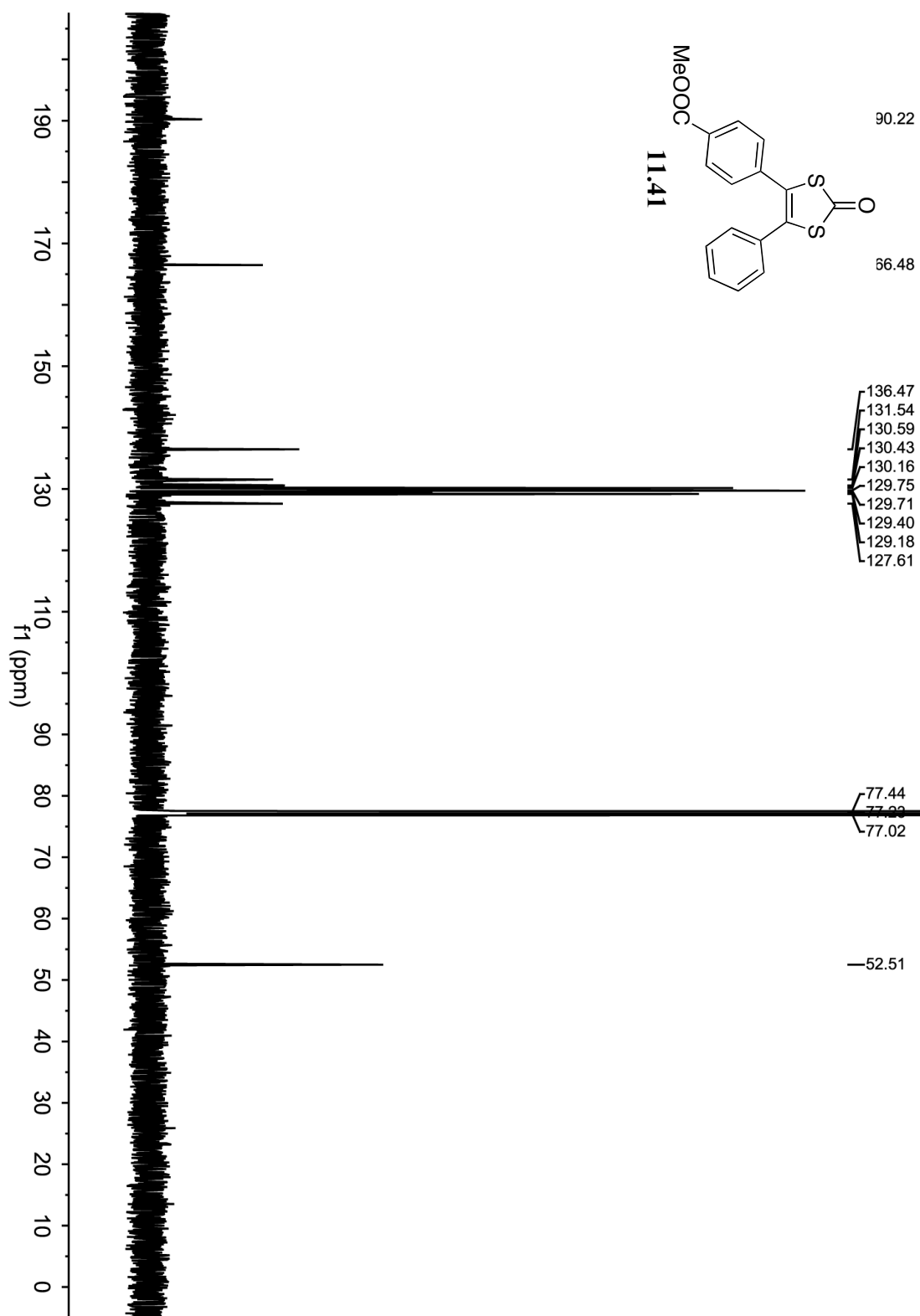


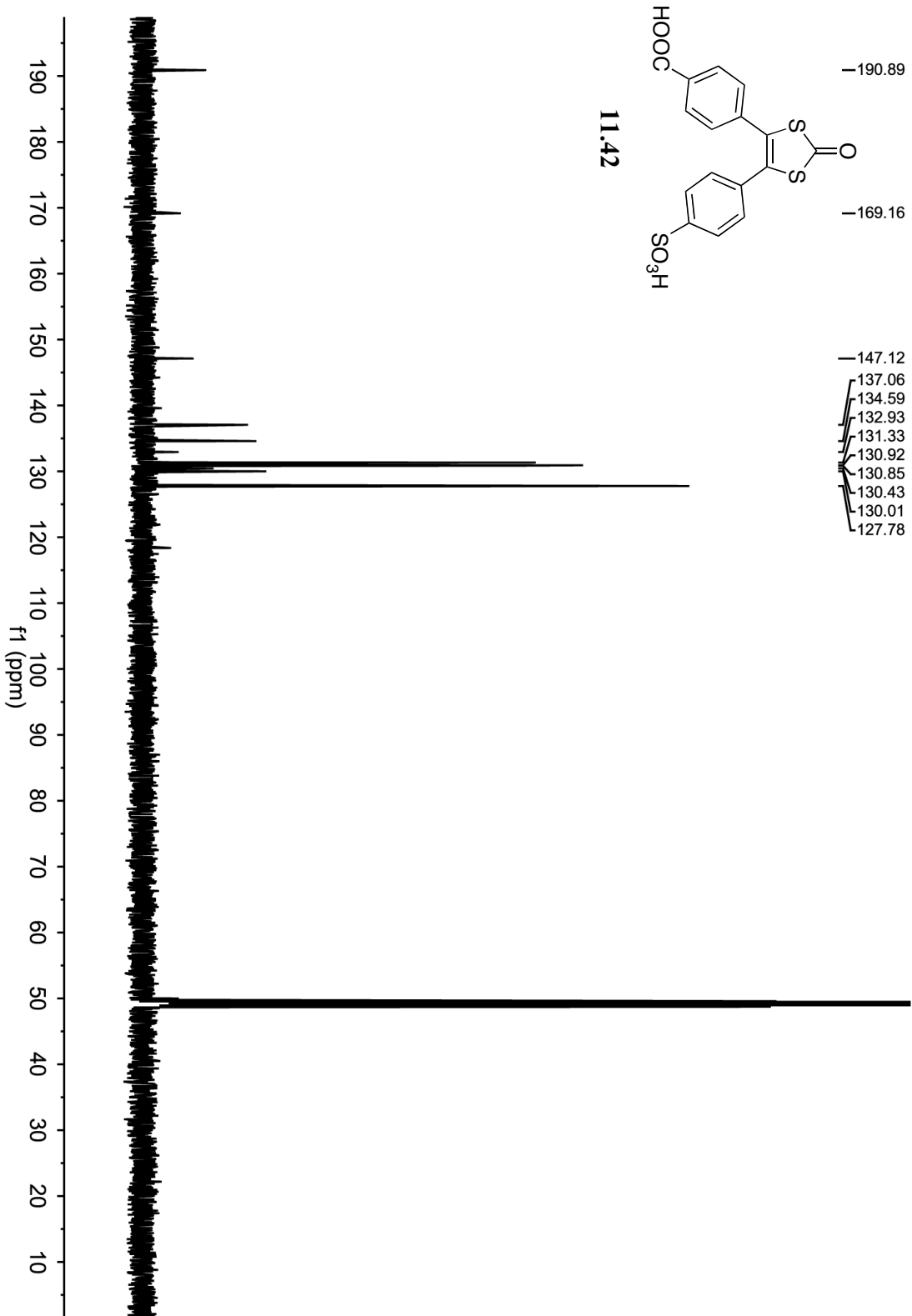


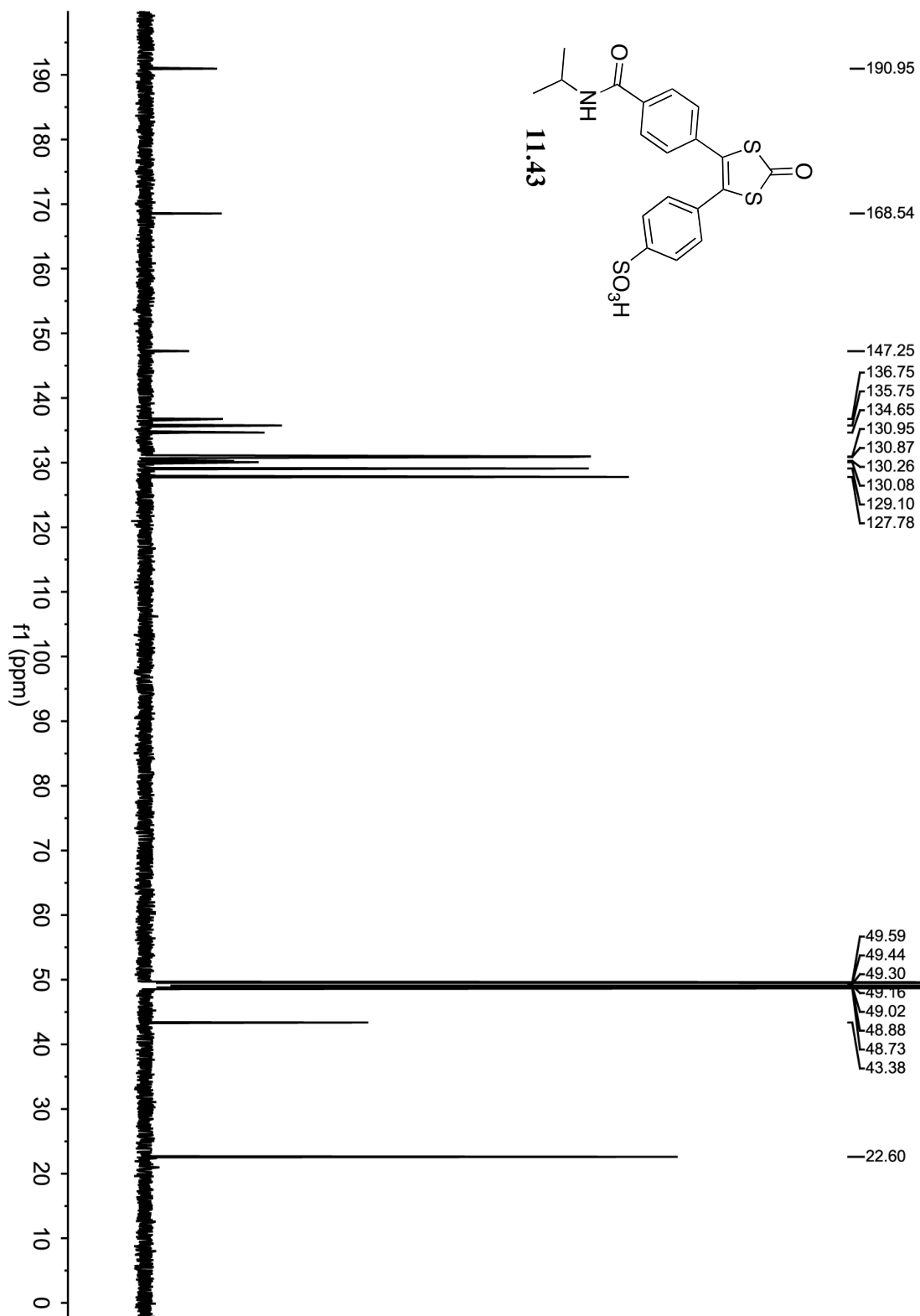


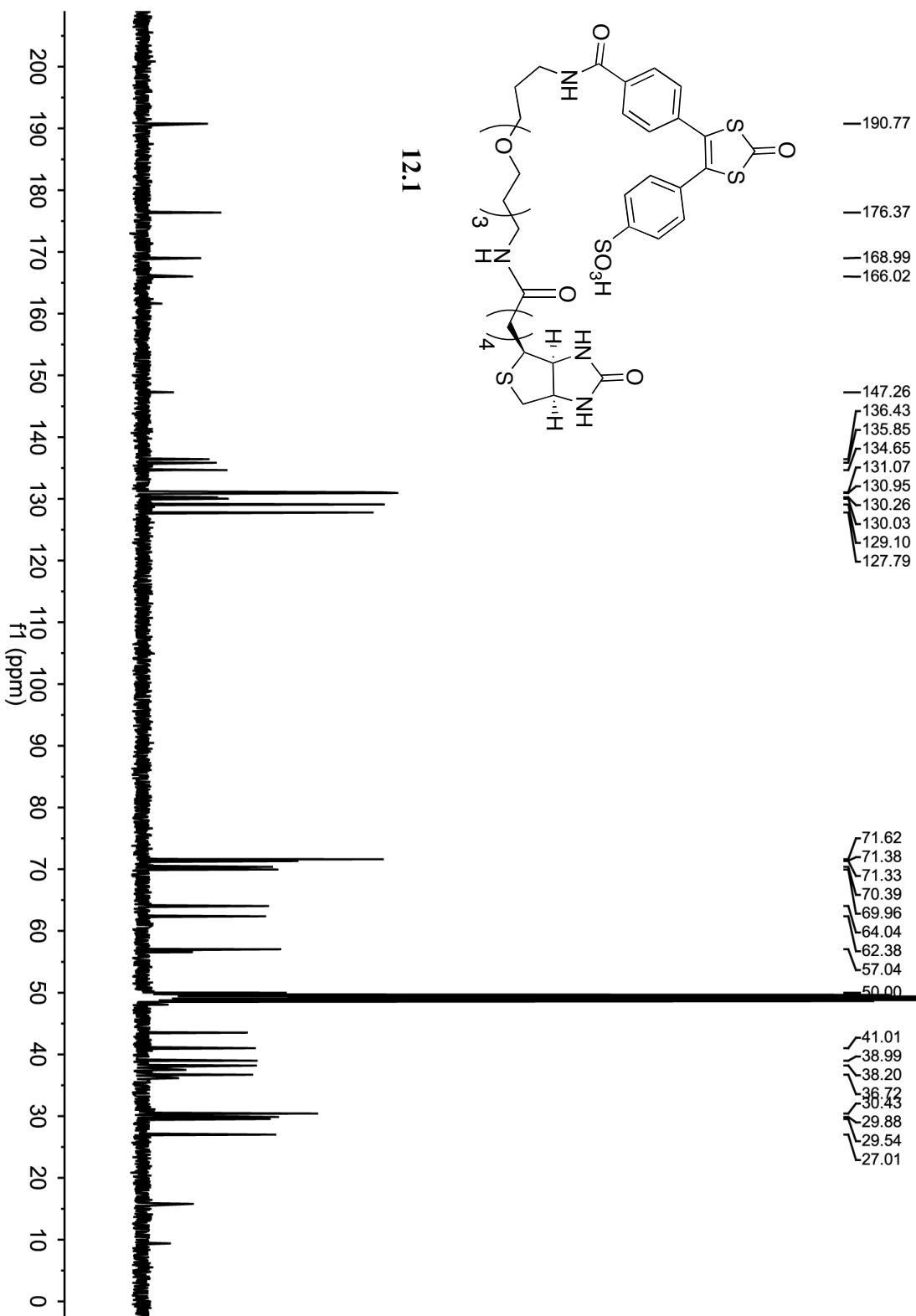


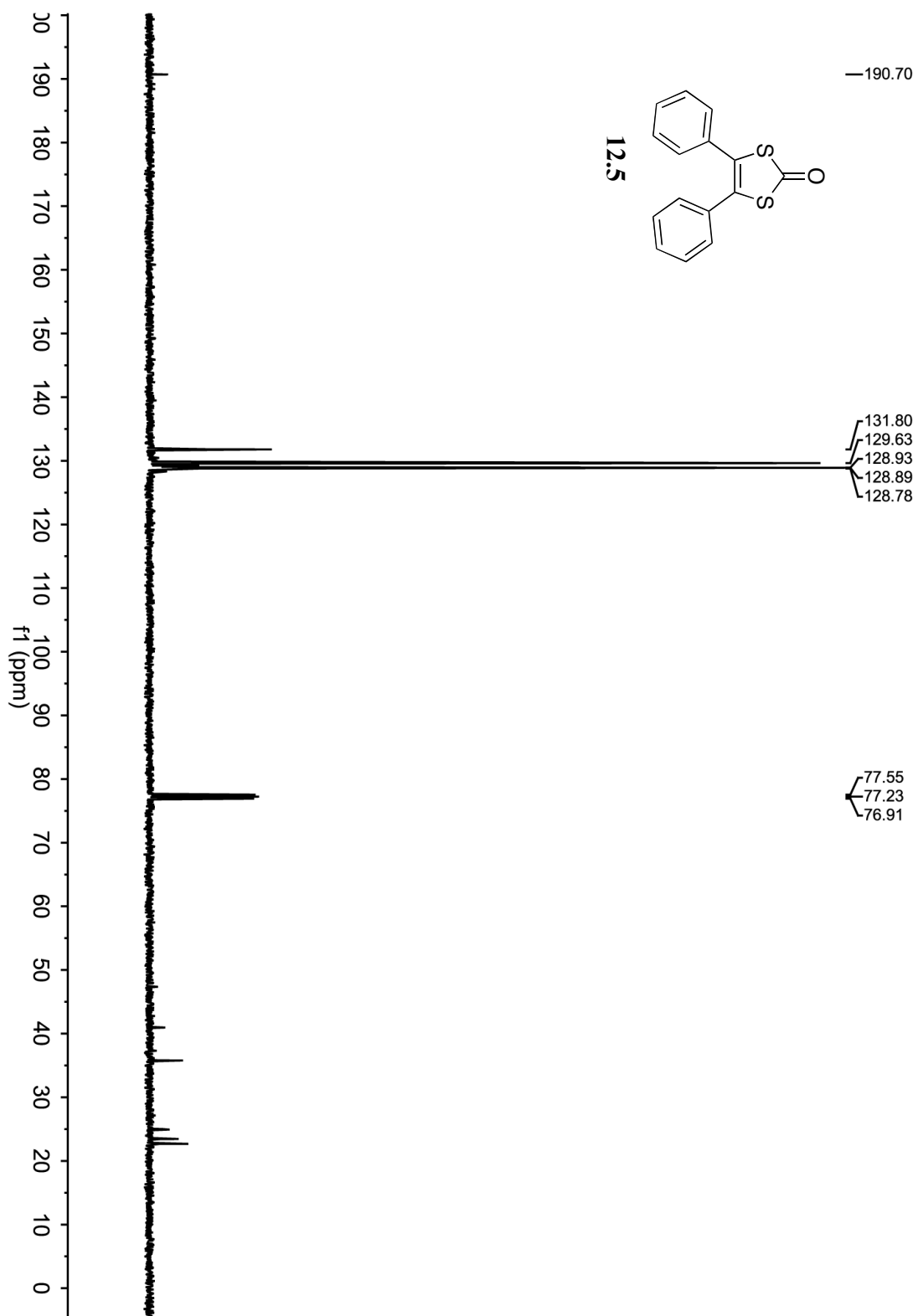


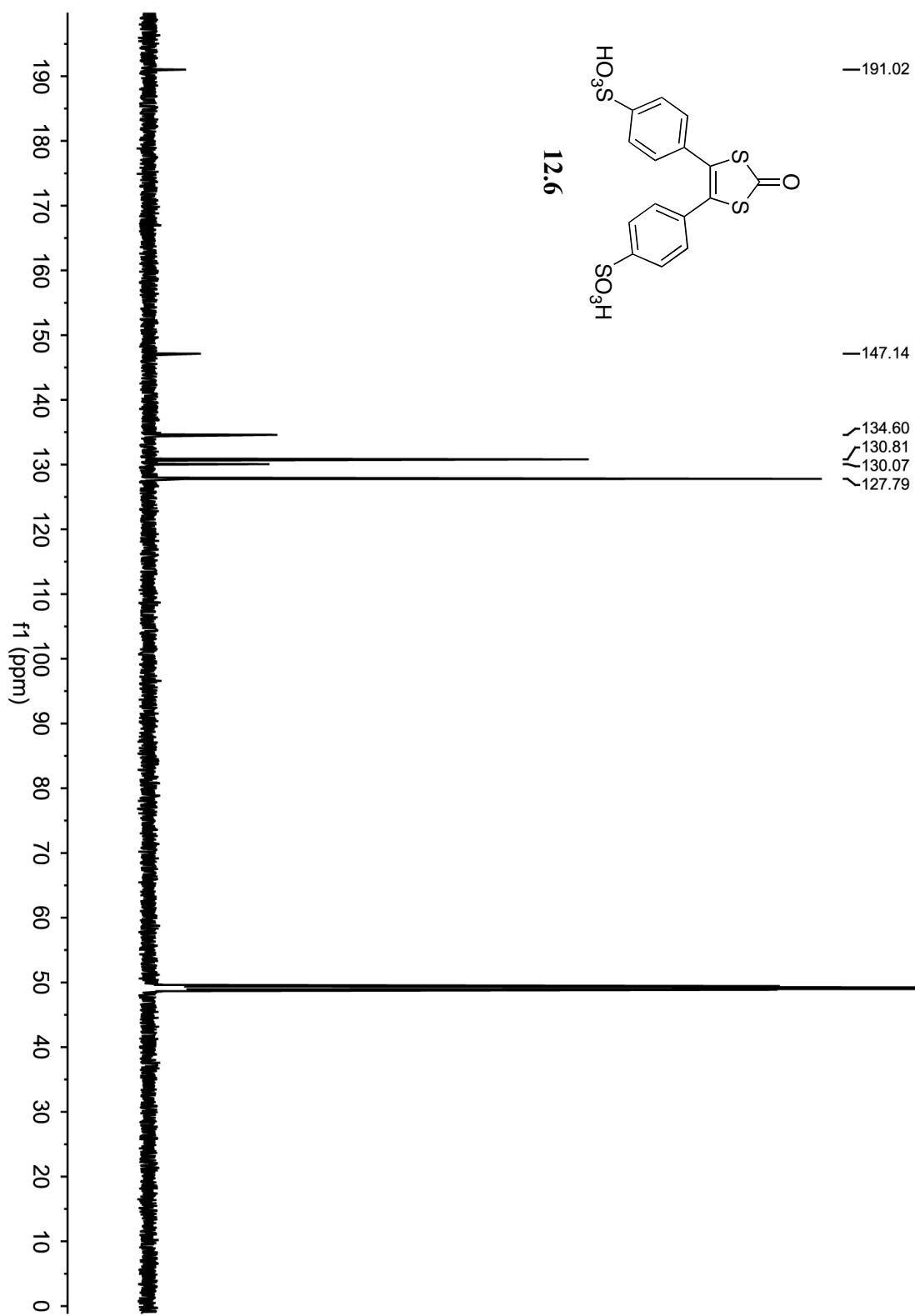






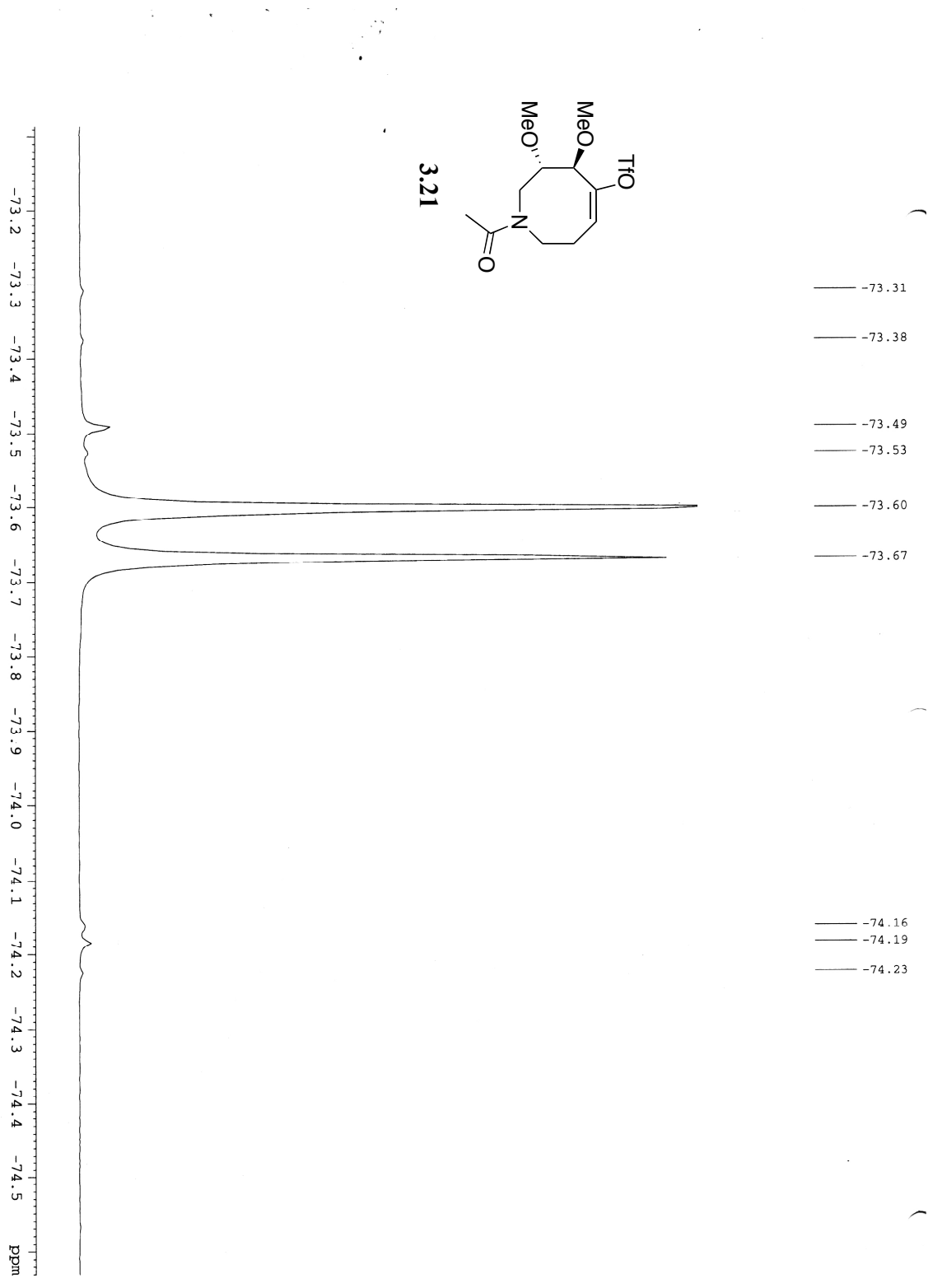




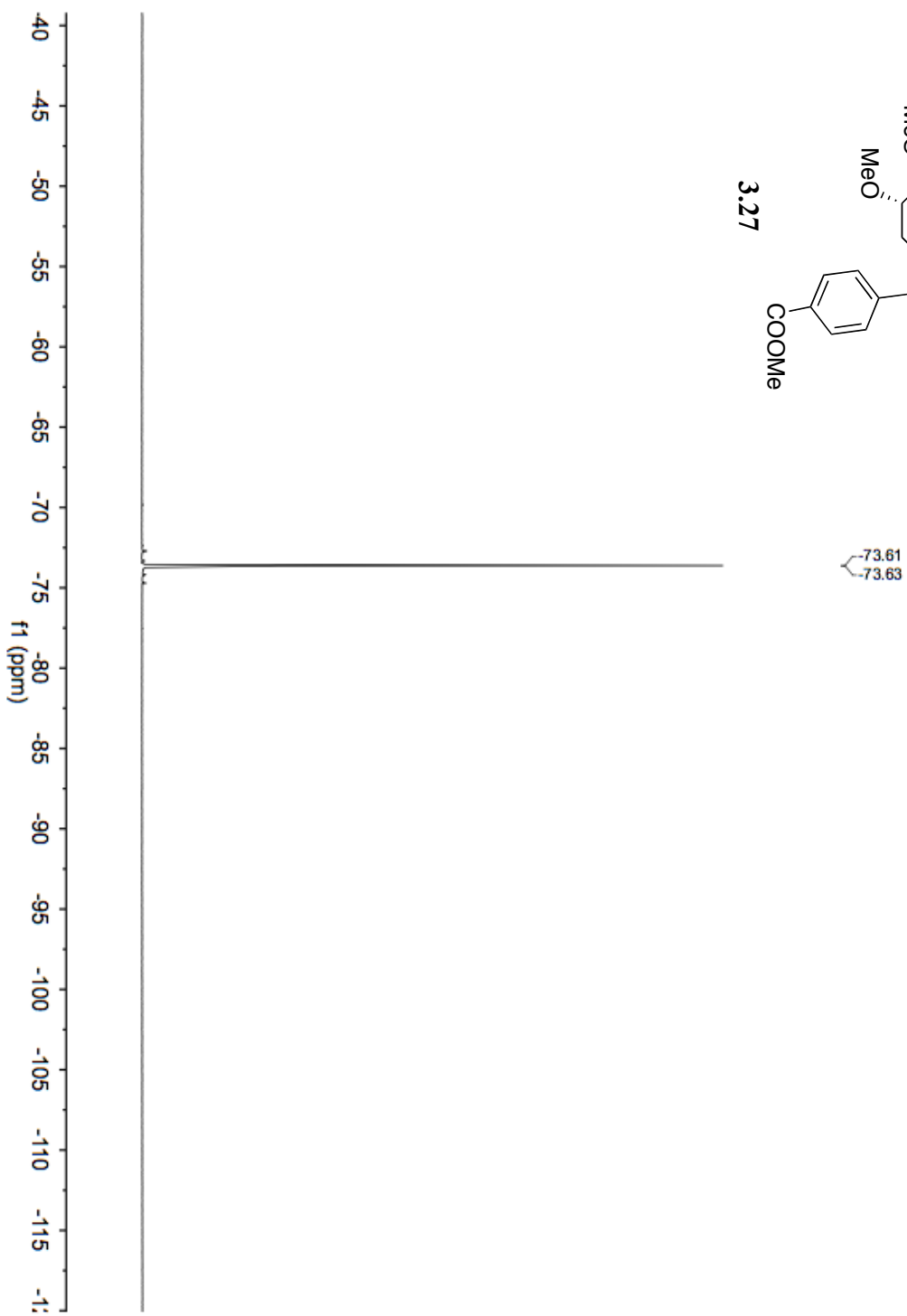
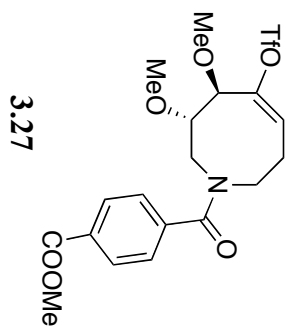


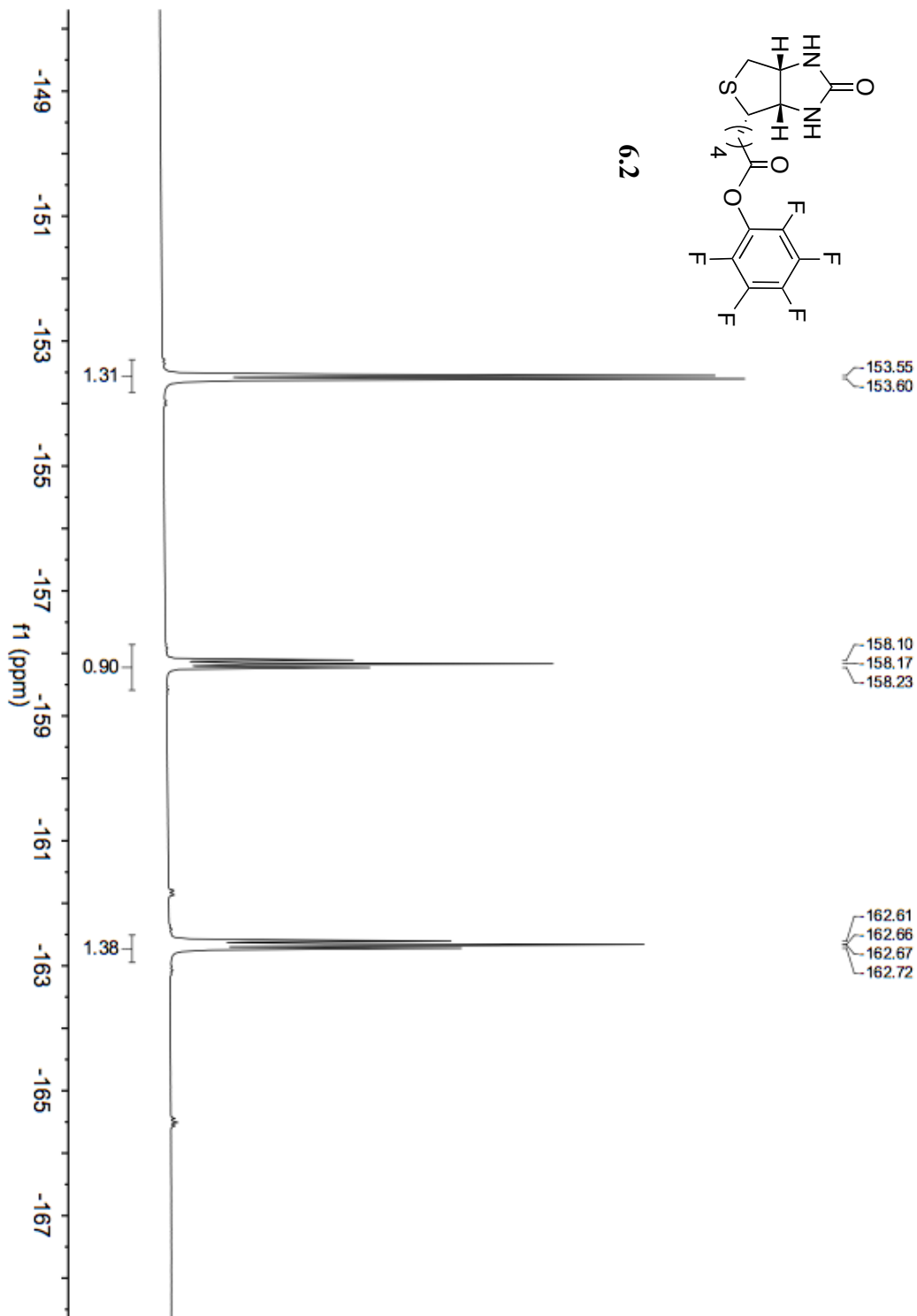
Appendix C

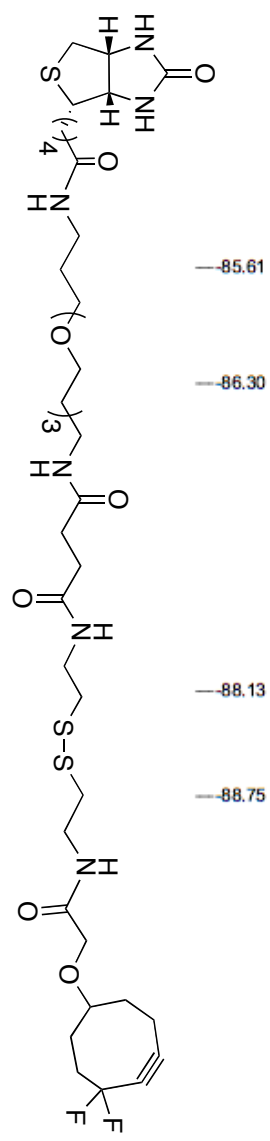
¹⁹F NMR Spectra



3.21

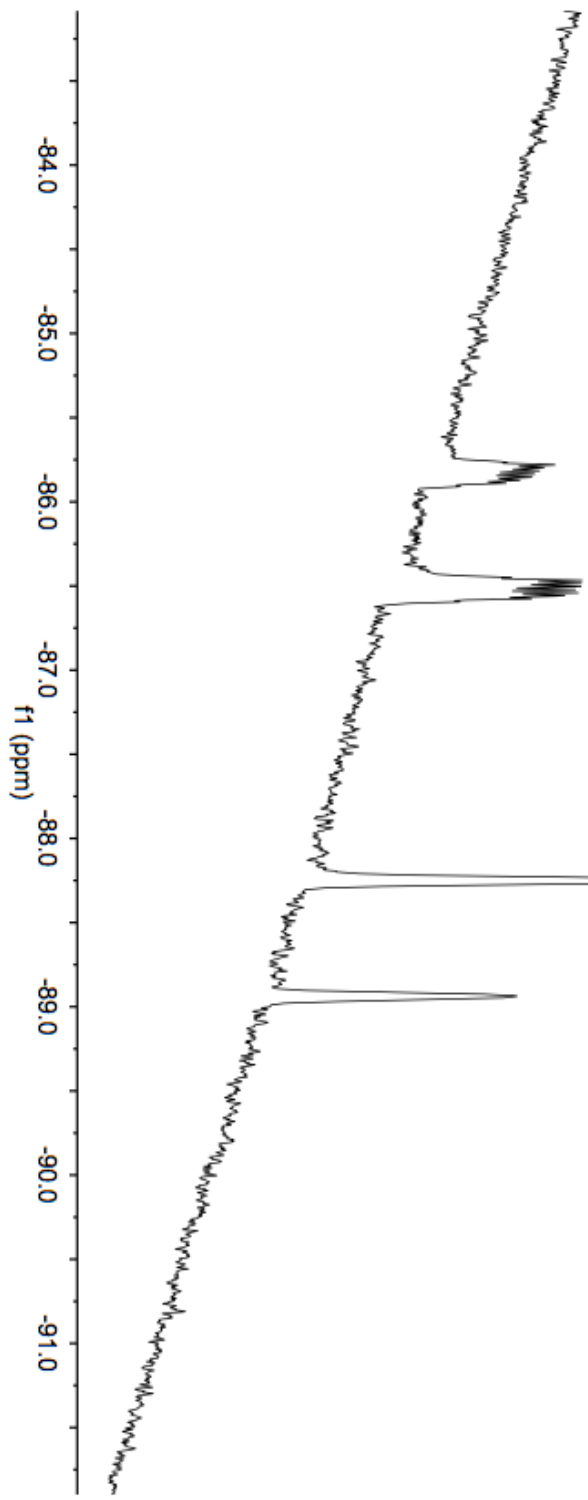


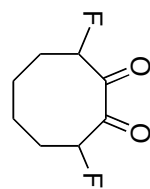




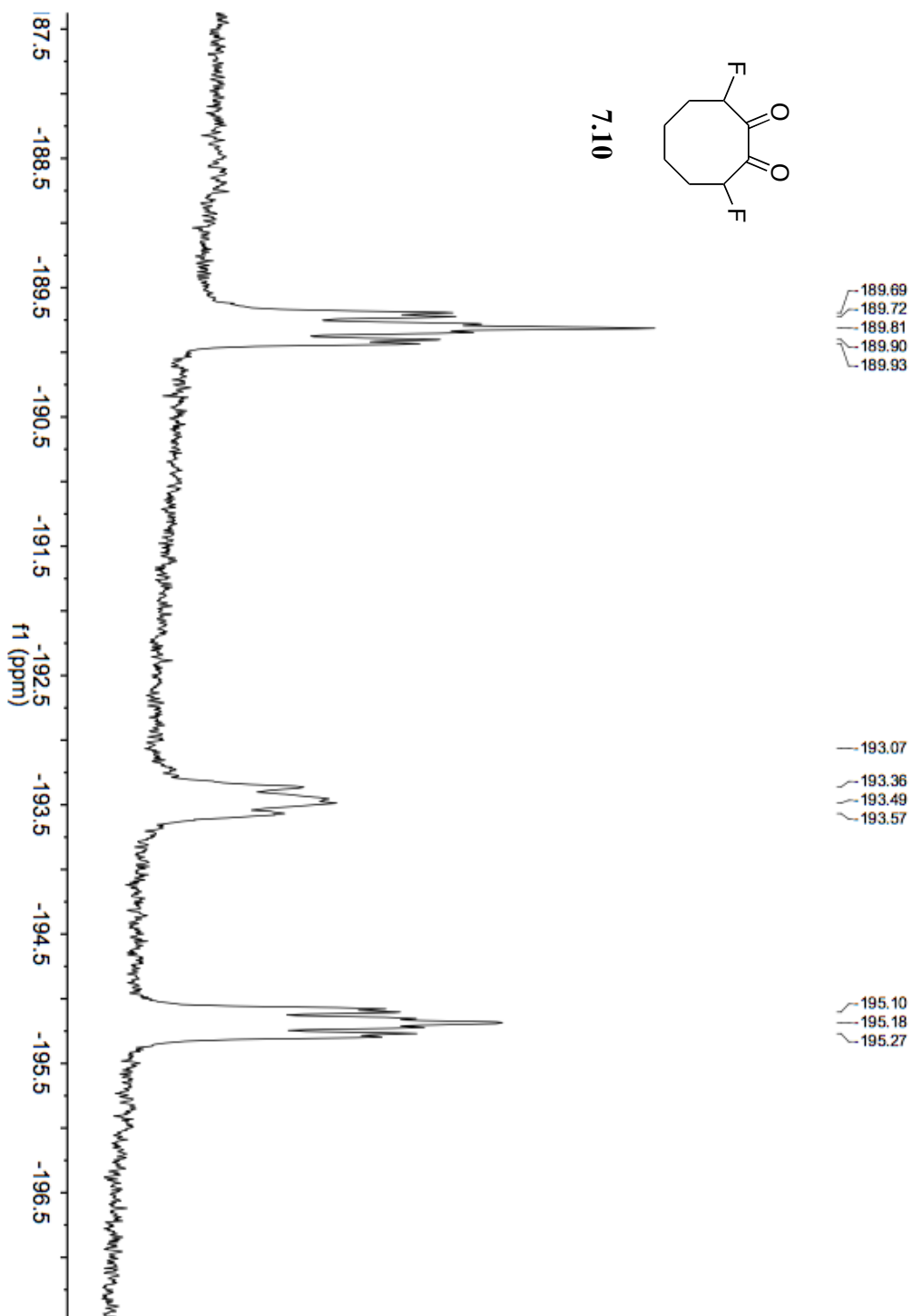
—85.61
 —86.30
 —88.13
 —88.75

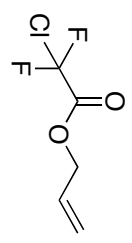
6.1



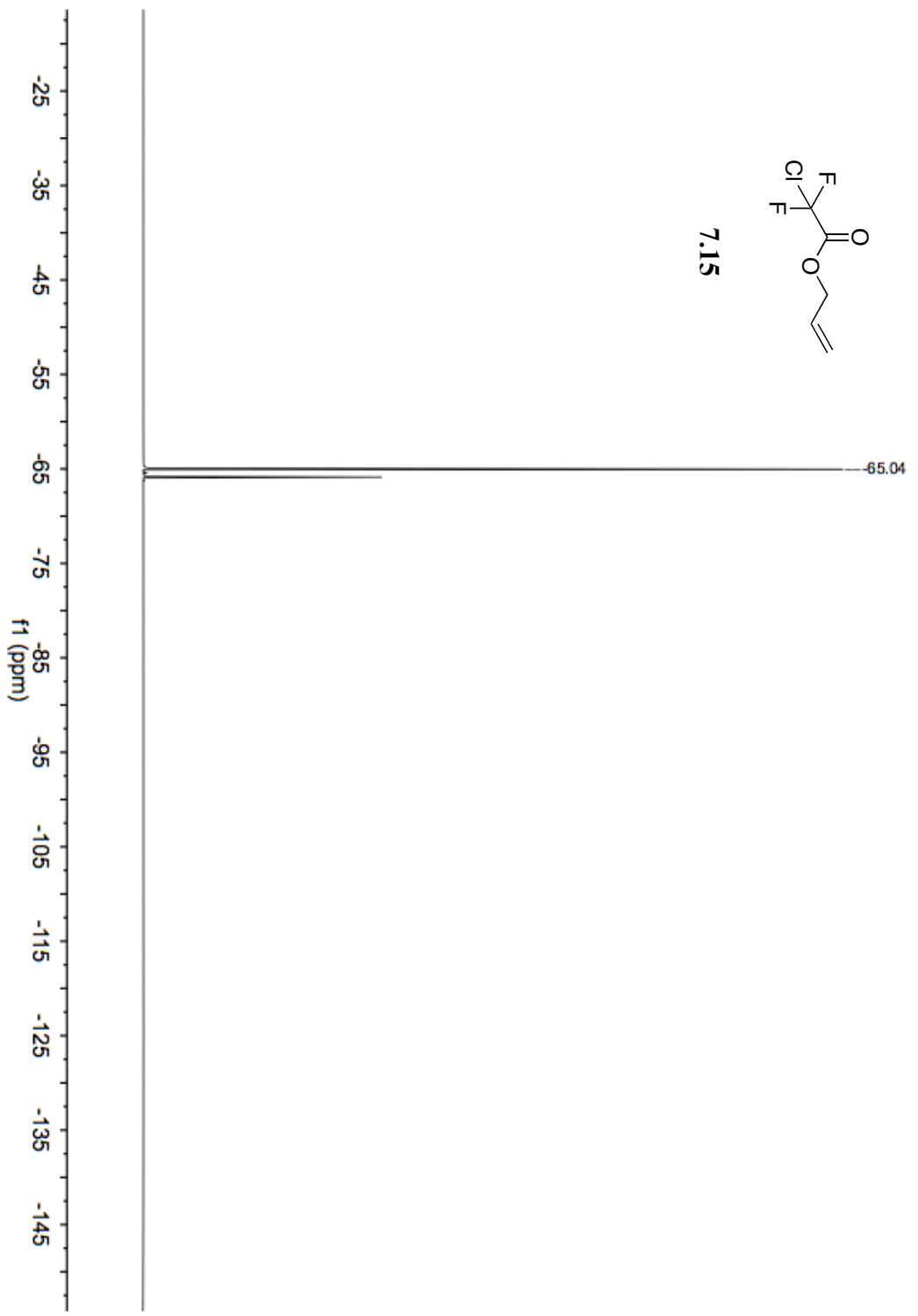


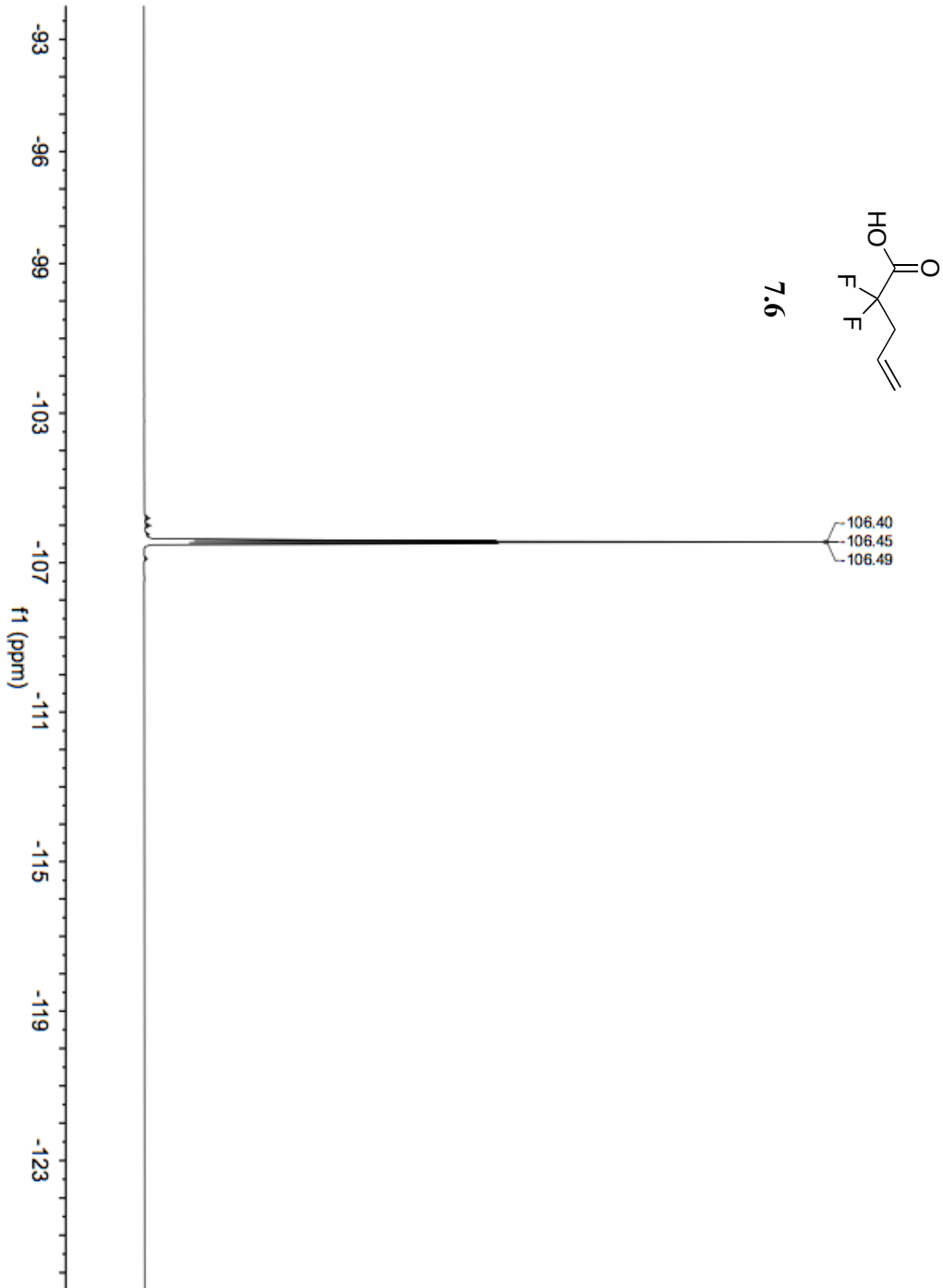
7.10

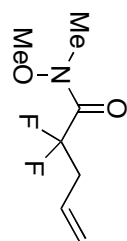




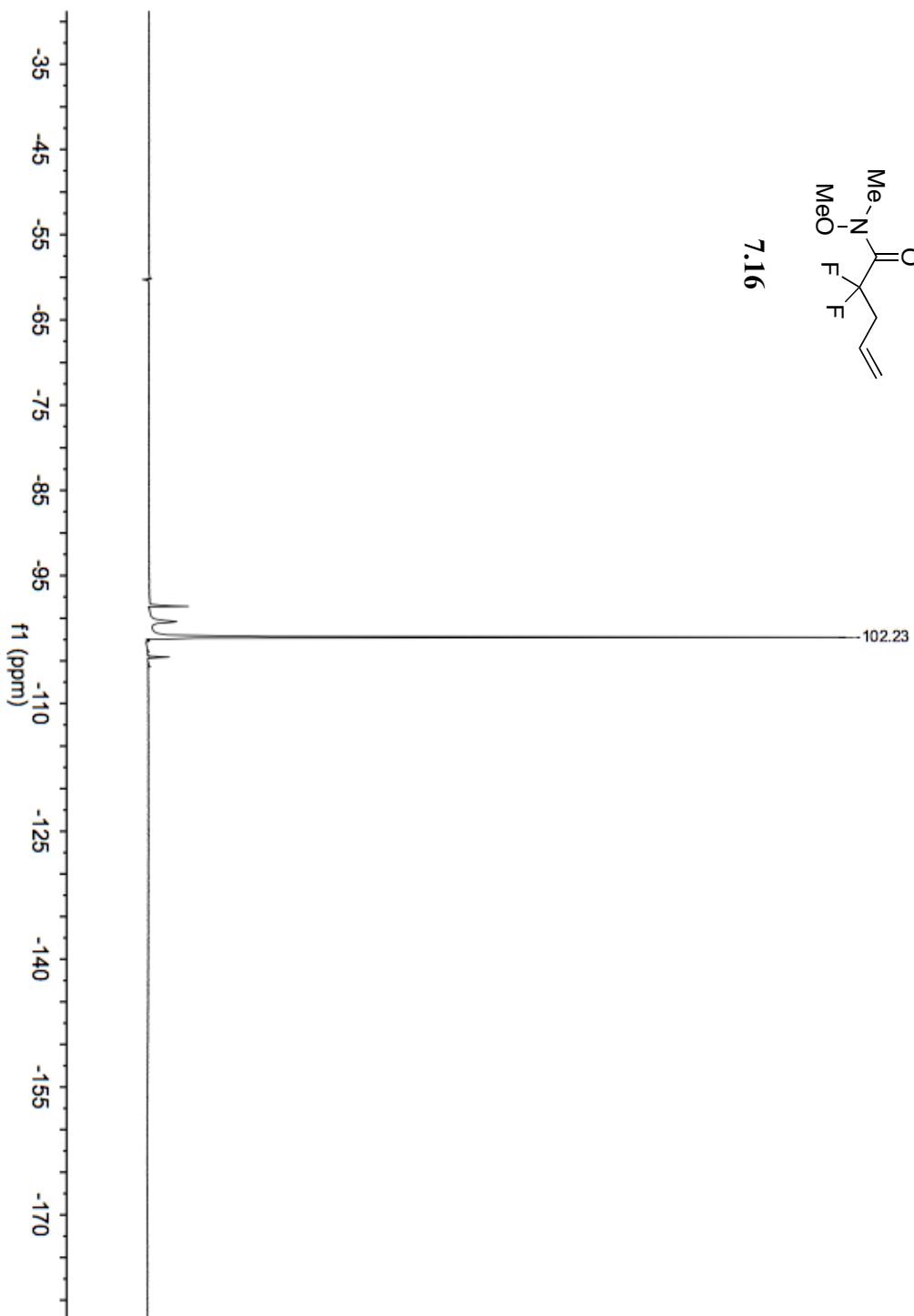
7.15

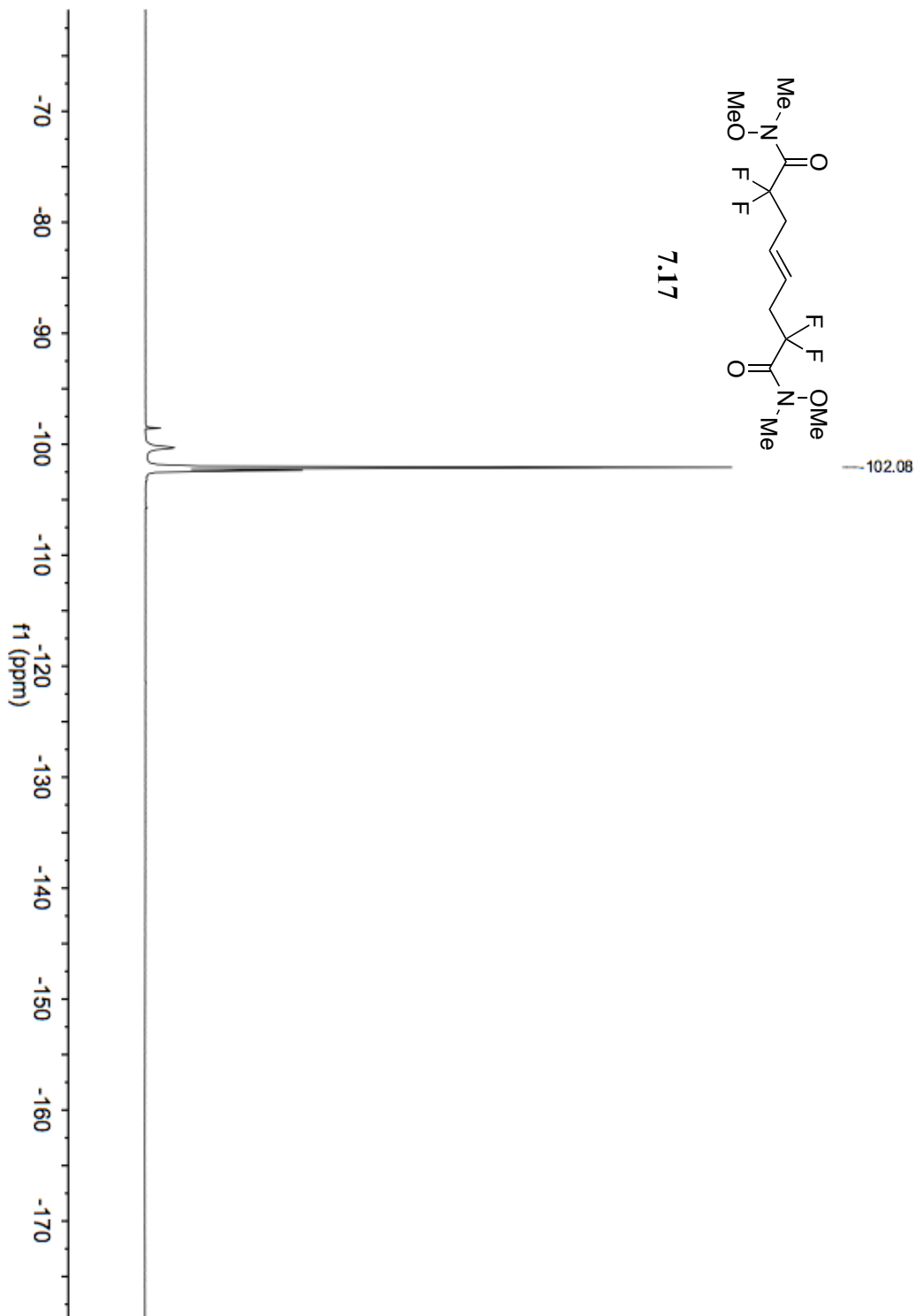


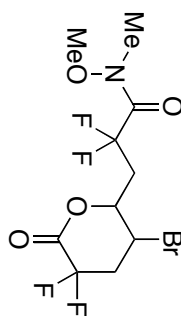




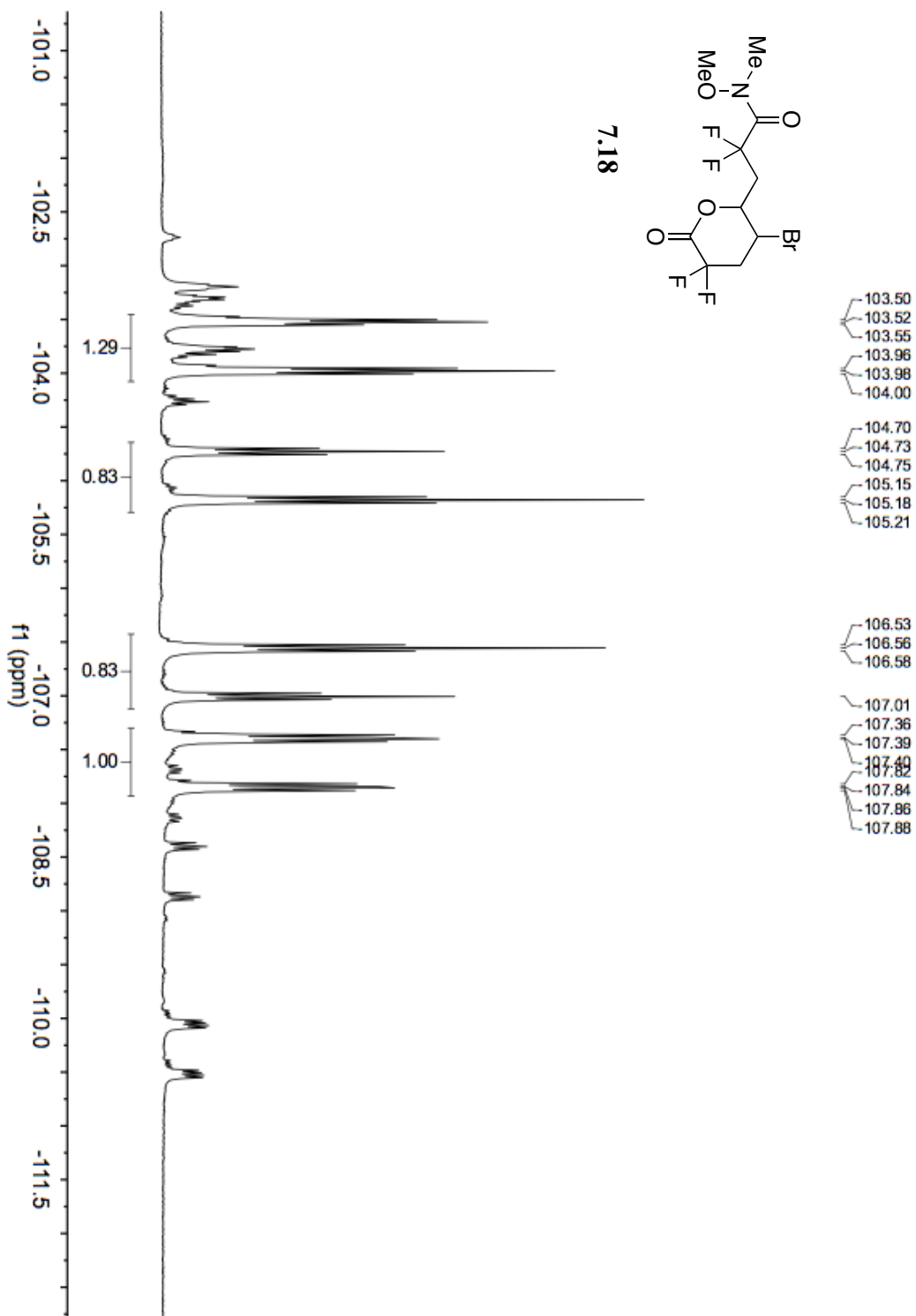
7.16

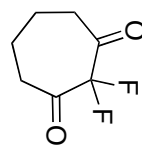




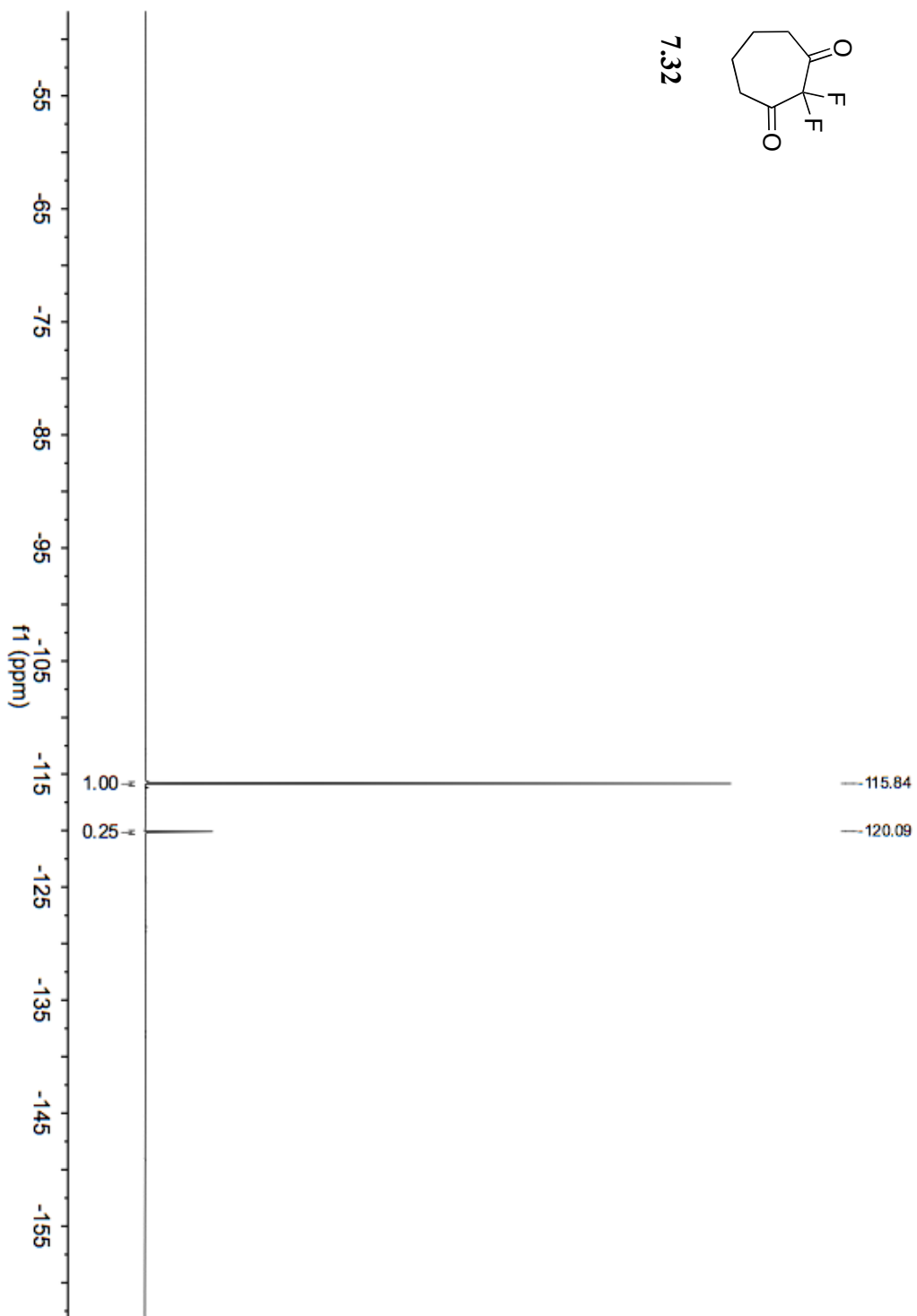


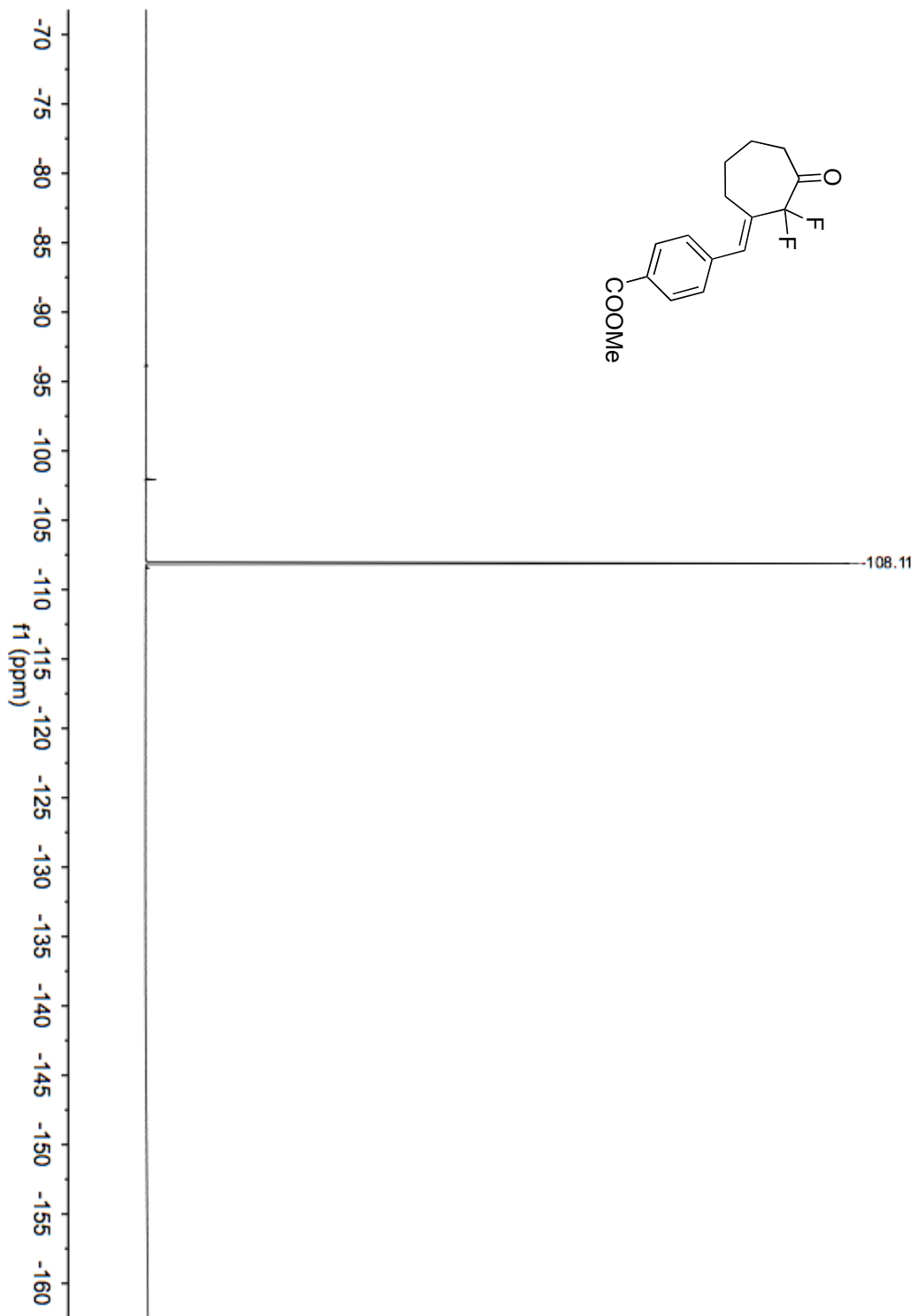
7.18

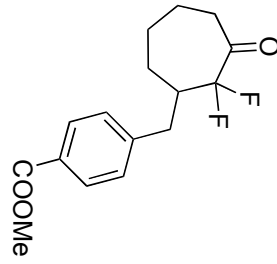




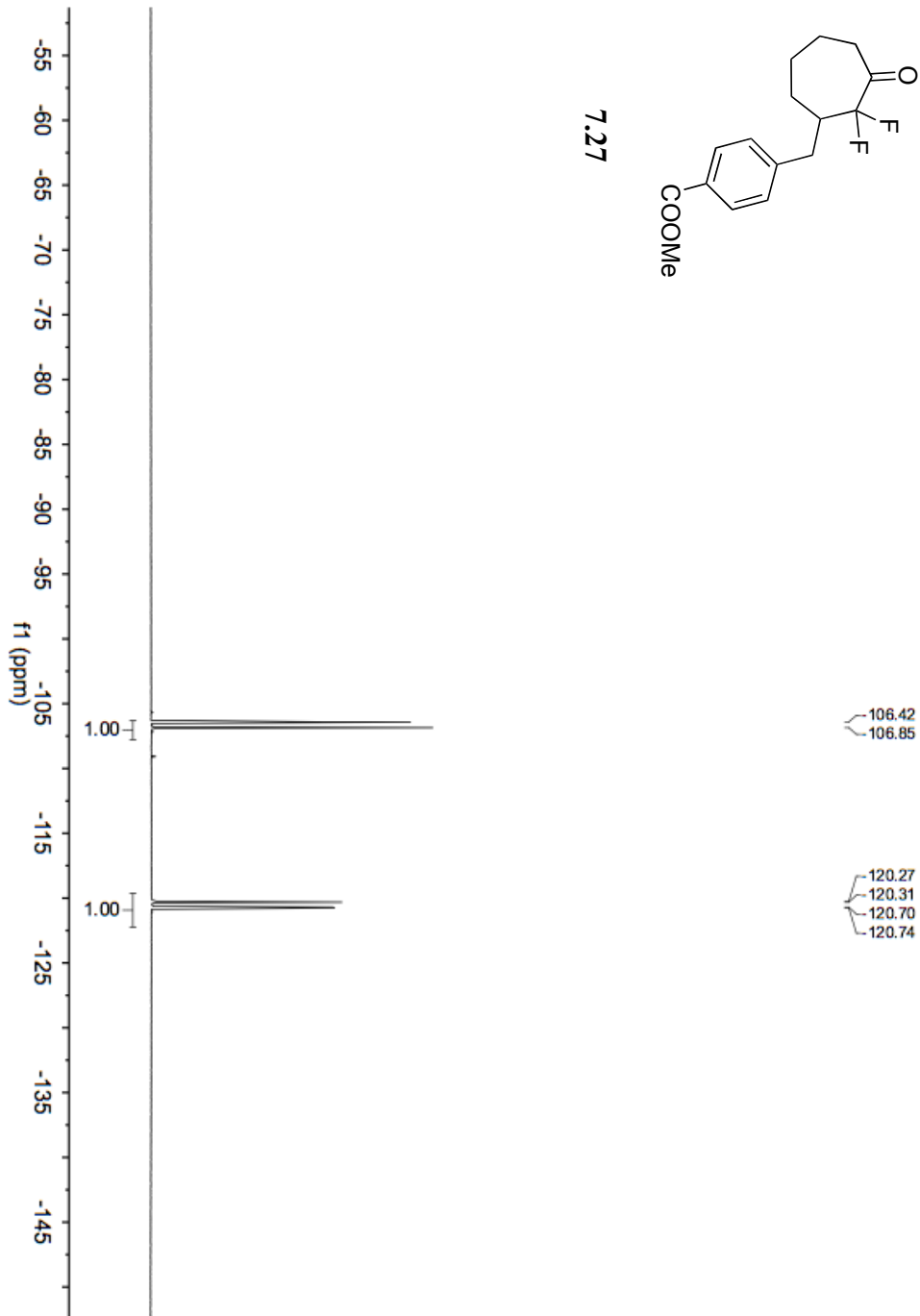
7.32

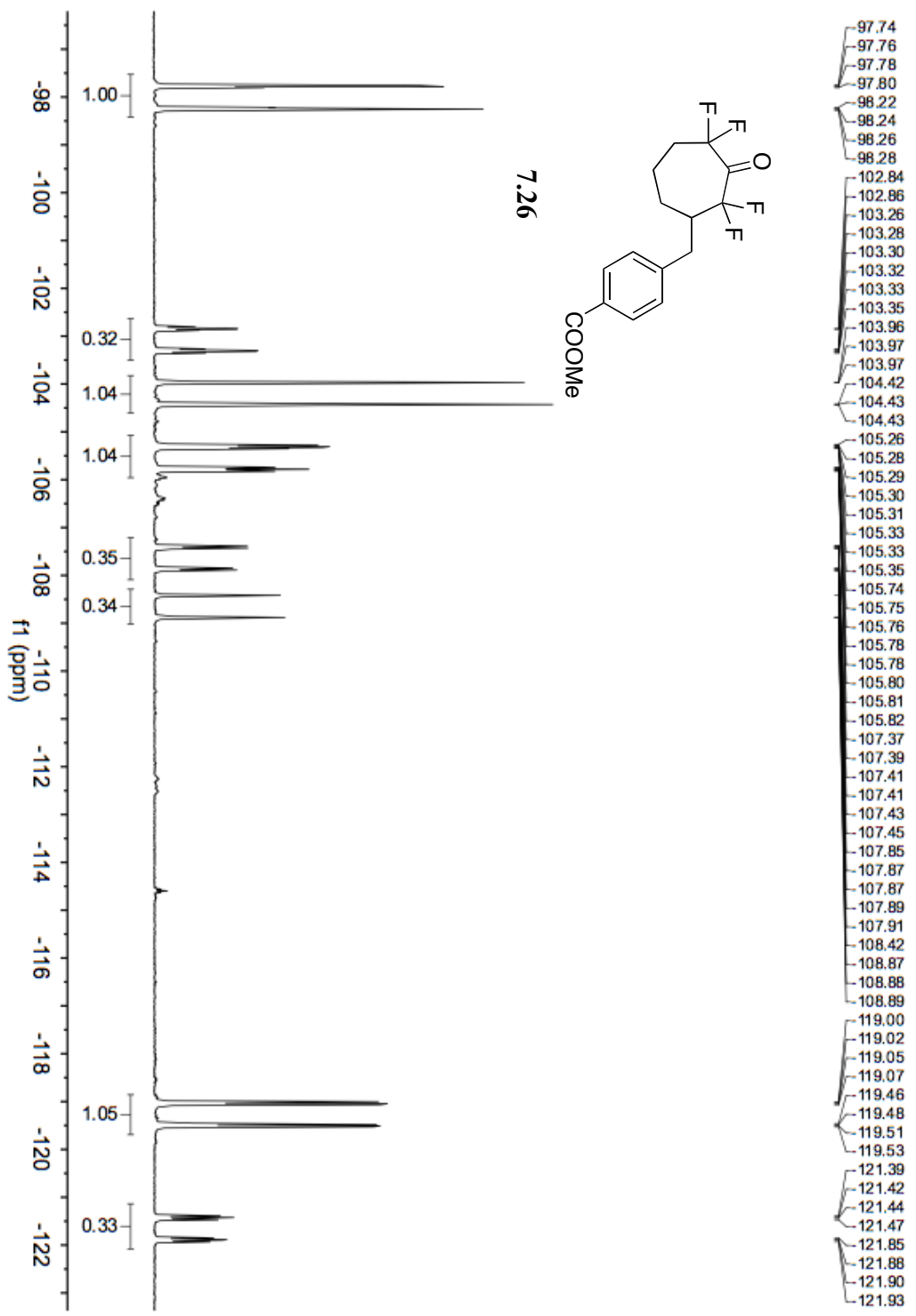


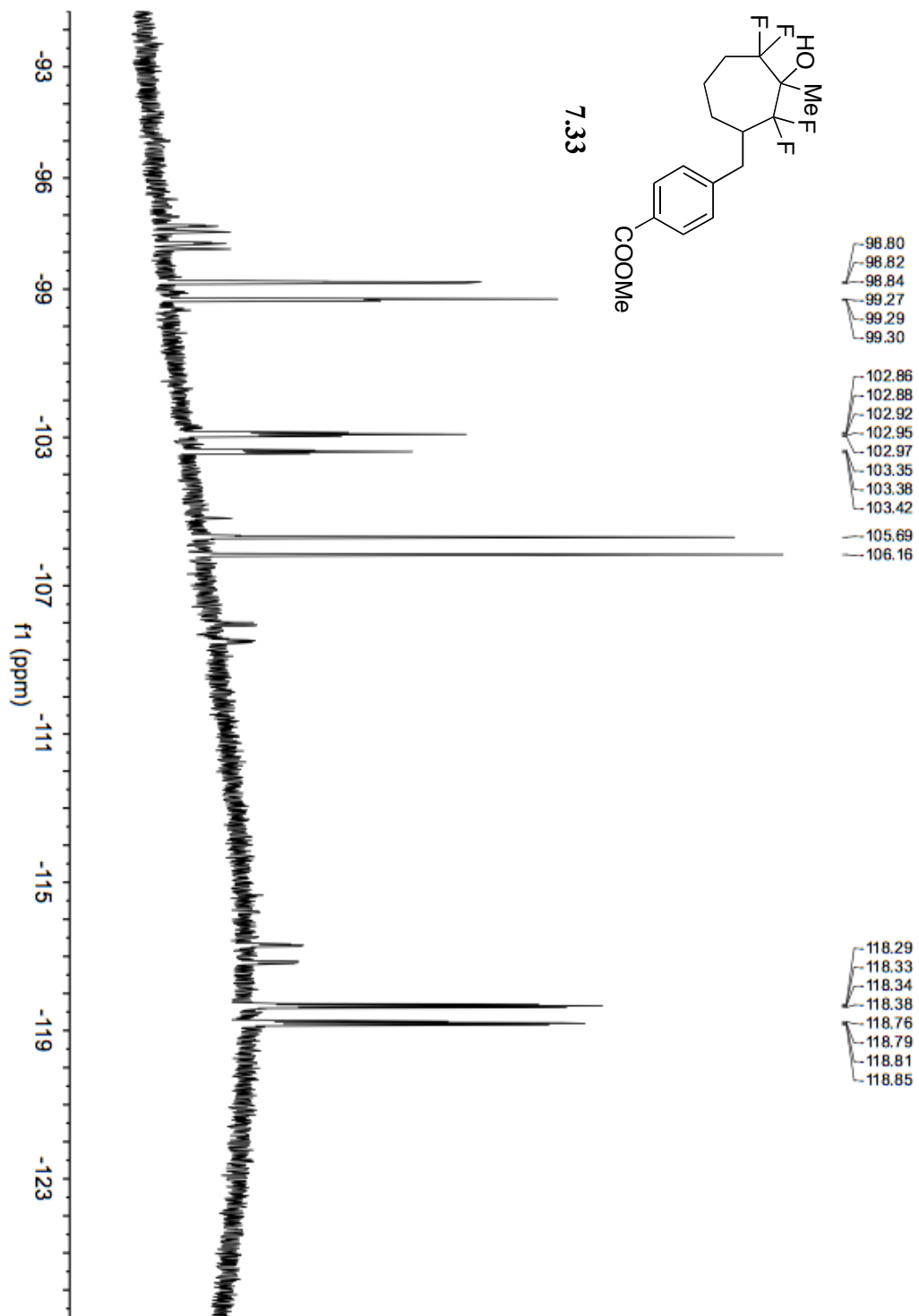


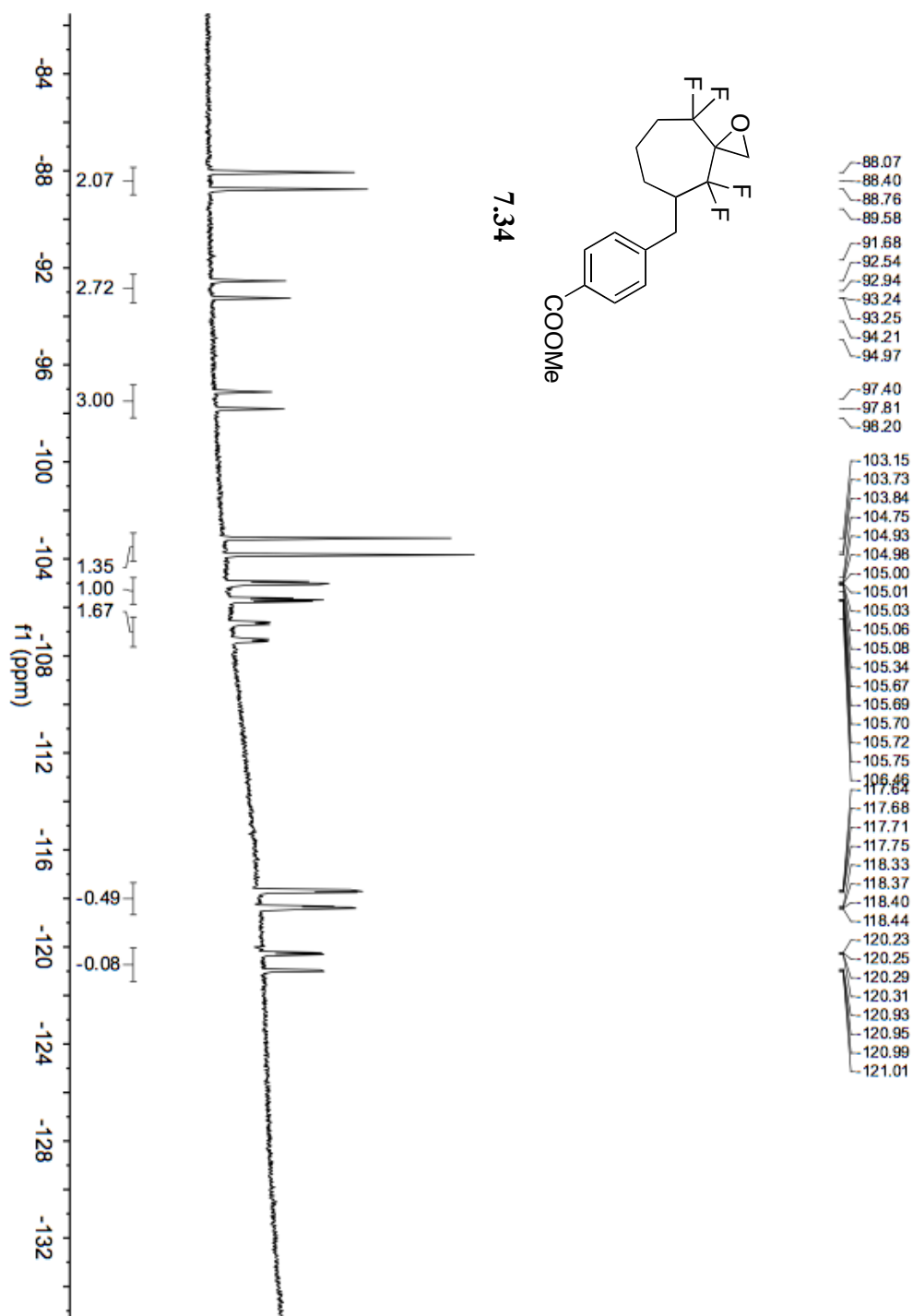


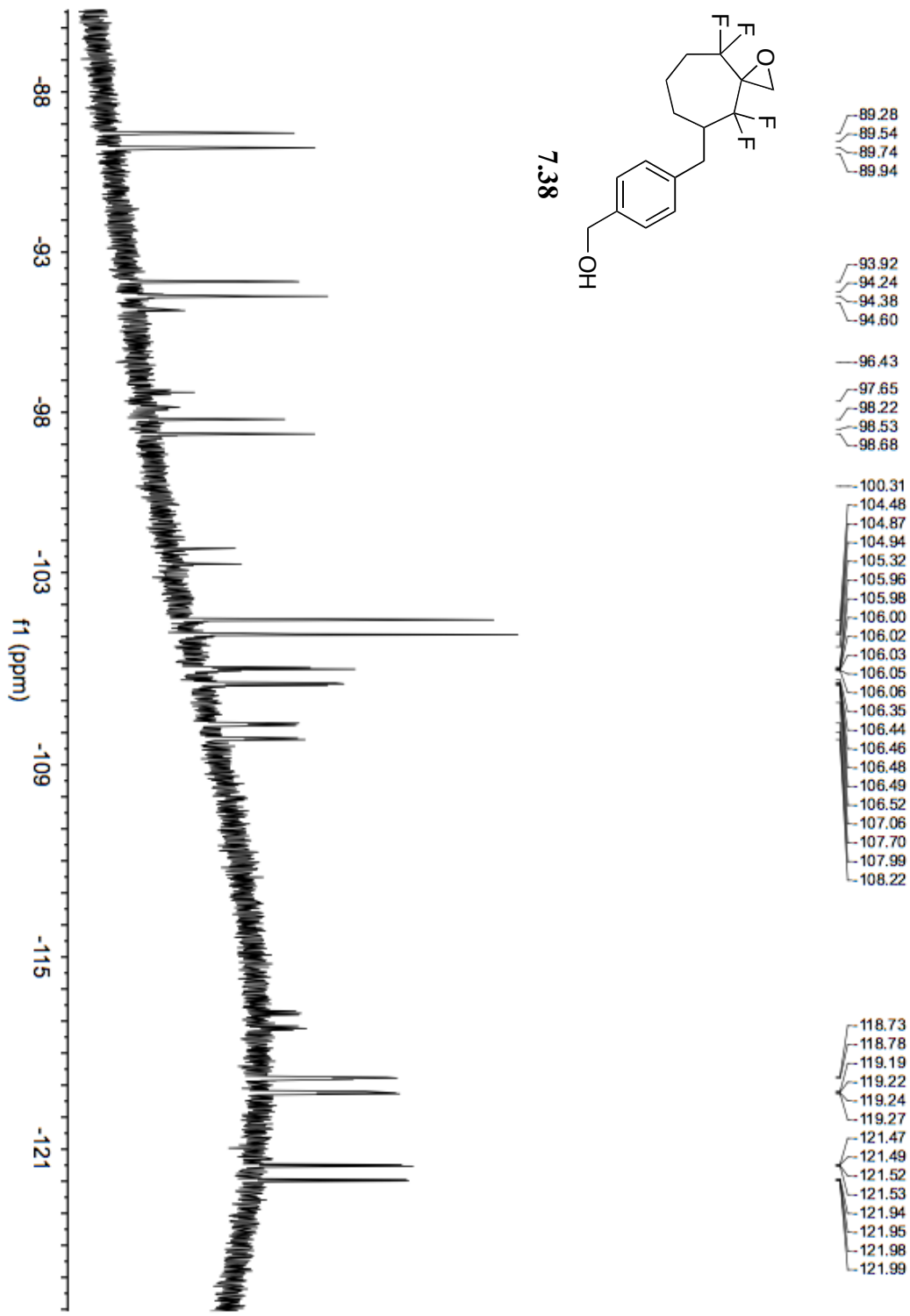
7.27

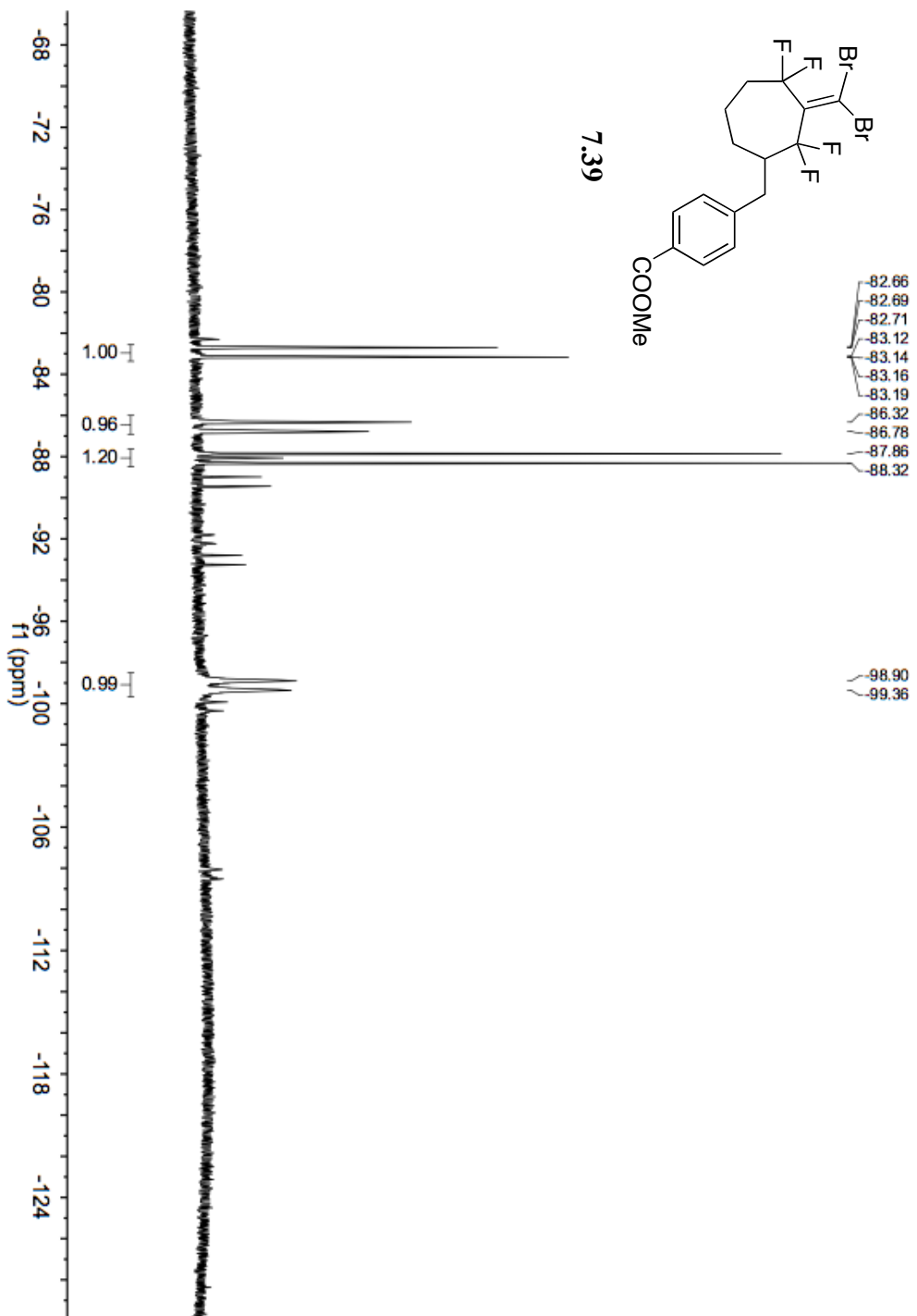


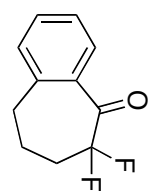




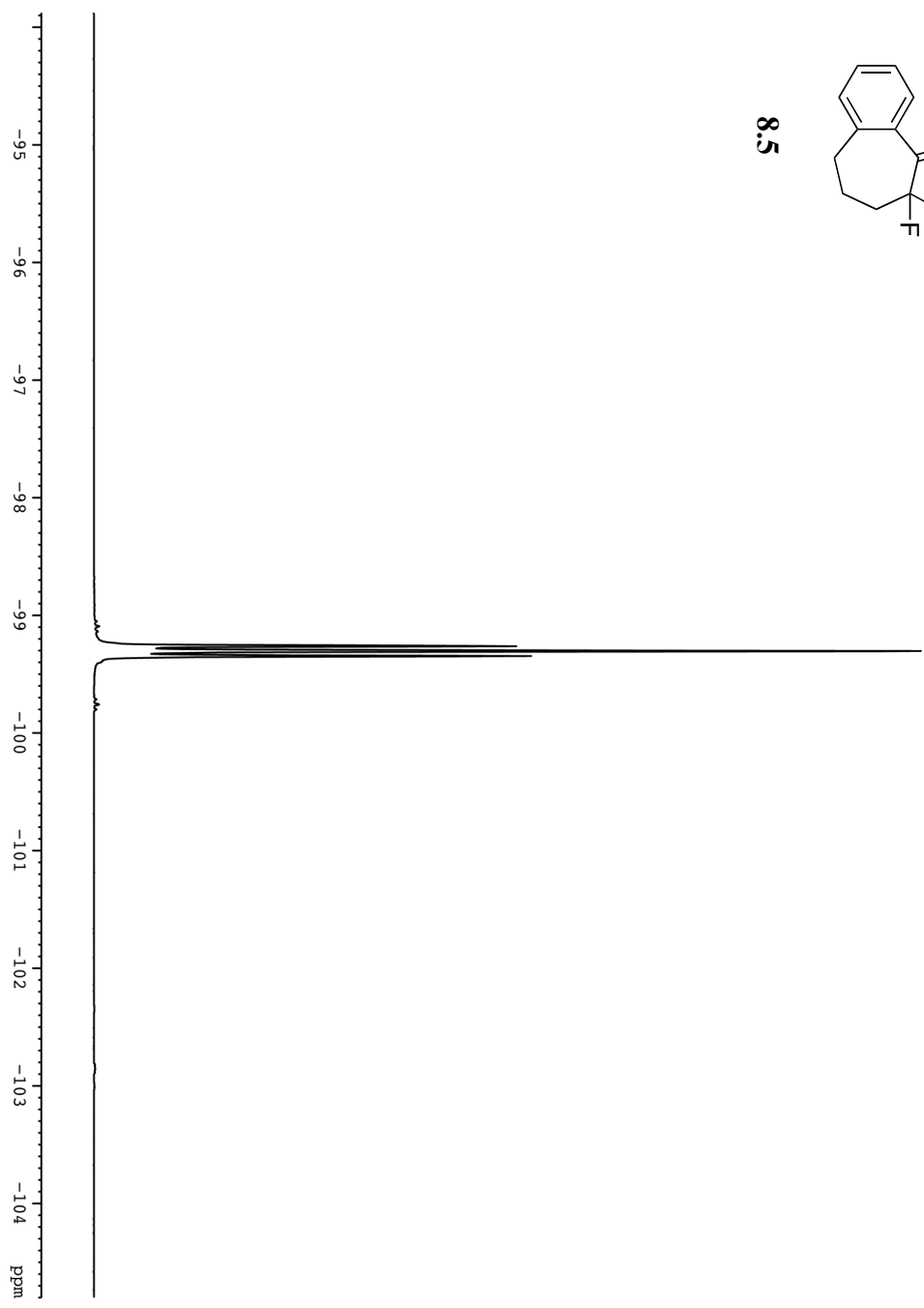


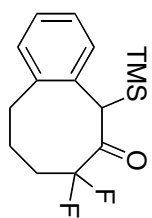




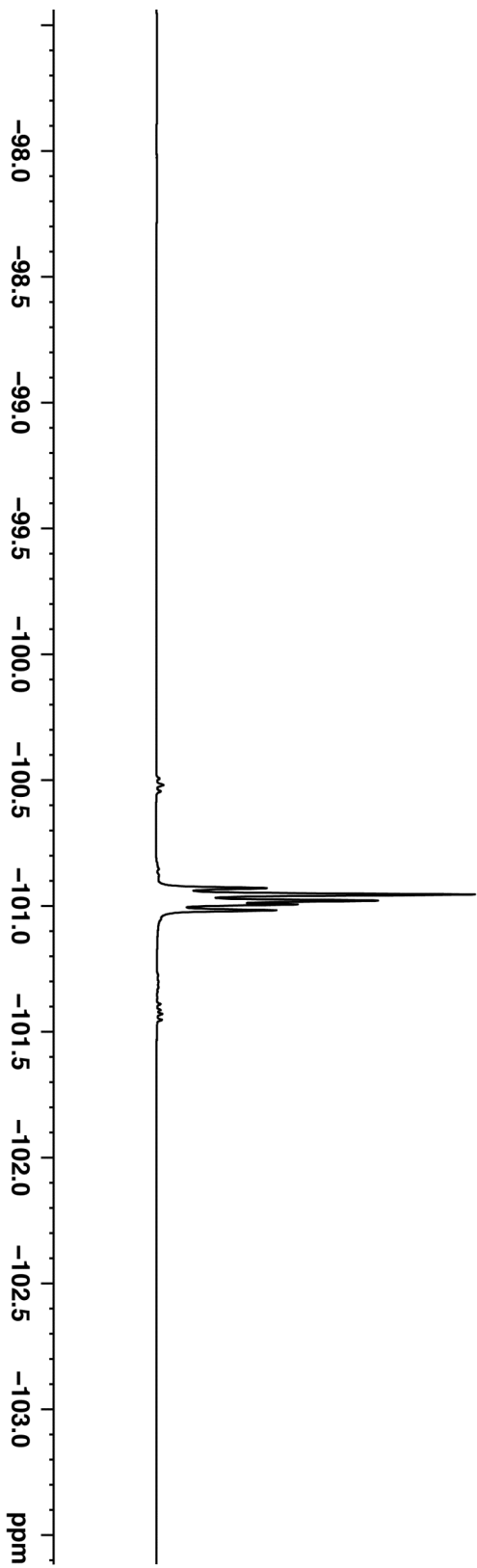


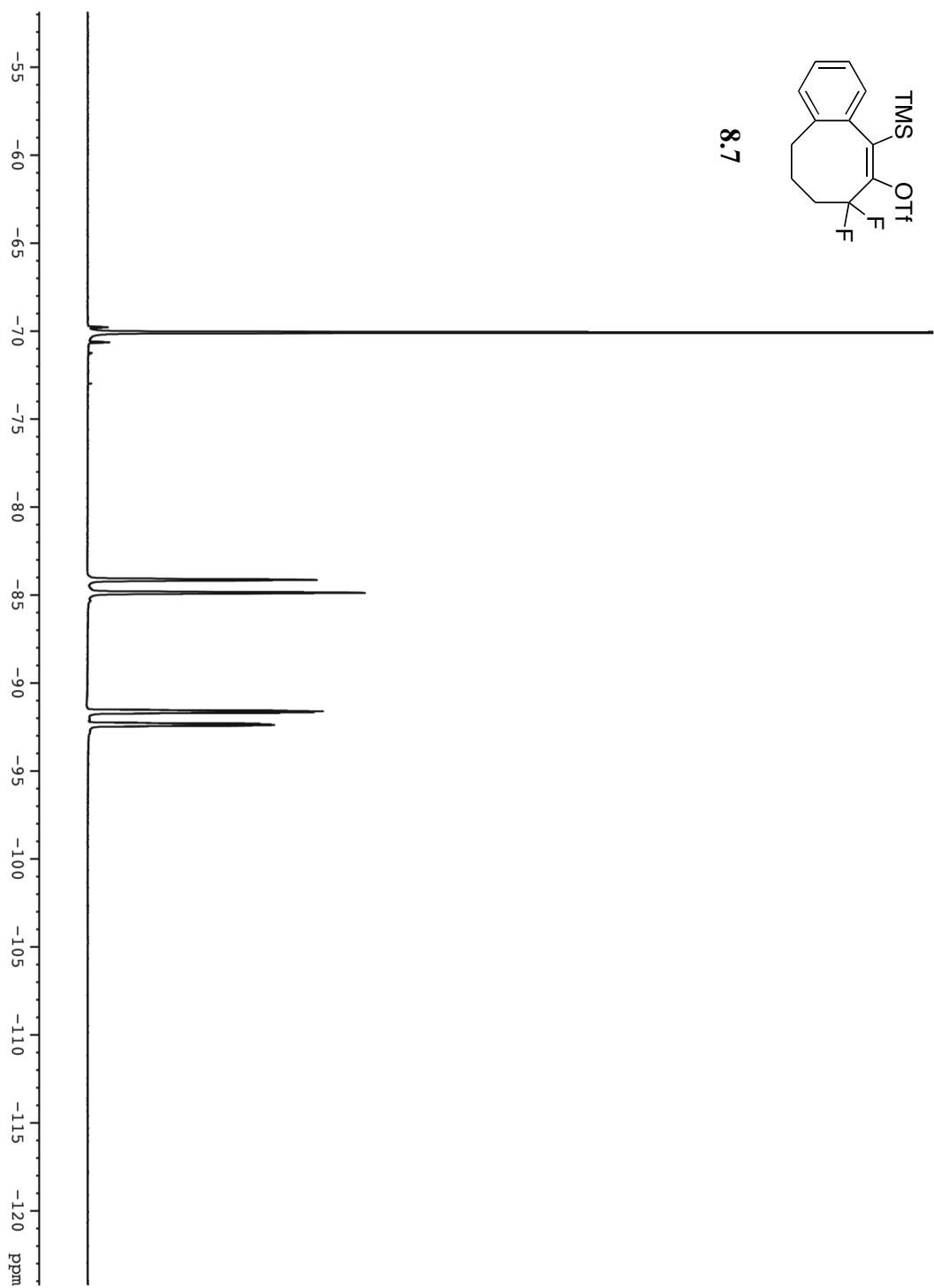
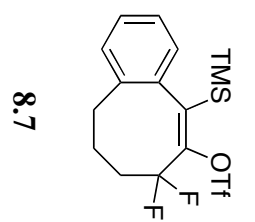
8.5

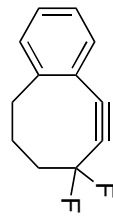




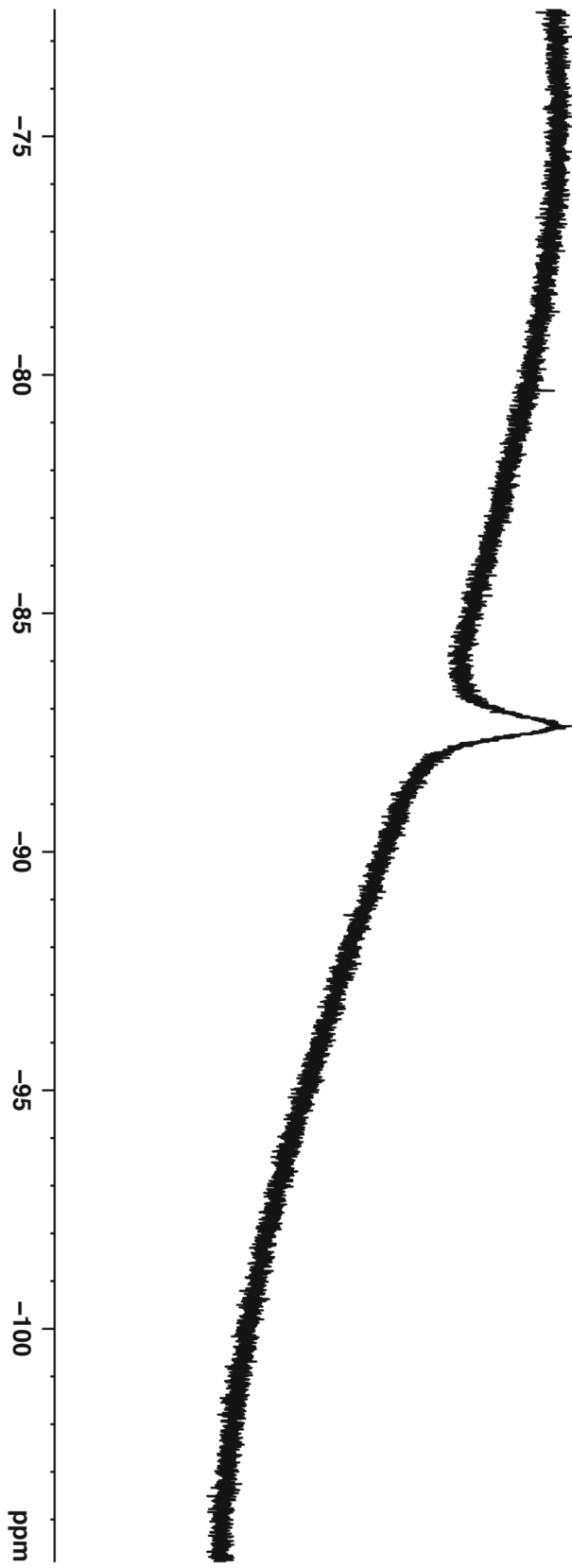
8.6

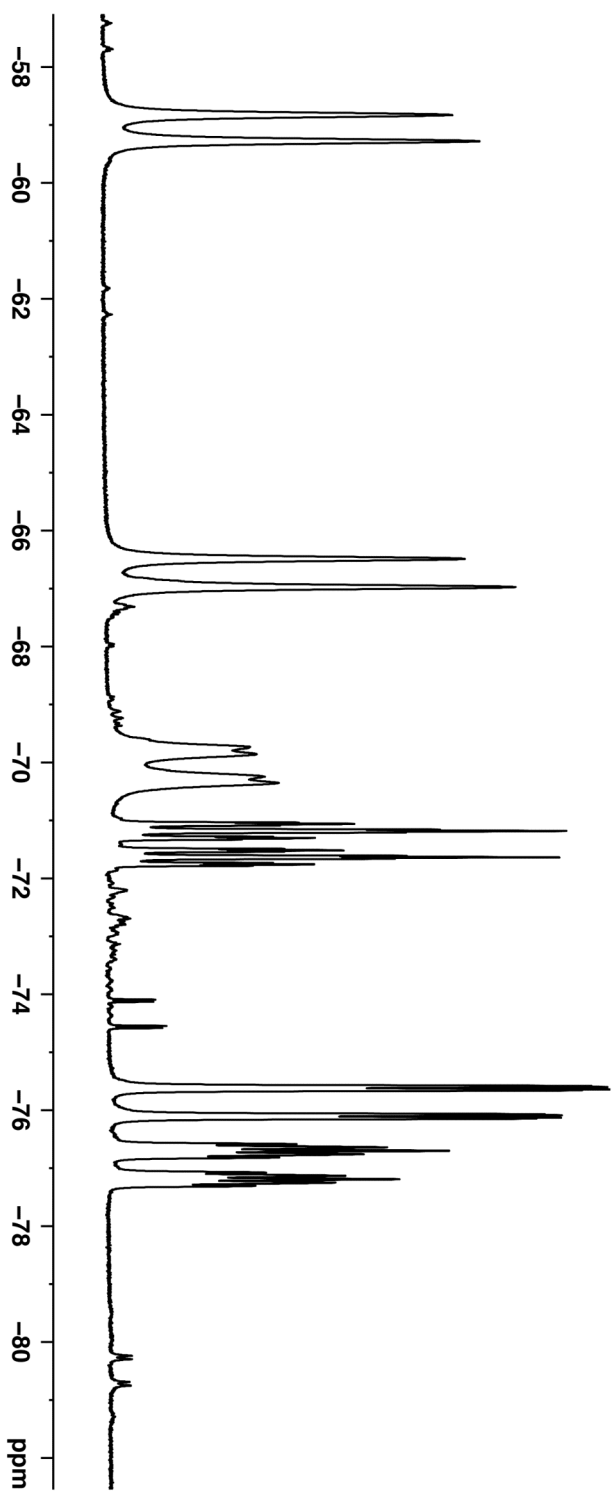
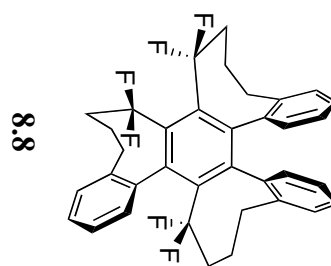


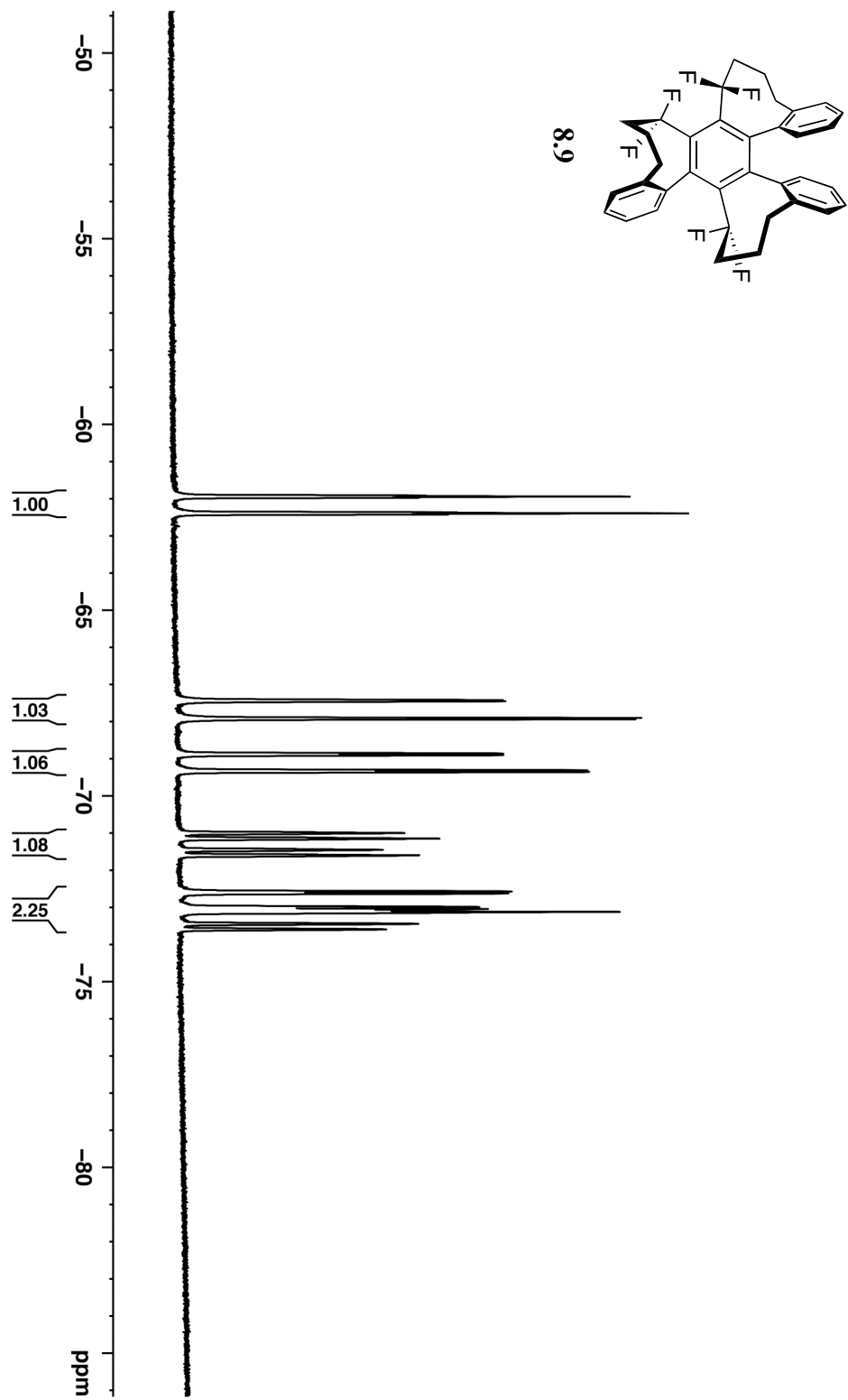


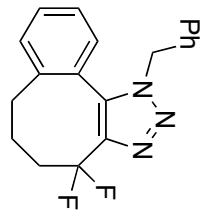


8.3

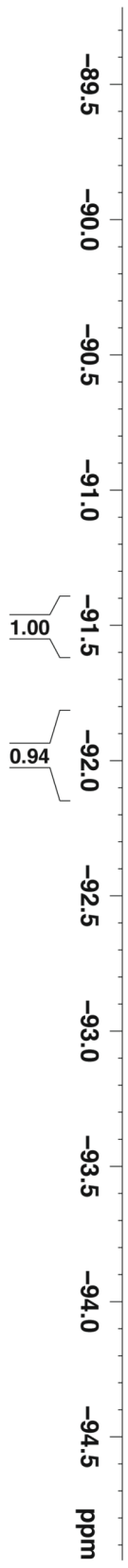


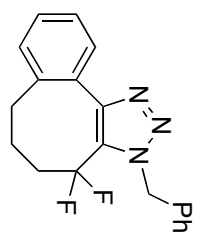




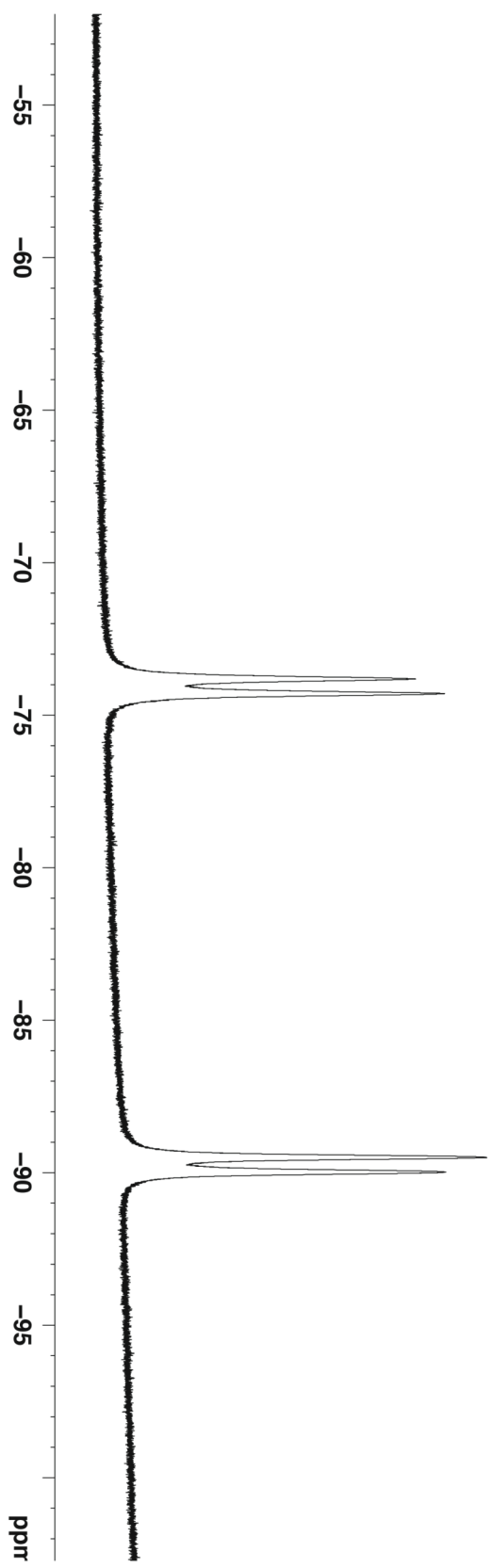


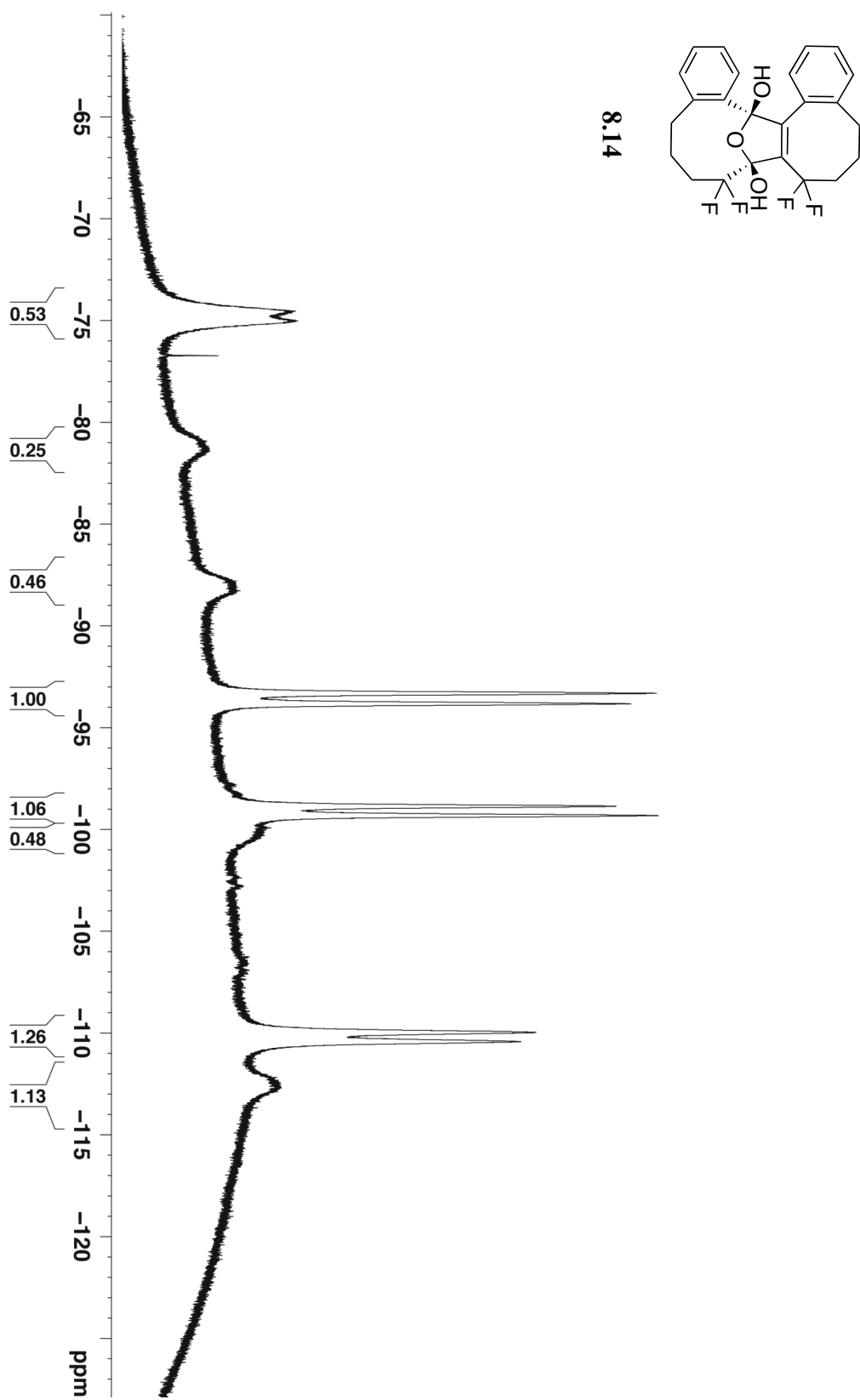
8.11

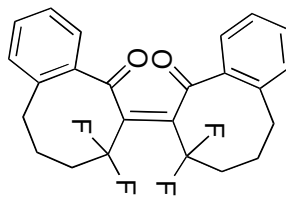




8.12

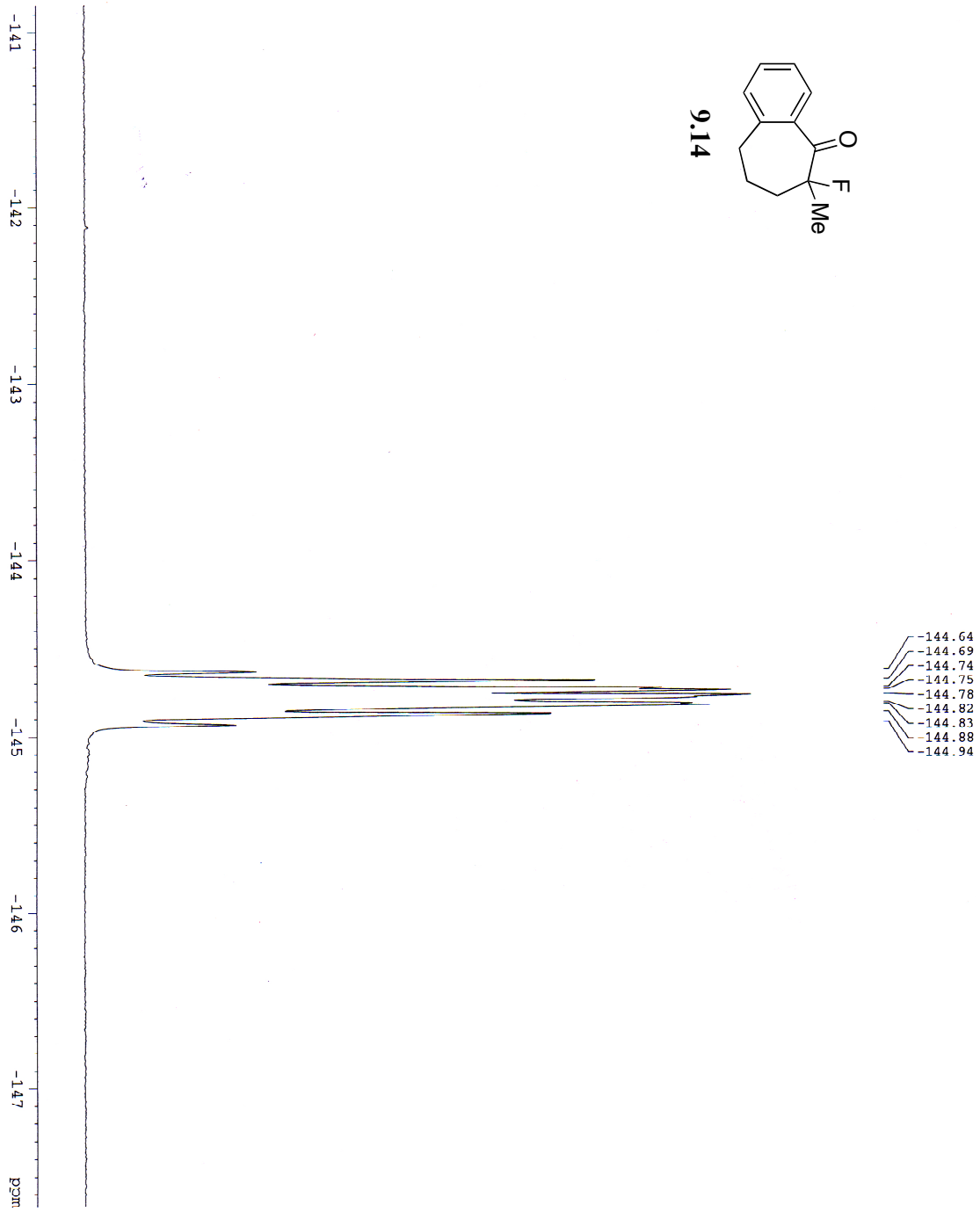
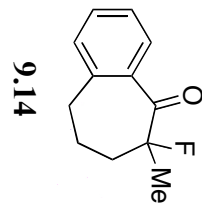


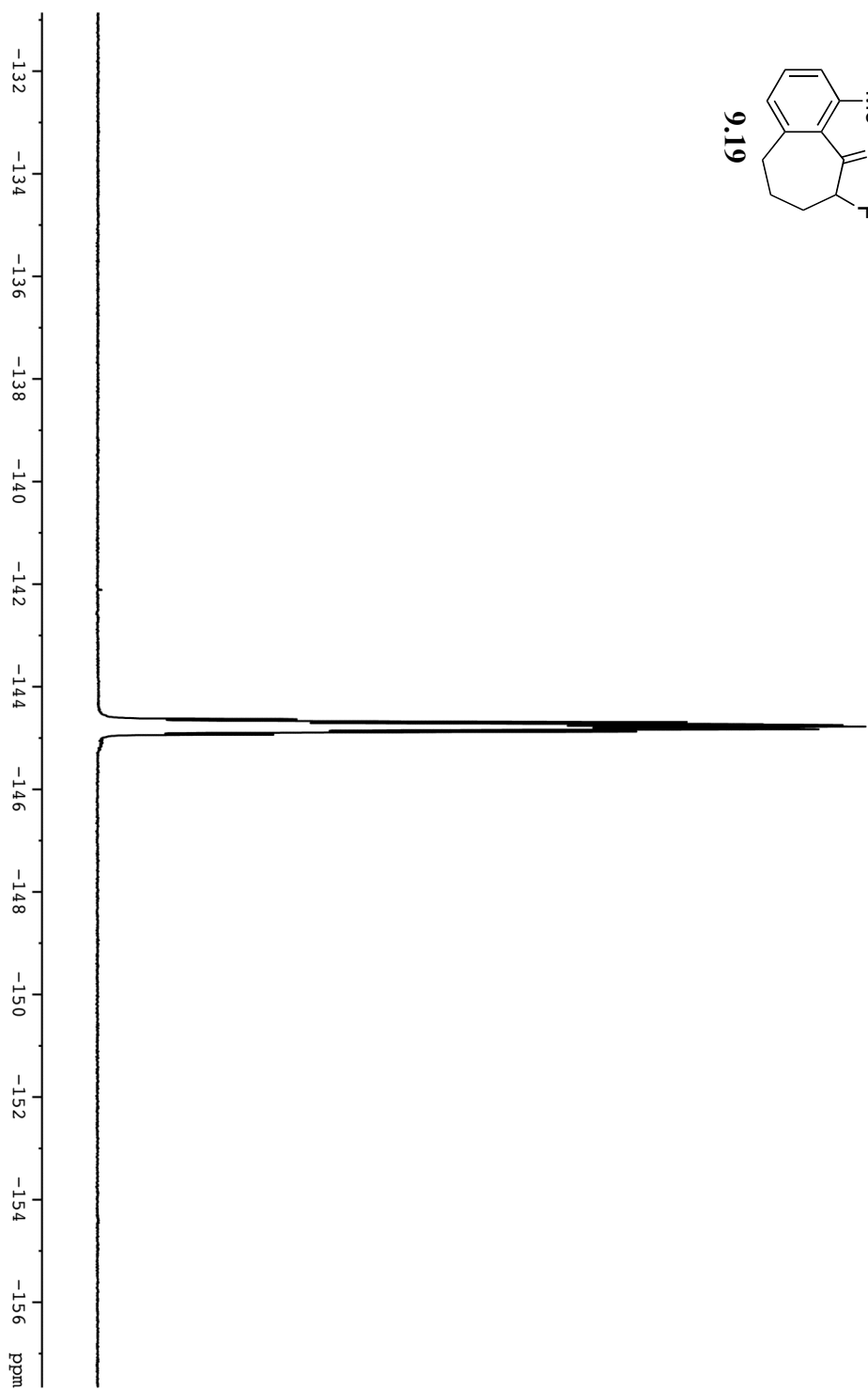
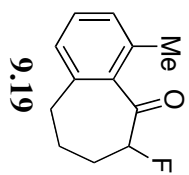


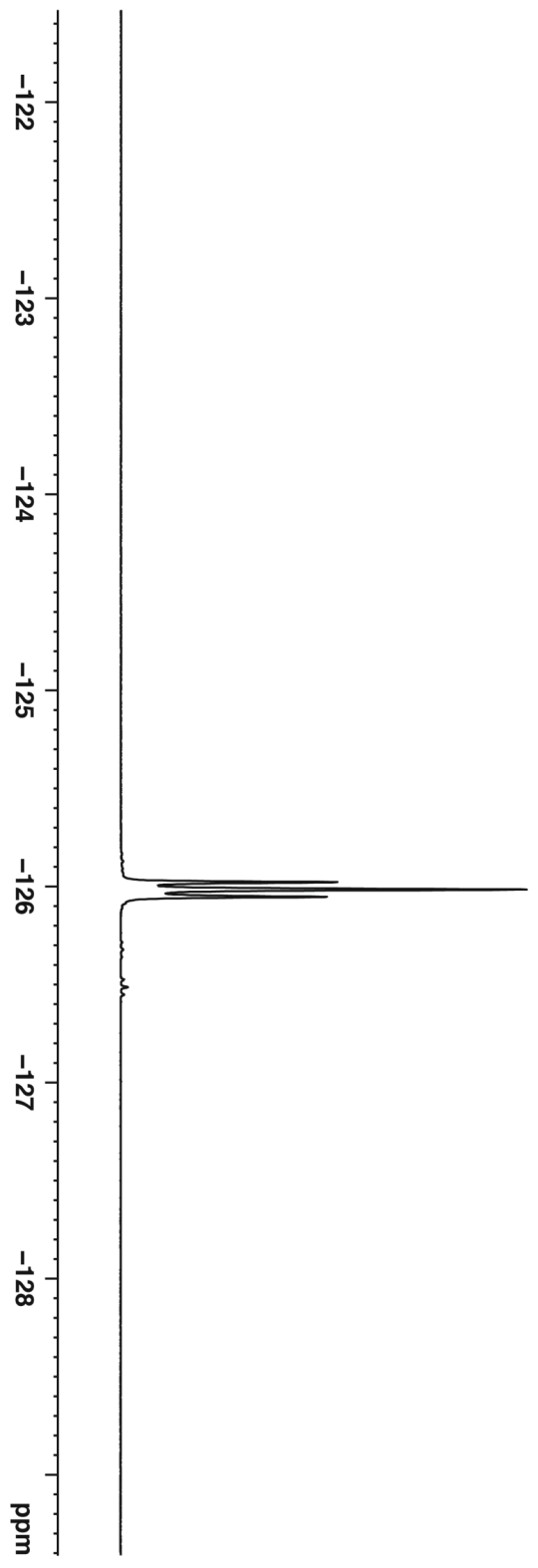
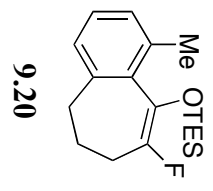


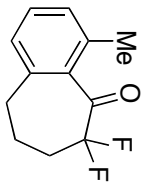
8.15



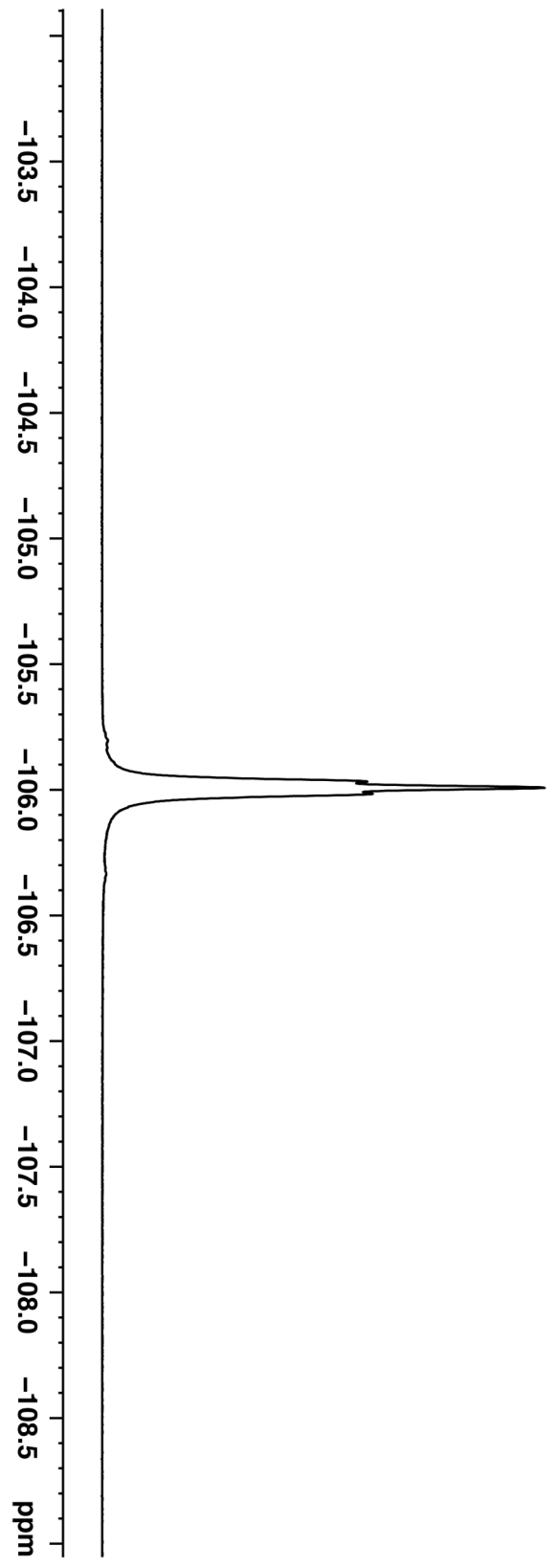


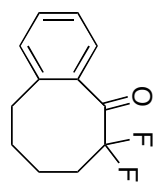




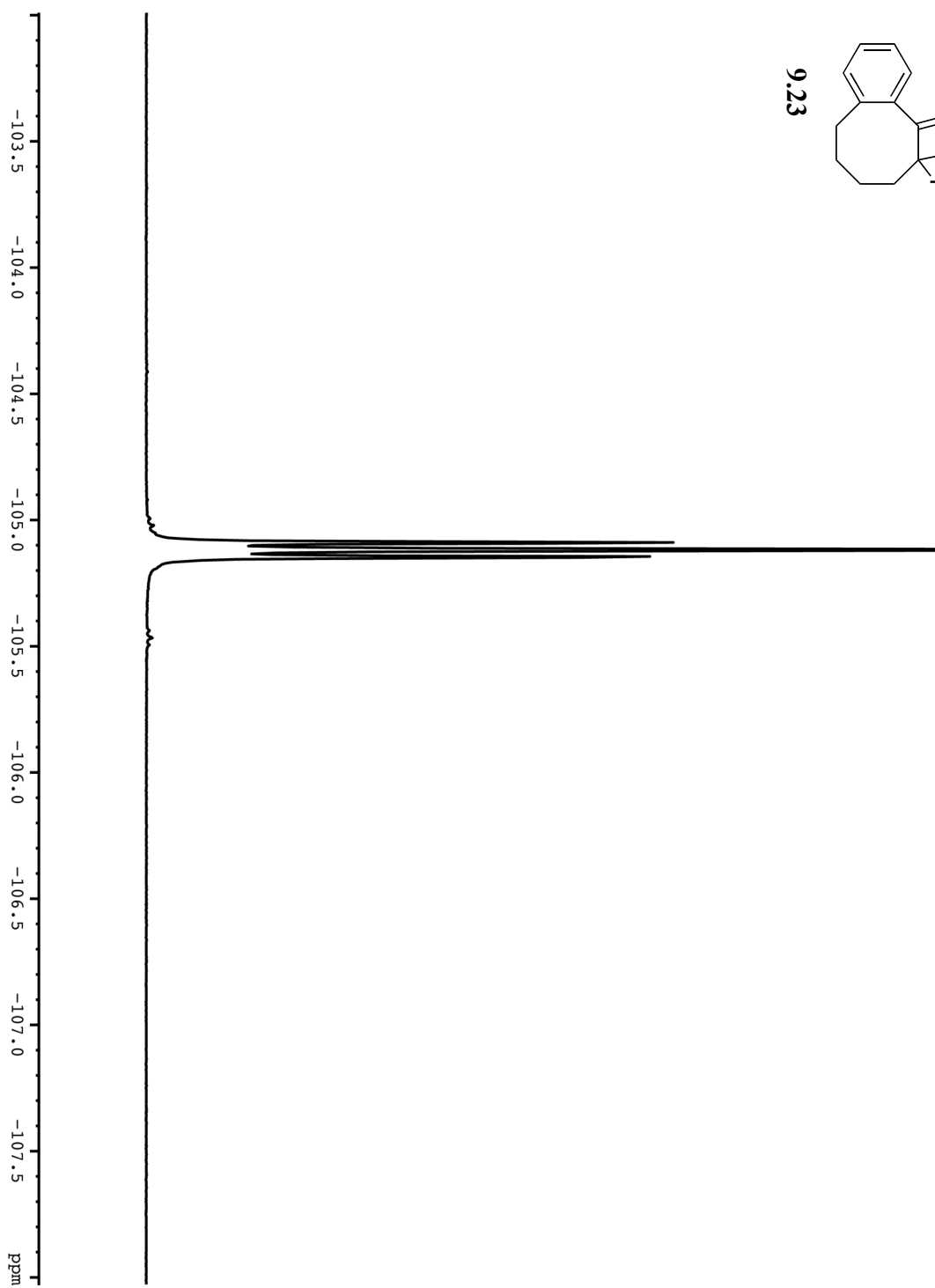


9.21

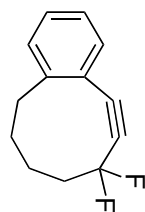




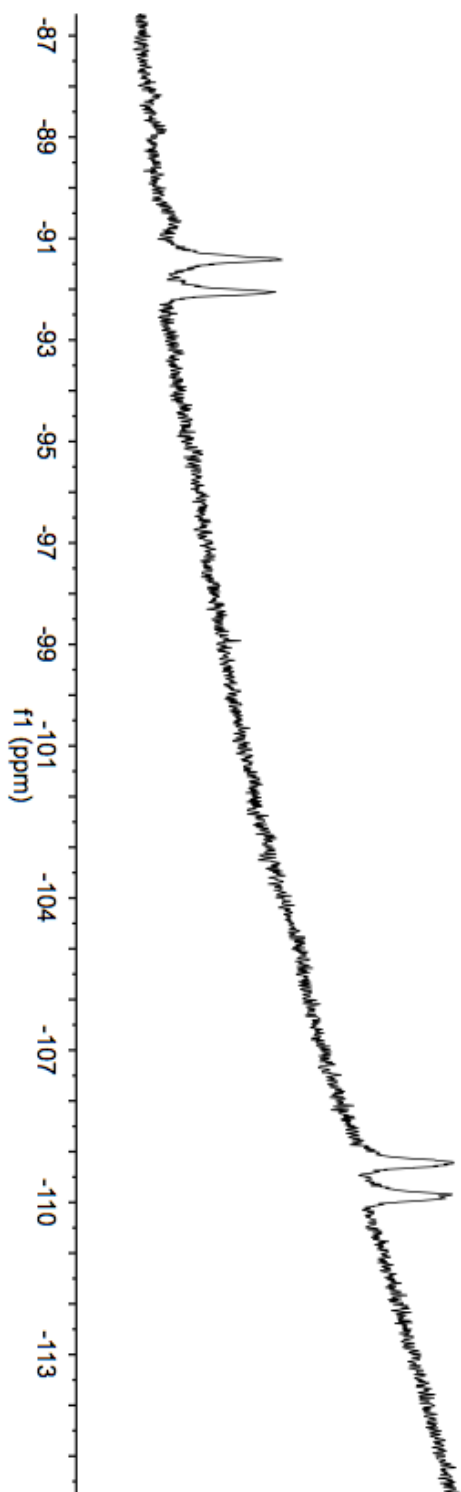
9.23



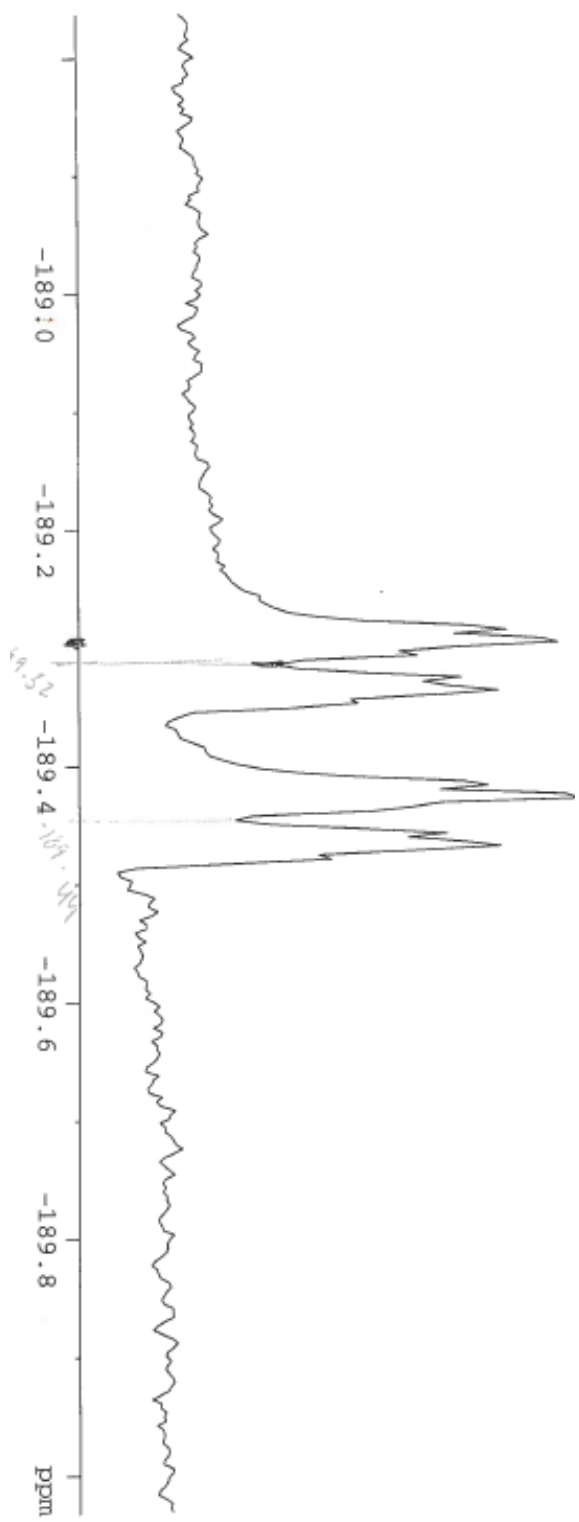
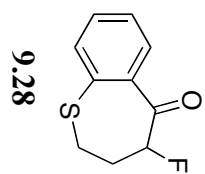
9.6

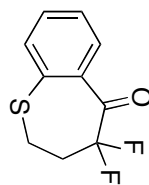


91.01
91.81
92.56

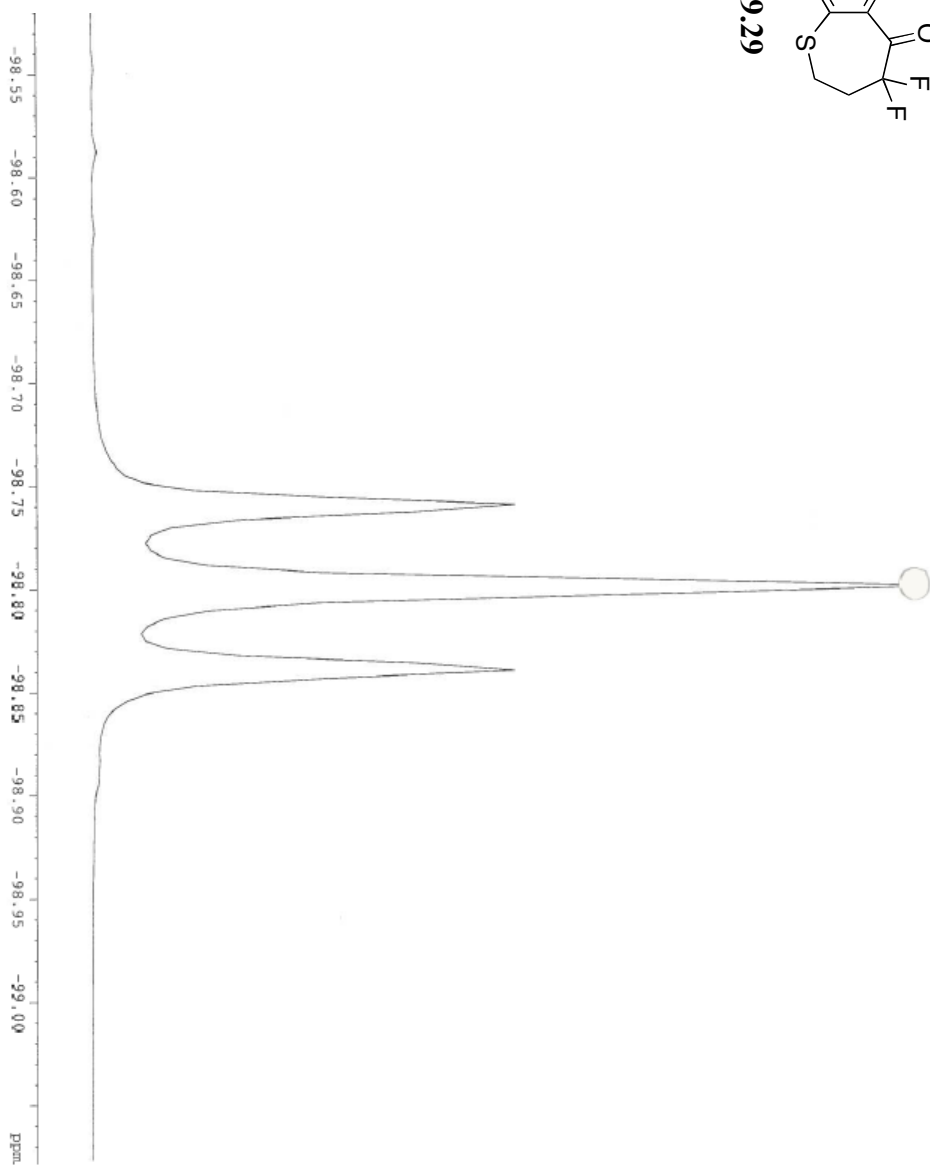


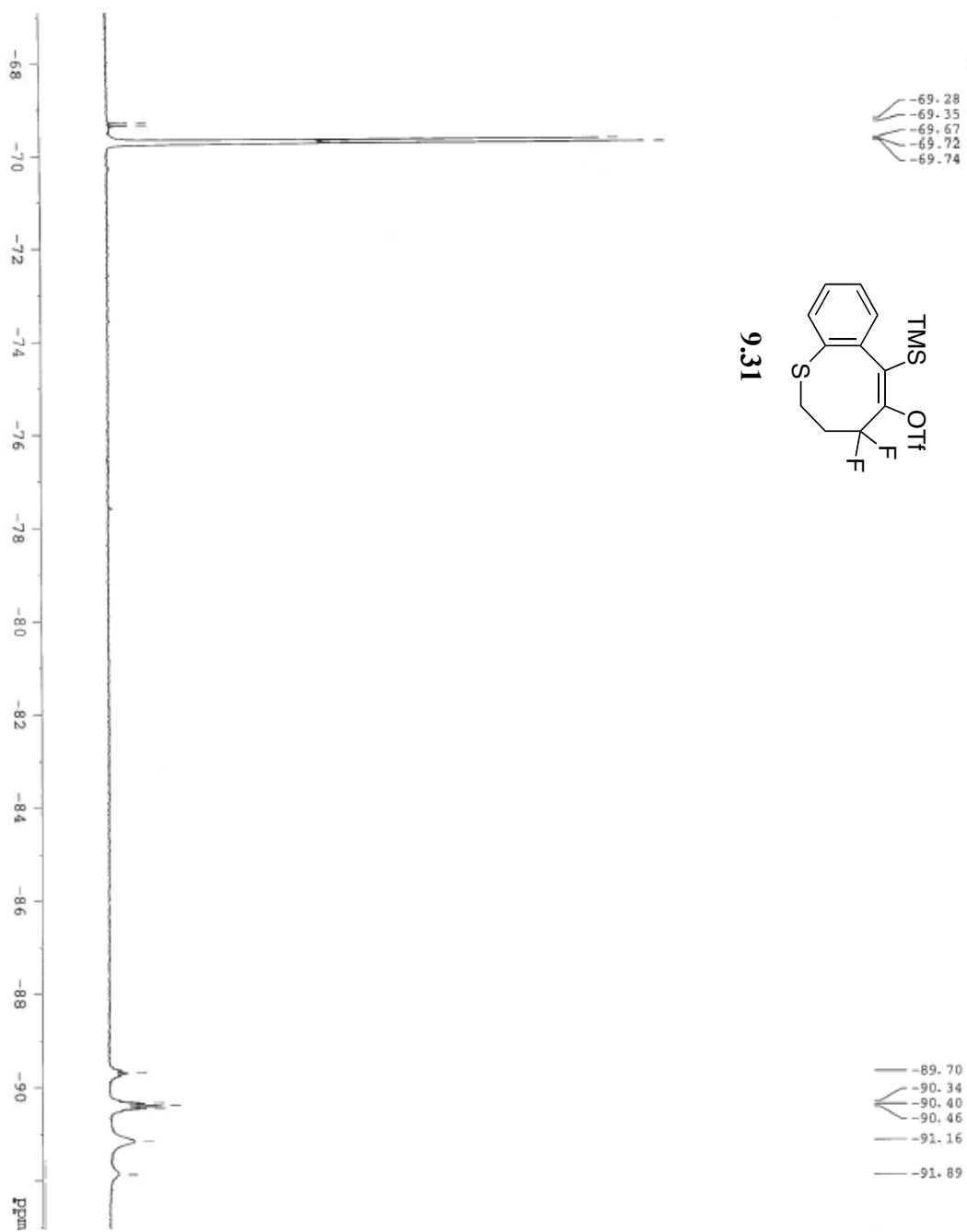
109.21
109.84

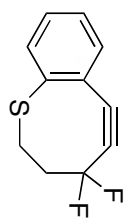




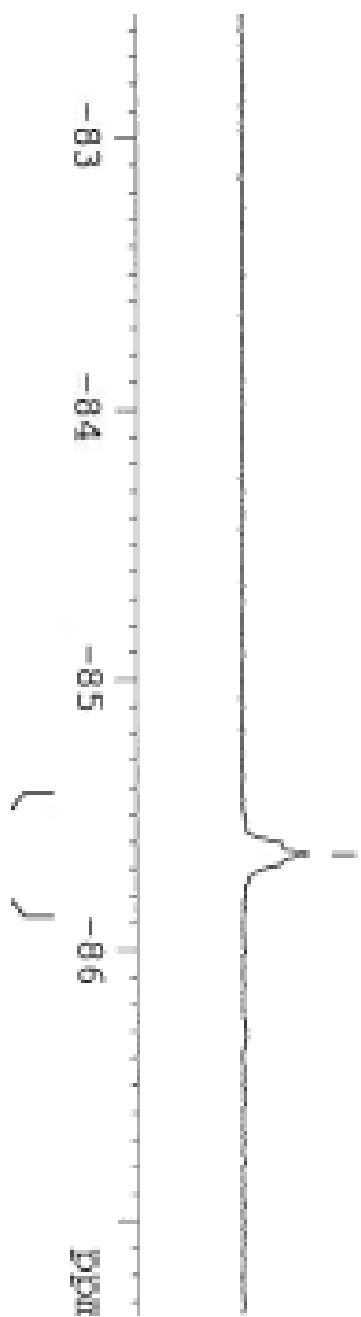
9.29

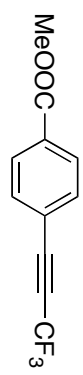




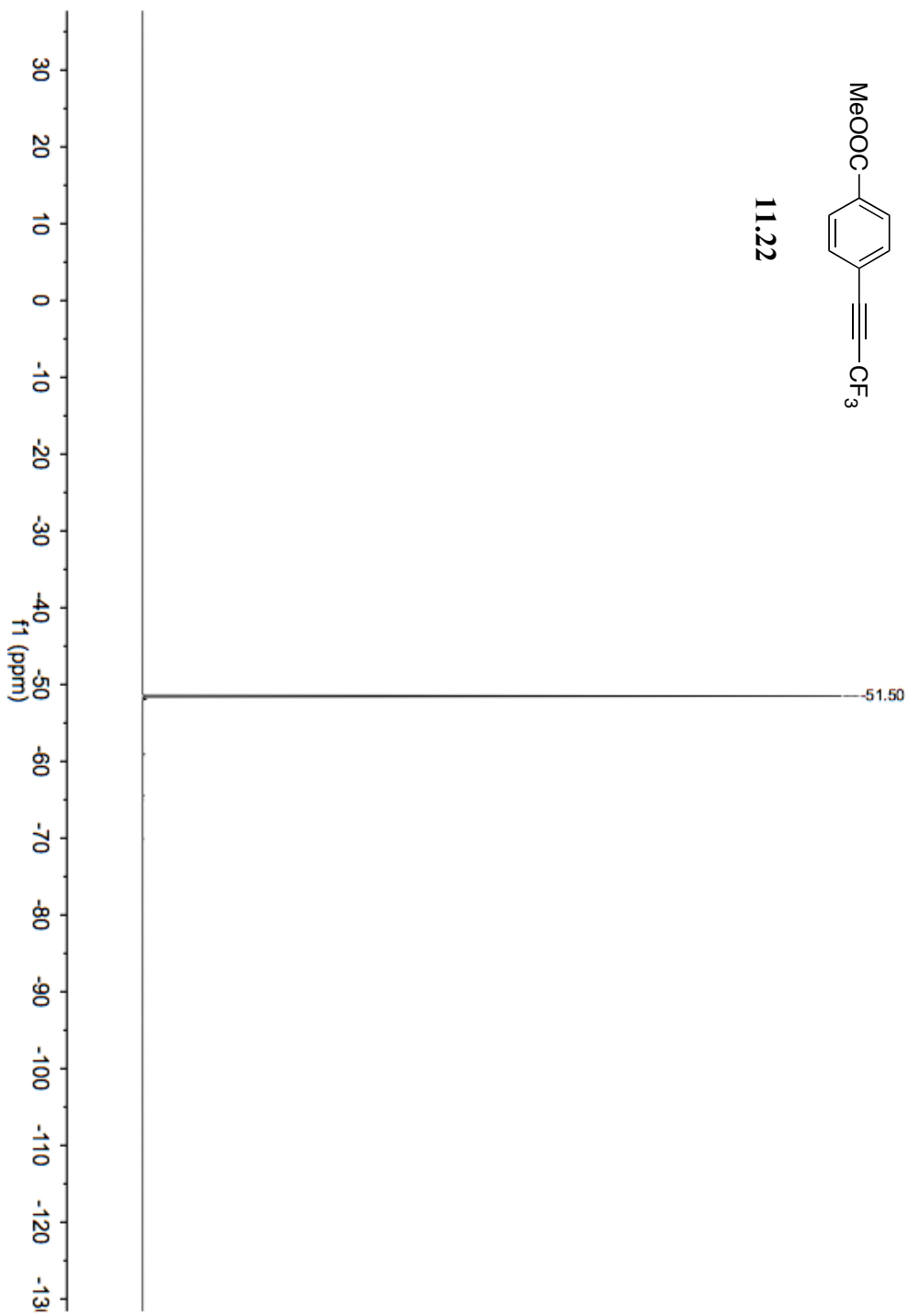


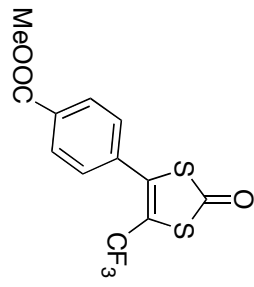
9.32



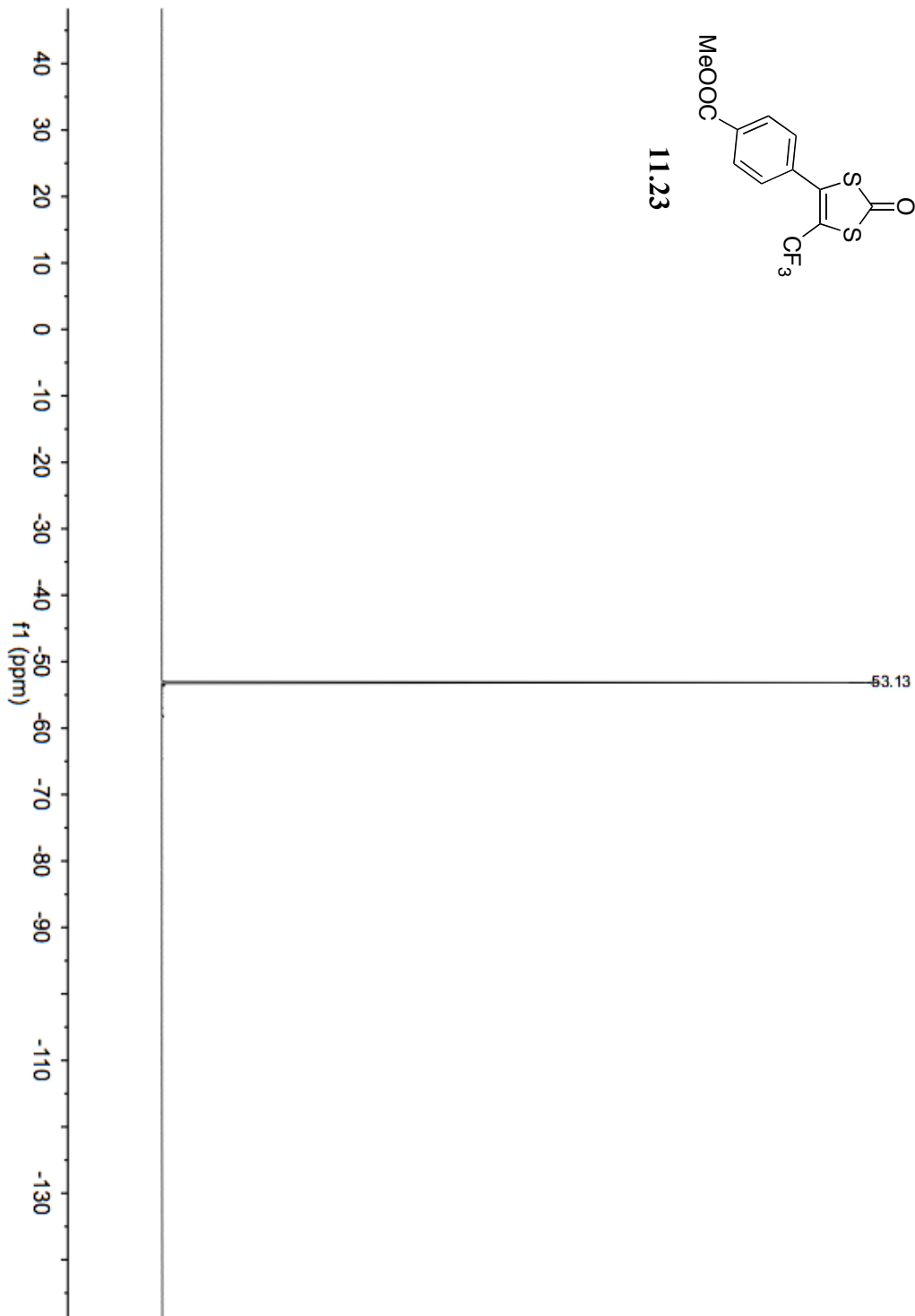


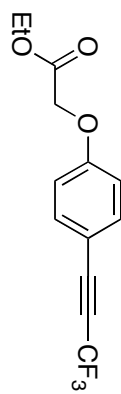
11.22



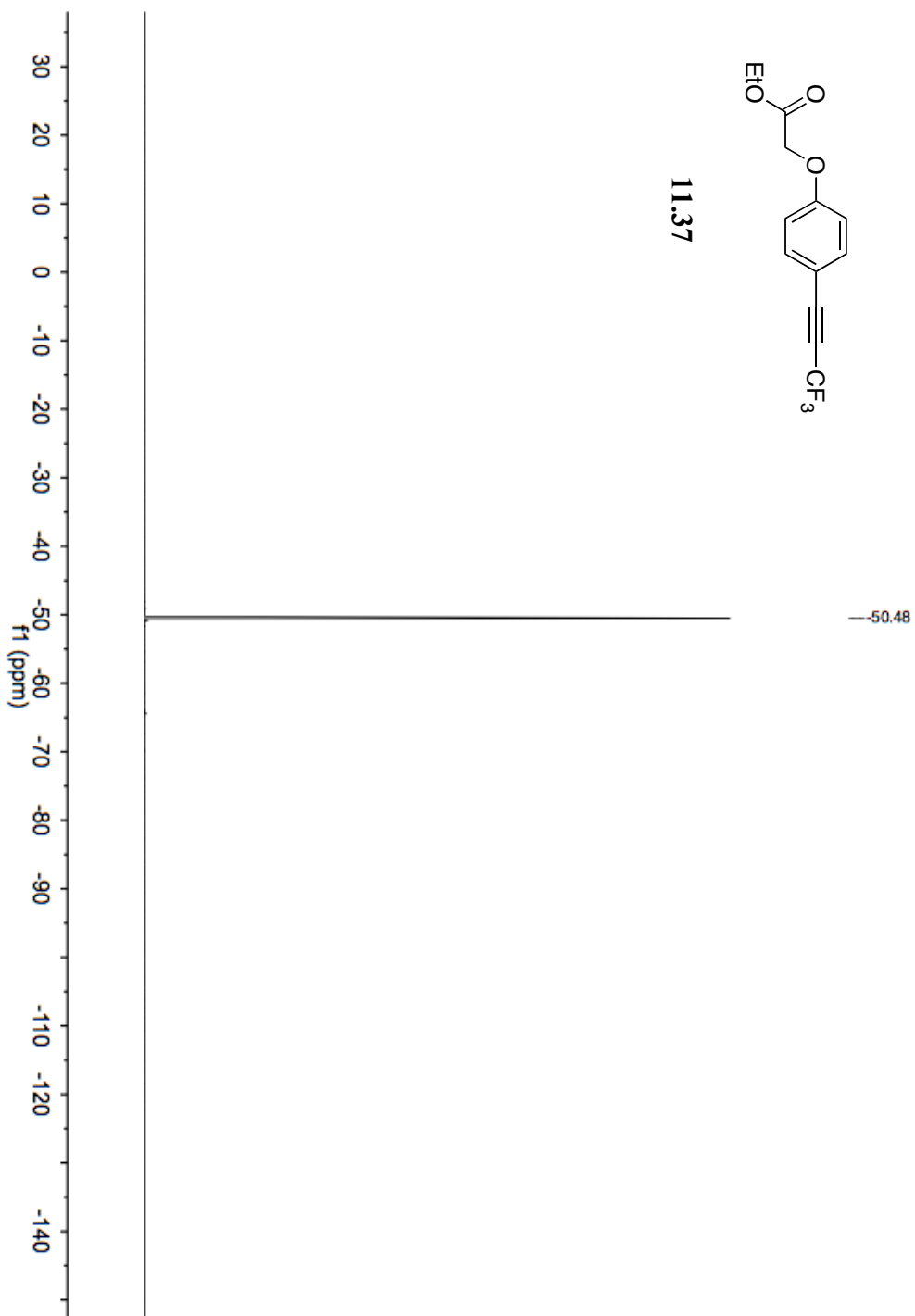


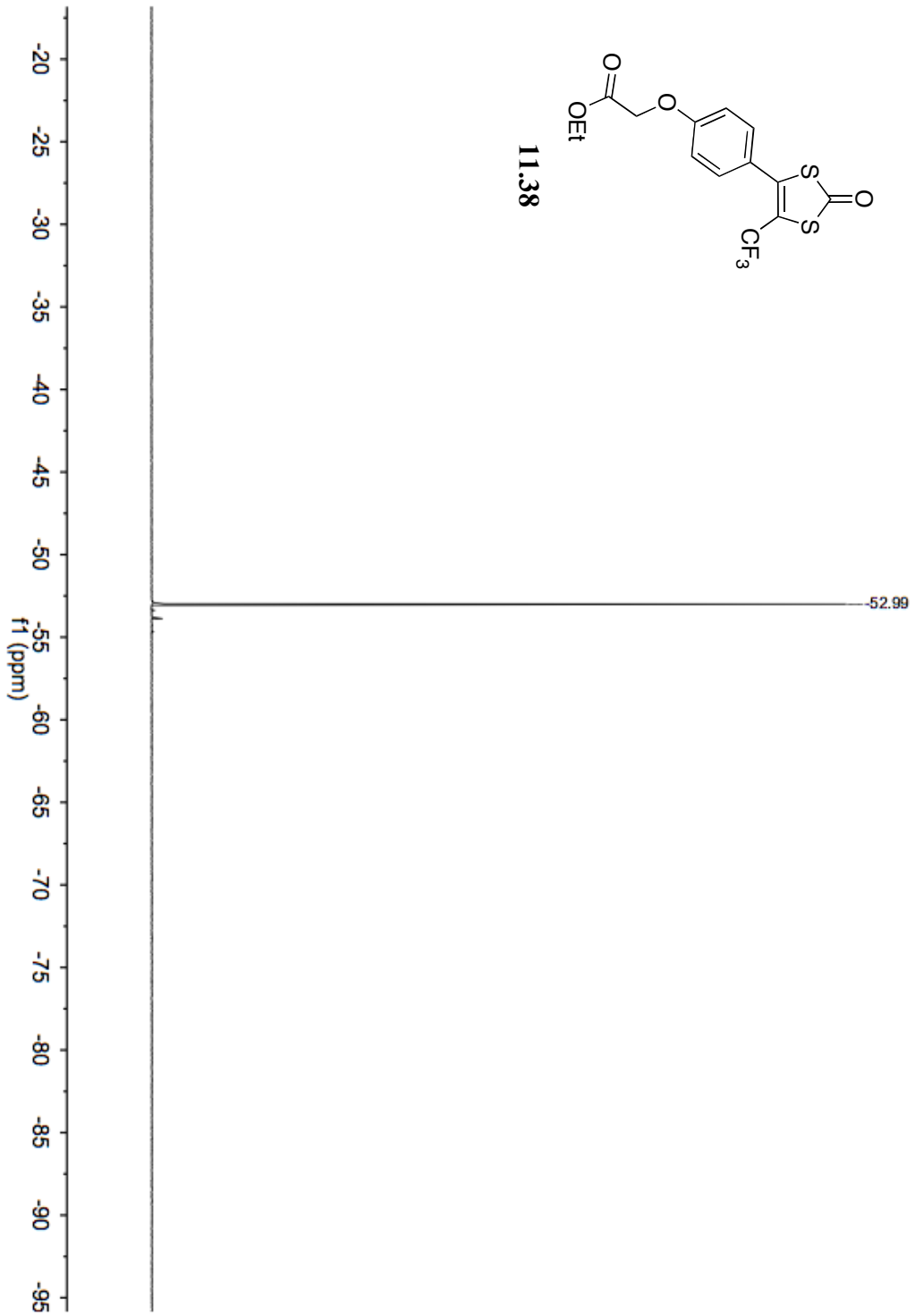
11.23





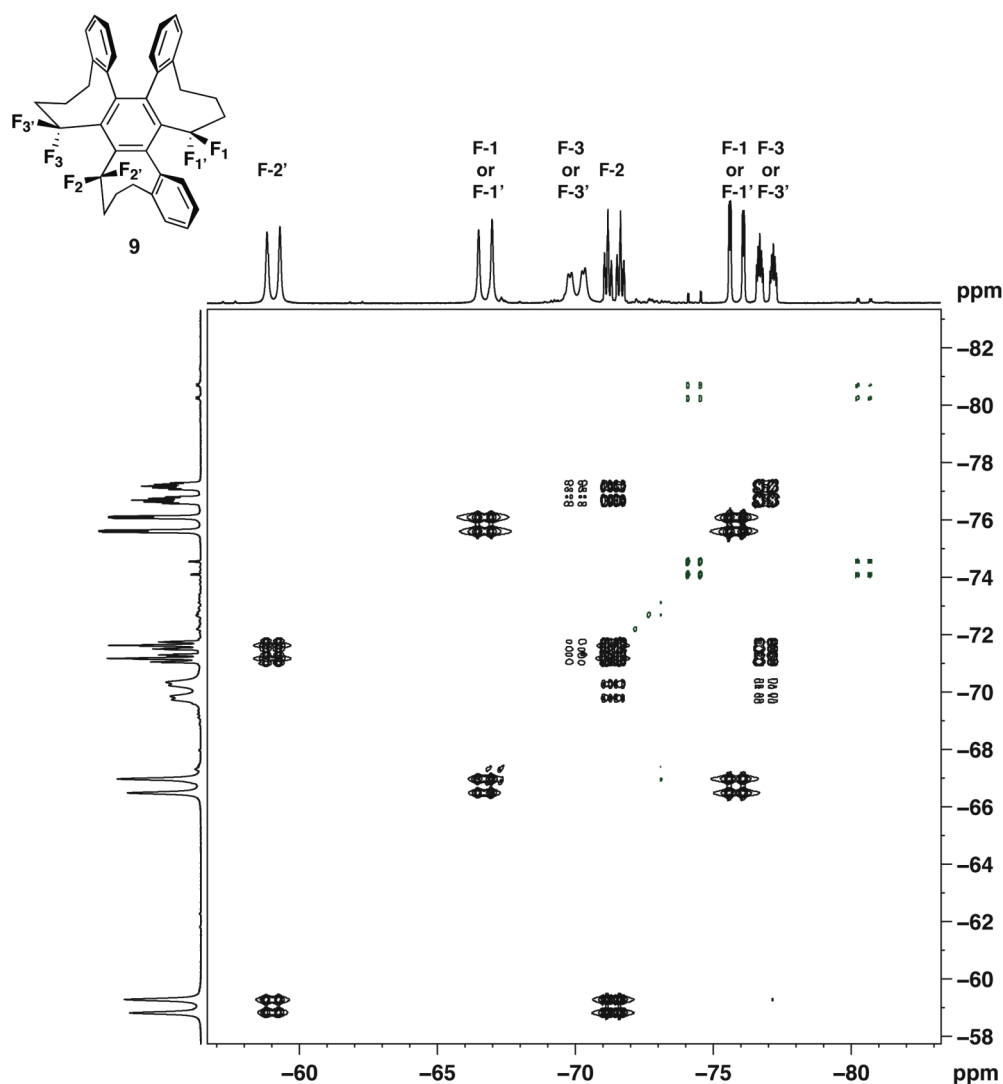
11.37





Appendix D

**2D NMR Spectra
HPLC Traces
UV/Vis/NIR Spectra**

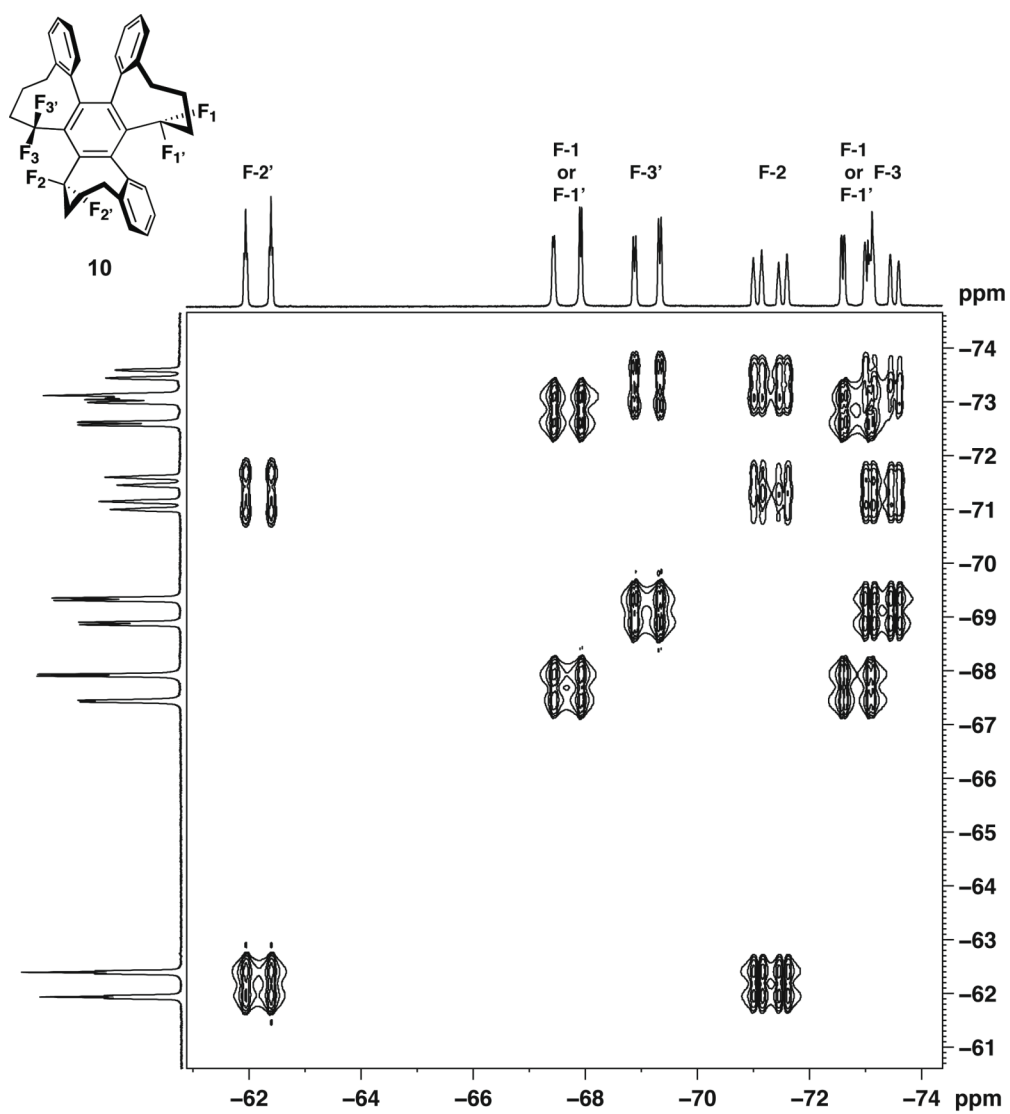


^{19}F - ^{19}F COSY spectrum of trimer **8.8**. COSY spectra demonstrate spatial interactions of ^{19}F because fluorine atoms exhibit significant through space coupling.^{1,2} The ^{19}F - ^{19}F NOESY spectrum of trimer **9** contains the same cross peaks observed in the COSY with decreased signal-to-noise.³ The green peaks represent an impurity.

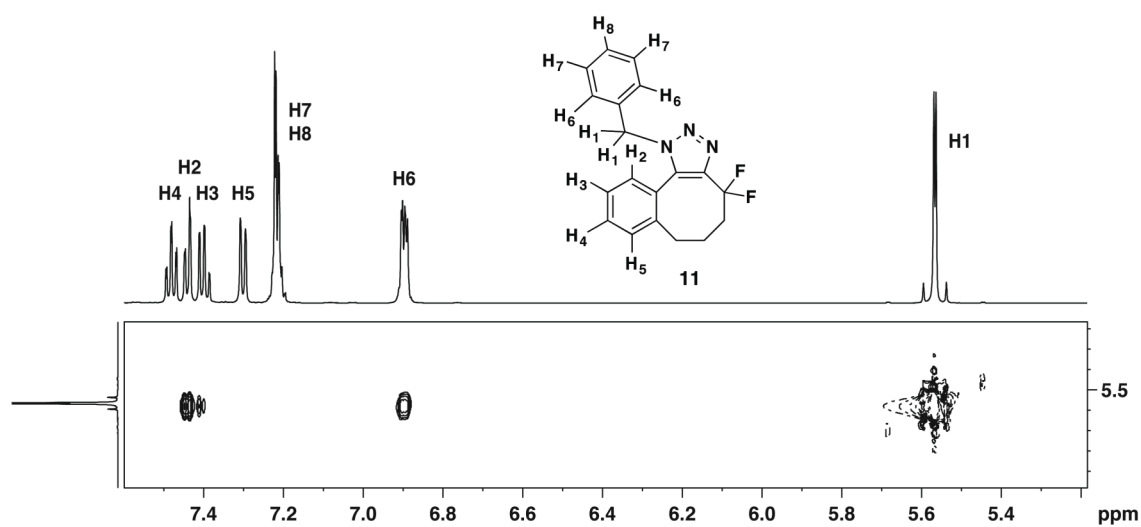
¹ Ng, S.; Sederholm, C.H. *J. Chem. Phys.* **1964**, *40*, 2090.

² ^{19}F - ^{19}F COSY spectra are known to exhibit ^4J coupling as opposed to the ^3J coupling traditionally observed in ^1H - ^1H COSY experiment due to the large through space coupling for fluorine atoms. See Buchanan, G.W.; Munteanu, E.; Dawson, B.A.; Hodgson, D. *Magn. Res. Chem.* **2005**, *43*, 528.

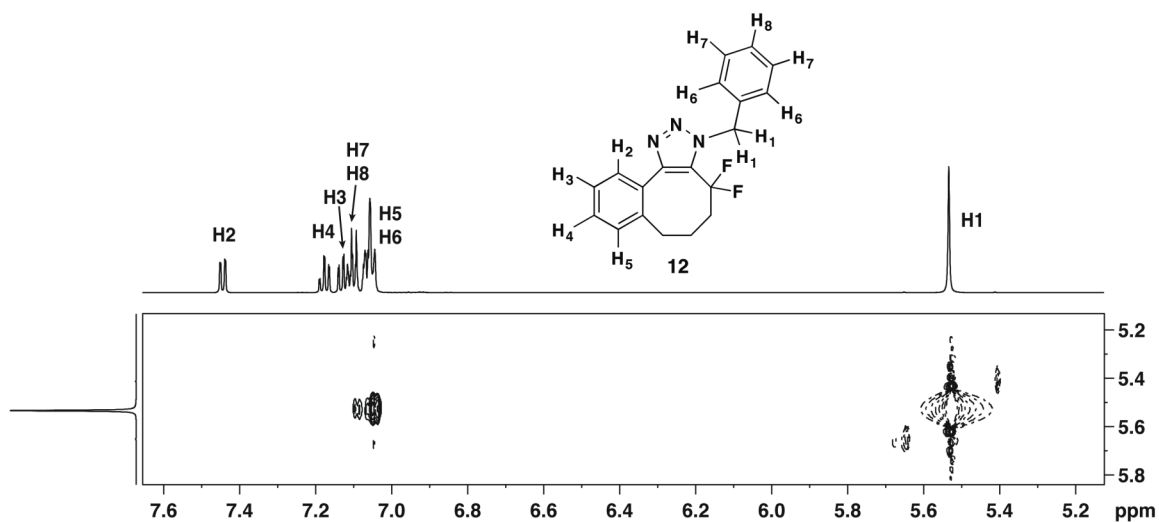
³ Battiste, J.L.; Jing, N.; Newmark, R.A. *J. Fluorine Chem.* **2004**, *125*, 1331.



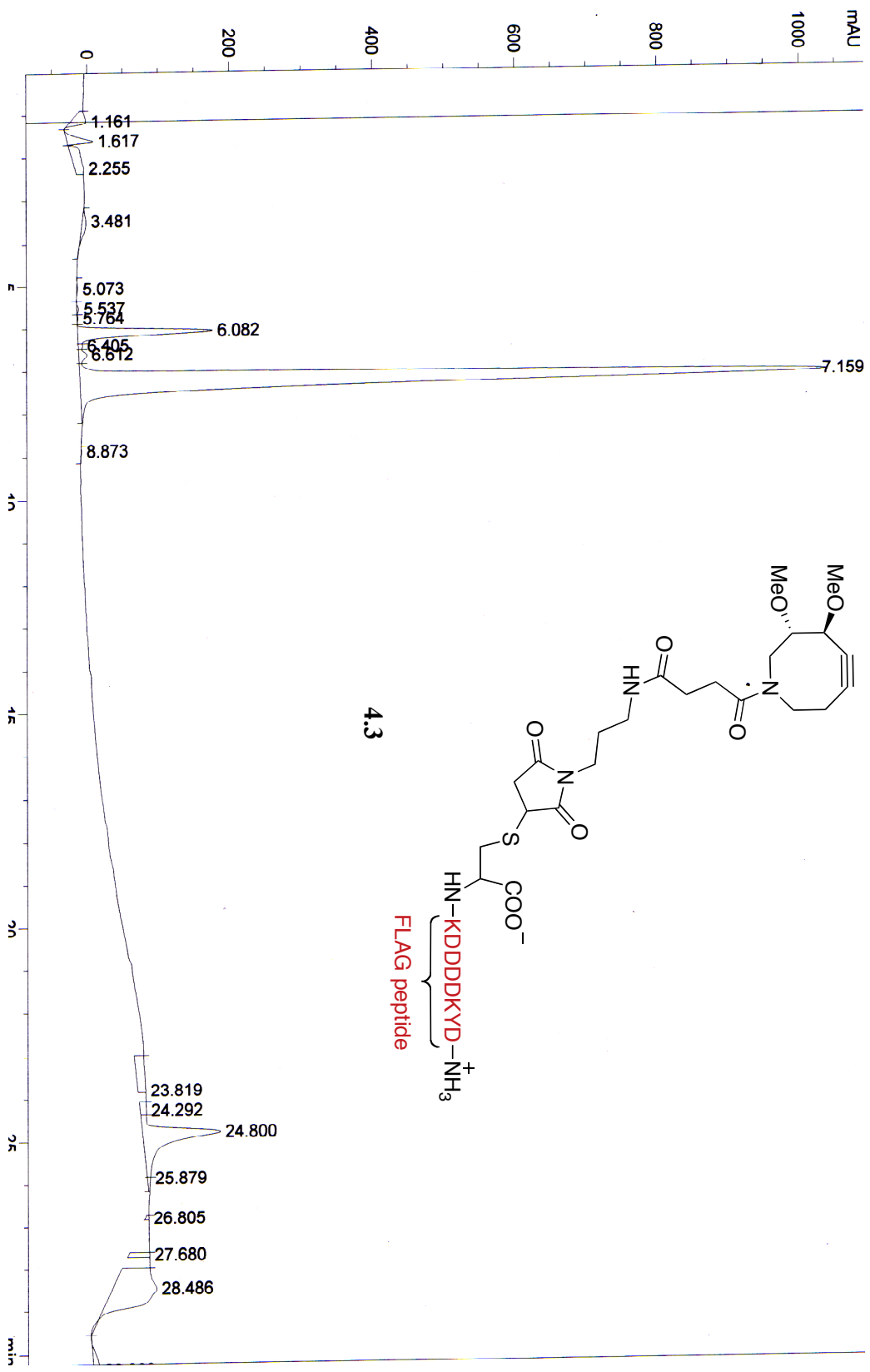
^{19}F - ^{19}F COSY spectrum of trimer **8.9**. COSY spectra demonstrate spatial interactions of ^{19}F because fluorine atoms exhibit significant through space coupling.^{1,2} The ^{19}F - ^{19}F NOESY spectrum of trimer **10** contains the same cross peaks observed in the COSY with decreased signal-to-noise.³

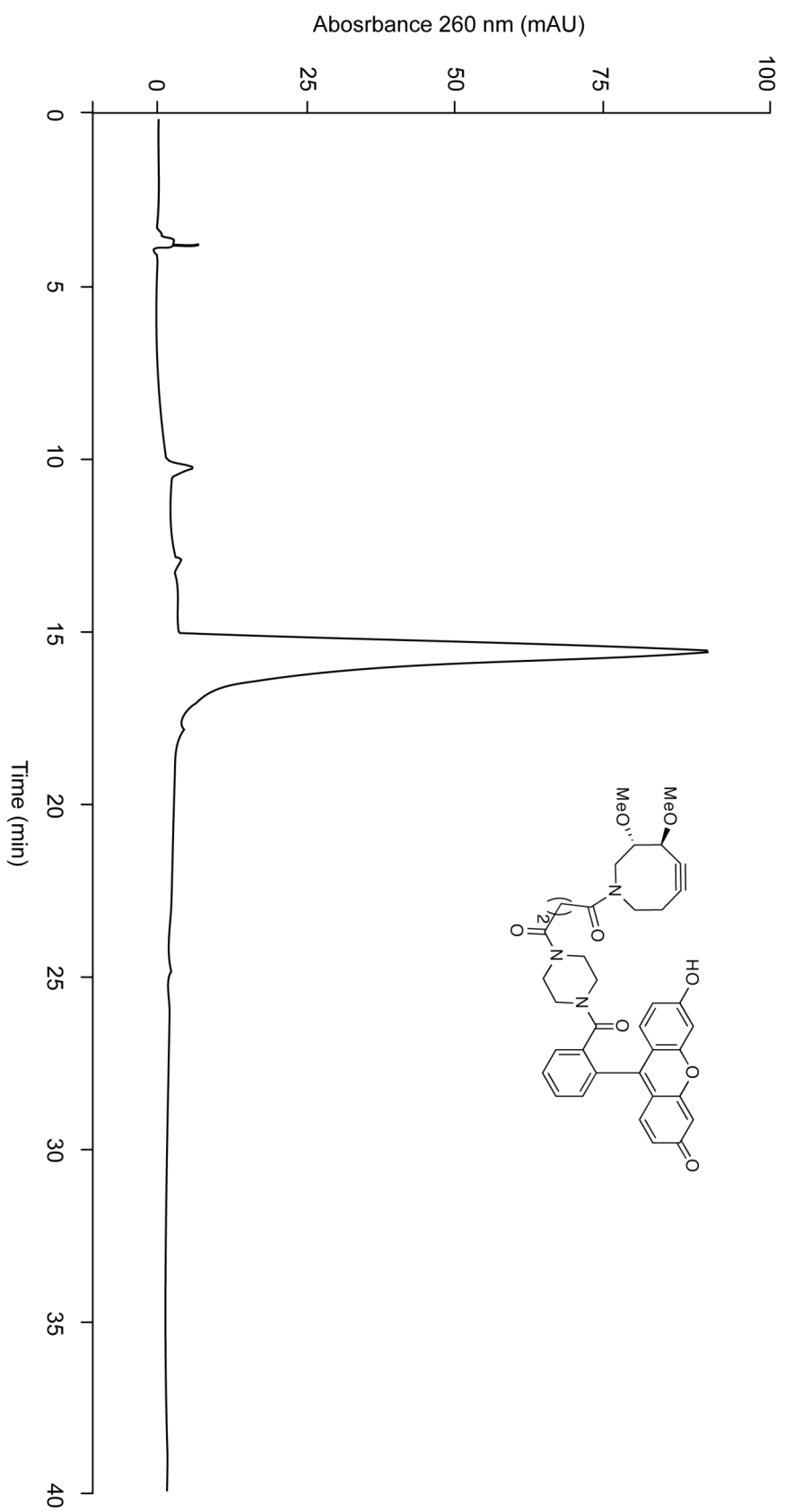


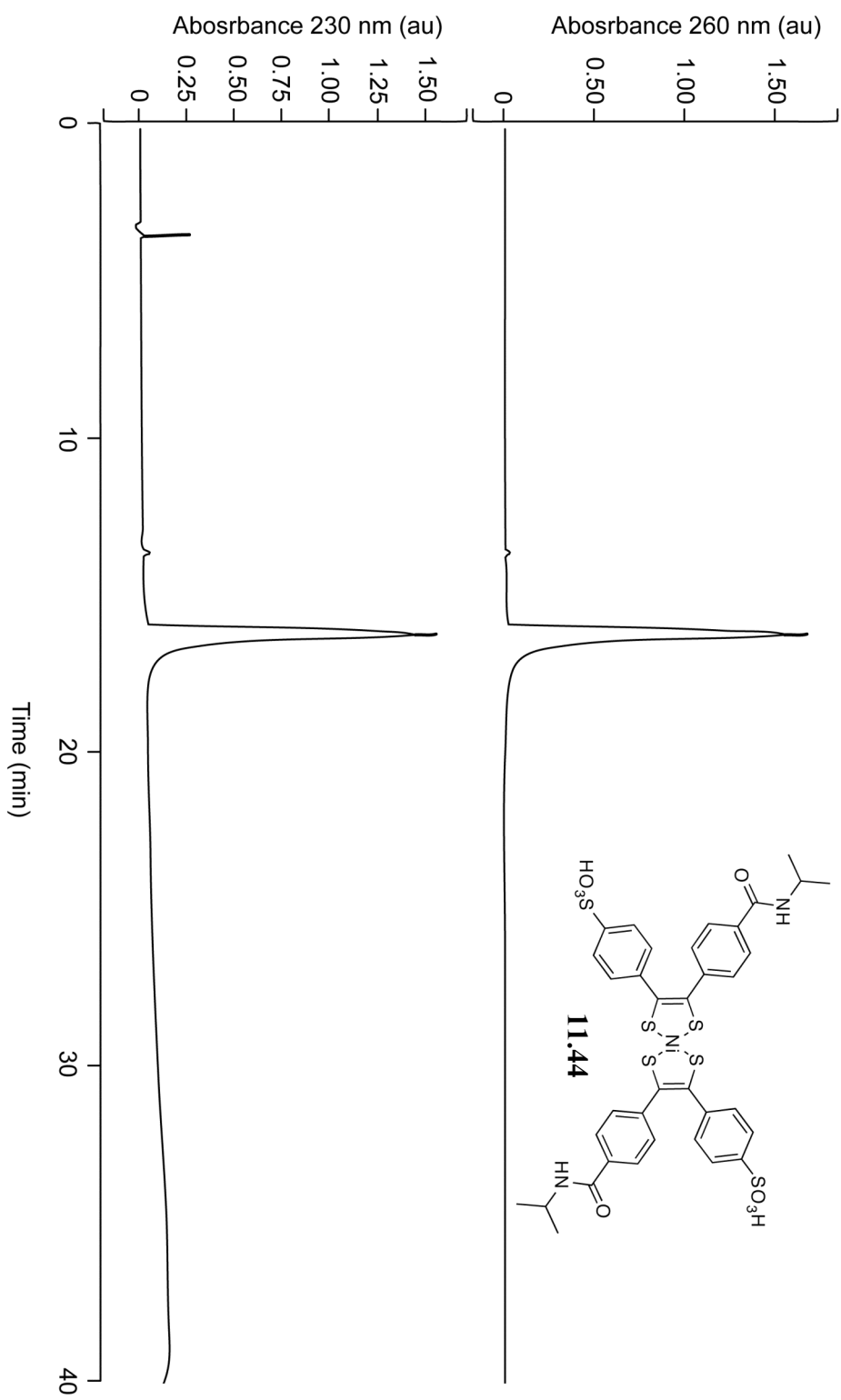
Portion of a ^1H - ^1H NOESY spectrum of triazole **8.11** depicting the interactions between benzylic protons H1 and other aryl protons within compound **8.11**.

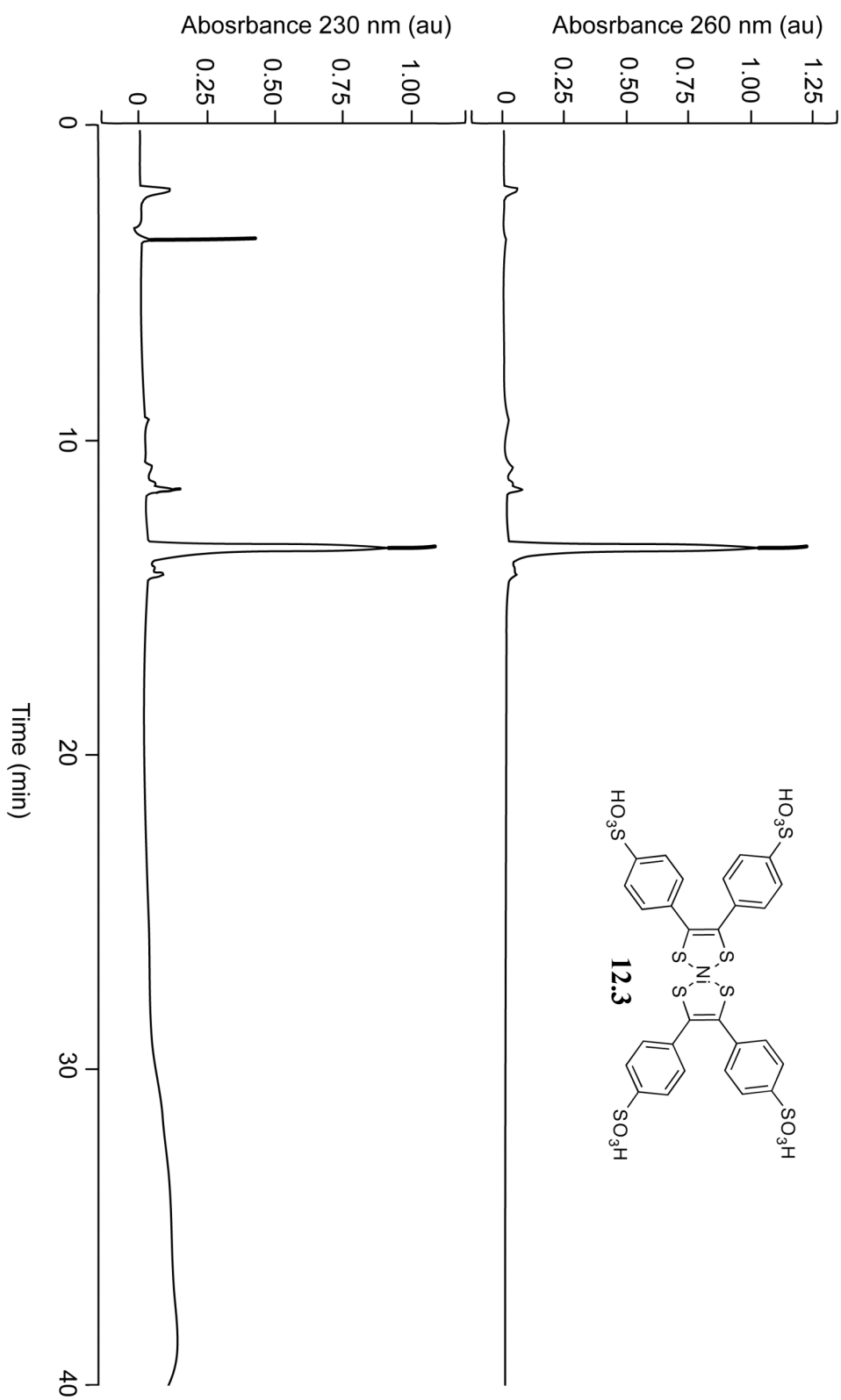


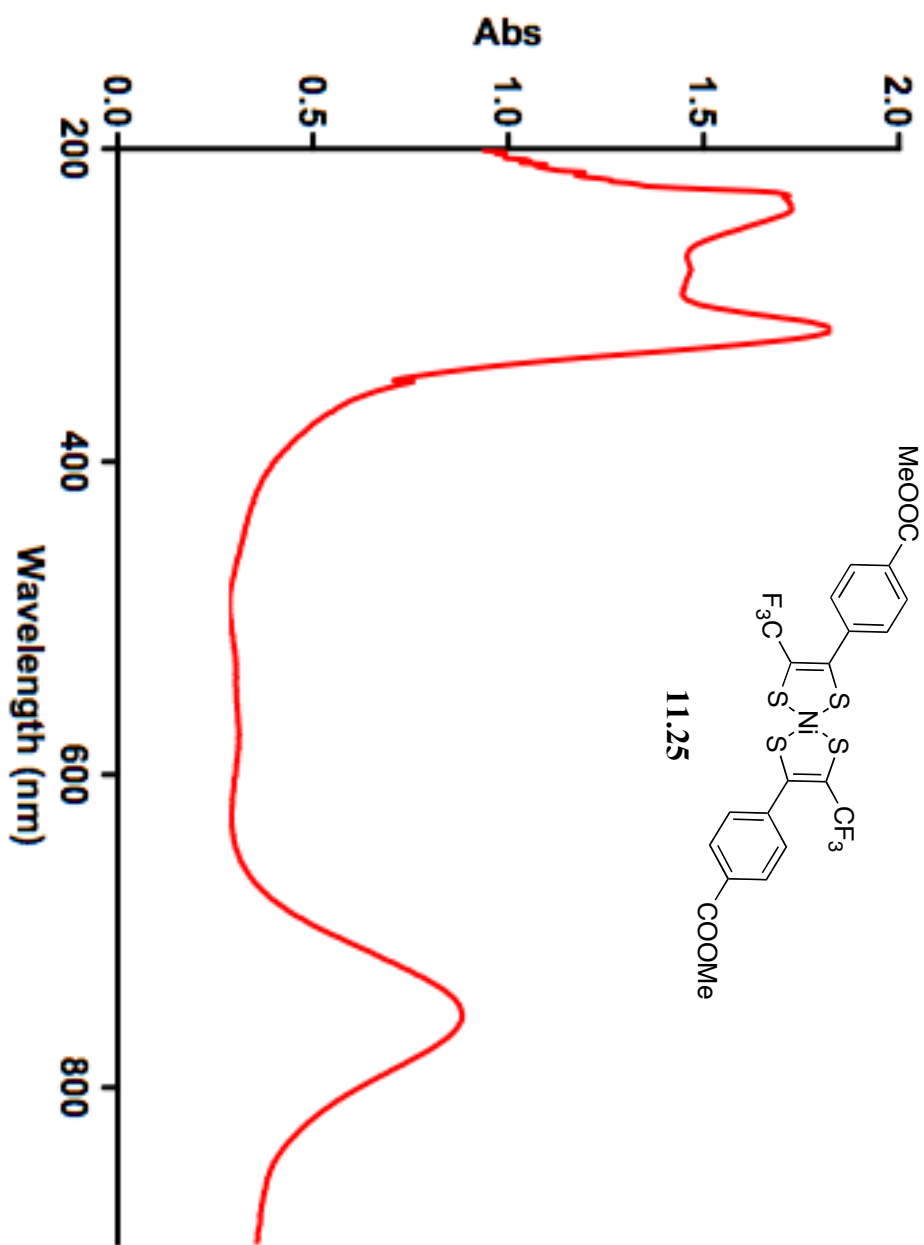
Portion of a ^1H - ^1H NOESY spectrum of triazole **8.12** depicting the interactions between benzylic protons H1 and other aryl protons within compound **8.12**.

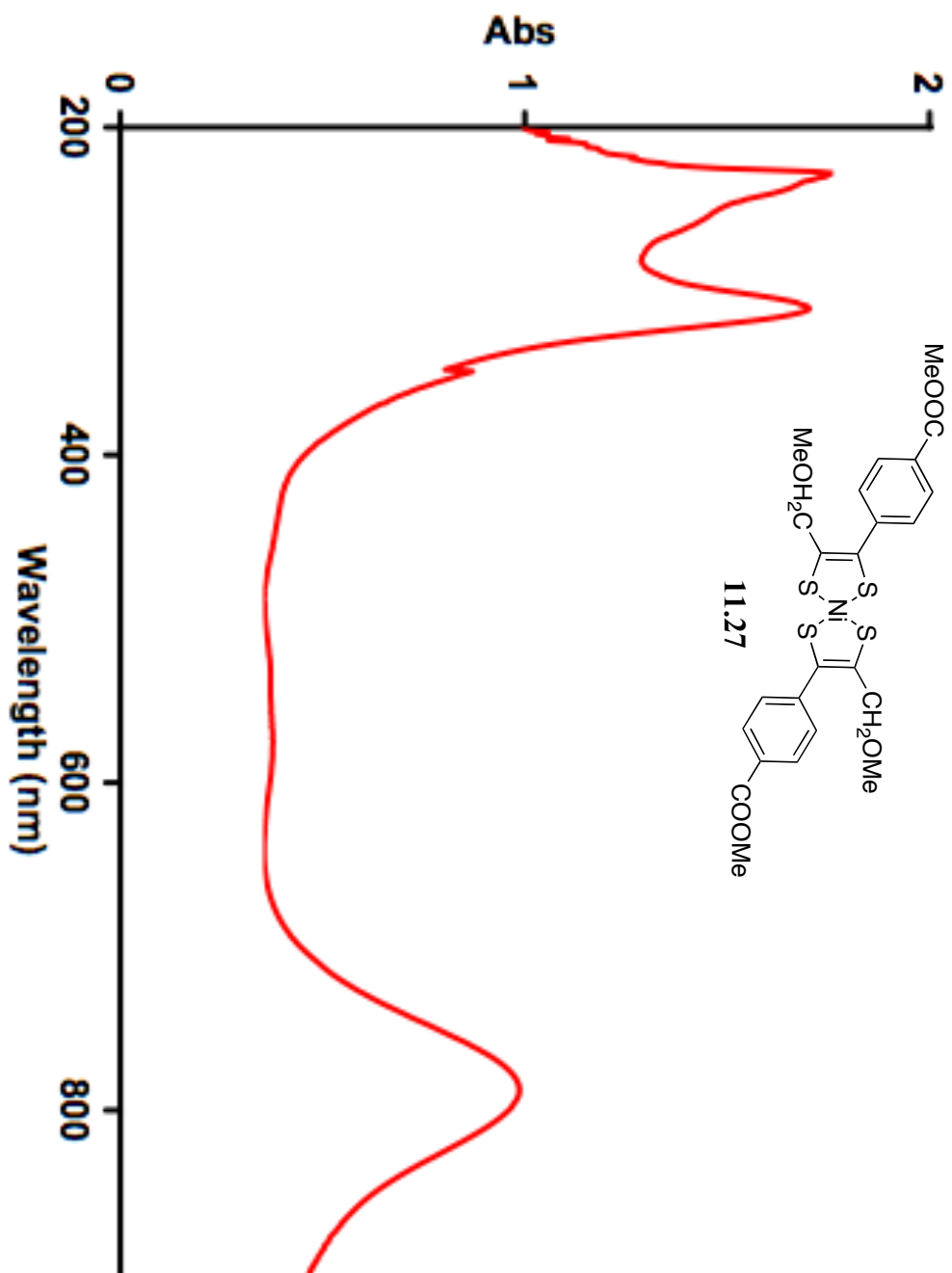


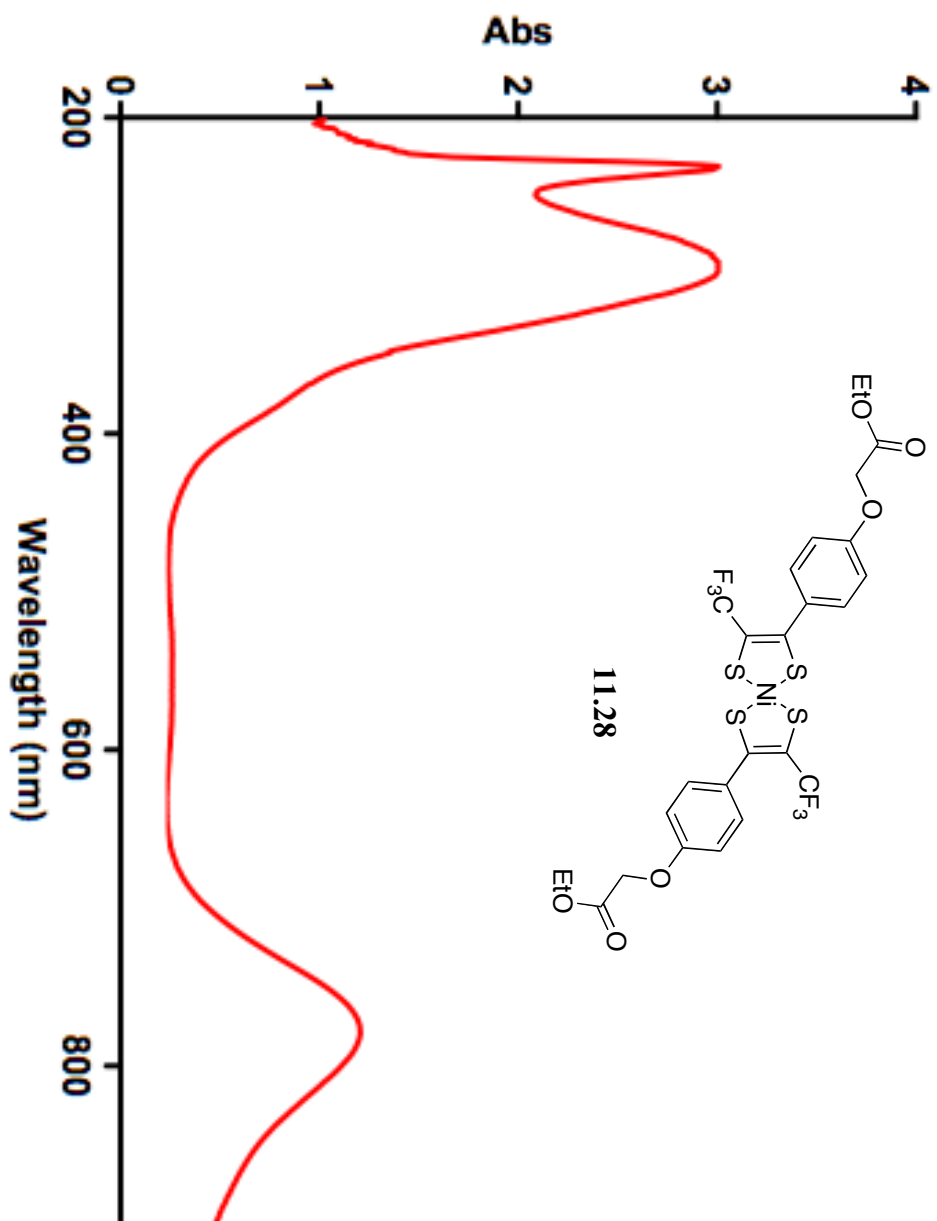


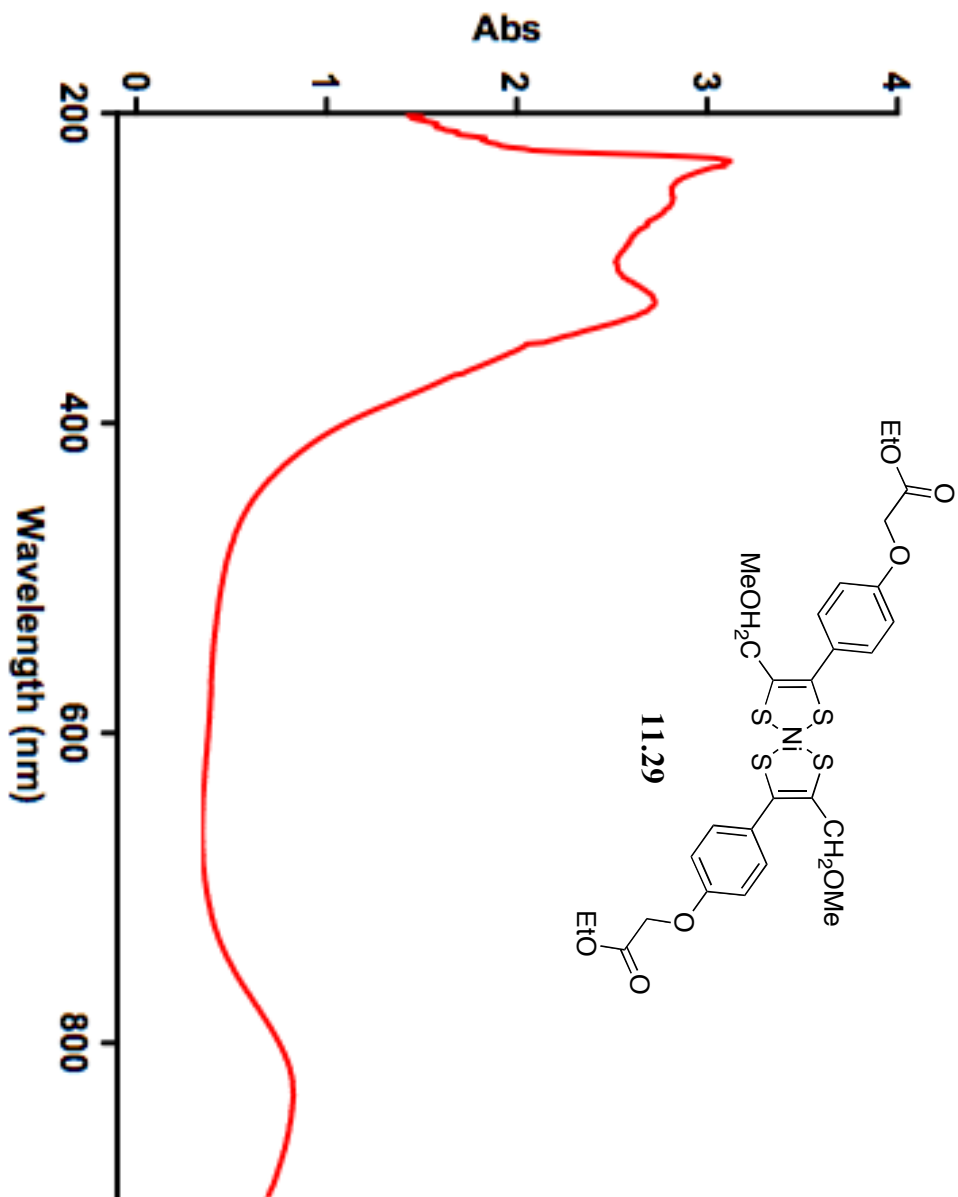


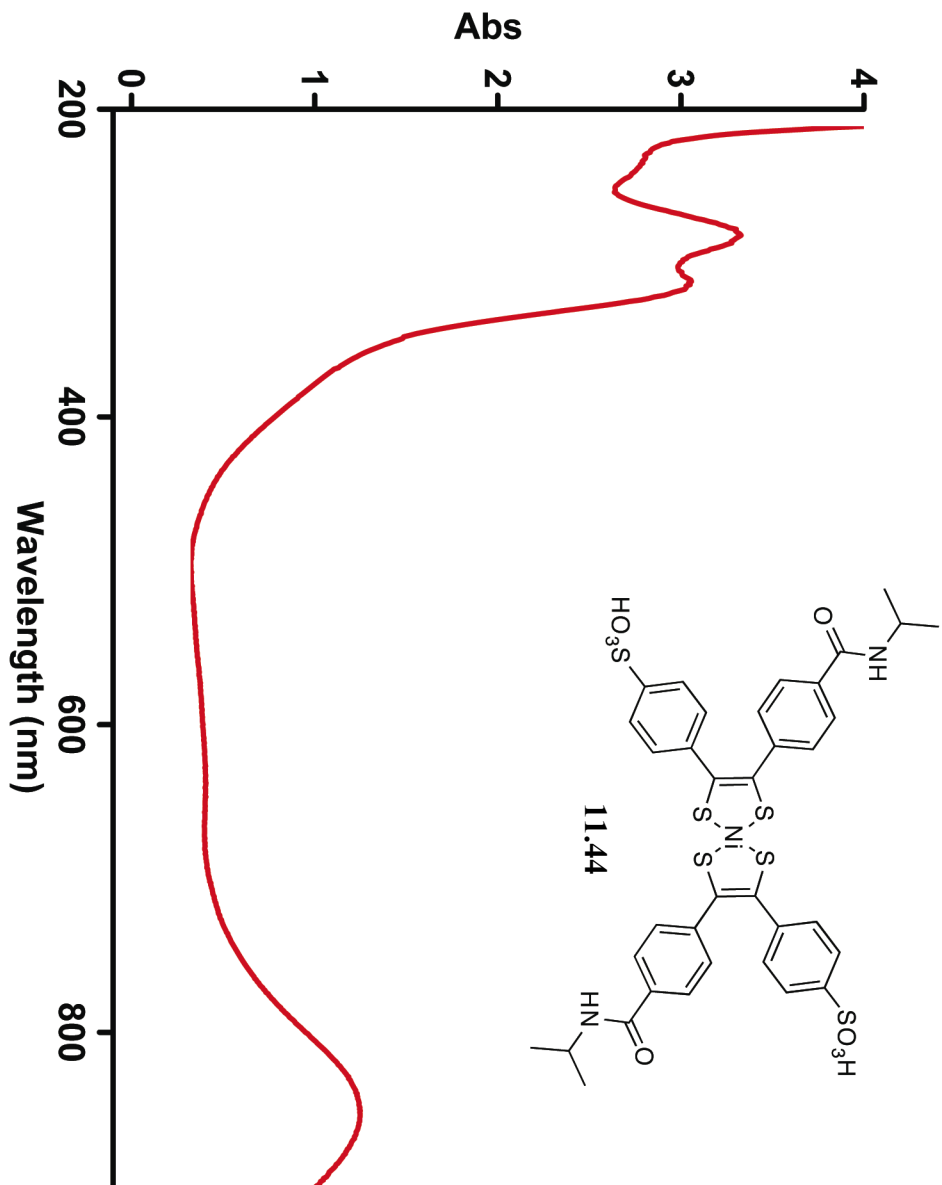


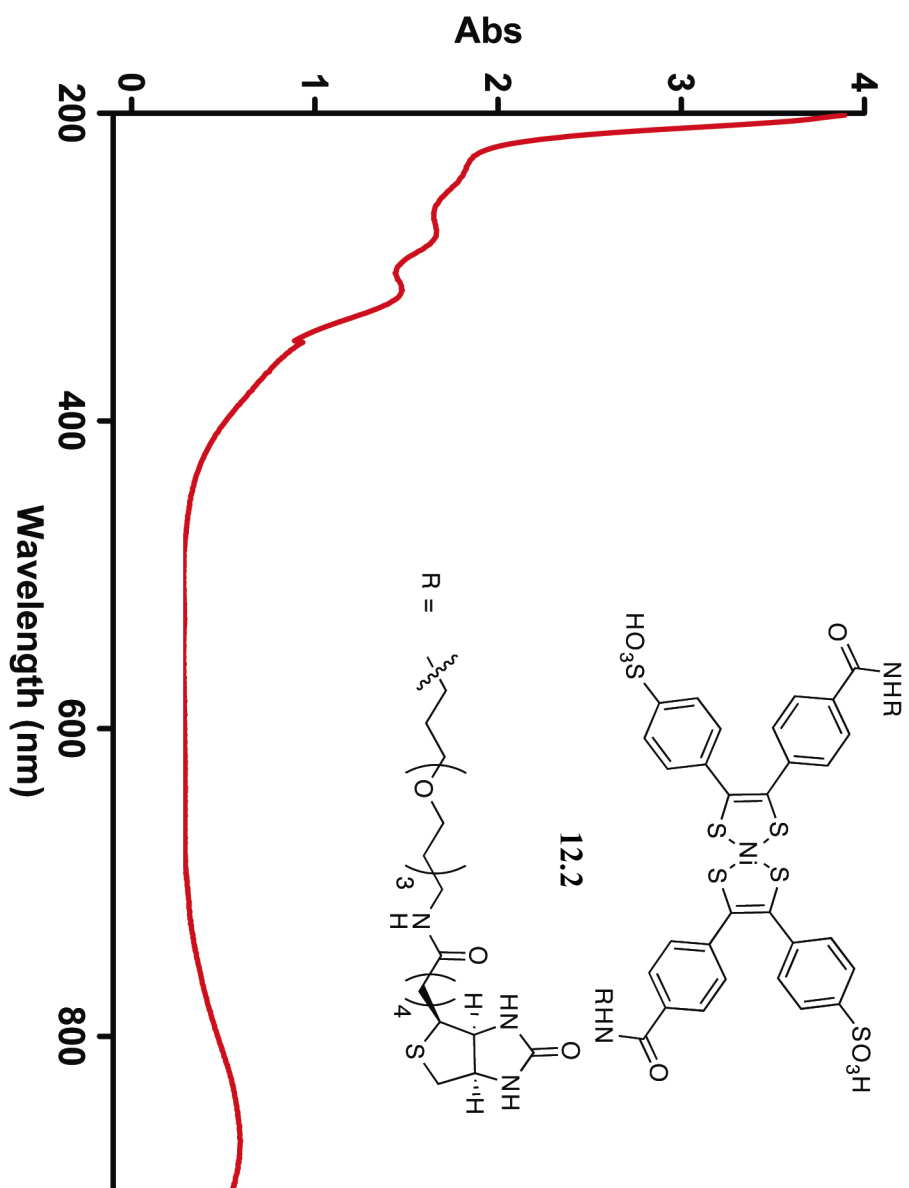


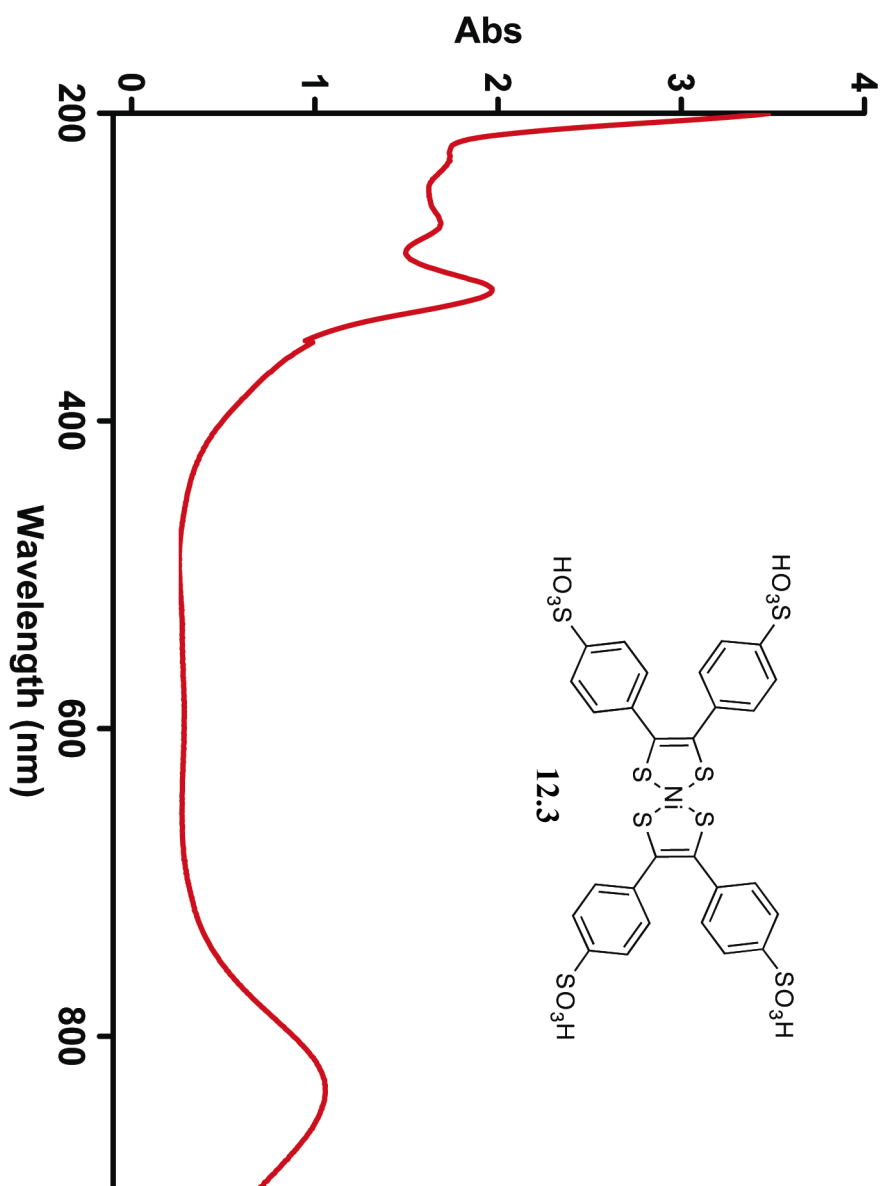












Appendix E

X-Ray Crystal Structure Data

Crystal data and structure refinement for DIMAC 3.35

Empirical formula	C13 H19 N O5	
Formula weight	269.29	
Temperature	150(2) K	
Wavelength	1.54178 Å	
Crystal system	Monoclinic	
Space group	P2(1)	
Unit cell dimensions	a = 5.5553(2) Å	a = 90°.
	b = 8.3543(3) Å	b = 95.758(2)°.
	c = 14.6808(4) Å	g = 90°.
Volume	677.91(4) Å ³	
Z	2	
Density (calculated)	1.319 Mg/m ³	
Absorption coefficient	0.848 mm ⁻¹	
F(000)	288	
Crystal size	0.12 x 0.08 x 0.04 mm ³	
Crystal color/habit	colorless prism	
Theta range for data collection	3.03 to 68.08°.	
Index ranges	-6<=h<=6, -9<=k<=9, -17<=l<=17	
Reflections collected	16229	
Independent reflections	2383 [R(int) = 0.0357]	
Completeness to theta = 67.00°	99.8 %	
Absorption correction	Semi-empirical from equivalents	
Max. and min. transmission	0.9669 and 0.9051	
Refinement method	Full-matrix least-squares on F ²	
Data / restraints / parameters	2383 / 1 / 175	
Goodness-of-fit on F ²	1.035	
Final R indices [I>2sigma(I)]	R1 = 0.0317, wR2 = 0.0828	
R indices (all data)	R1 = 0.0331, wR2 = 0.0841	
Absolute structure parameter	-0.02(16)	
Largest diff. peak and hole	0.168 and -0.122 e.Å ⁻³	

Atomic coordinates ($\times 10^4$) and equivalent isotropic displacement parameters ($\text{\AA}^2 \times 10^3$)

U(eq) is defined as one third of the trace of the orthogonalized U^{ij} tensor

	x	y	z	U(eq)
C(1)	8648(3)	10397(2)	2130(1)	28(1)
C(2)	11048(3)	10453(2)	1683(1)	27(1)
C(3)	11231(3)	9244(2)	906(1)	30(1)
C(4)	10346(3)	7704(2)	1235(1)	33(1)
C(5)	9337(3)	6820(2)	1703(1)	36(1)
C(6)	7987(4)	6339(2)	2468(1)	41(1)
C(7)	6780(3)	7889(2)	2767(1)	32(1)
C(8)	12407(3)	13124(2)	1910(1)	37(1)
C(9)	14068(4)	8197(3)	-29(1)	51(1)
C(10)	9797(3)	9560(2)	3690(1)	26(1)
C(11)	9370(3)	8545(2)	4517(1)	31(1)
C(12)	11367(3)	8691(2)	5307(1)	30(1)
C(13)	13372(3)	7505(2)	5253(1)	30(1)
N(1)	8505(2)	9242(2)	2887(1)	26(1)
O(1)	11274(2)	11993(1)	1290(1)	33(1)
O(2)	13677(2)	9206(2)	723(1)	35(1)
O(3)	11183(2)	10721(1)	3768(1)	32(1)
O(4)	13679(2)	6707(2)	4590(1)	41(1)
O(5)	14783(2)	7433(2)	6035(1)	42(1)

Bond lengths [Å] and angles [°]

C(1)-N(1)	1.4801(19)	C(8)-H(8A)	0.9800
C(1)-C(2)	1.545(2)	C(8)-H(8B)	0.9800
C(1)-H(1A)	0.9900	C(8)-H(8C)	0.9800
C(1)-H(1B)	0.9900	C(9)-O(2)	1.422(2)
C(2)-O(1)	1.4211(19)	C(9)-H(9A)	0.9800
C(2)-C(3)	1.535(2)	C(9)-H(9B)	0.9800
C(2)-H(2)	1.0000	C(9)-H(9C)	0.9800
C(3)-O(2)	1.4118(19)	C(10)-O(3)	1.237(2)
C(3)-C(4)	1.476(2)	C(10)-N(1)	1.343(2)
C(3)-H(3)	1.0000	C(10)-C(11)	1.519(2)
C(4)-C(5)	1.187(2)	C(11)-C(12)	1.528(2)
C(5)-C(6)	1.468(3)	C(11)-H(11A)	0.9900
C(6)-C(7)	1.542(2)	C(11)-H(11B)	0.9900
C(6)-H(6A)	0.9900	C(12)-C(13)	1.499(2)
C(6)-H(6B)	0.9900	C(12)-H(12A)	0.9900
C(7)-N(1)	1.4805(19)	C(12)-H(12B)	0.9900
C(7)-H(7A)	0.9900	C(13)-O(4)	1.207(2)
C(7)-H(7B)	0.9900	C(13)-O(5)	1.3239(19)
C(8)-O(1)	1.415(2)	O(5)-H(5)	0.8400
N(1)-C(1)-C(2)	116.90(12)	C(7)-C(6)-H(6A)	110.8
N(1)-C(1)-H(1A)	108.1	C(5)-C(6)-H(6B)	110.8
C(2)-C(1)-H(1A)	108.1	C(7)-C(6)-H(6B)	110.8
N(1)-C(1)-H(1B)	108.1	H(6A)-C(6)-H(6B)	108.8
C(2)-C(1)-H(1B)	108.1	N(1)-C(7)-C(6)	112.36(13)
H(1A)-C(1)-H(1B)	107.3	N(1)-C(7)-H(7A)	109.1
O(1)-C(2)-C(3)	106.16(12)	C(6)-C(7)-H(7A)	109.1
O(1)-C(2)-C(1)	108.39(12)	N(1)-C(7)-H(7B)	109.1
C(3)-C(2)-C(1)	114.87(13)	C(6)-C(7)-H(7B)	109.1
O(1)-C(2)-H(2)	109.1	H(7A)-C(7)-H(7B)	107.9
C(3)-C(2)-H(2)	109.1	O(1)-C(8)-H(8A)	109.5
C(1)-C(2)-H(2)	109.1	O(1)-C(8)-H(8B)	109.5
O(2)-C(3)-C(4)	113.68(14)	H(8A)-C(8)-H(8B)	109.5
O(2)-C(3)-C(2)	107.06(12)	O(1)-C(8)-H(8C)	109.5
C(4)-C(3)-C(2)	106.32(13)	H(8A)-C(8)-H(8C)	109.5
O(2)-C(3)-H(3)	109.9	H(8B)-C(8)-H(8C)	109.5
C(4)-C(3)-H(3)	109.9	O(2)-C(9)-H(9A)	109.5
C(2)-C(3)-H(3)	109.9	O(2)-C(9)-H(9B)	109.5
C(5)-C(4)-C(3)	157.53(16)	H(9A)-C(9)-H(9B)	109.5
C(4)-C(5)-C(6)	157.00(17)	O(2)-C(9)-H(9C)	109.5
C(5)-C(6)-C(7)	104.94(14)	H(9A)-C(9)-H(9C)	109.5
C(5)-C(6)-H(6A)	110.8	H(9B)-C(9)-H(9C)	109.5

O(3)-C(10)-N(1)	120.69(14)
O(3)-C(10)-C(11)	120.58(13)
N(1)-C(10)-C(11)	118.56(13)
C(10)-C(11)-C(12)	113.78(13)
C(10)-C(11)-H(11A)	108.8
C(12)-C(11)-H(11A)	108.8
C(10)-C(11)-H(11B)	108.8
C(12)-C(11)-H(11B)	108.8
H(11A)-C(11)-H(11B)	107.7
C(13)-C(12)-C(11)	113.20(13)
C(13)-C(12)-H(12A)	108.9
C(11)-C(12)-H(12A)	108.9
C(13)-C(12)-H(12B)	108.9
C(11)-C(12)-H(12B)	108.9
H(12A)-C(12)-H(12B)	107.8
O(4)-C(13)-O(5)	123.71(16)
O(4)-C(13)-C(12)	125.02(14)
O(5)-C(13)-C(12)	111.27(13)
C(10)-N(1)-C(1)	117.72(13)
C(10)-N(1)-C(7)	122.58(13)
C(1)-N(1)-C(7)	119.40(13)
C(8)-O(1)-C(2)	113.24(11)
C(3)-O(2)-C(9)	112.69(13)
C(13)-O(5)-H(5)	109.5

Anisotropic displacement parameters ($\text{\AA}^2 \times 10^3$). The anisotropic displacement factor exponent takes the form: $-2p^2 [h^2 a^* 2U^{11} + \dots + 2 h k a^* b^* U^{12}]$

	U ¹¹	U ²²	U ³³	U ²³	U ¹³	U ¹²
C(1)	25(1)	30(1)	30(1)	3(1)	0(1)	4(1)
C(2)	23(1)	30(1)	28(1)	4(1)	0(1)	0(1)
C(3)	24(1)	38(1)	28(1)	1(1)	1(1)	0(1)
C(4)	33(1)	34(1)	32(1)	-6(1)	2(1)	2(1)
C(5)	44(1)	28(1)	36(1)	-5(1)	5(1)	-1(1)
C(6)	54(1)	30(1)	41(1)	-1(1)	7(1)	-12(1)
C(7)	28(1)	36(1)	32(1)	0(1)	0(1)	-7(1)
C(8)	42(1)	29(1)	41(1)	1(1)	7(1)	-1(1)
C(9)	34(1)	82(2)	38(1)	-21(1)	7(1)	-2(1)
C(10)	23(1)	25(1)	32(1)	-2(1)	3(1)	3(1)
C(11)	30(1)	32(1)	32(1)	2(1)	1(1)	-1(1)
C(12)	32(1)	29(1)	27(1)	1(1)	2(1)	1(1)
C(13)	29(1)	31(1)	30(1)	3(1)	5(1)	-4(1)
N(1)	22(1)	27(1)	28(1)	1(1)	2(1)	0(1)
O(1)	35(1)	31(1)	32(1)	6(1)	1(1)	-3(1)
O(2)	25(1)	50(1)	31(1)	-8(1)	3(1)	-2(1)
O(3)	32(1)	31(1)	33(1)	0(1)	0(1)	-6(1)
O(4)	40(1)	46(1)	37(1)	-7(1)	7(1)	4(1)
O(5)	38(1)	51(1)	36(1)	-1(1)	-3(1)	14(1)

Hydrogen coordinates (x 10⁴) and isotropic displacement parameters (Å²x 10³).

	x	y	z	U(eq)
H(1A)	8333	11480	2365	34
H(1B)	7328	10149	1647	34
H(2)	12426	10278	2166	33
H(3)	10188	9596	347	36
H(6A)	9091	5894	2977	50
H(6B)	6753	5523	2269	50
H(7A)	5440	8181	2301	39
H(7B)	6081	7694	3351	39
H(8A)	11491	13214	2445	56
H(8B)	12453	14168	1609	56
H(8C)	14061	12773	2108	56
H(9A)	13516	7111	93	77
H(9B)	15797	8175	-110	77
H(9C)	13161	8610	-586	77
H(11A)	9229	7410	4325	38
H(11B)	7812	8864	4737	38
H(12A)	12049	9786	5309	36
H(12B)	10652	8536	5892	36
H(5)	15935	6802	5978	63

Crystal data and structure refinement for 5.29

Empirical formula	C ₂₀ H ₂₆ Br N O ₆
Formula weight	456.33
Temperature	100(2) K
Wavelength	1.54178 Å
Crystal system	Orthorhombic
Space group	P2(1)2(1)2
Unit cell dimensions	a = 14.0519(7) Å a = 90°. b = 22.4870(12) Å b = 90°. c = 6.6024(3) Å g = 90°.
Volume	2086.26(18) Å ³
Z	4
Density (calculated)	1.453 Mg/m ³
Absorption coefficient	2.993 mm ⁻¹
F(000)	944
Crystal size	0.05 x 0.05 x 0.02 mm ³
Crystal color/habit	colorless plate
Theta range for data collection	3.71 to 68.20°.
Index ranges	-16 ≤ h ≤ 16, -26 ≤ k ≤ 26, -7 ≤ l ≤ 6
Reflections collected	21596
Independent reflections	3704 [R(int) = 0.0418]
Completeness to theta = 67.00°	99.5 %
Absorption correction	Semi-empirical from equivalents
Max. and min. transmission	0.9426 and 0.8647
Refinement method	Full-matrix least-squares on F ²
Data / restraints / parameters	3704 / 0 / 257
Goodness-of-fit on F ²	1.054
Final R indices [I > 2σ(I)]	R1 = 0.0768, wR2 = 0.2003
R indices (all data)	R1 = 0.0899, wR2 = 0.2107
Absolute structure parameter	-0.06(5)
Largest diff. peak and hole	1.341 and -0.420 e.Å ⁻³

Atomic coordinates ($\times 10^4$) and equivalent isotropic displacement parameters ($\text{\AA}^2 \times 10^3$)

U(eq) is defined as one third of the trace of the orthogonalized U^{ij} tensor.

	x	y	z	U(eq)
C(1)	7102(5)	7020(3)	2113(13)	40(2)
C(2)	7618(6)	7149(3)	4086(13)	43(2)
C(3)	8433(5)	6724(3)	4654(13)	39(2)
C(4)	8095(5)	6452(3)	6632(13)	41(2)
C(5)	7023(5)	6587(3)	6732(12)	39(2)
C(6)	6352(6)	6157(3)	5688(11)	35(2)
C(7)	6561(5)	6025(3)	3444(11)	35(2)
C(8)	5499(6)	6666(3)	1495(12)	42(2)
C(9)	3881(6)	6216(4)	1368(13)	47(2)
C(10)	3372(7)	6747(5)	2170(20)	84(4)
C(11)	3867(7)	6173(4)	-932(15)	57(2)
C(12)	3546(7)	5639(5)	2260(20)	78(3)
C(13)	9747(6)	7235(4)	3322(17)	58(3)
C(14)	8448(5)	5592(4)	8545(14)	45(2)
C(15)	8716(6)	4955(4)	8455(15)	56(2)
C(16)	8920(6)	4659(5)	10208(18)	67(3)
C(17)	9178(9)	4081(6)	10210(20)	88(4)
C(18)	9204(7)	3760(5)	8410(20)	76(4)
C(19)	8988(9)	4034(5)	6640(20)	84(4)
C(20)	8718(9)	4624(5)	6659(17)	71(3)
N(1)	6386(4)	6551(3)	2250(10)	37(1)
O(1)	6970(4)	7152(2)	5773(8)	40(1)
O(2)	5294(4)	7090(3)	499(10)	48(1)
O(3)	4888(4)	6231(2)	2025(9)	46(1)
O(4)	9308(4)	7015(3)	5078(10)	49(1)
O(5)	8350(4)	5830(2)	6693(9)	45(1)
O(6)	8357(4)	5864(3)	10073(10)	57(2)
Br(1)	6233(1)	5417(1)	7215(1)	51(1)

Bond lengths [Å] and angles [°]

C(1)-N(1)	1.460(8)	C(9)-C(11)	1.522(13)
C(1)-C(2)	1.520(12)	C(10)-H(10A)	0.9800
C(1)-H(1A)	0.9900	C(10)-H(10B)	0.9800
C(1)-H(1B)	0.9900	C(10)-H(10C)	0.9800
C(2)-O(1)	1.439(10)	C(11)-H(11A)	0.9800
C(2)-C(3)	1.538(11)	C(11)-H(11B)	0.9800
C(2)-H(2)	1.0000	C(11)-H(11C)	0.9800
C(3)-O(4)	1.421(9)	C(12)-H(12A)	0.9800
C(3)-C(4)	1.518(11)	C(12)-H(12B)	0.9800
C(3)-H(3)	1.0000	C(12)-H(12C)	0.9800
C(4)-O(5)	1.445(9)	C(13)-O(4)	1.403(11)
C(4)-C(5)	1.538(10)	C(13)-H(13A)	0.9800
C(4)-H(4)	1.0000	C(13)-H(13B)	0.9800
C(5)-O(1)	1.424(9)	C(13)-H(13C)	0.9800
C(5)-C(6)	1.516(10)	C(14)-O(6)	1.188(11)
C(5)-H(5)	1.0000	C(14)-O(5)	1.342(11)
C(6)-C(7)	1.539(11)	C(14)-C(15)	1.482(13)
C(6)-Br(1)	1.953(6)	C(15)-C(16)	1.365(14)
C(6)-H(6)	1.0000	C(15)-C(20)	1.400(14)
C(7)-N(1)	1.442(9)	C(16)-C(17)	1.349(16)
C(7)-H(7A)	0.9900	C(16)-H(16)	0.9500
C(7)-H(7B)	0.9900	C(17)-C(18)	1.392(19)
C(8)-O(2)	1.193(10)	C(17)-H(17)	0.9500
C(8)-O(3)	1.348(9)	C(18)-C(19)	1.353(18)
C(8)-N(1)	1.367(10)	C(18)-H(18)	0.9500
C(9)-O(3)	1.481(9)	C(19)-C(20)	1.380(15)
C(9)-C(10)	1.488(12)	C(19)-H(19)	0.9500
C(9)-C(12)	1.500(13)	C(20)-H(20)	0.9500
N(1)-C(1)-C(2)	114.5(7)	O(4)-C(3)-C(2)	114.0(6)
N(1)-C(1)-H(1A)	108.6	C(4)-C(3)-C(2)	103.1(6)
C(2)-C(1)-H(1A)	108.6	O(4)-C(3)-H(3)	110.9
N(1)-C(1)-H(1B)	108.6	C(4)-C(3)-H(3)	110.9
C(2)-C(1)-H(1B)	108.6	C(2)-C(3)-H(3)	110.9
H(1A)-C(1)-H(1B)	107.6	O(5)-C(4)-C(3)	109.7(6)
O(1)-C(2)-C(1)	111.2(7)	O(5)-C(4)-C(5)	115.6(6)
O(1)-C(2)-C(3)	106.6(7)	C(3)-C(4)-C(5)	105.4(6)
C(1)-C(2)-C(3)	116.4(7)	O(5)-C(4)-H(4)	108.7
O(1)-C(2)-H(2)	107.4	C(3)-C(4)-H(4)	108.7
C(1)-C(2)-H(2)	107.4	C(5)-C(4)-H(4)	108.7
C(3)-C(2)-H(2)	107.4	O(1)-C(5)-C(6)	109.5(6)
O(4)-C(3)-C(4)	106.7(6)	O(1)-C(5)-C(4)	102.0(6)

C(6)-C(5)-C(4)	117.7(6)	O(4)-C(13)-H(13B)	109.5
O(1)-C(5)-H(5)	109.1	H(13A)-C(13)-H(13B)	109.5
C(6)-C(5)-H(5)	109.1	O(4)-C(13)-H(13C)	109.5
C(4)-C(5)-H(5)	109.1	H(13A)-C(13)-H(13C)	109.5
C(5)-C(6)-C(7)	116.2(6)	H(13B)-C(13)-H(13C)	109.5
C(5)-C(6)-Br(1)	111.2(5)	O(6)-C(14)-O(5)	123.8(8)
C(7)-C(6)-Br(1)	110.4(5)	O(6)-C(14)-C(15)	124.1(8)
C(5)-C(6)-H(6)	106.1	O(5)-C(14)-C(15)	112.1(8)
C(7)-C(6)-H(6)	106.1	C(16)-C(15)-C(20)	117.4(9)
Br(1)-C(6)-H(6)	106.1	C(16)-C(15)-C(14)	119.3(10)
N(1)-C(7)-C(6)	109.6(6)	C(20)-C(15)-C(14)	123.2(9)
N(1)-C(7)-H(7A)	109.7	C(17)-C(16)-C(15)	121.7(12)
C(6)-C(7)-H(7A)	109.7	C(17)-C(16)-H(16)	119.2
N(1)-C(7)-H(7B)	109.7	C(15)-C(16)-H(16)	119.2
C(6)-C(7)-H(7B)	109.7	C(16)-C(17)-C(18)	120.5(12)
H(7A)-C(7)-H(7B)	108.2	C(16)-C(17)-H(17)	119.8
O(2)-C(8)-O(3)	124.7(8)	C(18)-C(17)-H(17)	119.8
O(2)-C(8)-N(1)	124.9(7)	C(19)-C(18)-C(17)	119.6(10)
O(3)-C(8)-N(1)	110.3(6)	C(19)-C(18)-H(18)	120.2
O(3)-C(9)-C(10)	109.8(7)	C(17)-C(18)-H(18)	120.2
O(3)-C(9)-C(12)	101.8(7)	C(18)-C(19)-C(20)	119.5(12)
C(10)-C(9)-C(12)	113.9(10)	C(18)-C(19)-H(19)	120.2
O(3)-C(9)-C(11)	107.8(7)	C(20)-C(19)-H(19)	120.2
C(10)-C(9)-C(11)	113.5(9)	C(19)-C(20)-C(15)	121.2(11)
C(12)-C(9)-C(11)	109.3(8)	C(19)-C(20)-H(20)	119.4
C(9)-C(10)-H(10A)	109.5	C(15)-C(20)-H(20)	119.4
C(9)-C(10)-H(10B)	109.5	C(8)-N(1)-C(7)	120.7(6)
H(10A)-C(10)-H(10B)	109.5	C(8)-N(1)-C(1)	117.9(6)
C(9)-C(10)-H(10C)	109.5	C(7)-N(1)-C(1)	120.5(6)
H(10A)-C(10)-H(10C)	109.5	C(5)-O(1)-C(2)	107.9(6)
H(10B)-C(10)-H(10C)	109.5	C(8)-O(3)-C(9)	123.3(6)
C(9)-C(11)-H(11A)	109.5	C(13)-O(4)-C(3)	112.3(7)
C(9)-C(11)-H(11B)	109.5	C(14)-O(5)-C(4)	116.0(7)
H(11A)-C(11)-H(11B)	109.5		
C(9)-C(11)-H(11C)	109.5		
H(11A)-C(11)-H(11C)	109.5		
H(11B)-C(11)-H(11C)	109.5		
C(9)-C(12)-H(12A)	109.5		
C(9)-C(12)-H(12B)	109.5		
H(12A)-C(12)-H(12B)	109.5		
C(9)-C(12)-H(12C)	109.5		
H(12A)-C(12)-H(12C)	109.5		
H(12B)-C(12)-H(12C)	109.5		
O(4)-C(13)-H(13A)	109.5		

Symmetry transformations used to generate equivalent atoms

Anisotropic displacement parameters ($\text{\AA}^2 \times 10^3$). The anisotropic displacement factor exponent takes the form: $-2p^2 [h^2 a^* 2U^{11} + \dots + 2 h k a^* b^* U^{12}]$

	U ¹¹	U ²²	U ³³	U ²³	U ¹³	U ¹²
C(1)	45(4)	34(3)	40(4)	8(3)	-2(4)	-4(3)
C(2)	48(4)	37(4)	45(5)	-5(3)	6(4)	-7(3)
C(3)	34(4)	40(4)	43(5)	-6(3)	-3(3)	0(3)
C(4)	33(4)	46(4)	43(5)	-5(3)	-5(3)	-2(3)
C(5)	34(3)	44(4)	39(5)	0(3)	10(3)	0(3)
C(6)	39(4)	33(3)	33(4)	18(3)	0(3)	-4(3)
C(7)	36(3)	38(3)	30(4)	4(3)	-3(3)	0(3)
C(8)	53(4)	42(4)	30(4)	1(3)	4(3)	-7(3)
C(9)	43(4)	48(4)	49(5)	-9(3)	-13(4)	0(4)
C(10)	46(5)	79(7)	129(11)	-52(8)	-4(6)	-2(5)
C(11)	55(5)	51(5)	64(6)	0(4)	-13(5)	-7(4)
C(12)	45(5)	98(7)	92(9)	32(7)	-26(5)	-27(5)
C(13)	45(4)	41(4)	88(8)	19(5)	19(5)	3(3)
C(14)	24(3)	65(5)	45(5)	17(4)	3(3)	2(3)
C(15)	24(3)	72(5)	71(6)	10(5)	11(4)	2(4)
C(16)	50(5)	78(6)	72(7)	24(6)	15(5)	14(5)
C(17)	75(7)	86(8)	102(11)	51(8)	23(7)	23(6)
C(18)	56(5)	55(5)	117(11)	38(7)	4(6)	12(5)
C(19)	94(9)	55(6)	101(10)	-10(6)	10(7)	11(6)
C(20)	82(7)	63(5)	70(7)	3(5)	2(6)	5(6)
N(1)	32(3)	44(3)	36(3)	-3(3)	-8(3)	-6(2)
O(1)	38(3)	48(3)	34(3)	-10(2)	1(2)	2(2)
O(2)	42(3)	46(3)	55(4)	2(3)	-11(3)	2(3)
O(3)	38(3)	53(3)	47(3)	6(3)	-9(3)	-7(2)
O(4)	38(3)	53(3)	56(4)	3(3)	-4(3)	-6(2)
O(5)	34(3)	48(3)	53(4)	6(3)	2(2)	-1(2)
O(6)	44(3)	78(4)	50(4)	8(3)	7(3)	12(3)
Br(1)	39(1)	55(1)	59(1)	16(1)	-1(1)	-6(1)

Hydrogen coordinates ($\times 10^4$) and isotropic displacement parameters ($\text{\AA}^2 \times 10^3$).

	x	y	z	U(eq)
H(1A)	6789	7389	1643	47
H(1B)	7577	6905	1078	47
H(2)	7895	7558	3975	52
H(3)	8520	6411	3594	47
H(4)	8418	6661	7779	49
H(5)	6829	6629	8183	47
H(6)	5710	6348	5723	42
H(7A)	7233	5900	3286	42
H(7B)	6149	5697	2967	42
H(10A)	3426	6757	3645	127
H(10B)	2699	6726	1782	127
H(10C)	3655	7109	1595	127
H(11A)	4095	6548	-1515	85
H(11B)	3216	6096	-1394	85
H(11C)	4283	5847	-1367	85
H(12A)	3951	5315	1764	118
H(12B)	2886	5566	1848	118
H(12C)	3584	5659	3737	118
H(13A)	9884	6905	2398	87
H(13B)	10342	7435	3687	87
H(13C)	9321	7519	2653	87
H(16)	8880	4866	11460	80
H(17)	9344	3892	11446	105
H(18)	9371	3351	8417	91
H(19)	9023	3822	5399	100
H(20)	8531	4809	5429	86

Crystal data and structure refinement for Major Trimer 8.8

Empirical formula	C ₃₆ H ₃₀ F ₆	
Formula weight	576.60	
Temperature	100(2) K	
Wavelength	1.54178 Å	
Crystal system	Monoclinic	
Space group	P2(1)	
Unit cell dimensions	a = 9.0552(4) Å	a = 90°.
	b = 12.8869(6) Å	b = 103.344(2)°.
	c = 12.0073(5) Å	g = 90°.
Volume	1363.34(10) Å ³	
Z	2	
Density (calculated)	1.405 Mg/m ³	
Absorption coefficient	0.916 mm ⁻¹	
F(000)	600	
Crystal size	0.12 x 0.08 x 0.04 mm ³	
Crystal color/habit	colorless prism	
Theta range for data collection	3.78 to 68.17°.	
Index ranges	-10<=h<=10, -15<=k<=14, -14<=l<=14	
Reflections collected	12405	
Independent reflections	4349 [R(int) = 0.0149]	
Completeness to theta = 67.00°	99.9 %	
Absorption correction	Semi-empirical from equivalents	
Max. and min. transmission	0.9643 and 0.8980	
Refinement method	Full-matrix least-squares on F ²	
Data / restraints / parameters	4349 / 1 / 379	
Goodness-of-fit on F ²	1.038	
Final R indices [I>2sigma(I)]	R1 = 0.0274, wR2 = 0.0735	
R indices (all data)	R1 = 0.0282, wR2 = 0.0744	
Absolute structure parameter	0.07(7)	
Largest diff. peak and hole	0.247 and -0.132 e.Å ⁻³	

Atomic coordinates ($\times 10^4$) and equivalent isotropic displacement parameters ($\text{\AA}^2 \times 10^3$). U(eq) is defined as one third of the trace of the orthogonalized U^{ij} tensor.

	x	y	z	U(eq)
C(1)	6239(2)	3861(1)	280(1)	17(1)
C(2)	6327(2)	3431(1)	-776(1)	17(1)
C(3)	7552(2)	2772(1)	-842(1)	17(1)
C(4)	8631(2)	2496(1)	147(1)	18(1)
C(5)	8354(2)	2758(1)	1225(1)	18(1)
C(6)	7221(2)	3485(1)	1297(1)	18(1)
C(7)	5100(2)	4718(1)	394(1)	20(1)
C(8)	4213(2)	5371(1)	-584(1)	22(1)
C(9)	5138(2)	6080(1)	-1190(2)	25(1)
C(10)	6134(2)	5496(2)	-1861(2)	24(1)
C(11)	5223(2)	4600(2)	-2461(1)	22(1)
C(12)	4186(2)	4759(2)	-3503(1)	28(1)
C(13)	3141(2)	4002(2)	-3972(2)	34(1)
C(14)	3114(2)	3070(2)	-3402(2)	31(1)
C(15)	4148(2)	2899(2)	-2361(1)	24(1)
C(16)	5196(2)	3657(1)	-1886(1)	19(1)
C(17)	7656(2)	2411(1)	-2019(1)	17(1)
C(18)	6879(2)	1536(1)	-2504(1)	20(1)
C(19)	6867(2)	1255(2)	-3626(1)	23(1)
C(20)	7668(2)	1832(2)	-4247(1)	26(1)
C(21)	8496(2)	2682(2)	-3755(1)	24(1)
C(22)	8491(2)	2994(1)	-2643(1)	21(1)
C(23)	9501(2)	3856(2)	-2059(2)	29(1)
C(24)	10902(2)	3430(2)	-1178(2)	33(1)
C(25)	10871(2)	2280(2)	-920(2)	28(1)
C(26)	10126(2)	1971(1)	44(1)	23(1)
C(27)	9212(2)	2249(1)	2350(1)	21(1)
C(28)	10528(2)	2846(2)	3119(1)	25(1)
C(29)	10954(2)	3902(2)	2695(2)	28(1)
C(30)	9712(2)	4757(2)	2495(2)	29(1)
C(31)	8382(2)	4534(1)	3025(1)	25(1)
C(32)	8341(3)	4959(2)	4090(2)	37(1)
C(33)	7159(3)	4740(2)	4604(2)	42(1)
C(34)	5993(2)	4086(2)	4059(2)	38(1)
C(35)	6004(2)	3678(2)	2984(2)	29(1)
C(36)	7181(2)	3909(1)	2468(1)	22(1)
F(1)	5874(1)	5429(1)	1182(1)	25(1)
F(2)	4033(1)	4275(1)	902(1)	28(1)
F(3)	11210(1)	2193(1)	1030(1)	27(1)

F(4)	9961(1)	913(1)	21(1)	30(1)
F(5)	9674(1)	1275(1)	2129(1)	28(1)
F(6)	8148(1)	2025(1)	2983(1)	25(1)

Bond lengths [Å] and angles [°]

C(1)-C(2)	1.402(2)	C(18)-C(19)	1.393(2)
C(1)-C(6)	1.419(2)	C(18)-H(18)	0.9500
C(1)-C(7)	1.539(2)	C(19)-C(20)	1.373(3)
C(2)-C(3)	1.414(2)	C(19)-H(19)	0.9500
C(2)-C(16)	1.510(2)	C(20)-C(21)	1.381(3)
C(3)-C(4)	1.398(2)	C(20)-H(20)	0.9500
C(3)-C(17)	1.512(2)	C(21)-C(22)	1.395(2)
C(4)-C(5)	1.414(2)	C(21)-H(21)	0.9500
C(4)-C(26)	1.544(2)	C(22)-C(23)	1.506(2)
C(5)-C(6)	1.408(2)	C(23)-C(24)	1.553(3)
C(5)-C(27)	1.540(2)	C(23)-H(23A)	0.9900
C(6)-C(36)	1.516(2)	C(23)-H(23B)	0.9900
C(7)-F(2)	1.3794(19)	C(24)-C(25)	1.515(3)
C(7)-F(1)	1.3858(19)	C(24)-H(24A)	0.9900
C(7)-C(8)	1.516(2)	C(24)-H(24B)	0.9900
C(8)-C(9)	1.532(2)	C(25)-C(26)	1.520(2)
C(8)-H(8A)	0.9900	C(25)-H(25A)	0.9900
C(8)-H(8B)	0.9900	C(25)-H(25B)	0.9900
C(9)-C(10)	1.537(2)	C(26)-F(4)	1.371(2)
C(9)-H(9A)	0.9900	C(26)-F(3)	1.3815(19)
C(9)-H(9B)	0.9900	C(27)-F(5)	1.368(2)
C(10)-C(11)	1.503(2)	C(27)-F(6)	1.389(2)
C(10)-H(10A)	0.9900	C(27)-C(28)	1.535(2)
C(10)-H(10B)	0.9900	C(28)-C(29)	1.533(3)
C(11)-C(12)	1.395(2)	C(28)-H(28A)	0.9900
C(11)-C(16)	1.401(2)	C(28)-H(28B)	0.9900
C(12)-C(13)	1.386(3)	C(29)-C(30)	1.554(3)
C(12)-H(12)	0.9500	C(29)-H(29A)	0.9900
C(13)-C(14)	1.385(3)	C(29)-H(29B)	0.9900
C(13)-H(13)	0.9500	C(30)-C(31)	1.514(3)
C(14)-C(15)	1.396(2)	C(30)-H(30A)	0.9900
C(14)-H(14)	0.9500	C(30)-H(30B)	0.9900
C(15)-C(16)	1.388(2)	C(31)-C(36)	1.394(3)
C(15)-H(15)	0.9500	C(31)-C(32)	1.399(3)
C(17)-C(18)	1.384(2)	C(32)-C(33)	1.383(3)
C(17)-C(22)	1.400(2)	C(32)-H(32)	0.9500

C(33)-C(34)	1.391(4)	C(34)-H(34)	0.9500
C(33)-H(33)	0.9500	C(35)-C(36)	1.383(2)
C(34)-C(35)	1.396(3)	C(35)-H(35)	0.9500
C(2)-C(1)-C(6)	119.23(14)	C(9)-C(10)-H(10B)	110.2
C(2)-C(1)-C(7)	122.86(14)	H(10A)-C(10)-H(10B)	108.5
C(6)-C(1)-C(7)	117.90(13)	C(12)-C(11)-C(16)	118.98(17)
C(1)-C(2)-C(3)	119.76(14)	C(12)-C(11)-C(10)	119.89(17)
C(1)-C(2)-C(16)	123.63(14)	C(16)-C(11)-C(10)	120.06(14)
C(3)-C(2)-C(16)	116.58(13)	C(13)-C(12)-C(11)	121.08(18)
C(4)-C(3)-C(2)	120.59(14)	C(13)-C(12)-H(12)	119.5
C(4)-C(3)-C(17)	122.25(14)	C(11)-C(12)-H(12)	119.5
C(2)-C(3)-C(17)	117.14(14)	C(14)-C(13)-C(12)	119.87(16)
C(3)-C(4)-C(5)	118.68(14)	C(14)-C(13)-H(13)	120.1
C(3)-C(4)-C(26)	119.79(14)	C(12)-C(13)-H(13)	120.1
C(5)-C(4)-C(26)	121.45(14)	C(13)-C(14)-C(15)	119.63(18)
C(6)-C(5)-C(4)	120.04(15)	C(13)-C(14)-H(14)	120.2
C(6)-C(5)-C(27)	117.15(14)	C(15)-C(14)-H(14)	120.2
C(4)-C(5)-C(27)	122.77(14)	C(16)-C(15)-C(14)	120.69(18)
C(5)-C(6)-C(1)	119.66(14)	C(16)-C(15)-H(15)	119.7
C(5)-C(6)-C(36)	118.09(14)	C(14)-C(15)-H(15)	119.7
C(1)-C(6)-C(36)	122.05(14)	C(15)-C(16)-C(11)	119.74(15)
F(2)-C(7)-F(1)	105.50(12)	C(15)-C(16)-C(2)	119.14(15)
F(2)-C(7)-C(8)	105.79(13)	C(11)-C(16)-C(2)	121.08(15)
F(1)-C(7)-C(8)	104.84(14)	C(18)-C(17)-C(22)	119.83(14)
F(2)-C(7)-C(1)	107.14(14)	C(18)-C(17)-C(3)	120.58(14)
F(1)-C(7)-C(1)	106.94(12)	C(22)-C(17)-C(3)	119.52(15)
C(8)-C(7)-C(1)	125.17(14)	C(17)-C(18)-C(19)	120.53(15)
C(7)-C(8)-C(9)	116.69(13)	C(17)-C(18)-H(18)	119.7
C(7)-C(8)-H(8A)	108.1	C(19)-C(18)-H(18)	119.7
C(9)-C(8)-H(8A)	108.1	C(20)-C(19)-C(18)	119.84(16)
C(7)-C(8)-H(8B)	108.1	C(20)-C(19)-H(19)	120.1
C(9)-C(8)-H(8B)	108.1	C(18)-C(19)-H(19)	120.1
H(8A)-C(8)-H(8B)	107.3	C(19)-C(20)-C(21)	120.00(15)
C(8)-C(9)-C(10)	114.10(14)	C(19)-C(20)-H(20)	120.0
C(8)-C(9)-H(9A)	108.7	C(21)-C(20)-H(20)	120.0
C(10)-C(9)-H(9A)	108.7	C(20)-C(21)-C(22)	121.10(16)
C(8)-C(9)-H(9B)	108.7	C(20)-C(21)-H(21)	119.4
C(10)-C(9)-H(9B)	108.7	C(22)-C(21)-H(21)	119.4
H(9A)-C(9)-H(9B)	107.6	C(21)-C(22)-C(17)	118.62(16)
C(11)-C(10)-C(9)	107.64(13)	C(21)-C(22)-C(23)	121.51(15)
C(11)-C(10)-H(10A)	110.2	C(17)-C(22)-C(23)	119.45(15)
C(9)-C(10)-H(10A)	110.2	C(22)-C(23)-C(24)	111.72(16)
C(11)-C(10)-H(10B)	110.2	C(22)-C(23)-H(23A)	109.3

C(24)-C(23)-H(23A)	109.3	C(29)-C(30)-H(30B)	108.6
C(22)-C(23)-H(23B)	109.3	H(30A)-C(30)-H(30B)	107.6
C(24)-C(23)-H(23B)	109.3	C(36)-C(31)-C(32)	118.87(18)
H(23A)-C(23)-H(23B)	107.9	C(36)-C(31)-C(30)	121.07(15)
C(25)-C(24)-C(23)	115.71(15)	C(32)-C(31)-C(30)	120.06(18)
C(25)-C(24)-H(24A)	108.4	C(33)-C(32)-C(31)	120.9(2)
C(23)-C(24)-H(24A)	108.4	C(33)-C(32)-H(32)	119.5
C(25)-C(24)-H(24B)	108.4	C(31)-C(32)-H(32)	119.5
C(23)-C(24)-H(24B)	108.4	C(32)-C(33)-C(34)	119.73(18)
H(24A)-C(24)-H(24B)	107.4	C(32)-C(33)-H(33)	120.1
C(24)-C(25)-C(26)	116.37(15)	C(34)-C(33)-H(33)	120.1
C(24)-C(25)-H(25A)	108.2	C(33)-C(34)-C(35)	119.78(19)
C(26)-C(25)-H(25A)	108.2	C(33)-C(34)-H(34)	120.1
C(24)-C(25)-H(25B)	108.2	C(35)-C(34)-H(34)	120.1
C(26)-C(25)-H(25B)	108.2	C(36)-C(35)-C(34)	120.3(2)
H(25A)-C(25)-H(25B)	107.3	C(36)-C(35)-H(35)	119.9
F(4)-C(26)-F(3)	105.95(13)	C(34)-C(35)-H(35)	119.9
F(4)-C(26)-C(25)	108.11(14)	C(35)-C(36)-C(31)	120.35(16)
F(3)-C(26)-C(25)	104.26(14)	C(35)-C(36)-C(6)	121.61(17)
F(4)-C(26)-C(4)	110.10(14)	C(31)-C(36)-C(6)	118.03(15)
F(3)-C(26)-C(4)	107.63(13)		
C(25)-C(26)-C(4)	119.83(15)		
F(5)-C(27)-F(6)	101.29(13)		
F(5)-C(27)-C(28)	110.29(13)		
F(6)-C(27)-C(28)	108.35(13)		
F(5)-C(27)-C(5)	109.57(13)		
F(6)-C(27)-C(5)	107.21(12)		
C(28)-C(27)-C(5)	118.65(14)		
C(29)-C(28)-C(27)	117.64(14)		
C(29)-C(28)-H(28A)	107.9		
C(27)-C(28)-H(28A)	107.9		
C(29)-C(28)-H(28B)	107.9		
C(27)-C(28)-H(28B)	107.9		
H(28A)-C(28)-H(28B)	107.2		
C(28)-C(29)-C(30)	116.87(15)		
C(28)-C(29)-H(29A)	108.1		
C(30)-C(29)-H(29A)	108.1		
C(28)-C(29)-H(29B)	108.1		
C(30)-C(29)-H(29B)	108.1		
H(29A)-C(29)-H(29B)	107.3		
C(31)-C(30)-C(29)	114.75(15)		
C(31)-C(30)-H(30A)	108.6		
C(29)-C(30)-H(30A)	108.6		
C(31)-C(30)-H(30B)	108.6		

Symmetry transformations used to generate equivalent atoms.

Anisotropic displacement parameters ($\text{\AA}^2 \times 10^3$). The anisotropic displacement factor exponent takes the form: $-2p^2 [h^2 a^* 2U^{11} + \dots + 2 h k a^* b^* U^{12}]$

	U ¹¹	U ²²	U ³³	U ²³	U ¹³	U ¹²
C(1)	17(1)	14(1)	22(1)	0(1)	7(1)	0(1)
C(2)	18(1)	14(1)	19(1)	1(1)	5(1)	-3(1)
C(3)	19(1)	14(1)	19(1)	0(1)	7(1)	-3(1)
C(4)	20(1)	14(1)	22(1)	-2(1)	6(1)	0(1)
C(5)	17(1)	16(1)	20(1)	0(1)	3(1)	-2(1)
C(6)	20(1)	15(1)	19(1)	0(1)	7(1)	-2(1)
C(7)	21(1)	19(1)	21(1)	-4(1)	7(1)	1(1)
C(8)	19(1)	21(1)	25(1)	-3(1)	4(1)	6(1)
C(9)	27(1)	17(1)	29(1)	2(1)	1(1)	2(1)
C(10)	21(1)	21(1)	31(1)	8(1)	6(1)	1(1)
C(11)	21(1)	24(1)	23(1)	1(1)	9(1)	3(1)
C(12)	30(1)	34(1)	20(1)	7(1)	7(1)	10(1)
C(13)	30(1)	49(1)	20(1)	-1(1)	-2(1)	7(1)
C(14)	25(1)	37(1)	29(1)	-10(1)	-1(1)	-2(1)
C(15)	22(1)	24(1)	25(1)	-3(1)	6(1)	-1(1)
C(16)	16(1)	22(1)	19(1)	-2(1)	7(1)	3(1)
C(17)	19(1)	15(1)	18(1)	1(1)	5(1)	4(1)
C(18)	19(1)	19(1)	22(1)	1(1)	7(1)	0(1)
C(19)	23(1)	23(1)	23(1)	-6(1)	2(1)	1(1)
C(20)	27(1)	33(1)	16(1)	0(1)	5(1)	9(1)
C(21)	27(1)	26(1)	23(1)	8(1)	13(1)	6(1)
C(22)	19(1)	17(1)	27(1)	3(1)	8(1)	2(1)
C(23)	29(1)	20(1)	45(1)	-5(1)	20(1)	-7(1)
C(24)	27(1)	41(1)	34(1)	-10(1)	11(1)	-16(1)
C(25)	16(1)	38(1)	29(1)	-9(1)	5(1)	4(1)
C(26)	23(1)	21(1)	22(1)	-5(1)	0(1)	5(1)
C(27)	22(1)	19(1)	22(1)	0(1)	4(1)	2(1)
C(28)	26(1)	26(1)	21(1)	-1(1)	0(1)	3(1)
C(29)	29(1)	31(1)	24(1)	-4(1)	6(1)	-8(1)
C(30)	37(1)	22(1)	23(1)	3(1)	-3(1)	-10(1)
C(31)	38(1)	17(1)	19(1)	0(1)	1(1)	6(1)
C(32)	54(1)	27(1)	23(1)	-4(1)	-4(1)	12(1)
C(33)	65(1)	43(1)	19(1)	-2(1)	8(1)	26(1)
C(34)	48(1)	45(1)	25(1)	9(1)	18(1)	23(1)
C(35)	35(1)	28(1)	28(1)	6(1)	13(1)	10(1)
C(36)	30(1)	18(1)	17(1)	4(1)	6(1)	9(1)
F(1)	30(1)	20(1)	23(1)	-5(1)	0(1)	8(1)
F(2)	24(1)	34(1)	30(1)	2(1)	14(1)	5(1)
F(3)	20(1)	36(1)	24(1)	-7(1)	0(1)	6(1)

F(4)	35(1)	20(1)	34(1)	-3(1)	4(1)	8(1)
F(5)	34(1)	19(1)	30(1)	3(1)	3(1)	7(1)
F(6)	28(1)	25(1)	24(1)	7(1)	7(1)	-1(1)

Hydrogen coordinates ($\times 10^4$) and isotropic displacement parameters ($\text{\AA}^2 \times 10^3$).

	x	y	z	U(eq)
H(8A)	3493	5808	-285	26
H(8B)	3605	4898	-1162	26
H(9A)	5797	6527	-611	30
H(9B)	4431	6538	-1725	30
H(10A)	6430	5965	-2426	29
H(10B)	7069	5240	-1332	29
H(12)	4197	5397	-3897	33
H(13)	2445	4121	-4684	41
H(14)	2394	2550	-3717	38
H(15)	4136	2258	-1973	28
H(18)	6348	1124	-2068	24
H(19)	6307	665	-3961	28
H(20)	7653	1646	-5015	31
H(21)	9079	3061	-4180	29
H(23A)	8913	4316	-1662	35
H(23B)	9849	4273	-2641	35
H(24A)	11821	3576	-1466	40
H(24B)	11001	3817	-452	40
H(25A)	11929	2022	-730	33
H(25B)	10333	1920	-1626	33
H(28A)	10274	2954	3870	30
H(28B)	11440	2397	3252	30
H(29A)	11266	3790	1966	34
H(29B)	11851	4168	3257	34
H(30A)	10184	5419	2810	35
H(30B)	9324	4851	1660	35
H(32)	9137	5405	4464	44
H(33)	7144	5034	5326	51
H(34)	5193	3917	4418	45
H(35)	5199			

Crystal data and structure refinement for Minor Trimer 8.9

Empirical formula	C ₃₆ H ₃₀ F ₆	
Formula weight	576.60	
Temperature	100(2) K	
Wavelength	1.54178 Å	
Crystal system	Triclinic	
Space group	P-1	
Unit cell dimensions	a = 10.9610(4) Å b = 11.2443(4) Å c = 24.9515(9) Å	a = 90.207(2)°. b = 100.731(2)°. g = 115.162(2)°.
Volume	2722.88(17) Å ³	
Z	4	
Density (calculated)	1.407 Mg/m ³	
Absorption coefficient	0.917 mm ⁻¹	
F(000)	1200	
Crystal size	0.20 x 0.20 x 0.20 mm ³	
Crystal color/habit	colorless rod	
Theta range for data collection	3.62 to 68.10°.	
Index ranges	-13<=h<=13, -13<=k<=13, -26<=l<=29	
Reflections collected	46641	
Independent reflections	9620 [R(int) = 0.0356]	
Completeness to theta = 67.00°	97.5 %	
Absorption correction	Semi-empirical from equivalents	
Max. and min. transmission	0.8378 and 0.8378	
Refinement method	Full-matrix least-squares on F ²	
Data / restraints / parameters	9620 / 0 / 803	
Goodness-of-fit on F ²	1.028	
Final R indices [I>2sigma(I)]	R1 = 0.0428, wR2 = 0.1070	
R indices (all data)	R1 = 0.0464, wR2 = 0.1100	
Largest diff. peak and hole	0.931 and -0.549 e.Å ⁻³	

Atomic coordinates ($\times 10^4$) and equivalent isotropic displacement parameters ($\text{\AA}^2 \times 10^3$). U(eq) is defined as one third of the trace of the orthogonalized U_{ij} tensor.

	x	y	z	U(eq)
C(1)	8284(2)	8473(2)	5894(1)	18(1)
C(2)	7833(2)	9349(2)	6101(1)	19(1)
C(3)	8217(2)	9753(2)	6668(1)	19(1)
C(4)	9188(2)	9429(2)	7013(1)	18(1)
C(5)	9618(2)	8537(2)	6803(1)	18(1)
C(6)	9131(2)	8033(2)	6250(1)	17(1)
C(7)	7932(2)	7981(2)	5299(1)	20(1)
C(8)	9002(2)	8321(2)	5016(1)	22(1)
C(9)	8753(2)	7881(2)	4471(1)	27(1)
C(10)	7413(2)	7065(2)	4201(1)	31(1)
C(11)	6351(2)	6724(2)	4478(1)	28(1)
C(12)	6580(2)	7176(2)	5026(1)	21(1)
C(13)	5349(2)	6860(2)	5285(1)	24(1)
C(14)	4770(2)	7891(2)	5181(1)	26(1)
C(15)	5416(2)	9095(2)	5603(1)	24(1)
C(16)	6977(2)	9875(2)	5697(1)	21(1)
C(17)	7661(2)	10576(2)	6954(1)	23(1)
C(18)	8565(2)	12064(2)	7083(1)	28(1)
C(19)	9897(2)	12705(2)	6862(1)	29(1)
C(20)	10983(2)	12157(2)	7041(1)	24(1)
C(21)	10823(2)	11525(2)	7569(1)	22(1)
C(22)	11522(2)	12284(2)	8069(1)	27(1)
C(23)	11273(2)	11764(2)	8558(1)	31(1)
C(24)	10296(2)	10473(2)	8555(1)	30(1)
C(25)	9608(2)	9704(2)	8065(1)	25(1)
C(26)	9882(2)	10209(2)	7568(1)	20(1)
C(27)	10696(2)	8196(2)	7168(1)	21(1)
C(28)	12178(2)	9163(2)	7180(1)	26(1)
C(29)	12824(2)	8943(2)	6718(1)	29(1)
C(30)	12006(2)	8772(2)	6129(1)	28(1)
C(31)	10877(2)	7386(2)	5969(1)	24(1)
C(32)	11200(2)	6396(2)	5794(1)	32(1)
C(33)	10225(2)	5102(2)	5677(1)	37(1)
C(34)	8880(2)	4768(2)	5723(1)	34(1)
C(35)	8532(2)	5738(2)	5890(1)	25(1)
C(36)	9526(2)	7038(2)	6023(1)	20(1)
C(37)	5823(2)	5746(2)	8269(1)	21(1)
C(38)	5041(2)	6466(2)	8270(1)	22(1)
C(39)	5225(2)	7243(2)	8752(1)	22(1)

C(40)	6179(2)	7289(2)	9223(1)	26(1)
C(41)	7101(2)	6727(2)	9196(1)	32(1)
C(42)	6907(2)	5940(2)	8719(1)	25(1)
C(43)	5592(2)	4735(2)	7817(1)	21(1)
C(44)	5130(2)	3421(2)	7931(1)	23(1)
C(45)	5030(2)	2458(2)	7554(1)	27(1)
C(46)	5408(2)	2807(2)	7058(1)	31(1)
C(47)	5856(2)	4107(2)	6939(1)	29(1)
C(48)	5947(2)	5085(2)	7311(1)	24(1)
C(49)	6275(2)	6457(2)	7151(1)	28(1)
C(50)	4928(2)	6549(2)	6899(1)	29(1)
C(51)	3765(2)	5835(2)	7200(1)	26(1)
C(52)	3947(2)	6419(2)	7772(1)	24(1)
C(53)	4547(2)	8160(2)	8763(1)	23(1)
C(54)	3157(2)	7718(2)	8771(1)	28(1)
C(55)	2588(2)	8608(2)	8774(1)	37(1)
C(56)	3397(3)	9939(2)	8761(1)	43(1)
C(57)	4781(2)	10381(2)	8760(1)	38(1)
C(58)	5383(2)	9512(2)	8768(1)	27(1)
C(59)	6913(2)	10026(2)	8813(1)	34(1)
C(60)	7710(2)	10222(2)	9419(1)	38(1)
C(61)	6890(2)	9486(2)	9836(1)	30(1)
C(62)	6155(2)	7981(2)	9751(1)	28(1)
C(63)	8261(3)	6883(4)	9700(1)	29(1)
C(64)	7955(3)	5888(4)	10123(1)	33(1)
C(65)	8052(3)	4605(3)	9999(1)	35(1)
C(66)	7151(2)	3885(2)	9447(1)	42(1)
C(63A)	8649(10)	7382(9)	9514(4)	21(2)
C(64A)	8832(9)	6469(7)	9941(3)	26(2)
C(65A)	7665(10)	5170(10)	9967(4)	24(2)
C(66A)	7151(2)	3885(2)	9447(1)	42(1)
C(67)	7917(2)	4327(2)	8991(1)	26(1)
C(68)	8804(2)	3779(2)	8902(1)	34(1)
C(69)	9592(2)	4188(2)	8508(1)	35(1)
C(70)	9517(2)	5163(2)	8192(1)	32(1)
C(71)	8644(2)	5706(2)	8268(1)	26(1)
C(72)	7842(2)	5304(2)	8662(1)	22(1)
F(1)	7371(1)	9986(1)	5201(1)	24(1)
F(2)	7352(1)	11173(1)	5870(1)	26(1)
F(3)	6372(1)	10362(1)	6668(1)	26(1)
F(4)	7359(1)	10025(1)	7431(1)	27(1)
F(5)	10500(1)	6935(1)	7031(1)	24(1)
F(6)	10488(1)	8141(1)	7693(1)	26(1)
F(7)	4124(1)	7701(1)	7708(1)	33(1)

F(8)	2687(1)	5785(1)	7919(1)	31(1)
F(9)	6589(1)	7452(1)	10202(1)	45(1)
F(10)	4793(1)	7569(1)	9777(1)	33(1)
F(11)	8744(2)	8146(2)	9949(1)	34(1)
F(12)	9387(1)	6958(2)	9503(1)	31(1)
F(11A)	9045(6)	8634(6)	9749(3)	26(1)
F(12A)	9617(4)	7650(5)	9195(2)	28(2)

Bond lengths [Å] and angles [°].

C(1)-C(6)	1.407(2)	C(16)-F(1)	1.375(2)
C(1)-C(2)	1.410(2)	C(16)-F(2)	1.3795(19)
C(1)-C(7)	1.502(2)	C(17)-F(4)	1.374(2)
C(2)-C(3)	1.413(2)	C(17)-F(3)	1.3780(19)
C(2)-C(16)	1.539(2)	C(17)-C(18)	1.534(2)
C(3)-C(4)	1.413(2)	C(18)-C(19)	1.537(3)
C(3)-C(17)	1.541(2)	C(18)-H(18A)	0.9900
C(4)-C(5)	1.412(2)	C(18)-H(18B)	0.9900
C(4)-C(26)	1.516(2)	C(19)-C(20)	1.557(2)
C(5)-C(6)	1.406(2)	C(19)-H(19A)	0.9900
C(5)-C(27)	1.536(2)	C(19)-H(19B)	0.9900
C(6)-C(36)	1.502(2)	C(20)-C(21)	1.502(3)
C(7)-C(8)	1.396(2)	C(20)-H(20A)	0.9900
C(7)-C(12)	1.400(2)	C(20)-H(20B)	0.9900
C(8)-C(9)	1.384(2)	C(21)-C(22)	1.398(2)
C(8)-H(8)	0.9500	C(21)-C(26)	1.398(2)
C(9)-C(10)	1.391(3)	C(22)-C(23)	1.377(3)
C(9)-H(9)	0.9500	C(22)-H(22)	0.9500
C(10)-C(11)	1.378(3)	C(23)-C(24)	1.389(3)
C(10)-H(10)	0.9500	C(23)-H(23)	0.9500
C(11)-C(12)	1.397(2)	C(24)-C(25)	1.380(3)
C(11)-H(11)	0.9500	C(24)-H(24)	0.9500
C(12)-C(13)	1.510(2)	C(25)-C(26)	1.396(2)
C(13)-C(14)	1.542(2)	C(25)-H(25)	0.9500
C(13)-H(13A)	0.9900	C(27)-F(6)	1.3686(19)
C(13)-H(13B)	0.9900	C(27)-F(5)	1.3717(19)
C(14)-C(15)	1.529(2)	C(27)-C(28)	1.517(2)
C(14)-H(14A)	0.9900	C(28)-C(29)	1.530(3)
C(14)-H(14B)	0.9900	C(28)-H(28A)	0.9900
C(15)-C(16)	1.524(2)	C(28)-H(28B)	0.9900
C(15)-H(15A)	0.9900	C(29)-C(30)	1.538(3)
C(15)-H(15B)	0.9900	C(29)-H(29A)	0.9900

C(29)-H(29B)	0.9900	C(51)-C(52)	1.510(2)
C(30)-C(31)	1.513(3)	C(51)-H(51A)	0.9900
C(30)-H(30A)	0.9900	C(51)-H(51B)	0.9900
C(30)-H(30B)	0.9900	C(52)-F(8)	1.380(2)
C(31)-C(32)	1.394(3)	C(52)-F(7)	1.385(2)
C(31)-C(36)	1.395(2)	C(53)-C(54)	1.391(2)
C(32)-C(33)	1.380(3)	C(53)-C(58)	1.401(3)
C(32)-H(32)	0.9500	C(54)-C(55)	1.388(3)
C(33)-C(34)	1.385(3)	C(54)-H(54)	0.9500
C(33)-H(33)	0.9500	C(55)-C(56)	1.382(3)
C(34)-C(35)	1.386(3)	C(55)-H(55)	0.9500
C(34)-H(34)	0.9500	C(56)-C(57)	1.382(3)
C(35)-C(36)	1.393(2)	C(56)-H(56)	0.9500
C(35)-H(35)	0.9500	C(57)-C(58)	1.391(3)
C(37)-C(38)	1.408(2)	C(57)-H(57)	0.9500
C(37)-C(42)	1.415(2)	C(58)-C(59)	1.504(3)
C(37)-C(43)	1.506(2)	C(59)-C(60)	1.562(3)
C(38)-C(39)	1.416(2)	C(59)-H(59A)	0.9900
C(38)-C(52)	1.541(2)	C(59)-H(59B)	0.9900
C(39)-C(40)	1.405(2)	C(60)-C(61)	1.516(3)
C(39)-C(53)	1.508(2)	C(60)-H(60A)	0.9900
C(40)-C(41)	1.412(2)	C(60)-H(60B)	0.9900
C(40)-C(62)	1.537(2)	C(61)-C(62)	1.527(3)
C(41)-C(42)	1.407(3)	C(61)-H(61A)	0.9900
C(41)-C(63)	1.563(3)	C(61)-H(61B)	0.9900
C(41)-C(63A)	1.575(9)	C(62)-F(10)	1.376(2)
C(42)-C(72)	1.504(2)	C(62)-F(9)	1.377(2)
C(43)-C(44)	1.394(2)	C(63)-F(12)	1.380(3)
C(43)-C(48)	1.399(3)	C(63)-F(11)	1.385(4)
C(44)-C(45)	1.388(2)	C(63)-C(64)	1.516(5)
C(44)-H(44)	0.9500	C(64)-C(65)	1.526(4)
C(45)-C(46)	1.382(3)	C(64)-H(64A)	0.9900
C(45)-H(45)	0.9500	C(64)-H(64B)	0.9900
C(46)-C(47)	1.383(3)	C(65)-C(66)	1.527(3)
C(46)-H(46)	0.9500	C(65)-H(65A)	0.9900
C(47)-C(48)	1.394(3)	C(65)-H(65B)	0.9900
C(47)-H(47)	0.9500	C(66)-C(67)	1.500(3)
C(48)-C(49)	1.502(3)	C(66)-H(66A)	0.9900
C(49)-C(50)	1.539(3)	C(66)-H(66B)	0.9900
C(49)-H(49A)	0.9900	C(63A)-F(12A)	1.375(12)
C(49)-H(49B)	0.9900	C(63A)-F(11A)	1.376(10)
C(50)-C(51)	1.526(3)	C(63A)-C(64A)	1.529(12)
C(50)-H(50A)	0.9900	C(64A)-C(65A)	1.489(12)
C(50)-H(50B)	0.9900	C(64A)-H(64C)	0.9900

C(64A)-H(64D)	0.9900	C(69)-C(70)	1.374(3)
C(65A)-H(65C)	0.9900	C(69)-H(69)	0.9500
C(65A)-H(65D)	0.9900	C(70)-C(71)	1.374(3)
C(67)-C(72)	1.395(3)	C(70)-H(70)	0.9500
C(67)-C(68)	1.401(3)	C(71)-C(72)	1.389(3)
C(68)-C(69)	1.381(3)	C(71)-H(71)	0.9500
C(68)-H(68)	0.9500		
C(6)-C(1)-C(2)	120.01(15)	C(12)-C(13)-C(14)	111.54(14)
C(6)-C(1)-C(7)	116.55(14)	C(12)-C(13)-H(13A)	109.3
C(2)-C(1)-C(7)	123.43(14)	C(14)-C(13)-H(13A)	109.3
C(1)-C(2)-C(3)	119.21(15)	C(12)-C(13)-H(13B)	109.3
C(1)-C(2)-C(16)	118.83(14)	C(14)-C(13)-H(13B)	109.3
C(3)-C(2)-C(16)	121.93(14)	H(13A)-C(13)-H(13B)	108.0
C(2)-C(3)-C(4)	120.44(15)	C(15)-C(14)-C(13)	115.61(14)
C(2)-C(3)-C(17)	124.27(14)	C(15)-C(14)-H(14A)	108.4
C(4)-C(3)-C(17)	115.27(14)	C(13)-C(14)-H(14A)	108.4
C(5)-C(4)-C(3)	119.28(15)	C(15)-C(14)-H(14B)	108.4
C(5)-C(4)-C(26)	122.12(14)	C(13)-C(14)-H(14B)	108.4
C(3)-C(4)-C(26)	117.99(14)	H(14A)-C(14)-H(14B)	107.4
C(6)-C(5)-C(4)	119.84(15)	C(16)-C(15)-C(14)	116.15(14)
C(6)-C(5)-C(27)	119.99(14)	C(16)-C(15)-H(15A)	108.2
C(4)-C(5)-C(27)	120.02(14)	C(14)-C(15)-H(15A)	108.2
C(5)-C(6)-C(1)	120.47(15)	C(16)-C(15)-H(15B)	108.2
C(5)-C(6)-C(36)	120.82(14)	C(14)-C(15)-H(15B)	108.2
C(1)-C(6)-C(36)	118.70(14)	H(15A)-C(15)-H(15B)	107.4
C(8)-C(7)-C(12)	119.38(15)	F(1)-C(16)-F(2)	102.03(13)
C(8)-C(7)-C(1)	118.37(15)	F(1)-C(16)-C(15)	109.05(13)
C(12)-C(7)-C(1)	122.24(15)	F(2)-C(16)-C(15)	109.80(13)
C(9)-C(8)-C(7)	121.36(16)	F(1)-C(16)-C(2)	109.96(13)
C(9)-C(8)-H(8)	119.3	F(2)-C(16)-C(2)	108.68(13)
C(7)-C(8)-H(8)	119.3	C(15)-C(16)-C(2)	116.36(14)
C(8)-C(9)-C(10)	119.33(17)	F(4)-C(17)-F(3)	101.32(13)
C(8)-C(9)-H(9)	120.3	F(4)-C(17)-C(18)	109.14(14)
C(10)-C(9)-H(9)	120.3	F(3)-C(17)-C(18)	109.48(14)
C(11)-C(10)-C(9)	119.63(17)	F(4)-C(17)-C(3)	107.22(13)
C(11)-C(10)-H(10)	120.2	F(3)-C(17)-C(3)	110.10(13)
C(9)-C(10)-H(10)	120.2	C(18)-C(17)-C(3)	118.21(14)
C(10)-C(11)-C(12)	121.84(17)	C(17)-C(18)-C(19)	119.17(15)
C(10)-C(11)-H(11)	119.1	C(17)-C(18)-H(18A)	107.5
C(12)-C(11)-H(11)	119.1	C(19)-C(18)-H(18A)	107.5
C(11)-C(12)-C(7)	118.45(17)	C(17)-C(18)-H(18B)	107.5
C(11)-C(12)-C(13)	118.52(16)	C(19)-C(18)-H(18B)	107.5
C(7)-C(12)-C(13)	122.86(15)	H(18A)-C(18)-H(18B)	107.0

C(18)-C(19)-C(20)	116.37(15)	C(30)-C(29)-H(29A)	108.0
C(18)-C(19)-H(19A)	108.2	C(28)-C(29)-H(29B)	108.0
C(20)-C(19)-H(19A)	108.2	C(30)-C(29)-H(29B)	108.0
C(18)-C(19)-H(19B)	108.2	H(29A)-C(29)-H(29B)	107.3
C(20)-C(19)-H(19B)	108.2	C(31)-C(30)-C(29)	112.36(15)
H(19A)-C(19)-H(19B)	107.3	C(31)-C(30)-H(30A)	109.1
C(21)-C(20)-C(19)	111.55(15)	C(29)-C(30)-H(30A)	109.1
C(21)-C(20)-H(20A)	109.3	C(31)-C(30)-H(30B)	109.1
C(19)-C(20)-H(20A)	109.3	C(29)-C(30)-H(30B)	109.1
C(21)-C(20)-H(20B)	109.3	H(30A)-C(30)-H(30B)	107.9
C(19)-C(20)-H(20B)	109.3	C(32)-C(31)-C(36)	118.18(17)
H(20A)-C(20)-H(20B)	108.0	C(32)-C(31)-C(30)	119.51(17)
C(22)-C(21)-C(26)	119.17(17)	C(36)-C(31)-C(30)	122.19(15)
C(22)-C(21)-C(20)	120.01(16)	C(33)-C(32)-C(31)	121.73(19)
C(26)-C(21)-C(20)	120.56(15)	C(33)-C(32)-H(32)	119.1
C(23)-C(22)-C(21)	121.03(18)	C(31)-C(32)-H(32)	119.1
C(23)-C(22)-H(22)	119.5	C(32)-C(33)-C(34)	119.75(17)
C(21)-C(22)-H(22)	119.5	C(32)-C(33)-H(33)	120.1
C(22)-C(23)-C(24)	119.64(17)	C(34)-C(33)-H(33)	120.1
C(22)-C(23)-H(23)	120.2	C(33)-C(34)-C(35)	119.50(18)
C(24)-C(23)-H(23)	120.2	C(33)-C(34)-H(34)	120.2
C(25)-C(24)-C(23)	120.10(18)	C(35)-C(34)-H(34)	120.2
C(25)-C(24)-H(24)	119.9	C(34)-C(35)-C(36)	120.67(18)
C(23)-C(24)-H(24)	119.9	C(34)-C(35)-H(35)	119.7
C(24)-C(25)-C(26)	120.70(18)	C(36)-C(35)-H(35)	119.7
C(24)-C(25)-H(25)	119.6	C(35)-C(36)-C(31)	120.12(16)
C(26)-C(25)-H(25)	119.6	C(35)-C(36)-C(6)	118.86(15)
C(25)-C(26)-C(21)	119.26(16)	C(31)-C(36)-C(6)	120.95(15)
C(25)-C(26)-C(4)	124.15(15)	C(38)-C(37)-C(42)	119.88(15)
C(21)-C(26)-C(4)	116.57(15)	C(38)-C(37)-C(43)	124.82(15)
F(6)-C(27)-F(5)	102.60(12)	C(42)-C(37)-C(43)	115.30(15)
F(6)-C(27)-C(28)	108.22(14)	C(37)-C(38)-C(39)	119.31(15)
F(5)-C(27)-C(28)	110.18(14)	C(37)-C(38)-C(52)	122.97(15)
F(6)-C(27)-C(5)	109.22(13)	C(39)-C(38)-C(52)	117.70(15)
F(5)-C(27)-C(5)	111.48(13)	C(40)-C(39)-C(38)	120.00(15)
C(28)-C(27)-C(5)	114.42(14)	C(40)-C(39)-C(53)	117.64(15)
C(27)-C(28)-C(29)	116.55(15)	C(38)-C(39)-C(53)	121.97(15)
C(27)-C(28)-H(28A)	108.2	C(39)-C(40)-C(41)	120.19(16)
C(29)-C(28)-H(28A)	108.2	C(39)-C(40)-C(62)	116.36(15)
C(27)-C(28)-H(28B)	108.2	C(41)-C(40)-C(62)	123.44(16)
C(29)-C(28)-H(28B)	108.2	C(42)-C(41)-C(40)	119.12(16)
H(28A)-C(28)-H(28B)	107.3	C(42)-C(41)-C(63)	119.70(17)
C(28)-C(29)-C(30)	117.10(15)	C(40)-C(41)-C(63)	121.02(18)
C(28)-C(29)-H(29A)	108.0	C(42)-C(41)-C(63A)	112.2(4)

C(40)-C(41)-C(63A)	122.9(3)	F(8)-C(52)-C(38)	106.49(14)
C(63)-C(41)-C(63A)	28.2(3)	F(7)-C(52)-C(38)	107.57(13)
C(41)-C(42)-C(37)	120.26(16)	C(51)-C(52)-C(38)	125.14(15)
C(41)-C(42)-C(72)	122.07(16)	C(54)-C(53)-C(58)	119.99(17)
C(37)-C(42)-C(72)	117.66(15)	C(54)-C(53)-C(39)	122.94(16)
C(44)-C(43)-C(48)	119.35(16)	C(58)-C(53)-C(39)	117.07(15)
C(44)-C(43)-C(37)	117.95(15)	C(55)-C(54)-C(53)	120.29(19)
C(48)-C(43)-C(37)	122.41(15)	C(55)-C(54)-H(54)	119.9
C(45)-C(44)-C(43)	121.10(17)	C(53)-C(54)-H(54)	119.9
C(45)-C(44)-H(44)	119.4	C(56)-C(55)-C(54)	120.02(19)
C(43)-C(44)-H(44)	119.4	C(56)-C(55)-H(55)	120.0
C(46)-C(45)-C(44)	119.57(17)	C(54)-C(55)-H(55)	120.0
C(46)-C(45)-H(45)	120.2	C(55)-C(56)-C(57)	119.71(18)
C(44)-C(45)-H(45)	120.2	C(55)-C(56)-H(56)	120.1
C(45)-C(46)-C(47)	119.70(17)	C(57)-C(56)-H(56)	120.1
C(45)-C(46)-H(46)	120.1	C(56)-C(57)-C(58)	121.4(2)
C(47)-C(46)-H(46)	120.1	C(56)-C(57)-H(57)	119.3
C(46)-C(47)-C(48)	121.53(18)	C(58)-C(57)-H(57)	119.3
C(46)-C(47)-H(47)	119.2	C(57)-C(58)-C(53)	118.52(18)
C(48)-C(47)-H(47)	119.2	C(57)-C(58)-C(59)	120.38(19)
C(47)-C(48)-C(43)	118.72(17)	C(53)-C(58)-C(59)	121.01(17)
C(47)-C(48)-C(49)	120.85(17)	C(58)-C(59)-C(60)	112.45(16)
C(43)-C(48)-C(49)	120.12(16)	C(58)-C(59)-H(59A)	109.1
C(48)-C(49)-C(50)	109.43(14)	C(60)-C(59)-H(59A)	109.1
C(48)-C(49)-H(49A)	109.8	C(58)-C(59)-H(59B)	109.1
C(50)-C(49)-H(49A)	109.8	C(60)-C(59)-H(59B)	109.1
C(48)-C(49)-H(49B)	109.8	H(59A)-C(59)-H(59B)	107.8
C(50)-C(49)-H(49B)	109.8	C(61)-C(60)-C(59)	117.24(17)
H(49A)-C(49)-H(49B)	108.2	C(61)-C(60)-H(60A)	108.0
C(51)-C(50)-C(49)	113.42(15)	C(59)-C(60)-H(60A)	108.0
C(51)-C(50)-H(50A)	108.9	C(61)-C(60)-H(60B)	108.0
C(49)-C(50)-H(50A)	108.9	C(59)-C(60)-H(60B)	108.0
C(51)-C(50)-H(50B)	108.9	H(60A)-C(60)-H(60B)	107.2
C(49)-C(50)-H(50B)	108.9	C(60)-C(61)-C(62)	118.41(16)
H(50A)-C(50)-H(50B)	107.7	C(60)-C(61)-H(61A)	107.7
C(52)-C(51)-C(50)	116.51(15)	C(62)-C(61)-H(61A)	107.7
C(52)-C(51)-H(51A)	108.2	C(60)-C(61)-H(61B)	107.7
C(50)-C(51)-H(51A)	108.2	C(62)-C(61)-H(61B)	107.7
C(52)-C(51)-H(51B)	108.2	H(61A)-C(61)-H(61B)	107.1
C(50)-C(51)-H(51B)	108.2	F(10)-C(62)-F(9)	100.24(15)
H(51A)-C(51)-H(51B)	107.3	F(10)-C(62)-C(61)	109.20(14)
F(8)-C(52)-F(7)	105.36(13)	F(9)-C(62)-C(61)	109.96(15)
F(8)-C(52)-C(51)	106.19(14)	F(10)-C(62)-C(40)	107.09(14)
F(7)-C(52)-C(51)	104.62(14)	F(9)-C(62)-C(40)	110.19(15)

C(61)-C(62)-C(40)	118.55(16)	C(69)-C(68)-H(68)	119.0
F(12)-C(63)-F(11)	101.8(3)	C(67)-C(68)-H(68)	119.0
F(12)-C(63)-C(64)	109.6(2)	C(70)-C(69)-C(68)	119.63(18)
F(11)-C(63)-C(64)	110.1(3)	C(70)-C(69)-H(69)	120.2
F(12)-C(63)-C(41)	107.8(2)	C(68)-C(69)-H(69)	120.2
F(11)-C(63)-C(41)	106.6(2)	C(71)-C(70)-C(69)	119.49(19)
C(64)-C(63)-C(41)	119.5(3)	C(71)-C(70)-H(70)	120.3
C(63)-C(64)-C(65)	117.2(2)	C(69)-C(70)-H(70)	120.3
C(63)-C(64)-H(64A)	108.0	C(70)-C(71)-C(72)	121.62(18)
C(65)-C(64)-H(64A)	108.0	C(70)-C(71)-H(71)	119.2
C(63)-C(64)-H(64B)	108.0	C(72)-C(71)-H(71)	119.2
C(65)-C(64)-H(64B)	108.0	C(71)-C(72)-C(67)	119.73(16)
H(64A)-C(64)-H(64B)	107.2	C(71)-C(72)-C(42)	118.53(16)
C(64)-C(65)-C(66)	112.2(2)	C(67)-C(72)-C(42)	121.73(16)
C(64)-C(65)-H(65A)	109.2		
C(66)-C(65)-H(65A)	109.2		
C(64)-C(65)-H(65B)	109.2		
C(66)-C(65)-H(65B)	109.2		
H(65A)-C(65)-H(65B)	107.9		
C(67)-C(66)-C(65)	111.41(19)		
C(67)-C(66)-H(66A)	109.3		
C(65)-C(66)-H(66A)	109.3		
C(67)-C(66)-H(66B)	109.3		
C(65)-C(66)-H(66B)	109.3		
H(66A)-C(66)-H(66B)	108.0		
F(12A)-C(63A)-F(11A)	99.7(7)		
F(12A)-C(63A)-C(64A)	109.2(7)		
F(11A)-C(63A)-C(64A)	111.6(7)		
F(12A)-C(63A)-C(41)	115.7(7)		
F(11A)-C(63A)-C(41)	112.6(6)		
C(64A)-C(63A)-C(41)	108.0(7)		
C(65A)-C(64A)-C(63A)	119.9(7)		
C(65A)-C(64A)-H(64C)	107.3		
C(63A)-C(64A)-H(64C)	107.3		
C(65A)-C(64A)-H(64D)	107.3		
C(63A)-C(64A)-H(64D)	107.3		
H(64C)-C(64A)-H(64D)	106.9		
C(64A)-C(65A)-H(65C)	107.4		
C(64A)-C(65A)-H(65D)	107.4		
H(65C)-C(65A)-H(65D)	106.9		
C(72)-C(67)-C(68)	117.60(17)		
C(72)-C(67)-C(66)	123.43(18)		
C(68)-C(67)-C(66)	118.90(18)		
C(69)-C(68)-C(67)	121.92(18)		

Symmetry transformations used to generate equivalent atoms:

Anisotropic displacement parameters ($\text{\AA}^2 \times 10^3$). The anisotropic displacement factor exponent takes the form: $-2p^2 [h^2 a^{*2} U^{11} + \dots + 2 h k a^* b^* U^{12}]$

	U11	U22	U33	U23	U13	U12
C(1)	16(1)	15(1)	19(1)	3(1)	4(1)	2(1)
C(2)	16(1)	17(1)	21(1)	3(1)	3(1)	4(1)
C(3)	16(1)	15(1)	22(1)	2(1)	5(1)	4(1)
C(4)	16(1)	16(1)	19(1)	4(1)	6(1)	4(1)
C(5)	15(1)	17(1)	19(1)	5(1)	5(1)	4(1)
C(6)	16(1)	15(1)	19(1)	3(1)	5(1)	4(1)
C(7)	25(1)	15(1)	18(1)	4(1)	3(1)	9(1)
C(8)	25(1)	19(1)	22(1)	5(1)	4(1)	10(1)
C(9)	34(1)	26(1)	22(1)	6(1)	11(1)	13(1)
C(10)	43(1)	30(1)	18(1)	0(1)	5(1)	14(1)
C(11)	31(1)	23(1)	21(1)	1(1)	-1(1)	7(1)
C(12)	26(1)	15(1)	20(1)	4(1)	2(1)	7(1)
C(13)	22(1)	21(1)	22(1)	3(1)	1(1)	4(1)
C(14)	20(1)	28(1)	24(1)	2(1)	1(1)	7(1)
C(15)	22(1)	28(1)	23(1)	4(1)	1(1)	13(1)
C(16)	24(1)	20(1)	20(1)	2(1)	3(1)	10(1)
C(17)	20(1)	28(1)	22(1)	1(1)	3(1)	12(1)
C(18)	27(1)	26(1)	31(1)	-5(1)	0(1)	14(1)
C(19)	30(1)	19(1)	33(1)	2(1)	2(1)	8(1)
C(20)	22(1)	18(1)	27(1)	0(1)	6(1)	3(1)
C(21)	18(1)	23(1)	26(1)	-2(1)	3(1)	11(1)
C(22)	22(1)	28(1)	31(1)	-8(1)	-1(1)	13(1)
C(23)	31(1)	43(1)	23(1)	-11(1)	-5(1)	24(1)
C(24)	34(1)	48(1)	19(1)	3(1)	6(1)	28(1)
C(25)	23(1)	31(1)	24(1)	5(1)	7(1)	14(1)
C(26)	18(1)	24(1)	19(1)	0(1)	3(1)	11(1)
C(27)	26(1)	21(1)	17(1)	2(1)	4(1)	12(1)
C(28)	20(1)	27(1)	29(1)	0(1)	0(1)	11(1)
C(29)	20(1)	33(1)	33(1)	4(1)	6(1)	11(1)
C(30)	23(1)	35(1)	29(1)	10(1)	12(1)	14(1)
C(31)	29(1)	32(1)	17(1)	7(1)	8(1)	17(1)
C(32)	42(1)	46(1)	24(1)	7(1)	11(1)	31(1)
C(33)	62(1)	41(1)	25(1)	2(1)	8(1)	38(1)
C(34)	54(1)	23(1)	23(1)	0(1)	0(1)	18(1)
C(35)	32(1)	22(1)	19(1)	2(1)	3(1)	11(1)
C(36)	26(1)	22(1)	14(1)	4(1)	4(1)	12(1)
C(37)	18(1)	18(1)	24(1)	0(1)	5(1)	5(1)
C(38)	18(1)	22(1)	22(1)	1(1)	3(1)	6(1)
C(39)	18(1)	23(1)	23(1)	1(1)	4(1)	7(1)

C(40)	24(1)	28(1)	26(1)	-4(1)	-1(1)	13(1)
C(41)	25(1)	36(1)	34(1)	-12(1)	-6(1)	17(1)
C(42)	20(1)	22(1)	30(1)	-3(1)	2(1)	8(1)
C(43)	15(1)	20(1)	23(1)	-1(1)	1(1)	6(1)
C(44)	20(1)	21(1)	24(1)	2(1)	0(1)	7(1)
C(45)	24(1)	20(1)	34(1)	-3(1)	-2(1)	9(1)
C(46)	29(1)	33(1)	31(1)	-10(1)	-1(1)	15(1)
C(47)	24(1)	38(1)	22(1)	-2(1)	4(1)	11(1)
C(48)	16(1)	25(1)	24(1)	1(1)	2(1)	5(1)
C(49)	25(1)	25(1)	27(1)	4(1)	8(1)	5(1)
C(50)	31(1)	28(1)	25(1)	8(1)	7(1)	9(1)
C(51)	26(1)	25(1)	25(1)	3(1)	2(1)	10(1)
C(52)	22(1)	24(1)	26(1)	2(1)	5(1)	9(1)
C(53)	25(1)	29(1)	16(1)	0(1)	2(1)	14(1)
C(54)	24(1)	42(1)	18(1)	0(1)	2(1)	16(1)
C(55)	36(1)	67(2)	22(1)	-4(1)	0(1)	36(1)
C(56)	62(2)	57(1)	29(1)	-5(1)	-4(1)	48(1)
C(57)	58(1)	33(1)	25(1)	-1(1)	-2(1)	26(1)
C(58)	36(1)	29(1)	18(1)	0(1)	3(1)	15(1)
C(59)	35(1)	29(1)	28(1)	-1(1)	10(1)	4(1)
C(60)	28(1)	40(1)	33(1)	-6(1)	4(1)	5(1)
C(61)	33(1)	34(1)	23(1)	-6(1)	1(1)	17(1)
C(62)	31(1)	36(1)	21(1)	-1(1)	-1(1)	20(1)
C(63)	23(2)	34(2)	32(2)	-11(1)	-3(1)	17(2)
C(64)	38(2)	47(2)	20(1)	-2(1)	-4(1)	28(2)
C(65)	43(2)	43(2)	26(1)	2(1)	-1(1)	28(2)
C(66)	36(1)	52(1)	24(1)	4(1)	2(1)	7(1)
C(63A)	20(5)	14(4)	27(5)	-2(4)	-1(4)	6(4)
C(64A)	36(5)	18(4)	25(4)	3(3)	1(4)	14(4)
C(65A)	40(5)	16(4)	18(4)	3(4)	8(4)	14(4)
C(66A)	36(1)	52(1)	24(1)	4(1)	2(1)	7(1)
C(67)	21(1)	27(1)	24(1)	1(1)	-2(1)	6(1)
C(68)	31(1)	23(1)	40(1)	2(1)	-8(1)	12(1)
C(69)	27(1)	34(1)	45(1)	-10(1)	-1(1)	19(1)
C(70)	23(1)	40(1)	32(1)	-4(1)	5(1)	13(1)
C(71)	19(1)	24(1)	29(1)	2(1)	2(1)	6(1)
C(72)	18(1)	19(1)	24(1)	-4(1)	-1(1)	6(1)
F(1)	27(1)	24(1)	21(1)	7(1)	5(1)	11(1)
F(2)	28(1)	19(1)	30(1)	2(1)	2(1)	12(1)
F(3)	20(1)	32(1)	28(1)	-2(1)	1(1)	14(1)
F(4)	28(1)	36(1)	23(1)	3(1)	9(1)	16(1)
F(5)	32(1)	21(1)	22(1)	3(1)	4(1)	14(1)
F(6)	34(1)	29(1)	16(1)	4(1)	4(1)	16(1)
F(7)	45(1)	29(1)	27(1)	3(1)	2(1)	21(1)

F(8)	18(1)	42(1)	29(1)	4(1)	3(1)	10(1)
F(9)	64(1)	46(1)	26(1)	-3(1)	-13(1)	35(1)
F(10)	32(1)	44(1)	22(1)	4(1)	8(1)	14(1)
F(11)	27(1)	38(1)	34(1)	-17(1)	-8(1)	17(1)
F(12)	21(1)	37(1)	34(1)	-11(1)	-4(1)	15(1)
F(11A)	30(3)	15(3)	29(3)	-2(2)	-6(2)	10(2)
F(12A)	15(2)	30(3)	33(3)	-1(2)	6(2)	5(2)

Hydrogen coordinates (x 10⁴) and isotropic displacement parameters (Å²x 10³).

	x	y	z	U(eq)
H(8)	9919	8867	5202	26
H(9)	9491	8132	4282	32
H(10)	7229	6745	3828	37
H(11)	5439	6165	4291	33
H(13A)	5622	6837	5684	29
H(13B)	4621	5976	5132	29
H(14A)	4897	8201	4816	31
H(14B)	3767	7450	5169	31
H(15A)	4994	9700	5485	29
H(15B)	5171	8797	5957	29
H(18A)	8821	12252	7486	33
H(18B)	7987	12520	6944	33
H(19A)	10338	13662	6979	35
H(19B)	9644	12603	6457	35
H(20A)	10878	11499	6751	29
H(20B)	11920	12887	7087	29
H(22)	12180	13172	8072	33
H(23)	11766	12286	8895	37
H(24)	10101	10118	8890	36
H(25)	8940	8822	8066	30
H(28A)	12749	9136	7533	31
H(28B)	12227	10062	7173	31
H(29A)	12985	8148	6780	34
H(29B)	13736	9702	6748	34
H(30A)	11592	9405	6093	33
H(30B)	12645	8981	5873	33
H(32)	12115	6619	5755	39
H(33)	10475	4443	5565	44
H(34)	8201	3880	5640	41
H(35)	7606	5515	5915	30

H(44)	4880	3181	8273	27
H(45)	4704	1564	7635	33
H(46)	5359	2156	6800	38
H(47)	6109	4338	6597	35
H(49A)	6880	6672	6882	33
H(49B)	6767	7101	7478	33
H(50A)	5111	7491	6901	35
H(50B)	4626	6169	6512	35
H(51A)	2903	5804	6977	32
H(51B)	3642	4913	7222	32
H(54)	2596	6802	8775	33
H(55)	1642	8303	8786	45
H(56)	3003	10547	8752	52
H(57)	5334	11298	8755	45
H(59A)	7259	10881	8651	40
H(59B)	7098	9399	8600	40
H(60A)	8466	9957	9424	45
H(60B)	8141	11176	9541	45
H(61A)	6187	9811	9852	36
H(61B)	7523	9734	10199	36
H(64A)	7012	5660	10178	39
H(64B)	8599	6325	10474	39
H(65A)	7766	4020	10292	42
H(65B)	9023	4803	9998	42
H(66A)	6841	2923	9463	51
H(66B)	6323	4056	9372	51
H(64C)	9615	6296	9886	31
H(64D)	9114	6967	10306	31
H(65C)	6852	5333	9981	28
H(65D)	7901	4838	10320	28
H(66C)	7312	3147	9607	51
H(66D)	6151	3554	9296	51
H(68)	8865	3106	9119	40
H(69)	10183	3798	8455	41
H(70)	10064	5459	7923	39
H(71)	8588	6372	8046	31

Crystal data and structure refinement for Dimer 8.14

Empirical formula	C ₅₁ H ₅₂ F ₈ O ₈	
Formula weight	944.93	
Temperature	100(2) K	
Wavelength	1.54178 Å	
Crystal system	Triclinic	
Space group	P-1	
Unit cell dimensions	a = 10.9513(5) Å	a = 63.010(2)°.
	b = 14.9709(7) Å	b = 75.207(2)°.
	c = 15.4572(7) Å	g = 80.666(2)°.
Volume	2180.20(17) Å ³	
Z	2	
Density (calculated)	1.439 Mg/m ³	
Absorption coefficient	1.012 mm ⁻¹	
F(000)	988	
Crystal size	0.12 x 0.10 x 0.06 mm ³	
Crystal color/habit	colorless prism	
Theta range for data collection	3.28 to 68.36°.	
Index ranges	-13<=h<=13, -13<=k<=17, -18<=l<=18	
Reflections collected	38046	
Independent reflections	7750 [R(int) = 0.0245]	
Completeness to theta = 67.00°	97.9 %	
Absorption correction	Semi-empirical from equivalents	
Max. and min. transmission	0.9418 and 0.8882	
Refinement method	Full-matrix least-squares on F ²	
Data / restraints / parameters	7750 / 2 / 616	
Goodness-of-fit on F ²	1.025	
Final R indices [I>2sigma(I)]	R1 = 0.0336, wR2 = 0.0839	
R indices (all data)	R1 = 0.0358, wR2 = 0.0860	
Largest diff. peak and hole	0.347 and -0.428 e.Å ⁻³	

Atomic coordinates ($\times 10^4$) and equivalent isotropic displacement parameters ($\text{\AA}^2 \times 10^3$). U(eq) is defined as one third of the trace of the orthogonalized U^{ij} tensor.

	x	y	z	U(eq)
C(1)	3429(1)	8602(1)	-1061(1)	15(1)
C(2)	3980(1)	9348(1)	-837(1)	19(1)
C(3)	3214(1)	10276(1)	-813(1)	23(1)
C(4)	2680(1)	10975(1)	-1737(1)	24(1)
C(5)	1339(1)	10712(1)	-1679(1)	21(1)
C(6)	1118(1)	10683(1)	-2592(1)	19(1)
C(7)	539(1)	11530(1)	-3256(1)	25(1)
C(8)	250(1)	11550(1)	-4085(1)	29(1)
C(9)	521(1)	10708(1)	-4264(1)	28(1)
C(10)	1101(1)	9854(1)	-3618(1)	21(1)
C(11)	1409(1)	9834(1)	-2789(1)	16(1)
C(12)	2053(1)	8889(1)	-2105(1)	14(1)
C(13)	1359(1)	8350(1)	-1019(1)	14(1)
C(14)	40(1)	8052(1)	-772(1)	15(1)
C(15)	-934(1)	8796(1)	-1026(1)	17(1)
C(16)	-2184(1)	8542(1)	-758(1)	19(1)
C(17)	-2478(1)	7542(1)	-231(1)	21(1)
C(18)	-1518(1)	6801(1)	7(1)	21(1)
C(19)	-254(1)	7039(1)	-262(1)	17(1)
C(20)	754(1)	6223(1)	90(1)	20(1)
C(21)	860(1)	6037(1)	1135(1)	24(1)
C(22)	828(1)	6990(1)	1270(1)	21(1)
C(23)	1937(1)	7639(1)	688(1)	18(1)
C(24)	2159(1)	8174(1)	-429(1)	14(1)
C(25)	3978(1)	5930(1)	7351(1)	15(1)
C(26)	4773(1)	4934(1)	7801(1)	17(1)
C(27)	5046(1)	4190(1)	7358(1)	20(1)
C(28)	3897(1)	3804(1)	7258(1)	19(1)
C(29)	3503(1)	4448(1)	6247(1)	18(1)
C(30)	2105(1)	4733(1)	6291(1)	16(1)
C(31)	1372(1)	4145(1)	6154(1)	18(1)
C(32)	96(1)	4379(1)	6143(1)	19(1)
C(33)	-477(1)	5225(1)	6260(1)	19(1)
C(34)	234(1)	5821(1)	6398(1)	17(1)
C(35)	1513(1)	5584(1)	6426(1)	15(1)
C(36)	2235(1)	6247(1)	6613(1)	15(1)
C(37)	3373(1)	6772(1)	5813(1)	14(1)
C(38)	3215(1)	7417(1)	4777(1)	15(1)
C(39)	2910(1)	6981(1)	4231(1)	16(1)

C(40)	2760(1)	7563(1)	3262(1)	19(1)
C(41)	2884(1)	8590(1)	2835(1)	22(1)
C(42)	3171(1)	9030(1)	3374(1)	20(1)
C(43)	3352(1)	8455(1)	4342(1)	17(1)
C(44)	3813(1)	8938(1)	4859(1)	19(1)
C(45)	5272(1)	8890(1)	4642(1)	22(1)
C(46)	5902(1)	7866(1)	4735(1)	20(1)
C(47)	5655(1)	7016(1)	5762(1)	18(1)
C(48)	4355(1)	6612(1)	6240(1)	14(1)
C(49)	7370(1)	7795(1)	7563(1)	20(1)
C(50)	7342(2)	6677(1)	8115(1)	27(1)
C(51)	8624(2)	8219(1)	6987(1)	38(1)
O(1)	3190(1)	9169(1)	-2029(1)	15(1)
O(2)	4307(1)	7801(1)	-1021(1)	18(1)
O(3)	2324(1)	8197(1)	-2525(1)	16(1)
O(4)	2767(1)	5619(1)	7463(1)	16(1)
O(5)	3922(1)	6492(1)	7879(1)	17(1)
O(6)	1363(1)	6977(1)	6788(1)	18(1)
O(7)	6428(1)	8348(1)	7584(1)	23(1)
O(8)	3992(1)	5755(1)	9811(1)	30(1)
F(1)	4376(1)	8819(1)	43(1)	25(1)
F(2)	5072(1)	9647(1)	-1547(1)	24(1)
F(3)	3019(1)	7073(1)	955(1)	23(1)
F(4)	1824(1)	8370(1)	1029(1)	23(1)
F(5)	5908(1)	5167(1)	7851(1)	20(1)
F(6)	4153(1)	4458(1)	8778(1)	20(1)
F(7)	6477(1)	6208(1)	5733(1)	25(1)
F(8)	6049(1)	7275(1)	6387(1)	27(1)

Bond lengths [Å] and angles [°].

C(1)-O(2)	1.3985(15)	C(4)-H(4B)	0.9900
C(1)-O(1)	1.4156(16)	C(5)-C(6)	1.512(2)
C(1)-C(24)	1.5252(17)	C(5)-H(5A)	0.9900
C(1)-C(2)	1.5522(18)	C(5)-H(5B)	0.9900
C(2)-F(1)	1.3706(16)	C(6)-C(7)	1.398(2)
C(2)-F(2)	1.3752(16)	C(6)-C(11)	1.408(2)
C(2)-C(3)	1.5126(19)	C(7)-C(8)	1.382(2)
C(3)-C(4)	1.532(2)	C(7)-H(7)	0.9500
C(3)-H(3A)	0.9900	C(8)-C(9)	1.380(2)
C(3)-H(3B)	0.9900	C(8)-H(8)	0.9500
C(4)-C(5)	1.5516(19)	C(9)-C(10)	1.392(2)
C(4)-H(4A)	0.9900	C(9)-H(9)	0.9500

C(10)-C(11)	1.392(2)	C(29)-C(30)	1.5137(18)
C(10)-H(10)	0.9500	C(29)-H(29A)	0.9900
C(11)-C(12)	1.5218(17)	C(29)-H(29B)	0.9900
C(12)-O(3)	1.4131(15)	C(30)-C(31)	1.3958(19)
C(12)-O(1)	1.4243(15)	C(30)-C(35)	1.4108(19)
C(12)-C(13)	1.5372(17)	C(31)-C(32)	1.387(2)
C(13)-C(24)	1.3353(18)	C(31)-H(31)	0.9500
C(13)-C(14)	1.4854(17)	C(32)-C(33)	1.387(2)
C(14)-C(15)	1.4011(18)	C(32)-H(32)	0.9500
C(14)-C(19)	1.4025(19)	C(33)-C(34)	1.389(2)
C(15)-C(16)	1.3876(19)	C(33)-H(33)	0.9500
C(15)-H(15)	0.9500	C(34)-C(35)	1.3953(19)
C(16)-C(17)	1.387(2)	C(34)-H(34)	0.9500
C(16)-H(16)	0.9500	C(35)-C(36)	1.5245(18)
C(17)-C(18)	1.385(2)	C(36)-O(6)	1.4063(15)
C(17)-H(17)	0.9500	C(36)-O(4)	1.4297(15)
C(18)-C(19)	1.3954(19)	C(36)-C(37)	1.5328(18)
C(18)-H(18)	0.9500	C(37)-C(48)	1.3360(19)
C(19)-C(20)	1.5085(19)	C(37)-C(38)	1.4866(18)
C(20)-C(21)	1.541(2)	C(38)-C(39)	1.4016(18)
C(20)-H(20A)	0.9900	C(38)-C(43)	1.402(2)
C(20)-H(20B)	0.9900	C(39)-C(40)	1.3865(19)
C(21)-C(22)	1.527(2)	C(39)-H(39)	0.9500
C(21)-H(21A)	0.9900	C(40)-C(41)	1.385(2)
C(21)-H(21B)	0.9900	C(40)-H(40)	0.9500
C(22)-C(23)	1.5033(19)	C(41)-C(42)	1.388(2)
C(22)-H(22A)	0.9900	C(41)-H(41)	0.9500
C(22)-H(22B)	0.9900	C(42)-C(43)	1.3950(19)
C(23)-F(3)	1.3780(15)	C(42)-H(42)	0.9500
C(23)-F(4)	1.3924(16)	C(43)-C(44)	1.5053(19)
C(23)-C(24)	1.5081(18)	C(44)-C(45)	1.5428(19)
C(25)-O(5)	1.3991(15)	C(44)-H(44A)	0.9900
C(25)-O(4)	1.4197(15)	C(44)-H(44B)	0.9900
C(25)-C(48)	1.5317(17)	C(45)-C(46)	1.534(2)
C(25)-C(26)	1.5524(18)	C(45)-H(45A)	0.9900
C(26)-F(5)	1.3743(15)	C(45)-H(45B)	0.9900
C(26)-F(6)	1.3806(15)	C(46)-C(47)	1.5078(19)
C(26)-C(27)	1.5097(18)	C(46)-H(46A)	0.9900
C(27)-C(28)	1.5353(19)	C(46)-H(46B)	0.9900
C(27)-H(27A)	0.9900	C(47)-F(8)	1.3702(15)
C(27)-H(27B)	0.9900	C(47)-F(7)	1.3960(16)
C(28)-C(29)	1.5493(18)	C(47)-C(48)	1.5086(18)
C(28)-H(28A)	0.9900	C(49)-O(7)	1.2172(17)
C(28)-H(28B)	0.9900	C(49)-C(51)	1.492(2)

C(49)-C(50)	1.496(2)	O(2)-H(2)	0.8400
C(50)-H(50A)	0.9800	O(3)-H(3)	0.8400
C(50)-H(50B)	0.9800	O(5)-H(5)	0.8400
C(50)-H(50C)	0.9800	O(6)-H(6)	0.8400
C(51)-H(51A)	0.9800	O(8)-H(8X)	0.832(5)
C(51)-H(51B)	0.9800	O(8)-H(8Y)	0.827(5)
C(51)-H(51C)	0.9800		
O(2)-C(1)-O(1)	111.07(10)	C(9)-C(8)-C(7)	119.58(14)
O(2)-C(1)-C(24)	108.33(10)	C(9)-C(8)-H(8)	120.2
O(1)-C(1)-C(24)	104.19(10)	C(7)-C(8)-H(8)	120.2
O(2)-C(1)-C(2)	110.04(10)	C(8)-C(9)-C(10)	119.74(14)
O(1)-C(1)-C(2)	105.02(10)	C(8)-C(9)-H(9)	120.1
C(24)-C(1)-C(2)	117.96(11)	C(10)-C(9)-H(9)	120.1
F(1)-C(2)-F(2)	104.94(10)	C(11)-C(10)-C(9)	120.89(14)
F(1)-C(2)-C(3)	108.27(11)	C(11)-C(10)-H(10)	119.6
F(2)-C(2)-C(3)	108.30(11)	C(9)-C(10)-H(10)	119.6
F(1)-C(2)-C(1)	108.14(11)	C(10)-C(11)-C(6)	119.79(12)
F(2)-C(2)-C(1)	105.01(10)	C(10)-C(11)-C(12)	119.39(12)
C(3)-C(2)-C(1)	121.05(11)	C(6)-C(11)-C(12)	120.82(12)
C(2)-C(3)-C(4)	116.51(12)	O(3)-C(12)-O(1)	110.55(10)
C(2)-C(3)-H(3A)	108.2	O(3)-C(12)-C(11)	108.53(10)
C(4)-C(3)-H(3A)	108.2	O(1)-C(12)-C(11)	107.60(10)
C(2)-C(3)-H(3B)	108.2	O(3)-C(12)-C(13)	108.48(10)
C(4)-C(3)-H(3B)	108.2	O(1)-C(12)-C(13)	103.63(10)
H(3A)-C(3)-H(3B)	107.3	C(11)-C(12)-C(13)	117.90(10)
C(3)-C(4)-C(5)	112.93(12)	C(24)-C(13)-C(14)	130.27(12)
C(3)-C(4)-H(4A)	109.0	C(24)-C(13)-C(12)	108.75(11)
C(5)-C(4)-H(4A)	109.0	C(14)-C(13)-C(12)	120.85(11)
C(3)-C(4)-H(4B)	109.0	C(15)-C(14)-C(19)	119.41(12)
C(5)-C(4)-H(4B)	109.0	C(15)-C(14)-C(13)	119.47(12)
H(4A)-C(4)-H(4B)	107.8	C(19)-C(14)-C(13)	121.10(12)
C(6)-C(5)-C(4)	116.48(12)	C(16)-C(15)-C(14)	120.69(13)
C(6)-C(5)-H(5A)	108.2	C(16)-C(15)-H(15)	119.7
C(4)-C(5)-H(5A)	108.2	C(14)-C(15)-H(15)	119.7
C(6)-C(5)-H(5B)	108.2	C(17)-C(16)-C(15)	119.93(13)
C(4)-C(5)-H(5B)	108.2	C(17)-C(16)-H(16)	120.0
H(5A)-C(5)-H(5B)	107.3	C(15)-C(16)-H(16)	120.0
C(7)-C(6)-C(11)	117.88(13)	C(18)-C(17)-C(16)	119.67(13)
C(7)-C(6)-C(5)	118.35(13)	C(18)-C(17)-H(17)	120.2
C(11)-C(6)-C(5)	123.71(12)	C(16)-C(17)-H(17)	120.2
C(8)-C(7)-C(6)	122.10(14)	C(17)-C(18)-C(19)	121.37(13)
C(8)-C(7)-H(7)	118.9	C(17)-C(18)-H(18)	119.3
C(6)-C(7)-H(7)	118.9	C(19)-C(18)-H(18)	119.3

C(18)-C(19)-C(14)	118.90(13)	C(28)-C(27)-H(27A)	108.1
C(18)-C(19)-C(20)	119.88(12)	C(26)-C(27)-H(27B)	108.1
C(14)-C(19)-C(20)	120.88(12)	C(28)-C(27)-H(27B)	108.1
C(19)-C(20)-C(21)	109.64(11)	H(27A)-C(27)-H(27B)	107.3
C(19)-C(20)-H(20A)	109.7	C(27)-C(28)-C(29)	113.04(11)
C(21)-C(20)-H(20A)	109.7	C(27)-C(28)-H(28A)	109.0
C(19)-C(20)-H(20B)	109.7	C(29)-C(28)-H(28A)	109.0
C(21)-C(20)-H(20B)	109.7	C(27)-C(28)-H(28B)	109.0
H(20A)-C(20)-H(20B)	108.2	C(29)-C(28)-H(28B)	109.0
C(22)-C(21)-C(20)	114.52(11)	H(28A)-C(28)-H(28B)	107.8
C(22)-C(21)-H(21A)	108.6	C(30)-C(29)-C(28)	115.96(11)
C(20)-C(21)-H(21A)	108.6	C(30)-C(29)-H(29A)	108.3
C(22)-C(21)-H(21B)	108.6	C(28)-C(29)-H(29A)	108.3
C(20)-C(21)-H(21B)	108.6	C(30)-C(29)-H(29B)	108.3
H(21A)-C(21)-H(21B)	107.6	C(28)-C(29)-H(29B)	108.3
C(23)-C(22)-C(21)	116.16(12)	H(29A)-C(29)-H(29B)	107.4
C(23)-C(22)-H(22A)	108.2	C(31)-C(30)-C(35)	118.19(12)
C(21)-C(22)-H(22A)	108.2	C(31)-C(30)-C(29)	118.34(12)
C(23)-C(22)-H(22B)	108.2	C(35)-C(30)-C(29)	123.42(12)
C(21)-C(22)-H(22B)	108.2	C(32)-C(31)-C(30)	121.92(13)
H(22A)-C(22)-H(22B)	107.4	C(32)-C(31)-H(31)	119.0
F(3)-C(23)-F(4)	104.41(10)	C(30)-C(31)-H(31)	119.0
F(3)-C(23)-C(22)	108.26(11)	C(31)-C(32)-C(33)	119.68(12)
F(4)-C(23)-C(22)	106.98(11)	C(31)-C(32)-H(32)	120.2
F(3)-C(23)-C(24)	108.70(10)	C(33)-C(32)-H(32)	120.2
F(4)-C(23)-C(24)	107.03(11)	C(32)-C(33)-C(34)	119.42(12)
C(22)-C(23)-C(24)	120.34(11)	C(32)-C(33)-H(33)	120.3
C(13)-C(24)-C(23)	128.76(12)	C(34)-C(33)-H(33)	120.3
C(13)-C(24)-C(1)	109.41(11)	C(33)-C(34)-C(35)	121.34(13)
C(23)-C(24)-C(1)	121.83(11)	C(33)-C(34)-H(34)	119.3
O(5)-C(25)-O(4)	111.59(10)	C(35)-C(34)-H(34)	119.3
O(5)-C(25)-C(48)	108.71(10)	C(34)-C(35)-C(30)	119.44(12)
O(4)-C(25)-C(48)	104.03(10)	C(34)-C(35)-C(36)	118.99(12)
O(5)-C(25)-C(26)	109.49(10)	C(30)-C(35)-C(36)	121.57(11)
O(4)-C(25)-C(26)	104.31(10)	O(6)-C(36)-O(4)	111.05(10)
C(48)-C(25)-C(26)	118.51(11)	O(6)-C(36)-C(35)	107.52(10)
F(5)-C(26)-F(6)	104.58(10)	O(4)-C(36)-C(35)	107.58(10)
F(5)-C(26)-C(27)	107.84(10)	O(6)-C(36)-C(37)	108.82(10)
F(6)-C(26)-C(27)	108.51(11)	O(4)-C(36)-C(37)	103.78(10)
F(5)-C(26)-C(25)	108.02(10)	C(35)-C(36)-C(37)	118.04(10)
F(6)-C(26)-C(25)	105.00(10)	C(48)-C(37)-C(38)	131.06(12)
C(27)-C(26)-C(25)	121.65(11)	C(48)-C(37)-C(36)	108.96(11)
C(26)-C(27)-C(28)	116.61(11)	C(38)-C(37)-C(36)	119.68(11)
C(26)-C(27)-H(27A)	108.1	C(39)-C(38)-C(43)	119.51(12)

C(39)-C(38)-C(37)	119.46(12)	O(7)-C(49)-C(51)	120.45(14)
C(43)-C(38)-C(37)	121.03(12)	O(7)-C(49)-C(50)	122.53(13)
C(40)-C(39)-C(38)	120.76(12)	C(51)-C(49)-C(50)	117.02(13)
C(40)-C(39)-H(39)	119.6	C(49)-C(50)-H(50A)	109.5
C(38)-C(39)-H(39)	119.6	C(49)-C(50)-H(50B)	109.5
C(41)-C(40)-C(39)	119.77(13)	H(50A)-C(50)-H(50B)	109.5
C(41)-C(40)-H(40)	120.1	C(49)-C(50)-H(50C)	109.5
C(39)-C(40)-H(40)	120.1	H(50A)-C(50)-H(50C)	109.5
C(40)-C(41)-C(42)	119.87(13)	H(50B)-C(50)-H(50C)	109.5
C(40)-C(41)-H(41)	120.1	C(49)-C(51)-H(51A)	109.5
C(42)-C(41)-H(41)	120.1	C(49)-C(51)-H(51B)	109.5
C(41)-C(42)-C(43)	121.24(13)	H(51A)-C(51)-H(51B)	109.5
C(41)-C(42)-H(42)	119.4	C(49)-C(51)-H(51C)	109.5
C(43)-C(42)-H(42)	119.4	H(51A)-C(51)-H(51C)	109.5
C(42)-C(43)-C(38)	118.83(12)	H(51B)-C(51)-H(51C)	109.5
C(42)-C(43)-C(44)	119.64(12)	C(1)-O(1)-C(12)	110.73(9)
C(38)-C(43)-C(44)	121.24(12)	C(1)-O(2)-H(2)	109.5
C(43)-C(44)-C(45)	110.51(11)	C(12)-O(3)-H(3)	109.5
C(43)-C(44)-H(44A)	109.5	C(25)-O(4)-C(36)	110.81(9)
C(45)-C(44)-H(44A)	109.5	C(25)-O(5)-H(5)	109.5
C(43)-C(44)-H(44B)	109.5	C(36)-O(6)-H(6)	109.5
C(45)-C(44)-H(44B)	109.5	H(8X)-O(8)-H(8Y)	95.4(18)
H(44A)-C(44)-H(44B)	108.1		
C(46)-C(45)-C(44)	114.66(11)		
C(46)-C(45)-H(45A)	108.6		
C(44)-C(45)-H(45A)	108.6		
C(46)-C(45)-H(45B)	108.6		
C(44)-C(45)-H(45B)	108.6		
H(45A)-C(45)-H(45B)	107.6		
C(47)-C(46)-C(45)	115.66(11)		
C(47)-C(46)-H(46A)	108.4		
C(45)-C(46)-H(46A)	108.4		
C(47)-C(46)-H(46B)	108.4		
C(45)-C(46)-H(46B)	108.4		
H(46A)-C(46)-H(46B)	107.4		
F(8)-C(47)-F(7)	104.33(10)		
F(8)-C(47)-C(46)	108.23(11)		
F(7)-C(47)-C(46)	106.98(11)		
F(8)-C(47)-C(48)	109.01(10)		
F(7)-C(47)-C(48)	106.54(11)		
C(46)-C(47)-C(48)	120.57(11)		
C(37)-C(48)-C(47)	128.25(12)		
C(37)-C(48)-C(25)	109.48(11)		
C(47)-C(48)-C(25)	122.26(11)		

Anisotropic displacement parameters ($\text{\AA}^2 \times 10^3$. The anisotropic displacement factor exponent takes the form: $-2p^2 [h^2 a^* 2U^{11} + \dots + 2 h k a^* b^* U^{12}]$

	U ¹¹	U ²²	U ³³	U ²³	U ¹³	U ¹²
C(1)	15(1)	15(1)	17(1)	-8(1)	-3(1)	0(1)
C(2)	15(1)	23(1)	24(1)	-13(1)	-4(1)	-3(1)
C(3)	20(1)	24(1)	33(1)	-20(1)	-3(1)	-4(1)
C(4)	22(1)	16(1)	35(1)	-14(1)	-3(1)	-3(1)
C(5)	18(1)	15(1)	30(1)	-13(1)	-3(1)	1(1)
C(6)	13(1)	14(1)	23(1)	-5(1)	0(1)	-3(1)
C(7)	19(1)	14(1)	32(1)	-5(1)	-1(1)	0(1)
C(8)	24(1)	20(1)	27(1)	2(1)	-6(1)	3(1)
C(9)	27(1)	29(1)	19(1)	-3(1)	-7(1)	1(1)
C(10)	20(1)	20(1)	18(1)	-6(1)	-2(1)	0(1)
C(11)	13(1)	14(1)	16(1)	-4(1)	0(1)	-2(1)
C(12)	13(1)	13(1)	17(1)	-8(1)	-2(1)	-1(1)
C(13)	16(1)	10(1)	16(1)	-6(1)	-2(1)	0(1)
C(14)	15(1)	18(1)	13(1)	-8(1)	-3(1)	-3(1)
C(15)	18(1)	16(1)	17(1)	-8(1)	-4(1)	-2(1)
C(16)	16(1)	24(1)	20(1)	-12(1)	-5(1)	1(1)
C(17)	16(1)	29(1)	21(1)	-13(1)	-2(1)	-6(1)
C(18)	22(1)	20(1)	21(1)	-9(1)	-2(1)	-7(1)
C(19)	19(1)	17(1)	16(1)	-9(1)	-3(1)	-3(1)
C(20)	21(1)	14(1)	23(1)	-7(1)	-4(1)	-2(1)
C(21)	25(1)	18(1)	21(1)	-2(1)	-5(1)	-3(1)
C(22)	22(1)	23(1)	14(1)	-6(1)	-3(1)	-2(1)
C(23)	18(1)	19(1)	18(1)	-10(1)	-7(1)	2(1)
C(24)	14(1)	11(1)	18(1)	-8(1)	-3(1)	0(1)
C(25)	16(1)	15(1)	16(1)	-8(1)	-4(1)	-1(1)
C(26)	17(1)	17(1)	18(1)	-7(1)	-6(1)	-1(1)
C(27)	20(1)	16(1)	26(1)	-11(1)	-9(1)	4(1)
C(28)	22(1)	13(1)	24(1)	-9(1)	-7(1)	1(1)
C(29)	18(1)	16(1)	21(1)	-11(1)	-4(1)	0(1)
C(30)	18(1)	15(1)	14(1)	-5(1)	-3(1)	-2(1)
C(31)	24(1)	14(1)	15(1)	-5(1)	-4(1)	-3(1)
C(32)	23(1)	20(1)	14(1)	-4(1)	-5(1)	-9(1)
C(33)	17(1)	23(1)	16(1)	-5(1)	-5(1)	-3(1)
C(34)	17(1)	17(1)	14(1)	-4(1)	-3(1)	-1(1)
C(35)	17(1)	14(1)	12(1)	-3(1)	-3(1)	-3(1)
C(36)	16(1)	13(1)	15(1)	-6(1)	-4(1)	1(1)
C(37)	16(1)	11(1)	17(1)	-8(1)	-2(1)	0(1)
C(38)	12(1)	16(1)	16(1)	-7(1)	-2(1)	0(1)
C(39)	15(1)	14(1)	19(1)	-7(1)	-3(1)	-1(1)

C(40)	19(1)	23(1)	20(1)	-11(1)	-6(1)	0(1)
C(41)	23(1)	21(1)	16(1)	-4(1)	-6(1)	1(1)
C(42)	21(1)	14(1)	21(1)	-4(1)	-3(1)	-1(1)
C(43)	14(1)	17(1)	18(1)	-8(1)	-1(1)	0(1)
C(44)	24(1)	14(1)	21(1)	-8(1)	-3(1)	-2(1)
C(45)	24(1)	19(1)	25(1)	-9(1)	-4(1)	-7(1)
C(46)	17(1)	23(1)	21(1)	-11(1)	-1(1)	-5(1)
C(47)	16(1)	20(1)	21(1)	-11(1)	-5(1)	-1(1)
C(48)	18(1)	11(1)	16(1)	-8(1)	-3(1)	0(1)
C(49)	22(1)	22(1)	20(1)	-13(1)	-5(1)	0(1)
C(50)	33(1)	21(1)	29(1)	-12(1)	-10(1)	0(1)
C(51)	28(1)	29(1)	47(1)	-16(1)	9(1)	-1(1)
O(1)	13(1)	14(1)	17(1)	-7(1)	-2(1)	-2(1)
O(2)	14(1)	17(1)	22(1)	-10(1)	-3(1)	2(1)
O(3)	19(1)	15(1)	17(1)	-9(1)	-6(1)	3(1)
O(4)	16(1)	16(1)	15(1)	-6(1)	-4(1)	-2(1)
O(5)	24(1)	14(1)	15(1)	-8(1)	-6(1)	1(1)
O(6)	16(1)	18(1)	24(1)	-13(1)	-5(1)	2(1)
O(7)	20(1)	23(1)	28(1)	-14(1)	-4(1)	1(1)
O(8)	43(1)	21(1)	19(1)	-7(1)	-4(1)	9(1)
F(1)	23(1)	31(1)	29(1)	-17(1)	-11(1)	-1(1)
F(2)	14(1)	27(1)	34(1)	-18(1)	0(1)	-6(1)
F(3)	21(1)	27(1)	20(1)	-8(1)	-10(1)	4(1)
F(4)	28(1)	28(1)	21(1)	-16(1)	-5(1)	-3(1)
F(5)	19(1)	18(1)	26(1)	-10(1)	-10(1)	1(1)
F(6)	26(1)	16(1)	17(1)	-4(1)	-6(1)	-1(1)
F(7)	17(1)	24(1)	28(1)	-9(1)	-3(1)	3(1)
F(8)	27(1)	35(1)	23(1)	-13(1)	-7(1)	-12(1)

Hydrogen coordinates (x 10⁴) and isotropic displacement parameters (Å²x 10³).

	x	y	z	U(eq)
H(3A)	3753	10668	-701	27
H(3B)	2498	10059	-235	27
H(4A)	3259	10936	-2327	28
H(4B)	2645	11675	-1822	28
H(5A)	1159	10047	-1112	25
H(5B)	718	11210	-1530	25
H(7)	338	12109	-3135	30
H(8)	-132	12140	-4529	35
H(9)	313	10712	-4826	33

H(10)	1290	9276	-3745	25
H(15)	-737	9482	-1384	20
H(16)	-2836	9051	-936	23
H(17)	-3334	7366	-34	25
H(18)	-1724	6117	360	25
H(20A)	1576	6424	-375	24
H(20B)	536	5597	109	24
H(21A)	156	5626	1625	28
H(21B)	1660	5643	1281	28
H(22A)	49	7399	1086	25
H(22B)	765	6794	1983	25
H(27A)	5538	3605	7770	23
H(27B)	5592	4506	6690	23
H(28A)	3175	3797	7798	23
H(28B)	4098	3104	7340	23
H(29A)	3967	5073	5906	21
H(29B)	3779	4075	5834	21
H(31)	1758	3568	6066	22
H(32)	-383	3962	6056	23
H(33)	-1348	5396	6247	23
H(34)	-159	6403	6475	20
H(39)	2804	6279	4528	20
H(40)	2574	7258	2893	23
H(41)	2773	8992	2174	26
H(42)	3245	9735	3079	24
H(44A)	3487	8588	5584	23
H(44B)	3488	9647	4629	23
H(45A)	5577	9402	3960	27
H(45B)	5546	9068	5104	27
H(46A)	5609	7684	4284	23
H(46B)	6827	7935	4504	23
H(50A)	6511	6494	8556	40
H(50B)	7999	6420	8511	40
H(50C)	7497	6384	7642	40
H(51A)	8529	8954	6685	57
H(51B)	8947	7989	6466	57
H(51C)	9219	7994	7433	57
H(2)	4943	8013	-1482	27
H(3)	2864	7756	-2259	24
H(5)	3889	6104	8482	25
H(6)	1714	7305	6968	27
H(8X)	4117(18)	6322(7)	9734(14)	32
H(8Y)	3926(18)	5485(13)	10420(4)	32

Crystal data and structure refinement for Dimer 8.15

Empirical formula	C ₂₄ H ₂₀ F ₄ O ₂	
Formula weight	416.40	
Temperature	100(2) K	
Wavelength	1.54178 Å	
Crystal system	Triclinic	
Space group	P-1	
Unit cell dimensions	a = 7.5863(4) Å	α = 91.070(3)°.
	b = 8.9598(5) Å	β = 96.218(2)°.
	c = 14.6268(8) Å	γ = 104.754(3)°.
Volume	954.66(9) Å ³	
Z	2	
Density (calculated)	1.449 Mg/m ³	
Absorption coefficient	0.999 mm ⁻¹	
F(000)	432	
Crystal size	0.12 x 0.10 x 0.05 mm ³	
Crystal color/habit	colorless prism	
Theta range for data collection	3.04 to 68.25°.	
Index ranges	-9 ≤ h ≤ 9, -10 ≤ k ≤ 10, -17 ≤ l ≤ 16	
Reflections collected	16000	
Independent reflections	3374 [R(int) = 0.0180]	
Completeness to theta = 67.00°	97.7 %	
Absorption correction	Semi-empirical from equivalents	
Max. and min. transmission	0.9517 and 0.8895	
Refinement method	Full-matrix least-squares on F ²	
Data / restraints / parameters	3374 / 0 / 271	
Goodness-of-fit on F ²	1.036	
Final R indices [I > 2σ(I)]	R1 = 0.0322, wR2 = 0.0853	
R indices (all data)	R1 = 0.0351, wR2 = 0.0883	
Largest diff. peak and hole	0.272 and -0.204 e.Å ⁻³	

Atomic coordinates ($\times 10^4$) and equivalent isotropic displacement parameters ($\text{\AA}^2 \times 10^3$). U(eq) is defined as one third of the trace of the orthogonalized U^{ij} tensor.

	x	y	z	U(eq)
C(1)	12252(2)	2961(1)	6896(1)	18(1)
C(2)	12516(2)	1932(1)	7688(1)	19(1)
C(3)	14068(2)	1181(1)	7779(1)	18(1)
C(4)	14073(2)	193(1)	8511(1)	22(1)
C(5)	15486(2)	-508(2)	8708(1)	26(1)
C(6)	16916(2)	-244(2)	8167(1)	28(1)
C(7)	16912(2)	713(2)	7436(1)	26(1)
C(8)	15515(2)	1449(1)	7221(1)	20(1)
C(9)	15678(2)	2433(2)	6387(1)	21(1)
C(10)	14448(2)	1616(2)	5515(1)	23(1)
C(11)	12760(2)	2208(2)	5238(1)	21(1)
C(12)	11502(2)	2072(1)	5977(1)	21(1)
C(13)	12558(2)	4474(1)	7096(1)	18(1)
C(14)	13326(2)	5058(1)	8084(1)	18(1)
C(15)	12265(2)	5722(1)	8711(1)	18(1)
C(16)	13174(2)	6194(1)	9597(1)	20(1)
C(17)	12371(2)	6865(1)	10240(1)	23(1)
C(18)	10646(2)	7100(2)	10005(1)	25(1)
C(19)	9720(2)	6609(1)	9142(1)	22(1)
C(20)	10479(2)	5894(1)	8482(1)	19(1)
C(21)	9325(2)	5367(2)	7574(1)	24(1)
C(22)	9776(2)	6534(2)	6819(1)	30(1)
C(23)	11806(2)	7061(2)	6697(1)	25(1)
C(24)	12602(2)	5765(2)	6433(1)	22(1)
O(1)	11426(1)	1773(1)	8252(1)	28(1)
O(2)	14870(1)	4949(1)	8333(1)	27(1)
F(1)	9898(1)	2411(1)	5641(1)	29(1)
F(2)	10947(1)	526(1)	6182(1)	26(1)
F(3)	11843(1)	5208(1)	5567(1)	34(1)
F(4)	14446(1)	6370(1)	6350(1)	40(1)

Bond lengths [Å] and angles [°].

C(1)-C(13)	1.3367(18)	C(13)-C(24)	1.5202(17)
C(1)-C(2)	1.5217(17)	C(13)-C(14)	1.5271(17)
C(1)-C(12)	1.5269(17)	C(14)-O(2)	1.2172(16)
C(2)-O(1)	1.2144(15)	C(14)-C(15)	1.4925(17)
C(2)-C(3)	1.4933(17)	C(15)-C(16)	1.4041(18)
C(3)-C(4)	1.4027(18)	C(15)-C(20)	1.4071(18)
C(3)-C(8)	1.4128(18)	C(16)-C(17)	1.3806(18)
C(4)-C(5)	1.3819(19)	C(16)-H(16)	0.9500
C(4)-H(4)	0.9500	C(17)-C(18)	1.386(2)
C(5)-C(6)	1.386(2)	C(17)-H(17)	0.9500
C(5)-H(5)	0.9500	C(18)-C(19)	1.382(2)
C(6)-C(7)	1.384(2)	C(18)-H(18)	0.9500
C(6)-H(6)	0.9500	C(19)-C(20)	1.3992(18)
C(7)-C(8)	1.3960(18)	C(19)-H(19)	0.9500
C(7)-H(7)	0.9500	C(20)-C(21)	1.5070(18)
C(8)-C(9)	1.5157(17)	C(21)-C(22)	1.539(2)
C(9)-C(10)	1.5462(19)	C(21)-H(21A)	0.9900
C(9)-H(9A)	0.9900	C(21)-H(21B)	0.9900
C(9)-H(9B)	0.9900	C(22)-C(23)	1.523(2)
C(10)-C(11)	1.5247(18)	C(22)-H(22A)	0.9900
C(10)-H(10A)	0.9900	C(22)-H(22B)	0.9900
C(10)-H(10B)	0.9900	C(23)-C(24)	1.5014(18)
C(11)-C(12)	1.5040(17)	C(23)-H(23A)	0.9900
C(11)-H(11A)	0.9900	C(23)-H(23B)	0.9900
C(11)-H(11B)	0.9900	C(24)-F(3)	1.3621(15)
C(12)-F(1)	1.3705(15)	C(24)-F(4)	1.3853(16)
C(12)-F(2)	1.3894(15)		
C(13)-C(1)-C(2)	117.47(11)	C(6)-C(5)-H(5)	120.3
C(13)-C(1)-C(12)	128.58(12)	C(7)-C(6)-C(5)	119.80(12)
C(2)-C(1)-C(12)	113.73(10)	C(7)-C(6)-H(6)	120.1
O(1)-C(2)-C(3)	121.58(11)	C(5)-C(6)-H(6)	120.1
O(1)-C(2)-C(1)	116.93(11)	C(6)-C(7)-C(8)	122.28(13)
C(3)-C(2)-C(1)	121.48(10)	C(6)-C(7)-H(7)	118.9
C(4)-C(3)-C(8)	119.64(12)	C(8)-C(7)-H(7)	118.9
C(4)-C(3)-C(2)	115.06(11)	C(7)-C(8)-C(3)	117.59(12)
C(8)-C(3)-C(2)	125.24(11)	C(7)-C(8)-C(9)	116.26(11)
C(5)-C(4)-C(3)	121.22(12)	C(3)-C(8)-C(9)	126.13(11)
C(5)-C(4)-H(4)	119.4	C(8)-C(9)-C(10)	113.26(10)
C(3)-C(4)-H(4)	119.4	C(8)-C(9)-H(9A)	108.9
C(4)-C(5)-C(6)	119.47(12)	C(10)-C(9)-H(9A)	108.9
C(4)-C(5)-H(5)	120.3	C(8)-C(9)-H(9B)	108.9

C(10)-C(9)-H(9B)	108.9	C(20)-C(21)-C(22)	113.06(11)
H(9A)-C(9)-H(9B)	107.7	C(20)-C(21)-H(21A)	109.0
C(11)-C(10)-C(9)	115.11(10)	C(22)-C(21)-H(21A)	109.0
C(11)-C(10)-H(10A)	108.5	C(20)-C(21)-H(21B)	109.0
C(9)-C(10)-H(10A)	108.5	C(22)-C(21)-H(21B)	109.0
C(11)-C(10)-H(10B)	108.5	H(21A)-C(21)-H(21B)	107.8
C(9)-C(10)-H(10B)	108.5	C(23)-C(22)-C(21)	114.45(11)
H(10A)-C(10)-H(10B)	107.5	C(23)-C(22)-H(22A)	108.6
C(12)-C(11)-C(10)	113.26(11)	C(21)-C(22)-H(22A)	108.6
C(12)-C(11)-H(11A)	108.9	C(23)-C(22)-H(22B)	108.6
C(10)-C(11)-H(11A)	108.9	C(21)-C(22)-H(22B)	108.6
C(12)-C(11)-H(11B)	108.9	H(22A)-C(22)-H(22B)	107.6
C(10)-C(11)-H(11B)	108.9	C(24)-C(23)-C(22)	113.44(11)
H(11A)-C(11)-H(11B)	107.7	C(24)-C(23)-H(23A)	108.9
F(1)-C(12)-F(2)	103.67(10)	C(22)-C(23)-H(23A)	108.9
F(1)-C(12)-C(11)	110.31(10)	C(24)-C(23)-H(23B)	108.9
F(2)-C(12)-C(11)	108.22(10)	C(22)-C(23)-H(23B)	108.9
F(1)-C(12)-C(1)	109.52(10)	H(23A)-C(23)-H(23B)	107.7
F(2)-C(12)-C(1)	105.89(10)	F(3)-C(24)-F(4)	104.44(10)
C(11)-C(12)-C(1)	118.15(11)	F(3)-C(24)-C(23)	108.69(11)
C(1)-C(13)-C(24)	128.07(11)	F(4)-C(24)-C(23)	108.52(11)
C(1)-C(13)-C(14)	117.45(11)	F(3)-C(24)-C(13)	111.77(11)
C(24)-C(13)-C(14)	113.32(10)	F(4)-C(24)-C(13)	104.68(10)
O(2)-C(14)-C(15)	121.57(11)	C(23)-C(24)-C(13)	117.80(10)
O(2)-C(14)-C(13)	115.77(11)		
C(15)-C(14)-C(13)	122.66(11)		
C(16)-C(15)-C(20)	119.40(11)		
C(16)-C(15)-C(14)	115.14(11)		
C(20)-C(15)-C(14)	125.46(11)		
C(17)-C(16)-C(15)	121.25(12)		
C(17)-C(16)-H(16)	119.4		
C(15)-C(16)-H(16)	119.4		
C(16)-C(17)-C(18)	119.56(12)		
C(16)-C(17)-H(17)	120.2		
C(18)-C(17)-H(17)	120.2		
C(19)-C(18)-C(17)	119.70(12)		
C(19)-C(18)-H(18)	120.2		
C(17)-C(18)-H(18)	120.2		
C(18)-C(19)-C(20)	122.08(12)		
C(18)-C(19)-H(19)	119.0		
C(20)-C(19)-H(19)	119.0		
C(19)-C(20)-C(15)	117.92(12)		
C(19)-C(20)-C(21)	117.50(12)		
C(15)-C(20)-C(21)	124.58(11)		

Symmetry transformations used to generate equivalent atoms:

Anisotropic displacement parameters ($\text{\AA}^2 \times 10^3$). The anisotropic displacement factor exponent takes the form: $-2p^2 [h^2 a^* U^{11} + \dots + 2 h k a^* b^* U^{12}]$

	U11	U22	U33	U23	U13	U12
C(1)	15(1)	23(1)	16(1)	0(1)	4(1)	7(1)
C(2)	20(1)	18(1)	17(1)	-2(1)	3(1)	2(1)
C(3)	20(1)	16(1)	18(1)	-1(1)	1(1)	2(1)
C(4)	23(1)	20(1)	20(1)	1(1)	2(1)	0(1)
C(5)	31(1)	19(1)	24(1)	5(1)	-3(1)	4(1)
C(6)	27(1)	25(1)	34(1)	3(1)	-1(1)	12(1)
C(7)	24(1)	27(1)	29(1)	3(1)	6(1)	10(1)
C(8)	21(1)	18(1)	21(1)	0(1)	2(1)	4(1)
C(9)	19(1)	23(1)	23(1)	5(1)	8(1)	7(1)
C(10)	30(1)	23(1)	19(1)	3(1)	10(1)	11(1)
C(11)	27(1)	22(1)	15(1)	-2(1)	3(1)	7(1)
C(12)	20(1)	21(1)	21(1)	-1(1)	1(1)	6(1)
C(13)	17(1)	23(1)	16(1)	1(1)	4(1)	7(1)
C(14)	19(1)	16(1)	18(1)	3(1)	3(1)	3(1)
C(15)	22(1)	15(1)	16(1)	2(1)	4(1)	3(1)
C(16)	23(1)	18(1)	18(1)	3(1)	2(1)	2(1)
C(17)	32(1)	20(1)	15(1)	0(1)	4(1)	0(1)
C(18)	33(1)	20(1)	22(1)	1(1)	13(1)	5(1)
C(19)	24(1)	20(1)	25(1)	4(1)	8(1)	6(1)
C(20)	22(1)	16(1)	19(1)	2(1)	5(1)	4(1)
C(21)	19(1)	32(1)	23(1)	-3(1)	1(1)	10(1)
C(22)	37(1)	41(1)	20(1)	1(1)	-1(1)	24(1)
C(23)	39(1)	20(1)	17(1)	3(1)	2(1)	12(1)
C(24)	27(1)	26(1)	15(1)	3(1)	4(1)	9(1)
O(1)	29(1)	31(1)	26(1)	8(1)	13(1)	10(1)
O(2)	21(1)	36(1)	25(1)	-5(1)	0(1)	10(1)
F(1)	22(1)	44(1)	22(1)	-4(1)	-2(1)	13(1)
F(2)	30(1)	21(1)	23(1)	-2(1)	5(1)	-2(1)
F(3)	65(1)	32(1)	14(1)	1(1)	1(1)	26(1)
F(4)	32(1)	45(1)	48(1)	27(1)	18(1)	13(1)

Hydrogen coordinates ($\times 10^4$) and isotropic displacement parameters ($\text{\AA}^2 \times 10^3$).

	x	y	z	U(eq)
H(4)	13087	3	8878	26
H(5)	15478	-1165	9211	31
H(6)	17895	-719	8299	34
H(7)	17895	874	7067	31
H(9A)	16972	2714	6258	26
H(9B)	15341	3401	6531	26
H(10A)	15199	1735	4995	27
H(10B)	14037	498	5618	27
H(11A)	13165	3305	5087	25
H(11B)	12069	1617	4676	25
H(16)	14365	6049	9757	24
H(17)	12997	7163	10840	28
H(18)	10102	7596	10435	29
H(19)	8531	6762	8992	27
H(21A)	8014	5194	7662	29
H(21B)	9516	4368	7366	29
H(22A)	9085	6061	6227	36
H(22B)	9343	7453	6969	36
H(23A)	11971	7831	6216	30
H(23B)	12494	7578	7280	30